UNCLASSIFIED

AD NUMBER

AD221586

CLASSIFICATION CHANGES

TO: unclassified

FROM: confidential

LIMITATION CHANGES

TO:

Approved for public release, distribution unlimited

FROM:

No Foreign

AUTHORITY

22 Dec 1960 SoD memo; 10 May 66 per M. Kahn, DDC-IR

THIS PAGE IS UNCLASSIFIED

UNCLASSIFIED

AD 221 586

Reproduced
by the

ARMED SERVICES TECHNICAL INFORMATION AGENCY
ARLINGTON HALL STATION
ARLINGTON 12, VIRGINIA

UNCLASSIFIED

DISCLAIMER NOTICE

THIS DOCUMENT IS BEST QUALITY PRACTICABLE. THE COPY FURNISHED TO DTIC CONTAINED A SIGNIFICANT NUMBER OF PAGES WHICH DO NOT REPRODUCE LEGIBLY.

NOTICE: When government or other drawings, specifications or other data are used for any purpose other than in connection with a definitely related government procurement operation, the U. S. Government thereby incurs no responsibility, nor any obligation whatsoever; and the fact that the Government may have formulated, furnished, or in any way supplied the said drawings, specifications, or other data is not to be regarded by implication or otherwise as in any manner licensing the holder or any other person or corporation, or conveying any rights or permission to manufacture, use or sell any patented invention that may in any way be related thereto.

UNCLASSIFIED

SUMMARY TECHNICAL REPORT
OF THE
NATIONAL DEFENSE RESEARCH COMMITTEE

Classification cancelled
or changed to Unclassified 2 Aug 60
AUTH: Sec Def Memo
By Oberlies C Beebe
Signature and Grade
Date 22 Dec 60

This document contains information affecting the national defense of the United States within the meaning of the Espionage Act, 50 U.S.C., 31 and 32, as amended. Its transmission or the revelation of its contents in any manner to an unauthorized person is prohibited by law.

This volume is classified CONFIDENTIAL in accordance with security regulations of the War and Navy Departments because certain chapters contain material which was CONFIDENTIAL at the date of printing. Other chapters may have had a lower classification or none. The reader is advised to consult the War and Navy agencies listed on the reverse of this page for the current classification of any material.

UNCLASSIFIED

Manuscript and illustrations for this volume were prepared for publication by the Summary Reports Group of the Columbia University Division of War Research under Contract OEMsr-1131 with the Office of Scientific Research and Development. This volume was printed and bound by the Columbia University Press.

Distribution of the Summary Technical Report of NDRC has been made by the War and Navy Departments. Inquiries concerning the availability and distribution of the Summary Technical Report volumes and microfilmed and other reference material should be addressed to the War Department Library, Room 1A-522, The Pentagon, Washington 25, D. C., or to the Office of Naval Research, Navy Department, Attention: Reports and Documents Section, Washington 25, D. C.

Copy No.

236

This volume, like the seventy others of the Summary Technical Report of NDRC, has been written, edited, and printed under great pressure. Inevitably there are errors which have slipped past Division readers and proofreaders. There may be errors of fact not known at time of printing. The author has not been able to follow through his writing to the final page proof.

Please report errors to:

JOINT RESEARCH AND DEVELOPMENT BOARD
PROGRAMS DIVISION (STP ERRATA)
WASHINGTON 25, D. C.

A master errata sheet will be compiled from these reports and sent to recipients of the volume. Your help will make this book more useful to other readers and will be of great value in preparing any revisions.

UNCLASSIFIED

20229

SUMMARY TECHNICAL REPORT OF DIVISION 2, NDRC

RDB
Library Section

VOLUME 1

CLASS
CHANGED

EFFECTS OF IMPACT AND EXPLOSION

OFFICE OF SCIENTIFIC RESEARCH AND DEVELOPMENT
VANNEVAR BUSH, DIRECTOR

NATIONAL DEFENSE RESEARCH COMMITTEE
JAMES B. CONANT, CHAIRMAN

DIVISION 2
E. BRIGHT WILSON, JR., CHIEF

WASHINGTON, D. C., 1946

UNCLASSIFIED

UNCLASSIFIED

NATIONAL DEFENSE RESEARCH COMMITTEE

James B. Conant, *Chairman*

Richard C. Tolman, *Vice Chairman*

Roger Adams	Army Representative[1]
Frank B. Jewett	Navy Representative[2]
Karl T. Compton	Commissioner of Patents[3]

Irvin Stewart, *Executive Secretary*

[1]*Army representatives in order of service:*

Maj. Gen. G. V. Strong
Maj. Gen. R. C. Moore
Maj. Gen. C. C. Williams
Brig. Gen. W. A. Wood, Jr.
Col. L. A. Denson
Col. P. R. Faymonville
Brig. Gen. E. A. Regnier
Col. M. M. Irvine
Col. E. A. Routheau

[2]*Navy representatives in order of service:*

Rear Adm. H. G. Bowen
Capt. Lybrand P. Smith
Rear Adm. J. A. Furer
Rear Adm. A. H. Van Keuren
Commodore H. A. Schade

[3]*Commissioners of Patents in order of service:*

Conway P. Coe
Casper W. Ooms

NOTES ON THE ORGANIZATION OF NDRC

The duties of the National Defense Research Committee were (1) to recommend to the Director of OSRD suitable projects and research programs on the instrumentalities of warfare, together with contract facilities for carrying out these projects and programs, and (2) to administer the technical and scientific work of the contracts. More specifically, NDRC functioned by initiating research projects on requests from the Army or the Navy, or on requests from an allied government transmitted through the Liaison Office of OSRD, or on its own considered initiative as a result of the experience of its members. Proposals prepared by the Division, Panel, or Committee for research contracts for performance of the work involved in such projects were first reviewed by NDRC, and if approved, recommended to the Director of OSRD. Upon approval of a proposal by the Director, a contract permitting maximum flexibility of scientific effort was arranged. The business aspects of the contract, including such matters as materials, clearances, vouchers, patents, priorities, legal matters, and administration of patent matters were handled by the Executive Secretary of OSRD.

Originally NDRC administered its work through five divisions, each headed by one of the NDRC members. These were:

Division A—Armor and Ordnance
Division B—Bombs, Fuels, Gases, & Chemical Problems
Division C—Communication and Transportation
Division D—Detection, Controls, and Instruments
Division E—Patents and Inventions

In a reorganization in the fall of 1942, twenty-three administrative divisions, panels, or committees were created, each with a chief selected on the basis of his outstanding work in the particular field. The NDRC members then became a reviewing and advisory group to the Director of OSRD. The final organization was as follows:

Division 1—Ballistic Research
Division 2—Effects of Impact and Explosion
Division 3—Rocket Ordnance
Division 4—Ordnance Accessories
Division 5—New Missiles
Division 6—Sub-Surface Warfare
Division 7—Fire Control
Division 8—Explosives
Division 9—Chemistry
Division 10—Absorbents and Aerosols
Division 11—Chemical Engineering
Division 12—Transportation
Division 13—Electrical Communication
Division 14—Radar
Division 15—Radio Coordination
Division 16—Optics and Camouflage
Division 17—Physics
Division 18—War Metallurgy
Division 19—Miscellaneous
Applied Mathematics Panel
Applied Psychology Panel
Committee on Propagation
Tropical Deterioration Administrative Committee

UNCLASSIFIED

UNCLASSIFIED

NDRC FOREWORD

As events of the years preceding 1940 revealed more and more clearly the seriousness of the world situation, many scientists in this country came to realize the need of organizing scientific research for service in a national emergency. Recommendations which they made to the White House were given careful and sympathetic attention, and as a result the National Defense Research Committee [NDRC] was formed by Executive Order of the President in the summer of 1940. The members of NDRC, appointed by the President, were instructed to supplement the work of the Army and the Navy in the development of the instrumentalities of war. A year later, upon the establishment of the Office of Scientific Research and Development [OSRD], NDRC became one of its units.

The Summary Technical Report of NDRC is a conscientious effort on the part of NDRC to summarize and evaluate its work and to present it in a useful and permanent form. It comprises some seventy volumes broken into groups corresponding to the NDRC Divisions, Panels, and Committees.

The Summary Technical Report of each Division, Panel, or Committee is an integral survey of the work of that group. The first volume of each group's report contains a summary of the report, stating the problems presented and the philosophy of attacking them, and summarizing the results of the research, development, and training activities undertaken. Some volumes may be "state of the art" treatises covering subjects to which various research groups have contributed information. Others may contain descriptions of devices developed in the laboratories. A master index of all these divisional, panel, and committee reports which together constitute the Summary Technical Report of NDRC is contained in a separate volume, which also includes the index of a microfilm record of pertinent technical laboratory reports and reference material.

Some of the NDRC-sponsored researches which had been declassified by the end of 1945 were of sufficient popular interest that it was found desirable to report them in the form of monographs, such as the series on radar by Division 14 and the monograph on sampling inspection by the Applied Mathematics Panel. Since the material treated in them is not duplicated in the Summary Technical Report of NDRC, the monographs are an important part of the story of these aspects of NDRC research.

In contrast to the information on radar, which is of widespread interest and much of which is released to the public, the research on subsurface warfare is largely classified and is of general interest to a more restricted group. As a consequence, the report of Division 6 is found almost entirely in its Summary Technical Report, which runs to over twenty volumes. The extent of the work of a division cannot therefore be judged solely by the number of volumes devoted to it in the Summary Technical Report of NDRC; account must be taken of the monographs and available reports published elsewhere.

The research program of Division 2, first under the leadership of John E. Burchard and then of E. Bright Wilson, Jr., included studies of underwater explosions, of muzzle blast effects in high velocity guns, the terminal ballistics of concrete and plastic armor, and defenses against shaped-charge projectiles, to name but a few of the projects described in the Division's Summary Technical Report, which has been prepared under the direction of the Division Chief and has been authorized by him for publication.

The most dramatic example of the work of Division 2 was the study of bombs of the blockbuster type. The blockbuster was the exclamation point to a program of research aimed at establishing principles for the selection of weapons designed to achieve maximum damage against a given target for a given expenditure of energy. The Division's study on the effects of explosions in various types of soil is a project of great importance to a work in which any next war may involve atomic bombs and guided missiles. We join the nation in expressing gratitude for Division 2's valuable wartime achievements.

VANNEVAR BUSH, Director
Office of Scientific Research and Development

J. B. CONANT, Chairman
National Defense Research Committee

UNCLASSIFIED

UNCLASSIFIED

FOREWORD

THE PRINCIPAL OBJECTIVE of Division 2 was to place the use of weapons and of defensive materials on a quantitative, engineering basis. Scientific studies were therefore carried out on terminal ballistics, on explosions in air, earth, and water, and on certain properties of materials, with the object of providing the basic data necessary for the rational employment of bombs, projectiles, explosives, etc. At all times, the principle was kept uppermost that practical results would inevitably follow from a deeper scientific understanding of the physics and chemistry of the phenomena involved in the action of weapons.

It is hoped that the present volume will be useful to those groups who are carrying on work dealing with the design or employment of weapons. It should also be useful in the event of a future war in giving newcomers to the field a concise survey of the state of knowledge at the end of World War II.

The field of activity of Division 2 touched upon those of several other divisions, particularly Division 1, Ballistic Research, Division 8, Explosives, Division 11, Chemical Engineering, Division 17, Physics, Division 18, War Metallurgy, and the Applied Mathematics Panel. The work on the terminal ballistics of hypervelocity projectiles carried out at Princeton was naturally of importance to Division 1, which was developing means for producing these high velocities. The coordination with Division 8 was at all times very close; in fact, three of the contracts of Division 2, namely those with Cornell University (under J. G. Kirkwood), the Stanolind Oil and Gas Company (under Daniel Silverman), and the Woods Hole Oceanographic Institution, were originally assigned to Division 8. Divisions 2 and 11 and the Applied Mathematics Panel cooperated on various bombing problems, especially those dealing with the relative effectiveness of high-explosive and incendiary bombs. The contacts with Division 17 were concerned chiefly with the problem of neutralising land mines; those with Division 18 were related to the properties of metals at high rates of strain. One contract, with the California Institute of Technology, was transferred from Division 2 to Division 18.

The technical material which is described in this volume is the work of many people, not all of whom were connected with Division 2 of National Defense Research Committee. The work of many British laboratories needs to be especially mentioned, since the British were particularly effective in the fields covered by Division 2. Also, our own Service laboratories contributed much to this type of work. Among the Division 2 contracts, the largest were the Princeton University Station, directed by Walter Bleakney, and the Underwater Explosives Research Laboratory at Woods Hole, under Paul C. Cross. The Duke University contract, under Paul M. Gross, deserves special mention also, because of the successful development of the frangible projectile for gunnery training.

The preparation of this volume has been a cooperative effort by a group of men, all of whom were directly engaged during the war on the projects about which they have written. To these authors, R. A. Beth, P. W. Bridgman, P. C. Cross, C. W. Curtis, P. M. Gross, W. D. Kennedy, C. W. Lampson, A. E. Puckett, E. M. Pugh, W. G. Schneider, J. J. Slade, Jr., R. J. Slutz, J. G. Stipe, Jr., and M. P. White, goes the credit for the high level of technical writing in the chapters which follow. The successful coordination of this joint operation is due to Merit P. White who has very ably edited the volume and organized the separate chapters into a coherent whole.

E. BRIGHT WILSON, JR.
Chief, Division 2

UNCLASSIFIED

PREFACE

THIS VOLUME is not designed to be a detailed record of all work of Division 2. The time available for its preparation, no less than the type of reader for whom it is written, has prevented this. This report is designed for the use of individuals concerned with planning or directing investigations similar to those described here, for whom a knowledge of the methods of attack, the difficulties that may be encountered, and the results that have been accomplished will be useful. Furthermore, an extensive, although not necessarily exhaustive, bibliography is included. For those desiring only an overall view of the work of this Division, and as an introduction for those planning to read the entire volume, a "Summary" has been prepared, comprising Part I, immediately following the Table of Contents.

The content of this volume comes partly from the fact that Division 2, throughout World War II, has been mostly concerned with information, and not with the development or improvement of devices. This information has dealt with the performance of weapons and with defense against weapons. Some of it has been obtained by the Division through experimentation, some from tests by other organizations in NDRC, the Services, and among our Allies, and much information came from the field. Very early in the existence of Division 2 it was recognized that the value of any information obtained was a direct function of the use that was made of it, and that the potential users of this information were to a large extent organizations in the field. As a result, considerable thought was given to ways of getting information on weapon performance to such users in forms where it could and would be used. Because of the importance of these functions—getting, organizing, and dispensing information on weapons—not only in the existence of Division 2, but also to any other organization that undertakes the same problem, they are discussed in Part VII of this volume, "Liaison."

The research carried out by Division 2 is treated under five categories, Parts II to VI of this volume. Part II is concerned with explosions in air, water, and underground. Muzzle blast control is included with these. Part III covers terminal ballistics of steel armor, concrete, plastic protection, and earth, and the development of a frangible bullet for training of aerial gunners. Part IV is concerned with rather fundamental investigations on the properties of matter, in particular, the propagation of plasticity in solids, the behavior of steel under very large pressures, and the design of a supersonic wind tunnel. However, all research on supersonic problems done in the Division is discussed in Chapter 2 on explosions in air. Studies of protective measures are treated in the next part, Part V, except for those items that have been covered elsewhere in the volume. Part VI is concerned with application of information on weapon behavior and effectiveness to the problems of selecting weapons for specific targets, and with estimating the resulting damage.

Before concluding this already overlong preface, I wish to express my appreciation of the conscientious and painstaking efforts of my collaborators.

MERRITT P. WHITE
Editor

CONTENTS

CHAPTER		PAGE
	PART I	
	SUMMARY	3
	PART II	
	EXPLOSIONS	
1	Underwater Explosives and Explosions by *W. G. Schneider, E. B. Wilson, Jr.*, and *P. E. Cross*	19
2	Explosions and Explosives in Air by *W. D. Kennedy*	64
3	Explosions in Earth by *C. W. Lampson*	110
4	Muzzle Blast, Its Characteristics, Effects and Control by *J. J. Slade, Jr.*	133
	PART III	
	TERMINAL BALLISTICS	
5	Fundamentals of Terminal Ballistics by *R. A. Beth*	155
6	Terminal Ballistics of Armor by *C. W. Curtis*	160
7	Terminal Ballistics of Concrete by *R. A. Beth*	191
8	Terminal Ballistics of Plastic Protection by *J. G. Stipe, Jr.* . .	229
9	Terminal Ballistics of Soil by *J. G. Stipe, Jr.*	233
10	The Frangible Bullet for Use in Aerial Gunnery Training by *P. E. Cross* and *M. P. White*	242
	PART IV	
	PROPERTIES OF MATTER	
11	Design of Model Supersonic Wind Tunnel by *A. E. Puckett* . .	251
12	Behavior of Materials under Dynamic Loads by *M. P. White* .	255
13	Deformation of Steel under High Pressure by *P. W. Bridgman* and *M. P. White*	266
	PART V	
	PROTECTION	
14	Defense against Shaped Charges by *E. M. Pugh*	277
15	Structural Protection by *M. P. White*	283

PART VI

ATTACK

CHAPTER		PAGE
16	Target Analysis and Weapon Selection by *J. G. Stipe, Jr.*	305

PART VII

LIAISON

17	The Division 2 Technical Library by *R. J. Slutz*	337
18	Training of Operation Analysts by *J. G. Stipe, Jr.*	339
19	Weapon Data Sheets by *J. G. Stipe, Jr.*	342
	Glossary	473
	Symbols	477
	Bibliography	479
	OSRD Appointees	501
	Contract Numbers	502
	Project Numbers	503
	Index	505

PART I

SUMMARY

SUMMARY

Chapter 1

UNDERWATER EXPLOSIONS AND EXPLOSIVES

THIS CHAPTER treats the physics and chemistry of underwater explosions. In Section 1.2 there is a survey of the results of investigations made on underwater explosions including the properties of the shock wave, the bubble oscillations, the surface phenomena, and comparison of explosives.

The discussion of shock waves includes a treatment of the way in which they are produced, their shape, variation with weight and distance from charge, dependence on type of explosive, reflection from free, rigid, and deformable surfaces, and some numerical magnitudes which have been obtained.

The treatment of the oscillation of the gas bubble covers the reasons for this oscillation, the dependence of the period of the oscillation on several variables, the migration of the gas bubble under gravity and under the influence of free and rigid surfaces, the pressure pulses radiated during the minima in this oscillation and their properties.

Surface phenomena are described from the viewpoint of the theory of the domes and plumes above underwater explosions and the usefulness of these phenomena for various types of measurements. Underwater cratering is discussed briefly, as is the production of surface waves by underwater explosions. The results of the very extensive comparisons of different explosives for underwater effectiveness are summarized together with some remarks on the methods of statistical analyses used in connection with such comparisons. The theories which were developed to calculate shock-wave properties, surface phenomena, surface waves, etc., are briefly reviewed.

There is a section on damage produced by underwater explosions including some general considerations, the effect of target inertia, the effect of cavitation, diffraction effects, and the relation of shock-wave parameters to damage. Some theoretical and experimental investigations of several simple systems such as a steel diaphragm over an air cavity, the ball crusher gauge, and the simple crusher cylinder are discussed. The use of scaled models and the difficulties involved in their use are described.

The section on experimental methods for studying underwater explosion phenomena contains a description of a variety of underwater pressure gauges and their utilization, including both the electrical and mechanical types. Photographic procedures are described which were very fruitful in the study of underwater explosions. Experimental procedures are given for studying the generation of surface waves and for the location of underwater explosions (such as are useful in testing fuzes).

The final section contains a description of the research facilities at the Underwater Explosives Research Laboratory [UERL] of Division 2, NDRC, which was located at Woods Hole, Massachusetts.

Chapter 1 contains numerous references, the titles of which are contained in the bibliography.

Chapter 2

EXPLOSIVES AND EXPLOSIONS IN AIR

This chapter deals with the behavior of shock waves in air; in particular, the air blast from high explosives is described, and the ways in which the air blast performs militarily useful functions are examined.

During World War II, the techniques of measuring the highly transient phenomena associated with explosions, theories concerned with them, and applications of the information obtained were developed from very meager beginnings. The important role of blast in the functioning of bombs was truly appreciated only as the war progressed, and the development and use of very large blockbuster bombs was one consequence of this realization.

Experimental methods for measuring and investigating the properties of blast waves in air are described in this report. Electrical gauges, mechanical gauges, methods depending upon measurement of shock-wave velocity, and photographic methods are discussed, and the advantages and disadvantages of each method are pointed out.

The criteria for assessing the relative merits of weapons whose functioning depends upon air blast are based in part upon some observations of the blast damage accomplished by German bombs dropped on Great Britain, and British bombs on Germany, and in part upon semitheoretical studies of the response of structural elements to blast. For bombs that are

not too large, the near-miss effectiveness is approximately measured by the positive impulse in the blast. For very large bombs, and certainly for the atomic bomb, the peak pressure in the blast is considered the important factor.

In an effort to improve the blast performance of high-explosive bombs, several high explosives were studied to determine their merits for this purpose. Results are usually expressed as the relative peak pressures and relative positive impulses from equal volumes of the explosives being compared. Compilations of such data from several sources were made, and the results are expressed as average relative peak pressures and relative positive impulses. These data demonstrate a marked superiority of aluminized explosives over nonaluminized explosives. Estimates of the relative areas of blast damage to be expected of several of these explosives were made, and are shown graphically in Figure 4. It is shown, for example, that a bomb filled with tritonal is estimated to produce about 33 per cent more blast damage than would a similar bomb filled with TNT.

The metal case of a bomb reduces the blast from its explosive contents. It is shown that the relatively thick case of a *general-purpose* [GP] bomb reduces the damaging power per ton of bombs by about 60 per cent, compared with that obtainable from a *light-case* [LC] bomb. It is pointed out that the thinnest case consistent with safe handling and storage should be used for bombs intended to be detonated instantaneously on impact or burst in air by means of a proximity fuze.

The principle of similitude which permits the calculation of blast pressures, impulses, etc., from bombs of various sizes, from measurements with one size or weight, is stated, and its limitations discussed. The dependence of peak pressure and positive impulse on distance from the explosion are expressed graphically for bombs burst high above the ground, as well as for those on the ground. The advancement of theoretical work is described, and the extent to which it has been tested and checked by experimental results is outlined.

By experimental and theoretical investigation of the properties of the blast from bombs burst at various heights above the ground as well as on impact, it is shown that there exists some optimum height of burst such that the area of damage of a desired category can be maximized, and that, on the average, the area of demolition as well as of less severe damage can be approximately doubled by use of air-burst, rather than ground-burst, fuzes. The experiments show, moreover, that the optimum height is not critical, and that both demolition and less severe damage can be nearly maximized by a single optimum height of burst for a given size of bomb. Estimates are made for the air burst of an atomic bomb for which the peak pressure is the criterion of damage, and it is estimated that, if the bomb were burst at the optimum height, the damage would be about 90 per cent greater than if it were burst on the ground.

The relative effectiveness of explosives in enclosed spaces is quite different from that of explosives detonated in the open. It is shown that this difference is due to the relatively slow combustion of the products of the explosion, and that the order of merit of explosives in enclosed spaces is the same as the order of their heats of combustion. The significance of these results is that small GP bombs whose near-miss effectiveness is almost nil should be filled with one of the explosives found to be best in enclosed spaces. The poorest explosive tested under these conditions is Composition B, and the best, tritonal.

The history and present status of the development of slow-burning explosives [SBX] is described. Experimental results show that certain SBX materials, such as one consisting of aluminum powder and gasoline, dispersed and ignited by a high-explosive bursting charge, have promise of improved performance over high explosives as fillings of small (500- to 1,000-lb) bombs, whose main blast effect is obtained through direct hit and penetration of the target.

The application of explosives to the clearance of land mines by blast is described. Demolition devices in the form of "line" charges were developed by the Engineer Board for this purpose. The measurement of blast pressures and impulses from some of these devices is described, and the results are shown graphically. A theory of the responses of the fuzes of land mines to the blast from explosive charges has been devised; by means of this theory, together with blast measurements, the distances at which mines should be cleared by various demolition charges have been calculated. Comparison of these predictions with experimental observations of minefield clearance show good agreement for "point" charges, such as bombs, and poor agreement for line charges. More blast measurements and theoretical work are required in order to clear up these discrepancies.

Blast measurements which were made at various altitudes up to about 14,000 ft above sea level show

that the order of merit among the explosives tested is unchanged, but that the magnitudes of the pressures and impulses measured are less at high altitudes than at sea level. Good agreement with theoretical predictions is obtained.

The application of blast measurements to model-scale experiments with igloo-type storage magazines is described. The purpose of these tests was to assist in determining the minimum spacing between magazines, consistent with insuring that a disastrous chain of sympathetic detonations would not occur. Other measurements on the blast from rocket jets and from charges of various shapes are also briefly described.

Chapter 3

EXPLOSIONS IN EARTH

Before the beginning of World War II, the question of the effects of underground explosions on nearby structures was not particularly important, because the quantities of explosive involved were comparatively small. The use of large and powerful bombs and the development of long-range bombers to deliver them anywhere in the enemy's territory gave this problem immediate importance at the beginning of World War II. The existence of the atomic bomb and of various guided missiles for conveying it as well as conventional explosives to distant targets makes burial in the earth one of the most effective defenses for a future war. This means, in turn, that the effects of explosions in earth will be of even greater importance to both defense and attack than in the past.

Because of the lack of reliable information on the nature and magnitudes of the phenomena that accompany an underground explosion, a very extensive series of tests was carried out cooperatively by the Corps of Engineers, the Committee on Passive Protection against Bombing, and Division 2, NDRC. These tests were made both in free earth and adjacent to buried reinforced concrete structures comparable to fortification construction, in a wide range of soil types from loess to saturated clay, and at scales up to 1,000-lb charges detonated adjacent to structures with 5- and 10-ft walls. In free earth, transient measurements of pressures, accelerations, velocities, and earth movements were taken. Crater sizes and permanent displacements were determined after each test. With structures present, the same quantities were measured both on the structures and at distances from them. Structural damage was recorded and correlated with amount of explosive and its point of detonation with respect to the target.

These data have been analyzed and the results expressed by means of semiempirical equations and graphs. From these it is possible to predict, with an uncertainty of the order of 20 per cent, the pressures, impulses, accelerations, velocities, displacements, and crater sizes that will result from detonation of a given amount of explosive at a certain depth. In addition, the damage to structures comparable to those tested can be predicted with about the same order of accuracy.

Chapter 4

MUZZLE BLAST: ITS CHARACTERISTICS, EFFECTS, AND CONTROL

Muzzle blast may be considered either as a relatively mild explosion following shot ejection or as an extremely high-pressure jet of short duration preceded by a traveling shock. The strength of this shock may be high, and depends on the muzzle pressure of the powder gas at the time of shot ejection. Within this spherical shock the gun empties in a jet characterized by a large bottle-shaped central region bounded by stationary shocks in which the gas attains very high speeds, and by an external turbulent shell in which the powder gases mix with the outside air. In this mixing region an explosive burning of certain components of the powder gas may occur, giving rise to the characteristic flash of medium and large caliber guns. The main emptying action occurs within a time comparable to the travel time of the projectile, although the low-pressure stages of the flow continue much longer. The main blast is followed by a wave of rarefaction which produces some flow of air toward the muzzle.

With increasing powder pressures the severity of muzzle-blast effects becomes a limiting factor in the tactical use of guns of high muzzle velocity. The blast pressures often cause severe damage to structures near the muzzle and injuries and discomfort to personnel. Among the problems presented by muzzle blast is the raising of dust by guns firing at low elevations. In direct fire obscuration of the target is a serious handicap, since a gun is useless while it is enveloped in a cloud of dust. Unless powder pressures are to be limited or high-pressure guns are to be replaced by weapons less damaging to the vicinity of the emplacement, it is necessary to develop devices that will lessen the effects of blast.

The most successful of the muzzle attachments so far developed is the muzzle brake. Brakes have been developed which absorb over 90 per cent of the recoil energy of guns, and there are indications that very high-pressure guns can be rendered practically recoilless by means of such attachments. The reduction of recoil energy permits the use of light mounts with high-pressure guns. However, all brakes direct the blast intensity toward the rear of the gun, the back pressures produced rising with the efficiency of the unit; for this reason only brakes of moderate efficiencies have been utilized.

Since in most emplacements the elevation and traverse of a gun are limited, it is generally possible to design a muzzle attachment which deflects or deforms the blast in such a way as to ensure a substantial amount of protection to neighboring structures. Also, such devices are usually brakes, but they can be designed so that the braking action is negligible. It is possible to deflect the blast unsymmetrically without affecting the flight or yaw of the projectile, but provision must be made to take up the eccentric thrust on the gun produced by such deflection.

The slight upward deflection of the blast permitted by the strength of existing elevating mechanisms has been found moderately successful in solving the problem of target obscuration produced by dust. With elevating mechanisms constructed to take the unsymmetrical thrust, it is conceivable that the dust problem can be satisfactorily solved.

Brakes of low and medium efficiencies can be constructed which suppress flash or, at least, do not accentuate it. It may be possible to go to high efficiencies without enhancing flash.

These partial solutions of the blast problem will be less successful as pressures increase. The conduction of the gases to the rear of the gun would permit effective muffling of the blast, provided a sufficiently large fraction of the gas can be deflected through 180 degrees. A deflector capable of doing this is still in the preliminary stages of development, but experiments so far indicate the feasibility of deflecting a substantial fraction of the blast and conducting it to where it can be ejected at relatively low pressure toward the rear of the gun or up over the carriage. Such a disposal system would permit the utilization of the maximum braking action, and the saving in weight of recoil mechanism and mount that this would make possible would compensate for the weight of the added superstructure.

Chapter 5

FUNDAMENTALS OF TERMINAL BALLISTICS

Terminal ballistics, as distinguished from interior and exterior ballistics, deals with the interaction of the missile (bomb, projectile, etc.) and the target. While attention is usually focused on the effect of the missile on the target, resulting in penetration or perforation, the effect of the target on the missile causing deformation, rupture, shatter, fuze failure, etc., is often of great importance in determining the result of the missile-target interaction.

Chapters 6, 7, 8, and 9 of this volume describe the terminal ballistics of steel, concrete, plastic protection, and soil from the point of view of the work done on these subjects by Division 8 during World War II. Projectile deformation and shatter are especially significant in the study of steel and plastic protection targets. The development of a frangible projectile for aerial gunnery training, described in Chapter 10, depends on the complete shattering of the projectile at the target.

A distinction is made between perforation and penetration according to whether the missile does or does not pass completely through the target. This distinction applies particularly in the case of nondeforming missiles. The depth of penetration or the residual velocity after perforation depends not only on the material and thickness of the target, and on the mass, caliber, and shape of the projectile, but also on the impact conditions: striking velocity, yaw, and obliquity.

Chapter 6

TERMINAL BALLISTICS OF ARMOR

To serve as a basis for the development of better armor-piercing projectiles, studies have been carried out to determine how the energy required for perforation of a steel plate depends on mass, size, shape, and mechanical strength of the projectile components as well as the hardness, thickness, and obliquity of the target. Changes in these parameters were considered both as they alter the energy required for perforation directly when the projectile stays intact during the impact and indirectly as they control the extent of projectile deformation. Deformations play a particularly important role when the striking velocity is above 3,000 fps, that is, at hypervelocities. Although the practicality of projectile velocities in this

range has been well demonstrated, the difficulties in designing a nondeforming projectile still remain one of the principal obstacles to full attainment of the potential benefits of hypervelocity weapons.

Aside from a description of new techniques that have been developed for terminal ballistic studies (Section 6.3), the principal points discussed in Chapter 6 which includes reference not only to work done by Division 2, NDRC, but to investigations of other organizations as well, are the following:

NONDEFORMING PROJECTILE—ENERGY REQUIRED FOR PERFORATION (SECTION 6.5)

1. For nondeforming projectiles of a given shape, for a particular type of armor and for a specified angle of incidence, the "specific limit energy," WV_l^2/d^3, depends to a good first approximation only on the plate thickness expressed in calibers. Thus

$$\frac{WV_l^2}{d^3} = Cf\left(\frac{t}{d},\theta\right),$$

where W = projectile weight (lb),
V_l = minimum velocity to perforate plate (fps),
d = diameter or caliber of projectile (ft),
t = plate thickness (ft),
θ = angle of incidence,
C = constant for plates of a particular hardness,
$f\left(\frac{t}{d},\theta\right)$ = general function of $\frac{t}{d}$ and θ.

The advantage of this form is that it reduces the performance of projectiles of all sizes to a common basis.

2. The form of $f(t/d,\theta)$ depends on the mechanism of plate failure. Different mechanisms are discussed, but it is pointed out that there is no physical theory capable of predicting the exact form for plates of all thicknesses. A review is given of the empirical expressions for $f(t/d,\theta)$ now in common use.

3. In addition to plate thickness, the specific limit energy depends on plate hardness, there being an optimum value which results in maximum resistance to perforation. A perforation formula is given which includes hardness.

4. There is a slight "scale effect" in the sense that the specific limit energy for plates of a given caliber thickness decreases with increase in the size of the projectile. Although this contradicts the above equation, the discrepancy is not great since the effect is small.

5. Except for thin plate and large angles of attack, a perfectly nondeforming projectile requires less energy for perforation than one that deforms.

PROJECTILE DEFORMATIONS—SHATTER (SECTIONS 6.6.1 AND 6.6.2)

1. A projectile deforms progressively with increase in striking velocity. At the shatter velocity, which is somewhat above the velocity where the initial failure takes place, projectile deformation usually leads to an abrupt increase in the energy required for perforation. The dependence of the shatter velocity on the properties of the projectile, the plate, and on the angle of attack are discussed.

2. The effect of shatter in increasing the energy required for perforation is greatest at normal incidence (increase by as much as 100 per cent) but drops off with the angle of attack until at very large angles a shattered projectile may perforate with less energy than one that remains intact. The increase is significant, however, for angles at least as great as 45 degrees.

3. It is pointed out that, because of the occurrence of shatter, projectiles are sometimes able to perforate a target when fired over long distances but fail at point-blank range. As a result, the effect of firing a projectile at a velocity above its shatter velocity is usually to increase its effectiveness at long range at the sacrifice of good performance near the muzzle; there is no overall gain.

PROJECTILE PARAMETERS (SECTION 6.6.3)

1. Correct design of an armor-piercing projectile depends on a choice of the best values for its nose shape, length, density, strength of material, and, in the case of a subprojectile, its size. Section 6.6.3 considers how changes in each of these parameters affect (a) the striking energy, (b) the energy required for perforation when the projectile stays intact, and (c) the conditions under which deformation takes place.

2. Because of the greater density of tungsten carbide, projectiles made from this material have both a greater striking energy and a higher shatter energy than similar steel projectiles. If perforating ability is the criterion of goodness, tungsten carbide is undoubtedly a better projectile material than steel.

3. Regardless of the adjustment of parameters, a monobloc projectile made from present-day materials will not remain undeformed under all conditions of impact likely to be encountered in combat. This is

true for the attack of homogeneous as well as face-hardened plate.

PREVENTION OF SHATTER BY USE OF CAPS (SECTION 6.7)

Although the addition of a cap is very effective in preventing deformation of both steel and tungsten carbide projectiles, it is a detriment to perforating ability when it is not needed to avoid shatter or when shatter does not increase the energy required for perforation. Whether or not the cap is of benefit depends on the striking conditions. A general discussion of the comparative performance of monobloc and capped projectiles is contained in Section 6.7. Some protection for the nose of the projectile is always necessary if the striking velocity is extremely high.

HYPERVELOCITY PROJECTILES (SECTION 6.4, 6.5, 6.8)

1. Some of the advantages and disadvantages of different types of hypervelocity tungsten carbide cored projectiles are mentioned in Section 6.8. All have about the same terminal ballistic performance but differ in other respects.

2. On considering the interior and exterior ballistic behavior of subcaliber projectiles, it is seen that the striking energy decreases with decrease in diameter; less energy is required to make a hole of small diameter. However, since the striking and limit energies do not decrease at the same rate, there is usually an optimum diameter for the subprojectile.

3. Examples are given showing that tungsten carbide cored projectiles can perforate significantly thicker armor than conventional full-caliber steel projectiles fired from the same gun.

FUTURE STUDIES (SECTION 6.9)

1. As the power of guns is increased, better means must be found for keeping the projectile intact. Particularly for oblique attack, the problem of finding the forces involved in the plate-projectile interaction has hardly been touched. Once these forces are known, it should be possible to deduce the dynamic stresses produced in the projectile during impact and to design rationally against the resulting deformations.

2. More satisfactory methods should be devised for preventing decapping and breaking of projectiles by thin skirting plates.

3. Special attention should be given to high-angle attack. At the end of World War II, it was impossible with the best antitank guns and projectiles available to defeat the sloping plates on the front of German tanks except at very close range.

Chapter 7

TERMINAL BALLISTICS OF CONCRETE

A large amount of experimental work was done on the terminal ballistics of concrete during the war at scales from caliber .30 to 16 in. and with reinforced concrete targets from 3 in. to 23 ft thick. Penetration was studied as a function of striking velocity and obliquity, and the limit velocities for scabbing and perforation for various thicknesses and calibers determined. For a given projectile and target, penetration increases less rapidly with striking velocity than does the striking kinetic energy.

A scale effect was found for penetration in the sense that the penetration into a given target, in calibers, of similar projectiles at the same striking velocity increases with approximately the one-fifth power of the caliber.

Extensive tests were made, at caliber .50 scale and smaller, of the effect of concrete properties on penetration resistance. Some tests were also made of the effect of nose shape and the effect of projectile mass on penetration, perforation, and scabbing. Empirical formulas have been devised for representing these results.

In addition, experimental data were obtained on a number of other phenomena, including ricochet, sticking penetration, front and back craters, the effect of reinforcing, scab plates and meshes, layers and laminations, composite and spaced slabs, edge effects, the effect of explosions, and the effect of repeated fire.

A theory of concrete penetration was devised which agrees satisfactorily with the empirical penetration formula mentioned above and which gives the force resisting the missile during penetration as a function of depth and remaining velocity. Estimates of this resisting force are of importance in connection with the problem of projectile and bomb deformation against concrete targets. The theory, furthermore, furnishes a basis for computing the time of penetration for fuzing problems, and for computing the remaining velocity at any depth which is needed in the analysis of composite targets.

Preliminary development work has been done on an electromagnetic method for measuring projectile velocity as a function of time during penetration in a nonmagnetic and nonconducting target material like concrete.

A summary is given of analytical theories of penetration and perforation. This summary includes, as

special cases, all the theories which have so far been proposed for describing penetration and perforation.

Chapter 8

TERMINAL BALLISTICS OF PLASTIC PROTECTION

Plastic protection consists of a mixture of stone and a mastic binder backed by a thin plate of mild steel. It requires only a small amount of strategic material and has proved valuable as protection against small-arms fire and fragments.

The protective merits of plastic protection cannot be measured in terms of a simple ballistic limit, as is done with armor, mild steel, and concrete. At low striking velocities a small fraction of the incident missiles perforate the material, and at high striking velocities a larger fraction of the striking missiles perforate. At all ordinary velocities there is a definite probability of perforation, and this probability increases slowly with increase in striking velocity. This behavior can best be interpreted by statistical means, and such interpretation requires a large number of tests for the results to be significant.

The best present specifications of plastic protection require quartzite or flint gravel of fairly uniform size, at least three times the diameter of the missile to be stopped. This gravel is mixed with asphalt and a limestone filler, and the mixture is poured from a hot mixing oven into forms. The best proportions for the mix are approximately 60 per cent gravel, 10 per cent asphalt, and 30 per cent limestone dust, by weight. A backing plate of mild steel, having a weight per square foot of 10 to 30 per cent of the weight of the completed panel, is securely fastened to the material. A layer of expanded metal is placed inside and near the front to aid in holding the material in place and to provide additional structural strength. A panel of this type, of thickness nine to ten times the diameter of the incident missile, provides a fair degree of protection.

Chapter 9

TERMINAL BALLISTICS OF SOIL

Small-scale experiments have been performed to determine the effects of soil properties and projectile characteristics, especially nose shape and density, on penetration into soil over a wide range of striking velocities. The results of these small-scale tests have been correlated with the observed penetration of bombs and large projectiles into soil.

It is found that penetration increases with increase in velocity and for projectiles and bombs of normal shape is approximately proportional to the cube root of the weight of the missile. Penetration depth is also dependent on the nose shape of the projectile, blunt-nosed projectiles penetrating farther than sharp-nosed projectiles. This dependence on shape is very pronounced in rich clay but small in coarse sand. Except for striking velocity and nature of the target medium, stability of the projectile is perhaps the most important single factor in soil penetration. Blunt-nosed projectiles are usually stable and have long straight underground trajectories. Sharp-nosed projectiles usually turn sideways and have curved underground trajectories.

A summary of the known relations for penetration into soil, perforation of soil parapets by small-caliber bullets, and perforation of composite targets of concrete covered with earth is given in Weapon Data Sheets 2A*, 2A2a, and 2C1a, Chapter 19.

Chapter 10

THE FRANGIBLE BULLET FOR USE IN AERIAL GUNNERY TRAINING

The need for a realistic training procedure for flexible aerial gunnery was recognized in the late months of 1943. The development of a frangible bullet which can be fired from machine guns in a bomber at an attacking lightly armored target airplane fulfilled the requirements to a marked degree. This project was concerned with the development of the frangible bullet (T44) and associated equipment, and with some problems that arose in connection with the use of the procedure in a gunnery training program.

Experimental work with approximately one hundred types of bullets varying in composition, geometry, and density indicated that a thermosetting plastic with dense filler offered the best possibilities for a bullet that would (1) do minimum damage to the armor, (2) satisfactorily withstand field use and the loading process, (3) have reasonable flight characteristics, and (4) be amenable to relatively simple and economical production in the required quantity. For a particular thickness of armor, it appears that, to a fair approximation, the limit impact energy of such bullets is essentially constant regardless of mass or density.

The most suitable armor for the target airplane was found to be 24ST Dural in places where visibility was not in question, and multiplate bullet-resistant glass for locations where visibility was necessary. Up to

thicknesses of approximately 0.350 in., 24ST Dural is superior to armor steel, weight for weight, in defeating the frangible bullet.

A caliber .30 aircraft machine gun modified by addition of a piston booster was found to function quite satisfactorily as an automatic weapon firing the frangible bullet of weight 6.95 g at a muzzle velocity of 1,360 fps. The most satisfactory propellant found for the round with low loading density is DuPont SR4759 which is regarded as a compromise until a more suitable propellant can be obtained or the cartridge case changed to something other than the caliber .30 M-1 case.

A hit-indicator system was found to be quite effective in signaling to the gunner in the bomber when the target airplane is receiving hits. The signaling is effected by lights on the target airplane, which are activated by the impacts of the bullets on the target-airplane armor.

The most essential feature of the introduction of the frangible bullet into a training program is the requirement that, to a fair approximation, the gunner give to the best of his knowledge the same leads as he would give in combat for an equivalent situation. It was found that the solution to the problem lay in an appropriate scaling of airplane and bullet velocities with some changes in the gunner's sighting device. Calculations of the combat leads, using the velocities of combat airplanes and combat ammunition, and of the training leads, using training airplane and bullet velocities, showed that for the most important cases the lead angles are essentially constant for equivalent situations.

Field trials of the frangible-bullet technique have shown that it is a satisfactory procedure although definitely not free from significant limitations. It was found that an instructor's sight would be a material aid in the training program and such a device was developed.

Investigation of some of the psychological factors in sighting indicated that learning was comparatively rapid on a semisynthetic training device. There remains a real question as to whether such learning can be translated into a higher proficiency under conditions of air-to-air firing.

Some experimental work by the Ballistics Research Laboratory [BRL] of Princeton University Station of Division 2 on shapes of bullets other than that used in the present T44 round has indicated that a bullet with a secant ogive and boattail has less drag below 1,200 fps than does the T44 bullet. Preliminary investigations by this same group have shown that a caliber .50 frangible slug made from material of the same density as the T44 is inferior to the caliber .30 T44 in so far as velocity limit for perforation is concerned.

Chapter 11

DESIGN OF MODEL SUPERSONIC WIND TUNNEL

In order to obtain information needed for the design of a large supersonic wind tunnel to be built at the Aberdeen Proving Ground, a model wind tunnel having a 2.5-in. square working section was constructed at the California Institute of Technology. This tunnel was designed to operate at Mach numbers from 1.2 to 4.4. The specific problems that were solved are the following:

1. The pressure ratios and power requirements at various Mach numbers.
2. The design of nozzles to give supersonic flow in the working section.
3. The manner of supporting the model to avoid interference with the air flow around it.
4. Methods of observing the flow and of measuring the forces acting on the model.

Chapter 12

BEHAVIOR OF MATERIALS UNDER DYNAMIC LOADS

Under very rapidly applied forces, such as occur during impact or explosion, a structure may behave quite differently than under static or gradually applied forces. An investigation of these changes and of the factors governing them was one of the first problems attacked by Division 2 in the course of its study of structural defense. The effect of dynamic loading is particularly important in connection with the penetration and perforation of projectiles, in the response of elements of structures to blast or impact, and in the damage to ship's plating by blast or underwater shock. In addition, there are numerous other situations where strength under impulsive loading is important, for example, in the calibration of crusher cylinders for measuring chamber pressures in guns.

Two factors must be considered in any investigation of the effect of impulsive forces. First, there is a change in the physical characteristics of most materials. As the rate of deformation is increased the resistance to deformation also increases. Thus for soft

copper specimens the force required to produce a given deformation dynamically at a certain rate of straining was found to be of the order of 20 per cent greater than that required statically. Similar effects exist in steels. Furthermore, normally ductile materials are able to withstand stresses well above their elastic limits without permanent deformation if the forces are applied for short enough periods. The investigation of the change in material properties under dynamic loads was pursued experimentally with some analytical assistance.

The second important factor to consider in dynamic loading is the *propagation effect*. The effect of a force applied suddenly to a structure is not transmitted instantaneously throughout the structure, but with a finite velocity. Consequently, the more rapidly a force is applied the greater the tendency for the effect to be localized near the point of application. Thus a sudden tensile force on a wire tends to make it break at the loaded end. It is found that for instantaneously applied forces the occurrence of localized failure depends on the velocity produced by the force, or, in cases where the loading is produced by impact, the velocity of impact is the governing factor. In general, there appears to be a definite critical velocity of impact for a given structure loaded in a given manner. Above this critical velocity failure occurs at the loaded point with very little deformation or damage in the rest of the system. Below the critical velocity failure may or may not occur at the point of application of the load (depending generally on the geometry of the system), but the damage and deformation to the structure will not generally be confined to the neighborhood of the load. Consequently, the amount of energy that can be absorbed by a structure under impact is usually very much less for velocities above the critical than for those below.

The critical velocity of tensile impact for most ductile metals is of the order of 100 to 200 fps. In transverse impact on a thin member, such as a wire, the critical velocity is of the order of 300 to 600 fps. This effect may be important in the case of balloon mooring cables struck by planes, or for thin plates or diaphragms under blast loads.

Chapter 13

DEFORMATION OF STEEL UNDER HIGH PRESSURE

This investigation was a portion of the fundamental research program undertaken by Division 2 and directed at acquiring an understanding of the mechanism of armor penetration by projectiles. During such penetration the material adjacent to the projectile is subjected to stresses of the order of 500,000 psi and to exceedingly large deformations. Comparable stresses and deformations cannot be reproduced in such material by the normal methods of testing since rupture always intervenes. Consequently, such tests can furnish only estimates of the amount of strain-hardening and of the conditions that produce rupture during projectile penetration. However, under large hydrostatic pressures, rupture can be delayed sufficiently to allow both aspects to be adequately covered. The principal object of this investigation was to use this means of securing this information. During the first stages of the work another object was also in view, to determine whether or not the information acquired during tests under large hydrostatic pressure could be correlated directly with the ballistic performance of a material.

The following conclusions are drawn:

1. The region of high pressure in the neighborhood of a penetrating projectile is characterized by practically infinite ductility. This ductility is the result of the pressure and does not require any elevation of temperature.

2. This region of high pressure and high ductility surrounding a penetration is also a region of very severe strain-hardening. This hardening may be by a factor of two or three, depending on the type of steel. This factor appears to be smaller for steels of high normal strength; thus there is partial compensation.

3. This investigation has not revealed any significant correlation of the behavior under pressure with ballistic behavior. It appears that, in general, ballistic behavior is closely associated with fairly obvious characteristics, such as inhomogeneity, brittleness, presence of inclusions, etc., which can be investigated by standard methods.

4. The relation between applied force and the resulting deformation of a test specimen is not much affected by superposition of a hydrostatic pressure. In fact, the load to produce a given strain must be increased by an amount of the order of only 5 per cent for pressures of the order of 150,000 psi. On the other hand, the superposition of hydrostatic pressure increases very greatly the amount of deformation that can be produced before rupture, permitting investigation of regions not otherwise attainable.

5. The orientation of a specimen with respect to

the direction of rolling of the original plate has some effect on its rupture strength, but no observable effect on the load required for a given deformation.

6. The Brinell hardness of steel appears to be increased by about 5 per cent for an increase in hydrostatic pressure of 150,000 psi.

Chapter 14

DEFENSE AGAINST SHAPED CHARGES

The problem of providing protection against shaped-charge weapons has been studied in considerable detail. In the course of this investigation, a number of fundamental experiments and much theoretical work have been carried on simultaneously with the necessary engineering type of experiments.

As a shaped-charge jet penetrates the front of a target, the pressure it produces is so great that the strength of most target materials is unimportant and the process is governed primarily by the target densities. Materials of low density provide the greatest protection for a given weight. Densities from 100 to 150 lb per cu ft are practical. However, strength is desirable at the rear of a target to prevent the flow that tends to continue after the jet is used up.

The protection of armored vehicles was the problem considered to be the most important, because of the fact that light infantry weapons had been developed by the enemy that were capable of perforating and setting on fire any tank. Two practical protection devices were developed. The first was a set of removable steel panels containing plastic armor consisting of a quartz gravel, pitch, and wood-flour mixture (density, 125 lb per cu ft) designated HCR2. The second was a set of steel plates with hardened steel spikes welded onto them.

The panels were made to cover the majority of the most vulnerable areas of any M4 tank. The maximum protection of this type that could be applied without interfering with the operation of the vehicle added 11.7 tons. Construction was started on two sets of panels, one using homogeneous armor and the other using mild steel. In the mild-steel panels the front plates were backed by aluminum. It is estimated that because of its thicker basic armor and the smaller area needing protection, the M26 tank can be provided with equivalent protection by adding 7.1 tons.

The spikes provide protection by impaling the liner of the shaped-charge weapon and thus spoiling its performance. Protection of this kind can be provided against existing weapons with 4.1 tons for the M4 and 3.2 tons on the M26.

Because demolition hollow charges were being used against concrete fortifications, the protection of these structures was studied. Since concrete follows the density law and its density is low, it is a fairly good protective material itself. It was found that the weight of concrete needed for protection could be reduced by each or all of the following devices: increasing the strength of the concrete, providing an air space between two walls of concrete, using a steel scab plate on the back surface, and using a steel face plate on the front surface. The reduction in weight achieved with the first two devices is very small, but with the last two it is more significant. The scab plate also protects personnel against scabbing fragments from a wall perforated by a shaped-charge jet.

Chapter 15

STRUCTURAL PROTECTION

To study the principles of design and construction of defensive structures, both civil and military, was the original function of Division 2, and, although the chief concern of the division shifted from defense to attack as the war progressed, defense never became wholly unimportant. Much of the work that was done was of fundamental nature; most of this is discussed in the early chapters of this volume, especially those dealing with explosions, with terminal ballistics, and with the properties of matter. Under "Structural Protection," Chapter 15, are considered the experimental studies of structural behavior that are not treated elsewhere in the volume, and the methods of analysis and design of structures that have been developed.

Generally, the important problems of structural protection are: (1) to determine what attack will just defeat a structure (this is likewise the principal problem of attack) or how much damage to a structure will be caused by a certain attack, and (2) how the resistance of a structure to attack can be increased, or structures of increased resistance be constructed. The following experimental studies have been made (mostly discussed in Chapter 15): the effect of underground explosions on massive buried concrete structures, the damage caused by external and by confined explosions (briefly), the effect of contact explosions on concrete, and the behavior of reinforced concrete beams under impact. On the analytical side, both the elastic and the plastic types of behavior of structures have been

studied and reasonably simple methods of predicting the effect of a given impact or impulse on a structure or structural element devised. Comparisons with experiment for cases of plastic behavior are shown in the appendix of this chapter.

Impact or contact explosion generally causes both local and general damage. The local damage may consist of cratering on the side of the attack, scabbing on the far side, or even perforation of the target. Scabbing may be a very serious danger to personnel or equipment within a fortification or shelter. Its likelihood can be reduced by the use of scab plates or scab mesh on the inside face that are well tied to the interior of the wall. In the absence of such devices, the occurrence of scabbing is determined by the quantity and strength of explosive, on whether or not it is backed by earth or other material, and by the strength and thickness of the wall. Expressions for the limiting wall thickness for a given amount of explosive with and without backing are given. Expressions are also given whereby the size of craters can be predicted in a given situation.

General damage, distributed over the more distant parts of a target is caused by either contact or distant explosion, or by impact. The extent and distribution of the effect are determined by the characteristics of the structure and by the amount and distribution of the pressure exerted on the structure. When the duration of this impulsive load is short the impulse, or area of the active force-time relation, determines the effect. Methods of predicting this effect are discussed and their agreement with experiment shown to be adequate. In addition, the magnitude of impulse associated with a contact, air-backed explosion is shown to depend on the amount and kind of explosive, and on the shape of the explosive charge, the impulse being greater as the center of gravity of the charge is moved closer to the contact surface. An expression for predicting the amount of the impulse is given.

Chapter 16

TARGET ANALYSIS AND WEAPON SELECTION

The efficient prosecution of a war requires that weapons be selected for each target in such a way that the maximum damage results for a given expenditure of effort. The proper weapon and the necessary weight of attack using this weapon can be determined by careful analysis of the target and by application of the principles of weapon selection.

In bombing attacks, the physical damage to the target is usually measured in terms of the area damaged to a specified degree, and the efficiency of a particular weapon against the target in question is expressed by its *mean area of effectiveness* [MAE]. This quantity is the average expected area of damage for one bomb, divided by the weight of one bomb. The greater the MAE, the more efficient the weapon against the given target. The MAE for a particular combination of bomb and target may be determined in several ways; the most reliable method is by measuring the damage occurring in a large number of bombing attacks in which targets of the particular type were damaged.

Targets may be damaged by external air blast, confined blast, underground explosion, underwater explosion, fragmentation, debris, or fire. The target must usually be analyzed in terms of its vulnerability to several of these mechanisms, and that mechanism to which the target is most vulnerable selected. The weapon capable of causing the desired type of damage, and having the greatest MAE for the target under consideration, is usually best. In some cases the greatest overall efficiency is obtained by selecting some bomb other than that having the highest MAE for the target, since all bombs do not load to equal weights on aircraft. The bomb expected to cause the greatest damage per plane load can be determined from a knowledge of the MAE and the loading characteristics of each bomb under consideration, and should be selected for the greatest efficiency.

In many instances of bombing attack a knowledge of the mechanism of damage to which the target is most vulnerable will determine the best type and fuzing of bomb and frequently will also determine the most efficient size of bomb to be used. For example, air blast is most efficient if very large light-cased bombs are used and are fuzed for air burst; confined blast requires GP (occasionally SAP) bombs with short delay fuzing; underground explosion requires GP bombs with delay fuzing; depth bombs are especially designed for causing damage by underwater explosion and should be used with properly set hydrostatic fuzes; specially designed fragmentation bombs, with instantaneous or air-burst fuzes, should be used for targets vulnerable to fragments; incendiary bombs are for use against combustible targets.

A detailed discussion of the methods of applying a knowledge of the mechanisms of damage and a

knowledge of the characteristics of the target to weapon selection and determination of force requirements is given in Chapter 16. These principles are applied to military targets, transportation targets, and industrial targets. The results of many of the target analyses given in this chapter are given in abstract form in Section 6 of the Weapon Data Sheets of Chapter 19.

Chapter 17

THE DIVISION 2 TECHNICAL LIBRARY

Since the principal function of the division was the collection, analysis, and distribution of information on the performance of weapons, a library was essential to its existence. The organization of the library was designed to fit into the organization and functioning of the division as closely as possible. Classification of reports was by subject, with very complete cross referencing by subject (all the subjects touched on in each report were used), by author, by title, and by all reference numbers appearing on each report. This made it possible to locate a report of which only a fragmentary description was available; it was also possible to find all reports in the library that dealt with a particular subject.

The usefulness of the library was considerably increased by the preparation of abstracts of all reports as they were received. These abstracts were distributed promptly to the various research workers in the division, enabling them to request those reports of particular use to them, serving the purpose better than a simple acquisition list. The abstract of each report was also put on its principal subject filing card so that a subject search through the library was possible without an examination of all reports in the field in question, and was not handicapped by the absence of any reports that happened to be on loan.

The reports received were obtained from various sources. British reports on weapons and weapon performance came through the OSRD Liaison Office. Reports prepared by the American Services were obtained through Group A of the Liaison Office. Those members or associates of the division who were attached to, or in contact with, other research or investigating organizations were of great assistance in securing reports. By the end of World War II the contents of the library amounted to about 20,000 items.

Perhaps the most important requirement for a successful library is that it receive the serious and preferably the full-time attention of a capable individual and not, as tends to be the case, be given to the newest member of the organization as one of his minor responsibilities.

Chapter 18

OPERATIONS ANALYSTS

A training course for operations analysts, to act as consultants on weapon effectiveness and bomb selection, was given at the Princeton University Station of Division 2. The training program included lectures on the fundamentals of terminal ballistics and explosive effects, a review course in mechanics, and a special course in mathematical probability and its applications to bombing problems. Additional training by other organizations included instruction on the characteristics and effects of incendiaries by NDRC Division 11, on rockets by NDRC Division 3, on bombs and fuzes by the U. S. Navy Bomb Disposal School, further training in mathematical probability by the Applied Mathematics Panel, and a short course at the Army Air Forces School of Applied Tactics.

Approximately forty men were trained. They were assigned to operations analysis sections of several Army Air Forces, the Joint Target Group (AC/AS Intelligence), various naval organizations, and to other work where a knowledge of weapon performance was required.

The work of these men was very well received, and some of them were clearly influential in decisions taken at higher levels. Most of the men worked for the Army Air Forces, and all indications are that the Army Air Forces were well satisfied with their work in analyzing targets and determining their vulnerability.

Chapter 19

WEAPON DATA SHEETS

Division 2 has prepared a loose-leaf notebook giving, in compact and accessible form, quantitative information on the characteristics and performance of weapons. The emphasis has been on aerial bombing, but other weapons are included. This notebook was issued in loose-leaf form so that new material and revisions of old material could be added at frequent intervals.

The notebook was first published in July 1943. Fifty copies containing 15 Weapon Data Sheets and 6 Incident Summaries were issued then. The book finally included a total of 81 Weapon Data Sheets and 17 Incident Summaries. The final distribution, including the desk-size loose-leaf notebook, a pocket edition for field use, and bound copies of the final edition, reached a total of nearly 1,200 copies.

All sheets of the final edition, with one omission and a few minor corrections, are reprinted in Chapter 19 to serve as reference material for the other chapters of this report.

PART II

EXPLOSIONS

Chapter 1

UNDERWATER EXPLOSIVES AND EXPLOSIONS

1.1 INTRODUCTION

UNDERWATER explosions are of obvious military importance in connection with attack upon merchant and naval vessels, including submarines, and in the clearance of underwater obstacles both artificial and natural. In addition, they have recently been used for long-distance signaling. In order to utilize such explosions most effectively and in order to design the most efficient underwater weapons and to develop quantitative methods for determining explosive effectiveness in various weapons, it is necessary to have an understanding of the physics and chemistry of the phenomena involved.[a] For these reasons it was decided by the National Defense Research Committee [NDRC] that a laboratory for the investigation of underwater explosions should be set up. The Underwater Explosives Research Laboratory [UERL] was accordingly established, first under Division 8 (Explosives), by means of a contract with the Woods Hole Oceanographic Institution at Woods Hole, Massachusetts. In 1944, this contract was transferred to the jurisdiction of Division 2 (Effects of Impact and Explosion), as a consequence of reorganization of Division 8.

Before the founding of the Underwater Explosives Research Laboratory, work had been done on underwater explosions by the Naval Ordnance Laboratory [NOL], the David Taylor Model Basin [DTMB], the Submarine Mine Depot, and by various organizations in Great Britain.[1] The British work especially had clearly outlined the principal features of the phenomena to be studied and had, in addition, indicated some of the most promising directions for the development of instrumentation. In spite of this, however, the state of knowledge in 1941, when work was began under NDRC, was extremely rudimentary.

By the end of World War II, a large amount of information had been acquired, both by the British and by ourselves, concerning the nature of the explosion process, particularly as concerns the shock wave emitted by an underwater explosion. The relative effectiveness of various explosives had been measured. Furthermore, studies had been made, though not completed, on the so-called bubble phenomena, that is to say, the pulses emitted by the oscillating gas globe resulting from an underwater explosion. Some work had been done on the theory and mechanism of damage to structures but this work was very far from being complete.

[a] Pertinent to War Department Projects OD-03 and OD-131 and to Navy Department Projects NO-138, NO-223, NO-224, NO-237, NO-263, and NS-267.

1.2 SURVEY OF RESULTS OF UNDERWATER EXPLOSION INVESTIGATIONS

The term "high explosive" is used for those substances which are capable of undergoing an exceedingly rapid decomposition known as detonation.[2] This distinguishes a high explosive from propellants or "low" explosives which decompose by a process of rapid burning. In the detonation process, the reaction zone spreads through the material at a rate determined by the physical laws of conservation of mass, momentum, and energy. In the burning process, the rates of the chemical reactions involved are not fast enough to sustain a "detonation front," and hence the rate of conversion of reactants to products is limited by the rates of these chemical reactions.

1.2.1 Description of a Typical Weapon

A normal underwater weapon consists of a main charge of high explosive, for example, TNT, a booster charge, which is a small charge of a somewhat more sensitive explosive, and an initiator, which is a detonator cap containing a percussion or heat-sensitive explosive in very small quantity. The initiator or detonator cap is fired by the fuze mechanism. For example, in a depth charge this may be triggered by the hydrostatic pressure which causes a striker to hit the detonator cap and thus set off the very sensitive material in it. This small explosion detonates the booster charge which, in many weapons, consists of a few pounds of powdered TNT. The resulting explosion is then sufficiently powerful to detonate the main charge of less sensitive material. The chemicals contained in the detonator are too sensitive to be handled in any quantity, so that only a few grains are used. Mercury fulminate or lead azide are commonly used in detonator caps, often combined with a small quantity of tetryl. Either impact, as in concussion cap, or heat, as in an

electric cap, will cause these combinations to detonate, whereas cast TNT and other military explosives, suitable for the main charge, should not detonate with a comparable excitation.

1.2.2 Explosives Commonly Used for Underwater Weapons

The materials which have been most commonly used for the main filling in underwater weapons are TNT, amatol, minol, torpex, and HBX, whose compositions are given in Table 1. (Tritonal and RDX-Composition B are included since they were extensively used by the air forces against land targets.)

TABLE 1. Explosive compositions.*

Explosive	Component proportions†						
	AN	RDX	TNT	Al	CaCl₂	D-2	Wax
TNT	....	....	100	....	....	....	....
Amatol	40-80	....	60-20	....	....	....	....
Minol-2	40	....	40	20	....	....	....
Torpex-2	....	42	40	18	....	....	0.7
HBX-1	....	40	38	17	+‡	5	....
Tritonal	....	....	80	20	....	....	1
RDX-Comp.-B	....	60	40	....	....	....	....

AN ammonium nitrate
RDX Cyclonite, cyclomethylene trinitramine
TNT trinitrotoluene
Al aluminum metal, powdered
$CaCl_2$ calcium chloride
D-2 high-melting wax/nitrocellulose/lecithin = 84/14/2
Wax a variety of high-melting waxes have been used.

* For a summary of the properties of the more common explosives, see Data Sheet 1A1, Chapter 19.

† Production lots of mixtures may vary by as much as 1% from the listed proportions.

The introduction of aluminum into military explosives on a large scale was one of the outstanding developments of World War II. This addition very greatly increases the energy released on detonation and therefore the effectiveness of the charge. No other change in chemical composition produces nearly so great an enhancement of the effect as the introduction of aluminum.

Torpex was the most powerful military explosive used during World War II. HBX is a form of torpex in which a desensitizer has been incorporated to make the material less hazardous to handle.

A considerable number of other materials have, of course, been used, especially by enemy nations.

1.2.3 The Detonation Process

High explosives are chemical compounds containing large amounts of energy; that is to say, compounds which can undergo reaction to a set of products of considerably lower energy. This reaction in the ordinary type of high explosive does not require oxygen from the air but is a process which will go spontaneously without outside assistance once it is started. Most high explosives are organic nitro compounds; that is, they have the NO_2 group attached to carbon atoms in a molecule. The attachment is by way of the nitrogen atom. During the explosion reaction, the atoms in the molecule are partially broken apart and rearranged so that the normal products would be water, carbon monoxide, carbon dioxide, and nitrogen. In other words, the oxygen transfers from the nitrogen to hydrogen and carbon, to which it can be more strongly bound, thus releasing a very considerable quantity of energy. If aluminum is present, it has a strong attraction for the oxygen and, during the reaction, takes up all the oxygen needed from the other material. This process of decomposition and rearrangement of the atoms is exceedingly rapid in an explosive but is not instantaneous. Furthermore, even if the reaction velocity were infinite, the laws of conservation of matter, conservation of momentum, and conservation of energy would place a limit on the velocity with which the region of decomposition could proceed down a stick of explosive detonated at one end. This velocity in a solid high explosive is extremely great, of the order of 10,000 to 20,000 fps but it can be, and has been, accurately measured. Detonation velocity is an important property and one which is now quite well understood. For most military applications, it is not a measure of the power or usefulness of the explosive. Methods exist for calculating the detonation velocity of materials which have not been made in more than gram lots. What is required is the chemical formula of the material and the heat of combustion. These considerations of thermodynamics and hydrodynamics, namely, the conservation laws of mass, momentum, and energy, permit a computation of the detonation velocity which agrees quite well with that measured experimentally. For a more complete discussion of the detonation process and studies on detonation velocity, the reader is referred to the Summary Technical Report of Division 8.

As the detonation process proceeds down the stick of explosive, the solid explosive in front of the detonation wave is unaware of the existence of the explosion because the detonation wave is traveling with a velocity greater than the velocity of sound in the explosive material. Behind the detonation front, the pressure rises almost instantly to an exceedingly high value of the order of 2,000,000 psi.[3,4] If the explo-

sive is unconfined, this region of high pressure will rapidly expand into the surrounding medium, whether air or water, and thus fall ultimately to atmospheric pressure. If the explosive is contained in a metal case, the case is ruptured.

Under certain conditions, a high-order detonation such as described above does not occur. For example, if the initiation process is inadequate, the explosive may simply burn if open to the oxygen of the air. This burning is very fierce but a very much slower process indeed than detonation. The energy released may be actually greater than in the case of detonation but it is released over a relatively long time and, therefore, does not have the shattering effects of a true explosion. Even in the absence of oxygen, the decomposition may take place at a lower velocity or may begin and then die out, leaving a large mass of unreacted material. It is also possible that a fairly thin layer of material near the surface of the explosion may be blown away without decomposition. This layer would, therefore, not contribute its energy to the explosion. These questions of so-called low-order detonations are not completely understood but can usually be avoided by having a suitable booster.

As the detonation wave passes a given point in the explosive, there are left the gaseous products of the decomposition of the explosive at a very high pressure, moving with a considerable forward velocity. This pressure is sufficient to burst the container of the weapon without regard to the tensile strength of the metal; in other words, the metal has an effect on the situation only through its inertia, since its strength is utterly negligible compared with the forces which are acting upon it. In an underwater explosion, the thin containers normally used have very little influence on either the internal or external phenomena, so far as is known.

1.24 Properties of the Shock Wave

The very high pressure in the explosion products is communicated to the water immediately surrounding the charge, since the gaseous products naturally begin to expand at once and, therefore, to push against the surrounding water. It is often stated that water is incompressible but, of course, this is only a relative statement. Water is much less compressible than air but is considerably more compressible than, say, steel. Under the influence of the very great pressures produced in an explosion, a thin layer of the water around the charge is highly compressed and accelerated outward. This compression and outward motion is then transmitted to the next layer of water, and so forth, so that a wave of compression spreads out through the water, accompanying which the water acquires an outward mass motion.

Nature of the Shock Wave

The compression wave has certain very interesting properties. In the first place, it has a very steep front; in other words, the rise in pressure as the wave reaches a given point is practically instantaneous. This is partly because the explosion which produced the pressure wave was a very rapid event in itself. Even if a slower process were used to start the pressure wave so that it would not initially be steep-fronted, it would gradually become steeper as it traveled outward through the water, because the high-pressure portions of the wave travel faster than or "overtake" the preceding low-pressure portions. This overtaking effect follows from two consequences of the passage of the preceding low-pressure wave. First, the water behind the low-pressure wave is compressed and somewhat heated, and hence tranamits compression waves more rapidly than the water ahead of the low-pressure wave. Second, the water behind the low-pressure wave has acquired a mass motion forward so that the high-pressure portion is being propagated through a forward-moving medium. The high-pressure regions thus tend to catch up with the low-pressure regions and eventually to form a very steep front.

The steep front (see Figure 1) of the shock wave is followed by a region of decaying pressure which is to be expected because, as the explosion gases expand they will rapidly fall in pressure. In fact, this fall of

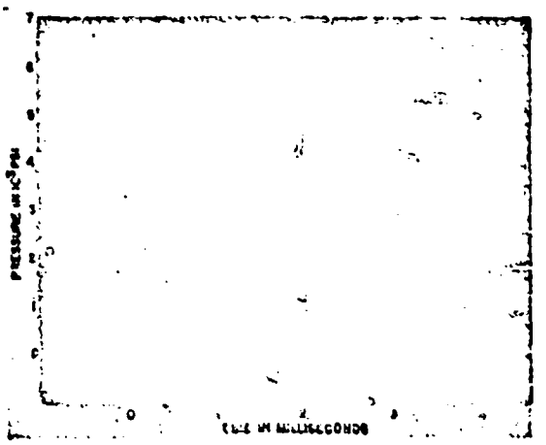

Figure 1. Oscillogram showing pressure-time curve recorded by piezoelectric gauge.

pressure with expansion is much more rapid than one might at first expect. If the gases formed by the explosion acted like gases at ordinary temperatures and pressures, the pressure would decay somewhat more rapidly than the volume increased according to the ordinary laws of gases. If one considers the properties of a gas with a density of, say, 100 lb per cu ft corresponding to a pressure of about 2,000,000 psi and a temperature of the order of 3000 C, one sees that these properties should deviate widely from those of a gas at 1 atmosphere pressure and room temperature. In fact, a considerable part of the high pressure exhibited by gas of this density is due to deviations from the ideal gas laws caused by the finite volume occupied by the individual gas molecules themselves, a volume which is normally neglected in discussions of gases at ordinary pressure. Therefore, as the gas expands, this contribution to the pressure is very rapidly lost and there is a very rapid decay of pressure with expansion. This decay of pressure in the explosion products shows up as a decay in the pressure behind the peak of the compressional wave traveling out through the water.

The compressional wave, when it has become steep-fronted, is called a shock wave and is responsible for at least a part, and probably a major part, of the damage caused to ships and structures by noncontact under water explosions.

If measuring instruments are located at some distance from an underwater explosion, nothing is observed at the actual time of the explosion except possibly a flash of light in some cases. At a finite time later, depending upon the distance from the charge, there is a sudden rise in pressure to a maximum value, which is called the peak pressure in the shock wave. After reaching the peak value, the pressure immediately begins to decay. The decay with time, at a given distance, is roughly given by an exponential expression of the form

$$P_t = P_m e^{-t/\theta},$$

where P_t is the pressure at time t and P_m and θ are constants, the peak pressure and time constant respectively, of the shock wave at the given distance. The rate of decay is commonly indicated by giving the value of θ which corresponds to the time required for the pressure to fall to $1/e$ of its original value, where e is the base of the natural logarithm or 2.718.

Suitable instruments might also be used to detect the motion of the water. This would be zero until the shock wave arrived at the point, upon which the water would immediately acquire a forward velocity. This forward velocity would decay as the pressure decayed. Because of this motion, the water through which the shock wave is passing possesses an outward momentum or impulse. This can be measured by obtaining the area under the pressure-time curve at a point and is one important characteristic of the shock wave. Another obviously important characteristic of the shock wave is the amount of energy which is propagated outward past any given point. To a fair degree of approximation, this is given by the area under the curve in which the square of the pressure is plotted against time, though more accurate expressions can be given. If the pressure were low, such as is the case with ordinary sound waves, the integral of the square of the pressure gives accurately the energy transported. The forward velocity of the water is proportional to the pressure and, therefore, the kinetic energy of the water is proportional to the square of the pressure.

Decay of the Shock Wave with Distance

If the explosive is in the form of a sphere or of a cylinder not too far different from a sphere in shape, the shock wave will spread out more or less uniformly in all directions, thus forming what is called a spherical wave. (See Figures 2 and 3.) The area covered

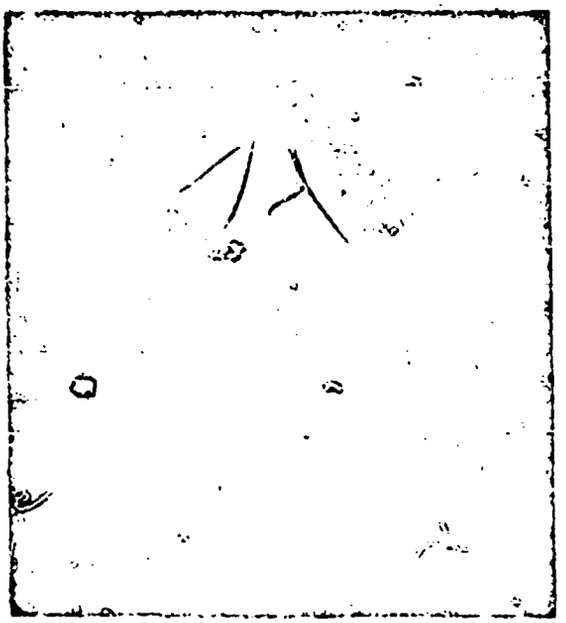

Figure 2. Flash photograph of ¼-lb spherical pentolite charge detonated at center.

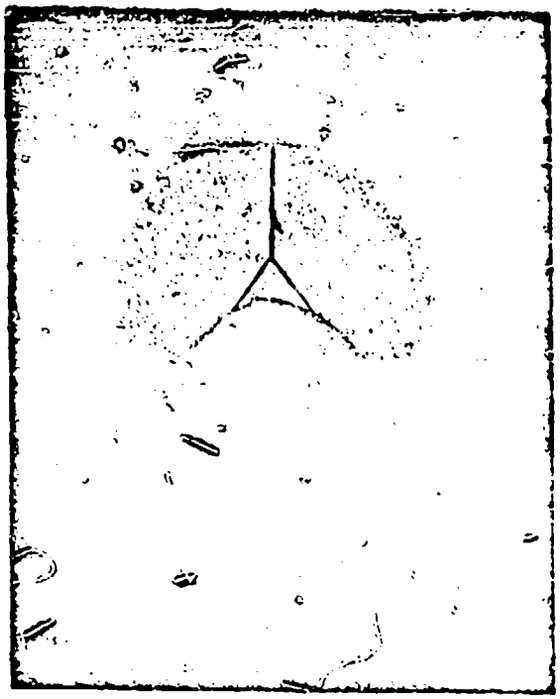

FIGURE 3. Flash photograph of ¼-lb symmetrical cast pentolite cylinder detonated at center.

by the wave will, therefore, increase as the square of the distance. Hence as the wave spreads outward from the source, it will decay and, if there were no dissipation, that is, no conversion of energy into heat with the passage of the wave, the total energy would remain constant over the whole spherical surface. Because of the increase in area of the sphere, however, the energy transported across the unit area would decrease as the square of the distance from the explosion. Connected with this would be a decay in the peak pressure which would follow an inverse first power law, since the energy, which is related to the square of the pressure, decays as the second power. The impulse or momentum would decay approximately as the first power since it is the area under the pressure-time curve. In actual fact, there is some dissipation, since the passage of the shock front will result in an irreversible transfer of mechanical energy into heat through the action of viscous forces, etc. This loss of available energy causes the decay of the energy transport to be somewhat more rapid than the inverse square of the distance, though the effect is not very great. Consequently, the decay of the peak pressure will be somewhat greater than the inverse first power.

The duration of the wave increases as the shock progresses outward because the high pressure in the front of the wave travels faster than the low pressure in the "tail" of the wave. The increase in the duration partly compensates for the extra decay of peak pressure with distance, thus bringing about the result that the impulse decays very nearly as the first power even when dissipation is considered.

ORDER OF MAGNITUDE OF SHOCK-WAVE PARAMETERS

Some numerical values of the various shock-wave parameters discussed above are presented in Table 2.

TABLE 2. Shock-wave parameters for 300 lb of cast TNT (density 1.52).

	Distance from charge (ft)			
	20	30	60	100
Peak pressure (psi)	6,150	3,900	1,820	1,030
Impulse* (psi-sec)	3.63	2.56	1.41	0.90
Energy flux* (psi-in.)	1,676	750	181	64
Time constant (msec)	0.45	0.50	0.57	0.61

* Measured to a time behind the shock front equal to 6.7 times the time constant.

THE LOW-PRESSURE TAIL OF THE SHOCK WAVE

At a time behind the shock front corresponding to five times the time constant, the pressure has fallen to 5 or 10 per cent of the peak value and thereafter decreases very slowly. This low-pressure region is commonly called the tail of the shock wave.[3] On theoretical grounds it is predicted that the pressure must eventually fall to zero and then go slightly negative, but at what time after the shock front this occurs is not definitely known.

To date, accurate measurements of the tail of the shock wave have not been made. This is due to the fact that the instrumentation was generally designed to measure the higher pressures in the early part of the shock wave and thus the necessary accuracy for measuring the very low pressures in the tail was not realized. For explosive comparison measurements this difficulty was overcome by measuring the impulse and energy flux to some arbitrary time after the shock front. It was convenient for this purpose to choose a time equal to some multiple of θ, the time constant. For example, at a time after the shock front equal to 8 θ, the pressure has fallen to approximately 5 per cent or less of the peak value. It should be pointed out, however, that, although the pressure in the tail of the shock wave is very low, if it lasts long enough there may be a considerable quantity of momentum in this portion of the wave. Whether or not this momentum, which is delivered at a low pressure, is important in damage is not known.

The Principle of Similitude

It is very fortunate that the peak pressure, duration, and other properties of the shock wave from charges of one size can be very simply related to the properties of the shock wave from a charge of a different size. The relation can be stated as follows:

If every linear dimension of an explosive charge is multiplied by the same factor k, then at a distance Rk from the larger charge, the peak pressures will be identical to the value at a distance R from the smaller charge, but the duration, the impulse, and the energy from the larger charge will be k times greater at these related distances. If two charges have approximately the same shape and one is k times larger in its linear dimensions than the other, its weight will, of course, be k cubed times greater. The law can, therefore, be approximately stated by using the cube root of the weight ratio as the scaling factor k. As an example, one might compare the shock wave from a 300-lb TNT charge with the shock wave from a charge weighing $\frac{3}{10}$ of a lb and having the same shape as the large charge. The scaling factor is then 10, the cube root of the weight ratio of 1,000. Consequently, one should expect to obtain the same pressure, about 6,000 psi, at a distance of 2 ft from the small charge as was obtained at 20 ft from the large charge. The duration, impulse, and energy at 20 ft from the large charge will each be ten times as great as the corresponding quantity 2 ft from the small charge. It is very important to note that this scaling law, by itself, does not tell anything whatsoever about the law of decay with distance. No matter what the latter law should be, this so-called similarity or scaling law would be expected to hold. What it does do is connect the law which governs the way in which the shock-wave properties change with distance with the law for the change of shock-wave properties with charge size. It is, of course, assumed that when the charge sizes change, the explosive type, density, etc., are kept the same. Mathematically stated, the similarity law is:

$$\text{Pressure} \quad P = f_1\left(\frac{W^{\frac{1}{3}}}{R}\right),$$

$$\text{Momentum} \quad I = W^{\frac{1}{3}} f_2\left(\frac{W^{\frac{1}{3}}}{R}\right),$$

$$\text{Energy flux} \quad E = W^{\frac{1}{3}} f_3\left(\frac{W^{\frac{1}{3}}}{R}\right),$$

$$\text{Time constant} \quad \theta = W^{\frac{1}{3}} f_4\left(\frac{W^{\frac{1}{3}}}{R}\right),$$

where W is the weight of the charge, R the distance from the explosion, and the f's unspecified functions. In actual fact, it is found both empirically and theoretically that the decay of peak pressure with distance in water does not deviate greatly from the inverse first power as mentioned above. If the decay were exactly inverse first power, the similarity law would lead to the conclusion that the peak pressure at a fixed distance would increase as the cube root of the charge weight. The dependence on distance of the shock-wave parameters must be determined experimentally, and equations expressing their dependence are approximate, but the similarity law is presumably very nearly exact.[4,7] Figure 4 illustrates the accuracy with which similarity scaling represents the features of the pressure-time relation for spherical pentolite charges of from 4 to 80 lb. The deviations in the tail of the curve are probably experimental error, since measurements in this region are as yet subject to error.

When targets or gauges, etc., are introduced into the picture, perfect scaling cannot be expected unless these objects are also scaled. That is to say, each of their linear dimensions should be multiplied by the scaling factor k. This extension of the similarity principle to targets as well as to shock-wave properties is called the *Hopkinson rule* and is subject to more uncertainty theoretically and experimentally than is the simple scaling law of the explosive charge and its shock wave. (See Section 1.3.3.)

1.2.5 Interactions of Shock Waves with Surfaces

Reflection at Free Surfaces

The effects of the free water surface on the explosion have been neglected so far. When a shock wave reaches a free surface it is reflected, not as a wave of compression but as a wave of reduced pressure or rarefaction. This is a familiar phenomenon with sound waves and holds true also for high-amplitude shock waves. The surface of the water is thrown upward with less resistance than is water deeper in the ocean. Consequently, there is propagated downward the rarefaction wave mentioned above. If the target or gauge is beneath the surface at some distance from the explosion, it will receive not only the direct wave from the source, but also a wave which has been reflected from the surface of the ocean and is therefore a rarefaction wave. The reflected wave will arrive at a somewhat later time than the direct wave because of the longer path. When it does arrive, being a wave

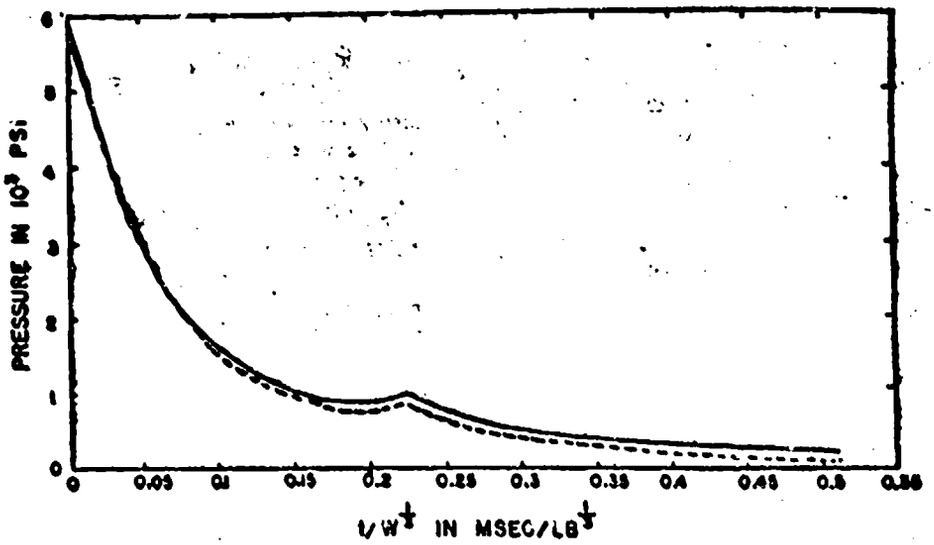

FIGURE 4. Similarity comparison of pressure-time curves for spherical cast pentolite charges of 4 lb and 80 lb.

of rarefaction, it will tend to cancel the pressure still being exerted by the tail of the original wave. A pressure-time curve showing this reflection is given in Figure 5. This is the phenomenon of "cutoff" and can be the limiting factor in the range of effectiveness of charges in shallow water. The time interval between the compression and rarefaction and, therefore, the resulting duration of the pressure pulse in shallow water can be at least approximately computed by using the known velocities of these waves and the geometrical direct and reflection paths. An approximate formula for the cutoff time, t, which applies when R, the horizontal component of the charge-to-gauge distance, is large relative to the depth, is

$$t = \frac{2gD}{cR},$$

where g and D are the gauge and charge depths and c is the velocity of sound.

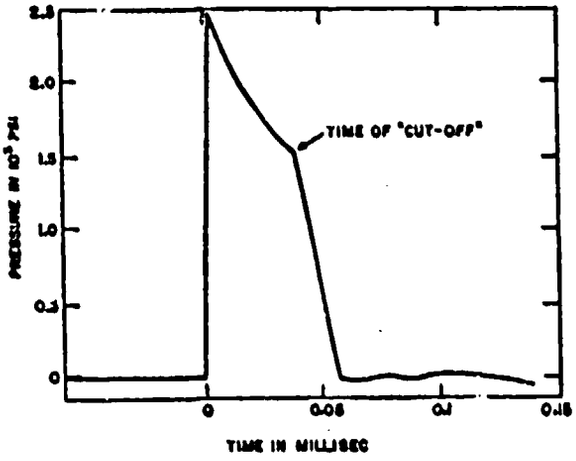

FIGURE 5. Reproduction of piezoelectric gauge pressure-time curve showing "cutoff" of pressure due to reflection at sea surface.

CAVITATION

There is another phenomenon of importance which complicates this surface reflection effect and that is the phenomenon of cavitation. The reflected wave from the surface is a rarefaction wave, but water will not withstand any appreciable tension. Although it is claimed that extremely pure water under laboratory conditions can support at least several hundred pounds per square inch of tension, the evidence seems extremely strong that ordinary sea water, which would normally contain many impurities, including air bubbles, etc., can sustain practically no tension. When tension is applied, what happens is that the water is torn apart and small bubbles appear which contain either air or water vapor. These bubbles have been photographed, as illustrated in Figure 6. The occurrence of cavitation therefore limits the amount of rarefaction which can be transmitted through the water. This limit is approximately equal to the total pressure (atmospheric plus hydrostatic plus shock wave) which is present. Any greater rarefaction, which would tend to cause actual tension in the water, results in cavitation.

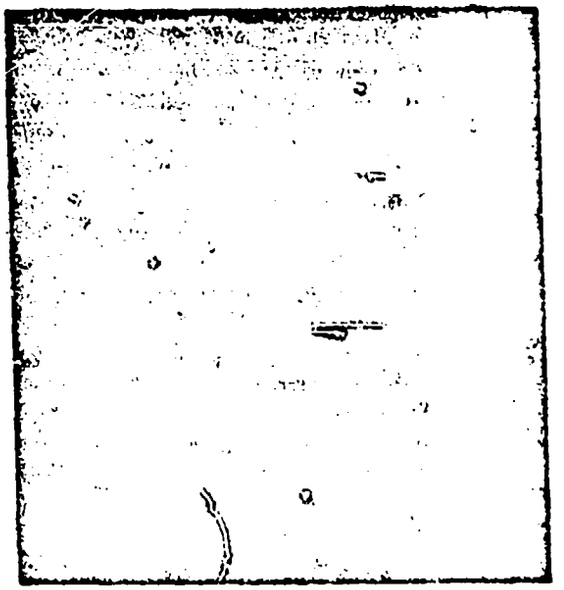

FIGURE 6. Flash photograph of shock wave reflected at free surface of sea.

REFLECTION AT RIGID SURFACES

When a shock wave impinges upon a rigid surface, it is reflected as a compressional wave. In other words, it is more or less completely reflected without great change in shape. If the incident wave strikes the wall head-on, it will be reflected back along the same line, with the result that the pressure immediately in front of the wall at the time of reflection will be the sum of the incident and reflected pressures. To a considerable degree of accuracy the peak pressure at the rigid reflecting surface will be twice the peak pressure of the incident wave in free water and the duration will be approximately that of the free wave, provided the surface is of infinite extent or at least so large that signals coming from the edges do not arrive during the times of interest.

The flash photograph of Figure 7 shows the reflected shock wave in front of a steel block as well as the initial shock front.

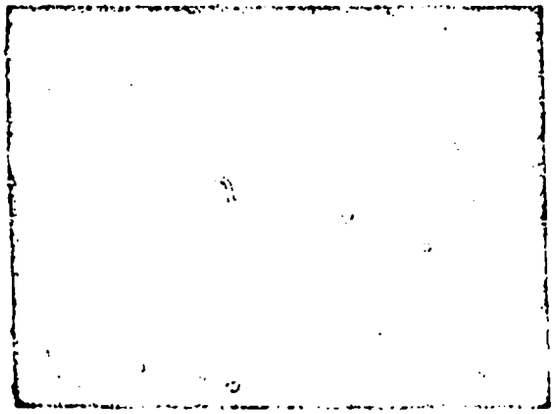

FIGURE 7. Flash photograph showing advance of shock wave around cylindrical steel block.

MACH REFLECTION

If the wave strikes at an angle, the phenomenon is similar to the acoustic case of the reflection of a sound wave, provided the intensity is not too great. For each

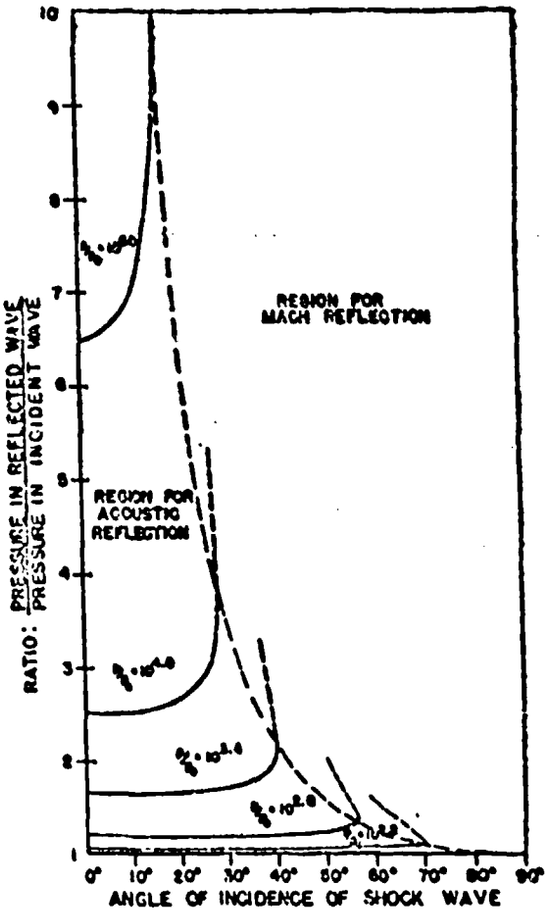

FIGURE 8. Plot showing theoretical prediction of conditions under which Mach reflection will occur.

angle there is, however, a theoretical lower limit to the pressure, above which simple acoustic-type reflection cannot occur.[8] What does occur instead is the so-called Mach effect. Theoretical studies have been made[9,10,11] of the phenomena which take place under

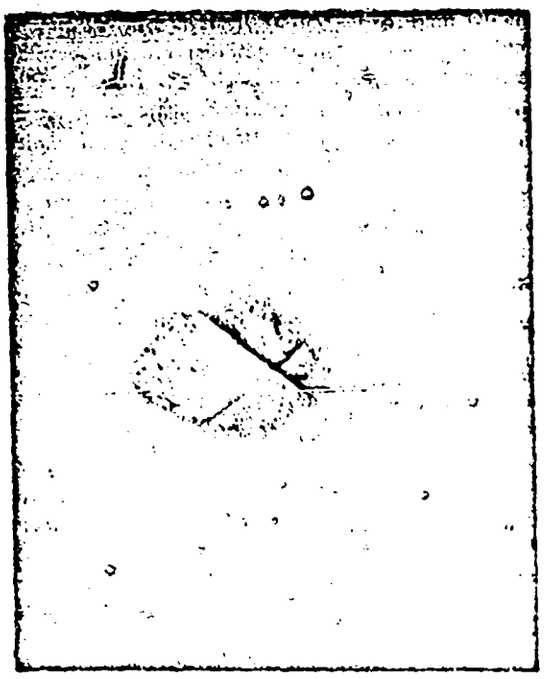

FIGURE 9. Flash photograph showing ordinary acoustic intersection of two shock waves.

conditions such that acoustic reflection can no longer occur. Some of the results on shock pressures in water are presented in Figure 8, reproduced from a Bureau of Ordnance report.[12] Note that the more glaring the reflection, the lower the pressure which is required to cause the Mach effect. When a Mach reflection takes place, there is also an incident and a reflected wave but these do not reach the surface. Instead, there is a transition region containing a wave running parallel to the surface, called the Mach "stem," which connects the junction of the incident and reflected waves with the surface. Figures 9 and 10 illustrate the difference between regular and Mach intersection of two shock waves.[13] These cases are essentially equivalent to the reflection cases since the reflected shock wave can be thought of as a second shock wave having its origin at an "image" charge behind the rigid surface. Experimentally, in this instance it is easier to study intersections of two shock waves than it is to achieve an ideal rigid reflector.

The pressure relations are not fully worked out theoretically for the Mach phenomenon, which is of more importance in air than in water (see Chapter 2), but it is known that the net result may be to cause the pressure exerted on a surface to be higher when the wave strikes at an angle than when it approaches head-on.[14]

MULTIPLE CHARGES

The enhancement of certain parameters in the Mach intersection zone of the shock waves from multiple charges suggests that a given weight might be more effectively used under certain conditions if divided into several properly placed and initiated parts.[15,16a] Clearly the meager data now available on this whole field should be supplemented.

INTERACTION OF SHOCK WAVE WITH A DEFORMABLE TARGET

Although it cannot be said that a full exposition of the phenomenon occurring when a shock wave reflects off either a free or a rigid surface is available, there is at least a considerable body of knowledge regarding these two types of events. When one considers the effect of a shock wave on a yielding surface such as the hull of a ship, the situation is much less satisfactory. If the surface is reasonably stiff, then one might use the rigid surface treatment, which would yield a doubling of the pressure in front of the surface. As soon as the hull plating begins to move, there will be sent out into the water a rarefaction wave because the moving hull will tend to pull the water with it. Because of the inertia of the metal, its motion may continue after the shock-wave pressure has fallen to a low value. The rarefaction wave sent out by the

FIGURE 10. Flash photograph showing Mach intersection of two shock waves.

moving plate will certainly reduce the applied pressure and may often cause it to become negative. This will be especially true for a light, thin plate. If the pressure does become negative, then cavitation will follow. The appearance of cavitation in front of a plate being damaged by an explosive wave has been photographically demonstrated (see Figure 11) and

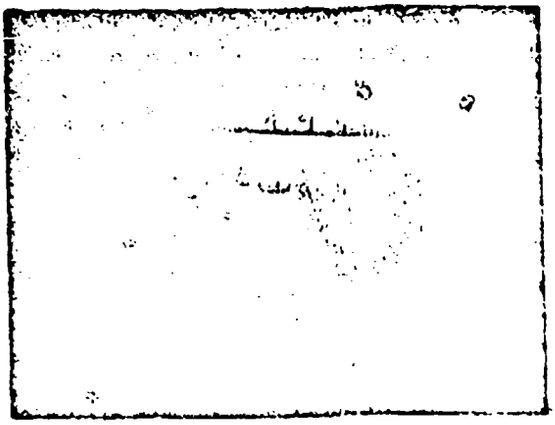

FIGURE 11. Flash photograph showing cavitation bubbles in front of thin air-backed diaphragm.

will profoundly modify the course of events. It is sufficient to say here that the effects of shock waves on yielding surfaces are complicated and not thoroughly understood.

1.2.6 Behavior of the Gas Bubble

OSCILLATIONS OF THE BUBBLE

The gas bubble formed by the products of the explosion will continue to expand for a considerable period of time after the explosion. Thus, for a 300-lb depth charge at, say, 50-ft depth, this time may be about 0.35 sec. Consequently the water which formerly occupied this space is moving outward during this whole time interval and when the bubble has reached its maximum expansion, the total displacement of the water is very considerable. In the example quoted, the maximum radius of the bubble would be about 17 ft and this figure represents the maximum displacement of the water which was originally in contact with the charge. This displacement is very much greater indeed than the quite small displacement of the water caused by the passage of the shock wave itself. The division of the phenomenon into two parts, a shock wave and then the so-called after flow or incompressive flow of the water, is an arbitrary but very convenient division. The phenomena in the shock wave itself are most closely related to acoustic theory, in which the compressibility of the water is the all-important factor. On the other hand, the flow of the water in the later stages is best treated by the approximation of incompressive flow. One simply regards this large mass of water as being pushed out by the expansion of the bubble.

The inertia of this large mass of moving water causes the expansion to go past the point of equilibrium so that the pressure within the gas globe falls far below the hydrostatic pressure at the given point, and the size of the gas globe increases to a maximum value considerably in excess of its equilibrium value at that depth. This overshooting phenomenon will result in a subsequent contraction of the gas as the hydrostatic pressure of the water brings the outward flow to rest and then reverses it. The water then flows into the cavity, compressing the residual gases and again the inertia of the process carries the bubble past its equilibrium radius, so that actually the gas bubble is compressed down to almost the size of the original charge, with a consequent building up of the gas pressure. This pressure increase eventually cushions the inflow, brings it to rest and then reverses the flow. The net result of this series of events is a pulsating phenomenon. The gas globe oscillates in size, becoming larger and smaller, with a period which is very considerably greater than the times involved in the shock-wave phenomena. For example, a 300-lb depth charge at 50 ft has a period of pulsation of approximately 0.70 sec. It is not difficult to devise a simple theory which yields a reasonably accurate calculation of the period of the motion.[17,18] By a simple consideration of the law of conservation of energy, it is found that the period is governed by the following formula:

$$T = KW^{\frac{1}{3}} Z^{-\frac{5}{6}},$$

where T is the period, W the charge weight, and Z the depth of the charge plus 33 ft. The term K is a constant characteristic of the explosive.

At the first contraction of the gas globe, there is a sufficiently high pressure produced in the gas to send out another compression wave through the water. This compression wave differs from the initial shock wave in that the pressure-time curve is not steep-fronted but is more or less symmetrical with respect to time.[34,37] The peak involved is not nearly so high as in the initial shock wave being of the order of $\frac{1}{10}$ to $\frac{1}{20}$ of that value, but the duration of this pulse is rather greater, with the result that the impulse involved

in the first of these bubble pulses is of the same order or even greater than that transmitted by the shock wave.[20,26] The successive bubble pulses become smaller and smaller so that there is little practical importance from a damage viewpoint in considering any beyond the first. The energy that is originally present in the outward flowing water, which is of the order of 50 per cent of the chemical energy, is gradually converted into heat by the formation of vortices or radiated as compressional energy of the bubble pulses. The first bubble pulse may contain approximately 5 to 8 per cent of the original chemical energy. It is seen from the formula above for the period that this bubble pulse phenomenon is a function of the depth below the surface whereas the shock-wave phenomenon is not, except for the surface cutoff. The effect of the depth arises because the force which causes the bubble to cease its expansion and go into a contractual phase is the hydrostatic pressure of the water which, of course, increases with depth.

Bubble Migration Due to Gravity and Effects of Surfaces

The large cavity filled with the burnt gases is naturally influenced by gravity and, in general, will rise under this force. The phenomenon is more complicated, however, because there is an interaction between the upward motion due to gravity and the expansion and contraction. Hydrodynamic theory predicts and experiment verifies that the most rapid upward motion takes place when the bubble is in its contractual phase. When the bubble is expanding, the upward motion is relatively slow, because of the large volume of water which must be displaced then. In the contracting phase, the accumulated momentum affects smaller and smaller masses of water so that the vertical velocity becomes very great. This rather complicated phenomenon has a number of important applications, as will be mentioned later.

The motion of the bubble is affected not only by gravity but also by the presence of free or rigid surfaces.[21,22,26-28] A free surface causes a net repulsion of the bubble which under certain favorable conditions may actually overcome the effect of gravity and drive the bubble downward. The depth at which the gravity rise is balanced by the free surface repulsion is known as the upper "rest" position and is realized only for small charges. A rigid surface, on the other hand, attracts the bubble, on the average, particularly so that the bottom may attract the bubble and under special cases may prevent the rise under gravity during the first few oscillations. Thus there will also exist a lower "rest" position.

It is difficult to give a simple, physical description of the cause of the attraction by a rigid surface and the repulsion by a free surface, although the effect was first predicted theoretically.[17] Some indication of the mechanism of this effect may be gained by remembering that, as the bubble expands during its oscillation, the water is pushed away and must flow somewhere. If a rigid surface is nearby, the water is prevented from flowing in that direction, so that the bubble is first repelled, but as the bubble begins to contract the reverse process occurs and the bubble is attracted to the rigid surface because water cannot flow in from that side directly. This explanation does not, however, indicate why the attraction during the contraction phase is larger than the repulsion during the expanding phase.[18,19] This difference is related to the interaction between the oscillatory motion and the overall motion of the bubble similar to the case of the interaction between gravity and the radial oscillation. This interaction causes the displacement of the bubble to be much more rapid during the contracting phase.

Damage Due to Bubble Phenomena

It is of great importance to determine whether the bubble phenomena are important in causing damage. In this connection there are three separate factors which should be considered: (1) the pressure pulses radiated at each minimum of the gas globe, (2) the outward radial mass motion of the water accompanying the expansion of the gas globe, and (3) the upward mass motion of the water resulting from the migration of the gas globe.

It has been demonstrated theoretically[17,21] that the pressure pulse radiated by the bubble at its minimum is greatest when the bubble migration is small. According to this result, known as the principle of stabilization, underwater mines should be located at the rest position to obtain the maximum damage at the surface of the water from the bubble pressure pulse. Thus, for a 300-lb charge the mine should be moored approximately 14 ft above the sea bed. However, preliminary measurements with 300-lb TNT charges at this location[28] indicated the effect to be very much less than predicted. Evidence of damage due to the bubble pressure pulse has been provided by photographs, taken with a high-speed motion picture camera, of a cylinder being damaged by a small charge.[28] Some of these photographs are reproduced

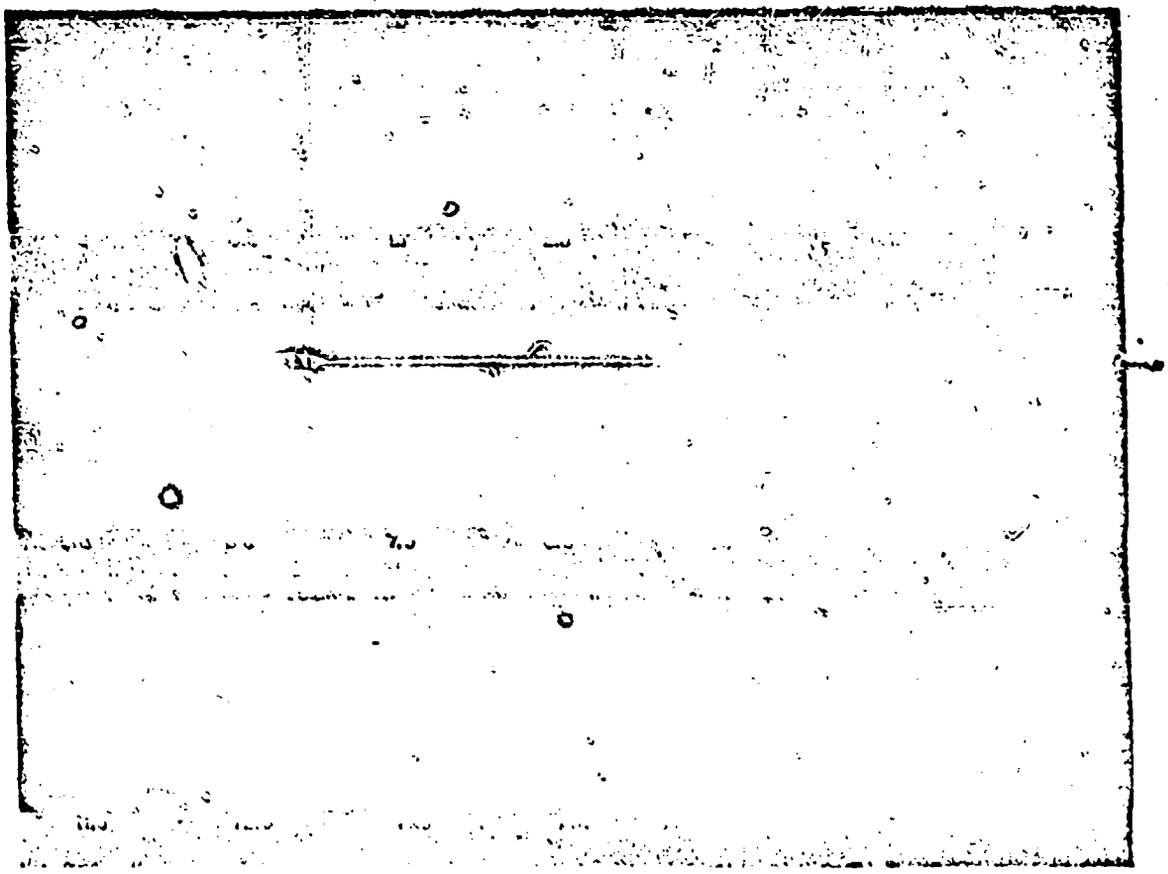

FIGURE 12. Photographs showing cylindrical model being damaged by explosion at depth of 400 ft. Numbers under photographs are times in milliseconds.

in Figure 12. It is to be noted that additional damage to the cylinder takes place shortly after the bubble reaches its minimum size. The bubble does not migrate perceptibly in these pictures because of the large hydrostatic pressure at the depth of the experiment. In general, however, where an explosion occurs under a target, because the gas bubble will migrate upward by as much as 15 ft (for 300 lb of TNT, at about 50-ft depth), the bubble pressure pulse originates at a point which is much nearer the target, and thus the damage due to the bubble pulse may be comparable to that caused by the shock wave. This effect has been demonstrated on a small scale[15,16,34] by experiments in which the damage to diaphragm gauges (see Section 1.3.2) directly above a charge was several times greater than the damage to similar gauges at the same distance from the charge but to one side.

Of considerable interest is an anomalously high pressure in the bubble pulse which has been observed at a depth of 20 ft for 300-lb TNT charges[32] and at a depth of 4 ft for ½-lb TNT charges.[29] Bubble pressures at these charge depths are at least five times as great as those at any other depths. The duration of this pressure pulse is relatively short, and the charge-depth range over which the phenomenon was observed was very narrow. No explanation for this behavior can be advanced at this time. It has been suggested that the bubble at these depths intersects the surface at its maximum expansion and sucks in air. On recompression, a second chemical reaction may take place giving rise to additional energy. Further investigation is needed.

Mention was made of the mass motion of the water accelerated radially outward as the bubble expands. It is claimed by German investigators that this radial mass motion of the water is the most important factor in damaging targets at close range. At greater distances it is not effective because, due to the spherical

symmetry of the system, the kinetic energy of the outflowing water falls off as the fourth power of the distance. The maximum kinetic energy of the water is very simply related to the cube root of the period of the bubble oscillation.[17]

In addition to the radial motion of the water, there is also an upward mass motion of the water resulting from the migration of the gas globe. The upward migration, which for 300 lb of TNT is of the order of 15 ft, occurs during the very short interval of time when the bubble is nearer its minimum size. Thus velocities in excess of 100 fps may be realized. If one visualizes a spout of water projected upward with this velocity and striking a ship, considerable damage might be expected to occur. There is, however, no direct evidence at present that actual cases of ship damage can be attributed to this cause.

From the preceding discussion it is apparent that much more information must be accumulated before it will be possible to assess the relative importance of the various factors which may cause damage. The experimental study is complicated by the fact that the bubble phenomena, due to their independence on gravity and the effects of free and rigid surfaces, cannot be scaled in any simple manner.

1.27 Surface Phenomena

One of the most spectacular effects of underwater explosions is the surface phenomena associated with them. If the charge is exploded at a fairly shallow depth, a great mass of water is thrown into the air. The more careful analyses of these effects show that they consist of several parts. If the charge is not too shallow, the first effect which is noticed is the radial spreading of a black ring, immediately followed by the formation of a "dome" of white spray thrown up off of the water. At a later time, of the order of seconds for 300-lb charges, high plumes of water break through the dome and rise to a much greater height. There may be several separate plume phenomena. Sometimes these plumes are black, as if they contained products of combustion, such as free carbon. It is currently assumed on the basis of very good evidence that the first effects are due to the arrival of the shock wave at the surface. This shock wave, as mentioned above, will be reflected from the free surface as a wave of tension. If one plots the pressures and tensions to be expected beneath the surface as a function of time, one sees that cavitation should occur at a small depth beneath the boundary, thus essentially peeling off a layer of water. This layer will possess a considerable upward velocity because of the passage of the shock wave upward and the reflected shock wave downward. A simple calculation shows that if there were no questions of air pressure or air resistance, this velocity would suffice to throw the water high into the air, of the order of twice the dome heights normally observed. On the other hand, if an unbroken layer were actually peeled off, it could rise only a very few inches under these same conditions because of the vacuum underneath it and the pressure of the atmosphere above it, forcing it down. It seems likely that the irregularities always present on the surface cause this layer to be broken into droplets almost immediately, so that the atmospheric pressure has access to the underside of the broken layer and therefore does not influence the phenomenon further. It is certainly reasonable to assume that air resistance is sufficient to account for the discrepancy between the observed dome heights and those calculated on this very simple basis.

The plumes presumably are masses of water forced up ahead of the rising bubble. It will be remembered that during the contractural phase of the bubble's oscillation, its rise under gravity is very great, so that the water immediately above the bubble can acquire a considerable upward velocity. Ultimately, the bubble itself will break the surface, adding the burnt gases and possibly solid particles from the reaction to the material thrown upward. Depending upon the exact phase of the bubble oscillation at the time of the breakthrough, the plume may be very high and narrow or spread out in a sidewise direction. If the explosion is deep enough so that several oscillations of the bubble can occur before the gases break the surface, then the bubble pulses can also contribute their own spray domes to the picture. It has even been observed that two separate domes can occur, presumably due to the sidewise migration of the bubble on its upward path due to special circumstances. The first dome, in this case, would come from shock wave and the second one from the first bubble pulse.

When charges are very deep, of the order of 100 ft multiplied by the cube root of the weight in pounds, the obviously visible surface effects, except for the ultimate coming to the surface of the broken-up gas globe, become increasingly difficult to detect. It has been claimed that this depth is critical and is a measure of the strength of the water to resist the tension wave but it seems more likely in the light of other experiments that, if the surface were rough enough and the phenomenon observed with a high-speed

camera, there would be some effect at almost any depth. The possible absence of an effect with a smooth surface may be due to the inability of the cavitated surface layer to break into droplets under these conditions. Much more study would be required to settle these points definitely.

A knowledge of the mechanism of the various surface effects is important for a number of indirect applications, such as the measurement of the shock-wave pressure, as will be seen later. It should be stated, however, that the height of the surface plumes and other observed phenomenon should not be interpreted in terms of the power of the explosive or the depth of the charge without very careful consideration of the detailed physics of the phenomenon. Otherwise, quite misleading results can be obtained. The use of surface effects to determine the depth of an underwater explosion will be discussed in more detail later.

1.2.8 Underwater Cratering

A charge exploded on the ocean bottom will produce a crater the dimensions of which will be a function of the size of the charge, the nature of the explosive, the depth of the water, and the hardness of the bottom. Not very much quantitative information is available for predicting underwater cratering, but some experiments[34,35] indicate that, roughly, a crater of approximately 5.8 cu ft per pound of TNT can be expected on a sand or mud bottom. Naturally, a rocky or hard bottom will give considerably less cratering. This cratering effect is important practically because little damage is done to massive underwater obstacles outside of the crater produced by an explosion. Cratering is more effective if the explosive is covered by a sufficient depth of water. This is to be expected because otherwise there is a very great loss of energy into the air. The scaling laws described above seem to hold at least approximately for these cratering phenomena. It is, of course, necessary that the sea bed be reasonably homogeneous. With this caution in mind, a rough estimate can be made by assuming that the volume is proportional to the charge weight and the dimensions proportional to the cube root of the charge weight under conditions where the depth of water is likewise proportional to the cube root of the charge weight.

1.2.9 Surface Waves

Another effect of an underwater explosion which is closely related to the surface phenomenon described above is the production of surface water waves. The expansion of the gas bubble and its rise under gravity displaces a considerable volume of water upward, leading to surface waves spreading out from a point above the explosion. It cannot be said that ordinary explosives are very efficient producers of such waves,[37,38] the energy going into them being a small fraction of the chemical energy. Nevertheless, it is possible with large explosions to produce waves having sufficient height to be useful for certain purposes.

The use of pressure-operated mines by the Germans resulted in an extensive investigation of the production of surface waves by conventional explosives. Such waves will cause pressure variations at the bottom which might be regulated so as to activate these mines. A fairly elaborate mathematical theory of the production of surface waves was developed[39,40,41] and tested experimentally.[37,42,43] The theory was based on incompressive hydrodynamics and treated the explosion as an ideal source. The effect of the bottom and of the free surface was taken into account by the use of image sources and a perturbation treatment. In order to get numerical results, it was assumed that the bubble reached a fixed effective volume instantly, remained constant during the bubble period, and then collapsed instantly to zero volume. In comparing the results of the theory with the rather scanty experimental data, it was found desirable to use an empirically determined effective bubble volume, in order to secure a good fit with experiment. More experimental data would be necessary in order to determine the limits of accuracy of this theory.

It was found that in order to get waves of more than a very few inches in amplitude at distances greater than 1,000 ft tremendous charges are necessary. Furthermore, these are more efficient if they are divided into a large number of smaller charges spread over a greater area. The reason for this is that the large lump charge produces a gas bubble whose diameter is greater than the depth of the water under most circumstances where these mines would be of interest. Consequently, a tremendous amount of energy is lost by venting to the atmosphere, whereas if the charge is divided into a large number of smaller charges each of these has a gas bubble which will not immediately vent. The waves also seem to be larger and it is reasonable to expect they would be if the charge is placed sufficiently deep.

1.2.10 Comparison of Explosives

One of the principal functions of UERL was the comparison of different explosives for effectiveness in

underwater weapons. Tests were also frequently made to prove that minor changes in composition of production fillings, especially of the desensitizer component, had no detrimental effect on explosive power. Early in the development of the laboratory, it was realized that production and loading techniques were important factors in determining the weapon performance. It was decided, therefore, to develop instrumentation applicable to testing the various weapons at full scale.

For this purpose the 76-ft wooden fishing schooner, *Reliance*, was equipped as a floating laboratory.[44] Because of its reasonably clear deck space and adequate booms, it has proved very well adapted to handling the heavy gear required for positioning the charge, gauges, cables, etc., for each shot. Electronic equipment for recording the piezo gauge signals was compactly installed in one hold. The other hold served as a work shop for mechanical gauge maintenance.

The full-scale service weapons used in most tests were loaded at the Naval Mine Depot, Yorktown, Virginia. When the pilot loading unit at Yorktown was completed and placed in charge of special officers, it became possible to get very detailed data on the individual test weapons. This was found to be essential to the proper interpretation of the *Reliance* measurements.

The tests were usually conducted in Vineyard Sound, where water of about 80-ft depth is available in several areas. The charge and gauges were set overboard by the *Reliance* crew so as to be strung out at known distances apart at a uniform depth, usually 40 ft. This was accomplished by use of a sea anchor applying tension to the gauge line, which was supported at appropriate places by surface floats, the *Reliance* being headed into the tidal current.

A typical layout, as shown in Figure 13, contained up to eight tourmaline piezoelectric gauges at various distances from the charge, each with its own electric cable to the vessel. In addition, a large number of ball crusher gauges and smaller numbers of Modugno and diaphragm gauges (see Section 1.4) were mounted along the main spacer cable. Several piston-type momentum gauges were also used. The charge was fired with an electric cable when all the gear had been put in position. The explosion would sever the gear into two portions (see Figure 13), the sternmost portion being cut loose from the vessel. After retrieving the forward portion of the gear, the *Reliance* then turned and picked up the rear set of buoys, gauges, etc. Although occasional trouble due to damage of floats was encountered, in general the *Reliance* was able to make one or more shots every day as a matter of routine.

The success of this type of work depended entirely upon the quality of the personnel involved and their strict adherence to the necessary precautions. Experience on the part of the scientific staff demonstrated that meticulous care in the handling of all types of gauges was required in order to secure accurate and reproducible results. The crew of the *Reliance* was very conscientious in carrying out instructions received from the scientific staff and, of course, there were always several scientists on board. It would have been impossible to do this type of work successfully with a crew which changed from day to day or which was not entirely conscientious in performing its duties. The captain of the *Reliance* commanded and coordinated the gear-setting operations, after which the scientific personnel conducted their work. The captain was directly responsible to a research supervisor in charge of the *Reliance* program.

A considerable number of different explosives were compared.[48-51] The quantities measured were the peak pressure, impulse, and energy flux in the shock wave as given by the piezoelectric gauges, the relative peak pressure as estimated from the mechanical gauges, and the relative impulse as estimated with the piston-type momentum gauges. Table 3 shows the average results of these explosive comparisons. In most cases, these numbers are averages over a fairly large number of different types of service weapons such as the Mark 6 depth charge, Mark 54 depth bomb and the Mark 13 aerial mine. The ratios of peak pressure are probably correct to 2 or 3 per cent. The various measurements on each different explosive have been reduced to a common density for that explosive, since the performance is a function of density of loading. The outstanding result of these investigations is the establishment of the importance of aluminum as a constituent of military explosives. This fact was well appreciated

TABLE 3. Results of explosive comparisons relative to TNT for constant volume of explosive.

Explosive*	Density (g/cm³)	Pressure ratio	Impulse ratio	Energy ratio
Torpex-2	1.71	1.16	1.27	1.53
HBX	1.65	1.13	1.25	1.45
Minol-2	1.64	1.08	1.26	1.40
Tritonal	1.70	1.05	1.18	1.19
RDX-Comp.-B	1.60	1.10	1.08	1.21
TNT	1.55	(1.00)	(1.00)	(1.00)

* See Table 1 for composition of explosives.

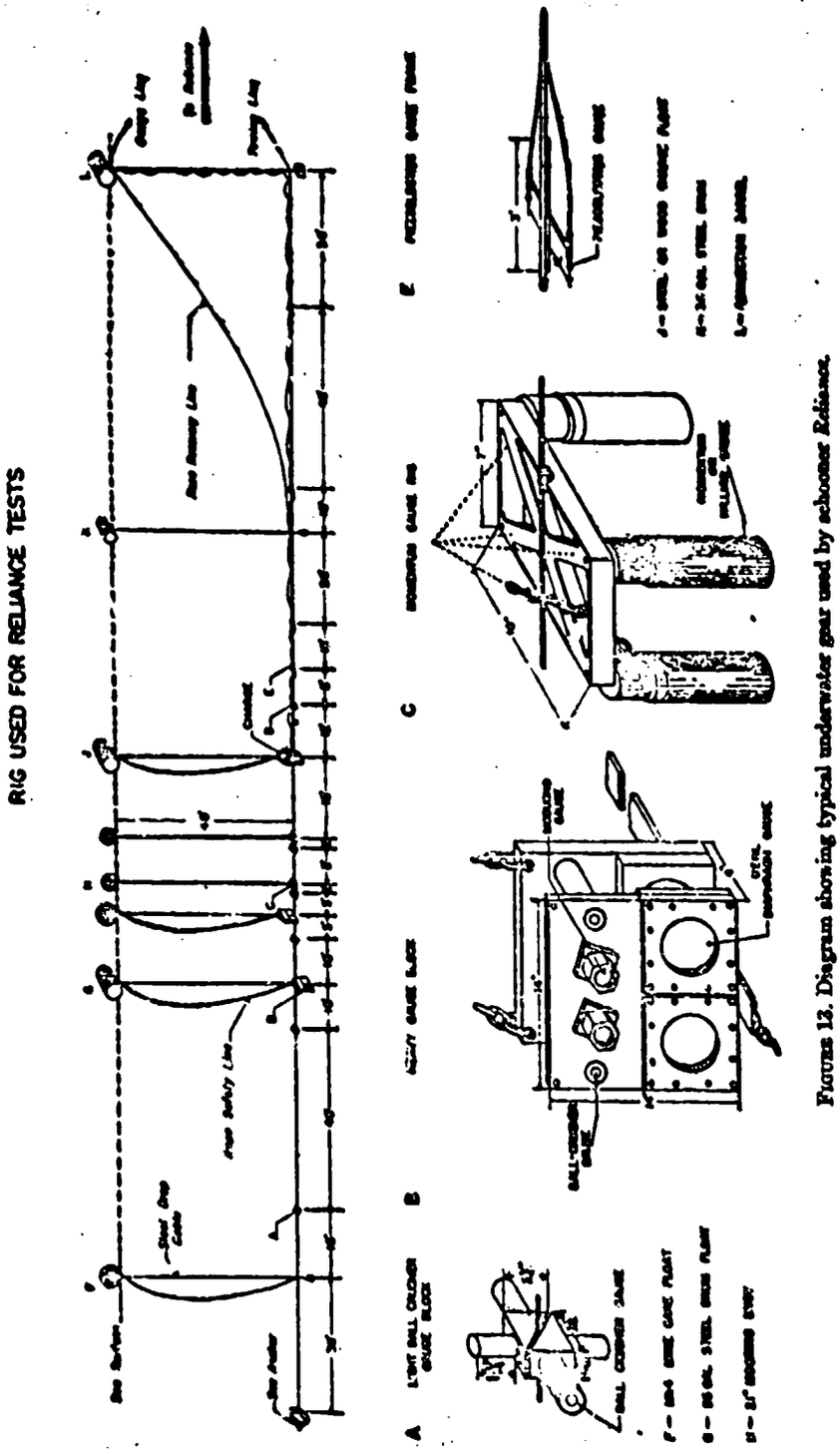

FIGURE 12. Diagram showing typical underwater gear used by schooner *Reliance*.

and utilized by both the Germans and the British[42] quite early in the war. Arguments on the basis of oxygen balance give very misleading results. For example, TNT is oxygen deficient from this viewpoint, so that the addition of aluminum to TNT makes the oxygen balance very much worse. Nevertheless, this addition increases the performance of TNT. The reason for this is the very great energy release when aluminum combines with oxygen. This energy is so large that it is advantageous to rob the carbon of oxygen and give this oxygen to the aluminum, even when there is not enough oxygen to convert all the carbon to carbon dioxide. There seems to be no good evidence that the water is involved appreciably in the reaction as has been sometimes suggested. The possibility of the reaction of water during an explosion could conceivably be settled by making especially smooth spherical charges and comparing their power with charges having rough surfaces. When the surface is smooth, the gas globe also is very smooth, whereas, with a rough charge surface there is some tendency for Munroe jet action to reproduce irregularities in the gas globe. With a smooth gas globe, it is very hard to see how sufficient mixing could take place for the water to enter the reaction to any great extent.

Torpex was the most powerful of the explosives actually used in any appreciable quantity. However, it is probably somewhat more sensitive than is desirable in a military explosive. For this reason, following certain British work, HBX was developed by the Bureau of Ordnance in cooperation with Divisions 8 and 2 of NDRC. HBX consisted essentially of torpex with 5 per cent of a desensitizer added (see Table 1).

Unfortunately, no general agreement has been reached as to whether it is peak pressure, impulse energy, or bubble energy which is the determining property of an underwater explosion for producing damage. Consequently, there is the possibility that two explosives might be tested, one of which was superior in one respect and another in another respect. On the basis of present information, it would be difficult to make a decision between such a pair of explosives. Fortunately, no such dilemma arose with the materials which were under consideration during the war. In most cases, the more powerful explosive as rated by one quality also ranks higher in all of the other qualities at the same time. This is not necessarily true, and evidence of deviations from this rule are seen in the table.

It will be noted that ratios of peak pressures for the commonly used explosives range up to about 1.16. It may well be asked whether a 16 per cent improvement in peak pressure is worth striving for. The importance of this 16 per cent improvement may be made more striking by considering the volume within which the peak pressure exceeds a certain minimum amount. This volume will be approximately 60 per cent greater for the explosive which has 16 per cent higher peak pressure at equal distances. To achieve such an improvement is worth a considerable effort from a military viewpoint.

The testing procedures described above were extensively used during World War II at UERL, and the results were in part responsible for the extensive use of torpex and HBX as aircraft depth-bomb fillings. In attacks against submarines the important factor in explosive effectiveness is the range at which the weapon is capable of disabling or sinking the submarine. For 250 lb of torpex, the range for sinking appears to have been 20 ft or more in attacks against most types of submarine encountered. Comparison of shock-wave parameters at 20 and 30 ft thus provides a reasonable basis for assessing explosive effectiveness for this purpose.

On the other hand, there is a certain amount of evidence that only about half as much torpex as TNT is required to produce equivalent damage in the case of contact explosions. As discussed in Section 1.2.6, this would seem to support the view that the mass flow of water against the target was the important factor for damage close to the charge. The energy available by this mechanism is related to the gas bubble energy which in turn is proportional to the cube of the bubble period. In fact, most German comparisons of explosives were based upon relative bubble period measurements. Since, on an equal-volume basis, the bubble period for torpex is 1.22 times that of TNT, the effectiveness of torpex in, for example, a contact torpedo war head, would be estimated to be about 1.8 times that of TNT. The preference on the part of most American submarine commanders for torpex war heads can be readily understood on the basis of this difference.

It is interesting to note that the radically different German and American procedures for comparison of explosives were probably valid and justified considering the prime use with which each side was concerned. The Germans were concerned with contact or near-contact weapons for use against shipping and the Americans with maximum lethal-range depth bombs for use against submarines.

Bubble period measurements were made at UERL

on small scale (½-lb) charges of tetryl, TNT, and torpex and on large scale (250-lb) charges of TNT and minol. The results were not, however, considered in connection with explosive comparisons.

1.211 Importance of the Use of Statistical Methods

The problem of comparison of explosives discussed above is an illustration of a type of situation often encountered where statistical analysis of experimental data is highly important. In many basic measurements, experiments can be performed with such precision that little consideration of statistical questions is necessary, but often in practical problems, especially in the comparison of explosives, all measurements cannot be performed with as high a degree of accuracy as would be desirable. This is due to the fact that it may be difficult to recognize and control all the factors which might influence the measurements. In deciding whether a new type of explosive is really superior to older types, one should bear in mind that service weapons loaded by normal procedures are not absolutely uniform and reproducible. For example, the weight, density, and quality of the cast explosive is noticeably variable. Therefore, it is obviously dangerous to base decisions on the measurements of a small number of charges. Furthermore, even when a sufficient number of experiments have been carried out, a careful statistical treatment of the data is desirable in order to determine the degree of confidence which can be associated with the results. There are a number of basic principles which are applicable to the problem of explosive evaluation.[53,54]

The first principle is that controls should always be used. That is to say, in any series of experiments in which new materials or new methods are being tested, there should be an ample number of tests on standard materials or methods. Thus, in testing explosives at UERL, charges of TNT were always included in each series, so that any variation of the test conditions, due to any cause whatsoever, which might change the absolute level of the pressures, impulses, etc., would at least largely cancel because ratios of these quantities to the corresponding quantities for TNT were always employed. In many cases the persons responsible for instrumentation may feel highly confident that they have brought under control all the variables which influence the result appreciably and that it is, therefore, unnecessary to employ controls. Experience has almost universally shown that this is not a safe procedure and that unknown forces of variation are very likely to appear, even with test methods which have been highly developed and long used. For example, at UERL the diaphragm gauges mentioned above were developed quite early to a state of high reproducibility. After several months' use of this gauge, a sudden shift in values occurred which proved very difficult to locate. A long search located the trouble as due to a change in the grade of lumber supplied for making the frames to hold the gauges. As a result of this experience, controls were rigidly required thereafter in all tests.

A second basic principle is that the controls and the test specimens should be measured under as nearly identical conditions as possible. This normally involves testing them at close intervals of time, because it is very difficult to reproduce, after a long interval, all the conditions which initially existed. It was, therefore, a standard practice at UERL to test explosives in strings. That is, a number of different explosives, including TNT as a standard, were tested either the same day or on successive days with the same equipment and methods. Furthermore, the order in which the different materials were fired was chosen by lot so as to minimize any possible effect of systematic changes of various variables with time. For example, if every day the explosives in a string had been fired in the same order, it might have been possible for a systematic error to enter because the temperature was always colder the first thing in the morning than later. Because the accuracy of the measurements and the reproducibility of charges were not sufficient to make one measurement of each substance adequate, the strings were repeated a number of times, in each of which the order was chosen independently by lot. The number of strings required was calculated in advance by standard statistical methods on the basis of the expected precision of the individual measurements and the desired overall accuracy.

In carrying out these repetitions to the strings, another principle was employed. Since the conditions under which explosives are used in practice are extremely variable, it is not sufficient to make tests under only one set of conditions. Thus it was at least conceivable in advance of the experiments that the relative merit of two explosives might be a function of the distance from the charge, the size or shape of the charge, etc. Since it was desired to obtain an overall answer to the question of how much better an explosive X is than TNT, the experiments had to be

performed over a range of conditions. Therefore, insofar as it was feasible, each string was measured under somewhat different conditions although, of course, every shot inside a given string was carried out under the same conditions. From string to string, some variable was changed which was not expected to cause any shift in the relative effectiveness of the explosive. By proceeding in this way it was possible to determine the effect of such variables. The ratios of explosive performance obtained in the different strings could still be averaged together to get an overall average ratio applicable to the range of conditions employed. The average would be more accurate and reliable than the results of any individual string.

A fourth principle was to choose by lot the values of any presumably unimportant variables which could not be controlled from measurement to measurement. For example, in using the diaphragm gauges, the steel plates could be used only once and the plates as received from the manufacturer might have been arranged in an order leading to a systematic variation of thickness or strength from one plate to the next. The plates of each lot were thoroughly shuffled, so that any accidental variations would enter the results as random error and not as a systematic error, tending to falsify the conclusions.

Every effort was made to avoid subjective errors. Frequently the explosive being tested was identified only by number, so that those carrying out the tests and analyzing the results would not know the identity of the materials. Thus there was little chance of the subconscious influence of prejudice on the answer. The frequency with which prejudice unintentionally influences the results of scientific experiments is not sufficiently appreciated.

Considerable attention was paid to the estimation of experimental errors from the data itself. Gauges were normally used in pairs, so that the differences between members of a pair when averaged over many experiments would give a good estimate of the reliability of a gauge. In this way, a decision could be made on the basis of a standard statistical argument as to whether a given observed difference between two explosives was likely to be real or merely the result of experimental error.

1.2.12 Absolute Values of Shock-Wave Parameters

Since the explosive comparison experiments were so designed that ratios were obtainable from identical gauges under conditions as nearly the same as possible for the various explosive compositions, small errors in the absolute calibrations tended to cancel. Nevertheless, considerable effort was expended to perfect the instrumentation so as to yield absolute values of the shock-wave parameters because of their importance in studies of damage processes.

Figures 14, 15, and 16 give the peak pressure, impulse, and energy flux respectively for charges of

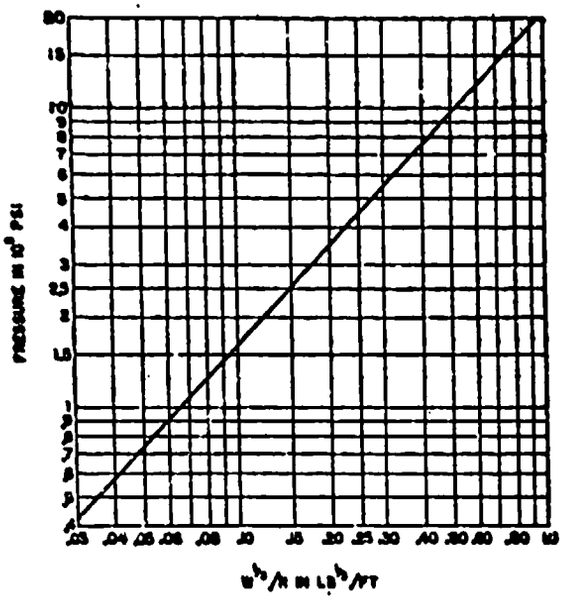

FIGURE 14. Plot of P versus $W^{1/3}/R$ for spherical cast TNT.

TNT as functions of $W^{1/3}/R$. Over the range of these measurements, the shock-wave parameters are represented with fair accuracy by the following linear equations

$$\text{Peak pressure} \quad P = 2.12 \times 10^4 \left(\frac{W^{1/3}}{R}\right)^{1.13} \text{ psi},$$

$$\text{Impulse} \quad I = 1.46 W^{1/3} \left(\frac{W^{1/3}}{R}\right)^{0.89} \text{ psi-sec},$$

$$\text{Energy flux} \quad E = 2.40 \times 10^3 W^{1/3} \left(\frac{W^{1/3}}{R}\right)^{2.05} \text{ psi-in},$$

where $W^{1/3}/R$ is expressed in $\text{lb}^{1/3}/\text{ft}$. Impulse and energy flux are calculated to the time $t = 6.7\theta$ sec only, i.e., 6.7 times the time constant of the shock wave. The energy factor given here is calculated on the acoustic approximation

$$E \cong \frac{1}{\rho c} \int P^2 dt$$

where ρ is the density and c the velocity of sound for sea water.

The true energy flux would include terms for the finite amplitude effect[28] and for the mass motion of the water radially outward from the charge surface (see Section 1.2.6). At the distances from the charge over which these equations are intended to apply,

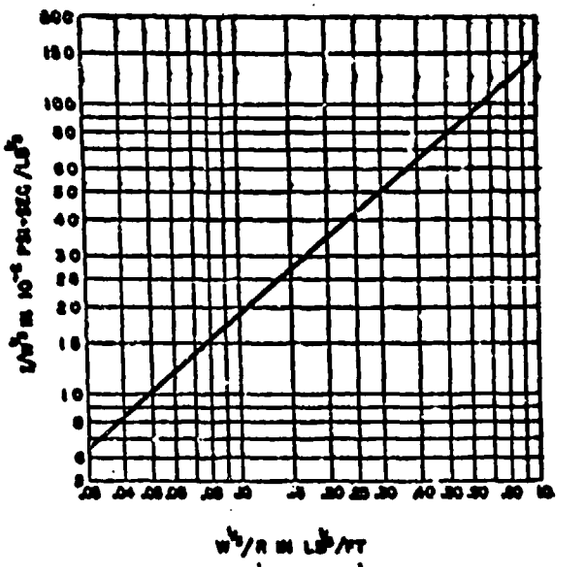

FIGURE 15. Plot of $I/W^{\frac{1}{3}}$ versus $W^{\frac{1}{3}}/R$ for spherical cast TNT.

neglect of these factors does not seriously invalidate the results. Experimental data is not yet available which would make possible the evaluation of the total energy flux over a complete bubble expansion.

Procedures employed to overcome various difficulties encountered in attempts to establish the absolute level of the piezoelectric results are described in Section 1.4.1. By the end of World War II it was believed that the controlling factor in limiting the precision of the absolute values was the difficulty of obtaining precise determinations of the piezoelectric constant of the tourmaline gauges. In principle, this calibration should be carried out under conditions closely approximating those in the shock wave being measured. Since a calibration of this type is extremely difficult to accomplish, several independent methods of estimating shock-wave peak pressures were employed to test the reliability of the piezoelectric results.

1. For four shots in which it was used, the optical distortion method described in Section 1.4.3 gave pressures which were approximately 10 per cent greater than those measured by the piezoelectric gauges. Unfortunately, sufficient work was not done to determine the accuracy of this method.

2. A second check which has the advantage of simplicity was provided by the measurement of the velocity of rise of the spray dome from the surface above an explosion. The pressure P at any point in the water is related to the propagation velocity of the shock wave U and the particle velocity u by the simple equation

$$P = \rho U u,$$

where ρ is the density of the water. Values of the shock-wave propagation velocity U are shown in Figure 17.[16] It has been shown[27,29] that to a good approximation $u = V/2$, where V is the velocity of rise of the spray dome. The factor ½ enters because

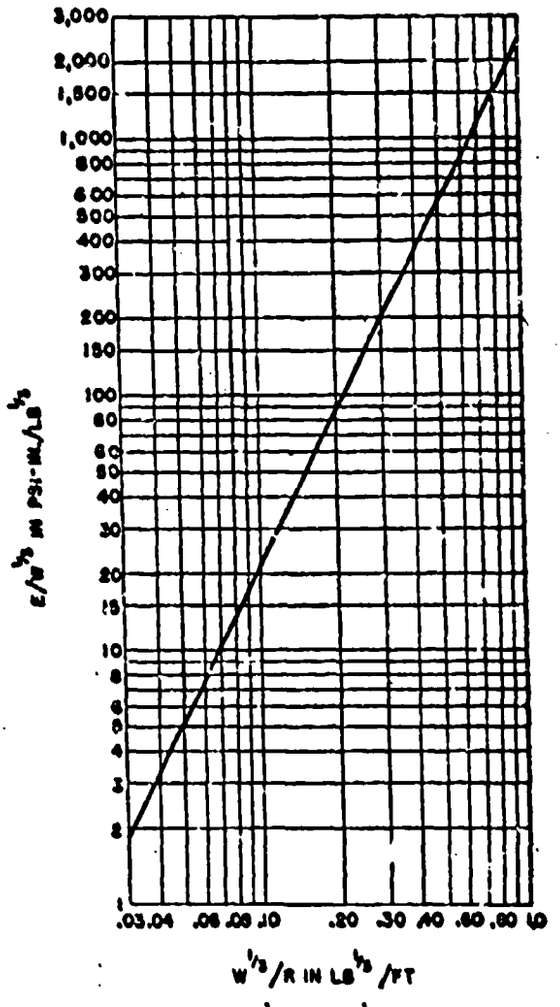

FIGURE 16. Plot of $E/W^{\frac{1}{3}}$ versus $W^{\frac{1}{3}}/R$ for spherical cast TNT.

the reflected rarefaction wave doubles the upward velocity of the spray. The latter was measured by means of a high-speed streak camera.[60,61] Table 4 shows a comparison of the pressures obtained by this method with the corresponding piezoelectric gauge values.

TABLE 4. Comparison of pressures from dome velocity and piezoelectric gauge measurements for TNT charges.

Charge weight (lb)	Distance to charge (ft)	Pressure (psi)	
		By dome velocity	By piezoelectric gauge
5.07	4.00	7,680	7,800
5.53	4.00	8,150	8,100

3. The ball crusher gauge, described in Section 1.4.2, provided a further check on the absolute-pressure level of the piezoelectric gauges. Pressures obtained with the ball crusher gauge on 300-lb charges were in agreement with the piezoelectric gauge values to within ±5 per cent.

4. Only a very rough check was made by measurement of the propagation velocity of the shock wave U. From the Rankine-Hugoniot conditions (see Section 1.2.13) and an equation of state for water,[54,62] the following approximate relation valid to a pressure of approximately 20,000 psi may be derived:

$$\frac{U-c}{c} = (5.4 \times 10^{-6})P.$$

The pressure is thus directly dependent on the quantity $U-c$ which, except at very high pressures, is small and therefore difficult to measure experimentally with the required accuracy.

5. An additional check on the calibration of the piezoelectric gauges was due to the reciprocity calibration method developed at the Underwater Sound Reference Laboratory [USRL] of Division 6, NDRC.[63] Some tourmaline gauges of the type used for the underwater explosion measurements were calibrated by this method and gave values in good agreement with those obtained by the usual static calibration methods.

1.2.13 Theoretical Studies of Shock-Wave Propagation and Intensity

Relation between Peak Pressure and Velocity of Propagation of Shock Waves

The velocity of propagation of a shock wave depends upon its peak pressure in a way that can be calculated. This velocity is higher than the velocity of sound when the peak pressure is high but approaches the velocity of sound as the peak pressure decreases. The mathematical relationship is based on the laws of conservation of matter, conservation of momentum, and conservation of energy. The resulting equations are known as the Rankine-Hugoniot relations.[64] Application of these relations requires, in addition, a knowledge of the effect of temperature and pressure on the density of water (or sea water).

Figure 17 shows the results of a calculation for sea water of the relation between the excess shock velocity (i.e., shock velocity minus sound velocity) and the shock wave pressure.[54,62] This relationship enters into any theoretical calculations on shock-wave propagation and also has direct practical applications. In Section 1.2.12 it is mentioned that measurements of shock-wave velocity, combined with the above law, were investigated as a possible independent check on other methods for measuring the absolute value of the shock-wave pressure. In any measurements involving times of propagation, such as in depth ranging (Section 1.4.5), this excess velocity must be considered if the pressure is considerably greater than acoustic levels.

Theoretical Calculation of Shock-Wave Properties

It proved to be possible to predict by purely theoretical methods the peak pressure and other shock-wave parameters as functions of distance from charges of various explosives. Work carried out under Division 8,[2,4] yielded estimates of the pressure within the explosive charge itself at the instant of complete detonation. As an approximation it was usually assumed that the pressure inside was the same throughout a spherical charge and that the burnt gases were at rest at that instant, although actually it was known that the mechanism was more complicated. With this starting point, it is a purely hydrodynamical problem, but a very difficult one, to calculate the events which occur in the surrounding water as the pressure wave is emitted.

The equation of continuity (conservation of matter) and the equation of motion (conservation of momentum) supply a set of differential equations for the motion of the water which, in principle, determine the events accompanying expansion of the explosion products once the boundary conditions are specified.[65] The boundary conditions are given on the one hand by semiempirical relations describing the way in which the pressure of the burnt gases falls off as the

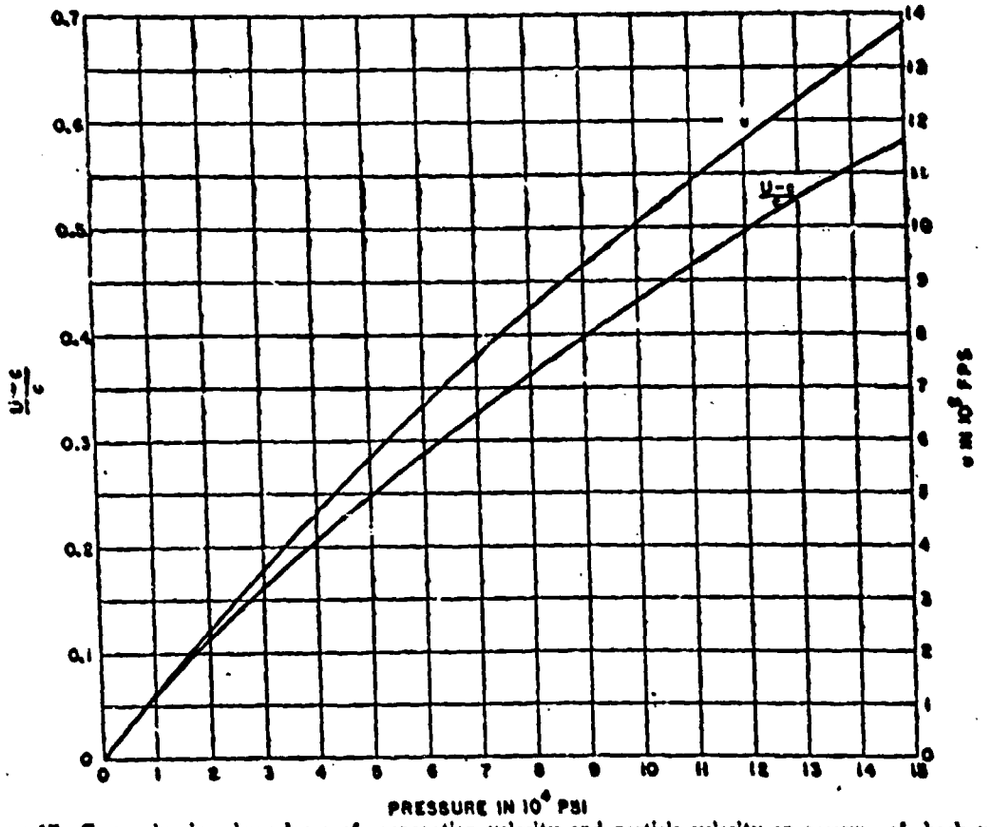

FIGURE 17. Curve showing dependence of propagation velocity and particle velocity on pressure of shock wave.

gas bubble expands,[64,67] and on the other hand by the Hugoniot relations between the shock-front pressure and velocity. It has not yet proven feasible, however, to solve differential equations exactly for this problem.

One procedure which was used to get an answer for one case (TNT) was numerical integration.[68-70] This led to reasonably good results but was so excessively laborious that it was not applied to other materials or to other densities of TNT.

An approximate solution was found at Cornell University which was remarkably successful.[71-74] In that solution, the pressure, etc., inside the explosion were obtained from a theoretical treatment involving numerous approximations, and the solution of the hydrodynamic problem of the propagated pressure wave necessarily required certain compromises with rigor. When these simplifications were made a complicated but tractable solution of the differential equations was obtained, and applied to a considerable list of explosives at several loading densities.[75-80] The results in terms of explosive comparison ratios relative to TNT for a few explosives are listed in Table 5. These values are to be compared with the corresponding experimental ratios shown in Table 3. The theoretical values

TABLE 5. Theoretically computed explosive ratios for constant volume comparison relative to TNT.

Explosive*	Density	Peak pressure ratio	Impulse ratio	Energy ratio
Torpex-2	1.70	1.10	1.16	1.28
Minol-2	1.65	1.05	1.11	1.17
RDX-Comp.-B	1.61	1.06	1.07	1.13
Amatol	1.55	0.94	0.92	0.87
TNT	1.59	(1.00)	(1.00)	(1.00)

* For composition of explosives see Table 1.

are somewhat lower than experiment but they do give the correct order of merit of the different explosives.

Later a different type of approximation was used which also enabled the peak pressure and impulse to be calculated as functions of distance and charge weight.[81-83] In this treatment, certain measured parameters of the shock wave at a given distance could be

used to compute the shock-wave parameters at other distances, hence the description of this theory as a propagation theory. This method was considerably simpler than the earlier procedure and had the advantage of being applicable to shock waves in air as well as water. (See Chapter 2.)

Figure 18 shows a comparison of the peak pressure versus distance curves for TNT for the theoretical calculations and for some measurements with piezo gauges at UERL. The agreement is really quite remarkable for so complicated a phenomenon. As a matter of fact, during the period in which the piezo gauges were still in a development stage at UERL the calculated results were usually the values utilized since they were regarded as more reliable than any experimental values then available.

The theoretical investigations at Cornell involved very difficult and abstract mathematical methods and it was not at all certain at the time they were undertaken that they would lead to results of any practical value. As a matter of fact, the investigations proved to be extremely useful, not only because of the direct applications of the numerical values of pressures, etc., but because the theory served as a guide and framework for the experimental work at UERL. There was constant competition between the experimental and theoretical workers in seeking the ultimate answers, and discrepancies which sometimes appeared lead to searches for errors and effects which otherwise might not have been suggested.

1.3 DAMAGE PRODUCED BY UNDERWATER EXPLOSIONS

1.3.1 General Considerations

The problem of predicting the damage to a given structure which will be caused by an underwater explosion is very difficult and has not yet been fully solved. In principle, the problem is nothing more than the application of Newton's laws of motion and of the resisting properties of the material. The difficulties arise from the complexity of the system of forces acting on an element of the structure as it is being deformed by the explosion. Usually the complete expression of these forces is not known or the solution of the resulting equations is not feasible. When simplifying approximations are made to render the problem tractable, some uncertainty is introduced as to the confidence with which one can apply the theoretical results to the interpretation of experiments on an actual structure. In view of the difficult nature of the problem, it is not surprising that reasonably complete theory is available for only certain simple, idealized target structures such as, for example, a circular steel diaphragm having its edge rigidly sup-

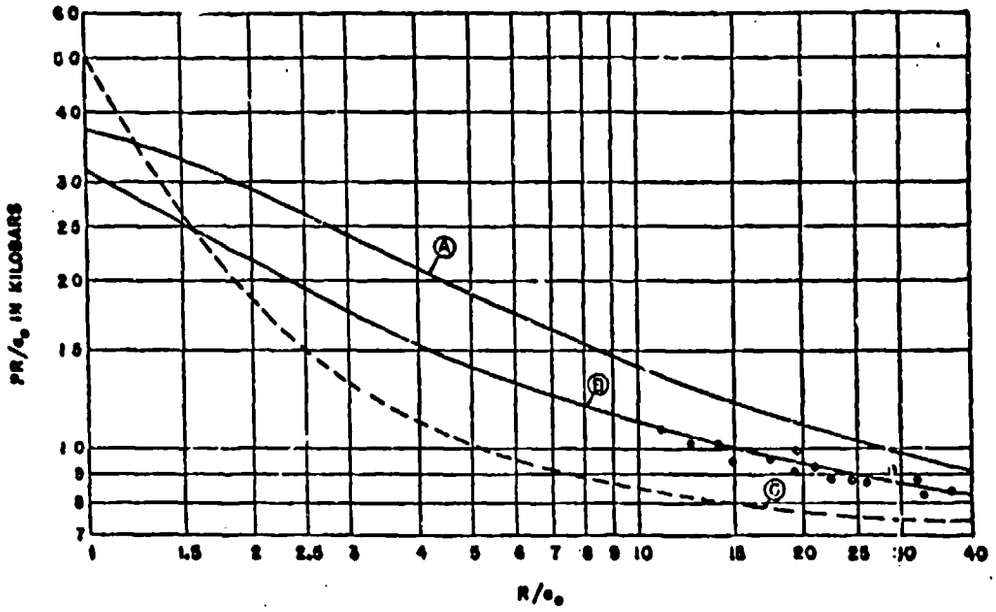

FIGURE 18. Curve of theoretically computed pressures for cast TNT versus distance from charge. Curve A: approximate analytical solution; Curve B: "propagation theory"; Curve C: numerical integration treatment.

ported. In the case of ship structures it is even difficult to state which properties of the explosion are the most important in producing damage in a given case. It is conceivable that under certain conditions the damage-determining factor could be shock-wave peak pressure, impulse or energy, the properties of the bubble pulses, or the incompressive flow of the water associated with bubble motion. Nevertheless, certain concepts of the damage theories at least define the limitations on possible hypotheses concerning the nature of the damage process.

The theories so far developed are primarily applicable to noncontact explosions, for example, a depth bomb exploded near a submerged submarine or a large aerial bomb exploded in the water at a distance from a merchant vessel but near enough to produce serious damage. Under these conditions, especially where the charge is at the same level as the target and not underneath it, the kinetic energy effects due to the incompressive flow of the water can probably be ignored, since, as pointed out in Section 1.2.6, these effects fall off as the fourth power of the distance, whereas the energy transported by the shock wave falls off only as the second power of the distance. For charges at a distance from a target, the double pulses are probably not important. In many cases, the explosion occurs too near the surface for those pulses to develop because venting occurs first. In other cases, such as in a deep attack on a submarine, bubble pulses might have to be considered, especially if the charge detonates underneath the target. This is a subject which needs further investigation.

The subject is particularly confused for contact or near-contact explosions. Under these circumstances, the shock-wave phenomena and flow phenomena occur almost simultaneously and the target, if close enough to the charge, will be subjected to quite a high pressure from the gas bubble itself.

Effect of Target Inertia

When a shock wave strikes a target of large area so that the effects of the edges do not need to be considered, a number of possibilities exist. If the target is quite massive so that its inertia is large and the time required for it to accelerate appreciably is large compared to the duration of the shock wave, the impulse of the wave will be completely absorbed by the target, and impulse will then be the deciding factor in determining the extent of damage. This is similar to the experiment in which a bullet strikes a ballistic pendulum. The period of the pendulum is long compared with the time of impact of the bullet and one thus measures the total impulse transferred by the bullet to the pendulum. Furthermore, one can treat the reflection of the wave as if the target were rigid, so that the pressure and likewise the impulse are essentially doubled by this reflection. The question as to whether or not damage takes place then becomes a problem of calculating whether the target is capable of absorbing the given amount of impulse without suffering permanent deformation. As a simple illustration, consider a completely free, air-backed plate upon which a shock wave impinges perpendicularly. If the plate has the mass M and the impulse in the shock wave has the value I, the plate acquires a momentum $Mv = 2I$, where v is the velocity acquired by the plate and the factor 2 occurs because of the reflection of the shock wave.

On the other hand, the damage process is different when the target plate is so light that its inertia does not prevent appreciable motion during the time of passage of the shock wave. In the limit when the plate is so light that it accelerates rapidly compared with the duration of the shock wave one might expect that the peak pressure would be the important damage determining factor. If the possibility of cavitation is ignored this would follow because the damage would be over before the pressure in the shock wave had fallen appreciably below its peak value. Under these conditions the ultimate duration of the shock wave would have no important bearing on the extent of the damage. This extreme situation is the sort that would be expected with a very large explosion, such as an atomic bomb. Here, the full duration of the wave is longer than the period of most target structures so that the damage is measured by the peak pressure and not by the impulse or duration.

Effect of Cavitation

Under certain circumstances cavitation can occur. This greatly complicates the treatment of the damage problem. When the target accelerates under the action of the shock-wave pressure, its motion forward tends to reduce the pressure in the water. If the target is light enough, this effect can be so pronounced as to cause the pressure to fall very rapidly below zero to negative values. In other words, the plate acquires sufficiently great velocity actually to pull away from the water or to cause the water to pull away from itself, resulting in the formation of cavitation bubbles. Figure 11 (see Section 1.2.5) shows such cavitation in front of a thin air-backed free plate accelerated by

a shock wave. A theory has been developed to take into account this phenomenon in the simple idealized case of a deformable diaphragm with supported edges. The net result of this theory is that the energy of the shock wave becomes trapped between the target plate and the receding layer of cavitation bubbles. This layer recedes because the plastic deformation of the moving plate absorbs its kinetic energy and thus arrests its forward motion. When this happens, the water which is moving forward piles up against the plate and the pressure once more rises to positive values so that the cavities begin to collapse. This boundary between solid water and cavitated water then recedes away from the target plate. The mathematics leads to the predictions that, under these circumstances, it will be the square root of the energy of the shock wave which is the determining factor for damage.

Edge Effects

The damage process for all actual cases is complicated by edge effects. A real target is not of infinite extent, so that the phenomena occurring around the edges of the target will influence the phenomenon at the center. A finite time is required for any disturbance to be propagated through either the sea water medium or the target structure so there will be a time factor in the influence of edge effects, but they will eventually act to influence the phenomena at any part of the structure. Thus, if the target is of small diameter, cavitation may never get started because the reduction in pressure at the center caused by the forward motion of the target plate may be eliminated by the flow of pressure in from the high-pressure regions around the plate. This diffraction effect was used to predict quantitatively the conditions under which cavitation will occur.[24,25] The predictions so obtained were successfully borne out by underwater photographic investigation of cavitation phenomena. (See Section 1.4.3.)

Relation of Shock-Wave Parameters to Damage

It is seen from the above discussion that peak pressure, the square root of energy, or impulse may each in its own domain be the determining criterion of damage. In all real cases, the mechanism will be some combination of these idealized ones. It is unfortunate that no more definite answer to this question has yet been made which is applicable to practical situations, because a knowledge of which of the characteristics is the important one would enable a determination of the optimum weapon size to be made.[26] Thus, if peak pressure is determining, the lethal radius will be proportional to the cube root of the charge weight on the basis of the similarity law; whereas, if impulse is effective, the lethal radius will increase approximately as the two-thirds power of the weight. Finally, with the square root of the energy, the lethal radius would increase approximately as the square root of the weight, that is, intermediate between the peak pressure and impulse cases. Since, in practice, one never gets either the pure peak pressure or the pure impulse cases but something intermediate, the square root law is normally not a bad approximation. Given the proper law to apply, one could calculate the optimum weapon size using knowledge of the modes of attack and the geometry of the target. Thus, it could turn out, with a very small target, that the important factor was the lethal volume, that is the volume around the explosion within which the target would be damaged. This lethal volume would vary as the cube of the lethal radius and, therefore, as the $\frac{3}{2}$ power of the weight if the square root law applied. Under these conditions, the probability of damage would increase more rapidly than the weight of the charge and would thus favor large charges. However, as the charge weight increases to large values, the increase in the time constant of the shock-wave decay would cause the damage-distance exponent to decrease toward the peak pressure-distance decay exponent which would ultimately make the lethal volume proportional to charge weight. The lethal volume criterion is certainly not the proper one to use in all cases. For example, if the depth of the target is known and the depth of the explosion can be accurately set, lethal area would be a more appropriate criterion. The problem is thus complicated but should be soluble if the conditions are known in detail.

1.3.2 Explosive Damage to Steel Plates

Although it should be clear from the above paragraph that the state of knowledge concerning damage to structures in general from underwater explosions is not in a satisfactory state at the present time, nevertheless, simple idealized systems have been effectively studied both experimentally and theoretically and provide a useful basis for further work. The simplest of these systems is the free air-backed plate. Some experiments have been performed on this type of system especially with the aid of underwater photography.[12] Complications here are the edge effects and the pro-

duction of cavitation under certain conditions, so that even this very simple system has not been fully treated theoretically.

Another simple system which has been treated is the ball crusher gauge in which a copper sphere is damaged by the pressure wave accelerating a piston. This is discussed in Section 1.4.2.

Circular Steel Diaphragm Experiments

The UERL diaphragm gauge described in Section 1.4.2 which consists of a clamped air-backed steel diaphragm has been extensively studied both theoretically and experimentally with quite satisfactory results. In the course of its use as an empirical measure of the effectiveness of various explosives,[14,21-23] a large amount of experimental data was obtained with a great variety of charge weights and distances. In addition, a number of special experiments were made on this gauge from the viewpoint of testing the applicability of theoretical results.

It was found, for example, that when the charge size was of the order of 300 lb or larger, the ratios of diaphragm gauge readings for various explosives were very closely proportional to the peak-pressure ratios from these explosives as measured piezoelectrically. However, there was empirical evidence that even with charges of this size the diaphragm gauge was not acting as a pure peak-pressure gauge; that is, its readings were somewhat influenced by the rate of decay of the pressure pulse. To explore this point, the data were analyzed to determine the effect of weight and distance on the damage to the diaphragm. It was found that over short ranges of weight and distance, the central indentation S of the diaphragm could be expressed as a simple function of the weight W and distance R, i.e.,

$$S = \frac{CW^m}{R^n},$$

where C is an empirical constant related to the gauge properties and m and n are empirical constants. Using this formula, one can investigate the relation between weight and distance which produces a given constant damage. If peak pressure were the only factor influencing the result, the similarity law would show that the distance for a given degree of damage should vary as the cube root of its weight. In other words, the ratio of the weight exponent to the distance exponent should be one-third. For large charges, the actual value was 0.4, showing that peak pressure was not the only factor influencing the results. If impulse had been the sole factor, the ratio would be approximately two-thirds as calculated from the known dependence of impulse on weight and distance. For small charges (about 5 lb), the exponents found with the diaphragm gauges were 0.6 and 1.2 for weight and distance respectively. The ratio of approximately one-half shows that in this region of charge weight the diaphragm gauge is measuring something between impulse and peak pressure.

Experiments were performed in which the time required for the diaphragm to receive its full depression was measured by means of an electric contact fitted into the gauge.[18] The experiments showed that the time was about 150 μsec, much shorter than the first bubble period, unless the gauge was mounted above a small charge. Consequently, the great bulk of the data obtained with these instruments as employed at UERL for explosive comparisons (i.e., gauge horizontal to side of charge) was not influenced by bubble pulses. This was further demonstrated by the time of action of the gauge as determined approximately from experiments in which the depth of submergence of the gauge and charge was varied.[20,21a] As the two were brought closer to the surface, a critical depth was reached at which the damage began to decrease with closer approach to the surface. The explanation of this decrease is that the shock wave reaching the diaphragm is cut off by the rarefraction coming from the surface. The time at which the pressure wave is thus cut off can be calculated from the geometry of the setup so that the depth at which the falling off in damage begins will give the maximum duration of the shock wave which is effective in causing damage. This time turned out to be of the order of 200 μsec for charges of a few pounds, in rough agreement with the value of 150 μsec obtained in experiments using the electric contact procedure. As mentioned in Section 1.4.3, it was found by photographic experiments that cavitation did not occur with these gauges under normal test conditions, although conditions could be devised which would result in cavitation.

When water-backed instead of air-backed diaphragms are damaged, the deformation is considerably less. This reduction is primarily due to the inertial resistance of the water which must be accelerated by the deforming plate.

Experiments were performed on the influence of diaphragm thickness and diaphragm weight in order to compare with the theory discussed below.

Experiments were also carried out which showed the influence of pieces of wood near the diaphragm

gauge to be very marked, so that wooden structures should be avoided in using these or other underwater pressure gauges.

Theoretical Calculation of the Plastic Deformation

A number of theoretical treatments of air-backed diaphragms were made during World War II.[94,95,96] The theory developed at Cornell University was based on a number of approximations and assumptions, including the idea that the deformation of steel could be approximately treated mathematically by assuming that its stress-strain curve was a horizontal straight line at the yield stress. Furthermore, it was assumed that the diaphragm could be treated as a membrane under a constant tension equal to the product of its thickness and the yield stress of the material. It was necessary to consider not only the reaction of the diaphragm to the load imposed upon it, a problem of plasticity, but also the effect of the deformation of the diaphragm on the load itself, since the moving diaphragm sends out a rarefraction wave. This correction is complicated by the diffraction effects from the region surrounding the diaphragm. The approximation was also made of linearizing the differential equations which were set up. Solutions were obtained which gave the deformation to be expected under any given condition of shock-wave attack, provided cavitation did not occur. These formulas were remarkably successful in predicting the experimental values which actually obtained over a very wide range of variables.[16,97] The theory also indicated the form of the dependence of the diaphragm deflection on the thickness[98] and the diameter of the steel plates, the effect of bubbles, etc. It was thus feasible, by use of the theory, to eliminate the effect of small unavoidable variations in plate thickness. Thus in making explosive comparisons at UERL it was customary to reduce all gauge readings to the corresponding reading for a standard thickness of diaphragm.

The conditions leading to cavitation were successfully derived,[94] but there still remains the very difficult problem of developing an accurate theory for predicting the damage under conditions of cavitation.

1.2.3 Some Remarks on the Use of Scaled Models

One of the most convenient methods of studying the phenomenon of damage by underwater explosion is the use of scaled models.[99-102] There has been much discussion and not a little experimentation in the past concerning the reliability of this method of investigation and it cannot be said that the issue with respect to explosion phenomena is completely clarified. However, a great deal more is understood now regarding the requirements for true scaling than was known at the beginning of World War II. At that time, for example, the phenomenon of bubble oscillations was not at all well known. Furthermore, the effect of rate of strain on the strength of materials was not appreciated. The evidence is now very strong that shock-wave properties scale, as described in Section 1.2.4, to a considerable degree of accuracy. It is not, of course, impossible that more refined investigations will detect small deviations from the scaling laws but the deviations should not be of great practical significance. It is also well known now that the bubble effects do not scale in the same way. Bubble effects, therefore, immediately put a limitation on the use of models for the study of underwater damage under conditions such that bubble or flow phenomena may be important. There are, however, other limitations. The most important limitation is the fact that it is almost never possible to build a model which is perfectly scaled from a large structure. For example, no really equivalent means of fastening the members together has been found. Rivets and welding are not easy to reproduce on a small scale. Neither is it usually practical to make the structural members of exactly the same shape in the model as in the prototype. It is also very difficult to reproduce the properties of heavy steel members on a small scale, since the operation of rolling out thin sheets influences the strength noticeably. In spite of all these difficulties, it is unquestionable that a great deal of essential information can be derived from model experiments.

Naturally, no model experiment is a complete substitute for a full-scale test on the actual structure of interest. On the other hand, the number of variables involved and the number of variables which are not easily controlled may be so great that a single large-scale test can be highly misleading. When an experiment involves either variables which cannot be accurately controlled or variables which take on many values in practice, one of which must be selected for the test, one has a statistical problem such that only a large number of experiments under a wide range of practical conditions can give a result of assured accuracy. Such a large number of tests is impractical if expensive full-scale structures have to be employed. It is for these reasons that model investigations are practically essential for the study of damage although

it is clearly very desirable to supplement them with a few well-chosen full-scale tests.

In general, the way in which the various parameters should be scaled can be deduced from the principles of dimensional analysis.[103] A more rigorous procedure requires a complete knowledge of the differential equations of motion of the system. Frequently it is not possible to scale properly every parameter or variable which occurs in the equations. When, for example, parameters such as gravity and density occur in the equations, rigorous scaling may not be possible or may be impractical to carry out experimentally.

In constructing a model, a great amount of knowledge and judgment must go into the design and into the decision as to which features of the structure are the essential ones. Thus, it may be important that the moments of inertia of certain members be accurately reproduced although it may not be necessary to reproduce the exact shape. On the other hand, it is not sufficient that the structure have the same static strength as the prototype because one is interested here in dynamic effects where the inertia of various members may be very important in determining their resistance to damage. The degree of perfection with which certain components of the model are fabricated may or may not be vital. Thus, in tests made at UERL on simple cylinders, it was found that the ability of these structures to withstand explosive attack was critically dependent on the degree of roundness of the cylinder, (see Section 1.3.4). A flat spot deviating from a perfect circle by as much as half the thickness of the material caused a definite weakening of the structure. On the other hand, this effect was not nearly so pronounced when the cylinders were ribbed in closer imitation to the construction of a submarine.

The influence of the effect of strain rate on the strength of the materials needs to be studied further in connection with the use of models. If it were not for this effect,[104] it would be expected that the Hopkinson law of scaling described in Section 1.2.4 should hold for shock-wave damage. Limited experiments at UERL on copper diaphragms of two sizes showed close agreement with the Hopkinson scaling law, in spite of the well-known rate of strain effect on the strength of copper. (See Chapter 12.) This may be a result of the fact that at both scales the rate of strain was fairly high and in a region where the strength is not changing rapidly with rate of strain although it differs materially from the static strength. Extrapolation of this scaled result to much larger structures might be slightly in error because of the strain rate effect. This rate of strain difficulty does not, however, invalidate relative experiments in which various variables such as method of construction of the model, distance of the charge, type of explosive, are compared at the same scale. The relative ease with which large numbers of experiments may be conducted with small-scale structures argues strongly in favor of the use of small models, or simple idealized targets, in the investigation of the fundamental nature of the damage process.

1.2.6 Explosive Damage to Steel Cylindrical Shells

Another type of simple system which has been studied extensively, both experimentally and theoretically, is the air-filled cylinder. Various models of such cylinders were designed and studied at UERL. These were roughly scaled to represent a section of a submarine hull between bulkheads and were constructed with or without internal ring supports analogous to the stiffener ribs of a submarine. The sizes were approximately one-tenth or one-twentieth of full scale in linear dimensions. A technique was evolved for rolling and fastening the cylindrical wall so that the maximum deviations from perfect circular cross section could be made as low as one-eighth of the wall thickness.

Cylindrical Models without Internal Ring Supports

The majority of the experiments with this type of cylinder were conducted with a model having a diameter of 5 3/16 in., an unsupported length of 8½ in. and wall thickness of 0.038 in. The ends, which consisted of circular steel plates 1 in. thick, were free to move inward on a central supporting rod as the cylinder was damaged.[81] These shells had a single longitudinal welded seam. In practice the charge was oriented relative to the cylinder so that the seam was on the far side of the cylinder, thereby minimizing the effect of unavoidable imperfections introduced by the welding.

One interesting series of experiments with this model consisted of damaging the cylinders with 25 grams of tetryl at various shallow depths. The results indicated that under certain conditions the bubble pulse may contribute greatly to the damage. This is illustrated by the photographs in Figure 19. All three cylinders shown were damaged with the same size of charge and at the same charge-to-cylinder distance

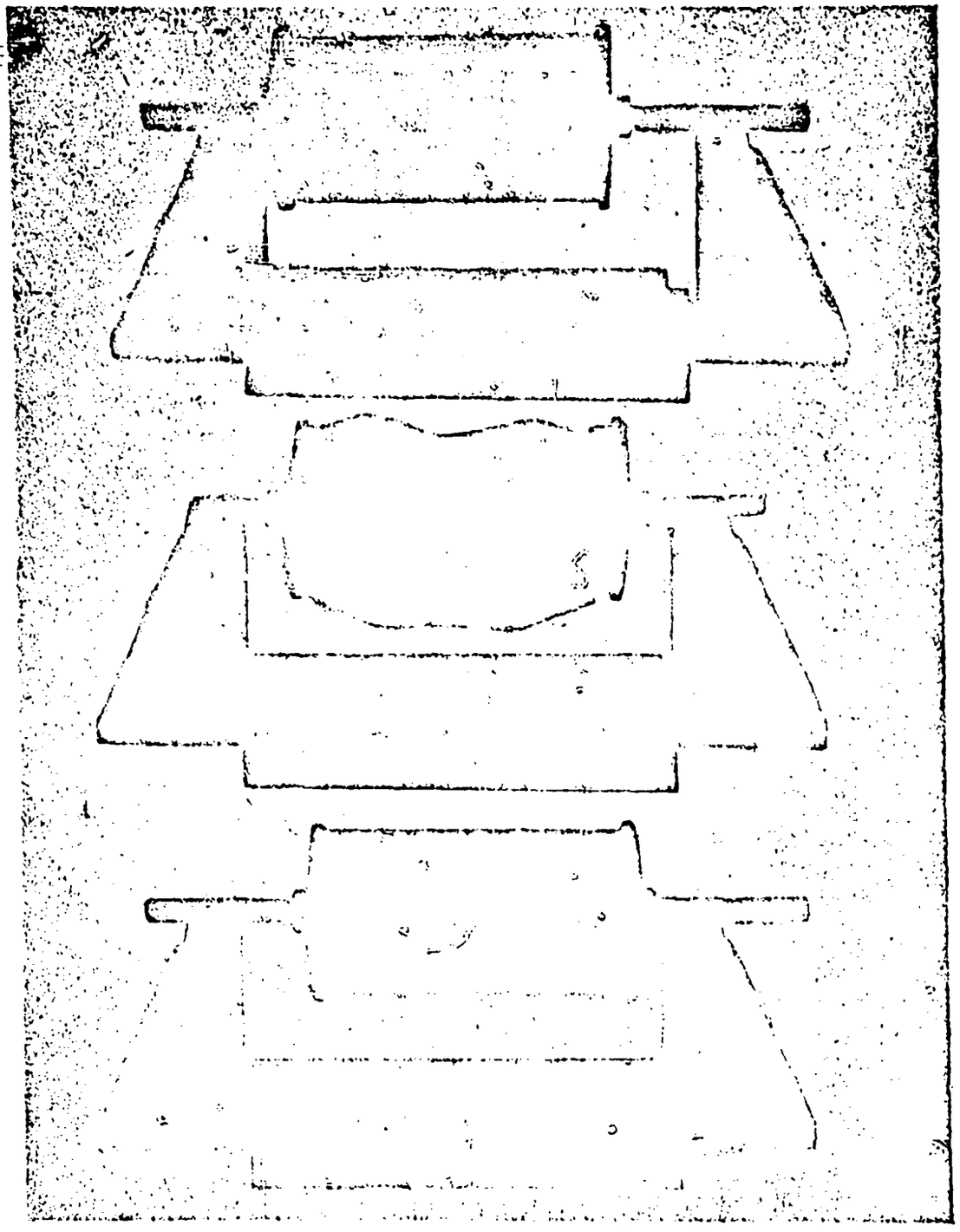

FIGURE 19. Photographs of cylindrical models showing effect of bubble damage in shallow water.

of 26 in. and with the charge vertically above the cylinder. They differed only in the depth of submergence of the charge-cylinder combination. In the first photograph, the charge was 1 ft beneath the surface so that the explosion bubble was vented before it could have emitted anything but the shock wave. Note the small amount of damage which is presumably the effect of the shock wave alone. In the third photograph, the system was submerged so that the charge depth was 5 ft. Hence the normal bubble pulse would develop, largely uninfluenced by the presence of the surface. The damage is considerably larger. In the second photograph, the depth of submergence of the charge was 2 ft, which presumably led to the bubble being repelled by the surface so that the bubble pulse came from a point practically in contact with the cylinder, resulting in its complete destruction. It is important to emphasize that the downward migration of the bubble due to free surface repulsion, observable with small charges, does not occur with charges greater than several pounds. This is a consequence of the relatively greater upward force of gravity on the larger gas globe. This is an example of a phenomenon which is not easily scalable, and illustrates the fact that extreme care must be exercised in the design and interpretation of model scale experiments.

Another series of experiments was designed to investigate the effect of slight deviations from a perfect circular cross section of the cylinder wall. This was accomplished by deforming the shell before mounting so that the curvature in certain local regions was altered. Deviations from a perfect circular cross section of ½- to 2-wall thicknesses did not greatly affect the extent of the damage in shallow water, but were important factors in determining the locations of the damage. In deep water, however, where a considerable hydrostatic load was superimposed on the explosive loading, these slight imperfections in the cylinder wall significantly increased the observed damage.

Cylindrical Shells with Internal Ring Supports

Later investigations were conducted with cylinders which had internal stiffener rings and the following dimensions: diameter 8⅝ in., length 8¼ in., and wall thickness 0.038 in. The stiffener ribs were of strength and at spacings appropriate to a scaled model of a submarine pressure hull. In shallow water experiments with these models, bubble pulse damage and the influence of imperfections were observed but found to be less severe than in the case of the unribbed cylinder. To study the effect of a superimposed hydrostatic load, the damage to cylinders of this model by 25-gram tetryl charges at various distances was determined at depths extending to 700 ft. The results are presented in Figure 20, in which the charge-to-cylinder distance at which a certain arbitrarily defined "critical" damage was inflicted by the explosion is plotted against the depth of submergence.[108]

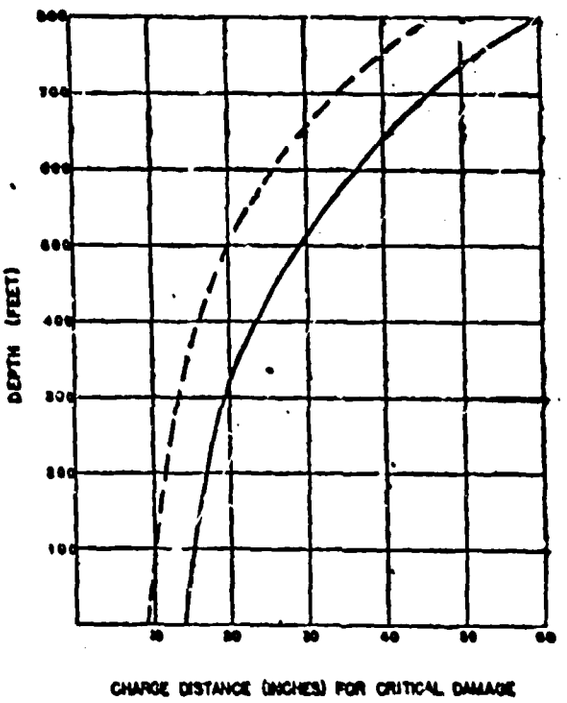

Figure 20. Plot of charge distance required to produce critical damage versus depth.

In order to distinguish between shock-wave damage and bubble-pulse damage to the ribbed cylinders, high-speed motion pictures (2,500 frames per sec) of the cylinder at the time of the explosion were taken. Such pictures were obtained for a number of different depths extending to 700 ft. Photographs for one test are shown in Figure 12 and have been referred to in a previous section. On the basis of a number of similar photographs obtained at other depths, there seems to be little doubt that with hydrostatic loading of the model an appreciable amount of additional damage is caused by the bubble pulse, apart from the damage caused by the shock wave.

Theoretical Treatment of Static and Dynamic Buckling of Cylinders

In conjunction with the experimental work on cylinder models at UERL, theoretical studies were carried out at Cornell. One result of these investigations was a revision of the theory of the static strength of cylindrical shells under hydrostatic pressure. An error was found in Love's fundamental theory of elasticity and an entirely new method of solving the equations of the resistance of a cylindrical shell was carried through to completion. The results were expressed in the form of tables which should be useful to submarine designers or designers of other externally loaded pressure vessels.[106]

At the same time, a beginning was made on the problem of the dynamic resistance of cylindrical shells to explosive loading.[107] From the results of this theory it would appear that pressures considerably greater than the static buckling pressures are required to initiate buckling for dynamic loading such as occurs with a decaying shock wave. Moreover, on the basis of the theory, one would not expect a superimposed hydrostatic load to effect the results to the extent indicated by experiment. (See Figure 20.) The reason for this discrepancy is not yet clear.

The theoretical treatment of explosive damage to cylindrical shells is much more difficult than is that of the circular diaphragm. One difficulty arises because of the instability of the cylinder shape. Once an indentation is produced, there is a tendency for collapse to occur because of the hydrostatic pressure alone.

1.3.5 Results of Other Damage Tests

Countermining of Horn Mines

Tests were conducted at UERL with some Japanese antiboat horn mines, as well as with some replica horns manufactured by the Gulf Research and Development Company, to determine the optimum conditions for countermining such mines in shallow water.[108] Sufficient damage must be caused by the countermining charge to damage a lead cylinder and crush an inner acid-containing glass vial. The damage process of the horns was such that the peak pressure of the shock wave was the important factor; the pressure necessary to activate the horn was found to be approximately 1,500 psi. Thus for a 30-lb charge in a depth of water of 5 ft the effective countermining radius for 50 per cent activation was 37 ft. Experience has shown that under the same conditions activation of all the mines would be reasonably certain at 27 ft or less. Supplementary work has shown that it is not likely that such a mine as the Japanese antiboat mine will be countermined by sympathetic detonation at distances as great as the distance at which it can be countermined through operation of the horn.

Improbability of Underwater Sympathetic Detonation

In general it is difficult to detonate underwater charges of the common explosives fillings or even booster charges, by the explosion of another charge. Thus in one series of tests,[109] small bare (but waterproofed) tetryl and TNT charges failed to detonate when as close as 5 ft from a 100-lb TNT charge. Another test[109] consisted of four trials, in each of which an unfused TNT-loaded GP bomb was placed nose to nose 4 ft from a Mark 13 mine loaded with 700 lb of torpex. In each case the explosion of the Mark 13 mine failed to detonate the charge of the GP bomb. On the other hand, the most sensitive detonator cap tested (U.S. Army Corps of Engineers special blasting cap, nonelectric) was sympathetically detonated when at a distance as great as 29 ft from the explosion of 100 lb of TNT.[109] In countermining actual underwater weapons, other factors, such as damaging or activating specific fuze mechanisms, must be considered. In the absence of any mechanism which can be activated by the shock wave it is unlikely that the explosive charge in such weapons can be detonated sympathetically.

If an occasion requires the detonation of a charge or charges following the explosion of a given charge, it is necessary to provide a mechanical firing mechanism which is activated by the shock wave from the given charge. Tests on one such device in shallow water at Woods Hole revealed an interesting dependence of the range at which it would respond on the nature of the bottom (hard sand or soft mud). It would be important to study piezoelectrically the nature of shock-wave transmission under these conditions.

1.4 EXPERIMENTAL METHODS FOR STUDYING UNDERWATER EXPLOSION PHENOMENA

1.4.1 Piezoelectrical and Other Electrical Methods

Piezoelectric Pressure Gauges

In making an experimental study of underwater explosions, it is obviously important to devise meth-

ods of determining the pressure in the shock wave at various locations around the explosion, preferably as a function of the time. It was early suggested by J. J. Thompson in England that piezoelectric crystals could be used to measure these very short-time phenomena. The British developed, after World War I, a large gauge made from a plate of tourmaline. This is a naturally occurring crystal which is piezoelectrically active, that is, when subjected to pressure an electric charge appears on the surfaces which can be measured by electrical instruments. Their large British tourmaline gauges were utilized in some extremely interesting investigations which served to outline the nature of the phenomena and the problems yet to be solved.[110] As the technique of using oscillographic equipment and vacuum-tube amplifiers progressed, it became clear that the gauge could be further improved. In the first place, it was desirable that it be made physically small because otherwise the time required for the wave to pass by the gauge was an appreciable fraction of the duration of the phenomena being studied. Furthermore, a great increase in the ruggedness of the gauge was necessary if the pressure near to charges was to be explored. These ideas led naturally to the development of very small tourmaline gauges consisting essentially of one or more small slabs of crystal with metallic coating on the appropriate faces connected to a cable, the whole unit being then insulated and waterproofed. Figure 21 gives a diagram of one of the latest models of underwater tourmaline pressure gauges. The size usually used for studying the shock wave from actual service weapons is about ½ in. in diameter. It was possible with these gauges to measure the shock wave reasonably close to the charge without losing the gauge. Thus, it was routine to place them 20 ft from a 300-lb depth charge where the pressure was about 6,000 psi. Pressures as high as 30,000 psi have been reliably measured.

Many hundreds of these units were made by the Stanolind Oil and Gas Company [SOG], a contractor to Division 2, by the Reeves Sound Laboratory, a subcontractor to the Oceanographic Institution, and by the staff at UERL itself. These sources supplied gauges to many other laboratories. They were used daily for the routine comparisons of different explosive compositions and for other studies at scales ranging from a few grams to hundreds of pounds of explosive. A complete description of their construction and use is available.[81,111,112]

In order that a piezoelectric gauge may be used for absolute pressure measurements it is necessary to calibrate the gauge. This is usually accomplished by measuring the charge generated by the gauge when it is subjected to a known change in pressure in a compression chamber which is filled with a suitable

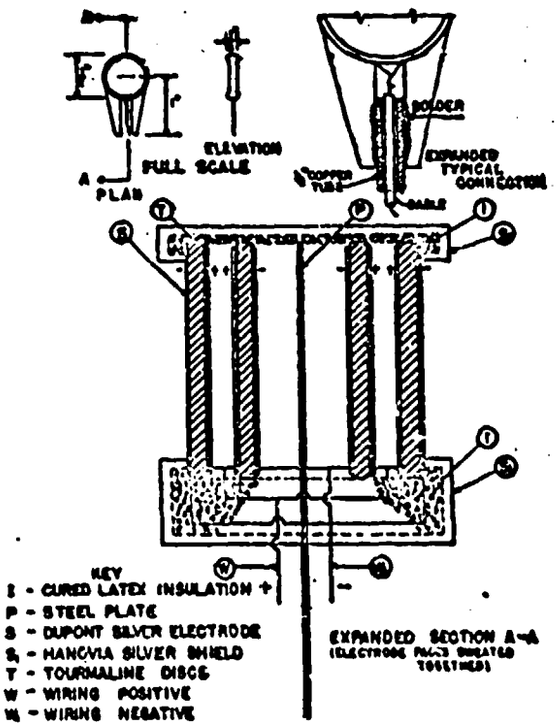

FIGURE 21. Schematic drawing showing dimensions and construction of tourmaline piezoelectric gauge.

liquid. The change in pressure in the calibration chamber is usually brought about by opening a needle valve when the chamber is under a known pressure, or by bursting a diaphragm covering an opening in the chamber. The main difficulty with this so-called static method is that the change in pressure cannot be made to take place sufficiently rapidly to compare with the very short time of rise of pressure which occurs in the shock wave. It is also not known to what extent reflections and oscillations in the pressure chamber may affect the results. Mounting of the gauge in the pressure chamber presents another problem. If the crystal element alone is mounted in the pressure chamber, it is not definitely known whether a calibration of this type will be the same after the crystal element is mounted on a cable and the whole assembly is waterproofed. When the completed gauge is to be calibrated, the gauge must be mounted in the

chamber through a gland nut on the gauge cable, a procedure which was found under certain conditions to give rise to spurious electric charge. In view of these problems independent methods of pressure measurements which would serve as a check on the piezoelectric gauge calibration were carried out, the results of which are mentioned in Section 1.2.12. On the basis of these results, together with a detailed study of the static calibration method, it was concluded that the static calibration of the tourmaline piezoelectric gauges, when carried out with the proper precautions, is adequate for most ordinary explosives work.

Tourmaline has a particular advantage among the various available crystals which show the piezoelectric effect in that it produces an electric charge when subjected to a hydrostatic pressure, that is, a pressure uniformly applied to all surfaces, whereas, most of the other materials commonly employed will show a charge only when they are compressed in one direction alone. Thus, quartz, Rochelle salt, and ammonium dihydrogen phosphate, a new material known as ADP, have been used for pressure gauges for underwater use but in each case they require a container designed to protect the edges of the crystal from the pressure. This makes the gauge more complicated and especially makes it more difficult to secure the high-frequency response that is necessary in order to record faithfully very short-time phenomena. Nevertheless, Rochelle salt and the ADP crystals have certain advantages, primarily their very much greater sensitivity. Rochelle salt in particular is 100 times as sensitive as tourmaline or quartz but has a very serious drawback in that it is highly temperature-sensitive so that it is very difficult to use it for quantitative measurements. Furthermore, the crystal is fragile and seriously affected by moisture. ADP is somewhat less sensitive than Rochelle salt, is less affected by temperature but is also fragile and moisture-susceptible. It proved to be quite convenient, however, for sound ranging setups where a more sensitive pickup was desired. The Road Research Laboratory [RRL] in Great Britain has successfully used quartz gauges for underwater work. Quartz would seem to have little advantage over tourmaline, since it is no more sensitive and requires a container.

Other Electrical Pressure Gauges

Early in World War II, considerable experimentation was carried out, especially by DTMB, on resistance-type pressure gauges.[113] The simplest form for this is a small radio resistor. The applied pressure of the shock wave compresses the resistance element and thereby changes its resistance by a small amount. These have an advantage over the piezo gauges in that they are of low impedance, whereas the crystal gauges are of very high impedance, and thus subject to the difficulties associated with high-impedance circuits. On the other hand, the resistance gauges which were tried were not very successful, partly because of their very low sensitivity which meant that an amplifier of very great gain was necessary. Another difficulty was the fragility of all those gauges which were tried and the fact that many of them showed hysteresis, that is to say, they did not come back to their original state after having been compressed. It is still not at all certain that further research could not develop a successful underwater resistance-type gauge.

In principle, it should be possible to make successful underwater pressure gauges using the condenser-microphone principle or the magnetostrictive principle. The latter effect was successfully used in underwater microphones but no effort was apparently made to adapt them to the high pressure and short durations encountered in shock waves. This could probably be done and might yield a gauge with many advantages.

Another principle partially investigated is based on the dependence of the conductance of sea water itself on pressure. The David Taylor Model Basin initiated some investigations at Catholic University on the effect of pressure and temperature on the conductivity of sea water but practical gauges were never developed. This is a promising principle and probably should be followed up.

Recording Methods for Electric Pressure Gauges

Since the tourmaline gauges are almost the only ones successfully used in this country, a brief description of the other components necessary for their employment will be given.[114] These additional components would not be greatly different for the other types of gauges but some modifications would be required.

The first problem is that of a suitable cable for transmitting the electric impulses from the crystal to the recording equipment. This proved to be a very difficult problem because ordinary rubber cables, for example, give rise to a signal themselves when compressed by the pressure wave. Furthermore, it is necessary that the cable be mechanically strong since it is

roughly handled in use and by the explosion. Its capacity and insulation resistance must be of the right magnitude and stable with time and treatment. Cables were finally found which satisfied all these requirements. Especially successful was the cable developed at DTMB which employed copper tubing as the outside shield.[115] Much thought was put into the problem of terminating the cable properly so that a length of, say, 600 ft would transmit faithfully the signal produced by the gauges. This involved the design of terminating networks which not only compensated for electric reflection at the ends of the cable but also minimized the distortions due to the dielectric absorptions of the cable insulation. This problem was quite successfully solved.[116] It is also necessary to have suitable vacuum-tube amplifiers with a broad range of frequency response, sufficient gain, high stability and reproducibility, and a linear response with amplitude. These were obtained by making small modifications of commercially available equipment.[116] The output of such an amplifier was fed into a *cathode-ray oscillograph* [CRO] tube which was equipped with an electronic time base so that the spot of the oscillograph swept across the screen horizontally with time and was deflected upward proportionately to the applied pressure. This trace was then photographed, with the result that the pressure as a function of time was permanently recorded. (See Figure 1.) In some cases, rotating drum cameras were used so that the motion of the film provided the time axis. Naturally, other auxiliary circuits such as oscillators for putting on timing marks to measure the time scale, calibration equipment for putting amplitude marks so that the pressure could be determined numerically, and test equipment were also necessary. With the total equipment in use for some time before the end of World War II, it was possible to make routine daily measurements on charges of a great range of sizes which were accurate to within perhaps 3 per cent as far as peak pressure was concerned. Furthermore, impulse measurements to better than 5 per cent and energy measurements to better than 7 or 8 per cent could be made. Many thousands of such records were taken at UERL during World War II.

A background of four years' experience in design and construction of instruments for recording explosion pressure-time curves in the field has shown the importance of factors which are of less concern in laboratory work. These considerations are doubtless familiar enough to all who have made such measurements, but the following discussion is included as a possible help to those who may be called upon to plan equipment for field tests.

Field measurements of underwater explosions must frequently be made under adverse conditions, both for the operator and for the equipment. Therefore, it is important that the equipment function properly under unfavorable combinations of temperature, humidity, and primary power-supply variations. For the sake of the operator, it is also important that the necessary controls be simple and straightforward, and that proper functioning of the equipment be easily determinable. The possible need for repair in the field with limited facilities should also be taken into account.

A particularly important consideration is the fact that explosions occur once and may involve considerable amounts of time, effort, and money. In these circumstances, equipment which fails an appreciable fraction of the time may be worse than useless.

These difficulties of field work underline the importance of mutual understanding on the part of the man who develops the equipment and the man who uses it. The former should know what will be required of the equipment and should have field experience; the operator should have some knowledge of the basic principles of the equipment in order to use it intelligently. When a new type of measurement is to be undertaken, the design of needed electronic equipment must be based on knowledge of field requirements and what is reasonably possible.

The actual design should then be developed to meet the requirements with a minimum of adjustments and a maximum of reliability. Large safety factors should be allowed, to take account of such things as tube variations, tolerances of component parts, and leakage currents. Good mechanical layout and construction and clean wiring may mean the difference between servicing in the field and stopping work until laboratory repairs can be made. It is also worth while to use standard and readily available components as far as possible.

The completed instrument should be tested under actual or simulated conditions and these results kept recorded on the instrument as a part of the service record. Routine tests and inspections of all equipment are valuable in maintaining it at peak performance and avoiding breakdown.

1.4.2 Mechanical Gauges

The piezoelectric gauges described above were indispensable for an accurate picture of the pressure as a function of the time where it was desired and

they were entirely practical for a wide range of uses. However, especially in the early days of their development and for many special applications even now, the necessity for long cables and electric equipment on shipboard made it desirable to have mechanical gauges which, with proper understanding of the theory of their response, enabled certain properties of the shock wave to be measured. Historically, the mechanical gauges were developed before the electric ones, though much of their theory was not known until later.

The Ball Crusher Gauge

Probably the most successful mechanical gauge is the so-called ball crusher gauge developed by NOL.[117] Figure 22 shows the construction of this simple gauge

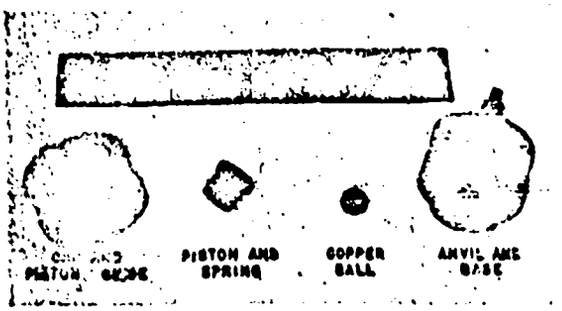

Figure 22. Construction of ball crusher gauge.

which, it is seen, consists of a copper ball held between an anvil and a light piston. The pressure wave, reaching the gauge, pushes the piston against the ball thus flattening it on two sides. The extent of the depression is measured and from it the peak pressure in the wave can be determined, provided some estimate of the duration of the pressure pulse is known. The ball crusher gauge, like all mechanical gauges, does not have a quick enough response time to measure peak pressure directly without further consideration. The static pressure required to produce a given deformation on the copper sphere can be measured but this cannot be converted directly into peak pressure in the shock wave without two corrections. In the first place, there is a correction of approximately 20 per cent due to the increased strength of the copper balls at high rates of strain such as encountered in exposure to a shock wave.[104,118,119] (See Chapter 12.) Another factor affecting the conversion of ball deformation to peak pressure is the inertia of the piston. Because of this inertia, the standard NOL gauge really responds to a combination of peak pressure and the rate of decay in the first 60 or 70 μsec of the shock wave. It will thus not register the same deformation and, therefore, not the same apparent pressure for 5,000-psi peak pressure from a small charge as for 5,000-psi peak pressure from a large charge unless this time factor is taken into account. Fortunately, the correction is not too critical provided the charge is of the order of the size of service weapons or larger and the theory is adequate to take care of the difference.[120] Therefore, when properly interpreted, ball crusher gauges can be used to give peak-pressure values reproducible to 2 or 3 per cent for the shock wave of a large charge. It is, however, necessary to be sure that the wave is not complicated by multiple peaks as is sometimes the case, especially off the end of the charge. It is this uncertainty of the form of the pressure-time curve from special situations that makes it highly desirable to have electric gauges in conjunction with the mechanical gauges. The ball crusher gauge is very convenient to use since it is self-contained, small, and easily read.

Theory of the Ball Crusher Gauge

The response of the ball crusher gauge to an explosion shock wave can be treated mathematically by simply applying Newton's laws to the motion of the movable piston.[121,122] The effective mass of the piston includes small correction factors for the mass of the copper sphere and for the mass of the water following the piston. The force acting on the piston is expressed in two terms. One term, $AP_m e^{-t/\theta}$ represents the force exerted by the shock wave on the piston of area A as a function of time. (See Section 1.2.4.) The other force term, λx, represents the resistance of the copper ball to plastic deformation. This has been found to be linear over a wide range of deformation, and λ, the proportionality factor which gives the force as a function of the piston displacement x, should be determined by appropriate calibration for each production lot of annealed copper spheres.

The spheres may be calibrated statically or dynamically. Since they are deformed at high rates of strain by the shock wave, it is necessary to apply a correction factor of about 20 per cent in case static calibrations are employed, i.e., the proportionality factor λ should be increased by 20 per cent over that determined statically. At UERL a dynamic calibration was employed in which the factor λ was computed from the deformation produced by a free falling weight which struck the sphere with known energy.[123,124] In this case the rate of strain effect is assumed to be the same as that encountered in the use of the gauge.

The solution of the differential equation of motion

for the piston is relatively simple. The ball deformation corresponds to the maximum value of the piston displacement. This maximum is reached in 160 or 170 μsec in the standard NOL gauge (effective piston mass about 16 grams, with ⅜-in. copper spheres). Since the decay of the shock wave may be appreciable during this time, especially for small charges, the deformation does not directly yield an estimate of peak pressure. Fortunately, the theory gives quantitatively the relation between deformation, peak pressure, and time constant so that true peak pressures can be computed from the deformations provided an estimate of θ, the time constant, is available. The dependence on θ becomes very small for large charges such as service weapons, for which the decay in pressure is small over the period of response of the gauge, so that the ball crusher gauge acts very nearly as a direct peak-pressure gauge under these conditions ($\theta \gg 170$ μsec.) It is, of course, necessary to remember that the simple form of the theory mentioned here assumes exponential decay of the shock wave. If the shock wave form is complicated (as it is off the ends of some service weapons)[91b,126] the interpretation of the gauge readings becomes considerably more complicated.[126]

Diaphragm Gauges

Another simple type of mechanical gauge is the so-called Modugno gauge,[127] which consists of a copper diaphragm about 1⅜ in. in diameter clamped over a small air space. (See Figure 23.) The pressure wave

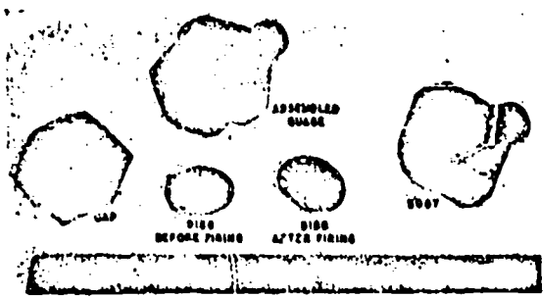

Figure 23. The Modugno gauge.

dishes in the soft copper diaphragm and the deformation can easily be measured. This deformation is quite reproducible but is not simply related to the applied pressure. In other words, the static pressure required to produce a given deformation is not simply related to the dynamic peak pressure which produces the same deformation. The gauge is, however, essentially a peak pressure gauge for charges of the order of 300 lb or greater and is quite convenient for relative measurements such as in the comparison of explosives.

A similar gauge was developed at the Explosives Research Laboratory of Division 8[128] and widely utilized at UERL.[13] This gauge consists of a cylindrical steel box with a steel diaphragm clamped over its front opening. (See Figure 24.) The pressure wave dishes the diaphragm and the central deflection is measured. For quite small charges of the order of a pound or so ($\theta \approx 60$ μsec), this gauge seems to measure a quantity moderately closely proportional to the impulse in the wave but with charges of 300 lb

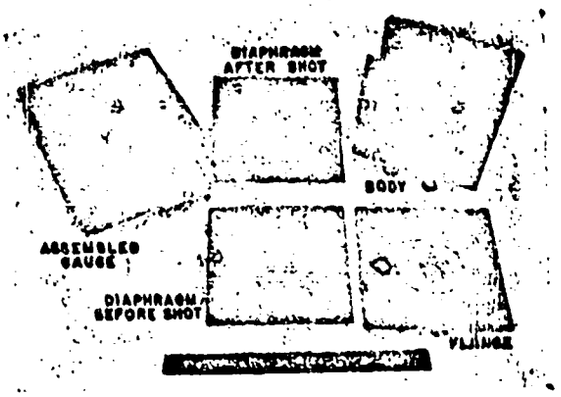

Figure 24. Assembly of underwater steel diaphragm gauge.

or greater ($\theta \approx 500$ μsec), it appears to be, both theoretically and experimentally, essentially a peak-pressure gauge, since the deflection time is of the order of 170 μsec. It is more reproducible when properly employed but not quite so convenient as the ball crusher and the Modugno gauges because of its larger size and weight. Because of its simplicity, however, in addition to its usefulness for measuring the relative effectiveness of different explosives, it proved to be a convenient gauge for experimental studies of the more fundamental properties of underwater explosions which are important in damage to steel plates. These studies, theoretical as well as experimental, were mentioned in Section 1.3.2.

Piston-Type Momentum Gauges

When used with large charges, all of the above mentioned gauges give an indication of the peak pressure. It is very desirable to have a mechanical gauge which can measure the impulse in the wave since impulse, under certain conditions, is a more important quantity than peak pressure in so far as damage is concerned. Hilliar in Great Britain developed such a

gauge just after World War I.[128] This gauge consists of a steel block with a long cylindrical hole. In the hole is a copper crusher cylinder such as used in gun gauges, and a steel piston. It differs from the ball pressure gauge in that the piston has considerable mass and length. Figure 25 shows the construction of one of these piston-type gauges. Since the piston is reasonably heavy, it takes a certain amount of time to accelerate. There is a gap between the end of the piston and the copper crusher so that the piston can accumulate momentum before striking the copper cylinder. By making certain simplifying assumptions, the mathematical treatment of this system is not difficult and shows that the deformation of the copper crusher cylinder can be interpreted in terms of the impulse in the shock wave up to a certain time. By having a number of these gauges with different piston masses and length of travel it is possible to block out, roughly, the form of the pressure-time curve by means of purely mechanical instruments. This gauge was used very successfully by Hilliar. However, it requires extremely careful handling and has not been so successful in the hands of investigators during World War II as it was with Hilliar. Nevertheless, it is a useful instrument. A number of variations on this design have been made but they all utilize essentially the same principle. The theory of piston gauges has been treated in some detail recently.[129]

The results of all types of pressure gauges are influenced by the way in which they are mounted and by the surroundings. Thus a gauge mounted in a large and very thick steel baffle will read approximately double the peak pressure which will be measured by a gauge in free water. This is because of the doubling of the pressure by the superposition of the incident and reflected waves. However, the baffle has to be 3 or 4 ft thick before this effect is detected by most mechanical gauges because these instruments require a certain finite time to operate and this time must be small compared with the travel time of the wave back and forth through the steel baffle. Gauges are also affected by their orientation relative to the oncoming wave. It is customary to use the mechanical gauges described above face-on to the explosion, except Hilliar and momentum gauges. The amount of inertia attached to the gauge, i.e., the massiveness of its mounting, has been found to be relatively unimportant. This has some influence on the results but fortunately the ball crusher gauges, at any rate, seem to function quite reproducibly with very little backing. In all cases it is desirable to mount the gauges as far from reflecting obstacles as possible. This is particu-

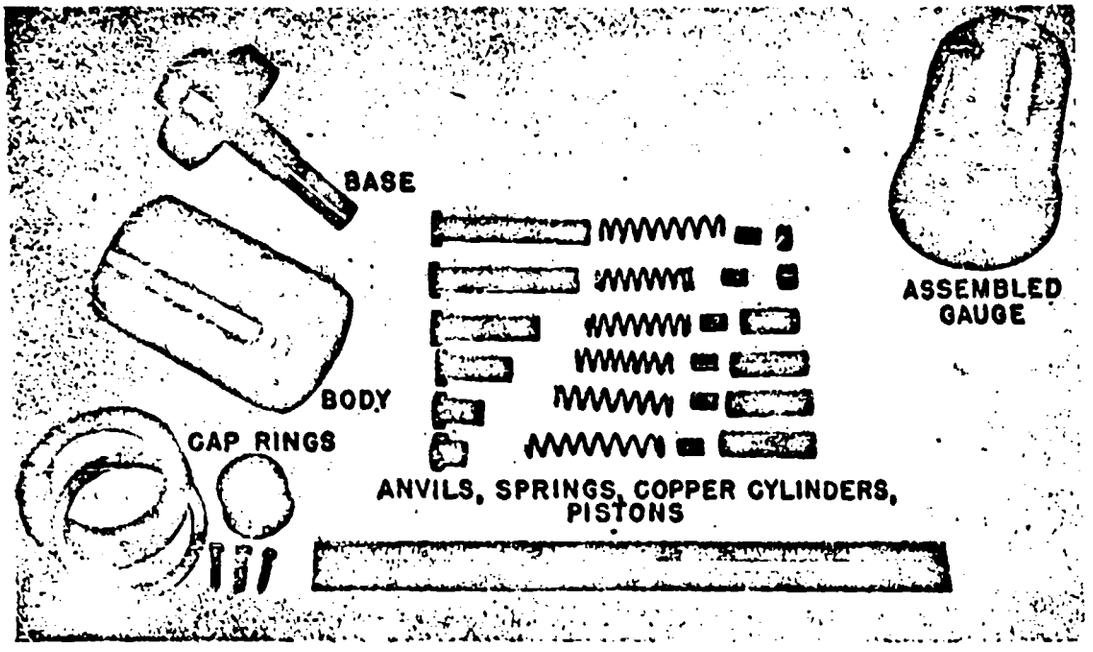

FIGURE 25. Assembly of Hilliar gauge.

larly true of the piezoelectric gauges which are capable of yielding the complete pressure-time curve. Nearby solid objects will reflect portions of the wave striking them and these reflections will be picked up by the piezo gauges. It is definitely bad to use wood for mounting any type of underwater pressure gauge.[121] Apparently this low density, soft material reflects a rarefaction wave and serious errors may be obtained if the pieces of wood are placed near any of the above gauges.

1.4.3 Photographic Methods

One of the most interesting and fruitful techniques for the study of underwater explosion phenomena is that of photography. Several photographic methods have been developed by means of which there have been obtained detailed pictures of a number of the phenomena which occur in connection with these explosions.

Flash Charge Photography

One of the most useful devices was the invention at the Explosives Research Laboratory of Division 8 of the explosive flash bulb. This source of illumination can be made to give a very bright flash of light lasting only a few μsec, which is a sufficiently short time to "stop" the shock wave in its rapid motion. This flash bulb consists of a spherical charge of high explosive surrounded by a very thin layer of argon gas in a transparent container. The explosive is detonated from its center by means of a Primacord fuze. Therefore, the detonation wave should reach all points of the surface of the sphere simultaneously, sending a shock wave through the argon gas. This shock wave heats the gas to an extremely high temperature and causes it to emit a flash of light. The duration is short because the time required for the shock wave to pass through the gas is very short. Synchronization of the firing of the flash lamp and the phenomenon to be studied is readily accomplished by means of the Primacord fuze. The flash charge and the charge being studied are both connected by predetermined lengths of Primacord to the same detonator cap, so as to explode the two charges at the proper time interval. Standard cameras can be utilized provided they are contained in a strong metal cylinder with a thick glass window to protect them from the explosions. Simple relays may be used to open the shutter before the event and close it shortly thereafter. Details of these techniques have been described elsewhere.[11] (See also Division 8, STR.)

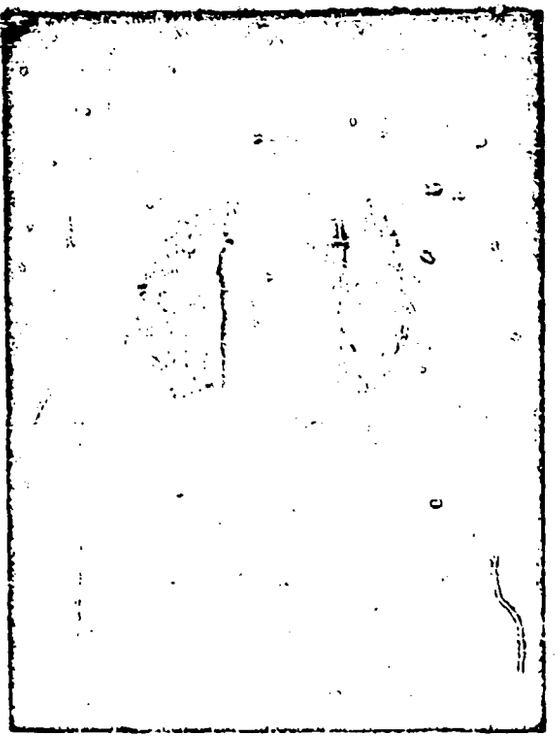

FIGURE 26. Flash photograph showing shock wave and gas bubble of long cylindrical charge detonated at one end.

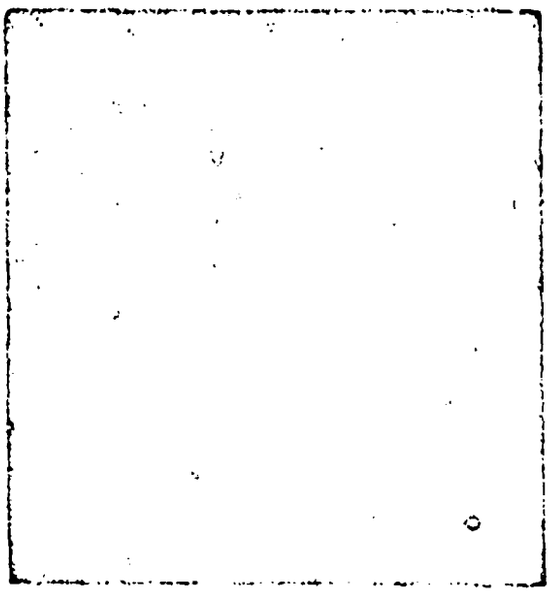

FIGURE 27. Flash photograph of 3½-in. equilateral cast pentolite cone detonated at apex.

Figure 2 (Section 1.2.4) shows an underwater explosion at a time when the bubble has expanded to a radius of about three times the radius of the original charge. The photograph shows clearly the outline of the original charge because enough light was emitted by its detonation to record its shape on the film. Later, when the flash charge was fired, the outline of the bubble and the silhouette of the shock wave were recorded. The shock-wave surface is quite smooth, which is also to be expected theoretically since any irregularities should rapidly smooth themselves out. Notice also that the bubble surface does not show pronounced irregularities.

The shape of the shock wave about the charge reflects the shape of the charge. Spherical charges (see Figure 2 and Figure 3, Section 1.2.4) give spherical shock waves, whereas elongated shapes (Figure 26) give distorted ellipsoidal shock waves with this broad end at the cap end of the explosive. Figure 27 shows a photograph of a conical charge detonated at the apex.

An example of the use of photographic techniques for quantitative studies is the evaluation of shock-wave parameters by the so-called optical distortion method.[122,123] Figure 28 shows the apparent distortion of a grid ruled on a Lucite sheet as viewed through a spherical shock wave. Several variations of the experimental setup are possible, but in the case illustrated the grid is in a plane through the center of the shock-wave sphere. It is possible to develop a theory which relates the displacement of the grid intersections from where they would appear in the absence of the shock wave (obtained by extrapolation of the lines outside the shock front) to the peak pressure and decay constant of the shock wave. A knowledge of the index of refraction of sea water as a function of pressure is required. It is necessary to design the experiment with great care so that all the distances and angles required in the theoretical analyses are known with sufficient precision. Results obtained by this method were quoted in Section 1.2.12.

Another promising application of flash photographic techniques involves a double exposure accomplished by the use of two flash charges detonated a known interval of time apart. From the two shock-wave silhouettes on the resulting photograph the mean propagation velocity can be measured and hence the peak pressure in the shock wave can be derived (see Section 1.2.12). This method has been explored but has not as yet fully developed.[13]

An important series of studies on cavitation was carried out using underwater flash charge photography. Illustrations have already been given of the cavitation produced when a shock wave is reflected by a free surface and when a thin air-backed diaphragm is damaged (Section 1.2.5, Figure 6 and Figure 11). Figure 20 shows the extent of the cavitated region under certain conditions of shock-wave attack on heavy free air-backed plates. In these cases, heavy steel disks were attached to air-filled pipe sections of larger diameter by very thin diaphragms so that the resistance to displacement was essentially all from the inertia of the heavy disk, the strength of the thin diaphragm being negligible. The extent and shape of the cavitated regions correspond roughly to those computed from the results of the theoretical analysis of the systems. The theory takes into account the time variation of the pressure at any point in the water due to the incident pressure wave, the reflected waves from the accelerating disk, and the diffracted waves from regions around the target.

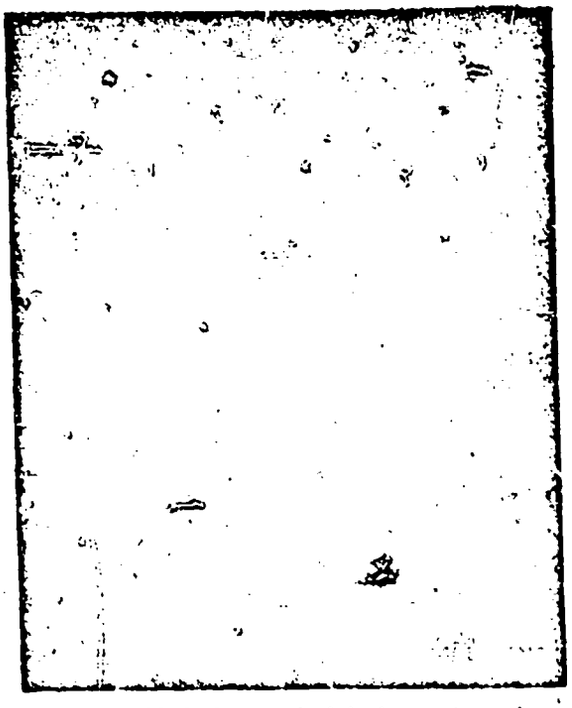

FIGURE 28. Flash photograph of shock wave traversing ruled grid.

The significance of these experiments is chiefly in the fact that they constitute an experimental verification of the essential correctness of the theory, including the effect of cavitation, for shock-wave interaction with this simple type of target. It is char-

FIGURE 29. Flash photographs showing cavitation in front of rigid air-backed free plate.

acteristic of the so-called fundamental approach to a problem that one should proceed step by step along a course of investigation in which general principles determining the phenomenon are postulated then tested under conditions which are as simple as possible. In this way false starts may be eliminated more efficiently, and if one eventually establishes the fundamental laws of nature which control the phenomena, the usually more complicated practical problems may then be attacked with confidence.

Since the occurrence or nonoccurrence of cavitation has an importance in determining damage to targets or response of gauges, many photographs designed to detect cavitation were taken at UERL. For example, cavitation was shown not to occur under the normal conditions of use of the mechanical gauges employed but was shown to occur when the cylindrical shell models were appreciably damaged.

The use of flash charge photography to show the Mach phenomenon of shock wave interaction was mentioned in Section 1.2.5.

HIGH-SPEED MOTION PICTURE PHOTOGRAPHY

In addition to the flash charge techniques for photographing underwater explosion phenomena, high-speed motion picture photography (100 to 3,000 frames per sec) has been successfully used. This requires intense light sources which must have durations at least as long as the phenomena being photographed. For this purpose, ordinary photographic flash bulbs have been used, and some progress has been made in the development of a suitable underwater flare. To date, high-speed motion picture techniques have been used primarily to study explosive damage to underwater targets (see Figure 12, Section 1.3.4) and to study the behavior of the gas bubble. From these photographs, measurements of the bubble radius and the bubble migration can be made.

As in the flash photography techniques, the camera is contained in a heavy watertight case equipped with a small window. In principle there is no limit to the size of charge which can be photographed, provided the water is of sufficient clarity and the lighting sufficiently intense. Considerable development has taken place to perfect intense underwater light sources and further developments are foreseen. However, the clarity of the water is a serious limitation since sea water, in general, is very turbid, and thus work with only very small charges can be carried out. Where larger charges or targets are to be photographed, the

experiments must be carried out in localities where the sea water is sufficiently clear, for example, in the Gulf Stream, or near the Bahama Islands or Cuba. The Underwater Explosives Research Laboratory has sent expeditions for photography work into each of these locations. There are other localities where the water is sufficiently clear during certain seasons of the year.

The photographic techniques for studying the damage process, as well as explosion phenomena in general, offer great promise and should be pursued further. Considerable thought should be given to the selection of a suitable location, and it would appear desirable for some branch of the military to establish facilities at the location, which preferably should be close to a shore laboratory.

1.4.4 Measurements of Explosion-Generated Surface Waves

Personnel of UERL have conducted experiments involving charges of from 300 to 30,000 lb to determine the efficiency of explosive generation of surface waves and the associated underwater pressure variations.[81] (See Section 1.2.9.) In general, the pressure variations on the bottom in shallow water were determined. These are simply related to the amplitude of the surface waves if the latter are assumed to be sinusoidal.[134] The present variations fall off with depth in a manner dependent upon the wavelength. The most successful measuring instrument was the NOL Mark 1 hydrophone in which the displacement of a diaphragm was measured electromagnetically. To check upon the absolute values observed with this hydrophone, other devices were developed at UERL but not extensively used. A sylphon differential pressure meter suitably protected against shock-wave damage gave results in good agreement with the NOL hydrophone. The pressure on the sylphon was recorded electrically through the output of a photoelectric cell, the illumination on which was determined by the sylphon distortion. Some photographic records of the surface waves were taken, but these were difficult to interpret satisfactorily.

1.4.5 Location of Underwater Explosions

One of the practical problems which UERL was able to solve satisfactorily was that of testing the fuzes on various types of underwater weapons to see whether they functioned under actual service conditions at the depths for which they were set. This problem provides an excellent illustration of the principle that practical problems can best be solved by making use of knowledge of the fundamental physics and chemistry of the problem rather than by relying on strictly empirical procedures. Thus observations have been made on the nature of the domes and plumes from underwater explosions at various depths (75 ft and less) and this procedure has been employed to estimate the depth at which various depth bombs and depth charges function. At the time these investigations were made, the bubble oscillation phenomenon was not known in this country so that the conclusions were based on purely empirical observations. Knowledge of the bubble oscillation phenomenon and its motion under gravity permits one to predict that the empirical method based on the time of appearance of plumes will be quite inaccurate at the depths of most interest.[135-138] Because of the rapid upward motion of the bubble during its contracting phase, the time interval between the beginning of the surface phenomenon and the break-through of the plume is not a sensitive function of the depth as had been assumed previously. The use of this time interval to determine depth can, therefore, not be recommended.

The knowledge gained from their studies of the physics of underwater explosions enabled the staff at UERL to devise a number of successful methods of solving this problem which turned out to be quite simple to apply.

The Sound-Ranging Method

The most obvious method is to set up a sound-ranging system, that is to say, a series of sound pickups connected to an oscillograph system, so that the time intervals between the arrival of the shock wave at the various pickups can be measured. If the time interval between the arrival of the shock wave from an underwater explosion at two known points and the shock velocity over this interval are accurately known, the location of the explosion is restricted to a surface defined by the observed time interval, this surface being a hyperboloid of revolution about the line joining the two points. Two independent time interval observations are required to locate the explosion on a curve which is the intersection of two such surfaces. Three independent time intervals (from four pickup stations) would be required to fix the location of the explosion as a known point in space.

In the system developed at UERL,[81] the arrival of the shock wave at three tourmaline piezoelectric gauges on a vertical line gave two independent time

intervals, and the results fix the explosion source as somewhere on a horizontal circle at depth D and of radius R, with the center on the vertical line through the gauges. (This system does not determine the direction of the explosion relative to the gauge line.) Additional time intervals from the arrival of surface and bottom reflections at the gauges may be used to obtain alternative values of the depth and to apply approximate corrections for deviations of the gauge line from the vertical. The gauge line was connected by 1,200-ft cables to recording oscillographs aboard a vessel holding the gear against the tide. A bomb target was towed 100 ft from the gauge line.

Several series of tests were conducted in Vineyard Sound on various fuze types in two types of aircraft depth bombs.[57,139-143] The bombs were dropped from airplanes traveling at about 150 knots at an altitude of about 100 ft. The results indicated that previous fuze-testing procedures were not valid, and that many of the fuzes tested under these conditions fired at considerably greater depths than they were supposed to, as determined by static calibrations in a pressure chamber. This malfunctioning confirmed suspicions which originated from an analyses of operational performance of the fuze types involved.

Methods Based on Observations of Surface Phenomena

In conjunction with tests at shallow depths, several methods of determining the depth of explosions shallow enough to produce surface upheavals have been developed. Many of these methods are modifications of the dome analysis methods.[49-144] This method is based on the shape of the dome and is, in principle, independent of the charge weight. The shape of the dome is treated as determined by the obliquity of the shock wave to the surface as a function of the horizontal radius from the center of the dome, and the depth may be readily determined by rather simple geometrical considerations. A determination of a distance scale for the photographs is required.

Several other methods employed the known relation between shock wave peak pressure and the spray particle velocity in the dome.[57,58,145] As applied, this method involved an empirical extrapolation to determine the initial spray velocity, because photographically observed velocities were often abnormally high for the first few tenths of a second. Use was made of the piezoelectrically determined dependence of the peak pressure on the distance from the bomb used. Both time- and distance-scaled motion pictures are required for these methods, and the calculations are sometimes tedious.

A very simple empirical method was devised at UERL following a study of the surface phenomena of a series of Mark 54 depth bombs (350 lb of torpex) detonated at various depths from 15 to 75 ft. The ratio h_D/d_D of the dome height to the diameter of the dome base at the time of the first plume phenomenon was found to be related to the depth by the empirical equation

$$\text{Depth (Mark 54)} = 19.4 \left(\frac{h_D}{d_D}\right)^{-0.67} \text{ ft.}$$

This method required neither time nor distance scales, and is recommended for use in the future for routine tests of production lots of fuzes. A calibration should be made, however, by firing at known depths, a series of the weapon in which the fuzes are to be used. Unskilled personnel can be taught easily the proper procedure for smoothing (or averaging out) irregularities in the dome contour so as to get reproducible measurements of the ratio h_D/d_D.

Determination of the Depth of Deep Explosions

For the location of deep explosions,[146] the sound-ranging procedure was successfully modified so that pressure pickups could be positioned as deep as 800 ft. A ½-lb charge was fired at a known position with respect to the ranging system within 2 sec after the weapon being tested had been detonated. By this means any deviation of the gauges from a vertical straight line, due to slight currents in the water, could be detected and corrected for. In addition, an independent and much simpler method was used,[146] namely the measurement of the period of the bubble oscillation, which is a simple function of the depth (see Section 1.2.6). This method gave results in excellent agreement with the sound-ranging method and is much easier to apply experimentally since only a single pickup and oscillograph circuit are required, and the pickup position is relatively immaterial.

An extensive investigation of the British Squid projectile was carried out by the UERL staff in Tongue of the Ocean in the Bahama Islands, utilizing a sound-ranging system and the bubble pulse method. As an example of the precision of these methods, Figure 30 shows the depth as a function of time for this weapon. It was possible to determine the location of an explosion 800 ft down with considerable precision.

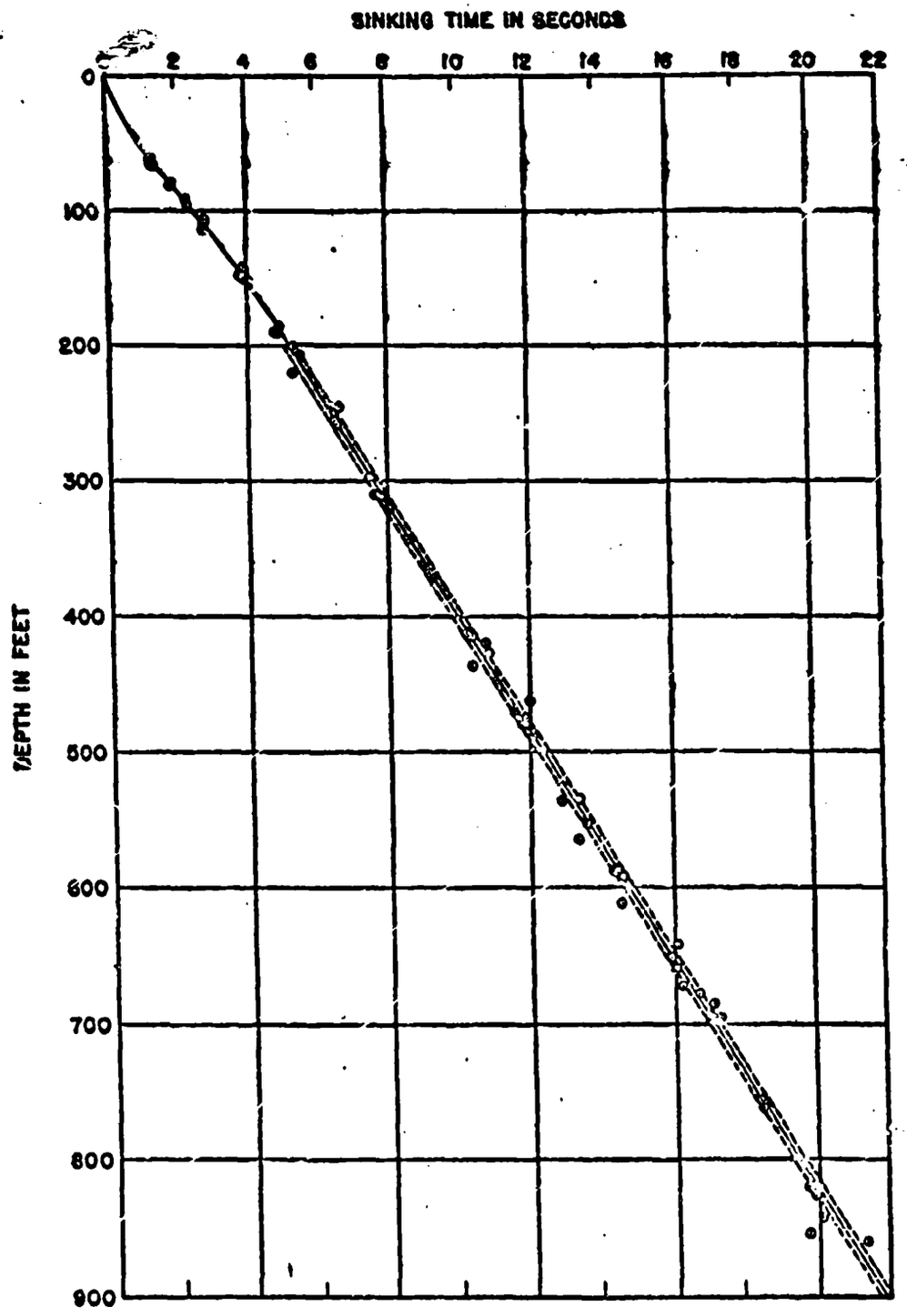

FIGURE 30. Plot of sinking time-depth curve for Squid projectile.

1.8 DESCRIPTION OF RESEARCH FACILITIES AT THE UNDERWATER EXPLOSIVES RESEARCH LABORATORY

It seems worth while to give a brief description of the facilities available at UERL because the experience gained in this undertaking might be useful to others planning to set up a laboratory for similar types of research. It should be stated that this laboratory was originally planned to be a very small group of perhaps half a dozen investigators but, as its problems multiplied, the project was expanded until it ultimately had a total staff of between 80 and 100 persons. Naturally, many things would have been done differently if the project had been planned for this size in its beginning stages.

The requirement which determined the location of the laboratory was the availability of a well-equipped research laboratory with water of at least 20-ft depth in which explosions could be set off immediately adjacent to the laboratory. Although experiments with charges larger than a fraction of a pound could not be made at the location next to the building, nevertheless, the possibility of carrying out small-scale experiments so conveniently was continuously utilized and was very important. It was, furthermore, necessary that there be deeper water at not too great a distance from the laboratory and that the surroundings not be built up to such an extent that the annoyance and damage caused by explosions would preclude work of this type. Questions of climate were considered but no location which seemed to be available met the ideal specifications in this regard.

The location at Woods Hole involved working at the Woods Hole Oceanographic Institution [WHOI], which possesses a well-equipped research laboratory with office space, machine and carpenter shops, storage rooms, electric supplies of various types and, most important of all, a history of experience in carrying out experiments at sea. The town of Woods Hole provided reasonably comfortable living conditions for the members of the staff and their families.

Explosives were stored on a nearby island on which magazines were constructed.[147] The storage of explosives is one of the most difficult problems encountered in setting up a laboratory of this type. Experience showed that it was absolutely essential that supplies of explosives and storage of weapons for testing should be readily available and under the direct control of the laboratory. Whenever it was necessary to rely on other agencies for such explosives, delays were almost inevitable.

Another essential feature of this laboratory was a casting or preparation house in which explosive charges were made up in the forms desired. This house was also located on the island and was of very simple construction. It contained melting kettles which were used for the preparation of cast charges of a great variety of shapes and sizes. This installation also was under the complete control of the laboratory and was thus able to provide the needed charges without the delays which are so common when the jurisdiction over the supply is different from that of the laboratory.

Explosives were fired underwater at a number of locations. Charges up to about half a pound were lowered to appropriate depths in the water adjacent to the institute dock. This was extremely convenient because short electric connections were possible to instruments in the laboratory buildings. Work can be carried out very much more rapidly when the firing point is readily accessible to the main laboratory as it was in this case. For work with mechanical gauges requiring larger charges, say up to 25 lb, two especially designed floats were built which could be moored in the harbor where the water was about 60 or 70 ft deep. These floats consisted of two pontoons connected by a deck with a central well and carrying a quadrupod mast for the cable blocks necessary for lowering the gear. In one model, the central well could be opened on one side by the removal of a portion of the deck. Charges were supported in the center of large steel rings to which were mounted the gauges. The ring could then be lowered and, if necessary for larger charges, floated from an oil drum out through the deck opening to a convenient distance from the moored raft.

A small pond was also prepared on the island for work with electric gauges on charges up to 5 lb. This had many advantages. An overhead cable was strung so that it was very convenient to launch the charges and equipment into the water. Furthermore, there were no waves or tide to contend with and a fixed installation could be set up on dry land. Experience showed that work could be done several times faster when land based than when based on vessels. However, for charges of the size of service weapons, it was necessary to work from shipboard and for this purpose the schooner *Reliance* was fitted out as described in the Section 1.9.10. This proved to be a

very successful arrangement but it was seldom possible to fire more than two large charges a day whereas dozens of the small ones could be shot in the same time from the land based location.

There were also available numerous beaches and locations of varying depth where special experiments such as on underwater cratering, effect of shallow shots, etc., could be carried out. This availability of varied types of water conditions was most helpful.

One of the important features of the organization of this laboratory was the fact that those responsible for the scientific and technical direction of the project had complete authority and control over the various services such as explosive supplies, preparation of charges, operation of the vessels, etc. This placed a considerable burden of a nonscientific character on the technical people but it was felt, and experience demonstrated that this was correct, that only in this way could complete coordination and rapid progress of the work be made possible. Experience at other laboratories where divided authority existed has demonstrated that such an organization is not a good one for scientific research. It is, of course, necessary that decisions such as, for example, the question of whether the weather is suitable for the safe operation of a vessel be left to the commanding officer of the vessel. However, if the commanding officer is responsible to the scientific director of the laboratory and not to some independent agency, he is more likely to make his decisions with the interest of the experimental project uppermost. It is also especially important that these Service groups feel that they are part of the scientific organization and not merely being assigned to a certain branch of work for a temporary period. The difference between successful and unsuccessful scientific work depends on small differences in the way in which numerous, not obviously important, precautions are followed through. The building up of the proper morale and spirit among the nontechnical employees is of the utmost importance in ensuring that the experiments are carried out in the way that is necessary to useful results.

Chapter 2

EXPLOSIONS AND EXPLOSIVES IN AIR

2.1 INTRODUCTION

2.1.2 Purposes of Investigation

EXPLOSIVES WERE employed in enormous quantities in weapons of many types throughout World War II. These weapons were used to cause injury to the enemy in specific ways. Some weapons, such as demolition bombs, depth bombs and charges, explosive-filled shells, etc., were devised and used for the attack of structures such as factories, dwellings, fortifications, ships, and so on; other weapons, such as fragmentation bombs and shells, were intended to incapacitate personnel; demolition charges, including "hollow" charges, were employed in contact with obstacles, such as bridges, buildings, fortifications, etc., in order to breach the obstacle or to impair the usefulness of the structures to the enemy; and certain specialized devices depending on high explosives in the form of long, narrow charges were used for the passage of mine fields. For all of these weapons, even in the beginning of World War II, there was a choice among a number of high explosives as fillings, and as World War II progressed a large variety of new explosives was developed.*

The choice of a high explosive to be used in a particular weapon was based on evaluation of a number of factors, among which a few were:

1. The use to which the weapon was to be put.
2. The requirement for sensitivity and stability of the high-explosive filling. (The stability and sensitivity of high explosives were investigated by Division 8, NDRC.)
3. The quantity of explosive required for the anticipated volume of production of the weapon.
4. The best or most powerful explosive for the purpose.

In order to select an explosive, then, it was necessary to evaluate, among other things, the power of the available explosives relative to each other, using as criteria those characteristics of performance most likely to be important in the contemplated use.

In the case of weapons such as demolition bombs which produce damage by virtue of the air blast from their explosion, the evaluation of various explosives relative to each other was accomplished by comparing the air-blast intensities from corresponding quantities of the explosives in question. The order of merit of explosives for this purpose was then taken as the order of their air-blast intensities.

As new explosives were developed, their performance in air blast was measured, and the body of knowledge so obtained gave a basis for suggesting still other explosives for trial. Thus, a second valuable product of the comparisons of explosives was the steady improvement in the power of available military explosives, until, by the end of World War II, the performance of a bomb filled with one of the best explosives was estimated to be about twice that of a similar bomb filled with amatol 50/50, the usual filling for demolition bombs at the outbreak of this war.

Studies of the behavior of shock waves, development of theories regarding them, and observation of the effects of weapons on targets made possible the prediction of the extent of damage to be expected from bombs of various fillings, and provided a basis for selection of bombs for tactical use in the way calculated to give maximum effect. Moreover, fundamental knowledge of the physical laws governing the propagation and reflection of shock waves made possible the development of a new and more effective way to use bombs of a given type: it was found that a bomb that bursts at the optimum height above the ground produces a blast wave of greater effectiveness than that from a bomb bursting on impact. This increase is estimated to correspond approximately to a doubling of the area of damage to be expected.[1]

Thus, a large bomb filled with a good explosive, fused so as to burst at the proper height, is estimated to be about four times as effective as the older types, fused instantaneously.

An important application of knowledge of the shock waves produced by explosions is in the evaluation of target vulnerability to various types of attack. By empirical or other means, the susceptibility of various targets to damage by blast has been estimated, and the blast intensities from various weapons determined. These data are useful in the design of structures to resist air attack. Similar use can be made of this in-

*Pertinent to War Department Projects OD-01, OD-03, OD-79, OD-145, and to Navy Department Projects NO-11, NO-12, NO-144, NO-208, NO-224, and NO-283.

formation in specifying factors in the safe handling, transportation, and storage of high explosives.

Throughout these investigations an important aim has been to broaden the fundamental knowledge concerning shock waves and explosives, for it is only on the basis of a good body of fundamental information that the development of new weapons can be successful.

2.1.2 History

Prior to the beginning of World War II, it was the usual practice to assess explosives for use as fillings for aerial bombs by two general types of measurements:

1. Tests were performed, such as the Trauzl lead block test, which assigned relative merits based on some property or properties of the explosive itself, or,
2. A bomb containing the explosive was detonated in an enclosure surrounded by panels of wood, steel, etc., in order to determine the number and penetrating power of fragments.

Data obtained from the Trauzl block test, plate-denting tests, and measurement of detonation velocities are associated with the *brisance* of the explosive. Although they provided information that is valuable for many purposes, the results are not directly pertinent to the *blast* damage effectiveness of explosives since the more brisant of two explosives is not necessarily the one that produces the greater blast intensity. Similarly, fragmentation in a very large blast bomb, in which the explosive to case-weight ratio is as great as possible, is usually not pertinent to the use to which such bombs are put.

Aside from the question of which explosive filling has the greatest blast effectiveness, there are several other ways in which air-blast measurements are essential and for which no other type of measurement suffices. For example, it is desirable to have a quantitative measure of the parameters that describe the shock wave in order that the intensity thus measured can be related by some means to the damage which the wave accomplishes. Without such information, the only way in which the effectiveness of a weapon can be estimated is by observing its effect on targets themselves. The effects of charge shape, thickness and composition of the case, etc., on the blast effectiveness of a weapon are best determined by measuring blast intensities. It is also important that the interactions of shock waves with their surroundings by reflection, absorption, etc., be quantitatively determined by means of blast measurements.

The development of blast-measuring techniques and their application to the evaluation of weapons was begun in England at the Road Research Laboratory [RRL] in 1938, and later, at the Armament Research Department [ARD]. In the United States, similar developments were undertaken in 1941 and 1942 by the Princeton University Station, Division 2, NDRC, the Ballistic Research Laboratory [BRL], Aberdeen Proving Ground, the David Taylor Model Basin [DTMB], and Harvard University [HU], Divisions 8 and 9, NDRC. Blast measurements using 4,000-lb bombs were first performed in the United States at Aberdeen Proving Ground in December 1942, with BRL, DTMB, and HU participating. In 1943, the development and operation of blast-measurement apparatus was undertaken by the Stanolind Oil and Gas Company [SOG]. At the same time, the HU group was transferred to the Underwater Explosives Research Laboratory [UERL] at Woods Hole Oceanographic Institution [WHOI].

The early applications of blast measurements were concerned with evaluation of the performance of new bombs, determination of the effects of booster design on performance, etc. As new explosive compositions became available, extensive comparative tests on bombs and charges of all sizes were carried out. By the end of 1943, the relative merits of several of the most important explosives had been determined, and, as a consequence, the older explosives (usually of the amatol type) had been replaced as service fillings by the newer, more powerful explosives. In Great Britain, particularly, the fullest advantage was taken of every means by which the blast effectiveness of bombs could be enhanced.

In addition to studies of the relative effectiveness of explosives, blast measurements were made in order to determine the effect of case-weight on blast, the properties of shock waves obliquely reflected from surfaces, the blast intensities from line charges, the blast from explosions in igloo-type storage magazines, and a number of other properties of explosions.

2.2 THE PHENOMENA OF EXPLOSIONS IN AIR

2.2.1 The Detonation of High Explosives

High explosives release their energy by a process called *detonation*, and low explosives, or propellants, by a process of *rapid burning*. The time required for the detonation of a quantity of high explosive is

much less than that for the burning of a like amount of propellant. With high explosives, the rate of detonation is not markedly affected by the particle size; with propellants, the grain size is all-important. The shattering effect of a high-explosive detonation is great; that of a propellant explosion much less. These distinctions are not completely clear-cut, however.

Several low explosives can be made to detonate; even black powder, under great pressure, may detonate under the proper conditions. The military uses to which high explosives are put depend upon their great shattering power (brisance) and their high rate of detonation.

Some high explosives, such as mercury fulminate, lead azide, etc., are very sensitive to heat, shock, etc., and can be easily detonated by a spark or other local application of heat. These explosives are used to initiate less sensitive explosives and are called *primers*. Other explosives that are less sensitive to shock and heat than primers but in which detonation can be initiated by primers, are used as *boosters*, i.e., intermediates between the primer and the main body of explosive, capable of being initiated by the former and of initiating the latter. The most important of the explosives used as boosters is tetryl. The main explosive filling is very insensitive to shock, heat, friction, etc., and must be detonated with the aid of a booster. The quantities of these three types of explosive in a given weapon differ greatly. (1) A very small quantity of primer, usually less than 1 gram, is used, (2) the booster weight is ordinarily of the order of a fraction of a pound to a few pounds, and (3) the bulk of the explosive content of a weapon is the insensitive main filling, which may constitute over 90 per cent of the total amount of explosive.

The explosion of the booster gives rise to a compression wave in the main explosive filling. If no further action were to take place, i.e., if detonation in the main filling did not occur, this compression would be propagated as a wave, at approximately the velocity of sound, through the explosive. However, if the compression is sufficient, chemical reaction of the explosive will take place as a consequence of the elevated pressure and temperature in the compressional wave. This chemical reaction is exceedingly rapid, and the chemical products of the reaction have a very high pressure and temperature. This zone in which the chemical reaction takes place, called the detonation wave, is propagated through the explosive at a velocity considerably in excess of the velocity of sound in the explosive and is preceded by a compression wave which it supports.

The velocity of propagation of the detonation wave, called the detonation velocity, depends on the chemical and physical properties of the explosive and, to some extent, on the dimensions of the mass of explosive and the degree of confinement. Most military high explosives have detonation velocities of the order of 5,000 to 8,000 m per sec, i.e., 16,000 to 26,000 fps.

Theories have been developed[2,3] that make it possible to compute the detonation velocity, the pressure and temperature in the detonation wave, and the chemical processes that occur. These theoretical results have been confirmed in large part by direct experiment. (See Summary Technical Report of Division 8.)

When the detonation wave reaches the interface between the explosive and the air that surrounds it (the charge unconfined) the products of the detonation, largely gases, expand with high velocity, pressure, and temperature. The boundary between the air and the hot compressed gases is sharply defined. The outer layer of the burnt gases is theoretically at a very high pressure (initially of the order of 10,000 psi). Behind this layer the pressure and temperature at a short time interval later decrease rapidly to lower values toward the interior of the charge. The rate of expansion of the luminous zone, presumably the hot burnt gases, continually decreases. Eventually another discontinuity emerges from the luminous zone and thereafter leaves it behind. This is the shock wave, a sharp discontinuous rise in pressure propagating through the air surrounding the explosion products. Throughout the expansion of the hot gases, the chemical composition of the reaction products changes as their pressure and temperature change.

If the charge is confined by a metal case, such as the steel case of a bomb, the case is expanded by the pressure of the hot gases. At first, the metal flows plastically, until the volume of the case has been increased considerably (about twofold for steel cases), and then rupture takes place. The resulting fragments of the case are propelled at high velocity, and since they are not at first retarded so much as is the shock front they precede the shock wave over a great distance from the charge. The acceleration of the fragments requires energy, of course, and a considerable fraction of the detonation energy of the explosive may be carried away by the fragments. As a result, the energy, and hence the pressure, etc., of the shock wave from a confined charge are considerably less

than from an uncased explosive charge. Extensive investigations of fragmentation have been carried out and are described elsewhere.[9,10]

At the boundary between the burning gases and the surrounding air, oxygen comes in contact with the hot reaction products. Since most explosives do not contain sufficient oxygen to burn the carbon and hydrogen (and aluminum) completely, the product gases are capable of further (slow) oxidation. These reactions may take place at the surface between hot gases and air, or they may occur within the flame region when mixing with the air takes place. In any event, these processes are slow compared with the very rapid detonation process. Additional energy is released by this means, and the shock-wave intensity is enhanced. The processes described are called *afterburning*. Of the total energy available for complete combustion of the explosive, only about one-third is produced by the detonation. Therefore, if afterburning were complete, the energy from that source would be about twice that from detonation.

2.2.2 The Propagation of the Shock Wave in Air

The rapid expansion of the mass of hot gases resulting from detonation of an explosive charge gives rise to a wave of compression called a shock wave which is propagated through the air. The front of the shock wave can be considered infinitely steep, for all practical purposes. That is, the time required for compression of the undisturbed air ahead of the wave to the full pressure just behind the wave is practically zero.

If the explosive source is spherical, the resulting shock wave will be spherical, and, since its surface is continually increasing, the energy per unit area continually decreases. As a result, as the shock wave travels outward from the charge, the pressure in the front of the wave, called the peak pressure, steadily decreases. At great distances from the charge, the peak pressure is infinitesimal, and the wave, therefore, may be treated as a sound wave.

Behind the shock-wave front, the pressure in the wave decreases from its initial peak value. Near to the charge, the pressure in the tail of the wave is greater than that of the atmosphere. However, as the wave propagates outward from the charge, a rarefaction wave is formed which follows the shock wave. At some distance from the charge, the pressure behind the shock-wave front falls to a value below that of the atmosphere, and then rises again to a steady value equal to that of the atmosphere. The part of the shock wave in which the pressure is greater than that of the atmosphere is called the *positive phase*, and, immediately following it, the part in which the pressure is less than that of the atmosphere is called the *negative* or *suction* phase.

The velocity at which the shock wave is propagated is uniquely determined by the pressure in the shock-wave front and the pressure, temperature, and composition of the undisturbed medium. The greater the excess of peak pressure over that of the atmosphere, the greater the shock velocity. Since the pressure at the shock front is greater than that at any point behind it, the wave tends to lengthen as it travels away from the charge, i.e., the distance between the shock front and the part at which the pressure in the wave has decreased to atmospheric continually increases. For a discussion of the theory of shock waves see the bibliography.[11]

A gauge that is capable of indicating the pressure instantaneously applied and that is fixed with respect to the charge will record the pressure in the wave as a function of time. The resulting pressure-time curve bears a close resemblance to the pressure-distance curve described above: there is an initial abrupt rise in pressure followed by a relatively slow decrease in pressure to a value below that of the atmosphere. The time elapsing between the arrival of the shock front and the arrival of the part in which the pressure is exactly atmospheric is called the *positive duration*, and this, like the length of the wave, increases as the wave travels away from the charge. A quantity of interest in the application of blast measurements is the *positive impulse* which is the average pressure during the positive phase, multiplied by the positive duration.

Associated with the propagation of the shock front is a forward motion of the matter behind the shock front and the conditions that determine the shock velocity also determine the particle velocity. In gases, such as air, the particle velocity for high-shock pressures is very high. For example, at about 3 atmospheres excess pressure in the shock front, the particle velocity immediately behind it is about 700 mph.

The temperature behind the shock front is also greater than that ahead of it because of the compression of the medium. Since this compression is irreversible, the temperature of the air through which the shock wave has passed and which has returned to

atmospheric pressure is somewhat greater than that of the undisturbed air prior to the arrival of the shock wave. This *irreversible heating* of the air is less, the smaller the excess pressure in the shock wave.

At a very great distance from the charge, the wave becomes acoustic, i.e., the pressure rise, temperature rise, and particle velocity are all infinitesimal, and the velocity of the wave is that of sound.

2.2.3 The Interaction of Shock Waves with Their Environment

Very weak shock waves, i.e., those of nearly acoustic strength, are reflected from plane surfaces in such a way that a geometrical construction of the wave system can be made in a very simple way. Consider a point source of the shock C (Figure 1) and, some distance from it, a plane reflecting surface S. The incident wave I, striking the surface, will be reflected from it in such a way that the reflected wave R may be considered to arise from a second image source C' on the opposite side of the reflecting surface, perpendicularly below the true source and equally distant from the surface.

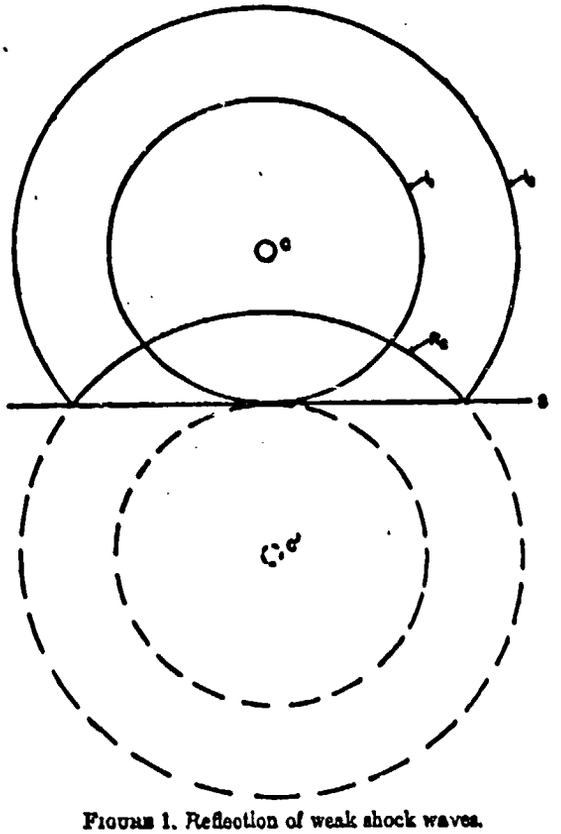

FIGURE 1. Reflection of weak shock waves.

Figure 1 shows two successive stages of this reflection process. In the first, I_1, the incident wave is just tangent to the surface. The excess pressure over that of the atmosphere at the reflecting surface is just double (for very weak shock waves) that of the incident wave where it is not in contact with the surface. At a later stage, the incident wave is represented at I_2 and the reflected wave at R_2 imagined to arise from the image source C'. Again the pressure at the line of contact of I_2, R_2, and the surface S is just double that of I_2. The angles at which the shocks I_2, R_2 meet the surface S are equal.

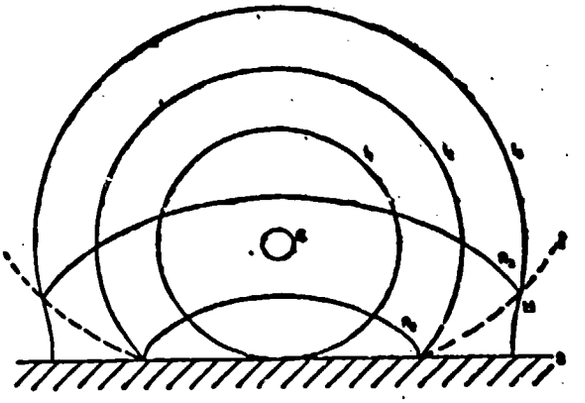

FIGURE 2. Reflection of strong shock waves.

When the pressure in the shock wave is appreciably above that of the atmosphere, the phenomena are different. One reason for this is that the pressure, density, and velocity of the air into which the reflected shock advances are not those of the undisturbed atmosphere. In Figure 2 are represented three successive stages in the reflection of strong shocks. In the terminology used above, the incident wave I_1 is first shown just as it touches the reflecting surface S. The excess pressure above that of the atmosphere at this point is more than twice that of I_1 elsewhere, and the magnitude of the increase of pressure over that of I_1 is determined by the strength of I_1. For example, if the peak (excess) pressure of I_1 is 100 psi, the reflected shock pressure is about 500 psi, a fivefold increase of pressure. (See data sheet 3A3 of Chapter 19.)

As the incident wave expands to some greater size I_2, the reflected wave R_2 also expands but the reflected wave is not spherical and cannot be constructed by the device used in Figure 1. The angles at which I_2 and R_2 meet the surface S are not equal, in

general, and the angle of the reflected shock R_2 depends upon the strength and angle of incidence of the incident shock.

At some distance from the charge C, determined by the distance of C from S and by the strength of the incident shock, a new phenomenon occurs. The intersection of R and I no longer lies on S but lies above it and follows some path, I. A new shock, M, the Mach stem, connects the intersection of R and I to the surface. The intersection of R, I, and M is called the *triple point*. As the shock system expands further, the Mach stem grows rapidly, tending to swallow up the two-shock system above it. If C is very close to the surface, but not on it, the Mach stem is formed almost directly under C, and, in a short time, has grown so that most of the shock system is a Mach stem, and only in a small region directly over the charge are R and I distinct. If the charge C is on the surface S, no separate reflection R is formed, and it can be considered that the entire shock wave is a Mach wave.

A very practical property of the reflection of shocks is that the pressure (and positive impulse) in the neighborhood of the triple point and in the Mach stem are considerably greater than those in I_2 or in the shock emitted when C is in contact with S. That is, if C is a bomb bursting above the ground represented by S, the intensity of the blast in the region M and just above it is greater, at a given horizontal distance from the bomb, than is the case if the bomb is burst in contact with the ground.

When a shock wave strikes a nonrigid obstacle, such as a building, the wave is reflected by the surfaces of the building in the various ways described above. The reflection from a nonrigid surface will not, however, conform quantitatively to that from a rigid surface such as that discussed above. At the instant the wave strikes the wall, the wall is accelerated and continues to accelerate as long as there is an excess of pressure on its outer surface. At first, the deformation of the wall is elastic, so that for insufficient excess pressure or insufficient positive duration there may be no permanent displacement of the wall. If the blast intensity is sufficient, the wall eventually deforms inelastically and suffers permanent displacement. If, for the wall in question, the displacement is greater than some critical amount, the wall will collapse.

A simplified picture of the processes of damage consists of a wall of indefinite extent which has a certain natural period of vibration. If a shock wave of very long duration strikes it, the wall can be considered to be subjected suddenly to a blast of constant pressure equal to the pressure in the shock wave enhanced by reflection. For sufficiently small pressures, the wall will deform elastically (the amount of the displacement being about twice that from a static pressure equal to the pressure in the reflected blast) and will not rupture. Some pressure must exist, however, such that the wall will collapse. For shock waves of finite duration, the wall may not collapse even though the pressure is equal to the critical pressure. Instead, the wall will acquire momentum from the shock wave and will vibrate, without reaching the amplitude corresponding to collapse. If the duration of the wave is very short compared with the time required for collapse, the momentum imparted to the wall must be sufficient to deform it beyond the critical limit. On the basis of reasoning such as this, the peak pressure is usually considered to be the determining factor in the damage produced in the blast from very large bombs, such as atomic bombs. For small bombs it is generally assumed that the positive impulse is the important quantity, since the duration of the blast is quite short. Unfortunately, neither operational experience nor experiment is adequate to test these criteria properly. A reference for a more detailed analysis of this problem is given in the bibliography[12] and the subject of damage is treated in Chapter 16 of this volume.

2.3 EXPERIMENTAL METHODS AND APPARATUS

2.3.1 Electrical Methods for Measuring Pressure versus Time

The Use of Piezoelectric Gauges

For the measurement of air-blast pressures the most common method employs piezoelectric gauges. Of all piezoelectrically active crystalline substances, those that have been used in gauges are tourmaline, quartz, Rochelle salt, and ammonium dihydrogen phosphate, [ADP].

A piezoelectric substance is one that produces on its surfaces an electric charge when the crystal is strained. In gauges, slabs of the crystal, cut in such a way as to produce the maximum charge, are provided with metallic electrodes. To these electrodes are attached the conductors of an electric cable which connects the gauge with the recording apparatus. The

fundamental advantageous property of piezoelectric gauges is their quick action that responds to transient pressure changes of very short duration.

Tourmaline is fairly abundant and can be obtained in rather large crystals. It differs from the others listed in that it produces a net electric charge when it is subjected to uniform hydrostatic pressure. Its sensitivity, in terms of the electric charge produced for unit pressures, is about the same as that of quartz. Quartz, like tourmaline, is fairly abundant and insoluble in water. Unlike tourmaline, however, if quartz is subjected to a uniform hydrostatic pressure, no net electric charge is produced on its surfaces. When quartz, Rochelle salt, or ADP, is used in a gauge, it is necessary to seal the edges of the crystal slabs from the blast pressure by a rigid housing, which is usually made of metal. Pressure, then, is applied only unidirectionally to the crystal slabs. Rochelle salt differs from quartz in its sensitivity; gauges made of Rochelle salt are about a hundredfold more sensitive than are those of the same size made of quartz. The disadvantages in the use of Rochelle salt are that it is soluble in water, and that there is a rather high temperature coefficient of pressure sensitivity. ADP is intermediate in temperature sensitivity and pressure sensitivity between quartz and Rochelle salt. Although all four crystalline materials have been successfully used in piezoelectric gauges, the tendency has been to turn finally either to tourmaline or to quartz.

One property that is possessed by all piezoelectric substances is pyroelectric activity. That is, these substances produce an electric charge as a result of a change in their temperature. Tourmaline produces a net charge when it is heated uniformly as well as nonuniformly. Quartz, Rochelle salt, and ADP, however, do not produce a net charge as a result of uniform heating. The charge produced by a temperature change of 1 C in tourmaline is about equal (and opposite in sign) to that produced by a pressure of 250 psi. For this reason, the piezoelectric crystal slabs in a gauge must be carefully protected by adequate thermal insulation from the effects of transient temperature changes.

A tourmaline gauge consists of a pile of disks of tourmaline, sawed from the crystal, and each provided with closely adhering metal electrodes on the sawed faces. The disks are so arranged in the pile that the charges produced on contiguous electrodes are of the same sign. Lead wires are soldered to the electrodes and attached to the electric cable. An electric shield surrounds the pile and is connected to the shield of the cable. Finally, the whole assembly is coated with a material that is a good thermal insulator.

The quartz gauge, which has been used very successfully in England by RRL and ARD, consists of a pile of quartz disks, provided with a thin metal cap or piston and sometimes with a plate of fused quartz to provide thermal insulation. The pile is mounted in a massive steel body, and a seal of viscous oil around the piston (at RRL) or a sheet of tin foil across the face of the gauge (at ARD) prevents leakage of air into the body of the gauge. References for the design, calibration, and use of tourmaline gauges[18-21] and quartz gauges[20-23] are given in the bibliography.

The gauges are calibrated by applying known pressures and observing the magnitude of the electric charge produced. Over very wide ranges of temperature and pressure, the pressure sensitivities of tourmaline and quartz gauges are constant. In measuring blast pressures, however, if the gauge projects into the flow of air behind the shock front, the wave is disturbed, and the gauge records the pressures of this disturbed wave which differ from those in the undisturbed wave. This difficulty is common to all gauges (not only piezoelectric ones) used in this way. It can be overcome by mounting the gauges flush with the surface of a rigid baffle, or of the ground; by this means, the gauge does not disturb the air flow and does record the true pressures in the wave.

In addition to the gauges themselves, coaxial electric cables, amplifiers, calibration circuits, and means of recording are necessary. The coaxial cables must be free from spurious electric signals when struck by shock waves and from distortions of the gauge signal arising from dielectric absorption.[24,25] Since the gauge generates an electric charge, the voltage of the output signal from the amplifier depends upon the electric capacity of the system and hence upon the length of the coaxial cable.

Amplifiers of adequate gain, low- and high-frequency response, stability, and linearity must be used. Since the electric signals usually obtained in this work are of the order of a few millivolts, the amplification required is considerable.

Calibration of the overall electric charge sensitivity of the cables, amplifiers, and recording apparatus, and of the time base must be made. These involve recording the output of the apparatus when an electric calibrating signal of known voltage (corresponding to a known electric charge) and another of known frequency are applied to the input of the apparatus.

Recording of the amplifier output voltage versus time is usually done by use of cathode-ray tubes and photographic recording of the traces on their screens. The very high range of frequencies which the cathode-ray tube can reproduce faithfully makes it particularly suitable for this work. It does, however, have the disadvantage of being rather insensitive, requiring considerable amplification of the low-level gauge signals. Time resolution is usually provided by moving the film in a direction perpendicular to the deflection of the trace on the cathode-ray tube. Although moving film is preferred, stationary film has been used by deflecting the cathode ray in the proper direction at a constant rate by means of an electronic single-sweep generator.

The oscillogram thus obtained can be interpreted as a pressure-time curve, by means of the calibrations of gauge-charge sensitivity and time. Figure 3 represents a typical oscillogram of a pressure-time curve.

In Figure 3, the atmospheric pressure prior to the arrival of the shock wave at the gauge is represented by the horizontal line P_o. At the time $t = 0$, the shock

FIGURE 3. Typical oscillogram of pressure-time curve.

wave arrives at the gauge and the pressure is almost instantaneously increased to P, the peak pressure. Thereafter, the pressure decays relatively slowly, until at t_o, the "crossing time," the pressure is again atmospheric. The time t_o is the positive duration of the wave. After t_o, the pressure decreases and a region of suction (S) follows the positive pressure phase. The pressure then again returns to atmospheric. The cross-hatched area bounded by $t = 0$, P, and t_o, is proportional to the positive impulse of the shock wave.

The advantages of the piezoelectric technique are the wide range of pressures at which the gauge may be used, its high-frequency response, its linearity with pressure, and the comparatively simple auxiliary apparatus. The disadvantages of the method are the relatively low sensitivity, the high time constant required of gauge, cable, and amplifier input circuit (necessitated by the fact that the gauge is a charge-generator), and the pyroelectric sensitivity of the gauge.

References to descriptions of apparatus for use with piezoelectric gauges are contained in the bibliography.[14,15,16,17,18,19,20]

The Condenser-Microphone Technique

The condenser-microphone gauge has been recently developed for use in measuring air-blast pressures. A condenser-microphone consists of two parallel metal plates mounted so as to be insulated from each other, and separated by a dielectric (air, mica, etc.). The two plates, which are the plates of a condenser, are connected to the associated electronic apparatus by means of an electric cable. Under the application of pressure, the dielectric between the condenser plates is reduced and the capacity of the condenser therefore increases.

In one type of apparatus, the gauge condenser is connected as part of a tuned circuit in a transmitter. The change in the resonant frequency of this circuit is linearly dependent on the pressure applied to the gauge over the range of pressures for which the gauge was designed. The output signal (frequency-modulated) of the transmitter is applied to the input of a receiver either via an electric cable or by radio transmission. The frequency-modulated signal is amplified, demodulated, and again amplified, and the output is applied to the recording apparatus. The gauge can also be used in amplitude-modulation devices. Either cathode-ray oscillographs or galvanometer oscillographs can be used for recording, depending upon the frequency-response requirements. Apparatus of these types has been used by BRL,[21] General Motors Research Division,[22] the Research Department, Woolwich,[23] Princeton University Station,[24] and the Explosives Research Laboratory.[25]

A modification of this system, developed at BRL,[21] is used to make a direct simple measurement of positive impulse. The frequency-modulated signal from the transmitter is caused to beat against an oscillator in the receiver. The resulting beat-frequency signal is amplified and "sharpened" to produce pulses of a few μsec duration. These pulses drive neon lights whose flashing is recorded on moving film. Since the frequency of the signal is proportional to the pressure applied to the gauge, the time integral of the pressure over the positive duration (i.e., the positive impulse) is proportional to the difference between the number of flashes and the number that would have occurred without a pressure pulse. Then the interpretation of the photographic record consists simply of counting dots.

The advantages of the condenser-microphone tech-

nique are: (1) the system has no inherent limitation on low-frequency response, i.e., it can respond to static pressures; (2) the gauge can be made relatively free from transient thermal effects; (3) the system has essentially no interference from cable signal, low-frequency pickup on cables, and microphonics, and does not require high impedance in the gauge circuit; and (4) it is particularly well adapted to the use of transmission by radio, thus replacing electric cables. The disadvantages of the system are: (1) the pressure range over which a particular gauge will operate is relatively small, thus necessitating the selection of a gauge to suit each expected condition; (2) the gauge has a natural period of vibration which limits its high frequency response; and (3) for use at distances of the order of 1,000 ft between gauge and recording apparatus, electronic apparatus (transmitter, power supply, or batteries, etc.) must be located at the gauge, thus complicating the problem of servicing. The further development of this method offers promise of a great improvement in the techniques of air-blast measurement.

The Resistor Gauge Method

A third device for measuring transient pressures depends on the change of electric resistance of an element under stress. In one form, the gauge consists of a resistance element that is hydrostatically compressed. In another, a resistance wire is formed in a spiral and cemented to the back of a diaphragm constrained at its periphery. When pressure is applied, the diaphragm is deformed, the wire is stretched and the resistance of the wire changes.

Associated with the gauge is a simple potentiometer circuit by means of which changes in resistance give rise to proportional changes in voltage. These voltage changes are amplified and recorded. The principal development of resistance-strain gauges of the diaphragm type has been effected by the Navy Department at DTMB.[36,37]

The advantages of the resistance type of gauge are, (1) the gauge has no limitation on its low-frequency response, i.e., it is capable of measuring static pressure; (2) the gauge and its method of operation are relatively simple; and (3) the gauge circuit is low impedance. The disadvantages of the system are, (1) the gauge is usually quite insensitive, thus requiring a rather high gain amplifier; (2) the gauge is subject to hysteresis; (3) there is a characteristic oscillation of the diaphragm which limits its high-frequency response; and (4) the pressure range over which a given gauge will operate is relatively small, and a gauge must, therefore, be selected to conform to the requirements of each use.

Other Electric Methods for Measuring Pressure as a Function of Time

Gauges based on magnetic properties have been used in numerous applications and have been proposed for use in measuring air-blast pressures. Several possible types have been suggested: moving-coil or moving-magnet gauges, moving diaphragm gauges, and magnetostrictive gauges. Some of these types offer possibilities for gauges of high-output voltage or of great compactness. One advantage would be the low-impedance characteristics.

2.2.2 Mechanical Gauges for Measuring Pressure, Impulse, etc.

Gauges Based on the Spring-Piston Principle

A gauge for measuring peak pressure has been designed that operates by recording the maximum extension of a spring acted upon by a moving piston which is accelerated by the action of a pressure pulse. If the natural period of the piston-and-spring is short compared with the duration of a transient pressure pulse, the maximum extension of the spring is proportional to the peak pressure of the pulse.

One gauge of this type which has been successfully used for measuring air-blast pressures is the Naval Ordnance Laboratory [NOL] ball crusher gauge.[38-40] This gauge consists of a massive block in which is fitted a sliding piston, a fixed anvil, and between them, a spherical copper ball. The plastic-flow characteristics of the ball give a very nearly linear resisting force. The maximum compression of this spring is measured by the permanent deformation of the ball. Although, in principle, the dimensions and mass of the piston and diameter of the ball can be chosen arbitrarily, in practice there is an upper limit to piston area per unit mass, and a lower limit to the size of ball. As a result, the gauge is best suited for measuring high peak pressures. The standard NOL gauge (as developed for underwater use) has been used successfully at air-blast pressures as low as 50 psi.

Another type of gauge[41] based on the same principle is the UERL spring-piston gauge. This consists of a moving piston, helical spring, and a simple means of recording the maximum stroke of the piston. This gauge can, in principle, be designed to measure blast pressures in any range where the positive duration is large, but the relatively delicate mechanism estab-

lishes a practical upper limit to pressure estimated to be about 100 psi.

For measurement of blast intensities from charges of moderate size with which the positive durations encountered are not extremely long, the spring-piston gauge is capable of precise measurement of positive impulse. For this purpose, the piston mass and spring strength are adjusted so that the natural period of the mass is about four times the positive duration of the blast. Under these conditions, the maximum compression of the spring is a measure of the positive impulse.

The Williams gauge[43] is a device that has been used for many years as an approximate peak-pressure indicator. It consists of a very light piston moving in a closely fitting cylinder and working against the air in the cylinder, which it compresses. The maximum compression is recorded by a simple device. The air in the cylinder behaves as a nonlinear spring. The chief difficulties with the gauge are that a very small friction (such as that caused by dust) introduces large errors in the readings and that the range of pressures which can be read with a given gauge is quite small. Moreover, the theory of the gauge operation is not completely developed.

The advantages of the ball-crusher gauge are, (1) simplicity of construction and operation, and (2) applicability to measurements of high pressure. The disadvantage is that the gauge is too insensitive to be used below about 50 psi. The advantages of the UERL spring-piston gauge are: (1) its applicability to the measurement of relatively low peak pressures; and (2) the high precision of results. The disadvantages are: (1) the gauge is relatively complicated, requiring fairly elaborate machine work; (2) it is only moderately rugged; and (3) very high blast pressures would be difficult to measure. The two types, ball crusher and spring-piston, complement each other in the ranges of pressure to which they can be best applied.

Gauges Based on the Free Piston Principle

For the measurement of positive impulse, gauges that employ a freely sliding piston with none but unavoidable retarding forces (such as friction) have been used.

In one form, the gauge, in addition to the freely sliding piston, is provided with a rotating drum carrying recording paper on which a stylus attached to the piston writes. The resulting record is a plot of the integral of impulse versus time. Thus, the impulse at any time is proportional to the slope of the curve at that time, and the positive impulse is proportional to the maximum (positive) slope of the curve. The gauge records the negative impulse as well and, in principle, is capable of yielding a pressure-time curve by two differentiations with respect to time. This gauge has been designed and used by UERL.[43]

Another type of gauge embodying the same principle had been developed by RRL.[43] In this gauge, the piston is split into two parts. The outer part receives on its surface the pressure of the blast, and pushes the inner section along the gauge. With the impulse thus acquired during the positive phase of pressure, the second part strikes a spring. The maximum compression of the spring, which is proportional to the impulse given to the piston, is recorded by an indicating pointer and scale. In the suction phase, the first, or outer piston, is decelerated without affecting the motion of the second part, which is vented to allow free motion of air past it.

Both types of free-piston gauge are quite precise and relatively simple to operate. The split-piston type gives a direct reading of positive impulse whereas the other gives records that must be interpreted by careful measurement. On the other hand, the records give more information concerning the blast wave. The principal disadvantage of the two gauges lies in their relatively complex mechanism. Another limitation is that the design of the gauge must be suited to the range of positive impulses that are expected, and the range for any one set of values of the mechanical variables such as piston area and mass is not sufficiently wide to cover all likely possibilities.

Damage Gauges

Peak-pressure gauges have been devised to operate on the principle that a thin diaphragm, stretched over a hole in a rigid plate, will rupture at a certain pressure when the diaphragm is subjected to a blast wave. If several such diaphragms are provided, covering holes of various sizes, the pressure required to rupture the diaphragm over a given hole will depend on the hole size. Hence, given a calibration of the device, the peak pressure of a blast wave is established as less than that required to break the diaphragm of the largest hole unbroken, and greater than, or equal to, the pressure required to break the diaphragm over the smallest hole broken. The pressure is thus bracketed as closely as is desired, simply by having a sufficient number of holes of graduated sizes.

One such device, the paper blast meter,[44] has been used for many years in the approximate measurement

of blast pressures. It consists of two boards clamped together, with a sheet of paper held tightly between them. Holes of about ten different sizes are bored through both boards, in register. The gauge is mounted with the plane of the diaphragm perpendicular to the direction of propagation of the wave, i.e., head-on to the wave. By virtue of the multiplication of pressure on reflection, the pressure exerted on the diaphragm is greater than that of the incident wave; proper account of this must be taken.

A more recent modification of this gauge is the *foilmeter*, which consists of a wooden or metal box with one open end over which is clamped an assembly similar to the paper blast meter but with aluminum foil instead of paper. Foil is used because it is much less sensitive than paper to changes in atmospheric conditions such as temperature and humidity. The box gauge can be oriented either face-on or side-on to the direction of propagation of the blast, since the box prevents the blast from acting on the reverse side of the diaphragm. The development, properties and use of foilmeters have been studied at the Princeton University Station[46] of Division 2.

The great advantage of this type of peak-pressure gauge is its simplicity. The operation and the interpretation of results are simple, and no elaborate machine work is involved. Its greatest limitation is that the precision of results is usually not high, and the limits within which the pressure can be bracketed with a reasonable number of holes are rather wide.

A gauge based on the principle of bracketing the pressure between those required to move and not to move spring-loaded pistons was developed at the (British) RRL. A box containing six pistons sealing holes in its front face, each held in place by a spring with known force, constitutes the gauge. A slight motion of a piston is detected by the displacement of an indicator piston, pushed by the first. In its present stage of development, this gauge is not capable of good precision. It also requires considerable machine work in construction.

2.2.3 The Shock-Wave Velocity Method

As was pointed out in Section 2.2.2 the shock-wave velocity is uniquely determined by the characteristics of the medium and the excess pressure in the shock wave. That is, under specified conditions, the pressure may be expressed explicitly in terms of the shock-wave velocity. (See Section 2.4.5, equation 8.) Advantage is taken of this relation to make very accurate measurements of peak pressures.

The measurement of shock-wave velocity requires detectors, gauges, etc., which record the precise times of arrival of the wave at various known distances from the charge. In addition, it is usually desirable to measure the velocity of sound in the medium under identical conditions to those existing at the time of the principal velocity measurement. The acoustic velocity is measured conveniently by firing a small explosive charge just prior to the firing of the main charge and observing the times of arrival of the acoustic wave at the same gauges used for the main measurement. Thus the measurements required to obtain pressures from velocities are those of distance and time. Both, however, must be measured very accurately, since the percentage of errors in the computed peak pressures are several times those in the measured velocity. This system has been adopted as a routine measurement by BRL.[48]

The measurement of shock velocity as a means of obtaining peak pressure offers the great advantage that the true peak pressure can be obtained without the uncertainties associated with gauges which must be calibrated by methods which often do not well simulate the conditions of use. As was pointed out above, the necessary measurements are those of distance and time. Very great accuracy of measurement of distance and time are required, especially at the lower pressures; because of the increased accuracy required, the practical lower limit of pressure determined by this method is about 3 psi; the complexity of apparatus required for velocity measurements is often as great as that for methods for obtaining pressure-time curves, and the latter method gives, in addition to peak pressure, the positive impulse as well as other useful information.

2.2.4 Other Experimental Methods

The Photography of Explosion Phenomena

The photography of explosion phenomena is a powerful experimental tool in this field. The detonation velocity, fragmentation processes, rate of expansion of the case, jets from hollow charges, the velocity of the flame, etc., have been extensively studied by the Explosives Research Laboratory of Division 8, NDRC. (See the Summary Technical Report of Division 8.)

The study of shock waves by photographic means has been a fruitful source of information. From flame velocities, the peak pressures very close to the charge have been obtained.[47] Shadow and schlieren photography of the shock waves just outside the flame have

produced information about the early stages of the expanding shock wave, particularly with regard to effects due to the shape of the charge.[48] Photographs of the shock waves at still later stages of their development have yielded information on their pressures, the nature of their reflections, the interactions of shock waves, etc.[49-53]

For many purposes, such as the study of the action of structures under loading by blast waves, the most convenient apparatus is a high-speed motion picture camera with a continuous source of light. Such cameras are available commercially and provide frame speeds up to 8,000 frames per sec. Still higher speeds have been attained by special cameras. For some purposes, cameras using rotating mirrors[54,54] (with stationary film) or rotating drums[55,56] carrying the film have been developed. These cameras are particularly valuable for studying self-luminous phenomena, such as detonation waves and flame.

Still pictures of shock waves can be taken by using an intermittent light source of very short intensity. Flashing lamps,[58] sparks,[59,61] and high-explosive charges[57] have been used as light sources. It is required that the duration of the flash be sufficiently short that the motion of the shock during exposure is not so great as to blur the photograph unduly. The light source is ordinarily placed behind the shock wave, facing the camera lens, and either the shadow or the schlieren technique[58] is used.

Another technique which has been of value in the study of shock waves, gas jets, etc., is that using interferometry.[59,60] In this method, the shock wave, jet, etc., which is being studied crosses one of two beams of an interferometer. Since the refractive index of the compressed air of the shock wave is different from that of the undisturbed air, the interference lines are caused to shift. Photographs of this phenomenon can be interpreted quantitatively in terms of densities of air in various parts of the domain pictured. The technique is particularly valuable, since it gives quantitative information, not only about the shock front but also about the region behind the shock front.

The Measurement of Strain

For measuring strains in objects subjected to the action of shock waves, a gauge consisting of a grid of resistance wire cemented between pieces of thin paper is very useful. The principle of operation has already been discussed. If a current is flowing through the wire when it is stretched or compressed, the potential across the wire will change as a result of the change in resistance caused by the strain in the wire.[61] (See Section 2.3.1). Such gauges are manufactured commercially. The paper and wire assembly is supplied cemented to a piece of felt cloth to facilitate handling. In use, the gauge is cemented to the surface of the object under test and is connected to the lead wires of the amplifying and recording apparatus. Oscillograms that can be interpreted as deflection-time curves are obtained.

Aside from the quantitative measurement of strain in the material itself, the strain technique is valuable as an aid in establishing the chronology of events that accompany explosions. The interactions of blast waves with target structures can then be analyzed, with the purpose of establishing the mechanism of damage to the target.

The Blast Tube

A very useful apparatus for the study of shock waves in air and for the calibration of air-blast gauges is the blast tube. This device consists of a long tube which is divided into two sections, the compression chamber and the expansion chamber, by an air-tight diaphragm. Compressed air is admitted to the compression chamber to build up the required pressure, and when the diaphragm is punctured by a knife it shatters and a shock wave is formed which is propagated along the expansion chamber. Gauges can be mounted in the expansion chamber and their characteristics under conditions similar to those under which they are to be used can then be studied. The blast tube was devised at Princeton University Station.[48,49,62-67] It has been used for gauge calibration by SOG[16] and by UERL.[18]

The relation between compression-chamber pressure and shock-wave pressure has been obtained theoretically and experimentally.[62-66] It was found that the experimental measurements lie about 6 per cent below those theoretically predicted. By inserting blocks into the compression chamber in order to shorten it, a shock wave can be produced whose pressure-time curve is very similar to those from explosive charges.[66]

The calibration studies of gauges in the blast tube reveal that the apparent gauge sensitivity decreases as the shock-wave pressure increases. This is interpreted to be due to the disturbance of the air flow by the gauge, so that the average pressure on the surface of the gauge is less than that of the undisturbed wave. Theoretical computations have been made by the Applied Mathematics Panel, OSRD,[49] which

show that the flow-effect hypothesis is reasonable.

By means of a blast tube of rectangular cross section, the reflections of plane shocks at oblique angles have been studied by photographic technique.[46] (See Section 2.4.5.)

2.6 ANALYSIS OF EXPERIMENTAL WORK

2.6.1 The Criteria of Blast Damage

The most conclusive way to test a weapon is to use it for its intended purpose, to do so many times, and to analyze and evaluate the results.[b] This is also the most expensive way to test it: the expenditure of lives, labor, and time may be very great, and the consequences of failure severe. The alternative is to determine those characteristics of the weapon by virtue of which its purpose is accomplished, to formulate these characteristics in terms of simple, observable quantities, and to measure those quantities under controlled conditions.

Under certain conditions a high-explosive [HE] bomb, detonating near structures, will demolish or seriously damage them. The means by which the bomb accomplishes its purpose is its air blast; there may be contributions from fragments, earth shock, and the fires it may cause. In order to compare the effectiveness of two bombs, it is then necessary to measure their air-blast intensities under identical conditions. If all parameters (peak pressure, positive impulse, etc.) of the blast from one are more intense than the corresponding properties of the blast from the other, the result is established: the first bomb is superior to the second (for use in the open) *provided* a sufficient number of such comparisons establishes the statistical validity of the result. (In Section 2.4.6, comparison of explosives in enclosed rooms is taken up, and it is shown that under those conditions, the order of effectiveness of explosives is different from that in the open.) If some properties of the first bomb are superior and others inferior to those of the second, the result of the test is indeterminate, unless some further information is available on the basis of which it can be established that one property is more important than another in the process of damage. For example, the fragment velocity from bomb A may be greater than that of B, and the blast peak pressure and impulse from B greater than those from A; if the bomb is to be used to accomplish blast damage, the superiority of the blast peak pressure and impulse from B would establish its superiority, other parameters of A and B being of equal value. If, however, it were necessary to choose between two intensive properties of the blast, such as peak pressure and positive impulse, the choice would be very much more difficult. Fortunately, in most cases the order of superiority on the basis of positive impulse is the same as that of peak pressure. (See Table 2.)

In order to obtain evidence that would establish the criterion of blast damage effectiveness of air-blast waves, careful studies[70] have been made by the British of many bombing incidents in Britain during the blitz. By examination of bomb fragments, it was possible to establish the size of bomb and to distinguish between bombs having explosive fillings containing aluminum and those which had nonaluminized fillings.[71] By this means the average area of damage was determined for each type of bomb, for each of four categories of damage: A (demolition); B (major irreparable damage); C (severe damage, requiring evacuation for a time); and D (minor damage, requiring only temporary evacuation). The mean radius for each type of damage was taken to be the radius of the circle whose area equalled the observed area of damage.

Static detonation trials of similar bombs, with air-blast measurements, provided the necessary information on the peak pressure, positive impulse, etc., which would be obtained, on the average, at distances from the bomb corresponding to the radii of the four classes of damage. It was decided on the basis of such data, that for British buildings the mean radius of A damage corresponded to 120 psi-msec of positive impulse, B damage to 72, and C damage to 40. This implies, of course, that it is the positive impulse, and not the peak pressure, which is of principal interest in blast damage. Although this was the best that could be done under the circumstances, it was not entirely satisfactory, since the number of incidents analyzed was relatively small (72 in all), the range of bomb sizes was not great (1,000 to 5,000 lb), the exact nature of the filling was in doubt, and the scatter of the measurements of damage area was large, as would be expected.

Proceeding on the basis of the *positive impulse criterion* so established, comparisons of bombs having various fillings were based principally on their relative positive impulses. It was found experimentally that to a good approximation, the positive impulse depends on the reciprocal of the distance from the bomb; this implies, of course, that the radii of a given

[b] See also Chapter 16.

category of damage from two bombs are proportional to the positive impulses from these bombs at a given distance, and hence that their areas of effectiveness are proportional to the squares of their positive impulses determined at a given distance.

The early British air attacks on German targets yielded further information. It had been realized that the area of damage of a given bomb would be less with German targets than with British, because of the heavier average wall construction of German buildings. Moreover, since the estimates of the effectiveness of these attacks depended on the interpretation of air-cover photographs, it was found that the distinctions among the A, B, C, and D classes of damage could not be drawn, and therefore two classes were defined and adopted, (1) *demolition* (at least one-third of load-bearing walls destroyed); and (2) *visible damage* (damage visible on good quality, air-cover photographs). The corresponding positive impulses for the mean radii for these types of damage were estimated to be 120 and 55 psi-msec respectively.

In the meantime, the development of heavier and heavier bombs progressed. The 4,000-lb *high-capacity* [HC] bomb was adopted very early and 8,000-lb and 12,000-lb HC bombs were soon developed. No such heavy bombs had been used by the Germans over England, and the extension of the incident studies, at best not conclusive, to such large bombs was not easily justified. Some experimental data were used[13] on the response of brick walls to pressure and simplifying assumptions made, obtaining a result that indicated that for bombs greater in size than the 4,000-lb HC bomb, the positive impulse criterion was probably no longer valid, and that, for bombs larger than the 12,000-lb HC, the peak pressure was probably of greater importance. Few bombs of these two larger sizes were used and they were sometimes mixed with other bombs and incendiaries. For these reasons, no very good test of the impulse criterion for very large bombs could be made from air-cover photographs. However, the few data which do exist[72-74] support this prediction that for such bombs the criterion is neither purely impulse nor purely peak pressure but something between the two.

More recently, a group composed of personnel from Divisions 2 and 11 of NDRC and from the Applied Mathematics Panel worked under directive AN-23 on the evaluation of the effects of weapons, both British and American, on targets. From careful analysis of strike and post-raid photographs, the *mean area of effectiveness* [MAE] of each of several types of bombs has been established.[75] (See Chapter 16.)

For very large bombs, e.g., the atomic bomb, where the blast duration is very long (of the order of a second), there can be little doubt that the peak-pressure criterion holds. That is, for each target structure, a certain peak pressure is required to rupture the walls, and for predicting the area of damage to be expected it should be sufficient to know the distances from the bomb at which the peak pressures are just adequate. Theoretical consideration of the problem of reactions of structures under blast loading has recently been reported.[76,77] (See Chapter 15.)

2.42 The Relative Effectiveness of Explosives in the Open

The most common military high explosives that have been used or considered for use as fillings for aerial bombs are listed in Table 1, together with their chemical compositions and densities; the compositions of actual fillings vary by a few per cent from those given. Similarly, the filling density given for each explosive is an average over a number of actual filling densities in various batches. The importance of filling density is twofold: explosives are usually compared on the basis of equal volumes, so that the greater the density, the more favorable the comparative blast effectiveness. Second, the filling density is a measure of the quality of the particular filling; a poor pour will have air cavities and the components of the mixture will segregate. Both of these faults lead to low overall densities.

An important division of these explosives into two classes can be made: (1) those that contain aluminum, and (2) those that do not. As can be seen from the relative blast intensities, the aluminum contributes heavily to improved blast performance.

The methods of comparing explosives on the basis of their air-blast intensities are essentially the same at all establishments where such work is done: the charges, consisting of identical containers filled with the explosives to be compared, are detonated while being supported in a fixed position on the testing field. Air-blast gauges, usually electric, are set up at several distances from the charge, and blast pressure-time records obtained. From these records, the peak pressures and positive impulses are computed. The conditions of the test are held the same from round to round, so that direct comparisons among the different explosives can be obtained. The results are usually reported as relative peak pressures and relative posi-

TABLE 1. Average densities and compositions of explosives.

Explosive	Average loading density (g/cm)³	Composition,* per cent by weight of: Ammonium nitrate	Barium nitrate	Ammonium picrate	Halite	PETN	RDX	TNT	Aluminum	Wax
Torpex (30% Al)	1.74	...	...	...	...	...	35	35	30	...
Torpex-2†	1.72	...	...	...	...	...	42	40	18	0.7‡
Minol-2	1.71	29	...	...	...	...	...	43	28	...
DBX	1.64	21	...	...	...	...	21	40	18	...
HBX†	1.63	...	...	...	...	...	40	23	17	5§
Tritonal 75/25‖	1.72	...	...	...	...	...	...	75	25	...
Minol-2	1.65	40	...	...	...	...	...	40	20	...
Tritonal 80/20	1.70	...	...	...	...	...	...	80	20	...
Trialen	1.64	...	...	...	...	...	15	70	15	...
Baronal	2.14	...	50	...	...	...	...	35	15	...
Comp. B	1.61	...	...	...	...	...	60	40	...	1‡
Pentolite	1.60	...	...	...	...	50	...	50	...	...
Ednatol	1.59	...	...	...	57	...	...	43	...	...
TNT	1.56	...	...	...	...	...	...	100	...	...
Pieratol	1.57	...	...	52	...	...	...	48	...	...
Amatex	1.55	44	...	...	...	...	6¶	50	...	...
Amatol 60/40	1.55	60	...	...	...	...	...	40	...	...
Amatol 50/50	1.55	50	...	...	...	...	...	50	...	...

*Under actual loading conditions, compositions vary by a few per cent from the average values given here.
†When 0.5% calcium chloride is added to torpex-2, it is called torpex-3; HBX contains 0.5% calcium chloride in addition to the other ingredients.
‡Not taken into account in percentages of other ingredients.
§D-2; desensitizing wax of the following composition: 9.9 parts Victory wax; 1.0 part nitrocellulose; 0.1 part lecithin.
‖Also may include 2% carbon black.
¶Varies between 5% and 6%, at the expense of ammonium nitrate.

tive impulses, referring all results to those from one type of filling, chosen arbitrarily as a standard. Several identical rounds of each type of explosive are usually fired in each series of tests in order to establish the statistical validity of the results.

It is found that the relative pressures and impulses are essentially independent of the charge-to-gauge distance, so that results obtained at a number of such distances can be considered as averages. Moreover, on the average, the results from various groups of experimenters are in agreement. The average relative peak pressures and positive impulses for all explosives considered are summarized in Table 2. These averages[78] include results from trials in the United States by UERL and SOG, both of Division 2, NDRC,* and by BRL, Aberdeen Proving Ground, as well as in Great Britain, by RRL and ARD. All results are reduced to the basis of the average loading densities listed in Table 1. The adjustment to relative peak pressures and relative positive impulses for differences in weights was made according to the empirical formulas

$$\frac{P_1}{P_2} = \left(\frac{W_1}{W_2}\right)^{0.6}, \qquad (1)$$

and

$$\frac{I_1}{I_2} = \left(\frac{W_1}{W_2}\right)^{0.67}, \qquad (2)$$

where P_1, P_2 are peak pressures from weights W_1, W_2 respectively, and I_1, I_2 are the corresponding positive impulses. For the usual variations in loading density, such corrections are of the order of 1 or 2 per cent as a rule.

A salient feature of the results in Table 2 is the sharp distinction between the aluminized and nonaluminized explosives: the aluminized explosives are, as a group, considerably superior to the nonaluminized ones. The increase in power is due to the high energy release of the oxidation of the aluminum. The chemical reactions in the detonation process have been studied theoretically.[66]

The addition of aluminum to explosives increases their bullet and impact sensitivity. (See Division 8, STR.) Because of this increased sensitivity, it was necessary to find some relatively insensitive alterna-

*Division 2, NDRC, reports dealing with the order of effectiveness of explosives and those of Division 8 which were transferred to Division 2 are given in references 70-92. A more complete bibliography of reports from all sources is given in reference 78.

tive to torpex-2. One explosive mixture whose sensitivity is satisfactory is HBX, which is made by the addition of D-2 wax to torpex-2. (See Table 1.) Another effect of addition of D-2 wax to torpex-2 is to decrease the air-blast intensity, largely because of the decrease in loading density. A similar mixture is torpex D-1, in which the desensitizer wax used (D-1)

TABLE 2. Peak pressure and positive impulse relative to those of Composition B (the comparison being on an equal volume basis).

Explosive	Relative peak pressure	Relative positive impulse
Torpex (30% Al)	1.13	1.21
Torpex-2	1.12	1.15
Minol-3	1.09	1.13
DBX	1.07	1.11
HBX	1.06	1.11
Tritonal 75/25	1.04	1.10
Minol-2	1.06	1.09
Tritonal 80/20	1.04	1.06
Trialen	1.02	1.06
Baronal	1.00	1.02
Comp. B	(1.00)	(1.00)
Pentolite	0.98	0.97
Ednatol	0.94	0.95
TNT	0.92	0.94
Picratol	0.90	0.90
Ainatex	0.88	0.85
Amatol*	0.86	0.80

*Applies to both amatol 60/40 and 50/50.

is somewhat lower-melting than is D-2. No detectable difference exists in blast intensities between HBX and torpex D-1. It has recently become the practice to add 0.5 per cent of calcium chloride to torpex-2, HBX, and minol-2, in order to reduce the gassing that is produced in aluminized explosives. No effect on the air-blast intensities has been observed as a result of the addition of calcium chloride.

The relative damaging power of explosives can be estimated, for bombs that are not too large, on the basis of the positive impulse criterion (see Section 2.4.1). Since the positive impulse has been shown to decrease linearly with increasing distance from the bomb, the relative damage radii are proportional to the relative positive impulse, and the relative *areas* of damage are estimated to be equal to the squares of the relative positive impulses. On this basis, and using data from Table 2, the bar graph in Figure 4 was obtained. The heights of the bars are proportional to the estimated relative damage areas. The chief confirmation of the improvement of aluminized over nonaluminized explosives comes from observations on the effectiveness of German bombs of both types in Brit-

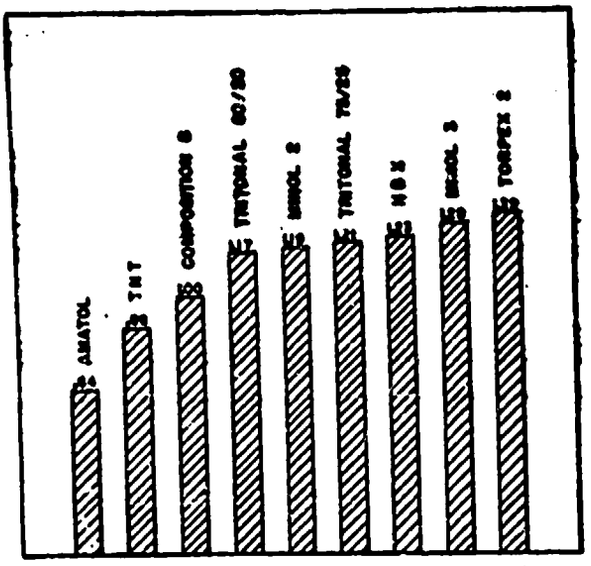

FIGURE 4. Estimated relative areas of damage based on relative positive impulse.

ain.[71] In those incidents, the aluminized explosives (consisting of trialen or aluminized hexanite, both of which should be inferior to HBX and superior to TNT in blast intensity) gave 50 to 100 per cent more damage area than did the nonaluminized explosives (TNT or amatol 60/40). The estimated improvement from HBX, over the average of TNT and amatol 60/40, would be about 65 per cent, which lies about midway between the observed values.

The influence of several variables on the blast intensities of explosives has been studied:

The Effect of Varying the Aluminum Content in Torpex, Minol, and Tritonal-like Compositions. Although torpex-2 contains 18 per cent aluminum, minol-2 20 per cent, and tritonal 20 per cent, these are not the aluminum concentrations that give the greatest blast intensities. By experiments with mixtures containing various percentages of aluminum, it has been shown that the optimum compositions contain: torpex, 30 per cent;[94] minol, 28 per cent;[94-96] and tritonal, 25 per cent.[97-100] As a result of these experiments, the British proposed to replace minol-2 and ordinary tritonal by minol-3 and tritonal with 25 per cent aluminum. (See Table 1.)

The Effect of Aluminum Grain Size on Blast Intensities. There are two reasons for the interest in the effect of aluminum grist size on blast intensities. (1) Because of mass-production processes for "atomizing" aluminum, some grists were in better supply than others, and (2) it was found[101] that use of the

coarser grists produced less sensitive explosives. Accordingly, tests were performed which showed that aluminum powder that passed a 50-mesh sieve and was retained on a 150-mesh sieve could be used in place of the Navy specification aluminum (30 per cent of which passed a 325-mesh sieve) in torpex without loss of power,[97] but with considerable gain[102] in insensitivity. Also, it was found[103] that minol-2, prepared from "36-mesh to dust" aluminum was equal in power to that prepared from "200-mesh to dust" material.

Effect of Bomb Case-Weight on the Order of Merit of Explosives. Static detonation trials of both aluminized explosives in the forms of "bare" and cardboard-cased charges and heavy-, medium-, and light-cased bombs showed no dependence, on the average, of the *relative* blast intensities on case-weight.[76]

Dependence of Order of Merit on Distance from the Bomb. On the average, the experimental evidence, based on blast-pressure measurements made over ranges of charge-to-gauge distance corresponding to pressures of most importance in producing damage, shows the relative peak pressure and relative positive impulses to be independent of distance.[76] Other experimental work,[103] however, indicates that, for very small distances from the charge, the order of merit may be very different from that in the range of distances wherein air-blast measurements are usually made.

2.4.3 The Principle of Similitude

By dimensional reasoning, the following principle of similitude was derived for explosions and explosives. If, of two charges of the same explosive, all of the dimensions of one are k times those of the other, the peak pressures measured at any distance from the smaller will be equal to those measured at k times that distance from the larger. Moreover, the positive impulse, energy, positive duration, etc., from the larger will be k times the corresponding quantities for the smaller, the distances from the charge being in the proportion $k/1$. This principle, of course, assumes that all other variables not so specified are the same in the two cases. The principle of similitude is not necessarily inviolate; it has required experimental verification.

The principle may be restated in terms of the *weights* of the charges, since the densities are presumed to be equal. If the weights of two geometrically similar charges of the same explosive are W_1 and W_2, the peak pressures at distances proportional to $\sqrt[3]{W_1}$ and $\sqrt[3]{W_2}$, respectively, will be equal and the positive impulses, durations, etc., will be proportional to $\sqrt[3]{W_1}$ and $\sqrt[3]{W_2}$, respectively, at those distances. This can be expressed as follows:

$$P = f\left(\frac{r}{W^{\frac{1}{3}}}\right)$$

$$\frac{I}{W^{\frac{1}{3}}} = F\left(\frac{r}{W^{\frac{1}{3}}}\right)$$

and

$$\frac{t_o}{W^{\frac{1}{3}}} = \phi\left(\frac{r}{W^{\frac{1}{3}}}\right) \qquad (3)$$

where P, I, and t_o are the peak pressure, positive impulse, and positive duration, respectively, measured at a distance r from W pounds of explosive, and f, F, and ϕ are unspecified functions of the variable $r/W^{\frac{1}{3}}$.

The similarity law as applied to air blast has not received an adequate test. For a range of charge weights from 8 to 550 lb, it has been found that the principle of similitude is applicable within limits of error of a few per cent.[104] By taking into account the effects of the case of bombs, differences in explosives, etc., it was shown[105] that the principle was applicable to blast measurements made by BRL on a range of charge sizes from 100- to 10,000-lb bombs. However, it has been found by British investigators that the positive impulses from 66-lb bare charges of Composition B[106] give values, predicted for 4,000-lb bombs by the similarity principle, that are considerably less than those actually obtained, the effect of the case being taken into account. Moreover, blast-pressure measurements at UERL, using very small bare charges, of the order of 2 to 4 lb in weight, lie well below those obtained elsewhere for larger charges of approximately the same shape. In order to test the principle properly, charges ranging in weight from 1 to 10,000 or 100,000 lb, and having identical shapes, explosive fillings, types of case, etc., should be detonated and blast-pressure measurements made under the same conditions by several investigators.

There are several quite reasonable qualitative arguments which would deny the exact applicability of the principle of similitude.

The Lack of Similarity of Afterburning. Afterburning, which was described in Section 2.2.1, is a term applied to the relatively slow combustion of the products of the chemical reactions in the detonation process, and involves the reaction of combustible products (carbon monoxide, hydrogen, methane, carbon, etc.) with atmospheric oxygen. That this process

actually does occur has been demonstrated experimentally.[107,108]

If this process (afterburning) occurs only at the periphery of the globe of hot gases, the extent of the reaction is determined by the area of the globe (approximately spherical). This means that the relative importance of the afterburning reaction would decrease with increasing charge-weight, since the ratio of area to volume of a sphere decreases linearly with increasing radius (i.e., charge-weight).

On the other hand, if mixing of atmospheric oxygen with the hot detonation products takes place, the burning is a volume and not a surface phenomenon. Since the elapsed time for a given process (e.g., expansion of the hot gases to a certain pressure and temperature state) is proportional to the cube root of the charge-weight (to a first approximation) the extent of a chemical reaction within the gas globe which has a finite reaction rate will be greater for longer elapsing time and the energy liberated will, therefore, be greater. By this mechanism, larger charges would be expected to give greater energies per unit weight of explosive. It has already been mentioned that the energy available from complete combustion of an explosive is of the order of three times that available from its detonation alone. Therefore, afterburning, at least in principle, may give rise to large departures from the principle of similitude. The scanty experimental evidence available indicates departures from the similarity principle in the direction predicted by this argument.

The Skin-Effect. If a sphere of explosive is detonated at its center, a spherical detonation wave, consisting of a chemical reaction zone of high temperature and pressure preceded at a small distance by a shock wave, will be propagated outward from the center of the charge. On reaching the surface of the charge (presumed to be unconfined, in air), the shock wave is reflected inward as a rarefaction. This rarefaction, or tension wave, will shortly meet the advancing chemical reaction zone and should tend to "freeze" the reactions by lowering the temperature and pressure in the reacting material. Thus a thin "skin" of undetonated explosive will be ejected from the charge, and the energy available will not be fully realized. Now the thickness of the skin is independent of the size of the charge; therefore, the fraction of the total weight of explosive which is in the skin decreases with increasing charge-weight. As a result of the skin-effect, departures from the similarity principle would be expected, and in a direction such that the blast intensity should increase disproportionately with increasing charge-weight. However, this effect should be most pronounced for very small charges, and should be negligible for large charges.

The presence of a heavy metal case around the charge would alter the phenomenon: on reaching the interface between metal and explosive, the shock wave is partly reflected as a compression, and partly transmitted as a compression in the metal. If the rarefaction wave reflected from the metal-air interface fails to meet the oncoming reaction zone before it has reached the metal, no skin-effect would be expected.

It is obvious that experimental work is required to test these hypotheses. For practical purposes, and over moderate ranges of charge size, the similarity principle can be applied, for want of more direct experimental results.

2.4.6 The Effect of a Case on the Blast Intensity from an Explosive Charge

It was pointed out in Section 2.2.1 that if the explosive charge is contained in a metal case, as in a bomb, the expansion, rupture, and projection of fragments of the case require energy which can come only from the energy released in detonation. This subtraction of energy reduces the amount that is available for the shock wave, and, therefore, shock-wave intensities from a cased charge are less than from a bare charge having the same net charge-weight.

A series of experiments using 8-lb charges of Composition B encased in cylindrical containers of various thicknesses was performed by RRL.[108,110] These results showed that both peak pressure and positive impulse from the explosive charge are reduced by the case, and that the reduction is greater, the greater the case thickness. It has been shown that the empirical equation

$$I_i = e^{-\left(1-\frac{W}{W_c}\right)} I_s, \qquad (4)$$

expresses RRL results within experimental error. Here I_i and I_s are the positive impulses from the cased and bare charges respectively, W and W_c are the weights of the explosive charge and total weight of cased charge, respectively, and e is the base of Naperian logarithms.

By making simple assumptions[108] about the partition of energy between shock wave and fragments, a somewhat different expression was derived from the above.

$$W' = \left(0.2 + \frac{0.8}{1 + 2M/W}\right) W, \qquad (5)$$

where W is the explosive charge-weight in a cased charge whose equivalent case-weight is M, and W' is the bare charge-weight whose blast pressure and impulse would be identical to those of the cased charge. However, it happens that both expressions give very nearly equal numerical results. The second expression has the advantage that it predicts the effect of case-weight on peak pressure as well as on positive impulse. The effect of case-weight on peak pressure and positive impulse are shown graphically in Figure 5 in terms of the weight of bare charge required to give equal blast intensity to that of a cased charge. For use in equations (4) and (5), the charge-weight ratio [W/W_c of (4), $W/(M+W)$ of (5)] is the "equivalent" charge-weight ratio, obtained by computing the ratio of charge-weight to total weight for a hypothetical cylindrical charge having the same weight as the charge-weight in the bomb, the same diameter as the cylindrical section of the bomb, and the same case thickness as that on the cylindrical section of the bomb. This amounts to assuming that the casing of the ogival nose and conical tail sections, which are relatively heavily cased, detract relatively little from the overall blast from the bomb, at least as far as measurements perpendicular to the bomb's equator are concerned. Table 3 lists "equivalent" and "actual" charge-weight ratios for some American and British bombs.[113]

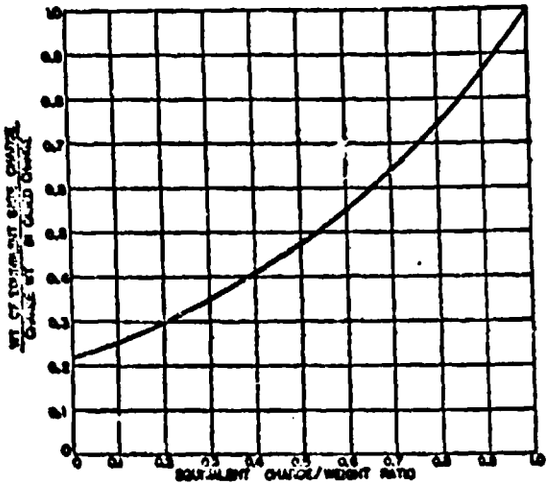

FIGURE 5. Effect of case weight on peak pressure and positive impulse.

Further evidence of the pronounced effect of the case-weight on blast pressures and impulses lies in a comparison of the blast from 500-lb *general-purpose* [GP] bombs and 350-lb depth bombs[24] and in the comparison of the blast from aluminum and thin steel cased bombs with those from bombs of standard case thickness.[113-116]

TABLE 3. Charge-weight ratios of American and British bombs.[113] R = charge-weight ratio.

Bomb	R (per cent) Equivalent cylinder	Actual
American bombs		
100-lb GP	0.67	0.50
250-lb GP	0.61	0.50
500-lb GP	0.65	0.51
1,000-lb GP	0.59	0.56
2,000-lb GP	0.64	0.53
500-lb SAP	0.36	0.31
1,000-lb SAP	0.34	0.32
1,000-lb AP	0.25	0.14
4,000-lb LC	0.82	0.80
British bombs		
250-lb GP	0.40	0.29
500-lb GP	0.37	0.31
1,000-lb GP	0.43	0.33
4,000-lb GP	0.35	0.30
250-lb SAP	0.21	0.17
500-lb SAP	0.20	0.18
500-lb MC	0.54	0.41
1,000-lb MC	0.62	0.47
4,000-lb MC	0.60	0.58
2,000-lb HC	0.81	0.72
4,000-lb HC	0.80	0.75
8,000-lb HC	0.75	0.68
12,000-lb HC	0.75	0.67

The important implication of these results is that a large blast bomb should have the minimum weight of metal casing consistent with safety in handling the bomb. For such a bomb, the best fuzing is proximity *variable-time* [VT] fuzing; there is no danger of breakup of a thin case, since the bomb functions either in mid-air or instantaneously on impact. The minimum case thickness is, therefore, that necessary to avoid injury to the bomb in handling prior to the attack.

The improvement in blast performance obtainable with thin steel or aluminum cases over the standard bombs is illustrated in Table 4, where relative areas of damage from a fixed quantity of explosive encased with various thicknesses of metal and from equal total weights of bombs of various case-weights are estimated, using the positive impulse criterion. (See Section 2.4.1.) It should be emphasized that experiment shows no significant difference in the effect of a case for various explosive fillings. Hence, improvements obtained by reducing the case-weight are in addition to improvements obtained from better explosives (see Section 2.4.3) or by proximity fuzing (see Section 2.4.5).

TABLE 4. Estimated relative areas of damage from bombs of various case thicknesses.*

A. Charge-weight equal for all bombs.

Type of bomb	Total weight / Wt of charge	Equivalent cylinder C/W ratio	Estimated relative damage area
Bare charge	1.00	1.00	1.00
Aluminum case	1.10	0.93	0.88
Thin steel case	1.18	0.90	0.83
LC bomb	1.25	0.82	0.71
GP bomb	1.88	0.64	0.49

B. Total weight equal for all bombs.

Type of bomb	Charge weight / Total weight	Equivalent cylinder C/W ratio	Estimated relative damage area
Bare charge	1.00	1.00	1.00
Aluminum case	0.90	0.93	0.76
Thin steel case	0.87	0.90	0.69
LC bomb	0.80	0.82	0.53
GP bomb	0.53	0.64	0.21

*The same type of explosive filling is assumed throughout.

2.43 Reflection of Shocks and the Mach Phenomenon

THE RANKINE-HUGONIOT EQUATIONS

Relations (the Rankine-Hugoniot equations) that express the application of the laws of conservation of mass, momentum, and energy to a shock wave are

$$\rho(U-u) = \rho_0 U,$$
$$p - p_0 = \rho_0 U u,$$
$$\Delta E = \tfrac{1}{2}(p+p_0)\left(\frac{1}{\rho_0} - \frac{1}{\rho}\right), \qquad (6)$$

where U is the velocity of the shock front, ρ, p, u are the density, pressure, and particle velocity behind the shock, ρ_0, p_0 are the corresponding quantities in the undisturbed medium in front of the shock, and ΔE is the change in energy content in crossing the shock front. All pressures are absolute, not gauge, pressures.

These equations can be combined to produce the following explicit dependence of the velocity of propagation U on the pressure in the shock p and the pressure p_0 and velocity of sound c_0 in the undisturbed medium (a perfect gas)

$$\frac{p}{p_0} = \left(\frac{2\gamma}{\gamma+1}\right)\left(\frac{U^2}{c_0^2}\right) - \left(\frac{\gamma-1}{\gamma+1}\right) \qquad (7)$$

where γ is the ratio of specific heats at constant pressure and constant volume. For air, at pressures (and corresponding temperatures) not exceeding 300 psi, γ is very nearly constant and equal to 1.40. The velocity-pressure relation for air for these pressures then becomes:

$$\frac{p}{p_0} = \frac{7}{6}\frac{U^2}{c_0^2} - \frac{1}{6}. \qquad (8)$$

As pointed out in Section 2.3.3, this equation is the basis for a very accurate method for determining peak pressures. For temperatures corresponding to pressures higher than 300 psi, $\gamma \neq 1.40$; the properties of air to 15000 K have been computed and tabulated.[13,19]

HEAD-ON REFLECTION OF SHOCKS

The reflection of shocks from plane surfaces was briefly described in Section 2.3.3; a more detailed analysis is presented below.

When a shock strikes a plane reflecting surface head-on, the properties of the reflection phenomenon obey not only the Rankine-Hugoniot equations, but the added requirement that no matter can cross the boundary between the surface and the gas. Hence, the particle velocity behind the reflected shock as it leaves the surface must be zero with respect to the wall. Figure 6A[4] depicts a plane incident shock I just

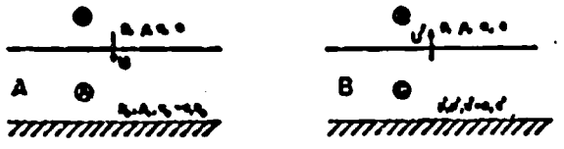

FIGURE 6. Reflection of shock from plane surface. A. Incident shock before reflection. B. Shock after reflection.

before striking a wall W. In the region B, behind the shock, the pressure, density, particle velocity, and velocity of sound are p, ρ, u, and c, respectively, and the corresponding quantities in front of the shock (i.e., in the undisturbed medium A) are p_0, ρ_0, $u_0 = 0$ and c_0 respectively. Upon striking the wall, the shock R is reflected and travels away from the wall into the compressed region B. The pressure, density, and local velocity of sound behind the reflected shock (i.e., between R and W in the region C) are denoted by p', ρ', c'. The particle velocity u' equals zero, as mentioned above.

The pressures in the regions A and C are related to the pressure in B by:

$$\xi = \frac{p_0}{p}, \qquad \xi' = \frac{p'}{p}.$$

It should be noted that

$$\xi \leq 1, \qquad \xi' \geq 1.$$

By application of equations (6), and assuming an ideal gas, the compression ratio ξ' of the reflected

[4] The figures and notations are due to von Neumann whose exposition of this subject is particularly clear.

shock can be obtained in terms of that of the incident shock ξ.

$$\xi' = \frac{(3\gamma - 1) - (\gamma - 1)\xi}{(\gamma + 1)\xi + (\gamma - 1)}. \qquad (9)$$

Again γ refers to the ratio of specific heats at constant pressure and at constant volume. If γ is taken to be constant and equal to 1.40 over the whole range of pressure, it can be seen that

$$1 \leq \xi' \leq 8, \text{ when } 1 \geq \xi \geq 0.$$

That is, according to their relation for very strong incident shocks, the pressure in the reflected shock may be as much as eight times as great as the pressure in the incident shock. For very weak shocks, the excess pressure $(p' - p_0)$ in the reflected shock is about double that in the incident shock $(p - p_0)$. However, for very strong shocks in air $\gamma \neq 1.40$, and it is no longer possible to get an accurate solution using the approximation assuming air to be an ideal gas.

Oblique Reflection of Shocks: Regular Reflection

The theory of the oblique reflection of shocks from plane surfaces has been presented. Consider an incident plane shock I which meets a wall W at an angle α. (See Figure 7.) A reflected shock R is formed at the wall at some angle α'. With notation similar to

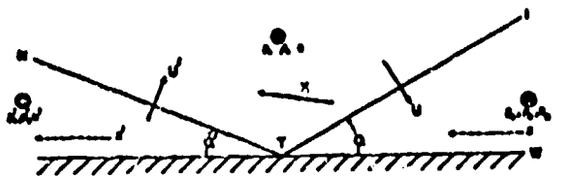

Figure 7. Oblique reflection of shock from plane surface.

that of the previous section, A, B, C are the domains in front of the incident shock, between the two shocks, and behind the reflected shock, respectively. The gas in these domains has pressures p_0, p, p', densities ρ_0, ρ, ρ', and local sound velocities c_0, c, c', respectively. The velocity of propagation of the incident shock with respect to the gas in A is U, and that of the reflected shock, also with respect to the air in A, is U'. If the frame of reference is taken fixed with respect to the line of contact with the wall T, gas can be considered as flowing into the shock with the velocity s. This flow is turned (in the direction x) by the oblique shock I and its velocity is changed. Since there can be no component of flow normal to the wall, behind R, the strength of R and the angle α' must be such that the flow is again turned parallel to the wall in the direction s'.

By application of the Rankine-Hugoniot equations and ideal gas laws to the above simple geometrical picture, the strength and angle of α' of the reflected shock R have been computed as functions of the strength of I and its angle.[118,119] Several remarkable properties of obliquely reflected shocks are predicted by this theory.

1. For a given strength of incident shock (measured by ξ), there is some angle of incidence $\alpha_{extreme}$ such that the type of reflection described above cannot occur for $\alpha > \alpha_{extreme}$.

2. For each gaseous medium, there is some angle α_1 such that for $\alpha > \alpha_1$ the strength of the reflected shock is greater than it is for head-on reflection. For air (approximated as an ideal gas with $\gamma = 1.40$) $\alpha_1 = 39° 22'$.

3. For a given strength of incident shock, there is some value for $\alpha = \alpha_{min}$ such that ξ' is a minimum.

4. The angle of reflection α' is an increasing monotonic function of the angle of incidence α. For $\alpha \leq \alpha_1$, $\alpha' \leq \alpha$ and for $\alpha = \alpha_{extreme}$, $\alpha' > 0$.

These properties of obliquely reflected shocks of finite strength ($\xi < 1$) may be contrasted with corresponding properties of acoustic waves (in which $\xi = 1$).

1. Acoustic reflection occurs for $0 \leq \alpha < 90°$.
2. $\xi = \xi'$ for all values of α.
3. Same as 2.
4. $\alpha = \alpha'$ for all values of α'.

The theory of regular reflection received exhaustive tests in experiments at the Princeton University Station.[49] A "shock tube," consisting of a pipe of rectangular cross section partitioned by a destructible diaphragm, was employed. (See Section 2.3.4.) In one section, the compression chamber, compressed air was admitted to build up the desired pressure. In the other section, the expansion chamber, the air was at atmospheric pressure or below it. When the diaphragm was punctured, it was shattered, and a plane shock wave was propagated through the expansion chamber. A "wall," which could be set at any desired incidence with the shock wave, was held firmly in the expansion chamber. By means of transparent windows, the shock-wave system and the wall were photographed in profile, using a spark as a light source. Shock strengths were computed from measured shock velocities.

The theory of regular reflection was verified for a wide range of pressures and angles of incidence. The

prediction that no two-shock (i.e., regular) reflection could exist above $\alpha = \alpha_{extreme}$ was quantitatively confirmed.

Mach Reflection

In a series of papers, E. Mach[121-123] and collaborators reported experiments on the interaction of shock waves arising from intense sparks.[120-124] Their experiments were as follows. To a glass plate, tinfoil electrodes were cemented, so that one or more sparks from a battery of Leyden jars would follow preset patterns on the glass surface. Parallel with the first plate and a few millimeters from it a second plate was supported, coated on its inner surface with soot. When a spark occurred, the soot just opposite it was blasted clear of the plate. They observed that if the electrodes were so arranged that two sparks, one long (the linear spark), the other quite short (the point spark), occurred simultaneously, not only was the soot cleared away opposite the sparks themselves, but a thin line of soot was deposited between the point and line sparks in the shape of a parabola, the point being the focus, the line the directrix. The line of soot was interpreted to be the locus of intersection of the plane and cylindrical shocks from the two sparks. However, at the two ends of the parabolic line, the line broadened into fans or V's, regions from which soot was partly cleared. This is called the Mach *V-ausbreitung*, or simply the Mach V.

Experiments of this type were repeated[125] at Harvard in 1941, particular attention being directed to study of the V. Using an arrangement similar to Mach's, with an "angular" spark S (angle between two sparks $= 2\alpha$) and a linear spark S' opposite the angle, it was found that with angles less than $2\alpha =$ 110°, no V was formed, but that a ridge of soot bisecting the angle was formed instead. As 2α was increased over 110°, a V was formed, and the angle (2ϕ) of the V was found to increase as α was increased. (See Figure 8.) Moreover, lines 1, 1', 2, 2', and 3 were observed in the soot. Lines 1 and 1' were obviously the loci of intersection of the shocks from

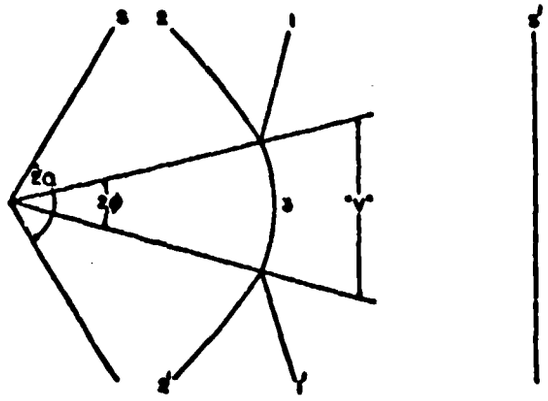

Figure 8. Illustrating shock waves from intense sparks (Mach V).

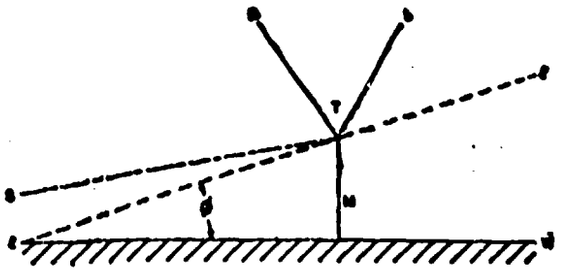

Figure 9. Mach reflection from rigid wall.

S and S' lying above and below the axis of symmetry, respectively, and 2 and 2' were thought to be loci of intersection of the portions of S and S' on opposite sides of the axis of symmetry. In the V region, only one shock, 3, was observed.

Similar experiments were performed[126] with refined technique, and photographs were obtained showing the instantaneous picture of the shock system from an angular spark. Photographs of three-shock systems involving shocks related to 1, 2, and 3 in Figure 8 have been obtained by many investigators. The reflection was photographed[21] of shocks arising from explosive sources; reflection of the bow waves of projectiles in flight from plane surfaces was photographed at BRL.*

It was pointed out above that regular (i.e., two-shock) reflection cannot occur at angles $\alpha > \alpha_{extreme}$. Some other shock system must replace it; such a system is the three-shock system composed of the incident I, reflected R, and Mach M shocks (see Figure 9).†

It has been demonstrated experimentally[48] that, in addition to the three shocks I, R, and M there is a "slipstream" S, which is a boundary between regions of different particle velocity and different density but of the same pressure. It was also found that, when $\alpha > \alpha_{extreme}$ a Mach wave M is formed at the wall which grows as the shock system moves along the

* Work of A. C. Charters and R. N. Thomas of BRL.

† Note that one can think of obtaining the configuration of Figure 8 (i.e., intersection of shocks) by removing the wall W in Figure 9 and replacing it by the mirror image of the shock system above the wall.

wall, and the locus of the triple point T is a straight line, $l - l$.

The theory for Mach configurations in shock systems is only partly developed. A number of workers[118,127-130] recently have contributed to the present state of its advancement. However, there is a large body of experimental work on the Mach wave system, and empirical correlations have been found which make the results very useful for practical military purposes.

The Application of Oblique Reflection in Air-Burst Bombs

The proposal that the effectiveness of bombs might be increased if they were detonated at some height above the ground, rather than on the ground, was advanced early in the war. However, the properties of oblique and Mach reflection were not understood at that time, and the improvement in performance was supposed to arise from a reduction of the screening effect of one building on another. A model town was built of brick, earth, and heavy timbers, and blast measurements were made[121,122] by RRL with gauges located among the buildings and charges detonated at various heights above the streets. The results indicated that peak pressures were considerably greater from a charge burst at the optimum height than from a ground-burst charge, and that the area of damage of the B category could be more than doubled by air burst, if the impulse criterion was assumed to apply. (See Section 2.4.1.) The optimum height for maximizing B damage from 4,000-lb bombs was taken to be 200 ft (a figure later shown to be much too great).

A number of 4,000-lb HC bombs were provided with proximity fuzes, set to function at about 200 ft above the ground, and were dropped in British raids over Mayen and Spezia. For a number of reasons, only a few of the bombs functioned properly over appropriate target areas, with interpretable post-raid air-cover photography. These incidents were evaluated and it was decided that, since the two bombs (out of 10 dropped) which could be located and which functioned properly at 190 ft above ground level gave less demolition, but twice as much visible damage as would impact-burst bombs, the performance did not justify its introduction into service. This decision, of course, was based on three misconceptions: (1) that shielding, or rather the absence of shielding, was solely responsible for increased damage area; (2) that the optimum height of burst should be 200 ft (instead of 40 to 70 ft as was later demonstrated); and (3) that demolition could not be increased, but only reduced by air burst. It is, however, surprising that so important a decision was made on such poor grounds; the performance of two bombs was the whole basis for the decision. In spite of this, in the light of later experimental evidence, the performance of the bombs was just what would be expected from a burst so high above the optimum.

In 1943, it was urged that the blast-measurement groups at UERL and Princeton undertake further studies of the properties of air-burst charges, and this time, the basis of the proposal was not shielding, but the properties of obliquely reflected shock waves, even in the absence of a built-up area. In December 1943 there was begun at UERL a study of the effect of height of burst on the peak pressures and positive impulses in the blast, measured at a few set horizontal distances from a small charge detonated at various heights above the ground;[144-145] gauges were placed at a few heights above the ground. Somewhat earlier, the Princeton University Station had undertaken similar studies, with several gauge-to-charge distances, the gauges being mounted flush with the ground.[139-140] The work[49] using the shock tube with a photographic technique that was described above was also begun in this period. The UERL work, in collaboration with SOG included cardboard-cased charges of 2-, 12-, and 42-lb weight; that of Princeton University Station included largely ½-lb TNT engineer blocks. All results were in agreement: as the height of burst was increased, the peak pressure and positive impulse measured at a fixed horizontal distance increased to maximum values and then decreased. The height of burst required to produce a maximum area of specified damage, i.e., the optimum height of burst, depended to some extent on the magnitude of the peak pressure or positive impulse of the area of which it was desired to maximize. For demolition-type damage, the height of burst was such that the range of heights at the optimum for a 4,000-lb *light-cased* [LC] bomb was estimated to be 40 to 70 ft. The maximum (particularly for positive impulse) was found to be so broad that the optimum height was not critical: variations from it of as much as ±20 per cent produced within 10 per cent of the optimum positive impulse.

Finally, these studies were followed by full bomb-scale tests. UERL and SOG measured the blast from bombs ranging in size from 350-lb depth bombs to 2,000-lb GP bombs supported at various heights above the ground.[146-147] The earlier small charge results

were confirmed and the increase in area of damage from air-burst over impact-burst bombs was predicted to be 50 to 100 per cent. The UERL work is summarized[98] and an empirical method for expressing the results by means of a few parameters is reported.[149]

In the meantime, when British investigators learned of the early UERL results, the question of air burst was reopened and the assessment of the raids on Mayen and Spezia was re-examined.[149] It was concluded that the burst at 200 ft gave B damage slightly less than for ground burst, and about twice as much less serious C damage, and that the Spezia incident was fully in accord with the model town experiments.[121] When the Static Detonation Committee compared[150] the early UERL and RRL[121] results it concluded that they were broadly in agreement. A commentary[151] was issued which stated the history of the British experience and reconciled it with UERL results. Additional information about the effect of air-burst bombs was obtained from V-1 bombing incidents in Britain.[152]

Two new series of blast measurements on air burst were undertaken in England. In one, 67-lb bare charges of Composition B were detonated at various heights above the open ground, with gauges at various distances from the charge and at two heights above the ground.[153] These results were in fair agreement with the previous work at UERL and Princeton University Station. Quantitative differences in the measured quantities among the results of the four laboratories were found, and although these have not been fully explained to date, all results are in approximate agreement in the optimum heights of burst and the magnitude of the increased effectiveness to be expected. In a second series of trials[154] a one-seventh scale model town was constructed and 8-lb charges of Composition B were fired at various heights above streets and buildings, with gauges recording the blast at various points in the city. These experiments confirmed the earlier work in that blast pressures and impulses were found to be maximized by air burst. Moreover, the presence of buildings did not alter this advantage. Earlier work[155] had also shown that the increases in effectiveness due to air burst could be obtained with obstacles in the path of the blast.

The general subject of "Air Burst for Blast Bombs"[21] was treated at a symposium in Washington, D. C., sponsored by Division 2, NDRC, for the purpose of presenting the subject to representatives of the Services. The topics included an introductory explanation, the experimental background, the interpretation of results in terms of expected damage, and performance of existing VT fuzes in this application. The theory of the Mach effect, the experimental verification of the theory of oblique reflection, and an empirical method for correlating the experimental results were also described.

The direct outcome of the experimental results is a set of curves expressing the dependence of peak pressure and positive impulse on the height at which the charge is detonated, with gauges located at various horizontal distances from the charge and at various heights above ground. If, from other sources, the magnitudes of peak pressure and positive impulse required to produce a specified degree of damage are known the experimental results afford a means of establishing the height of burst (the optimum height) required to maximize the damage and of predicting the gain in area of damage to be expected from air burst.

A blast pressure gauge, which is located at some height h_g above the ground at a distance d measured horizontally from the charge, will record one of two general types of pressure-time record, depending upon whether the gauge is within, or outside of, the Mach region. This is illustrated in Figures 10A and B. Figure 10A shows the single-peak type of pressure-time record obtained when the gauge is flush with the ground, or when the triple point T (at which the Mach wave and incident and reflected waves meet)

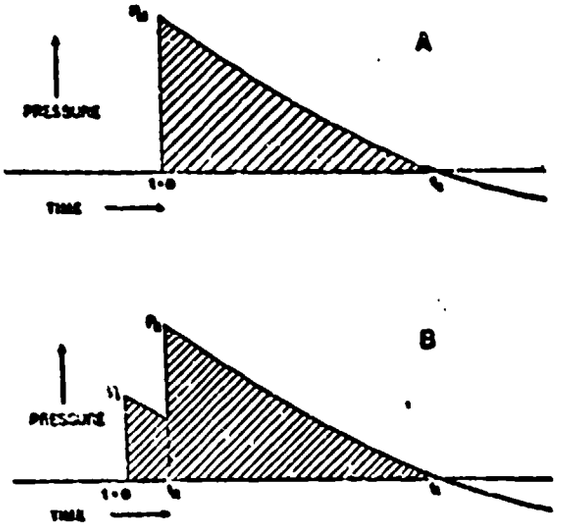

FIGURE 10. Pressure-time curves recorded below and above triple point. A. Single-peak gauge record. B. Double-peak gauge record.

is higher than the gauge. Figure 10B represents a double-peak record, such as is obtained when the height of the gauge is greater than that of the triple point. The incident peak pressure is P_I, the reflected peak pressure P_R, and the Mach peak pressure P_M. The positive impulses in the two cases are proportional to the areas of the crosshatched parts of the figures. The times t_R and t_O are, respectively, the reflection time and positive duration of the wave. If the gauge is above the triple point, the nearer it approaches the triple point, the smaller is t_R. By plotting the reflection time at a given gauge versus the charge height, the charge height at which the triple point is just at the gauge can be determined (i.e., t_R is just zero). Thus the path of the triple point can be determined for each charge height, and a family of curves, such as those in Weapon Data Sheet 3A8[168] of Chapter 19 can be obtained.

the meanings of some of the symbols are as follows. Other symbols are defined on the figure itself.

C	explosive charge
h_c	height of charge
I	incident shock
R	reflected shock
M	Mach shock (stem)
S	slipstream
T	triple point
y	height of stem
$l-l$	path of triple point
$\alpha_{extreme}$	limiting angle for regular reflection
d_e	distance on ground corresponding to $\alpha_{extreme}$

For simplicity, the stem is shown as a vertical straight line, although this is not always the case. Note that the definition of α is given a special extension when a Mach shock is formed, and that α may be obtuse.

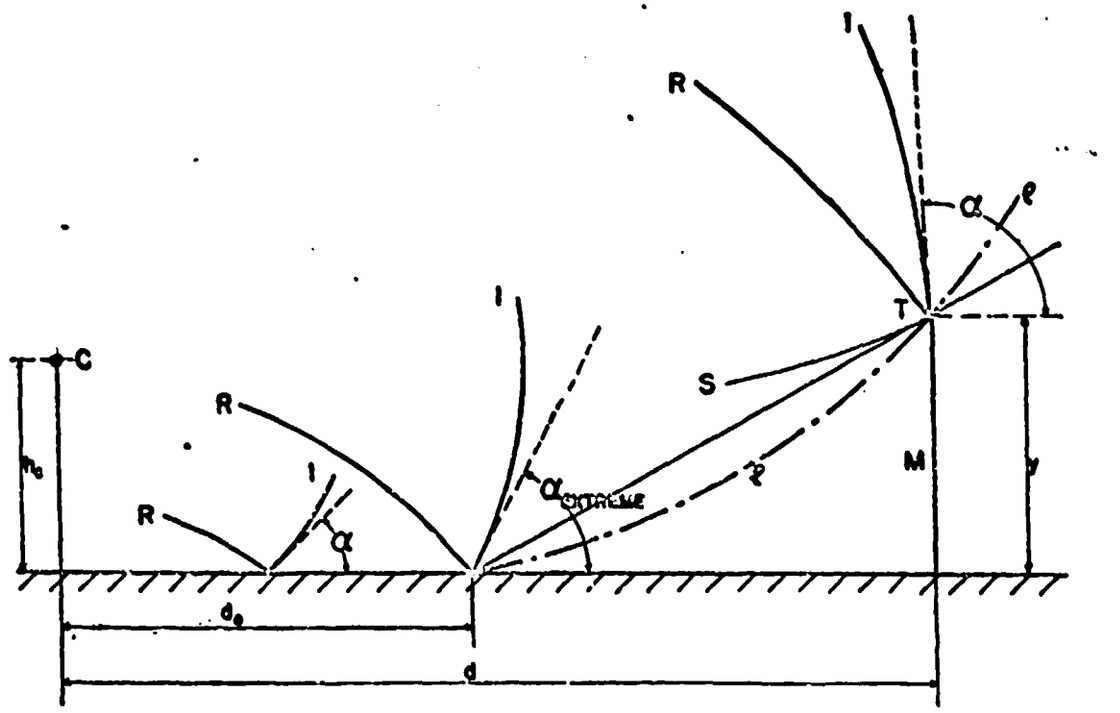

FIGURE 11. Geometry of Mach reflection.

It was[168] found that, if the path of the triple point was expressed in terms of ϕ and $\alpha - \alpha_{extreme}$ (see Figure 11), the paths of triple points from all sizes of charge, at all heights above the ground, at all distances from the charge could be represented by a single curve, to a satisfactory approximation. In Figure 11,

In Figure 12, the dependence of d_e, the horizontal limit of regular reflection, on the charge height h_c is shown, and values of $\alpha_{extreme}$ are indicated. The linear dimensions are normalized by the scaling factor $\sqrt[3]{W}$ where W is the weight of charge; d_e, of course, depends upon the pressure-distance function

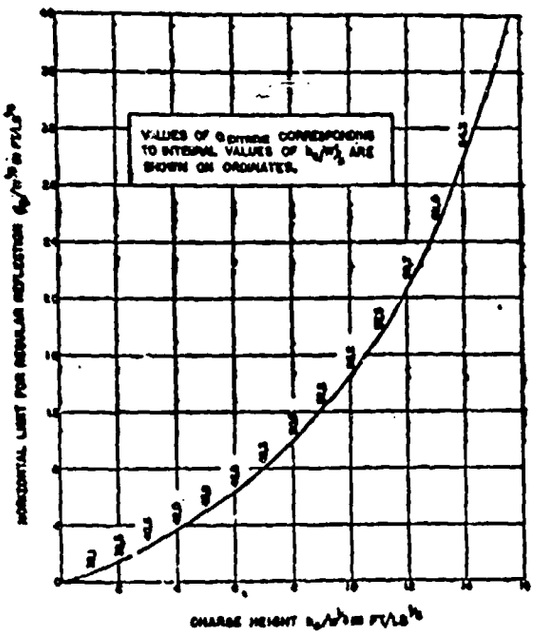

FIGURE 12. Theoretical limit for regular reflection versus charge height.

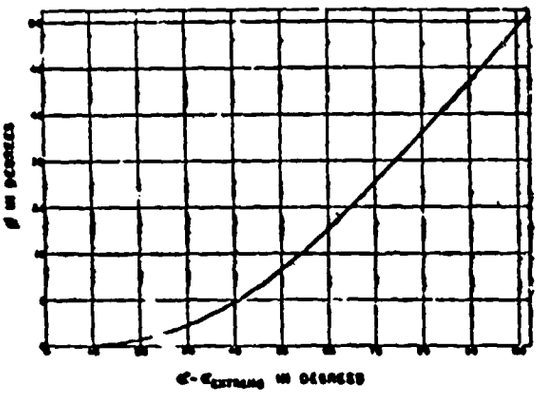

FIGURE 13. ϕ versus $\alpha - \alpha_{extreme}$

of the explosive charge. With the aid of Figure 12 together with Figure 13, which shows the dependence of ϕ on $\alpha - \alpha_{extreme}$, the paths of triple points can be computed.

The particularly practical applications of these results is based upon the experimental fact that the pressure at the gauge is maximized when the height of charge is 0.9 of that required to cause the triple point to pass through the gauge.

The height of charge which gives the maximum positive impulse at a gauge is somewhat greater, in general, than that required to make the triple point pass through the gauge. However, the optimum height is not critical, so that for moderate ranges of degrees of damage the same height of burst can be used to maximize the damage, whether the criterion of damage be peak pressure or positive impulse.

Figure 14 represents the expected radii of two types of damage as functions of the height of burst of a 4,000-lb LC bomb filled Composition B. These curves were estimated from experimental results on the assumption that the mean radius of demolition, maximum radius of demolition, and mean radius of visible damage correspond to impulses of 120, 90, and 55 psi-msec, respectively. These impulses would be produced midway up a wall 50 ft high, side-on to the blast from the bomb in question at the distances and charge heights shown.

The salient features of Figure 14 are:

1. The expected radii of damage are increased, on the average, about 45 per cent at the maxima so that the expected *areas* of damage would be increased by about 100 per cent on the average.

2. The height of burst required to maximize the radius of damage is not critical, and is roughly the same for both categories of damage considered. A height of burst of 30 to 100 ft would produce within 10 per cent of the maximum obtainable damage; the optimum height would be 50 to 60 ft.

The percentage increase in area of damage is greatest for the most severe type of damage (demolition).

That air burst improves the performance (i.e., blast damaging power) of a bomb has been demonstrated in actual raids, as has already been mentioned. The Spezia incidents showed that an air-burst 4,000-lb bomb detonating at about 200 ft above the ground reduced demolition and doubled the area of visible damage compared with previous experience with ground-burst bombs. This is precisely what the experimental results would predict for a bomb burst so high above the ground. The V-1 incidents, in which the bombs burst above the ground (as a result of striking trees, etc.) at about the optimum height, add further confirmation of the improvement from air burst.

It has been announced that the atomic bombs used over Hiroshima and Nagasaki were burst well above the ground. If the atomic bomb were similar to a charge of 20,000 tons of TNT as far as blast is concerned and if the peak pressure required to demolish a representative Japanese building were 5 psi, the optimum height of burst would be about 2,700 ft, and the area of demolition would be about 4.9 square

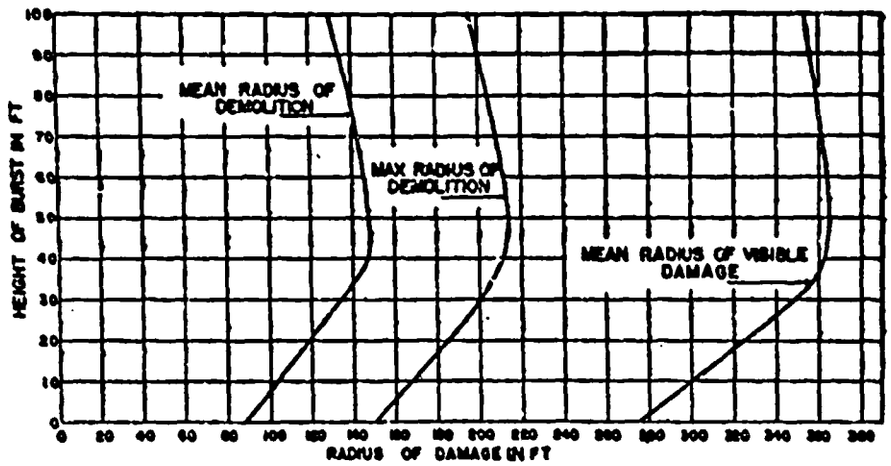

FIGURE 14. Damage radius from 4,000-lb bomb burst at various heights (estimated).

miles. Were the same bomb burst at ground level, the area of demolition would be about 2.6 square miles (using again the assumption that 5 psi is critical for demolition). This computation indicates a possible 90 per cent increase of the effectiveness of an atomic bomb by air burst. Weapon Data Sheet 3-A-9[166] of Chapter 19 was used for this computation.

A simple argument which shows that it is physically reasonable that damage should be increased by air burst is as follows: If a bomb is burst very high above the ground, so that the reflection from the ground occurs much later than does the incident shock wave at a gauge also high above the ground, the free-air peak pressure exists in the approximately spherical shock wave. If the same bomb bursts on the ground, only one (hemispherical) wave is produced, but the pressure in the wave is the same as that from a bomb of twice the weight, burst in free air. (See Section 2.2.3.) According to equation (1), the pressure at a fixed distance from a bomb of twice the weight would be about 1.5 times that of a bomb of equal weight, both being burst in free air. Now suppose the bomb is burst at the optimum height above the ground. The shock wave from the image charge (C', Figure 2) will add to that from the bomb, and will give at least twice, and, for very strong shock waves, several times the pressure from the unit charge. If it is assumed that the pressure is just doubled, the pressure observed near the triple point will be 2.0 times that from the unit charge. Hence, by raising the bomb from the ground to the optimum height, the pressure measured near the ground at a fixed distance away is increased by the factor $2.0/1.5 = 1.3$. Since, for strong shocks, the increase on reflection may be much more than twice, this estimate is conservative.

Since the blast intensity is greater in a lateral direction when the bomb is air-burst than when it is ground-burst, it is necessary that the intensity measured above an air-burst bomb be less than that from a ground-burst bomb, since the total energy should remain constant. This is actually the case, since above an air-burst bomb the gauge is high above the triple point and the reflected wave does not reinforce the incident wave. Hence air burst can be considered as a means of introducing asymmetry into the distribution of blast intensity around the bomb, in such a way that in the lateral direction, where the targets are located, the blast is more intense, while in the vertical direction, where there is no target, the blast is less intense.

At this point, estimates of the cumulative effect of the improvements from filling, case-weight, and air burst may be summarized. In Figure 15, the estimated relative areas of damage from 4,000-lb bombs of various fillings, case thicknesses, and fuzings are represented as bars whose heights are proportional to estimated relative *areas* of damage. A thick-cased bomb of the GP type (c/w ratio about 53 per cent) filled with amatol 50/50 and fuzed instantaneously was the standard demolition bomb used by this country at the beginning of World War II. A very thin-cased bomb fuzed instantaneously filled minol-3 was the latest type used by the British. Both the U. S. and Great Britain were about to introduce proximity fuzing in 4,000-lb and larger LC bombs when World War II ended.

It should be emphasized that this comparison involves only *blast* bombs. For many purposes, such as damaging subsurface water, gas, and electric mains, attack of very strong, i.e., blast-resistant structures, interdiction of roads, railroads, and bridges, and attack of troops by fragments, a large blast bomb is unsuited.

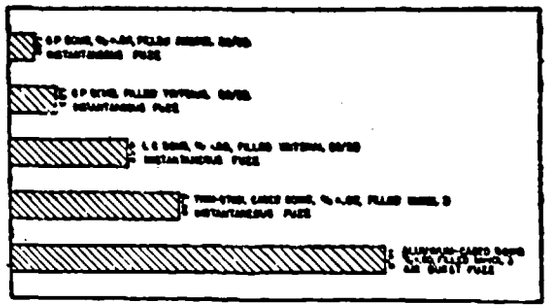

FIGURE 15. Estimated relative areas of blast damage from various 4,000-lb bombs.

The proximity fuzing of bombs of the 2,000-lb GP type and smaller is not profitable for purposes of increasing the structural damage areas, since the area of effectiveness of these bombs, in general, is less than the plan area of a target building, and they, therefore, function best by penetrating the target and bursting within it. However, an entirely different purpose is served by bursting fragmentation bombs above the ground: it has been shown that for the attack of troops in slit trenches, and of aircraft protected by revetments, the fragmentation effectiveness is increased by air burst.

2.4.5 Blast in Enclosed Rooms

HIGH EXPLOSIVES

Thus far, the experimental results that have been discussed have had to do with the blast damage effectiveness of the shock wave emitted by a charge detonated in the open, and it was asserted that for such application, the large thin-cased bomb with a VT fuze is the best type. In this section, the properties of bombs burst *within* a target structure will be considered.[166]

When a charge is detonated inside a building, the initial shock wave is identical with that obtained in the open. When this shock wave strikes the walls that surround the charge it is reflected and the reflected wave bounds back and forth among the walls, floor, and roof until its energy has been completely transformed into heat or until there are no longer confining walls, i.e., until the structure is demolished. In addition, the hot gases from the detonation are thoroughly mixed with air, and the afterburning process is greatly facilitated by the retention of the hot gases, at high pressure, by the walls. As a consequence, a pressure-time curve determined by means of a gauge placed inside a building is similar to that in Figure 16A, which is a reproduction of an actual gauge record, obtained as described above. The initial shock wave and the reflections may be imagined to be superimposed on a "hump." This hump is due to the relatively gradual building up of pressure inside the structure as a result of the heat energy released by the explosion, both from the original detonation and from afterburning. The decay of the shock wave (and consequent transformation of its energy into heat) can be seen as the damping out of the pressure peaks toward the tail of the wave.

An estimate of the pressure rise in the enclosed room which arises from the explosion of a quantity of high explosive can be made, using certain simplifying assumptions.[167] If the walls of the room are perfectly rigid, nonconductors of heat, without windows or other vents, and if all of the available energy of the explosive is realized in the initial detonation and subsequent afterburning, the pressure rise Δp in psi is

$$\Delta p = \frac{8.8H}{V}, \qquad (10)$$

where H is the total heat of combustion of the explosive in kilocalories and V the volume of the room

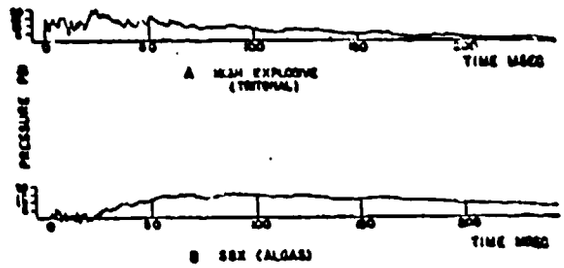

FIGURE 16. Pressure-time curve recorded for charge detonated within building.

in cubic feet. For a given (large) room, the total positive impulse I must be proportional to the heat evolved:

$$I = \text{constant} \times H. \qquad (11)$$

Suppose, for example, that a 500-lb bomb bursts inside such a building, whose volume is 100,000 cu ft. The bomb contains 267 lb of TNT, which has a heat of combustion of 3.6 kilocalories per gram; the

final pressure rise, computed by means of equation (10), is 38.7 psi. Of course, since an actual building is far from the type assumed for these purposes, the pressure computed can give only a very rough measure of the true pressure.

In order to establish the order of merit for explosive fillings for bombs that burst inside target structures, a series of experiments was performed by SOG in collaboration with UERL.[155] Five different explosives, in the form of bare charges of three charge-weights of each explosive were fired in a heavy reinforced concrete structure. Piezoelectric gauges were used to record the pressure-time curves of the blast. Figure 16A is typical of the oscillograms so obtained. The positive impulse was computed as a function of time of integration, and the results are expressed as relative positive impulses versus time. Figure 17 is reproduced from a report on relative effectiveness of explosives fired in nearly closed rooms.[155] At very small times, the relative positive impulses are approximately those given in Table 2, Section 2.4.2; i.e., they correspond to those observed in the open. However, at later stages in the pressure-time curves, the cumulative positive impulses relative to each other change from the open air values, and, finally, the order of merit is quite different from that in the open.

Equation (11) predicts that the relative positive impulse (measured to very long times) depends linearly on the energy liberated by the explosion. Figure 18, in which the relative positive impulses are plotted versus the relative heats of combustion (TNT having been chosen the standard explosive), shows clearly that the simple theory is confirmed. The order of merit of explosives in enclosed rooms is directly proportional to their heats of combustion.

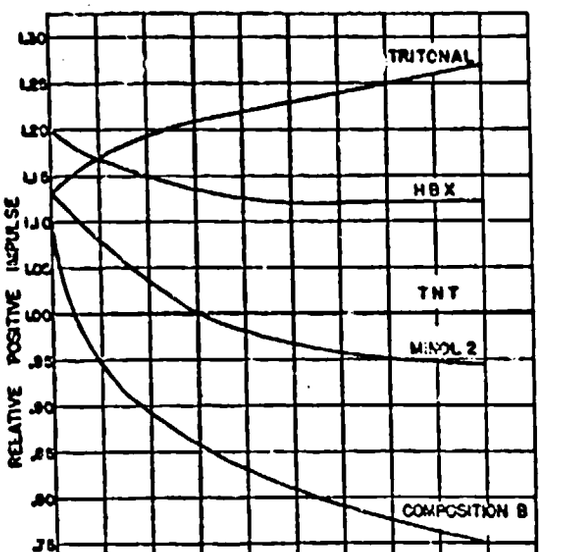

FIGURE 17. Dependence of relative positive impulse on time of integration.

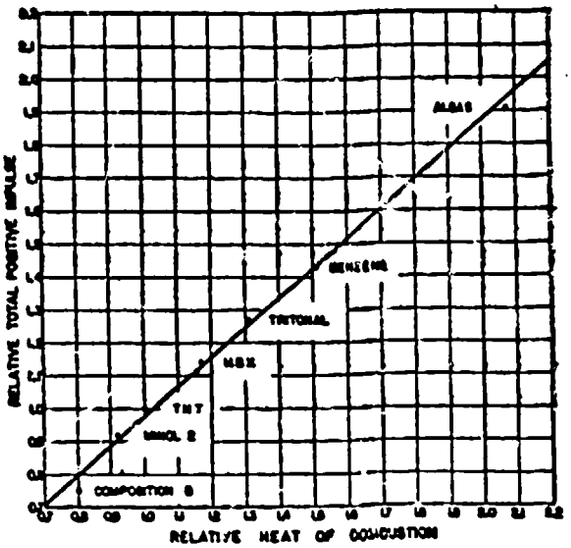

FIGURE 18. Dependence of relative total positive impulse on relative heat of combustion.

In the case of minol-2, the change in relative positive impulse (with TNT as a standard) from the open air value (1.16) to the enclosed room value (0.91) is very marked; whereas minol-2 is one of the best explosives for open air effectiveness, it is one of the poorest for confined blast. Tritonal and HBX, on the other hand, are good explosives both in the open and inside buildings. In the open, Composition B is about midway up the scale of explosives, its positive impulse being about 6 per cent better than that of TNT; in enclosed rooms, however, Composition B is the poorest of the explosives tested.

The concrete chamber used in the tests described above was only slightly vented, with about 1 sq ft of opening per 500 cu ft of volume. A more usual venting would be about 1 sq ft per 150 cu ft of volume. Experiments[156] carried out in a test chamber in which venting could be varied over wide ranges showed that the order of the relative positive impulses was not very dependent on the degree of venting.

From model-scale tests of the rupture of brick walls resulting from the explosion of a charge within a structure, it was[157] concluded that the rupture of the

walls occur over relatively long periods of time, and that the integration of the pressure-time curves in the enclosed blast experiments to long times (i.e., over the whole positive duration, or nearly so) is justified.

It is implied by equation (11) that the scaling law for enclosed blast should be

$$\frac{I_2}{I_1} = \left(\frac{W_2}{W_1}\right)^m, \qquad (12)$$

where I_1 and I_2 are total positive impulses from W_1 and W_2 pounds of explosive respectively and the exponent m should be equal to unity. In practice, it was[165] found that $m = 0.9$; this further supports the conclusion that in enclosed rooms the pressures produced are directly proportional to the energy released and that the heat of combustion of explosives is a good measure of their effectiveness under such conditions. The exponent m from open-air blast measurements is about 0.67; in the enclosed-room experiments the transition from the open air to the enclosed-room type of scaling occurred at times of the order of 20 to 40 msec after the beginning of the pressure-time record. This time is shorter than that observed[166] to elapse between detonation and rupture in their model-scale experiments.

Slow-Burning Explosives

It had long been realized that if the energy of complete combustion could somehow be utilized to produce blast many combustible substances offered possibilities of greatly improving the blast performance of bombs. As was shown in the foregoing part, the blast impulse in enclosed rooms is proportional to the heat of combustion of the explosive. Such substances as paraffin, gasoline, aluminum, etc., have heats of combustion two or three times as great as those of ordinary high explosives. It was proposed that a combustible such as aluminum powder be dispersed and ignited in air, and that if the combustion were sufficiently rapid, the resulting blast would be several times as energetic as that from a corresponding quantity of high explosive.

The advantages of a filling for bombs which could be dropped from low-flying aircraft and fuzed to burst inside a building after a short delay without injury to the aircraft from fragments were recognized in Britain, and experiments directed to this end were performed.[160]

It was found[161] that flake aluminum could be dispersed and ignited by a tetryl booster of a few pounds weight, and that the resulting burning produced pressures which, if the bombs were inside a building, would demolish it. The effectiveness in the open was practically nil, owing to the slowness of combustion, and consequent lack of a shock wave. Even compared[162,163] to the usual HE fillings (e.g., minol-2) in enclosed rooms, these *slow-burning explosives* [SBX] bombs were inferior. However, their principal object was accomplished: the fragments were few and very short range, so that low-flying aircraft would not be endangered. Combustibles other than aluminum, such as coal dust and a mixture of aluminum powder and gasoline were tried, but without the partial success of the early flake-aluminum bombs.

When it was found that the flake aluminum bombs would function properly only when the flake aluminum was unpolished[164] and that the amount of such aluminum available was entirely inadequate, the project was dropped by British workers.

A different point of view was held by some persons in the United States. It was hoped to obtain a bomb that would be quite *superior* to an ordinary high-explosive bomb in enclosed rooms by taking advantage of the high heat of combustion possessed by many combustibles. The use of several substances, such as paraffin, gasoline, petroleum, aluminum, etc., was proposed for this purpose.[165] It was realized that the problem lay in dispersing the combustible quickly in an adequate volume of air, and igniting it in such a way that a very rapid combustion would occur.

Another proposed use of the SBX principle was in sabotage devices: a small burster containing high explosive could be inserted in bags of flour, etc., and cause a dust explosion. Divisions 11 and 19 of the NDRC were particularly concerned with this use of SBX, and experiments were carried out, at the Maryland Research Laboratories,[166-169] using a burster consisting of a small charge of granular TNT and magnesium powder encased in an aluminum tube (the burster was named Lulu), and, at the Factory Mutual Research Corporation,[170-172] using a charge consisting of a pressed mixture of sulphur and aluminum powder (called Salex) dispersed and ignited by a small charge of tetryl.

A study was undertaken of various combustible materials for use as SBX.[166,168,172] Many small-scale experiments (with about two pounds of combustible) using flake and powdered aluminum, flour, coal dust, benzene, 50/50 gasoline/aluminum powder, etc., were performed.[172] It was concluded that the use of liquid hydrocarbons or their mixtures with aluminum powder were suitable for SBX and, with the proper weight and kind of burster, were capable of giving blast im-

pulses considerably in excess of those from equal volumes of HE charges fired under the same conditions, i.e., in enclosed rooms. The apparently contradictory result that in these experiments the gasoline/aluminum powder mixture was well dispersed and ignited and that in the British experiments it was not might be explained by the difference in the burster, which was found to be exceedingly important.

Further tests[168] on a larger scale (up to about 40 lb of combustible) confirmed the earlier finding that a mixture of aluminum and gasoline (containing 28 to 38 per cent of gasoline by weight) could be well dispersed and ignited by a suitable burster, and that the resulting total positive impulse was considerably greater than that from an HE charge of the same volume. The use of gasoline improves the loading density of a charge containing aluminum powder and is itself one of the best combustibles.

A typical pressure-time oscillogram from an SBX charge (weighing 10 to 11 lb) fired in an enclosed room is represented in Figure 16B. The scales of pressure and time are the same for Figures 16A (high-explosive charge, 13.5 lb of tritonal) and 16B (SBX charge, 10 to 11 lb of aluminum/gasoline mixture). The differences between the two are clearly discernible: the shock wave from the burster of the SBX charge has a very low pressure but, as the combustible burns, the pressure builds up to a hump and persists at a high level for a long time relative to the positive duration of the blast from the high explosive.

The relative total positive impulses (on an equal-volume basis) from SBX, consisting of benzene, and of aluminum/gasoline (Algas), are plotted in Figure 18 versus their relative heats of combustion. The data plotted for SBX are from only an intermediate size, using about 6.5 lb of benzene or about 10 to 11 lb of Algas. Larger charges gave more erratic results, the proposed explanation of which had to do with the disproportionately small burster and possibly with the presence of water in the structure when they were fired. The experimental results for these two SBX materials fall remarkably well on the straight line that expresses the results from high explosives. This indicates that the combustion of the SBX was advanced toward the same degree of completion as was that of the HE charges.

The improvement obtainable from the Algas over that from the best of the high explosives can be expressed in terms of the sizes of buildings which bombs filled with each could presumably demolish: the Algas bomb should demolish a building of 55 per cent larger volume than that which the tritonal bomb could demolish.

Although SBX requires further study to make certain that it is advantageous from a military point of view, the small-scale results show great promise and suggest future lines of experimentation.

From observations of the effect of bombs on targets, the AN-23 Group[68] concluded that the effectiveness of a 500-lb GP bomb in a direct hit is about 10 times that from a near-miss. This ratio decreases as the bomb size increases, and large blast bombs whose effective damage area is greater than that of a given target structure, are less effective in direct hits than in near-misses. With such bombs, a direct hit demolishes the target structure, but the walls of the building struck shield adjacent buildings from the blast, absorbing the energy in the blast. For 500- and 1,000-lb GP bombs, it is, therefore, more important to increase their direct-hit effectiveness rather than their near-miss effectiveness. The use of SBX may well offer this advantage: its improved performance in a direct hit may more than compensate for its lack of near-miss effectiveness (for SBX is practically without effect in the open).

A compromise filling for small (500- or 1,000-lb) GP bombs is suggested by the applicability of equation (11) which has been experimentally verified: a conventional high explosive having an increased aluminum content (such as TNT/Al, 60/40, or even 40/60) should be markedly superior to tritonal in enclosed rooms and not much less effective in the open. Thus the same bomb might be practically as good for cratering, earth shock, etc., and very much better for demolition by a direct hit. Mixtures such as TNT/Al, 60/40, have been tested in bombs in the open[68] and were found to give blast impulses about equal to those from tritonal. The total blast impulse from TNT/Al, 60/40, should be about 20 per cent greater than that from an equal volume of tritonal, both being measured in enclosed rooms. The corresponding increase for TNT/Al, 40/60, would be about 50 per cent.

An additional advantage to the SBX type of filling lies in its presumably greater incendiary effect. Flame temperatures remain very high for longer periods from SBX than from conventional HE.

2.4.7 The Variation of Peak Pressure and Positive Impulse with Distance from the Charge

THEORY

In the study of explosions and the shock waves resulting from them, one of the most important and,

at the same time, one of the most difficult problems was to obtain the laws that govern the propagation of the shock waves through the air. The need for a theoretical solution to this problem was acute, both because no fundamental understanding of explosion phenomena was possible without it, and because the experimental difficulties in measuring the pressure in a shock wave close to a charge were great, and the experiments liable to serious error. On the other hand, the theoretical difficulties were also great and, at best, simplifying assumptions had to be made.

By applying the equations of hydrodynamics, with additional simplifying assumptions, an approximate solution was obtained[174,175] for the propagation of blast waves in air. The straightforward numerical integration of the equations of hydrodynamics is exceedingly laborious and was, therefore, applied only to a limited extent.[176,177] In all these procedures, the problem was simplified by assumptions and the exact Hugoniot curve for air was not used. As a result of the limitations imposed by the approximations, an accurate numerical solution for the propagation equations, from the surface of the charge outward to any desired distance from it, could not be obtained. Asymptotic solutions were obtained for the propagation at low pressures, where the assumption could be made that the entropy change across the shock front could be neglected. Other assumptions led to solutions valid for regions close to the charge.

More recently, a new theory was devised[178,182] which involves an assumption concerning the shape of the energy-time curve, which amounts to assuming that the pressure-time curve for the blast wave at large distances is linear (during the positive phase). The theory allows use of the exact Hugoniot curve for air[117] and makes it possible to compute the peak pressure, positive impulse, and energy of the shock wave as a function of distance from the charge, over any desired range of distance.

In its first form, the theory required two experimentally measured quantities, such as the pressures at two distances, the pressure and impulse at one distance, etc., in order to evaluate two constants of integration of the theory. Later, the necessity of using experimental values was eliminated[183] by considering the thermodynamic properties of the explosive and of the detonation products. Two alternative assumptions concerning the detonation state were presented. In one, the "instantaneous" detonation state, the explosive was imagined to be converted into its products at high temperature and pressure, contained in its original volume. In the second, the Chapman-Jouguet conditions were assumed to apply. Of the two hypothetical states, experimental evidence favors the Chapman-Jouguet detonation state.

Experimental Results — Free-Air Pressures and Impulses

The theoretical work applies only to the detonation of a charge in free air, i.e., with charge and gauges well removed from reflecting surfaces such as the ground. Unfortunately, relatively few studies of the variation of peak pressure with distance in free air have been made. Moreover, until quite recently, the effects of the flow of air past the gauge on the recorded pressure were not recognized, so that the absolute values of pressure from much of the earlier experimental work are in doubt, particularly at higher pressures.

Recent experimental determinations of peak pres-

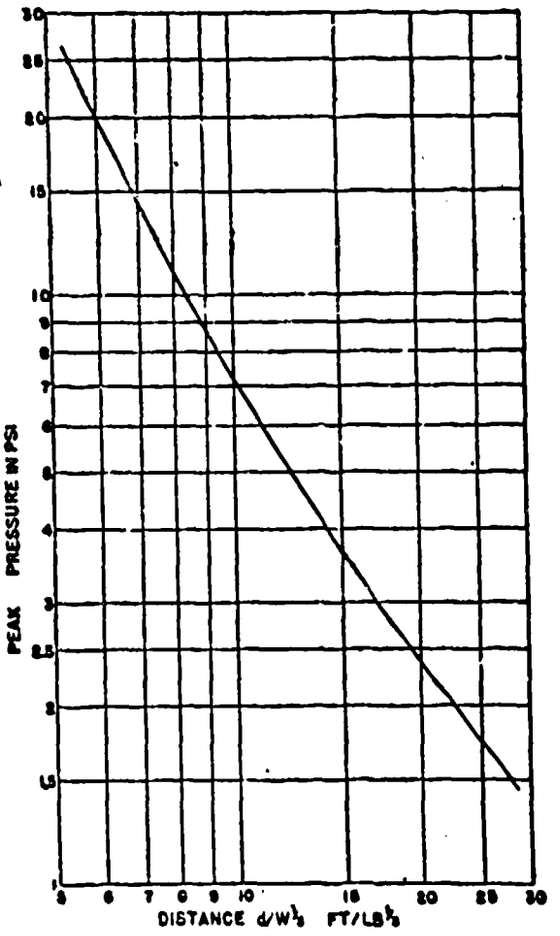

Figure 19. Logarithmic plot of free air pressure versus distance curve for cast TNT.

sures as functions of distance from the charge in free air are those of UERL,[87,88,90] Princeton University Station,[184] ARD,[183] and SOG.[91] The charges used by UERL were cylindrical cast TNT (3.5 to 41.7 lb), those by ARD were cylindrical cast Composition B (67 lb), those by SOG were cylindrical cast TNT (11 lb), and those by Princeton University Station were rectangular blocks of pressed TNT (0.5 lb). The agreement among UERL, ARD, and SOG results is excellent (after taking into account the differences due to the use of Composition B by ARD). Moreover, these results fit the theoretical curve[183] within experimental error. The curve obtained by Princeton University Station, however, is different from the others, being steeper and crossing the theoretical curve. There is good reason to believe that the Princeton University Station curve is not in error, but that a real difference exists because of the shape of the charges. Since the cylindrical charge shape is more symmetrical, and less likely to give special results, it is not surprising that experiments using them are in better agreement with theory. Figure 19 is a logarithmic plot of the free-air pressure versus distance curve for cast TNT, with the scale of distances normalized by dividing by the cube root of the charge-weight.

Available data on the dependence of positive impulse on distance in free air are even fewer than for peak pressures. Only the data of UERL[87,90] and SOG[91] are available for this purpose. The data from UERL are internally consistent and lie 6 per cent below the theoretical curve, on the average. The SOG data lie, on the average, 14 per cent above the theoretical curve. Thus, it is again true that the theory is in agreement with experimental determinations of positive impulses, within the uncertainty of the latter. Figure 20 is a plot of the positive impulse versus distance in free air for cast TNT charges, with both quantities divided by the cube root of the weight of the charge.

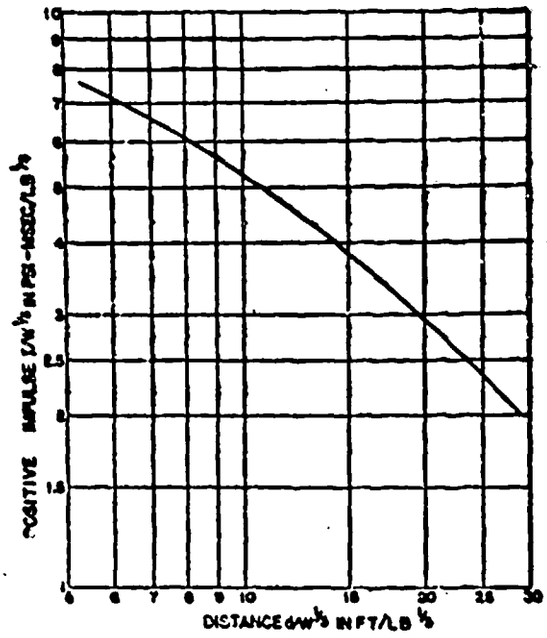

FIGURE 20. Logarithmic plot of positive impulse versus distance in free air for cast TNT charges.

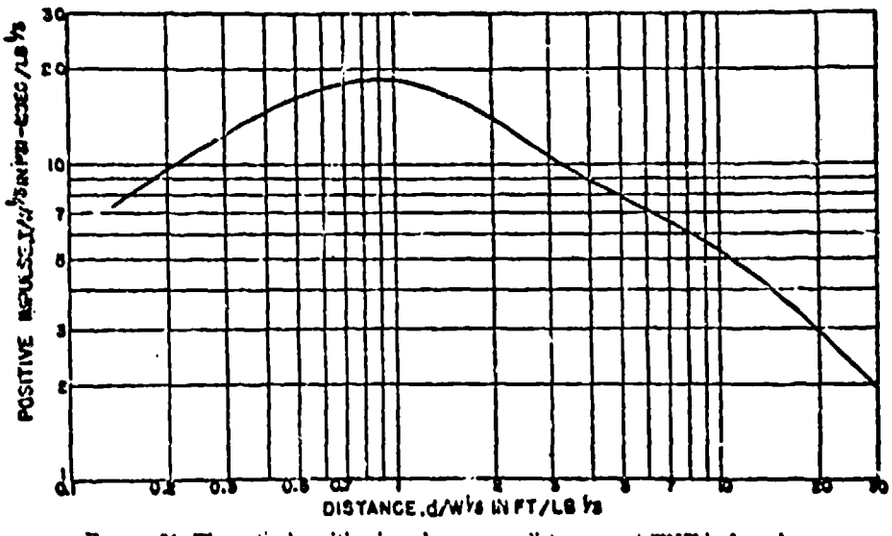

FIGURE 21. Theoretical positive impulses versus distance, cast TNT in free air.

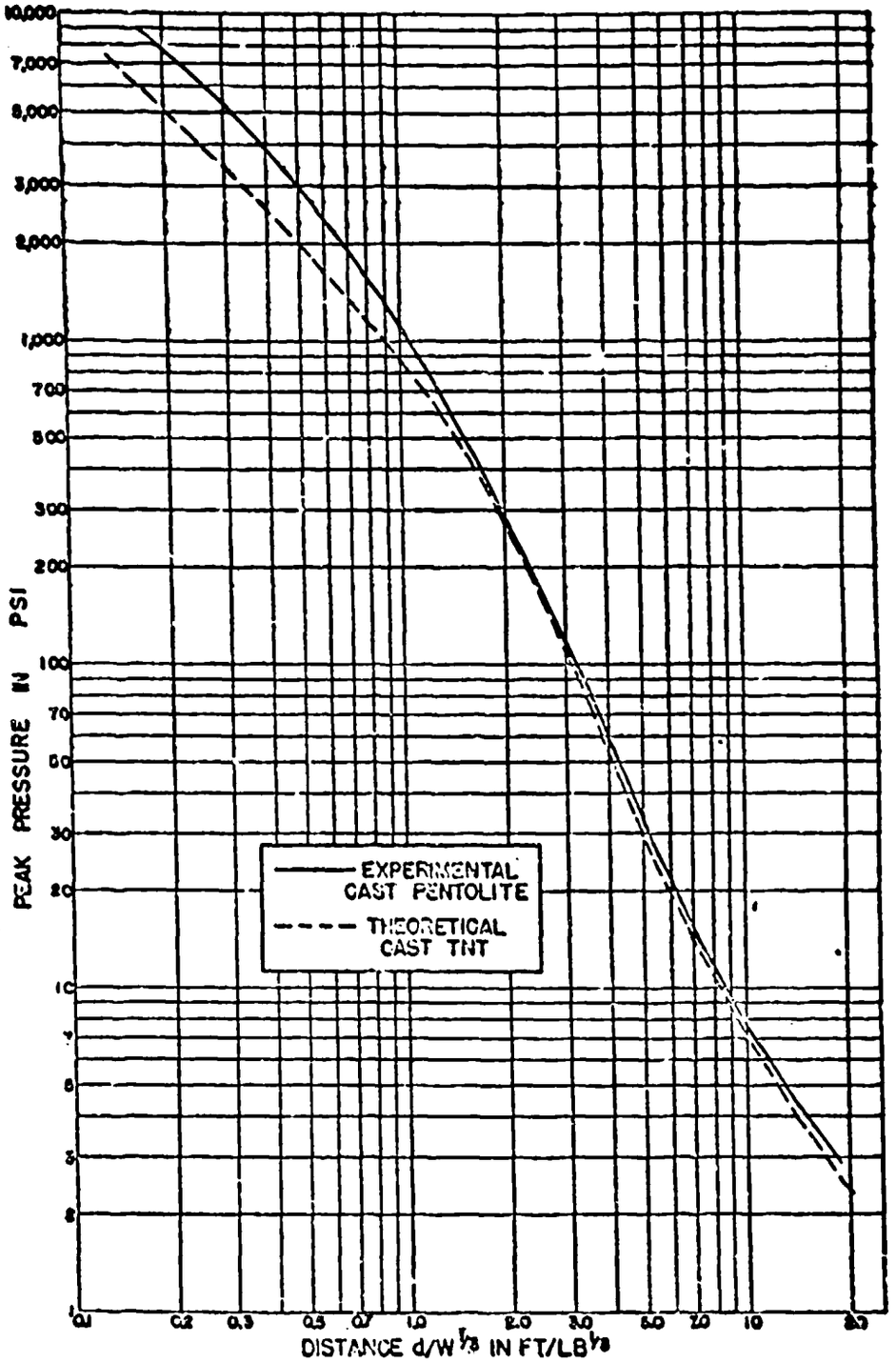

FIGURE 22. Pressure-distance curves, experimental (———) and theoretical (– – –).

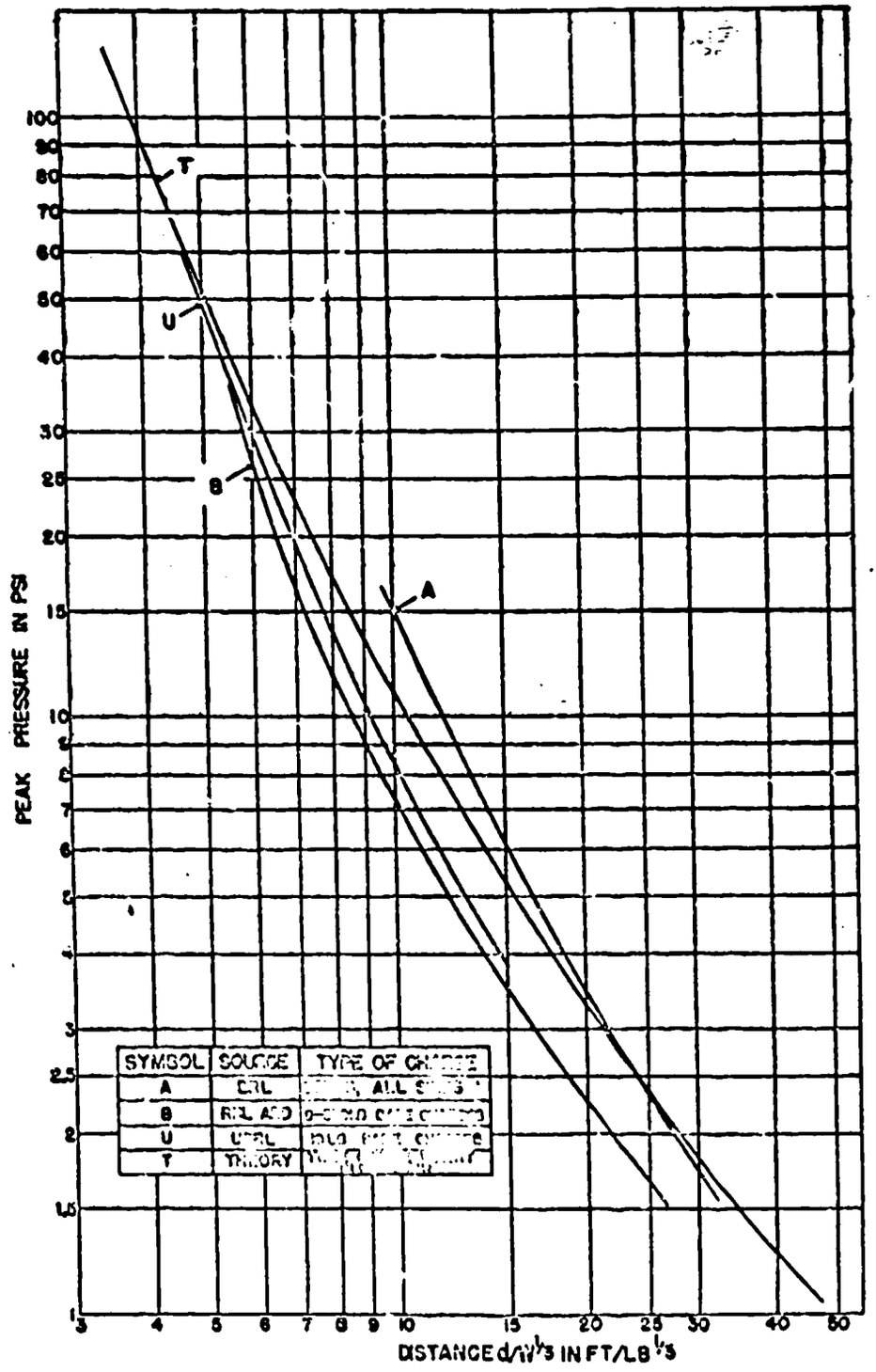

FIGURE 23. Pressure-distance curve (experimental and theoretical) for ground-burst blast of bare charges.

The theory predicts a very interesting behavior of the positive impulse at small distances from the charge: as the distance from the charge is increased, beginning at its surface, the positive impulses first rise and reach a maximum, then decrease. Figure 21 is a plot of the theoretical positive impulse versus distance curve for spherical charges of cast TNT on a at the greater distances on both piezoelectric gauge measurements and velocity measurements. The smooth curve of Figure 25 represents these data; no comparison with theory is available, since the new theory[168] has not been applied, numerically, to pentolite. On the same graph, however, the theoretical pressure-distance curve for cast TNT is plotted for comparison.

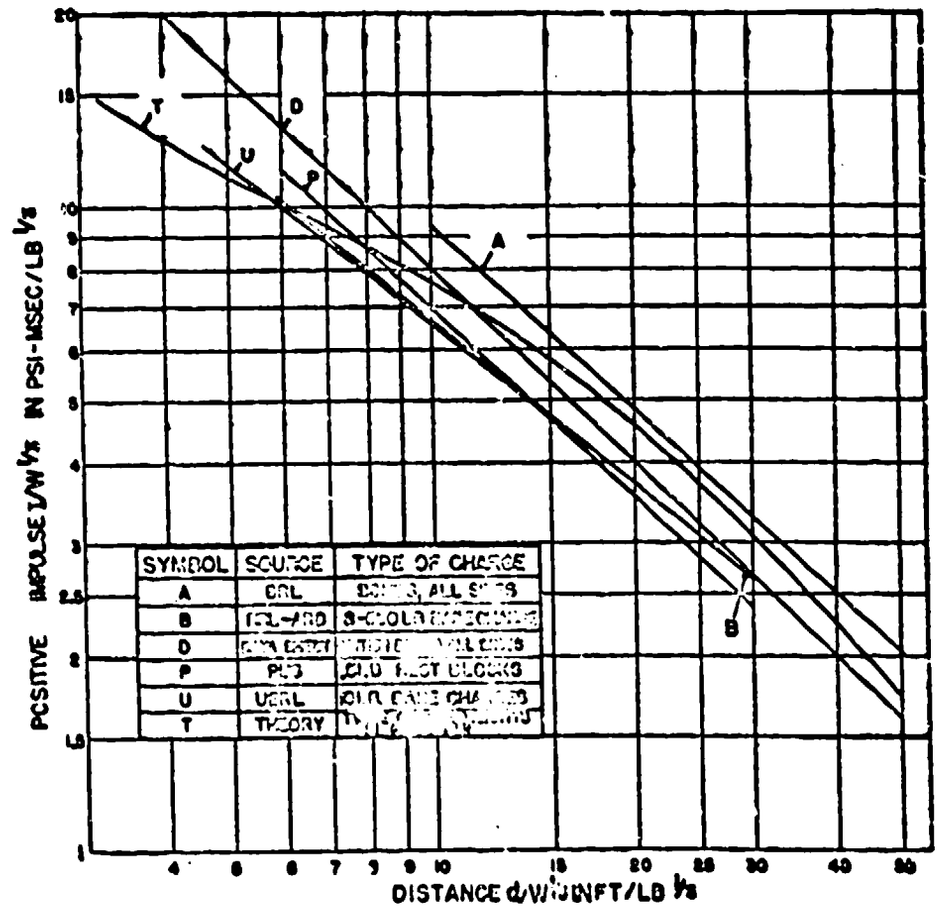

FIGURE 24. Experimental positive impulses versus distance curves (on ground) from various sources.

smaller scale than that of Figure 20 and with a greater range of distance. The existence of the maximum, which occurs at about 1 ft from a charge weighing 1 lb, has never been confirmed by experiment, since pressures at this distance are in excess of 1,000 psi.

Measurements of peak pressure, very close to the charge,[183] at intermediate distances,[186] and in the range[90] covered by Figure 19, using in all cases spherical charges of pentolite, centrally initiated, have been made. Those close to the charge are based on shock-velocity measurements (see Section 2.3.3) and those

EXPERIMENTAL RESULTS — GROUND-LEVEL PRESSURES AND IMPULSES

As described in Section 2.4.5, a charge detonating on the ground produces a blast wave having the pressures and impulses that a charge of twice the weight would give in free air, providing there were no crater, and providing the ground were a perfect reflector of the shock wave. In practice, of course, craters are formed, and the ground absorbs energy from the shock wave as it proceeds. Moreover, differences in soil can cause different degrees of energy absorption.

... rather more scatter in results can be ... is found when the charges are resting ... d than when they are detonated in free ... result of such uncertainties, the free-air ... can serve only as a theoretical upper limit to ... st intensity for ground-burst charges.

Experimental measurements of ground-burst blast pressures and impulses are available from several sources. In order to obtain a representative sample of these measurements, some results from British Laboratories (RRL and ARD), UERL, Princeton University Station, and BRL have been compiled, averaged, and plotted in Figures 23 and 24. A large range of soil conditions, climate, charge sizes, and a narrow range of gauge heights are involved. All BRL measurements were made with the bomb supported a short distance off the ground, and a correction for this was necessary. For measurements where bombs or other cased charges were used, the results have been adjusted so that all plotted values refer to bare charges. Differences in explosives were also taken into account by use of the data of Section 2.4.2.

In Figure 23, the highest curve (pressure versus distance) is that from BRL results[105] on bombs of all sizes, charge-weight ratios, etc., adjusted by use of a function such as that of Figure 5 for the effect of the bomb case. The next higher curve is that from bare charges of Composition B, varying from 8 to 550 lb but mostly about 67 lb.[104,106,187-189] Data from RRL and ARD were averaged for this curve. The effect of the difference in blast between TNT and Composition B was taken into account. The curve for 10-lb bare charges of TNT, determined both by means of piezoelectric gauges and the shock-wave velocity technique[190] is almost indistinguishable from the British bare-charge results. The theoretically predicted curve is also plotted. This curve was obtained by taking the free-air pressures for a doubled charge-weight and should represent an upper limit, since the ground is not a perfectly rigid reflector. Although the evidence from the difference between the curves from large charges and small is by no means convincing that the principle of similitude does not hold exactly, the direction in which deviations from exact scaling occur is the one which fits the reasoning of Section 2.4.3.

In Figure 24 (positive impulses versus distance) the curve on which Weapon Data Sheet 3A2*[97] of Chapter 19 is based is considered the most generally applicable one for moderately large charges. This curve was obtained principally from many British measurements of the blast from bombs of all sizes, the effects of the case being taken into account. The next lower curve is that from a large number of British measurements of the blast from bare charges of Composition B.[104,106,187-189] The curve from UERL measurements of the blast from 10-lb charges of TNT[190] is very close to the British bare-charge curve. The BRL results[105] from bombs and large bare charges are somewhat higher than those represented by Weapon Data Sheet 3A2*. The Princeton measurements in which ½-lb rectangular blocks of TNT were used[141] are very close to the British and UERL bare-charge results, but the latter curves are not so steep. Effects that are due to the special charge shape may be involved. A theoretical curve, based on the free-air curve from theory but using doubled charge-weight, is also given. A striking difference between this curve and the experimental ones is that the latter are straight lines, whereas the theoretical curve is concave downward. Presumably, the special reflection and absorption effects of the ground are responsible for this difference. In Figure 24, as in Figure 23, the curves seem to be progressively higher, the larger the weight of charge.

An interesting feature of these curves is the lower rate of decay with distance of both pressure and impulse for bare charges as compared with bombs and the greater rate of decay for ground-burst charges than for free-air charges (compare Figures 19 and 20). For comparison, the curves obtained by using the free-air results for charges of doubled weight (to take into account ground reflection) are also plotted in Figures 23 and 24.

2.4.3 The Air Blast from Line Charges; Mine Field Clearance

Theory

The basic principles of the theory[191] of propagation of shock waves from explosive sources in air and water have been applied to a line charge, i.e., to a charge one of whose dimensions is much greater than the other two. This theory[192] takes into account the finite detonation velocity of the explosive and is applicable to an infinitely long cylindrical stick, initiated at one end. By assuming the detonation velocity infinitely great, a simplified set of equations is obtained which is applicable at rather large distances from the charge. The theoretically predicted pressure and impulse versus distance curves for an infinitely long cylindrical charge of cast TNT detonated in free air are given in Figures 25 and 26. The scales of im-

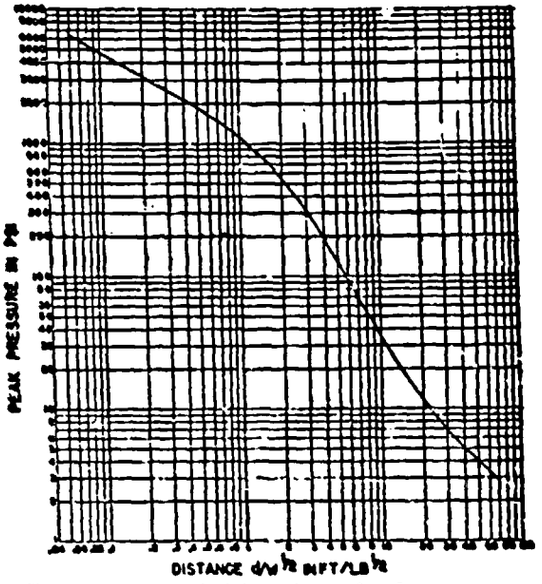

FIGURE 25. Theoretical dependence of peak pressure on distance from line charge of cast TNT.

pulse and distance are normalized by dividing each by $\sqrt[3]{W}$, where W is the charge-weight per foot; the square root rather than the cube root is the scaling factor for line charges.

The general shapes of the pressure and impulse versus distance curves for line charges are very similar to those for point charges (compare Figures 21, 23). The principal difference is that, for line charges, the rate of decrease of peak pressure and positive impulse with distance is less than for point charges. There is a predicted maximum in the positive impulse versus distance curve for line charges, as well as for point charges. The existence of this maximum has not been demonstrated experimentally for, as is the case with point charges, measurements of positive impulse so close to the charge are very difficult. In both cases, the maximum is predicted to occur at a distance from the charge where the peak pressure is of the order of 1,000 psi. The possible existence of this maximum may have a great practical importance in clearing mine fields by use of explosives. (See part 2 below.)

CLEARANCE OF MINE FIELDS BY EXPLOSIVES

Land mines constitute one of the most effective defensive weapons; their use in very large numbers often practically immobilized the mechanized units of advancing armies and exacted a large toll of killed and injured troops and crippled vehicles. One of the most acute problems in ordnance was the development of means of detecting, removing, and exploding land mines sown by the enemy. To do this, many devices were employed, none with complete success. Among other methods of mine field clearance, an important one used explosives; the blast from explosive charges was capable of causing the fuzes of some types of mines to function. For physical properties of line charges, see Weapon Data Sheet 1A7b of Chapter 19.[156]

Two general types of mines were used. (1) Anti-tank mines were so devised that the pressure of a

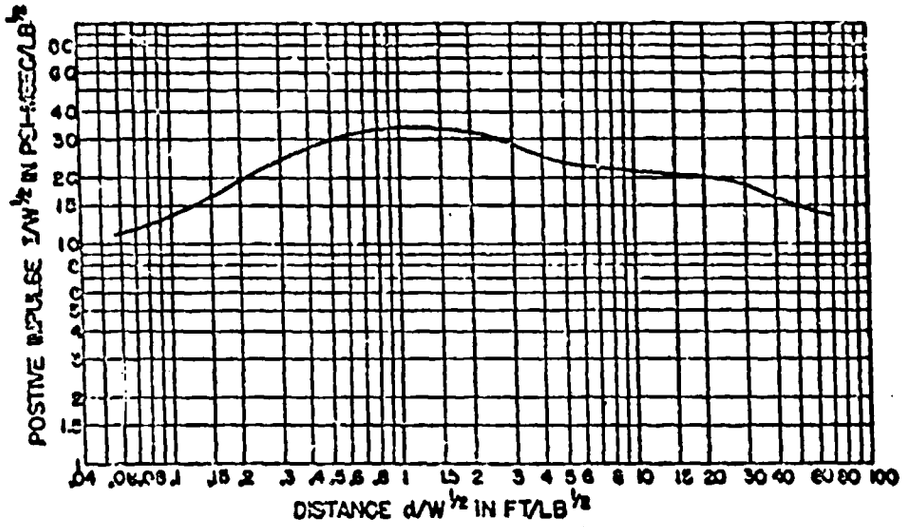

FIGURE 26. Theoretical dependence of positive impulse on distance from line charge of cast TNT.

heavy vehicle such as a tank would explode the mine, but the weight of a man was insufficient. (2) Antipersonnel mines were fitted with trip wires, triggers, etc., which would cause the fuze to function even if they were only slightly disturbed. Both types of mines were usually used in the same field; the antitank mines made the passage through the field hazardous for armored vehicles, and the antipersonnel mines were equally hazardous for the sappers who entered the field in advance of tanks to detect and disarm the mines. In addition, the field was usually under enemy fire.

Explosives in the form of bombs, and other special point charges, line charges, and "plane" charges were used or tested. Aerial bombing of mine fields, using navy depth bombs and 500-lb GP bombs, was tested,[102] and static trials of bombs suspended at various heights above a mine field to simulate air-burst bombs were carried out. Alternate explosive fillings (TNT and tritonal) were evaluated for mine field clearance.[104] It was found that air-burst bombs cleared mines to a greater distance than did ground-burst bombs, and that bombs filled with tritonal were more effective than those filled with TNT. (Similar tests, using rocket heads filled TNT and torpex-2[105] showed that torpex was markedly superior to TNT.) On the whole, however, aerial bombing of mine fields was considered an ineffective method, largely owing to the scatter in the points of burst, which necessitated a very heavy bombing to insure that a continuous path would be cleared. Even under the conditions of the test, when the target mine field was well marked, many bombs missed it entirely.

For use in clearance of mine fields, line charges of several types were developed by the U. S. Army Engineer Board, at Fort Pierce, Florida, and the A. P. Hill Military Reservation, Virginia. Antipersonnel mine-clearing devices were line charges of low weight of explosive per foot, intended to be launched by a variety of means over a mine field, and detonated. Some of these devices were: (1) detonating cord cable kit, M1,[106] consisting of a coil of flexible explosive "rope" composed of 13 (and later 19) strands of Primacord detonating fuze; (2) infantry snake, mine-clearing antipersonnel M1,[107] consisting of an assembly of corrugated magnesium-alloy channels bolted together and filled with two rows of paper-wrapped explosive charges; and (3) a flexible hose[103,106-206] (the infantry hose), 1 in. in diameter, which could be laid across the mine field and filled, *in situ*, with a liquid explosive. The detonating cord was launched through the air by means of a rocket; the infantry snake skidded along the ground, propelled by a rocket mounted in its nose; and the flexible hose was to be paid out by a rapidly rolling wheel or by a rocket launched from an armored vehicle toward the mine field.

For clearance of antitank mines, much heavier explosive charges must be used than for antipersonnel mines, both because of the relative insensitivity of the former to blast, and because a wide lane is required for large vehicles. Some of the line charges developed for clearing antitank mines were: (1) snake, M2A1,[208] and M3[206] consisting of overlapping corrugated steel or aluminum plates bolted together to form two parallel troughs in which special cartridges of explosive were placed; (2) a flexible hose[207] (the dragon or tank hose) similar to the infantry hose but of 3-in. diameter; and (3) the projected line charge [PLC] consisting of a cloth tube containing plastic explosive (Composition C3) provided with an axial nylon rope and constricted at short intervals by tying with twine. The snakes were assembled in the rear and then towed to the edge of the mine field, whence they were pushed by a tank into the field, and then detonated. The tank hose was to be launched by projection from a rocket tube mounted on a tank. The PLC was to be tied to a rocket (the coiled charge and rocket being towed by a tank to the edge of the mine field) and launched through the air.

For clearance of S mines, which were very blast resistant, a plane charge, consisting of a mat of woven Primacord, was developed.[103,106-206] This charge (the carpet-roll torpedo) was to be launched by rockets propelling the roll across the mine field and unrolling as it went.

All of the weapons described were capable of clearing mines, but each had its disadvantages. The chief difficulty was that a charge that was capable of clearing an adequate path was heavy and cumbersome, and in the process of laying the charge, personnel were exposed to enemy fire. Detonation of a large charge near a tank endangers the tank and occupants. However, the *blast* effect inside the tank is not normally hazardous to personnel.[208]

In order to test mine field clearing devices, mines simulating certain enemy types in all possible respects were developed and produced in quantity. These dummy mines were filled with inert material, and the fuze was so arranged that it could be determined, after the test, whether or not an actual mine fuze would have functioned. The universal indicator mine[209,210] was developed by the Gulf Research and Develop-

ment Company, Division 17, NDRC, to serve, as its name implies, as a mine that could be calibrated against any type of actual mine. The results of tests using the universal indicator mine could be used to predict the clearance of most types of mines with which it had been compared. Mine fields consisting of these and other indicator mines were laid out in the way best calculated to yield results of statistical validity, and the explosive charge being tested was detonated among them. The mines were then uncovered and their fuzes examined.

Experimental data on the clearance of many types of mines by various types of explosive charges are contained in the reports of the U. S. Army Engineer Board;[192,193,195-204] these data have been analyzed statistically and reported by the Statistical Research Group, Princeton University.[211] It is clear from these data that type of soil, time since burial, depth of burial, and moisture in the soil are all important factors in determining the distance from the charge at which a mine may be detonated by blast.

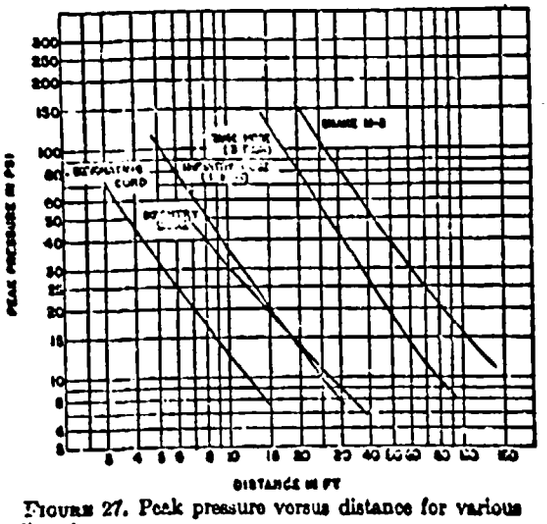

FIGURE 27. Peak pressure versus distance for various line charges.

Although it was known from experiment that the blast from line charges was capable of detonating mines, there was at first no way other than trial and error to predict the performance of new types of charges, or of old types with new explosive fillings. Two things were needed: first, an applicable theory of the functioning of mines, relating the physical properties of the fuzes to the parameters describing the intensity of the blast, and second, measurements of the peak pressure and positive impulse in the blast from various line charges.

A simple theory of the response of simulated Tellermine 43 [TMi-43] to blast was developed;[212] this was later applied to the response of the universal indicator mine.[213,214] These theories require a knowledge of the pressure-distance and impulse-distance curves for each explosive charge to which the theory is to be applied.

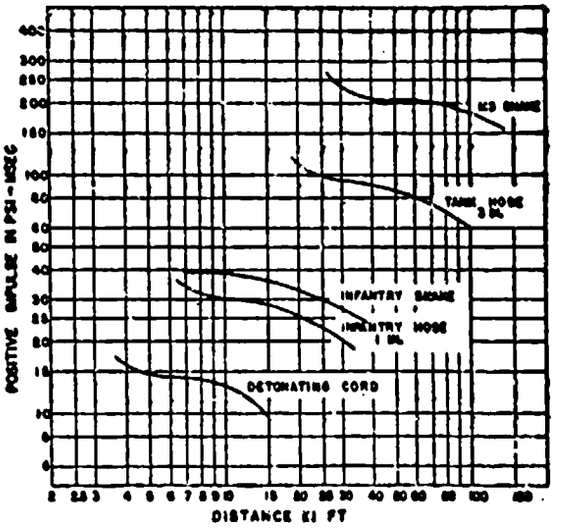

FIGURE 28. Positive impulse versus distance for various line charges.

In Great Britain investigations of the functioning of German mines and simulated mines, theoretical studies of their response to blast loading,[215] development of line charges, and measurement of the blast intensities from line charges[218,219] have been carried out.

If mines are more deeply buried than 2 in. below the surface of the ground, it is found that, in a narrow belt just beyond the crater from the explosive charge, a large fraction of the mines are not detonated, and, indeed, many mines are rendered more sensitive and, therefore, hazardous. Beyond this region it is found that essentially all mines are cleared for a certain distance; at still greater distances, the fraction of mines detonated falls off rapidly. This phenomenon (of low expectation of detonation near the crater) is called the "skip effect" or "probability dip." It constitutes a serious disadvantage of the explosive method of clearing mine fields, since it is precisely in and adjacent to the crater that tanks must travel. Many hypotheses have been advanced to account for the skip effect, but none has been verified by experiment. It may be that the existence of a maximum in the impulse versus distance curve (Figure 26) is somehow

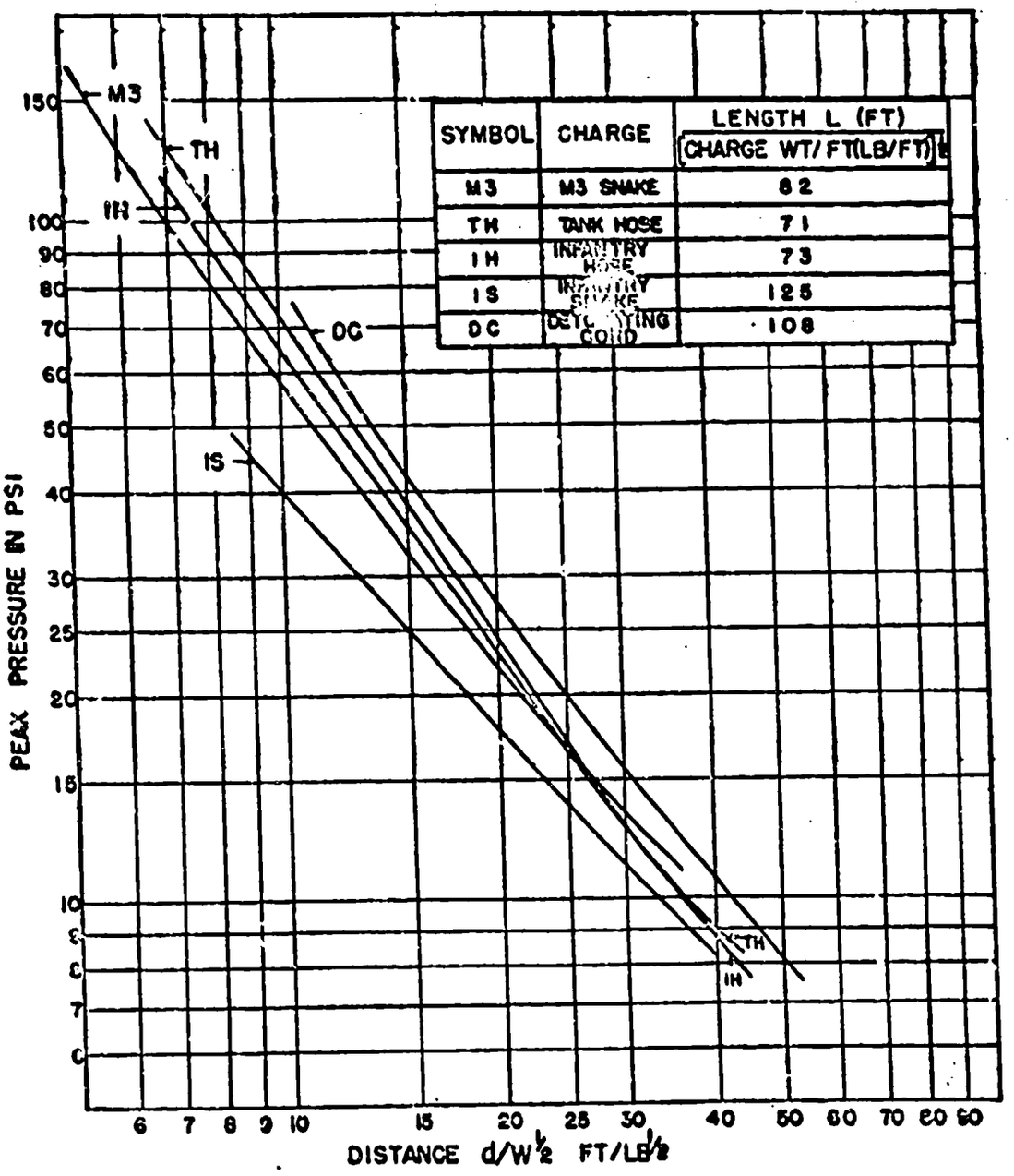

FIGURE 29. Peak pressure versus distance for line charges.

responsible for the effect. Another hypothesis is that earth-borne shock is responsible; the skip effect is not observed with air-burst point charges.

EXPERIMENTAL PEAK PRESSURE AND POSITIVE IMPULSE VERSUS DISTANCE CURVES

Blast pressures and positive impulses were measured along the perpendicular bisectors of several of the line charges mentioned above.[100] In Figures 27 and 28 these results are plotted as functions of distance from the charge. In Figures 29 and 30 the same results are represented on a reduced scale by dividing the distances and positive impulses by the square root of the charge-weight per foot, in each case. The ratios of lengths of charge L (ft) to square root of weights

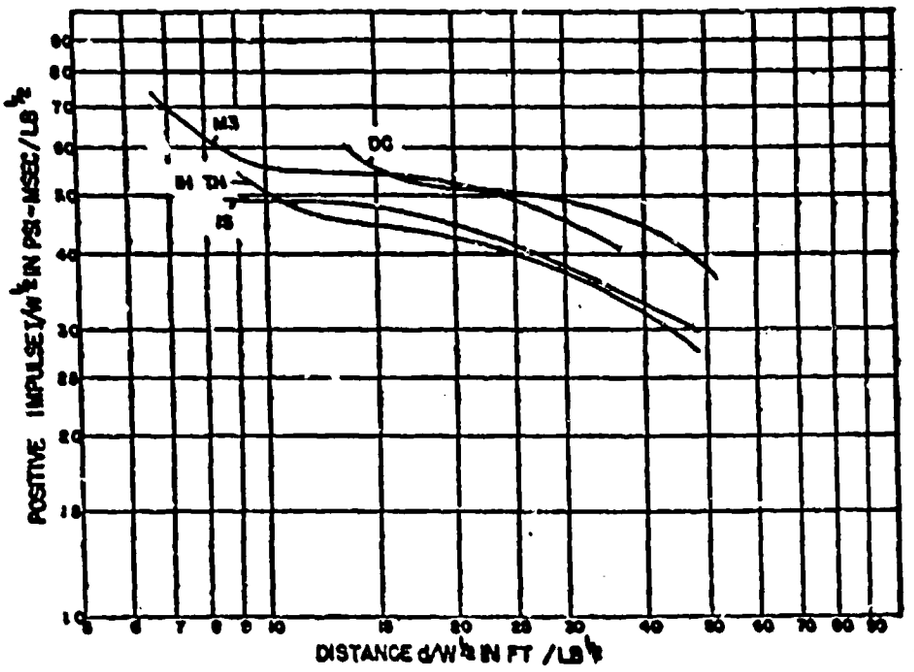

FIGURE 30. Positive impulses versus distance for line charges.

per foot, W^l (lb per ft)^l are indicated for each charge. In Table 5 the data on the physical properties of the line charges used are listed.

British measurements[218,219] have shown that, over a great part of the length of the line charge, the pressures and impulses measured along lines perpendicular to the charge are independent of the position along the charge. Near the ends of the charge, however, this is not true.

TABLE 5. Dimensions and weights of line charges.*

Charge	Explosive	Wt exp. per foot (lb/ft)	Length (ft)	Case material	Case wt per foot (lb/ft)
Detonating cord	PETN†	0.078	30	Fabric	0.032
Infantry snake	TNT/NG 93½/1½	0.64	100	Magnesium alloy	0.54
Infantry hose (1-in. hose)	EL389B‡	0.47	50	Impregnated Fiberglas	0.040
Tank hose (3-in. hose)	EL389B‡	4.5	154	Impregnated Fiberglas	0.15
M3 snake	Amatol 80/20	14.4	320	Aluminum	0.4

*The lengths of charge, weights, etc., are those used in blast measurement tests.[186] In actual weapons, other lengths may be used, as well as inert sections which do not contribute to the blast.

†Thirteen strands of Primacord detonating fuse contained in a woven, impregnated outer jacket. Pentolite 50/50 is more commonly used as an explosive filling for the detonating cord.

‡EL389B has the composition: nitroglycerin (NG) 60.0%, DNT oil 27.6%, TNT 11.5%, stabilizer 0.6%.

The application of the square root scaling principle to the 1- and 3-in. liquid-filled hose was found to be roughly applicable. Since the charges were not infinitely long, it was necessary also to scale the lengths of the charges in the same way, i.e., to keep $L/W^{\frac{1}{3}}$ fixed. That the blast pressures and impulses from charges of all types do not fall on the same curves when the impulses and distances are reduced by the square root of the charge-weight per foot (see Figures 29, 30) is due to a combination of the effects of different values of $L/W^{\frac{1}{3}}$, different charge-weight ratios, different explosive fillings, and different cross-sectional shapes of charge. Experiments show that, for pressures measured opposite the center of the charge, $L/W^{\frac{1}{3}}$ is essentially "infinite" if it is greater than about 80 $ft^{\frac{1}{3}}/lb^{\frac{1}{3}}$.

A remarkable feature of the impulse versus distance curves is the inflection in slope. There is a range of distance from the charge over which the impulse changes very little; this is predicted by the theory.[191] No quantitative comparison with the theoretical prediction can be made because of unknown effects of the differences in filling, case, and shape, and because the

theory applies to detonation in free air, whereas all of the line charges were fired on the ground. An approximate estimate of the ground-level values for TNT from the theoretical results for free air can be obtained by computing the pressures and impulses from twice the weight of charge.

There are several methods by which the effectiveness of the line-charge weapons can be increased. Almost any explosive gives greater blast than amatol 80/20. For example, aluminized explosives might increase the width of cleared path by about 30 per cent or possibly more. The skip effect might also be reduced with superior explosives. The case-weight should obviously be held to a minimum; the M2A1 snake, made with steel plates, is less effective than is the M3 snake, which is made with aluminum; the latter has a total weight 3,000 lb less. Utilizing air burst, if it were feasible, would also increase the effectiveness of line charges, as has been shown by experiment.[220]

The theory[213-216] can be applied to predict the clearance of certain mines calibrated against the universal indicator mine, as well as to the TMi-43 indicator mine. In Table 6 a few predictions so calculated are compared with experimental results. Although the theory gives good agreement with experiment for point charges, it predicts too wide a cleared path for line charges; the fault may lie with one of the simplifications of the theory, namely, that the pressure-time curve can be considered linear. Experiment[100] shows that, in the region of interest, the pressure-time curves are more nearly exponential than linear.

The use of line charges, such as sections of M3 snakes, has been proposed as a demolition device to be used against defended towns: it was suggested that charges could be pushed into streets by tanks and detonated after withdrawing the tanks. Computations of the expected areas of damage from these devices using the impulse criterion for blast damage indicate that the line charge, so used, would have a higher MAE per ton, than would ordinary bombs using the same filling. This, however, is not ordinarily an economical method of delivering explosive.

2.4.9 The Effect of Atmospheric Pressure on Peak Pressures and Positive Impulses

Almost all measurements of blast pressures have been made at elevations not far above sea level. Some uses for explosives, however, might involve the detonation of charges far from sea level, and consequently at low atmospheric pressures. That both temperature and pressure affect the propagation of blast waves is known from dimensional arguments. Expressions have been obtained for such effects.[221]

The theory of propagation[181] of shock waves from explosive sources in air and water has been applied to the propagation of blast waves in regions where atmospheric pressure and temperature were different from those at sea level.[222] It was assumed that the energy delivered by the explosion to the atmosphere was the same at all altitudes. It is predicted that both peak pressure and positive impulse are less the greater the altitude; the change of shapes of the pressure-distance and impulse-distance curves were computed.

The blast measurement groups of the SOG at Tulsa, Oklahoma, measured the blast from charges fired at three elevations above sea level: 650, 6,600, and 14,100 ft, in order to determine the effect of atmospheric pressure on the pressures and impulses from three kinds of explosives; tritonal, TNT, and blasting gelatin were used.[91] Blast measurements were made at four distances from the charge in free air. Within the experimental error, it was found that the effects of changes in atmospheric pressure on peak pressure and positive impulse are independent of distance from the charge and nature of the explosive, and that the results are not significantly different from theoretical prediction.

TABLE 6. Comparison of clearance of indicator mines with that predicted by theory.

A. Point charges[213] TMi-43 indicator mine.

Charge	Depth of burial (in.)	Distance for 50% clearance (ft) Observed	Computed
AN-M[illegible]-2 (89-lb TNT)	3	21	26
	4	19.5	19
	6	14	17
Bare TNT, 8-lb	4	3.7	4.5
Bare TNT, 64-lb	4	17	18.5

B. Line charges[214] Universal indicator mine

Wt of charge (lb/ft)	Depth of burial (in.)	Distance for mine reading equal to 0.080 in. (ft) Observed	Computed
4.5	2	28	37
	4	23	32
	6	20	26
10	2	28	62
	4	25	56
	6	22	52
15	2	30–53	72
	4	36–45	74
	6	28–37	69

The effects of the atmospheric pressure on the blast, expressed as the average peak pressures and positive impulses relative to those near sea level are given in Table 7. The theoretical predictions for cast TNT are also included for comparison.

Although the experiments showed no significant differences in the effect of altitude on pressures and impulses depending upon the nature of the explosive or gauge-to-charge distance, the theory predicts that over a very wide range of distance (much wider than that in the experiments) the effects depend upon both the kind of explosive and the distance from the charge.

TABLE 7. Effect of atmospheric pressure on peak pressure and positive impulse.*

Altitude	6,600 ft.		14,100 ft.	
Average atmospheric pressure (in. of mercury)	24.43		18.04	
Average temperature (F)	76		38	
	P_2/P_1	I_2/I_1	P_3/P_1	I_3/I_1
Experimental[91]	0.93±.026	0.97±.039	0.87±.038	0.87±.027
Theoretical[222]	0.90	0.93	0.82	0.87

*Subscripts refer to elevation (ft) above sea level: 1 = 650 ft, 2 = 6,600 ft, 3 = 14,100 ft.

2.4.10 Miscellaneous Experimental Results

THE EFFECT OF CHARGE SHAPE ON THE BLAST

Most explosive charges of military importance are not spherical in shape, and for some applications, it is important to know the blast intensities in all directions from the charge. Unfortunately, very few studies have been made of the blast pressures in various directions around charges; comparisons of explosives, for example, have usually been based upon measurements along lines perpendicular to the axis of the charge, i.e., approximately in the plane of its equator.

In one series of trials, the ARD[223] measured the blast in various directions around 500-lb MC bombs which were supported with their axes horizontal a few feet from the ground. It was concluded that over the range of measurement (which was from 30 to 80 ft from the bomb) the pressure and impulse versus distance curves were not significantly different in different directions.

That the blast pressures (and impulses) are not equal for all orientations around the charges for some charge shapes, was demonstrated for rectangular blocks of TNT,[224] and for cylindrical charges of various explosives[93] in which two proportions of cylindrical height to diameter were used. These measurements were made at distances roughly corresponding to those in the bomb trials mentioned above (i.e., after allowing for the difference in weights). Although the effects varied considerably, depending on the explosive used, in general it was found that the blast pressures and impulses measured opposite the base of the charge were greater than those opposite the "side," when the charge was a squat cylinder having a diameter equal to twice its height.

Another series of trials,[225] using German 1,000-kg bombs of elliptical cross section, showed that the blast measured perpendicular to the major axis of the charge was more intense than that perpendicular to the minor axis.

These blast measurements for bombs and small charges were made at relatively great distances from the charge, and, in many cases, asymmetries in the pressures were found as described above. Other measurements[226] of flame velocities very close to the charge (from which pressures could be computed) showed a marked asymmetry when cylindrical charges were used. Photographs of the shock wave[48] close to cylindrical bare charges with flat ends showed complicated wave patterns, which were interpreted as the interactions of the shock waves from the cylindrical and plane parts of the charge. Several shocks could be observed, particularly off the corners and base of the charge. In the measurements of blast pressures opposite the base of cylindrical charges[94] the pressure-time oscillograms exhibited second and even third shocks closely following each other in the positive phase, in addition to the initial peaks. It can be inferred that these extra shocks correspond to the shock waves photographed very close to the charge.

There is need for further work along these lines. The evolution of the shock waves from charges of several shapes, beginning at the surface of the charge and extending to large distances from it, should be studied systematically.

THE BLAST MEASURED NEAR THE BREECH OF A ROCKET LAUNCHER

Blast pressures were measured[227] near the jets from 5-in. spin-stabilized rockets in order to provide data that could be used in designing the mountings of such launchers on aircraft and other vehicles. It was thought that the air blast caused by the jets might be responsible for damage to exposed aircraft surfaces, for example.

These measurements were made at various distances

behind the breech, and 6 to 12 in. off the axis of the launcher. One gauge, placed on the axis, and about 10 ft behind the breech, recorded about 0.4 psi; the highest pressure measured was about 1 psi. The pressure-time records consisted of high-frequency (about 6- to 10-kc) oscillations enduring for 100 msec or more. These oscillations were interpreted to be due to turbulence surrounding the jet.

The Blast from Model Igloo-Type Explosive Storage Magazines

The problem of storage of large quantities of high explosives became very acute at the end of the war. Existing magazine facilities were inadequate, and construction of new magazines would require greatly increased storage areas, if the previous standard intermagazine distances were to be used.

On behalf of the Army-Navy Explosives Safety Board, tests of the effects of full-scale magazine explosions on adjacent magazines were carried out at Arco, Idaho, in the autumn of 1945. Blast-pressure measurements, as well as many other types of measurements, were made. "Target" magazines, placed at the standard spacing, as well as at proposed closer distance from the exploded magazines, were found to survive the blast. In order to study further the characteristics of explosions of igloo-type storage magazines, one-tenth scale model tests were carried out later at UERL.

Reinforced concrete model igloos were constructed at the University of Illinois[228] under contract with Division 2, NDRC, and were tested by UERL.[a] In one test the igloos were arranged in a manner closely patterned after that used on the full-scale tests, and blast-pressure measurements were made. It was found that the blast pressures measured in these model tests were in good agreement with those of the full-scale tests, using the cube root scaling law. However, the damage to target magazines was more severe in the model tests than in the full-scale tests. Although this difference might have been due to failures to conform to the model laws or to differences in the construction details of the model and full-scale igloos, it is also possible that the greater damage in the model tests was due to a difference in the type of soil, with corresponding difference in the earth shock transmitted.

The model tests demonstrated that the effect of the earth cover on an exploded magazine is to reduce greatly the air blast from the explosion of its contents. Tests simulating the piling of explosives in earthen revetments demonstrated that the revetment afforded little, if any, protection to adjacent igloos from the blast. The shape of the pile of explosives simulating that in an igloo (a long narrow pile), and also arranged in a revetment in a less elongated pile, was found to affect the distribution of blast pressure around the charge. The pressures measured opposite the middle of the elongated pile were higher than those obtained opposite the side of the shorter pile. The presence of an earth cover, in other tests, also affected the asymmetry of the blast; the blast from the uncovered end with the door was found to be considerably more intense than that from the thickly covered rear. These observations might be useful in so arranging magazines that the strongest part of a target igloo is opposite the part of its neighbor from which the greatest blast intensity is expected.

The probabilities of certain types of chains of sympathetic detonations in a magazine field have been computed for various probabilities that one magazine could be sympathetically detonated by the accidental explosion of a neighboring magazine.[230] It was concluded that, in a two-dimensional uniform array of magazines, if the chance that a single transfer will take place are one in five, say, the probability that no more than four magazines will explode is not less than 0.53. The dying out of chains of sympathetic explosions in a magazine area cannot be counted upon as an insurance that no catastrophe will occur if the magazines are arranged uniformly in two dimensions.

2.8 SOME PROPOSALS FOR FUTURE WORK

The foregoing account of the theory and experiments dealing with air blast from explosives clearly shows that there is need for more work in this field. A few lines of investigation which seem necessary to improve existing knowledge of shock waves in air are indicated in the following.

The applicability of the cube root scaling to point charge explosions and of square root scaling to line charges should be thoroughly studied, and, if these scaling principles are found not to be strictly applicable, the causes of this failure should be investigated. This involves determination of the peak pressure and positive impulse versus distance curves over a wide range of distance from the charge and for a wide range of charge-weights.

The afterburning phenomenon should be studied further, and an attempt should be made to obtain com-

[a] These results have not yet been formally reported. An informal report on one test is in reference 229.

plete detailed information on the chemical processes that occur and the basic principles involved. Afterburning should be studied using a variety of explosives.

The effects on the blast of the shape of the charge, of the weight of case and of the material of which the case is made should be investigated, using a variety of explosive fillings.

Comparisons with theoretical predictions of blast from explosive charges should be made, using both point and line charges, the measurements being made sufficiently close to the charge to test the existence of predicted maxima in the impulse versus distance curves.

The pressures and impulses in all directions from line charges should be measured, and the effects of length of charge, cross sectional shape, and weight and material of case on the blast should be investigated.

The properties of the negative phase (suction) from both point and line charges should be studied. The origin and properties of the "secondary" peak which is usually observed at or after the positive duration time should also be investigated.

The measurements of pressures and impulses from shocks obliquely reflected from plane surfaces should be continued and extended to include the whole experimentally accessible region around an air-burst charge. Photographic studies of the reflections of shocks should be pursued further.

The refraction of shock waves around corners should be explored, and the particular applications of this information to evaluation and design of protective barricades and to the penetration of blast into holes and slots should be made.

The reactions of simple systems under blast loading should be investigated and theoretical work should go hand in hand with the experiments. The ultimate purpose of such work should be to establish well-defined criteria by which weapon effectiveness can be assessed.

The subject of detonation in gaseous mixtures has been experimentally and theoretically attacked. Further work in this field, however, is needed. The air blast from gas-explosion sources should be measured.

New experimental techniques are needed for much of this work. The condenser-microphone gauge is very promising for application where the use of piezoelectric gauges is difficult. Methods of pressure-time measurement very close to explosive charges must developed. Apparatus for measuring transient temperatures and particle velocities would be very useful. Existing photographic techniques should be improved and such measurements as explosion flame spectra at high speed undertaken. New mechanical gauges would supply much needed apparatus for certain purposes.

These problems, and many others, have an obvious bearing on present or potential military applications. However, the study of air-blast phenomena should be undertaken, at least in part, with the point of view of acquiring a body of information which affords a really broad understanding of their nature and which provides sufficient factual basis for development of weapons in ways not now foreseen.

Chapter 3

EXPLOSIONS IN EARTH

3.1 INTRODUCTION

3.1.1 Object of the Investigation

THE PRIMARY purpose of the investigations described in this chapter was to determine the effect of subsurface explosions on massive underground structures, such as fortifications, in order to provide a rational basis of design for structures to resist such attack and also to disclose the possibilities of such methods of attack on enemy structures.* The investigation of these problems was undertaken by the Committee on Passive Protection Against Bombing [CPPAB] (later the Committee on Fortification Design [CFD]) of the National Research Council at the request of the Fortifications Section of the Office of the Chief of Engineers, U. S. Army. This section of the Office of Chief of Engineers is charged, among other things, with the design of field and coastal fortifications. Up to the beginning of World War II, coastal and field fortifications were designed to resist artillery fire. However, the advent of the long-range heavy bomber introduced an unknown element into the protection problem; namely, the effect of large quantities of high explosive detonated near to, or in contact with, the walls of a structure. The forces and their distribution about the structure are much different in this case from those produced by the impact of a projectile. Also, the probability of damage from a near miss by a bomb is much greater than that from a shell, even one of large caliber, since the shell carries a small amount of explosive compared to the bomb. A quantitative knowledge of the magnitude and duration of the forces imposed upon the structure by this form of attack is obviously very important to the fortification designer and was one of the chief objectives of the investigation. This information, once acquired, can obviously be used in reverse in order to formulate practical methods of attack on enemy installations. Some quantitative idea of the magnitudes of forces and the laws of propagation are essential to the planners of aerial attack on targets such as bridges, dams, and underground installations in order that adequate sizes of bombs and density of attack be used to insure a reasonable chance of success.*

If industries and military installations are in the future placed underground to protect them against even more destructive explosives than have been generally used, then the propagation of earth shock and its effect on structures becomes the primary concern of both the designer and the attacker of such installations.

3.1.2 Previous Investigations

Before 1939, essentially the only systematic investigations of the effect of underground explosions had been a study of the remote effects of quarry blasts, which had been undertaken by some explosive manufacturers and the U. S. Bureau of Mines in order to establish the limits of distance for certain varieties of superficial damage to dwellings.[3-7] These investigations have had very little bearing on the problems of military damage but may be more valuable when future problems of protection are considered.

In 1940 the problem of underground damage became of immediate and pressing interest to the British, who initiated a program of experiments to determine crater radii, earth movements, accelerations, and damage radii from bombs. These were more or less ad hoc experiments designed to furnish answers to pressing problems as they arose and did not attempt a systematic study of the phenomena. Considerable data were accumulated on the dimensions of craters and of the magnitudes of the earth movement, both transient and permanent, for various arbitrary depths of explosive charges.[8-16] A series of controlled experiments was carried out at full scale on the damage inflicted to underground piping and at a model scale on damage to buildings.[17,18] A survey of the state of knowledge at the end of 1941 concerning underground experiments is given in a report[19] containing some average curves for earth movement and wall damage as functions of distance and size of charge, together with an inference as to the validity of model laws for scaling results.

The British had, of course, collected a wealth of information on damage to structures from actual bombing incidents, but the complexity of these re-

*Pertinent to War Department Projects OD-03, OD-79, CE-5, CE-6, and to Navy Department Projects NO-12 and NO-263.

sults together with lack of knowledge as to the exact depth, point of impact, and frequently even the size of bomb, made correlation difficult and in some cases impossible. The interpretation of such data is aided greatly, of course, by a knowledge of the laws of variation of underground effects with distance, charge size, depth of charge, and kind of soil which can only be obtained by systematic experimentation.

2.13 The CPPAB-CFD, Division 2, NDRC Program

It became evident in 1941, during the course of American experiments on bombing of fortification elements, that considerable damage to a fortification might be caused by a near miss penetrating into the earth adjacent to the structure and exploding there. This observation was consistent with the experience of the British on damage to foundation walls derived from actual bombing incidents. Proposals for protection against such incidents by means of burster slabs and spaced walls were made and tried out at reduced and full scales. The results were sometimes quite unexpected and led to the conclusion that a systematic study of the phenomena occurring underground subsequent to the explosion of a buried bomb was necessary. The Humble Oil Company of Houston, Texas, at the conclusion of some discussions with members of the CPPAB voluntarily undertook to conduct some measurements on the transient displacements and pressures in earth at various distances from a buried charge of dynamite.[30] This work was preliminary in character and was mainly concerned with techniques of measurement of these quantities. The results were sufficiently encouraging to warrant the continuance of the work with the purpose of investigating the effects from larger charges, up to 1,000 lb of TNT.[31] The results from these tests were difficult to interpret because the charges of different weights were not buried at depths proportional to the size of charge and because, as was learned later, the soil in this locality had unusual transmission characteristics, coupled with the presence of a very shallow water table which gave an abrupt change of characteristics with depth. The results of these experiments made it clear that the phenomena were indeed complicated and that only a large-scale systematic test which followed the principle of investigating one variable at a time while holding all the others constant would yield the kind of data that would permit a quantitative evaluation of the influence of the various parameters. After certain preliminary programs had been carried out at the Princeton Station of Division 2 to investigate problems of instrumentation and choice of target types, a large program was organized for the systematic study of effects of underground explosions.

The objectives of these projected experiments were (1) to determine the magnitudes of the measurable physical effects from an underground explosion as functions of distance, depth, soil type, size of charge, etc., (2) to measure the damage inflicted on a target model as a function of these same quantities, and (3) to obtain, if possible, a correlation between (1) and (2) in such a manner as to permit predictions to be made as to the damage that might be inflicted by a bomb or other explosive charge under a given set of conditions. An additional objective was that of accumulating sufficient background information so that intelligent experiments could be planned for a particular problem if objective (3) could not be completely attained.

The magnitude of this program grew to alarming proportions as the final plans neared completion and it was decided to omit the investigation of the depth effect and to place all charges at the scaled depth expected to give maximum effects and damage as determined by preliminary experiments. The choice of a target model was attended by considerable perplexity but the problem was finally solved by the decision to use a target that simulated a structural element rather than a complete structure in the hope that analysis and application of the results would be facilitated. The target chosen was essentially a reinforced concrete box without top or bottom and with massive side walls. An extensive construction program was initiated at Camp Gruber, Oklahoma, under the supervision of the Corps of Engineers, designed to furnish a complete scale range of the selected type of target in order to determine, among other things, if any scale effect existed which would prevent the use of models to settle specific questions. It was essential in such a program, involving so much cost and labor, that as much information as possible be accumulated from each test, an objective that was greatly facilitated by the cooperation of the Geophysical Research Corporation of Tulsa, Oklahoma, and of the Humble Oil and Refining Company of Houston, Texas, in providing personnel and equipment for recording transient velocities, displacements, accelerations, and earth pressures. This equipment was in addition to the Mobile Oscillographic Laboratory[32] and personnel

provided by the Princeton University Station, Division 2, NDRC. The program involved the detonation of about 100,000 lb of explosive in units ranging from 8 to 3,200 lb per shot and the construction of over 50 target structures ranging in size from one-fifth to full scale. The full-scale targets had front walls of 5-ft thickness and 25-ft span, the other walls being identical in span but less thick. The experimental work started in August 1943, occupied about four months, and involved the taking of approximately 10,000 records which were equally divided between transient measurements and those taken after the shot. The analysis of these data was completed in June 1944, at which time a report on the tests and analysis was rendered to the Office of the Chief of Engineers.[23]

At this time (June 1944) the CFD ceased to exist and Division 2, NDRC, undertook to continue this research particularly along the lines suggested in the above-mentioned report; namely, investigating the effect of soil type and depth of charge and gauge on the results. This involved no change in personnel or policies, inasmuch as the relations between Division 2, NDRC, and the CFD had always been very close and the personnel of the Princeton Station had directed and carried out much of the previous work.

In order to carry out this second program, arrangements were made with the Humble Oil and Refining Co. to carry out investigations of the effect of charge and gauge depth in two radically different types of soil. One soil was the heavy clay found along the Gulf Coast of Texas and the other was loess, a light aeolian-deposited soil found in the vicinity of Natchez, Mississippi. Since the previous investigation had shown the model law to be obeyed, only one size of charge was used in this program (64 lb TNT). Concurrently with this work a parallel program was carried on at Princeton at a smaller scale to check the effects in a third type of soil. Also, a program of measurement of the comparative effectiveness of various kinds of explosives was carried out at small scale.[24] The experimental work in these programs was completed in July 1945 and the analysis of the data completed in November 1945.[25] The interpretation of the results is handicapped by the absence of any theory as to the propagation of explosion waves in a plastic material such as earth, but empirical analysis has succeeded in separating out fairly well the effects of the different parameters of charge and target geometry and the soil type from the data. A correlation with a simple theory of damage to structures has been made which gives the influence of some of the target and charge parameters on the degree of expected damage. (See also Chapter 15 of this volume.)

3.2 PHYSICAL PHENOMENA IN EARTH THAT ACCOMPANY AN UNDERGROUND EXPLOSION

3.2.1 Phenomena near the Explosion

Detonation of a charge changes its solid material almost instantaneously into an equal mass of gas at very high pressure which immediately begins to expand. This expansion imparts a high radial velocity to the earth particles adjacent to the charge and produces a high transient pressure in the medium. The high initial velocity of the earth carries it past the point of pressure equilibrium, due to inertia, so that after a certain time the motion is arrested and a reverse motion is imparted. If the pressure in the gas bubble were not relieved the pressure at remote points would reduce to a value equal to the permanent stress in the medium due to the presence of this sphere of high-pressure gas. There are two factors that tend further to reduce the final pressure; one of these is the cooling of the gas in the gas bubble due to thermal conduction to the medium and the other is the relief of pressure due to the break-through of the gas bubble to the surface of the earth, or to the leakage of the gas into the surrounding earth. If the charge is buried at such a depth that the gas pressure is quickly relieved by motion of the medium above the charge, the peak pressure will be reduced. This effect is illustrated in Figure 4, which shows the results of an experimental determination of the quantity called the coupling factor of the explosive charge as a function of its depth below the surface. If the charge is within a certain depth, called the camouflet depth, the material above the gas bubble will be thrown out and a crater will be formed. A large proportion of the earth will, of course, fall back into the hole, thus masking the true dimensions, but excavations of craters have shown that the sides at and below the depth of the charge are highly compressed and discolored from the action of the hot gases in the bubble.

3.2.2 Propagation of the Pressure Wave

Earth in the vicinity of the high-pressure gas bubble acts as a plastic rather than an elastic medium which means that Hooke's law is not obeyed and that the

strains are not proportional to the stresses. This characteristic of earth as a medium for the transmission of pressure waves is illustrated in Figure 1, which shows an experimentally obtained dynamic stress-strain curve for a certain variety of silty-clay soil

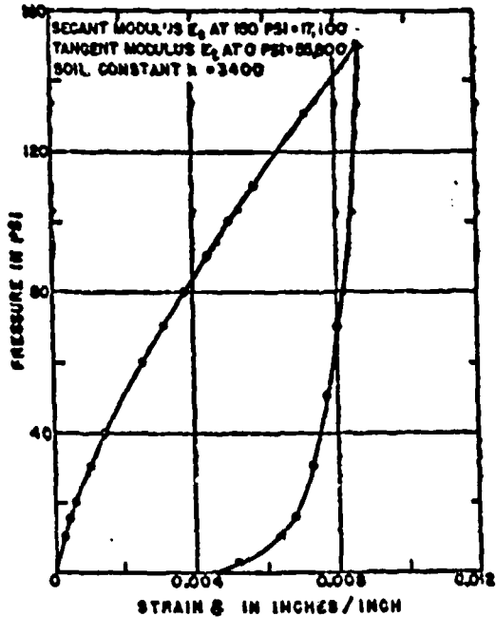

FIGURE 1. Experimental dynamic stress-strain relation for silty-clay soil.

found in Oklahoma. The net effect of this plastic behaviour of the medium is to cause pronounced distortion of the pressure wave as it is propagated away from the explosion. From the theory of wave propagation in solids discussed in Chapter 12 of this volume it is known that the velocity of an incremental pressure difference is proportional to the square root of the slope of the position it would occupy on the stress-strain curve, from which it can be readily seen that the velocity of the peak of the wave will be less than that of the initial part of the wave. The greater slope of the unloading portions of the stress-strain curve, except at very low pressures, indicates that the back of the wave has a higher velocity than the front.

The effect of these properties of the stress-strain curve is that the wave suffers a continual change of shape in the rear as well as the front. The peak is simultaneously retarded with respect to the front of the wave and eaten away by the more rapid rarefaction part following it. The low speed of the tail of the wave results in an overall spreading out of the wave in space and time in addition to these other changes. These effects are shown in a series of experimental pressure-time curves in Figure 2.

When these radial pressure waves meet the surface of the earth they are reflected with a reversal of phase. In practice, the wave is so spread out in time and space that this reflection is progressive and the reflected part subtracts from the compression wave below it to produce an increase of attenuation of the pressure with distance near the surface rather than a clear-cut incident and reflected wave. The boundary conditions at the surface require the existence of an

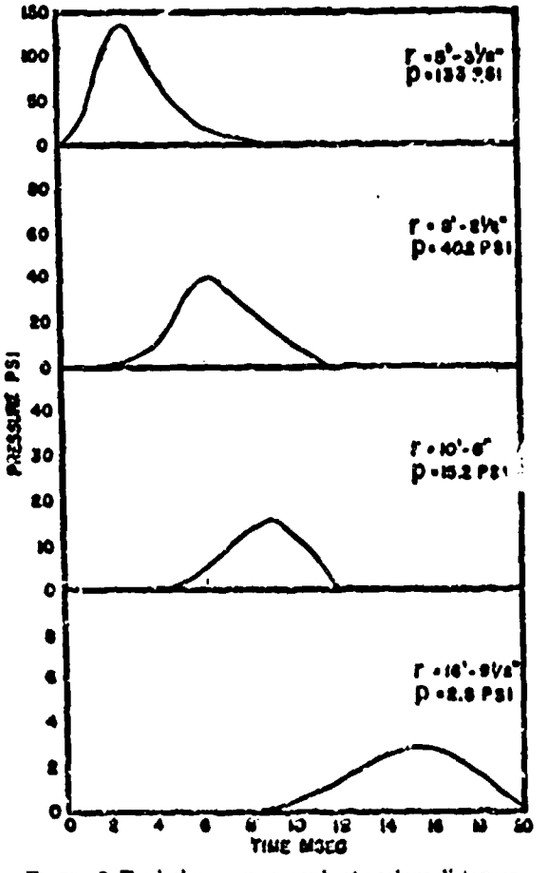

FIGURE 2. Typical pressure records at various distances from 8-lb TNT charges.

auxiliary set of surface waves, sometimes called Rayleigh waves. These waves travel at a lower speed and with less attenuation than the direct compressional waves and are responsible for the majority of surface effects at very remote distances from the explosion, such as window rattling and possibly plaster crack-

ing. The behavior of these waves is interesting from a theoretical point of view but since in the vicinity of the charge their magnitudes are negligible compared with the direct compressional waves, their importance in the study of military damage is minor. It may be that with large enough charges their effects at remote distances may move up into the military damage category but for normal explosives and bombs this is certainly not true.

3.2.3 Effect of Soil Characteristics

The magnitude of the transmitted pressure wave from an explosive charge is profoundly influenced by the properties of the soil through which it passes. Certain soils, such as wet clay, are very good transmitters of pressure while other soils such as silty loam and loess are very poor transmitters of pressure. The ratio of transmissibility between the two extremes may be as large as 100 to 1. This large ratio does not mean that the radii of damage from bombs in soil are in these ratios but, as will be shown later, these damage radii have a maximum ratio of approximately 2 to 1. The transmissibility of soil is expressed quantitatively by a number called the soil constant k, which is correlated roughly with the initial slope of the stress-strain curve and is ordinarily called the initial modulus of elasticity, although the material is plastic and not elastic. The magnitudes of other phenomena in the medium, such as particle velocity, acceleration, transient motion, and impulse, are found to be proportional to some function of this soil constant, which thus turns out to be the quantity that is most descriptive of the propagation qualities of the soil.

Referring to Figure 1, the stress-strain curve for a typical soil, one can deduce two facts, readily verified by experiment, which are (1) the finite area enclosed by the stress-strain loop implies that considerable energy is dissipated per unit volume of material so that the waves must be rather rapidly attenuated, and (2) the displacement of the point of intersection of the unloading curve with the abscissas of the graph implies that the medium is left with a permanent strain or displacement after the passage of the wave. If the material were elastic, the peak pressure would decrease as the inverse distance, while experimentally it is found that in earth near the charge, the permanent displacement and the peak pressure decrease in magnitude approximately as the inverse cube of the distance from the charge, indicating that the rate of energy dissipation in earth is very large.

The magnitudes of pressure, acceleration, and transient displacement near the crater may be very large. For example, in a typical silty-clay soil and for a 1,000-lb charge of TNT, the peak pressure near the edge of the crater may be 1,000 psi, while the acceleration is about 180 times the acceleration of gravity and the transient displacement may be as much as 4 ft.

The magnitude of pressure, acceleration, etc., inside the crater is not known except by inference, the reason for the uncertainty being the difficulty of making measurements in this region. Normally everything in this region is destroyed, including any equipment that may be placed there.

3.3 THE MODEL LAW

The model law, when referred to in connection with physical tests, is a term generally applied to a set of rules derived through dimensional reasoning by which the results of a set of properly designed experiments can be extended to larger or smaller scales of phenomena. The term *scale effect* has been somewhat loosely applied to any deviations from the model law that arise in an analysis of experimental results derived from models. The presence of such effects, which apparently do occur in some classes of experiments, such as those on projectile penetration discussed in Chapters 5, 6, and 7, greatly complicates the analysis of the results. Fortunately no such effects have been detected in underground explosion testing and the model law results can be extended with an accuracy as good as that of the original measurements.

If it is assumed that the velocity of propagation of the effect of an explosion in earth depends only on the stress and not on such quantities as the rate of deformation, then the effect of an increase in all dimensions of the experiment by the length scale factor S results in an increase of the time of propagation to an equivalent point by the same factor S. It is then possible to make a table (Table 1) in which any quantity such as pressure, impulse, velocity, etc., is represented by its dimensional components of mass M, length L, and time T, and to arrive at an expression for the relative magnitude of this quantity in the new system which is expanded in length scale by the factor S. In the present experiments $W^{\frac{1}{3}}$, the cube root of the weight of explosive charge in pounds, has been selected as being a length characteristic of the scale of the experiment. This may seem dimensionally misleading but it merely means that there has been chosen for reference a unit of length whose cube is

TABLE 1. Model law relations.

Quantity	Symbol and quantity in original system	Scale factor A	Quantity in the new system
Length	L	S	SL
Mass	M	S^3	S^3M
Time	T	S	ST
Force	F	S^2	S^2F
Pressure	P, p	1	P, p
Energy	E	S^3	S^3E
Velocity	u, v	1	u, v
Total impulse	I'	S^2	S^2I'
Impulse per unit area	I	S	SI
Displacement	D	S	SD
Acceleration	a	$1/S$	a/S

proportional to the weight or volume of the charge. Then if an experiment is performed with a charge-weight of W_1 lb and it is required to know the effects that would occur with a charge-weight of W_2 lb, the scale ratio $S = (W_2/W_1)^{\frac{1}{3}}$, and at the distance Sr, the magnitudes of the quantities in question can be determined from the original measurements at distance r multiplied by the factors given in the table. The model law, of course, tells nothing of the manner in which the quantities vary with distance but states only that if the effect is of magnitude E_1 in the experimental system at a distance r from the charge, then in the new system the effect will be AE_1 at a distance Sr from the charge, A depending on the quantity in question and being given in Table 1.

An example that illustrates the use of the model law is the comparison of the peak pressures produced by the explosion of 1 and 1,000 lb of the same explosive. It is assumed that experiment has shown that at a distance of 4 ft from the 1-lb charge the peak pressure is 80 psi. The length-scale ratio between the two cases is $(1{,}000/1)^{\frac{1}{3}} = 10$ and Table 1 shows that the scale factor for pressure is 1; consequently, at a distance of 40 ft ($= Sr$) from the 1,000-lb charge the peak pressure is again 80 psi. This is equivalent to the statement that if $r/W^{\frac{1}{3}}$ is the same for the two cases then the pressure is the same.

A comparison of the impulses per unit area I for these two weights of explosive at the scaled distances 4 and 40 ft is made in the same way, except that, from Table 1, the scale factor for impulse per unit area is S ($= 10$). Thus, if the impulse per unit area from a 1-lb charge at 4 ft is found to be 0.2 psi-sec then at 40 ft from a 1,000-lb charge the impulse per unit area is 2 psi-sec. This comes about by virtue of the fact that, although the peak pressures at these scaled distances are the same, the time scale of the phenomena is multiplied by 10, the scale *factor*, so that the duration of the pressure is increased tenfold. The impulse, being proportional to the product of pressure and time, must then be increased by a factor of 10 as indicated.

It will be noted in this chapter that most of the experimentally determined quantities have been represented by empirical equations which have as coefficients a constant, and various combinations of the parameters k, W, ρ, r, and λ which are identified in Table 2.

The manner in which these parameters enter into the empirical equations has been determined very simply by equating the dimensions on both sides of the equality sign. The variables were determined from physical considerations, but the manner in which they entered the equation was determined by dimensional considerations. The form of these equations was, of course, tested against the experimental data in each case and found to be correct to the first order of approximation. The test for correctness consisted in determining to what extent the dimensionless constant in the equation really was constant for widely varying values of the parameters.

TABLE 2. Parameters of the empirical equations.

Symbol	Name	Dimension	Units
k	Soil constant	$ML^{-1}T^{-2}$	Psi
W	Charge-weight	L^3	Lb
ρ	Soil density	ML^{-3}	Lb-sec^2/in.^{4} $= \frac{\text{lb per cu in.}}{\text{acc. } g \text{ (in./sec}^2\text{)}}$
r	Distance	L	Ft
λ	$r/W^{\frac{1}{3}}$	1	Dimensionless unit of distance from charge

This section would be incomplete without a specific mention of target and damage relations to the model law. One of the primary objectives of the experimental program was, of course, to determine the accuracy of the model law as applied to target damage. The chief cause of the initial uncertainty was the fact that there are certain things in nature that do not scale, the chief offender being the effect of gravity. By changes of density of component materials efforts to overcome this defect can be made, but it is not easy to find structural materials of comparable strength and with greatly different densities. Consequently, if gravity is a controlling factor in an experiment, modification of the model law must be made. It was found experimentally, as had been inferred but not proved, that the impulsive forces involved in the damaging of a massive structure are very large compared to gravity

forces, so that essentially no deviation from the model law was detected. The conclusion is then that structural dimensions can be scaled, at least over a factor of 5 and probably 10, without encountering any deviation from the model law as far as explosive damage is concerned.

4.4 THE CHARACTERISTICS OF EARTH

Earth as a transmission medium for mechanical effects is characterized as a nonelastic or a plastic medium. Its transmission properties vary with moisture content, grain size and shape, composition, history, and possibly other factors. These effects combine to make the properties with respect to local position variable with depth, location, and weather. A 25 per cent dispersion in the measured effects from individual shots in a small area is the best consistency that has so far been attained. Reliable results can only be obtained by taking repeated measurements and averaging the results. In a region with variable soil types the individual results may vary by a much greater factor than 25 per cent. However, if the average soil constant of that locale is determined by a seismic method (discussed later) the results will not diverge very greatly from the 25 per cent consistency level.

4.4.1 Wave Propagation

The nature of earth as a transmission medium can be most readily understood by an examination of the stress-strain curve for a typical silty-clay soil. This stress-strain curve, which is shown in Figure 1, was determined by dynamic measurement described in detail elsewhere.[1] This figure shows that the slope of the loading part of the stress-strain curve decreases with an increase of pressure while the unloading part of the curve decreases in slope with a decrease in the pressure. The result of such a shape of the stress-strain curve is to produce dispersion in the transmitted compressional wave in such a way as to prohibit the formation of a true shock wave. (See Chapter 12 for discussion of wave propagation.) This is because the decrease of slope at higher pressure levels corresponds to a lower propagation velocity for the peak of the wave than for the lower pressure levels. This is indicated by the equation

$$v(p) = \left(\frac{1}{\rho}\frac{dp}{d\delta}\right)^{\frac{1}{2}}. \qquad (1)$$

In this equation ρ is the density of the medium (weight per unit volume divided by the acceleration of gravity), p is pressure or stress, δ is strain, and v is the propagation velocity of the pressure level corresponding to the point where $dp/d\delta$ is measured; consistent units must be used.

This variable velocity causes a continual change of shape of the wave as it progresses away from the source as is discussed in the introduction to this chapter and in Chapter 12.

The area between the loading and unloading parts of the curve of Figure 1 represents the energy absorbed per unit volume of the soil passed over by the wave. This must cause an attenuation of the amplitude and energy of the wave as it progresses away from the charge. Calculations indicate that this energy loss is consistent with the experimentally determined rates of decay of pressure and displacement of the soil. The rate of propagation of the initial part of the wave, or of very small amplitude waves, is determined by the initial slope of the stress-strain curve. This corresponds to the velocity determined by seismic refraction shooting. The fact that there is a rough correlation between the soil constant and the propagation velocity indicates that the general shape of the stress-strain curve is preserved in many soils even though the magnitude of the soil constant varies over large ranges.

The density of the soil has only a small range of variation in comparison with the other parameters. The degree of compaction on the other hand has an appreciable effect on the stress-strain relation which, in a nonstratified medium, produces a continuous increase of velocity with depth. The effect of this continuous change of velocity is to produce a curved transmission path. This was experimentally found to be the case in thick beds of loess encountered in the vicinity of Natchez, Mississippi.[18]

The moisture in the soil is probably the most important variable and produces the greatest effect on the transmission of pressure. Moisture content can change rapidly with depth, particularly at the boundary of the water table. This rapid variation of velocity produces refraction and possibly reflection effects, although these latter have not been definitely separated out of the data. The velocity of transmission through a water-soaked soil may be appreciably higher than the velocity through water itself. This corresponding high transmissibility appears in the data as a very high soil constant for wet soils.

Another effect which appears to be a general one is the presence of a low-velocity layer very near to the surface of many soils. This effect is not thoroughly

understood but may be due to a layer of aerated and highly compressible soil near the surface which has inherently a low velocity, or it may be due to an upward bulging of the surface layer which retards the horizontal transmission of pressure. The attenuation of the pressure wave is greatly increased in this shallow layer, as shown by the fact that the exponent of the pressure-distance curve (discussed later) changes from —3 to —4 in this region.

A great amount of work has been done on the problem of predicting the soil transmission character from an examination of the grain sizes and distribution, together with moisture content. The samples used were obtained by test borings. Core samples have been taken and tested for moduli of elasticity under rather careful control,[21] but the correlation of these results and the transmissibility of the soil as measured by explosion trials have proved very poor. It may be that the act of removing the soil from its place, even if carefully done, completely changes its stress-strain characteristics from those obtained in situ. The correlation of directly measured results with those obtained by seismic refraction shooting is very much better.

The transmission properties of rock for very high pressures have not been studied with the same techniques applied in this work. Probably a systematic study would reveal many features common to both media; however, the closer approach to elastic conditions for rock would be expected to modify the results in many details.

8.5 EXPERIMENTAL METHODS

The physical effects, resulting from the detonation of an explosive charge underground may be divided into two classes: (1) transient effects which must be measured as functions of time, and (2) permanent effects which may be measured subsequent to the explosion.

The transient quantities are:

1. Pressure.
2. Impulse per unit area.
3. Particle velocity.
4. Particle acceleration. This may be measured directly or obtained by a time differentiation of 3.
5. Particle displacement. This may be measured directly or obtained by a time integration of 3.
6. Velocity of propagation of the pressure wave.

The permanent effects which may be measured after the explosion are:

7. Permanent earth displacement at or below the surface.
8. Crater size.
9. Damage to structures in the vicinity of the charge.

All of the effects listed with the exception of 6 and 8 can be measured on a structure underground, but the magnitudes of these quantities are determined by the characteristics of the structure as well as of the earth.

The methods of measurement of these quantities are in general quite straightforward, although in most cases very elaborate equipment is needed because of the necessity for the simultaneous measurements of many quantities. Simultaneity of the measurements is desirable because the inhomogeneous nature of the medium, earth, makes impossible the exact repetition of any experiment. To obtain good correlation between quantities it is very desirable to measure them all from a single shot. An example of the efforts made in this direction was the systematic measurement of 32 transient quantities per shot in the experiments conducted in Oklahoma. Of course, the results of many shots were averaged to obtain the performance of the soil and structures but a factor characteristic of each shot can be obtained as a result of the number of simultaneous measurements.

8.5.1 Testing Procedure

The general experimental procedure is to drill a hole somewhat larger than the diameter of the explosive charge to the appropriate depth, place the charge, and fill the hole with water or thin mud as a tamping agent. The pressure gauges are placed at the bottoms of smaller holes drilled to the proper depth and the holes filled to the top with water. A slightly different procedure has to be used for the velocity and acceleration gauges, since it is found that for consistent results these instruments must be cemented in place. The coupling to the earth appears to be variable unless this procedure is followed. This makes it extremely difficult to place these instruments at appreciable depths because of the recovery problem. For this reason almost all the measurements of particle velocity and acceleration were taken at depths ranging from 6 to 18 in. from the surface.

8.5.2 Transient Measurements

The transient mechanical effects are translated by an electromechanical gauge, characteristic of the par-

ticular quantity in question, into an electric charge or voltage which is amplified electrically and applied to a recording oscillograph. This may operate on either the electronic (cathode-ray) or the electromagnetic principle. The time rate of variation of most of the quantities in small-scale work is great enough so that cathode-ray oscillographs are desirable recording agents, but for large charges high-frequency electromagnetic or piezoelectric oscillographs may be used. The high-frequency requirements are less severe than are required for air-blast recording but the requirements at the low-frequency end of the spectrum are slightly more severe.

The records of the oscillograph deflections may be obtained on moving film or paper cameras, drum cameras with film or paper, or still cameras using a single sweep on the cathode-ray tubes. All these methods have been used, with film recording predominating for *cathode-ray oscillographs* [CRO] while paper recording is more often used for electromagnetic oscillographs.

Detailed descriptions of the apparatus used during the investigation reported here are given in published reports.[22,23]

The electromechanical gauges may in general be divided into three types; that is, (1) piezoelectric, (2) electromagnetic, and (3) variable-resistor gauges. A list of the measurable transient quantities together with the type of gauge used in its measurement is given in Table 3.

TABLE 3. Measuring instruments.

Quantity	Gauge principle
Pressure	Piezoelectric, variable resistor
Impulse	Piezoelectric, variable resistor
Particle velocity	Electromagnetic
Particle acceleration	Electromagnetic, piezoelectric, variable resistor
Particle displacement	Electromagnetic

The pressure gauges are of two types: (1) piezoelectric and (2) variable resistor of which the piezoelectric is the more successful, in general, although the variable-resistor gauges are more rugged and can be used closer to the explosive charge. The piezoelectric gauges are similar to those used in air-blast recording and consist of a stack of tourmaline crystals with appropriate electrodes and connections covered with a waterproof coating of rubber compound. Since these gauges are sensitive to hydrostatic pressure, no housing need be provided. The resistor gauges operate through the change of resistance of a coil of wire due to hydrostatic pressure. The coil of wire is housed in an oil-filled container to which the pressure is transmitted by a neoprene diaphragm.[22] This gauge is rugged but insensitive, the chief difficulty being the tendency of the oil column to be set into oscillation by a peaked pressure wave.

The particle velocity gauges operate because of the motion of a coil in a magnetic field, the generated voltage being proportional to the velocity of relative motion.[22] These gauges have been very successful, inasmuch as it is found that differentiation of their records gives values of acceleration consistent with direct measurements and the integration of the records gives values of displacement which are also consistent with directly measured values. Direct measurements of acceleration were made with piezoelectric and electromagnetic accelerometers[1] of which the piezo type is the more useful because of its ruggedness.

Transient displacement of the earth was measured by a coil on an inverted spring pendulum which was coupled to two coils excited in phase opposition. Displacement of the coil generates a voltage proportional to its displacement.[18] This instrument was quite successful, the chief difficulty being the necessity for accurate leveling and the change of damping constant with temperature. This was the only oil-damped instrument used, the others being electromagnetically damped.

Since all of the measured quantities, except pressure, are vector quantities, it is necessary to use all the instruments except the pressure gauges in pairs at each station, one to measure the radial horizontal component and the other to measure the vertical component. Only a single pressure gauge was used at each station. All piezoelectric gauges are subject to the vexatious effect of cable signal which is the spurious charge generated in the insulation of cables when put into motion. Special cables can be obtained in which the effect is reduced to a minimum; in addition, protection to these cables must be provided so that they are disturbed as little as possible by shaking and by falling debris. A cable manufactured by the British, called Telecon, seems to be the best so far obtained from the standpoint of absence of cable signal.

Broad-band amplifiers with very long time constants must be provided for the recording of the electric outputs of gauges, particularly the pressure gauges, since sometimes with big charges the effects

are of relatively long duration while for small-scale testing the times to the peak are frequently very short. These require cathode-ray oscillographs for their recording, but the particle velocities and earth motions are sufficiently slow for electromagnetic oscillographs of reasonably good frequency response to be used successfully.

The multiplicity of amplifiers and recording channels generally means that a special truck must be provided to accommodate the apparatus both in transit and in use.[22] A separate gasoline-driven power supply of good regulation is necessary to supply electric current to the apparatus.

3.6 RESULTS IN EARTH IN ABSENCE OF STRUCTURES

3.6.1 Variation of Peak Pressure in Free Earth

The pressure in earth from the detonation of an explosive charge on or below the surface is propagated as a wave that is characterized by a continuous change of shape and length with distance from the charge. (See Figure 2.) This change of shape is a result of the spherical divergence of the wave and of the character of the stress-strain relation of the medium which causes the higher pressures to be propagated more slowly than the low-pressure levels of the wave. (See Section 3.3 and Chapter 12.)

The magnitude of the peak pressure of the wave is determined by essentially five factors: (1) the distance from the charge, (2) the character of the soil, (3) the coupling of the explosive energy to the soil, (4) the kind and amount of explosive, and (5) the depth of gauge if it is less than a critical depth.

The general equation that is found to fit all the results obtained in the range of distances $2 \leq \lambda \leq 15$ is

$$P = FEk\lambda^{-n}, \qquad (2)$$

where P = peak pressure in psi.
$\lambda = r/W^{\frac{1}{3}}$ = distance in feet divided by the cube root of the weight of explosive charge in pounds.
k = a constant characteristic of the soil.
F = a coupling coefficient determined by the depth of burial of the charge.
E = an energy factor determined by the type of explosive.
n = an exponent whose value is determined by the depth of the charge or gauge.

The normal value of the exponent n is 3 except for depth of charge or gauge less than a critical value of approximately $\frac{1}{2}W^{\frac{1}{3}}$ ft. For depths less than this the exponent approaches the value 4. The cause of this increased attenuation near the surface is not very well understood but may be due to surface yielding or to a

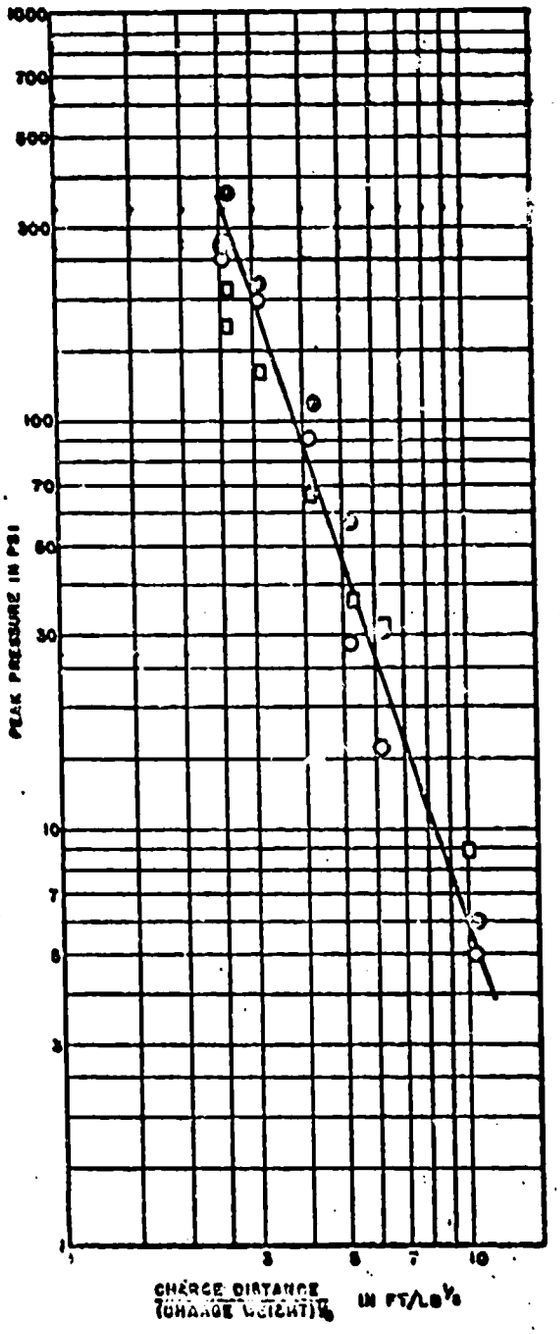

FIGURE 3. Peak pressure in earth as function of charge distance (1,000 lb TNT).

reflection of the pressure wave from the surface in the opposite phase which reduces the peak-pressure level as the distance from the charge increases. The value of 3 for the exponent at depths greater than this critical one is well established by many tests conducted in several different types of soil. Figure 3 shows the variation of peak pressures from 1,000-lb TNT charges as function of distance factor λ, obtained at Camp Gruber, Oklahoma.

The explosive factor E has been determined for several types of explosives[24] with the results shown in Table 4.

TABLE 4. Explosive factors for pressure.

Explosive	Explosive factor E
TNT	1.00
Amatol	1.04
Comp. B	1.04
Tritonal	1.17
Minol 2	1.34
HBX 2	1.39

For experiments using TNT, the explosive factor is unity and can be omitted from the equations. See Data Sheet 3B3 of Chapter 19 for summary of data on peak pressures in earth.

The coupling factor F is a function of the depth of burial of the charge and is shown in Figure 4 with the

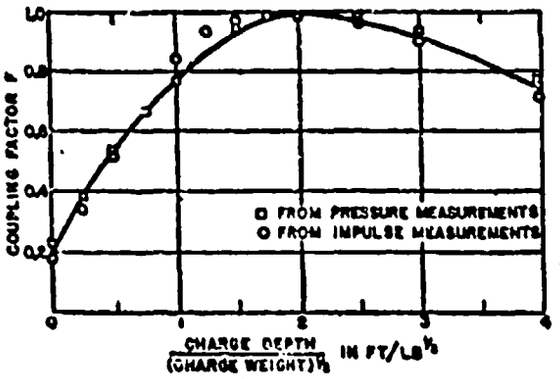

FIGURE 4. Explosive coupling factor as function of charge depth in clay silt.

abscissa in units of $d(ft)/W^{\frac{1}{3}}(lb)$. This curve seems to have a maximum value at a depth of burial corresponding to $d/W^{\frac{1}{3}} = 2$ and to fall off rather rapidly at smaller depths and rather slowly at greater depths. The reason for the lower value at the more shallow depths is apparently due to the escape of gases before the material of the medium near the explosion has reached the limit of its outward expansion. It is believed that for deeper gauges this fall-off at greater depths of charge will be more gradual or not even occur. No data exist to prove or disprove this point, however. The most striking feature is the almost linear rate of fall-off at charge depths less than the critical depth of $\frac{3}{2}W^{\frac{1}{3}}$ ft and the relative constancy for greater depth.

For charges of TNT buried at depths of approximately $2W^{\frac{1}{3}}$ ft and with gauges at a depth greater than $\frac{3}{2}W^{\frac{1}{3}}$ ft the equation for pressure as a function of distance reduces to

$$P = k\lambda^{-3}. \qquad (3)$$

This simple form of the empirical equation for variation of pressure with distance allows the transmission charactoristics of the soil to be expressed by a single parameter k, which is called the soil constant. If λ is taken as a dimensionless variable, then k has the dimensions of a modulus of elasticity. The range of values of k encountered in the experiments represents the variations in the soil if it is assumed that the same energy per pound of explosive is released at every shot. The assumption as to the constancy of energy release in a properly boostered charge is verified by other explosive tests. Any systematic variation in k with the weight of explosive charge would be evidence of the presence of a scale effect. No such variation is detected in any of the data.

The soil constant may vary over a range of more than 100 to 1, depending on the type and condition of the soil, whereas the coupling factor does not show a range of variation exceeding about 7 to 1. This fact indicates that the type of soil is the most important single variable governing the transmission of pressure.

TABLE 5. Soil constants for pressure as function of soil type and location.

Soil type	Location	k(min)	k(max)	k(avg)
Loess	Natchez, Miss.	400	1,700	800
Clay silt (loam)	Princeton, N. J.	1,300	2,500	2,000
Silty clay	Camp Gruber, Okla.	1,300	9,000	5,100
Clay, unsaturated	Houston, Tex.	10,000	20,000	15,000
Clay, saturated	Houston, Tex.	50,000	150,000	100,000

Table 5 shows measured values of the soil constant for different types of soil. See also Table 13 for a more extensive tabulation of soil constants based on measured seismic velocities.

The general variability to be expected in soils can be seen from the range of the maximum and minimum values of k given in Table 5 for each soil type. This range of variation is probably due to local conditions of moisture content and composition. The

largest variable other than the type of soil seems to be its moisture content, a factor varying in a somewhat unpredictable manner. In some localities the soil constant varies rapidly with depth (Figure 5). This has occurred in situations in which a shallow water table was present so that the moisture content and velocity of transmission varied over a large range quite near the surface.

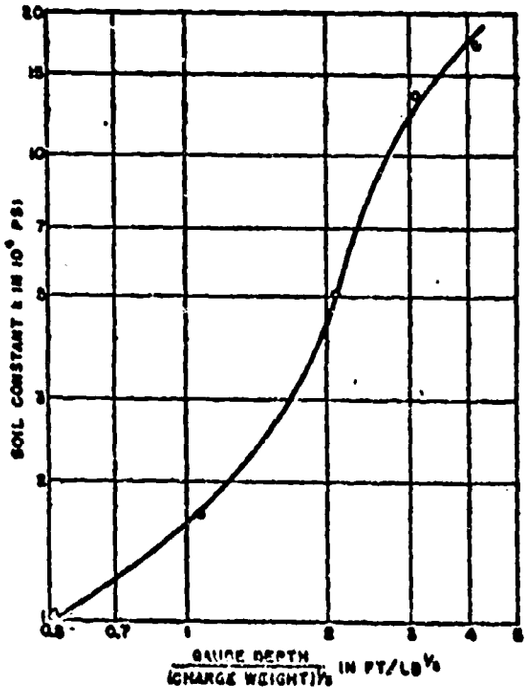

FIGURE 5. Variation of soil constant with gauge depth in Texas clay.

A correlation has been found between the soil constant k and the velocity of propagation of a seismic wave in the material. This is the velocity of a low-amplitude wave, corresponding to a sound wave in air, and is to be distinguished from the velocity of the peak of a finite wave. The initial slope of the stress-strain curve is associated with the velocity of very low-amplitude waves. The seismic velocity of these low-amplitude waves is obtained by shallow refraction shooting, using very small charges. This is a modification[17] of the technique used by geophysical prospectors in search for oil. Such explorations can be carried out very easily and cheaply compared to the direct method of measuring explosion pressures. The result of the correlation, which is accurate to the order of ±25 per cent, is

$$k = \tfrac{1}{32}\rho v^2, \qquad (4)$$

where k = soil constant in psi,

ρ = density of the soil = $\dfrac{\text{lb per cu in.}}{384 \text{ in. per sec}^2}$

v = velocity of seismic wave propagation in in. per sec.

This equation has been found to hold within an average accuracy limit of 25 per cent over a very wide range of soil types and values of the soil constant k.

These correlations indicate that the general shapes of the stress-strain curves are similar in all the soils measured so far. The basis of this statement is that the peak pressure and consequently the soil constant is governed by the shape of the overall stress-strain curve, while the seismic velocity is indicative only of the initial slope.

Exhaustive tests of soil properties at the site of explosion tests made by the U. S. District Engineer Office at Tulsa, Oklahoma, have shown no satisfactory correlation between transmission of explosion waves and the characteristics of the soil determined by the customary methods of soil mechanics.[18] It may be that the act of removing soil for test, no matter how carefully performed, disturbs its elastic or plastic properties enough to give questionable results. The site of the tests contains soils of an extremely heterogeneous character and the possibility exists that a more general study would yield positive results.

Tests in the field have shown that the peak pressure exerted against a massive target due to reflection will be about twice the pressure in free earth.[18]

3.5.2 Variation of Impulse per Unit Area in Free Earth

The positive impulse per unit area of a pressure wave in earth is the forward momentum carried by a unit cross section of the wave and is given by the time integral of the pressure up to the time T_0, at which the pressure falls to zero in the tail of the wave; i.e.,

$$I = \int_0^{T_0} p\,dt. \qquad (5)$$

Experimental determination of the impulse in free earth from the charge has shown that it obeys an empirical equation of the following form:

$$I = E'Fk'W^{\frac{1}{3}}\lambda^{-4/3} \qquad (6)$$

where I = impulse per unit area in psi-sec,
E' = explosive factor for impulse,
F = explosive coupling factor (Figure 4),
k' = a constant, characteristic of the soil type,
$W^{\frac{1}{3}}$ = cube root of the weight of charge,
$\lambda = r/W^{\frac{1}{3}}$ = distance in feet from the charge divided by the cube root of the weight of charge in pounds.

The explosive factors E' do not have the same values for impulse as for peak pressures. This is not surprising, since the impulse is more influenced by the behavior of the gaseous products after detonation than is the peak pressure. With one exception, the explosives fall in the same order of merit but with slightly different ratios. This is shown in Table 6.[24]

TABLE 6. Explosive factors for impulse.

Explosive	Explosive factor E'
TNT	1.00
Amatol	1.04
Comp. B	0.97
Tritonal	1.27
Minol 2	1.38
HBX 3	1.50

The explosive coupling factor F is the same as for peak pressure and is given in Figure 4 for the various depths of burial of the charge.

As in the case of peak pressure, if the explosive is TNT and the depth of burial is of the order of $2W^{\frac{1}{3}}$ ft, then the impulse per unit area can be expressed by the simple empirical equation:

$$I = k'W^{\frac{1}{3}}\lambda^{-2/3}. \qquad (7)$$

In this equation only one arbitrary parameter is present which may be associated with the transmissibility of the soil. The constant k' in this equation turns out to have a much smaller range of variation for different soils than does the soil constant k. Its measured values are given for different soil types in Table 7.

TABLE 7. Soil constants for impulse for various soils.

Soil	Location	k' (avg)
Loess	Natchez, Miss.	1.60
Clay silt (loam)	Princeton, N. J.	4.77
Silty clay	Camp Gruber, Okla.	5.44
Clay	Houston, Tex.	6.64

The impulse constant k' has also been found to be correlated with the soil density and the seismic velocity. The degree of correlation is not so good as for the pressure soil constant but still affords a rough guide to the magnitude of the expected impulse. The relationship between k', ρ, v, and k with a probable error of approximately ±35 per cent is:

$$k' = 1.15\rho v = 5.5\rho^{\frac{1}{2}}k^{\frac{1}{2}}, \qquad (8)$$

where k' = soil constant for impulse,
k = soil constant for pressure (Table 5),
ρ = density of soil (lb-sec^2 per in.^{4}),
v = velocity of seismic wave propagation in in. per sec.

It is obvious that such correlations can be no better than rough guides to the transmission qualities of the soil. Nevertheless, in the absence of any better tests, these correlations are very useful.

Consequently, equations (6) and (7) become:

$$I = 5.5E'F\rho^{\frac{1}{2}}k^{\frac{1}{2}}W^{\frac{1}{3}}\lambda^{-2/3}, \qquad (6')$$

and

$$I = 5.5\rho^{\frac{1}{2}}k^{\frac{1}{2}}W^{\frac{1}{3}}\lambda^{-2/3}. \qquad (7')$$

One would expect the impulse experienced by a massive target to be approximately twice the impulse in the incident wave. Experimentally, this ratio is found to be considerably more than 2, a phenomenon that has been explained qualitatively.[25] It comes about through the fact that the earth against the target may be left with a more or less permanent deformation which may exert a residual pressure of long duration. This residual pressure in the tail of the wave is included in integrating the pressure as a function of time, with the result that the impulse is considerably increased. This ratio of reflected to direct impulse has been found experimentally to average about 2.8 to 1,[25] but is subject to considerable fluctuation, since a relatively slight deflection of the target will relieve this residual pressure to a considerable degree.

Figure 6 shows the variation of impulse with distance from a 1,000-lb TNT charge. See Data Sheet 3B3 of Chapter 19 for summary of data on impulses in earth.

3.6.3 Variation of Particle Velocity in Free Earth

The maximum particle velocity of a wave is closely related to the peak pressure of the wave through the following equation (see Chapter 12 for further discussion),

$$u = \frac{1}{\rho}\int_0^p \frac{dp}{c(p)}, \qquad (9)$$

where u = the particle velocity in in. per sec,
p = pressure in psi,
P = peak pressure in psi,
ρ = the soil density = $\frac{\text{lb per cu in.}}{\text{acc. } g \text{ (in. per sec}^2\text{)}}$,
$v(p)$ = velocity of wave propagation in in. per sec as function of the pressure [equation (1)].

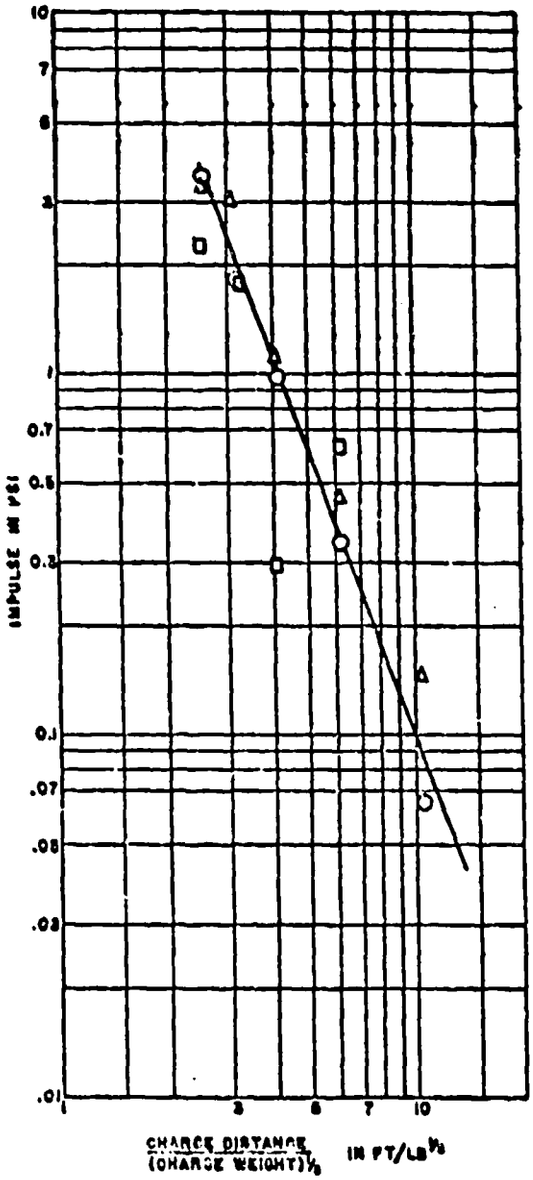

FIGURE 6. Impulse in earth as function of charge distance (1,000 lb TNT).

If the stress-strain curve is of the form indicated by experiment in clay-silt soil then the particle velocity can be expressed as

$$u = \frac{Bk^{\frac{1}{2}}}{\rho^{\frac{1}{2}}} \lambda^{-\frac{1}{2}}, \tag{10}$$

where k = soil constant for pressure in psi (Table 5),
$\lambda = r/W^{\frac{1}{3}}$ (ft/lb$^{\frac{1}{3}}$),
ρ = density $\left(\frac{\text{lb-sec}^2}{\text{in.}^4}\right)$,
B = numerical constant which has the theoretical value of 0.7 for this particular stress-strain curve.

The maximum particle velocity measured by instruments on the surface of the earth is complicated by a general yielding of the surface, the reflection of pressure waves from the surface, and by the presence of surface waves that are necessary to satisfy the boundary conditions at the surface. These effects combine to give a functional form to the empirical expression for this quantity that is somewhat different than the derived expression above.

In a particular series of tests these empirical results are:

$$u_h = 7{,}050\lambda^{-2} + 8.25\lambda^{-1} \text{ in. per sec}, \tag{11}$$

$$u_v = 3{,}200\lambda^{-2} + 9.85\lambda^{-1} \text{ in. per sec}, \tag{12}$$

where u_h is the maximum horizontal component of the radial velocity and u_v is the vertical component. Since the components differ continually in phase and amplitude, the maximum value of the radial velocity cannot be found by a simple vector addition of the components. The difference of the value of the exponent of the leading term from the theoretically derived value is ascribed to the influence of the surface effects upon the wave amplitude and rate of decay. This assumption has not been verified, however, because of the extreme difficulty of measuring the particle velocities at appreciable depths below the surface. The expressions can be written in slightly more general terms since the average density and soil constant have been determined for the region in which these measurements were taken. Here $\rho = 0.00015$ lb-sec^2 per in.^{4} and $k = 5{,}100$. Then:

$$u_h = \frac{k^{\frac{1}{2}}}{\rho^{\frac{1}{2}}}(1.2\lambda^{-2} + 0.0015\lambda^{-1}) \text{ in. per sec}, \tag{13}$$

$$u_v = \frac{k^{\frac{1}{2}}}{\rho^{\frac{1}{2}}}(0.55\lambda^{-2} + 0.0017\lambda^{-1}) \text{ in. per sec}. \tag{14}$$

Figure 7 shows experimental data on particle veloc-

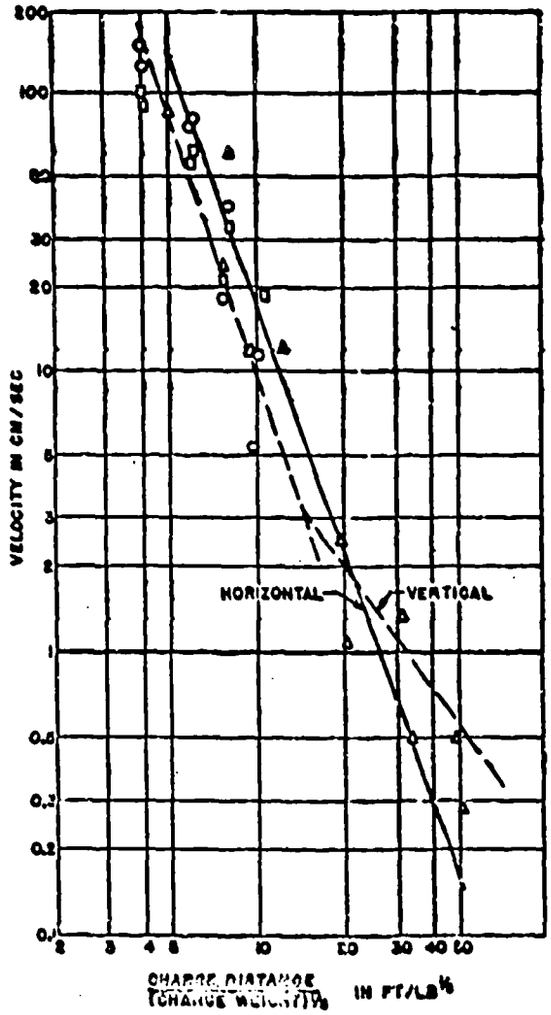

FIGURE 7. Maximum particle velocities in earth as functions of charge distance (64 lb TNT).

ity as a function of distance for 64-lb TNT charges.

This graph and the empirical formulas give the experimental values of the particle velocity at the surface resulting from the explosion of a charge of TNT buried at a depth of $2.1W^{\frac{1}{3}}$ ft beneath the surface. Unfortunately, no data exist concerning the manner of variation with depth of burial of the charge or with type of charge. It is believed that these quantities are affected by the depth of burial in somewhat the same manner as the pressure, since there is a direct theoretical relationship between pressure and particle velocity. In the absence of measured data then, one would apply the coupling factors and explosive factors to the particle velocity in the same manner as for pressure in order to obtain the most probable values for conditions other than those for which the data were taken.

The theoretical value of the maximum particle velocity is appreciably less than that experimentally determined at the surface. This discrepancy is in the right direction since a reflection from the surface would be expected to give the surface particles a higher velocity than that predicted for particles at depths not affected by surface reflections.

3.6.4 Variation of Particle Acceleration in Free Earth

An extensive series of measurements in one location gave particle accelerations near the surface resulting from the detonation of charges of TNT buried at depths $2.1W^{\frac{1}{3}}$ that can be expressed by the empirical equation[28]

$$a_g = \frac{k}{\rho W^{\frac{1}{3}}}(120\lambda^{-4} + 0.3\lambda^{-2} + 0.04\lambda^{-1}) \times 10^{-6}, \quad (15)$$

where a_g = horizontal or vertical acceleration in units of gravity (384 in. per sec^2),
k = soil constant in psi (Table 5),
ρ = soil density (lb-sec^2 per in.^{4}),
W = weight of explosive charge in pounds,
$\lambda = r/W^{\frac{1}{3}}$,
r = distance from the charge in ft.

This experiment also showed that the variation of acceleration with depth of burial of the charge is the same as the variation in peak pressure so that the coupling factor derived from pressure measurements may be applied to particle accelerations. It is also inferred, but not directly shown by experimental data, that the acceleration varies with type of explosive in much the same way as does the pressure, so that the explosive factors for pressure can be applied to situations in which explosives other than TNT are used (Table 4).

The acceleration is, of course, a vector quantity that must be specified in direction or by components along a set of axes. Experimentally it has been found that at the charge depth used the horizontal and vertical components of acceleration are approximately equal to each other at every distance. The angle of emergence of the acceleration vector is consequently at 45 degrees to the surface.

Figure 8 shows some experimentally obtained values of acceleration as function of distance for 64-lb TNT charges which were measured in the Oklahoma tests.

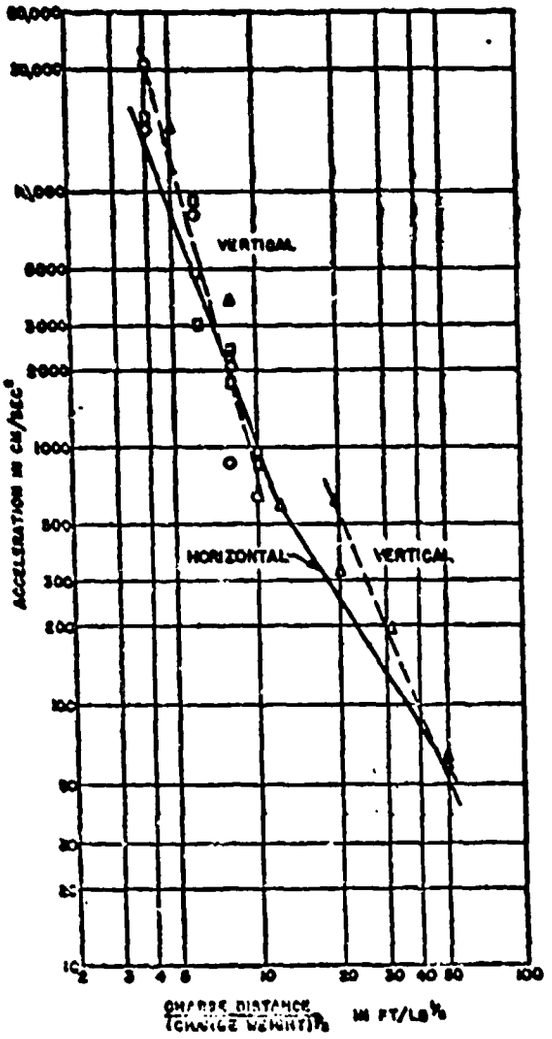

FIGURE 8. Maximum particle accelerations in earth as functions of charge distance (64 lb TNT).

8.5 Variation of Particle Displacement in Free Earth

The displacement of the particles in the medium due to the passage of a compression wave can be found by integrating the strain in each spherical shell over which the wave extends at the moment of maximum displacement. A first approximation is to assume that the maximum displacement of each particle occurs before appreciable negative velocity is attained by the particles. If this assumption is made, the displacement D at any radius r is,

$$D = \int_r^\infty \delta dr. \tag{16}$$

If one introduces the empirical pressure-distance and stress-strain curves, it is possible to derive an expression of the following form for the maximum displacement:

$$\frac{D}{W^{\frac{1}{3}}} = \frac{k^{\frac{1}{3}}\lambda^{-2}}{8} \tag{17}$$

where $\lambda = r/W^{\frac{1}{3}}$,
D = displacement in feet,
W = weight of charge in pounds,
k is given in Table 5,
r = distance in feet.

This displacement is presumably in a radial direction at depths below the surface.

The experimental values of transient displacement derived from direct measurement and from integration of the particle velocity-time records can be expressed by the following empirical equation:

$$D_h = W^{\frac{1}{3}}(3.94\lambda^{-2} + 0.0018\lambda^{-1}) \text{ ft (horizontal)}, \tag{18}$$

$$D_v = W^{\frac{1}{3}}(1.05\lambda^{-2} + 0.0027\lambda^{-1}) \text{ ft (vertical)}. \tag{19}$$

The maximum horizontal and vertical displacements at the surface are not necessarily attained simultaneously but, except at the greater distances, the displacements are approximately in phase. Then, approximately, at the near distances one finds the total transient displacement to be

$$D_r = 4W^{\frac{1}{3}}\lambda^{-2} \text{ ft}. \tag{20}$$

The value derived from equation (17), taking the average value of k to be 5,100, turns out to be:

$$D_r = 2.15W^{\frac{1}{3}}\lambda^{-2} \text{ ft}. \tag{21}$$

The ratio between these values is 1.86, which indicates that the assumptions made in the derivation are probably approximately correct. This rough derivation allows one to make estimates of the displacements for types of soil other than that in which the present measurements were made.

Experiment shows that the permanent horizontal displacement is approximately one-third the maximum transient displacement given by the equation above. This is slightly less than would be indicated by the stress-strain curve, but again the effect of the surface introduces a modifying factor so that direct predictions from the stress-strain curve would probably be somewhat in error.

If the dependence of displacement on the numerical value of $k^{\frac{1}{3}}$ [equation (17)] is accepted, then a plot of λ vs $(D/W^{\frac{1}{3}})(1/k^{\frac{1}{3}})$ can be made which would allow estimates of displacements in soils with different values of k. Such a plot is shown in Figure 9 with horizontal and vertical components shown separately.

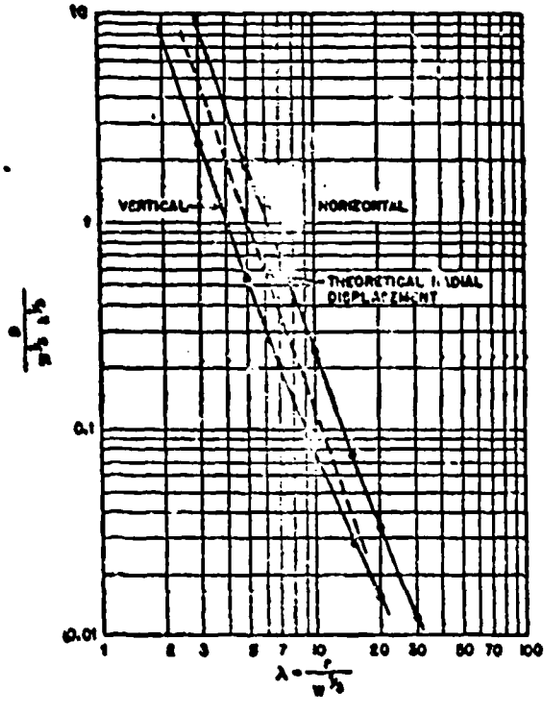

FIGURE 9. Transient earth displacements at surface as functions of charge distance. Displacement in thousands of feet, weight in pounds, distance in feet, k as in Table 5.

3.6.6

Crater Sizes

The size of the crater produced by a buried charge has been shown experimentally to be much less sensitive to type of soil and kind of explosive than to the depth of burial of the charge. The exact mechanism of crater formation is not understood well enough to allow any theoretical predictions to be made concerning the factors governing the size, but it has been demonstrated quite conclusively that the model law is obeyed and that predictions of size based on empirical data are reasonably reliable. (See Data Sheets 3B1 and 3B1a of Chapter 19 for diameters and depths of earth craters.)

The crater size can be considered to be equal to the product of an explosive factor E'', of a depth factor C, of a soil factor k'' (which equals $1.3k^{1/18}$), and of the cube root of the charge-weight, $W^{\frac{1}{3}}$.

The radius of the crater in feet is then

$$R(\text{ft}) = 1.3CE''k^{1/18}W^{\frac{1}{3}}. \qquad (22)$$

The explosive factors E'' for some military explosives are given in Table 8. The factors are ratios of the radius of crater produced with the given explosive to the radius of crater produced by TNT.

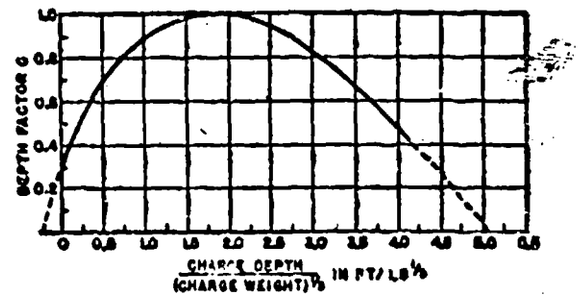

FIGURE 10. Depth factor for cratering by explosives.

The depth factor (Figure 10) varies over a wider range than do the others. It displays a maximum value at a charge depth of approximately $2W^{\frac{1}{3}}$ ft, descending quite sharply toward zero as the charge depth approaches zero. The decline with increasing charge depth beyond the optimum is slower, but an extrapolation of the measured part of the curve indicates that at about $5W^{\frac{1}{3}}$ ft the crater radius approaches zero with the formation of a camouflet.

Figure 11 shows types of crater and the approximate dimensions that might be expected from the explosion of a 500-lb bomb.[26]

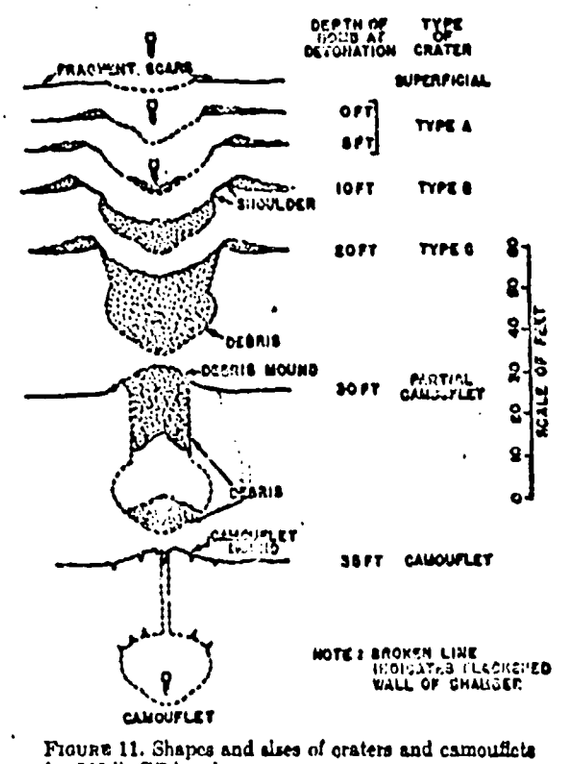

FIGURE 11. Shapes and sizes of craters and camouflets for 500-lb GP bombs.

TABLE 8. Crater radius as a function of type of explosive (ratios to TNT craters).

Explosive	$E'' = \frac{CR_X}{CR_{TNT}}$
TNT	1.00
Amatol	0.98
Comp. B	1.02
Tritonal	1.11
Minol	1.14
HBX 2	1.16

3.6.7 Comparison of Explosives

The orders of effectiveness of different types of explosives for the production of various underground effects have been given in various tables throughout the report, but it may be desirable to collect these results in one paragraph for convenient reference. Such comparison is given in Tables 9 and 10 where the values of peak pressure, impulse, crater radius and crater volume for the various explosives are compared to those for TNT at the same distance and depth of burial of the charge. The standard deviation of these ratios is approximately 5 per cent.

The comparison in Table 9 is on the basis of equal weights of the explosive charges. If the comparison is made for equal volumes, slightly different values, which are shown in Table 10, are obtained because of the different densities of the explosives. For comparison of effectiveness of bomb fillings, for example, where the volume is fixed, the comparison on an equal-volume basis is more useful.

3.7 DAMAGE TO BURIED CONCRETE STRUCTURES

From a military standpoint the physical phenomena in the medium, the laws of propagation, etc., are all subordinate to the degree of damage that will be produced under a given set of circumstances. The solution of this problem requires that satisfactory answers be obtained to two principal questions: (1) what are the magnitudes and durations of the forces acting on a structure and (2) what are the effects of such forces on a particular structure? These are extremely knotty questions, both of which involve a detailed knowledge of the behavior of structures under impulsive loads. The first and principal part of this chapter is concerned with the task of acquiring answers to the first of these two questions, and it is evident that no less effort must be spent on the answer to the second question. Some of these questions are treated in Chapter 15 of this volume. It is obvious that a complete answer would, in the limit, involve experiments with every conceivable type of structure which is, of course, an impractical procedure. It is equally obvious that some type of structure must be investigated experimentally in order to be able to make any predictions that are based on other than theoretical evidence.

3.7.1 Description of Programs

Two types of damage experiments were made. In the first of these, charges were detonated at distances

TABLE 9. Comparison of explosives (equal weights, equal distances).

Explosive	Peak pressure of X / Peak pressure of TNT	Impulse of X / Impulse of TNT	Crater radius of X / Crater radius of TNT	Crater volume of X / Crater volume of TNT
TNT	1.00	1.00	1.00	1.00
Amatol	1.04	1.04	0.98	0.95
Comp. B	1.04	0.07	1.02	1.07
Tritonal	1.17	1.27	1.11	1.39
Minol	1.34	1.39	1.14	1.47
HBX 2	1.39	1.50	1.15	1.51

TABLE 10. Comparison of explosives (equal volumes, equal distances).

Explosive	Peak pressure of X / Peak pressure of TNT	Impulse of X / Impulse of TNT	Crater radius of X / Crater radius of TNT	Crater volume of X / Crater volume of TNT
TNT	1.00	1.00	1.00	1.00
Amatol	1.08	1.09	0.99	0.97
Comp. B	1.12	1.05	1.04	1.14
Tritonal	1.33	1.47	1.16	1.55
Minol 2	1.44	1.51	1.17	1.60
HBX 2	1.49	1.53	1.18	1.63

from reinforced concrete targets greater than one crater radius; and the pressures, accelerations, velocities, and displacements on the target face and in free earth were recorded while the target damage was measured. In the other series of tests, charges were detonated in contact with the walls of buried, reinforced concrete structures. No transient effects were measured. Damage was recorded and correlated with size of charge and thickness of wall.

Damage from Noncontact Charges

The great variety in fortification structures makes it impossible to select a typical target for study. Consequently, it was decided to use a target that would represent a structural element, rather than a complete structure. It was believed that the results obtained would in this case be more definite and at the same time more susceptible to theoretical analysis. If this turned out to be true, then extensions of the analysis to more complex structures would be practical. The structure finally selected for study after an extensive series of preliminary tests at small scale on various structure types, was essentially a reinforced concrete box with open top and bottom, represented in Figure 12. The front and back were of different thicknesses, the latter being two-thirds of the front thickness. The side walls were of equal thickness and 0.42 as thick as the front. These targets were built in five sizes or scales, namely, 0.2, 0.4, 0.6, 0.8, and 1.0, the last being the so-called full-scale target, intended for use with a 1,000-lb charge. The reason for the large number of sizes was to determine whether or not a scale effect, or consistent variation of effect with size of target, could be found. The absence of such an effect would make the use of small, inexpensive targets practical and reliable.

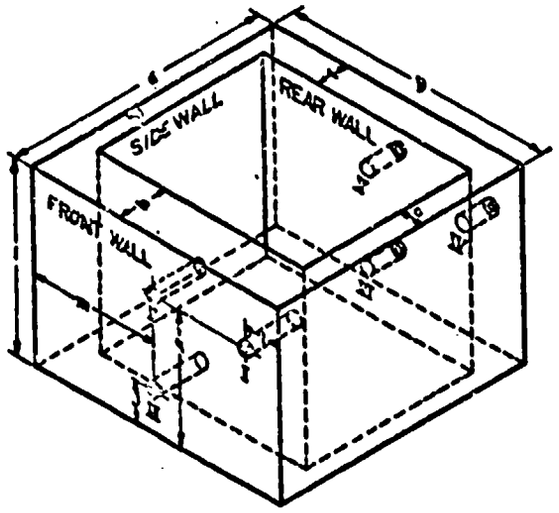

Figure 12. Dimensions of scaled concrete targets.

a	ft 2S8	i	ft 17.5S
b	ft 2S8	j	ft 4S
c	ft 2S	k	ft 12.5S
f	ft 3S	l	ft 3S
h	ft 5S	m	ft 12.5S

Gauge positions in rear symmetrical with front.

In all, 16 targets of the 0.2 scale, nine of the 0.4 scale, three of the 0.6 scale, seven of the 0.8 scale, and seven full-scale were constructed and tested. The magnitude of this project, which was carried out by the Tulsa District of the U. S. Corps of Engineers, can be visualized when it is realized that the full-scale targets were 25 ft on a side and 17 ft deep, with a front wall 5 ft thick and the other walls in proportion. The bottom of the target was 25 ft below ground level. The reinforcement of the full-scale targets consisted of a two-way mat of 1⅛ in. square deformed bars at 15-in. centers in each face of the front wall and comparable reinforcement in each of the other walls. The average compressive strength of the concrete used was about 3,400 psi, measured on 6-in. cylinders. More detailed information on target characteristics and resulting damage are given elsewhere.[28]

On each target there were mounted three piezoelectric pressure gauges on the front face and one on the rear face, by means of which pressures were determined as functions of time. It was found that the pressure exerted on the front face of such a structure is approximately twice that measured in free earth at the same distance, and that the impulse per unit area is approximately 2.8 times that in free earth. The fact that impulse is more than doubled (one would normally expect more nearly exact doubling) is believed to be due to the packing of the earth against the front face of the target, resulting in a more sustained application of pressure than in free earth at the same distance.

Thus, the pressure and impulse per unit area on a massive target in earth can be represented by the following expressions, provided normal explosives are used at depths of the order of $2W^{\frac{1}{3}}$ and at distances from the target between $2W^{\frac{1}{3}}$ and $15W^{\frac{1}{3}}$, both in feet:

$$P_r = 2kE\lambda^{-2}, \tag{23}$$

$$I_r = 15\rho^{\frac{1}{2}}k^{\frac{1}{2}}E'W^{\frac{1}{3}}\lambda^{-4/3}. \tag{24}$$

In the above equations P_r and I_r are the reflected peak pressure and impulse, k is the soil constant for pressure (Table 5), E and E' are explosive factors for pressure and impulse respectively (Tables 6, 8, 9, 10),

λ is $r/W^{\frac{1}{3}}$ (r is distance in feet; W is charge-weight in pounds), ρ is density of earth in lb-sec^2 per in.^{4} and averages 0.00015.

The term damage is qualitative and not susceptible to very definite measurement. A number of possible measures of damage were considered; among these the most significant are the total width of cracks in the front face and the amount of permanent bending of the front face. Both of these were used as measures of damage to the targets.

The testing procedure was to detonate a charge at a predetermined distance from the front target wall, and to measure the crack widths and deflections of the front face, the pressure and impulse on the front face, and the acceleration given to the target. Simultaneously, pressure, impulse, acceleration, and displacement were measured in free earth on the side of the charge opposite the target. Since the target is more or less damaged at every shot, it is apparent that only one set of measurements can be made on one target and that several targets must be used in order to obtain damage as a function of distance.

Damage from Contact Explosions in Earth

At the end of the test program described above the undamaged walls of the targets used in it were subjected to contact, earth-backed explosions. In addition, a series of tests on specially constructed targets was made at the same time. The latter tests were made at four scales on hollow reinforced concrete box structures with floors and roofs. The scales were 0.2, 0.37, 0.63, and 1.0. Three 0.2-scale structures were built and one each of the other sizes. The full-scale target was 47x47 ft in plan and 28 ft high. Its four walls were respectively 10, 11, 12.3 and 13.5 ft thick. The roof thickness was 9.5 ft and the floor thickness 4.75 ft. The other targets were in proportion. Reinforcing steel was arranged in mats and amounted to about 75 lb per cu yd. Concrete strength was 3,400 psi. The earth was excavated to about one-third the height of target and back-filled against the structure to its full height after construction. The full-scale structure was exposed to the effect of 2,000-lb *general-purpose* [GP] bombs (1,080-lb charges) exploded in contact at the center of each side. Underfloor explosions were also tried.

After each test the dimensions of cracks and the area of interior surface scabbing were recorded. From the latter it was possible to determine the so-called *scabbing limit* of concrete walls subjected to contact explosion with earth backing. A more complete discussion is given elsewhere.[28]

3.7.2 Representation of Results

Damage from Noncontact Charges

The results of this series of tests are best represented in a dimensionless plot showing either front-face crack width c or front-face deflection X_0 divided by a quantity of the same dimension, such as $W^{\frac{1}{3}}$, as a function of the important independent variables, namely, W, distance from charge, a factor characteristic of the soil, and factors characteristic of the target. The most

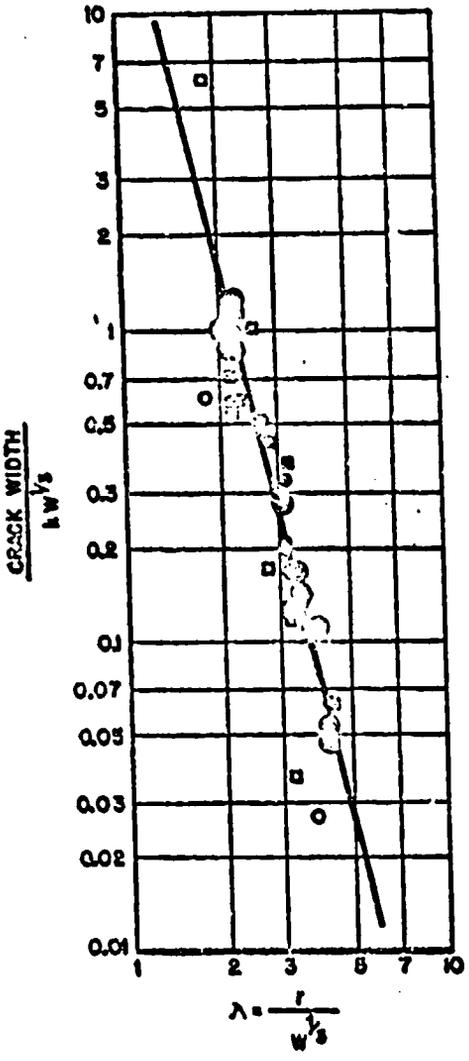

FIGURE 13. Total width of front wall cracks as function of distance and size of crater. Crack width in inches $\times 10^4$, weight in pounds, distance in feet, k as in Table 5.

important characteristic soil factor is k (Table 5). The charge distance is best expressed as $\lambda = r/W^{\frac{1}{3}}$.

Figures 13 and 14 give the results obtained in this series of tests. The first shows $c/kW^{\frac{1}{3}}$ as function of λ. Note that c is the total crack width in inches, and

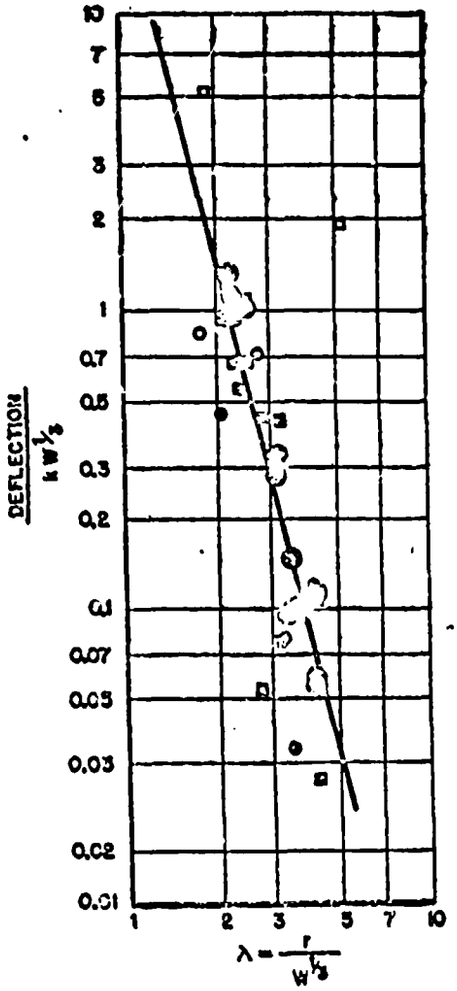

FIGURE 14. Permanent front wall deflection as function of distance and size of charge. Deflection in inches × 10^4, weight in pounds, distance in feet, k as in Table 5.

that k is the soil constant for pressure (Table 5). The other figure gives $X_o/kW^{\frac{1}{3}}$ as a function of λ. It is significant that there appears to be no consistent deviation with target scale. This indicates that target damage obeys the model law and that small-scale tests can be used for predicting the effects on full-sized structures. Straight lines have been fitted to these points by least squares. In Figure 13 the slope of the line of best fit is −4.52, and with 95 per cent confidence its slope lies between −3.85 and −5.19. This indicates that peak pressure is not the principal damaging factor since that varies approximately as the inverse cube of distance. The solid line shows the least squares fit and has the equation

$$\frac{c}{kW^{\frac{1}{3}}} = \frac{\lambda^{-4.5}}{250}. \qquad (35)$$

Similarly, the straight line of Figure 14 has the equation

$$\frac{X_o}{kW^{\frac{1}{3}}} = \frac{\lambda^{-4.5}}{300}. \qquad (36)$$

A theoretical analysis of the behavior of the structures tested has been made and is discussed in the following section of this chapter and in Chapter 15, Section 15.5.3.

TABLE 11. Damage categories for 5-ft wall of box structure and corresponding distances of 1,000-lb charge in earth for which k = 5,000 (Table 5).

Damage	Crack width (inches)	Charge distance λ	Charge distance (crater radii)
Heavy	5	2	1
Moderate	1	3.5	1.5
Light	0.1	5	2.5

Three categories of damage have been defined for the 5-ft reinforced concrete wall. These definitions in terms of crack width are shown in Table 11, together with the corresponding distances of 1,000-lb charges, assuming that the structure and the soil are similar to those of the present series of tests. When this is not the case, use must be made of Weapon Data Sheet 6A5 of Chapter 19 or of an analysis corresponding to that discussed in Chapter 15.

CONTACT CHARGES

From the investigation of the effects of earth-backed contact explosions on reinforced concrete walls that were made at the same time, it was concluded that the scabbing limit, or thickness at which scabbing of the far surface of a wall barely occurs in case of a contact earth-backed explosion, is given by the following expression

$$T = 1.4W^{\frac{1}{3}}, \qquad (37)$$

where T is wall thickness in feet and W is charge-weight in pounds.

3.7.3 Theories of Damage to Buried Structures

There is a simple theory for predicting the extent of damage to a buried structure when exposed to a near-

by explosion in earth.[22e] In this approach it is assumed that the impulse acting on the front face of the target puts it into motion. The velocity of motion is proportional to the total impulse divided by the mass of the front face. The kinetic energy of the front face can then be computed. A fraction of this energy is assumed to be used in causing plastic deformation of the front wall; from this the amount of bending and the width of cracks in this wall can be calculated. At two points in this analysis undetermined proportionality factors are introduced. These can be combined into a single factor whose magnitude can be found from experiment and must be assumed to remain the same in other situations. This method gives a relation between crack width, λ, charge-weight, and soil constant that is of approximately the same form as equation (25), namely,

$$\frac{a}{kW^{\frac{1}{3}}} = \frac{13Q}{S}\lambda^{-6}, \tag{28}$$

where Q is a constant, the *utilization factor*, to be determined experimentally. The value of k is given in Table 5. The strength factor S is given by the expression

$$S = \frac{2ad^2N\sigma W^{\frac{1}{3}}}{LH}, \tag{29}$$

where a is the thickness of the target wall in inches, d is the diameter of reinforcing bars in the target in inches, N is the number of bars in one wall that are stretched by the deformation of that wall, σ is the yielding stress of the reinforcing steel in psi, L is the horizontal span of the wall in inches, and H is its vertical dimension in inches. In order to make equation (28) agree with equation (25) Q must equal 0.06. From the way in which equation (28) was derived, this indicates that the crack width is only 6 per cent of what it would be *if* all the impulse in the pressure wave were used to produce plastic deformation.

It should be pointed out that measurements of pressure and impulse have not been made closer to the explosion than correspond to $\lambda = 2$ or 3. Consequently, any attempt to develop an analysis based on these measurements must recognize this limitation on its applicability. It appears, in fact, that for very near or contact charges the damage does not follow the same law that would be predicted from the effects of explosions beyond one crater radius. This is well illustrated in the curves of Data Sheet 6A5 of Chapter 19, which are almost horizontal in the region of small charge distances.

Because the utilization factor Q is so small in this case there is considerable uncertainty when equation (28) is applied to any situation that differs very much in respect either to soil characteristics or to structural characteristics from the tests that have been made. For this reason it seemed desirable to make a somewhat more elaborate analysis with the hope that a closer correlation between its predictions and the measured effects might be attained. Such an analysis was made but, unfortunately, not in time to appear in any published report; consequently it appears in Section 15.5.2 to which reference should be made. This analy-

TABLE 12. Tabulation of constants for various soils.

Soil type	Seismic velocity (fps) min	Seismic velocity (fps) max	Soil constant k (psi) min	Soil constant k (psi) max
Top soil (light dry)	600	900	262	590
Top soil (moist, loamy silt)	1,000	1,300	812	1,370
Top soil (clayey)	1,300	2,000	1,420	3,370
Top soil (semiconsolidated sandy clay)	1,250	2,150	1,510	4,150
Wet loam	....	2,600	....	5,600
Clay (dense wet, depending on depth)	3,000	5,900	8,850	34,100
Rubble or gravel	1,970	2,600	6,400	11,100
Cemented sand	2,600	3,200	9,700	12,600
Water-saturated sand	....	4,600	....	22,500
Sand	4,600	8,400	26,200	87,000
Sand clay	3,200	3,800	10,000	13,900
Cemented sand clay	3,800	4,200	17,800	21,700
Clay, clayey sandstone	....	5,000	....	45,000
Loose rock talus	1,250	2,500	1,750	7,000
Weather-fractured rock	1,500	10,000	3,100	140,000
Weather-fractured shale	7,000	11,000	63,000	156,000
Weather-fractured sandstone	4,250	9,000	23,500	116,000
Granite (slightly seamed)	....	10,500	....	160,000
Limestone (massive)	16,400	20,200	300,000	590,000

sis differs from the one that has been described in that the pressure pulse is assumed to continue during a large part of the deflection time of the target wall. The wall is assumed to be deformed continuously, at the same time exerting a force on the remainder of the structure which is pushed backward thereby. The inertia and passive resistance of the earth behind the rear wall of the structure are considered as well as the possibility of simultaneous plastic bending of the rear wall.

3.8 RECOMMENDATIONS FOR FUTURE WORK

Much remains to be done on both experimental and theoretical aspects of underground explosion phenomena. The importance of these problems is very great, inasmuch as future protection of critical installations from high explosive and atomic bombs will almost certainly involve burial in the earth. A knowledge of the factors that affect damage to possible targets exposed to the effects of possible weapons will be equally important to the attacker and the defender. The following problems appear to be the most important:

1. Development of a reasonably reliable and simple theory for predicting the effect of an explosion in free earth and on a structure. In particular, this should be applicable at great distances from the charge, since the atomic bomb will be effective at very great distances. Both plastic and elastic media (earth and rock) must be considered.

2. Continuation of the experiments on wave propagation that have been discussed, with particular attention to the following questions: (a) the propagation of waves in rock, (b) the propagation of waves produced by explosion near an interface between rock and earth or by explosion in a stratified medium, and (c) the propagation of waves at large distances from an explosion occurring at a relatively small-scaled depth in earth with and without an underlying rock stratum.

3. Continuation of the experiments on structural damage that have been discussed, with particular attention to the following questions: (a) the damage to relatively weak structures at great distances from an explosion, (b) the damage to structures at various depths of burial instead of nearly flush with the ground surface, as in the tests that have been made, (c) the relation between damage to complete structures and to structural elements. (For example, less damage would be expected to an isolated section of a tunnel than to an equal length of the complete structure, because of the difference in continuity.)

Chapter 4

MUZZLE BLAST, ITS CHARACTERISTICS, EFFECTS, AND CONTROL

41 INTRODUCTION

DURING WORLD WAR II medium-caliber guns with very high muzzle velocities and rates of fire were developed, and the trend continued toward an increase in these properties.* These high-pressure guns were at first used for defense against aircraft, but later they were adapted for use in direct fire against armored vehicles and pillboxes. Against these targets the guns were fired at low elevations, and soon offensive and defensive tactics were developed which required digging in the gun so that at times the muzzle barely cleared the ground.

With some guns that saw action in World War II the muzzle-blast problem had already become acute. On land the blast tore up the ground ahead of the muzzle and raised great clouds of dust that not only obscured the target but also revealed the gun position to the enemy. At times the obscuration problem became critical, for in direct fire the target must be seen and, when the target is a moving vehicle, the strike of the projectile must be sensed. A high rate of fire is a useless luxury when the gun is enveloped in a cloud of dust. At sea, where the decks are crowded with high-velocity guns as a means of defense against air attacks, the blast effects of a ship's own guns often produced more damage than that inflicted on it by enemy action. The crews were injured by the cumulative effects of the blasts and structures were heavily damaged.

As muzzle velocities increase, limitations appear in the tactical uses of high-pressure weapons. A gun that injures its crew, tears up neighboring structures with greater certainty than enemy fire, reveals its position through excessive flash, smoke, and dust, while effectively concealing that of the enemy, obviously needs something to tone down its performance. With the development of new types of weapons, such as rocket projectiles, it would seem that the modern high-pressure gun is already obsolescent unless something is developed to suppress the violence of the blast.

The only attachments that have been used to any extent in controlling blast in medium-caliber guns are muzzle brakes and simple cone or blunderbuss extensions to the muzzle of some antiaircraft guns to reduce the intensity of the flash. Silencers and compensators have been used on small arms. Muzzle brakes are not intended primarily to reduce blast effects in the neighborhood of the muzzle. They were originally devised as supplements to recoil mechanisms, though at present, when the design of recoil mechanisms offers no particular difficulties to the ordnance engineer, muzzle brakes are used primarily to reduce recoil energy so as to permit the mounting of high-pressure guns on lighter carriages.

Although work has been done on muzzle brakes in many places for many years, the Germans were the first, during World War II, to make extensive use of them. They introduced a variety of muzzle attachments but all these were eventually supplanted by the familiar 2-baffle brake which has been copied so extensively by other armies. This brake is a simple, sturdy unit of medium efficiency. The British developed high-efficiency brakes for use on the 6-pounder and 17-pounder, but the back blast from these brakes was too severe on the gun crews, and they made extensive use only of a modification of the German brake.

The only American brake put into the field in moderate quantities was the M2 brake on some of the later 76-mm guns mounted on tanks and tank destroyers. Little thought was given to the development of muzzle attachments until late in World War II. This lack of interest was due to the conviction that existing recoil mechanisms were adequate to absorb the recoil energy of the high-pressure guns. No great attention seems to have been given the possibility of reducing the weight of the mount through the use of a muzzle brake, and great objection was made to the blast effect produced toward the rear of the gun when any blast deflector is attached to the muzzle. Eventually, gun crews became accustomed to the back blast from the M2 brake on the 76-mm gun, and they were demanding the brake principally, it seems, because the Germans were using it.

A demand arose for the development of muzzle attachments when it was observed that under certain conditions the standard type of brake greatly reduces obscuration from dust, and some who had not felt the

*Pertinent to War Department Projects OD-154 and OD-160, and to Navy Projects NO-144 and NO-208.

need of a brake, as such, advocated its use for the relief of the dust situation. Toward the end of World War II a few experimental mounts were designed in which a brake was an integral part of the assembly.

Early in 1944, at the request of the Army Ground Forces, Division 2 agreed to attempt the development of a muzzle attachment that would suppress the raising of dust. Contracts for this work were given to Princeton University, the General Electric Company [GE], and the California Institute of Technology. At the beginning it was decided that the three contractors were to work on different phases of the project. At the Princeton Station the development was to be attempted of a light attachment that could replace the standard brake as a field modification and that might possibly give immediate partial relief from obscuration; at GE a correlation was to be attempted between the properties of high-pressure transient jets and proper sequences of steady-state jets, a high-pressure steam "gun" emptying into an evacuated chamber being proposed; and at the California Institute of Technology the basic work for a long-range program was projected. This separation of the project was not always adhered to. For instance, while the steam apparatus was being assembled, GE engineers constructed a medium-pressure .50-caliber air gun on which some 50 muzzle attachments were tested over a dust table. This turned out to be extremely valuable in arriving at conclusions about the potentialities of field attachments.

The development of deflectors for the suppression of dust was to proceed without regard for the braking action of the attachments. Soon after the initiation of these contracts, Division 2 undertook to study the properties of muzzle brakes at the request of the Ordnance Department, and the contract for this work was given to the Franklin Institute.

As part of the muzzle-blast investigations under Division 2, Princeton University Station also accepted a contract for the study of the characteristics of high-pressure jets by the interferometric method. This work was undertaken at the request of the Bureau of Ordnance of the Navy.

During the progress of these investigations it has became apparent that recoil, obscuration from dust and smoke, and flash must be looked upon not as isolated problems, but as components of a muzzle-blast problem that must be considered in the design of gun and mount assembly. So long as one persists in thinking of solutions in terms of appliances which may be screwed on to the muzzles of existing guns the blast problem presents itself as a series of problems with more or less incompatible solutions. For instance, a high-efficiency brake may raise a great deal of dust and induce flash; a good diffuser which protects the ground from the severity of the blast may nevertheless lead to serious obscuration; or a deflector that is effective in reducing obscuration may be a mediocre brake and induce flash in a normally flashless round. Since only one attachment may be used on a gun at a time, a more or less incomplete solution of only one of the component problems may be obtained or, at most, it may be possible to obtain only a small overall improvement in some group of blast effects, unless the drastic changes required to control blast as a whole are contemplated.

The simplest problem pertaining to muzzle blast is that of the muzzle brake, if one disregards the other blast effects. The action is well understood and it is relatively a simple matter to design a brake of high efficiency. It is another matter, however, to utilize a high-efficiency brake; the braking action that may be utilized is limited by the back blast which the gun crew can stand. The problem of the utilization of high-efficiency brakes can be considered as the problem of rendering the deflected jet innocuous. This, however, is the problem of the control of blast as a whole, for if the deflected jet is made harmless, the blast of the gun is reduced to that of the weakened residual jet. The piping of the deflected gases through ducts parallel to the gun tube to where they can be expelled harmlessly to the rear of the crew or up over the carriage presents no difficult engineering problems. The great problem that has been encountered is in the development of a deflector that reduces the forward jet to the magnitude where the superstructure is justifiable.

The necessity for resorting to extreme measures in controlling blast is seen in the failure of simple attachments to reduce blast effects satisfactorily. With increasing pressures and larger calibers the partial results now obtained become even less obvious. For instance, a diffuser that has been developed which eliminates the flash from a flashing round in the 76-mm gun produces no obvious effect on the flash of a 90-mm gun.

It is now possible to construct a deflector that reduces the residual blast to that of an extremely low-pressure gun and that controls the deflected gases so that they can be piped backwards.

4.2 MUZZLE-BLAST CHARACTERISTICS

The blast that follows shot ejection may be considered either as a mild explosion or as an extremely high-pressure transient jet. It is a mild explosion with respect to the mass of the detonated charge. The gas generated by the burning of the powder expands considerably in the gun tube and loses a large fraction of its energy in accelerating the projectile to muzzle velocity before it is released into the atmosphere at shot ejection. However, the gas still retains a great deal of energy at this time. At the muzzle it is moving with the velocity of the projectile under a pressure of 500 to 1,000 atm and heated to a temperature around 1500 K. The time it takes the gun to empty is of the order of magnitude of the travel time of the projectile, about 6 msec in the 3-in. gun. The most obvious characteristics of the blast, as shown, for instance, by spark photographs, are a strong almost spherical air shock and, within it, the greatly expanded jet from the muzzle. The evolution of this jet is determined by the flux of gas out of the muzzle and, in its earliest stages, by the flight of the projectile which interferes with its formation; and the flux out of the muzzle is determined by the state and velocity distributions of the gas within the tube at shot ejection.

4.2.1 Motion of the Gas within the Tube after Shot Ejection

The problem of the emptying of a gun is the continuation of the classical problem of interior ballistics that begins at detonation of the charge and ends with shot ejection. In some respects it is a simpler problem since there is practically no burning of the powder and the gas is expanding without the restraint of the projectile. The solution of this problem has been placed on a satisfactory basis.[1-5]

Figure 1 shows typical pressure and velocity curves during the principal part of the emptying time. Curves 1 show conditions at the time of shot ejection. Because of the high temperature the velocity of sound in the gas behind the projectile at shot ejection is very high, generally higher than the muzzle velocity, so that the sudden pressure drop which occurs at the muzzle is propagated back against the stream as a wave of rarefaction. At the muzzle this wave moves slowly relative to the tube, but it acquires speed as it reaches the slower moving gas within the tube. Curves 2 and 3 show the pressure and velocity distributions as the rarefaction front moves toward the breech, this front being marked *b* and *c*. Curves 4 show conditions as the rarefaction front reaches the breech, where it is reflected and moves forward riding the outflowing gas until it comes out at the muzzle. Most of the emptying action takes place while this rarefaction front is in

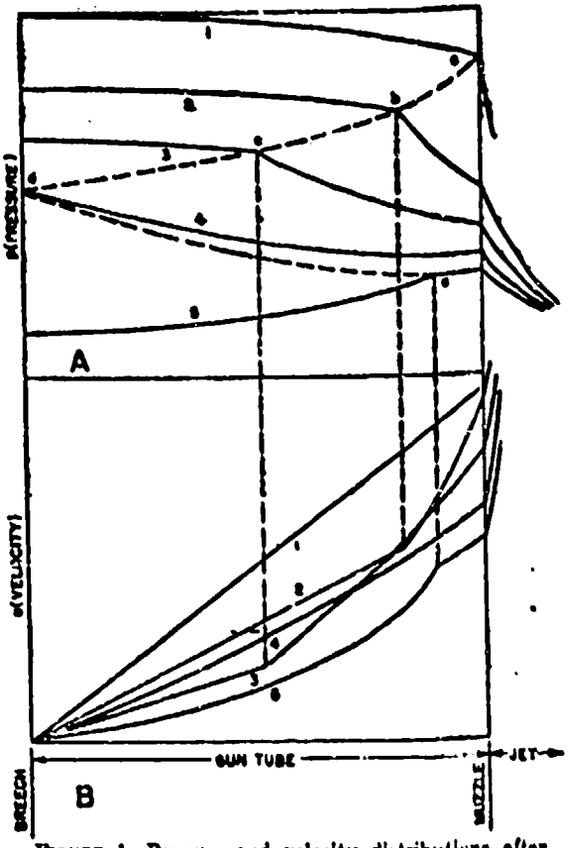

FIGURE 1. Pressure and velocity distributions after shot ejection. A. Pressure-distance distribution. B. Velocity-distance distribution.

the tube. An important phenomenon occurs when this front emerges in the jet; a description of it will be given after the jet has been described. In the problem of the blast the important results are those that give the outflow of the gas from the muzzle.

4.2.2 The Blast Characteristics

The characteristics and evolution of the blast are known qualitatively, principally through spark photographic studies of the burst from small arms and of high-pressure steady-state and transient jets.[6-7]

Figure 2 is a sketch showing the relevant features of the burst from a caliber .30 rifle firing service ammunition. The sketch is based on a spark photograph taken about ⅛ msec after shot ejection, when the bullet no longer interferes with the blast.

The air shock that envelops the jet is marked *a*. The strength of this almost spherical shock is greatest in front near the bore axis and attenuates gradually toward the rear. As the shock front recedes from the muzzle the center of the surface moves forward along the bore axis because the surface elements where the shock strength is greater recede faster.

As the gas crosses the oblique shock *c*, its speed is checked in the direction perpendicular to the shock surface so that the streamlines are violently deflected toward the bore axis. Most of the gas that crosses the shock *c* also goes through the oblique shock *e*, where the streamlines are deflected away from the bore axis. A typical streamline that crosses these shocks is

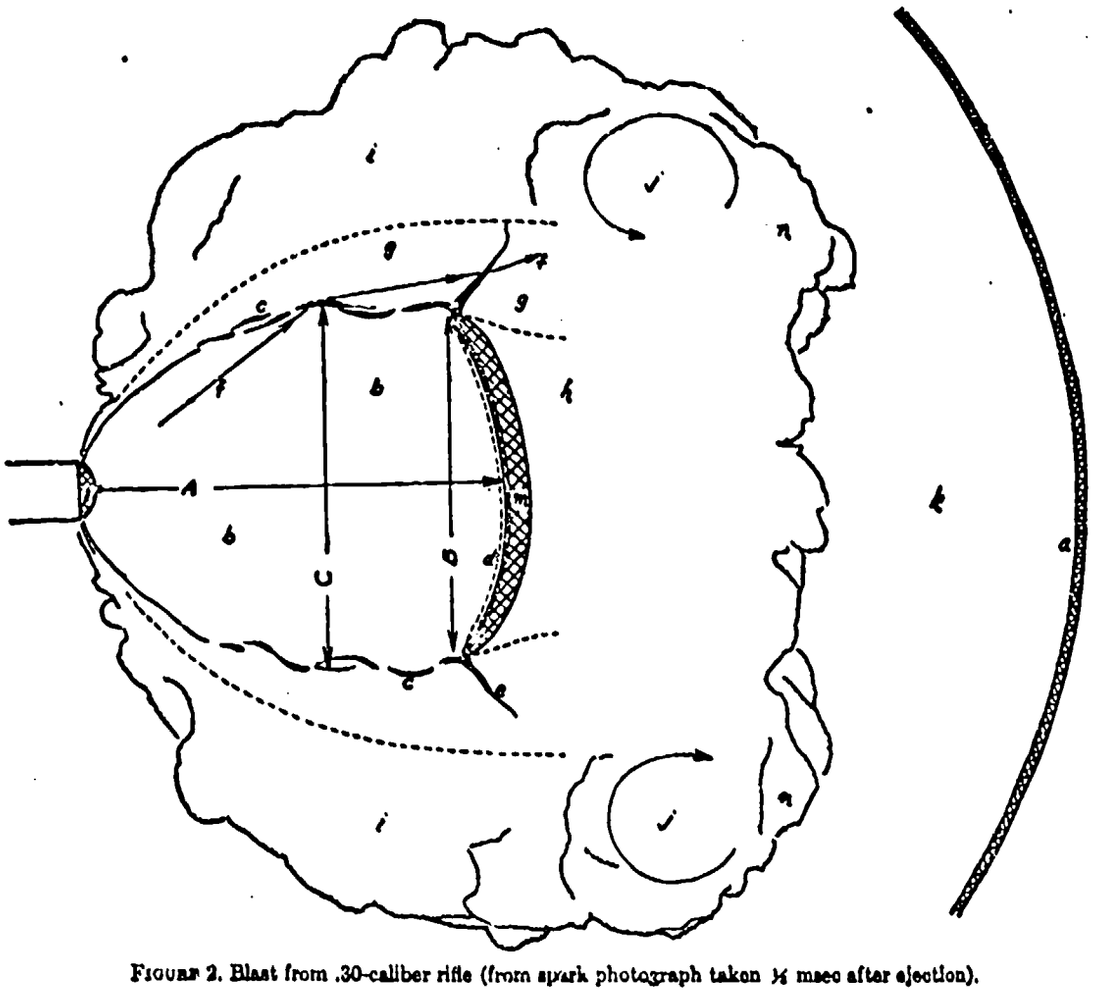

FIGURE 2. Blast from .30-caliber rifle (from spark photograph taken ½ msec after ejection).

The expansion of the jet takes place in the region marked *b*, which has been called the *bottle*. This bottle is bounded by the cylindrical oblique shock *c* and the normal shock *d*. The gas leaves the muzzle with the local speed of sound and expands freely as if there were no atmospheric constraint until it crosses the shocks. Within the bottle the velocity of the gas increases steadily as it moves away from the muzzle and becomes highly supersonic before entering the shocks, marked *f*. The stream becomes subsonic on crossing the normal shock *d*. The dotted line is roughly the boundary of the supersonic flow. The boundary between the relatively slow-moving gas in the region *h* and the fast-moving gas in the region *g* is very sharply defined near the intersection of the shocks.

Surrounding the jet boundary there is a highly turbulent shell *i* in which the outer lamina of gas mixes with the outside air. At *j* this turbulent mix-

ing region forms a strong annular vortex called the *smoke ring* by analogy with the smoke rings blown out by smokers. This smoke ring is a vortex in the jet and need have no smoke in it, of course; when it does it can be seen clearly.

In the region *k* close to the bore axis may be seen unburned powder particles traveling at very high speeds as indicated by their bow waves and wakes. Even in the stage of the burst shown by this sketch a few of these particles break through the traveling shock *a* into the still air ahead.

A time photograph of the blast taken in a dark chamber will show a muzzle glow at *i* and a glow, called primary flash, in the region *m* behind the normal shock. Neither of these is due to burning of the gases, since neither of these two regions comes in contact with the air. Muzzle glow and primary flash are observed even when the gun empties into a nitrogen atmosphere. The same change in composition of the gases taking place within the tube which accounts for muzzle glow also accounts for primary flash. The action is inhibited as the gas enters the relatively cold bottle and starts again as the gas enters the normal shock, where the temperature rises to a value near that at the muzzle. The unburned powder particles no doubt contribute to the phenomenon by being heated to incandescence in going through these regions of high temperature. The burning of the powder gases, called secondary flash, which is the principal element of the flash in medium- and large-caliber guns, occurs in the turbulent mixing region. It begins in the forward region *n* of the smoke ring and travels backward until the whole turbulent shell is involved. The smoke ring continues to burn as it moves forward, so that a time exposure of the burst from a 90-mm gun, for instance, taken at night produces a carrot-shaped fogging of the plate some 3 tube lengths along the bore axis and 1 tube length across.

In the earliest stages of the blast, from the time of shot ejection to the time when the projectile is 10 to 15 calibers from the muzzle, the shock *a* takes on a variety of forms, depending on the condition of the tube. For instance, if the tube is worn so that gas leaks past the projectile while it is traveling in the tube, the early shock has the form of the outer surface of two intersecting spheres, the smaller one ahead of the bullet; if the tube is new the shock is open ahead of the projectile and does not close until the projectile is 4 or 5 calibers from the muzzle. In any case, by the time the blast has attained the stage shown in Figure 2, the shock smooths out into a nearly spherical shape.

The jet cannot develop its characteristic shape, of course, until the bullet is beyond the point at which the shock *d* would normally occur at the existing muzzle pressure. The expanding gas attains extremely high speeds and when the projectile is close to the muzzle a shock forms at its base; relative to the gas, the projectile travels toward the gun at supersonic speed. This shock eventually detaches itself from the base and becomes the shock *d*. In the .30-caliber firings the shock becomes steady at a distance of about 15 calibers from the muzzle. This distance is marked *A* in Figure 2. At first the diameter *B* is the greatest diameter of the bottle and is equal to *A*. The distance *A* remains constant while *B* shrinks until $B = 0.5A$. While this is taking place the maximum diameter of the bottle drifts toward the muzzle and attains the final value $C = 0.7A$. Beyond this point the bottle shrinks without appreciable change in shape. Since the rate of emptying of the gun is greatest at shot ejection and attenuates very rapidly at first, the most damaging fraction of the blast comes out before the jet has attained a quasi-stationary shape.

Spark photographs record only sharp changes in pressure and density. Small density changes can best be observed by interferometry. An interferometer is essentially an optical system that splits a beam of light into two beams and recombines them in such a way that corresponding points of the two beams coincide finally. The interferometer is adjusted to give alternating zones of interference and reinforcement of light (fringes) on a photographic plate. If the density of the medium through which one of the beams passes is altered, a shift in these fringes is observed, the amount of the shift depending on the density change. If one of the beams is made to pass through a jet, a distorted fringe pattern is obtained from which the density distribution throughout the jet may be computed. A number of methods have been developed to obtain the density distribution from the observed fringe shifts. The computations are laborious and require the use of modern mechanical aids.[8,9]

By an extension of the results so far obtained on jets of moderate pressures, it is possible to draw a qualitative picture of the density distribution in the jet from a gun. Figure 3 shows this distribution at two sections: *A* is the distribution along the bore axis, and *B* is that at a section through the bottle normal to the bore axis. Besides the fluctuations indicated behind

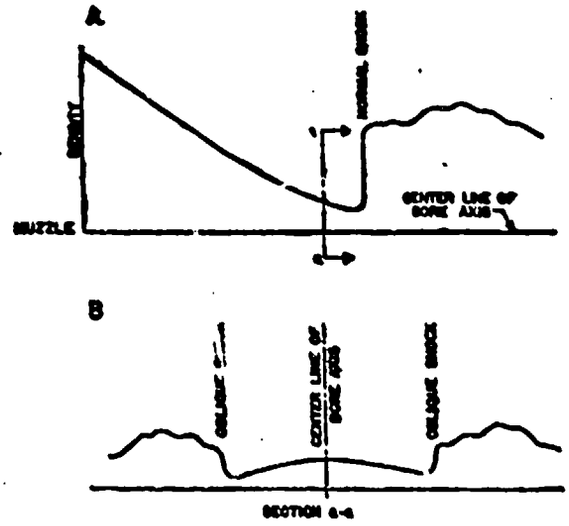

FIGURE 3. Density distributions in jet. A. Longitudinal distribution. B. Diametral distribution.

the shocks, minor fluctuations are observed within the bottle. These fluctuations lead to the waviness of the shocks observed in spark photographs and shown in Figure 2.

By inserting probes into the jet it is found that the streamlines within the bottle, before they are deflected by the oblique shocks and in the regions not too near the muzzle, are practically straight and converge in a point on the bore axis close to the muzzle,[9] as shown by the solid lines in Figure 4. The extension

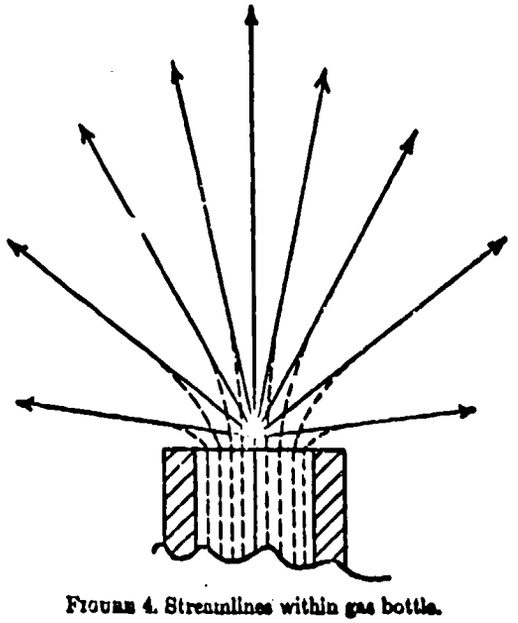

FIGURE 4. Streamlines within gas bottle.

of these streamlines into the muzzle is indicated by the broken lines in the figure.

Peak-blast pressures, as measured by gauges placed at varying distances from the muzzle, attenuate uniformly with distance in the manner characteristic of all explosions. The scaling of blast pressure according to caliber requires a knowledge of the muzzle velocity and the state of the gas in the tube at shot ejection. The latter is not accurately known for most guns. Figure 5 shows the results of scaling the blast recorded for a number of guns to .50-caliber scale.[10]

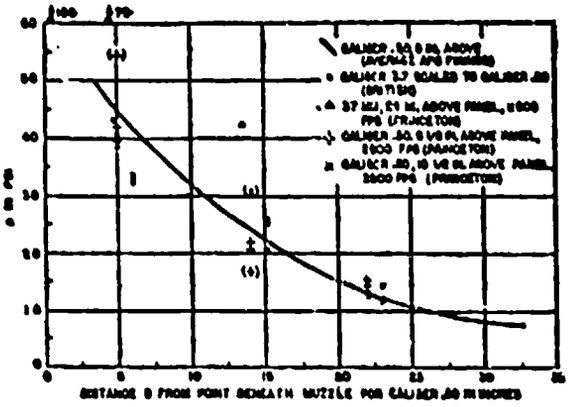

FIGURE 5. Attenuation of blast pressures with distance (.50-caliber scale).

4.2.3 The Terminal Rarefaction

The two curves marked 5 in Figure 1 show the state of the gas within the tube just before the rarefaction front reaches the muzzle after reflection at the breech. In Figure 6A the pressure curve is continued along the axis of the jet and beyond the normal shock. This shock is almost stationary relative to the tube but moving upstream with a relative speed determined by its strength. The rarefaction front will meet this shock at some point A. What happens after the encounter may be seen by referring to Figure 6B. The top diagram shows a shock and rarefaction wave moving relative to the still gas between them. The rarefaction front has a velocity c determined by the temperature of the gas into which the wave advances and the shock has a velocity V determined by this temperature and the ratio of the pressure before to that after it. The bottom diagram shows conditions after the encounter. The rarefaction wave is now traveling through the higher pressure gas behind the shock with a velocity $c' - u_1$ and the shock now moves with velocity $V' + u_2$; where u_0, u_1, u_2 are the local

particle velocities, as indicated in the figure. Because of the nonlinearity of the flow the interaction of the two waves is not very simple, but roughly it may be said that the rarefaction gets through the shock without essential changes.[21] After the interaction the bottle attenuates more rapidly.[5,6] The rarefaction is propagated in all directions and superposes the velocities behind it throughout the neighborhood of the muzzle.

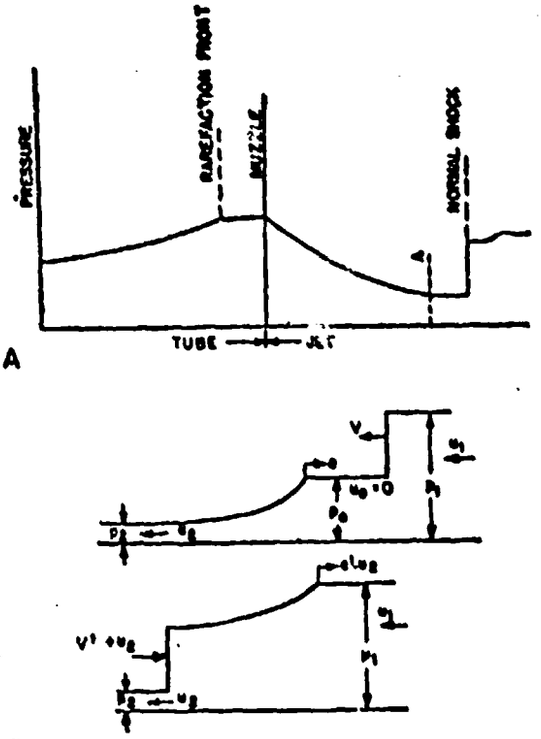

FIGURE 6. Terminal rarefaction in gun blast. A. Pressure distribution before emergence of rarefaction front. B. Interaction of shock and rarefaction wave.

4.1 BLAST EFFECTS

The effects of the blast near the muzzle are those of a mild explosion modified by the axial direction of the flow of gas, the interference by the projectile with the jet in the early stages of the blast, and the retardation of the outflow of gas by the length of the tube. For a given gun and type of projectile, muzzle-blast severity increases with muzzle velocity, but it is more accurate to consider the blast as a function of the charge weight, the projectile weight, and the ratio of the length of the tube to the caliber of the gun. Muzzle-blast effects increase with increasing charge mass and decrease with increasing length of tube, although increasing the tube length increases the velocity.

4.2.1 Recoil

The recoil of a gun is due to the backward pressure of the gas on the breech. Recoil begins at detonation of the charge and is ended by the action of the recoil mechanism. The recoil characteristics of a particular gun depend principally on the mount. For instance, the 37-mm antitank gun M3 recoils 20 in. whereas the 76-mm gun mounted on the M18 vehicle recoils only 12 in. The recoil energy of a gun, however, depends on the same quantities that determine blast severity; that is, on the charge weight, the projectile weight, and the length of the tube in calibers. The recoil energy would be the kinetic energy of the recoiling parts after the emptying of the gun, if these were mounted on level, frictionless runners parallel to the bore axis. Recoil energy is usually computed by equating the momentum of the recoiling parts to the momentum of shot and powder at the time of shot ejection; there is, however, an increment of energy given the recoiling parts by the pressure on the breech during the emptying of the gun after shot ejection, which may be considerable in high-pressure guns. Recoil energy is most simply measured by mounting the recoiling parts on a free swinging pendulum.[4,13-17]

The reduction of recoil energy by means of a muzzle brake, as distinguished from the mere reduction of recoil length by a recoil mechanism, depends on the utilizable energy of the blast; that is, on the kinetic and available internal energy of the gas as it comes out of the muzzle.

4.2.2 Blast Damage

Damage to structures by muzzle blast is due principally to the effect of the sudden blast pressure, but close to the muzzle an important contributing element is the reversal in pressure that accompanies the terminal rarefaction. Near the muzzle the effects of this reversal are quite obvious. For instance, on firing a 3-in. gun at low bore heights over a blast mat, the pins that hold down the edges of the mat are often torn out and the loosened mat folded towards the gun. If enough pins are pulled out the mat may wrap itself around the gun. The edges of the mat may be 10 feet from the muzzle when this happens.

The action may be visualized by considering a box with a closed lid, not hermetically sealed, placed near the muzzle. The initial blast pressure will tend to close the lid tighter and to crush in the walls. The peak pressure, however, is of extremely short duration and will merely give the walls and lid an initial inward impulse. The smaller but still high pressure behind the shock front will cause a flow of air into the box and build up the pressure inside. When the rarefaction wave comes, the lid will tend to fly open because of the relief of pressure outside which is of relatively long duration. When account is taken of the fact that most structures are stronger against pressure applied from outside, it will be seen that the rarefaction may account for a great deal of the damage of the blast.

Injury to personnel from a single round is probably due to the peak pressures. A membrane as light as an ear drum may be broken by the impact of the shock wave. Repeated firings, even when the pressures are far below critical, produce more subtle effects.

4.13 Dust and Obscuration of Target

When a gun is fired over dry ground, a cloud of dust rises explosively near the muzzle. Fast motion pictures may be used to study the rise and motion of this cloud.[1] When the gun fires at low elevation and low bore height the blast scours the ground in a characteristic parabolic pattern. In the absence of wind the compact cloud takes on the motion of the blast; it drifts forward, expanding slowly, its outer boundaries swirling in the direction of the vorticity of the smoke ring. Gravity eventually settles out the dust particles but this thinning out of the cloud may be very slow if the dust is fine. Any wind, of course, imparts its motion to the cloud and diffuses it.

Though the motion and attenuation of the dust cloud may be recorded by motion pictures, the processes by which dust particles are picked up and transported cannot be observed; but the laws of mechanics that govern the motion of individual particles and the statistical laws that describe the average behavior of a large collection of particles are well known, of course. Theoretical studies have been made which lead to a satisfactory understanding of the scouring of the ground by the blast and the raising and diffusion of dust.[6,7,18,19] The principal conclusions regarding the raising of dust by the blast are the following:

1. Pressure changes in the jet and air behind its front contribute little to the motion of a dust particle except insofar as these changes cause the air surrounding the particle to move. This statement is true even for strong shocks.

2. In the absence of turbulence a dust particle always has the velocity of the surrounding air superposed on its characteristic settling velocity.

3. The scouring of the ground is produced by the high-speed jet. Viscosity makes the air adhere to the surface particles. These are dragged with the current and act as an abrasive.

4. Turbulence scours the ground and diffuses dust that it picks up, but these processes are relatively slow. The principal function of the turbulence is to keep dust in the air from settling out.

5. Dust that has been picked up by the jet is held in suspension by the turbulence in the smoke ring and mixing layer surrounding the bottle and is transported upward by the larger scale currents in these regions.

6. Dust is picked up and may be raised a considerable distance whenever a wave of rarefaction can penetrate the ground before complete reflection. The velocities of the air behind a wave of rarefaction are opposite to the direction of propagation of the wave and cause an explosive rising of the dust.

The explosive rise of the dust caused by the terminal rarefaction can be observed in fast motion pictures. The amount of dust raised by this wave is considerably less than the amount picked up by the scouring action of the jet, but, coming after the main blast, it tends to stay close to the gun. The main traveling shock develops a rarefaction region behind it. On penetrating porous ground it raises dust a very small distance above the surface. This shock contributes to the raising of dust by preparing the ground for the blast that follows.

The obscuration of the target by the dust cloud is by no means simply related to the amount of dust raised. Obscuration is characterized by its intensity and its duration. Both these elements are greatly affected by meteorological conditions. A dense compact cloud that produces total obscuration may not be objectionable when a strong side wind sweeps it away quickly from the line of sight. On the other hand a diffuse dust cloud of great extent which produces incomplete obscuration for a relatively long time may be quite objectionable. An extremely tenuous cloud may produce severe obscuration because of the scattering of light by the small dust particles, since the eye can distinguish only the contrast between the transmitted and reflected light.

Since obscuration as it affects military weapons is a field phenomenon, the measurement of obscuration is a statistical field problem. The character of the obscuration associated with the blast of a particular gun is not something that can be determined in the laboratory; it is obtained as an average of the results of firing the gun under a great variety of field conditions. Since the larger guns must fire into fixed impact areas within small traverse ranges, it is difficult to obtain an adequate variety of conditions.

The obscuration due to a particular round may be measured in various ways. A direct and simple method is for one or more observers with stop watches to record the duration of total obscuration. This method is quite satisfactory when the gun is fired without muzzle attachment, for then the dust cloud usually has well-defined boundaries so that visibility is assured as soon as the cloud is swept away by the wind. If there is no wind the cloud attenuates as gravity settles out the dust and visibility continues to improve after the target is first visible. Muzzle attachments generally introduce secondary effects by dividing the jet; a period of clearing may be followed by a secondary obscuration as the wind sweeps the dust raised to one side of the gun into the line of sight. Motion pictures, particularly with color film, taken at 32 or 64 frames a second are fairly satisfactory in giving a permanent and general view of the phenomenon, but the analysis of a series of films is laborious and there is surprising variability in the results obtained by different observers.

A rather elaborate method for measuring obscuration in the field has been developed.[1,6,20] An instrument which consists essentially of a phototube and a suitable current amplifier has been built around a Heiland recording oscillograph. A strong light, placed some 200 ft ahead of the gun, is focused so as to give a bright image on the phototube cathode, the instrument being placed behind the gun. To make a measurement, the light is turned on and the shutter adjusted to give the proper current through the recorder. The light is then blocked off by a card to give the no-light trace on the record. When the card is removed the gun is fired. Thus the record shows full-light and no-light traces and the variable trace due to the dust that rises between the light source and the phototube. One channel of the recorder is used to make a time trace by driving it with a relaxation oscillator. Other channels are used with switches so that observers may record the time at which they first see the target and thus establish the visibility level of the record.

The blast also contributes to obscuration in an extended sense by causing the gunner to flinch; during the time it takes him to recuperate from the effects of the detonation the target is generally obscured and his sense of its direction impaired. Even when sighting through a telescope he may not be able to take advantage of brief intervals of clearing.

4.5.5 Flash

The flash from a medium-caliber high-pressure gun is brief but of great intensity. At night it lights up the surrounding country vividly and may produce complete blindness for a few seconds. Secondary flash, being produced by the burning of the hydrogen and carbon monoxide in the jet, is in effect a secondary explosion which increases the blast pressures. With high rates of fire, flash adds considerably to personnel discomfort.

4.6 THE PARTIAL CONTROL OF BLAST BY FIELD ATTACHMENTS

When any device is attached to the muzzle of a gun it interferes with the free expansion of the jet. The thrust of the gas on the attachment modifies the recoil energy of the tube, flash is affected by the change in shock pattern and the diffusion of the jet, the shape and concentration of the dust cloud and its obscuration characteristics are altered, and the distribution of blast pressures near the muzzle are modified by the change in the shape of the shock front and the redistribution of strength along it. The purpose of muzzle attachments is to produce favorable changes in some or all the above-mentioned effects.

A distinction has been made between attachments that may be used on existing guns and those that require more or less drastic changes in the construction of the gun and mount assembly. The former are called field attachments. Strictly, no muzzle attachment is a field modification on a gun. Small devices, such as the service muzzle brake, require the cutting of a thread at the muzzle and the placing of a counterweight on the breech block so as to allow the elevating mechanism to function freely. However, any attachment comparable to a standard muzzle brake in size and weight may be used as a field modification on a gun prepared to take the brake. The devices that may be constructed to modify the blast effects of a gun range continuously from simple field modifications to those that must be incorporated in the original de-

sign of gun and mount; however, those devices will be called field attachments which require for their use only the cutting of a muzzle thread, the counterweighting of the breech block, and the possible strengthening of the elevating mechanism.

The reduction in blast effects that may be obtained by the use of field attachments can be expected at best to be incomplete, since through such devices the gas is still ejected in the neighborhood of the muzzle with little, if any, lengthening of the emptying time. It was seen that in a gun firing without muzzle attachment the greatest blast intensity occurs near the bore axis and tapers off gradually toward the rear. A blast deflector merely breaks up this concentration of the blast; it can do this in many ways, but it reduces the overall blast effectiveness only by the relatively small amount of energy made unavailable by the added shocks and turbulence which it produces and, perhaps, by the slight retardation of the jet when the deflector has a large capacity. Present knowledge of the deflection of a supersonic jet is qualitative and still meager.[4,8]

A field attachment that modifies the blast of a given gun satisfactorily cannot be expected to continue to show desirable properties when scaled up to higher calibers or when the powder pressure is increased. For instance, in the problem of obscuration, a device on the 76-mm gun that produces a transparent dust cloud may be acceptable even when it greatly lengthens the time of partial obscuration. A like deflector on a 90-mm gun may produce a comparable diminution in the amount of dust raised, but the resulting cloud can produce complete obscuration for a greater time than does the cloud raised by the gun firing without attachment. A great reduction in the density of the dust cloud cannot be considered an improvement when the severity and duration of the obscuration are not diminished.

The size of a deflector suitable for a field modification is greatly restricted. Upper limits were taken as 10 lb for the 37-mm gun, 80 lb for the 76-mm gun, and 140 lb for the 90-mm gun.[21] In constructing small-scale models of these attachments it is usually difficult and impractical to construct an exactly scaled model, but if the scale is maintained the upper limit for the .50-caliber gun would be about 0.4 lb and for the .30-caliber gun about 0.08 lb. The sizes of the models built in the various projects involved in this program depended on the objectives of the particular investigations. At Princeton, for instance, the object was to develop a field modification for immediate use, and few models were designed and fewer constructed in the larger calibers that could not have been brought down to the proper weights by economical design; whereas at the Franklin Institute, where the investigation was more basic, muzzle brakes were used on the .50-caliber gun which weighed 16 lb and were reducible to 5½ lb.[27]

4.41 Muzzle Brakes

A muzzle brake consists essentially of a *diffuser* and a *baffle*. The diffuser is an extension of the muzzle which allows the gas to expand and guides it toward the baffle surface; the baffle is a plate which deflects radially the gas it intercepts. On being deflected the gas exerts a pressure on the baffle surface opposed to the pressure of the powder gas on the breech. This forward pressure counteracts to some extent the momentum of recoil. For a given gun the effectiveness of a brake depends on the fraction of the jet deflected and on the vector momentum of the deflected gas when it leaves the brake. Brakes are most successful, of course, on guns that have a severe blast. In high-velocity guns an appreciable increment in muzzle velocity is obtained only by increasing the charge considerably.[28] The greater powder pressure leads to greater recoil energy, but this increase is not so great as the increase in the available energy of the blast.

A diffuser-baffle system with a number of variable elements has been investigated at length on the .50-caliber gun.[6,12-16] The generalized 1-baffle brake is shown in Figure 7. The effect on recoil of variations in the elements marked C, D, E, L, N, S in the drawing was determined. In this investigation the plate diameter Q of the baffles is large and the effect of varying it was not considered. The flange around the diffuser, or nozzle, is not essential and in most of the brakes with non-zero reversal angle it was curved backward to permit free expansion of the deflected gas.

A selection from the results of this investigation is given in Table 1. These results are for the flat 1-baffle brake and for the powder load adjusted to give a breech pressure of about 30,000 psi and a muzzle velocity near 2,500 fps. The last column shows the per cent reduction in recoil energy obtained by the various combinations of elements. This quantity is

$$R = \frac{100(E_1 - E_2)}{E_1},$$

where E_1 is the recoil energy of the gun firing without a brake and E_2 the recoil energy obtained when

TABLE 1. Effect of varying certain elements on the efficiency of a single-baffle brake, .50-caliber gun ($D = 0$, $P = 30{,}000$ psi).

Group	Variable	S (calibers)	C (degrees)	L (calibers)	E (degrees)	N (calibers)	R per cent reduction in recoil energy
I	Baffle spacing (S)	0.5	0	0	..	1.1	31.4
		1.0	0	0	..	1.1	55.1
		2.0	0	0	..	1.1	65.8
		3.0	0	0	..	1.1	68.4
II	Nozzle angle (C) $L = 2.25$	2.5	0	2.25	..	1.1	67.5
		2.5	10	2.25	..	1.1	62.1
		2.5	30	2.25	..	1.1	73.8
		2.5	50	2.25	..	1.1	70.0
III	Nozzle angle (C) $L = 4.5$	2.5	0	4.5	..	1.1	67.5
		2.5	10	4.5	..	1.1	63.3
		2.5	20	4.5	..	1.1	70.8
		2.5	30	4.5	..	1.1	70.2
IV	Diffuser cone angle (E)	2.5	30	2.25	..	1.1	73.8
		2.5	30	2.25	5	1.1	70.6
		2.5	30	2.25	10	1.1	70.6
		2.5	30	2.25	15	1.1	70.6
V	Orifice diameter (N)	2.5	0	2.25	..	1.1	67.2
		2.5	0	2.25	..	1.5	63.3
		2.5	0	2.25	..	2.0	55.3
		2.5	0	2.25	..	2.5	50.9

the brake is used. The weight of the recoiling parts is maintained constant.

Usually R is called the efficiency of the brake; but it must be borne in mind that it is the efficiency of the combination of gun, round, and brake. For example, a combination of muzzle-brake elements that leads to an efficiency of about 70 per cent on the .50-caliber gun, firing a round for which $P = 30{,}000$ psi and $v = 2{,}500$ fps, yields an efficiency of only about 50 per cent when used on the .30-caliber rifle, firing a service round[16] for which $P > 50{,}000$ psi and $v = 2{,}700$ fps. As has been pointed out, this variation in effectiveness is due to the difference in emptying characteristics of the two guns.

The effect on efficiency of varying the powder load is indicated in Table 2. The first column ($P = 30{,}000$) shows the values of R listed for Group I in Table 1.

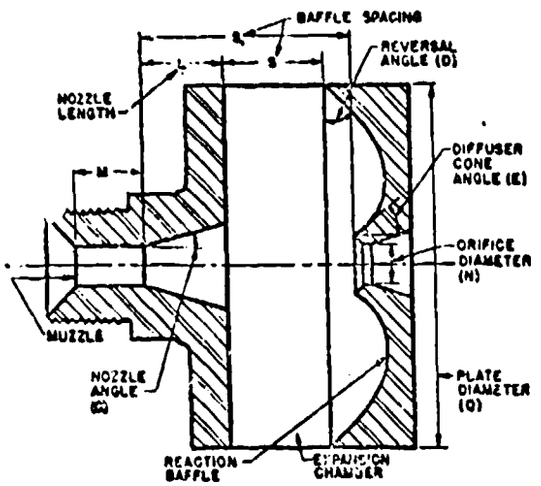

FIGURE 7. Muzzle brake. The principal design variables.

TABLE 2. Effect on efficiency of varying powder load, flat 1-baffle brake without diffuser, .50-caliber gun.

S (calibers)	R (per cent) $P = 30{,}000$ (psi)	$P = 40{,}000$ (psi)	$P = 50{,}000$ (psi)
0.5	31.4	34.0	36.2
1.0	55.1	55.3	57.2
2.0	65.8	67.9	69.0
3.0	68.4	70.4	72.0

From the point of view of the interception and deflection of the jet as well as from that of the design of brakes, a convenient parameter is S_1, with $M = 0$, shown in Figure 7. For example, in Group IV of Table 1 the efficiency of the brake is lowered by the addition of a diffuser cone.[b] This reduction is observed when $S + L$, the distance to the back of the plate, is maintained constant. This result is to be expected

[b] In this investigation the baffle orifice cone is called diffuser cone; however, with respect to the deflected gas it is a compresser.[16]

since the jet is now intercepted nearer the muzzle where the expansion is less. Maintaining S_1 constant will show the effect of the diffuser cone on the deflected blast.[8] Again, the third entry in Group II shows a significant gain in efficiency, as compared to the fourth entry in Group I, obtained by the introduction of a nozzle. However, in Group I, $S_1 = S = 3$ calibers and in Group II, $S_2 = S + L = 4.75$ calibers, and at least part of this improvement must be attributed to the greater spacing.

From the data obtained in these tests requirements for brakes of low, intermediate, and high efficiencies have been proposed. These requirements are shown in Table 3.

TABLE 3. Muzzle brake requirements.

	Low efficiency	Intermediate efficiency	High efficiency
Efficiency (per cent)	30–35	65–70	86–91
Number of baffles	1	1	2
No. 1 baffle spacing (caliber)	0.5	2–2.5	2
No. 2 baffle spacing (caliber)	.....	.....	1
Reversal angle D (degrees)	—30–0	0	30–45
Nozzle angle C (degrees)	0	15–20	20–30
Nozzle length L (caliber)	0	2.25–4.0	2.25–4.0

It should be observed that efficiencies ranging from 87.4 per cent for $P = 30{,}000$ psi to 89.4 per cent for $P = 50{,}000$ psi have been obtained with a single baffle with $D = 30$ degrees.[16,17]

An empirical formula has been devised to predict the efficiency of muzzle brakes. The results obtained by the use of this formula agree quite well with the results of tests on the brake designs used in this investigation, as is shown by Figure 8. The two curves

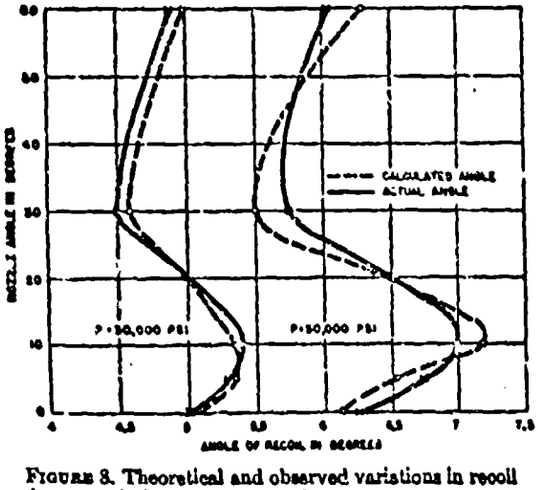

FIGURE 8. Theoretical and observed variations in recoil due to variations in nozzle angle.

of the figure, one for $P = 30{,}000$ psi, the other for $P = 50{,}000$ psi, show the computed and observed angles of recoil due to variations of the nozzle angle for a flat baffle spaced at 1.25 in. The known ballistic quantities used in this formula are net bore area, muzzle velocity, weight of recoiling parts, weight of projectile, and weight of charge; besides these, the muzzle pressure at shot ejection must be computed and the

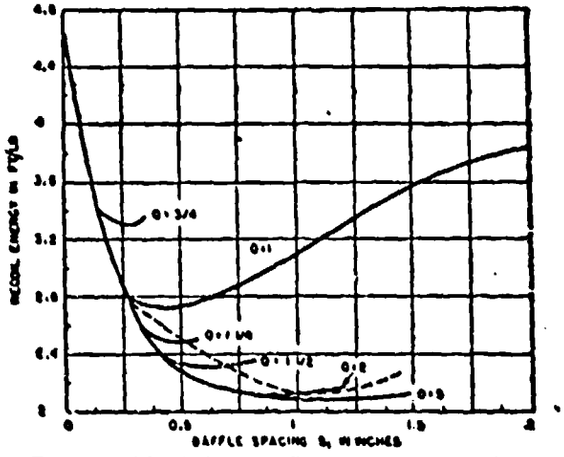

FIGURE 9. Muzzle brake. Effect on recoil of varying baffle diameter and spacing.

mean muzzle velocity of the gases estimated or adjusted to give results agreeing with experiment. The muzzle brake quantities are reduced to three areas and three angles which characterize the expansion and deflection of the jet. These quantities are found from the geometry of the brake according to rules empirically determined from results obtained with the .50-caliber gun. No comparison has been made with other calibers.

The weight of a brake is greatly influenced, of course, by the plate diameter Q. As has been pointed out, the maximum weight of a field attachment suitable for a given gun is severely restricted, and the design problem starts with this restriction. A preliminary investigation of the effects on recoil energy due to variations in Q has led to a number of conclusions concerning the construction of deflectors in general and brakes in particular. These tests were carried out with flat baffles on a .30-caliber rifle.[18] Some of the results obtained in this investigation are shown by the solid curves of Figure 9 where the recoil energy obtained by using single plates of various diameters is plotted against S_1, the plate distance from the muzzle. The curve for the 5-in. plate envelops those for the

smaller diameters. Very near the muzzle all the curves coincide, showing that in that region the plate diameter $Q = 0.75$ in. is adequately large to yield the braking efficiency that can be obtained with baffle spacings not exceeding 0.13 in. At a spacing of about 0.13 in., the curve for the 0.75-in. plate leaves the envelope, and the distance of the point of departure increases with increasing diameter. Beyond the point of departure all the curves are very much like that for the 1-in. baffle, which is plotted to $S_1 = 2$ in.

The effect of a second baffle is shown in the case where a 1-in. first plate is fixed 0.3 in. from the muzzle. The dotted line in Figure 9 shows the recoil energy curve obtained by varying the second baffle spacing. Some such investigation presumably led to the proportions of the German 2-baffle brake.[8]

From these results, aided by spark photographs of the deflected gases, the following general conclusions have been drawn regarding the size and effectiveness of brakes:

1. If the length of a brake is fixed, then the greatest efficiency is obtained by using a single baffle of adequately large diameter.

2. The weight of a brake may be greatly reduced by using two or more baffles within the fixed overall length. This reduction in weight is achieved by sacrificing efficiency, but the reduction in efficiency is negligible when two baffles are used.

3. The maximum amount of gas that may be utilized by any brake is close to that deflected by a single baffle of adequately large diameter placed at 4 calibers from the muzzle.

A qualitative analysis of the flow through a deflector confirms these conclusions.[8] A type of brake designed on the basis of the results of this investigation is described in the next section.

With the protection against muzzle blast afforded gun crews by existing guns, only brakes of medium efficiency can be utilized. The utilizable efficiencies may be obtained from light attachments, such as the 2-baffle service brake used on the British 17-pounder.

4.4.2 Deflectors for the Protection of Structures Against Blast Damage

Any deflector that deforms the blast relieves blast pressures in some directions, accentuates them in others. Deflectors of moderate size may be used as aids in protecting structures only if there are directions available toward which the blast intensity may be directed. It is not sufficient, however, to deflect the blast

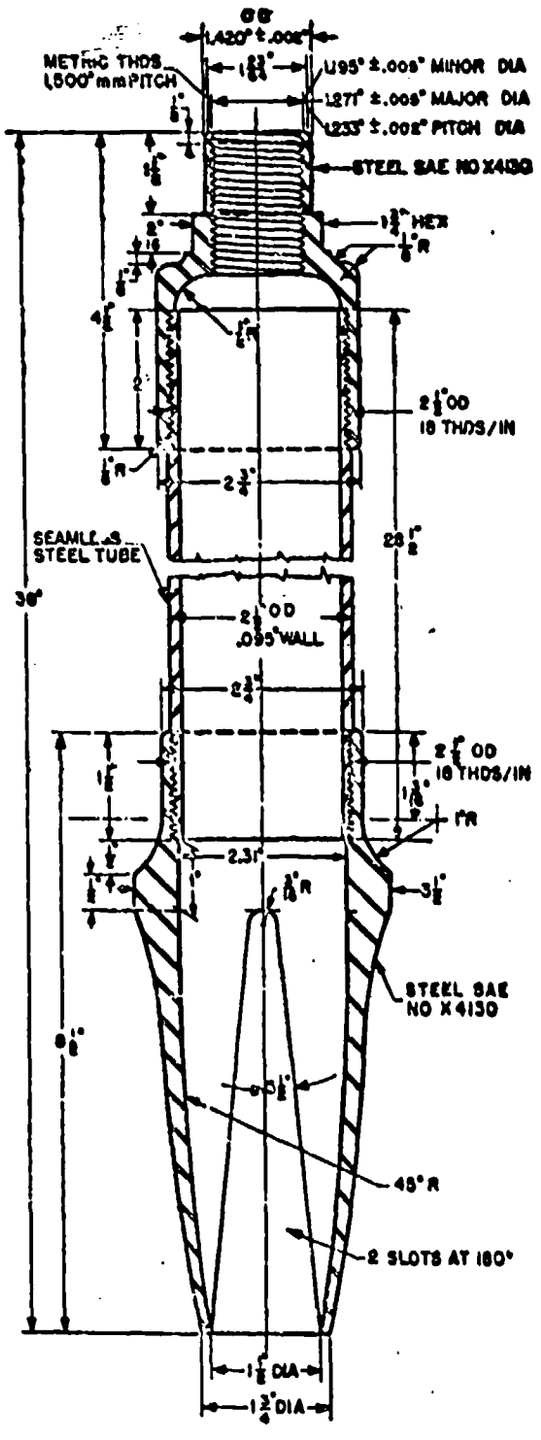

FIGURE 10. Blast deflector for 20-mm A/C cannon.

does the standard service brake. This last effect must be taken into account in the problem of dust because no field attachment can eliminate obscuration when the gun fires from the dug-in position. It is possible to prevent serious obscuration only by placing a sufficiently large blast mat under the deflector. If it is possible to dig the gun in it is certainly practicable to spread a mat before it. At low bore heights the principal function of the deflector is to protect the mat from the blast effect.

The 4-baffle deflector shown in Figure 11 has exhibited the best overall performance in the tests to which it has thus far been subjected.[6,10,24] At normal bore heights its performance is not distinguishable from that of the 2-baffle unit, although close to the ground it produces somewhat greater obscuration. However, it showed marked improvement over all the deflectors tested in protecting a mat from blast damage at extremely low bore heights. It seems quite certain that a properly constructed canvas mat can be used with this unit.

What has been said regarding multiple baffling in connection with muzzle brakes applies equally well to all deflectors. This 4-baffle unit is about 25 per cent lighter than the 2-baffle deflector of comparable performance. It is not so efficient a deflector or brake as the 2-baffle unit, but the greater strength of the forward jet produces no noticeable effects on the dust at normal bore heights and its efficiency as a brake is probably as great as can be utilized when gun pressures exceed their present values. It shows a tendency to inhibit flash.

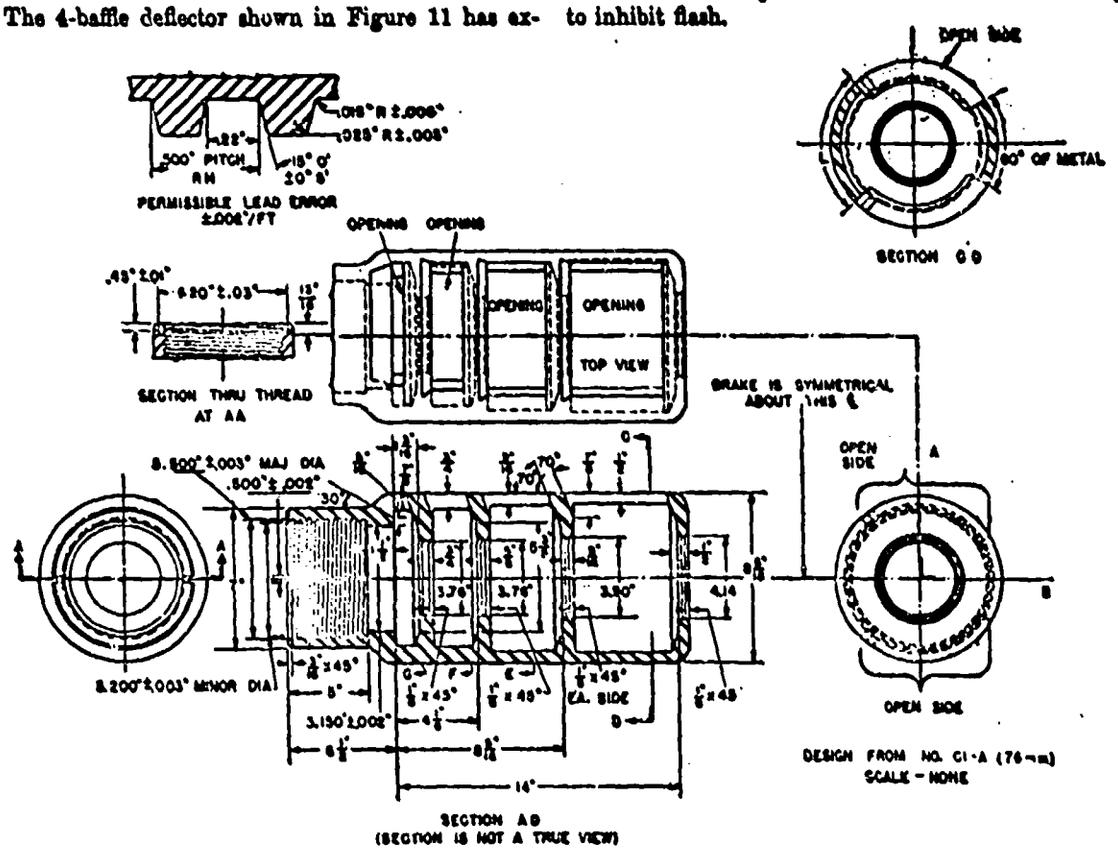

Figure 11. Four-baffle deflector for suppression of dust.

The deflector shown in Figure 12 has a large cavity and the port area, although adequately large, is small compared to the wall area.[6,7] This deflector suppresses the effects of the terminal rarefaction quite satisfactorily at low bore heights. As constructed, its general performance is not so good as that of other deflectors but it can be greatly improved by properly shaping and spacing the baffles. As has already been indicated, the suppression of the rarefaction wave is due to the large cavity and relatively small ports. The effectiveness of

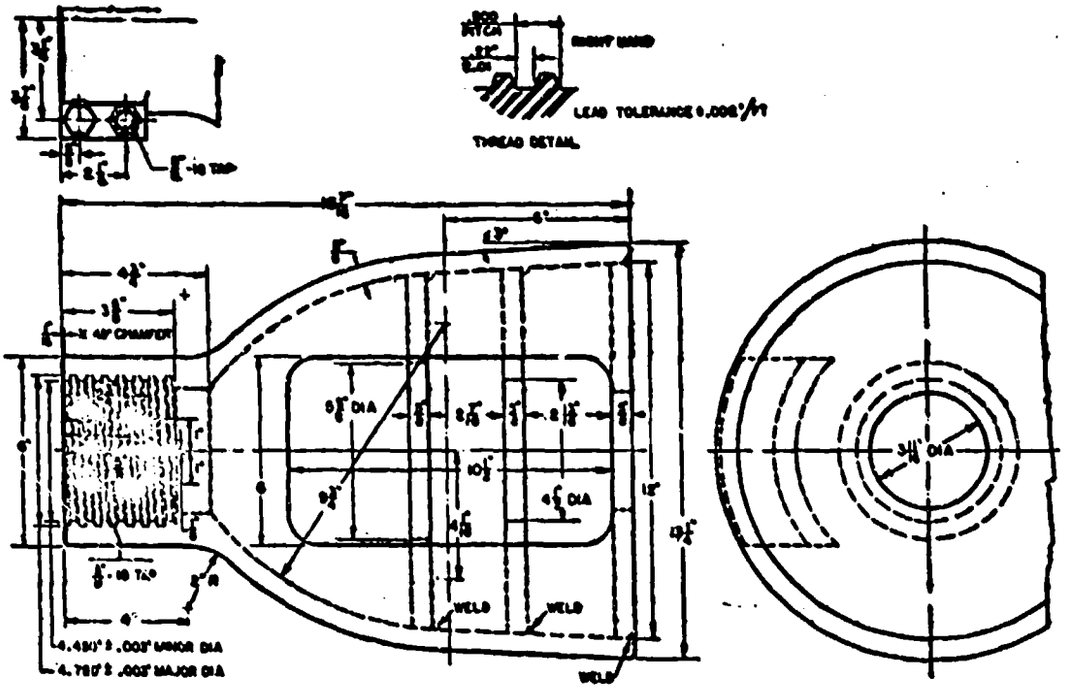

FIGURE 12. Deflector of large capacity for suppression of dust.

any deflector in the dust problem is enhanced by a sufficiently great increase of its radial dimensions without an increase of the port area, but whether the improvement in visibility justifies the increase in weight has not been determined. Besides the disadvantage of increased weight, deflectors of large capacity induce flash. When firing flashless long-primer ammunition in the 76-mm gun, a brilliant flash was always observed when the deflector shown in Figure 12 was used.

When the length of a deflector and the number of baffles is predetermined, the diameter of the baffles as well as the spacing may be determined experimentally for maximum braking action as was indicated in connection with Figure 9. The port area then is made as large as practicable. In the 4-baffle deflector the baffles were spaced as shown in Figure 11 in an attempt to produce uniform flow through the ports rather than to give maximum braking action. A more effective means of distributing the flow is to vary the diameters of the baffle holes as shown in Figure 13. This method, however, diminishes the efficiency of the unit as a deflector. Uniformity of flow can be achieved by varying the port areas as shown in Figure 13.[4] The capacity of this deflector is increased by increasing the

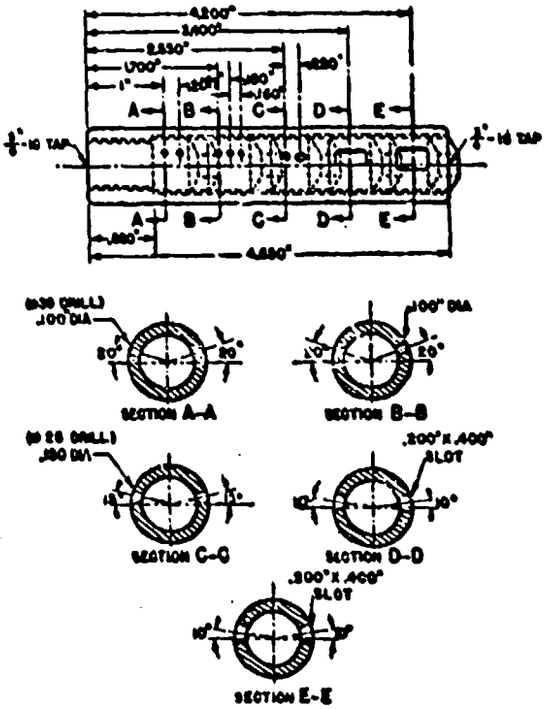

FIGURE 13. Arrangement of ports to ensure uniform distribution of outflow from deflector.

length without increasing the diameter. This deflector has received no full-scale tests.

4.6.3 Deflectors for the Suppression of Flash

The suppression of flash and smoke is a problem of powder chemistry, but muzzle attachments have a great effect on the production of flash. It has been observed that multiple-baffle deflectors of small capacity and with small baffle hole diameters and large port areas tend to inhibit flash. The deflector shown in Figure 11 completely suppresses flash in the 37-mm gun, and an 8-baffle deflector similar to this completely suppresses the flash from a flashing round in the 76-mm gun 80 per cent of the time. The flash produced the rest of the time is weak and due to localized burning of the deflected jet.[8-24] The 8-baffle deflector did not show any obvious diminution in the flash of the 90-mm gun, but the intensity of the flash from this gun is so great that even a great reduction could not be detected by the eye.

4.8 THE CONTROL OF BLAST

Satisfactory deflection of the gas may be achieved with relatively small muzzle attachments. The most efficient of these permit a residual jet to go through the forward hole which, by itself, produces unobjectionable blast effects in guns at least as large as the present 90-mm gun. The problem these deflectors leave unsolved is that of the disposal of the deflected jet. The most successful of muzzle attachments is the muzzle brake, but its usefulness is limited by the great blast pressures and other blast effects produced toward the rear of the gun when high efficiencies are utilized. The dust problem can no doubt be solved by using a sufficiently large attachment which deflects the jet straight up. Such a deflector would be a mediocre brake and, because of the great downward thrust at the end of the tube, its use would require radical changes in the gun and mount assembly with a substantial overall increase in weight. So long as the blast, however deflected or deformed, is ejected in the neighborhood of the muzzle there will be muzzle-blast problems.

Assuming that the desired fraction of the jet can be deflected through 180 degrees and carried in one or more ducts so as to eject it up over the carriage or sufficiently far to the rear of the gun, then near the muzzle the only blast effects would be those of the weak residual jet. In passing through the long ducts and through expansion chambers that might be provided the deflected jet would lose considerable pressure; the disposal system, in effect, could be an effective muffler. The design of such a disposal system would present no grave difficulties. Consider, for example, the simple system in which the jet is subjected to an axially symmetrical deflection and the duct is the space between the outer surface of the gun tube and the inner surface of a concentric thin-walled tube of sufficiently large diameter. This duct would recoil with the gun and would have to fit into a second tube fixed to the part of the mount that moves as a unit with the recoil slide; that is, the first tube would recoil with the gun into a second tube fixed to the mount but elevating and traversing with the gun. Beyond the juncture of the tubes the flow would be divided and carried by two ducts which might turn upward and possibly forward over the vehicle. The thrust produced by the secondary deflection of the gas could always be directed so as to produce no rocking of the carriage.

Assuming the possibility of such deflection the maximum braking action would be available, and the saving in weight of recoil mechanism and mount would compensate for the weight of the disposal system. However, the silhouette of the gun would be increased.

Such a disposal system can be justified only if a sufficiently large fraction of the blast can be turned through 180 degrees. One method of controlling the jet is to construct a valve that closes the forward hole of the deflector immediately after the base of the projectile has gone through. A valve that shuts off the forward flow within 1 msec after shot ejection has been constructed for the .30-caliber gun.[8] The scaling of such a valve to large calibers presents difficulties, though not insurmountable ones. A valid objection to the use of such a device is that a valve is subject to malfunction. Deflection of a substantial portion of the jet through an angle greater than about 120 degrees by means of a static deflector has been found difficult. A 1-baffle deflector with cone diffuser of extremely large size can be constructed which gives satisfactory results, but multiple baffling to reduce the size leads to jet separation with consequent decrease in efficiency.[8]

Close to the termination of this investigation an efficient and reasonably compact 180-degree deflector was being developed.[8] The method of designing the inner surfaces of a 4-baffle unit is sketched in Figure 14. The dotted lines a, b, c, d and d' emanating from the mid-point of the muzzle are approximately the

asymptotes of streamlines in the bottle of the free jet. The lines d, d' are elements of the boundary of the minimum residual jet which goes through a circle of 1.1-caliber diameter placed at 4 calibers from the muzzle. This will be the actual residual jet, provided the

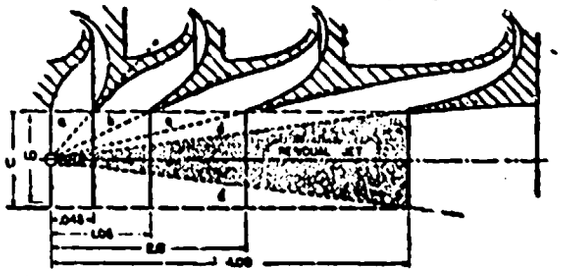

FIGURE 14. The 180° blast deflector. Design of inner surfaces. Dimensions are in calibers.

gas is allowed to expand freely at the muzzle and no shocks from the inner surfaces of the deflector enter the shaded region between d and d', for an oblique shock that enters this region always deflects streamlines from outside into the shaded area. To ensure that shocks do not enter this region or, if they enter, that they be weak it is necessary that the lips of the baffle cones be as thin as it is practicable to make them and that the elements of these cones coincide with the streamlines as closely as possible. From this initial direction the surfaces curve away gently so as to compress the intercepted gas gradually.

The layout of the inner surfaces is still a matter of trial and experience since there are no known methods of ensuring the isentropic compression and turning of a 3-dimensional supersonic jet. It seems unlikely, furthermore, that a static deflector can be constructed to maintain isentropic flow at all stages of a transient jet. Practically, the compression and deflection of a supersonic jet can be accomplished only through a system of oblique shocks; these cannot be avoided, but if the compression is gradual it may be possible to turn the stream without producing a normal shock. The minimum requirement in the present problem is that a normal shock that may occur in the passage between two baffles shall be weak enough not to drift down below the baffle cone lip, where it would alter the central flow. Once the gas is compressed to where its speed is subsonic it will follow the curved path more readily. The attempt to turn the gas as nearly isentropically as possible is desirable, however, for two reasons: (1) through adiabatic flow the greatest braking action will be obtained, and (2) the tendency to flash will be diminished.

After the gas is turned through 180 degrees it is allowed to expand into the ducts. The transition section also requires careful consideration. Even if it is not possible to maintain adiabatic flow, it is necessary that the transition be gradual to minimize turbulence. By maintaining a sharp boundary between the air in the ducts and the powder gas until the pressure is substantially reduced, secondary burning may be avoided. It is anticipated that burning within the disposal system and flash on ejection of the gases will prove troublesome to control unless, perhaps, a liquid spray is used within the system.

The ideal spacing of the baffles is that which distributes the flow uniformly between the passages. In view of the intensity of the flux of gas out of the muzzle while the base of the projectile travels through the deflector it will be difficult to avoid an excess of gas going through the passages closest to the muzzle. The spacing shown in the sketch of Figure 14 is such as to make the openings normal to the mid-streamlines approximately equal.

The only deflector of this type constructed was a 2-baffle brake with 30 degree reversal angle.[8] The residual jet was about the weakest that has been obtained even though the width of the passages had been reduced to 0.07 in. at the point where the gas had been turned through 120 degrees. It seems quite certain that through this small area the speed of the gas was already subsonic and that no loss in flow would have resulted from further turning. The braking efficiency was 63.5 per cent. It has already been explained that brakes on the .30-caliber rifle have low efficiencies and that a brake configuration that yields 50 per cent efficiency on this caliber will yield 70 per cent on the .50-caliber gun. Since there can be no throttling of the gas in the passages as there is in brakes with large baffle spacings, the efficiency will increase with increasing reversal angle and with proper expansion before ejection.

4.6 CONCLUSIONS

The blast problems that arise with increasing pressures in the modern medium-caliber high-velocity guns require for their solution a detailed knowledge of the phenomena associated with the emptying of a gun if the solution of these problems is to be raised from the trial and error stage. Methods of treating the interior ballistics of a gun after shot ejection have now been developed and a working knowledge, mostly

qualitative, of the blast characteristics has been accumulated. Simplified formulas on which to base the rational design of muzzle attachments are still to be developed; but progress has been made in the understanding of the extent to which muzzle-blast effects may be modified by various types of attachments, and general predictions regarding the efficacy of new designs can now be made.

The most successful muzzle attachments are the muzzle brakes, but because of the high blast pressures they produce at the rear of a gun only brakes of medium and low efficiencies are generally utilizable. These may be constructed as light units. So long as only moderate braking efficiencies are required, attachments may be constructed that inhibit flash or, at least, that do not accentuate it. Freedom from obscuration of target is more difficult to ensure, but the seriousness of the problem may be diminished. By taking advantage of the strength of the elevating mechanism, the blast may be turned slightly upward and this is sufficient to reduce obscuration substantially at normal bore heights. At low bore heights, slight upward deflection is insufficient to ensure visibility of target, but by proper diffusion of the deflected jets it is possible to use a mat in combination with the deflector so that obscuration will result only under most adverse conditions. These improvements can be expected to be less obvious when the powder pressures are increased substantially above their present values.

The full utilization of the breaking action of the blast and a more definite solution of the blast problem in general may be achieved by disposing of the gases toward the rear of the gun or up over the carriage. A disposal system of this sort must be incorporated in the design of gun and mount assembly. Since full-braking action is utilizable in this scheme, the great reduction that may be made in the weight of recoil mechanism and mount may be sufficient to allow a reduction in weight of the whole assembly. High-pressure guns can be rendered practically recoilless by the use of such a disposal system.

By properly shaping the inner surfaces of the deflector the blast can be delivered to the return ducts without tendency to burn, but it is not certain that burning would not occur as the gas mixes with the air in the ducts. To prevent burning it might be necessary to use a spray. In field guns the transportation of sufficient liquid to prevent burning would present, perhaps, a grave problem, but at sea the problem of spraying the gas in ducts would be minimized should salt water prove suitable for the purpose.

Since the equivalent of the obscuration problem does not occur at sea, it should be possible to obtain a substantial reduction of the blast effects in a ship's guns with relatively compact deflector-duct systems.

4.7 RECOMMENDATIONS

The modern high-pressure medium-caliber gun already has great competition in the many weapons that have recently been developed, but it is assumed that the highly mobile gun and the multiple gun antiaircraft battery will continue to maintain their places in the midst of the new weapons. The survival of such guns will no doubt depend largely on the success with which their blast is brought under control.

Investigations of blast effects and of the potentialities of blast deflectors would be greatly aided if the scaling laws of blast phenomena were known. To determine these and at the same time augment our present knowledge of the emptying of guns, the following programs are recommended:

1. The theoretical investigation of the interior ballistics of a gun after shot ejection should be continued until a working method for determining the flux of momentum through the muzzle is derived.

2. The systematic measurement of interior ballistic quantities should be continued. Records should be read for times after shot ejection at least as long as the time of travel of the projectile. This work should be done on small arms as well as on guns of large caliber and should include a range of caliber, tube lengths, relative powder loads, and rates of burning of powder.

3. Work should be initiated for determining the distribution of momentum in the blast, that is, in transient jets of short duration. This problem presents many difficulties but some solution should be attempted.

4. A ballistic pendulum should be constructed capable of carrying the larger of the medium-caliber guns. Such a pendulum would greatly facilitate investigations of recoil problems.

Field attachments comparable to the present muzzle brakes will no doubt continue to be used for a long time. For instance, when a gun crew is adequately protected by armor plate and the gun fires at high elevations it might be possible to use a high-efficiency brake. It seems unlikely that small muzzle attachments that exhibit properties vastly different from those already observed can be constructed, but the following programs would be profitable:

5. Full-scale models of brakes similar to that de-

scribed in Section 4.5 should be constructed with various reversal angles. It is believed that these brakes will tend to suppress flash.

6. The effect on flash of simple multiple-baffle units should be investigated in various calibers.

7. The feasibility of strengthening elevating mechanisms and balancing existing guns to take deflectors of larger capacity which give the blast greater upward deflection than those that have already been tested should be investigated. Deflectors similar to that shown in Figure 13 should be constructed to full scale.

It seems quite certain that great reduction in blast effects cannot be achieved with anything less than 180-degree deflection of a large fraction of the blast, followed by the effective muffling of the deflected gas. It is still speculative to what extent blast can be controlled by such means. One final program is strongly recommended:

8. A 180-degree deflector such as that described in Section 4.5 should be constructed in a caliber no smaller than 90 mm. Disposal systems should be investigated which expand and cool the deflected gas before the eventual baffling and ejection to the point where burning and flash will not occur. If burning cannot be prevented within such a system by proper expansion, the effect of sprays should be investigated.

PART III

TERMINAL BALLISTICS

Chapter 5

FUNDAMENTALS OF TERMINAL BALLISTICS

5.1 INTRODUCTION

THE ABILITY of a weapon to neutralize an objective depends, at least partly, on the relation between the amount of protection possessed by the target and the power of the weapon. Only the attacking missile and, within limits, its condition when it reaches the target, and the portion of the target that is attacked are under the control of the offense: the type, arrangement, and extent of the protection are at the disposal of the defense. This competition between the power of a given attack and the strength of passive protection supplies the subject matter of terminal ballistics. Specifically, terminal ballistics is concerned with phenomena occurring at the target. Other divisions of the general subject of ballistics, interior and exterior, deal with the phenomena in the gun and the phenomena of free flight respectively. This subdivision of the subject matter of ballistics into three parts is useful even though the distinctions are not always sharp or even applicable in all cases as, for example, with rockets or aerial bombs.

5.2 THE WORK OF DIVISION 2 IN TERMINAL BALLISTICS

Different phases of terminal ballistics were studied by Division 2, NDRC, during World War II, the selection of problems and the emphasis placed on the various research programs being determined by practical considerations arising from the needs of the Armed Services. These needs, of course, changed with the favorable progress of this war and the resulting general trend from defense to offense.

Thus the terminal ballistics work of Division 2 was concentrated on certain selected problems rather than on an attempt to cover all of the unsolved problems in the field. In most cases the object of the research was basic information by which operational designs or procedures might be improved and made more effective, rather than the development of a particular device or gadget. Correspondingly, the work was planned and organized primarily in terms of the target material rather than according to the missiles considered. Thus Chapters 6, 7, 8, and 9 describe work on different target materials. However, Chapters 10 and 14, which are concerned with particular missile-target interactions and form part of the terminal-ballistics work of Division 2, did result in the design of a very special bullet for training aerial gunners and in the design of special methods of protecting tanks against shaped-charge missiles.

Chapters 6, 7, 8, and 9 describe the terminal ballistics of steel, concrete, plastic protection, and earth from the point of view of the work done in Division 2 during World War II. Much allied work from other sources is included in the text and references in order to give a connected picture without, of course, pretending to give a complete review of all outside work on the same general subject. After some early study of the terminal ballistics of ordinary and armor steels in general, the principal emphasis in the work on steels was placed on exploring the phenomena at high striking velocities (Chapter 6). These studies furnish a factual basis for assaying future trends in the development of both arms and armor as well as suggesting some of the specific features of projectile design for hypervelocities. An extensive study of the terminal ballistics of concrete (Chapter 7) was initiated by the Committee on Passive Protection Against Bombing [CPPAB] (later the Committee on Fortification Design [CFD]) to obtain information on which a rational design of protective structures, bomb shelters, and fortifications could be based. The information gained was also of value for the analysis of offensive operations. In this same connection, work was done on the terminal ballistics of earth and soils (Chapter 8). Another research program, of particular interest to the Navy and Merchant Marine, dealt with determining the kind and degree of protection afforded by plastic protection (British plastic armor) against small-arms fire (Chapter 9). Little or no work was done during World War II by Division 2 on the terminal ballistics of rock, stone, gravel, brick, wood, and other special materials which are of military interest in this field.

It is the purpose of the present chapter to outline the scope of terminal ballistics and to discuss in a general way some of the principal phenomena and concepts involved.

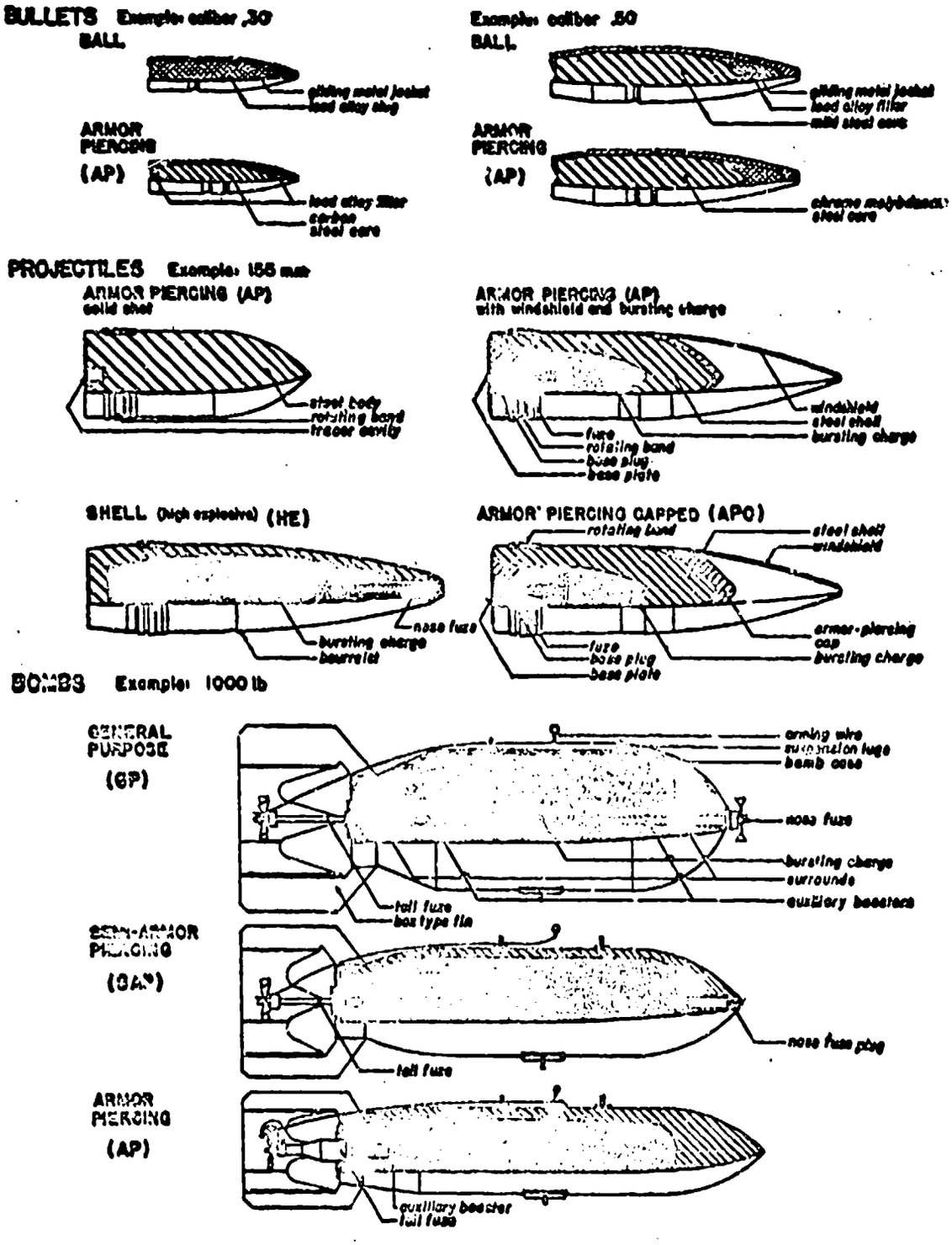

FIGURE 1. Typical bullets, projectiles, and bombs.

5.3 MISSILES

Some of the conventional types of missiles are shown in Figure 1. Besides bullets, projectiles, and bombs, however, shaped-charge weapons, rockets, fragments, etc., may be considered missiles in a broad sense.

5.3.1 Missile Properties

The principal properties of a nondeforming projectile are its weight W, caliber D, and shape. If a projectile deforms, these items change during penetration and are therefore not sharply defined. If only subsidiary parts of a projectile deform, such as windshield, cap, or jacket, reasonably good estimates of penetration can often be obtained by using only the weight, caliber, and shape of the nondeforming part of the projectile.

A derived projectile parameter which is particularly useful in comparing phenomena at different scales is the caliber density D, defined as W/d^3. This is a constant for similar projectiles of different calibers. For a given type of missile the value of D will remain within a narrow range for exterior ballistic reasons, i.e., in order to achieve satisfactory flight characteristics. This fact is an aid in estimating the weight of a hypothetical attacking missile of assumed caliber. Thus, both foreign and American armor-piercing [AP] bombs and conventional steel projectiles have caliber densities that usually lie in the interval

$$D = 0.45 \text{ to } 0.65 \text{ lb per cu in.},$$

with $D = 0.55$ lb per cu in. as a reasonably good average value. For semi-armor-piercing [SAP] bombs the range is

$$D = 0.20 \text{ to } 0.35 \text{ lb per cu in.},$$

with $D = 0.27$ lb per cu in. as an average. The charts given in Figure 2 will facilitate estimates involving caliber density.

5.3.2 Missile Deformation at Impact

The missile depends for its action on the kinetic and chemical (explosive) energy it carries to the target. Attention is restricted to the case in which the missile reaches the target mechanically intact since there are separate treatments of the remote effects of an explosive missile transmitted to the target by air blast, earth or water shock, and fragments. Furthermore, the mechanical performance of the missile against the target before any explosion takes place stands in the forefront of our interest.

At impact there is a competition between missile and target in which not only the target but also the missile may yield in varying degrees. Thus a steel projectile may shatter against armor, and a general-purpose [GP] bomb or high-explosive [HE] shell may deform or rupture against concrete. In both cases a considerable indentation into the target may still be achieved, even though it is less than would be produced by a nondeforming missile. Some of the typical features of Service missiles that are involved in the question of deformation or breakup may be seen in Figure 1. Thus, the function of an armor-piercing cap is to improve the terminal ballistic performance of a projectile against an armor target by inhibiting the breakup or shatter of the remainder of the missile. A windshield is added to the nose of some projectiles to improve their exterior ballistics; against targets like armor or concrete this windshield is crushed and swept away during the first stages of penetration. Interior ballistic considerations have resulted in the provision of a soft metal jacket on small-arms bullets to give the barrel a longer life when many rounds have to be fired; against steel armor or concrete these jackets are soon torn off even when the core remains intact.

Except for some cases at high obliquity against thin plates, shatter or deformation handicaps a missile with respect to the target. The breakup of small-caliber AP cores in plastic protection was found to be an essential factor in the performance of the latter as a target. When fragments from an explosive shell or bomb are considered as individual missiles their target effect is greatly influenced by breakup; this is true to such an extent that it is difficult to devise experimental methods for recovering fragments intact for the purpose of assaying their original size, shape, and weight distributions as functions of direction from the shell or bomb. The extreme case of complete projectile shatter without sensible effect on the target was proposed and given a satisfactory practical solution in the frangible bullet for gunnery training (see Chapter 10).

5.4 IMPACT CONDITIONS

The principal impact conditions which need to be specified are striking velocity v_0, the striking obliquity or angle of incidence θ, and the yaw. The last two are defined in Figure 3, together with several other terms relating to the geometry of impact. Bombs and pro-

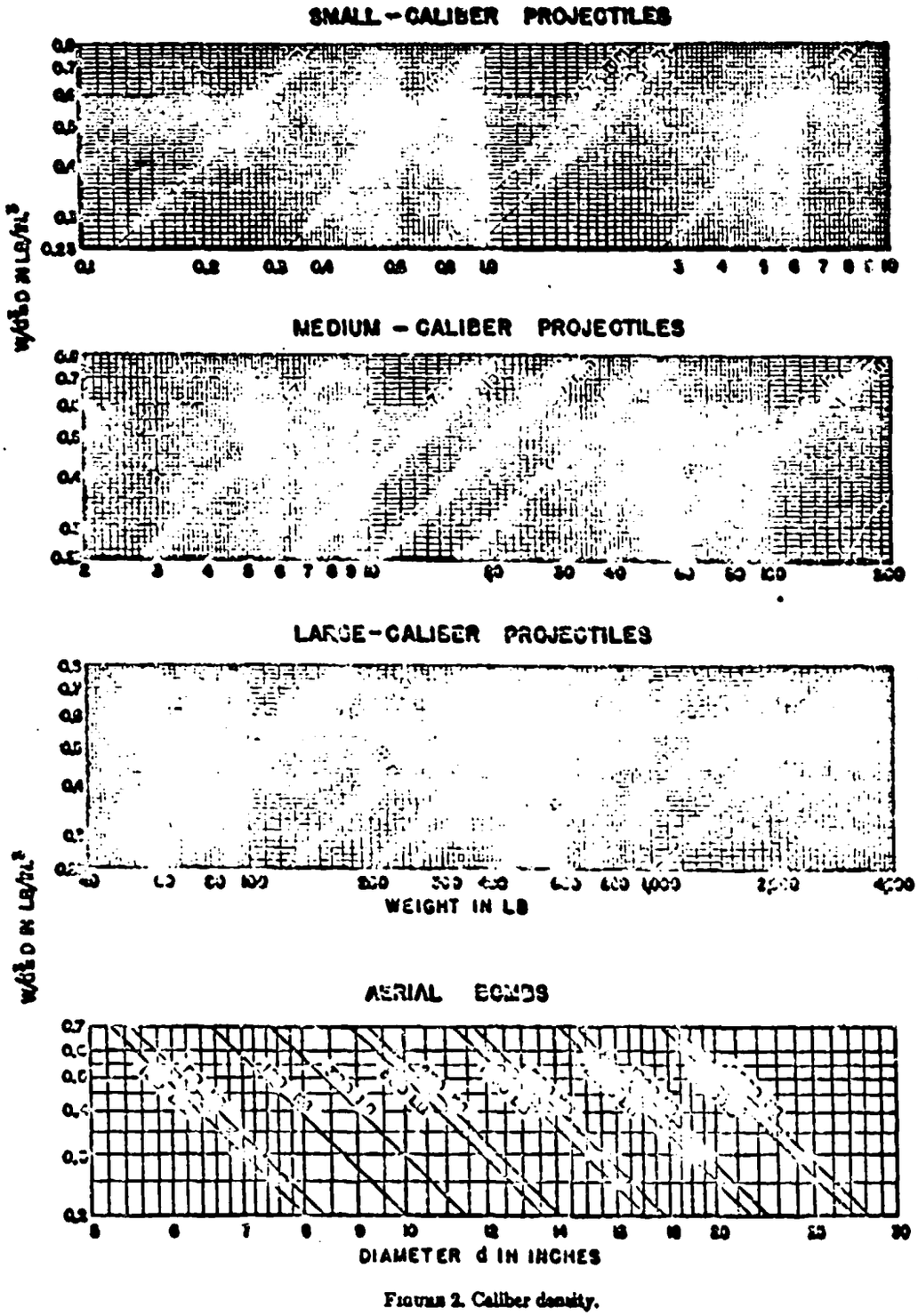

FIGURE 2. Caliber density.

jectiles are designed to minimize yaw in flight, and it may be assumed in most terminal-ballistic problems that the yaw is zero unless otherwise observed or specified. Increasing yaw tends to decrease the penetrating

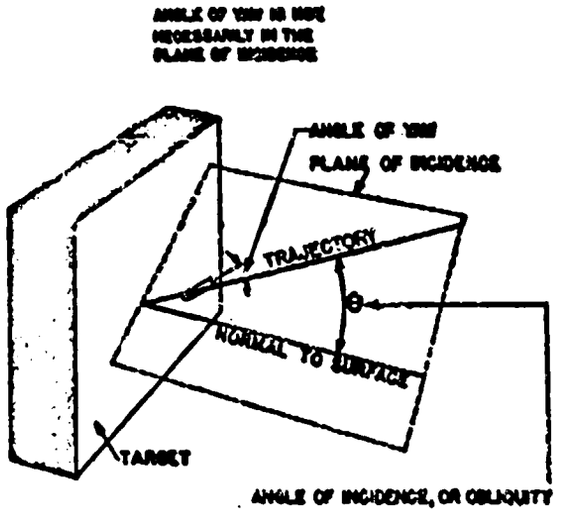

FIGURE 3. Geometry of impact.

ability of a projectile or bomb and to increase its chances of deformation and breakup.

The performance of a projectile against a given target usually increases with striking velocity and decreases with increasing obliquity. However, each of these factors also tends to increase the likelihood of projectile shatter, which can, in some cases, exactly reverse the expected trends. Thus a projectile that defeats a plate at a certain striking velocity may shatter at a higher velocity and fail to defeat it. On the other hand, a projectile that ricochets intact at a certain obliquity may actually produce deeper indentations or even perforation at a greater obliquity if this causes shatter.

8.5 RESULTS OF IMPACT — PENETRATION AND PERFORATION

In considering the effects on the target it is useful to distinguish between penetration and perforation, particularly when the projectile remains in one piece and does not break up. With breakup of the missile some parts may pass through the target while others are stopped. In a strict sense the term *penetration* is reserved for the entry of a projectile into a target without passing through it. The phrase "penetration into a massive target" or simply "massive penetration" is often used when there is no bulging or rupture of material at the back face of the target, this being taken as evidence that the penetration in such cases does not depend on the finite thickness of the target. The term *perforation* is used specifically when the projectile passes completely through the target slab or plate. In the transition region between massive penetration and perforation the proximity of the back face of the target permits a greater penetration than would be obtained with a thicker target under the same conditions. In other words, in the transition region the penetration is expected to depend on the target thickness, while massive penetration is assumed not to depend on target thickness.

In an idealized way Figure 4 shows the difference in the character of the perforation hole made by a nondeforming projectile in concrete and steel. With a brittle or frangible target, like concrete, both front

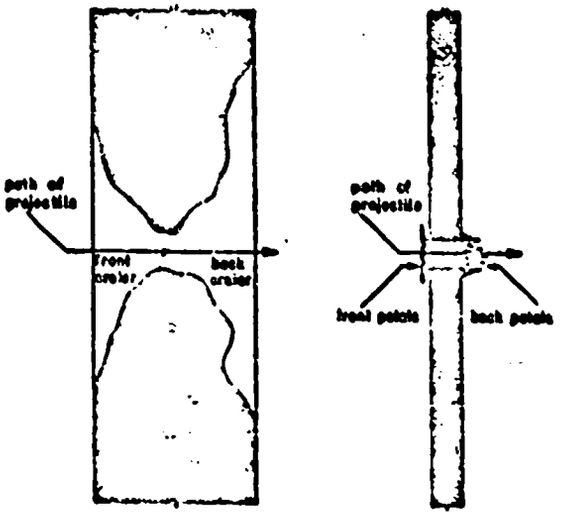

FIGURE 4. Perforation of thin concrete target and of steel target.

and back craters are formed; the material ejected from the front crater is called *spall*, while that from the back crater is called *scab*. With a tough or ductile target, like steel, the displacement of material from the path of the projectile usually results in the formation of front and back petals rather than a separation of the material from the target as spall and scab.

Chapter 6

TERMINAL BALLISTICS OF ARMOR

6.1 INTRODUCTION

PERFORATION of steel has been studied more extensively than that of any other material, but until World War II few tests had been made with plates thicker than twice the caliber of the projectile. Up to that time there had been little interest in heavier plate since it could not be defeated with the Service weapons then available. As practical methods were developed for obtaining higher projectile velocities the situation changed. It then became necessary not only to extend investigations to thicker plate but to find better means of preventing projectile deformation. It is now possible to perforate homogeneous armor almost 10 calibers thick, but the problem of armor perforation has by no means been completely solved.[a,b]

6.1.1 Trend to Hypervelocities

It has always been true that methods of defense have advanced to neutralize the destructive power of existing weapons. During World War II, for example, tanks were made less and less vulnerable by progressively increasing the amount and improving the arrangement of the protective armor. Before World War II, the principal antitank weapon of the United States was the 37-mm gun; at the end of the war a 90-mm gun firing a high-velocity, tungsten carbide cored projectile was being used, and more effective weapons were being developed.

Improvements not only in tank armor but in all types of passive protection may be expected to continue and guns must likewise be made more effective to match these improvements. There are three conventional methods by which greater effectiveness can be obtained:

1. As better methods of handling guns are developed, their maneuverability is increased. This permits the replacement of small weapons by guns and projectiles of larger caliber.

2. By continued improvements in design, guns of all calibers can be made more powerful.

3. The ability of any gun to perforate armor can usually be increased by the use of special projectiles of the subcaliber type.

Merely increasing the size of a gun obviously offers only a partial solution to the problem; advances must come mainly from the development of more powerful guns and of better subcaliber projectiles. Advances along either of these lines involve the use of what are now termed hypervelocities, velocities in excess of 3,000 fps. The practicality of projectile velocities in this range has already been well demonstrated; numerous gun and projectile combinations resulting in hypervelocities have been developed and certain of these have been successfully used in combat. Possibilities for substantial improvements have not been exhausted, however.

6.1.2 Hypervelocity Projectiles in World War II

The possibility of the practical use of hypervelocities was well recognized before 1941, but suitable methods for obtaining these velocities had not been worked out. The idea of the tapered-bore gun[c] as well as the subcaliber projectile[b] for standard guns was not new, and efforts were continually being made to overcome gun erosion so that the power of conventional guns could be increased without unduly shortening their life.

Interest in unconventional methods of gun and projectile design was intensified in 1941 because of a report from the Libyan campaign in North Africa that the Germans were using a hypervelocity, tapered-bore gun as an antitank weapon. Actually this gun was not extensively used, but it did lead to a momentary setback in morale and consequently provided a spur to programs for the development of hypervelocity weapons in the United States, England, and Canada. Before the end of World War II all countries had successfully employed in combat high-velocity, tungsten carbide cored projectiles which were provided for guns of various calibers. The principal Service type of the Americans, *hypervelocity armor-piercing* [HVAP], and of the Germans, *armor-piercing* [AP 40], was the composite rigid; that of the British, *armor-piercing discarding sabot* [APDS], was the discarding sabot. It is perhaps worth noting that none of these projec-

[a] Pertinent to War Department Projects OD-75, CE-5, and CE-6; and to Navy Department Project NO-11.

[b] See Chapter 5.

[c] See Weapon Data Sheets 2C3, 2C3a, 2C4, 2C5*, 2C5a, 2C6, 2C7 of Chapter 19.

tiles required modification of standard guns; the guns could therefore be used to fire alternatively projectiles of conventional and subcaliber types. The development of other methods had been brought to a successful conclusion but these methods were not widely used in the theaters of operation.

In the United States the work in devising and developing methods for obtaining hypervelocities was carried out by Division 1, NDRC, and the Army Ordnance Department. Additional studies of the terminal-ballistic aspect of the problem were made by Division 2, NDRC.

The need for a program to investigate the terminal-ballistic phase had been emphasized by another report from the Libyan campaign. It appeared that guns firing 2-pounder AP shot were much less effective at point-blank than at longer ranges. This apparently anomalous behavior resulted because at the high velocity near the muzzle the shot completely disintegrated on impact, but at greater distances, having lost some of its velocity in flight, it remained intact.[3] The reduction in penetrating ability due to breakup of the shot far offset any advantage that might have been expected because of its greater striking energy at the muzzle. Thus there was early recognition of the fact that a projectile might become less rather than more effective when its velocity is increased. The difficulty in designing a nondeforming projectile still remains one of the principal obstacles to the use of hypervelocity weapons.

6.1.3 Studies of Armor Perforation in Division 2, NDRC

Initial Hypervelocity Program

When the hypervelocity program was first originated in Division 2, NDRC, at the request of the Army Ordnance Department under project OD-75, it was described as an "investigation of the penetration of homogeneous and face-hardened armor at striking velocities of 3,000 fps and above. Tests were to be made at t/d [thickness of plate/diameter of projectile] ratios between 2 and 4 and at angles of obliquity ranging from 0 degree to the maximum within the capacity of the equipment. Plate hardnesses were to be such as to give Brinell readings of 250 or above."[20]

Soon after work was begun, August 1942, it was recognized that the original directive was too limited. Actually, the tests were not restricted to plates less than 4 calibers thick nor were all firings conducted at velocities above 3,000 fps. The hypervelocity problem is not so much one of determining projectile performance in a particular range of velocities as it is of discovering the effect of increasing the velocity from low to high values.

General Terminal-Ballistic Program

Terminal-ballistic studies at high velocities represented for Division 2, NDRC, a natural extension of earlier investigations using velocities that could be obtained with conventional guns and projectiles. In the earlier work, which was carried out for the U. S. Naval Ordnance Department under project NO-11 and for the Corps of Engineers, U. S. Army, under projects CE-5 and CE-6, interest centered mainly in the properties of the plate and its ability to resist perforation. In the later work, the experimental range of velocities was extended from 3,000 to 5,500 fps and the emphasis was shifted from a study of plate behavior to considerations of projectile performance, particularly as it is affected by deformation. The program was originally planned and continued to be an empirical study of the general problem of projectile impacts against armor over the complete range of practical velocities. It was impossible, however, to consider all types of targets and to investigate all variables in projectile design. The tests were mainly limited to impact conditions likely to be encountered in combat and were not primarily intended to study basic physical phenomena.

Purpose

The purpose of the work was to test the feasibility of using hypervelocity projectiles to defeat armor protection and to study the factors controlling perforation. The ultimate goal was to obtain data that would indicate the impact conditions under which projectiles of different types would be most effective and would serve, at least in part, as a basis for projectile design.

6.1.4 Scope of Present Report

The discussion in the following sections is limited mainly to those aspects of the terminal-ballistic problem covered by the work of Division 2, NDRC, but reference will be made to parallel work of other research groups. The report is not intended as a complete record of all contributions nor as a comprehensive review of all phases of the subject. For total coverage of tests relative to high-velocity impacts, reference should be made to British and Canadian reports[4] mentioned in the British Ordnance Board Proceedings, to papers by Frankford Arsenal, and to firing

records of the Aberdeen Proving Ground. Other organizations in the United States that have made important contributions to the general problem of armor perforation but have not been concerned with hypervelocities are Watertown Arsenal, Naval Research Laboratories [NRL] and the Naval Proving Ground at Dahlgren.

6.2 PROBLEM OF ARMOR PERFORATION BY INERT PROJECTILES

Although a concise statement of the problem of armor perforation could be made, it would, through the omission of details, be misleading. Instead of a definition, a brief discussion will be given of the general problem.

Neither the general problem of discovering the most efficient means of piercing armor nor the more specific problem of designing a projectile to perforate the maximum thickness of plate can be solved by terminal-ballistic considerations alone. The ability of an armor-piercing projectile to defeat a particular target depends as much on the power and size of the gun and the range over which the projectile is fired as it does on the plate-projectile properties that control perforation. Considering a given gun, the energy available from the powder is expended principally in overcoming frictional and engraving forces acting on the projectile during its travel through the gun, in heat transferred through the walls of the barrel, and in supplying kinetic energy to the powder gases and to the projectile.[4] Part of the energy possessed by the projectile at the muzzle is lost to air resistance in flight, and only the remainder is available for piercing armor. It is the province of interior ballistics to transfer as great a portion of the original energy into the muzzle energy of the projectile as possible, of exterior ballistics to reduce losses due to air resistance, and of terminal ballistics to use the remaining energy in the most effective way for perforating the target and producing subsequent damage. It is unfortunate that changes in projectile design desirable from a terminal-ballistic point of view may be detrimental to its interior and exterior ballistic behavior.

A projectile can best use its striking kinetic energy for perforation if it remains entirely undeformed during impact. This basic idea is an almost intuitive concept which is confirmed by trials reported profusely throughout the literature.[5,6] Only one case is known to the writer in which this is apparently not true.[5] In the attack of thin plate at very high angles of obliquity, a projectile of conventional nose shape may ricochet if it remains intact and require more energy for perforation than a projectile that shatters. Even under these exceptional conditions of attack, however, it is likely that if a nondeforming projectile of any nose shape were possible it could be designed to perforate with less energy than one that deformed.[7,8] Although there is general acceptance of the idea that a projectile should be kept intact if possible, a feeling still persists in some quarters that this is of little importance for high striking velocities. This is implied in a well-known ordnance book, which states that "if very high striking velocities are obtained, penetration is little affected by the material of which the projectile is composed." It is conceivable that this might be true at sufficiently high velocities, but it is not true up to 5,000 fps, which is higher than the velocity of any present-day projectile in practical use. In general, the thickness of armor that can be defeated by a projectile with a given striking energy will fall between the limit thicknesses corresponding to the extreme cases of a nondeforming projectile on the one hand and a perfectly plastic projectile on the other.

Although the nondeforming projectile represents the ideal, this cannot be attained in practice, at least not under all conditions of impact likely to be encountered by projectiles fired from present-day guns. It is therefore necessary to accept some sacrifice, which usually appears through the addition of an armor-piercing cap. Although the projectile proper may be kept essentially intact by this means, there is still some loss in penetrating power due to the disintegration of the cap itself. The cap will lead to improved performance only for conditions of impact at which the uncapped projectile deforms badly and the deformation greatly increases the energy required for perforation. To assess the feasibility of using a cap, one must know the performance of both the uncapped and capped projectile over a wide range of striking conditions. For the uncapped projectile it is necessary to determine (1) the energy required for perforation when no deformation occurs, (2) the conditions under which deformation takes place, and (3) the effect of the deformation in limiting perforation. For the capped projectile one must find the extent to which the above factors are affected by the addition of the

[4] The energy of rotation of the projectile and recoil of the gun are usually neglected.

protective material. All three factors are altered by changes in the projectile parameters. It is therefore convenient to resolve the investigation into separate studies of the individual variables, both as they affect the energy required for perforation directly when the projectile stays intact and indirectly through projectile deformation.

The parameters of a projectile are most easily specified by giving first the projectile type (monobloc, capped, or jacketed). If the discarding pieces of a sabot are not considered, all practical projectiles fall into one of these three categories, which are pictured schematically in Figure 1. Both the capped and the jacketed projectiles are formed by adding protective material to the monobloc, so that the monobloc is not only the simplest type but is the basis of the other two. It is customary to consider first the performance of the monobloc and then to determine the effect of the cap or jacket in modifying its behavior.

As far as its performance as an undeformed projectile is concerned, the monobloc is completely specified if its size and shape are uniquely defined and its density given. The size is given by stating the diameter (or caliber) of the projectile; the quantities defining the shape are then made independent of size by expressing them as multiples of the diameter (i.e., in calibers). Classification according to shape is conventionally made by considering the body and the nose separately. Since the body is usually in the form of a circular cylinder with a square base, it can be specified, except for details, by one quantity, the caliber length. A variety of nose shapes (tangent ogival, secant ogival, conical, double-radius ogival, and combination of tangent ogive and cone) have been used; one of the most common is the tangent ogive shown in Figure 1. From the size and shape parameters and the density one can determine, either by direct integration or by methods developed for rapid numerical calculation,[8] the mass, volume, center of gravity, and moments of inertia. Mass and density are not independent; in practice it is usual to give the mass. Thus when the projectile can be taken as a rigid body the variables commonly considered are mass, diameter, nose shape, and total projectile length.

If the projectile deforms, the strength of the material must also be taken into account. A complete investigation of this factor would include not only terminal-ballistic tests relative to the occurrence, causes, and effects of deformations resulting from changes in the projectile's strength, but also studies leading to the development of higher strength materials. The latter aspect of the problem is as important as the first, but its solution is essentially the responsibility of ferrous and powder metallurgists rather than that of ballisticians. This phase of the subject will not be treated in the present report. Discussion will be confined to questions concerning the dependence of performance on such quantities as projectile hardness and bend (transverse rupture) strength.

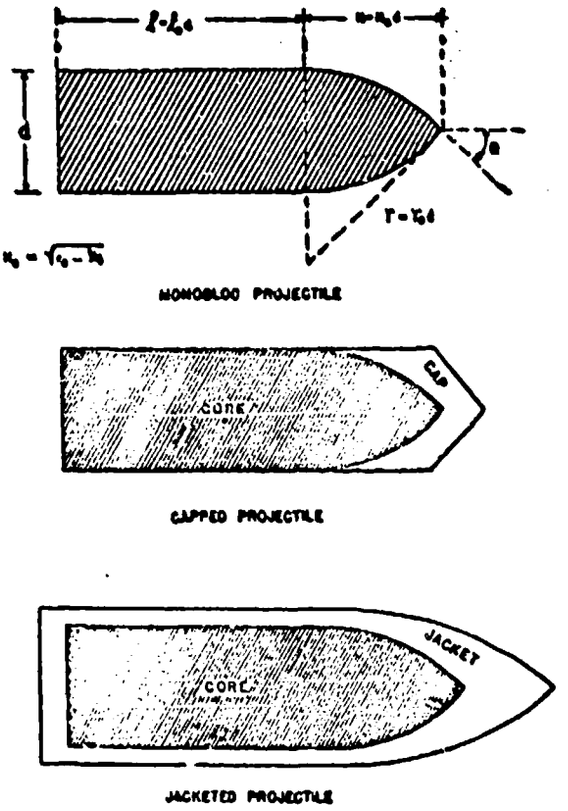

FIGURE 1. Idealized projectile types.

No completely satisfactory system for specifying caps and jackets has been devised, but just as with the core their effectiveness must depend, at least to some extent, on the mass, size, shape, and strength of the protective material.

The effect of changes in the projectile parameters discussed above usually depends on the hardness, thickness, and arrangement of the plates making up the target. Whether the principal emphasis falls on the projectile or on the target depends on whether the interest is in offense or defense.

In summary, the terminal-ballistic problem of armor perforation is essentially one of determining

how the energy required to defeat a steel target depends on the mass, size, shape, and mechanical strength of the projectile components as well as the hardness, thickness, and arrangement of the plates composing the target. The problem is complicated not only by the large number of variables involved but by the likely occurrence of projectile deformation. The solution to the problem, which can be obtained only in a practical sense, must be combined with solutions to the problems of exterior and interior ballistics before answers are possible to more general questions such as how to design a projectile to perforate the maximum thickness of plate, or what is the most efficient gun-projectile combination to neutralize a given objective. Actually no completely rational system of projectile design has been devised, but there is available a great deal of qualitative and semi-qualitative information on the effect of changes in various parameters.

6.1 EXPERIMENTAL TECHNIQUES FOR TERMINAL-BALLISTIC STUDIES

In problems concerned only with the perforation of armor the quantity of most direct practical interest is the energy absorbed by the plate. Logically, however, terminal-ballistic studies should begin with a measurement of the forces resisting the bullet during penetration. Until the nature of these forces, which is only partially understood at present, is completely known it seems unlikely that an exact theory of projectile penetration will be developed. Furthermore, a knowledge of force and time is needed for problems in fuze design and for determining the stresses in a projectile leading to its deformation. Only average forces can be calculated from the total energy absorbed unless assumptions are made concerning the mechanism of penetration.

Unfortunately it is experimentally very difficult to determine the forces of the plate-projectile interaction because of the extremely short time of impact. Only a few attempts at direct measurement have been made and these were all carried out for normal incidence of the projectile. For studying impacts against steel an optical method has been developed by which a shadow of the base of a penetrating projectile is recorded on a rotating drum camera.[9,10] By a suitable analysis the position, velocity, and deceleration of the projectile may be deduced as functions of time from the photographic record. A second method[11] of measuring deceleration during impact should be mentioned, although it can be used only with nonmagnetic and nonconducting target materials like concrete. (See also Section 7.7 of Chapter 7.) The method consists in magnetizing the projectile and recording the electromotive force induced in two suitably placed coils by means of a cathode-ray oscillograph [CRO]. The target is placed between the two coils in a region where the induced electromotive force is dependent only on the velocity of the bullet and not on its position. With a linear sweep for measuring time, the trace on the oscillograph is a line, each point of which is displaced a vertical distance proportional to the velocity. The deceleration is obviously obtained as a function of time by measuring the slope of the line at various points.

The present report deals mainly with the total energy absorbed by the plate. This quantity is determined from a knowledge of the projectile's striking energy and the energy it retains after perforation, that is, the residual energy. Of particular interest is the energy absorbed when the plate just succeeds in stopping the projectile. If the striking energy is above this limiting value, the projectile will usually perforate; if it is below, it will fail. Sometimes, however, the projectile fails at the higher energy and succeeds at the lower.

The limit energy is conventionally measured either by "bracketing" or by the method of residual velocities. To determine a bracket, firings are conducted by varying the projectile's striking velocity until shots are obtained close to, but on either side of, the limit; the limit energy is then calculated from the average value of the bracketing velocities and the projectile's mass. The method of residual velocities[12] is more elegant but, because of practical difficulties, is restricted mainly to normal attack by nondeforming projectiles. In this method several projectiles are fired at different velocities above the limit and the striking and residual velocities measured for each shot. If the residual energies are plotted as a function of the striking energies, the points representing the different shots fall on a straight line and extrapolation of this line to the striking energy axis gives the limit energy.

In the conventional terminal-ballistic range the equipment consists of guns for propelling the projectiles to the target, means for supporting and orienting the plate, apparatus for measuring striking and residual velocities, and auxiliary devices such as microflash and spark units for observing the projectile be-

fore, during, and after perforation. Each investigator naturally has his own techniques; only those used by Division 2, NDRC, will be described.

6.11 Projectile Propulsion

For studying the effect of impacts, any method of firing is satisfactory provided the projectile arrives at the target in good condition, without yaw and with sufficient velocity. Ease in performing and preparing for a test is often the principal consideration in choosing between possible methods.

The use of a smoothbore gun was suggested by the need for firing simple projectiles. Actually the manufacture of projectiles consumes a great deal more time, effort, and money than the carrying out of a plating trial. Thus any simplification in the design of a projectile which does not affect its perforating ability represents a tremendous saving. Aside from this saving, simplification is at times necessary; for example, in studying the effect of jackets, unjacketed projectiles must be fired for comparison. The smoothbore gun does not require the use of a rotating band or jacket and makes the problem of cap attachment much simpler since the cap is not subjected to centrifugal forces. Lack of rotation has been shown[13] to have a negligible effect on the projectile's perforating ability.

Such a gun has been successfully used for work at model scale[14] (.244 caliber) over a four-year period. Yaw is avoided by placing the muzzle of the gun within 6 in. of the target, which is mounted on a ballistic pendulum to allow measurement of the striking velocity. Since blast from the gun would affect the pendulum, the projectiles are fired through a piece of rubber covering a hole in a metal blast shield. By using an oversized chamber and long barrel, unjacketed tungsten carbide projectiles, having a caliber density about twice that of conventional steel projectiles, have been fired at velocities up to 3,850 fps.

In order to attain higher velocities and to work with larger calibers, composite rigid and sabot projectiles have been used in standard guns. Tapered-bore guns or guns with tapered muzzle attachments are not only complicated in themselves but require jacketed projectiles that are difficult to manufacture. The composite rigid is usually the easiest hypervelocity type to make but often cannot be used because of the jacket. Any type of subprojectile (monobloc, capped, or jacketed) can be used with a sabot. Much simpler sabots can be used for terminal-ballistic tests than are required for combat since extreme accuracy is not important and yaw can be reduced at the target by setting the gun at a minimum yaw distance. The principles of sabot design are given in a report[15] by the Division 1, NDRC group at the University of New Mexico.

6.12 Plate Suspension

Test has shown[16] that the method of plate support is of secondary importance in controlling the energy required for perforation. Thus, in the extreme case of a rigid support on the one hand and perfectly free suspension on the other, a free plate weighing only six times as much as the bullet required 9 per cent more energy for perforation. It is probable that the difference would be less for plates of reasonable size. The lateral dimensions of the plate are likewise not of prime importance provided the extent is sufficient to include the principal region of plastic deformation. The insensitiveness of these factors implies that (1) no form of springs, cushions, or nets can add substantially to the stopping power of a target and, (2) except in terminal-ballistic tests requiring high absolute accuracy, variations due to differences in the type of support or the extent of the plate need be of no concern if the lateral dimensions are at least 25 calibers. Actually, tests are often performed with plates smaller than this and it is likely that little error is introduced by so doing, but definitive experiments covering this point are lacking so this remains a moot question.

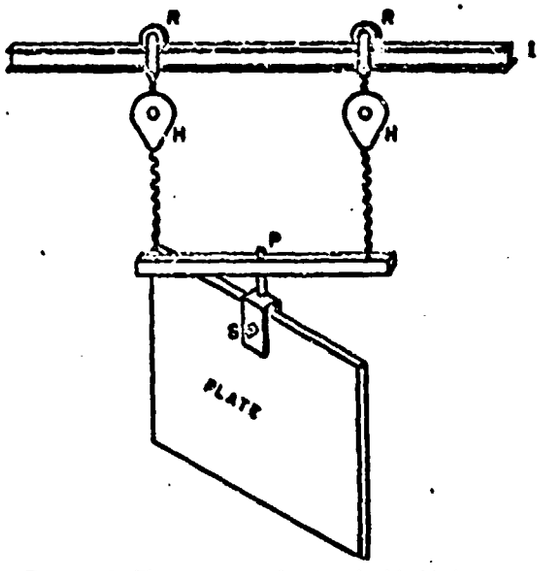

FIGURE 2. Plate support for terminal-ballistic tests.

One type of plate support that has proved convenient for plates weighing up to 1 ton is shown schematically in Figure 2. The plate can be shifted either laterally or vertically and turned so as to allow any angle of attack. Several shots can easily be taken on the same plate without shifting the position of the gun. In order to determine the angle of incidence a protractor is magnetically attached at the expected point of impact before each shot. The protractor is set by adjusting an index arm so that it is in line with the muzzle of the gun as seen in a mirror which is parallel to the face of the plate.

6.2.5 Velocity Measurements

The principal criterion for the goodness of velocity measuring equipment is the attainment of accurate determinations *at the target*. In order to avoid the vagaries involved and the time consumed in making corrections for velocity lost in flight, the equipment should measure as nearly as possible instantaneous values rather than average values over long base lines. Measurement of instantaneous values, or their approximate determination by means of a short base line, has the further advantage that higher striking velocities can be obtained because the gun can be fired at short range; this is particularly important when light windshields are omitted to simplify the projectiles.

Measurement of both striking and residual velocities can be made for normal impact by means of a double ballistic pendulum.[16,17] A transmission pendulum supports the target, and a terminal pendulum stops the projectile after perforation. For the pendulums described in the reference, the overall probable error in a velocity measurement made with the transmission pendulum is 0.10 per cent and with the terminal pendulum is 0.06 per cent. These are probable errors of the apparatus only and do not include errors in the results due to inhomogeneity of the steel plates, spalling of the plates, etc.

A second instrument,[18,19] which also fulfills the requirement of being able to determine an essentially instantaneous velocity with good accuracy, measures the time of passage of a projectile over a very short (1 to 4 ft) known distance. The base line is defined by two light beams, each of which consists of a narrow sheet covering an area of about 1 sq ft. As the beams are successively interrupted by the projectile, electric pulses are generated by phototubes and transmitted to a spiral chronograph which measures the time between their reception. Figure 3 shows the physical arrangement of the light beams and photocells. When the light beams are placed close to the target the quantity measured can usually be taken as the striking velocity without correction. A determination of the velocity can be made within 30 sec after the shot with an accuracy of better than 0.4 per cent. The principal limitations of the light beams and photocells are that they do not operate reliably with projectiles traveling at speeds near the speed of sound, and they cannot be successfully used for measuring residual velocities.

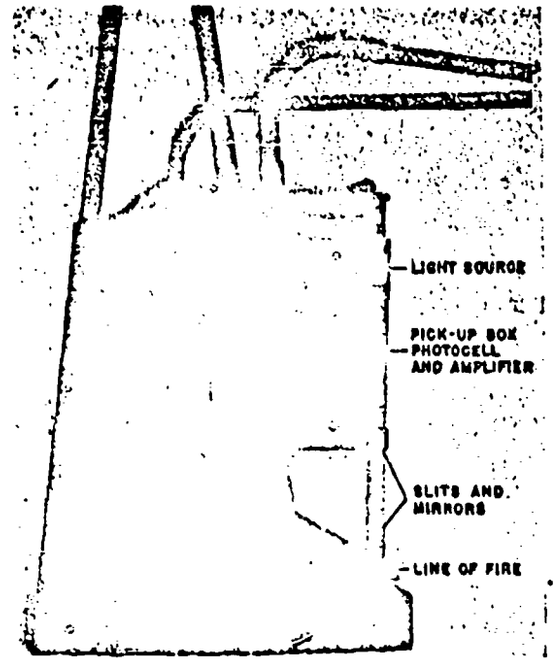

FIGURE 3. View of light beams and photocells for measurement of projectile velocities.

The heart of the above equipment is the spiral chronograph which was developed to measure time intervals of a few msec to an accuracy of better than 1 μsec. During the lapse of time between the two pulses a spiral is traced out on a cathode-ray tube at a constant known angular velocity; the spiral trace starts with the first pulse and stops with the second, so that the number of revolutions appearing on the cathode-ray tube screen is a direct measure of the time interval. A picture of one of the spirals with blanking spots at 5-μsec intervals is shown in Figure 4. A long persistent screen is used on the chronograph so that a visual reading of the spiral is obtained as well as a photograph.

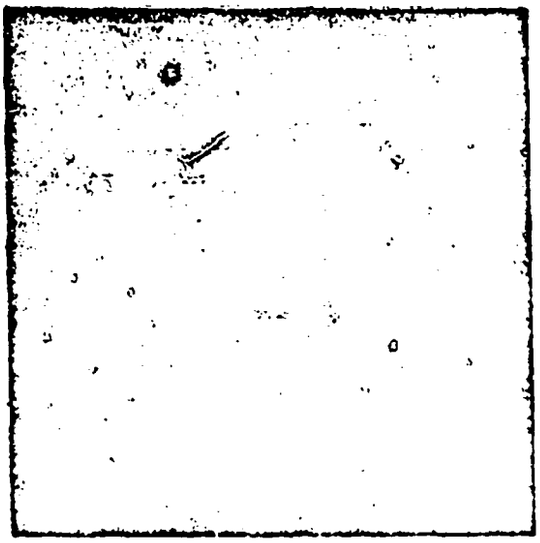

FIGURE 4. Photograph of spiral chronograph trace.

Since light beams and photocells cannot be successfully used for measuring projectile velocities behind the plate, special equipment has been developed for this purpose. The method involves taking spark shadowgraphs of the projectile at two successive positions along its path. From these pictures and the geometry of the optical system, it is possible to find the distance traveled by the projectile between exposures. To determine the time between exposures and thus the residual velocity, light from the two sparks used to produce the shadowgraphs is allowed to fall on phototubes which actuate the spiral chronograph. This apparatus has the advantage that in addition to measuring the residual velocity it furnishes a record of the condition of the projectile immediately after perforation of the plate. Although the base line is variable it is never over 2 ft. The accuracy of measurement is comparable to that obtained with the light beams and phototubes, but the time required for making a determination is considerably longer.

6.3.4 Auxiliary Apparatus

It is often useful to know the condition of the projectile before and during impact as well as after perforation. For this purpose spark shadowgraphs and microflash photographs are used. Examples of such pictures are shown in Figures 6 and 9. In this connection mention should be made of the multiple-spark apparatus[20,21] developed in England under the auspices of the Armament Research Department [ARD]. With this equipment, which is based on the optical method of Schardin and Crans, a series of spark pictures is taken showing the projectile at successive intervals during its penetration cycle. Since times between exposures are measured, the striking velocity, residual velocity, and an estimate of the deceleration at different stages of penetration can be obtained.

6.4 DEPENDENCE OF STRIKING ENERGY ON EXTERIOR AND INTERIOR BALLISTIC BEHAVIOR

Several attempts have been made [2,6,22] at calculating the size of core for a subcaliber projectile that will lead to perforation of the greatest single thickness of homogeneous armor. This problem is similar to that of finding the best length of projectile or the best density of material. In these problems changes always occur in the mass and sometimes in size of the projectile components and as a result there are variations in the projectile's striking kinetic energy as well as in the absorption of this energy by the plate. Thus the maximum energy that can be obtained at the muzzle of a given gun depends on the total mass of the projectile and, if a sabot type is being considered, the fraction of the total muzzle energy not wasted in the carrier varies with the relative masses of the subprojectile and the discarding pieces. Of the energy possessed by the subprojectile, a certain portion will be lost in flight, and the mass and size of the subprojectile are factors controlling the extent of this loss.

The difficulty in calculating how the relative distribution of energy changes with variations in the size and mass of the projectile components lies in the fact that the ballistic behavior cannot be exactly described by simple analytical expressions. Although tables and graphs are routinely used[23,24,25] to compute the performance of particular projectiles, these will not be employed in the present discussion. Approximate expressions will suffice for purposes of illustration, but it is not proposed that these be used for purposes of exact design.

6.4.1 Muzzle Energy of Subprojectile

An increase in muzzle velocity can always be obtained with a given bore and chamber by decreasing the mass of the projectile and employing a quicker burning powder. The following relation gives an estimate of the total muzzle energy that can be supplied

to a projectile of mass M without exceeding the safe maximum pressure of the gun:

$$e\left(1+\frac{1}{3}\frac{C}{M}\right)=e_p\left(1+\frac{1}{3}\frac{C}{M_p}\right), \qquad (1)$$

where e_p is the muzzle energy of a standard full-caliber projectile of mass M_p and C is the powder load. The muzzle energy e_s of the subcaliber projectile is given by

$$e_s=\frac{M_s}{M}e, \qquad (2)$$

where M_s is the mass of the subprojectile. If the subcaliber projectile varies only in size, its "caliber density" will remain constant and consequently

$$\frac{M_s}{R^3}=M_p, \qquad (3)$$

where $R\ [=d_s/d_p]$ is the ratio of the diameter of the subprojectile to that of the gun. This assumes that all projectiles have the same shape as a given prototype.

The total mass of the projectile M depends on the type of carrier used; for a particular type, the mass of the carrier $M_c(R)$ will vary in a definite way with the ratio R. Thus,

$$M=M_s+M_c(R)=M_pR^3+M_c(R). \qquad (4)$$

By combining equations (1), (2), (3), and (4), the ratio of the muzzle energy of the subprojectile to that of the standard full-caliber projectile can be determined for a given gun in terms of the ratio R. This energy ratio will be designated $E(0)$, where the zero in parentheses is intended to imply that the value is for point-blank range. Thus,

$$E(0)=\frac{e_s}{e_p}. \qquad (5)$$

This is a definite function of R for a given gun and projectile type. Values of $E(0)$ are given in Table 1 for R values ranging from 1 to 0.54. The gun in this case is the 37-mm M3, the projectiles are scale models of a particular steel projectile,* and all values are relative to the performance of a full-caliber 1.95-lb projectile having a muzzle energy equal to that of the 37-mm M51. It will be noted that the velocity is also directly related to R, increasing as R decreases.

As one would expect, the velocity of the subprojectile increases but its kinetic energy decreases as its diameter becomes smaller. If the caliber density of the prototype were increased, not only would the muzzle energy of the complete projectile be increased for subcaliber projectiles of all sizes [equation (1)], but a greater fraction of this energy would reside in the subprojectile [equation (2)].* The mass could be increased either by using for the core a denser material, such as tungsten carbide, or by increasing the length of the projectile.

* It is usually not necessary to increase the weight of the carrier in direct proportion to the increase in the mass of the subprojectile.

TABLE 1. Performance of subcaliber steel projectiles as a function of core diameter.

Diameter ratio R	Muzzle velocity V_0 (fps)	Range (yd)					
		0		1,000		2,000	
		$E(0)$	$T(0)$	$E(1{,}000)$	$T(1{,}000)$	$E(2{,}000)$	$T(2{,}000)$
(37-mm)							
1.00	2,851	1.00	1.00	1.00	1.00	1.00	1.00
0.90	3,216	0.93	1.09	0.93	1.09	0.93	1.09
0.80	3,637	0.83	1.18	0.82	1.16	0.81	1.15
0.70	4,112	0.71	1.25	0.69	1.22	0.67	1.19
0.60	4,628	0.57	1.30	0.53	1.22	0.49	1.15
(20-mm)							
0.54	4,946	0.47	1.29	0.43	1.20	0.38	1.09

$R=\dfrac{\text{subprojectile diameter}}{\text{gun diameter}}$.

$E(z)=\dfrac{\text{energy of subprojectile at range } z}{\text{energy of similar full-caliber projectile at range } z}$.

$T(z)=\dfrac{\text{limit plate thickness of subprojectile at range } z}{\text{limit plate thickness of similar full-caliber projectile at range } z}$.

6.4.2 Energy Loss Due to Air Resistance

In many cases a hypervelocity projectile loses energy in flight at a greater rate than do projectiles fired at lower velocities. As a result, the hypervelocity projectile may perforate more armor at the muzzle but lose this advantage if fired over a long range. This has happened so often in practice that it is sometimes felt that a hypervelocity projectile is necessarily a short-range projectile and that its ineffectiveness at long ranges is due to the high velocity at which it is fired. Actually an increase in velocity is in itself an advantage; the poor performance that has been observed has always resulted because the hypervelocities were attained by using projectiles having low ballistic coefficients.

For air of standard density the fractional loss in energy for a projectile traveling a distance dx is given by:

$$\frac{de(x)}{e(x)} = -\frac{2K}{C}\,dx, \qquad (6)$$

where $e(x)$ is the energy of the projectile at range x,
K is the "drag coefficient,"
$C[=M/id^2]$ is the ballistic coefficient for a projectile of mass M, diameter d, and form factor i.

Thus, if the drag coefficient K were independent of the velocity, the fractional rate of change of energy with distance would also be independent of velocity. Actually, however, for velocities above the velocity of sound, K decreases as V increases so that the *fractional energy loss is less the higher the velocity*. In other words, if the power of a gun is increased not only will the muzzle energy of the projectile be greater but there will be a smaller fractional loss in energy over a given range.

To determine the magnitude of this effect the variation of K with velocity must be known. For projectiles with a $^{5}/_{10}$ secant ogive (G_2 Siacci table), K can be represented fairly well by $k(V^2)^{-3/2}$ in the velocity range between 2,000 and 4,500 fps. Substituting into equation (6) and integrating yields

$$F(x) = \frac{e(x)}{e(0)} = (1-\delta x)^{3/2}, \qquad (7)$$

where $F(x)$ is the fractional energy retained at range x (ft), and

$$\delta = \frac{k'}{CV_0^2},$$

k' is a constant, C the ballistic coefficient, and V_0 the muzzle velocity.

An increase in either the muzzle velocity or the ballistic coefficient results in an increase in the energy retained at a given range. For a subcaliber projectile, C decreases in direct proportion to R;[1] if the muzzle energy of the subprojectile were constant and thus independent of R, the increase in V_0 would slightly more than balance the decrease in C, but since the muzzle energy decreases with decrease in R, the value of $F(x)$ is somewhat less for a sub- than a full-caliber projectile.

By expressing $E(x)$, the ratio of the striking energies of the sub- and full-caliber projectiles at range x, in terms of the fractional energy retained by each projectile

$$E(x) = \frac{e_s(x)}{e_p(x)} = \frac{e_s(0)}{e_p(0)}\,\frac{F_s(x)}{F_p(x)} = E(0)\,\frac{F_s(x)}{F_p(x)}. \qquad (8)$$

Values of $E(x)$ are given as a function of R in Table 1 for 1,000- and 2,000-yd ranges, together with the values of $E(0)$ that were discussed in the previous section.

It will be noted that the ratio of the striking kinetic energy of a subcaliber projectile to that of the full-caliber projectile decreases with increase in range, and that the rate of decrease is greater the smaller the subprojectile. For example, with R equal to 0.7, the values of $E(0)$, $E(1{,}000)$, $E(2{,}000)$ are 0.71, 0.60, 0.67 respectively, while with R equal to 0.54 they are 0.47, 0.43, 0.38. Thus if hypervelocities are obtained by using a subcaliber projectile, the performance relative to that of a similar full-caliber projectile is likely to deteriorate with range. This does not mean, of course, that the range performance of a tungsten carbide cored subprojectile will necessarily be worse than that of a full-caliber steel projectile; in fact it will usually be better, because the mass, and therefore the ballistic coefficient, of the subprojectile will be increased by using tungsten carbide. Any increase in the mass of the prototype, either by an increase in density or in length, will lead to a larger value of $F(x)$, which means smaller energy losses in flight.

6.4.3 Stability

The necessity of maintaining stability is one of the factors setting a lower limit to the diameter of a subprojectile or an upper limit to its length. At the muz-

[1] From equation (3) and the definition for the ballistic coefficient

$$C = \frac{M}{id^2} = \frac{M_p R}{id_p^2} = C_p R,$$

where a constant C_p is the ballistic coefficient for the full-caliber projectile having a diameter equal to the gun diameter d_p.

xle of a fixed gun the stability factor S of a subcaliber projectile is given by

$$S = \frac{\pi^2 R^2 \rho A_0^2}{K_M \rho_a n^2 B_0}, \qquad (9)$$

where ρ = average projectile density (strictly, the equation applies only to projectiles of uniform density),

A_0 = dimensionless coefficient proportional to moment of inertia about projectile axis [$A = \pi \rho d^5 A_0$],

B_0 = dimensionless coefficient proportional to moment of inertia through center of gravity and perpendicular to projectile axis [$B = \pi \rho d^5 B_0$],

K_M = overturning moment coefficient,

ρ_a = density of air,

n = distance along barrel per turn of rifling measured in calibers of gun.

As indicated by this equation, S decreases with decrease in R.[8] Due to changes in A_0, B_0, and K_M, S also varies with projectile length, decreasing rapidly as the projectile is made longer. Thus, if the projectile is to be stable, that is, if S is to have a value at least equal to 1, there is a maximum projectile length for each value of R; as R becomes smaller the maximum length expressed in calibers likewise decreases and it would appear that the caliber length must necessarily be less for sub- than full-caliber projectiles. This problem is complicated, however, by terminal-ballistic considerations. The tendency of a projectile to break on impact increases with its length and this breakage may degrade its perforating ability. It appears that in many guns the twist of the rifling is sufficiently large that the length of a full-caliber projectile is limited by projectile breakage rather than stability. For these guns the full-caliber projectile can be scaled down without producing instability; S then plays the role of a limiting factor for determining the smallest value of R that can be used. Only for values of R less than this is the stability factor important for determining the length of the projectile.

Although it appears from equation (9) that the stability factor increases with an increase in the density of the material, which would provide a further reason for using tungsten carbide, this equation applies strictly only to monobloc projectiles. For jacketed projectiles the core must be kept well forward to gain full advantage of the heavier material.

[8] The stability factor does not decrease quite so rapidly as R^2, because for supersonic velocities K_M, like the drag coefficient, decreases as the velocity increases. The velocity that can be obtained with a given gun increases with a decrease in R, so K_M likewise decreases slightly.

6.4.4 Striking Energy

The greatest striking energy can be obtained from a given gun by using a full-caliber projectile made from the most dense material possible and having the greatest length consistent with the maintenance of stability. The advantage of the sub- over the full-caliber projectile for perforating thicker armor results solely from its terminal-ballistic performance which must be considered in the determination of an optimum size. It is also clear that terminal-ballistic results should be considered in deciding upon the best projectile length.

6.5 STEEL AS A PROTECTIVE MATERIAL

Section 6.4 deals with the dependence of striking energy on the principal projectile parameters. There remains the problem of determining the energy required for plate perforation as a function of both the plate and projectile properties. The present section is concerned with the relative effectiveness of armor protection and with the limit energy for a nondeforming projectile. Except for the effect of changes in projectile size and weight, this section deals only with the properties of the plate.

6.5.1 Effectiveness of Armor Protection

Comparison with good quality reinforced concrete, which for economic reasons is the usual basic material in fixed fortifications, furnishes an idea of the relative effectiveness of steel as a protective material. To afford equal protection against nondeforming projectiles of small and intermediate calibers, homogeneous armor need be only about one-sixth as thick as concrete. The armor has the added advantage that, due to its hardness, it is more likely to deform or shatter the projectile and thus further reduce its perforating ability. Furthermore, spalling and cracking are not as likely with good quality armor as with concrete, so that it is better able to withstand repeated attack. Even though antitank guns were greatly improved after 1940, it was still possible in 1945 to build highly maneuverable armored tanks that were immune to frontal attack except at very short range.

The type of armor protection most commonly used consists of a single plate of homogeneous armor and

the present report deals mainly with this type of target. Face-hardened armor is appreciably better than homogeneous only if the hard surface succeeds in shattering the projectile. Shatter can often be prevented by the use of an armor-piercing cap and when the cap accomplishes its purpose the advantage of face-hardened armor largely disappears. At the end of World War II, the face-hardening process was rarely being used except for heavy plates in naval construction. It might be profitably used in small sizes, however, if it were protected by a thin, spaced plate for cap removal.

6.5.2 Perforation Energy—Mechanisms of Plate Failure

If the energy required for perforation by projectiles of a given shape depends only on the size of the projectile, the strength and thickness of the plate, and the angle of attack, a dimensional analysis indicates that the perforation formula must have the form

$$\frac{e_l}{d^3} = \bar{C} f\left(\frac{t}{d}, \theta\right) \text{ or } \frac{WV_l^2}{d^3} = Cf\left(\frac{t}{d}, \theta\right), C = 2g\bar{C}, \quad (10)$$

where e_l (limit energy) = minimum energy required for perforation,
W = projectile weight,
V_l = limit velocity,[b]
d = maximum projectile diameter,
t = plate thickness,
$\bar{C}$ = measure of strength of plate material expressed as force per unit area,
g = acceleration due to gravity,
$f(t/d,\theta)$ = general function of t/d and θ,
θ = angle of incidence.

Although there are indications that this equation is not exactly correct, it is sufficiently true to provide a simple basis for correlating experimental data. Thus, in Division 2, NDRC, Data Sheet 2C3 of Chapter 19, the results of proof firing of monobloc projectiles of various sizes against homogeneous armor are represented by plotting the *specific limit energy* WV_l^2/d^3 against the plate thickness expressed in calibers t/d. The measured values fall within a narrow band for each angle of attack; the spread of the bands is due mainly to scatter in the data and only in small part to failure of equation (10).

The form of the function $f(t/d,\theta)$ depends on the mechanism of plate failure. Ideally a failure may be classified as either a plugging or a ductile type, but cases sometimes occur in practice that combine the elements of both.

Plugging Failure

When complete cylindrical plugs are punched out of the plate, experiment indicates[26] that $f(t/d) = (t/d)^2$. Although this form is compatible with the assumption that perforation is resisted by a constant shearing stress acting over the surface of the cylindrical plug during ejection, this picture is undoubtedly too simple. A large resisting force probably acts on the projectile only during the initial stages of penetration and then drops to a negligible value when the plug is formed.

Members of the Watertown Arsenal Ballistics Laboratory have investigated the mechanism of plug formation[26,27] and suggest that the plug is not necessarily formed by crack propagation but may be produced by plastic deformation along a surface of maximum shear. The deformation is confined to a narrow region in the neighborhood of this surface because the rapid rate of increase in the stress does not allow time for heat conduction. As a result there is a large temperature rise in the region of maximum shear where the greatest strains occur. The temperature rise reduces the stress required for deformation and thus facilitates further deformation. Once started, the process is unstable so the plug merely slips out of the plate. This amounts to saying that in an adiabatic process the stress-strain curve in shear has a maximum and that the negative slope beyond the maximum corresponds to instability.

The mechanism of plugging is different from that of spalling. Spalling, which consists of the ejection from the back face of the plate of a thin circular disk or irregular flakes considerably larger than the caliber of the projectile, usually results because of planes of weakness arising from excessive inclusions and inhomogeneities. Plates having such planes of weakness are usually eliminated during proof firing.

Ductile Failure

With homogeneous plate in the usual hardness range and projectiles having conventional nose shapes, the plate material is plastically deformed over a wide region about the point of impact; a smooth petaled

[b] Two limit velocities are in common use: (1) minimum striking velocity required for complete perforation with zero remaining velocity ["Navy limit" (U.S.) and "critical velocity or W/R limit" (British)]; (2) minimum striking velocity required to produce a hole through which light can be seen, the projectile being removed if necessary ["Army limit" (U.S.) and "ballistic limit" (British)]. Unless otherwise specified, the "Navy limit" will be used in this report.

hole is produced and no material is thrown from the plate.[23]

In the case of very thin plates (less than ¼-caliber), $f(t/d)$ is equal to $(t/d)^3$ whether the plate petals or plugs. It has been suggested by members of the U. S. Naval Proving Ground[10] that in the ductile failure of a thin plate most of the projectile's energy is expended in bending back the petals. With the additional assumption that the width of the petals is proportional to the thickness of the plate, the correct form for $f(t/d)$ results.

If very thick plate is used, most of the displaced material is pushed laterally aside rather than forward as in the case of thin plates. Ideally, if there were only lateral displacements and provided the inertial forces of the plate material were negligible, it would be expected that $f(t/d) = (t/d)$. This is equivalent to assuming a constant pressure on the nose of the projectile. The pressure has been interpreted[21] as the hydrostatic pressure necessary to expand a cylindrical hole in the plate by moving the material sidewise until the radius of the hole is equal to that of the projectile. Although approximately true, this ideal form of $f(t/d)$ is never exactly realized in practice even for thick plate, one reason being that with projectiles of conventional nose shape some of the material is always pushed forward as well as sidewise. During petal formation at the back of the plate the forward motion produces cracking and bending instead of lateral plastic deformation.

Present Status of Plate Penetration Theory

At the present time there is no physical theory of armor penetration capable of predicting the exact form of $f(t/d,\theta)$ for all plate thicknesses. Although the basic ideas and some of the details have qualitative explanations,[24] usable forms for $f(t/d,\theta)$ must be obtained from firing data.

4.4.3 Perforation Formulas—Normal Impact

Even for the simplest type of impact (normal incidence, ductile failure, nondeforming projectile) no general analytical expression has been developed that systematizes the results of all recent firing tests, but approximate formulas can be used over restricted ranges in the t/d values.[4,8,9,10,11] These approximate empirical formulas are satisfactory for practical purposes if they are not extrapolated beyond the region of experimental values used for determining the constants of the equations.

One-Parameter Expressions—Terminal-Ballistic Coefficients

As a method of reporting experimental data and as a means of removing, to a first approximation, effects due to changes in the weight and size of the projectile and to variations in the thickness of the plate, values are often given for ballistic coefficients.[1] The ballistic coefficients in common use are k, F, and C, which are calculated from the following equations:

$$\frac{WV_1^2}{d^3} = 1.933 \times 10^6 k^2 \left(\frac{t}{d}\right)^{1.5}, \tag{11a}$$

$$\frac{WV_1^2}{d^3} = F^2\left(\frac{t}{d}\right), \tag{11b}$$

$$\frac{WV_1^2}{d^3} = 1.728 \times 10^6 C\left(\frac{t}{d}\right)^{1.43}, \tag{11c}$$

where multiplying factors have been used so that W is expressed in pounds, V_1 in feet per second, t in feet, and d in feet. Equation (11a) for k is commonly employed by the U. S. Army; equation (11b) for F, by the U. S. Navy; and (11c) for C, by the British Ordnance Departments.

All three of these expressions are special forms of equation (10) in which $f(t/d)$ has been set equal to $(t/d)^a$ and a assigned a constant value. Since, as pointed out in the last section, a is equal to 2 for very thin plate and has a value near 1 for thick plate, any equation in which a is fixed requires that the ballistic coefficient itself depend on plate thickness. F in fact is often written as $F(t/d)$. Results obtained with mild steel plate[21] indicate that in going from plate 0.3 to 2.0 calibers thick, k^2 decreases by 23 percent, C by 18 per cent, and F^2 increases by 49 per cent. Although ballistic coefficients are insensitive to reasonable changes in weight and diameter of the projectile, they can rarely be assigned constant values for the purpose of extrapolating over a wide range in plate thickness.

Two-Parameter Formulas

As a second approximation for $f(t/d)$, numerous formulas have been proposed that permit the adjustment of two parameters rather than one. Among these are[4,8,9,10,11]

$$\frac{WV_1^2}{d^3} = C\left(\frac{t}{d}\right)^{1.43}. \tag{13}$$

[1] These coefficients are not to be confused with the ballistic coefficient used in exterior ballistics. The latter was used in Section 6.4.2.

where $\log C = C_0 - n\frac{t}{d}$,

$$\frac{WV_1^2}{d^3} = C_0\left(\frac{t}{d}\right)^n, \quad (13)$$

$$\frac{WV_1^2}{d^3} = C_0\left(\frac{t}{d} - n\right), \quad (14)$$

$$\frac{WV_1^2}{d^3} = C_0\left(\frac{t}{d} + n\right)^n. \quad (15)$$

For a range in t/d values from 0.5 to 2.0 there is very little to choose between these four equations so far as accuracy in representing firing data is concerned. Despite the very different forms, the differences in predicted values are of the same order of magnitude as the errors made in measurement.

The region of particular interest for hypervelocity projectiles is for plate thicker than 2 calibers. Although equations of the type (13), (13), (14), and (15) give acceptable results for t/d between 0.5 and 2.0 when the parameters are adjusted for this region, they are likely to lead to serious errors if they are extrapolated to large values of t/d without readjustment of C_0 and n. In Figure 5 are given results obtained[18] with .244-caliber projectiles against homogeneous armor (BHN 255) 1.5 to 6.2 calibers thick. Since the points in this logarithmic plot of WV_1^2/d^3 against t/d fall on a straight line, it is apparent that the data in this range of plate thicknesses can be represented by an equation of the type of equation (15). For the projectile with a 1.5-caliber ogive the equation is

$$\frac{WV_1^2}{d^3} = 2.73 \times 10^6\left(\frac{t}{d}\right)^{1.55}. \quad (16)$$

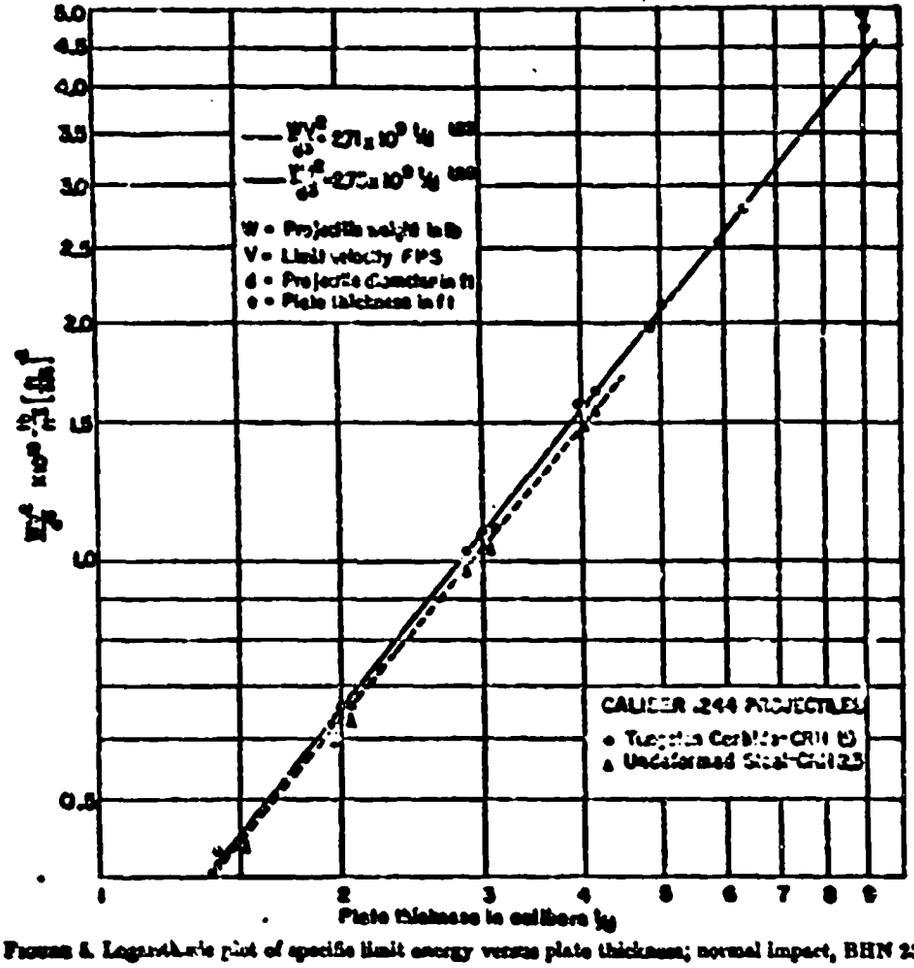

FIGURE 5. Logarithmic plot of specific limit energy versus plate thickness; normal impact, BHN 255 armor.

A general equation of the type of equation (15), with C_0 and n adjusted for the range in plate thickness between 0.5 and 2.0, is given in Section 6.5.6. For .244-caliber projectiles against homogeneous plate (BHN 255) this equation becomes:

$$\frac{WV_r^2}{d^3} = 1{,}728\left(694\frac{t}{d} + 603\right)^2. \qquad (17)$$

In the region of t/d between 1.5 and 2.0 the limit velocities predicted by equations (16) and (17) for projectiles with the same caliber density never differ by more than 3 per cent, which is quite acceptable agreement, considering that the two equations were established independently from entirely different sets of firing data[36] and with projectiles having slightly different nose shapes. For plate 6 calibers thick, however, equation (17) leads to a limit velocity 24 per cent too large. On the other hand, the value of n in equation (16) must be decreased slightly (to approximately 1.16) and the value of C_0 increased to obtain acceptable values for t/d between 0.5 and 1.5. In this regard it may be noted that for all plate thicknesses greater than 0.5 the value of n for plate of this hardness is less than that used in equations (13) and (15) for calculating ballistic coefficients and slightly larger than that used in equation (14). If n were exactly equal to unity, the energy required to displace a given volume of plate material would be constant regardless of the diameter of the hole; since n is almost equal to unity, this is approximately true.

In summary, there are several two-parameter formulas that give acceptable agreement with experiment for plate between 0.5 and 3.0 calibers thick, but an attempt to extrapolate these equations to predict values for thick plate without readjustment of the parameters may lead to serious error. For plate thicker than 1.5 calibers, an equation of the type of equation (13) with n approximately 1.25, is in agreement with measurements made for one hardness of plate.

6.5.4 Perforation Formula—Oblique Impact

By limiting the discussion to nondeforming projectiles the case of oblique impact is almost excluded. For angles of attack near 40 degrees it is impossible with projectile materials now available to keep any monobloc type undeformed at velocities much above 2,500 fps, even when the attack is against soft homogeneous armor. Perforation limits can therefore be determined for a nondeforming projectile at oblique angles of incidence only with relatively thin plate.

The problem of oblique attack is complicated by the fact that the projectile is acted on by transverse forces which tend to turn its axis away from the normal to the plate as the nose passes through the front face and toward the normal as it leaves the back. This motion is evident from the spark shadowgraphs in Figure 6. As a result of this angular motion the axis of the hole usually makes a larger angle with the normal to the face of the plate than the angle of incidence and the hole is elliptical in shape; the size of the hole and the energy absorbed by the plate is greater than if the projectile had not turned. At sufficiently large angles the projectile ricochets and in this case very little of the projectile's striking energy is absorbed by the plate; it is merely redirected. As one might expect, no satisfactory general perforation formula exists for oblique attack by a nondeforming projectile, but equations have been reported[38] for one particular case in which the attack was against very thin plate.

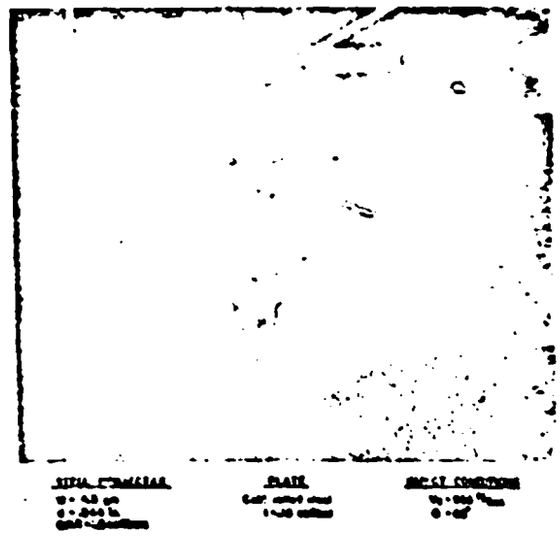

FIGURE 6. Motion of projectile during perforation of thin plate at oblique angle.

6.5.5 Plate Hardness

A good index of the terminal-ballistic performance of armor is its hardness, which is usually specified by the *Brinell hardness number* [BHN]. After the limit energy has been correlated with the average hardness of a plate, the chief variation in the plate's behavior

results from inhomogeneities introduced either by poor heat treatment or by inclusions of foreign material. Defects resulting from inclusions are particularly deleterious if the plate has been extensively rolled. The defects are then spread out so that planes of weakness are produced which result in laminations. In the following discussion it will be supposed that all plates are clean and uniformly hardened.

The resistance of a plate increases with its hardness up to the point where brittle failures set in.[43,44] As the hardness is increased, the petals at the front and back faces are first broken off and with further increase plugs are ejected. Concurrently with a change from a ductile- to a plugging-type failure, the energy required for perforation by a nondeforming projectile decreases. Thus there is an optimum hardness for a given set of impact conditions, and several investigations[34,44] have been carried out to determine its value.

A perforation formula including the hardness of the plate as a parameter has been proposed[34] by members of the National Physical Laboratory (England). This formula is based on firings carried out with scale models of the 2-pounder AP shot (caliber density, 0.603 lb per cu in.; nose shape, 1.4-caliber radius with "swell") against plates having nominal BHN of 250, 300, 350, and 450, and ranging in thickness from 0.5 to 2.0 calibers. All shots were at normal incidence.

$$\frac{WV^2}{d^3} = 1{,}728\left(43.4\sqrt{B}\,\frac{t}{d} + 747 - \frac{54{,}000}{B_0 - B}\right)^2, \quad (18)$$

where B is the Brinell hardness number, B_0 is a constant for a projectile of a given size, and W, V, d, and t have the usual units of lb, fps, and ft, respectively.

This formula agrees with the following observed facts:

1. The curve of limit energy against hardness has a broad maximum. This means that the exact value of the hardness is not critical and indicates why it is difficult experimentally to determine an optimum value.

2. The optimum hardness increases with t/d and, as indicated by the increase in B_0, decreases as the caliber increases. The variation of B_0 with the size of the projectile will be considered in the next section. The change in optimum hardness with the projectile's size, together with the fact that it is more difficult to make good quality hard plate in large than small sizes, are reasons for the common practice of making heavy armor softer than light armor.

6.56 Scale Effect

Nearly every terminal ballistic test involving projectiles of different diameters shows that for a given t/d there is a slight tendency for the specific limit energy to decrease as the caliber of the projectile increases.[27,28,45] In other words, if two projectiles exactly the same except for size are fired against plates of identical armor having the same caliber thickness, the larger projectile has a slightly lower limit velocity. This scale effect contradicts equation (10), although not seriously since the effect is small.

Three possibilities have been proposed as explanations:

1. The simplest proposal is simply that, due to difficulties in heat treatment, the quality of thick plates is inferior to that of thin plates, so comparisons at the same t/d result in an advantage for the large calibers. In certain cases this may play a part, but it is not the complete explanation.

2. A second suggestion is that the effect is due to the decrease in the rate of strain of the target material with increase in caliber, smaller stresses being required to produce the same strain at a lower rate of strain. As a result of rapid rate of strain measurements[46] it has been shown that in armor this effect is too small to account for the observed differences in ballistic limits. Furthermore, the scale effect has been produced in static punching experiments.[47]

3. The third, and most reasonable proposal, depends on the observation that size effects occur also in slow bend and impact test of notched bars.[48-51] Specifically, if d is a linear dimension of the specimen, then the work required to fracture similar specimens is not proportional to d^3. It is significant that the size effect in static tests, just like the scale effect in armor, increases with brittleness: it is larger the greater the hardness of a given steel. Since size effects have been observed for fracture but not with plastic flow it appears likely that the region near the back face is the one responsible for the scale effect. Except for very hard or inferior plate this is the only region in which cracking occurs. It has been suggested that size and therefore the scale effect may be connected with the occurrence of inclusions, which are present to some extent even in good quality armor.

The scale effect has been included in equation (18) by allowing B_0 to be a function of the diameter of the projectile:

$$B_0 = 500 - 160 \log_{10} \frac{d}{d_2}, \quad (19)$$

where $d_2 = 0.1304$ ft. Although a correction due to

a change in the caliber of the projectile is usually small, it may become important for hard, thin plate since the scale effect increases with plate hardness and with a decrease in the caliber thickness. As an indication of the magnitude of the effect, a change in d by a factor of 2 results in a 6 per cent change in the specific limit energy for 1 caliber thick plate with BHN 250.

6.3.7 Applications of Perforation Formulas — The Sabot Projectile

The perforation formulas just discussed are useful for predicting optimum projectile performance and in addition, under conditions where the projectile does not deform, they have the following applications:

1. Corrections of firing trial results to a common hardness basis.
2. Determination of the optimum hardness for a plate.
3. Assessment of the effect of changes in the design of a projectile on its perforating ability.

With regard to the last point, it will be noted that all the perforation formulas indicate that with a given striking energy a greater thickness of plate can be perforated with a small than a large projectile. This advantage of a subcaliber projectile is partially offset, however, by the fact pointed out in Section 6.4.2 that the striking energy of a subprojectile decreases with its diameter.

Equation (16)[1] will serve to estimate the relative importance of these two conflicting factors. If $T = t_s/t_p$, where t_s is the limit plate thickness for the subcaliber projectile and t_p is the limit for a similar full-caliber projectile, then in terms of the ratio of the striking energies E the perforation formula becomes:

$$T = R\left(\frac{E}{R^3}\right)^{1/1.25}. \qquad (20)$$

As previously used, R is the ratio of the diameter of the sub- to that of the full-caliber projectile. Values of T calculated for steel projectiles fired from a 37-mm gun are listed in Table 1 for values of R from 1.00 to 0.04 and for ranges of 0, 1,000, and 2,000 yd. Corresponding values of T have also been calculated by assuming that the steel of the subprojectile is replaced by tungsten carbide. The values for the tungsten carbide cored projectiles are contained in Table 2, where, as in Table 1, all results are given relative to the performance of a prototype full-caliber steel projectile, which is used as the standard.

Although the figures given in Tables 1 and 2 are merely illustrative, they indicate the fact, borne out by experience, that in cases where projectile deformation is not a factor a considerable increase in perforating ability results from the use of subcaliber projectiles. They also show the effect of changing the weight and size of the subprojectile.

Thus, by increasing the weight of the subprojectile, the replacement of steel by tungsten carbide leads to a real improvement; not only can a greater thickness of plate be perforated at the muzzle but the relative advantage of the tungsten carbide cored projectile increases with range. It will be noted that when deformations are not considered the advantage of the tungsten carbide[2] is due solely to its greater density, which leads to a higher striking energy, and that it does not result because less energy is required for perforation.

With regard to the size of the subprojectile, Table 1 indicates an optimum diameter for the steel projectile at each range considered. This best diameter increases with increase in range and at a given range decreases with an increase in density of the core material. Fortunately the choice of diameter is not critical; the "optimum" shifts slowly with range and at a given range the thickness of plate perforated does not decrease rapidly for small changes in the diameter near the best value. The most suitable diameter in any particular case depends on the approximate range over which the projectile is to be fired and on the exact type of carrier and subprojectile being considered. For particulars, reference should be made to the original reports.[14,22]

Strictly, Tables 1 and 2 apply only to normal attack by monobloc projectiles, but the same trends with weight and size are apparent when jacketed or capped projectiles are used as prototypes. This results since the general form of the perforation equation does not change appreciably as protective material is added to the core.

6.4 PERFORMANCE OF MONOBLOC PROJECTILES

A general discussion of projectile deformations with particular reference to their dependence on striking

[1] Plates thinner than 1.4 calibers will not be considered in the present application. For plate having a BHN 250 and with no change in projectile diameter greater than 2, the scale effect should always be small. It will be neglected here.

[2] The advantage is slightly exaggerated in the present case because of the assumption that no heavier carrier is needed for a tungsten carbide than a steel core.

TABLE 2. Performance of subcaliber tungsten carbide projectiles as a function of core diameter. (Performance relative to full-caliber steel projectile of similar shape, with the same standard as used in Table 1.)

Diameter ratio R	Muzzle velocity V_0 (fps)	Range (yd)					
		0		1,000		2,000	
		E (0)	T (0)	E (1,000)	T (1,000)	E (2,000)	T (2,000)
(37 mm)							
1.00	2,265	1.04	1.68	1.16	1.12	1.34	1.26
0.90	2,555	0.99	1.14	1.10	1.24	1.26	1.39
0.80	2,870	0.92	1.27	1.01	1.37	1.15	1.52
0.70	3,210	0.83	1.41	0.90	1.50	1.00	1.64
0.60	3,532	0.70	1.53	0.74	1.59	0.80	1.69
(20 mm)							
0.54	3,665	0.61	1.58	0.62	1.61	0.65	1.66

R = subprojectile diameter / gun diameter

$E(z)$ = energy of tungsten carbide subprojectile at range z / energy of similar full-caliber steel projectile at range z

$T(z)$ = limit plate thickness of tungsten carbide subprojectile at range z / limit plate thickness of similar full-caliber steel projectile at range z

conditions will be given before considering effects due to changes in such projectile parameters as length, nose shape, and strength of material. Changes in these parameters are important mainly because they control deformations of the projectile; to a limited extent, however, changes in length and nose shape also effect the energy required for perforation even when the projectile remains intact.

4.6.1 Projectile Deformations — Dependence on Impact Conditions

On impact, the stresses in a projectile, and therefore its tendency to deform, increase continuously with increase in striking velocity. Although details of the resultant progressive disintegration change with variations in projectile characteristics, the general pattern is the same for all. On striking the plate at velocities below a certain critical value, whose magnitude depends on the properties of the projectile, the type of armor, and the angle of attack, the projectile stays intact. As the velocity is increased above this value the projectile deforms progressively[1] until at a sufficiently high velocity it completely disintegrates almost immediately on impact.

At a velocity (really, within a narrow range of velocities) somewhat above the velocity at which the initial failure takes place, the hole made in the plate changes from one of approximate projectile diameter with smooth sides to one that has a rough jagged surface and is greatly oversize. These two types of holes are shown in Figure 7. Concurrently with a change from a small to an oversized hole there is usually an abrupt increase in the energy required for perforation. When an oversized hole is produced the nose of the projectile is always in several small pieces.

The initial failure may occur either in the nose or in the body of the projectile. If it occurs in the body there is usually a considerable difference between the velocity at which it first takes place, the rupture velocity, and that at which there is a significant, abrupt change in the character of the hole—the shatter velocity. In this case there is apparently little correlation between the rupture and shatter velocities. If, on the other hand, the initial failure takes place in the nose, this leads directly to shatter, which occurs with projectiles of conventional nose shape at velocities only slightly higher than the rupture velocity; shatter as defined here[m] corresponds roughly to the point

[1] An exception to this statement sometimes, though rarely, occurs when the initial failure takes place in the body of the projectile. Projectiles have been observed[7] to break across the body and fail to perforate the plate at a low velocity and yet perforate whole at a slightly higher velocity.

[m] Because of the close correlation between the rupture and shatter velocities in the case where initial failures take place in the nose, values reported for the shatter velocity sometimes correspond to the velocity at which the initial failure occurs and sometimes to the velocity at which the nose completely disintegrates.[6,43] In fact, it has been proposed,[42] with some reason, that what has here been called the rupture velocity for nose failures be defined as the shatter velocity. The term shatter velocity as used in the present report has the meaning originally assigned to it by Milne and Hinchliffe.[3] Shatter velocity defined in this way has practical importance because it corresponds more closely than the rupture velocity to the point at which there is an abrupt change in the energy absorbed by the plate, but it is difficult to measure and often has only statistical significance.[44]

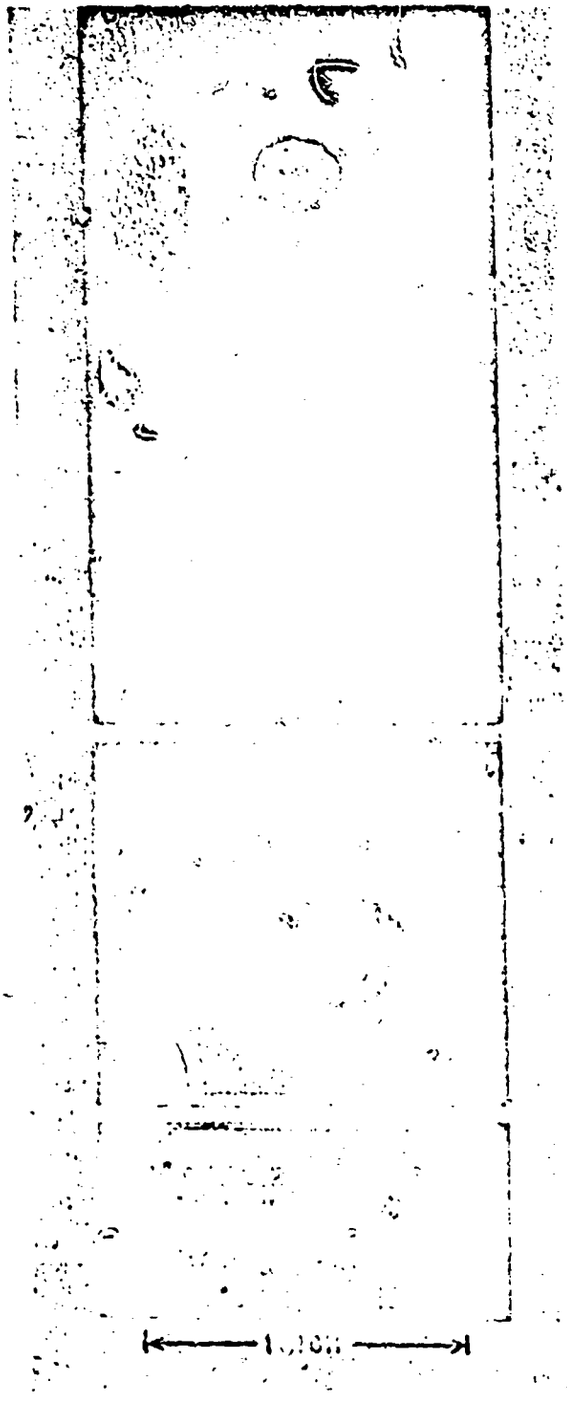

FIGURE 7. Holes produced by shattered and non-shattered steel cores in .50-caliber arrowhead projectile. A. View of exit side of holes. B. Same holes after sectioning. Exit side of holes to the left.

at which the whole nose of the projectile is removed.

As the angle of attack is changed, the values for the two critical velocities likewise change. For a particular projectile and type of armor, they may be represented by curves[53-56] such as shown in the schematic graph of Figure 8, where the striking velocity is given as a function of the angle of attack. Both curves have their greatest values for normal incidence and drop off with

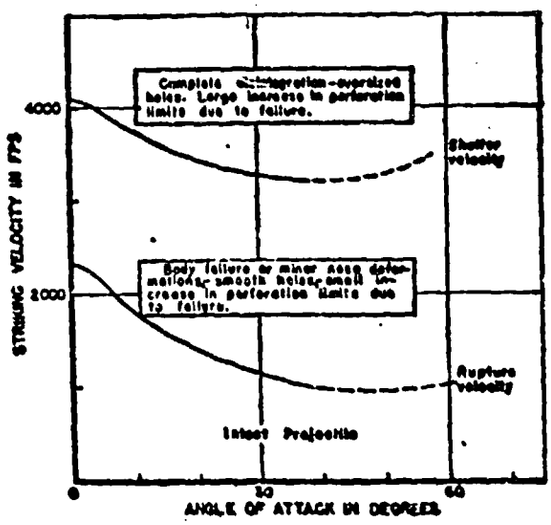

FIGURE 8. Schematic graph of critical velocities. Values correspond to those for tungsten carbide projectile.[55]

increase in the angle of attack; very few tests have been made for large angles, but at least in one case[54] the curve for the shatter velocity flattens out for intermediate angles and rises slightly for large angles.

These curves are given in terms of the striking conditions. Their exact positions depend on nose shape, projectile length, and strength of projectile material. It seems unlikely that they depend to any considerable extent on the size of the projectile or its density, but these factors have not been thoroughly investigated. They are displaced to lower velocities when the plate hardness is increased[56] but, at least for plate over 1 caliber thick, are relatively insensitive to changes[a] in plate thickness.[5]

Examples showing the dependence of projectile deformation on striking conditions are given in Figures 9, 10, 11, 12, and 13. It is evident from the spark shadowgraphs of Figures 9 and 10, showing a tungsten carbide projectile just as it emerged from the back of the plate, that the projectile remained com-

[a] As an exception to this, body failures in tungsten carbide sometimes decrease with increase in plate thickness.[55]

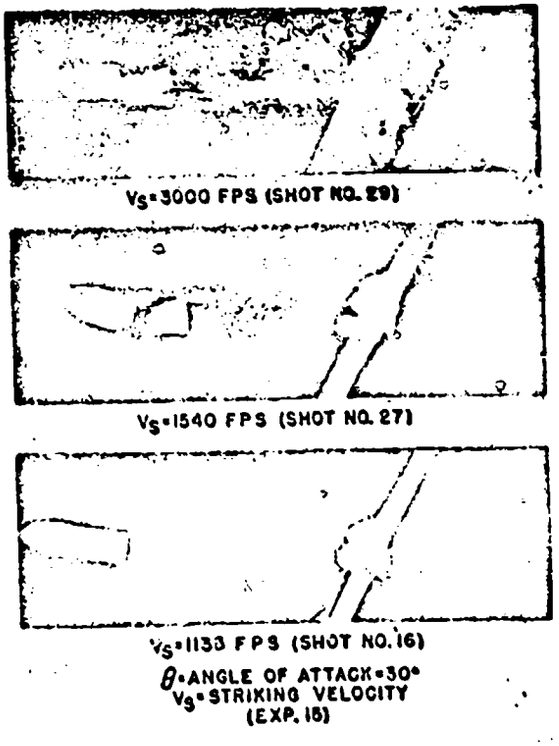

FIGURE 9. Dependence of projectile breakup on striking velocity. A .244-caliber tungsten carbide projectile ("standard"; 1-1TR) after perforating ½-in. cold-rolled steel (Rockwell B 94).

pletely intact when the striking velocity and angle of attack were small but broke across the body when these quantities were increased.[36] In another series of shots[37] extending to higher velocities than used for the pictures of Figures 9 and 10, the projectile was fired into very thick armor; the pictures reproduced in Figure 11 are X-ray photographs taken through sections cut from the armor after the impacts. For a particular angle of attack—note the shots at 0 and 30 degrees—only body failures occurred at the low velocities, but at the highest velocity the projectile broke into many small pieces. The diameter of the holes is considerably larger than the original projectile diameter and the depth of penetration is much less than would occur with an intact projectile. At normal, the penetration is no greater for a striking velocity of 4,200 fps than for 2,600 fps.

In contrast to the behavior of tungsten carbide, which suffered a body fracture, the recovered steel projectiles shown in Figure 12 first underwent plastic deformation which resulted in a bulge near the bourrelet; this bulge grew with increasing velocity. The first separation was the removal of the tip of the nose and at a slightly higher velocity the projectile was recovered in several pieces. Pictures of plate sections showing essentially these same stages of progressive disintegration are reproduced in Figure 13.

6.6.2 Effect of Projectile Deformation on Perforating Ability

Except at very large angles of impact, the increase in perforation energy resulting from the onset of shatter is considerably greater than the increase produced by the body failures and the minor nose deformations which occur in the region between the rupture and the shatter velocities. This effect of shatter is greatest at normal incidence where the increase in perforation energy may be as great as 100 per cent. Although the effect decreases as the angle of attack

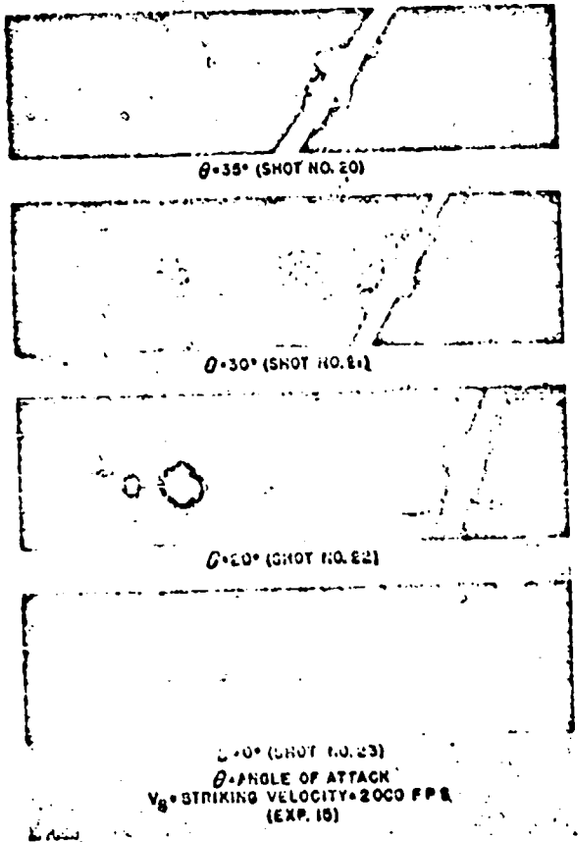

FIGURE 10. Dependence of projectile breakup on angle of attack. A .244-caliber tungsten carbide projectile ("standard"; 1-1TR) after perforating ½-in. cold-rolled steel (Rockwell B 94).

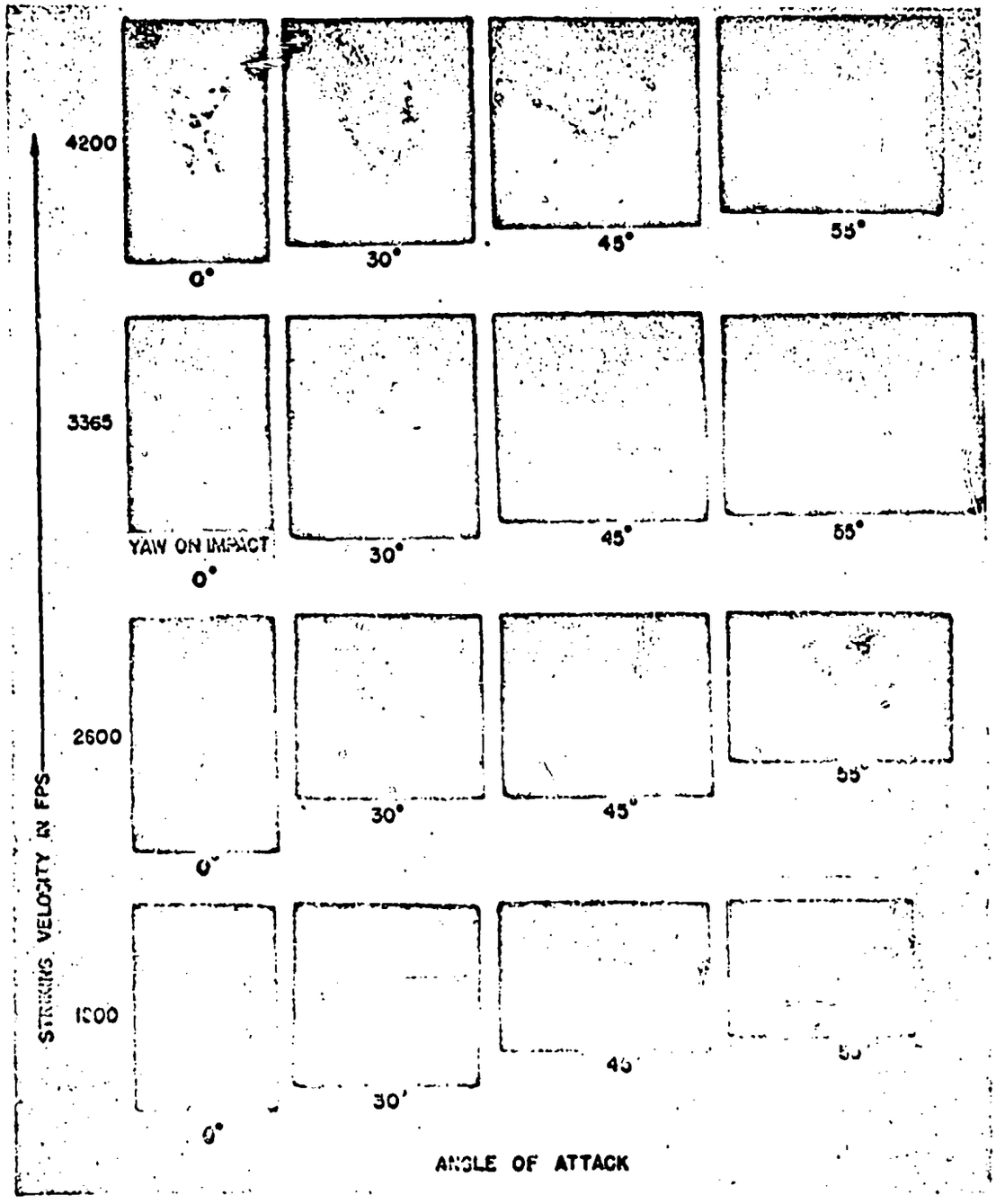

FIGURE 11. X-ray photographs of penetrations by .244-caliber tungsten carbide projectile into homogenous armor (BHN 206).

LCS projectile:
- Composition: 75 per cent tungsten carbide, 25 per cent cobalt
- Hardness: Rockwell A 85
- Transverse rupture strength: 375,000 psi
- Density: 13.0 g per cu cm
- Mass: 6.9 g

CONFIDENTIAL

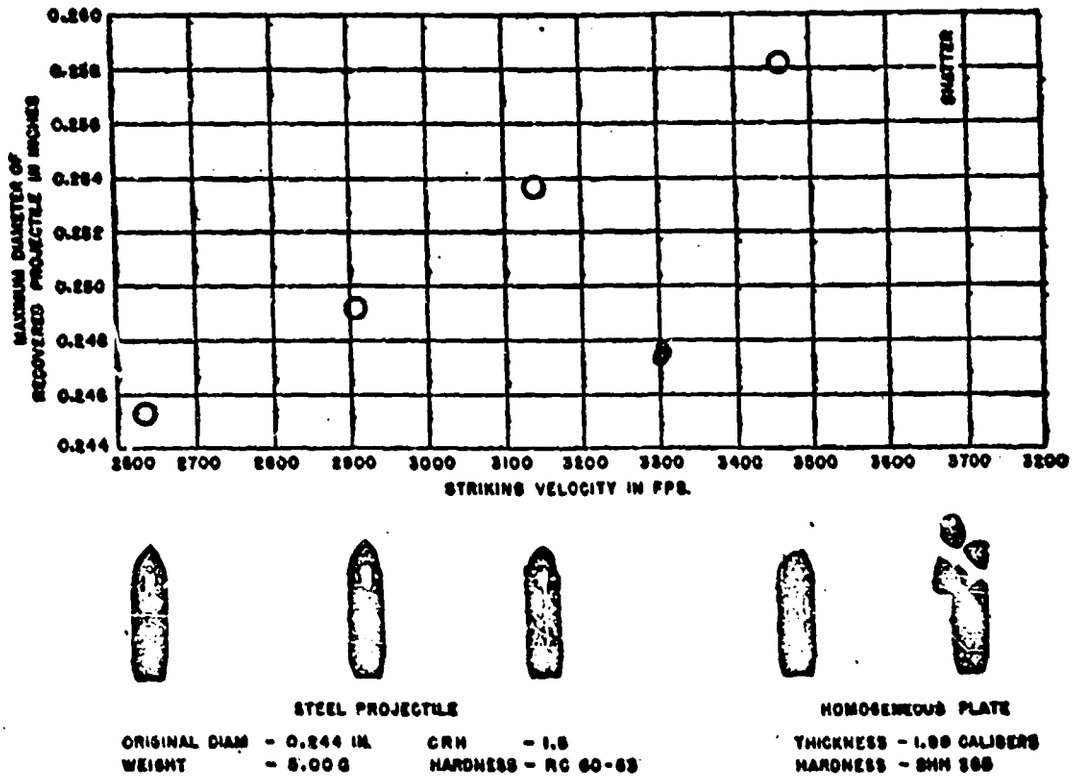

FIGURE 12. Deformation of steel projectiles as function of striking velocity (0° obliquity).

increases until at very large angles (greater than 50 degrees for 1-caliber plate) the energy required for perforation by a shattered projectile may actually be less than for a projectile that remains undeformed,[8] it is still significant for angles of attack at least as great as 45 degrees.

When a projectile is fired at a velocity above its shatter velocity its performance as a function of range (or striking velocity) may conveniently be described by means of graphs such as shown in Figure 14. In this graph[3] the performance is given for a particular angle of attack in terms of the striking velocity and thickness of plate; by means of three curves, the shatter-velocity curve, the curve representing the limit velocity with shatter, and the curve for the limit velocity without shatter, the graph is divided into four regions. These regions are designated by Roman numerals and indicate the following results:

I No perforation, no shatter.
II Perforation, no shatter.
III No perforation, shatter.
IV Perforation, shatter.

All four of these results do not occur for all thicknesses of plate. Thus if the plate is thin, result III cannot be obtained regardless of the striking velocity; even though shatter occurs it does not prevent perforation and the projectile will defeat thin plate at all velocities above its limit as an unshattered projectile. For thick plate, result II is missing; it is impossible in this case to perforate the plate without shatter and with shatter only at very high striking velocities. With plates of intermediate thickness, between 0.8 and 1.35 in. in the present example, all results are possible; the projectile can perforate plates of these thicknesses at relatively low velocities (at long range) but will fail at higher velocities (at short range) because of shatter. At still higher velocities perforation can again be achieved in spite of shatter, although, as in the case illustrated, these velocities are often above the muzzle velocity of the gun. When perforation can be obtained at velocities above and below but not within a certain interval, the interval is called a *shatter gap*.

The shatter velocity in the above example is much

higher than usually encountered because the graph is based on data obtained at normal incidence with a sharp-nosed projectile. With projectiles having more conventional nose shapes, or in oblique attack, shatter may occur at velocities even below the muzzle velocities of full-caliber projectiles fired from standard guns. It was mentioned in the introduction that the 2-pounder projectile used by the British in the Libyan campaign failed to perforate German tanks when fired at point-blank range but was successful at long ranges. This resulted from the occurrence of a shatter gap which extended well below 3,000 fps.

Graphs similar to that of Figure 14 may be drawn for oblique angles of incidence as well as for normal. As the angle of attack is increased, more energy is re-

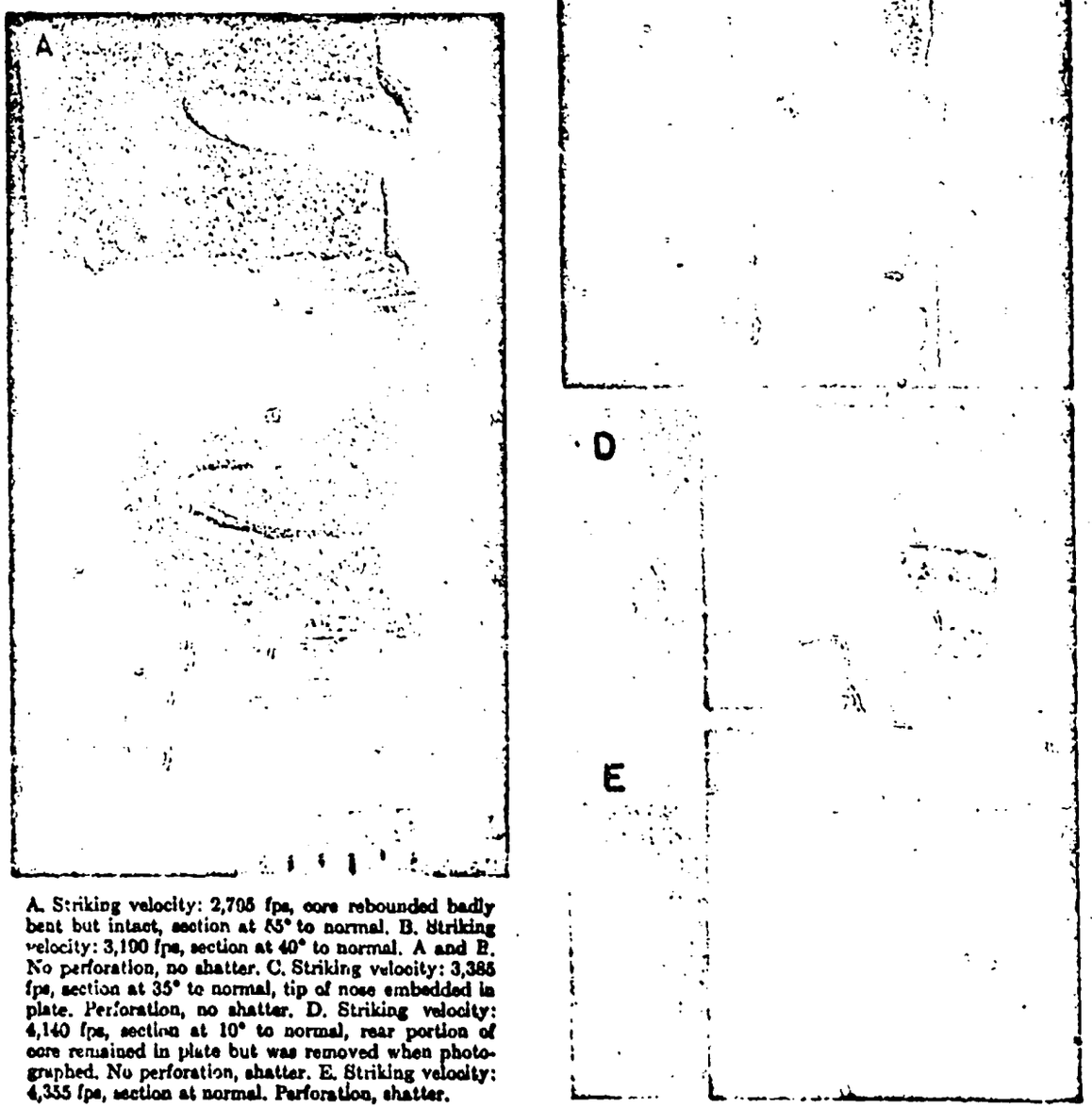

A. Striking velocity: 2,705 fps, core rebounded badly bent but intact, section at 55° to normal. B. Striking velocity: 3,100 fps, section at 40° to normal. A and B. No perforation, no shatter. C. Striking velocity: 3,385 fps, section at 35° to normal, tip of nose embedded in plate. Perforation, no shatter. D. Striking velocity: 4,140 fps, section at 10° to normal, rear portion of core remained in plate but was removed when photographed. No perforation, shatter. E. Striking velocity: 4,355 fps, section at normal. Perforation, shatter.

FIGURE 13. Transition from unshattered to shattered projectile with increasing velocity (0° obliquity).

quired for perforation, so the two curves representing the limit velocities are displaced upward; on the other hand, the shatter velocity decreases with increase in the angle of incidence so this curve is displaced downward. The result of these displacements is illustrated by the curves for 0, 20 and 30 degrees, reproduced[5] in Figure 15. The results of shots at 20 degrees for a thickness of plate including a shatter gap are shown in Figure 13. At the larger angles the shatter gap occurs at lower velocities and with thinner plate, but its extent is less because the difference between the

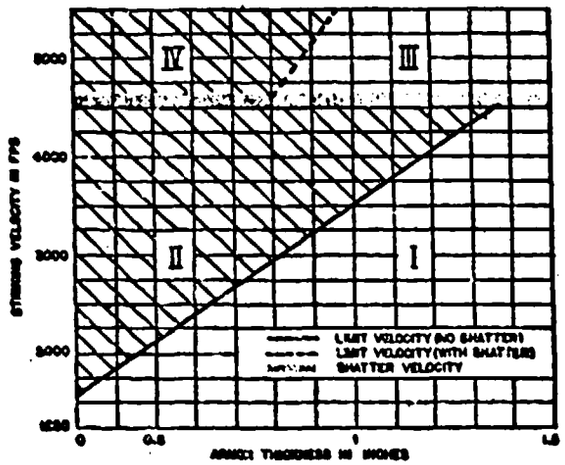

FIGURE 14. Perforation limits and shatter velocities at 0° obliquity. Steel cores of .244 caliber against homogeneous armor, BHN 255-295.[63]

Region I: No perforation, no shatter.
Region II: Perforation, no shatter.
Region III: No perforation, shatter.
Region IV: Perforation, shatter.

energy required for perforation with and without shatter has decreased. Thus with increase in the angle of attack it becomes more difficult to prevent shatter since it occurs at lower velocities (at least for $\theta < 40$ degrees) but its effect in limiting perforation becomes less.

The effect of firing a projectile at a velocity above its shatter velocity is only to increase its effectiveness at long range at the sacrifice of good performance near the muzzle; there is no overall gain. Particularly at hypervelocities, prevention of shatter for angles at least up to 45 degrees is the principal problem in the design of armor-piercing projectiles. Avoidance of less extensive deformation, such as a simple body failure, is of secondary, although sometimes not negligible, importance.

6.4.3 Projectile Parameters

As mentioned in the introduction of this chapter the parameters of a monobloc projectile may be considered as its size (diameter d), its length (either total length or length of cylindrical section l_c), its nose shape (specified for tangent ogive by the caliber radius r_o), its density and strength of material (usually measured in terms of hardness and bend or transverse rupture strength). The shape parameters are shown in Figure 1.

To be able to specify a completely rational projectile design the effect of changes in each of these quantities on perforation limits should be quantitatively known; at present it is usually possible to indicate only the trends to be expected.

Strength of Material

Projectile failures obviously result from a lack of mechanical strength. The causes of failure are reviewed in a series of reports from the Watertown Arsenal.[54,55,64] It is pointed out that a failure usually occurs as a result of (1) shearing stresses in the nose, (2) lateral expansion near the bourrelet produced by axial compressive stresses, or (3) tension in the outer layers of the body resulting from bending. To resist the shearing and compressive stresses and thus prevent nose failures the material should have a high hardness; to prevent body failures it should have a high-bend (or transverse-rupture) strength. Un-

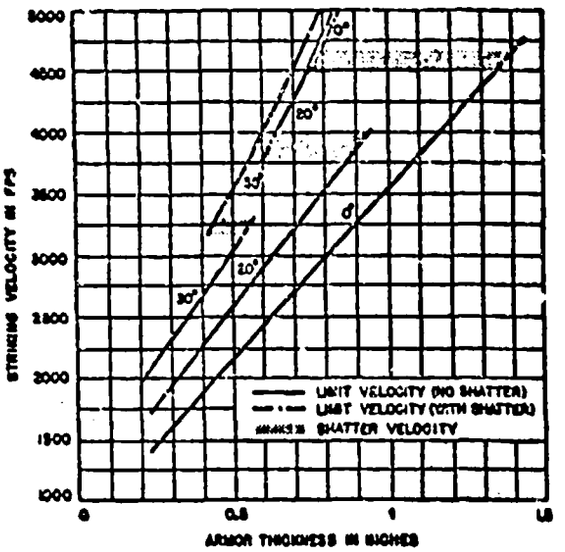

FIGURE 15. Perforation limits and shatter velocities at 0°, 20°, and 30° obliquity. Steel cores of .244 caliber against homogeneous armor, BHN 255-295.[63]

fortunately maximum bend strength usually cannot be obtained simultaneously with maximum hardness. To alleviate this difficulty steel projectiles are given a differential heat treatment. The nose is kept hard but the body softened to allow plastic deformation, which relieves the tensile stresses in the outer fibers. By this means it is often possible to prevent body failures in steel projectiles without increasing the likelihood of nose failures. This is essential because a nose failure leads immediately to shatter, which is much more disastrous than a body failure.

In the case of cemented tungsten carbide projectiles, the highest transverse-rupture strength that can be obtained, even by sacrificing hardness,* is so low that body failures occur at extremely low velocities. Thus the initial failure taking place at the rupture velocity is invariably a fracture across the body. The nose remains intact, however, until the shatter velocity is reached, whereupon the whole projectile disintegrates. A series of tests[57,58] carried out with cemented tungsten carbide projectiles of different compositions has shown that, as one would expect, the shatter velocity increases with increasing hardness, while the rupture velocity is increased by an increase in transverse-rupture strength. Since by changing the composition a decrease in transverse-rupture strength always accompanies an increase in hardness, the shatter velocity can be raised by this means only at the expense of lowering the rupture velocity. This decrease in the rupture velocity is usually of no practical importance, however, since it is so low in any case that body failures cannot be prevented with projectiles of conventional length under conditions of impact likely to be encountered in combat.

For perforation of single thicknesses of homogeneous armor the best composition of tungsten carbide is the one giving the highest hardness. High hardness is obtained by cementing the tungsten carbide particles together with a small amount of binder and this, fortunately, leads to a high density, which is an added advantage. If the target consists of spaced plates, other considerations indicate that a different choice may be advisable.[57]

Nose Shape

Although the ultimate reason for projectile failure is low mechanical strength, the shatter and rupture velocities may also be varied by changes in other parameters. While mechanical strength is important only with respect to deformations, changes in the other variables may also affect the energy required for perforation when the projectile stays intact, or the energy and velocity with which the projectile strikes the plate.

Changes in nose shape will not affect the striking energy, provided the total projectile weight is kept constant and a windshield is used to keep the external contour the same. Thus the two most important criteria of goodness are: (1) high shatter velocity and (2) low perforation energy for the intact projectile.[41,52,60-66]

In Table 3 are given the shatter velocities against homogeneous armor at 0, 15, 22.5, and 30 degrees for steel projectiles having tangent ogives with caliber radii of 3.0, 1.5, 1.27, and 1.0, and also for a projectile with a 0.2-caliber spherical tip used in conjunction with 1.27-caliber tangent ogive.[52,62] At normal, the projectile with the largest caliber radius, that is, the one with the most pointed nose, has the highest shatter velocity. At 30 degrees the situation is reversed; of the projectiles with a simple tangent ogive, the one with the smallest caliber radius now has the highest shatter velocity. Thus, as far as avoidance of shatter is concerned, it is an advantage to make the projectile quite pointed for normal attack but blunt for a 30-degree angle of incidence. For larger angles of attack the order may again reverse.[62]

TABLE 3. Dependence of shatter velocities (fps) on nose shape and angle of attack. Steel projectiles, homogeneous plate (BHN 341).*

Angle of attack (degrees)	Caliber ogive				
	3.0	1.5	1.27	1.0	1.27 and 0.2†
0	4,000‡	3,400‡	....	....	....
15	....	3,200	3,050	2,600	2,350
22.5	....	2,750	2,600	2,500	2,200
30	2,000‡	2,400	2,350	2,450	2,200

*Values taken from Watertown Arsenal results given in reference 62. These are actually rupture velocities.
†Double radius ogive with spherical tip.
‡Estimated from results in reference 62.

If the shapes are rated on a basis of the energy required for perforation when the projectile stays intact, the large-radius ogive is again best at normal. Thus in normal attack of homogeneous armor 4 calibers thick the limit energy of a projectile with a 1.5-caliber radius is 15 per cent greater than for one with a 5.0-caliber radius;[61] this advantage decreases with

* Although attempts have been made at adjusting the hardness and transverse-rupture strength along the length of a tungsten carbide projectile, these trials have not proved successful.[64]

plate thickness, but the difference is still 4 per cent for 1-caliber plate. At high obliquities, projectiles with a large radius ogive have a greater tendency to scoop; since this leads to a higher limit energy, a blunt-nosed projectile becomes best under these conditions.

On a basis of both ratings, high shatter velocity or low limit energy, a large radius has an advantage for near-normal attack but not for oblique attack. Obviously a choice of the best shape cannot be made unless the conditions of impact are exactly specified. A relatively blunt nose, 1.25- to 1.5-caliber radius, is usually chosen because of the difficulty of avoiding shatter at obliquities between 30 and 45 degrees. Even with a blunt nose, however, shatter cannot be prevented at high striking velocities without the use of a cap.

The above discussion was concerned with a single radius ogive. It will be seen from Table 3 that a rounded tip leads to lower shatter velocities at all angles of obliquity; since this shape in no case results in an appreciably lower limit energy, a rounded tip should be avoided. Flat-ended projectiles are even more likely to shatter so that they can only be used at very low velocities and therefore against very thin plate; under these conditions, however, they require considerably less energy for perforation than projectiles with ogival heads.[39]

Length

Because of a decrease in the weight of the projectile, a decrease in length leads to a lower striking energy and a higher striking velocity. The writer knows of no tests which show the exact dependence of the shatter velocity on length, but it seems unlikely that it is appreciably affected. Certainly if the projectile is too short it will fail by shatter because of the high striking velocity. This furnishes a basis for an absolute lower limit for the length; an upper limit is set by stability considerations.

If body failures occur for lengths intermediate between these two extremes, a choice must be made between the greater striking energy obtained with a long projectile and the smaller tendency toward body failures resulting from a short projectile. As an example of the effect of length on the occurrence of body failures,[40] a decrease in the body length of a tungsten carbide projectile from 2.75 to 1.25 calibers increased by over 300 per cent the energy at which it could be fired through homogeneous plate at 30 degrees without breaking. Since a body failure usually does not greatly increase the energy required for perforation, it is often difficult to decide on the best length[39] unless the projectile can and must be kept completely intact.

Conventional lengths for monobloc steel projectiles and tungsten carbide cores are about 3.5 calibers overall, with body lengths a little over 1 caliber shorter. The cores for capped steel projectiles are usually shorter than 3.5 by ½ to 1 caliber.

Density

As with an increase in length, an increase in density of the projectile results in a higher striking energy but a lower striking velocity; the lower striking velocity reduces the likelihood of shatter.

The most important change in density encountered in projectile design occurs when tungsten carbide is substituted for steel. It is interesting that it is the high density of tungsten carbide, rather than its better mechanical properties, that is responsible for its superior perforating ability. Although the shatter velocity of a tungsten carbide projectile is not much greater than that of a good steel, it can have almost twice the striking energy without shattering because of its greater weight. Thus the high density of tungsten carbide leads to two distinct advantages: (1) a greater striking energy and (2) a higher shatter energy. It is essential, of course, that an increase in density not be accompanied by a decrease in strength; lead, for example, is a poor projectile material in spite of its high density.

Another effect of a change in density, or more precisely of a change in weight, is of secondary importance, but will be mentioned for the sake of completeness. This effect is concerned with the energy required for perforation when the projectile does not shatter. Equation (10) should apply in this case and this equation assumes that the limit energy is independent of the weight of the projectile. This has been shown to be true[41] for normal attack of plate thicker than 1.5 calibers but for thinner plate the limit energy increases slightly with increase in projectile weight.[37,41] For 1-caliber plate an increase in weight by 50 per cent increased the limit energy of a projectile with a 1.5-caliber radius by slightly more than 8 per cent.

Size

A change of size is obviously of importance in design only in the case of subcaliber projectiles. As a result of the increase in striking velocity with a decrease in size, shatter often occurs before the optimum diameter calculated by the method of Section 6.5 is

reached. A case in which the occurrence of shatter determines the most suitable size for a subcaliber capped steel projectile is considered in Section 6.8. The shatter velocity of a monobloc steel projectile is so low at obliquities that even a full-caliber projectile of this type is ineffective if fired from a present day standard gun in the important range between 20 and 45 degrees. Monobloc tungsten carbide projectiles might conceivably be used in subcaliber sizes if the striking velocity was limited to values below about 3,000 fps and the attack restricted to homogeneous plate. If the projectile and gun were the types considered in calculating Table 2, a muzzle velocity of 3,000 fps would correspond to a subprojectile to gun diameter ratio of 0.75.

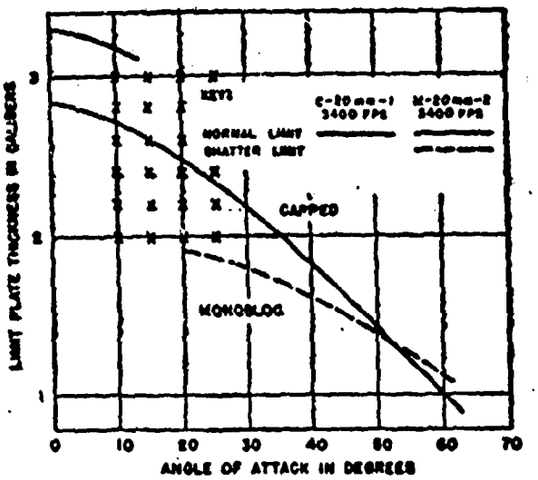

FIGURE 16. Comparative performance of capped and monobloc projectiles against homogeneous armor.

6.7 COMPARATIVE PERFORMANCE OF CAPPED AND MONOBLOC PROJECTILES

The purpose of the cap is to prevent shatter. In cases where the monobloc does not deform badly or where shatter aids perforation, the use of a cap is a detriment. On the other hand, if deformation greatly reduces the perforating ability of the monobloc, then the cap, by keeping the main body of the projectile intact, may decrease the limit energy for the projectile as a whole despite some loss in penetrating ability due to its own disintegration. Thus the limit energy may be either increased or decreased by the attachment of a cap and unless the conditions of impact are exactly specified, no answer can be given to the question of whether a capped or a monobloc projectile perforates a greater thickness of armor.

For attack of face-hardened plate the cap is useful at all striking velocities. Against soft homogeneous plate (BHN 250) the monobloc has the advantage at low velocities (less than approximately 2,500 fps for steel projectiles), but the capped projectile can perforate thicker plate at velocities above the shatter velocity of the monobloc at normal incidence (for steel projectiles usually above 3,500 to 4,500 fps, depending on nose shape). Whether or not the cap is of benefit at velocities intermediate between these two extremes depends on the angle of attack.

A comparison of the performance of a capped and a monobloc steel projectile of equal total weights is given in Figure 16 for a particular striking velocity in the intermediate range.[6.66] The graph indicates the thickness of plate perforated by each projectile as a function of the angle of attack. For small angles the monobloc perforates thicker plate. The advantage of the capped type, whose piercing element remains intact at all obliquities, begins at and is greatest for an angle just larger than that at which the monobloc shatters. As the angle is increased beyond the critical angle for shatter the difference between the thickness of armor perforated by the two types gradually decreases until it becomes zero. At still greater angles (greater than 55 degrees in the present case) the shattered monobloc perforates the most armor. Thus in the intermediate velocity range the monobloc is superior at large and small but not at intermediate angles; the capped projectile becomes superior at smaller angles as the velocity is increased.

Although the exact amount by which the shatter velocity is raised by means of a cap depends on many factors, particularly cap weight, there is no doubt as to the general effectiveness of the method for reducing deformations. To cite one case,[6.67] a particular cap (27 per cent of core weight) increased the shatter velocity of an uncapped projectile fired against homogeneous armor from less than 2,400 fps to approximately 4,100 fps; the cap was equally effective in increasing the shatter velocity at all angles of attack from 0 to 60 degrees. The addition of the cap in this case reduced the perforating ability of the projectile only for plate less than 2 calibers thick because even at normal incidence the uncapped projectile could perforate plate no thicker than this without shatter. For 1-caliber plate at normal incidence the cap increased the limit

velocity by 10 per cent and the limit energy by 54 per cent. This effect of the cap in increasing the limit velocity becomes less for thicker plate.[66]

The relative performance of a number of full-caliber monobloc and capped steel projectiles is shown in the graphs of the Division 2, NDRC, Data Sheets 2C3a (Chapter 19). These are standard projectiles fired from standard guns at velocities below 3,000 fps. The curves, which give the thickness of homogeneous armor that can be perforated at various ranges, were purposely not begun at zero range because the projectiles had not been tested at velocities as high as the muzzle velocities. Extrapolations would probably be justified for both the capped and monobloc projectiles at 0 degree obliquity and for the capped but not the monobloc at 30 degrees. For example a test[8] of the monobloc 37-mm M74 showed that at point-blank range it would shatter and perforate only 2.2 in. at 30 degrees while extrapolation of the 2C3a graph indicates that it should defeat 3-in. plate. Another point is that the performance of the monobloc projectiles is worse at long ranges than that of the capped projectiles. This might appear to contradict earlier statements that a monobloc is better at low velocities. The cause for the poor performance of the monobloc in this case, however, is not its poor terminal-ballistic behavior but the fact that only the capped projectiles have windshields.

The above examples are for steel projectiles. That the addition of protective material is also effective in the case of tungsten carbide cores was well demonstrated during the development of a hypervelocity projectile for the 6-pounder, 7-cwt, 57-mm gun.[68] During this development, a comparative terminal-ballistic test was carried out with projectiles of two types. One had a comparatively heavy steel windshield and Duralumin pad covering the nose of the tungsten carbide core while the other had only a light Duralumin windshield. At 4,150 fps, which was the muzzle velocity of the gun, the projectile with the heavy steel windshield was able to perforate approximately 25 per cent more armor at all but near-normal obliquities.

Actually the tungsten carbide cored projectiles used in the 57-mm gun were jacketed rather than capped. In either case, however, the essential feature necessary for good performance is sufficient protective material surrounding the nose of the core. The portion of the jacket surrounding the sides of the core apparently has little effect in controlling breakup,[69] and presumably this is also true for the material behind the core. In cases where the core does not shatter, however, material behind the core often contributes to the penetration by giving the core a boost from behind when it strikes the plate.[8] Thus the results given for perforation limits of tungsten carbide cored projectiles in the Division 2, NDRC, Data Sheet 2C6 of Chapter 19 are sometimes less than would be computed from equation (16), not only because of a slight scale effect but also because of contributions from the jacket.[9] It should be pointed out that the band in this graph marked "capped" should apply to any projectile which has sufficient material to protect the nose whether it has a cap in the conventional sense or not.

6.8 HYPERVELOCITY PROJECTILES

As previously indicated, armor-piercing projectiles are conventionally classified as monobloc, capped, or jacketed, and either steel or tungsten carbide is customarily used for the piercing element (core). Conceivably any of these six possible types might be employed as a full-caliber or as a subcaliber projectile,[a] but, with the exception of small arms ammunition, the only types used in combat during World War II were full-caliber capped and monobloc projectiles made entirely of steel and jacketed tungsten carbide projectiles in both full and subcaliber sizes. Except for experimental purposes and in the case of one gun, the German 88-mm, steel projectiles were not used at hypervelocities. The possibility of a hypervelocity, subcaliber steel projectile will be discussed, however, in order to compare results with those obtained with tungsten carbide cored projectiles which were used exclusively at hypervelocities.

6.8.1 Steel Projectiles

Normally the full-caliber steel projectiles have muzzle velocities below 3,000 fps. The monobloc is ruled out for use at higher velocities because of the likelihood of shatter. The capped projectile is less likely to shatter than the monobloc and can be successfully used as a full-caliber projectile in somewhat more powerful guns, but only a small advantage is gained by using it as a subcaliber projectile.

The graph in Figure 17 shows the thickness of armor that can be perforated at the muzzle of a 37-mm

[9] Following customary practice, the specific limit energies and caliber plate thicknesses in this graph are based on core weight and diameters.

[a] As used here, subcaliber means that the diameter of the projectile in flight is less than the diameter of the gun.

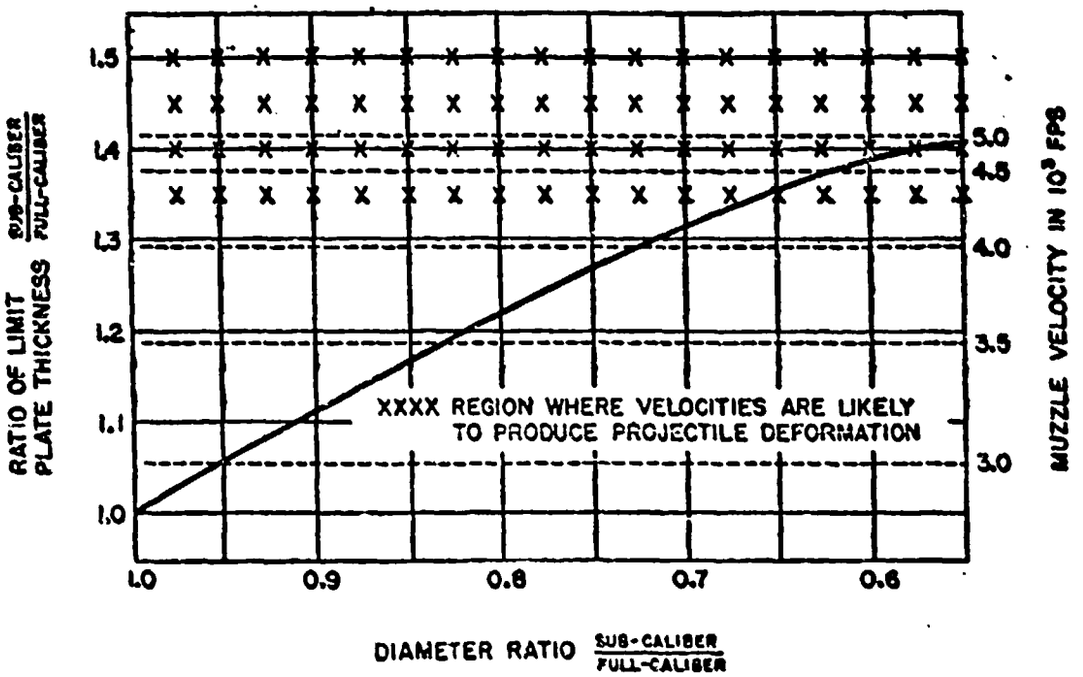

FIGURE 17. Perforation limits as function of diameter of subcaliber projectiles. Homogeneous armor attacked at point-blank range.

gun by subcaliber capped steel projectiles of the same shape but different sizes.[6] This curve was calculated by the method outlined in Section 6.5 but is based on a perforation formula obtained from firing trials with a projectile of the particular type and shape considered in this example; the curve should hold at obliquities as well as at normal. It will be noted that even though the cap in this case is very heavy (27 per cent of core weight), shatter sets in before the optimum diameter is reached. In order to avoid shatter at the muzzle the subprojectile to gun diameter ratio should not be greater than about 0.7; furthermore, at 2,000 yd a core of this size would give better performance than smaller cores even though deformation is not a factor at this range. If a subprojectile with a diameter ratio of 0.7 were a scale model of the full-caliber projectile, it should perforate approximately 30 per cent more armor at the muzzle and 20 per cent more at 2,000 yd. Actually, however, it is not necessary to use a cap as heavy as this for the full-caliber projectile; the cap of the 37-mm M51 is only 14 instead of 27 per cent of the core weight. Consequently the advantage at the muzzle of the subcaliber projectile over the M51 is only 18 rather than 30 per cent, and this advantage decreases with increase in range. In this example the muzzle velocity for the full-caliber projectile is 2,900 fps; in the case of a more powerful gun, the subprojectile would be limited to even larger diameters and its advantage would be still less. In fact, if the power of guns is increased any considerable amount above the present level even the full-caliber projectile will be unsatisfactory unless means of increasing the strength of steel are found.

6.8.2 Tungsten Carbide Cored Projectiles

There are three conventional types of jacketed tungsten carbide projectiles: (1) the folding skirt projectile, (2) the composite rigid or arrowhead, and (3) the sabot. Due to their very small total weight all have muzzle velocities in the hypervelocity range even when fired from standard guns. Likewise all have about the same terminal-ballistic performance which is determined to a first approximation by the size and weight of the core. In other respects each has its own advantages and disadvantages.

Folding Skirt. This projectile is fired through a tapered bore which may either be built into the gun or added to a standard gun by means of a special muzzle attachment. The taper serves to swedge down flanged

skirts, which extend from the main body of the projectile so that the emergent caliber is much less than the original diameter. In this way the accelerating pressure of the powder gases is allowed to act on a large area while a small area is presented to the resisting pressure due to air resistance. The principal disadvantages of this means of obtaining hypervelocities is that the taper prohibits the use of standard ammunition.

Composite Rigid. This is merely a light-weight full-caliber projectile with a tungsten carbide core having a diameter approximately half that of the gun. Due to a very low ballistic coefficient it rapidly loses velocity in flight so that it is effective only over a very short range.

Sabot. The principal disadvantage of the sabot is the danger that the discarding pieces will strike friendly troops. Although the high ballistic coefficient of the subprojectile makes it effective over a much longer range than the composite rigid, it is not so accurate at the present stage of development.

That practical projectiles of these designs are significantly superior in perforating ability to conventional full-caliber types has been demonstrated both in combat and by plating trials. The most recent estimates for the performance of various armor-piercing projectiles against German tanks[18] indicate that for every gun considered (75-mm, 77-mm, 90-mm, 17-pounder, 3.3-in.) the composite rigid and sabot projectiles are more effective than the corresponding full-caliber steel projectiles. Contrary to the opinion that tungsten carbide projectiles are inferior at oblique angles of incidence, their superiority exists at 55 degrees obliquity as well as at normal, although not to the same extent.

A second example showing the increase in perforating ability to be expected from the use of tungsten carbide cored projectiles is given in the graph of Figure 18, which is based on firing trials carried out by Division 2, NDRC. This graph indicates the thickness of homogeneous armor that can be defeated at the muzzle of a 37-mm gun as a function of the angle of attack. Limit thicknesses are given for three projectiles: (1) full-caliber capped steel 37-mm M51, (2) subcaliber capped steel, and (3) subcaliber jacketed tungsten carbide, model of 6-pounder *discarding sabot* [DS] Mark I. A description of these projectiles is given in Table 4. The full-caliber type is the standard service projectile for this gun; the sub-

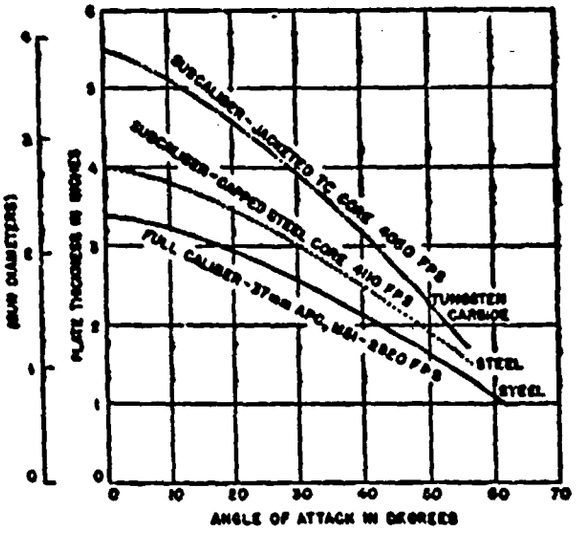

FIGURE 18. Comparative performance of sub- and full-caliber projectiles. A 37-mm M3 gun, point-blank range, homogeneous armor BHN 260 ± 20. See Table 4 for complete projectile descriptions.

TABLE 4. Description of projectiles whose perforating ability is given in Figure 18.

Projectile type	Full-caliber capped-steel 37-mm M51 APC				Discarding sabot, capped-steel subprojectile				Discarding sabot, jacketed tungsten carbide subprojectile (Model of 6-lb DS, Mark I)		
Components	Complete	Windshield	Cap	Core	Complete	Subprojectile			Complete	Subprojectile	
						Windshield	Cap	Core		Jacket	Core
Weight (lb)	1.87	0.03	0.23	1.61	0.85	0.01	0.14	0.53	0.88	0.23	0.43
Diameter (in.)	1.46	....	....	1.46	1.46	....	....	1.02	1.46	0.95	0.72
Muzzle velocity (fps)	2,920				4,110				4,050		

caliber steel projectile is the one whose performance was discussed in the preceeding section; the tungsten carbide cored projectile is representative of good design for this type, although the writer has seen no report indicating that the diameter of the core has been adjusted for optimum size. At normal the tungsten carbide cored projectile is able to perforate 60 per cent more armor than the full-caliber projectile; while the advantage drops with obliquity, it is still 22 per cent at 55 degrees.

69 FUTURE STUDIES

A person thoroughly familiar with the results of the many plating trials carried out during the past few years should be able to suggest a good basic design and reasonable values for the parameters of either a full or a subcaliber projectile to be fired against simple targets from a present-day gun. Adjustment of the parameters on a basis of firing trials may well be necessary, however, before acceptable performance is obtained. The designer will find his task difficult (1) if the power of the gun is much above the present level, (2) if the main armor of the target is protected by a thin skirting plate, or (3) if the armor plate is set so that it can be struck only at a large angle of incidence.

If higher striking velocities are to be employed, better means must be found for keeping the projectile intact. Every effort should be made to increase the strength of projectile materials and more satisfactory methods should be devised for preventing the decapping[48] and breaking of projectiles[71] by skirting plates.

Special attention should be given to high-angle attack. At the end of World War II it was impossible with the best antitank guns and projectiles available to defeat the sloping plates on the front of German tanks except at short range.

At the present time projectile design must be carried out almost entirely on a basis of empirical results. Particularly for oblique attack, the fundamental problem of finding the forces involved in the plate-projectile interactions has hardly been touched. Once these forces are known it should be possible to deduce the dynamic stresses produced in the projectile during impact and to design rationally against the resulting deformations.

Chapter 7

TERMINAL BALLISTICS OF CONCRETE

7.1 INTRODUCTION

7.1.1 The Work of CPPAB and CFD

RESEARCH ON the terminal ballistics of concrete[a] was begun at Princeton late in 1940 under the auspices of the Committee on Passive Protection against Bombing [CPPAB].[1] This Committee was appointed by Frank B. Jewett, President of the National Academy of Sciences, on June 24, 1940, to supervise the execution of a one-year contract entered into July 1, 1940, by the United States of America and the National Academy of Sciences. This contract called for the National Academy of Sciences to make reports to the Chief of Engineers, U. S. Army, covering "the basis of design of structures to provide protection to personnel and installations, both military and civil, against bombing by aircraft." The contract was subsequently renewed by the Corps of Engineers in July 1941, July 1942, and July 1943. In the latter contract, terminating October 31, 1944, the name was changed to Committee on Fortification Design [CFD] to correspond more closely to the then-current objectives of the committee's work.

Almost from the beginning this work was closely integrated in many of its phases with the research programs of Sections B and S of Division A of NDRC and later of Division 2 after the reorganization of NDRC in January 1943.

7.1.2 Purpose of the Investigation

In the first instance the research on concrete was undertaken to create a better quantitative basis for the design of defensive structures, as has just been discussed. As World War II progressed and the emphasis shifted from defense to offense, many further implications of the knowledge gained began to appear. Basic knowledge concerning the terminal ballistics of concrete is needed in predicting the effects of our own weapons on the enemy's fortifications, bunkers, submarine pens, and other concrete structures. It is extremely important to realize that an attacking bomb or projectile may be handicapped or even defeated by such things as ricochet, deformation, rupture, improper fuzing, etc., and to avoid overestimation caused by a lack of understanding of the phenomena of terminal ballistics. Not only the advantageous choice and use of attacking weapons but also their design must be based on terminal-ballistic information. For example, the design of concrete-piercing projectiles and bombs to carry the maximum amount of high explosive without deformation and rupture against concrete requires estimating the nature and magnitude of the forces encountered during concrete penetration. Similarly, the best fuzing to detonate the projectile at maximum penetration or after perforation depends on the time of penetration or perforation; indeed, the question of fuze initiation also depends on a knowledge of the setback forces at impact, particularly in the case of very thin slabs. These examples and general remarks are perhaps sufficient to suggest the nature and relative importance of terminal-ballistic studies of concrete and their bearing on offensive as well as defensive activities.

Beyond these particular applications the study of the terminal ballistics of concrete is of long-range importance because it sheds additional light on the general problems of penetration and perforation. Heretofore only steel (including armor) had been studied extensively and perforation rather than penetration stood in the forefront of interest. This was partly because of the difficulty in obtaining both the high velocities and the nondeforming projectiles required to produce massive penetrations beyond the nose height of the projectile. With concrete targets, ordinary projectile velocities and ordinary armor-piercing [AP] projectiles are adequate to secure penetrations beyond the bourrelet in massive targets. Hence the simpler and more fundamental problem of massive penetration could be studied extensively. Furthermore, the existence of a marked scale effect and the brittle rather than ductile nature of the target material serve to widen the range of phenomena considered in the theoretical treatment of penetration and perforation.

7.1.3 History of the Problem

It was probably surprising to everyone to discover that although extensive use of concrete had been made in fortifications and notably in the Maginot Line and

[a] Pertinent to War Department Projects CE-5 and CE-6 and to Navy Department Project NO-32.

[b] See Weapon Data Sheets 2A1, 2A3, 2A5, 2B1, 2C1, 2C1a of Chapter 19.

the West Wall, no evidence could be found in available documents of any very serious experimental work on the terminal ballistics of concrete since the time of the Metz Committee, 1835. In view of the early period in which this work was done and the many uncertainties which surround it, it was concluded that a serious program should be entered into on the terminal ballistics of concrete.

The history of the problem of the terminal ballistics of concrete before 1940 is adequately covered in a CPPAB report[2] discussing the theoretical and experimental results then available for the solution of the penetration problem in concrete, steel, wood, earth, and sand. This report surveys the theories of penetration, the problem of rupture (scabbing), and of perforation without rupture, and the effect on penetration of the physical properties of the target. It also includes a substantial bibliography of those sources from which material was actually used in preparing the report, beginning with Robins in 1742 and concluding with British Air Raid Precaution [ARP] publications of 1939. The principal authors cited include Robins, Euler, Morin, Poncelet, Piobert, Didion, Martin de Brettes, v. Wuich, Resal, Levi-Civita, Pétry, deGiorgi, Cranz, Thompson, Scott, Peres, Milota, Gaede, Vieser, Heidinger, Skramtajew, Montigny, Speth, Bazant, Gailer, Harosy, and Hayes.

7.1.4 Principal Contributions

Both experimental and theoretical work was done on the terminal ballistics of concrete by Division 2 of NDRC and the afore-mentioned associated organizations. Small- or model-scale experiments were carried out at Princeton, while large-scale tests were made at the Aberdeen Proving Ground, where the necessary facilities were made available by the Corps of Engineers and the Ordnance Department, U. S. Army. In compiling and reporting the experimental observations, great emphasis was put on making complete and accurate tabulations of all principal and auxiliary data. The results have been found to be useful as source material for problems of many kinds and, it is hoped, may form the bases for better analyses of the phenomena of penetration and perforation in concrete than have yet been made.

The course of the work during World War II may be outlined by the following brief summaries of the principal contributions. The bibliography for this chapter includes not only these references but also lists related work by the Army, Navy and by British organizations.

1. *Final Report, National Research Council, Committee on Fortification Design*, John R. Burchard, December 1944.

While this is chronologically the last of the CPPAB and CFD reports, it is put first here because it contains a complete final review of the history, projects, and reports of these committees from their inception to the end. Work on the terminal ballistics of concrete formed part of the activity of these committees.

2. *Terminal Ballistics*, H. P. Robertson, CPPAB Interim Report, January 1941.

A critical survey of previous work in the field of penetration and perforation is given. The report contains extensive references to earlier work.

3. *Final Report for the year ending June 30, 1941*, Part 1, CPPAR.

This report contains the small-caliber penetration data of the first Princeton "Concrete Properties Survey," the object of which was to obtain experimental information on the effect of concrete properties on penetration resistance. The then current theories of concrete penetration are discussed and the data are analyzed in terms of the classical Poncelet theory. The first evidence suggesting the existence of the *scale effect* for concrete penetration is presented and discussed on page 48 of this CPPAB report.

4. *Penetration of Projectiles in Concrete*, Richard A. Beth, CPPAB Interim Report No. 3, November 1941.

This report suggests the use of an empirical penetration formula for concrete of the form $\epsilon_c = KDV^\alpha d^\beta$, where ϵ_c is the nose-corrected penetration in calibers, D is the caliber density of the nondeforming projectile, V is the striking velocity, d is the caliber, and K, α, and β are constants. The factor d^β represents the scale effect.

5. *AP Bomb Test—Comment*, Richard A. Beth, CPPAB Interim Report No. 9, April 1942.

Bibliography, data, and discussion of tests with 12-in. AP projectiles, weighing 1,000 lb, striking heavily reinforced concrete slabs of three thicknesses, 36, 60, and 81 in., at 1,000 fps and 20 degrees obliquity. The .45-caliber penetration data obtained on unreinforced 1-ft cubes of the same concrete are also given and an attempt is made to evaluate the scale effect according to the type of formula suggested above.[4] This involves a suggested method of making allowance for the density of reinforcing steel on penetration.

6. *A Brief Summary of Recent Data on Penetration in Concrete at Various Scales*, Richard A. Beth, CPPAB Interim Report No. 18, June 1943.

A summary review of penetration data at .45-caliber, 37-, 75-, 155-mm, 12-, and 16-in. scales. The data are analyzed and correlated in terms of empirical formulas of the form suggested above.[4] Scale-effect graphs are given. Some data on sticking, scabbing, and perforation of concrete by inert projectiles are given.

7. *Penetration and Explosion Tests on Concrete Slabs—Report I: Data*, Richard A. Beth and J. Gordon Stipe, Jr., CPPAB Interim Report No. 20, January 1943.

This report contains complete data and some preliminary analyses in the form of graphs of extensive tests on 39 reinforced concrete slabs at .45- and .50-caliber, 37- and 75-mm, 3-in., and 155-mm scales. Penetrations, perforations, obliquities, and explosions are included.

8. *Penetration and Explosion Tests on Concrete Slabs—Report II: Crater Profiles*, J. Gordon Stipe, Jr., CPPAB Interim Report No. 21, January 1943.

Eleven large prints of measured crater profile drawings which are reproduced at smaller size in reference 7.

9. *Resistance of Laminated Concrete Slabs to Perforation*, Robert J. Hansen, CPPAB Interim Memorandum M-9, May 1943.

Report on tests made at 37-mm scale to find the reduction in perforation limit velocity produced by pouring concrete slabs in successive layers rather than monolithically. A lowering of limit velocity by not more than 5 per cent per construction joint was found.

10. *Terminal Ballistics and Explosive Effects* (Appendix to the *CPPAB Final Report for the year ending June 30, 1943*), CFD Report, Oct. 1943.

This report contains a description of terminal-ballistic phenomena with concrete, steel, armor, and other target materials, together with a compilation of considerable quantitative information on these subjects in the form of tables, graphs, and nomograms. It was originally written to assist the Corps of Engineers in the preparation of a new fortifications manual.

11. *Concrete Properties Survey*, Richard A. Beth, J. Gordon Stipe, Jr., M. E. DeReus, and J. T. Pittenger, CFD Interim Report 27, July 1944.

This report consists of three separately bound parts: *Effect of Concrete Properties on Penetration Resistance, Appendix A—Preparation and Physical Tests of Concrete*, and *Appendix B—Penetration Data*.

In order to explore the effect of various concrete properties on penetration resistance, 154 1-ft cube targets representing about 75 different concretes were made and tested for penetration resistance, using non-deforming hardened steel .50-caliber model-scale projectiles. Tests were made at normal incidence with striking velocities from 600 to 2,000 fps. The earlier Concrete Properties Survey data[5] were neither so extensive nor so accurate as these newer data and should therefore be regarded as preliminary or auxiliary to the data of this report. Summary tables of the data and a discussion and analysis of the results are contained in the first part of the report; the two appendices contain complete descriptions and original data on the parts of the work indicated by their titles.

12. *Ballistic Tests on Concrete Slabs*, J. Gordon Stipe, Jr., M. E. DeReus, J. T. Pittenger, R. J. Hansen, CFD Interim Report 28, June 1944. (The separately bound *Appendix A—Tables of Data* contains full tabulations of all original ballistic and concrete data.)

Perforation, scabbing, and penetration tests were made on 133 concrete slabs in this companion program.[11] The same .50-caliber projectiles were used and slabs from 3 to 18 calibers thick were tested. These small-scale tests were planned to supplement the information at larger scales,[7] particularly with respect to the effect of slab thickness, concrete strength, aggregate gradation and size, various schemes of reinforcement, scab plates, and obliquity of incidence. The following relations were found: $e/d = 1.23 + 1.07z$ and $s/d = 2.28 + 1.13z$, where e/d and s/d represent the thickness that can be perforated and scabbed respectively, in calibers, and z is the penetration depth in calibers into massive concrete of the same characteristics at the perforation or scabbing-limit velocity. These relations show good agreement with the data except at obliquities above 40 degrees.

13. *Repeated Fire and Edge Fire Effects on Small Concrete Slabs*, J. Gordon Stipe, Jr., CFD Interim Memorandum M-12, July 1944.

The number of rounds required for perforation of reinforced concrete slabs by repeated fire attack with .50-caliber model-scale projectiles was tested for two

thicknesses of concrete, two reinforcing schemes, and for different distances from the slab edge.[12] Tables of ballistic data and many observed crater profile drawings are included.

14. *Composite Slabs*, J. Gordon Stipe, Jr., CFD Interim Memorandum M-13, June 1944.

A method of estimating the perforation-proof thickness of slabs composed of concrete and steel, soil and concrete, and of the three materials is proposed.

15. *Penetration Theory: Estimates of Velocity and Time during Penetration*, R. A. Beth, OSRD-4720, NDRC Report OTB-7, February 1945.

This paper summarizes the theory of the variation of the resisting force R during projectile penetration for three cases: (1) R is a constant (the Robins-Euler theory), (2) R is a function of the remaining velocity v only (sectional pressure theories), and (3) R is a function of the penetration depth x only (sectional energy theories). The functional form of R is not known, but there are reasons for believing that the actual curve for R will fall between those predicted for cases (2) and (3). A knowledge of R would be a step toward solving problems of fuze and projectile design and the design of composite targets.

16. *Concrete Penetration*, Richard A. Beth, OSRD-4856, NDRC Report A-319, March 20, 1945.

An attempt is made to revive the Poncelet hypothesis by postulating a force law of the form $R = a(x) + bv^2$ for concrete penetration, and $a(x)$ and b are evaluated from the .50-caliber penetration data[11] and some additional data on the effect of projectile mass and nose shape given in an appendix. Calculations of resisting force, time, and remaining velocity during penetration are made. The theoretical consequences of a further generalization of the Poncelet force law, $R = a(x)v^{1.5} + b(x)v^2$, in which the first term is able to take account of the concrete scale effect, are worked out in an appendix.

17. *An Electromagnetic Method for Measuring Projectile Velocity during Penetration*, R. A. Beth and E. J. Schaefer, OSRD-5175, NDRC Report A-329, June 1945.

The method consists in magnetizing the projectile and recording the electromotive force induced in suitably disposed coils during deceleration in a nonmagnetic and nonconducting target material, like concrete, by means of a cathode-ray oscillograph equipped with a linear time sweep. The report outlines the theory and design of the coils, the equipment used, and describes preliminary experimental work including the methods of stablizing the magnetic moment of the projectiles against the effects of impact.

18. *Penetration Theory: Separable Force Laws and the Time of Penetration*, Richard A. Beth, OSRD-5258, NDRC Report A-333, June 28, 1945.

This report considers the consequences of assuming a separable force law of the form $R = cg(x)f(v)$ as an alternative to the generalized Poncelet force law.[13] General formulas are given for penetration as a function of striking velocity, remaining velocity as a function of depth during penetration, and for time of penetration. A number of special cases are tabulated, including all of the classical theories of penetration. A separable force law for perforation leads to a relation between limit, striking, and residual velocities of the form $F(v_l) = F(v_s) - F(v_r)$, which is independent of the projectile mass and the target strength under certain plausible assumptions.

19. *Ballistic Tests on Concrete Slabs, II, Effect of Nose Shape*, J. Gordon Stipe, Jr., OSRD-6638, NDRC Report A-112M.

This report gives additional supplementary .50-caliber data of reference 12, particularly with respect to the effect of nose shape on scabbing and perforation.

20. *Final Report on Concrete Penetration*, Richard A. Beth, OSRD-6459, NDRC Report A-388.

This report summarizes the work on concrete penetration and perforation which has been done at Princeton during World War II. It then proposes an approximate theory of concrete penetration which corresponds to the present state of knowledge on the subject.

7.2 PHYSICAL DESCRIPTION OF PHENOMENA

Some of the principal phenomena resulting from the impact of inert nondeforming projectiles on reinforced concrete slabs are illustrated in Figures 1 and 2. Each drawing represents a section through the slab in the plane of incidence of the projectile (see Figure 3, Chapter 5) and is drawn to scale from measurements of an actual shot. They are arranged to show the effects of slab thickness, striking velocity, and obliquity. The data were obtained in the penetra-

tion and explosion tests on concrete slabs and are displayed in somewhat different form in Data Sheet 2A3, Chapter 19.

Figures 1 and 2 are based on observations made with 37-mm AP projectiles, with cap and windshield removed. The projectile weight was about 1.70 lb, which gives a caliber density D of 0.554 lb per cu in.

722 Scale Effect

Qualitatively similar results have been observed with projectiles of various calibers from 0.30 to 16 in. and with AP and semi-armor piercing [SAP] bombs. Quantitatively, however, because of the scale effect in concrete, the effects illustrated are produced at progressively somewhat lower striking velocities as the caliber or scale is increased for projectiles of the same form and caliber density and for targets of the same concrete composition, strength, age, and thickness in calibers. These scale effect results invalidate the rule of thumb resulting from earlier theories that under similar circumstances penetration is proportional to caliber. For large changes in caliber this effect can be a serious one. In round figures the massive penetration measured in calibers for large projectiles is 100 per cent greater than that for small projectiles in going from .50 caliber to 16 in., and 50 per cent

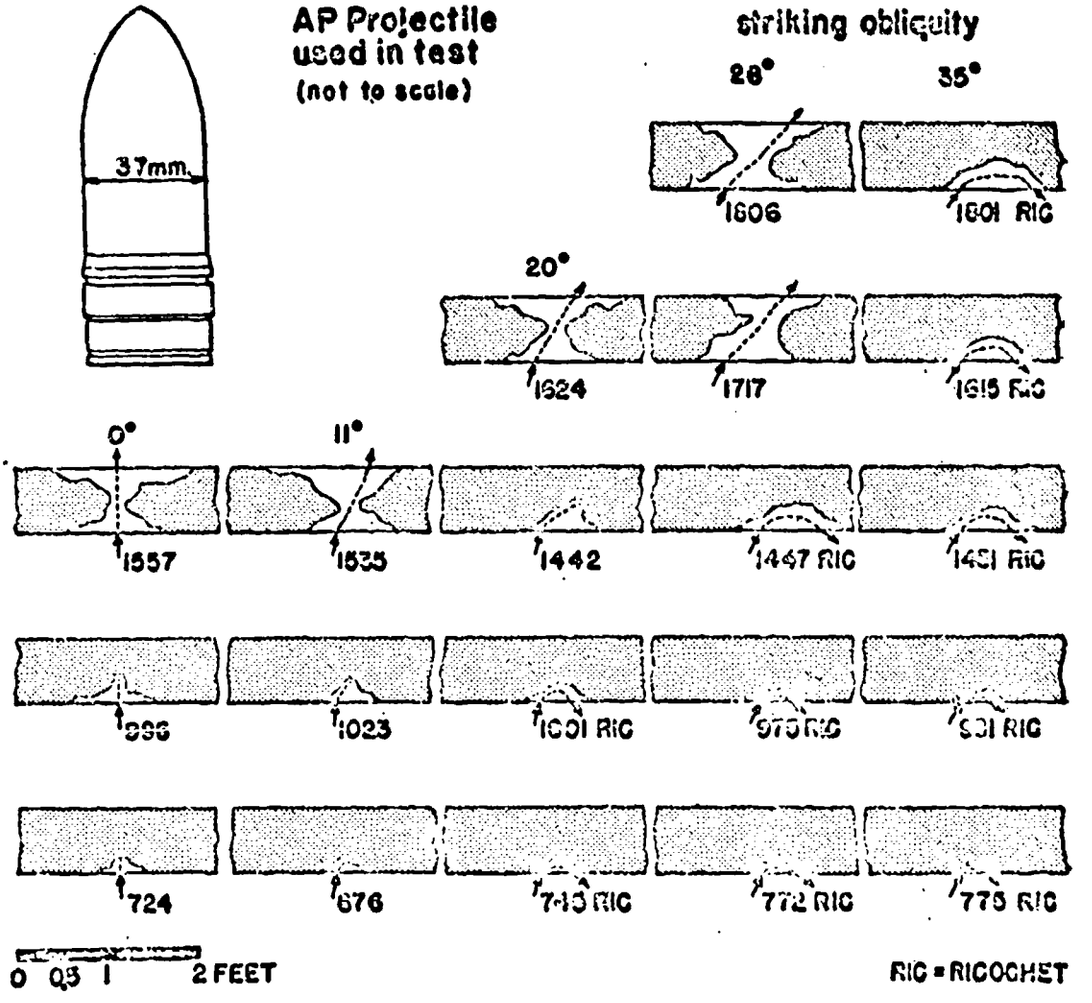

FIGURE 1. Thin slab. Profiles of actual craters. Slab: thickness, 8.9 in.; compressive strength, 5,700 psi. Projectile: 37-mm M80; weight, 1.70 lb; cap and windshield removed. Striking velocity (fps) shown for each impact.

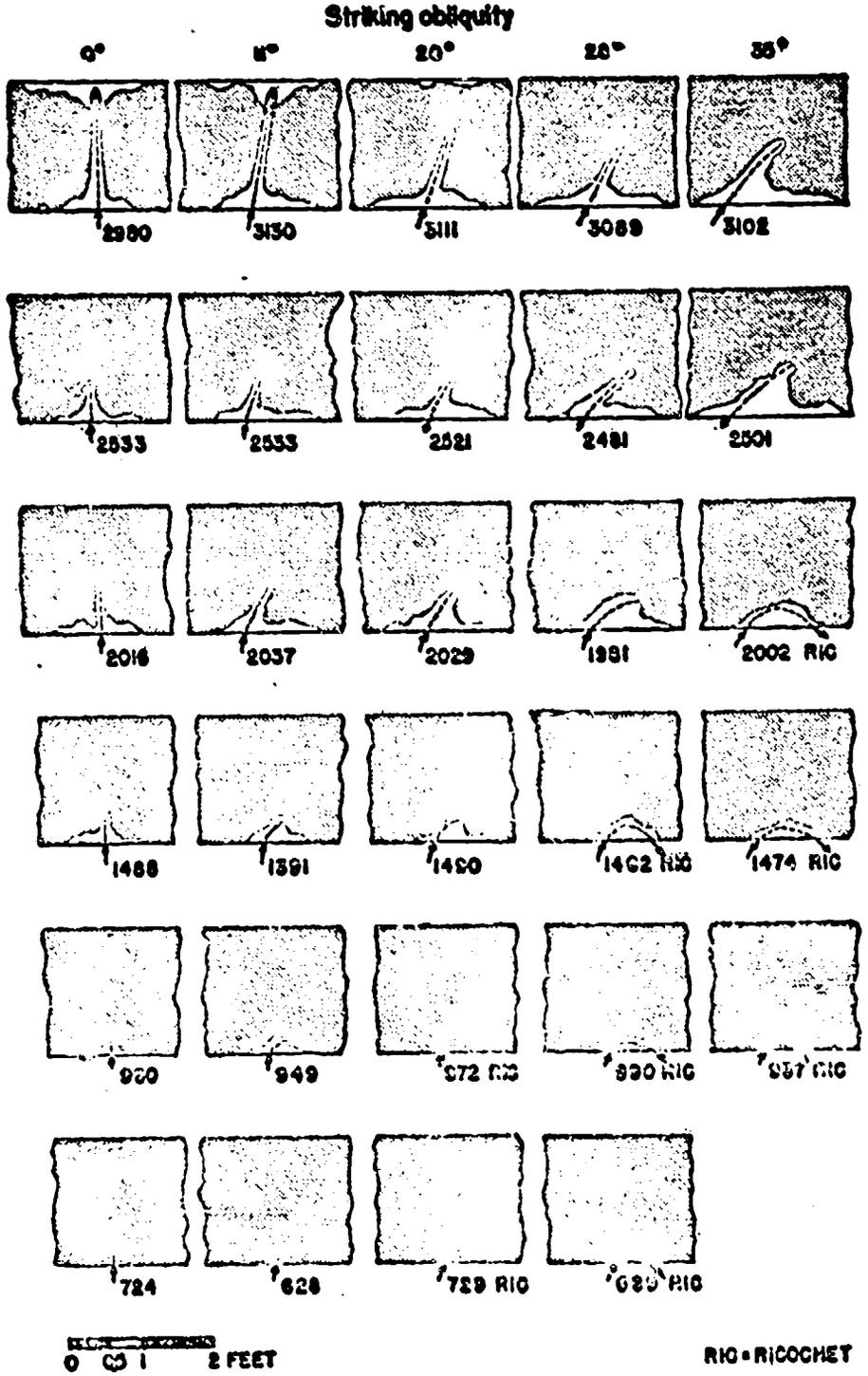

FIGURE 2. Thick slab. Profiles of actual craters. Slab: thickness, 22 in.; compressive strength, 5,700 psi. Projectile: 37-mm M80; weight, 1.70 lb; cap and windshield removed. Striking velocity (fps) shown for each impact. Stuck projectiles actually shown.

greater in going from 1- to 6-in. calibers, for otherwise similar circumstances.

Being made from observations on actual shots, Figures 1 and 2 show not only the general trends found by varying striking velocity and obliquity for two typical thicknesses of slab, but also exhibit the kinds of random variations from an idealized norm which are found even under well-controlled conditions. It is convenient to make an arbitrary division into front- and back-face phenomena for the purposes of discussion.

222 Front-Face Phenomena

Front Crater; Spalling

Pieces of concrete, called spalls, are ejected from the region surrounding the point of impact thus leaving the front crater seen in the drawings. The size of the crater formed increases rapidly with increasing striking velocity up to 1,200 or 1,500 fps for ordinary AP projectiles and less rapidly at still higher striking velocities. Its shape is roughly conical but very irregular. The presence of a reinforcing layer or mat

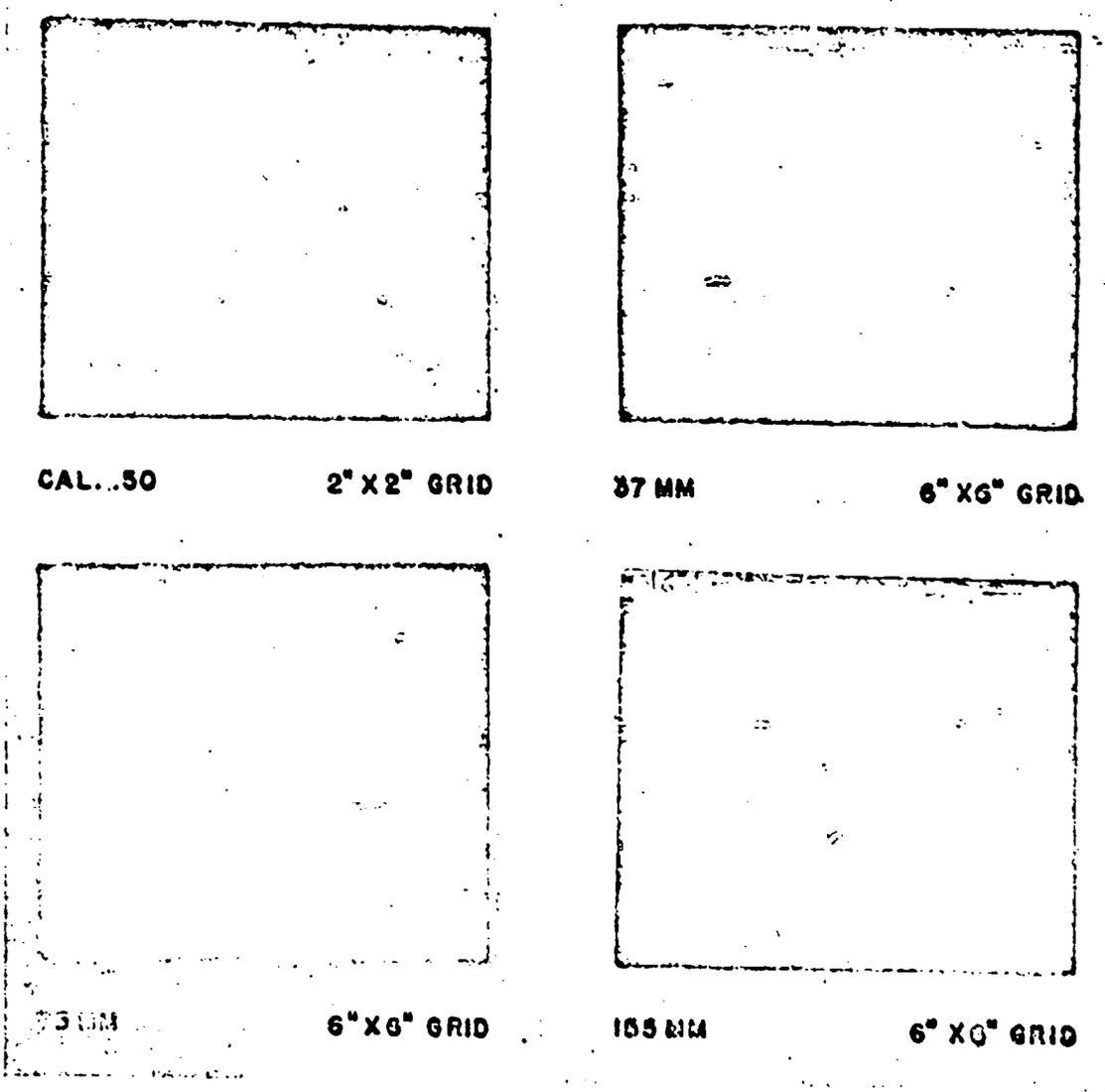

Figure 8. Spall craters in concrete due to AP projectiles striking normally at approximately 1,050 fps. All photographs to same scale in calibers. Cord grids placed in front of craters show original size.

[illegible] restricting effect [illegible] crater. The photographs [illegible] appearance of typical front-face craters [illegible]. Those illustrated were produced by the impact of .50-caliber, 37-, 75-, and 155-mm projectiles, respectively. The photographs have been reproduced at different scales so that the projectile diameters have the same absolute size for all of the photographs.

Penetration

For a given missile and target the average normal penetration may be expected to increase with striking velocity according to a smooth curve. Actually the random variations of individual shots from the ideal mean curve may be as great as 10 or more per cent in penetration. In Section 7.3.3 the mathematical representation of the penetration curve will be discussed for "massive" targets, that is, targets so thick that the concrete does not begin to yield (scab) on the back face. When scabbing (see next section) sets in, penetrations begin to increase more rapidly with striking velocity than indicated by the curve for massive penetration.

At striking velocities up to about 1,000 fps a normally incident projectile does not penetrate beyond the crater which it forms, and the deepest point of the nose impression appears roughly as the apex of the sloping crater sides. At higher velocities a nondeforming projectile begins to form a cylindrical penetration hole beyond the crater, provided the target is thick enough. This is illustrated particularly in the crater profiles on the left side of Figure 2.

Obliquity tends to reduce the penetration depth as measured perpendicular to the target face although the slanting or curved path length of the projectile in the target may be almost the same as in the case of normal incidence. With ricochet (see below) this path length may be even greater than for the normal case. For practical purposes, however, the depth reached below the face of the target seems more significant than the slant depth. The drawings show that this perpendicular depth decreases in a regular way with increasing obliquity, although the random variations of individual shots from an idealized average curve have been found to be even larger than in the previously discussed case of normal penetration. This, together with the fact that relatively much fewer experimental data are available and the fact that it is expected that the perpendicular penetrations at various obliquities depend on both nose shape and projectile length in a complicated way, has made it much more difficult to establish general rules or formulas for penetrations at obliquities.

Sticking

In a thick slab, if the penetration hole goes deep enough beyond the front crater, the projectile is likely to stick, that is, be held tightly at or near its maximum penetration without falling out of the penetration hole or rebounding from the target. Experience indicates that a projectile must penetrate at least 3.5 to 4.5 calibers before it will stick, the larger factors apparently being required for thicker slabs. Such penetrations will ordinarily be attained at normal incidence with striking velocities in the region between 1,000 and 2,000 fps, the value depending on the actual weight and caliber of the nondeforming part of the projectile, the strength and penetration resistance of the concrete, and the thickness of the slab. The velocity at which sticking sets in with a given projectile-target combination is called the *sticking limit*. The sticking limit increases with increasing obliquity. A number of cases of sticking are shown in the upper two rows of Figure 2.

The phenomenon of sticking is of special importance with explosive projectiles or bombs. It is felt that the maximum effect of detonation is secured when explosion takes place at the deepest penetration that can be attained by the inert missile before detonation. It is practically impossible to fuze accurately enough for this if the projectile rebounds. In general the fuze time should be made long enough to allow perforation or the maximum penetration to be reached before the missile detonates. If the fuze setting is greater than the time required for either perforation or maximum penetration, the maximum damage will be secured except in the case of rebound, while if the fuze setting is shorter the projectile will be definitely handicapped with respect to the target in almost all cases. The mass and striking velocity of bombs are usually too low for sticking penetration; if the target is too thick to be perforated, a bomb will rebound instead of sticking.

Ricochet

Examples of ricochet may be seen in the lower right half of each of the Figures 1 and 2. Ricochet will occur for a given striking velocity when the obliquity becomes great enough. Conversely, for a fixed obliquity or angle of incidence different from normal there is a limiting velocity, the *ricochet limit*, below

which ricochet occurs and above which the projectile digs into the slab without ricochet. It will be noted that the ricochet limit increases sharply with obliquity.

Ricochet greatly handicaps the missile with respect to the target and thereby enhances the protection afforded by the slab while decreasing the relative effectiveness of the projectile. This applies particularly to explosive projectiles or bombs when the fuze setting is such that the detonation takes place when the missile is no longer in contact with the target. The lateral and turning forces exerted on the projectile or bomb during ricochet also pose difficult problems for the fuze designer.

Although perforation and ricochet cannot, by definition, occur simultaneously, it is possible to have a scab thrown off from the back of the slab when the projectile ricochets. With sufficiently thin slabs the front and back craters so formed have been observed to overlap in such a way as to leave a clear hole through the slab, even though the projectile remains on the attacking side of the slab and therefore does not perforate in the true sense.

7.23 Back-Face Phenomena

Back Crater; Scabbing

For a given target slab a progressive increase of striking velocity produces, first, cracking on the back surface, followed by scabbing of increasing extent. Scabbing consists of the ejection of pieces of concrete from the back of the slab opposite to the impact point thus leaving a back crater after the shot. The lowest velocity for which scabbing will occur is called the *scab limit* for any particular missile-target combination. The scab limit increases slowly with obliquity for angles up to 10 or 15 degrees and more rapidly for larger angles.

Figure 4 shows the appearance of typical back-face craters at various scales, namely .50-caliber, 37-, 75-, and 155-mm. As with the front-face craters shown in Figure 3, the photographs have been reproduced to the same scale in calibers. The back-scab crater is usually wider and shallower than the front-spall crater, although both tend to be very irregular and to show large departures from symmetry, smoothness, and reproducibility. In reinforced concrete often only the cover (the concrete layer outside or beyond the back-face reinforcing mat) is actually projected away from the slab, while a considerable amount of badly broken and cracked target material may be retained within the reinforcing mat. On the other hand, as may be seen in Figure 4, the back mat tends to widen the area of cover which is loosened and thrown off, especially when insufficient shear steel is provided for tying each lateral bar to the body of the slab at closely spaced intervals.

Below the scab limit a concrete slab or wall will offer adequate protection to personnel or equipment not in direct contact with the slab and therefore not directly subjected to whatever mechanical shock may be transmitted through it. However, as soon as scabbing sets in, pieces of considerable size and velocity may be thrown off. Thus scabbing is the first serious source of danger to the objects which the slab is intended to protect. In this light the scab limit rather than the perforation limit is often used as the principal criterion in the design of protective concrete.

Perforation

The *perforation limit* is the lowest velocity at which the projectile or bomb just passes completely through the slab. Like the scab limit it is lowest for normal incidence and it increases with obliquity in a roughly similar way. Beginning at the scab limit, penetrations increase more rapidly with striking velocity than in massive concrete, the excess being largest just before perforation is attained. Hence the perforation limit is found to be markedly lower than the velocity required to penetrate a distance equal to the slab thickness in massive concrete of the same characteristics.

Perforation is especially dangerous in the case of explosive projectiles and bombs that are fuzed to detonate after perforation. The missile may be expected to produce the maximum damage to personnel and equipment when this explosion, fragmentation, and blast take place within a space entirely enclosed, and supposedly protected, by concrete walls and roof. The residual velocity of a projectile, after perforating such an enclosure, is usually insufficient to carry the projectile through the far wall and out again even if the direction of the trajectory is favorable; therefore the fuze time need only be made sufficiently long to secure maximum damage.

Limit Velocities

It should be emphasized that the limit velocities for scabbing and perforation as they have been defined here are idealized mean values at which the missile will just begin to scab or to perforate the concrete slab in question. Actually the values are not sharp; repeated tests under well-controlled conditions show the same kind of random fluctuations as have

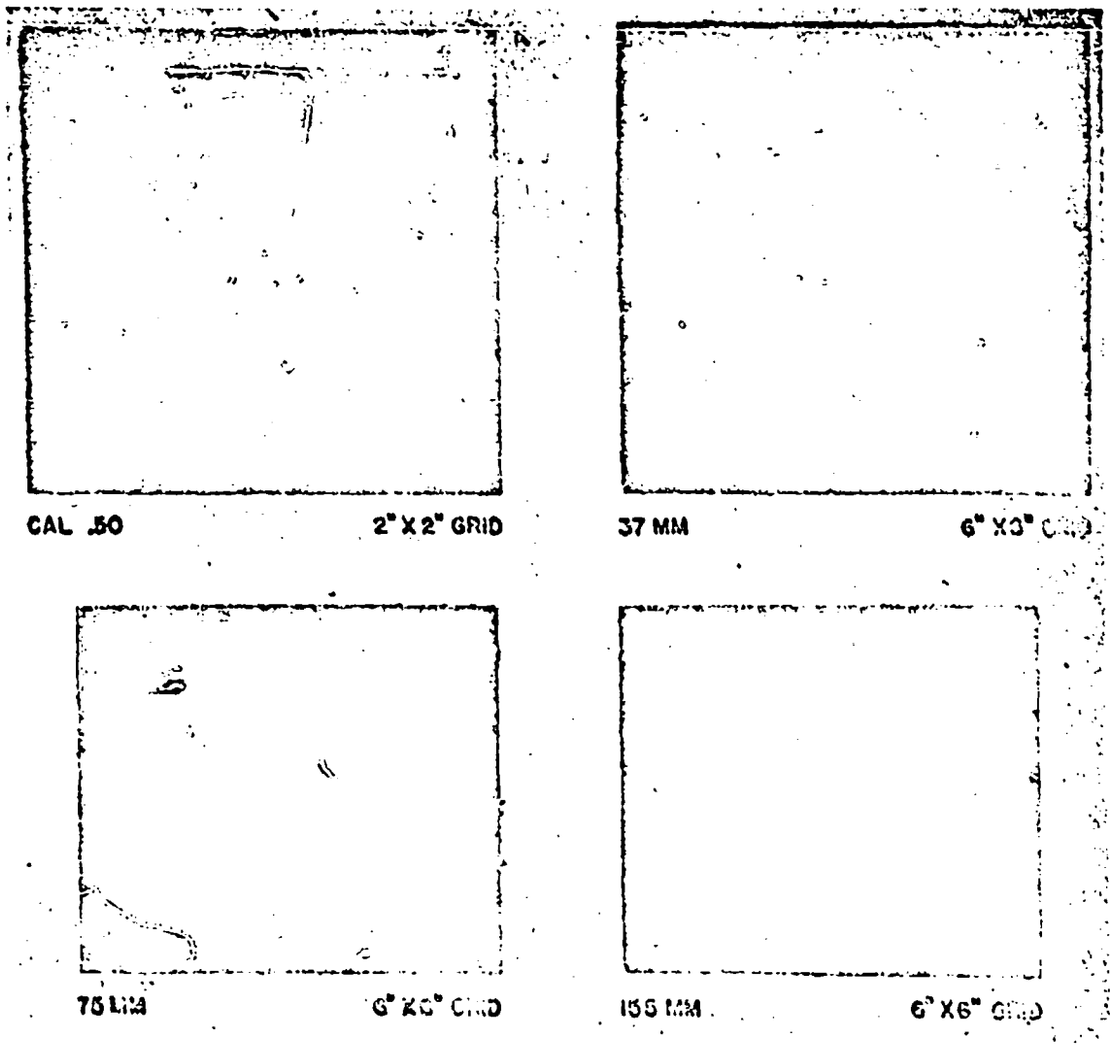

FIGURE 4. Scab craters in concrete due to AP projectiles striking normally at velocities slightly above perforation limit. All photographs to same scale in calibers. Cord grids placed in front of craters show original size.

been mentioned in connection with the other concrete phenomena. (Compare with Chapter 8.) In practice it is necessary to allow for these uncertainties by using an appropriate "safety factor" or "ignorance factor" to ensure that scabbing or perforation either will or will not take place accordingly as the purpose is attack or defense.

LIMIT THICKNESSES

It is often convenient, in dealing with these phenomena for design purposes, to consider the striking velocity fixed and to ask for the slab thickness that will just be scabbed or just be perforated. Here again the terms scab-limit thickness and perforation-limit thickness are used for the idealized mean thicknesses without allowance for uncertainties.

7.2.4 Important Characteristics of Concrete Targets

The terminal-ballistic behavior of a concrete target depends on the nature and quality of the concrete and on certain construction features such as size, reinforcement, etc. This is well illustrated by some of the phenomena already described and shown in Figures 1, 2, 3, and 4. A deeper understanding of these as well as some of the other phenomena to be dis-

cussed may be gained by reviewing some of the more important and typical characteristics of concrete targets.

Thickness and Quality of Concrete

Some idea of the order of size of the concrete targets under discussion may be gained from the fact that practically all of the experimental work has been done on slabs whose thickness falls somewhere in the range from 3 to 18 calibers. The perforation thickness of good reinforced concrete (say, 5,000-psi cylinder strength) for normally incident AP projectiles at 2,000 fps may, because of the scale effect (see Section 7.2.1), be as low as 9 to 12 calibers for .50-caliber[24] and run as high as 16 to 18 calibers for 16-in.[21] projectiles. These statements are merely intended as a guide to the order of magnitude of the thicknesses under discussion; whenever possible the actual design of protective structures, estimates of weapon performance, or other theoretical work should be based on a more detailed consideration of the factors involved.

One of these factors is the quality of the concrete. In general, the selection of materials, mix design, methods of placing, etc., which govern the quality of concrete for civil construction have a similar effect on the ability of concrete to resist the effects of projectile impact. Extensive experimental tests at .50-caliber[11] and smaller scales[8] were made during World War II to study the effect of concrete properties on penetration resistance. Many suggestive correlations appear in the data but, as may be expected, it is difficult to find a general quantitative formulation for them.

A case in point is the effect on penetration of changes in compressive strength. This is important because compressive strength is perhaps the most common engineering designation of the quality of concrete. The small-caliber tests, confirmed by some evidence at larger scales, suggest the following approximate rule of thumb:[28] for a given projectile and striking velocity the normal depth of penetration is inversely proportional to the square root of the compressive strength of the concrete. For example, an increase of 10 per cent in compressive strength will reduce penetrations by about 5 per cent under otherwise similar circumstances. This rough rule seems to hold whenever the kind, amount, and size distribution of the aggregate component remains essentially unchanged, and the increase in compressive strength is secured by an increase in the cement content of the mix or by an increase in the age of the target tested. But an exception has been found with differences in strength occasioned by different curing conditions.[11] Compared to otherwise similar moist-cured concrete, dry-cured targets showed up to 20 per cent increase of penetration resistance while the nominal compressive strength measured on companion cylinders cured with each target, decreased by 40 to 50 per cent.

The experimental tests also show that penetration is affected by changes in the aggregate component of the concrete in the sense that an increase in the size and amount of aggregate put into the concrete tends to decrease penetrations. But it is not clear what aggregate parameter would be most appropriate for a quantitative formulation of this effect, especially when differences in scale or caliber have to be considered.

The .50-caliber tests on several dozen targets[11] indicate the order of magnitude of the effect to be as follows: with concretes up to 4,000-psi compressive strength, penetrations decreased by about 20 per cent when the aggregate was changed from fineness modulus 3.0, ⅛-in. maximum size, and 65 per cent by volume, to fineness modulus 5.0, 1-in. maximum size, and 75 per cent by volume. For 7,000-psi concrete the effect seems to be smaller.

Even among the three specific aggregate parameters named it is hard to decide, on the basis of experimental data, which is the most appropriate for describing the effect. Concrete technologists insist that a reasonably smooth gradation of aggregate sizes, from coarse stones and gravel down to fine sand, must be used in making good concrete. The water-cement ratio determines the compressive strength of the resulting concrete, independent of the amount and sizes of aggregate used. For a given water-cement ratio, an amount of water-cement paste somewhat in excess of that needed just to fill the voids in the dry aggregate is usually provided. Less paste will obviously result in porous concrete and too great an excess may result in nonuniformity, a tendency toward segregation, and an unwarranted increase in cost. An increase in the aggregate size, which tends to decrease the proportionate volume of the interstitial spaces (since a smooth gradation down to the finest sand is still required), also tends to decrease the water-cement paste required, and thereby tends to increase the percentage by volume of solid aggregate in the resulting concrete. A consequent difficulty is the impossibility of making accurately scaled-down concrete for model tests in which the relative volumes of aggregate and paste are

maintained.[11,22,43] Furthermore, a proper adjustment of the gradation and the amount of water-cement paste requires a certain degree of correlation without, however, compelling a unique relationship to exist among the three aggregate parameters named above. Obviously the same would be true for any other aggregate parameter which might be devised. This is the reason for the difficulty in obtaining a clear experimental indication of the appropriate aggregate parameter affecting penetration, namely, it is not possible to vary any one over a very wide range and still maintain the others constant. Some progress might be made by using statistical methods, but sufficient data for this are not now available.

Theoretical considerations have not given a clear solution of the aggregate problem either. Energy considerations suggest that the proportionate volume of aggregate in the concrete should play a role, since the energy required per unit volume to crush a stone aggregate of good quality is undoubtedly greater than that required to crush a unit volume of the interstitial mortar. Since compressive strength is mainly a measure of the quality of the interstitial cement, the above-mentioned experimental observation that the effect of aggregate changes seems to be less with concretes of high compressive strength tends to support the crushing energy considerations just described. Some English interpretations of concrete penetration data[22,43] suggest that the aggregate effect and the scale effect (see Section 7.3.1) arise from the same cause and that penetration is, in fact, a function of the dimensionless ratio of caliber to (maximum) aggregate size. It may be possible to reconcile this interpretation with the energy consideration discussed above by assuming that the degree of crushing of aggregate, and hence the energy required, is in some way a joint function of aggregate and projectile size. On this basis the scale effect also should be less pronounced with concretes of high compressive strength and greater with weak concretes. This has not yet been observed, but it is doubtful whether the available data are adequate to show the effect if it does exist.

The material of which the aggregate is composed can have some influence on penetration resistance, as shown by small-caliber tests,[11] but no quantitative laws connecting this effect with physical properties of the aggregate material have as yet been found.

On the other hand, tests of special cements or admixtures have so far shown no significant improvement in the penetration resistance of the resulting concrete in relation to the compressive strength. Usually, if the same trouble and expense were applied in making a richer mix or in making the slab thicker, a much greater increase in protection would be secured.

As far as protective construction (fortifications, bomb shelters, etc.) is concerned, the net result of the small-caliber tests is as follows: Taking for granted that modern methods of mix design and field procedures in handling and placing are used and that a clean, hard aggregate (e.g., quartz or traprock, etc.) can be selected, it is advantageous to use as large a fineness modulus and as large a proportionate volume of aggregate as possible in the concrete. The maximum aggregate size chosen will, of course, be limited in the usual way by the availability of a reasonably good gradation below the maximum, the spacing of the reinforcing bars, and the thickness of the section to be poured. The change of compressive strength, and hence of penetration resistance, with water-cement ratio was found, approximately, to be such that for a given amount of cement about the same protection against perforation can be secured whether a thick slab with high water-cement ratio and weak concrete or a thinner slab with low water-cement ratio and strong concrete is made.[11]

Reinforcement

As a material, concrete is much stronger in compression than it is in tension. When overstressed by static loading it fails in a brittle rather than in a ductile manner. Under the impact of bombs and projectiles it exhibits the same general characteristics, which are quite different, by and large, from the toughness and ductility shown by most metals.

When a massive concrete slab suffers a direct hit the penetrating missile crushes the concrete ahead of it and tends to drive the detritus forward and sidewise. During deep penetrations most of this crushed material is ultimately driven aside because of the reaction of the compressed and confined material ahead of the missile and because of the pointed nose shape of bombs and projectiles. This sets up strong radial pressures and circumferential tensions around the penetration hole which result in pronounced radial cracking because of the weakness of the concrete in tension. The forces are easily able to crack up quite large masses of concrete unless sufficient reinforcing steel is present to inhibit the spreading of the cracks and to offer tensile strength bridging the cracks that are formed. With inadequate reinforcing, the structural collapse following the cracking due to a single shot may breach a wall or roof completely.

Thus the principal function of steel reinforcement in concrete protective structures is to inhibit mass cracking, as well as splintering, scabbing, and spalling (see below), which result from a direct hit or explosion, and to supply structural, tensile, or flexural strength. The effect of reinforcing steel in resisting penetration along the path of the projectile in concrete is too small to warrant any large increase in percentage of steel or in complication of the reinforcement pattern for this purpose.[8] See also Section 15.2.5 of Chapter 15, where impact tests on reinforced concrete beams are discussed.

For protective construction it is felt that reinforcing steel need not exceed about one percent of the total volume of the concrete and that deformed bars should be used if available. Small bars with close spacing are somewhat preferable to large bars with wide spacing, but the choice should also take into account practical considerations such as the relative difficulty of bending and placing the steel. The advantage to be secured by the use of large maximum-sized aggregate has been mentioned, and the spacing of reinforcing bars should not be so small as to make the proper placing and consolidation of the concrete difficult. While closer spacing tends to reduce the width and extent of cracks which *intersect* the plane of the reinforcing, it must also be remembered that very close spacing has been observed to create planes of weakness *along* which the concrete tends to crack and separate as a result of impact or shock. The latter tendency was found to be particularly severe when sheets of expanded metal were tried as reinforcing in burster slab tests.

Some typical reinforcement patterns are shown in Figure 5. The concrete cover over the face mats should be as thin as practicable in order to reduce spalling and scabbing as much as possible. Figure 6 shows the effect of front-cover thickness on spall formation in the case of some 75-mm tests. The striking velocity for the upper two photographs was about 1,900 fps, and about 1,400 fps for the lower two. Spalling of the front cover is also shown in Figure 3. Similarly Figure 4 shows the way in which the scab formed from the back cover is thrown away from the slab while a great deal of the broken-up scab material formed within the reinforcing is retained by the back-face mat. Figure 4 also illustrates how the back-face reinforcing acts to extend the area of scabbing along the plane of weakness formed by the mat. It is therefore particularly important to reduce the thickness of the back cover in protective construction. (See discussion of scab plates and meshes below.)

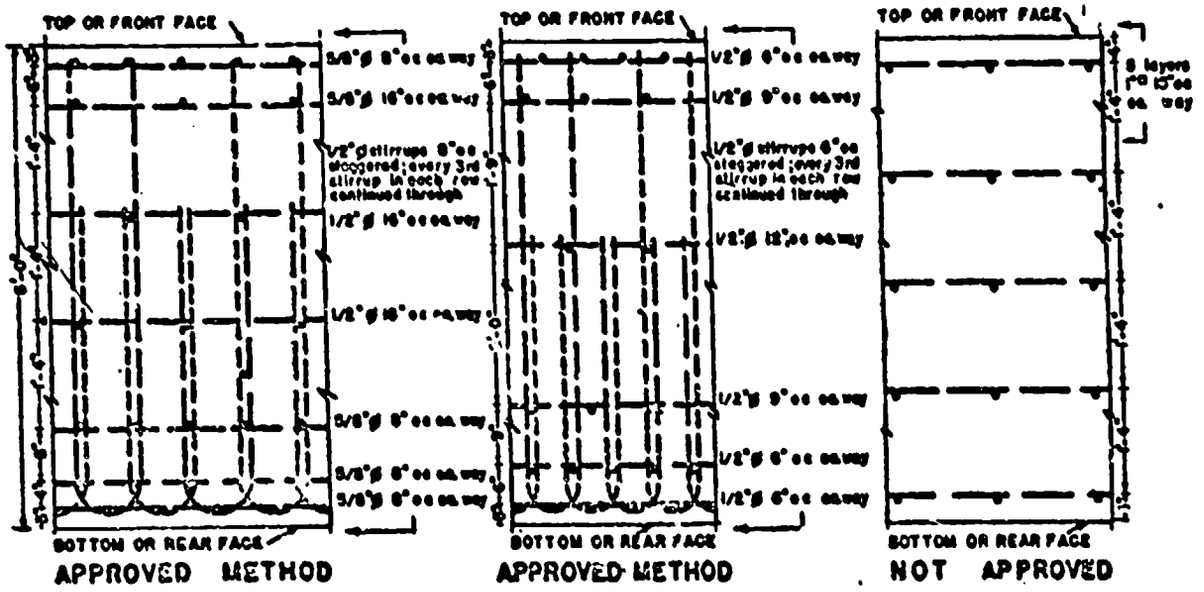

FIGURE 5. Methods of reinforcing 6-ft protective wall or roof slab. (From Fortifications, Mines and Demolitions Branch, Office of the Chief of Engineers.)

Besides restricting the size of front and back cracks and increasing the resistance to repeated hits by holding broken-up concrete in place, the face mats also serve their usual structural purpose in providing flex-

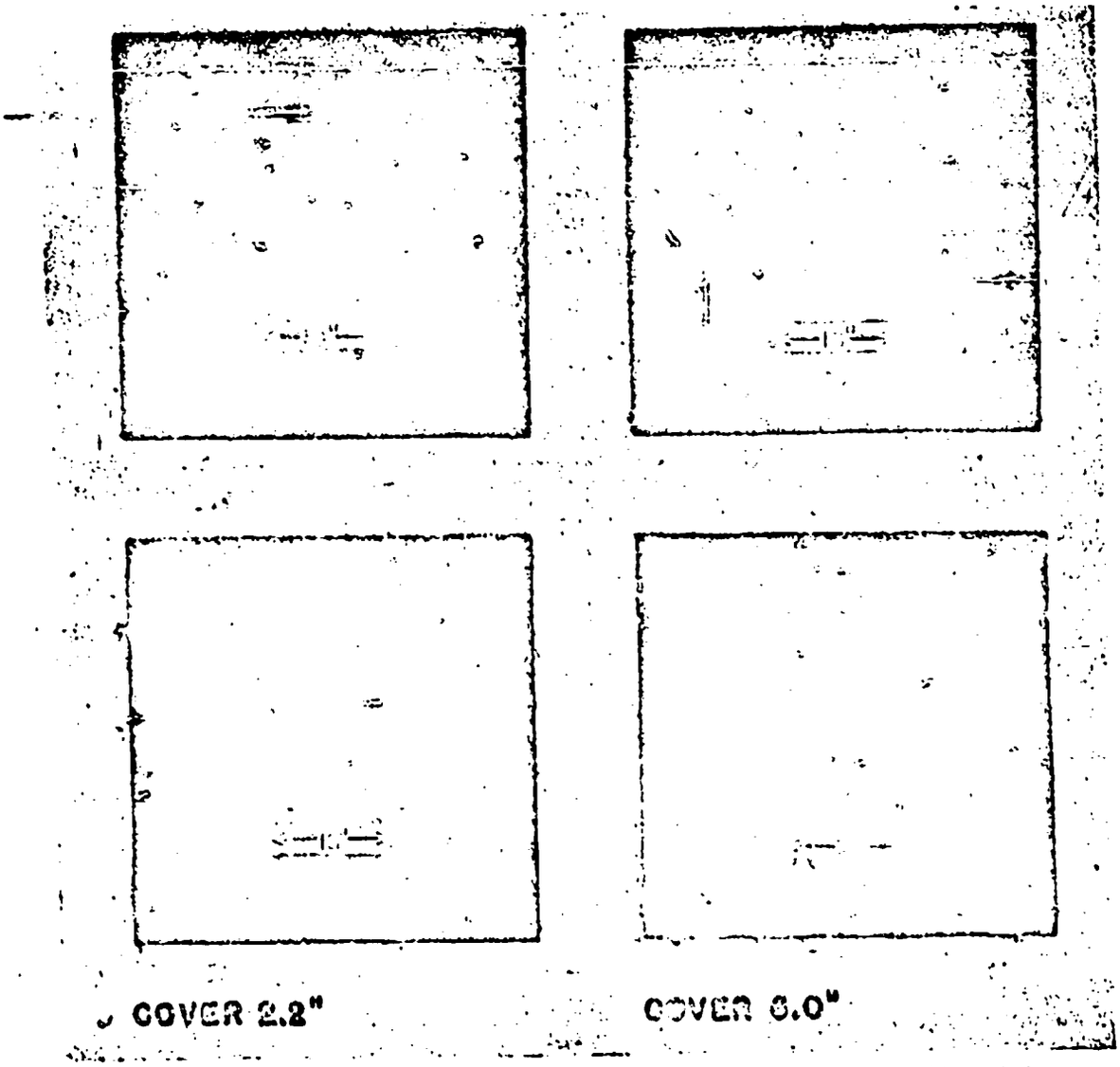

FIGURE 6. Effect of cover on front-face crater formation. The upper photographs are at higher velocity.

ural strength for the slab. A slab tends to recoil and vibrate after impact, so that tensile reinforcing is needed in the front face as well as in the back face.

In protective construction more internal reinforcing is used than in civil construction. Shear steel is required to tie the face mats to the body of the slab at frequent intervals in order to promote their anticratering functions as described above; an effective system is to tie the face mats together by shear steel running through the whole thickness of the slab. Additional reinforcing mats similar to the face mats and parallel to them are provided in the interior of the slab as shown in Figure 5. These supply tensile strength to resist the cracking occasioned by the penetration forces previously described, and are particularly valuable in holding cracked or broken concrete in place to resist repeated fire (however, see Section 7.2.7). In American practice these interior mats are usually somewhat more closely spaced near the surfaces of the slab (see Figure 5), while an equal spacing is sometimes advocated in England.

Scab Plates and Meshes

Steel plates are often attached to the back face of concrete slabs, particularly roofs, to inhibit scab ejec-

tion and to retain scab material in the case of direct hit. In order to function properly such scabbing plates must be attached by strongly welded lugs or heavy bolts at frequent intervals as shown in Figure 7. Spot welding to the shear steel has been found to be inadequate.[7] Tests have shown the shock of a deep penetration to be sufficient to break such welds over a wide area; the result can be worse than having no scab plate at all if the plate itself is thus added to the ejected of a burster slab is increased by this backing over what it would be as an unbacked roof slab.

In small-scale tests a scab mesh embedded in the back surface of the slab has given excellent results in retaining scab material from contact explosions on the front side of the slab.[64] The mesh was placed in contact with the form for the back-slab face and was tied to the internal reinforcing structure. In permanent construction it would be necessary to use bituminous

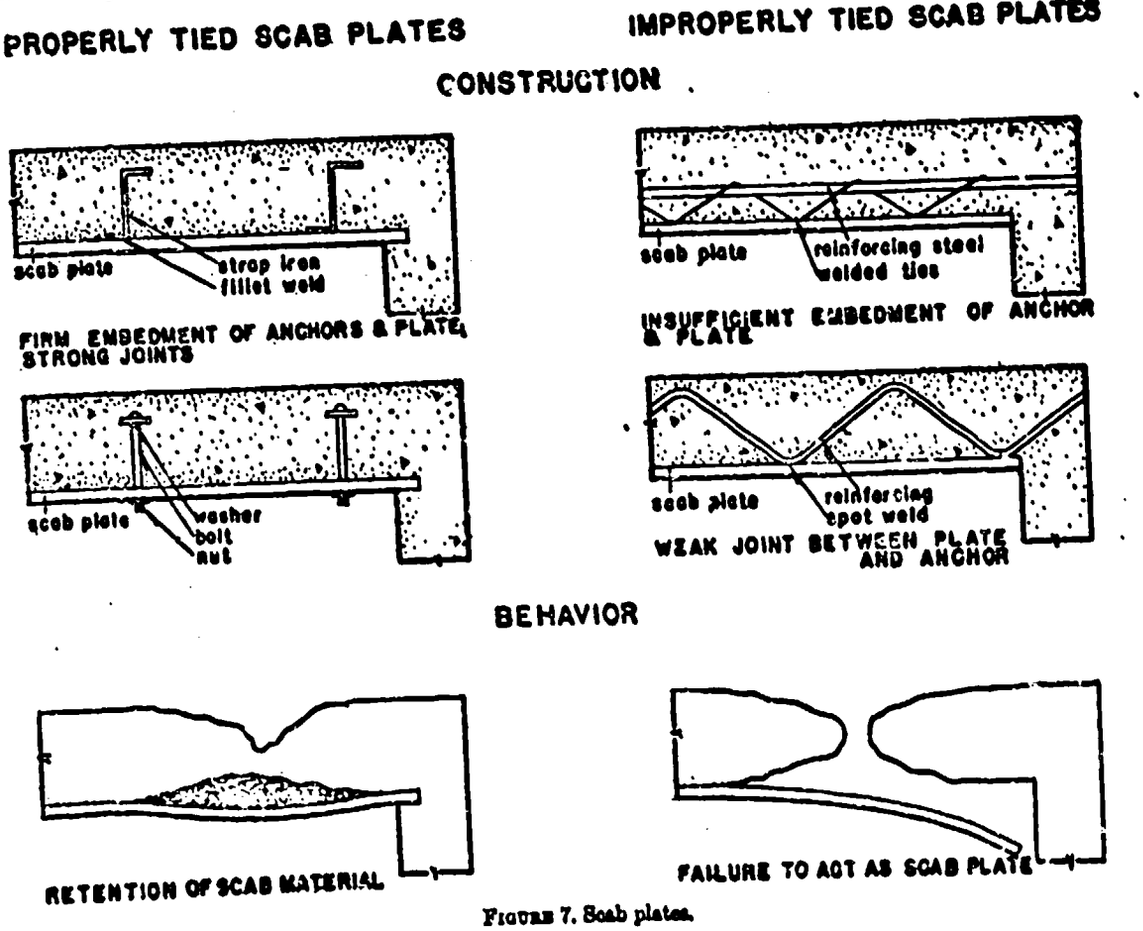

FIGURE 7. Scab plates.

concrete scab. Besides being firmly attached, the scab plate should be made in one continuous sheet if possible (or securely welded together at the seams of adjoining sheets), with the edges embedded in the supports as suggested in Figure 7.

It is believed that a well-designed scab plate will add from 5 to 10 per cent to the scabbing and perforation resistance of a concrete slab. In the case of a burster slab the earth on which it rests forms a backing. There is evidence that the perforation resistance paint or other means to prevent the exposed portions of this mesh from being weakened by rust. In effect, the idea behind the scab mesh is to prevent the damage that may be caused by flying scab pieces by reducing the thickness of the back cover to zero (see the discussion of Figure 4 above). It should be emphasized that more extensive and larger scale tests of the scab mesh idea are needed before it can be either recommended or discarded as far as full-scale protective construction is concerned.

Layers and Laminations

If a thick slab is constructed in several layers or laminae its resistance to perforation tends to be less than for a monolithically poured slab of the same dimensions and quality. On the basis of 37-mm tests with a total slab thickness of 1 foot, it is estimated that the perforation limit velocity will be lowered by not more than 5 per cent per construction joint.[9] The outer layers should be at least 2 to 3 calibers thick and reasonable care should be taken to secure good mechanical contact between the layers by cleaning and washing off the surface with water before each new layer is poured.

In new construction, pouring in layers or lifts may be justified for several reasons in spite of the indicated decrease of efficiency in the concrete used. Limitations of equipment and length of working shift may make monolithic pouring impractical. With very thick slabs it may even be a net advantage to pour the mass in sections with sufficient time between pours for setting and cooling, because the heat generated during setting may cause mass temperature strains and cracking with a resulting impairment of penetration resistance.[21] With old construction it is sometimes desired to increase the thickness and protective value of existing walls, roofs, or burster slabs by adding a layer of new concrete.

For design purposes with either old or new construction, it is suggested that, assuming clean contact between layers, the above-mentioned allowance of 5 per cent in limit velocity per construction joint will be found to be on the safe side.

Spaced Slabs

Model-scale tests have shown that a double slab construction with an air space between the slabs may actually be more resistant to scabbing, perforation, and contact explosions than the same amount of concrete poured as a single slab.[14] In .50-caliber tests a double slab system, consisting of a 6-in. front slab separated by a ¾-in. air space from a 1-in. back slab, was slightly more resistant than a single slab 7 in. thick. The combination of a 3- and a 1-in. slab with a ¾-in. air gap had approximately the same resistance to perforation or scabbing as a single slab 4 in. thick. The combination of a 3- and a 1-in. slab with no air gap was less resistant than a single slab 4 in. thick, in agreement with the 37-mm laminated slab results mentioned above.

It was originally expected that the scabbing of the first slab into the air space between the two slabs would result in a net decrease in the scabbing and perforation resistance of the combination. The anomalous fact that this decrease in resistance usually does not take place appears to be due to the fact that the projectile perforating the first slab with a low residual velocity tends to tumble in the air space between slabs and strike the second slab with large yaw.

The spaced slab construction appears to be very promising on the basis of the model-scale tests, but, as in the case of the scab meshes discussed above, more extensive and larger-scale tests are needed to decide the real merits of the idea.

Composite Slabs

Some preliminary work has been done on the problem of designing composite slabs of concrete and steel, or of soil and concrete, to resist perforation by inert projectiles.

The simplest method consists of the following empirical procedure.[14] It is assumed that the limit thickness or proof thickness for each of two materials at the required limit velocity is known. The composite slab of this limit velocity will consist of a fraction a of the proof thickness of the first material in contact with a fraction b of the proof thickness of the second material. A graph is made by plotting a against b. The required values of a and b should lie on a smooth curve whose end points on the axes are fixed because, by definition, $a = 1.00$ when $b = 0$, and $a = 0$ when $b = 1.00$, and the curve should be such that a decreases monotonically as b increases and vice versa. In general, the curve may be expected to lie in the vicinity of the straight line $a + b = 1.00$.

A plot of some .50-caliber data for combinations of concrete and steel suggests that these curves may be practically the same no matter for what particular limit velocity they are made, and an approximate mean curve has been given. For similar .50-caliber data on soil and concrete, it was felt to be more appropriate to express the a for soil as a fraction of the mean penetration distance in soil for the limit velocity. Then the a versus b curves showed a falling trend with increase in limit velocity such that the curve falls above or below the straight line $a + b = 1.00$ by varying amounts, according as the limit velocity is below or above about 1,400 fps. A more complete investigation, including data for larger calibers, should be made.

A second method of designing composite slabs has been suggested, based on making estimates of the remaining velocity of the projectile as it reaches each layer of different material after the first.[15] This re-

quires having an adequate knowledge of the variation of velocity as a function of depth during penetration and perforation (see Section 7.4) and making suitable simplifying assumptions concerning the possible interaction of the two adjacent materials as the projectile crosses an interface.

7.2.5 Edge Effects

If a projectile or bomb strikes near an edge of a concrete slab it tends to be deflected toward the edge, to achieve deeper penetration, and to break out concrete toward the edge. The effect depends not only on the striking obliquity and the nearness to the edge, but also on the design of the reinforcing used near the edge.

It was concluded from .50-caliber tests at normal incidence that the edge effect is quite small at distances greater than 6 calibers from the edge but may be appreciable at 4 calibers.[18] The highest striking velocity in these tests was about 2,000 fps and there was evidence that the edge effect increased, that is, occurred farther from the edge, with increase in striking velocity. This agrees with the mechanically plausible expectation that the edge effect should actually depend directly on the normal depth of penetration in calibers in relation to the distance from the edge in calibers. Weaker concrete permits deeper penetrations and, presumably, greater edge effects. Because of the scale effect (see Section 7.2.1), the normal caliber penetration for a given striking velocity increases with caliber; hence, for a given striking velocity the edge effect may be expected to increase with caliber. Fragmentary data from full-scale tests[16] indicate the possibility of the edge effect occurring as far as 15 projectile diameters from an edge and increasing in normal penetration by as much as 40 per cent, compared to penetration in massive concrete at 8 calibers from an edge. These interpretations of the small amount of full-scale data available were purposely made on the safe side for the design of protective construction and thus probably overestimate the edge effect at larger scales.

Due to the edge effect, embrasures, firing ports, and doors are the weakest parts of a structure.[20,21] They are the natural points of attack and therefore merit particular attention in the design of fortifications and other defensive structures. Further full-scale tests on the edge effect and means of reducing it are needed.

7.2.6 Effect of Explosions

The previous sections have dealt principally with the effects of inert impact on a reinforced concrete target. With explosive bombs and projectiles the effect of the explosion is superimposed on the inert effects preceding the instant of detonation. The effect of the explosion on the target is conditioned by the position which the missile has reached at the time of detonation and the deformation, if any, which the missile may have suffered in the process.

The influence of sticking penetration, ricochet, perforation, and residual velocity on the results of detonation have already been discussed in Sections 7.2.2 and 7.2.3. If a missile remains intact during perforation and detonates within a protective structure it will cause the maximum damage of which it is capable. This is the primary intention of the attack. Short of complete perforation, scabbing offers the next most serious possibility of damage within a heavy concrete structure. Figure 8 shows, at the top, front and rear views of a reinforced concrete slab 19 in. thick after the inert impact of a 75-mm projectile at 1,250 fps.[7] The lower pictures show the same slab after the static detonation of a simulated high-explosive [HE] projectile containing a little over 2½ lb of TNT in the penetration hole. The incipient scab of the upper photograph has been thrown off, leaving a wide rear crater down to the back reinforcing mat, and there is a clear hole through the slab. The front crater has been widened and the reinforcing thrown out from the crater.

A useful quantity in dealing with explosive projectiles and bombs is the caliber charge density D_e defined by:

$$D_e = \frac{c}{d^3}, \qquad (1)$$

where c is the weight of the charge in pounds and d is the maximum diameter or caliber in inches. From the definition of caliber density D ($D = w/d^3$), it is evident that

$$D_e = D \cdot \frac{c}{w}, \qquad (2)$$

where c/w is the charge-weight ratio of the missile. Since higher charge-weight missiles in general have smaller caliber densities, D_e tends to be more nearly the same than either D or c/w for HE missiles. Its value seldom goes above $\frac{1}{10}$ lb per cu in., and many HE shells, SAP, and general-purpose [GP] bombs have caliber charge densities D_e approaching this value.

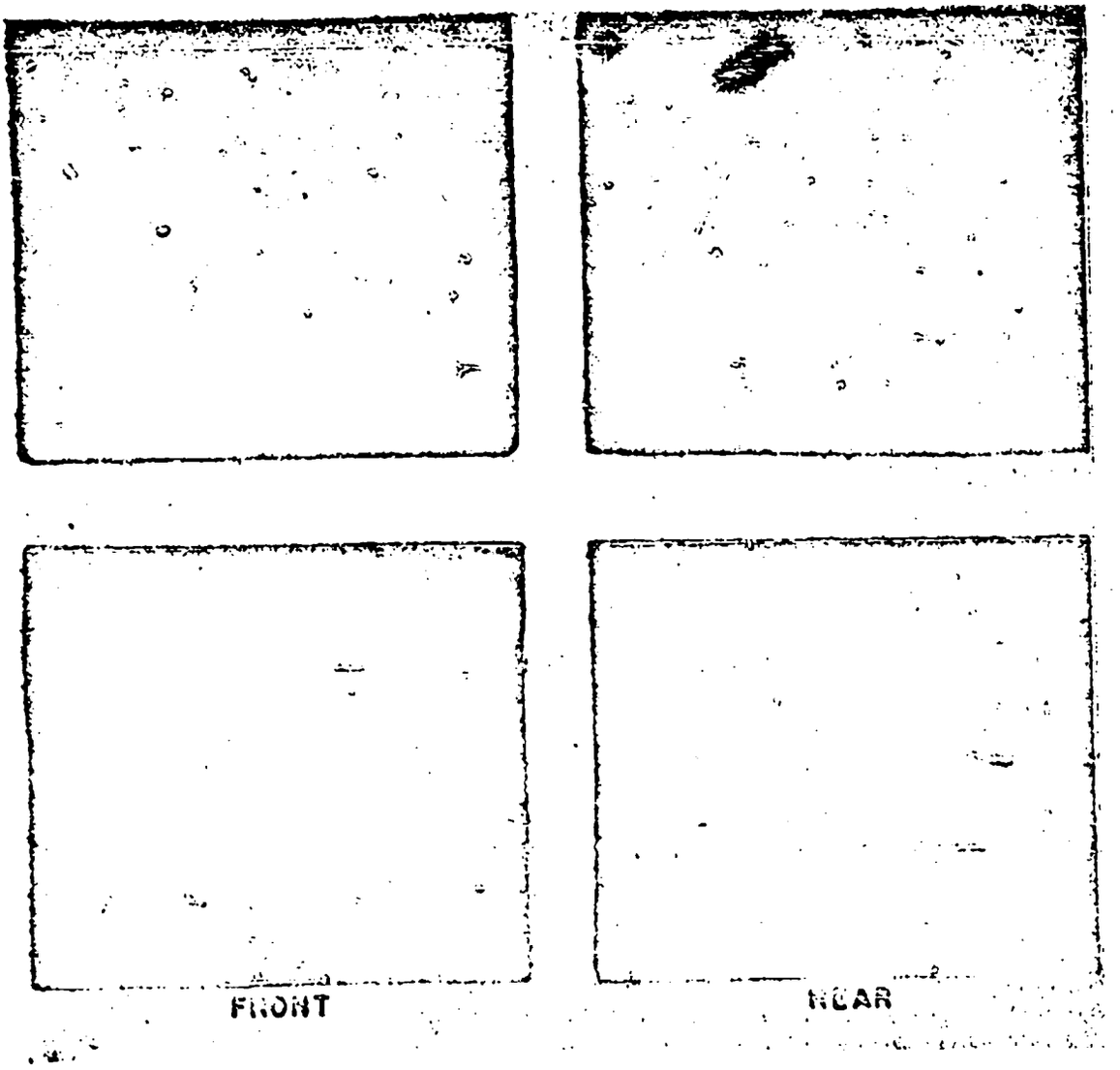

FIGURE 8. Front and rear view of typical crater before and after static detonation of HE projectile.

The simulated projectile whose effects are shown in the lower two photographs of Figure 8 had a value of D_e of about $^1/_{10}$ lb per cu in., and it was statically detonated at the maximum penetration previously produced by an inert projectile. It is generally felt that these conditions will produce as severe an effect on a concrete target as may be gotten in combat from any of the usual explosive missiles for the caliber and striking velocity used. In this sense, Figure 8 illustrates the maximum effect that may be expected from an explosive missile when the inert penetration before detonation is near the scabbing limit for the slab.

The effect of an explosion following inert penetration into a massive concrete target is illustrated in Figures 9 and 10.[1] The crater profiles of Figure 9 are based on measurements of three actual shots[1] with caliber charge densities of about 0.007, 0.07, and 0.11 lb per cu in. respectively, reading from top to bottom. The black area in each case represents the additional concrete removed by the explosion following the inert penetration outlined by the white area.

It is evident that the increase in penetration depth produced by the explosion is fairly small. According to a rough rule of thumb this increase in depth of hole is only about ½ caliber or less for common types of HE missiles.

It might be expected that this additional penetration depth would increase with the depth of the preceding inert penetration because of the increasing confinement of the explosive charge. In spite of attempts to do so, this expected tendency has not been found in the available observations, but it must be admitted that the data show considerable fluctuations from the mean. The nature of these fluctuations is suggested by the irregular outlines of the actual crater profiles in Figure 9. At least until more data on this point become available it may be assumed as a first approximation that the increase in depth, Δs calibers, due to an explosion, is independent of the depth of inert massive penetration attained before the detonation. This even seems to give fairly good estimates when the missile detonates on the surface of the concrete without penetrating appreciably before detonation.

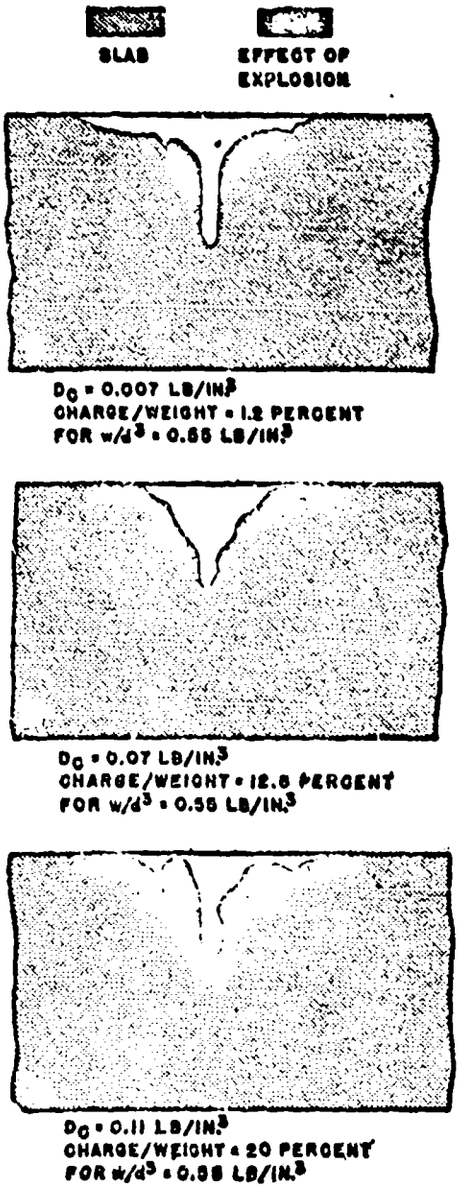

FIGURE 9. Effect of penetration of inert projectiles plus detonation of explosive projectiles in reinforced concrete.

A small amount of data, such as that shown in Figure 8, for different caliber charge densities, has led to the suggestion that the increase in depth Δs may be estimated from

$$\Delta s = 0.6(10D_e)^4 \text{ calibers.} \qquad (3)$$

Additional data are needed to test this relationship. This formula has been expressed in terms of the quantity $10D_e$ to facilitate making mental estimates of Δs, since, for the most effective HE projectiles and bombs, $10D_e$ will be nearly unity, as discussed above.

The crater profiles of Figure 9 show that the lateral effect of the explosion is relatively larger than the increase in depth of the penetration hole. The increase of front crater was also shown on the left side of Figure 8. The effect of different types of reinforcing on the widening of the front crater is illustrated in Figure 10, where the bottom photographs, showing the crater after detonation, are reproduced to the same scale as the corresponding views before detonation at the top. The removal of concrete and the widening of the front crater are particularly important with repeated fire (see Section 7.2.7) or in case the weakened wall or slab is subjected to subsequent attack of any kind.

The effect on concrete due to the explosion of a bomb or other charge in contact with the slab and at various distances from it in air is discussed in Section 15.2. Similarly the effect of underground explosions on reinforced concrete slabs and walls is discussed in Section 3.7.

In connection with the design of fortifications and other protective structures, attention is drawn to some model-scale tests of contact explosions on concrete.[44] These indicated that an advantage would be gained for the defender by utilizing the scab-mesh and spaced-slab constructions discussed in Section 7.2.4 against contact explosions. Larger scale tests of these construction methods are needed.

During World War II, a considerable amount of

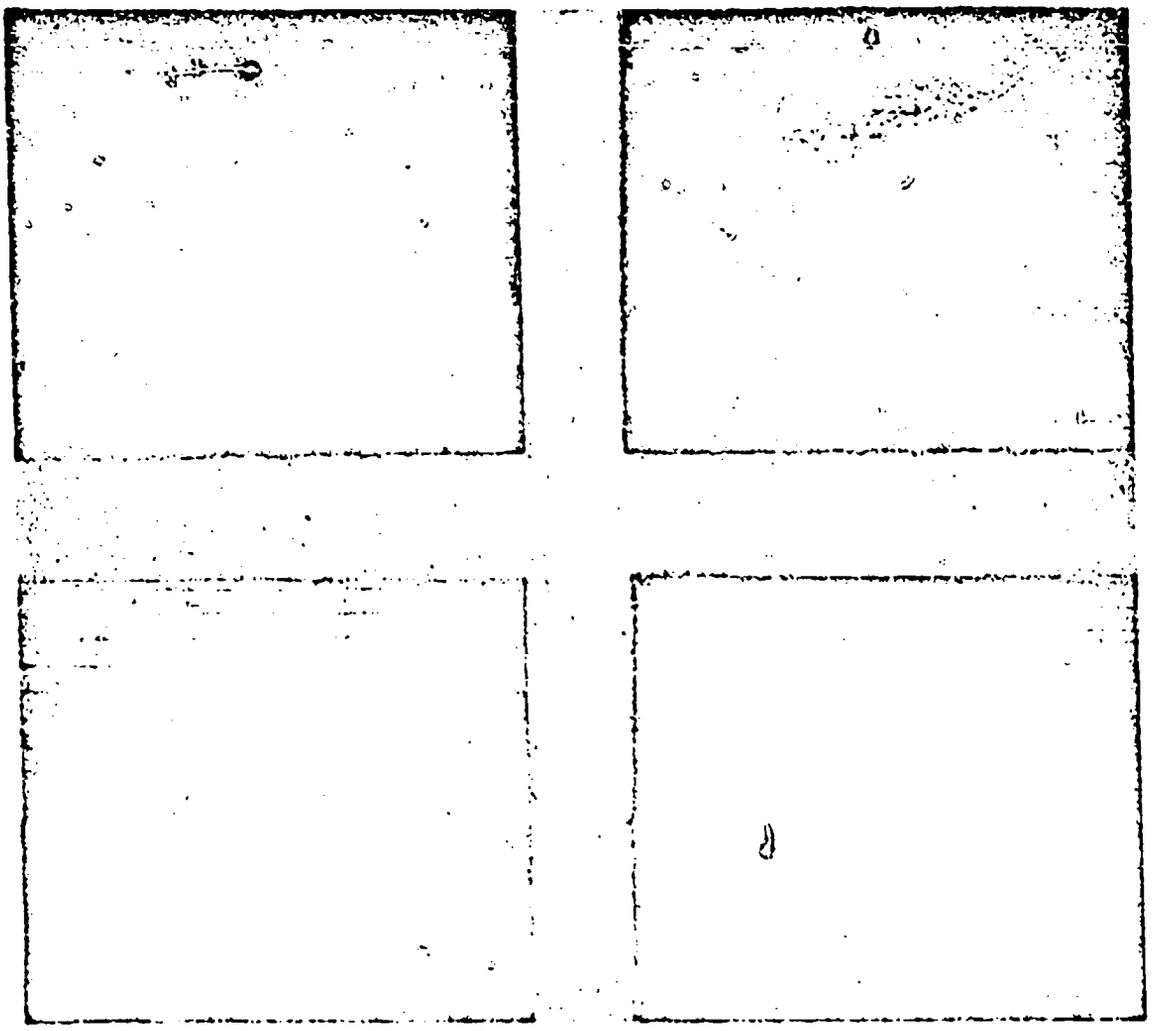

FIGURE 10. Front craters before and after static detonation of HE projectiles, showing effect of different types of reinforcing.

development work was done on both sides toward increasing the effectiveness of explosive missiles against concrete. The Germans developed special anticoncrete projectiles[51,57] for artillery fire (150-mm, 210-mm, etc.) as well as a number of hollow charge projectiles and bombs which could be used against concrete as well as armor.[58] In England, and to a lesser extent, in the United States, there was interest in increasing the size, caliber density, and striking velocity of bombs for attacking concrete, especially heavy protective construction like the German submarine pens. A large amount of work was done on methods of breaching concrete antitank walls and reducing other concrete defenses. (See Section 7.2.7.)

While no specially designed anticoncrete HE projectiles were developed in the United States during World War II, a very interesting compromise solution was worked out to make use of standard HE projectiles with a special nose fuze for attacking concrete.[28] To obtain the maximum explosive effects that have been described above, two things are necessary: (1) the missile must remain essentially intact during the inert penetration stage preceding detonation, both to promote maximum inert penetration and to keep the charge and fuze in condition for high-order detonation, and (2) the fuze must provide sufficient delay to permit maximum penetration (or, in the best case perforation) before detonation. The latter is obviously

a fuze design problem. It turns out that the former, also, is dependent to a great extent on the mechanical design of the fuze element, in the sense that the fuze contours, strength of parts, and method of attachment to standard HE projectiles (e.g., 90-mm or 105-mm) can be made to increase the missiles' resistance to deformation against concrete, and indeed, to reduce the probability of deformation to a practicable minimum under field conditions.

For maximum effect the fuze delay should be at least as great as the time of penetration. On the other hand, it should not exceed this total time of penetration by too much in case the projectile rebounds from the target without sticking or in case of ricochet (see Section 7.2.2).

Very little work has been done on direct measurement of the time of penetration and not enough is known about the theory of penetration for computing this time very accurately (however, see Section 7.4). Until a better experimental or theoretical basis becomes available, it is suggested that the total time of penetration t_1 be estimated from [14,16,18]

$$t_1 = \frac{2x_1}{v_0}, \qquad (4)$$

where x_1 is the depth of maximum penetration and v_0 is the striking velocity. A consistent set of units is implied; for example, if x_1 is in ft and v_0 in fps, t_1 will be in sec. This relation would be exact if the force resisting penetration were a constant. However, there are reasons for expecting that the estimate of t_1 so obtained will not be too far wrong in the actual case in which the force during penetration is not strictly constant. The relation given is at least simpler and even probably more accurate than some relations based on an assumed law of resisting force that have been suggested.[14,16,17] Equation (4) has some physical basis and makes allowance in the right direction for both x_1 and v_0. It is certainly better than assuming t_1 to be a constant regardless of caliber.

7.2.7 Effect of Repeated Fire

The effect of repeated hits on reinforced concrete depends on the dispersion of the points of impact and the degree to which the slab reinforcement tends to hold the debris in place to offer resistance to later shots. Small dispersion, for example, such that successive hits fall within the spall crater of the first shot, is advantageous for the attack, if the object is to perforate the slab as soon as possible with at least one projectile, as is often the case when a strong point is to be neutralized and particularly when explosive projectiles are available. If the object is to make a breach of given size as, for example, in an antitank wall, a relatively greater fire power is needed and the distribution of hits will be determined by the width of gap desired.

Model-scale repeated fire tests have been made with .50-caliber nonexplosive projectiles.[13] Successive impacts were placed within a 5-in. diameter circle, that is, within a 5-caliber radius circle measured from the first impact point. Thus the later shots fell well within the spall-crater radius of the first shot. The striking velocity was kept approximately constant, about 1,400 fps for successive rounds. Crater profiles were measured at frequent intervals during the firing and the number of inert shots required to perforate slabs of various thicknesses were found. The data show that the additional depth of penetration due to each impact was in every case less than the penetration of the first round and that the number of rounds required for perforation increased roughly as the cube of the thickness. This is perhaps physically plausible on the assumption that equal increments of energy delivered by successive shots remove roughly equal increments of concrete from the hole. However, it is then striking that the relation was found for perforation rather than penetration and also that it holds (roughly) down to the single-shot perforation thickness. It was also concluded that multiple-layer internal reinforcing increased the resistance of the slab to repeated fire attack, relative to that offered by similar slabs without internal reinforcing mats, in line with the previous discussion (Section 7.2.4) of the tendency of reinforcing to hold cracked and broken concrete in place.

Some data at larger scale have been obtained on the effect of repeated inert fire under field conditions.[19] The less strictly controlled conditions make the analysis of these tests more difficult. It had been concluded,[19] however, that the depth of penetration with repeated fire increased at a rate somewhere between the second and fourth roots of the number of shots, and that perforation could finally result when the target thickness was only 2 or 3 calibers greater than the total depth of penetration so attained. Within the accuracy involved, these results tend to confirm the previously stated model-scale findings for larger calibers.

It should be emphasized that these results were found for normal, or nearly normal, incidence. The depth of penetration for repeated fire measured per-

pendicularly to the slab face will undoubtedly decrease with increasing obliquity, probably in about the ratio that the single-shot depth decreases. However, for higher obliquities approaching the ricochet angle, or angles at which the first projectile tends to turn and follow a curved path in the concrete, the repeated fire depth may be expected to show less decrease due to obliquity than the single-shot depth, because, within the craters produced by the first shots, the actual striking angle tends to be altered to favor succeeding rounds. Similar effects may be expected for the increased number of rounds required for perforation as the obliquity is increased.

Edge effects for repeated fire have been studied experimentally and crater profiles determined with .50-caliber inert projectiles; some observations are available at larger calibers in the reports already cited. In a general way the results follow the description given above and in Section 7.2.5.

Extensive tests[44] were made in England during World War II on the breaching of reinforced concrete antitank walls by repeated fire using various specific combinations of inert AP shot and HE shell. The idea behind this pick-and-shovel tactic is that the solid projectiles will achieve maximum penetration, cracking, and breaking up of the concrete, while the less penetrative explosive projectiles will be more effective in removing rubble and cutting reinforcing from the section of the wall to be breached. This in turn permits the solid shot to reach deeper layers of the solid wall and the process is repeated until the required breach is made.

Some of the conclusions drawn from the British test, listed and summarized in the reference given,[44] are as follows. Short ranges (1,000 yd or less) are desirable, since random hitting is considerably reduced and the effect of the increased striking velocity is very marked. HE shells must be used in addition to the AP shot in the proportion of 1 HE shell to 4 or 5 AP shot. They are necessary to cut the reinforcing and clear the rubble. HE shells must not be fired too early or too late. One or two rounds after each ten rounds of AP give the best results. If the firing of HE shells is postponed too long, all the concrete will have fallen away and only the reinforcement will be left, in which case it is difficult to hit and destroy. The number of HE shells should be kept to the minimum necessary to cut the reinforcement and clear the rubble. An excess of HE will reduce the rubble to fine dust, which does not give a good grip to tank tracks. Craters will also be formed, making passage of the gap difficult. The less the reinforcement, the more resistant the wall is to battering and the more shot and shell are required to break it up. For this situation, test observations run counter to the usual conclusions (Section 7.3.4) that reinforcement tends to hold the cracked and broken concrete in place. If, however, the reinforcement is very heavy, additional shells are usually required to cut it.

This is probably the best method for breaching a wall with gun fire. The results obtained suggest that similar combination shot and shell methods would also be advantageous for neutralizing a concrete-protected strong point whenever repeated fire must be used. In this case the primary object would not necessarily be to create a breach, but to get one or more explosive projectiles to detonate within the bunker or fortification being attacked.

7.3 ANALYSIS OF EXPERIMENTAL WORK

In Section 7.2 the more important terminal-ballistic phenomena for concrete have been described. A number of more or less quantitative conclusions have already been drawn from the experimental observations discussed.

It is the purpose of this section to show how some of the more important phenomena may be summarized and correlated by graphs, diagrams, and empirical formulas. The empirical formulas will, in turn, form the basis for the theory of concrete penetration to be discussed in Section 7.4.

Throughout this section considerable emphasis is put on recommendations for further work, both experimental and analytical. The method of Section 7.3.3 for analyzing the normal penetration curve was devised toward the end of World War II. Normal penetrations form the point of departure for the analysis of scabbing, perforation, the effects of obliquity, etc. It is felt that the methods of Section 7.3.3 will form a much more accurate basis for estimating normal penetrations than the various methods heretofore used and that the analyses of Sections 7.3.4, 7.3.5, 7.3.6, and 7.3.7 can be much improved by using the new method for normal penetrations. It seems logical to make a number of recommendations for further experimental work in conjunction with the description of the analysis of past experiments.

7.3.1 Ballistic Limits

A graphical summary of the way in which the various ballistic limits (perforation, scabbing, sticking,

and ricochet) vary with striking obliquity and velocity may be given in the form shown in Figures 11 and 12. Each such diagram refers to a particular target and projectile combination; the examples given are based on the same concrete slab and projectile as

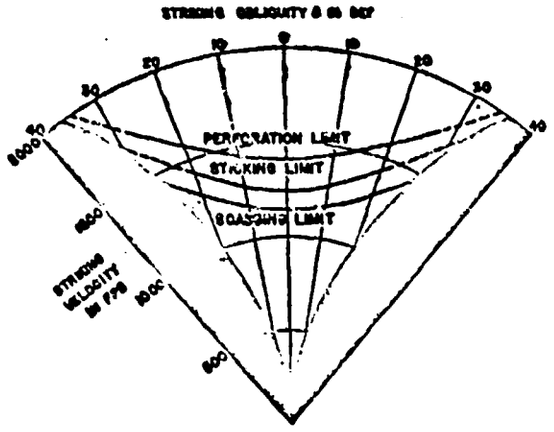

FIGURE 11. Thin-slab ballistic limits. Based on data of Figure 1. Target, 8.9 in. thick; projectile, 37-mm M80, weight 1.70 lb.

the crater profiles shown in Figures 1 and 2, and in Data Sheet 2A3 of Chapter 19. The general form of the curves shown may be expected to be similar for any perforable concrete target and nondeforming inert projectile or bomb of conventional type.

The graphs are symmetrical about the zero obliquity radius and only one half of the diagram would ordinarily be needed to present the information. The complete diagrams are given here to emphasize the fact that the perforation, scabbing, and sticking limit curves all cross the zero obliquity axis normally. This fact must be remembered when diagrams are made showing obliquities on only one side of $\theta = 0$ degree.

These diagrams also show that the perforation, scabbing, and sticking limit velocities increase faster than secant θ with obliquity θ. This has led to attempts to express the ratio of the oblique to the normal limit in each case as a constant power of sec θ, the exponent being greater than unity. However, this yields only very rough agreement because the best exponent to fit the data for each limit appears to vary with both obliquity and slab thickness.

A comparison of Figures 11 and 12 shows that the sticking, scabbing, and perforation limits do not always occur in the same order for various slab thicknesses. Perforation, of course, always occurs at a higher velocity than scabbing, since both are essentially back-face phenomena (see Section 7.2.3). But for a sufficiently thick target, sticking depends on the depth of penetration beyond the front face and is, therefore, classed as a front-face phenomenon (see Section 7.2.2). As the slab thickness is decreased, the scabbing-limit velocity decreases until the scabbing-limit curve begins to pass the sticking-limit curve, which is believed to change only slowly, if at all, down to this particular slab thickness. With a further decrease in slab thickness the sticking-limit velocities as well as the scab-limit velocities decrease, although the scab-limit velocities decrease more rapidly. Thus with the thin slab, Figure 11, sticking occurs at higher velocities than scabbing, but at lower velocities than with the thick slabs, Figure 12. If the slab is sufficiently thin, sticking will presumably not occur at any velocity, since the slab will be perforated before sticking can take place.

Ricochet is also a front-face phenomenon (see Section 7.2.2), and by definition, cannot occur simultaneously with either sticking or perforation. However, as shown in Figure 11, ricochet of the projectile and scabbing of the target can occur simultaneously.

It is interesting to speculate on the course these curves should take with increasing velocity and obliquity: for example, on how the sticking- and ricochet-

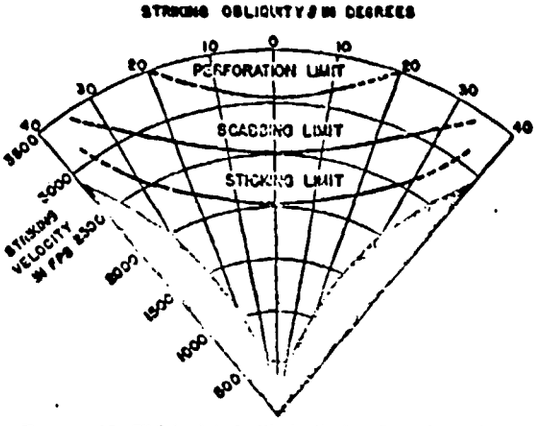

FIGURE 12. Thick-slab ballistic limits. Based on data of Figure 2. Target, 22 in. thick; projectile, 37-mm M80, weight 1.70 lb.

limit curves approach one another, or on the expected curvature of the sticking-limit curve. However, this is not important until significantly higher striking velocities are used on concrete. For the situations which are at present of practical interest the various limit curves may be expected to exhibit the general

characteristics shown in Figures 11 and 12 and discussed above.

7.3.3 Vulnerable Areas

The polar diagrams just described show the various ballistic limits as functions of striking velocity and

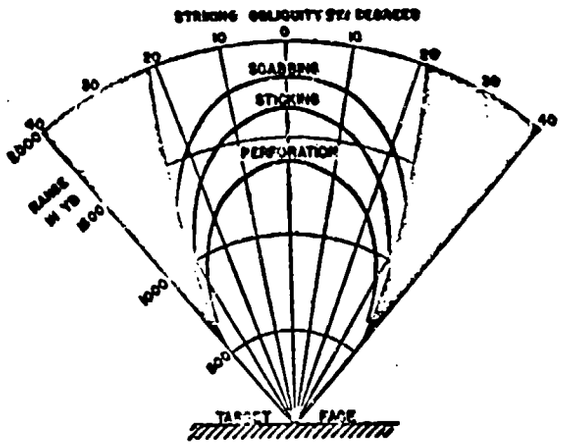

FIGURE 13. Thin-slab vulnerable areas. Based on data of Figure 1. Target, 8.9 in. thick; projectile, 37-mm M80, weight 1.70 lb, muzzle velocity 2,900 fps.

obliquity for a specific target and a specific projectile. If, in addition, the muzzle velocity of the gun and the range-velocity relation of the projectile are known or assumed, it is possible to construct the vulnerable-area diagrams shown in Figures 13 and 14.

A vulnerable-area diagram is, in effect, a map laid out with range and obliquity relative to the target face as polar coordinates. This map shows the outlines of the areas within which the gun must be placed to obtain sticking, scabbing, or perforation, or to avoid ricochet, assuming the target to be a vertical wall and the trajectory to be horizontal at striking. As is obvious from Figure 12, the thick slab cannot be perforated at all by the gun of the present example for which the muzzle velocity, that is, the maximum velocity available, is only 2,900 fps. The vulnerable area for scabbing is much smaller than that for sticking.

As the slab thickness is decreased, the scabbing area increases while a perforation area appears and likewise grows. It is thought that the sticking region changes very slowly until the boundary of the scabbing region overtakes it and that then, with further decrease in slab thickness, the sticking region expands also, although not so rapidly as the scabbing area. For sufficiently thin slabs the phenomenon of sticking probably disappears entirely and the projectile either falls on the front or gun side of the slab or else perforates the slab. As shown in Figure 13, scabbing occurs at greater ranges than sticking for the thin slab while the converse is true for the thick slab (2½ times as thick) of Figure 14. Comparison of the two figures also shows that sticking occurs at greater ranges (i.e. lower striking velocities) for the thin slab than for the thick slab.

A vulnerable-area plot of the type shown in Figures 13 and 14 contains practically all of the essential information needed in either an operational analysis of the estimated effect of a single inert shot attack on a concrete target or in designing a concrete slab to resist this specific attack. Analogous diagrams for steel and armor plate have been used for the design of armored vehicles and tanks. Their use is suggested in a similar way in the design of fortifications. The difficulty lies in making quantitative predictions of the various vulnerable and ricochet areas for arbitrarily selected gun, projectile, and slab. Nevertheless, even semiquantitative maps of this type will help to clarify the fortification designer's problem.

If, for example, a seacoast fortification is being designed against 16-in. naval gunfire, only the deep-water areas from which an enemy might conceivably fire such weapons need be outside the area defined by

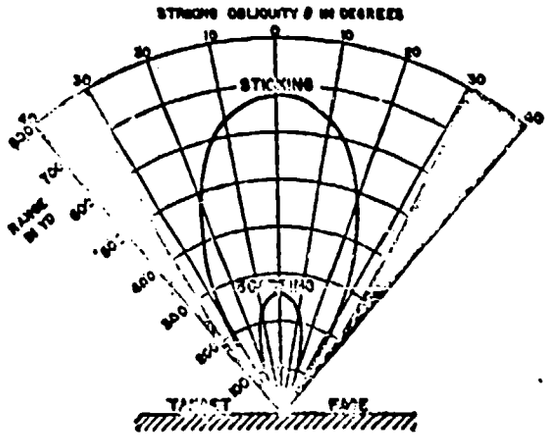

FIGURE 14. Thick-slab vulnerable areas. Based on data of Figure 2. Target, 22 in. thick; projectile, 37-mm M80, weight 1.70 lb, muzzle velocity 2,000 fps.

the scabbing and ricochet limits. The designer's problem is to choose the site, orientation, and slab thicknesses so that this will be true for each wall of the fortification. Since this end is to be achieved at the lowest cost for materials and construction, it would, for example, be concluded in this case that the land-

ward walls need not be as thick as the seaward walls, or that even the seaward walls can be reduced in thickness by orienting them so that the deep-water areas fall within the ricochet regions for these walls.

According to this method of analysis, vulnerable-area diagrams, of the type shown in Figures 13 and 14, are made for each wall of the proposed fortification or bunker. The vulnerable-area diagram for the whole structure is composed of the separate diagrams for the walls placed in the proper relative positions to one another. The composite diagram is then placed on a map of the terrain or region chosen for the site, so that the vulnerable areas will actually appear as regions on the map. Vulnerability to other forms of attack can be similarly analyzed.[24]

How can a vulnerable-area diagram be made for an arbitrary gun, projectile, and concrete target? One may assume that the range-velocity relation for the gun and projectile are known or can be found. The question then reduces to the problem of making a ballistic-limit diagram (of which Figures 11 and 12 are examples) for the particular projectile and target, because from this a vulnerable-area diagram can be constructed, using in addition only the range-velocity relation.

The problem of predicting ballistic limits for any projectile (even assuming it to be inert and nondeforming) at any obliquity and against a given concrete target is by no means completely solved. Present procedures are based on the following ideas. In the first place, predictions are based on experimental test data rather than on theory. Empirical rules found from penetration observations permit fairly good predictions of massive penetration as a function of striking velocity (at least for normal incidence) in terms of concrete properties, and projectile mass, caliber, and nose shape. Experimental data on sticking, oblique penetration, and ricochet are also available, but further work on empirical formulas describing these phenomena is needed. Finally, it turns out that fairly good linear empirical relations can be set up between massive penetration at a given striking velocity and the thickness of a slab of the same concrete that can be (1) scabbed and (2) perforated. Over a wide range, these relations seem to be independent of concrete properties and even hold fairly well at obliquities up to 40 degrees.

If this work on concrete is compared with the corresponding work on steels and armors for nondeforming projectiles, the most striking contrast is the emphasis on penetration in both the experimental and theoretical work on concrete, whereas the work on steel dealt almost exclusively with perforation. This stems from the fact that massive penetration is much easier to observe and interpret with concrete than with steel. Penetrations beyond the bourrelet of the projectile and up to 10 calibers are easily produced at ordinary velocities in concrete (i.e. below 3,000 fps), whereas with plain and armor steels it is difficult to make systematic massive penetration measurements even up to 2 calibers without projectile shatter or deformation. For such depths the special phenomena near the face of the target and those caused by the entry of the projectile nose into the target probably still play a major role, making the observations more difficult to interpret.

It is felt that the theory of massive penetration should be less complicated than the theory of perforation, because in the former only the front-face effects are present, while in the latter the back-face effects must also be considered. Furthermore, if penetration is being studied, almost every shot gives a point on the graph; with perforation a number of bracketing shots are needed to determine one perforation limit. It is very difficult to produce identical concrete targets at different times and places, much more difficult than in the case of steels, and hence it is very advantageous to base the terminal-ballistic studies on experimental penetration curves, each of which is obtained from a single target, rather than to depend solely on the relation between perforation limits as determined for different targets. It is felt that the best method of comparing the terminal-ballistic properties of concrete targets lies in comparing the respective penetration curves obtained with the same projectile rather than in comparing the usual engineering specifications and strength tests. It is felt that the perforation limit for a given concrete target is, for practical purposes, uniquely determined by its thickness and its massive penetration curve as obtained with the same projectile.

Besides this connection with ballistic limits, the penetration curve is of direct practical importance in analyzing the effect of explosive missiles and the effect of repeated fire.

7.3.3 The Dependence of Penetration on Striking Velocity

A great deal of attention has been devoted to the problem of finding a suitable empirical formula to represent the observed massive penetration in con-

crete of an inert nondeforming bomb or projectile as a function of striking velocity at normal incidence.* This is needed not only for smoothing (since individual penetrations exhibit experimental scattering from the mean) and for interpolation (since it is practically impossible to obtain any specific striking velocity by adjusting the powder load) but also for extrapolation, for example, to estimate accurately the massive penetration that would be obtained in the concrete of a given slab for the striking velocity at which scabbing and perforation are actually observed. (See Section 7.3.5.)

Lacking an adequate theory of penetration, it is believed that, of the empirical relations that have been proposed, the following is the most satisfactory both for simplicity and for accuracy of representation.[20]

$$G(z) = cV^{1.80}, \tag{5}$$

$$\text{where } G(z) = z^2/4 \quad \text{for } 0 \leq z \leq 3.00 \text{ calibers} \\ = z - 1.00 \text{ for } z \geq 3.00 \text{ calibers}, \tag{6}$$

and z = nose depth at the end of penetration, in calibers,

V = striking velocity in fps divided by 1,000,

c = constant for a given target and projectile.

This formula relates z and V for normal nondeforming penetration into a massive concrete target. For numerical purposes it is convenient to express V in thousands of fps and to define the units of c accordingly so that $G(z)$ will be a dimensionless quantity.

Table 1 gives values of $V^{1.80}$ for V up to 3.0. The values given correspond to striking velocities at intervals of 100 up to 3,000 fps. This table will greatly facilitate the application of equation (5) to penetration data.

TABLE 1. Values of $V^{1.80}$ for concrete penetration formula, equation (5).*

v (fps)	$V^{1.80}$	v (fps)	$V^{1.80}$	v (fps)	$V^{1.80}$
100	0.016	1,100	1.187	2,100	3.802
200	0.055	1,200	1.388	2,200	4.134
300	0.115	1,300	1.604	2,300	4.478
400	0.192	1,400	1.832	2,400	4.835
500	0.287	1,500	2.075	2,500	5.203
600	0.399	1,600	2.330	2,600	5.584
700	0.526	1,700	2.599	2,700	5.977
800	0.669	1,800	2.881	2,800	6.381
900	0.827	1,900	3.175	2,900	6.797
1,000	1.000	2,000	3.482	3,000	7.225

*v = striking velocity in fps. $V = v/1000$ = striking velocity in thousands of fps.

* See references 2, 3, 4, 6, 11, 15, 16, 18, 20, 22, 23, 33, 34, 36, 40, 44, 47, 50, 52.

Refinements of the empirical approximation represented by equation (5), particularly for values of z below 2.00 calibers, could undoubtedly be made, but the formula suggested has the advantages that it is simple in form, that it takes account of face and nose effects in a reasonable way, and that it involves a single parameter c. The latter is very important because it permits direct comparison of any two sets of penetration data, regardless of the particular striking velocities used in obtaining each.

For the analysis of concrete penetration data (normal incidence, inert and nondeforming projectile, massive concrete target), graph paper, as shown in Figure 15, based on equations (5) and (6), may be used. The ordinates are laid off at distances given by the function $G(z)$ and labeled with values of z, the abscissas are similarly laid off at distances proportional to $V^{1.80}$ and labeled with the corresponding values of v. According to equation (5), the observed points of any particular set of penetration data will be on or near a straight line through the origin; the slope of this straight line will be proportional to the parameter c. Graphical determination of this mean straight line offers a simple procedure for smoothing, interpolating, and extrapolating for any given set of observed penetration data. The plot not only displays the magnitude of the random experimental errors involved, but also shows just how well the empirical equation (5) is able to represent the mean of the observations. When a sufficiently large number of such

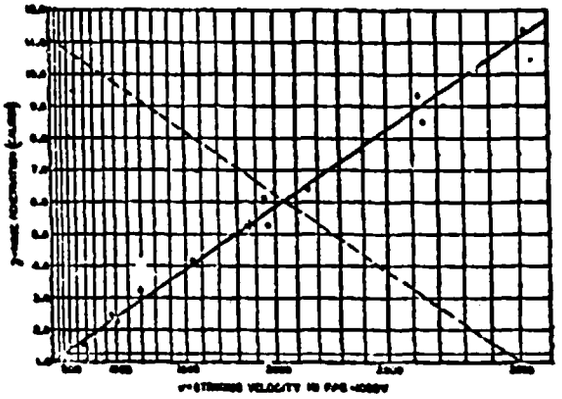

FIGURE 15. Graph on which $G(z) = cV^{1.80}$ represents straight line with slope c through origin for plotting normal penetration in concrete of nondeforming projectile as function of striking velocity. Typical set of field data is plotted (37-mm 1.65-lb AP projectile, data on page A-35 in reference 7). Center of gravity of plotted points is marked +. For dashed line see Section 7.4.6.

plots have been made they should be reviewed to search for systematic deviations from the formula, equation (5). If found, these may in turn lead to improvements in the formula.

For numerical evaluations of the parameter c referring to a specific projectile-target combination, it is suggested that the following formula is suitable both for simplicity and for the relative weighting of data:[20]

$$c = \frac{\Sigma G(s)}{\Sigma V^{1.50}}. \qquad (7)$$

This gives the slope of a straight line passing through the origin and through the center of gravity of the plotted data points (marked + in Figure 15). It also takes some account of the fact that absolute experimental errors tend to increase with distance from the origin, but not so fast as the coordinates themselves.

7.3.4 The Dependence of Penetration on Projectile Mass, Caliber, and Nose Shape, and on Target Properties

The method just outlined gives a satisfactory representation of the relation between striking velocity and penetration for a wide range of data regardless of target properties and projectile mass, caliber, and nose shape, such that changes in these only affect the parameter c in equation (5).

Analysis of the experimental data bearing on these effects[19] leads to the following empirical penetration formula, based on equation (5):

$$G(s) = KNd^{0.20}DV^{1.50}, \qquad (8)$$

where K = penetrability of the concrete,
N = nose-shape factor for the projectile,
d = caliber or maximum diameter of the projectile (in.),
$D = w/d^3$ = caliber density of the projectile (lb per cu in.).

The caliber-density factor D approximates very well the effect of projectile mass on penetration as far as present data go. Additional data on the effect of projectile mass are greatly needed; these should be obtained under carefully controlled conditions, keeping the other factors as constant as possible while only the projectile mass is varied over a wide range.

The scale-effect factor $d^{0.20}$ represents quantitatively the important effect described in Section 7.2.1 within the accuracy of present data, in which D and N usually have different values for the calibers to be compared. Additional data on the scale effect, with careful controls to keep K, D, and N constant for the different calibers, and with the larger calibers going well above 155 mm, will probably be required in order to improve this scale-effect formulation. Beyond this, a better understanding of the physical causes underlying the scale effect is needed.

The .50-caliber data on the effect of nose shape on penetration are analyzed in the report cited above.[20] This analysis results in the recommendation that the nose-shape factor N be estimated from

$$N = 0.72 + 0.25\sqrt{n - 0.25}, \qquad (9)$$

when n is the radius in calibers of a tangent-ogive projectile nose. The dimensionless quantity n is often called *caliber radius head* [crh] in British work; it is denoted by r_0 in Figure 1 of Chapter 6. The radical in this formula is the nose height in calibers for the case of a tangent ogive. If the actual projectile does not have a tangent-ogive nose, this formula for N will probably still give satisfactory results provided n is estimated from an ideal tangent ogive which would most closely approximate to the actual nose shape.

A considerable amount of small-caliber data is available for evaluating the effect of concrete properties on the penetrability K. These data have not as yet been analyzed by the method of Section 7.3.3, and this should be done. The method of analysis used in reporting the .50-caliber data of the last Princeton Concrete Properties Survey evaluated a "penetration parameter" for each concrete. Examination of the ideas behind this earlier and less accurate method of analysis shows that the penetration parameter there used is, in general, proportional to the penetrability K as defined here. Hence the curves given in the report cited may be interpreted as showing how K varies with various concrete properties, although the numerical value of K will be different from that given for the old penetration parameter. More accurate values of K for each of the concretes should be calculated by the center of gravity method of equation (7), which with equation (8) leads to:

$$K = \frac{\Sigma G}{Nd^{0.20}\Sigma DV^{1.50}}. \qquad (10)$$

The caliber density D in lb per cu in. has been put inside the summation in the denominator to take account of variations in projectile mass. Values of K in the interval from 2.0 to 5.0 have been found from typical sets of data.[20]

7.3.5 **Analysis of Perforation and Scabbing Data**

As mentioned near the end of Section 7.3.3, the analysis of experimental observations on perforation has been based on the massive penetration curve obtained with the same concrete and projectile at lower striking velocities. Using the penetration observations, one can estimate, by extrapolation, the hypothetical nose penetration s_i in calibers that would be obtained in a massive target of the same properties at the observed perforation limit velocity v_i. The actual thickness of the target perforated at this limit velocity is denoted by e and its thickness in calibers by e/d.

Perforation tests were made with .50-caliber model-scale projectiles on 133 concrete slabs[18] ranging in thickness from 3 to 18 calibers in compressive strength from 1,500 to 7,000 psi, and in maximum aggregate size from ¼ to 2 calibers. A large variety of reinforcing schemes was also investigated. It was found that within practical limits e/d is a linear function of s_i and that this function is the same within about 10 per cent regardless of the target variations tested. The mean relationship,

$$\frac{e}{d} = 1.23 + 1.07 s_i, \tag{11}$$

was found for perforation.

The scab limit velocity v_s was also determined for each slab and the massive penetration s_s corresponding to this striking velocity was estimated. As for perforation, linear relations were found between the scab-limit thickness e/d in calibers and s_s, the mean relationship being

$$\frac{e}{d} = 2.28 + 1.13 s_s. \tag{12}$$

The values of s_i and s_s used in obtaining these linear relationships were estimated by a method which is probably less accurate than that described in Section 7.3.3. Using still older and probably even less accurate methods of estimating s_i and s_s, the relations[19]

$$\begin{aligned} \frac{e}{d} &= 1.32 + 1.24 s_i \\ \frac{e}{d} &= 2.12 + 1.36 s_s, \end{aligned} \tag{13}$$

had previously been obtained for 37-mm, 75-mm, 3-in., and 1.55-mm data.[7] It is not known whether the apparent differences between these relations and those determined at the .50-caliber scale are real or whether they are due to differences in the methods used in estimating s_i and s_s. The question should be resolved by basing the required extrapolations of the massive penetration data on the method described in Section 7.3.3 and recomputing both the small- and large-scale data.

At the beginning of World War II the concept of a proof factor was used for perforation and scabbing questions. It was felt that the ratio of the limit thickness for perforation to the massive penetration depth at any striking velocity would be practically constant, that is, about 3/2 or 4/3. The results described tend to eliminate the concept of proof factors and to replace them by the idea that the difference (instead of the ratio) between perforation-limit thickness and massive penetration at the same velocity is more nearly a constant in the case of concrete targets. Analogous statements can be made for scabbing. The constant difference hypothesis would hold exactly if the coefficients of s_i and s_s in the last terms of equations (11) and (12) were unity, in which case the perforation difference or defect would be about 1½ calibers and the scabbing defect about 2½ calibers. It is possible that the suggested re-evaluation of the data using the methods of Section 7.3.3 would lead to some such formulation, but until then the perforation and scabbing defects mentioned can only be thought of as rough approximations for thin slabs.

It should also be pointed out that the linear approximations, equations (11) and (12), cannot hold for very thin slabs less than about 2 or 3 calibers in thickness. The actual relations must be curved so as to pass through the origin, that is, so that e/d goes to zero with s_i and so that e/d goes to zero with s_s. It is likely that a composite function $G_i(e/d)$ of the type given in equation (6) for $G(s)$ will be found to be proportional to s_i and another similar composite function $G_s(e/d)$ will be proportional to s_s. To the extent that the thickness defect hypotheses discussed in the previous paragraph holds, the word proportional should be replaced by equal.

According to this reasoning, it will be seen that the combination of the penetration equation (5) with the relations at present represented by equations (11) and (12) leads to equations of the form

$$\begin{aligned} G_i\left(\frac{e}{d}\right) &= c_i V_i^{n_i}, \\ G_s\left(\frac{e}{d}\right) &= c_s V_s^{n_s}, \end{aligned} \tag{14}$$

connecting the limit thicknesses e and e with corresponding limit velocities V_i and V_s. The evaluation

of the functions G and the constants c and a and their relation to the corresponding quantities in equation (5) depends on further data and analysis along the lines indicated above.

7.3.6 The Dependence of Penetration, Ricochet, Scabbing, and Perforation on Obliquity

The data analyses discussed in the last three sections deal exclusively with the phenomena at normal incidence. Much less is known about the effect of obliquity on penetration, scabbing, perforation, and the occurrence of ricochet. In combat, however, some degree of obliquity is almost always present and it is very important not to ignore its effects. The general character of some of these effects was described in Sections 7.3.1 and 7.3.2, and illustrated, particularly, in Figures 11, 12, 13, and 14.

With oblique penetration the principal quantity of practical interest is the component of penetration perpendicular to the target face s_p measured in calibers. For theoretical analyses other facts, such as slant depth and the curvature of the projectile path in the target, are also of interest and have often been recorded in data tabulations.

For a given projectile and target the perpendicular component of penetration s_p is a function of two variables, namely, the striking velocity and the obliquity. This alone makes the analysis of oblique penetration much more difficult than in the case of normal penetration which depends on only one variable, the striking velocity. In addition, much less experimental work has been done, and the experimental scattering is greater for oblique fire than for normal fire, probably due to the fact that the turning forces, causing the projectile path to curve away from the direction of incidence, are more erratic in their effect on s_p than the force variations which produce experimental errors in normal penetration. For these reasons no generally applicable empirical formula has yet been found to express s_p as a function of striking velocity and obliquity.

The studies that have been made so far indicate that the ratio s_p/s, where s is the penetration at normal incidence at the same velocity, is less than $\cos\theta$ but approaches $\cos\theta$ as the striking velocity is increased. This is plausible on the assumptions that the resisting forces are roughly independent of depth and that the asymmetric forces deflecting the projectile from the direction of incidence act mainly near the surface of the target. As the striking velocity is increased, the time that these turning forces act on the projectile is decreased and thus its deviation from its original direction is decreased.

A rough idea of the decrease in penetration of ordinary AP projectiles caused by obliquity for striking velocities from 1,000 to 2,000 fps can be gained from the following tabulation based on a partial analysis[28] of the data:

θ	0°	5°	10°	15°	20°	25°	30°	35°
$\frac{s_p}{s}$	1.00	0.95	0.89	0.82	0.75	0.67	0.58	0.47

The values of s_p/s for any particular obliquity θ tend to decrease for smaller striking velocities and to increase toward $\cos\theta$ as an upper bound for higher striking velocities.

Even though they are probably the best available, there is some hesitation in giving these values because they seem to imply a greater accuracy than is at present justified. One reason for the large scatter of the experimental points probably lies in the less accurate methods of estimating s, the penetration at normal incidence for the striking velocity at which s_p was observed. Now that the method of Section 7.3.3 is available, a thorough review of all good obliquity data should be undertaken.

The following points are suggested for such a review. At first only data obtained with AP projectiles of conventional shape and mass, for which penetrations at normal incidence on the same face of the same target were also recorded, should be analyzed. The data should be grouped by calibers. From the normal incidence penetrations, the s corresponding to the striking velocity for each s_p should be estimated, using the method of Section 7.3.3. For some calibers, data on concretes of widely different strengths are available; it is probable that the effects of obliquity can be better represented as functions of s rather than striking velocity. Hence, it is suggested that the analysis be made in terms of the function

$$f(s,\theta) = \frac{s_p}{s\cos\theta}. \qquad (15)$$

This function can be evaluated for each data point. The attempt to find an empirical formulation should be guided by the fact that $f(s,\theta) = 1.000$, by definition, and by the expectations that $f(s,\theta) < 1.000$ for $\theta > 0°$ and $f(s,\theta) \to 1.000$ for $s \to \infty$. It may be hoped that $f(s,\theta)$ will be found to be sufficiently independent of the strength or penetrability of the concrete to permit an empirical formulation (or graphs or tables)

in terms of $f(s,\theta)$ for all concretes, whereas a unified formulation in terms of a function of striking velocity and θ does not seem, a priori, so promising.

In conducting obliquity tests it is possible to choose θ quite accurately while the striking velocity for each shot cannot be controlled so accurately. For the analysis of results it is a great advantage to conduct all obliquity tests at one or more fixed angles. Obliquities of 11°, 20°, 28°, and 35° have been so used in 37-mm, 75-mm, 3-in., and 155-mm scale tests[7] to get a good distribution of cos θ values; at the .50-caliber scale multiples of 10° were used.[12]

The effect of nose shape and projectile length will undoubtedly be noticeable, particularly at low velocities and high angles. The analysis for such effects should be based on the results of the obliquity analysis for projectiles of conventional form and mass as outlined above.

Some quantitative idea of the angles and velocities at which ricochet begins may be gained from Figures 11 and 12 (which refer to a 37-mm projectile of conventional type) and from Data Sheet 2A5 of Chapter 19. Ricochet limits will undoubtedly be found to be sensitive to projectile nose shape and length, as well as to concrete strength.

The relations (11) and (12) for perforation- and scabbing-limit thicknesses hold also for oblique impact up to 40° according to extensive .50-caliber tests,[12] provided the estimated s_1 and s_2 values are replaced by the corresponding values of s_θ for the obliquity and limit velocities in question. The graphs in the report cited suggest certain systematic deviations from the relations (11) and (12) with obliquity, but these are within the accuracy claimed for the relations up to about 40°.

Thus the prediction of oblique scabbing and perforation is based on the estimation of oblique penetration in quite the same way as in the case of normal incidence. Improvements in the analysis may be sought by first improving the accuracy of prediction for oblique penetration along the lines suggested above, based on better evaluations of the function $f(s,\theta)$. This in turn, should lead to a better analysis of oblique perforation and scabbing data.

7.3.7 Nomograms for Estimating Penetration, Scabbing, and Perforation of Concrete Targets

Data Sheets 2A1, 2B1, and 2C1 of Chapter 19 deal with penetration, scabbing, and perforation, respectively, of reinforced concrete by AP projectiles and AP and SAP bombs. These nomograms were devised in 1943[10] according to the best methods of data analysis then available. The left halves of the three diagrams, including the striking velocity scale, are identical, and are based on an empirical formula according to which the nose-corrected penetration in calibers is (approximately) proportional to the caliber density, to the three-halves power of the striking velocity, to a graphical scale effect function (given in Figure 18 of the report cited), and inversely proportional to the square root of the compressive strength of the concrete. The "ladder" transfer from *B* to *C* scales in Data Sheet 2A1 takes account of the ½-caliber nose correction used in the diagram up to this point. In Data Sheets 2B1 and 2C1 the corresponding ladder scale embodies the relations (13) which were used for scabbing and perforation.

No final revision of these data sheets was ever made, but it is felt that a considerable improvement would result from the material discussed in previous sections.

7.4 THEORY OF CONCRETE PENETRATION

The motion of a projectile is at all times governed by the laws of dynamics. This fact is known with greater precision than any of the specific observations and measurements which have so far been discussed in this chapter. The experimental conclusions and empirical formulas given in previous sections have, however, not made use of Newton's laws of motion.

The aim of a theory of penetration is to go beyond empirical formulas and to establish a quantitative connection between the forces acting on the projectile during penetration and the observed behavior. The nature of these forces is not well understood for any target material. In many respects the theory is at least as well developed for concrete as it is for steel or other materials.

The phenomena of projectile penetration involve not only very high stresses, producing strains far beyond the elastic limit, but these occur under impact conditions at very high velocities. During the penetration cycle the velocity decreases very rapidly to zero. Relatively little progress has been made toward direct experimental observation of the dynamic phenomena *during* the penetration cycle.

While the ensuing discussion explicitly refers to concrete as the target material, the general point of view as well as many of the details may, with appropriate modification, be applied to the theory for steel and other materials.

7.4.1 The Need for a Theory of Penetration

The importance of an analytical study of such phenomena, as an extreme case of the strength and failure of engineering materials, should not be underrated. Some of the ways in which an adequate theory of penetration is of practical importance for the problems of terminal ballistics are the following.

A theory of penetration is needed to establish sound correlations, that is to deepen and extend the analysis of experimental data beyond the methods described in Section 7.3. In a fundamental sense, a proper attention to the theory of penetration is needed in planning and conducting all experimental work, lest the work devolve into a series of isolated ad hoc tests aimed at answering specialized questions and thus obtaining results which can never be correlated. Sufficient data on actual projectile masses, diameters, and shapes, on striking velocities, on actual penetrations and target properties, etc., should always be recorded to furnish the basis for examining the interrelations among different tests and for theoretical analysis.[7.11,12]

A theory of penetration is needed to give information about the resisting forces which cause projectile and bomb deformation; on this a more rational design against deformation could be based. At present there exists only very meager knowledge of the conditions of striking velocity, obliquity, and target thickness under which present bombs and HE projectiles will fail, nor is it known how to apply information gained by actual test with one missile to other service missiles. The "practical" expedient of testing all missiles against targets of all thicknesses is impractical. This is perhaps a typical example of how the lack of theory costs time and money in multiplying the tests needed and, even then, fails to provide generally applicable information.

A theory of penetration is needed to provide information concerning the setback forces available for fuze initiation (especially with thin slabs) and the time thereafter to maximum penetration or to perforation, in order to secure the maximum effect from the detonation of a given missile (see Section 7.2.6). The lateral and turning forces encountered in oblique impact need also to be better understood, both as causes of fuze failures and as causes of missile deformation.

A theory of penetration is needed for predicting the remaining velocity of a projectile after penetrating a given thickness of a target material for designing composite targets, as discussed in the last paragraph of Section 7.3.4. Similarly a theory of perforation is needed to give information on the residual velocity after perforation, for example, in order to estimate the distance covered before detonation of a time-fused missile.

A better understanding of the way in which the resisting forces vary with depth in the target, with projectile shape, and with velocity is needed for the analysis of oblique penetration and perforation data. (See Section 7.3.6.)

7.4.2 The Equation of Motion

The fundamental problem of terminal ballistics is to account for the observed penetration at normal incidence and zero yaw of a nondeformable projectile into a uniform massive target. Under these idealized conditions the projectile penetrates in a straight line coincident with the direction of incidence and the rectilinear motion is governed by a single differential equation expressing Newton's second law of motion, namely,

$$\frac{w}{g}\frac{d^2x}{dt^2} = \frac{w}{g}\frac{v\,dv}{dx} = \text{force acting on projectile.} \quad (16)$$

The first expression on the left is the usual product of mass times acceleration; the second form, which is the rate of increase of the kinetic energy with distance, is often more useful for penetration problems. The force acting on the projectile during penetration is, of course, negative when x is measured in the direction of motion.

With yaw or oblique incidence lateral forces tend to deflect and turn the projectile. While equation (16) still governs the forward component of motion of the center of gravity, additional equations based on the second law of motion must be written for the lateral motion and for the rotation of the projectile about a transverse axis. In addition, the force functions to be used with the several equations are, in general, dependent on the components of position and velocity involved in all of the equations. This problem is vastly more complicated than the fundamental simple case for which equation (16) was written. Attention will be restricted for the present to the simple problem specified at the outset.

7.4.3 Scale Relations

In order to compare the relations at various scales or calibers in a simple way, it is advantageous to eliminate w and x by introducing the caliber density D and the caliber penetration s, as has been done in

many of the discussions of Section 7.3 and 7.5. Equation (16) can then be written in the form:

$$Dv\frac{dv}{ds} = -R = -\frac{\pi g}{48}P, \qquad (17)$$

where P is the resisting pressure in psi and g is the acceleration due to gravity or 32.174 ft/sec^2.

In the absence of a scale effect, the force function R will be independent of caliber. When a scale effect exists, as in the case of concrete (and probably to a lesser extent with steel), R will depend on the caliber d. This, however, will not affect the integrability of the equation of motion (16) because, for a nondeforming projectile, d is constant during the motion represented by the equation.

7.4.4 The Law of Force

A mean value of the force resisting a projectile during penetration can easily be found by dividing the striking kinetic energy by the observed depth of penetration. For concrete targets this mean force divided by the cross-sectional area of the projectile may be from 30,000 to 100,000 psi. This calculation corresponds to the assumption that R is constant in equation (16), but if it is made for different depths of penetration (same projectile and target) the mean pressure values are found to increase with depth, that is, penetration increases less rapidly than the striking kinetic energy. If the resisting force were constant during each penetration, then R would have to assume different but constant values for different striking velocities. This does not seem likely from a physical point of view and, hence, it is concluded that R is not constant, but varies during the penetration cycle. The crux of the penetration problem lies in finding out how the force varies during penetration, and in elucidating the physical phenomena involved.

It is common to assume that R depends on the instantaneous velocity, or on the depth in the target, or on both, that is

$$R = R(z,v). \qquad (18)$$

The scale effect dependence on d need not be expressly shown here because d does not vary during penetration.

A possible dependence of R on other variables during the motion cannot be excluded on a priori theoretical grounds. The resistance arises from an interaction between the moving projectile and the material of the target which must be displaced. A pattern of motion or flow must be set up in the plastically disturbed or crushed region of the target, while elastic effects are propagated with finite velocity beyond the disturbed region. In general, the instantaneous motion of individual target particles in the flow region will neither be exactly parallel or perpendicular (radial) to the motion of the projectile, although both assumptions have been made in simplified armor-perforation theories. As the projectile advances into the disturbed region the direction and rate of motion of each particle changes continuously and others are set into motion at depths beyond that reached by the nose of the projectile. In this process some of the energy and momentum transferred from the projectile to target material at earlier stages in the penetration cycle will serve to reduce both the crushing and inertial resistance of the target at later stages. At each stage the disturbed region extends laterally and well ahead of the actual penetration hole.

Thus, the resistance R may well depend on the deceleration dv/dt and on the "previous history" of the motion, as well as on z and v directly. The penetration cycle may involve a transient stage at the beginning, during which the disturbance or flow pattern in the target material is set up, and a subsequent quasi-steady-state stage, during which the projectile-target interaction depends in some continuous way on the relative motions of the projectile and the target material in its neighborhood. It is even possible that some motion of the target material continues for a brief time after the forward motion of the projectile has ceased. It is not clear how these considerations may be put into mathematical form and no definite suggestion involving other variables than those in equation (18) has as yet been formulated, let alone integrated and compared with experiment.

The nature of the physical phenomena causing the scale effect are also not understood. Among the suggestions that have been made are the following. (1) If the target is not homogeneous, but actually varies in penetration resistance with depth, R will depend on the absolute depth x rather than on the caliber depth z as assumed in equation (18). (2) R may depend on the ratio of caliber to some characteristic length associated with the granular structure of the target, for example, the mean aggregate size in concrete or the grain size in steel. (3) The flow pattern of displaced target material and, hence, the resisting force, may be a function of the projectile velocity measured in calibers per sec, that is, v/d. Thus a functional relation may exist between the resisting pressure and the rate, in calibers per sec, at which the plastically deformed

or crushed region advances into the previously undisturbed target material.

7.4.5 The Relation between Theory and Experiment

The interrelation of theory and experiment in the concrete penetration problem is schematically shown in Figure 16.[36] The first three of the four boxes in the Experiment column have been covered in previous sections, particularly Section 7.4. The Theory column begins with postulating a law of resisting force which, when inserted in the relation $F = ma$ and integrated, leads to a rational penetration formula. This theoretical formula is to be compared with experiment as indicated by the line marked *A*. The last box in each column indicates the direction in which fundamental progress should be sought, and the lines *B* and *C* show the cross connections which should then be examined.

In the next section a law of resisting force, based on five assumptions is suggested for concrete. The equation of motion can be integrated analytically and the resulting penetration formula agrees satisfactorily with the empirical formula, equation (8), which was set up in Section 7.3.4. Thus, within the approximations involved, the connection *A* in Figure 16 is established.

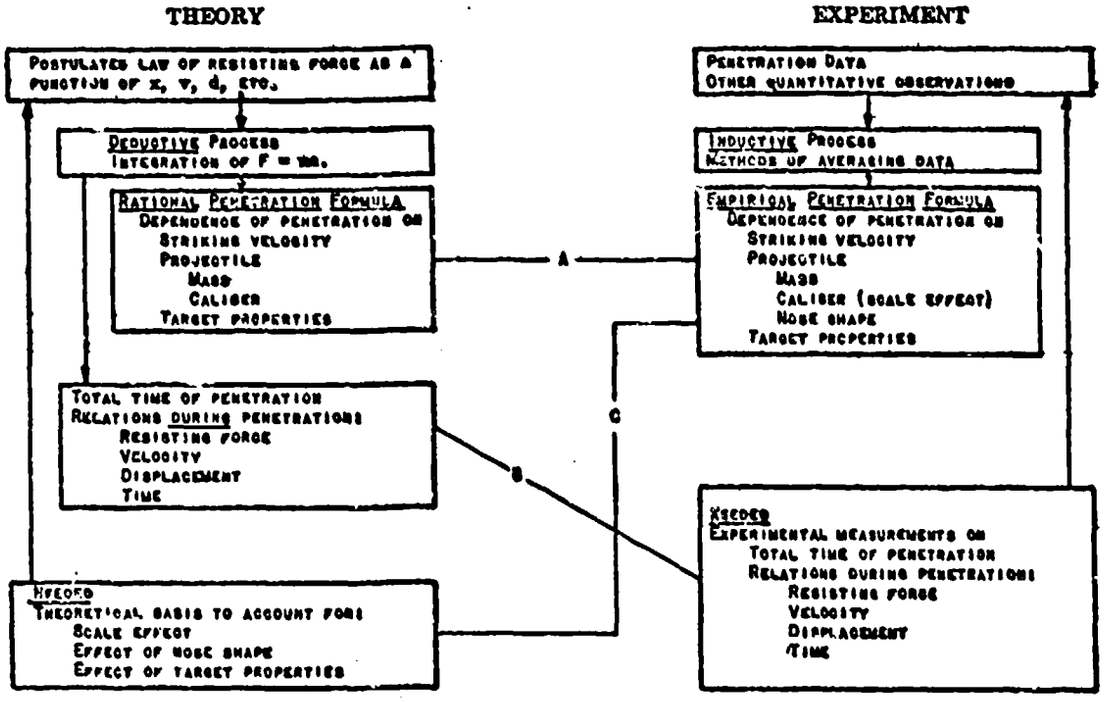

FIGURE 16. Interrelation of theory and experiment in penetration problem. Separation between columns is almost complete in our present knowledge. Lines *A*, *B*, and *C* emphasize connections which should be examined in order to make progress toward more unified structure.

7.4.6 A Theory of Penetration for Concrete

The following theory of concrete penetration[36] is offered as a good approximation for the experimental data now available. It is the best that can be recommended in the present state of knowledge on the subject.

The theory of penetration for a nondeforming projectile of conventional form penetrating a massive concrete target without yaw in a direction normal to the target face (zero obliquity) can be based on the following assumptions:

1. The force per unit area resisting the forward motion of the projectile in the target can be represented to a very good approximation by a separable force law[18]

$$R = cg(z)f(v), \tag{19}$$

where z is the depth of nose penetration measured in

calibers and v is the remaining velocity at each instant.

2. The depth dependence of R can be approximated by

$$g(s) = \frac{s}{2} \text{ for } 0 \leq s \leq 2.00 \text{ calibers},$$
$$= 1.00 \text{ for } s \geq 2.00 \text{ calibers}. \qquad (20)$$

This assumption is an attempt to take account of the entry of the pointed nose of the projectile into the target and the effect that the escape of target material during crater formation may have on R.

3. The velocity dependence of R can be approximated by

$$f(v) = v^{2-\alpha}, \qquad (21)$$

where α is a constant. Both the fractional exponent needed for fitting the data and the fact that $f(v)$ then goes to zero with v are unsatisfactory from a physical point of view. These defects are associated with the basic lack of knowledge concerning the physical causes of the velocity dependence of R, discussed in Section 7.4.4.

4. The constant c is inversely proportional to

$$KNd^{\beta}, \qquad (22)$$

where K is the penetrability of the concrete, N is the nose-shape factor for the projectile, d is the caliber and β a numerical exponent. The form of the assumed scale-effect dependence on d is again unsatisfactory, but until a better understanding of the underlying physical phenomena is attained (see end of Section 7.4.4) it will be difficult to improve this formulation.

5. An excellent representation of concrete penetration data at all scales is obtained by assigning the values

$$\alpha = 1.80 \text{ and } \beta = 0.20. \qquad (23)$$

According to these five assumptions the law of force, equation (18), becomes:

$$R = \frac{g(s)}{KN}\left(\frac{v}{d}\right)^{0.20} \times \text{constant}. \qquad (24)$$

The numerical values of α and β given in equation (23) were found from concrete penetration data without assuming $2 - \alpha = \beta$. The fact that they give a force law in which the velocity dependence and the scale dependence can be combined in the single factor $(v/d)^{\beta}$ may be significant in connection with the problem of the cause of the scale effect as discussed at the end of Section 7.4.4.

The equation of motion (17), with the above relation for R, can be integrated by separation of the variables[2,18] from the initial conditions at impact ($s = 0$ and $v = v_0$) to the final conditions at the end of penetration ($s = s_1$ and $v = 0$).

With a hybrid system of units[16] that is convenient for practical numerical computations, and making the arbitrary constant on the right side of equation (24) equal to $(1{,}000)^{1.80}/1.80$, the resulting *penetration formula* is:

$$G(s_1) = KNd^{2.20}DV_0^{1.80}, \qquad (25)$$

where $G(s_1) = \int_0^{s_1} g(s)\,ds$,
$= s_1^2/4$ for $0 \leq s_1 \leq 2.00$ calibers,
$= s_1 - 1.00$ for $s_1 \geq 2.00$ calibers,
s_1 = final maximum nose penetration of the projectile in calibers (dimensionless),
K = penetrability of the concrete (units are such as to make $G(s_1)$ dimensionless),
N = nose factor for the projectile (dimensionless),
d = caliber or maximum diameter of the projectile (in.),
D = weight of projectile/d^3,
= "caliber density" of the projectile in lb per cu in.,
V_0 = $v_0/1{,}000$ = striking velocity of the projectile in thousands of fps.

By dropping the subscripts on s and V, equation (25) becomes identical with the empirical formula, equation (8), obtained from analyzing normal penetration data (without using the equation of motion) in Section 7.3.4. Thus the connection marked A in Figure 16 is established.

In the units given above, the resisting force per unit maximum cross-sectional area of the projectile is, from equations (17), (24), and (25)

$$P = \frac{263{,}820}{KN}\left(\frac{V}{d}\right)^{0.20} g(s) \text{ psi}, \qquad (26)$$

where V is the instantaneous remaining velocity of the projectile in thousands of fps, and d is in in.

Integrating the equation of motion to find the relation between v and s during penetration gives

$$\frac{G(s)}{G(s_1)} + \left(\frac{v}{v_0}\right)^{1.80} = 1. \qquad (27)$$

It can be shown[18] that the values of v and s which satisfy this equation for given values of v_0 and s_1 will lie on a straight line having intercepts $(0,s)$ and $(v_0,0)$ in Figure 15 of Section 7.3.3. For the sample set of data plotted in Figure 15 the maximum nose

penetration z_1 is 11.1 calibers when the striking velocity v_0 is 3,000 fps. The dashed line shows the relation between z and v during this penetration according to equation (27). Thus the remaining velocity when the nose of the projectile has reached a depth of $z = 8.0$ calibers is, approximately, $v = 1{,}560$ fps. This method of estimating the remaining velocity may be used in the analysis of composite slabs discussed at the end of Section 7.2.4.

The time σ in msec from the instant of impact to any depth z during penetration may be computed from[18]

$$\frac{V_0\sigma}{x} = \frac{1}{z}\int_0^z \frac{dz}{\left[1-\frac{G(z)}{G(z_1)}\right]^{1/1.56}} = \text{dimensionless function of } z \text{ and } z_1, \quad (28)$$

where x is the nose penetration in feet ($x = zd/12$). The total time of penetration, σ_1 msec, can be determined from [18]

$$K = \frac{V_0\sigma_1}{x_1} = \frac{1}{z_1}\int_0^{z_1} \frac{dz}{\left[1-\frac{G(z)}{G(z_1)}\right]^{1/1.56}} = \text{dimensionless function of } z_1 \text{ only}, \quad (29)$$

where x_1 is the maximum nose penetration in ft ($x_1 = z_1 d/12$). The right sides of these equations are universal functions for concrete, independent of the target and projectile parameters K, N, d, and D. Thus, by numerical evaluation of the integrals, a graph can be made for finding values of $V_x\sigma/x$, and $V_0\sigma_1/x_1$. Then the determination of σ or σ_1 is reduced to a simple slide-rule operation. This method of estimating penetration times may be used to solve problems regarding fuze settings for attacking concrete.

7.5 ADDENDA

7.5.1 The Solenoid Method for Measuring Phenomena during Penetration

As indicated in the last box on the right side of Figure 16, the most promising way of improving the present understanding of penetration would be to obtain direct experimental observations of phenomena *during* penetration. Until these are obtained, theoretical considerations, such as those given in Section 7.4.4, will continue to be tentative and speculative. Even measurements of the total time of penetration alone would be most helpful.

The experimental work[17] deals with an experimental method of measuring velocity as a function of time during penetration in nonmagnetic and nonconducting media like concrete. The basic ideas involved in this method are as follows:

The electromotive force induced by a longitudinally magnetized projectile (considered as a point dipole with a magnetic moment of M electromagnetic units) moving with a velocity v cm per sec along the axis of an idealized circular coil of N turns and r cm radius, is

$$e = kvf(x) \text{ volts}, \quad (30)$$

$$\text{where } k = \frac{6\pi MN}{10^9 r^3} \text{ volt-sec/cm}, \quad (31)$$

$$\text{and } f(x) = \frac{x}{(1^2+x^2)^{5/2}} = \text{dimensionless position function}, \quad (32)$$

where x is the instantaneous position of the dipole on the coil axis measured in coil radii from the center of the coil. The position function $f(x)$ is plotted in Figure 17. In the absence of a resistant target, v is sensibly constant and x is proportional to the time t measured from the instant $t = 0$ when the dipole is at the center of the coil. For this case Figure 17 is a

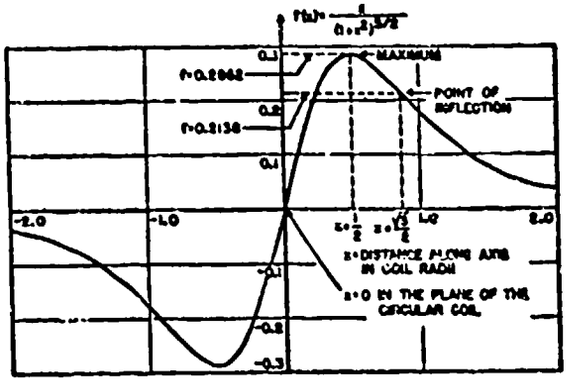

FIGURE 17. Position function $f(x)$ for single coil.

picture of the form of the emf pulse as a function of time as commonly obtained from each coil in the solenoid method of measuring projectile velocities. If the projectile strikes a resistant target (nonmagnetic and nonconducting) placed near the coil, the emf pulse will be changed because v changes and because x is no longer proportional to t. On the assumption that the magnetic moment M does not materially change after impact it is possible to deduce the projectile velocity as a function of time from an accu-

rately recorded oscillographic trace of the emf pulse as a function of time.

A more direct determination of velocity as a function of time can be obtained by using two identical coaxial coils connected in opposition and spaced a distance of 0.90 diameter apart. Measuring x (in coil radii) from the point on the common axis midway between the coils, the induced electromotive force becomes

$$e = kvF(x) \text{ volts} \tag{33}$$

where $F(x) = f(x + 0.90) - f(x - 0.90)$. (34)

This two-coil position function is shown in Figure 18, together with the two single-coil components of which

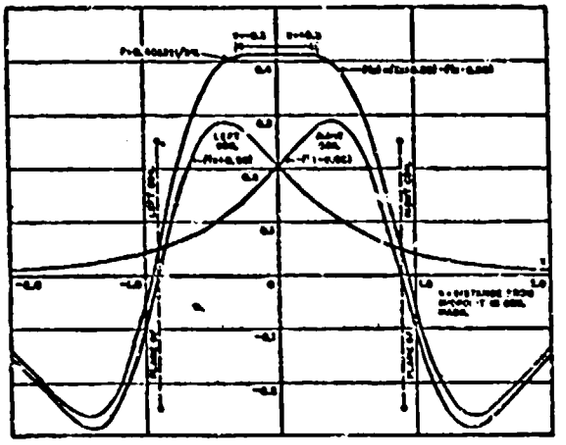

FIGURE 18. Position function $F(x)$ for two opposing coils, 0.90 diameter apart.

it is composed. The flat-top region of the graph illustrates the fact that $F(x) = 0.4085$ and is constant within $\pm \frac{1}{3}$ per cent, while the dipole is in the interval,

$$-0.3 < x < 0.3, \tag{35}$$

between the coils. Hence, *in this interval*, equation (33) becomes

$$e = 0.4085kv \text{ volt}, \tag{36}$$

that is, the induced electromotive force is proportional to the projectile velocity at each instant and is *independent of* x to a very good approximation. The oscillograph trace will give directly the velocity as a function of time while the magnetic center of the projectile is in the interval (35); the target should therefore be placed so that the decelerations to be observed occur in this interval.

It is of some scientific interest to point out that this two-coil arrangement is very closely related to a two-coil arrangement specified by J. C. Maxwell[18] for obtaining a nearly uniform magnetic field gradient near the axis midpoint. Maxwell's spacing between coils is $\sqrt{3}/2 = 0.866$ diameter; the 0.90-diameter spacing is a compromise which serves to extend the useful interval (36) somewhat without materially affecting the constancy of $F(x)$ for practical purposes. The underlying connection between the present arrangement and Maxwell's becomes clear if the dipole is considered as moving in the magnetic field of a current flowing in the coils and the rate of work done on the dipole is equated with the additional power required by the current to overcome the induced electromotive force.

The two-coil arrangement not only has the advantage over the single-coil system of greatly simplifying the routine analysis of the recorded oscillograph traces, but it makes it easier to assess the accuracy of the resulting $v(t)$ curves and to recognize imperfections in the recording system which might otherwise lead to erroneous $v(t)$ curves.

Experimental work using the two-coil system is reported in reference 17, particularly the aspects of the initiating and recording system and the problem of stabilizing the bullets to reduce the change in magnetic moment during impact to a minimum. Satisfactory performance was obtained with .50-caliber Service AP bullets, and the problem of stabilizing model-scale artillery type bullets had just been begun when the work was interrupted in order to transfer the available personnel to a more important problem.

7.5.2 Summary of Analytical Theories of Penetration and Perforation

The theory of concrete penetration presented in Section 7.4 is one among many that have been considered analytically. The following summary of the various mathematical possibilities is presented to aid those who will carry forward the theory of penetration and perforation, either for concrete or for other materials.

Summary of Integrable Force Laws

The various integrable forms of $R(z,v)$ that have been proposed may be summarized under two general classes of analytical force laws[18]

$$\text{Separable:} \quad R = a \cdot g(z) \cdot f(v), \tag{37}$$

$$\text{Generalized Poncelet:} \quad R = a \cdot g(z)v^{\beta} + b \cdot \gamma(z)v^{2}. \tag{38}$$

Since a nondeforming projectile is considered, d will remain constant during the motion. Hence any scale

effect dependence of R on d need not appear explicitly in these hypothetical force laws in order to permit the formal integration of the equation of motion, equation (17). Relations for penetration and perforation obtained by integrating this equation are collected in Table 2. Figure 19 shows some of the theories which fall under these two general classes of force laws, as special cases. Thus, the classical theories[2] of Robins-Euler, Poncelet, and Pétry may be considered as special cases of either equation (37) or equation (38).

The constants a and b have been written as factors separate from the functions of s and v in these equations. In this way $g(s)$, $\gamma(s)$, and $f(v)$ can be thought of as dimensionless functions which may remain the same for a given type of target (such as steel or concrete) while the constant parameters a and b absorb the necessary physical dimensions and have different values for different targets of the same type. Both the relations between v and s during penetration and the relations for residual velocity after perforation have been put in a form not involving a, b, and D in Table 2 in the expectation that this form would be invariant for all targets of one type.

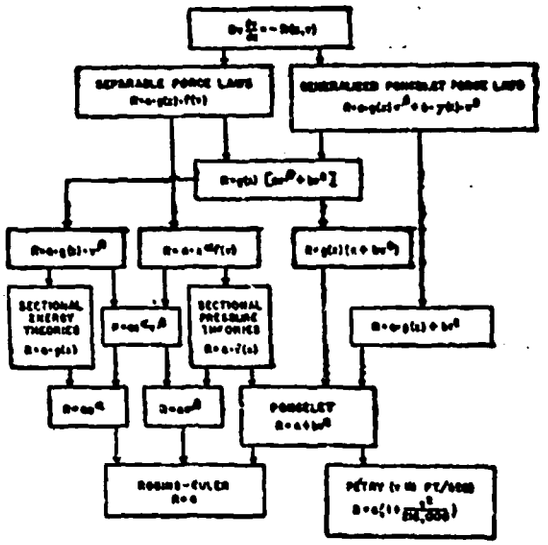

FIGURE 19. Classification of penetration theories. There are shown some of the theories obtained by successive specialization (indicated by arrows) of the two general analytical force laws of Table 2.

TABLE 2. Summary of analytical theories of penetration and perforation.

	Separable force laws $Dv\frac{dv}{ds} = -a\cdot g(s)\cdot f(v)$	Generalized Poncelet force laws $Dv\frac{dv}{ds} = -\left[a\cdot g(s)v^{\beta} + b\cdot\gamma(s)\cdot v^{2}\right]$
Penetration		
Penetration formula (Relation between v_0 and s_1)	$D\cdot F(v_0) = a\cdot G(s_1)$	$D\cdot v_0^{2-\beta} = (2-\beta)\,a\cdot G(s_1)$
Relation between v and s during penetration	$\frac{F(v)}{F(v_0)} + \frac{G(s)}{G(s_1)} = 1$	$\left(\frac{v}{v_0}\right)^{2-\beta}\cdot M(s) + \frac{G(s)}{G(s_1)} = 1$
Perforation		
Limit velocity	$D\cdot F(v_l) = aG_c$	$Dv_l^{2-\beta} = (2-\beta)aG_c$
Residual velocity	$F(v_r) = F(v_0) - F(v_l)$	$v_r^{2-\beta}\cdot M_c(s_c) = v_0^{2-\beta} - v_l^{2-\beta}$
Where	$F(v) = \int_0^v \frac{v\,dv}{f(v)}$	$M(s) = e^{\frac{(2-\beta)b}{D}\int_0^s \gamma(s)\,ds}$
	$G(s) = \int_0^s g(s)\,ds$	$G(s) = \int_0^s M(s)\cdot g(s)\,ds$
	$G_c = \int_0^{s_c} g_c(s)\,ds = \text{constant}$	$M_c(s) = e^{\frac{(2-\beta)b}{D}\int_0^s \gamma_c(s)\,ds}$
		$G_c = \int_0^{s_c} M_c(s)\cdot g_c(s)\,ds = \text{constant}$
		e = base of natural logarithms

If the function $g(z)$ has some form such as is suggested in Figure 20, it can take account of target face and projectile nose effects, at least qualitatively. (Compare item 2 in Section 7.4.6.) For small values of z, the resistance R must be smaller than after the full projectile nose has entered the target and after target material can no longer escape from the original target volume as petals or spall. In the deeper layers of the target the displaced material is more confined and $g(z)$ may level off to a fairly constant maximum value (which may be made unity by defining the parameter a properly). As soon as the material at the back face of the target begins to yield or rupture, R must begin to decrease, perhaps very rapidly or even abruptly as is suggested by the dashed curve for $g_e(z)$ in Figure 20. In the region of massive penetration, $g_e(z)$ and $g(z)$ should coincide, the position of the dashed portion of $g_e(z)$ being determined by the distance from the back face of the target. The depth z_e at which $g_e(z)$ becomes zero will be near e/d, but it may be greater than e/d with a ductile material like steel or it may be less than e/d with a brittle material like concrete.

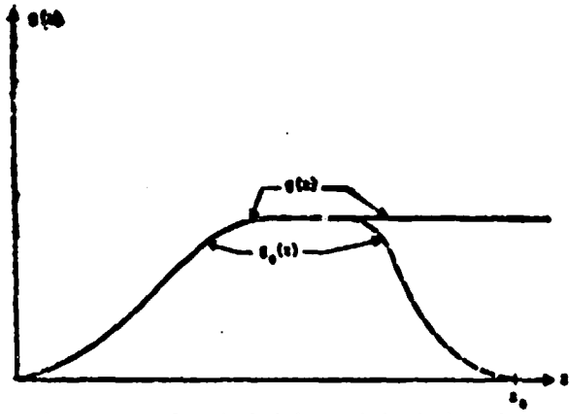

FIGURE 20. Hypothetical form of depth dependence function $g(z)$ in equation (37) or (38).

The first term on the right in equation (38) represents the crushing resistance of the target, while the second term represents the inertial resistance of the displaced target material in the sense of the classical Poncelet theory.[22] The problem of the form that $\gamma(z)$ should have is more elusive than that for $g(z)$. It may be plausible to give $\gamma(z)$ and $\gamma_e(z)$ forms similar to those suggested for $g(z)$ and $g_e(z)$ in Figure 20, and for similar reasons; certainly $\gamma_e(z)$ should also become zero for some value of z near e/d.

TIME OF PENETRATION

In addition to the relations shown in Table 2, the time-depth relation during penetration can be calculated from one or both of the two expressions

$$12\,\frac{t}{d} = \int_0^z \frac{dz}{v}, \tag{39}$$

$$12\,\frac{t_1 - t}{d} = D\int_0^v \frac{dv}{R}, \tag{40}$$

provided either that v can be expressed as a function of z in equation (39) or that R from equation (17) can be expressed as a function of v in equation (40). The latter is especially useful for sectional pressure theories, for which $R = af(v)$, as shown in Figure 19. Particular interest attaches to the total time to maximum penetration z_1 which is important in estimating fuzing times. It has been suggested[13,14,15] that the dimensionless combination

$$K = \frac{v_0 t_1}{z_1} = 12\,\frac{v_0 t_1}{z_1 d} = \int_0^1 \frac{d(z/z_1)}{v/v_0}, \tag{41}$$

is a useful parameter for such problems since its value will be near 2.0, as may be seen by regarding K as the ratio of the striking velocity v_0 to the average velocity during penetration z_1/t_1. The dimensionless quantity K used in equation (29) of Section 7.4.6 is the same as K in equation (41), although different units were used for velocity and time.

Chapter 8

TERMINAL BALLISTICS OF PLASTIC PROTECTION

8.1 INTRODUCTION

PLASTIC PROTECTION is the American name for a material originally developed by the British and called by them *plastic armor.*[a,b] This material has been further developed both abroad and in this country, and has proved useful as a protective material requiring relatively small amounts of strategically important materials. Its chief use is for protection against small-caliber bullets or fragments.

8.1.1 Description of the Material

Plastic protection consists of a layer of stones embedded in a mastic of asphalt and filler, backed by a thin plate of mild steel and having a layer of expanded metal embedded in the mixture near the front face. The approximate proportions by weight for the main component are: 60 per cent stone, 30 per cent limestone dust filler, 10 per cent asphalt or other bituminous binder. These materials are thoroughly mixed at a temperature high enough for the asphalt to become molten and to wet the filler and stone, and the mixture is then poured into molds or onto backing plates. The stone-bitumen mixture can be poured from the mixing oven directly against the wall of a structure; this is sometimes done to protect certain parts of a ship from strafing attack by planes. In its most common form plastic protection is furnished in slabs that can be bolted to the walls of structures or fitted together to form walls around objects to be protected.

8.2 BALLISTIC BEHAVIOR OF PLASTIC PROTECTION

Plastic protection is a mixture of hard stones and soft bituminous filler. Because of this heterogeneous nature, it must be expected that projectiles of a particular variety striking various points on the surface of the material will penetrate in different ways and that the depth of penetration will vary over a wide range. Projectiles will be deflected by the stones, will yaw, and may be broken if they suffer glancing impact against a stone at a high velocity. Thus the process of penetrating into a slab of given thickness at a given striking velocity can occur in a large number of ways, some of which may result in perforation of the slab by the projectile or parts of a broken projectile, others not. Consequently, there is no sharply defined limiting velocity for perforation. One can only specify that, for a given thickness of plastic protection, bullets striking with low velocity will generally be stopped, only a small fraction perforating. As the striking velocity is increased, the fraction perforating the slab will increase, and at very high striking velocities a large fraction of the bullets striking the target will perforate. If, on a graph, a plot is made of the proportion of the striking bullets that perforate, as a function of striking velocity, the result will be similar to each of the curves of Figure 1.

8.2.1 Statistical Interpretation of Perforation Data

The large variety of ways in which a bullet can penetrate plastic protection, some of them leading to perforation and others not, can be treated statistically.[1] If all details of the mechanism were known, all methods of penetrating could be determined and the fraction of these leading to perforation could be found for each striking velocity and for each slab. This information is not known, and the results must be found experimentally by firing a large number of bullets and counting the perforations to determine the percentage through. This must be done for a number of striking velocities to determine one of the curves shown in Figure 1, and must be repeated at several striking velocities for slabs of different thickness, or weight per unit area, to determine a full set of curves. Each point on one of these curves is an average value of the percentage through, and to be reliable each point must be based on a large number of rounds fired. Standard statistical methods may be used to determine the reliability of each point and thus to determine the reliability of each curve or series of curves.

The determination of the ballistic properties of plastic protection by the statistical treatment referred to above requires firing a large number of rounds if

[a] Pertinent to War Department Projects CE-5 and CE-6 and to Navy Department Projects NO-11, NO-12, and NS-145.

[b] For definition of ballistic terms, see Chapter 5.

[c] See Weapon Data Sheet 2C2 of Chapter 19.

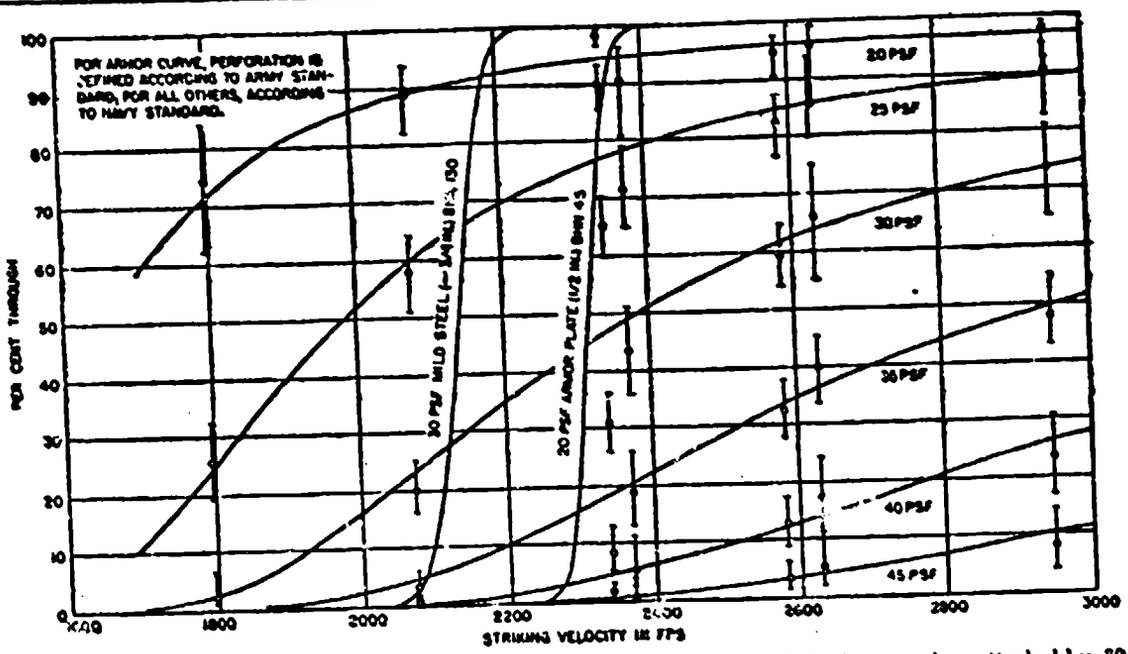

FIGURE 1. Per cent through as function of striking velocity for various weights of plastic protection, attacked by .30-caliber AP M2 bullets at normal incidence. Curves for ¼-in. mild steel and ½-in. armor plate are included for comparison. (Shape of mild steel curve is estimated.)

the result is to be reasonably reliable. This has been done for only one type of plastic protection and using only one bullet, the .30-caliber armor-piercing [AP] M2. The results are shown in Figure 1. Curves for mild steel and for armor plate are included in the figure for comparison. The steepness of the curves for mild steel and for armor show why perforation-limit velocities for these materials can be determined simply by bracketing; the difference between the velocity for complete protection and the velocity for certain perforation is small. The phenomenon is entirely different from that of perforation of plastic protection and statistical methods are not usually necessary.

The curves show that at low striking velocities plastic protection is not so good as an equal weight of mild steel or armor plate, since the steel and armor stop all bullets, while a few get through the plastic protection. At higher velocities the plastic protection is better than either the mild steel or armor, since it stops some of the bullets while the other materials are perforated by all bullets that strike with high enough velocity. As a specific example, the curves show that plastic protection having a weight of 30 lb per sq ft is inferior to mild steel of the same unit weight for .30-caliber AP M2 bullets striking normally with velocities below 2,120 fps, but is superior to the mild steel at higher velocities. At a striking velocity of 2,250 fps all the bullets will perforate the mild steel while only 40 per cent of them (on the average) will perforate the plastic protection.

STATISTICAL METHODS

Different statistical treatments of the data have been suggested.[1] The most promising method is based on the hypothesis that the percentage through may be represented as a normal probability integral function of the thickness, or weight per unit area, for a given striking velocity, but present data offer no proof that this method is better than others. Mathematical details of the statistical methods of analysis and interpretation of the perforation data for plastic protection are also given.

8.2.2 Behavior at Obliquities

The comparison between plastic protection and mild steel or armor, shown in Figure 1, is for bullets striking at normal incidence. At obliquities other than normal, the comparison is even more favorable to plastic protection at high velocities and just as good or slightly better at low velocities.

RICOCHET

Fewer ricochets are observed from plastic protec-

tion than from mild steel or armor when both are subjected to oblique attack under the same conditions. For .30-caliber AP M2 bullets striking with a velocity of about 2,800 fps, ricochets have not been observed for obliquities of 45° from the normal and it is necessary to increase the obliquity to 60° from the normal before a majority of the bullets begin to ricochet. The other bullets are embedded in the slab. This behavior is much better than that of mild steel or armor plate for uses in which prevention of ricochet is desirable.

8.2.3 Protection against Explosions

No extensive tests of the protective value of plastic protection subjected to explosions have been made. Slabs of British Mark II plastic armor, 1¾ in. thick, with a 20-gauge mild steel face plate and 5/16-in. mild steel backing plate have been tested by contact explosion of hand grenades and mortar bombs.[3] A British-type 36M hand grenade was detonated in contact with such plastic protection; no perforations were observed, and the backing plate was only slightly bent. Similar results were obtained by detonating grenades 15 in. from the panels, and by detonating a grenade in contact with panels and over a joint between panels. A British 2-in. Mark I mortar bomb was fired to strike panels of plastic protection with a velocity of 210 fps. The bomb detonated instantaneously, and although the front of the panel was damaged, only slight bending of the backing plate was observed. There were no perforations.

8.2.4 Protection against Shaped Charges

The use of plastic protection for protection against shaped charges is discussed in Chapter 14.

8.3 SPECIFICATIONS OF COMPONENTS

Extensive tests of plastic protection have been made only with the .30-caliber AP M2 bullet. Such tests have been made of plastic protection of several different compositions, and limited tests have been made using large missiles.

The best specification of components, based on these tests, is as follows.

1. The stone size should be at least three times the diameter of the missile to be stopped. Flints and quartzites are the most effective of the easily available stones.

2. The stone content should be approximately 60 per cent by weight, the mastic approximately 40 per cent.

3. The mild steel backing plate should be between 10 and 30 per cent of the weight of the panel.

4. The thickness of panel should be 9 to 10 times the diameter of the missile to be stopped.

8.3.1 Effect of Variation of Components

The effect of varying the thickness, or weight per unit area, of plastic protection is shown in Figure 1. The effects of varying some of the other specifications have been studied by testing panels with small-caliber bullets, and the results of these tests are outlined below. These results are tentative, since the large number of tests needed to establish statistically significant differences have not been made.

Type of Stone

Test panels have been made using a wide variety of types of stone. The results of testing these panels show rather conclusively that flint and quartzite are better than other easily available materials, and that softer or weaker stones are not satisfactory.

Similar tests have been made of panels containing steel balls in a plastic binder.[3] No direct comparisons between this and the normal variety of plastic protection have been made.

Size of Stone

Panels made of stone of several sizes have been tested, and panels using stone of uniform size and stone of graded sizes have been tested. The results of these tests show that the average dimensions of the stone should be at least three times the diameter of the attacking bullet, and that the use of stone of a more or less uniform size results in slightly better protection than is provided by an equal quantity of stone graded in size up to a maximum of about three times the bullet diameter.

Type of Mastic Binder

Several mastic binders have been used, and a choice between asphalt and coal-tar pitch cannot be made on the basis of present knowledge. A few panels were made for experimental purposes using gelatin binder and these were definitely inferior to those made with asphalt or coal-tar pitch binders. Tests of slabs made with different types of asphalt indicate that the binder should have a high tensile strength, but this conclusion is based on a small amount of data and the tests do not include materials of a very high tensile strength. It is quite possible that after a certain tensile strength is reached, a further increase in tensile

strength of the binder will add very little to the protective value.

Proportions of Materials

Slabs have been made using various proportions of stone and mastic binder. It has been found that the best protection for a given weight of material per square foot is given by a mixture containing between 55 and 65 per cent of stone by weight. If the stone component is more than 70 per cent by weight there may be difficulty in pouring the mixture into vertical molds. Most plastic protection used at present contains about 60 per cent of stone by weight.

Backing Plate

Slabs made with and without backing plates have shown by test that a backing plate adds materially to the protection. Without a backing plate, material may be ejected from the back face, while a backing plate tends to keep the material in place and thus aids the material in stopping the bullet.

A number of tests have been made in attempts to find a substitute for steel to be used for the backing plate. The only satisfactory materials are other metals; these are usually more expensive but may be used if a nonmagnetic material is needed. They have no advantage over steel in terms of protection. Armor plate is slightly better than mild steel for use as a backing plate, but the extra protection can be attained more economically by using mild steel and a thicker slab of plastic protection. Plywood, fiber board, and similar materials are definitely inferior to steel.

In the present designs of plastic armor, the backing plate is usually from 10 to 30 per cent of the weight of the slab. The optimum thickness has not been determined.

Front Plate or Expanded Metal Reinforcing

Slabs have been made with and without a front plate of mild steel or armor. If the slabs are of equal weight per square foot (those without the front plate being thicker) the protective value is not significantly different for bullets striking normally. For bullets striking with obliquity, more ricochets occur from slabs having a front plate.

Expanded metal or some similar material is usually placed in the slab of plastic protection as an aid in holding the material together under heavy attack and to act as reinforcing for additional structural strength. It has been found that the addition of a layer of expanded metal is advantageous and that it is somewhat better to place the material near the front of the slab than to place it in the center.

8.4 RECOMMENDATIONS FOR FUTURE WORK

Plastic protection is a new material and has not been investigated thoroughly. It is a promising material for protection against small-arms fire and against fragments, and does not use large quantities of strategically important materials. For these reasons further investigations of plastic protection are highly desirable.

The usual means of determining the ballistic merit of a material in terms of thickness required to stop missiles having given characteristics and striking velocity cannot be used in studying the behavior of plastic protection. Statistical methods of analysis and interpretation must be used, and these methods require a large number of tests if the results are to be significant.

Chapter 9

TERMINAL BALLISTICS OF SOIL

9.1 INTRODUCTION

SOIL HAS BEEN USED more in military protective construction than any other material, from the parapet and parados of a foxhole to the large embankments used in major fortifications and the earth cover above deep underground storage of matériel. The use of very large bombs capable of deep penetration into soil requires a knowledge of the factors controlling the penetration of a missile into soil. The advent of the atomic bomb gives increased importance to a knowledge of these factors, since one obvious countermeasure to it is construction deep under ground. New weapons must be designed that are capable of penetrating to great depths so that buried enemy targets may be neutralized by deep explosion. Furthermore, it is essential to know what depth of burial will make our own vital points relatively safe against the weapons expected from the enemy.[a,b,c]

9.1.1 Studies of Soil Penetration

Most of the work on penetration into soils prior to World War II consisted of the determination of parameters in empirical equations that had been developed for other materials, with no systematic attempt to find whether the assumptions implied in the form of these equations were valid in the case of soils.

The early work on penetration into soils done in World War II consisted chiefly of ad hoc tests of specific projectiles or bombs, usually over a very limited range of velocities, and compilations of the depths of penetration of bombs dropped onto various soils. In many instances the dimensions and weight of the missile, the striking velocity, or the characteristics of the soil were not included in the reported data so that the results of these special tests cannot be correlated with each other or reduced to general relations. In 1943 the Committee on Passive Protection Against Bombing [CPPAB], National Research Council, in preparing a report on terminal ballistics and explosive effects,[10] found that the information available on penetration of bombs and projectiles into soil was entirely inadequate. Consequently, at the request of the Office of the Chief of Engineers, U. S. Army, the committee (later called the Committee on Fortification Design [CFD]) initiated a study of the terminal ballistics of soils. This was carried out by the committee in cooperation with Division 2, NDRC, and employed the Ballistics Laboratory of the Princeton University Station of Division 2. The results were reported to the Chief of Engineers, U. S. Army.[1] This test consisted of a systematic, though limited, study of the effects of striking velocity, projectile shape and weight, and soil type and condition on the penetration of projectiles and bombs into soils and into composite targets of earth and other materials. The Road Research Laboratory [RRL] of the Department of Scientific and Industrial Research (British) has also recognized the inadequacy of earlier information on penetration into soils and has made a systematic study of the effects of several variables on projectile penetration into soils, chalk, and gravel.[2,3]

9.2 PHYSICAL PHENOMENA THAT ACCOMPANY PROJECTILE PENETRATION

The penetration of projectiles and bombs into soils is characterized by wide variations in penetration observed under apparently identical conditions. These variations are attributed to instability and tumbling of the projectile and to the curved trajectory usually observed near the end of the penetration path. The penetration is dependent on many of the physical properties of the soil, such as the grain size and distribution, the density and degree of compaction, the moisture content, and the presence of large stones or voids. For example, a projectile will penetrate from two to three times as far into rich clay as into coarse sand; thus stratification of the soil or other variations in composition along the trajectory will have an appreciable effect on the depth of penetration.

Projectiles penetrating a cohesive soil generally form conical craters, wide at the entrance and tapering for nearly the full length of the penetration path. A large mass of soil is displaced by the projectile, the

[a] Pertinent to War Department Projects CE-5 and CE-6 and to U. S. Navy Project NO-12.

[b] See Chapter 5 for general discussion of terminal ballistics.

[c] See Weapon Data Sheets 2A2*, 2A2a, and 2C1a in Chapter 19.

soil in front of the projectile being compacted and sometimes pulverized. Near the surface, projectiles meet a comparatively small resistance to motion, since the surface breaks away and relieves the compaction. Farther below the surface the soil has been compacted by the overburden so that the resistance to deformation and to penetration increases with depth. If a projectile strikes soil at high obliquity it will tend to curve toward the surface, attempting to stay in a region of small resistance to motion. If the obliquity is great enough, the projectile will ricochet (see Weapon Data Sheet 2A5 of Chapter 19).

Ordinary projectiles are unstable in end-on motion through earth and tend to assume a side-on attitude. Once a projectile starts turning sideways, the forces resisting forward motion are asymmetrical with respect to the projectile and the trajectory will be curved. The projectile may even come to rest with the nose pointing back toward the point of entry. Blunt-nosed projectiles are more stable in motion in soils, with the possible exception of sands and gravel, than sharp-nosed projectiles; since they topple less quickly they present a smaller area to the soil and therefore have less resistance to motion.

Projectiles striking coarse sand at high velocity crush the sand into a fine powder. Jacketed Service bullets striking coarse sand at velocities above about 1,800 fps have the jacket stripped from the core and at higher velocities the jacket is torn into small pieces. At lower velocities the jacket is not stripped but is deeply scored.

9.3 EXPERIMENTAL INVESTIGATIONS OF PENETRATION INTO SOIL

Experimental investigations of penetration into soils require a knowledge of the shape and weight of the projectile used, its striking velocity and obliquity, the characteristics of the soil, and the effects achieved. The striking velocity of the projectile may be measured with any of the standard chronographs that have been developed for this purpose. Physical characteristics of the soil should be determined, including the classification of the soil, the grain size and distribution, the moisture content, the bulk density, and the dry density. Physical properties of the soils, such as the shearing strength, the compressibility, the bearing strength, and the Proctor needle penetration pressure, have not yet been related to penetration resistance, but if an analysis of the results is to be attempted in terms of the physical properties of the target, measurement of these and other properties should be made by the standard methods used in soil mechanics.

The effects on the target normally include the depth of penetration, the diameter of the conical crater at several depths, information on toppling of the projectile and curvature of the path, and any other data that may be desirable for special purposes. The objective of experimental work on penetration of projectiles and bombs into soils is to relate the measured effects on the target to the characteristics of the projectile, the striking angle and velocity, and the properties of the target.

9.3.1 Experimental Work at Princeton

In the fall of 1943 CFD of the National Research Council initiated a series of tests on terminal ballistics of soils using the range facilities of the Princeton University Station, Division 2, NDRC. The results of these tests were reported in July 1944 to the Chief of Engineers, U. S. Army.[1]

Penetration Tests

Penetration tests were made by firing .50-caliber special projectiles into a box filled with soil or into a mound of soil with a smooth face; all firings were horizontal and normal to the target surface. Velocities from 500 to 3,000 fps were obtained by using different powder charges, and the velocity of each round was measured by an Aberdeen-type chronograph using metal foil screens. Solid steel projectiles having various nose shape,[4] .50-caliber jacketed Service ammunition, and ½-in. steel spheres were used. Ogival-nosed projectiles of 1.5-caliber radius and having three different masses were fired to determine the effect of mass on penetration.

Sand, loam, and a rich clay were used as target materials. The characteristics of these soils as used are given in Table 1. The sand and the loam were placed in a large wooden box, 4 ft square and 2 ft deep, having a cloth face supported by wide-mesh wire screening on the aiming side. The rich plastic clay was stiff enough to hold its shape and was built into a mound about 5 ft wide, 8 ft long, and 2 ft high with a smooth vertical face on one side.

Two or three projectiles were fired into each target, using well-separated aiming points. Each projectile

[4] Flat, hemispherical, ogival of 1.5-caliber radius, and ogival of 3.1-caliber radius.

TABLE 1. Physical characteristics of soils used in ballistic tests at Princeton.

Type of measurement	Target material		
	Sand	Loam	Clay
Mechanical analysis (% by weight)			
Coarse sand, larger than 0.25 mm	90	36	14
Fine sand, 0.05 to 0.25 mm	10	28	9
Silt, 0.005 to 0.05 mm	0	22	19
Clay, smaller than 0.005 mm	0	14	58
Plastic limit, moisture (% by weight)	...	21	32
Liquid limit, moisture (% by weight)	...	27	60
Plastic index	...	6	28
Properties of the soils as used for penetration tests			
Moisture (% of dry weight)	3	18	35
Dry weight (lb per cu ft)	100	108	84
Proctor needle pressure (psi)	150	200	40

was then recovered by digging along the trajectory by hand, and the position of the projectile and the length of trajectory measured. A projectile can be recovered easily in clay because the crater remains open after penetration. The craters in sand collapsed and careful digging was necessary to find the projectiles without changing their positions.

The target was rebuilt and recompacted for each group of shots. Measurements of the density, compaction, and moisture content were made at frequent intervals.

Penetration Tests in Sand. All six types of projectiles were fired into sand at velocities of 500 to 3,000 fps. All of the projectiles were unstable and toppled at striking velocities above 800 fps. The trajectories were curved and the projectiles were frequently found to have undergone lateral motion from the point of impact as great as one-half the penetration. In some cases the path of the projectile through the sand could be determined by traces of discoloration, crushed or dried sand, or warm places in the sand, but in most instances the only measurements that could be made were the final position of the projectile with respect to the entrance point and its orientation.

There was a wide scatter in the data for penetration of each of the projectiles into sand. Penetration depths and lateral offsets differing by more than 30 per cent were common for rounds fired under supposedly identical conditions.

No appreciable difference in the penetration of projectiles having the same mass but different nose shape was found. Projectiles having the same size and shape but different masses penetrated to different depths in sand, the lighter projectiles, of course, penetrating less. Projectiles having ogival noses of 1.5-caliber radius, equal lengths, and masses differing by 30 per cent had penetrations differing by 11 per cent at same velocity. The ½-in. spheres had a mass 27 per cent of the mass of the projectiles with hemispherical noses and at the same velocity penetrated about 65 per cent as deep as those projectiles.

The .50-caliber ball M2 Service projectiles showed severe scoring of the copper jacket when fired into sand at low velocities. At velocities above about 1,600 to 1,800 fps the jackets were stripped from the cores, and at higher velocities the jackets were torn to small pieces.

Tests were made by firing into sand targets having different compactions and different water contents. These are related by the fact that the dry unit weight (weight per unit volume of dry component) due to a given compaction depends upon the moisture content of the soil. Changing the dry unit weight either by compaction or by changing the moisture content had approximately the same effect on penetration. Targets of low dry unit weight allowed greater penetration of the projectiles than highly compacted targets; increasing the dry unit weight from 91 to 103 lb per cu ft resulted in a decrease of about 20 per cent in penetration depth.

Penetration Tests in Loam. The penetration tests in loam soil were similar to those in sand. The same projectiles were fired over the same range of velocities, and penetration depths and lateral offsets were measured for each round. No tests were made of loam targets having different compactions or moisture contents.

The results were similar to those found in the tests of sand targets. The projectiles were unstable and toppled in the soil, the long-nosed projectiles becoming unstable at slightly lower velocities than the flat- and hemispherical-nosed projectiles. The scatter in the data for rounds fired under apparently similar conditions was not so great as in sand.

The blunt-nosed projectiles penetrated farther in the loam soil than did the sharp-nosed projectiles of the same mass. Compared to the projectile having an ogival nose of 1.5-caliber radius, the flat-nosed projectiles showed an increase in penetration of 15 to 20 per cent, the hemispherical-nosed projectiles showed an increase of about 7 per cent, and the projectiles having ogival noses of 3.1-caliber radius showed a decrease in penetration of less than 5 per cent. The blunt-nosed projectiles were stable in motion at higher striking velocities than were the sharp-nosed projectiles, and the

lateral offsets of the blunt-nosed projectiles were smaller.

Very few of the projectiles of different mass were fired into the loam target. The results were similar to those found in sand, but the small quantity of data do not allow definite conclusions.

The .50-caliber ball M2 Service bullets were fired into loam soil at velocities varying from 1,000 to 2,700 fps. Only a few rounds were fired, but the results were similar to the results in sand, with the jackets stripping from the cores at velocities above about 2,200 fps.

Penetration Tests in Clay. Penetration tests in rich plastic clay were made by firing the various types of projectiles into a mound of clay having a smooth vertical face on the aiming side. The craters remained open after the penetration and it was possible to trace the complete trajectory of each round. The blunt-nosed projectiles were usually stable in motion in clay, traveling for almost the entire length of the trajectory before toppling. The sharp-nosed projectiles toppled and moved sidewise through the clay.

The difference in penetration depth for the projectiles having different nose shapes was very pronounced in clay. Compared with the projectile having an ogival nose of 1.5-caliber radius, the flat-nosed projectiles of the same mass penetrated 60 per cent farther, the hemispherical-nosed projectiles penetrated about 15 per cent farther, and the ogival projectiles having an ogive radius of 3.1 calibers showed a decrease of about 5 per cent in penetration.

Projectiles having different mass but the same nose shape showed different penetrations, the light projectiles penetrating to smaller depths when fired at the same velocity. Only a few very heavy projectiles were fired, and the light projectiles having ogival nose shape of 1.5-caliber radius were unstable and showed wide variations in penetration, so that no exact conclusions can be drawn from the data for projectiles of this shape and of different masses. The ½-in. spheres had a mass 27 per cent of the mass of the projectiles with hemispherical noses and penetrated about 68 per cent as far as these projectiles.

A number of .50-caliber ball M2 Service bullets were fired into the plastic clay. None of the jackets was stripped.

No tests were made using clay targets of different compaction. An attempt was made to test the penetration resistance of dried powdered clay but this was not successful.

Perforation Tests

Tests were made using parapets built of soil, with sloping front and back faces. These parapets were tested by repeated fire, using .50-caliber ball M2 Service bullets, and the number of rounds required to perforate parapets of various sizes was determined. No chronograph was used, the velocities being determined from a calibration of the gun in terms of the powder charge. It was found that parapets with sides sloping one vertically on one and one-half horizontally were not good protection except for impact more than 12 in. (24 calibers) below the top of the soil; projectiles striking nearer the top curved upward and came out of the top of the parapet.

A cover of tarpaulin or similar material, stretched tightly over the top of the parapet and anchored to the base, increases the resistance to perforation by repeated-fire attack. The increase in protection varies with different soils and is greater for dry soils than for wet soils.

Perforation of Sand in Bags. Sand bags were simulated by building a box with two cloth sides and filling it with sand. The box was tapered, being thicker at one end than at the other, so that different thicknesses of sand could be tested. It was found that the cloth held the sand in place and thus caused an increase in resistance to motion of the projectile and of the mass of sand around the projectile. Rounds fired at velocities just below the perforation limit velocity caused a very tight packing of the sand against the rear cloth face. Rounds fired at slightly greater velocities perforated the target and ripped a hole several inches in diameter in the back cloth face; sand was ejected from the back of the target with sufficient velocity to cause a sandblasting effect on lumber 4 or 5 ft away.

The thickness of sand between two cloth faces needed for protection is the same or slightly less than the depth of penetration of the projectile into the same sand with no confinement. Tightly packed sand gives much more protection than the same thickness of loose sand, and moist sand is slightly better than dry material.

Composite Targets. A number of tests were made by firing vertically downward onto concrete slabs covered with loam soil. Concrete slabs 1½, 3, and 4½ in. thick were used and various thicknesses of soil were placed on top of the different slabs. The .50-caliber solid steel projectiles were used in all tests, and the striking velocity of each round was measured. The results have been reported to the Chief of Engineers, U. S. Army.[4]

CONFIDENTIAL

9.3.3 Penetration by Bombs

Many measurements of depths of penetration of bombs into soils have been made. These data have usually been obtained by probing into the crater and there is no way of knowing whether the probe was stopped by the nose, tail, or tail fins of the bomb, or by a large rock. Bombs usually take a J-shaped trajectory under ground, curving forward in the direction of the line of flight of the aircraft. If the curvature is great a probe will not follow the path to the base of the bomb and the trajectory- and penetration-path length cannot be measured without excavation. British measurements of bomb trajectories in chalk have been reported and show typical underground paths.[6]

Published compilations of bomb penetration data should be consulted for additional information.[6,7] In using these compilations, care must be used in comparing the results of measurements made by different methods and in comparing penetrations into soils that are not completely described.

9.3.3 Penetration by Large-Caliber Projectiles

There is very little reliable data on the penetration of large-caliber projectiles into soils. The experimental methods are difficult because the underground trajectories of large artillery projectiles are so long that considerable excavation is necessary. If small projectiles are used to minimize the difficulties of excavation the projectiles may be moved or lost with consequent loss of data. Furthermore, it is not known whether or not there exists a scale effect that may impair the reliability of predictions based on small-scale tests.

Some data on penetration of large projectiles have been recorded.[6,8] Most of the information on penetration by large-caliber projectiles into soils is based on the extrapolation of small-scale experiments conducted as described in Section 9.3.1. The available data on penetration by large projectiles and bombs must be used to confirm the methods of extrapolation.

9.3.4 Penetration by Rocket Projectiles

Rocket projectiles perform in the same way as other projectiles in penetration, with the possible exception of different stability due to the long body. Many present rockets are simply modifications of ordinary projectiles with rocket motors attached.

Experimental work on penetration of rocket projectiles into soil is described in Volume 1 of the Summary Technical Report of Division 8, NDRC. These experiments show that control of underground motion can be achieved by properly shaping the nose of the rocket.

9.4 RESULTS OF TESTS

No complete theoretical treatment of penetration into soils has been developed. The experimental work using projectiles having the same nose shape and different masses, described in Section 9.3.1, shows that the penetration of these projectiles at a given velocity is not proportional to the mass of the projectile. Thus soil penetration does not follow a relation based on a sectional-pressure theory (see Chapter 7). If penetration is not directly proportional to the mass of the projectile, the obvious conclusion is that the resistance to motion is not dependent on the velocity alone but must also depend on depth. This might be expected for soils, since the compaction increases along the path.

Empirical relations between the striking velocity, projectile mass, projectile nose shape, type of soil, and length of penetration path have been devised and are presented graphically in Data Sheets 2A2* and 3A2a of Chapter 19.

9.4.1 Dependence of Penetration on Striking Velocity

The dependence of the length of the penetration path in soil on the striking velocity of the missile is given graphically in Data Sheet 2A2*. No analytical expression for these empirical curves has been found. The dependence of the penetration path length on the velocity is different for each soil and for each projectile shape in the same soil, and the differences cannot be treated by simple multiplicative factors.

9.4.2 Dependence of Penetration on Projectile Mass

The small-caliber penetration data described in Section 9.3.1 show that the penetration-path length is not directly proportional to the projectile mass. An analysis of the penetration data for projectiles having the same shape and different masses shows that the penetration is proportional to a power of the mass between 0.25 and 0.40. The value ½ gives a good fit to the data and one then obtains:

$$x = W^{\frac{1}{2}} f(v),$$

or

$$\frac{x}{d} = \left(\frac{W}{d^3}\right)^{\frac{1}{3}} f(v), \qquad (1)$$

where x is the penetration-path length in in., d is the

projectile diameter (or caliber) in in., W is the projectile weight in lb, and $f(v)$ is the function expressing the dependence of penetration on velocity.

The small amount of data for penetration of large-caliber projectiles into soils and the available data for penetration of bombs into soils have also been studied and have been found to be in agreement with equation (1). The value of the exponent of the weight has not been determined with great accuracy, largely due to the scatter in the available data. The value ⅓ fits the data well enough to allow penetration predictions having an accuracy of ±20 per cent.

Equation (1) is considered reliable for projectiles having caliber densities W/d^3 between 0.15 and 0.65 lb per cu in. This equation must be used with the curves given on Data Sheet 2A2* of Chapter 19 which give $f(v)$ as a function of the striking velocity v. For soils having compositions differing from those listed on the data sheet, and for projectiles of other nose shapes, one must interpolate between the curves.

9.4.3 Dependence of Penetration on Projectile Nose Shape

The curves given in Data Sheet 2A2* of Chapter 19 show the different dependence of penetration on striking velocity for projectiles of three nose shapes. The penetration is always greater for blunt-nosed projectiles since these show less tendency to topple and therefore usually have straighter underground trajectories than do sharp-nosed projectiles.

9.4.4 Shape of Underground Trajectory

Most projectiles and bombs have curved underground trajectories, so that the final depth of penetration is less than the length of the penetration path. For striking obliquities of 30 degrees or less, measured from the normal to the surface, the underground trajectory of bombs is such that the final depth below the surface is 70 to 90 per cent of the penetration-path length. For striking obliquities greater than 65 or 70 degrees from the normal to the surface, the missile is likely to have a very short underground trajectory and to ricochet. For intermediate obliquities the penetration is usually shallow with a large forward offset.

Very little is known about the magnitude of the offset of bombs in underground travel except that this offset, the tail of the J-shaped trajectory, is generally in the direction of flight of the aircraft dropping the bomb. A graphical representation of a number of observed offsets is given in a British study of bomb penetration.[8]

Bombs and projectiles striking hard or resistant layers of soil are usually deflected. If a bomb strikes a horizontal layer of rock or other resistant material near the end of its normal underground trajectory, it will tend to travel along the hard surface.

9.4.5 Perforation of Soil Parapets

Soil parapets used for protection should be built with sides having a slope no greater than 1 on 1½ to insure against slipping when struck by projectiles. For protection against single hits, the thickness along the line of fire should be at least three times the expected penetration-path length in a large mass of the same soil, and to resist repeated fire of 10 hits close together the thickness along the line of fire should be about five times the expected penetration-path length of a single hit. The addition of a tarpaulin stretched tightly over the surface of the parapet and anchored to the base will increase the protective value. For .50-caliber bullets adequate protection is not provided except for levels 12 in. or more below the top of the soil because the bullets curve upward and come out of the top with appreciable residual velocity. No information is available on the distance below the top for protection against larger projectiles.

9.4.6 Perforation of Sand in Bags

Sand in bags is a good material for stopping small-caliber bullets. The sand should be very tightly packed in the bags, and the protection is better if the material is moist. Sand parapets should be built so that the thickness is at least as great as the expected pentration of the attacking weapon into a large mass of the same sand with no confinement.

9.4.7 Perforation of Composite Targets of Concrete and Soil

Composite targets of concrete and soil should always be constructed with the soil on the attacker's side. If the concrete has Q per cent of the thickness needed for protection with no soil cover, then soil having a thickness of $100 - Q$ per cent of the penetration-path length to be expected in a large mass of the same soil should be used to provide adequate protection. If the protection is against bombs or projectiles having striking velocities below 1,000 fps, the thickness of the soil should be about 25 per cent greater. If the protection is against high-velocity weapons the soil thickness may be slightly less.

If the thickness of soil cover over concrete is great enough to retain the projectile, there is always the

possibility of a tamped side-on explosion of a delay-fused projectile that fails to perforate the concrete. (See Chapter 3 for discussion of explosions in earth.)

9.4.4 Model Tests of Soil Penetration

Much valuable information on penetration into soils can be obtained by model testing. Equation (1) and the curves of Data Sheet 2A2* of Chapter 19 indicate that for model tests of penetration into soils the model projectiles must be geometrically similar to the prototype and of the same density. Comparison of data for bombs and for small-caliber projectiles indicates that if the soil particles are small compared with the projectile, scaling of the soil is not necessary. No investigation has been made of the effect of overburden on a soil on penetration. This may be important in small-scale studies of deep penetrations.

9.5 THEORIES OF PENETRATION INTO SOILS

A number of theories have been suggested to represent the performance of projectiles penetrating resisting mediums. The more important of these theories are reported in the bibliography.* (See also Chapter 7 of the present volume.)

9.5.1 Sectional-Pressure Theories

Most of the theories suggested for penetration into soil are based on the assumption that the pressure, or force per unit area, resisting the projectile motion is dependent on the velocity of the missile and not dependent on the depth of penetration. This assumption leads to the conclusion that if the target characteristics, striking velocity, and projectile shape are held constant the final depth of penetration is directly proportional to the sectional pressure (weight divided by cross-sectional area) of the projectile. Such theories are called *sectional-pressure theories* and predict that for projectiles of the same diameter and striking velocity but of different masses the penetrations into a given target should be directly proportional to the masses of the projectiles. As shown in Section 9.4.2, this is not in agreement with the experimental facts. This indicates that penetration into soil does not follow a sectional-pressure theory and that the force resisting the motion varies with depth.

Penetration into soil can still be described by a sectional-pressure theory if the dependence of the resisting force on depth be attributed entirely to the increase in cross-sectional area presented to the soil by toppling of the projectile, the resisting force being the product of the force per unit area which is dependent only on the velocity and the cross-sectional area of the projectile as presented to the soil, which increases as the projectile topples. According to this hypothesis the penetration of spheres into soils should follow a simple sectional-pressure theory (since spheres cannot topple). No data on penetration of spheres of different densities are available, and no test of this hypothesis has been made.

9.5.2 Sectional-Energy Theories

If the pressure resisting the motion of a projectile through soil depends on the depth of penetration and not on the velocity of the missile, the final depth of penetration must be some function of the striking kinetic energy of the projectile divided by its cross-sectional area. Theories based on this assumption are called *sectional-energy theories*. One conclusion from such theories is that for projectiles having the same shape and diameter the final depth of penetration into a given target must be proportional to the striking kinetic energy of the projectiles. Comparison of the penetrations of projectiles having different masses and fired at velocities such that the striking kinetic energy will be the same, shows that penetration into soils does not follow a sectional-energy theory. It appears, therefore, that the force resisting the motion does not depend on the depth alone.

9.5.3 Requirements of Penetration Theory for Soils

A satisfactory theory of penetration into soils must cover the instability and consequent toppling of projectiles. The resisting pressure, or force per unit area, may depend upon the velocity, the depth, or both. In any case, the total force resisting the motion is the product of this pressure and the cross-sectional area presented to the soil by the projectile, and so must increase as the projectile topples.

In Section 9.5.1 it was shown that the pressure, or force per unit area, resisting the projectile motion is not dependent on the velocity of the projectile alone, and in Section 9.5.2 it was shown that this pressure is not dependent on depth alone. One may expect any satisfactory theory of penetration into soils to include a force that depends upon both the depth of penetration and the velocity of the missile at all points along the trajectory.

16 RECOMMENDATIONS FOR FUTURE WORK

Since burial in earth is one of the most obvious protections against aerial attack and was being used on an increasingly large scale at the end of World War II, it can be expected to be one of the primary defensive devices of the future. The introduction of the atomic bomb will undoubtedly accelerate this trend. While present knowledge of the terminal ballistics of earth is not by any means complete it is probably adequate in most respects for present needs, or, at any rate, is consistent with the state of knowledge in comparable fields. But since the development of weapons and of defense against weapons will not maintain the status quo it is necessary to examine present knowledge in the light of future needs.

The following possibilities seem important:

1. First-priority targets, such as command and communications centers, shelters for very important personnel, etc., may be at very great depths, possibly hundreds of feet; other important targets, including power stations, vital manufacturing plants, stores of weapons, or other equipment, will also be buried. The two questions that will arise are: Can the enemy's protection be defeated by any means? Have we adequate protection against the enemy's weapons?

2. High-explosive (as contrasted to atomic) weapons will continue in use. No doubt these may be larger and contain a more powerful explosive than present weapons and may be delivered to the target by other means, but their mode of action will be no different. Such weapons may be capable of very great striking velocities and penetrations greatly exceeding those now possible.

3. Atomic weapons may be designed for creating earth shock. To do this they will have to be able to penetrate to very great depths to achieve maximum efficiency. The mechanism within the bomb must be able to withstand the resulting deceleration without either failure or premature action.

4. The fuzes used with high-explosive weapons of the future will be capable of finer adjustment than present fuzes in order to cause detonation at the most desirable point of an underground trajectory. With deep penetrations this will be an important consideration.

5. Bombing accuracies will be far better than are now possible. On this account, and because individual weapons will be very much more expensive and complex than are present bombs, it will be economical to have weapons that are equipped with adjustments for securing optimum performance against specific targets. In order to take full advantage of the potentialities of future weapons it must be possible to predict their trajectory and behavior before exploding.

On account of the probabilities that have been mentioned, the following investigations ought to be made:

1. Penetrations into mediums other than those already studied, such as gravel and soft rock, ought to be investigated. It is probable that soft earth is an extreme case, in that penetration in it is governed by its density while steel and concrete are equally extreme in the other direction in that penetration is governed by strength. For intermediate materials, such as soft rock, both strength and density may be of comparable importance. Of course, the striking velocities must cover a range extending far above those now used.

2. The time-distance relation during penetration will be needed for accurate fuzing of weapons. This requires either a better knowledge of the mechanics of penetration than we now have or a large number of direct measurements of the time-distance relation during actual penetrations. Such measurements might be a necessary preliminary to the development of a penetration theory. Again, a wide range of striking velocities, including high velocities, must be used.

3. A knowledge of the forces and decelerations of projectiles in earth and soft rock is needed. A penetrating weapon must have a case strong enough to withstand the greatest forces acting on it. On the other hand, excessive strength is generally undesirable since it reduces the amount of explosive. Furthermore, the fuzes and other mechanisms designed to operate just prior to detonation must be able to withstand the greatest decelerations to which they are subjected.

4. The stability of a projectile in earth is of great importance. Present projectiles tend to turn sidewise during penetration. This effect is generally undesirable since it reduces the total penetration considerably. On the other hand, instability may sometimes be desirable for limiting penetrations. Presumably, instability depends on the density of the medium and on the weight and dimensions of the projectile, especially its nose shape. It is known from small-scale experiments that blunt-nosed weapons are the more stable. Stable underwater rockets have been developed and many are found to be stable in earth. A systematic study of this problem is recommended with the aim of designing weapons of maximum stability.

5. The existence of a scale effect should be tested, since small-scale experiments are far more economical than large.

6. The influence of gravity, i.e., of the earth pressures due to gravity forces, needs study if very great penetrations are under consideration. Under normal penetrations, gravity pressures are so small in comparison to the dynamic forces opposing the motion of a projectile in earth that only the latter are important. On the other hand, if penetrations are of the order of hundreds of feet, the influence of the static earth pressure may be considerable.

7. The resistance of targets composed of earth in combination with other materials, especially concrete, needs study at large scales to supplement and confirm the results of the small-scale tests that have been made.

Chapter 10

THE FRANGIBLE BULLET FOR USE IN AERIAL GUNNERY TRAINING

10.1 INTRODUCTION

THE INVESTIGATIONS presented here are the results* of an attempt to solve the problem of training aerial gunners by having them fire live ammunition at an attacking pursuit airplane, thus simulating the conditions of combat. It was hoped that a bullet could be found that would be able to withstand the stresses in the firing process but be defeated by relatively light armor and therefore be suitable for use in a training program.

The project had its initiation in the late spring of 1942 and was carried out on an unofficial basis by Division 2 at Princeton and Duke Universities. In March 1944, the project was brought under official NDRC auspices and was carried on under a contract (OEMsr-1284) at Duke University and under subcontracts with the Bakelite Corporation and the American Time Products Company.

Many other groups contributed significantly to the technical and organizational aspects of the project. These included the Frangible Bullet Project, Laredo Army Air Field, Laredo, Texas; the Remington Arms Company, Bridgeport, Connecticut; the Explosives Department, E. I. DuPont de Nemours Company, Wilmington, Delaware; the Air Technical Service Command, A.A.F., Wright Field, Dayton, Ohio; the Ballistics Research Laboratory [BRL], Aberdeen Proving Ground; Frankford Arsenal and the Philadelphia Suboffice of the Ordnance Department; Operations, Commitments, and Requirements, A.A.F. Headquarters, and Air Ordnance A.A.F., Washington, D. C.; the Schnacke Manufacturing Company, Evansville, Indiana; Eglin Field and Buckingham Field, Florida, and the Fort Worth Headquarters, Training Command, A.A.F.

10.2 FUNDAMENTAL INVESTIGATIONS

10.2.1 The Plastic Bullet

As a result of preliminary tests carried out at Duke and Princeton Universities under Division 2, in which ceramics, bakelites, glasses, and various light metals were tried, it was concluded that a bullet consisting of a dense material in a plastic binder might have the desired qualities of frangibility and resistance to firing stresses.[1-4] Arrangements were therefore made with the Bakelite Corporation to supply molded materials for fabrication into bullets, which were then tested for their suitability. The tests included measurement of the limit impact velocity of the bullets against a given target metal, their ability to withstand loading and firing, and their stability in flight. It was decided that a composition designated as Bakelite RD-42-93 and consisting of 200-mesh lead powder in a thermosetting phenolic-resin binder was the most promising, and it was therefore adopted for the production of a frangible bullet, subsequently called the T44 bullet by the Ordnance Department. The bullet produced from the plastic is approximately of the same shape as the .30-caliber M2 ball bullet, weighs 6.95 ± 0.11 g (1.07 ± 1.5 grains) and has a specific gravity of 6.93. The ballistic tables for the bullet were determined at Aberdeen Proving Ground, and the ballistic coefficient on the basis of the T44 Siacci functions was found to be 0.163. The bullet may be fired through a Springfield rifle or .30-caliber Browning AC M2 machine gun with a muzzle velocity as high as 2,400 fps without showing signs of breakup or damage. The limit impact velocity of the T44 bullet against ¼-in. 24ST Dural armor plate is 1,750 ± 20 fps in comparison with 1,390 ± 20 fps for a .30-caliber ball bullet reduced to the mass of the T44 bullet. It was decided, on the basis of the requirements for pilot safety involved and the protection that could be afforded by the permissible weight of armor on the fighter plane, that a muzzle velocity of 1,360 fps was allowable for the T44 bullet. This gives ballistic performance such that a sight can be adjusted so that the leads (on a reticle diameter basis) required of the student gunner can be made practically identical with those required in combat with .50-caliber ammunition. The maximum practical firing range for the T44 bullet as now in use is about 700 yd and the maximum contact range is about 600 yd.

A number of variables in the production and use of the frangible bullets have been studied. It has been determined that variations in the lead-powder filler do not produce significant variations in the limit im-

*Pertinent to War Department Project AC-73.

pact velocity of the bullets and that considerable variation is possible in the time, temperature, and pressure during the molding process without appreciably affecting the resulting bullet. Similarly, no significant change occurs in finished bullets subjected to accelerated aging by heat or cold treatment. No difference was found in the limit impact velocity of bullets fired at room temperature and at —68 C against armor at room temperature.

On impact against light armor the frangible bullets break into fine particles. High-speed motion pictures show that the bullet disintegrates within 0.19 msec after impact against Dural armor at a velocity of about 1,300 fps.

In view of the desirability of having as broad a basis as possible for selection of the type of frangible bullet to be used in production, experiments for this purpose were carried out at the Division 3 Ballistics Laboratory at Princeton University, in addition to those carried on at Duke University. The Princeton laboratory made velocity-loss and time-of-flight measurements for six types of .30-caliber frangible bullets to determine their suitability. One of the bullets tested has the shape of .30-caliber M1906 ball and is similar to the T44 bullet in current use. Only one of the other five bullets tested showed a drag significantly less than the T44. This bullet, which had a secant ogive and boattail, showed a marked advantage over the T44 only for velocities below about 1,800 fps. However, this is the velocity range of interest since the T44 is fired at a muzzle velocity of 1,860 fps. A determination of stability factors and more precise time-of-flight measurements over longer ranges are necessary to indicate more clearly whether a bullet of this type offers a distinct advantage over the T44.

The Princeton Ballistics Laboratory has also done some preliminary work on a .50-caliber frangible bullet. The ballistic coefficient G_1 of this bullet was found to be approximately 0.25, which would give an acceptable "match" with the combat case for types of attack other than pursuit curve. However, data obtained for the limit impact velocity of the .50-caliber bullet against 24ST Dural show that it would not be safe to fire this ammunition at the present type of armored target planes when using a muzzle velocity as high as 1,860 fps.

10.2.2 The Reduced-Range Scheme

The problem of obtaining hits in aerial gunnery requires solution of a problem involving three vectors: the bullet-velocity vector, the bomber-velocity vector, and the fighter-velocity vector. By suitable reductions in all three vectors a reasonable facsimile of combat is achieved. The limiting factors are the minimum speed of the bomber and the amount of protection that the fighter can carry. These resulted in the choice of a bullet having a muzzle velocity of 1,860 fps. Ballistically, the training bullet should match the .50-caliber API-M8 bullet, now used in combat, as nearly as possible.

Perfect scaling is not possible because of the speed limitations that have been mentioned. While the trainer-bullet velocity is approximately half the combat-bullet velocity, the speed of the bomber can be reduced to only about 70 or 75 per cent of its combat speed. Higher trainer-bullet speeds would be possible only with heavier target protection. The lack of scaling is compensated for by changing the size of the reticle sight ring so that the gunner's leads on a "rad" basis, that is, in terms of the radius of the sight ring, are the same in training as in combat.

10.2.3 Armor

Along with experiments to determine a bullet suitable for air-to-air firing, certain other problems associated with use of the bullet came within the scope of this project. One of these is the ability of armor[1,2,6,8,9] of different types to withstand impact of the frangible bullet. This was investigated with the view to determining the type and thickness of armor necessary to use in armoring a plane to protect the pilot and essential plane parts. Different armor plates were compared on the basis of their limit impact velocities.[b] Limit impact velocities at normal incidence (90 degrees) were obtained for all plates and at other angles of incidence for some plates, since certain parts of the target plane need only be protected from hits by bullets striking at an angle of 45 degrees or less.

Three general types of armor were studied: first, Dural armor plate of various types (thicknesses 1/16, 3/32, 1/8, 3/16, 1/4, 5/16, 3/8, 1/2, and 3/4 in.); second, steel armor manufactured by the Jessop Steel Company (thicknesses 3/32, 1/8, 5/32, and 3/16 in.); and third, Doron, which consists of laminated layers of closely woven fiber glass bonded with plastic (thicknesses of 8/64, 13/64, and 26/64 in.).

Of the Dural plates tested, Alcoa 24ST and Reynolds .301T were found to be the only types that could

[b] The velocity of the bullet that damages a test plate sufficiently to produce a scatter pattern of 5 to 10 fine perforations on a sheet of 30-lb drug bond paper 6 to 8 in. behind the target.

be used efficiently in armoring a target plane in terms of protection afforded and weight of metal.

Bare 24ST Dural plate is superior to Alclad plate of equal thickness. It was also found that, within limits, higher-strength materials, as measured by static-testing procedures, are superior to those of lower strength. Preliminary tests indicate that multiple-thickness armor is slightly less effective than a single sheet of comparable thickness. Low temperature (—50 C) increases the limit impact velocity of ¼-in. 24ST Dural by about 50 fps for the .30-caliber bullet T44, although the armor appears to become somewhat more brittle. Temperature cycling has no perceptible effect on limit impact velocities. Experiments on firing more than one shot at the same area of armor indicate that several single shots fired in slow sequence at armor known to resist one such shot do relatively little more damage than one shot, but a machine-gun burst of an equal or reduced number of shots hitting the same spot may perforate the armor.

The Jessop steel armor is more resistant, on a weight for weight basis, than the 24ST Dural armor in thicknesses of Dural greater than 0.350 in. In lower thicknesses, the Dural is more effective.

The limit impact velocity of ⅛-in. Doron is about the same as that of ⅛-in. 24ST Dural plate. However, the damage inflicted on Doron by impact of bullets is so great that the maintenance problem involved in using such material in armoring a plane prohibits its use.

Experiments with 5-ply $1\frac{7}{64}$-in. multiplate glass of the type used around the cockpit of the target airplane showed that this provides adequate protection against the T44 round, since the limit impact velocity of such glass is above 1,000 fps. The second of two shots hitting the same small area of the plate with a velocity of approximately 1,550 fps can perforate the glass, but will not do so if the shots hit as much as 1½ in. apart. A sheet of Plexiglas back of 5-ply $1\frac{5}{32}$-in. multiple glass increases its limit impact velocity, as previously defined, by about 300 fps.

10.24 Propellant

One of the difficulties experienced with the T44 round as loaded in a .30-caliber M1 case was the procurement of a satisfactorily functioning propellant.[1,9,10] With the relatively low muzzle velocity of the round (1,360 fps) only a small powder charge (of the order of 0.80 to 0.95 g) is used, and because of the considerable air space, relatively low pressures prevail during the burning of the powder.

The primary requirements of a propellant suitable for use with the T44 bullet were found to be (1) that it have low position sensitivity (as regards its location in the case with respect to the primer location), (2) that it burn relatively completely, and (3) that in firing the round the modified machine gun function properly. The position sensitivity and approximate amount of unburned powder remaining after firing were determined for a number of different Hercules and DuPont powders. It was found that the small-grain fast-burning powders leave little unburned powder in the gun, but that the muzzle velocity obtained with them is quite sensitive to the position of the powder in the case, whereas the large-grain longer-burning powders leave considerable unburned powder in the gun but are relatively position insensitive. The tests indicate that the requirements of low position sensitivity, proper gun functioning, and small unburned residue are incompatible in the round as used at present and that some compromise must be made. It was felt that, in the light of these requirements, DuPont No. 4759 powder was the best of those tested.

Since a wide range of temperatures, varying from room temperature to approximately —50 C are encountered in the use of the T44 round, the average muzzle velocity was determined for nine production lots of T44 rounds at 25, 0, and —50 C. The average temperature coefficient between 0 and 25 C for the eight lots loaded by the Western Cartridge Company and St. Louis Ordnance Plant is about 4.5 fps per degree centigrade. This value is considerably higher than that of the one lot from the Frankford Arsenal (temperature coefficient = 2.8 fps per degree centigrade).

In firing the T44 production rounds, it was found that the standard deviation of the average muzzle velocity was frequently greater than the acceptable standard deviation of 30 fps. One of the factors that might contribute to the deviation was the variation in moisture content of DuPont No. 4759 powder. Since little information was available on the effect of moisture on this particular powder, experiments were carried out to determine (1) the effect of exposure to constant relative humidities on the weight of powder and (2) the muzzle velocity obtained with powder conditioned at different relative humidities. It was found that for powder conditioned two days at a relative humidity of 70 per cent subsequent conditioning at 85 per cent relative humidity increases the

weight of the powder approximately 0.15 per cent. Firing tests show that the average muzzle velocity may be expected to decrease about 9.8 fps per 0.10 per cent increase in moisture content of the powder.

10.3 MODIFICATIONS OF PLANE AND ACCESSORY EQUIPMENT

10.3.1 The Machine Gun

The regular .30-caliber AC M2 machine gun will not function as an automatic weapon[1,2,9,11-16] when the T44 round is fired through it with a muzzle velocity of 1,360 fps, since the momentum and muzzle blast are considerably smaller than that of the standard .30-caliber round. In view of this, two modifications of the gun were made, one of which (the piston gun) has been found satisfactory under experimental field conditions.

In the piston gun, the muzzle blast is trapped in a cylinder-piston assembly and the pressure developed gives the barrel and associated parts the required energy for automatic operation. The rate of fire of the piston gun is influenced by the type of nozzle on the gun, but the rate does not vary significantly for small variations in powder charge. The dispersion of shots on a ground target is considerably less with the modified piston gun and T44 round than with the .50-caliber machine gun and .50-caliber ammunition. However, comparable dispersion occurs in air-to-air firing.

Comparison of average muzzle velocities of rounds fired through new and used barrels showed that there was no significant variation in the average muzzle velocity due to difference in barrels.

10.3.2 The Plane

The solution to the problem of firing live ammunition at a real airplane[1] must involve a compromise between the weight of the armor that can be put on the target plane and the limit impact velocity of the bullet used against such armor. Therefore, the decision as to the weight and velocity of the bullet and the armoring of the airplane had to be considered simultaneously.

As a first approximation, successful aerial gunnery requires the proper solution of a sighting problem involving the bullet-velocity vector, the bomber-velocity vector, and the fighter-velocity vector. It appears that a reasonable facsimile of combat can be obtained by proper scaling or reduction of all these vectors. The limit of the reduction factor is set by the lowest speed at which it is practical for the bomber to fly. It is necessary also to consider the additional weight of armor permissible on the fighter plane. Finally, the matching conditions between combat and training conditions require a bullet with as high a ballistic coefficient as practicable.

In general, the most important type of attack from the standpoint of training is the pursuit-curve approach of the fighter. In such an attack, if firing is excluded during and after the breakaway, the sections of immediate vulnerability are those surfaces that are visible from a cone defined by a solid angle of 12 degrees and centered along the line of flight of the airplane. The first two types of target planes were armored for use solely with pursuit-curve attacks. The first consideration was always the complete protection of the pilot compartment and the most vulnerable parts of the airplane. A secondary consideration was the limitation of damage to a minimum.

Three types of target airplanes have been produced to date. The first was an A-20 airplane armored under the supervision of the Aircraft Laboratory, ATSC, Wright Field. The last two types are modified P-63 airplanes produced by Bell Aircraft Corporation and designated as RP-63-C and RP-63-G. The last type of airplane (RP-63-G) was armored so as to be usable for other than near pursuit-curve approaches in training and also to allow for the possible higher impact velocities in the B-29 training program. It is not contemplated, however, that continued fire will be directed against the armored airplane from any angle other than those involved in pursuit-curve or near pursuit-curve approaches.

The only difficulty of significance that has arisen in connection with the armor protection is an occasional failure of the cooling duct louvers on the RP-63 type airplane to afford adequate protection for the radiator located behind the louvers. A new louver has been designed which presumably will solve this problem. In general, it has not been necessary in field practice to replace any piece of armor because of excessive damage on surfaces where complete protection was intended. As far as is known only three pieces of 1-in. bullet-resistant glass have been replaced because of bullet damage.

10.3.3 The Hit Indicator

An essential feature of the target airplane is a hit-indicator[1] system. The primary features of the system used are as follows:

1. An impulse pickup placed on the armor plates so that an electric impulse is developed by the gauge when the plate is struck.

2. An amplifier unit by means of which the generated signal is amplified.

3. A thyratron-controlled trigger circuit and associated counter, relay, and lamps for signaling to a gunner when a hit has been made and allowing scoring of such hits.

The installation used in the RP-63-C target airplanes was furnished, with the exception of the wiring of airplane and signal lamp, by the Sperry Gyroscope Company. The gunner signal lamp is mounted in the cannon tube and may be seen easily within a cone of solid angle of about 30 degrees centered about the long axis of the airplane.

The functioning of this installation was somewhat unreliable because of spurious triggering and difficulty in proper adjustment of the time-delay relays; therefore considerable work was done toward designing an improved hit-indicator system. The American Time Products Company and the Bell Aircraft Corporation have designed amplifiers. The Duke project has constructed two sets of low-cost pickup units, each of which appears to have considerable promise when used with proper filters in the amplifier.

10.2.4 Use of Coupled Instructor's Turret

It became obvious in connection with the broad training program being developed for use with the T44 frangible bullet that the development or modification of several accessory pieces of equipment would help to improve the training. Thus, it was pointed out by Army personnel that it would be desirable for the instructor to be able to criticize the student at the actual time an attack is made. The best way to do this seemed to be through the development of an instructor's or slave turret[1,16] driven by the student's turret.

It was decided that the most immediate solution of this problem would result from the adaptation to this purpose of the central-station fire-control system developed by the General Electric Company [GE] and used on B-29 airplanes. In this adaptation, the gunner's turret controls another turret in which an instructor may observe the action of the student while firing at the attacking plane. An upper-rear turret of the B-29 was modified so that it would carry an instructor and would reproduce the movements in both azimuth and elevation of a Martin turret which would be operated by a student gunner. The Martin turret was fitted with the necessary selsyn generators to enable it to drive the instructor's turret in proper alignment.

An N8-A gun sight mounted in a deflectometer was attached to the sight yoke of the instructor's turret. A camera was mounted so that it was possible to make photographs and visual observations simultaneously.

Measurements were made to determine the accuracy with which this instructor's turret follows the driving turret. These measurements indicate that the accuracy of alignment of the two turrets is such that no significant errors in the evaluation of the student gunner would result.

Further preliminary work has been done in this general connection in arranging a selsyn-controlled range system so that the range setting on a computing sight in the Martin turret is reproduced on a computing sight mounted in the instructor's turret. Such a system should also prove of value in the B-29 training program.

10.2.5 Modification of K-15 Sight

Another investigation of equipment accessory to the training program involved a study of the possibility of modification of the K-15[1] sight for use with this bullet. The operation of the K-15 sight was therefore studied to determine the feasibility of making a simple adaptation of it for this purpose.

The sight and a motion-picture camera were mounted on a revolving turntable fitted with a fixed pipper. The camera was focused on a semicircular graduated scale, and photographs were made of the positions of the gyro reticle and the fixed pipper at various predetermined rates of rotation and ranges. Thus the combat leads developed for various settings of the sight can be determined from the photographs.

The most convenient method of modifying the K-15 sight for use with the T44 bullet at training speeds is by adjustment of the target-span handle (changing the effective wing span, and therefore the apparent range, of the target plane). The analysis of the data showed such a modification feasible if the following assumptions are made:

1. The fighter and bomber velocities are properly scaled so that the fighter paths in combat and in training are identical.

2. The fighter flies a lead-pursuit curve so that the lead ratio is 1.41 and the tracking-rate ratio is 0.71.

It must be pointed out that for pursuit-curve training, the maximum range for which the sight can be

used is about 450 yd on the present basis of modification without making changes in the internal electric system of the sight.

The data also revealed that there are time lags in the sight which may in some cases prove to be too large for the most effective use of the sight in combat gunnery.

10.4 FIELD TRIALS

The first field trials[1] of the frangible bullet were made using the armored A-20 target plane and a YB-40 bomber at Buckingham Army Air Field at Fort Myers, Florida. These tests proved the general validity of the use of the frangible bullet as a training procedure for aerial gunners. The major part of the remaining field trials of experimental nature have been carried out by the Frangible Bullet Project of the Laredo Army Air Field at Laredo, Texas, using the A-20 and RP-63-C target planes.

Some of the general limitations of the frangible bullet technique as brought out by field trials are listed in the following:

1. The long time of flight of the present frangible bullet, as compared to the time of flight of .50-caliber M8 ammunition, necessitates large prediction and deflection angles which accentuate the errors of all sights. The increased time of flight also gives the target aircraft more time to depart from a given plane of action.

2. The frangible bullet T44 is not stable if shot forward from an airplane going faster than 250 mph. This may be of concern in future training. This lack of stability can be remedied to a large degree by decreasing the pitch of the lands in the barrels through which the frangible bullet is fired.

3. The breaking of tips of the frangible bullets causes some trouble in gun malfunction.

10.5 PSYCHOLOGICAL ASPECTS

In the course of the development of the frangible-bullet technique and in its practical application to the training situation, questions frequently arose as to the psychological implications[1] of the scaling procedure used in connection with it, both with respect to the modification of sights and the alteration of plane speeds. In an attempt to obtain sound background information which would help in orienting the program in these matters several series of psychological experiments on the development and analysis of gunnery skills were run with untrained subjects. Tests were made with 61 subjects and involved 350 experimental sessions, representing some 23,000 pointing or tracking trials. The main types of trials included were pointing at a fixed target with variable deflections, tracking a moving target, and pointing with continuously varying deflections at a moving target.

Some of the many points of significance for the general gunnery-training problem brought out by these investigations are the following:

1. The desirability of some method, such as the instructor's or slave turret, for providing the student with a knowledge of his errors at the time of training.

2. Any evaluation of the relative contribution to the final overall firing errors attributable in a given sight mechanism to, say, tracking versus ranging should be based upon performance after training of gunners in the use of the mechanism. This would indicate that if it were possible to choose between automatic radar control of one or the other of these functions in the sight, this decision should be reached on the basis of trials by gunners trained on the basic sight mechanism and the results of such trials should be weighed along with engineering and design considerations.

3. Skill in tracking once acquired through training seems to be retained for a period of at least six weeks. On the other hand, there is a lack of retention of the skill acquired in the case where the student was trained to point a machine gun quickly at a target and at the same time give accurately a predetermined lead deflection away from the target.

Because of the limitations in number of subjects involved in these experiments, the conclusions indicated in the foregoing material must be regarded as preliminary in nature. However, they illustrate the possibilities of obtaining information of prime importance to a gunnery-training program from psychological experiments on student gunners, provided these are carried out with test equipment closely paralleling the gunnery situation itself. Such information should have important implications not only for the training program but in relation to such matters as the design and choice of sight mechanisms.

10.6 RESULTS

10.6.1 Closeness of Matching between Trainer and Prototype

An analysis of the general considerations that will result in reasonable matching of the leads used with

the frangible bullet with those required in combat shows that with proper adjustment of airplane velocities and sight reticle, and for pursuit-curve attacks, the match can be made quite satisfactorily.[1,17-21] Theoretical calculations of leads required of gunners firing at the target plane making attacks along curves of pursuit show that the leads, on a rad basis, are the same in combat and in training if the adjustments previously mentioned are made. The types of attacks considered were lead-pursuit and pure-pursuit attacks against bombers, parallel flight of fighter and bomber, support fire from a bomber formation against a fighter attacking a particular plane in the formation, and finally, fighter-fighter attacks.

10.62 Status of Project

The role that the frangible bullet can play in such matters as sight design and modification, study of aerial tactics, particularly in relation to fire from formations, in fighter-versus-fighter gunnery training and in certain naval gunnery-training problems has been studied.[1]

The status of the technique in the training of gunners in bombers as of V-J Day may be summarized as follows:

1. From the small beginning in November 1944 bullet production rose to a production capacity of from 40,000,000 to 45,000,000 per month in August 1945.

2. Some 800 armored target airplanes were produced for training by the spring of 1945. Prior to V-J Day, 450 additional planes with improved armor had been ordered; all but 30 of these were cancelled after V-J Day.

3. About 11,000 bomber missions, in which some 13,000,000 rounds of frangible-bullet ammunition were fired by student gunners, were flown in the seven gunnery-training schools in the United States.

4. It was stated just prior to V-J Day that all firing from the air in the gunnery program of the Training Command would thereafter be with frangible bullets.

10.7 POSSIBILITIES AND LIMITATIONS OF THE TECHNIQUE

The limiting factors at present are the minimum bomber velocity and the maximum weight of protection that can be added to existing planes for use as targets. Some improvement in the latter is possible by the use of specially designed target planes in which the protecting armor contributes to the structural strength of the plane instead of being simply added weight. With such improved protection, bullet velocities can be increased several hundred fps over the present velocities. This will permit closer scaling of plane and bullet velocities and reduce the modifications now needed in the sight and the compromises in the technique.

However, there is a limit to progress in this direction, due to the fact that combat-plane speeds and combat-bullet velocities will continually increase, making it increasingly difficult to build target planes strongly enough protected to withstand the bullet velocities required for matching.

PART IV

PROPERTIES OF MATTER

Chapter 11

DESIGN OF MODEL SUPERSONIC WIND TUNNEL

11.1 INTRODUCTION

THE FLIGHT VELOCITY of artillery projectiles has been for many years well in excess of the velocity of sound in air, which is about 1,100 fps. Aerodynamic data relating to the flight performance of a projectile can be obtained by studying its trajectory, but this is a slow and expensive method. In a wind tunnel, the projectile may be held stationary, while air is moved past it at high velocity, permitting the easy and quick determination of the aerodynamic forces acting on the model. For this reason, the desirability of a large supersonic wind tunnel became apparent several years before World War II. The construction of such a tunnel at Aberdeen Proving Ground was decided upon by the Ordnance Department.*

However, due to the rather special properties of air flow at supersonic speeds, certain of the design requirements for such a wind tunnel were not clearly understood. For this reason NDRC contracted with the California Institute of Technology in 1941 to construct a small-scale supersonic wind tunnel,[1] and in it to study the design and instrumentation problems connected with the construction and operation of a large supersonic wind tunnel. The specific problems which it was proposed to study were:

1. The compressor pressure ratios and power requirements at various air speeds.

2. The method of designing a nozzle to produce supersonic flow in the test section. Unlike a subsonic wind tunnel, the air speed in the test section of a supersonic wind tunnel is determined not only by the pressure drop through the tunnel, but also by the shape of the channel immediately upstream from the test section. Analytical methods are available for the design of this "nozzle"; it was desired to check these and to determine any necessary corrections. Each Mach number requires a particular shape and size of nozzle.

3. A method of supporting a model in the test section in such a way that the flow around the model remains essentially equivalent to that around the projectile in free flight. This problem is considerably more difficult in supersonic than in subsonic conditions.

4. Methods of observing the flow around a model and of measuring the forces acting on it. These consist principally of a *schlieren* optical system which makes

* Pertinent to War Department Project OD-24 and to Navy Department Project NO-3.

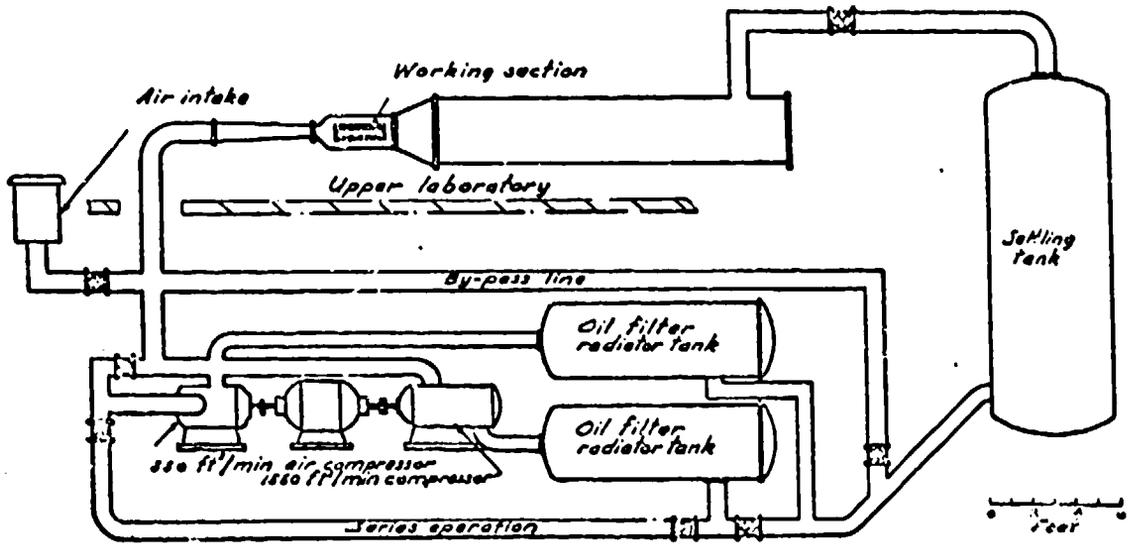

FIGURE 1. Compressor piping.

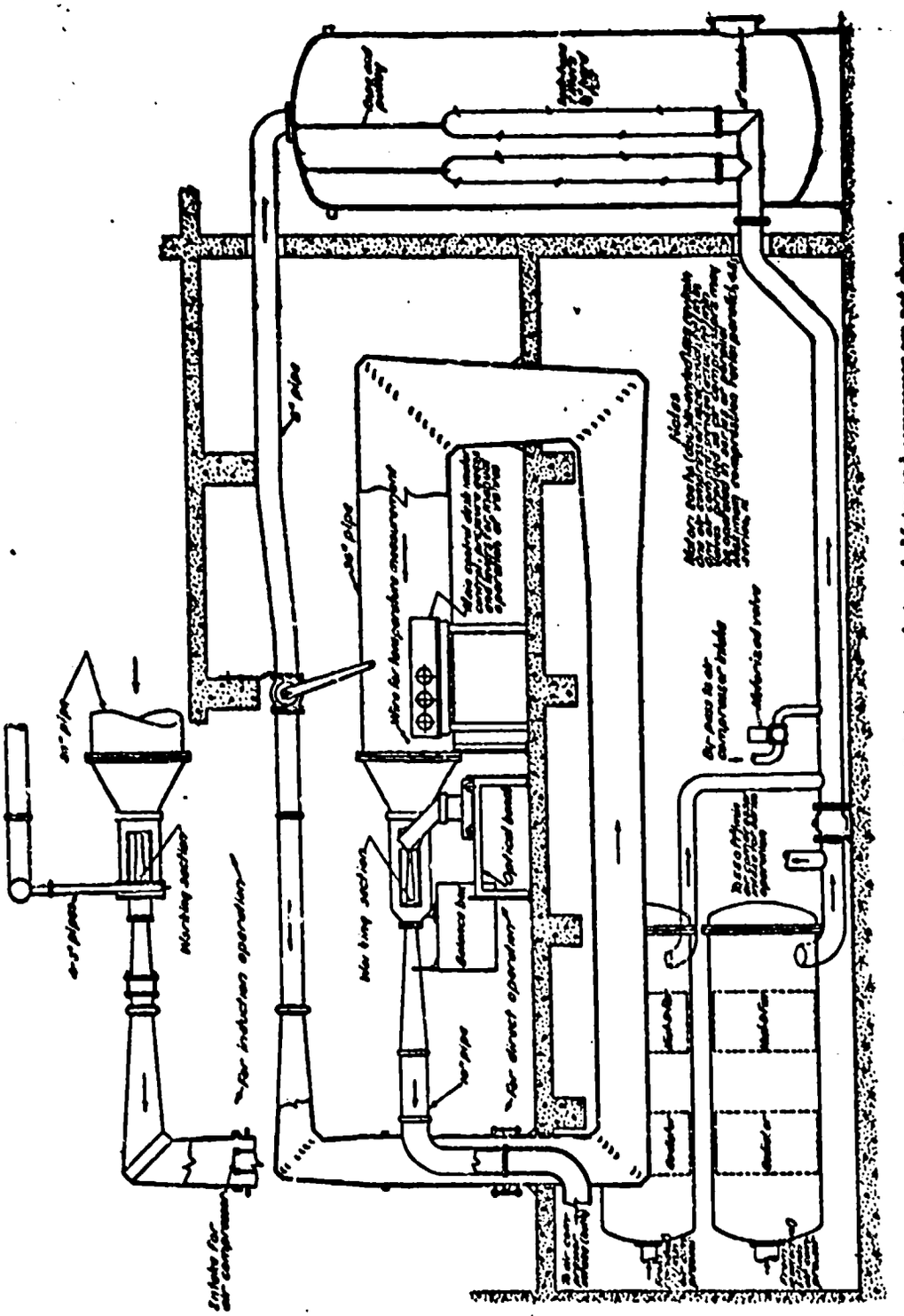

FIGURE 2. General layout (vertical section) of supersonic tunnel. Motor and compressor are not shown.

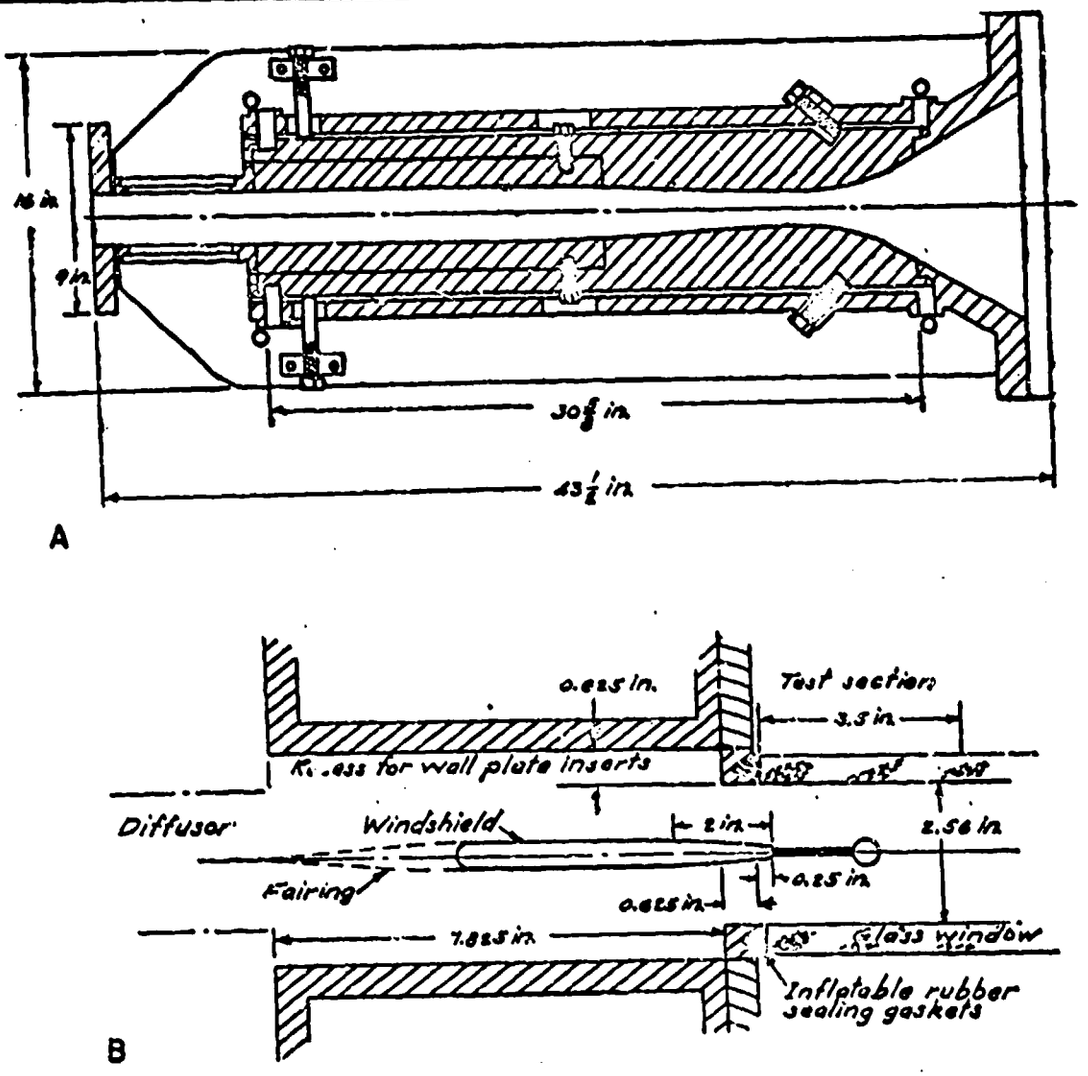

FIGURE 3. Working section. A. Vertical section. B. Horizontal section on test section axis.

visible the density gradients in the air in the test section and a balance system on which the model is suspended.

The small wind tunnel was constructed with a test section 2.5 in. square. It was operated through a range of Mach numbers from 1.2 to 4.4. (Mach number is the ratio of throat-section air speed to the local speed of sound.) Sufficient information was obtained on all of the above points to permit furnishing definite design data for the large supersonic wind tunnel at Aberdeen Proving Ground. Figures 1, 2, and 3 give details of construction.

11.2 PRINCIPAL RESULTS

The most important results of the above investigations can be summarized briefly.

1. In the determination of the pressure ratios necessary to operate the tunnel, it was found that a pressure recovery from the test section to the end of the diffuser can be effected by an amount comparable to that through a normal shock wave. In other words, a portion of the kinetic energy of flow at the test section can be converted to potential energy or pressure, thus diminishing the pressure difference to be overcome by the compressor. Curves of compressor

pressure ratio versus Mach numbers were obtained.

2. It was found practical to support projectile models by a single strut from the rear. This strut is connected to the balance system, which enters the channel to the rear of the model. The part of the balance system in the channel is shielded from the direct airstream by a windshield of special shape. It was found necessary to expand the channel around the windshield at low Mach numbers in order to avoid producing disturbances in the flow at the test section. Correct combinations of windshield shape and channel shape were found at all Mach numbers. A typical installation is shown in Figure 4 as viewed with the schlieren apparatus at a Mach number of 2.4.

3. The method of designing nozzles using the method of characteristics[2,3,4] was found to be satisfactory, although the existence of a boundary layer of retarded air along the nozzle walls necessitates some corrections.

4. The presence of walls in the test section does not affect the flow around the model if the latter is small enough. The permissible size of model depends on the Mach number, becoming less as the Mach number decreases toward 1. A blunt model 0.33 in. in diameter can be used in the 2.5-in. test section down to a Mach number of 1.8; below this speed, the problems of model size and support system make testing very difficult if not impractical. The relation of Mach number to permissible model size was determined.

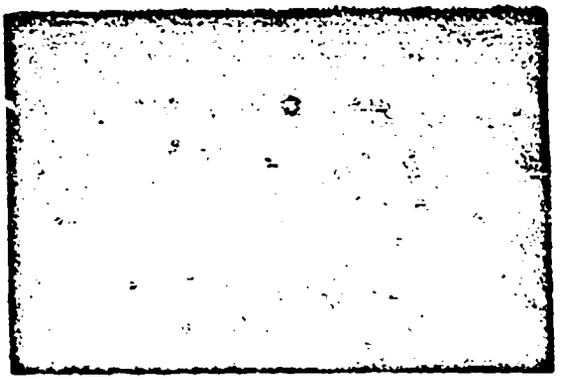

FIGURE 4. Schlieren photograph of flow at Mach number of 2.4.

11.3 CONCLUSIONS

The practicality and utility of a supersonic wind tunnel for investigating problems in ballistic aerodynamics was demonstrated. Various aspects of the design and instrumentation problems associated with such a wind tunnel were studied and satisfactory solutions found in all cases in the range of Mach numbers from 1.2 to 4.4.

Chapter 12

BEHAVIOR OF MATERIALS UNDER DYNAMIC LOADS

12.1 INTRODUCTION

12.1.1 Purpose of Investigation

EXPERIMENTAL AND theoretical investigations of the behavior of materials under dynamic conditions* were first undertaken by Division 2 as part of its program of fundamental research on the mechanism of projectile penetration and perforation. During the passage of a projectile through armor the material in the vicinity of the penetration receives very severe and very rapid distortion. It was believed that a knowledge of the effect of deformation rate on the relation between stress and strain and on the occurrence of brittle rupture would be useful in any study of projectile penetration. During the progress of the work, various ad hoc military applications were made. These were generally experimental comparisons of impact strengths of materials, e.g., light alloys for airplane construction tested at low temperatures, steels to be used in underwater plating of naval craft, metal components of projectile fuzes, and small crusher cylinders or spheres for measuring explosive pressures in guns. A large part of the work was also concerned with two fundamental problems: (1) the manner in which plastic strain is propagated and (2) the effect of impact velocity on mechanical properties of metals.

12.1.2 Previous Investigations

EXPERIMENTAL WORK

For some time it had been believed that rate of straining or rate of stressing of a material has an effect on its stress-strain relation and on its resistance to failure. In 1904, Hopkinson[1] concluded that a soft steel can endure a stress several times exceeding its elastic limit without plastic deformation, provided the duration of loading is made sufficiently short. More recently, so-called notch-impact tests, intended mostly as a measure of the brittleness or notch-sensitivity of a material (not of the behavior under impact) have been much used. A number of investigators have, in addition, attempted to study the effect of deformation rate on the stress-strain relations of various metals.[2-11] The latest of these researches employed rotary-type testing machines,[8-11] capable of speeds up to about 200 fps and using specimens generally similar to standard tensile specimens. In those investigations in which forces were measured during each test, it was generally found that the dynamic force as a function of deformation was somewhat higher than the static force.[8-12]

THEORETICAL WORK

No analysis of the tensile impact test was attempted in the years preceding World War II. The propagation of elastic waves in materials was well understood, of course, but almost no attention was paid to waves in nonlinear media other than gases, which had been treated by Riemann[13] in the 1860's. In 1930, L. H. Donnell[12] showed that a longitudinal wave in a wire or bar with nonlinear stress-strain relation would suffer a continual change of shape due to the unequal speeds of the different levels of stress.

12.1.3 Progress of Work during the War

A considerable part, but by no means all, of the work done in this field during World War II was done by Division 2. In the following brief account, the work of other agencies will be included in order to give a fairly complete if not detailed picture.

The situation is complicated by the large number of organizations involved and by the variety of problems attacked. Within Division 2, work was done at the following laboratories: University of Pennsylvania, Carnegie Institute of Technology, California Institute of Technology, Massachusetts Institute of Technology, Westinghouse Research Laboratories, and Princeton University. Outside of Division 2, published work was done by NDRC Division 18, by Watertown Arsenal Experimental Laboratory, and by the British, especially at Fort Halstead by the Armament Research Department [ARD] of the Ministry of Supply. The methods of attack were partly experimental, partly analytical. The problems covered may be divided broadly between two classes: (1) those dealing with the manner in which plastic stress and strain are propagated (these received mostly analytical treatment with experimental verification) and (2) those concerned with the manner in which the stress-

*Pertinent to War Department Project OD-57 and to Navy Department Projects NO-7, NO-11, and NS-109.

strain relation of a material is affected by the impact velocity (these were treated experimentally, but with analytical explanation and discussion).

UNIVERSITY OF PENNSYLVANIA AND CARNEGIE INSTITUTE OF TECHNOLOGY

The first work in this field in the division was begun in September 1941, at the University of Pennsylvania. This project was transferred to the Carnegie Institute of Technology in November 1942 and ended in May 1944. The experimental work consisted in compression of small copper spheres and cylinders of the types used for determining explosive pressures in guns. Later, armor steels were tested. The apparatus consisted of a rotary testing machine capable of a peripheral speed of 100 fps. Dynamic force-deflection curves were obtained. In addition, theoretical investigations were made dealing with the propagation of plasticity in the compression-test specimens, with the propagation of the plastic zone in a thick plate due to an expanding cylindrical hole, and with the effect of an impulse on the material of a plate.

CALIFORNIA INSTITUTE OF TECHNOLOGY

Work was undertaken at the California Institute of Technology in March 1942 and consisted of the following:

1. Tensile impact tests on short specimens (up to 12 in.) of various metals, mostly steels, in a rotary impact machine capable of peripheral speeds up to 200 fps. The force-time relation during each test was obtained.
2. The development of analytical methods of treating the propagation of plasticity under impact in wires and bars, including the specimens tested in the rotary machine.
3. Experiments on long wires in a guillotine-type machine mainly for the purpose of testing the theory developed in (2) above.
4. Pure strain rate tests in which propagation effects were eliminated.
5. Compressive impact.
6. Rapid loading tests.
7. Miscellaneous experiments and analyses concerned with lateral impact on plates and beams and with perforation of plates.

In January 1944, the contract with the California Institute of Technology was transferred to Division 18, NDRC. Reference should be made to the STR of that division for a discussion of all the experimental work (both before and after the transfer) done under this contract. The theoretical work is discussed in the present volume.

MASSACHUSETTS INSTITUTE OF TECHNOLOGY

Experimental investigations of the behavior of metals at high strain rates were carried out between July and November 1942. The apparatus used consisted essentially of a piston fitting a cylinder containing explosive. Detonation of the explosive stretched and broke the tensile test specimen. These tests were intended only for comparison with those obtained by other division contractors and have not been published by the division.

WESTINGHOUSE RESEARCH LABORATORIES

From November 1942 to August 1944, experimental work on stretching of steel and nylon specimens at moderate rates of strain was pursued. These tests were primarily concerned with the propagation of the zone of yielding in materials having well-defined yield points.

12.2 THE PROPAGATION OF PLASTICITY IN SOLIDS

12.2.1 Plasticity

A plastic material is one that can be given a permanent deformation by the application and subsequent removal of external forces. The stress-strain relation of such a material (as obtained by means of the simple tensile test, for example) is usually curved, but with a straight initial portion. The removal of load gives an unloading line that is usually straight and parallel to the first part of the loading curve (Figure 1). Generally similar relations are obtained in other kinds of stressing, e.g., simple compression, biaxial or triaxial loading, etc. Most plastic materials are elastic up to a certain stress, the elastic limit, defined as the highest stress that can be reached in a stressing-straining cycle without leaving permanent strain. Normally, the elastic part of the stress-strain relation is linear.

12.2.2 Elastic Waves

The behavior of elastic materials under static forces or under impact is quite well known. For example, when a uniform wire or rod receives a longitudinal impulsive stress less than the elastic limit, the effect is to produce in the specimen a longitudinal stress wave which maintains its form and which travels along the

specimen with constant speed. The speed is equal to

$$c = \sqrt{\frac{E}{\rho}},$$

where E is Young's modulus, the ratio of stress to strain, and ρ is density, or mass per unit volume (weight per unit volume divided by g, the acceleration of gravity). Since stress and strain are related, such a

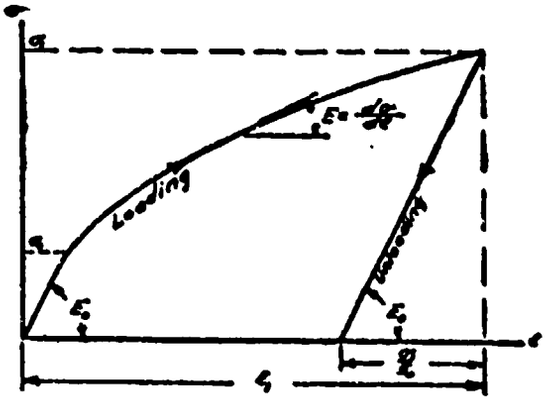

FIGURE 1. Stress-strain relation.

wave of stress is simultaneously a wave of strain. The stress σ, strain ϵ, and particle velocity V at a point of a wave in an elastic medium are related. For the uniform bar or wire at a point where the elastic waves are all moving in the same direction, the relation is:

$$\frac{\sigma}{E} = \epsilon = \frac{V}{c}.$$

A wave of this type travels unchanged until it meets a discontinuity of some kind, such as a fixed end, a free end, a change of section, or a change of material characteristics.

At a fixed end or at a free end the wave must be reflected totally. In the first case the reflected stress wave is exactly like the incident wave except for its direction of travel. In the vicinity of the fixed point, stress and strain are increased by the combination of parts of incident and reflected waves. Particle velocity, on the other hand, is diminished in this region due to interference of the waves. At the fixed point, stresses and strains are exactly doubled and particle velocity is exactly zero. At a free end, the reflected stress wave is the negative of the incident wave, stress and strain being of opposite sign to those of the original wave. Particle velocity, however, is in the same direction as in the original wave. In the vicinity of the free end, there is interference between the two waves in respect to stress and strain and reinforcement in respect to particle velocity. Exactly at a free end, the particle velocity is doubled, and stress and strain are permanently zero.

12.2.3 Plastic Waves[18-21]

In a plastic material the situation is complicated for the following reasons:

1. There is no longer a linear relation between stress and strain; in addition, the relations are different for increasing and for decreasing stress.

2. A wave does not maintain its form as it progresses. Rather, the front or region of increasing stress tends to become longer and longer, at least in normal cases.

3. The unloading wave travels faster than the wave front or loading wave, catches up to it, and tries to eat it away. This introduces complications into the analysis.

A wave of stress moving along a uniform member can be thought of as a series of very small waves, one superimposed upon the other. Each wavelet, of amplitude $\Delta\sigma$ and superimposed on a stress σ, has a velocity dependent upon its position in the stress-strain relation. In fact, its velocity will be a function of the stress σ, according to the following relation:

$$c(\sigma) = \sqrt{\frac{1}{\rho}\frac{d\sigma}{d\epsilon}}.$$

In this expression $d\sigma/d\epsilon$ is the slope of the engineering stress-strain curve at the stress σ. Since, in a normal plastic material this slope decreases with increasing stress, each stress wavelet moves slower than the immediately lower one. The strain at any point of the wave front is, of course, that corresponding to the stress at that point according to the stress-strain relation. The stress wavelet $\Delta\sigma$ gives rise to an increment of particle velocity

$$\Delta V = c\,d\epsilon.$$

Thus, the particle velocity V corresponding to a stress σ or to a strain ϵ in the increasing part of a wave front is:

$$V = \sqrt{\frac{1}{\rho}}\int_0^{\epsilon}\sqrt{\frac{d\sigma}{d\epsilon}}\,d\epsilon = \sqrt{\frac{1}{\rho}}\int_0^{\sigma}\frac{d\sigma}{\sqrt{\frac{d\sigma}{d\epsilon}}}. \qquad (1)$$

The quantity $d\sigma/d\epsilon$ is obtained as a function of either σ or ϵ by graphical differentiation of the engineering stress-strain relation.[18,19-21] Equation (1)

can be used to obtain the stress and strain resulting from a tensile or compressive impact velocity V, provided the corresponding stress-strain relation is used. See Section 12.2.8 below for a discussion of compressive impact.

12.2.6 Critical Tensile Velocity

In tension, the engineering stress-strain relation becomes horizontal at the ultimate strength of the material. If equation (1) is integrated to this point, the velocity so calculated is the critical tensile impact velocity. It would be expected that tensile impact at a velocity exceeding this critical velocity will always result in immediate necking and failure, with very little deformation away from the zone of necking. At velocities less than the critical, rupture may occur anywhere in the specimen, after reflection from a fixed boundary has occurred, and all of the member must participate in the deformation. Thus the energy required to break a member in tension is expected to be small at velocities above the critical. Experimentally, this conclusion is found to be correct. For most ductile materials the agreement between the critical velocity calculated according to the static stress-strain relation by equation (1) agrees well with that found experimentally in either the rotary- or the guillotine-type machine. This indicates (1) that the theory of equation (1) is at least approximately correct, (2) that the static and dynamic stress-strain relations for these materials are nearly the same. However, for one class of materials, mostly soft steels, which have a so-called yield-point at which a finite increase in strain occurs with constant or even decreasing stress, the agreement between observed and calculated critical velocities is not good. The conclusion is that the static and dynamic stress-strain relations differ considerably for such materials. This conclusion is supported by comparisons of dynamic and static deformation forces obtained in rotary machines[4,10-12] and was also reached by Hopkinson[1] on the basis of quite different experiments (Section 12.1.2). The critical tensile impact velocities of most ductile materials are of the order of 100 to 200 fps.

12.2.7 Reflection of Plastic Waves

The reflection of a plastic wave at a discontinuity resembles generally the reflection of an elastic wave. The problem is much more difficult to handle analytically in the plastic case but has been solved.[22-24] The reflection of a stress wave at a fixed end in an elastic member gives rise to stresses and strains that are exactly double those in the incident wave. If the material is plastic, the maximum reflected stress is less than twice and the reflected strain more than twice the maximum stress and strain in the incident wave.

12.2.8 The Unloading Wave

Normally, a stress wave has not only a front of increasing stress, but also a back part or tail in which the stress diminishes to zero. The behavior of the back of a plastic wave depends on the unloading stress-strain relation of the material. Normally, this unstressing relation is linear, but is steeper than the major part of the loading or stressing part of the relation. Consequently, the unstressing part, or tail, of the traveling wave tries to behave like an elastic wave and to move with a greater velocity than the plastic front. This means that if the member is long enough the tail of the wave will always catch the front and will tend to pass through it. Such a process is not possible; the back of the wave passes partly through the front and reduces it somewhat, is reflected from it, and returns as an elastic wave toward its starting point. At the starting point (the point of original impact) this reflected wave is again reflected and retraces its way to the more slowly moving plastic front. When the plastic front is reached by the new unloading wave the whole process repeats itself. At every such repetition the intensity of the plastic wave front is reduced, until it disappears or is reduced to the elastic limit of the material. The portion of the member in which this complicated process has taken place shows a nonuniform distribution of permanent strain. Near the point of impact the strain left in the member is that corresponding to the impact velocity as given by equation (1). At the point where the rear of the wave first overtakes the front of the wave the permanent strain begins to decrease and continues to decrease to the point in the member where the unstressing wave was reflected to the rear. Following this there is a short section of the member in which the permanent strain is constant; this is followed by a section of decreasing strain, then by a short section of constant strain, and so on. The stepped distribution of permanent strain in a specimen is illustrated in Figure 2. It is of interest to note that the stepped distribution of strain was observed experimentally only after its occurrence had been predicted from analysis.[16] For a more complete discussion of the behavior of the unstressing wave, reference should be made to the bibliography.[16,22,23]

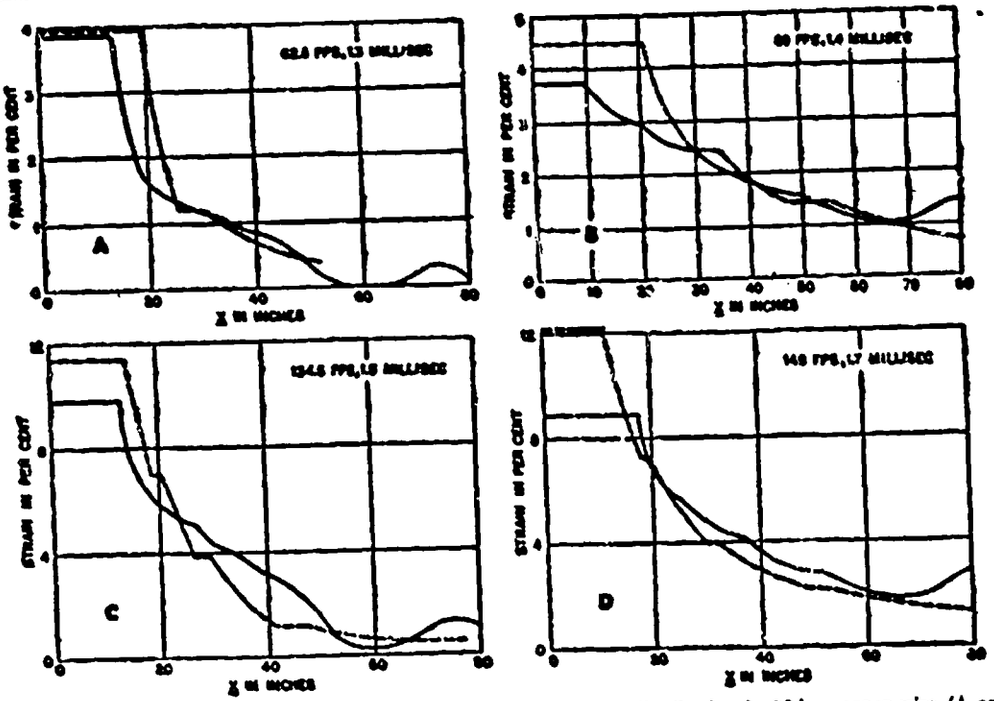

FIGURE 2. Theoretical (——) and experimental (——) curves of strain distribution in 80-in. copper wire (A and C) and in 80-in. aluminum wire (B and D).

12.2.7 Analysis of Impact Tests on Short Specimens

As stated above, although tensile impact tests had been carried out for several years before World War II there had been no attempt to analyze their results, it being assumed merely that the force deflection obtained dynamically gave the dynamic stress-strain relation of the material directly. It is now known that this assumption is not exactly correct. It is, however, possible to use the static stress-strain relation in calculating the expected relation between force and extension during a test. Any differences between the calculated and the observed relations can be taken to be at least partly due to differences between static and dynamic stress-strain relations. Unfortunately, the conditions of loading during a test are sometimes somewhat uncertain and may give rise to effects that obscure the results of such analyses. Of value in the analysis of impact tests is the explanation given for the existence and the method of calculating the critical impact velocity. Another contribution of plastic analysis to the impact tests is in connection with the afterflow or continuation of deformation that occurs in a tensile specimen after it breaks. Ordinarily this effect is small; however, occasionally it becomes important.[25] The theory of plastic wave propagation has also been used to aid in discussing the significance of measurements of energy required to break a specimen during the tensile test.[26]

12.2.8 Compressive Impact on a Uniform Member

The analysis of wave propagation in tension applies equally well in compression, provided the stress-strain relation is of the same form, i.e., concave downward. However, for large strains the compressive stress-strain curve must become concave upward (due to the fact that cross-sectional area increases under compression) and the analysis that has been outlined does not exactly apply. Some attempts at solving this problem have been made.[26,27] In the region where the stress-strain curve is concave upward a stress increment tends to move faster than the stress immediately smaller. Thus, a wave front tends to become steeper, not flatter, as it progresses. This change of shape can continue until an infinite stress gradient exists at the wave front. An infinite stress gradient, which may be thought of as a wave with a vertical front, then moves along the member. This is a kind of shock wave whose

characteristics, including speed and the relation between stress and impact velocity, are known. With increasing impact velocity the impact stress increases according to the shock-wave relations just mentioned and the material of the member acquires a velocity equal to the velocity of impact. However, above a certain striking velocity this is no longer true because the material is not strong enough to acquire the full velocity of the impact but tends to slough off sidewise against the striking body, while immediately in front of this region the member continues to approach the striking body. Thus the member behaves partially like a fluid. With increasing impact velocity this behavior is emphasized more and more until, at a velocity equal to or exceeding the speed of an elastic wave in the member, the behavior is exactly like that of a fluid, the impact pressure being dependent only on the density of the material and the velocity of impact, and not on its strength. In this limiting case,

$$\sigma = \rho V^2.$$

This theory has not been verified experimentally because of the velocities involved. Compression impact tests[25] on fairly long specimens were made at the California Institute of Technology project at velocities up to about 300 fps, and the results are outlined in the STR of Division 18. The calculated critical compressive impact velocity for a particular annealed copper is 600 fps and for hot-rolled 1018 steel, 1,500 fps.[26]

12.2.9 Transverse Impact on a Thin Wire

This problem was first treated for the plastic case by English investigators, but was also solved at the Princeton Station of Division 2. It is found that two distinct propagations occur in the wire. There is a stress wave propagated as in normal longitudinal impact. There is also a kink that moves along the wire away from the impact point. In this case also there is a critical velocity, above which deformation is confined to the vicinity of the point of impact. The critical velocity in transverse impact is greater (by a factor of 2 or 3) than for longitudinal tensile impact. For materials whose tensile strain at the ultimate stress is small compared to unity, the following expression gives the approximate ratio between the transverse critical velocity V_1 and the tensile critical velocity V of equation (1):

$$\frac{V_1}{V} = \left[\frac{2}{V}\sqrt{\frac{\sigma_u}{\rho}} - 1\right]^{\frac{1}{2}} . \qquad (2)$$

In the above expression σ_u is the ultimate tensile stress, and ρ is density (weight per unit volume divided by g, the acceleration of gravity). For the annealed copper of the previous section having a critical compressive velocity of 600 fps, the critical transverse impact velocity is calculated to be 450 fps while the critical tensile velocity is only 160 fps.

A practical application of this analysis is to the problem of the behavior of balloon mooring cables when struck by aircraft. (During World War II, certain German planes were equipped with cable cutters on the leading edges of wings.) The critical transverse impact velocities of steels are in the range 250 to 600 fps and thus are within the range of operating speeds of aircraft.

12.2.10 Behavior of Thin Diaphragms under Impulsive Pressure

If a thin diaphragm receives a sudden impulse of short duration it tends to move bodily, with constant velocity in the direction of the impulse. However, the edges of the diaphragm cannot move and therefore give rise to stresses and deformations which are propagated inward with constant speed. Until these reach a point on the sheet, that point has not been affected by the boundaries and has moved exactly as though there were no boundaries. Thus it can be seen that, immediately after such an impulse a diaphragm has a shape resembling a pie plate, being flat over the central region and with curved or sloping edges. The kink that separates the flat and the sloping areas moves inward, diminishing the former and enlarging the latter. (This shape occurs for any uniformly distributed pressure, even if not of short duration.)

If the diaphragm is long and narrow, the influence of the short sides of its behavior can be neglected except in their vicinity. Such a diaphragm when subjected to an impulse (of very short duration) behaves exactly like the wire discussed in the preceding section except that it is necessary to consider the interaction of stresses and kinks from two edges meeting at the center. An additional consideration is that the stress-strain relation for a member that is unable to contract in one dimension (like the diaphragm) differs somewhat from the normal tensile relation. Thus there is a critical impulse for such a diaphragm—the impulse that gives it a velocity equal to the critical transverse velocity of the material according to equation (2), making due allowance for the lateral restraint. An impulse per unit area exceeding this would be expected to cause immediate failure at the boundary.

The behavior of a circular diaphragm is generally the same, but more difficult to analyze. There is a critical impulse per unit area equal or approximately equal to that for the long, narrow diaphragm. Experiments with such diaphragms subjected not to impulsive pressure but to suddenly applied, nearly constant pressure show clearly that the central part of such a diaphragm remains flat until reached by the kink coming from the edge. The characteristic shape of a dynamically loaded and distorted, but unbroken, diaphragm differs markedly from the shape of a statically loaded one, being very much more conical.[20] Identical results are obtained in the case of diaphragms subjected to shocks from underwater explosions. (See Chapter 1.)

It must not be assumed that an impulse smaller than the critical impulse will not break a diaphragm. The significance of critical impulse is that a greater impulse will cause failure at the boundary with very little absorption of energy, while smaller impulses can result in failure at the center but with considerable absorption of energy.[20]

12.2.11 Lateral Impact on Beams

This problem has been solved analytically for the plastic case and the results found to agree reasonably well with experiments.[20,21] The solution is based on that obtained by Bousinnesq[22] for the elastic case. Due to the fact that bending is the governing factor rather than tensile stress as in the case of the thin wire, the results differ considerably from those obtained for the wire. In particular, it is found that for a constant impact velocity on a very long beam the quantity y/t (deflection divided by time after impact) is a function of the quantity x/t^2 (distance from the point of impact divided by the square of the time). In other words, all deflection curves obtained during the first stages of impact at constant velocity on a long beam can be reduced to a single curve if deflections are divided by the time and distances from the impact by the square of the time. There is found to be an impact velocity below which no permanent bending will occur. This depends only on the material and the cross-sectional shape of the beam but not on its size. For structural steel I beams the elastic limit velocity is about 25 fps. Over a certain range of velocities just above this value, permanent bending will occur only in the vicinity of the point of impact. Over a range of velocities immediately higher there will be two regions of permanent bending (of opposing curvatures), one under the force, the other moving along the beam. For still higher velocities there will be three zones of permanent bending, etc.

12.2.12 Concentrated Impact on Plates

This problem was attacked both experimentally and theoretically in the California Institute of Technology project.[23-26] The experiments were made in the guillotine-type machine on ¼-in. steel plates 7 in., 2 ft, and 6 ft in diameter, at velocities ranging from 0 to 200 fps. Two theories were developed, one considering only plastic bending of the plate, the other ignoring bending strength and considering only tensile stresses in the plane of the plate. The experimental results appear to lie between the results of the two theories but somewhat closer to the bending theory. It was concluded that any satisfactory theory of the behavior of plates under concentrated impact would have to involve both bending and extensional effects.

12.2.13 Applications of Theory to Penetration and Explosion Phenomena

At the Carnegie Institute of Technology there were developed analyses applying to the mechanism of projectile penetration in thick plates[26] and to the effects of an explosion in contact with a plate.[27] In the first case, the propagation of stress and deformation in a very thick plate due to an expanding cylindrical hole is studied. This is based on and is an extension of work dealing with a similar problem in which propagation effects are ignored.[28] The second analysis deals with the propagation of a plane pressure pulse across the thickness of a plate, with the reflection of the pulse on the far side and with the spalling that occurs there as a result.

Some experimental work on the mechanism of projectile penetration was carried out at the California Institute of Technology.[29]

12.3 EFFECT OF IMPACT VELOCITY ON MECHANICAL PROPERTIES OF MATERIALS

The object of this work was to determine in what way and how greatly the mechanical properties of a material, such as yield strength, ultimate strength, strain at rupture, etc., are affected by the impact velocity at which deformation is produced. Most of this work was at very rapid rates of straining in which specimens 6 to 12 in. long were broken at velocities up to 200 fps. One series of tests was run at much lower rates, of the order of a fraction of an inch per

minute. Nearly all tests were on metals, mostly steels; one series employed nylon. The work was almost entirely experimental but with analyses aimed at explaining or interpreting the experimental results.

The work was conducted under four contracts, of which the largest, at the California Institute of Technology, was transferred to NDRC Division 18 in January 1944. The experimental work carried out at the California Institute of Technology both before and after this transfer is outlined in the STR of Division 18 to which reference should be made.

12.2.1 High-Speed Compression Testing

This work was started under contract with the University of Pennsylvania and was transferred to the Carnegie Institute of Technology in the fall of 1942. The original purpose was to determine the difference in the force required to compress copper crusher spheres and cylinders by a given amount dynamically and statically. Crushers are used for measuring the explosive pressures in guns, being placed in a cylinder closed at one end and with a piston or plunger closing the other end and in contact with the crusher. The far side of the piston is connected to the chamber of the gun whose pressure is to be measured. Explosion forces the piston against the crusher, compressing it by an amount that is used as the measure of the maximum pressure in the gun. The crushers are calibrated statically and it was believed that the static force-deformation relation might not be reliable in giving the impulsive force. Work was not confined to copper crushers, however; specimens of armor steels were also tested.

Apparatus

The testing machine[43,44] (Figures 3, 4, and 5) consists essentially of a heavy steel wheel which is

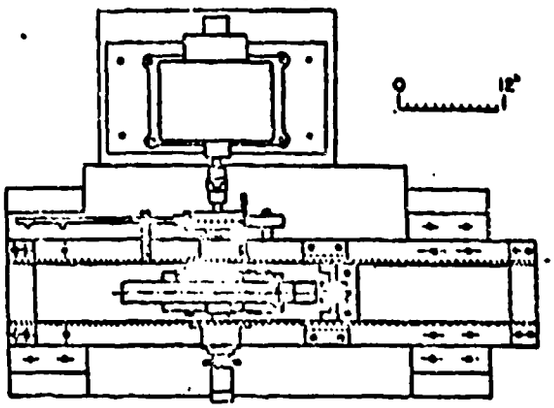

Figure 3. Top view of high-speed compression machine.

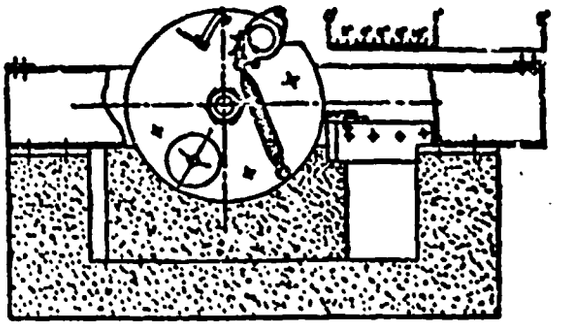

Figure 4. Side view of high-speed compression machine.

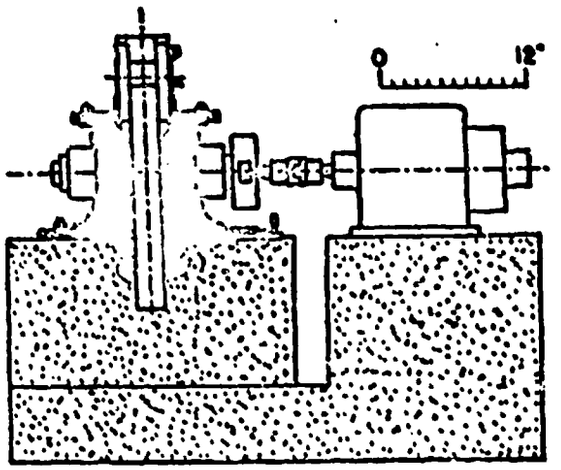

Figure 5. End view of high-speed compression machine.

rotated at the desired speed by a ¾-hp d-c motor. Peripheral speeds ranging from about 7 to 100 fps are possible, although all tests have been in the range between 16 and 60 fps. Near the periphery of the wheel are two horns mounted on bearings. Normally, these are cocked back within the circumference of the wheel but when released by a solenoid trigger they are swung out beyond the periphery by two heavy coil springs into position for striking and compressing the specimen. The hammer is supported between the horns and fits into a niche in the wheel when in the retracted position. A ⅝-in. notched steel rod passes through the hammer and the two horns, holding the former in place. The amount of compression of the specimen is limited by two adjustable hammer stops which are struck by the hammer after the desired compression has taken place. The rod supporting the hammer is then sheared off at the notches, allowing the hammer to be withdrawn from the neighborhood of the wheel by two coil springs to which it becomes attached upon impact.

The force applied is measured by a two-crystal quartz piezoelectric gauge mounted between the hammer stops. The specimen to be compressed is normally from ⅛ to ½ in. long and is placed directly on top of the crystal unit. The charge generated on the crystals by the compression force is fed into the horizontal component of a cathode-ray oscillograph [CRO], giving the spot a horizontal displacement proportional to the force. Calibration of the crystal and oscillograph is obtained by applying a known static force to the crystal and releasing it suddenly, at the same time photographing the horizontal displacement of the oscillograph spot. The vertical component of the oscillograph trace is the deformation of the specimen, being controlled by a beam of light, aimed at a photoelectric cell connected to the vertical component of the oscillograph, which is cut off by the motion of the hammer during impact.

Experimental Results

Force-deformation curves have been obtained for small-arms copper cylinders, copper spheres, and for cylinders of armor steel. In each material the dynamically obtained relation is from 15 to 30 per cent above the static relation (i.e., the force required dynamically is greater by this amount than the static force to give an equal deformation). Furthermore, the dynamic curve is not smooth but consists of a series of steps presumably corresponding to the successive reflections of the stress wave at the end of the test specimen.

Table 1 summarizes the results[40-44] obtained for 0.400-in. copper cylinders of a particular brand. It will be noted that the magnitude of the speed effect appears to change very little over the whole range of dynamic tests, being about 25 per cent. Other brands of copper cylinders of the same dimensions as those in Table 1 and also supplied by Frankford Arsenal were tested and found to give similar results.

Table 1. Speed effect in 0.4-in. copper crusher cylinders by compression impact, set: 0.12 in.*

Rate of strain (sec^{-1})	Average ratio of dynamic to static stress
30	1.23
470	1.26
705	1.24
940	1.30
1175	1.28
1410	1.28
1645	1.29

*Furnished by Frankford Arsenal. Designation of metal: 1942 P. O. 42-25501-Lot 2, annealed in October 1942.

Tests on copper spheres showed much more variation between similar specimens than did the tests on cylinders; there appeared to be a speed effect averaging about 30 per cent.[44] Because of the lack of reproducibility of results, spheres appear to be less suitable for use as crushers than do cylinders.

Measurements on specimens of homogeneous armor 0.375 in. long and 0.171 in. in diameter showed a speed effect of between 20 and 25 per cent for strain rates up to 1,500 sec^{-1}. These results were obtained during the early stages of the project and are not believed to be as reliable as the results on copper.

Analyses of Tests

A calculation of the expected force-time relation during dynamic compression of copper cylinders was made,[41] using the method of analysis based on plastic wave propagation that is described in Section 12.2. This shows that the force during impact should contain a number of small steps instead of being perfectly continuous; these steps are observed in the experiments. The calculated force is found to be smaller than the measured force and the amount of this difference, which is approximately the amount given in Table 1, is believed to be due to a difference in the static and dynamic stress-strain relations of the material.

A calculation has been made of the amount of additional deformation produced in a specimen after removal of the dynamic load and due to its own inertia.[42] It was found that this additional flow is negligible in situations corresponding to the normal uses of copper crusher gauges.

Tests on Long Specimens

Compression tests on specimens about 12 in. long were conducted at the California Institute of Technology. These were designed to investigate the propagation phenomena under compressive loading by methods similar to those used in tension and to attempt to correlate the results with analysis.[43]

12.3.2 High-Speed Tensile Testing

Practically all of the high-speed tensile tests[40-41] made for the division were carried out at the California Institute of Technology. Since all experimental work under this contract is reported in the STR of Division 18, to which this project was transferred in January 1944, only a brief description of the equipment used and of the nature of the tests will be given here.

Apparatus

Two types of testing machines were used. One is a rotary machine capable of peripheral speeds up to about 200 fps and used with specimens up to 12 in. long. This machine consists of a large wheel with two fixed horns near the periphery. Impact is produced by mechanically inserting a yoke directly under the

Figure 6. Rotary impact testing machine.

wheel which permits contact of the horns with the tup, which is attached to one end of the test specimen. The specimen is thereby stretched and broken in tension, causing the fixed end to exert a force on the steel dynamometer to which it is attached. The extension of the dynamometer alters the resistance of its wire winding. This impresses a potential on a CRO and permits recording the dynamometer force as a function of time. This machine has been used for investigating the effect of impact velocity on the force-time relations of various materials. Figure 6 shows details of the rotary machine.

The other is a guillotine-type machine (Figure 7) and is used for specimens of lengths up to several feet in tension, for compression, and for lateral bending of beams and plates. It is therefore used mainly for investigating propagation phenomena, although conclusions regarding the impact-velocity effect can be obtained from it as well as from the rotary machine. The machine consists of a pair of vertical steel rails between which slides a hammer attached to very heavy rubber bands. A tensile specimen passes through a hole in the center of the hammer and has at its lower end a steel block too large to pass through this hole. The upper end of the tensile specimen is attached to the framework of the machine. No measurement of the force in the specimen is normally made, although such measurements are possible. In making a test, the hammer is raised between the guide rails by means of a winch, thus stretching the rubber bands. When the hammer is released it accelerates rapidly, acquiring a velocity of any amount up to about 200 fps, depending on the distance raised and on the number of rubber bands. The velocity at the time of striking the specimen is measured electrically. The hammer is brought to rest by a braking system attached to the rails of the machine.

1222 Low-Speed Tensile Tests

These were carried out at the Westinghouse Research Laboratories and comprised two series of tests.[21,22] In the first series, nylon fibers and flat strips were stretched at rates ranging from 0.0042 to 8.70 in. per sec. The specimen gauge lengths were 2 and 3 in. The object of this series was to study the behavior of a material having a very definite yield point subjected to various rates of stretching. Such a material does not stretch uniformly from the beginning as do materials that have no definite yield point. Instead, plastic stretching for the full amount of the yield stretch first occurs suddenly at one point of the specimen. From this section two yield fronts travel toward the ends of the specimen. Between them the material

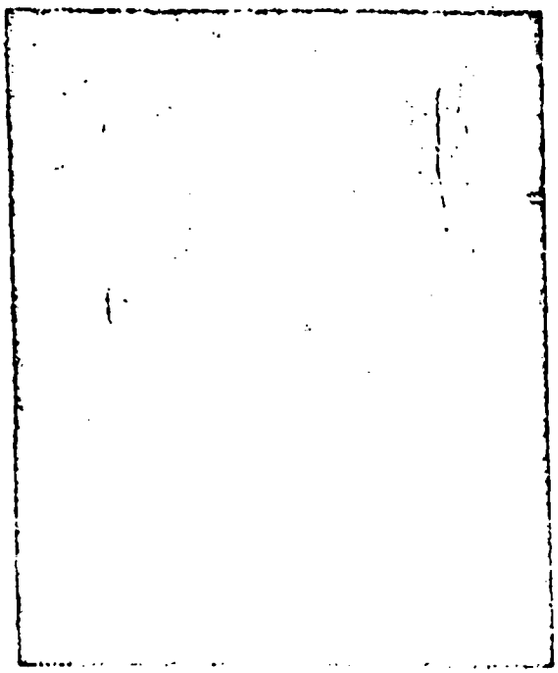

Figure 7. Vertical impact testing machine.

has its full yield stretch; beyond them there has been no plastic yielding at all. Not until the entire specimen has been covered by the advancing yield fronts does uniform deformation begin, which continues until necking occurs. This behavior is characteristic of mild steels.

The second series of tests was conducted on the mode of yielding of mild steel at rates of stretching ranging from 7.3×10^{-6} to 1.64×10^{-3} in. per minute. The variables studied were eccentricity of loading, length-to-width ratio of the specimen, speed of stretching, and rigidity of the testing machine.

Certain preliminary work on the propagation of yielding in materials having a well-defined yield point was carried out at the California Institute of Technology.[64]

12.2.4 Pure Strain Rate Tests

In investigations of longitudinal impact the results have generally been expressed as force-time curves during stretching, obtained at definite impact velocities. These results cannot be used to determine the effect of rate of straining on mechanical properties, in particular on the stress-strain relation, because in each test the rate of straining varies over very wide limits. Consequently, the results of longitudinal impact tests must be expressed in terms of impact velocity and not in terms of rate of straining.

In order to investigate the effect of pure strain rate[65,66] on the properties of materials, special equipment was devised at the California Institute of Technology in which a tubular specimen was employed. Deformation was obtained by means of fluid pressure within the specimen. Strain rates up to about 200 in. per in. per sec were attained. See also the Division 18 STR.

12.2.5 Preliminary Work on Rapid Loading

Some preliminary tests[67,68] have been carried out at the California Institute of Technology on rapid loading in contrast with impact loading. In impact loading, some particle or section of a structural member is almost instantaneously set into motion, whereas in rapid loading a particle or section is set into motion more or less gradually. It has been shown in the pure strain-rate tests that the proportional limit of a material is increased with increasing rate of strain. The work on rapid loading was directed primarily at determining the time that a given stress could be maintained at a given value when reached rapidly, without causing permanent deformation. The preliminary tests were not conclusive, but indicated the desirability of continuance of the study.

Chapter 13

DEFORMATION OF STEEL UNDER HIGH PRESSURE

13.1 INTRODUCTION

THE OBJECT of this investigation was to examine the behavior of steel, especially armor steels, under conditions somewhat comparable to those occurring during projectile penetration, namely, involving large deformations and high stresses.* Before the initiation of this work in the Division it was known that under hydrostatic pressures of the order of 300,000 to 500,000 psi the ductility of ordinary steels is greatly increased and that there are measurable increases in superficial hardness.[1] Also, it had just been established at the Naval Research Laboratory [NRL] that the average pressur[illegible] the nose of a projectile while penetrating armor [illegible] is of the same order.[2] It was therefore evident that an adequate understanding of the process of armor penetration would have to consider the modification in the properties of the steel brought about by the stresses generated by the projectile; this was the reason for the initiation of this investigation.

13.1.1 Lack of Correlation between Ballistic Behavior of Armor and Its Ordinary Mechanical Properties

At the beginning it was hoped that measurements of the effect of hydrostatic pressure on the mechanical properties of armor plate might afford an immediate answer to a question that was at that time of great practical importance, and the first measurements were directed toward this end. The problem was to explain the frequent lack of correlation between the ballistic performance of a piece of armor under actual firing tests and the ordinary mechanical properties of the plate as determined on small specimens cut from it. It was hoped that the effect of hydrostatic pressure on various properties, such as tensile strength, ductility, and hardness, might, by adding new physical properties to the list of properties already known, make it possible to effect a correlation between ballistic behavior and the complete set of properties in those cases where the correlation was not possible with the more restricted set.

The early measurements were made with this immediate practical purpose in view, but it was some time before the measurements could be applied to answering the question directly because of the difficulty of obtaining samples of plates that had failed in the ballistic test. By the time such samples were obtained, so much practical experience had been gained by other investigators that the matter was felt to be well understood and the problem no longer important. The apparent lack of correlation between ballistic behavior and ordinary mechanical properties appeared only in plates that had rather large-scale mechanical defects or chemical inhomogeneities.

13.1.2 Long-Range Significance of Investigation

The principal purpose of the investigation shifted therefore from the original one, involving matters of immediate practical importance, to one of more long-range significance, for it was still obvious that a satisfactory analysis of the process of armor penetration would have to take account of the behavior of the plate during penetration. A systematic investigation was therefore indicated in which the effect of such variables as heat treatment and composition, especially carbon content, would be determined. Such an investigation was carried out.

13.2 MECHANISM OF DEFORMATION UNDER LARGE HYDROSTATIC PRESSURES

The deformation of a material is determined by the internal stresses. These, in turn, are normally produced by a set of external loads. The state of stress at a given point can be best understood by thinking of a very small cube within the body surrounding the point. On each face of this cube there acts a stress whose direction is not generally normal to the face. As the cube is rotated about the given point of the body the stresses on its several faces will, in general, change in both magnitude and direction. It can be shown, however, that there is one orientation of the cube for which the stress on each face is perpendicular to that face. The three directions in the body that are perpendicular to the faces of this cube are called the *principal directions* at the point, and the corresponding stresses on the faces of the cube are the *principal*

* Per inant to War Department Projects CE-5 and CE-6 and to Navy Department Project NO-11.

stresses. Since the cube is very small, the stresses on opposing pairs of faces are equal. Hence there are three principal stresses at each point of a body. One of these is the biggest and another the smallest of all the stresses found when rotating the cube about the point in consideration. Several particular states of stress may be mentioned. In *hydrostatic stress* not only are the three principal stresses at a point equal to each other (and have the same sign), but there is no change in the stresses acting on the faces of the imaginary cube as it is rotated. A *uniaxial* state of stress occurs during the ordinary tensile or compressive test. In this case two of the principal stresses are zero and the third is equal to and parallel to the stress applied externally to the specimen. Any two states of stress can be combined simply by superposition. If the principal directions are the same in both states or one is in the hydrostatic state, the principal directions are not changed by such superposition.

The behavior of a ductile material such as steel under loads is affected by two distinct mechanisms, *deformation* or *flow*, and *rupture*. The deformation of a ductile material depends primarily on differences between principal stresses, and thus is only moderately affected by a superimposed hydrostatic pressure. The rupture of such a material, on the other hand, depends primarily on the absolute magnitudes of the stresses acting. Consequently, a superimposed hydrostatic pressure will tend to inhibit the rupture that a second system of forces tends to produce.

Thus, if the standard tensile test is used on a ductile material and is arranged so that the whole apparatus can be immersed in fluid under pressure, the following results are expected: under small superimposed pressures the normal stress-strain relation is obtained. If this is represented not in the usual way but in terms of *true stress* and *natural strain*[b] the relation consists of a straight initial portion (elastic region), a curving transition range near the end of which necking begins, and a more or less straight final portion having a positive slope and ending at the rupture point. The slope of this line is the so-called rate of strain-hardening, corresponding to the fact that deformation causes an increase in hardness or in resistance to further deformation. The point of rupture is the point at which the steadily increasing stress required for deformation attains the value necessary for tensile failure.

Under a large hydrostatic pressure the relation between strains and the additional applied tensile stress will be nearly unchanged. Slightly increased stresses may be required at a given stage of deformation because of the internal frictional resistance caused by the exterior pressure. However, rupture will be considerably postponed. The stress-strain relation will then continue to a value of the applied stress exceeding the normal rupture stress by an amount greater the greater the hydrostatic pressure. In this way it is possible to attain deformations very much exceeding those normally reached in tensile tests. Since very large strains occur in the neighborhood of projectile penetrations it is desirable to know how much strain-hardening occurs, and whether there is a continuous increase of stress with deformation or a leveling off at some limiting stress.

113 APPARATUS AND METHODS OF MEASUREMENT

The tensile specimen used has a gauge length of approximately 0.47 in., a diameter of about 0.180 in., and an overall length of 1.10 in. It is mounted in a double-yoke mechanism which exerts a tensile force on the specimen when the yoke is compressed. This assembly is placed in the cylinder of the high-pressure apparatus and is completely immersed in the pressure-transmitting fluid (*i*-pentane was used in these tests). Within the cylinder there is also an electrical device (called a *grid* because of its shape) for measuring the tensile force, and a manganin resistance gauge for measuring the pressure. A piston, advanced by a hydraulic press, produces hydrostatic pressure in the fluid and at the same time compresses the yoke, stretching the specimen. The use of spacers between piston and yoke or different quantities of fluid permits changing the mean hydrostatic pressure. Pressures up to 450,000 psi can be reached with the equipment used.

The pressure and the force on the specimen are measured electrically during a test. The distortion of the specimen can be determined from the movement of the piston after making corrections for the deformation of the mechanism. In addition, the final dimensions and shape of the specimen are recorded at the end of a test. From these data are obtained the stress-strain relations under hydrostatic pressure. It should

[b] The *true stress* equals the tensile force divided by the actual minimum cross-sectional area, not the original area. The *natural strain* is equal to $\log_e A_0/A$, where A_0 is the original cross-sectional area and A the area after deformation. In plastic flow the ratio of areas is equal to the ratio of lengths, since volume is conserved.

be noted that during necking of the specimen the strain along the specimen cannot be determined from the total extension, since the strain is not uniform. Consequently, only the strain at the end of the test, when measurements can be made in the open, is known. Thus a series of points below the necking point and a single arbitrary point beyond can normally be obtained from a single specimen.

Tests of superficial hardness, one-sided compression, and punching shear were also made in the apparatus just described by substituting suitable mechanisms for the yoke.

More detailed descriptions of the equipment and technique are given elsewhere.[1,3,5,a,b,c]

13.4 TEST PROGRAM

13.4.1 Tensile Tests

In all, 35 different steels, mostly armor plate, were tested in this program. Nearly 350 individual tests were made. These are divided into five series described below.

First Series

In this series,[3] 56 tests were made on 24 different Navy armor steels, all ballistically satisfactory. Nearly all of these tests were made either at atmospheric pressure or in the highest pressure range possible, namely, 300,000 to 450,000 psi at the end of a test. A number of specimens were cut with different orientations in the original plate, in order to allow investigation of the effect of orientation on behavior.

Second Series

In this series,[4] four types of Navy armor (two of them included in the first series), all ballistically satisfactory, received 36 tests. This series was tested at hydrostatic pressures ranging from atmospheric to about 225,000 psi. The effect of specimen orientation with respect to the original plate was examined more extensively than in the first series.

Third Series

In this series,[5] 62 tests at hydrostatic pressures ranging from atmospheric to 200,000 psi were made on four Navy armor steels, one of which had been tested before. Two of the new plates were not acceptable ballistically.

Fourth Series

In this series,[6] 49 tests were made at hydrostatic pressures ranging from atmospheric to 400,000 psi on samples of four Navy armor steels of inferior ballistic performance.

Fifth Series

In this series, 140 tests were made as follows: 10 on a 0.34C steel as received, 62 on a 0.45C steel in seven different heat treatments and as received, 8 tests on a 0.68C steel as received, and 60 tests on a 0.90C steel in six heat-treatments and as received. These were made at hydrostatic pressures ranging from atmospheric to 400,000 psi. The object of this series of tests was, of course, to determine the effect of variation of composition and heat treatment of steels on their behavior under large hydrostatic pressures.*

13.4.2 Hardness Tests

These tests[3,4] were made only during the early part of the work, since it was felt that the change of superficial hardness with pressure (in the Brinell scale, roughly 5 per cent for a pressure increase of 150,000 psi) was too small to be important in the present state of penetration theory. Hardness tests were made on 16 different Navy armor steels that were also included in the tension program.

13.4.3 One-Sided Compression Combined with Hydrostatic Pressure

The apparatus was completed just before the end of the contract under which this work was performed. Consequently, tests were made on only one type of steel.[6]

13.4.4 Punching Combined with Hydrostatic Pressure

These tests were performed at hydrostatic pressures[6] ranging from atmospheric to 225,000 psi on three heat treatments each of the 0.45C and 0.90C steel used in the last series of tension tests.

13.4.5 One-Sided Compression of Steel to Large Strains (without Hydrostatic Pressure)

Tests were made on three specimens cut in mutually perpendicular directions from one piece of armor steel.[7] These were compressed to a final length approximately 5 per cent of the original length.

13.5 RESULTS

13.5.1 Phenomena Investigated

The measurements were aimed primarily at investigating two different aspects of the effect of pressure on tensile phenomena. The first aspect embraces the

* See Table 1 and Figures 1 to 5 of this chapter for details of treatment and results of the tests of the 0.45C steel.

phenomena of strain-hardening which occur before rupture in the region of plastic flow. The second aspect covers the phenomena of rupture. In general, different types of measurement were made for the two kinds of phenomena. In the study of strain-hardening, several specimens were stretched by different amounts, allowing the *flow stress* to be determined as function of strain. The flow stress is closely connected with the so-called *true stress* defined as the total tensile force divided by the cross-sectional area of the neck. This true stress should more properly be called the *average true stress*, because the stress is not constant across the section, but varies by virtue of the deviation of the neck from a straight cylindrical contour, the degree of departure of the stress from uniformity being greater the greater the curvature of the contour at the neck. The method of correcting the true stress for this lack of uniformity so as to obtain the significant flow stress has been discussed in detail elsewhere.[8,9]

Relation Between Flow Stress and Strain in Tension

When flow stress is plotted against natural strain (Section 13.2), an approximately linear relation is found at stresses above that at the initiation of necking. By performing the experiment under hydrostatic pressure it is possible, because of the very much greater range of strain attainable under pressure without fracture, to establish this relation with much greater accuracy than would be possible from measurements made at atmospheric pressure only. To a first approximation, the relation between flow stress and strain is independent of the hydrostatic pressure under which the experiment is made, and the results have usually been represented on this basis. Recently, however, in some work done at Harvard University for the Watertown Arsenal the accuracy of the measurements has been sufficiently increased to disclose a small effect of pressure on the relation between flow stress and strain, the flow stress for a given strain being slightly increased by pressure.[10]

Phenomena of Fracture

The second aspect of tensile phenomena under pressure, fracture, itself presents two aspects; the first is the way in which the strain at which fracture occurs is affected by pressure, which may be expressed otherwise as the effect of pressure on ductility; and the second is the change in the geometrical appearance of the fracture with pressure. The effect of pressure on ductility may be exhibited graphically by plotting the strain at fracture against the hydrostatic pressure at the instant of fracture. The geometrical character of fracture is in general complicated, but at least one aspect of it lends itself to numerical representation. At atmospheric pressure the fracture of the steels studied here is usually of the cup-cone type. The bottom of the cup is sharply enough defined in these experiments to permit measurement, and the fracture may be characterized by the ratio of the area of the tensile part to the total cross-sectional area of the break.

Table 1. Schedule of heat treatments applied to 0.45C steel.

No.	Description	Temp. (F)	Time (hr)
1	Normalized	1650	½
2	Annealed, fine-grained	1500	½
3	Annealed, coarse-grained	1900	½
4	Brine-quenched, spheroidized	1500	½
		1300	10
5	Brine-quenched, tempered	1500	½
		600	1
6	Brine-quenched, tempered	1500	½
		600	1
7	Brine-quenched, tempered	1500	½
		900	1

13.12 Effect of Hydrostatic Pressure on Tensile Properties

As illustrations of the effects discussed in this section Figures 1 to 5 are presented.[8] These show the results of measurements made on samples of a medium carbon steel (composition: 0.45C, 0.83Mn, 0.016P, 0.037S, 0.19Si) that had received the various heat treatments listed in Table 1.

Ductility

The largest effect of hydrostatic pressure is on ductility; at pressures of 350,000 to 450,000 psi the elon-

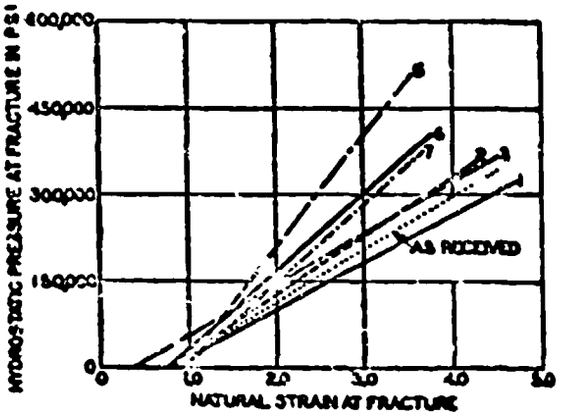

Figure 1. Effect of hydrostatic pressure on ductility of 0.45C steel with heat treatments listed in Table 1.

gation tolerated at the neck of a tension specimen may run to hundredfolds. At these extreme elongations the specimen loses its geometrical regularity and the situation becomes dominated by adventitious factors such as the presence of minute inclusions in the steel. In the region of less extreme elongations, that is, up to natural strains of 4 or 5, corresponding to elongations of 50- or 100-fold, the strain at fracture usually increases linearly with hydrostatic pressure, although exceptions have been found in which the increase was more rapid than linear.[6] The rate of increase of ductility appears to be greater for the softer steels; among those that have been studied in the present program the increase of natural strain at fracture caused by a pressure of 150,000 psi may be as much as 8 or as little as 0.8, as shown in Figure 1. Other steels are known for which the increase in ductility is much less, while the ductility of cast iron is not appreciably increased by the pressures that have been tried.

Strain-Hardening

Strain-hardening can be pushed much further under hydrostatic pressure than at atmospheric pressure because of the much greater strains possible without fracture. For all the steels that have been studied in this investigation the flow stress is approximately a linear function of the natural strain, at least up to strains of 3 or 4, and is approximately, but not entirely, independent of the hydrostatic pressure[10] (Figure 2). The rate of increase of flow stress with strain is in general greater for the harder steels, although there are examples of crossing of the curves not to be explained by experimental error. However, the rate of increase for the harder steels is not greater

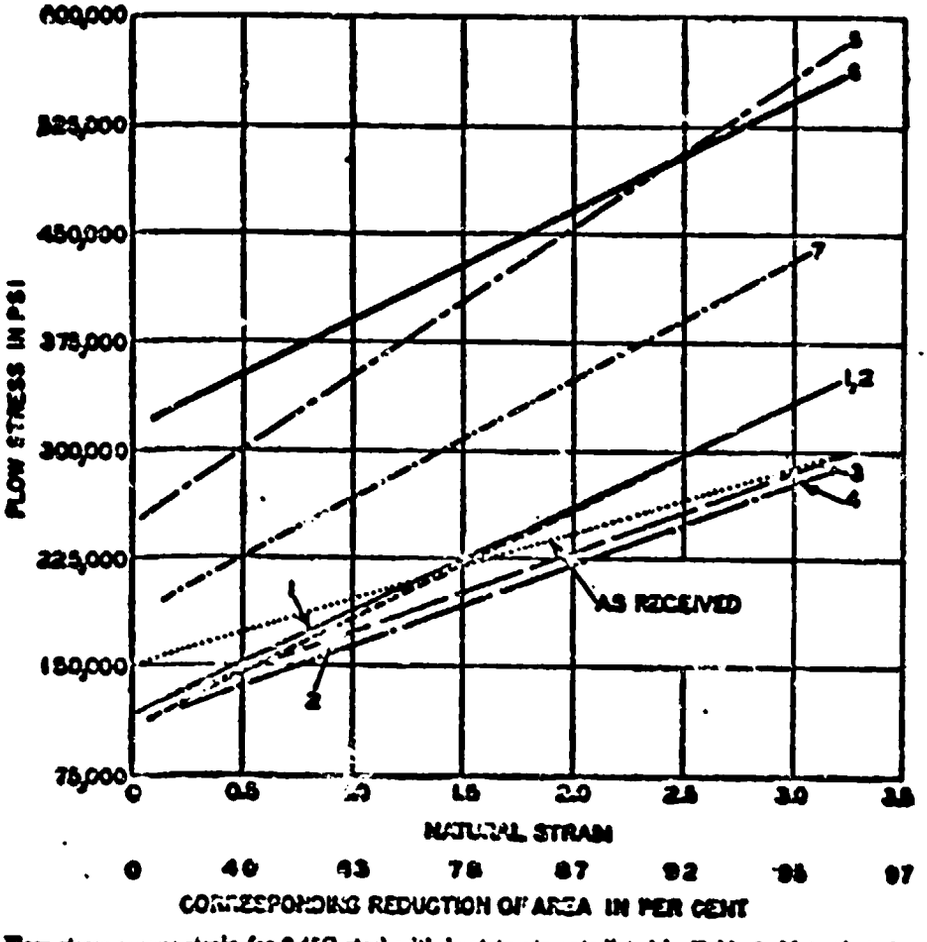

FIGURE 2. Flow stress versus strain for 0.45C steel with heat treatments listed in Table 1. Note that slopes of lines, i.e., rates of strain-hardening, are to a first approximation the same.

in proportion to the absolute values of flow stress. Thus the flow stress of a typical soft steel may increase from 100,000 to 300,000 psi or by a factor of 3 for a strain increase of 3; whereas a harder steel, e.g., treatment 5 of Figure 2, increases from 250,000 to 550,000 psi, or by a factor of 2.2, for the same range of strain.

Flow Stress at Fracture

By combining the results of the two previous paragraphs it can be concluded that the flow stress at fracture is a linear function of the hydrostatic pressure prevailing at the moment of fracture (Figure 3). The rate of increase of flow stress at fracture shows less dependence on the nature of the steel than do the factors from which it is derived; as a rough average, there is an increase of flow stress at fracture of 300,000 psi for an increase of hydrostatic pressure of 375,000 psi for any value of the flow stress.

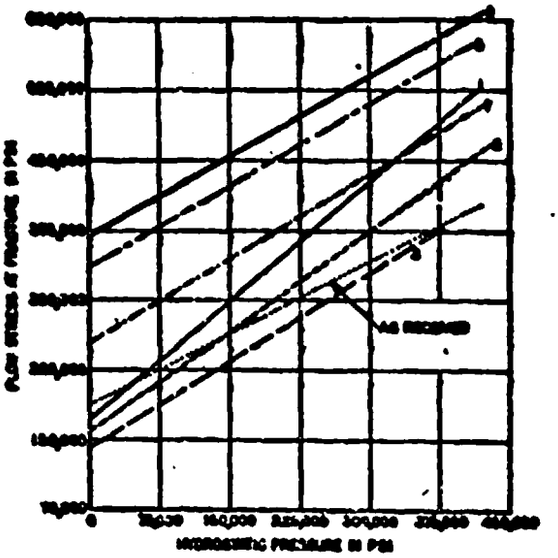

Figure 3. Relation between flow stress at fracture and hydrostatic pressure for 0.45C steel with heat treatments listed in Table 1. This figure is obtained by combining curves of Figures 1 and 2.

Orientation of Specimens

With respect to the orientation of the specimen in the original plate, the following appears to be true. The flow properties, which determine the form of the stress-strain relation, appear to be the same for all orientations. However, the rupture strength is less for specimens taken perpendicular to the original surface of a plate. For such specimens fracture occurs at smaller elongations and lower stresses than for specimens taken in either of the directions parallel to the plate surface, between which there appears to be no difference. The differences between different directions with respect to fracture phenomenon become smaller at higher pressures and probably disappear above 250,000 psi.

Effect of Pressure on Flow Stress

The method of these experiments has not been accurate enough to permit a satisfactory study of the

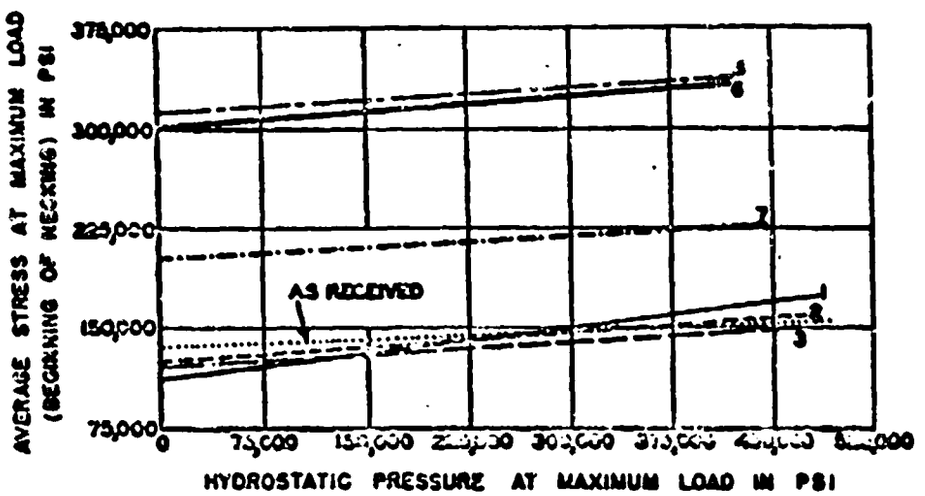

Figure 4. Ordinate is calculated by dividing total load at maximum by original cross-sectional area and multiplying by 1.221, which corresponds to assumption that initiation of necking occurs at strain of 0.2. Average stress at maximum load is essentially the "tensile strength."

effect of hydrostatic pressure on plastic flow in the initial region of small strains, before the initiation of necking, i.e., up to the maximum load. The effect of pressure on the maximum or the so-called tensile strength has, however, been established (Figure 4). It appears that the flow stress at the maximum load increases linearly with the hydrostatic pressure, and the amount of increase, with a few exceptions, is approximately the same for all steels, independent of the absolute stress. The flow stress at the maximum load increases by approximately 20,000 to 25,000 psi for an increase of hydrostatic pressure of 450,000 psi. Thus the magnitude of this effect is much less than that of any of the other effects that have been mentioned.

The stress at which plastic flow first begins seems to be increased by pressure by approximately the amount by which the flow stress at maximum load is increased.

Appearance of Fracture

The appearance of the tensile fracture[4,11] varies with pressure. Practically all the steels that were studied in this program show the normal cup-cone type of fracture at atmospheric pressure. With increasing hydrostatic pressure the tensile part of the break, that is, the bottom of the cup, occupies a progressively smaller part of the total cross section, and entirely disappears at a certain pressure beyond which the fracture is entirely by slip along curved shear surfaces (Figure 5).[4] Up to the pressure at which the tensile part vanishes the ratio of the tensile part of the area to the total area is roughly a linear function of pressure. Figure 5 shows several exceptions to this rule, in which the tensile part of the fracture persists to higher pressures than would have been extrapolated from measurements only at lower pressures. In general, the pressure at which the tensile area disappears is higher the harder the steel.

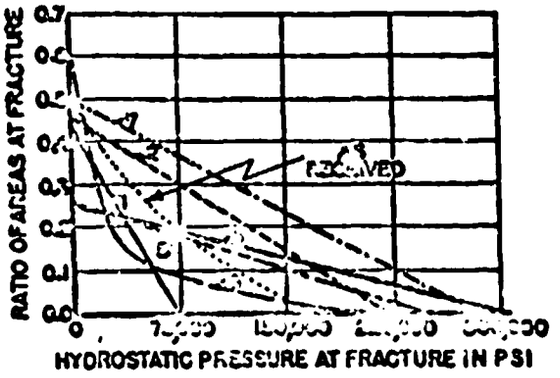

Figure 5. Effect of hydrostatic pressure on type of fracture obtained in tension. Ordinate shows ratio between area of tensile portion of break and total cross-sectional area.

12.5.3 Effect of Hydrostatic Pressure on Superficial Hardness

This question was examined only in the earlier tests of this program.[5,6] For the samples of 16 types of Navy armor tested the effect of a pressure of 150,000 psi was to increase the Brinell hardness by an amount which fluctuated irregularly around 5.7 per cent. The effect is obviously not large and presumably is related to the increase in plastic flow stress in tension that is caused by pressure. Because this effect is comparatively small, it was not studied further.

12.5.4 Effect of Hydrostatic Pressure on Flow under One-Sided Compression Stress

This study was only barely started in this program.[6] Numerical values have been obtained for one armor-plate steel. For plastic shortening up to 10 per cent, hydrostatic pressure appears to increase the compressive flow stress linearly and by about the same amount as the increase of stress at initial plastic yield in tension or as the increase of Brinell hardness.

12.5.5 Effect of Hydrostatic Pressure on Behavior under Punching Forces

This phenomenon[6] has been studied only for the three softest heat treatments of the 0.45C and 0.90C steels used for the tensile program, at pressures up to 225,000 psi. The effects are similar to the effects of pressure on tensile behavior in that there is a great increase in ductility. As the pressure is increased, the punched material has to be forced through greater distances before it breaks clear; at the higher pressures there is a gradual disappearance of the phenomena of fracture until eventually, as shown by other tests at pressures somewhat higher than those used here, the punching may be moved through the entire thickness of the plate without loss of coherence. Strain-hardening is an accompaniment of the punching process. This strain-hardening is of the same order of magnitude as would be expected from a crude comparison with the strain-hardening in tension. The total force required to start the plastic movement of the punched disk also increases with pressure by the same order of magnitude as the corresponding tensile

effect. The work required to expel the punched disk is greater by 25 to 30 per cent at pressures of 200,000 psi than at atmospheric pressure.

1116 Compression of Steel under Simple Longitudinal Stress to Large Strains

The method of Taylor and Quinney,[28] amounting to compressing in stages with reshaping between stages to minimize the extraneous components of stress arising from friction, was applied to an armor-plate steel to produce a final compressive natural strain of 3, or reduction of length to 5 per cent of the original. After the initial stages the true compressive stress rises linearly with natural strain. This is unlike the behavior of copper for which the true compressive stress approaches a constant value for large strains.[7] The rate of strain-hardening of this steel in simple compression is somewhat less than its rate in simple tension, and the absolute values of flow stress in compression are less than in tension.

PART V

PROTECTION

Chapter 14

DEFENSE AGAINST SHAPED CHARGES

14.1 INTRODUCTION

THE FACT THAT hollow explosive charges (designated shaped charges for security reasons) can defeat thick steel plates or other protection has long been known; however, no attempt was made to make military use of this fact until the beginning of World War II, when all combatants introduced weapons employing this principle. Artillery shells of various calibers and rocket-propelled projectiles for antitank work were encountered most frequently. Large demolition charges for defeating concrete fortifications also appeared. Though many of these weapons were ineffective because of faulty design, improvements were made rapidly. A joint Army-Navy-NDRC Committee on Shaped Charges, organized to study and promote the use of hollow-charge weapons in early 1943, considered the threat great enough to warrant setting up a project to study countermeasures.[a,b]

A shaped-charge weapon consists essentially of a hollow liner of inert material, usually metal or glass, and of conical, hemispherical, or other shape, backed on the convex side by explosive. A container and a detonating device are included (Figure 1). When detonation occurs the liner is compressed against itself, giving rise to a jet of metal or glass particles moving outward along the axis of the liner at very high velocities. This jet is able to achieve great penetration into any near target.

The performance of the hollow-charge projectile differs from that of other projectiles in that the thickness of material it can perforate is essentially independent of its striking velocity. In fact, hand-placed charges may perform somewhat better than the projectile type because they can be more readily detonated at the best distance from the target surface. Hand-placed hollow charges have been used against both tanks and concrete fortifications. The fact that performance is independent of velocity and therefore of range would appear to make these charges ideal for antitank artillery. However, when hollow-charge projectiles are caused to rotate by the rifling in the guns from which they are fired, their performance drops 30 to 50 per cent against solid homogeneous armor and much more than that against spaced armor or low-density targets. Nonrotated fin-stabilized hollow charges can be made to perform as well when fired dynamically as when they are fired statically. This accounts for the popularity of rocket-propelled low-velocity projectiles such as the American and German bazookas. These weapons are light, easily constructed, and remarkably effective. They can be carried by infantrymen almost as easily as rifles and under good conditions can perforate and set on fire any tank. If these weapons had been well designed at the beginning of World War II, they would have been a serious menace.

14.1.1 The Experiments

Since the static performance of a hollow charge always equals or surpasses its performance when fired dynamically, it was decided to start the search for protective devices using a small charge of standard construction that could be detonated statically. Although liners of various shapes and materials were being used, a charge employing the steel-cone liner (with 1⅝-in. base diameter, 42° cone angle) of the M9A1 rifle grenade was adopted, partly because these cones were available in large quantities and partly because steel cones were being used in the majority of weapons. Pentolite (50 PETN/50 TNT) was adopted for the explosive.

The experiments were devised with two purposes in view; first, to determine the effectiveness of materials or combinations of materials that gave promise of providing low-weight protection; and second, to investigate the fundamental laws governing the penetration and perforation process. The division was not sharp between these two types since most experiments contributed to both programs.

14.2 THEORY OF JET PENETRATION

Figure 1 shows a cross-sectional view of the head of an American bazooka which contains a typical hollow charge. When this weapon strikes a target, the base fuze, operating on the inertia principle, detonates the charge from the rear. A detonation wave travels forward and collapses the steel-cone liner, starting at its apex. The collapse of the cone squirts forward a long, narrow jet of steel at velocities from 10,000 to 30,000

[a] Pertinent to joint Army-Navy Project AN-1.
[b] See Data Sheets 3A5 and 3A6 of Chapter 19.

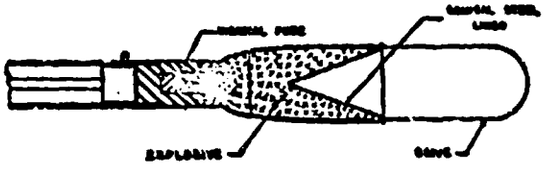

FIGURE 1. Head of American bazooka showing typical shaped charge with conical steel lining.

fps.[9,20] This process is illustrated by the series of high-speed radiographic photographs[8,14,15] in Figure 2. The photographs were taken of detonating charges in various stages and are arranged to show the sequence of events in one charge. The last picture shows a jet perforating some steel plates. Early in the process of its formation, the jet breaks up into fine particles but retains its jetlike characteristics out to great distances. There is a gradient in the velocities of the particles along the jet, the particles in front moving faster than those at the rear.[8,16] This causes the jet to lengthen and reduces its average density with time.

When a jet strikes a target of armor plate or mild steel, pressures of around a quarter-million atmospheres are produced at the point of contact. These pressures are so far above the yield strength of steel that the target material flows out of the path of the jet as would a fluid. There is so much sidewise momentum associated with the flow that the diameter of the hole produced is considerably larger than that of the jet and depends mainly upon the strength of the target material, since the radial flow of the material is eventually stopped by the strength of the target. Thus a larger hole is made in mild steel than in armor plate. However, the depth of penetration into a very thick slab of mild steel will be only slightly greater than that into homogeneous armor.

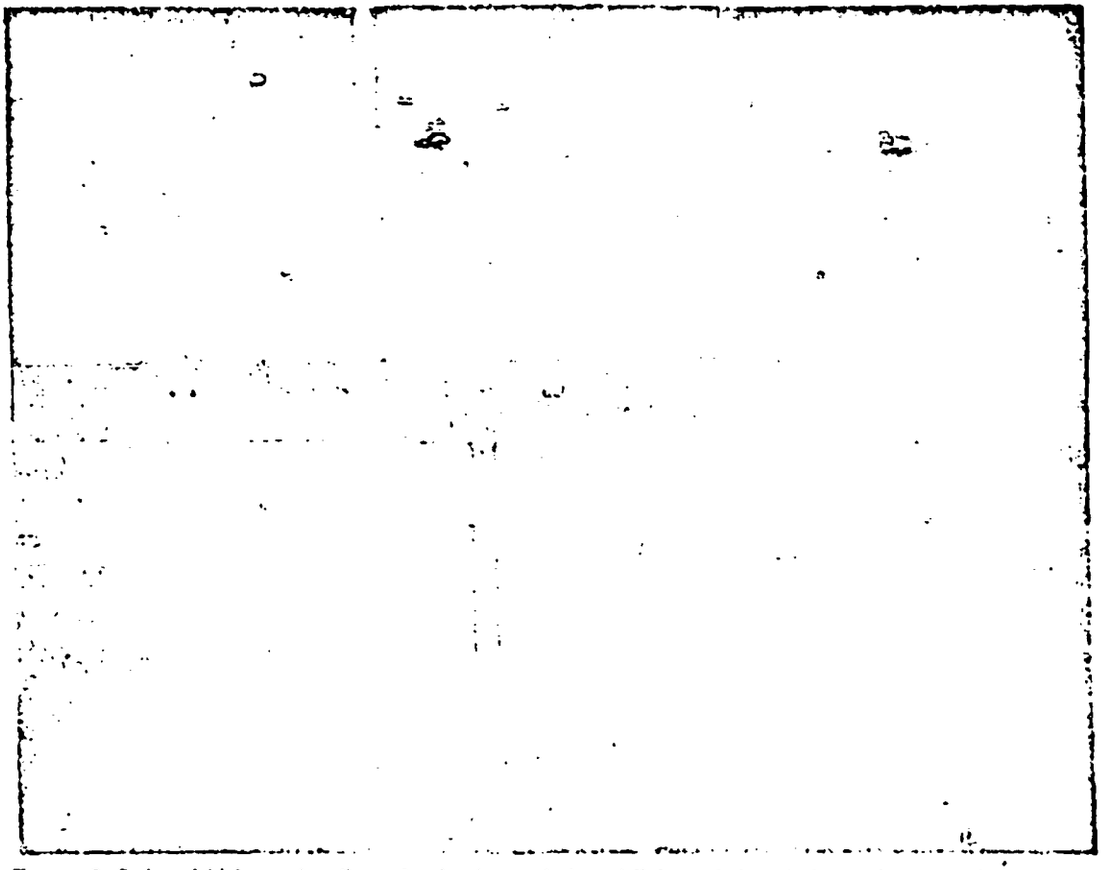

FIGURE 2. Series of high-speed radiographs showing conical steel linings of shaped charges in progressive stages of collapse, to illustrate formation of jet and slug. Last of the series shows jet from one such liner after perforation of two steel plates. (Aberdeen Proving Ground photographs.)

As the jet particles strike they are carried off radially with the target material. Thus the jet is used up from the front and becomes shorter and shorter until finally the last jet particle strikes the target and the primary penetration process stops. The actual penetration continues for a short time, especially in weak targets, because the kinetic energy imparted to the target material by the jet must be dissipated. The additional penetration caused by this afterflow is called secondary penetration. Its magnitude depends upon target strength. It is mainly responsible for the small differences observed between the depths of penetration in mild steel and in homogeneous armor, although there is probably some difference in the primary penetrations as well.

Since the pressures produced by the jet are much greater than the yield strengths of most target materials, both the target and the jet can be considered as fluids in calculating the rate of penetration. Simple hydrodynamic theory shows that the rate of penetration is proportional to the jet velocity. However, the rate at which a given length of jet is used up is also proportional to the jet velocity. Thus the depth of penetration is almost independent of jet velocity. This supposes, of course, that the low-velocity jets are nevertheless able to produce such high pressures that the hydrodynamic theory holds. Though the faster jets do not produce deeper holes, they produce wider holes than the slower jets. The depth of primary penetration P' is obviously proportional to the length of jet l, since the length determines how long the penetration process will last. Since primary penetration is nearly independent of strength, the process is controlled only by inertia, which depends upon the density ρ of the target and the average density ρ_j of the jet. Actually, the primary penetration P' is proportional to*

$$l\sqrt{\frac{\rho_j}{\rho}}.$$

An increase in standoff increases the length of jet l and decreases the average jet density ρ_j, while the product of the two quantities remains substantially constant. Therefore, from the above equation it appears that the primary penetration increases with standoff. However, due to slight asymmetries and irregularities in construction of charges, which vary from charge to charge, the jets waver and spread somewhat. This effect tends to reduce the effectiveness of the jets, but only at large standoffs. Consequently, at small standoffs an increase in standoff improves performance, while for large standoffs the reverse is true. There is an additional reason for the rapid increase in penetration as the charge is moved away from near contact with the target. The jet changes character as it travels away from the charge. When the jet first emerges from the liner, its density is near the density of the liner and it behaves like an incompressible fluid. Hence, at the point of contact with the target, the jet spreads out and its force is exerted over a wider area than the original jet cross section. On the other hand, at large standoff the jet separates into widely spaced particles which do not affect each other and which suffer no radial spreading until after they strike the target. The total force is thus concentrated on an area equal to the jet cross section.

Armor can be protected from shaped-charge attack by covering the armor with a material that will use up the jet before it strikes the armor. The rate at which the jet is used up is proportional to $\sqrt{\rho}$, where ρ is the density of the target material. If low-density materials are used for protection, they must be made thicker than those of higher density. However, *lower total weight of protection is provided with low-density materials.* In fact, the weight of the protection required against a given weapon is roughly proportional to $\sqrt{\rho}$. For example, if the density of the material used to provide protection against a given weapon is reduced by a factor of 4, the thickness must be approximately doubled and the weight can be approximately halved. For practical reasons it is not advisable to use materials having densities much lower than twice that of water.

When low-density materials are used to protect steel, the residual penetrations into the steel can be calculated approximately from the fact that the reduction in penetration caused by a slab of given thickness is proportional to the square root of its density. A more reliable method makes use of the curve of residual penetration into steel versus standoff of

* The point of contact of a fluid jet with the target moves through the target at a velocity U. If the jet has an absolute velocity V, its velocity relative to this point is $V - U$. The pressure at this point due to the jet is the same as that due to the target material, which has a relative velocity U toward this point. Thus, by Bernoulli's theorem

$$\tfrac{1}{2}\rho_j (V-U)^2 = \tfrac{1}{2}\rho U^2 \quad \text{or} \quad \frac{U}{V-U} = \sqrt{\frac{\rho_j}{\rho}}.$$

But primary penetration equals the penetration velocity U times the time of penetration $l/(V-U)$,

or

$$P' = U\,\frac{l}{V-U} = l\sqrt{\frac{\rho_j}{\rho}},$$

where l is the length of the jet.

the weapon. This curve, a characteristic of the weapon, must be known in order to achieve reliable results.

14.3 EXPERIMENTAL PROGRAM

Experiments on the general problem of protection against shaped charges were started in August 1943, and by October 1943 a plastic armor (gravel with a pitch-mastic binder) had been found that was much lighter than the homogeneous armor required for equal protection. In cooperation with the Flintkote Company, which made the plastic armor, a series of tests was started which improved this protection and further reduced its weight. A wide variety of aggregates was tried, of which pure quartz gravel in a mastic of pitch and wood flour proved best. This was designated HCR2. At the same time a series of tests was planned and carried out, mostly at the Aberdeen Proving Ground,[4] to determine whether or not practical use could be made of this material against existing weapons. Some tests were made on models of ship structures and these were supplemented by a test carried out on a larger scale at the Norfolk Navy Yard for the purpose of investigating this means of providing ships with protection against torpedoes having shaped-charge warheads. However, it seemed improbable that this type of torpedo attack would become serious in World War II and the project was dropped. It appeared that shaped-charge weapons could be most effectively used against tanks and therefore the protection of tanks was the major problem. Shaped charges were also being used to neutralize concrete fortifications. The protection of concrete structures was considered next in importance to the protection of armored vehicles.

14.3.1 Tank Protection

The problem of protecting tanks[1,11-27] was made difficult by the fact that the Germans (probably with their own heavily armored Tiger tank in mind) had started using bazookas and new shaped-charged weapons called Panzerfausts, the latter capable of perforating 8 to 10 in. of armor plate, while the tanks in use by the American Army could be defeated by weapons capable of perforating only 2 in. of armor. To complicate the problem further, the American tanks could stand very little additional weight. The thickness of protective material was also limited by the requirement that tanks must be able to pass over Bailey bridges. The German decision to use large charges probably saved many casualties, for in order to make the charge large they had to sacrifice muzzle velocity which made their weapons so inaccurate that it was very difficult to hit a tank even from close range. Probably because of this fact, Allied tank losses to shaped-charge weapons were so light that the necessary tests at Aberdeen were given a low priority, reducing considerably the progress made on the protection problem as a whole.

Plastic Armor for Tank Protection

The original plan for protecting tanks called for a set of small steel panels filled with plastic armor (HCR2) that could be fastened to the outside surface of any M4 tank in an emergency. It was hoped that by making the panels small the area damaged by a direct hit from any type of projectile would be small; that is, the damage would be confined to one or two of the panels. Tests at Aberdeen showed that:

1. HCR2 panels are very effective against artillery-type hollow-charge projectiles that are stabilized in flight by rotation.

2. HCR2 panels are less effective against nonrotated fin-stabilized projectiles, especially when these are fused to explode close to the surface. While steel is defeated most easily by shaped charges that explode to standoffs of 1 or 2 calibers, HCR2 is defeated most easily by those that explode close to the surface.

3. Many of the shaped-charge weapons found in the field are capable of larger penetrations than reports had indicated.

4. The HCR2 must be contained in large and strong steel panels to prevent excessive damage by projectiles. A heavy face plate is needed to prevent high explosive [HE] and high-explosive antitank [HEAT] shells from penetrating into the panels and blowing them apart.

This information could only be obtained by making tests at a proving ground where facilities were available for trying all types of projectiles. It could not have been inferred from laboratory tests.

The new information showed that, considering the weight of the HCR2, the steel panels, and the fastening devices, from 8 to 12 tons are required to protect the M4 tank adequately against the largest enemy shaped charge, the Panzerfaust. It is estimated that 7.1 tons on the heavy tank M26 will provide the same

[4] Some tests were also made at the NDRC Division 8 Explosives Research Laboratory, Bruceton, Pennsylvania, and one early test was made by the Armored Board at Fort Knox.

protection against shaped charges as 11.7 tons on the M4. The weight of the protection added is only 16 per cent of the total on the M26 as compared to 34 per cent on the M4. The thickness of panel on the turret is only 10¾ in. on the M26 compared to 13¾ in. on the M4.*

For the M4 tank this added weight seemed excessive, but it was the best solution available and it was decided to make up a set of panels for test. The work of designing the panels was carried out by the Flintkote Company in cooperation with the Office of the Chief of Ordnance in Detroit, Michigan. An M4 tank with the new horizontal suspension and a wide track was sent to Rutherford, New Jersey, to enable the Flintkote Company to fit panels to it. The track and suspension system of this vehicle is capable of carrying much heavier loads than is the narrow track and the vertical suspension used in early models. Demountable panels, to be filled with HCR2, made entirely of homogeneous armor plate welded together, were designed with ½-in. sides and ¾-in. face plates. The construction of these was only partially completed by the end of World War II.

The design and construction of panels that could be easily mounted and removed, and at the same time withstand combat conditions, turned out to be an engineering problem that took a great deal of time. In the meantime, reports began coming in that more and more Allied tanks were being lost to enemy shaped charges. Therefore, a type of panel was designed that could be made up in a few weeks, using ¾-in. mild steel instead of homogeneous armor. The face plate was strengthened by placing 2 in. of 24ST aluminum alloy directly in back of it, that is, between the face plate and the HCR2. Tests with the standard charge had indicated that a few inches of aluminum in this position in the panels would improve the shaped-charge protection as well as offer a means of improving the ballistic properties of the panels. These panels were fastened to the tank by cables to absorb shocks. One set was completed and was tested just after World War II ended. It was found that with some modification this set of panels would be quite satisfactory, although it is believed that the armor-plate panels would be more satisfactory.

* These weights and thicknesses are based upon the latest information obtained from statistical studies on the performance of these weapons. Less than 10 per cent of the largest weapons, the Panzerfausts, should come within an inch of perforating the basic armor protected by HCR2 even at normal incidence. The panels made and tested were somewhat thinner.

Spikes for Tank Protection

As soon as it was discovered that excessive weight of any kind of armor would be required to provide protection to the M4 tank, a search was started for a different principle of protection. Since the Panzerfaust and most other weapons detonate very close to the surface, and since no shaped-charge weapon functions well if its liner is distorted, spikes that would perforate the windshields and the liners were considered. After many disappointments, a design of spikes was found that could be expected to defeat all existing shaped-charge weapons[1,16] although fairly effective weapons could be developed specifically for use against this design. It would add only 3.2 tons to the M26 tank and 4.1 tons to the M4 tank, including the ¾-in. armor plate to which the spikes would be welded.

The final design for defeating all weapons was not tested, but the designs that were tested and proved successful against the various weapons were close enough to it to leave very little doubt as to its efficiency. This design calls for spikes made of 1-in. diameter rod, rolled from armor-plate alloy and hardened to *Brinell hardness number* [BHN] 400. The spikes have blunt points and are welded to armor plate in a pattern made up of equilateral triangles, 2.5 in. between centers. The spikes are 7.5, 8.0, 8.5 in. long, arranged so that no two adjacent spikes have the same length. The staggered lengths make it possible to defeat smaller-diameter projectiles with a given spacing. When a small-diameter projectile strikes a spike pattern normally and midway between two spikes of equal length, a slight symmetrical distortion of the liner is produced which does not greatly reduce its penetrating power. However, with spikes of unequal lengths, no such difficulty is encountered. The spike pattern weighs much less and takes less space than the HCR2 panels. It is less vulnerable and probably will not need to be changed when weapons with greater penetrating power are produced. At present it appears to be the best solution.

It has one limitation, however, in that a shaped-charge projectile designed with a nose fuze sensitive over a wide area would be able to defeat spikes on panels.

14.13 Concrete Fortifications

Fairly large shaped charges have been used to neutralize pillboxes and other concrete fortifications.[4,18-21] These have generally been hand-placed charges of large diameter; large artillery shells could

also be used. The Corps of Engineers requested a study of the problem of making concrete structures that would be better able to withstand such attacks.

Based upon designs furnished by the Corps of Engineers, a long series of small-scale model tests was performed. The effect of increased strength of concrete, air spaces in the concrete, scab plates at the rear, and face plates on the front were all investigated. The weight of concrete needed for protection can be reduced by each of these devices. However, the effects are rather small, so that the most economical solution appears to be the use of more concrete. The scab plate is very practical for other reasons, since it greatly reduces the spalling due to perforation.

14.2.3 Weapon Data Sheet

In the course of this work data were collected, and so far as possible correlated, on the design and performance of Allied and enemy shaped-charge weapons. There is a vast variety of designs. Liners are conical (with apex angles from 20 to 80 degrees), hemispherical, parabolic, and made of combinations of these shapes. They are constructed of a variety of metals and sometimes of glass. Many different explosives are used; those having high detonation velocities are preferred; the shapes and degrees of confinement of these explosives vary widely. The method of fuzing varies and affects performance. Unfortunately, the available information was, and still is, scanty and unreliable. Data Sheets 3A5 and 3A6 of Chapter 19 allow estimates of the performance of shaped-charge weapons.

14.2.4 Standard Charge Improvement

The performance of individual weapons varies widely even when they are selected from the same lot. These variations, mentioned in Section 14.2, make it difficult to obtain reliable information on the protective qualities of different materials and devices. If a more consistent charge were developed it would help greatly in such experiments.

In cooperation with the DuPont Eastern Laboratory and the Delaware Ordnance Depot, an attempt was made to develop more consistent standard charges.[1,22,23] The primary purpose of this research was to create a better tool for making protection experiments, although the study was also worth while for indicating how much improvement in performance is possible through improved construction.

Out of every lot of standard charges two or three were fired as controls. X-rays of the control charges revealed that all had flaws or air pockets. Statistical comparison of the photographs with the performance of these charges indicates that nonsymmetrical flaws are more detrimental than symmetrical ones. However, the correlation was not good enough to justify more definite conclusions, since other factors are as important as the flaws. For the next series of standard charges a new mold was made in which the liner could be very accurately aligned. The performance of this series was superior, especially at large standoff, and analysis showed that the average waver of the jet was reduced by about 40 per cent. Attempts were also made to improve the consistency of the standard charges by carefully selecting the steel for a series of cones from one heat of steel. Decarburizing the steel cones was also tried. Neither of these appeared to produce significant improvement. All of the cones used in standard charges were made by a mass production drawing process and were not as perfect as desired. It was evident that if the cones were accurately made and accurately aligned in the mold, and if the charge could be cast without flaws (especially eccentric flaws), the performance of these charges could be made much more consistent.

14.2.5 Statistics

Since consistent charges were not available, it was necessary to develop a statistical method of treating the results obtained with the charges available. The methods developed and used are treated in detail elsewhere.[1,23]

Chapter 15

STRUCTURAL PROTECTION

15.1 INTRODUCTION

PROTECTION CAN BE classified, somewhat arbitrarily, as being either civilian or military protection, although many structures can be placed in both categories. Most considerations applying to one class apply also to the other. The difference is mostly in dimensions and in function. Military structures may run to greater thicknesses than do civilian although there is considerable overlap. Military structures are generally designed to resist several different forms of attack, namely, blast, fragmentation, earth shock, shaped charge, and attack by high-explosive [HE] or armor-piercing [AP] projectiles. Not all forms of attack may be important in one situation, but normally more than one must be considered. Civilian protective structures, on the other hand, are mainly intended to give protection against blast, fragments, or debris. Furthermore, civilian protection must include consideration of means of strengthening or otherwise protecting existing structures or installations.

At the beginning of World War II, protection had very high priority since there was considerable uncertainty whether or not attacks would be made on the American continent. As World War II progressed and it became more and more apparent that no such attacks were to be expected, protection became less important. This does not mean that protection will not be of very great importance in the future. In fact, if there is another war, this country must be prepared for early attack. Presumably, such attack will be directed at centers of production, communication, and government. The problem of preparing adequate protection for the essential functions and for the populations of such potential targets should be given high priority, not when the danger of attack becomes apparent, *but from now on.*

The original concern of Division 2, and its principal concern until 1943, was with defense. As World War II proceeded emphasis shifted gradually and continuously to attack. This change of interest caused only comparatively minor changes in projects. Certain kinds of work, particularly that dealing with the properties of materials, became relatively less important than before. Certain new projects dealing with the performance or with the effectiveness of specific weapons or with the possibilities of enhancing their performance were added to the Division. However, most of the work of the Division was equally useful in defense or attack.

This chapter describes those parts of the program of the Division that are concerned with protection or defense and that are not discussed elsewhere in this volume. Brief references will be made to such discussions whenever necessary for completeness. The following chapters of this volume contain information especially pertinent to the present chapter: Chapter 3 on explosions in earth; Chapters 6, 7, 8, and 9 on terminal ballistics of armor, concrete, plastic protection, and earth; Chapter 14 on defense against shaped charges; Chapter 16 on target analysis and weapon selection; and Chapter 19 on data sheets on effects of fire, impact, explosion. The following subjects are discussed in the present chapter: the damage to concrete structures from contact explosions; damage to light structures from blast, especially internal blast; experiments on the impact behavior of reinforced concrete beams; theoretical analyses of the behavior of structures and structural elements under impact and blast; applications of the information acquired to problems of structural protection; and recommendations for future investigation.

15.2 EXPERIMENT

A very extensive series of tests was conducted by Division 2 and the Committee on Passive Protection Against Bombing [CPPAB] (later the Committee on Fortification Design [CFD]) on various aspects of protection. The terminal ballistics of armor, concrete, plastic protection and earth was studied at the Princeton University Station. The effects of explosions on concrete structures were investigated at Princeton and at Camp Gruber, Oklahoma, in collaboration with the Army Corps of Engineers. The protection of concrete structures against shaped-charge attack was studied at Carnegie Institute of Technology in cooperation with Division 8, NDRC. Tests on the behavior of reinforced concrete beams under impact were made at the University of Illinois.

15.2.1

Effects of Blast

In addition to the very extensive series of transient measurements of the various phenomena of blast and blast propagation that are discussed in Chapter 2 of this volume, some studies of the effect of blast on structures have been made.

Static Detonation Tests of Wood-Frame Dwelling Houses

Three typical small wood-frame dwelling houses were constructed by the Corps of Engineers at Aberdeen Proving Grounds and subjected to the effects of 500-lb general-purpose [GP] bombs (containing 60/40 amatol), detonating in the air and under ground, and to the effects of 250-lb very lightly cased TNT charges (equivalent in explosive weight to 500-lb GP bombs), detonating in air.[1] The tests were analyzed by the CPPAB and members of Division 2. Transient measurements of blast pressure and displacements were made. The air-blast detonations were at distances from houses ranging from 500 down to 95 ft. The below-ground detonation (there was only one) occurred at distances ranging from 17.5 to 60 ft from the three houses.

The following conclusions were drawn.

1. Extensive damage to similar structures can be expected at distances less than 30 ft from either ground shock or air blast, the former being slightly more serious. Chimneys were never damaged by blast, but were susceptible to earth shock. Cement-block basement walls fail badly due to earth shock. Other types of foundation walls, e.g., solid concrete, might be somewhat superior although no great difference is likely.

2. Despite very severe damage on the side of a structure facing an explosion there was never serious collapse, although considerable sagging occurred. This is very significant since most of the casualties produced in HE attacks on Britain and Germany were due to structural collapse. This would naturally be a much mor mmon occurrence with the brick bearing-wall construction, so universal in Europe, than with the wood-frame construction of the houses of the present tests. On the other hand, the protection against fragments afforded by the wooden houses is somewhat less than by the 12- to 18-in. brick walls common in Europe.

3. The frequent collapse of chimneys because of earth shock suggests that home shelters should not be located near chimneys.

Confined Blast

In order to supplement the measurements of transient pressures resulting from the detonation of charges in confined spaces[2] that are discussed in Chapter 2 of this volume, other experiments on the damaging power of such confined explosions were carried out at Princeton. The structure in which these tests were made had a reinforced concrete floor, roof, and columns. It was about 6.5 ft square and 4 ft high; thus it was approximately a ⅛ scale model. The interior was completely enclosed by brick filler walls, 1 course thick bonded to the concrete structure on bottom and sides, but not at the top.

The charges consisted of 22 and 44 g of tetryl and were detonated at the center of the enclosed space. The deflection of one wall was recorded as a function of time during each test. Damage was evaluated at the end of each test. In addition, ½- and 1-lb charges of TNT were exploded outside the structure at 3 ft from the center of a brick wall.

The 44-g tetryl charge at the center of the chamber blew out one wall completely and the major portions of the others. Analysis of the record of motion indicates that the wall accelerated during the first 35 msec following the explosion, at which time the center displacement was about 2 in. After that the velocity remained essentially constant. This deflection, and corresponding interval of time, are believed to correspond to complete disruption of the wall, at which point much of its ability to confine the gas would have disappeared. The 22-g charge caused cracks in all walls that essentially destroyed their strength, but did not blow any wall out. Following this, the external detonation of ½- and 1-lb charges of TNT 3 ft from the centers of already cracked brick walls showed no appreciable additional effect, thus illustrating the ability of confinement to enhance the effect of blast. Finally, a ½-lb charge of TNT detonated within the structure, completely wrecking it.

The corresponding full-scale effects are the following:

1. One and a quarter pounds of explosive within a similar structure 12 ft high and 20 ft square, with 12-in. brick walls, would cause serious wall cracking.

2. Two and a half pounds would blow out the walls but would not injure the frame, although detonation in contact with the floor would certainly injure it.

3. Fifteen pounds would cause complete destruction.

4. Thirty pounds of TNT detonating outside at a

distance of 10 ft from a wall would not injure it seriously.

These conclusions are limited in their applicability by two factors; first, most structures have openings of one kind or another that permit venting and reduce the degree of confinement; second, by the fact that the single-course brick wall of the model test is not exactly similar to a 13-in., 3-course wall. Whether the 1-course wall is weaker or stronger is difficult to decide, although it is believed to be stronger so far as bending as a whole is concerned.

15.2.2 Underground Explosions

Extensive tests on massive buried reinforced-concrete structures, representing elements of fortifications were carried out at scales ranging from $^1/_8$ to full, and are discussed in Chapter 3. The full-scale target was a concrete box 25 ft square in plan and 17½ ft deep without floor or roof. The side walls of the full-scale structure ranged in thickness from 2.1 ft to 5 ft. The charge used in the full-scale tests was 1,000 lb, corresponding to the effect of a 2,000-lb GP bomb. Charges were detonated at distances ranging from contact to where only minor damage resulted. In another series of tests, scaled targets with floor and roof were exposed to contact explosions. The largest of these structures was 47 ft square and 28 ft high, with walls ranging from about 10 to 13.5 ft in thickness and with a 9.5-ft roof. At the same time a very extensive series of measurements of the transient phenomena that accompany an explosion in earth was made in order to facilitate extension of the results obtained to situations not exactly similar to those of the tests.

Relations between damage, structural characteristics, distance of explosion, type of soil, and amount of charge have been determined and are given in Chapter 3, where these investigations are fully discussed. A method of analysis for predicting the effect of an underground explosion on a massive buried target has been developed that gives results of the same order as those observed. This is described in Section 15.5.2.

15.2.3 Contact Explosions on Concrete

In addition to the investigations of the effects of explosions on massive, buried concrete structures described in Chapter 3, and to the studies of the additional cratering caused by the explosion of projectiles after partial penetration of concrete slabs that are discussed in Chapter 7, certain more or less fundamental studies of the mechanism of crater formation in concrete, and of the factors that control it, were made jointly by the CFD and Division 2 at Princeton. The factors that were investigated are the kind of explosive, the shape of charge and point of initiation, the closeness of contact with the concrete surface, and the strength of the concrete. In connection with this program, the relation between the impulse exerted by explosion of a contact air-backed charge and the size and shape of the charge was obtained from an impulse pendulum constructed for this purpose. Some investigations of the effect of using spaced slabs and of employing a scab-mesh (without concrete cover) to control scabbing were made.

Scabbing

The phenomenon of scabbing[3] consists in the violent separation of a mass of material from the opposite face of a plate or slab subjected to an impact or impulse. The scabbing due to impact of a projectile on a concrete slab is discussed in Chapter 7, while scabbing caused by contact earth-backed detonation is described in Chapter 3. The scabbing that is produced in a concrete slab by an air-backed explosion is discussed here. Scabbing is undoubtedly due to the propagation of a compression wave from one face to the other, and its subsequent reflection as a tensile wave. A material that is weak in tension, like concrete, may be unable to withstand the stresses produced, causing large pieces to be thrown off with considerable velocity. No complete analysis of the mechanism of scabbing has been made; such an analysis would not be entirely reliable because the behavior of brittle materials under tension is somewhat unpredictable in that considerable variation may occur from one test to the next. The tendency to scab decreases rapidly with an increase in slab thickness, and, of course, increases with an increase in the amount or effectiveness of the explosive.

For concrete of about 4,000-psi compressive strength, the scabbing limit for ½-lb TNT demolition blocks (1¾x1¾x3¼-in.) standing on end and initiated at the top is approximately 8 in. For the same blocks lying flat the limit thickness is about 10 in. This difference is due to the greater impulse exerted by the flat charge. By use of the model law discussed in Chapter 8, it is possible to predict the limit scabbing thicknesses for similar charges of TNT (or an equivalent explosive) of other sizes. Thus, for end-on and side-on detonation, respectively,

$$T_e = 0.85W^{\frac{1}{3}}, \quad (1)$$

and

$$T = 1.0W^{\frac{1}{3}}. \quad (2)$$

In these expressions T is the scabbing-limit thickness in feet for concrete of normal strength (about 3,000-4,000 psi) and W is the weight of charge in pounds, having about the same proportions as the demolition blocks. For other proportions, interpolation or extrapolation is necessary. This can probably be done most safely in terms of the impulse of the explosions, assuming for example that the scabbing limit depends only on the impulse produced. On this assumption,

$$T = 0.2J^{\frac{1}{2}}, \qquad (3)$$

where T is scabbing limit in feet and J is the impulse caused by the explosion. This quantity is discussed in Section 15.2.4 and methods of predicting it are given. It must be pointed out, however, that the relation between thickness and impulse that is shown has not been verified, and is offered only for want of anything better. The relation between scabbing limit and concrete strength has not been determined; it is believed that the limit thickness does not vary greatly with changes in strength.

The scabbed volume is shallower and broader than the front-face crater. Its volume in a 5-in. slab subjected to end-on detonation of ½-lb demolition blocks was from four to six times that of the crater. The presence of earth, or other backing material, in contact with the rear slab face tends to prevent scabbing.

Control of Scabbing

Scabbing of the interior of a concrete structure from impact or contact explosion is usually less serious than would be the penetration of the same missile and its subsequent confined explosion. However, since scabbing may be produced by contact explosion of high-capacity weapons unable to penetrate, and is a serious danger to personnel or equipment exposed to it, means of preventing or controlling scabbing are desirable in many situations.[8] Since the scab is shallow, it is not greatly affected by interior reinforcing of the slab unless the latter is near the inside face. If there is a layer of steel bars near the inner face it will generally cause a plane of weakness that facilitates scabbing. If the reinforcing layer is moved nearer the face of the slab the amount of scabbed material decreases. For a layer of steel bars, or a steel mesh, against the slab face, a scab may form but will not leave the slab provided the bars or mesh are firmly tied to the interior reinforcing. An alternative is to use a scab plate which must also be tied in to the interior reinforcing. No information on the design requirements of such antiscabbing devices is available. See also Section 7.3.3 of Chapter 7. Another scheme, much used by the Germans in the roofs of pillboxes and covered gun emplacements, is to place small steel I-beams either side by side, or separated and with curved steel soffit plates between lower flanges, on the bottom faces. These serve three purposes, as antiscabbing protection, formwork during the placing of concrete, and enhancement of resistance to perforation by bombs or projectiles. A double wall of concrete with air or some packing material between the sections also offers more resistance to scabbing than does a single wall with the same amount of concrete. The resistance to projectile perforation is also slightly increased. This scheme has two principal objections: first, detonation of an HE shell in the inner space will be much more destructive because of the confinement than if it detonated at the bottom of its normal crater in a solid wall; second, the cost of construction is increased by the complications of a double wall.

Cratering

A crater is produced at a point of impact or impulse, or by an internal explosion. Craters in earth are discussed in Chapter 3, craters in concrete from projectile impact in Chapter 7. Craters are also produced in concrete by contact or near-contact explosions; these are the subject of this section.[3-6]

Presumably, a crater is produced by an explosion as the result of very high, very concentrated forces underneath the explosion. These force material inward, causing breakup and displacement of a cone of material surrounding the inward moving region. No complete investigation of the mechanism of cratering has been made. The normal shape of a crater produced by contact explosion is quite different from that of a scab. The shape is nearly but not exactly conical. The depth is approximately 0.5 and the diameter 2.5 times the cube root of the volume (expressed in the same units).

Since the crater is caused by the explosive pressures its size will be affected by anything that affects the magnitude, the duration, or the distribution of explosive pressures. For contact charges of a constant amount of a given explosive, a change of shape of the charge has considerable effect on its cratering ability. A change of shape also affects the impulse produced by a given amount of explosive, as will be discussed later. Thus it is logical to assume that some relation exists between the impulse and the cratering power of a given charge. However, it is clear that other factors will also affect the situation, since the impulse exerted

by an explosion is the time integral of the total force exerted on the whole surface of the slab, whereas the crater is caused by the very large pressures in the immediate vicinity of the charge and only so long as they exceed the confined compressive strength of the material. An extensive series of tests[4] has shown that good correlation exists between impulse and crater volume, but the rather serious scattering of data indicates that other factors are important. This relation is approximately

$$V = 1.5J, \tag{4}$$

for charges on end and detonated at the end away from the slab, and

$$V = 1.2J, \tag{5}$$

for charges lying on their sides and detonated at one end. V is the crater volume in cu in. and J is the total impulse of the explosion in lb-sec, discussed later. The concrete is assumed to be of normal strength, of the order of 4,000 psi.

The crater volume is affected by a number of factors whose influence is not perfectly understood. For example, the volume is dependent on the concrete strength; preliminary tests indicate that it varies approximately inversely as the square root of the strength.[3] Thus, increasing the strength by 50 per cent will decrease the crater volume by about 25 per cent.

The orientation of the charge is very important inasmuch as it affects the impulse very strongly, as shown later. Thus side-on detonation of demolition blocks gives volumes about 25 per cent larger than does end-on detonation.

The point of detonation of the charge appears to be very important, and is believed to be responsible for much of the lack of correlation in the series of tests on which equations (4) and (5) are based. Preliminary tests[5] on concrete and steel plates using demolition blocks on end and detonated either at the top or at the bottom gave the following results: impulses were affected only slightly; initiation at the bottom gave impulses 4 per cent greater than at the top. However, initiation at the top gave greater damage; in mild steel, crater volumes were doubled, and in concrete they were nearly quadrupled over those for base initiation.

Some tests[4] made with different explosives indicate that there is close correlation between crater volume and both velocity of detonation in the explosive and the so-called "plate denting index" used by explosive technicians as a measure of the *brisance* of an explosive. As detonation velocity increases from 22,500 fps (TNT) to 25,500 fps (Comp. B), the crater volume for a given weight and shape of charge increases by about 60 per cent. These are only tentative relations, however.

11.24 Impulse Delivered to a Slab by a Contact Explosion

When a charge detonates near a flat surface, pressures are exerted on the surface that may cause it to move or may damage it. For contact charges the same effects occur. In this case the damage may be characterized either as *local* or as *indirect*. The first depends very much on the intensities of pressure acting, as well as on the durations. Indirect damage can occur in portions of the target structure that are distant from the charge; it depends mostly on the impulse, or total integral with respect to time of the force acting on the structure.

The direct measurement of pressures from contact charges is extremely difficult because of the intensities that occur. It may be possible by indirect methods to obtain some idea of intensities, i.e., from comparison of crater dimensions in materials of different strengths. Impulse, however, can be measured quite easily. Such measurements are useful in dealing with the indirect damage resulting from contact explosions, and are also related to the local damage, such as cratering, since some of the factors altering pressures must also affect impulse. However, as shown in the discussion of the relation between impulse and crater volume given in the previous section, the extent of local damage can be greatly changed by such things as changing the point of initiation, which results in only secondary changes in impulse.

The impulse from a contact explosion is the time integral of the total force exerted on the target. This must include both the very intense instantaneous pressures under the charge and the longer lasting pressures surrounding the charge following the explosion. The impulse will certainly depend on the kind of explosive and on the shape of the charge used. Thus a long, thin stick of explosive perpendicular to a surface will deliver a smaller impulse than the same stick lying flat, or the same amount of explosive in a short, wide cylinder. In other words, to increase impulse by adding explosive, it should be added in contact or near contact for the greatest effect. The impulse is affected by confinement. Thus a given amount of charge in a crater is confined on the sides and must expand more in a vertical direction than if it were on

a plane surface.[9] This effect may result in an apparent difference in behavior between strong materials and weak materials, since the formation of a crater may be an essentially unstable process which proceeds more rapidly with an increase in size.

The Impulse Pendulum

For measuring explosive impulses an impulse pendulum[7,8] was constructed at Princeton. This is essentially a steel frame about 12 ft high from which is pivoted a steel member supporting two pieces of armor plate which are placed back to back and separated by the thickness of the pivoted supporting member. An impulse normal to the surface of one piece of plate will cause the plates and their support to swing about the pivot. The amount of swing can be measured and used to calculate the impulse. Different sizes of plate can be used; the largest were 2 ft square and 3 in. thick, weighing approximately 1,200 lb (two plates). Charges can be detonated at the center of one plate and their impulses measured.

For the charge sizes (up to 2.3 lb) and plate sizes (18 to 24 in. square) that have been used there appears to be no effect of plate size. Thus, for a plane surface, the impulse delivered is found to be dependent on the weight of charge, the type of explosive, and a geometrical shape factor. Dimensional considerations indicate that if other things are kept constant the total impulse is directly proportional to charge weight.[9] The relative effectiveness of different explosives can be represented by explosive coefficients; several of these are shown in Table 1.[4]

Table 1. Relative explosive factors for impulse.

Explosive	Factor
TNT	1.00
Tritonal 80/20	1.03
Tetrytol 50/50	1.04
Comp. B	1.07
Pentolite 50/50	1.07
C-3 Plastic explosive	1.14
HBX-2	1.22
Tetryl	1.58

Tests have been made for a large variety of charge shapes. From these it appears that the geometrical parameter can be taken as $h/\sqrt{A}$, where h is the dimension of the charge perpendicular to the target surface and A is the sectional area of charge parallel to the surface. For a cylindrical charge with its axis parallel to the surface, A can be taken as its plan area (diameter times length). Thus impulse can be expressed as the product of charge-weight times the explosive factor given in Table 1, multiplied by a function of the shape factor $h/\sqrt{A}$. For TNT (either pressed or cast) the following relation for impulse has been determined:

$$\frac{J}{W} = \frac{180}{1 + \dfrac{0.87h}{\sqrt{A}}}, \qquad (6)$$

where J is the impulse expressed in lb-sec. This is based on experiments in which $h/\sqrt{A}$ ranged from 0.25 to 5.4.

An important result of this investigation is the knowledge that considerable differences in impulse can be obtained with a given charge simply by changing its orientation. For example, a TNT demolition block weighs ½ lb and is 1.75 in. square by 3.25 in. long. On end, its shape factor is 1.86; on one side it is 0.74. From equation (6) the corresponding impulse factors are 70 and 110. Thus end-on and side-on impulses from a block are 35 and 55 lb-sec.

The effect of changing the point of initiation of the charge was investigated.[9] The effect on impulse was found to be very small, amounting to only 4 per cent in the case of demolition blocks on end. Base initiation gave the greater impulse. The effect of small standoff was not studied. It is probable that the effect of standoff on impulse is much less than the effect on local damage discussed in a previous section.

13.2.5 Impact Tests of Reinforced Concrete Beams

At the University of Illinois an extensive test program was conducted on the behavior of small reinforced-concrete beams under impact.[10-12] The tests were arranged in seven series, each series designed to determine the effect of varying some beam parameter. In all, 435 beams were tested. Impact was produced by hammers, weighing from 7 to 50 lb, striking the beams centrally at velocities up to about 100 fps. The hammers were accelerated by compressed air driving a piston.

The following sets of tests were made:

Series 1. *Effect of type of contact between hammer and beam.* Interposed bearing plates of three sizes and weights were employed to transmit the impact to the beams. A few tests were made without bearing plates.

Series 2. *Effect of amount and grade of longitudinal reinforcing steel with light web reinforcement.* One group of beams had no web reinforcing.

Series 3. *Effect of amount and grade of longitudinal reinforcing steel with heavy web reinforcement.*

Series 4. *Effect of type of web reinforcement, including ordinary U-stirrups, spirals, and welded units.*

Series 5. *Effect of concrete strength, with stirrups.*

Series 6. *Effect of artificial scabbing planes, beams with and without stirrups.*

Series 7. *Effect of varying beam spans.*

The beams of series 1 to 5 were 4 in. wide, 5¼ in. deep, and 47 in. long on 42-in. span with the impact applied at midspan. A detail of a typical beam is given in Figure 1. The beams of series 6 were identical to these except for the addition of 2½ in. of concrete and two ⅜-in. bars added to the bottom. The beams of

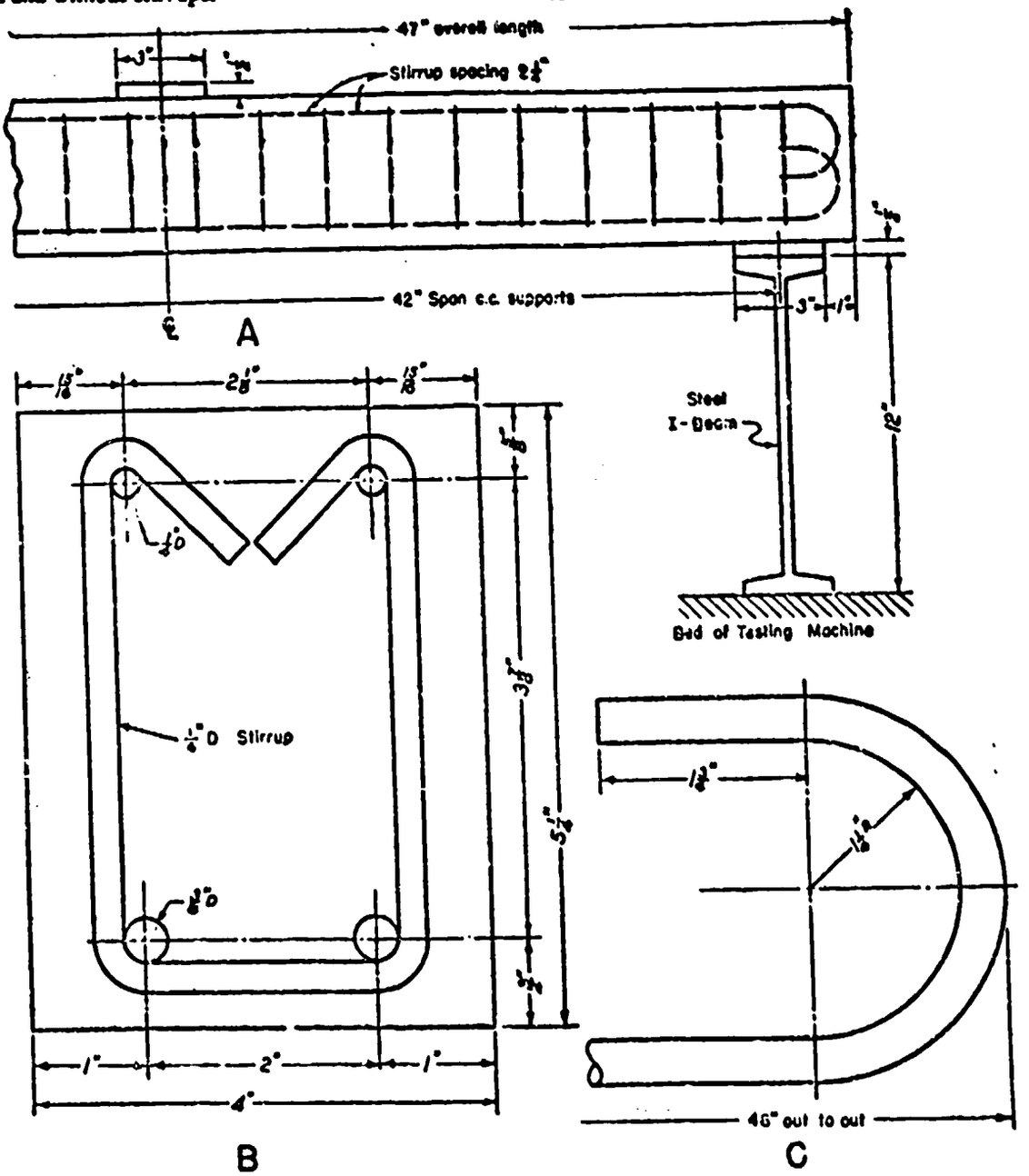

FIGURE 1. Typical details of test beams. A. Elevation. B. Cross section. C. Detail of hook at end of bar.

series 7 were of identical section to that shown in Figure 1. They varied in length by 2-ft increments from 30-in. to 126-in. and provided spans of 2, 4, 6, 8, and 10 ft. Except for series 5 all beams were made of concrete of the same mix, intended to give a compressive strength of 4,000 psi. The concrete was cured moist for 7 days, then stored until the beams were tested at the age of about 28 days. Generally, twelve beams of a kind were poured at the same time to provide for impact tests with three hammer weights, each at four velocities. Two 4x8-in. control cylinders were made with each batch of three beams and were stored with them and tested at the same time.

Testing Procedure

The beams were tested in the pneumatic impact-testing machine that is illustrated in Figure 2. The ends of the beam were supported on short lengths of 12-in. steel I-beam transverse to the length of the test beam, and were clamped in such a way that the ends of the test beam were held down during the test but were not restrained against rotation.

In all the tests except those of series 1 the impacts were applied through a 4x8x½-in. steel bearing plate embedded in a thin layer of plaster of Paris at the midspan of the beam.

The natural frequency of each beam was measured both before and after impact in order to secure a simple, quantitative measure of the extent of damage produced by impact.

The velocity of the hammer was measured just before impact. In order to limit the stroke of the hammer and to prevent it leaving the pneumatic cylinder, a stop was placed beneath the test beam which limited the deflection of the beam under the heavier impacts. Because the air pressure in the piston was not released during impact and was reduced by only about 6 per cent because of the increase in volume as the hammer was driven downward, a continued static force was exerted on the hammer, and consequently on the beam, after impact. Not only did this static force resist recovery of the beam after impact, but it contributed to the deflection, increasing it beyond the amount that would have occurred under impact of the hammer at the same velocity but without air backing. This effect is discussed further in Section 15.5.1.

After impact, the permanent deflection was recorded, and a sketch made of the beam showing the extent of spalling or scabbing and the pattern of cracks. Photographs were taken of all beams to record the visible damage. After the second determination of natural frequency, the beam was loaded statically to failure to determine by what amount the load-carrying capacity had been diminished by the impact.

Conclusions

Effect of Weight of Bearing Plate. Three weights of bearing plate, 0.04, 1.7, and 19 lb, were used. With the 7.5 and 18-lb hammers the greatest damage was produced with the 1.7-lb plate; with the 50-lb hammer the greatest damage occurred with heavy plate; but with all three hammers, the tendency to scabbing was greatest with the light plate.

As would be expected, the permanent deflection of the beam decreased with an increase in the weight of bearing plate, and the greatest change occurred with the lightest hammer. With the 50-lb hammer the effect of the bearing-plate weight was very small.

Effect of Repeated Impact. Several beams of series 1 were subjected to a repetition of impact. Even after a light impact, the second blow increased the deflection as would be expected, since each blow adds roughly the same amount of energy to the beam; if one blow causes plastic deformation the second may be expected to cause additional deformation. A rapid increase in structural damage seems likely with repeated impacts.

Effect of Variations in Amount of Reinforcing Steel. The role of longitudinal reinforcing is to resist bending of the beam as a whole, whereas the web reinforcement serves to maintain the integrity of the beam. Under concentrated impact, as in the present series of tests, there is a strong tendency for the beam to be broken up in the vicinity of the blow. Such breaking up can completely destroy the bending strength of a beam by removing the concrete surrounding the tensile bars at the section of the greatest bending moment. Consequently, for impacts of this kind, web reinforcing is very important in order to confine the concrete after it cracks; it also tends to prevent buckling of longitudinal steel when vibration of the beam puts it into compression. Various arrangements of web reinforcing were tried. There appeared to be little difference between these provided they were capable of the two functions just mentioned, restraint of concrete after cracking, and restraint of longitudinal steel against buckling. It should be mentioned that since a beam will vibrate upward as well as down, both top and bottom bars go into compression. It should also be pointed out that beams or panels subjected to distributed impulsive loads are very much less liable to local breakup, and the principal function of any web

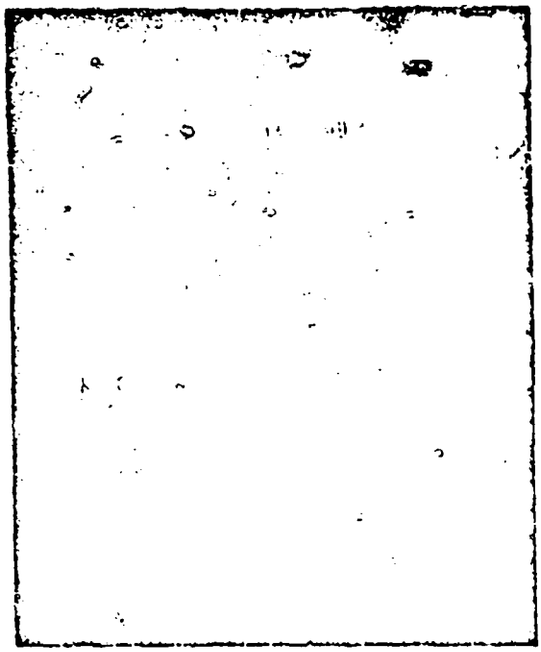

FIGURE 2. Pneumatic testing machine with beam in place for test with 50-lb. hammer

reinforcing is then to prevent buckling of longitudinal steel.

The heavy hammers tended to produce vertical cracks (similar to those occurring during static loading tests), whereas the lighter hammers tended to cause the diagonal cracks characteristic of scabbing. The velocity of impact appears to be the most important factor in scabbing; the lightest hammer at the highest velocities caused extensive scabbing and spalling.

There is some indication that an increase in the hammer velocity tends to cause a decrease in the initial slope, yield load, and maximum load obtained in the static test following impact. This effect would be expected since the higher velocity impacts would tend to produce more extensive cracking throughout the beam.

Effect of Concrete Strength. The compressive strength of the concrete had only a secondary influence on the action of the beams except for the impacts of greatest energy, for which the intermediate-strength concrete appeared to offer the greatest resistance. With low-strength concrete, the principal phenomenon accompanying failure appeared to be crushing of the concrete immediately under the bearing block. With the high-strength concrete, there was a wedging and splitting action beneath the bearing block, a chunk of concrete being forced down into the beam, spreading the stirrups and longitudinal steel apart. This action would have been much less serious if the stirrups had been complete loops instead of U-shaped, as in this particular test.

In general, it may be said that the concrete serves four functions: (1) it furnishes mass (the greater the mass of the beam, the less energy is given to it, other things being equal), (2) it furnishes compressive strength to balance the tension of the stretched longitudinal bars, (3) it keeps this tension at a distance from the compression portion of the beam, which is necessary for bending strength, and (4) it is the medium for transferring the impulsive load to the beam. For amounts of longitudinal steel such as used here (about 1.5 per cent at the bottom of the beam), the steel yields more than the concrete, even for concrete of moderate strength. (Note that a beam may be overreinforced for elastic deformation and at the same time underreinforced for plastic.) Thus, changing the concrete had little effect on the bending strength of the member, but would be expected to affect the local failure occurring under the load.

Effect of Artificial Scabbing Planes. Horizontal planes of weakness were introduced near the bottoms of beams with the thought that under impact, separation would occur at this section and that the scabbed material would carry away from the beam most of the energy given it, avoiding further damage to the beam. Unfortunately, practically no scabbing was caused in any of the experiments and it is impossible to draw any conclusions as to the possible efficacy of this scheme. These beams were, however, decidedly unsatisfactory since they were considerably weaker statically than beams of the same total depth without scabbing planes.

Effect of Span Length. These tests furnished only a partial answer to the question as to the effect of span on the impact resistance of a beam, since the results were complicated by the effect of the continuously acting air pressure in the cylinder of the hammer. The force so applied was, for the higher pressures and longer beams, of the same order as the static strength of the beams, hence the additional deflection due to this alone was too great to neglect. However, some of these results have been analyzed by the theory of plastic action discussed later in this chapter and illustrated in Section 15.5.1. Since this analysis gives results that agree generally with the observations it is concluded that the analysis is reliable. According to this theory the general or distributed damage (plastic

bending) decreases with an increase in span. This conclusion is partly supported by the results of these tests, since it was found that at low impact velocities, corresponding to low air pressures, resistance of beams increased with span. However, local damage is nearly independent of span.

The deflected shapes of the beams were determined after impact and found to be approximately linear from the span center to each support, with a short curved portion in the vicinity of the span center. There was also a small negative curvature in the outer portions near the supports.

Reference should be made to Sections 15.3.2 and 15.5.1, which discuss the analysis of these tests.

15.3 THEORY AND ANALYSIS

Because of the great variety of structures, materials, attacking agents, and conditions of attack, no experimental study can be complete. Thus, it is desirable to develop a method of analyzing structural behavior, in order that the results of the limited number of experiments that can be made may be used with confidence in predicting the behavior of structures of types that have not been investigated or that are subjected to situations that have not been studied experimentally. A method of analysis must fulfill certain requirements:

It must be simple and straightforward enough for use by the individuals who will have to use it, or else be reducible to graphs or tables for such use. It must give results that are reasonably reliable, possibly within a factor of 2, although this will depend on the particular situation; an empirical parameter introduced to make the analysis fit observation is permissible, but its presence limits the applicability of the analysis to situations similar to the ones for which agreement has been achieved, making extrapolation to other situations uncertain. An analysis must recognize the conditions of the problem; if the conditions of ultimate failure of a plastic structure are desired, then even a very good elastic analysis is of limited usefulness until the relation between the results of the analysis and the ultimate plastic state of the structure is known.

Elastic versus Plastic Design

Almost without exception, structures and structural elements exhibit both elastic and plastic behavior.[8] For loads below a certain load, removal of the load allows the structure to return to its original state; this is the definition of elasticity. (The relation between load and deflection is usually linear, but does not need to be.) For loads greater than the elastic limit, removal of the load does not result in the structure returning to its original state. The shape of the load-deflection relation is well known; an example is the stress-strain curve for structural steel. Normally, by far the greatest part of the area beneath the curve, which represents work done on the structure, is under the plastic portion; for mild steel or for an underreinforced concrete beam the total elastic energy is of the order of 1 per cent of the total deformation energy.

A static load is usually a specified *force;* occasionally it may be a specified deflection. A static load will seldom, if ever, be specified as a given amount of energy. A dynamic load, on the other hand, usually is applied either through impact by a mass having a given velocity, or as a force having a given variation with time. In each case the effect is to load the structure by giving it a definite quantity of *energy* (which may depend on the characteristics of the structure). This is the fundamental difference between static and dynamic loads; the former is usually a definite *force* capable of doing any amount of work within limits, while the second amounts to giving the structure a definite amount of *energy* whose amount may depend on the structure, but which, once given, must be handled by the structure to the best of its ability.

Ordinary engineering design nearly always is based on the assumption of elastic behavior in the structure. There are several reasons for this. In the first place the loads are generally static and the difference between the elastic-limit load of a structure and the greatest load it can take is not very large; the ratio is generally of the order of 1/2. In the second place, loads on ordinary structures may be removed and applied a large number of times. Unless stresses are kept well below the elastic limit, repeated loading will cause gradual deterioration and eventual failure. Finally, large deflections cannot be tolerated in most structures intended for everyday use, partly because cracking and noticeable sagging are not attractive.

Structures intended for protection against explosion or impact have been analyzed both elastically and plastically. The British used plastic analysis in designing certain air-raid shelters. The resistance of a plate or slab to a projectile is, of course, based on its plastic resistance, not its elastic strength. On the other hand, calculations based on elastic theory have been used in

the design of certain fortifications for the Corps of Engineers.

A structure can be designed for ultimate conditions either by means of what may be termed a plastic analysis, which attempts to take account of the actual mechanism of deformation of the structure, or by what may be called an elastic analysis, based on the usual elastic theory of structural design, but in which the permissible stresses are chosen, on the basis of experience, to yield an estimate of the true ultimate strength. Each method has certain advantages and disadvantages. The plastic analysis is the more realistic and rational. In situations where it can be applied but for which actual empirical information is lacking it is the more reliable. Its principal disadvantages are that it is entirely unfamiliar to most engineers, that at present it has been applied specifically only to certain comparatively simple design problems, and that some intuition and experience are needed by anyone applying it. The elastic method of analysis, although not especially simple in application, is more familiar to engineers than is the plastic method. It can also be applied to practically any type of structure. It has the disadvantage that it can be used to predict ultimate conditions only by the use of hypothetical allowable stresses of the order of ten times the actual ultimate strengths of materials. These hypothetical stresses can be reliably obtained only by comparison of elastic analysis with experiment. Where experiment is lacking, the use of hypothetical stresses based on other structural situations is risky.

To sum up: (1) A method of analysis designed to allow prediction of ultimate resistance is required for many problems of military design. (2) By the use of hypothetical design stresses (well above the actual ultimate strengths), the ordinary method of analysis, based on elastic theory, can be used for this. This can be applied to more situations and can be used by designers of less experience than can plastic analysis. (3) A method of analysis, based on the actual behavior of structures in the plastic state, has been developed. This is more rational than the elastic method in that it does not require the use of empirical factors.

15.3.1 Elastic Response of Structure to Impact or Impulse

The methods of determining the elastic behavior[13-18] of a structure under dynamic loading are based on the assumption that the relation between force and deflection (or stress and strain) is linear. A linear system is one for which force and deflection are proportional and for which removal of load results in a return to the original state. Such a system, when disturbed dynamically, tends to oscillate in its so-called *natural modes* or shapes of vibration. The natural modes of a stretched string are well known and consist respectively of one loop, two loops, three loops, etc., having progressively higher frequencies. When this system is disturbed and allowed to oscillate, all or most of the modes are excited and the resulting motion, although very complicated in appearance, consists only of combinations of these modes and frequencies. When a continuing disturbance is given to the string it acts in a definite way on each mode, and the response of the whole string can again be expressed as the sum of the responses of all its modes. Exactly similar considerations apply to any linear system. Such a system has natural modes, or shapes of vibration, each with a definite frequency. There may be an infinite number of modes (characteristic of so-called continuous systems such as the stretched string or a beam), or a limited number of modes, as in the case of a weightless spring supporting a series of weights. In general, the number of modes is equal to the number of quantities needed to describe the possible configurations of the system. Thus a system that consists of a spring supporting two masses that can only move vertically can be described completely by giving the vertical position of each mass, and has, therefore, two degrees of freedom and two modes.

The general problem of finding the elastic response of a system to a disturbance first requires determining the modes and frequencies of the system. Frequently, only the modes of lowest frequency are needed. Next, the effect of the disturbance on each mode is determined, and finally the total effect is found by combining the various mode effects. An exact mathematical solution is always possible but is frequently very difficult and tedious. There are various ways of simplifying the work. One is by using approximate shapes for the modes and determining from these shapes what the approximate frequencies are, then using these shapes and frequencies exactly as though they were the actual ones. This method, known as the Ritz-Rayleigh method, is a very useful one. It is necessary that the chosen mode shapes be possible ones and as close as possible to the real ones, and that important modes are not left out. Model tests facilitate mode and frequency determination. The reader who desires to apply the elastic method is referred to the references listed at the beginning of this section.

15.5.2 Plastic Response of Structure to Impact or Impulse

An analysis of the plastic behavior[9,13] of a structure is concerned with predicting the effect of a load that is sufficient to exceed the elastic limit of the material, usually by a considerable amount. There are various possible approaches to this problem. One is based on a mathematically exact analysis in which every attempt is made to represent the physical properties of the material correctly, either by equations or by graphs. This analysis must follow the structure through all phases of its response, and usually becomes extremely complicated as a result. This method is used in the plastic wave propagation studies discussed in Chapter 12. This approach has certain advantages in that strange and unexpected phenomena may be revealed by it that would not normally be discovered, such as the critical velocity of impact. The disadvantage is that the amount of labor involved in application is considerable and only very much idealized problems can usually be solved. Furthermore, in practical cases the various damaging agents involved and the characteristics of the structure are not usually known with any exactness. For this reason, another approach has been found to be more satisfactory in handling most practical problems.

An approximate method has been used for dealing with the plastic response of structures to impact or impulse that generally resembles the elastic method outlined above. First, the nature of the response of the structure is guessed at. This is the simplest and also the most critical part of the analysis. For complex structures it may be necessary to complete the analysis using several alternatives and to select the best one finally. The next step is either to calculate the amount of energy given to the structure during the impact or impulse and to use this to determine the final condition of the structure, or to set up a relation between the various forces known to be acting, the internal resistance to deformation, and the inertial reactions of the structure. These methods are shown in Sections 15.5.1 and 15.5.2 respectively. Although these methods are far from exact, examination of Figures 3 and 4 shows that in these cases at least, reasonable agreement with observation was obtained.

15.6 RECOMMENDATIONS FOR FUTURE WORK

The development of civilian protection can be put into three categories; there is much to be done with respect to each. These are (1) acquiring basic information, (2) applying that information to design and construction, (3) making overall plans for securing protection.

15.6.1 Fundamental Research

The information now available on the effects of weapons on structures is far from negligible and has mostly been acquired during World War II. However, it is not adequate, and will certainly be made less and less adequate now as weapons are developed. In general, the researches that have been described in this chapter should be extended and made more definite and more complete.

Because of the atomic bomb and the expected development of weapons of higher striking velocity and greater accuracy, protection by burial will probably become increasingly important. On this account the effectiveness of explosions at great depths and at great distances from deeply buried structures becomes important, and methods of securing maximum protection must be sought. Also, the effects of pressures of long duration on exposed structures must be determined, and means of minimizing these effects discovered.

15.6.2 Applications to Structures

Development in this direction has been much less than that on basic problems. In the case of ordinary structures it is desirable to determine what changes in existing structures and what changes in design and construction practice will most increase the resistance against air blast and earth shock. An examination of structures damaged and destroyed in England and Germany indicates that certain kinds of structures are peculiarly susceptible to large-scale collapse, for example the thin, concrete barrel-arch roof. Multistory structures with load-bearing brick or masonry walls are more vulnerable to internal or external blast than are frame buildings. Light beam connections may allow collapse that would have been prevented by heavy connections. Such considerations as these indicate that without great cost it may be possible to increase the blast resistance of cities by significant amounts. The economic advantages or disadvantages of such a plan should be investigated. In any event, it is very desirable that the relative safety of structures be determined in order that the more important facilities may not be left in the more dangerous places.

15.4.3 Overall Organization of Protection

Since most parts of this country will be vulnerable to attack in any future war it is of very great importance that protection for possible targets be planned. Since such protection will require extensive planning and a very long time to complete, it seems desirable to begin the task immediately. Such a plan will involve a great many things that have no connection with the present discussion. However, the following must be considered: (1) the various aspects of protection must be decided on, i.e., surface shelters, buried structures, methods of strengthening or protecting existing buildings, changes in building codes for bettering future construction; (2) the various standards of design and construction needed for the items enumerated above, i.e., methods of analysis, design loads, design stresses.

15.5 APPENDIX

15.5.1 Plastic Analysis of Reinforced Concrete Beams under Impact.

UNIFORM, SIMPLY SUPPORTED BEAM STRUCK AT CENTER BY WEIGHT W

Following the contact of the weight and beam the former is decelerated and the latter speeded up until they move together. Ordinarily, this will occur very quickly, in a time short compared to the total time required for the beam to come to rest again. Consequently, the reactions of the supports will be small compared to the force acting between the beam and weight. The shape of the beam is assumed to be parabolic or sinusoidal throughout the whole process, including both the period of acceleration under impact and the subsequent period of deceleration due to the plastic resistance of the beam to bending.

If the beam deflects sinusoidally its average deflection at any instant, taken over the whole span, is approximately ⅔ its maximum deflection at the instant. Similarly, its average velocity and average acceleration are, respectively, ⅔ the velocity and acceleration at the center. Furthermore, the average of the square of the velocity over the whole span is ½ the square of the center velocity.

The following symbols are defined:

F = the force between beam and weight at any instant,
t = time (variable),
T = duration of impact,
W = weight of striking body,
w = total weight of beam,
R = central force to overcome plastic resistance of beam (assumed constant),
V_0 = striking velocity of weight,
v_0 = common velocity of weight and beam at time T,
v = velocity of beam at point of impact at any time,
x = maximum permanent center deflection,
$E_0 = \frac{1}{2}WV_0^2/g$ — (initial energy of W),
E = total impact energy available for bending beam (the difference between E_0 and E is used up in producing local damage at the point of impact),
P = average force due to pressure on piston (tests of Section 15.2.4),
$E_b = E$ plus work done by P during deflection.

During the first stage of the impact the impulse acting on W must equal its loss of momentum: therefore,

$$\int_0^T F\,dt = \frac{W}{g}(V_0 - v_0). \tag{7}$$

The work done by F on the beam up to any instant t must be approximately equal to the kinetic energy acquired by the beam at that time; therefore,

$$\int_0^t Fv\,dt = \frac{wv^2}{4g}. \tag{8}$$

This expression can be differentiated, yielding $F = (w/2g)\,(dv/dt)$ which is substituted in equation (7).

Since $$\int_0^T \frac{dv}{dt}\,dt = v_0,$$

this gives $$v_0 = \frac{V_0}{1 + \frac{w}{2W}}. \tag{9}$$

Finally, the total energy given to the system consisting of the beam and weight is

$$E = \frac{E_0}{1 + \frac{w}{2W}}. \tag{10}$$

The energy given by equation (10) is available for bending the beam. Although the shape of the beam under dynamic bending will differ somewhat from the static shape the difference can be ignored in this approximate analysis. The relation between force and deflection of a beam can be determined by calculation with sufficient accuracy for present purposes; however,

there are usually available results of loading tests that cover the plastic range. From these the relation between deflection and external work can be found.

The procedure to be followed is then:

1. Calculate E_0, the striking energy of W,
2. Calculate the available energy from equation (10),
3. From the deflection-work relation obtained statically and the amount of energy available determine the permanent center deflection.

A similar process can be followed for other kinds of impacts or for impulses. For example, if the falling weight is not a single mass, but is distributed uniformly along the length of the beam (falling debris would be so treated) the energy available is

$$E = \frac{E_0}{1 + \frac{w}{W}}. \tag{11}$$

From a concentrated impulse J, of very short duration, acting at the center of span the available energy is

$$E = \frac{J^2 g}{w}. \tag{12}$$

From a uniformly distributed impulse of very short duration, the available energy is

$$E = \frac{4}{\pi^2} \frac{J^2}{w}. \tag{13}$$

Analysis of Impact Tests Discussed in Section 15.2.5

The relation between work and deflection in the plastic range for a reinforced concrete beam can generally be represented quite accurately by an equation of the form

$$x = \frac{1}{R}(E_0 - \epsilon), \tag{14}$$

where R is a constant equal to the average central force required to cause plastic bending of the beam. The quantity ϵ is small, and corresponds to the fact that a small amount of energy can be absorbed elastically by the beam without causing any permanent deflection. E_0 is the total energy supplied, normally equal to E.

An approximate value of R for beams that are not too heavily overreinforced and of normal proportions can be obtained in the following way if tests are not available.

1. For a simple span the effective bending length L' is less than the actual span L by approximately twice the depth of beam d.

2. The average plastic yielding moment is approximately $\frac{7}{8} \times \sigma \times A_s \times d$, where σ, A_s, and d are the average plastic strength of reinforcing, the total area of tensile steel, and the depth of beam to tensile steel, respectively. Then,

$$R = \frac{3\sigma A_s d}{L - 2d}. \tag{15}$$

The tests described in Section 15.2.5 can not be treated directly by use of equation (10) because of the fact that during the entire deflection time there was transmitted to the beam an additional force due to the air pressure in the cylinder acting through the hammer. If E is the energy available at the instant of impact, then by the time the system has come to rest an additional amount of work has been done equal to the average piston force P multiplied by x, the center deflection of the beam. Consequently, the energy used up by the beam exceeds the initial energy supplied by W by the amount Px. This leads to the following approximate relation between E_0, the energy of deformation, and E, the energy available from the falling weight:

$$E_0 = \frac{E}{1 - \frac{P}{R}}. \tag{16}$$

Then, for the present tests, equation (10) is replaced by

$$E_0 = \frac{E_0}{\left(1 + \frac{w}{2W}\right)\left(1 - \frac{P}{R}\right)}. \tag{17}$$

This, with equation (14), permits prediction of the permanent deflection produced in the tests under discussion.

One series of these tests has been analyzed. The analysis is outlined in Table 2, and the results of the analysis shown in Figure 3, which allows comparison between observation and prediction. The results appear to be adequate for engineering purposes; however, the consistently too-large effective energy predicted for the heavy hammer, and too-small effective energy for the light hammer indicate that the analysis can be improved. The difference is believed partly due to the fact that at equal effective energies the light hammer does more local damage than does the heavy hammer, on account of the higher velocity of the former. An additional reason is that the deformed shape of the beam depends somewhat on the velocity of impact; at the higher striking velocities of the light hammer the proportion of the beam participating in the deflection is less, hence the loss of energy is less, than for the heavy hammer.

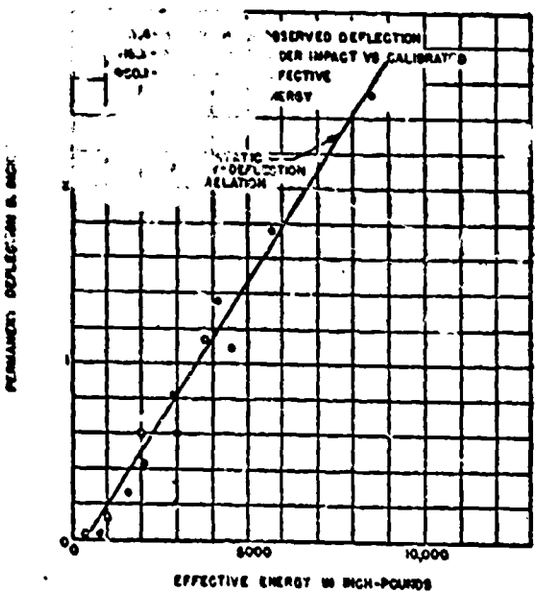

FIGURE 3. Relation between observed and predicted permanent deflection of reinforced concrete beams. See Table 2.

15.5.2 A Theory of Damage to Buried Structures from Underground Explosions

CHARACTERISTICS OF THE STRUCTURE

The structure is assumed to be a buried or partly buried, hollow, reinforced-concrete box, one of whose faces is exposed to a nearby underground explosion. The inside plan dimensions of the box are $L \times D$ (L is the unsupported length of the front wall), while H is the inside height. The front-wall thickness is a, that of each side wall b, and of the rear wall c. The ratio of the cross-sectional area of the reinforcing steel stretched during deflection of a wall to the total corresponding cross-sectional area of that wall is p, and is not necessarily the same in all walls or in the two principal directions of a wall. The concrete structure whose behavior will be analyzed here has no floor or roof; the same method can be applied to structures with floor and roof. The average yielding stress of the reinforcing steel in the plastic range is σ (intermediate between yield and ultimate strengths).

SYMBOLS

The following symbols are defined:

ρ and ρ_c = densities of earth and concrete respectively, or weight per unit volume divided by the acceleration of gravity (unit: lb sec^2 per in.^{4}),

P = pressure on face of structure at any time t,

P_0 = peak pressure (unit: psi),

I = impulse per unit area on face of structure,

t = time,

L = unsupported length of front target wall (unit: in.),

L' = effective length of front target wall for bending resistance (L' is less than L by an amount depending on the wall thick-

TABLE 2. Analysis of impact tests of reinforced concrete beams.*,†

W Weight of hammer (lb)	p Maximum air pressure (psi)	V_0 Striking velocity of hammer (in. per sec)	E_0 Striking energy of hammer (in.-lb)	P' Steady force after impact due to air pressure (lb)	E_b Total energy available for bending beam (in.-lb)	z Observed permanent deflection (in.)
50.1	100	233	3,580	490	1,630	0.265
50.1	150	268	5,400	735	3,040	0.614
50.1	200	332	7,130	980	4,630	1.081
50.1	300	404	10,300	1,470	8,500	2.532
18.1	100	384	3,450	490	868	0.028
18.1	200	537	6,780	980	2,110	0.417
18.1	250	597	8,300	1,225	2,920	0.803
18.1	300	653	10,150	1,470	4,140	1.355
18.1	350	708	11,700	1,720	5,650	1.764
7.4	100	592	3,360	490	405	0.023
7.4	200	838	6,700	980	980	0.128
7.4	300	1,025	10,000	1,470	1,990	0.590
7.4	400	1,180	13,200	1,960	3,770	1.151

* Data from Table 5 of Reference 12.

† Beams 4×5¼-in. on 72-in. span. Tensile reinforcing is 2¼-in. round bars at depth of 3⅛ in. (Figure 1). Yield point and ultimate strength of steel are 51,000 and 77,000 psi. R (plastic resistance of beam) = 3,050 lb from static tests or 2,900 lb from equation (14).

‡ After impact, air pressure is approximately 04 per cent of initial pressure and acts on area of 5.21 in.^{2}

ness, here the difference is taken as $(\frac{3}{4})a$, where a is front-wall thickness),

M = plastic bending moment of a strip of front face of unit width, approximately equal to $\frac{1}{4}\sigma_p a^2$ (unit: in.-lb per in.),

M' = plastic bending moment of a strip of rear wall of unit width,

R = reaction on each side wall from a strip of front wall of unit width, during deformation (unit: lb per in.),

R' = reaction on each side wall from a strip of rear wall of unit width, during deformation,

m = mass of unit area of front wall $= a\rho_c$,

m_1 = mass, per unit area of front face, of the remainder of the structure,

m_1' = mass, per unit area of front face, of the remainder of the structure with the exception of the rear face,

x = center deflection of the front wall at any time t (unit: in.),

x_m = permanent center deflection of front wall,

y = displacement of remainder of structure at any time t (unit: in.),

s = distance along a front-face strip measured from a side wall (unit: in.),

C = sum of crack widths in convex side of deformed wall (unit: in.),

k = soil constant, defined in Chapter 3 (unit: psi),

W = weight of charge (unit: lb),

r = distance of charge from front face (unit: ft),

$\lambda = r/W^{\frac{1}{3}}$.

A consistent system of units must be used. Here, all quantities will be in pounds, seconds, inches, except r, distance from charge to target, which must be in feet in order to fit the empirical equations for dependence of pressure and impulse on charge distance that are discussed in Chapter 3 and will be used.

The Explosion

A charge weighing W lb explodes at a distance r ft from the front face of the target and at about the depth of the center of the face. The pressure acting on the front face is assumed to decrease linearly with time from its initial peak value, so that

$$P(t) = P_0\left(1 - \frac{tP_0}{2I}\right), \tag{18}$$

for t less than $2I/P_0$, while P is zero thereafter. For explosives equivalent to TNT, P_0 and I at the center of the target face are given by the expressions below, which are discussed more fully in Chapter 3,

$$P_0 = \frac{2k}{\lambda^2}, \tag{19}$$

and

$$I = \frac{25\rho^{\frac{1}{3}}k^{\frac{1}{3}}W^{\frac{2}{3}}}{\lambda^{\frac{4}{3}}}. \tag{20}$$

For near explosions P_0 and I over the greatest part of the front face will be less than at the center of the face. Consequently, in using equations (19) and (20) for calculating damage, a 25 per cent reduction will be made to allow for this. This reduction will be too great for distant charges and probably too small for near charges.

Physical Behavior of Structure

The pressure acting on the front wall of the structure deforms it plastically, and is in equilibrium with its inertial resistance, its plastic resistance, and the reaction of the remainder of the structure. In other words, the work done to the front face of the structure by the pressure must be equal to the kinetic energy given the wall, plus the energy absorbed in plastic bending, plus the work done by the wall in moving the rest of the structure. Similarly, the reaction of the front wall on the rest of the structure plus the pressures applied directly to the rest of the structure are in equilibrium with the inertial and other forces opposing the motion of the rest of the structure. There are two possibilities here; either the entire remainder of the structure moves as a solid, pushing back the earth behind it, or the rear face is deformed plastically by the pressure of the earth behind it, against which it is pushed. Normally, both possibilities must be considered. The one most likely to occur is that which causes less damage to the front wall.

Case 1—No Rear Wall Damage. Consider a strip of the front wall of unit width, and extending from one side wall to the other. Under the impulsive pressure this strip will bend, assuming an approximately sinusoidal shape; in addition, the side walls to which the strip is attached will move in the direction of the pressure. $y + x \sin \pi z/l$ is the displacement of any point z of this strip. Its velocity and acceleration are, respectively, $dy/dt + dx/dt \sin \pi z/L$ and $d^2y/dt^2 + d^2x/dt^2 \sin \pi z/L$.

During an infinitesimal interval of time dt, the external pressure acting on the entire strip does an amount of work,

$$\Delta E = dt \int_0^L \left(\frac{dy}{dt} + \frac{dx}{dt} \sin \frac{\pi z}{L}\right) P dz,$$

$$\Delta E = LP \left(\frac{dy}{dt} + \frac{2}{\pi} \frac{dx}{dt}\right) dt. \quad (21)$$

During an infinitesimal interval of time dt, the energy expended in bending the strip plastically is equal to the plastic bending moment multiplied by the total change of curvature (provided there is no reversal of curvature),

$$\Delta E_p = \frac{d}{dt} Mx \frac{\pi^2}{L^2} \int_0^L \sin \frac{\pi z}{L} dz dt,$$

$$\Delta E = \frac{2\pi M}{L} \frac{dx}{dt} dt. \quad (22)$$

The total kinetic energy of the strip at t is

$$E_k = \frac{m}{2} \int_0^L \left(\frac{dy}{dt} + \frac{dx}{dt} \sin \frac{\pi z}{L}\right)^2 dz,$$

and the increase in this quantity during an interval dt is

$$\Delta E_k = \frac{mL}{2} \left[2 \frac{dy}{dt} \left(\frac{d^2y}{dt^2} + \frac{2}{\pi} \frac{d^2x}{dt^2}\right) + \frac{dx}{dt} \left(\frac{2}{\pi} \frac{d^2y}{dt^2} + \frac{d^2x}{dt^2}\right) \right] dt. \quad (23)$$

The sum of the two end reactions of the strip is

$$2R = PL - m \int_0^L \left(\frac{d^2y}{dt^2} + \frac{d^2x}{dt^2} \sin \frac{\pi z}{L}\right) dz$$

$$= L \left(P - m \frac{d^2y}{dt^2} - \frac{2}{\pi} m \frac{d^2x}{dt^2}\right). \quad (24)$$

In an interval of time dt, these reactions do work on the rest of the structure equal to $2R$ multiplied by the distance moved in that time,

$$\Delta E_r = \frac{dy}{dt} L \left(P - m \frac{d^2y}{dt^2} - \frac{2m}{\pi} \frac{d^2x}{dt^2}\right) dt. \quad (25)$$

Equating the work done on the front wall to the sum of the plastic work, the increase in kinetic energy, and the work done on the rest of the structure, yields

$$m \left(\frac{d^2y}{dt^2} + \frac{\pi}{4} \frac{d^2x}{dt^2}\right) = P - \frac{\pi^2 M}{L^2}. \quad (26)$$

The left side of equation (26), the equation of motion of the front wall, is the average inertial force per unit area of the wall. The first term on the right is the pressure, or applied force per unit area. The second term is the average force per unit area required to overcome the plastic bending resistance of the strip, and corresponds to the force that is transmitted to the remainder of the structure by the ends of the strip.

The plastic-bending resistance of a beam is somewhat greater than is calculated on the basis of the actual span. For example, in Section 15.5.1 the effective span was taken as the actual span less twice the thickness. In the present case the thickness is rather large compared to the span, and the effective span will be assumed to be less than the actual span by ¾ the thickness. Hence, in equation (26) L will be replaced by L', assumed equal to $L - \frac{3}{4} a$, and

$$m \left(\frac{d^2y}{dt^2} + \frac{\pi}{4} \frac{d^2x}{dt^2}\right) = P - \frac{\pi^2 M}{L'^2}. \quad (26')$$

If the back wall of the structure is not deformed the resistance of the earth behind it must be considered. This consists of two parts, a passive pressure, and an apparent mass that can simply be added to the mass of the structure. The first is taken as the average hydrostatic force due to a fluid of density 50 per cent greater than that of earth. The apparent mass is taken as a mass of earth in contact with the rear wall and of depth (perpendicular to the wall) ¼ its height. Neither contribution is large in the case of the structures considered. Then the equation of motion of the rear portion of the structure is

$$2R + 2bP = \frac{3\rho g H}{4} (L + 2b) + m_1 L \frac{d^2y}{dt^2}. \quad (27)$$

From equations (24), (26'), and 27), one obtains

$$m \frac{d^2x}{dt^2} = AP - B, \quad (28)$$

$$A = \frac{1.275 \left(\frac{m_1}{m} - \frac{2b}{L}\right)}{\frac{m_1}{m} + 0.19}, \quad (29)$$

$$B = \frac{0.636 \left[19.78 \frac{M}{L'^2} \left(1 + \frac{m_1}{m}\right) - \frac{3}{2} \rho g H \left(1 + \frac{2b}{L}\right)\right]}{\frac{m_1}{m} + 0.19} \quad (30)$$

Equation (18) can be combined with equation (28)

and integrated to give

$$m\frac{d^2x}{dt^2} = AP_0 - B - \frac{AP_0^2}{2I}, \qquad (28')$$

$$m\frac{dx}{dt} = (AP_0 - B)t - \frac{AP_0^2t^2}{4I}, \qquad (31)$$

$$mx = (AP_0 - B)\frac{t^2}{2} - \frac{AP_0^2t^3}{12I}. \qquad (32)$$

A maximum in x occurs when

$$t = \frac{(AP_0 - B)4I}{AP_0^2},$$

which is normally later than the time $t = 2I/P_0$, at which P becomes zero, and the equation (18) ceases to hold. In this case it is necessary to solve equation (28) with P equal to zero, making this solution continuous with equations (31) and (32) at the time $t = 2I/P_0$. When this is done the maximum value of x is given by

$$x_m = \frac{A^2I^2}{2Bm}\left(1 - \frac{4B}{3P_0A}\right). \qquad (33)$$

Case 2—Rear Wall Yields Plastically. The equation of motion of the front wall is the same as before, namely,

$$m\left(\frac{d^2y}{dt^2} + \frac{\pi}{4}\frac{d^2x}{dt^2}\right) = P - \frac{w^2M}{L'^2} \qquad (26')$$

The two side walls are assumed to be displaced an amount y against the resistance due to the bending of the rear wall. Their equation of motion is

$$2R + 2bP = m_1'L\frac{d^2y}{dt^2} + 2R_1. \qquad (34)$$

From equations (24), (26'), and (34) one obtains by the same process as before

$$x_m = \frac{A'^2I^2}{2B'm}\left(1 - \frac{4B'}{3P_0A'^2}\right), \qquad (35)$$

$$A' = \frac{1.275\left(\frac{m_1'}{m} - \frac{2b}{L}\right)}{\frac{m_1'}{m} + 0.19}, \qquad (36)$$

$$B' = \frac{0.636\left[19.76\frac{M}{L'^2}\left(1 + \frac{m_1'}{m}\right) - \frac{4R_1}{L}\right]}{\frac{m_1'}{m} + 0.19}. \qquad (37)$$

Front-Face Crack Width

When a slab is bent there is a surface within it that does not stretch, called the neutral surface. This is close to the concave side of the slab. Since concrete is brittle, bending causes cracks to open on the convex side of a slab. At any spot the average total crack width per unit length of slab surface will be approximately equal to the distance from the neutral surface, which is about ¾ the slab thickness, multiplied by the curvature of the slab in the direction in which the crack width is measured. If x_m is the center deflection, L the length of span, $3a/4$ the depth of the neutral surface, and C the total amount of stretch or the crack width in the distance L, then

$$C = \frac{3ax_m}{L}. \qquad (38)$$

Illustration

Consider the buried concrete structures whose tests are reported in Chapter 3, and the results shown in Figures 13 and 14 of that chapter. These structures are at scales varying up to 25x25 ft in outside plan dimensions and 17.5 ft high. The front, side, and rear walls are respectively 5, 2.1, and 3.33 ft thick. The value of p (proportional steel area) is approximately 0.0014 for each wall. These structures were damaged by 1,000-lb TNT charges at various distances in earth. The value of k (soil constant) for the area in which these tests were made is 5,000 psi. Then,

$W^{\frac{1}{3}} = 10$,

a, b, and c are respectively 60, 25, and 40 in.,

$L = 250$ in. and $L' = 205$ in.,

$m = 60\,\rho_s$,

$m_1 = 140\,\rho_s$ and $m_1/m = 2.33$,

$m_1' = 60\,\rho_s$ and $m'/m = 1.0$,

$2b/L = 0.2$,

$M = (\frac{3}{4})\,\sigma pa^2 = 270{,}000$, if $\sigma = 70{,}000$ psi,

$M/L'^2 = 6.4$ psi,

$R_1/L = 3\,\sigma\,pc^2/L'^2 = 10.6$ psi (this is found from the plastic bending moment in the back wall, which is approximately $(\frac{3}{4})\,\sigma pc^2$, and the relation between the maximum bending moment and the uniform load $2R_1/L$ per unit length, on a beam of effective span L'; thus $(2R_1/L)\,(L'^2/8)$ equals $(\frac{3}{4})\,(\sigma pc^2)$),

$\rho gh = 11.8$ psi,

$$A = \frac{1.275 \times 3.13}{2.63} = 1.08,$$

$$B = \frac{0.636(10.78 \times 6.4 \times 3.33 - 11.8 \times 1.8)}{2.52}$$

$= 100$ psi,

$$A' = \frac{1.375(0.3)}{1.19} = 0.86,$$

$$B' = \frac{0.636(19.78 \times 6.4 \times 2 - 42.4)}{1.19} = 113 \text{ psi},$$

For Case 1 (nondeforming rear wall),

$$\frac{x_m}{kW^3} = \frac{1}{12.5\lambda^3}\left(1 - \frac{\lambda^3}{60}\right). \tag{39}$$

For Case 2 (rear wall bends plastically)

$$\frac{x_m}{kW^3} = \frac{1}{22\lambda^3}\left(1 - \frac{\lambda^3}{43}\right). \tag{40}$$

It can be seen that Case 2 is the more likely. Equation (40) is plotted in Figure 4 together with the experimental points from the tests of these structures. It can be seen that the analysis predicts too little damage at large distances and too much damage at near distances. The reason for this is not clear, but may be associated with the fact that the nearer the charge to the target the less uniform the loading becomes, while for distant explosions the loading is very nearly uniform. It will be recalled that impulse and pressure were both arbitrarily reduced by 25 per cent to allow for the nonuniformity of pressure over the entire target. For distant charges this overestimates the reduction and for near charges it probably underestimates it.

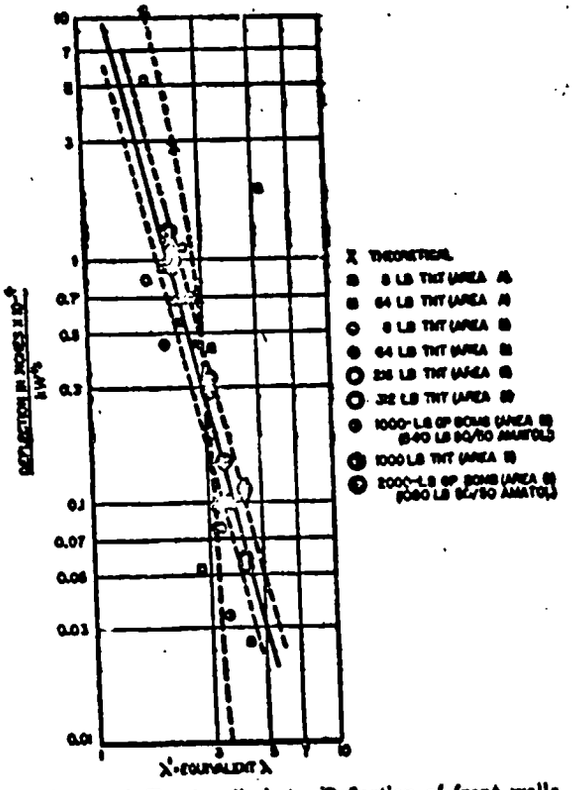

FIGURE 4. Front-wall shots. Deflection of front walls as function of λ'.

PART VI

ATTACK

Chapter 16

TARGET ANALYSIS AND WEAPON SELECTION

MODERN WARFARE is a specialized branch of engineering, and the proper prosecution of a war requires that available weapons be used at the highest efficiency possible under the prevailing operating conditions. The objective of the attacker is to inflict the maximum of damage with a given expenditure of effort. His tools are the various weapons developed by his technicians and supplied by his industry. It is desirable (1) to have efficient weapons, (2) to have a sufficient but not excessive selection of weapons, (3) to use weapons as effectively as possible, and (4) to know the effectiveness of the weapons used.[a]

16.1 INTRODUCTION

In order to make intelligent weapon selections one must know the characteristics of the weapons and understand the mechanisms by which they inflict damage on a target. In this chapter, first the characteristics of the most common weapons are briefly described, then each of the usual mechanisms of damage is discussed from the point of view of efficiency of the weapon. In Section 16.9 this information on weapons and mechanisms of damage is used to make detailed analysis of and weapon selection for several typical target types, and this section serves to illustrate the application of the principles described in the earlier sections of this chapter. The chapter is concluded by a few suggestions for further work on the effects of weapons on targets.

The most widely used report of Division 8 is the looseleaf notebook *Weapon Data — Fire, Impact, Explosion*. This notebook consists of Weapon Data Sheets containing quantitative information on the characteristics of weapons, the mechanisms by which they act on targets, and the selection of weapons for attack of certain target types. The final edition of this notebook, published as OSRD Report No. 6053, is reproduced as part of Chapter 19. Frequent references to individual Weapon Data Sheets are made throughout this chapter, and the sheets should be used as supplements to the material presented here.

A thorough understanding of the behavior of weapons requires knowledge of the fundamental phenomena of explosions and terminal ballistics as described in earlier chapters of this volume. References to pertinent sections of these chapters will be made, and although the present chapter can be studied independently, it is suggested that the reader make himself familiar with the more important points of the earlier chapters.

[a] Pertinent to joint Army-Navy Projects AN-23, AN-28, AN-29 and to Navy Project NO-267.

16.2 EFFECTIVENESS OF WEAPONS

During World War II considerable attention was given to the effectiveness and the proper use of weapons. This study was started by the British, with interest originally on defense in various civil and military establishments, and was eventually concerned with air, land, and sea warfare. Before the entrance of the United States into World War II, studies, likewise for defense, were initiated at Princeton at the request of the Army Corps of Engineers. As World War II progressed, there was a continued change of interest and eventually, the work at Princeton under Division 2 was primarily concerned with aerial attack. However, other methods of attack are discussed in this chapter. The following aspects of this work were most important: (1) the continued acquisition and correlation of information on the effectiveness of aerial weapons based on the experience of the British under German attacks, the results of tests of weapons in Britain and in the United States, and the examination and study of the effects of Allied bombing; (2) the preparation and distribution of data sheets on the characteristics and performance of various weapons (see Chapter 19); (3) the training of operations analysts in methods of target analysis and weapon selection (see Chapter 18); and (4) collaboration with the Joint Target Group (AC/AS Intelligence) in preparing recommendations for the aerial war in the Pacific, and with the United States Strategic Bombing Survey in drawing conclusions from the European theater.

16.2.1 Methods of Studying Effectiveness of Weapons

To use his weapons efficiently, the attacker must know the effectiveness of the weapons against various types of targets. Two methods have been used to study

the effectiveness of weapons: (1) synthesis of the effects of the weapons on separate components of structures, as determined by special tests, into a composite picture of the expected damage to the complete structure, and (2) study of damage caused in actual attacks. The first method has the advantage of applicability to a wide variety of targets, and the disadvantage of such complexity for most structures that it is difficult to use. The second method has the advantage of giving direct information, and the disadvantages of difficulty in determining the extent of the damage to enemy targets, and uncertainties in using the results to predict damage to a different type of target. A combination of the two methods, using one to supplement the other, has been found to be most effective.

Synthesis of Effects on Structural Components

Model- and full-scale tests have been made to determine the effects of explosion, fragments, fire, and other mechanisms of damage on various components of structures such as columns, beams, roofing, floor slabs, and wall panels. The results of such tests can, in principle, be used to predict the effect of any weapon on a structure having components of known characteristics. This type of engineering analysis has been attempted for industrial buildings, but, except for special cases, the complexity of the targets and the interrelations of the various types of damage have made the problem too difficult for ready solution.

Damage involving only one simple component of a target, such as the perforation of armor plate or concrete slabs, or the cratering of open ground, can be studied by direct and simple experiment, and the results can be applied to predicting damage to actual targets.

Study of Damage in Actual Attacks

Many studies have been made of the damage suffered by targets under attack by various weapons. Bombing attacks have been made on enemy installations, and by study of aerial photographs taken before and after the raid skilled photointerpreters can make very good estimates of the damage. The methods used in photointerpretation studies must be checked by intelligence reports on enemy-held targets and by detailed study when such targets fall into our hands. Ground surveys of the damage received by enemy factories, cities, and military installations have been made after these targets were in the hands of our own forces. This method of evaluating the effectiveness of weapons has a weakness in that the targets have usually been attacked by several weapons and it is frequently extremely difficult to attribute damage to a specific weapon.

Studies have been made by constructing models or copies of enemy installations and attacking these with the weapons to be evaluated. This method yields very useful information for attacking specific target types.

Studies of British buildings damaged by German air raids have been made, and where the size and type of weapon can be determined these yield useful information. One important function of these damage studies has been to check the methods used in photointerpretation by estimating the damage to the same structure by both ground and aerial surveys.

Controlled Experimental Attacks. A direct comparison of the effectiveness of different bombs can be made by selecting several enemy targets as nearly alike as possible and attacking each target with one of the weapons to be evaluated. By a study of aerial photographs taken before and after each attack, the relative effectiveness of the weapons can be determined. This method of studying the effectiveness of weapons has the advantage of damaging enemy targets and avoids the necessity of constructing prototypes. It has the disadvantage of relying entirely upon photointerpretation for the evaluation of damage.

Combination of the Two Methods

As stated above, the best method of studying the effectiveness of weapons is a combination of methods (1) and (2). Knowledge of the performance of explosives, the distribution of fragments, the ability of a missile to perforate a target, and other action of weapons on targets can be used to interpret the damage observed in terms of the characteristics of the weapon. Sufficient information on the fundamentals of weapon performance and the various mechanisms of damage possible with each weapon will enable one to correlate the observed damage from a number of different attacks and to draw general conclusions that may be used in planning future attacks to utilize the capabilities of the weapons in the most effective manner.

16.3 TYPES OF WEAPONS—THEIR CHARACTERISTICS

In order to evaluate the performance of weapons, the characteristics of the weapons must be known. Weapons may be used for explosive effect, for perfora-

tion or penetration (sometimes followed by explosion), for fragmentation, fire starting, or other effects. Airborne weapons, artillery and naval guns, and special-explosive weapons will be described separately.

16.3.1 **Airborne Weapons**

HIGH-EXPLOSIVE BOMBS

High-explosive [HE] bombs (see Weapon Data Sheet 1A3a* of Chapter 19) are of several types, the main difference being in the strength of the case. Bomb cases must be able to withstand the impacts to which they are subjected, for if a bomb case is ruptured before the explosive detonates a low-order explosion is likely to result. Low-order explosions are a relatively slow burning of the explosive and have very little effect compared to that of a proper high-order explosion.

Bombs that are to be used for penetration of resistant targets must have strong bodies, and the thickness of the case required for this strength leaves room for only a small quantity of explosive. Bombs that explode on contact or in the air need a body only for handling and so may have very thin cases, leaving room for a large quantity of explosive. These extremes and intermediate types of bombs may be described by the *charge-weight ratio*, which is the weight of the explosive charge divided by the total weight of the filled bomb.

Light-Cased [LC] *Bombs.* Light-cased bombs have a thin case and a charge weight ratio of about 80 per cent. The thin case cannot withstand severe impact and the bombs must be fuzed to explode instantaneously on contact with a light surface or to explode in the air above a target. As shown below in Section 16.5.1, bombs that damage a target by exterior blast are more efficient in large sizes than in small sizes; consequently, LC bombs are made only in large sizes. They should be used wherever maximum explosive effect is desired and penetration is not necessary.

General-Purpose [GP] *Bombs.* General-purpose bombs have cases somewhat thicker than those of LC bombs and a charge-weight ratio of about 50 per cent. The case is strong enough to withstand impact on most industrial construction and the bombs can penetrate into soil without deformation or rupture of the body; however, GP bomb cases will break up if the bombs are dropped on heavy concrete slabs (see Weapon Data Sheet 2C1a in Chapter 19). General-purpose bombs are available in a wide range of sizes. Since they can withstand impacts they can be used with delay fuzing.

Semiarmor-Piercing [SAP] *Bombs.* Semiarmor-piercing bombs have heavy cases and a charge weight ratio of about 30 per cent. The cases have sufficient strength to perforate medium armor or reinforced concrete without deformation. These bombs can be used with delay fuzing for attacks on targets protected by medium armor or reinforced concrete.

Armor-Piercing [AP] *Bombs.* Armor-piercing bombs have very heavy cases and contain only a small quantity of explosive. The charge-weight ratio is usually 10 to 15 per cent. These bombs are designed to perforate heavy armor plate without deformation or rupture of the case, and should be used with delay fuzing for attacks on targets protected by heavy armor.

INCENDIARY BOMBS

Incendiary bombs (see Weapon Data Sheets 1A3b, 1A3c of Chapter 19) are of two types: the intensive type and the scatter type. Bombs of the intensive type burn as a unit and confine their intense heat to a relatively small area. They are usually small (2 to 10 lb) and are dropped in clusters. Bombs of the scatter type are somewhat larger than those of the intensive type and are usually dropped singly. These bombs explode on impact and throw chunks of gasoline gel or other sticky highly inflammable material in all directions. The purpose of incendiary bombs is to start fires, and the choice of one or the other type depends on whether chunks of burning gasoline gel scattered over a small area or a number of smaller bombs scattered over a wider area will be more effective.

Incendiary Bomb Clusters. The small intensive-type incendiary bombs are packed in clusters that may be loaded on aircraft like the larger bombs. These clusters may be quick-opening or aimable: the quick-opening clusters open a short distance below the aircraft and the small bombs are scattered over a wide area, while the aimable clusters are dropped from high altitudes and open at an altitude of about 5,000 ft, scattering the bombs over a relatively smaller area.

SPECIAL-PURPOSE BOMBS

In addition to the HE and incendiary bombs described above, there are several types of bombs designed for special purposes (see Weapon Data Sheets 1A3a*, 1A3d of Chapter 19). Some of these are the fragmentation bombs, depth charges, and aerial torpedoes described below. Other special-purpose bombs such as chemical bombs and pyrotechnics are not discussed here since they are not used to create physical damage.

Fragmentation Bombs. Fragmentation bombs have

a fairly thick steel case that is broken up into small pieces, or fragments, by detonation of the explosive filling. The bodies of most types of fragmentation bombs are made of a helix of steel bar wrapped around a thin inner case; this results in fragments of a fairly uniform size dependent on the size of the steel bar. Since fragmentation bombs are designed to damage a target by missiles from the bomb case, they are always fuzed to explode on contact or in the air above the target.

The most used fragmentation bombs are small (4 to 20 lb) so that a large number of them may be carried to give good coverage over the target area. Some targets are only vulnerable to heavy fragments of high velocity; for these, larger fragmentation bombs are required. The small fragmentation bombs are packed in clusters for convenience in loading on aircraft.

For low-altitude attack with fragmentation bombs, small parachutes must be attached to the individual bombs. This slows the descent so that the attacking aircraft will be out of the danger zone before the bombs explode.

Depth Bombs. Depth bombs are designed for maximum underwater-explosive effect. Since the case must only withstand impact on water, it is thin and the charge weight ratio is approximately 70 per cent. Depth bombs carry hydrostatic fuzes that can be preset to cause detonation at any desired depth. These bombs may also be equipped with instantaneous nose fuzes so that they can be used as small LC bombs against surface targets.

Depth bombs have flat noses to prevent ricochet on striking water when dropped from low altitudes, and to give a better underwater trajectory. Some of the earlier models had round noses, but these can be equipped with a flat false nose.

Aerial Torpedoes. Aerial torpedoes are designed for launching from low-flying aircraft. They are similar in design and action to ship-launched torpedoes. Aerial torpedoes have a nose shaped to prevent ricochet when dropped from very low altitudes and to give underwater trajectories that are near the surface for a long distance.

Aircraft Rockets

Aircraft rockets were still in the process of development at the end of World War II. Most aircraft rockets now in use are essentially artillery projectiles propelled by rocket motors. They are used in low-level or diving attack at short range. Rockets can be aimed more accurately than bombs, but have the disadvantage of less explosive effect due to their smaller size.

Aircraft Gunfire

The small machine guns carried by most military aircraft can be used for strafing attack from low altitude, and are effective against light targets that are vulnerable to small-arms fire. Guns as large as 75 mm have been mounted in aircraft to function as airborne artillery. The relative merits of these guns and airborne rockets have not been determined.

14.2.2 Artillery

Artillery projectiles may be solid steel shot for piercing armor, or may be shell filled with explosive or other material. Armor-piercing projectiles are designed specifically for holing resistant targets, and are frequently equipped with a cap which protects the sharp nose in the first stages of impact against hard armor. The larger sizes of AP projectiles contain a small amount of explosive and can cause some damage by fragments after entering a target. Such projectiles must have an explosive that is insensitive to impact and must be fuzed with a short time delay.

High-explosive projectiles cause damage by explosive effect and by fragments. They must have a body strong enough to stand the forces acting when the projectile is fired from the gun. Such projectiles are usually fuzed for instantaneous action when striking the target.

Some projectiles have a hollow charge in the nose to perforate the target by action of the Munroe effect (see Chapter 14).

There are many other types of artillery projectiles, such as smoke shell, illuminating projectiles, etc., but since these do not cause physical damage to targets they are not considered here.

Small Arms

Small arms include rifles, machine guns, and similar weapons. They are effective only against light targets or personnel.

Rockets

A large variety of rockets have been developed for use in World War II. Most of these are essentially some type of artillery projectile or bomb propelled by a rocket motor. Rockets may be fired from individual launchers carried by hand or from multiple launchers carried by trucks, tanks, or small ships. Rockets may have solid heads for piercing targets, explosive heads, or may have a hollow charge in the head for holing the target. (See Chapter 14.)

Very large rocket projectiles have been used in World War II, the most striking example being the V-2 rocket employed by the Germans. This weapon carried a large explosive charge and was essentially an LC bomb with rocket propulsion.

16.3.3 Special-Explosive Weapons

There are many types of special-explosive weapons (see Weapon Data Sheets 1A7a, 1A7b of Chapter 19). Most of these are explosive demolition charges designed for some special purpose. Demolition charges come in a wide variety of sizes and may be combined into very large charges. There is great flexibility in their use subject to the limitation of hand placement.

Line Charges

Snakes are demolition charges built into a line charge several hundred feet in length. They may be pushed by tanks or propelled by a rocket motor. The shape of these charges makes them suitable for clearing paths through obstacles and mine fields. Line charges of less explosive power may be made of Bangalore torpedoes or braided Primacord. These may be used to clear narrow paths through light obstacles such as barbed wire.

Beach Clearance

A variety of special demolition charges have been developed for clearing mines and obstacles from beaches preliminary to a landing operation. Many of these devices are described in the references listed on Weapon Data Sheet 6D2 of Chapter 19.

16.4 EFFICIENCY OF WEAPONS—MEAN AREA OF EFFECTIVENESS

To compare the efficiencies of various weapons in damaging a target, some quantitative measure of the efficiency is needed. It would be desirable to measure the damage in terms of loss in effectiveness of the opposing forces, loss in productive capacity, destruction of stores and matériel, or other factors which are the ultimate objectives of both strategic and tactical attack. These factors are difficult to measure quickly and accurately, so the physical damage to the target is usually measured as it has been found to be related to these quantities. Such important factors as loss in productive capacity can be estimated from the physical damage to the target, but such estimates are not included here.

16.4.1 Mean Area of Effectiveness—Efficiency

In bombing attacks the physical damage to the target is usually measured in terms of the *area damaged* to a specified degree, and the efficiency is measured by the *mean area of effectiveness* (MAE). This quantity is the average expected area of damage for one bomb, divided by the weight of the bomb, and is usually expressed in acres per ton or thousands of square feet per ton of bombs.[b] The *radius of damage* is the radius of a circle of area equal to the average expected area of damage (MAE times weight of bomb). Since the damage area is not exactly circular, one expects to find as much damaged target at distances greater than the radius of damage from the bomb as there is undamaged target at distances less than the radius of damage from the bomb.

The MAE is a measure of the efficiency of the bomb on a weight basis. Bombs having large MAE values will cause large areas of damage per ton of bombs dropped on the target area, and by consideration of the loading characteristics of aircraft (see Section 16.6.1) the MAE may be used to determine the most efficient bomb in terms of area damaged per aircraft.

For a single bomb striking the target, the average area damaged is the MAE times the weight of the bomb. If a large number of bombs are dropped with random distribution in the target area, the fraction f of the target expected to be damaged is given by (because of overlapping)

$$f = 1 - e^{-MD}, \qquad (1)$$

where M is the MAE, D is the density of bombing in weight per unit area, and $e = 2.718\cdots$ is the base of natural logarithms. For nonrandom bomb distribution the relation is more complicated.

For some types of damage, MAE values can be determined from a knowledge of the action of the bomb; for example, the MAE for cratering is the area of the crater divided by the weight of the bomb. For other types of damage the mechanism of damage is complex and more accurate values of the MAE are determined by analysis of data from actual bombing raids. For example, if an attack has been made on a rail yard, reconnaissance photographs will show the

[b] Some references use MAE in square feet per bomb to describe the average area damaged per bomb. Such values must be divided by the weight of the bomb to be consistent with the MAE values used here. Some of the Weapon Data Sheets of Chapter 19 use MAE defined as area per unit weight and others use area per bomb. In each case it is clear which definition is used.

number of cars present and the number of cars damaged, determining the fraction f that are damaged. The area of the rail yard and the number of bombs falling within the yard can also be determined from photographs, and determine the bombing density D. Using these value of f and D the value M of the MAE may be calculated by equation (1). If a large quantity of such data is available, the average of such computations is quite reliable.

For many mechanisms of damage, the average radius of damage per bomb can be expressed as some power of the weight of explosive charge. If the radius of damage is proportional to w^p, where w is the weight of explosive, the area of damage is proportional to w^{2p} and the MAE, or area of damage divided by the weight of the bomb, is proportional to Rw^{2p-1}, where R is the charge weight ratio of the bomb. Therefore, for bombs of the same type, having the same charge weight ratio, the MAE is an increasing or decreasing function of the weight of explosive, depending on whether p is greater or less that 0.5. If the MAE is an increasing function of the weight of explosive, the greatest efficiency is obtained by using large bombs: if it is a decreasing function of the weight of explosive, the greatest efficiency is obtained by using small bombs. Thus a knowledge of the values of the exponent p and the minimum size of bomb that will produce some damage can be used to determine whether large or small bombs are the more efficient, and that is frequently all that is needed to make a weapon selection. If $p = \frac{1}{2}$, the MAE is not dependent on the weight of the charge.

Probable Damage

The probable damage to a target can be estimated from the value of the MAE of the particular bomb and target combination considered.

For estimating probable damage, targets may be divided into two types: those targets, usually small, that can receive the desired damage by a single bomb hit; and those targets, usually large or composed of many small targets, that require many hits if the desired damage is to be obtained. There are many intermediate types falling between these extremes, but only the two types will be considered in detail.

Individual Targets. If a target can be damaged to the desired extent by a single hit, the probability of causing at least this damage is the probability of obtaining at least one hit on the target with the proper bomb. The probable area of damage is the MAE times the weight of the bomb. For some individual targets, such as bridges, the probable damage depends upon whether or not a hit is obtained, and the expected area of damage has little meaning.

Individual targets may be attacked by single aircraft, by several aircraft making successive attacks, or by small formations of aircraft. The type of attack used should be that requiring the least force for a given probability of a hit.

Large or Compound Targets. Large targets or targets composed of many individual units are usually attacked by a formation of aircraft dropping bombs in a more or less uniform pattern. The size of the bomb pattern depends on the type of formation and method of dropping. This method of attack applied to very large target areas is called *area bombing.*

A typical example of bombing of a compound target is an attack on an industrial area containing several buildings. If the same type of bomb is carried by each of the aircraft the expected fraction of damage to each building is given by equation (1) where M is the MAE of the bomb for the building and D is the density of bombing. The expected *area of damage* to an individual building is the expected fraction damaged times the area of the building, or expected area damaged equals

$$A_1 f_1 = A_1(1-e^{-M_1 D}), \qquad (2)$$

where A_1 is the area of the building and M_1 is the MAE of the bomb used in the building considered. Some of the buildings will suffer more damage than predicted and others will experience less damage, but the *expected* area damaged in each building is given by equation (2). The total expected area of damage for the entire target area may be determined by applying equation (2) to each of the buildings and summing the results for the entire target system. Such a procedure will tend to average out the individual variations from building to building, the averaging being better for larger target areas, and if the values of the MAE and the bombing density are accurately known this gives a reliable picture of the overall damage to the target system.

The calculations described above assume that the density of bombing is uniform over the entire target area, which of course implies that the uniform pattern of bombs must cover the entire area. If the bombing density is not uniform, equation (2) may be applied to each individual building, using the values of M and D for that building, and the total expected area of damage will be the sum of the individual expected areas for all buildings.

Most industrial targets contain individual components of different importance. The expected area of damage for each component may be computed by equation (2) and weighted by multiplying this value by some numerical measure of the importance of the target. For example, if a target component of area A_1 has an importance I_1, then

$$\text{Weighted expected area of damage} = I_1 A_1 f_1, \quad (3)$$

and a measure of the effectiveness E of the attack is

$$E = \frac{I_1 A_1 f_1 + I_2 A_2 f_2 + I_3 A_3 f_3 + \cdots}{I_1 A_1 + I_2 A_2 + I_3 A_3 + \cdots}, \quad (4)$$

where both numerator and denominator are summed for all components of the target. The numerical values for the importance of the different target components must be assigned by someone familiar with the details of the target being attacked. The relation between the effectiveness E and the actual effect on the target, such as loss of productive capacity of an industrial target or decrease in defensive strength of a military target, can only be determined by a large amount of experience and data.

16.5 DAMAGE MECHANISMS

A knowledge of the various mechanisms for damaging targets is essential for making weapon selections or critically evaluating damage, and in many cases such knowledge is all that is needed for weapon selection. The most important mechanisms for damaging targets are air blast, confined blast, underground explosion, underwater explosion, fragmentation, and fire. Each of these will be considered separately here, with particular attention to bombing problems; however, the principles given here may be applied to any weapon causing damage by one of these mechanisms.

16.5.1 Air Blast

When a bomb detonates in air (see Chapter 2), the very rapid expansion causes a compressional wave of great intensity and very abrupt rise, called a *shock wave*, to spread out from the source of the explosion with a velocity initially much greater than the velocity of sound. This shock wave is characterized by a very sudden rise in pressure to the peak pressure, then a gradual decrease from this maximum value to a pressure below atmospheric pressure, followed by an increase to atmospheric pressure as shown in Figure 1. As the weight of the explosive charge is increased, the distance at which a given peak pressure of the shock wave occurs increases as the cube root of the charge-weight. At distances from two bombs which are proportional to the cube roots of the charge weights, the pressures will therefore be the same but it is found that the positive impulse will be greater for

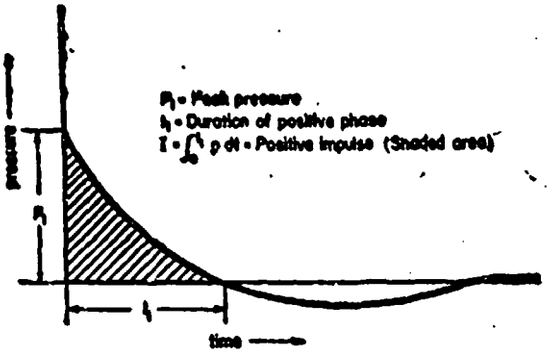

FIGURE 1. Shock wave due to explosion in air, showing change in pressure with time.

the larger charge by the ratio of the cube roots of the charge at these scaled distances. Furthermore, the peak pressure and particularly the positive impulse is larger at equal charge-weight for bombs which have light cases than for bombs having heavy cases.

Air blast damages a target by action of the shock wave on the target. If the shock wave strikes an object that will break very quickly, damage will occur if the peak pressure is sufficient, and the duration of the wave is not important. If the target is yielding, as are most buildings, with a characteristic period long compared to the duration of the shock wave, then the shock acts on the target for its full duration and damage is due to the momentum given to the target. This type of damage is a function of the positive impulse of the shock wave, which is the time integral of the excess above atmospheric pressure from the beginning of the shock to the time at which the pressure first falls to atmospheric pressure. The positive impulse is shown by the shaded area in Figure 1. Weapon Data Sheets 3A1, 3A2*, 3A2a, and 3A3 of Chapter 19 can be used to predict the peak pressure and positive impulse as functions of weight of explosive charge and distance from explosion.

For bombs having 8,000 lb or less of ordinary explosive the duration of the shock wave is usually much less than the natural periods of normal structures, and damage is due to the impulse exerted by the blast rather than to the peak pressure of the shock wave. It has been found experimentally that the distance from an explosion at which a given impulse is pro-

duced increases roughly as the ⅔ power of the weight of explosive. Applying the reasoning of Section 16.4.1 with $p = ⅔$, one sees that the area within which the impulse equals or exceeds a given value is proportional to the ⅔ power of the weight of explosive; thus the MAE for damage due to impulse, or effective area per unit weight, is approximately proportional to $Rw^{⅔}$ where R is the charge-weight ratio of the bomb and w is the weight of explosive charge. Since bombs having a large charge-weight ratio also use the explosive more efficiently (Chapter 2) the increase in efficiency is even greater than indicated here. One sees that for greatest efficiency in damaging a target by action of the impulse of the shock wave, bombs having large charge-weight ratio and large weight of explosive charge should be used. The LC bombs have these characteristics and are recommended in all cases where external air blast will be the most effective damaging agent. Instantaneous fuzing must be used to ensure detonation before breakup.

Airburst Bombs

The distance over which the impulse exerted by the blast wave exceeds a given value can be increased by detonation of the bomb above ground (see Chapter 2 and Weapon Data Sheets 3A7, 3A8, 3A9 of Chapter 19). Special fuzes must be used to obtain airburst.

16.5.2 Confined Blast

In some instances it is desirable to have a bomb detonate inside a building to cause damage by confined blast. Since LC bombs can not perforate any but very light roofs the GP bombs should be used, with short delay fuzing to cause detonation inside the building. The reasoning given in Section 16.5.1 still applies and large bombs are more efficient than small bombs up to the size that will completely destroy an entire unit.

At present, it is not possible from theory to predict whether confined blast with small bombs or external blast with large bombs is the better choice. However, operational data on Japanese targets indicates that 4,000-lb bombs, instantaneously fuzed, are more effective than 500-lb GP bombs with short delay fuzes against aircraft factories and similar structures.

Penetration into Structure

Case Strength. In order to cause damage by confined blast, a bomb must penetrate into the target (see Chapters 6, 7, 8, 9). This requires perforation of a structure that may be very light, in the case of a factory or warehouse, or very heavy, in the case of a fortification. Weapon Data Sheets 2C1-2C8 of Chapter 19 give information on the perforation of various materials by bombs and projectiles, and may be used to select a weapon capable of reaching the interior of the target. In general, LC bombs can be used only for extremely light roofing, GP bombs can be used for ordinary construction, SAP bombs are needed for unusually heavy industrial construction, reinforced-concrete fortifications, and lightly armored targets, and AP bombs are needed against heavily armored targets.

Explosive Sensitivity. Some explosives are very sensitive to impact and will detonate when the weapon strikes a target, regardless of the fuze delay. More insensitive explosives must be used for filling weapons that are to penetrate into a target before exploding.

16.5.3 Underground Explosion

When a bomb or shell explodes underground (see Chapter 3) the case expands and breaks as in air, but the expansion is slower because of the surrounding earth. A roughly spherical compression wave called an earth shock wave is generated, by the expanding case and by continued pressure of the gaseous products of explosion, and travels out into the surrounding medium in all directions, decreasing in intensity as it does so. When this earth shock wave reaches the surface it is reflected, lifting and cracking the soil and projecting a large mass of broken soil into the air. Except in very deep explosions a crater is formed and becomes partially filled with the broken earth that falls back almost vertically. The soil near the explosion is permanently displaced, and transient displacements may occur at some distance from the explosion.

Targets can be damaged by displacement of the foundation, by earth shock damage to underground walls, or by cratering. All these effects can be caused by underground explosions. General-purpose bombs can penetrate into the ground without damage to the case and should be used with the proper fuze delay to cause detonation at the desired depth.

Cratering

Many targets can be damaged by cratering (see Weapon Data Sheets 3B1a*, 3B1b of Chapter 19). Experiments have shown that all dimensions of a bomb crater are approximately proportional to the ⅓ power of the weight of explosive; thus the diameter of a bomb crater is proportional to $w^{⅓}$, the plan area is proportional to $w^{⅔}$, and the MAE for area cratered is proportional to $Rw^{-⅔}$, by the reasoning given in Section 16.4.1. This means that for maximum *area* cratered per unit weight of bomb, small bombs of large

charge-weight ratio should be used. General-purpose bombs are the bombs of greatest charge-weight ratio that can penetrate into soil without deformation. Fuze delays of 0.01 sec for the 100- to 500-lb GP bombs and 0.025 sec for the 1,000- to 4,000-lb GP bombs allow enough penetration for satisfactory crater formation. If the soil is resistant to penetration longer delays are satisfactory, but for soils allowing deep penetration longer delays may result in camouflet or incomplete craters.

Reasoning similar to the above shows that the volume of a crater is proportional to the weight of explosive. Therefore, if the objective of an attack is to crater large volumes instead of large areas, the efficiency, or volume per pound of explosive, is practically independent of the weight of the charge. This means that GP bombs of any size may be used with no great difference in efficiency of forming large crater volumes.

There is no available data to show whether scaling laws applied to craters of ordinary bombs can be used to predict crater formation by bombs containing very powerful explosives.

Displacement of Structural Components

Building columns and foundations, small bridge piers, and similar structural components can be moved by motion of the foundation soil, and such displacements may weaken the structure sufficiently to cause collapse or to require demolition (see Weapon Data Sheet 3B2 of Chapter 19). The required displacements can be caused by underground explosions in many cases.

Experiments have shown that the radius from an underground explosion at which a given surface displacement is attained increases about as the 0.45 power of the weight of explosive for GP bombs up to 2,000 lb in weight. Applying the reasoning of Section 16.4.1 one finds that the efficiency, or lethal area per unit weight, is proportional to $Rw^{-0.1}$ and the greatest efficiency will be obtained by using small bombs of large charge-weight ratio, provided that the bomb is large enough to cause the desired displacement. However, the exponent of w is so small that intermediate bomb sizes may be used with no great loss in efficiency. General-purpose bombs should be used to insure penetration into the soil without damage to the case, and should be fuzed with sufficient delay to allow enough penetration for a well-tamped explosion, but the fuze delay must not be too great or the explosion will occur too deep to cause much displacement near the surface. Fuze delays of 0.01 sec for the 100- to 500-lb GP bombs and 0.025 sec for the 1,000- to 4,000-lb. GP bombs are satisfactory for most purposes.

Damage to Underground Walls

Targets having underground walls can be damaged by earth shock acting on the walls (see Weapon Data Sheet 6A5[a] of Chapter 19). Experiments have shown that the radius for damage by earth shock is not a simple power function of the weight of explosive. However, graphical analysis of the data from a large number of tests shows that the optimum size of bomb for damaging a wall of thickness t ft is that giving a scaled thickness $t/w^{\frac{1}{3}}$ of 0.4 to 0.5, where w is the weight of explosive in pounds. The analysis also shows that for bombs smaller than this size the efficiency decreases very rapidly with decreasing weight of charge, while for larger than the optimum size bombs the efficiency is almost as great as for the optimum. Therefore, the greatest efficiency will be obtained by matching the weight of explosive to the thickness of the underground wall so that $t/w^{\frac{1}{3}}$ is about 0.4, or $w = 16t^3$, and by using the first size larger bomb than computed. Since the bombs must penetrate into the ground before explosion, GP bombs with short delay fusing should be used. The optimum fuzing should cause detonation at about the depth of the center of the wall.

16.5.4 Underwater Explosion

When an explosive detonates under water (see Chapter 1), the high pressure produced compresses the water and causes a compressional wave of high intensity, called a shock wave, to spread out from the source of the explosion. This shock wave can cause damage to ships or other structures under the water provided they are close enough to the source of the wave. Furthermore, the expanding gases from the explosion, after producing the shock wave, continue to exert pressure on the water, forcing it outward. The compressional wave is, therefore, followed by a flow of the water which can be treated as an incompressible flow. It is certainly possible that this flow causes damage and, in fact, it has been postulated by some that this is more important in causing damage than the shock wave itself. This is a question which has not been fully clarified. The bubble of burnt gas will overexpand, because of the inertia of the flowing water, and then contract under the influence of hydrostatic pressure. As the bubble nears its minimum size, a second compression wave is emitted which, although much less intense than the original shock wave, has a greater duration and, therefore, considerable momentum and energy.

If the explosion is deep enough, there may be a number of expansions and contractions with a pressure pulse emitted at each minimum. With shallow explosions, these do not occur because the gas bubble reaches the surface and vents before the subsequent contraction can occur. These so called bubble pulses can also cause damage under proper conditions.

When the shock wave strikes a target such as a ship, one or several things may happen. The structure may fail quickly before the pressure in the shock wave has decayed very far. This would be true of a brittle material or a system having a very small natural period and insufficient strength to resist the high pressure (of the order of thousands of pounds per square inch) in the shock wave. It may be, however, that the period of the structure is longer than the short duration of the high-pressure phenomenon, in which case the *impulse* of the wave may be absorbed and may be the determining factor for damage. There is one possible complication, probably quite important in practice. This is that the target, upon being accelerated by the pressure wave, may move with sufficient velocity to pull away from the water or to pull part of the water away from itself, causing cavitation in front of the target. This has been clearly demonstrated by photography for certain ranges of conditions. In this case, it is indicated that it is the *energy* of the shock wave that determines the damage produced. Therefore, there are three possible situations, theoretically, regarding damage produced by the shock wave; namely, damage produced by pressure, by momentum or impulse, or by energy. In the first of these cases, the radius of damage would increase as the cube root of the weight, in the second as the $\frac{2}{3}$ power approximately, and in the third as the $\frac{1}{2}$ power approximately. Experimentally, all three of these situations can be approximately realized but it is not clear which of them is the correct assumption for normal ship damage. The square root law being intermediate between the extremes seems to be a good rough approximation as far as our present knowledge is concerned.

Bubble damage, that is, damage caused by the later pressure pulses from the oscillating bubble, is believed to be important for charges located under the target since gravity causes the gas bubble to rise and there is also an attraction by the target drawing the bubble toward it. These conditions are probably also favorable to damage caused by the incompressive flow of the water. It is clear that a great deal of work remains to be done concerning the mechanism of damage by underwater explosions.

The case of a bomb does not have to be extremely strong to withstand impact on water, and bombs of high charge-weight ratio should be used for maximum efficiency. Depth bombs have been specially designed for use in aerial attack. These bombs have a charge-weight ratio of about 70 per cent and are equipped with hydrostatic fuzes that can be preset to cause explosion at any desired depth.

Special charges for underwater demolition are provided with waterproof cases and a wide choice of firing devices, and may be fitted together to make very large explosive charges.

Fragmentation

When a bomb explodes in air, the case is broken up into a large number of small fragments. Thin bomb cases result in very small fragments while thick cases result in fairly large, heavy fragments. The fragments leave the bomb with an initial velocity that is approximately inversely proportional to the square root of the ratio of the weight of case to the weight of explosive charge, and are slowed in their travel through air by a resisting force proportional to the average cross-sectional area of the fragments and to the square of their velocity. When fragments strike a target their ability to perforate it is the same as that of any other projectile of the same size and shape (see Chapters 6, 7, 8, and 9), but since fragments from any given bomb vary in size and shape the ability to perforate must be treated by statistical methods. Most fragments from a bomb of average shape are ejected laterally; thus the greatest density of fragments is in a thin disk-shaped spray around the bomb.

Thin-cased bombs eject fragments having a higher initial velocity than those from bombs having thick cases, but the fragments are very light and so are slowed in their travel through air more than heavy fragments. Furthermore, the fragments are so small and light that they have little ability to perforate resistant targets. For these reasons, bombs having thick cases are the preferred agents for causing damage to a target by fragments. The specially designed fragmentation bombs have thick cases. The body is made of a helix of square steel bar wrapped around a thin inner lining, and on explosion of the bomb this bar breaks into large heavy fragments of fairly uniform size. Fragments from GP bombs are lighter on the average and have such a wide variation in size that many small and ineffective fragments are included.

Bombs must detonate in air if their fragments are to be effective, and so should be equipped with instan-

taneous or air-burst fuzes; the air-burst fuzing is preferable for targets having shielding on the sides but at present can be used only on certain bomb types. The helical case of fragmentation bombs is not designed for perforation, so these bombs cannot be used for targets under cover. General-purpose bombs must be used for fragmentation damage on such targets.

Small, dispersed, and unprotected targets such as personnel, unarmored vehicles, and grounded aircraft are vulnerable to fragments. Any fragmentation weapon exploding near one of these targets can cause damage; the small 20-lb fragmentation bomb is most efficient. The larger fragmentation bombs are effective at a greater distance from the target but are not as efficient in lethal area per unit weight as the small bomb. Targets having heavy construction are not easily damaged by the fragments from the 20-lb bomb, and the 90- or 260-lb or other fragmentation bomb yielding large fragments must be used. General-purpose and SAP bombs are a good second choice, and the GP bomb may be more efficient against some targets. Targets of very heavy construction are not easily damaged by fragments from the standard fragmentation weapons and should be attacked by using some other mechanism of damage.

16.5.6 Fire

Many targets are combustible and where this is the case fire is usually the most effective agent (see Division 11 STR). Fires can be started by HE bombs or by the specially designed incendiary bombs. The incendiary bombs are more efficient in starting fires and should be recommended for all targets where fire is chosen as the mechanism of damage to be used. However, the fire-starting capabilities of HE bombs should not be ignored in estimating the effects of these weapons on combustible targets.

Concentration of Fire Sources

All types of incendiary bombs are effective in starting fires. The choice between the different types of bombs depends upon the desired distribution and intensity of sources of fire. The scatter-type incendiary bombs are usually filled with a gasoline gel mixture that ignites and spreads over a small area when the bomb bursts on impact. The small intensive-type bombs are dropped in aimable clusters that open at an altitude of about 5,000 ft spread over a larger area, and result in small sources of fire scattered so that for each of the present clusters there is one fire source for every 2,000 to 5,000 sq ft. These small bombs can also be dropped in quick-opening clusters that open a few hundred feet below the aircraft and spread the bombs over a large area, and for each cluster dropped from 10,000 ft there is an average of one fire source for every 20,000 to 50,000 sq ft. It is seen that these three types can be used to cause wide variations in concentration of fire sources. In general, a high concentration of fire sources is needed for targets that are not highly combustible and a wide spread or low concentration is allowable for highly combustible areas.

Vulnerability of Targets to Fire

The effectiveness of incendiary bombs in starting fires depends to a large extent upon the combustibility of the roof of the target (see Weapon Data Sheet 6B2 of Chapter 19). Once a fire is sufficiently well established to cause serious damage, the extent of its spread does not depend on the origin of the fire but on the combustibility of the roof, the height of the building (height of upper story in multistory buildings), and the amount and combustibility of the contents. Fires are usually limited to the fire division within which they start, where a fire division is defined as an area of a building separated from other areas by fire walls or air gaps. A fire well established in a fire division having a combustible roof usually burns out the entire fire division, while a fire well established in a fire division having a noncombustible roof usually burns out only part of the fire division.

The expected area of damage due to incendiary bombs for one fire division of an industrial building with a combustible roof is the area of the fire division times the probability of starting a fire; for an industrial building having a noncombustible roof the expected area of damage is that part of a fire division that will be burned out by a well-established fire (see graph on Weapon Data Sheet 6B2 of Chapter 19) times the probability of starting a fire. Thus the MAE for damage by fire depends upon the roof, the height, the contents, and the area of the fire division.

Roof. For the purpose of estimating fire damage to buildings, roofs may be described as combustible, noncombustible, or fire-resistant. The type of roof is usually determined from examination of photographs, knowledge of building construction practices, and other information. The probability of starting a serious fire in a building with combustible roof is about fifteen times the probability of starting such a fire in a building with noncombustible or fire-resistant roof.

Height. The probability of starting a fire that can cause serious damage depends strongly on the eave

height of the building or the height of the upper story for multistory buildings. Low buildings are much more vulnerable to fire starting than buildings with high roofs. The relative probabilities of starting a serious fire in buildings having heights of 10, 25, or 50 ft are approximately 1, 0.5, and 0.1. For buildings having heights of more than 50 ft to the eaves the probability of starting a serious fire is negligibly small.

Contents. As would be expected, the combustibility of the contents of a building has a great effect on the probability of starting a serious fire that will spread through the fire division. The combustibility of the contents is frequently described by the *occupancy rating*, or per cent of the floor area that is covered by combustible material. The probability of starting a serious fire is approximately three times as much for an occupancy rating of 45 per cent as it is for an occupancy rating of 5 per cent.

Incendiary Effects of High-Explosive Bombs

A study of damage to buildings has shown that the probability of starting a fire by action of an HE bomb is approximately ⅛. Thus for combustible-roof-type buildings, the average fire damage due to HE bombs is ⅛ of the area of the fire division, and for buildings having noncombustible roofs the average fire damage is ⅛ of the area that will be burned out (see graph on Weapon Data Sheet 6B2 of Chapter 19). If the bomb starts a fire, the structural damage and the fire damage will affect the same parts of the building, and only the fire damage should be considered. In the five out of six instances when no fire is started the structural damage due to the HE bomb is the only damage occurring. Thus the average expected damage for industrial buildings attacked by HE bombs is ⅝ of the expected area of structural damage plus ⅛ of the area expected for fire damage, provided that the area damaged due to one fire is equal to, or greater than, the area damaged by one explosion.

High-explosive bombs may damage the fire wall separating fire divisions, and if this occurs fire may spread from one division to the next. It is necessary that a 500-lb bomb strike within 30 or 40 ft of the wall to cause sufficient damage for interdivision fire spread.

High-explosive bombs may also be used in incendiary bomb attacks to cause damage to water mains, to block streets with debris, and to hinder and discourage fire fighters.

16.6 LOADING EFFICIENCY

The actual combat application of weapons at the highest efficiency is not so simple as described in Sections 16.4 and 16.5. There the efficiency of bombs for various mechanisms of damage was described as a function of the weight of the bomb, and it was shown that if the mechanism of damage to a target is known this information alone will often determine the most efficient size of bomb and the best fuzing. Such selections are based on the efficiency in terms of bomb weight, and are not necessarily selections of the most efficient weapons per plane load.

16.6.1 Loading of Bombs on Aircraft

The following example of the cratering efficiency per aircraft will illustrate the importance of the loading characteristics of aircraft in using bombs at the greatest efficiency. The diameter of the average crater formed in loam soil by bombs detonating at the optimum depth may be determined from Weapon Data Sheet 3B1a[4] of Chapter 19, and the area of the crater may be calculated from this diameter. The first column of Table 1 gives the nominal weights of the four smallest GP bombs, the second column gives the area of the average crater formed by each bomb detonating at the optimum depth in loam soil, and the several double columns give the number of bombs carried in normal loading and the total area cratered (assuming no overlap of craters) for some typical bombers. Section 16.5.3 shows that the smallest bomb is the most efficient for area cratering if the efficiency is measured in terms of the bomb weight, but Table 1 shows that this is not necessarily true where the efficiency is measured in terms of the plane load. The 100-lb GP bomb is the most efficient for normal loading on the B-24,

Table 1. Area cratered per plane load of various general-purpose bombs.

GP bomb	Crater area (ft^2)	B-29		B-24		B-17E		B-17F, G		B-23O, D	
		No.	Area (ft^2)	No.	Area (ft^2)	No.	Area (ft^2)	No.	Area (ft^2)	No.	Area (ft^2)
100-lb	310	80	24,800	52	16,140	20	6,200	38	11,780	12	3,720
250-lb	530	56	29,860	24	12,720	14	7,420	20	10,600	8	4,240
500-lb	830	40	33,200	12	9,960	8	6,640	12	9,960	6	4,980
1,000-lb	1,360	12	16,320	8	10,880	4	5,440	6	8,160	3	4,080

B-17F, and B-17G; the 250-lb GP bomb is the most efficient for the B-17E; and the 500-lb GP bomb is the most efficient for the B-39, B-25C, and B-25D. The importance of considering loading characteristics of aircraft is shown by the fact that the 1,000-lb bomb is more efficient than the 100-lb bomb for normal loading on the B-25, while on a weight basis the 100-lb bomb is approximately twice as efficient as the 1,000-lb bomb for area cratering.

16.6.2 Efficiency of Artillery Attack

The efficiency problems in artillery attack require consideration of the rate of fire and mobility of the weapons instead of the loading characteristics as considered for aircraft. The size of gun increases as the size of the projectile increases, and the amount of explosive carried per shell increases approximately as the cube of the projectile caliber. The rate of fire usually decreases as the size of the gun increases, and the mobility decreases as the weight of the gun increases. All of these factors and the operating range influence the efficiency of artillery weapons.

If the objective of an attack is a bombardment of a prescribed weight of the explosive per unit area, the results can be achieved by use of a large number of small rapid-firing guns operating at short range or by use of a smaller number of large guns firing more slowly at long range. The small guns and their ammunition are more mobile, and operational conditions may prejudice against exposing the number of and positions of the relatively immobile large pieces. However, the use of large guns makes a heavy attack possible from a reasonably long range, using a comparatively small number of weapons. The decision as to which method is the more efficient is a difficult one, depending on many factors; a detailed treatment of the problem will not be attempted here.

If the objective of an artillery attack is to perforate a resistant target such as a concrete-enclosed gun emplacement, the objective can be attained by a single direct hit from a large gun or by repeated hits in a small area using smaller projectiles (see Section 7.2.7). Here, the number of hits required for each projectile size can be estimated with some accuracy. The effects of mobility, rate of fire, and other factors must be considered as in area bombardment.

16.7 FORCE REQUIREMENTS

The force required to cause a desired degree of damage to a target depends upon the extent of the damage desired, the accuracy of delivery, and the MAE of the weapon against the target. If these factors are known the necessary force can be determined.

16.7.1 Bombing Attack

The force required for a given expectancy of causing a desired level of damage to a particular target will depend on the type of target, the MAE against this target of the weapon chosen, the level of damage sought, and the method and accuracy of the attack. A target may be a single unit, such as a ship, a bridge, or an important fortification, a collection of such units, or simply an area vulnerable to attack. Against a single target one hit may be sufficient, or a number of hits may be needed. In any event, the required number of hits can be determined.

Bombing can be by individual aiming of each bomb, by individual aiming of each string of bombs from a plane, or bombing by groups of planes, each dropping a single bomb or a string of bombs upon signal from the leader. The probability of achieving the desired number of hits with a given force, or the number of bombs that must be dropped for a given probability of achieving the desired number of hits, must be determined by statistical methods.[16.8.3] Briefly, the method is as follows: for individual aiming, the dispersion of bombs about the aiming point usually follows the normal probability curve, which can be used to calculate the expectancy of achieving at least the desired number of hits. In order to make this computation it is necessary to know the accuracy that can be expected in the bombing attack; this accuracy varies greatly with training, experience, incentives, and conditions under which the attack is made, but its expected value can be determined for a given situation.

For large formations of planes dropping bombs on signal the distribution of bombs differs from the normal error distribution and for a group so large that the size of the bomb pattern is large compared with the normal aiming error, the bomb distribution can be considered as a random pattern covering the target and surrounding area. In this case, the probability of getting one hit on a single target entirely within the area covered by the bombing pattern is the area of the target (or its vulnerable area) times the density of bombing, or number of bombs per unit area in the pattern. This method of bombing is not economical for isolated targets, but may be used against an area containing a large number of individual targets. The area of the bomb pattern is somewhat greater than the

size of the formation at the instant of bomb release.

When the target does not consist of individual units on which direct hits must be achieved, but instead contains areas of vulnerability to which a single bomb can be expected to cause a certain area of destruction, equation (1) of Section 16.4.1 may be used to determine the required density of bombing. This equation is

$$f = 1 - e^{-MD}, \qquad (1)$$

where f is the fraction of the target receiving the specified degree of damage, M is the MAE of the bomb used for the specified degree of damage of the target considered, and D (in reciprocal units to M) is the density of bombs. Knowing f and M, one can calculate the required density. From this density and a knowledge of the method of bombing to be used by the attacking force the number of bombs and planes can be determined. This method may be used to determine force requirements for attacks on industrial or urban areas, airport runways, or other targets where a desired level of damage is required but in which there are no specific vital spots to which damage must be caused.

16.7.2 Other Methods of Attack

The general considerations that have been outlined above apply equally to types of attack other than bombing, such as artillery, rocket, guided missile, torpedo, and other attacks. For individually aimed weapons the dispersion usually follows the normal error curve or an equivalent relation; the numerical factors that express the exact shape of this curve depend on the accuracy of aiming or control and on any factors that can affect the behavior of the weapon between the end of aiming or control and the time of striking. In any event, a knowledge of the expected distribution of hits, obtained from the past performance of the weapon and of the size and location of the target allows one to calculate the number of tries for a given expectancy of obtaining not less than the specified number of hits.

When weapons are used for general bombardment or area attack, in which aiming is not directed at individual targets, the required density of attack is determined by equation (1) for an expected level of damage due to attack by weapons of known MAE.

16.8 SELECTION OF TARGETS

Nearly every target contains a number of components of differing importance and vulnerability, and vulnerable to different damage mechanisms. The selection of the best component to attack must be based on the critical nature of the component and its physical vulnerability to the various damage mechanisms available in the form of weapons. A detailed knowledge of the entire target complex is required for intelligent target selection.

16.8.1 Strategic Targets

A strategic aerial campaign will be concerned first with the selection of target systems for attack, such as oil production, transportation, or steel. The choice of the systems to receive concentrated attack is made at the highest levels, on the basis of the relation between the effort required and the effect on the enemy. Estimates of the effort and effect must be made by those familiar with weapon analysis and with the whole internal economy of the enemy.

Every target system contains a large number of components of varying vulnerability to attack. The selection of the particular components of a system to be attacked in order to achieve the desired effect on the system is normally made at field command level, again on the basis of analyses by weapon analysts and economic analysts. The components chosen must, of course, be those for which the least effort is needed for the required effect. The number and choice of components of targets depend primarily on three kinds of facts: the relative importance of the components to the functioning of the system, the physical vulnerability of the components to damage, and the ease with which they can be hit. Although certain components of a system may be absolutely vital to its operation they may be so well protected and difficult to hit as to make very unsatisfactory targets.

Consider, for example, the planning of attacks on transportation. All existing means of transportation must be examined. It may be that all will require attack in order to reduce the flow of material to its destinations; on the other hand it may be that all supplies are controlled at some point by a particular system and that the desired effect can best be attained by attacks on this system only. In attacking a particular system it is essential to examine it carefully in order to select those parts of it on which to concentrate. In the case of rail transportation, for example, there are fuel or power supplies, locomotives and rolling stock, and right of way. Locomotives can be damaged while idle or while in operation and their repair and maintenance facilities can also be destroyed. Rolling stock can be attacked in large concentrations in freight yards. In attacking the right of way it is usually de-

sirable to select the bottlenecks that are by-passed with the most difficulty and are most difficult to repair. The choice of target points will depend on the time for which operation is to be stopped.

Several typical strategic targets are discussed from the point of view of vulnerability and weapon selection in Section 16.8.

16.8.2 Tactical Targets

A tactical attack is intended to be followed immediately by an advance of one's own forces into enemy territory or to interfere with the enemy's attempts to advance. In either case the objective is to destroy or damage fortifications or other defenses, transportation and communication facilities, and military supplies. The weapons and methods of attack are basically the same as in strategic operations, although they may be used under somewhat different conditions. The selection of targets according to importance, vulnerability, and ease of hitting must be made, using the principles discussed for strategic targets. The principal difference between strategic and tactical operations is in the length of time involved, the former being concerned with months and years, the latter with hours and days.

The attack of several typical tactical objectives is discussed from the point of view of physical vulnerability and weapon selection in Section 16.9.

16.9 WEAPON SELECTION

The broad general principles governing the selection of weapons to be used are similar for both strategic and tactical objectives. The primary concern must always be the efficiency, or damage for the effort expended.

The choice of bomb and fuze for the most efficient aerial attack on a target can frequently be made from a knowledge of the mechanism for obtaining the desired damage. The difficulty in making a weapon selection on this basis is the choice of a target and the choice of damage mechanism. The choice of a target must be made by using all available information and should include consideration of the vulnerability of the different targets to bombing. Once a target has been selected the type of damage desired must be decided upon. Where a target can be damaged by several mechanisms, the types of damage and the relative efficiencies of the different mechanisms must be compared.

In this section, weapon selection for aerial attack on typical military targets, transportation targets, and industrial targets will be described.

16.9.1 Military Targets

Military field targets differ from other targets in that the attack is always tactical and never strategic. The objective is temporary or permanent neutralization of the installations.

Small, Lightly Protected Targets

Small, lightly protected targets[4] are vulnerable to almost any explosive weapon detonating near them, and can be damaged by various missiles (see Weapon Data Sheet 6D3 of Chapter 19). If the targets are small and widely dispersed, the most efficient weapon for attack would be one just large enough to destroy one target provided that the aiming accuracy were such that a single shot could be reliably expected to hit the target. This is actually never the case so that the choice between many small weapons and a few large ones depends entirely on the MAE of the weapons. If the MAE (per ton) is larger for the large weapons and the given type of target, then a few large bombs will be more efficient than many small ones and vice versa. This is a very important point which has often been confused, so that an example may be in order. Suppose that it is important to destroy a small wooden shack by high-altitude attack. Since, in this type of attack, there is very little probability that any individual bomb will strike the target, all that can be done is to drop a considerable number of bombs which will form in a more or less random pattern which should blanket the target. Therefore, the chance that the target will be destroyed is the chance that at least one bomb falls within a critical distance of the target, this distance depending upon the size of the bomb and the strength of the target. If, for purposes of illustration, it is assumed that the target will be destroyed by a 100-lb bomb falling less than 20 ft away or by a 4,000-lb bomb exploding less than 150 ft away, the problem is equivalent to the following one:

A number of circles equal in radius to the destructive radius of the bomb are dropped at random over the target. What is the probability that at least one of these circles will cover or touch the target? It turns out that this probability is given by equation (1) where f is in this case to be interpreted as the probability of destruction of the target. In this equation, M is the MAE, that is the area of the circle

within which damage is to be expected divided by the weight of the bomb and D is the density of bombing in terms of weight per unit area. If the same total weight per unit area is dropped, the choice between the larger and the smaller bomb will depend upon the value of the MAE. If the figures given above are correct for the given target, then in this case the larger bomb would be superior since its MAE is, in this example, larger. This will not always be the case. For example, if the target were protected by a revetment, then clearly the MAE for any reasonable size bomb would be the area of the circle of the revetment and would not increase as the size of the bomb increased. In this case, the smaller bomb is obviously indicated. In many cases, such light targets are vulnerable to fragments, in which case the fragmentation bomb or small-arms bomb can be recommended. If close attack is possible, airborne rockets are effective.

Personnel. Personnel are vulnerable to direct hits by projectiles and to near misses by bombs. Men in the open or with partial shielding are attacked most efficiently by small fragmentation bombs. Any bombing attack is likely to cause personnel to seek cover, and a heavy, sustained attack of any kind will tend to prevent operation of all but protected gun positions.

The vulnerability of men to damage by fragments from bombs depends on whether they are standing in the open, prone in the open, or shielded by trenches or other protection. Men standing in the open are most vulnerable, of course; men prone in the open are much more vulnerable to fragmentation bombs fuzed instantaneously than are men in trenches, and are about five times as vulnerable to fragments from air-burst-fuzed 500-lb GP bombs as are men in trenches. Present air-burst fuzes cannot be used on small fragmentation bombs, so a direct comparison of these and the 500-lb GP bomb is not possible.

Weapon Data Sheet 6D3 of Chapter 19 gives the average lethal area per bomb for various bombs against personnel. The average maximum distance for incapacitation is 40 ft for the 20-lb fragmentation bomb and 90 ft for the 500-lb GP bomb, where both are fuzed for instantaneous detonation. Air-burst fuzes should always be used for bombing men in trenches.

Vehicles. Small unarmored vehicles are vulnerable to small weapons, and fragmentation bombs are efficient agents for damaging them in aerial attack. The average lethal area per bomb is given for various bombs in Weapon Data Sheet 6D3 of Chapter 19. The 20-lb fragmentation bombs are the most efficient of present bombs if the efficiency is measured on a weight basis, and should be used if available unless plane loading factors strongly favor other bombs. Severe damage can be caused at an average maximum distance of 45 ft from a 20-lb fragmentation bomb or 115 ft from the 500-lb GP bomb.

Aircraft. Grounded aircraft are vulnerable to damage by fragmentation bombs, strafing, and fire damage due to close hits by gasoline-gel-type incendiary bombs. If aircraft are parked in a line so that many can be attacked on one run, strafing is effective and efficient. In this or any other disposition of grounded aircraft in the open, small fragmentation bombs are the most efficient on a weight basis. Lethal areas per bomb are given in Weapon Data Sheet 6D3 of Chapter 19, which shows that the average maximum radius for severe damage is 45 ft for the 20-lb fragmentation bomb and about 160 ft for the 500-lb GP bomb. The lethal area per pound of bomb, or efficiency, is twice as great for the 20-lb fragmentation bomb as for the 500-lb GP bomb, and the 20-lb fragmentation bomb packed in clusters is usually more efficient per plane load.

Aircraft parked in revetted enclosures are shielded against fragments from the side, and should be attacked by bombs using air-burst fuzes so that the source of fragments is well above the top of the revetments. Small fragmentation bombs are effective if enough are dropped to give a reasonable expectation of hits inside of the revetments.

Resistant Targets

Resistant targets, such as fortifications, covered gun emplacements, and protected ammunition stores, are not vulnerable to the small fragmentation bombs recommended above for small, lightly protected targets and must be attacked by weapons capable of greater effect.

Gun Positions

From the point of view of vulnerability (see Weapon Data Sheet 6D1 of Chapter 19), gun positions may be divided into three types: (1) guns in the open with no protective shielding other than that provided by the gun mount, (2) guns surrounded by revetments or other protective walls but open on top, and (3) guns enclosed by heavy protective construction, such as concrete or steel pillboxes, or gun turrets of ships. These three types must be examined for their vulnerability to the several possible mechanisms of damage discussed in Section 16.5. Guns are heavy and present a small area and are not vulnerable to air

blast. They are obviously not vulnerable to damage by fire unless a combustible substance such as gasoline gel is actually placed on the gun or the ammunition stored by the gun can be exploded. This leaves as possible mechanisms of damage, underground explosions and direct hits by missiles such as fragments or projectiles. The two mechanisms cannot be used together, because delay fuzing is needed for underground explosion and instantaneous or air-burst fuzing is needed for effective fragment distribution. The more efficient of the two mechanisms must be decided upon.

Open Gun Positions. Open gun positions[8] have no protection and are vulnerable to damage by fragments from bombs exploding some distance away. They are vulnerable to damage by cratering, earth displacement, or projected debris from cratering in rocky soil. The underground-explosion effects are not great except in or close to the crater, but the damage by fragments can occur at some distance from even a small fragmentation bomb. Therefore, it is concluded that fragmentation is the most efficient mechanism of damage to open gun emplacements. This is in agreement with the results of a detailed study of vulnerability of guns reported in abstract form in Weapon Data Sheet 6D1 of Chapter 19. There it is seen that the MAE for damage by fragmentation is roughly ten times that for damage by underground explosion. This study used data for damage to guns by fragments from GP bombs; similar data for fragmentation bombs is not available in sufficient quantity for detailed analysis. On dividing the lethal area by the bomb weight in pounds for MAE comparisons of fragmentation damage against guns in the open, one finds that for medium (75-mm to 120-mm) and heavy (150-mm and larger) guns the 100-lb GP bomb is the most efficient, and the 90- and 260-lb fragmentation bombs are almost as efficient as the 100-lb GP. Any of these bombs, with instantaneous fuzing, may be selected for attack, and consideration of the aircraft loading of these bombs will enable the most efficient bomb per plane load to be selected.

Weapon Data Sheet 6D1 does not give numerical values for the vulnerability of light (20-mm and 37-mm) guns to damage by fragmentation. The bombs selected for the medium and heavy guns may be used, but since these guns are of lighter construction it is reasonable to expect that the smaller 20-lb fragmentation bomb will also be efficient for attacking light guns in the open. If there is no shielding around the guns, there is no advantage in using air-burst fuzes.

Guns of all sizes are vulnerable to direct hits by artillery projectiles or rockets. The operational conditions must determine whether this method of attack is preferable to bombing.

Guns in Revetments. Revetted gun[8] positions are vulnerable to damage by underground explosion or by fragments or other missiles, as are open gun positions. The important difference lies in the protection provided by the revetment. Experience has shown that even large bombs cause no appreciable damage to such guns unless they strike inside of the revetted area or outside but within about 4 ft of the inside edge of the revetment. If the revetment is circular with the gun at the center, a bomb having a radius of damage smaller than the radius of the revetted area plus 4 ft will act on the gun as if it were in the open, and a bomb having a radius of damage equal to or greater than the radius of the revetted area plus 4 ft will have a lethal area equal to the revetted area plus the area of a band 4 ft wide drawn around the revetment. This means that the largest efficient bomb will be that bomb having a radius of damage equal to the radius of the revetment plus 4 ft. The only instance in which larger bombs would be more efficient is with air-burst fuzing for detonation above the level of the revetment so that the protection provided is nullified. In the case of guns in revetments, as for guns in the open, the radius of damage by fragments from a bomb having instantaneous fuzing is greater than that for damage by underground explosion of the same bomb with delay fuzing.

The values of MAE per bomb for unserviceability and for temporary unserviceability due to fragment damage are given for several bombs and for different sizes of revetted gun emplacements in Weapon Data Sheet 6D1 of Chapter 19. Dividing these values by the bomb weight for comparison on a weight basis indicates that for light guns the 20-lb fragmentation bomb is the most efficient instantaneously fuzed bomb for 20- and 30-ft diameter positions, and is slightly less efficient than the 500-lb GP bomb fuzed for air burst; the 90-lb fragmentation bomb and 100-lb GP bomb are of about equal efficiency, and are a better selection than any of the other bombs listed, including the 500-lb GP bomb with air-burst fuzing.

Similar computations for fragmentation damage to medium and heavy guns in revetted positions give the same results, except that the 90-lb fragmentation bomb and 100-lb GP bomb have about the same efficiency, on a weight basis, as the 20-lb fragmentation bomb for small positions. There is not much data

on damage to heavy guns, but the larger fragmentation bombs are probably more efficient than the 20-lb bomb for attack on heavy guns having thick steel parts.

The efficiency comparisons above are for efficiency in terms of area of damage per pound of bomb. The efficiency in terms of area damaged per plane load must be determined by a further calculation using the areas given in Weapon Data Sheet 6D1 and the method of calculation described in Section 16.6.1.

Enclosed Gun Positions — Fortifications. Strong points of resistance frequently have gun positions enclosed in protective structures of armor or reinforced concrete.* Such structures are vulnerable to damage by underground explosion and are also vulnerable to damage by projectiles or bombs that perforate the top or side walls and detonate inside, damaging the gun or other mechanisms by heavy fragments. Both attacks require delay fuzing, but cannot be made with the same weapon without loss in efficiency of one or the other mechanisms; perforation requires the strength available only in thick bomb or projectile cases, and the consequent low charge-weight ratio is inefficient for underground explosion. Instantaneously fuzed bombs making direct hits on the roof can cause damage by contact explosion, but this damage is minor in comparison with the damage due to delay fuze action of the same bomb.

The most severe damage can be caused by a bomb or projectile perforating the roof or side wall and detonating inside the structure. SAP or AP bombs are required for all but thin fortification roofs, and AP projectiles should be used in attacking the side walls. Less rugged bombs or projectiles are likely to suffer case failure and fail to perforate. Weapon Data Sheets 2C1 and 2C1a of Chapter 19 may be used to determine the smallest bomb or projectile capable of perforating concrete of known strength and thickness, and Weapon Data Sheets 2C3 and 2C5* may be used to select the smallest weapon capable of perforating a known thickness of armor plate. The area of the target vulnerable to such an attack by bombing is the inside plan area of the structure, and since almost any explosive weapon capable of perforating the roof and detonating inside will destroy or severely damage the gun or other mechanism, the probability of neutralizing the position is the probability of obtaining a perforating hit in this area.

Delay-fuzed bombs striking outside a reinforced-concrete structure but close to the side walls may breach or collapse the walls by transmission of the shock of the explosion through the soil. The damage is not so severe as that caused by perforation plus subsequent internal explosion, but may be quite sufficient to neutralize the position. Weapon Data Sheet 6A5* of Chapter 19 may be used to determine the radius of damage to underground reinforced-concrete walls by underground explosion; the curve marked breaching should be used in making estimates of vulnerable area, and any lesser damage resulting from detonations farther from the wall should be considered a bonus. The area vulnerable to such an attack is roughly a band around the outside of the structure, having a width equal to the radius of damage. The shape of this area around corners of the structure must be estimated, and the band may be of varying width due to different thicknesses of the side wall.

Figure 2 is a schematic diagram of a typical reinforced-concrete fortification and shows the areas vulnerable to bombing attack by perforation of the roof and by earth-shock damage to the side walls. Approximately, the probability of a hit within either area is proportioned to the area. To determine the more efficient of the two methods of attack the vulnerable areas per plane load of bombs must be determined. For bombs capable of perforating the roof, the vulner-

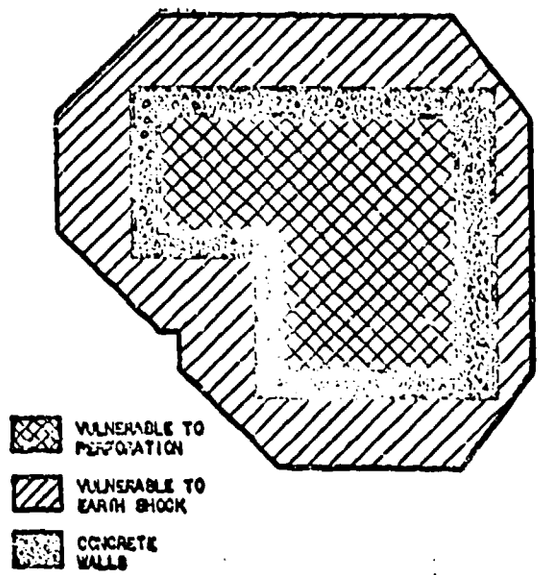

FIGURE 2. Reinforced concrete fortification, showing areas vulnerable to bombing attack. The inside plan area is vulnerable to perforation by bombs. The outside area, having width equal to the radius of damage, is the vulnerable area for earth shock damage to the side walls of the structure. The shape of this area near corners must be estimated.

able area is the inside plan area of the target plus the area vulnerable to earth-shock damage by the same bomb (since both use the same fuzing). The area vulnerable to earth-shock damage alone for bombs that cannot perforate the roof is determined as indicated above. These may be compared for all possible bomb selections to find that bomb for which the target has the largest vulnerable area per plane load. For the usual type of structure, it will be found that the most efficient bomb is the smallest bomb capable of perforating the roof.

Since the damage due to explosion in earth near the target is not so severe as damage due to perforation and explosion, it may be desirable to make the computation described above with weighted values for the different types of damage. For example, if the earth-shock damage is considered half as desirable as the damage by perforation, all areas for earth-shock damage should be halved in the computation of efficiency.

Other Resistant Targets. Other types of resistant targets are protected ammunition stores, command posts, armored vehicles, etc. Any resistant structures built of reinforced concrete may be analyzed for attack by the method used above. Underground structures may be attacked by earth-shock action against the walls or roof or by perforation of the composite roof of concrete covered with soil. (See *Composite Targets* in Section 9.3.1.) It must be remembered that earth shock can act on the roof as well as on the side walls, and that a bomb striking the roof but failing to perforate usually comes to rest in a position suitable for a tamped side-on contact explosion, with possibilities of severe damage.

Armored vehicles are vulnerable only to direct hits or very near misses by bombs. They are such small targets that direct hits by bombs are difficult to obtain, and they can usually be attacked more efficiently by rocket fire from aircraft or by artillery fire.

Military Obstacles

There are many types of military obstacles, varying in resistance from light wire barricades to heavy concrete and earth antitank walls. Most obstacles are vulnerable only to direct hits or very near misses, and are so small that hits are difficult to obtain by bombing or artillery fire. Hand-placed demolition charges are the most effective method of dealing with obstacles, but this technique cannot be used at a distance.

Wire Barricades. Paths through barbed-wire barricades can be cleared by dropping a line of instantaneously fuzed bombs across the barricade, by demolition rockets, or by line charges such as snakes or Bangalore torpedoes placed through the wire. Radii for clearance of wire by these weapons are given in Weapon Data Sheet 6D2 of Chapter 19. Bombs should be dropped by flight perpendicular to the line of the barricade, using minimum intervalometer setting so that the circles of clearance will overlap to provide a clear path through the barricade.

Obstacles. Bombing has proved to be ineffective against obstacles of concrete, stone, and steel, unless a direct hit is obtained. The clearance of obstacles by demolition charges is a specialized technique and will not be treated here. The references listed in Weapon Data Sheet 6D2 should be consulted.

Underwater Obstacles. Underwater obstacles can be cleared by detonation of suitable demolition charges. Special charges and techniques have been developed. The references listed on Weapon Data Sheet 6D2 should be consulted.

Land Mines. Bombing is not a satisfactory method for clearing land mines. Paths can be cleared through some mine fields by detonation of line charges on the ground, small line charges such as the Bangalore torpedo or the *infantry snake* being used to clear narrow paths, while larger line charges carrying several pounds of explosive per foot, such as the *demolition snake*, must be used to clear paths for tanks.

Precise data on the clearance of land mines by line charges are not available in enough quantity to allow generalizations. The available information indicates that for large charges the width of path cleared is proportional to the square root of the weight of charge per foot, as would be expected from model-law considerations. This means that several parallel line charges, properly spaced, can clear a wider path than a single charge having the same total weight of explosive per foot. This cannot be carried to the extreme of a large number of lines of small explosive content, however, since a certain minimum weight of explosive per foot in each line is necessary to detonate the mines.

The distance from an explosive charge at which land mines will be detonated depends, among other things, on the sensitivity of the mine to shock and its depth of burial. One rarely knows what type of mines are to be cleared or the depth of burial, so the choice of explosive weapons for clearance is at best a guess. The radius of clearance is not definite, but is usually given as the distance at which 50 per cent of the mines will be detonated. Some live mines are always left inside this radius. Mines near the limiting radius of

clearance may have shear wires holding the striker pin partially but not entirely cut. Such mines are not fired but are left in a more sensitive condition than before the attempted clearance.

Numerous mechanical devices have been developed for clearing paths through mine fields. Most of these simply apply a heavy load to the ground and cause the mines to function normally. Many of these devices are quite effective, but have the disadvantage of being vulnerable to damage by explosion of large mines.

16.5.2 Transportation Targets

The object of attacks on a transportation system is to paralyze the system. This may be accomplished by destroying or damaging terminals, carriers, transportation lines, or fuel supplies, and may be furthered by damaging construction and repair facilities and by attacks on plants manufacturing the carriers. Experience has shown that transportation cannot be permanently stopped. The best that can be achieved is temporary stoppage, and studies of each individual objective will show whether the most efficient method is to cause many short delays by light attacks at frequent intervals or to cause long delays by very heavy attacks that do not require frequent repetition.

Rail and Highway Transportation

Rail and highway transportation can be affected by attacking the terminal facilities, the carriers, or the roadway. The selection of the most important of these requires a detailed knowledge of the transportation system, its uses, and the repair and replacement facilities available. The carriers and roadway are usually more easily damaged than the terminal facilities. Cutting highways or rail lines is a quick method of stopping the flow of men and supplies, but, except for large bridges or tunnels, repairs or bypasses can be made quickly. Destruction of railway cars and locomotives or vehicles used in highway transportation does not cause such immediate results as line cutting, but if coordinated with attacks on manufacturing and repair facilities such attacks can have a lasting effect on transportation.

Rail Lines — Highways. Traffic may be temporarily stopped by direct damage to a rail line[7] or roadway, and even though such blocks are quickly repaired the right of way is so easily damaged that this method of stoppage is important for tactical use (see Weapon Data Sheet 6F2 of Chapter 19). Railway lines and highways are on the ground, and the obvious mechanism of damage is underground explosion.

Highways can be blocked by cratering. It was shown in Section 16.5.3 that for area covered by cratering, small bombs are more efficient on a weight basis than are large bombs. The bombs used must be large enough to form a crater across the full width of the roadway, and the block will not be successful unless made in a location where detours are difficult. The cratering of roadways on good level ground allowing short easy detours has nuisance value only.

Rail lines can be damaged by underground explosion. It is not clear whether the most useful damage is due to cratering or to displacement of the tracks, but since the bomb and fuze selection for both mechanisms is the same no choice between the two is necessary. The radii of damage for several GP bombs acting on railway track by underground explosion are given in Weapon Data Sheet 6F2, and may be used to estimate force requirements for a particular target. Even though small bombs cause more area cratered per pound than do large bombs, it is usually possible to make repairs on several craters simultaneously; thus one large crater may require more hours (but less man-hours) to repair than several small ones. If a line is cut in three or more places and the craters are large enough to require heavy equipment for efficient repair, it is necessary that some of the damage be repaired before equipment can be brought up to the others.

Lines of more than two tracks are seldom completely blocked by one bomb hit, and even in cases where all lines have been blocked, at least one track can be open to traffic in a very short time. For this reason, bombing of rail yards is a poor method of stopping through traffic.

Long-delay fuzes are not advisable since cutting of rail lines is usually a short term tactical maneuver and the full force of the attack is needed at once to stop the flow of traffic. Delay fuzes of ½ to 1½ hours may be used for nuisance value, but longer delays have no marked advantage. For tactical operations the enemy would continue to operate over bombs with long-delay fuzes.

Bridges. The most vulnerable points of a railway or highway system are the bottlenecks formed by bridges[8] or tunnels (see Weapon Data Sheet 6F3 of Chapter 19). Bridges are generally the more numerous and more easily damaged of the two. Low-level attacks may be made against the piers or abutments of bridges, using large GP bombs with long-delay fuzing to allow the attacking aircraft to escape before the explosion. Attacks from high altitudes may be made against the

bridge superstructure, using large GP bombs with very short fuze delays. Direct hits on the superstructure are then necessary.

Bridge abutments may be damaged by earth shock due to underground explosion behind the abutment walls. The radius of damage for various bombs can be determined by use of Weapon Data Sheet 6A5* of Chapter 19. The bomb must perforate the abutment and explode behind, or penetrate the soil behind the abutment and then explode. Bridge piers may be damaged or moved, causing the bridge to collapse, by a crater undermining the pier or by displacement of the pier. Such effects are very difficult to achieve against piers anchored to bed rock. Both piers and abutments are small targets, requiring high accuracy for successful bombing attack. Such accuracy is usually obtainable only from minimum altitudes and so can be used only if defenses are light. Large GP bombs (SAP bombs for perforation of heavy abutments) must be used.

Bridge superstructures must be attacked by bombs fuzed instantaneously or short delay, so attack must be made from medium or high altitude for safety of the aircraft. Precision bombing is necessary to obtain direct hits, and guided missiles may be used to advantage. Through-type bridges, having most of the superstructure above the roadway, require instantaneous or nondelay fuzing to damage the bridge frame. Deck-type bridges, having most of the superstructure below the roadway, require a short fuze delay of about 0.01 sec for detonation of the bomb in the structure.

Weapon Data Sheet 6F3 of Chapter 19 gives bomb and fuze recommendations for attacking a number of typical bridge types. This is based on analysis of more than 150 incidents of bomb damage to bridges in all theaters of operation of World War II. It will be noted that for minimum altitude attack on piers and abutments the recommendation assumes that a fighter bomber will be used and specifies that the largest bomb the aircraft can carry be loaded; for such an attack this is obviously the most efficient plane load. For medium- or high-altitude attack on bridge superstructures, the recommendation is generally the 1,000-lb GP bomb for single-track bridges and the 2,000-lb GP bomb for double-track bridges. At the time this Weapon Data Sheet was prepared, the 2,000-lb GP bomb was the largest available, having a case that could withstand impact on a bridge. The 12,000- and 22,000-lb bombs have been used successfully against very large viaducts, but unless the targets are extremely wide and heavily built these bombs are excessively large. The 4,000-lb GP bomb has not been used in combat for attack of bridges, but should prove to be a useful weapon for damaging heavy piers or abutments or for high-altitude attack on the superstructures of bridges more than 16 ft wide.

Tunnels. Tunnels[9] are bottlenecks in transportation systems second only to bridges in importance for attack (see Weapon Data Sheet 6F4 of Chapter 19). The blockage of tunnels may be more difficult to repair than damage to bridges, but the targets are usually less vulnerable. Tunnels may be blocked by collapsing the side walls by underground explosion in the soil near the tunnel lining; explosions inside the tunnel itself cause comparatively little damage. Weapon Data Sheet 6F4 gives the maximum distance from the tunnel lining at which a bomb causes sufficient damage to block passage. The bomb must penetrate through soil or rock and then explode near the tunnel, so GP or SAP bombs must be used, the SAP bombs being required for soft rock. If the tunnel is so deep that bombs cannot penetrate to within the lethal distance, such attacks are useless.

Tunnels may also be blocked by taking advantage of the steep slopes usually present at the portals and causing slides of these slopes. Such tunnel blocks are sometimes easy to repair. If the retaining walls around the portal are collapsed, the slide may be of such magnitude that reopening of the tunnel will be difficult.

Landslides. If conditions are favorable, landslides[10] may be caused in road cuts or on roads along mountain sides. Such slides are possible only if the soil is in a nearly unstable condition, as after a long rainy spell, but may make very successful road blocks requiring a long time for repair. The selection of slopes vulnerable to bombing is a special problem requiring a thorough knowledge of soil stability, and detailed references should be consulted.

Blocking of Right of Way. Attempts have been made to block rail lines and highways by bombing of buildings close to the right of way, and in some cases large areas of important rail centers have received very heavy bombing. Such methods were generally unsuccessful because there are usually rail and highway bypasses around large cities, and the bombing effort required to block all alternate routes was so large as to be inefficient and impracticable.

Carriers. Railway and highway transportation can be reduced by destruction or damage of the carriers.[1] This is not very efficient in the case of highway transportation because of the large numbers of relatively small vehicles, usually dispersed because of variations

in traffic requirements. Railway transportation can be seriously harmed by damage or destruction of freight cars and locomotives, the locomotives usually being more critical (as well as more difficult to damage). A knowledge of the relative availability of freight cars and locomotives is necessary to determine which will be the more profitable target.

Strafing and rocket attack are both effective on locomotives, especially if they are hit while in operation so that secondary damage from an exploding boiler will occur. Hits with rockets are more effective but also more difficult to attain, and of the two methods strafing is probably preferable with present accuracies. Strafing and rocket attack are of little or no value against other forms of rolling stock.

Locomotives and freight cars can be destroyed or damaged by bombing, and such attacks are usually more efficient when directed against the high concentrations of rolling stock common in freight yards.

Freight Yards. Freight yards are a very good target if the objective is damage of rolling stock. Freight cars can be damaged by blast, fragments, undermining by cratering, or by fire. Data to show which of these mechanisms is the most efficient are not available, and one must rely on analysis of attacks. Such an analysis shows that instantaneous fuzing is probably best, indicating that blast or fragmentation is the damage mechanism to be preferred. Fuze delays of 0.01 sec, however, are almost as effective as the instantaneous fuzing and probably cause damage by debris and by undermining of cars. If damage to tracks in the freight yards is desirable, the 0.01-sec delay fuzing will serve the double purpose of damaging freight cars and tracks. The 1,000- and 500-lb GP bombs are both effective; the smaller bombs do not cause severe enough damage. The 500-lb GP bomb is about 25 per cent more efficient than the 1,000-lb GP against freight cars, and the 1,000-lb GP is slightly more efficient than the 500-lb GP in damaging locomotives.

Radii for different categories of damage to locomotives are given in Weapon Data Sheet 6F2 of Chapter 19. The MAE can be determined by taking the area of a band, having the radius of damage as a width, drawn around the locomotive, adding the plan area of the locomotive, and dividing this total area by the bomb weight. Consequently, the MAE depends upon the size of the locomotive.

Analysis of data on the effects of bombs on freight cars has led to an MAE value of 0.29 acre per ton for the 500-lb GP bomb and 0.23 acre per ton for the 1,000-lb GP bomb, both being for fuze delays of 0.01 sec and for attack on European-style wooden box cars. Both bombs are effective against the shops, controls, and signal equipment, and warehouses usually found near freight yards.

Studies of a number of bombing attacks on freight yards in Italy show that with 500-lb GP bombs fuzed 0.01-sec delay, a bombing density of 1.5 to 2.0 tons per acre in the target area is sufficient to disrupt a freight yard completely. Obviously, transportation facilities which are expected to be captured later should not be over-destroyed.

Repair Facilities. Attacks on railway and highway systems should be followed up by attacks on the facilities used for repair of locomotives, freight cars, and other equipment. The repair shops are similar to machine shops or factories using heavy equipment, and should be attacked by the same methods. Attacks on heavy industrial plants are discussed in Section 16.9.3 below.

Fuel Supplies. All types of transportation require fuel for operation, and damage or destruction of these supplies can have an important effect on movement of materials.

Air Transportation

The volume of material carried by air transportation is usually much smaller than that handled by other methods, but the materials carried are frequently critical. The attack of aircraft in flight is difficult, and there is no roadway to attack, so that efforts must be concentrated on airports, fuel supply, and manufacture of aircraft.

At an airport, attacks on runways, grounded aircraft, repair shops, and fuel storage are all effective. These targets are frequently close together, but since the damage mechanisms for the various targets are different they cannot all be attacked efficiently by the same weapon. Grounded aircraft are attacked most efficiently by fragmentation bombs which have no effect on runways, while runways and landing areas are most efficiently attacked by cratering bombs which have comparatively small radii of damage to grounded aircraft.

Strategic bombing with the stoppage of aircraft transportation as an objective can be directed at aircraft production. Fuel production and storage are also important targets. The tactical attack of an airfield, with temporary neutralization as an objective, can be accomplished by first cratering the runways and then strafing or using fragmentation bombs to destroy the grounded aircraft.

Runways and Landing Grounds. The obvious mechanism of damage to be used in attacking runways and landing grounds[12] of airports is cratering by underground explosion (see Weapon Data Sheet 6F1 of Chapter 19). General-purpose bombs should be used to ensure penetration into the soil without case failure, and fuze delays of at least 0.01 sec or more for the 100- to 500-lb GP bombs, or 0.025 sec or more for the 1,000- to 4,000-lb GP bombs should be used to allow enough penetration for efficient cratering. Since most airports are built on a base of well-compacted soil, bombs will not penetrate too far for effective cratering even with very long fuze delays.

In planning a cratering attack, one must decide whether the objective is maximum area of craters, maximum volume of craters, or maximum number of craters. A statistical study of actual attacks on runways 200 to 300 ft in width shows that an average of 8 craters per 1,000 ft of length usually leaves the runway temporarily inoperative for fighter planes, while an average of 5 or less craters per 1,000 ft of runway length usually leaves the strip serviceable. More than 8 craters per 1,000 ft are needed for wider runways. The same study shows that for temporary unserviceability the number of craters rather than the area or volume cratered is the controlling factor. This means that as long as the bomb selected is large enough to form a damaging crater in an airport runway, the most efficient weapon for temporary tactical damage to runways is that bomb that can be loaded on aircraft in the largest numbers. All GP bombs, from the 100-lb to the largest sizes, cause craters large enough to damage runways, and any of them can be used with the delay fuzing recommended above. For runways paved with concrete more than 9 in. thick, the 250- or 500-lb GP bombs are the smallest that can be used for perforation of the paving without damage to the bomb case.

If the runways are to be made inoperative for more than a few hours, the number of craters is not the only criterion for successful attack, although in any case at least 8 hits per 1,000 ft of runway length (more for runways wider than 300 feet) are needed for unserviceability. The repair facilities available to the enemy must be considered. The use of small bombs results in a larger area cratered per pound of bomb than is caused by large bombs, and all GP bombs cause about the same crater volume per pound. Many small craters can be repaired simultaneously by several crews of men, and the small craters can usually be repaired without the heavy equipment needed for efficient repair of large craters. A compromise must be made between the desire for a large number of craters to ensure immediate inoperability and the desire for large craters (requiring more aircraft to carry the required number of large bombs) needed for long repair times. Whatever the weapon selection, the best that can be done is to make the runways unusable for the short time needed to repair craters.

Grounded Aircraft. Bombing and strafing attack on grounded aircraft[4] was considered in Section 16.9.1. Fragments provide the best mechanism of damage, and the most efficient present bomb is the 20-lb fragmentation bomb, fuzed for instantaneous action. For aircraft protected by revetments, bombs using air-burst fuzes are more efficient. However, air-burst fuzes are adapted for use only in large bombs, and small fragmentation bombs have efficiency comparable to that of larger bombs using air-burst fuzing.

Buildings — Repair Facilities. Damage to runways and landing grounds is always of a temporary nature, and damage or destruction of grounded aircraft is only effective until the enemy can bring in new planes. Both of these attacks are therefore of tactical value in that they make an airfield temporarily ineffective, but do not have appreciable long-term strategic value. More permanent damage to an airport can be caused by attacks on the buildings, repair facilities, and stores. Such installations are best attacked by the methods used for industrial buildings and warehouses, discussed in Section 16.9.3.

Water Transportation

Water transportation can be affected by attacking the terminal facilities and the carriers. Air attacks on such objectives do not always yield large dividends for the force used because ships are small moving targets difficult to hit, and docks and harbors are of such heavy construction that substantial forces carrying large bombs are necessary to cause appreciable damage. However, the importance of water transportation makes it an important strategic target. Ships may be attacked by gunfire, rockets, and torpedoes, and the usefulness of harbors, channels, or even larger areas may be very seriously affected by mining.

Dock and Harbor Facilities. Dock and harbor installations are usually so heavy that they are vulnerable only to direct hits or very near misses by large bombs. Warehouses and other buildings near docks can be damaged by the methods used for other industrial buildings, and if a large fire can be started great

damage can result. Mining of harbor entrances is difficult but effective.

Docks are vulnerable to damage by underwater or underground explosion; the latter is undoubtedly the more efficient. Large GP bombs with delay fuzing should be used. The radius of damage to docks depends upon their size and type of construction and each important target should be studied carefully by someone familiar with its construction and with the effectiveness of bombs. If ships are at the docks at the time of the attack, they are an additional target vulnerable to the weapons used against the harbor installations, and if sunk in the harbor they may form effective blocks to movement of other vessels or to use of facilities.

Ships. Ships[12] can be sunk or severely damaged by bombs, torpedoes, mines, and by gunfire or rockets. The most effective methods of attack from the air are bombing and torpedoes launched from aircraft; operational conditions frequently determine which method is to be used. Unless the target is known before weapons are loaded on a plane, weapon selection for the attack of ships is at best a qualified guess.

Ships are small moving targets difficult to hit from the air except by minimum altitude or dive bombing, and these methods may result in great losses if used against heavily gunned vessels. Unarmored merchant vessels are vulnerable to direct hits or very near misses by GP bombs fuzed for detonation inside of the ship, explosion below the water line and above the keel line being the most effective. Discriminating fuzes that function with a short delay if the bomb hits the ship but will not function on water impact may be used with hydrostatic fuzes so that near misses may damage the ship by underwater explosion. The vulnerable area for damage or sinking by one or more direct hits is the area of the ship as seen from the bomber; using the combination of discriminating fuze and hydrostatic fuze gives the added possibility of damage by near misses and the vulnerable area is increased by a band of small width, drawn around the ship. No accurate information on the width of this band, or near-miss distance, is available. To cause optimum damage by underwater explosion a bomb must detonate far enough below the surface so that the force of the explosion will not be wasted in the air above. The minimum depths for formation of bubbles by underwater explosion, given in Weapon Data Sheet 3C2 of Chapter 19, are satisfactory.

Most warships and large merchant ships are divided into compartments, and several compartments must be flooded to cause sinking. In general, this requires several hits at different points.

Division 2 has not made a study of the vulnerability of ships to bombing attack. A very good study, based on a careful analysis of the vulnerability of the various types of ships and the probability of obtaining multiple hits that will cause flooding of several compartments, has been made by the Navy.[13]

16.9.2 Industrial Targets

Each type of industrial target requires special study so that bombing efforts may be directed toward destruction of the most critical and most vulnerable components. Compromises are frequently necessary. For example, the air compressors of a steel mill are very critical, for if the flow of air to the blast furnaces is stopped the furnaces may freeze and be damaged beyond repair. These compressors are a small target, difficult to hit, and are of such heavy construction that a direct hit by a very large bomb is necessary to cause serious damage. Thus the air compressors, while very critical, are a relatively poor target and more loss in steel production per sortie can be caused by damage to other parts of the steel mill.

Factory Buildings and Machinery

Factory buildings[14] can be damaged by external blast, confined blast, displacement or undermining of the structure by underground explosion, and by fire (see Weapon Data Sheets 6B1, 6B2, and *Incident Summaries* of Chapter 19). Machinery and materials in the buildings can be damaged by falling debris or by collapse of parts of the building, by displacement due to blast or earth shock, by fragments, or by fire. The area damaged by underground explosion is generally smaller than the area damaged by air blast from the same bomb, and air blast is accompanied by fragments capable of damaging machinery. The most promising damage mechanisms for factory buildings and machinery are air blast and fire. Fire should be chosen as the damage mechanism when attacking combustible buildings or buildings with combustible contents; under all other conditions HE bombs should be used for blast effect on the structure and fragmentation and debris damage to machinery.

In causing damage by blast it is necessary to decide whether internal or external blast is better, since different fuzings must be used. Each has certain advantages and disadvantages. Internal blast, being somewhat confined, is more destructive to a structure than is an equal external blast (see Section 15.2.1 of Chap-

ter 15). However, on account of that confinement, its effect on a nearby structure is reduced. For this reason, a bomb larger than needed to damage one structure is inefficient if used for internal blast. Bombs must have cases heavy enough to perforate roofs without failure; this means that about half of the weight of a bomb will be wasted so far as explosive power is concerned. However, the fragments from the case will be effective damaging agents against the contents of most factories. The delay fuzing required for internal explosion means that near misses will crater and will be relatively ineffective in regard to both fragments and blast.

When external blast damage is desired, LC bombs with instantaneous or air-burst fusing are used. These give very small fragments and since bombs detonate outside of structures the damage to contents from fragments is small. Small bombs that make hits on structures, being unconfined and detonating at roof level, generally do much less damage per pound of explosive than those that penetrate before exploding. For external blast, efficiency of bombs increases with size throughout the range of HE sizes that are now in use (up to about 8,000 lb of explosive).

The choice between internal and external blast must be made after consideration of all the factors involved, particularly the amount and kind of contents, and their vulnerability to fragments, the size and strength of buildings and their separation. Analysis of attacks on Japanese industrial targets indicates that the use of large LC bombs for external blast is more efficient than 500-lb GP bombs detonated inside the structure. This increase in effectiveness should be even more marked if air burst were used for the large bombs.

Bombs fuzed with slight delay for internal blast effect will cause damage from very near misses, within the so-called *near-miss distance*, in about one out of ten cases. For the 500-, 1,000-, and 2,000-lb GP bombs against normal light factory construction the near-miss distances are respectively 15, 20, and 35 ft. For large LC bombs fuzed instantaneously or for air burst the effective distance (near-miss distance would be a misnomer here) is much greater, being about 80 ft for the 4,000-lb LC bomb with instantaneous fuzing. The effect of a particular bomb on a particular size and type of structure can be expressed in terms of the MAE (Section 16.4.1); the optimum size of bomb for causing structural damage can be determined by comparing MAE's. However, it must be remembered that damage to contents may be more important than structural damage, and generally requires fragmenting bombs exploding internally except where structural debris can damage contents, e.g., a heavy roof.

In general, it is concluded that for small HE weapons ($< 2{,}000$ lb) confined blast due to bombs exploding inside buildings is the most effective damage mechanism. This requires that the bombs be capable of perforating the roof without damage, so GP bombs must be used. Fuzing must be of sufficient delay to cause detonation below the roof and above the floor level, and thus depends on the height of the building. Nondelay fuzing causes detonation just below the roof and is best for targets whose construction is such that a major collapse of the roof can result. A fuze delay of 0.01 sec causes detonation 8 to 10 ft below the roof and is the best choice for most structures. A fuze delay of 0.025 sec causes detonation 20 to 25 ft below the roof and is effective for buildings having roof heights of 40 ft or more with machinery vulnerable to fragments near floor level, and should also be used for multistory buildings. The SAP bombs are necessary for attacks against buildings having unusually heavy roof construction. (See Data Sheet 2C1a of Chapter 19.)

Weapon Data Sheet 6B1 of Chapter 19 has a table of MAE's for several bombs against industrial buildings. Values given for the 500-lb GP bomb are determined by analysis of a large quantity of data, and values of the 4,000-lb LC bomb are also based on analysis. The values given for the 1,000-lb and 2,000-lb GP bomb are estimated from the MAE for the 500-lb GP bomb on the assumption that the MAE is proportional to the weight of explosive charge in the bomb, which has been shown by experience to be approximately correct. Analysis of recent data indicates that the larger bombs are proportionately a little more efficient than the 500-lb bomb, so that the MAE values for the 1,000- and 2,000-lb GP bombs, given in Weapon Data Sheet 6B1, should be increased by a few per cent. Furthermore, the greater near-miss areas for larger bombs indicate an additional superiority, since the probability of an effective hit is greater.

Light machinery within a building may be damaged by falling debris if part of the building collapses, and most machinery will be damaged by fragments from GP bombs exploding inside of the building, although effective and simple protection has been obtained by concrete walls surrounding each piece of equipment. Fragmentation bombs are not normally used with delay fuzing and have comparatively weak cases; hence, they are not suitable for creating fragment damage within a structure.

Very heavy machinery, as found in some industries, is not severely damaged by fragments and does not suffer irreparable damage from falling debris unless a heavy structural member strikes part of the mechanism. Such heavy equipment can be made inoperative by displacement due to underground explosion, but this is usually easily repaired. Some types of heavy machinery cannot be destroyed by HE bombs unless direct hits are obtained.

Warehouses—Storage Depots

Warehouses and other stores of supplies may be attacked using the weapons employed in attacking factory buildings. The structures are similar and are subject to damage by the same mechanisms. As shown in Section 16.5.6, the combustibility of the contents of a building is a very important item in the starting of fires by incendiary bombs and in the spread of these fires. If combustible materials are known to be stored, incendiary bombs are usually the best choice except for buildings having roofs that are highly fire-resistant.

Domestic Construction

Residential areas usually consist of a large number of very small well-separated structures. Although such structures are frequently combustible, each is a separate fire division and fires will not generally be spread from one unit to the next unless a conflagration is started. Small incendiary bombs scattered over the entire areas are the most effective weapon. The structures are usually so small that for present sizes of GP bombs near-miss damage is comparable to or greater than that due to direct hits. Therefore the greatest damage per ton of HE bombs will result if large bombs, fuzed for air burst, are used. The most effective of the present HE weapons is the 4,000-lb LC bomb with air-burst fuzing. If GP bombs smaller than the 100-lb size or LC bombs larger than the 4,000-lb size are developed their performance must be evaluated, that of the small GP bombs for direct hits, and of the large LC bombs for air burst.

Utilities

Utilities such as electric power, gas supply, water supply, sewage systems, and telephone and telegraph service are important targets in strategic warfare. Attacks may be directed at lines or at sources. The lines are usually not attacked as separate targets but are damaged as part of a general attack on an industrial target or area. Sources such as electric power plants and water supply and purification systems are good primary objectives.

Underground Piping. Underground piping, whether gas lines, water lines, sewage lines, or telegraph lines, is vulnerable to damage by underground explosion. Weapon Data Sheet 6E1 of Chapter 19 gives radii of damage to cast iron and to ceramic piping as a function of the weight of explosive charge for bombs exploding underground. Radii of damage to underground electric cables are not given; these cables are usually sheathed in lead, are quite flexible, and have been found undamaged even inside bomb craters.

Overhead Wiring. Overhead wiring is not a satisfactory target for bombing. Most observed damage to wiring can be attributed to debris or fragments.

Electric Power Plants. Electric power plants are usually either hydroelectric or operated by steam turbines. In either case the power plant itself is attacked in the same manner as any other heavy industrial structure by using large GP bombs fuzed with short delay for damaging the buildings by blast and the machinery by debris and fragmentation. Fragments can damage the windings in generators or the motors of turbines, and difficult and expensive repairs are necessary if only a few fragments enter one of these machines. Hydroelectric power plants can be put out of operation for long periods by damaging or destroying the dams, penstocks, or controls for water flow. The penstocks and controls are vulnerable only to direct hits, and most dams are exceedingly difficult to damage even with large and special weapons; equivalent loss in production of electric power can usually be obtained more easily by other means.

Transformer Substations. Transformers, switches, and other equipment in substations are highly vulnerable to damage by heavy fragments. A single fragment can perforate the case of a large transformer, short-circuit the windings, and cause the insulating oil to leak out. The entire transformer must be replaced. Fragmentation bombs equipped with instantaneous fuzes are the best weapon for attacking electric power substations or outdoor transformer installations at an electric power plant. The small 90-lb fragmentation bomb is most efficient for attacking small and medium sized transformers; large transformers having thick steel cases require the heavier fragments from the 90- and 260-lb fragmentation bombs for effective damage. GP bombs can also be used. Transformer installations are small and therefore difficult to hit in bombing. The large numbers of bombs needed for a reasonable assurance of several hits require that the resulting strategic effects must be compared with the effects of an equal tonnage of bombs dropped on some other target.

Special Industrial Targets

The discussion of factories and machinery, at the beginning of this section, applies to many kinds of industries operating in ordinary buildings. There are many other types of industry, e.g., steel manufacture and oil refining, that employ special plants and equipment and therefore need special study and planning for a successful bombing attack. Individual vulnerability analysis should be made of all important industrial targets in order to select the best objectives for attack and the most efficient weapon for damaging these objectives. For some types of assembly and light manufacturing, bombing of buildings, as discussed above, is satisfactory unless analysis of the target shows that special conditions exist. For other types of industry, requiring highly specialized construction and equipment, a detailed analysis is necessary for efficient strategic operations.

No attempt will be made here to give a detailed analysis of a wide variety of targets. One example, Japanese steel production, will be discussed and the important points in the analysis brought to the attention of the reader. Similar analyses may be made of any other strategic target systems.

The Japanese Steel Industry. The Japanese steel industry was an important strategic target in World War II. Before this war started, steel was produced in Japan from imported ores and in Manchuria from local ores. Most of the fabrication plants were located in Japan proper, and drew on Japanese steel production, Manchurian steel production, and imported iron and steel for supplies. Soon after World War II started, foreign imports of ores and of iron and steel were almost entirely cut off, and the main source of supply was the Manchurian ore.

After the imports of steel were stopped, the capacity of the fabrication plants in Japan was much greater than was needed to handle the steel produced locally and in Manchuria. This meant that steel fabrication plants were very poor strategic targets, since the work done by any one plant could be transferred to another plant with no overloading of facilities. The bombing of steel producing units in Japan and in Manchuria would have a much greater effect on production of finished products. Steel could be produced in Manchuria and shipped to Japan, or ores and coal could be shipped to Japan for local production. Approximately 12 tons of ore and coal are needed to produce 1 ton of steel, and since shipping was critical the effects of destruction of steel furnaces in Manchuria would be multiplied about twelvefold when considered as an effect on production of finished products in Japan.

This analysis of the wartime Japanese steel industry is somewhat naive in that all details are not fully considered, but a more thorough analysis leads to the same conclusion: the greatest loss in finished steel products in Japan, for a given bombing effort, could be achieved by destruction of steel mills in Manchuria. Recent history has shown this conclusion to be correct.

Bombing of Steel Mills. There are four principal operations in the production of steel, and the basic pieces of equipment for each operation, in the order of the operations, are:

1. Coke ovens, in which coke is produced from coal with various gases as by-products;
2. Blast furnaces, which are used for the reduction of iron ore to relatively pure iron;
3. Steel furnaces, in which the iron is alloyed with other materials, principally carbon, to form steel;
4. Blooming mills and rolling mills, in which steel is rolled to the shapes necessary for structural or mechanical use.

In most steel industries all four of these processes are carried out on one site and all are integrated for producing a continuous flow of finished steels from the raw materials. Each process is dependent on a continuous and regulated flow of products from the preceding process.

However, in the Japanese steel industry the first two steps were frequently carried out near sources of ore and coal in Manchuria, and the iron produced by the blast furnaces was shipped to Japan for conversion into steel and rolling into the required structural shapes. As stated above, the Manchurian production was the most important from a strategic point of view, so the primary objectives of strategic bombing of the Japanese steel industry should be the coke ovens and blast furnaces in Manchuria. These two targets will be considered separately below to select the one best suited for efficient bombing attack.[14] See Weapon Data Sheet 6C1 of Chapter 19.

Coke Ovens. Steel cannot be produced without coke for use in the blast furnaces, so the destruction of coke producing facilities directly affects the production of steel. From the point of view of bomb damage, coke ovens can be classified into two types: the older type, which can be repaired after a bombing hit with only the directly damaged portions requiring repair;

and the modern type, which undergoes excessive cracking as a result of cooling and therefore requires complete relining if cooled for repairs or cooled because of loss of control resulting from bomb damage. Damage to the older type of ovens is essentially limited to the radius of damage of the bomb, while an entire section of the newer type is damaged by a single effective bomb hit. Most coke ovens, both older and modern types, are built in batteries of four or five sections, each section being about 50 ft wide and 100 to 120 ft long and made up of some 30 to 40 ovens. The plan area for bombing attack is therefore 5,000 or 6,000 sq ft, although part of this area is masked by control equipment and loading chutes. Cooling for repairs, repairing the ovens, and reheating may require several months.

The tops of the sections of ovens are made of good quality brickwork about 3 ft thick. The 500-lb GP bomb is the smallest that can perforate the top without damage to the case, and if the top of the section is known to be more than 3½ ft thick the 500-lb SAP bomb or the 1,000-lb GP bomb must be used. Delay fuzing will assure detonation inside of the oven section, and 0.025-sec delay is recommended. A delay of 0.01 sec is not recommended because some bombs may have the fuzing mechanism initiated by overhead loading cranes and detonate before reaching the inside of the ovens. Since the bombs will be brought to rest within the ovens, delays longer than 0.025 sec are satisfactory but have no advantage.

Near misses more than about 2 ft from a section of ovens do not cause damage to the ovens. The auxiliary equipment may be damaged by near misses or direct hits, but since repairs can be made in a much shorter time than that required to repair ovens such damage is not serious except when it causes loss of control of the ovens, resulting in cooling and cracking. The important factor is not the area of primary damage but the time required for repair.

Blast Furnaces. The blast furnace plant consists of the furnace, charging equipment and storage and mixing bins, hot-blast stoves, blowing plant, and other handling equipment. The blast furnace cannot operate if any of the equipment related to it is damaged or destroyed. Destruction of some of the equipment will cause production to stop or to proceed at a reduced rate, but the furnace can be emptied and cooled slowly without damage. Destruction or serious damage to the furnace, *all* of the hot-blast stoves connected to one furnace, or to the blowing plant can cause operations to stop immediately, with "freezing" and consequent complete loss of the furnace. Such damage necessitates abandonment of the furnace and new construction requiring several months.

Blast furnaces cannot be damaged except by direct hits of large bombs, exploding inside the furnace. Hits on the side of the furnace will ricochet, so the area vulnerable to direct hits is the top of the furnace, or about 300 sq ft. The 2,000-lb GP bomb is the smallest bomb that can be expected to cause serious damage; a fuze delay of 0.025 sec is recommended to cause detonation inside of the furnace.

Hot-blast stoves heat the air for blast furnace operation. There are usually four of these, placed close to the furnace, but only two or three are used at any one time and one stove or connections to stoves at other furnaces can keep the furnace in operation while emptying and cooling. Therefore all four must be destroyed or seriously damaged to put one furnace out of operation. The stoves are of heavy construction and a direct hit by a 1,000- or 2,000-lb GP bomb, fuzed for 0.025-sec delay, is needed for each stove that is damaged. Four hits are needed to put a furnace out of operation. Each stove has a vulnerable area of about 300 sq ft.

The blowing plant furnishes air under pressure for operation of blast furnaces, and usually several furnaces receive compressed air from one blower. Thus destruction of one blowing plant may cause freezing of several furnaces. The blowing equipment is of very heavy construction and it is unlikely that a near miss by a 2,000-lb GP bomb will cause sufficient damage to stop or delay blast furnace operations. The target is so small that direct hits on the equipment are unlikely. No incidents of bomb damage to blowing plants have been reported.

Selection of Target. In the special case of the Japanese steel industry, analysis of the industry has shown that the best target from an economic point of view is the iron production in Manchuria. Further analysis of this as a target shows that the coke ovens and related equipment, the blast furnaces and related equipment, or both, are suitable targets. Severe damage or destruction of either target will require several months for repairs or rebuilding. The coke ovens can be damaged by smaller bombs than are needed for damage to the blast furnaces and related equipment, and present a vulnerable area many times as large. It is therefore concluded that the best targets for attack are the coke ovens. These present a vulnerable area of 5,000 to 6,000 sq ft per section and a direct hit by a single 500-lb GP bomb, fuzed 0.025-sec delay, will

cause such damage to one section that several months will be required for repairs.

16.10 RECOMMENDATIONS FOR FUTURE WORK

In any future war, new weapons, more complex and more powerful than those used in World War II, will be employed. Strategic warfare will probably be much more important than tactical operations. The vulnerability of targets to new weapons will be so different from vulnerability to present weapons that a large part of present knowledge of the effects of weapons on targets is already obsolete. However, mechanisms of damage will not be changed by the introduction of new weapons and the principles of selecting weapons to act by the most effective mechanism will remain the same.

The directions along which studies of weapon effectiveness should be continued are not entirely certain. It is true that present knowledge of the weapons used in World War II is far from exact or complete and, even though such weapons may soon be surpassed by others, there is reason to believe that analyses of the data obtained in Europe and Japan will be useful. High-explosive and incendiary weapons will continue to be effective. It is very probable that their power will be improved, and it is certain that methods of delivery will be greatly changed. It can be expected that aiming accuracies and velocities of impact will be greater in the future than they have been. These considerations will undoubtedly alter some of the recommendations that appear in this chapter.

Further study and analysis of the effects of bombing in Europe and Japan may be useful. However, the results of these studies will be of great value only if they are interpreted and applied by men trained in the fundamentals of terminal ballistics and explosive effects and capable of estimating the performance of new weapons from a knowledge of the performance of old ones. The training of such men, as outlined in Chapter 18, is recommended.

PART VII

LIAISON

Chapter 17

THE DIVISION 2 TECHNICAL LIBRARY

17.1 INTRODUCTION

SINCE THE PRINCIPAL functions of Division 2 were the acquisition, analysis, and distribution of information on weapon performance a means of collecting, sorting, and preserving the reports containing this information, especially those reaching the division from outside, was of utmost value to it. This need was recognized soon after the formation of the division, or rather, soon after the formation of its predecessor, Section B of Division A, NDRC. A library for the use of the division was set up at the division office in Princeton and made the primary responsibility of one man. This library grew rapidly and by the end of World War II contained about 20,000 items. Since it played a very essential part in the functioning of Division 2, and since such a library is an essential part of any organization having similar functions, it was felt desirable to describe its operation in this volume.

17.2 ORGANIZATION

The Division 2 library was organized with particular attention to its ability to assist a search for all reports relating to a particular subject. The essential need for this was found to be a well-maintained subject reference system. Listing merely key words that appeared in the titles of reports was insufficient; instead it was necessary to assign the work to a person with reasonable acquaintance with the technical field covered, so that he would be able to make an intelligent selection of subject references. In this library the cataloguing was done according to the subject classification. As an example of the form which that classification took, the following were the main categories:

1000-1999	Weapon Description,
2000-2999	Impacts,
3000-3999	Explosions,
4000-4999	Armor,
5000-5999	Structural Behavior,
6000-6999	Materials Testing,
7000-7999	Experimental Apparatus,
9000-9999	Miscellaneous.

The way this was worked out in detail is illustrated by considering a particular number, such as, say 3101;

3—Explosions
31—Air Blast
3101 Blast-Pressure Measurements.

The fineness with which subject classification is carried out is limited only by the ability of the classifier. It was found that for maximum convenience in locating reports it was well to have not more than a few dozen in each subject group so that it would not take too long to look through all of the reports of a group. In the subject classifications used, it turned out that one classification had 300 reports in it and another had 200, but few of the others had more than 20 or 30. No need was found for any particular order within a subject group, so that reports were simply added in the order received, although provision was made to put closely related reports, such as addenda or successive progress reports, consecutively. Thus each report was assigned a number having two parts, the first of which indicated the subject group while the second indicated merely the number of the report within the group. A typical number would be, say, 3101/52, which would mean the fifty-second report on air-blast pressure measurements. When the next report was received on the same subject, it would ordinarily receive the number 3101/53, but if it was particularly closely related to, say, 3101/47 then it would receive the number 3101/47.1.

It was found unnecessary to extend the subject classifying to the reports within one group, since that would make for unnecessarily complicated reference numbers, and since each subject group did not contain many reports.

It turned out to be very important not to limit the subject classification of a report to its primary subject but to make plentiful cross references to subsidiary subjects, because seldom is a report found that agrees exactly in subject with the breakdown used for classification but, instead, contains parts of several classes. If these subject cross references had been omitted the subject index would have been much less useful. For the same reason, when a report such as a progress report consisted of several parts by different authors, care was taken to catalogue it according to the subject

of each part, and to prepare author and title cross reference for each part as well.

It was found convenient to the operations of the library to have a ready means of distinguishing its reference numbers from others that might be used in connection with a report. Thus each of the Division 2 classification numbers was prefixed by a pair of letters to supply this indication. The letters PF (Princeton Files) were used, so that a complete number would be PF-3101/52.

Considerable care was taken to see that the cross references made were as extensive as possible. Thus not only were cross reference cards prepared for the author and the title of each report, but cards were also prepared for each of the various reference numbers that it contained. This was done even though certain reports contained fifteen or more such reference numbers. The effort was found to be repaid by the greater number of times that reports could be located from fragmentary information.

17.3 REPORT ABSTRACTS

A technical abstract was made of each report as it was received. This had a dual purpose; it was used on accessions lists which were distributed to the research workers in the division to let them know that new reports had been received in their fields, and it also was put on the subject reference cards, thus permitting a subject search without the necessity of obtaining the actual reports from the files or calling them in from loan.

17.4 CONTENTS

The major supplier of reports to the library was the OSRD Liaison Office, which did an excellent job of obtaining and forwarding reports secured from the various British organizations. Through this means were received regularly the reports of the Static Detonation Committee and the Anti-Concrete Committee of the Ministry of Supply, the Underwater Explosions Subcommittee of the Admiralty, and the Research and Experiments Department of the Ministry of Home Security. Group A of the OSRD Liaison Office performed the same function for reports issued by American Service groups, including intelligence reports in the field of the Division.

These sources were supplemented by information especially obtained by Division personnel in the course of various foreign missions. Thus early in World War II the Division Chief, during a trip to England, obtained permission to have reproductions made of a number of analyses of bomb-damage incidents in England prepared by the Ministry of Home Security. Also the several operations analysis groups, some of whose personnel had been trained by the Division (Chapter 18), sent back material expected to be useful to the Division's work, and the same was done by several of the various bomb-damage surveys. Through these sources the library was able to keep abreast of the information in the field of the Division, generally receiving reports shortly after they were written.

17.5 SECURITY

One of the problems that required most careful consideration for its solution was that of maintaining appropriate security in the functioning of the library. It was found that this could best be solved not by limiting the library to coverage of a very narrow field, but by having the library cover a broad field, supplying to the individual research worker only information pertinent to his problem. Thus the librarian would have a large enough field from which to locate related information for the research worker.

The accessions lists were handled in a special way because of the requirement of security. Instead of putting on one list all reports received by the library, it was necessary for the librarian to keep a tabulation of the interests of the various workers, and notify them only of the various reports in their fields. Thus the report titles and abstracts reproduced were sorted so that only appropriate ones reached each individual.

Chapter 18

TRAINING OF OPERATIONS ANALYSTS

18.1 INTRODUCTION

THERE HAS BEEN a clear need for men, trained in the principles of damage assessment and weapon selection, to work with operations officers in combat zones and with planning and intelligence organizations at various headquarters. These men act as consultants in weapon selection and operations planning, and aid in evaluating the damage caused by various operations.

As the personnel of Division 2 acquired information and experience on the performances of weapons it became more and more evident that men with such knowledge would be of great use to those engaged in planning operations. In late 1942, operations analysis sections were being set up at various air force headquarters, and Division 2 undertook to find and train men in the principles of weapon selection for such an assignment. In the spring of 1943 six men were brought to Princeton to be trained as operations analysts; all were later employed by the air forces as consultants in operations, working with planning groups in the theaters.

The work of this first group of men was so well received that there were requests for additional men of similar training and abilities. Other groups were formed and were trained at Princeton; by August 1945, five groups had received formal training and several men unable to come to the Princeton University Station at the time of one of the regular training courses received individual training. Most of the men were civilians, although one group was composed entirely of naval officers.

Approximately forty men received training in bomb selection and damage assessment and, except for those of the last group, nearly all were assigned to service with one of the air forces or with some other organization where a knowledge of the effects of bombing was needed. Men worked with at least eight of the various air forces, with the Joint Target Group (AC/AS Intelligence), with the Research and Experiments Department, Ministry of Home Security (British), and in various naval organizations. The last group of men completed their training in August 1945. Two of these had orders to report for duty and others were awaiting orders when Japan surrendered.

One man, accompanying landing forces so that he could make observations on the effects of bombing before these effects were erased or changed by clean-up operations, was killed in action. The fact that he took the risk of going in with a landing force for the opportunity of making direct and immediate observations of the effects of bombing is an example of the sincerity and thoroughness of the work of all of these men.

18.1.1 Liaison Provided by Training

One important result of sending these trained men to the field was the liaison provided between field operations personnel and research organizations in this country. The men who had been through the training program described above were familiar with the research activities of various organizations and therefore knew where to seek information and advice on problems as they occurred, and were receptive to such information. Most of the men working on weapon selection and damage assessment had the common background of the training program and were personally acquainted with each other. This provided an informal liaison between sections, and the men were interested in and receptive to ideas developed in sections other than their own.

The training program was very useful to Division 2, in that reports and personal communications from men working in the field provided a contact between those engaged in research and those applying the results of research. Such contact was especially helpful in guiding the programs of Weapon Analysis (see Chapter 16) and Weapon Data Sheets (see Chapter 19).

18.2 THE PRINCETON TRAINING PROGRAM

All men receiving formal training at the Princeton University Station went through a six-to-eight-week course of study, supplemented by visits and short training courses with other organizations.

18.2.1 Selection of Men for Training

Men to be trained as operations analysts for work with the air forces must have good background knowledge of engineering structures, mathematics, and applied physics. Most of the men selected for training were trained as engineers or architectural engineers and had some professional experience in one of these fields. Men were also selected for emotional maturity, physical fitness, pleasing personality, and ability to work well with others, because all of these traits are important in acting as a field consultant to higher echelon combat officers.

18.2.2 Training at Princeton

All the men had a review course in mechanics and a special course in mathematical probability and its application to bombing problems. The men were trained to find and use reference material on weapon effects and required to make detailed studies of many of the operations reports and damage studies available in the Division 2 library. The men received lectures on effects of air blast and underground explosions, terminal ballistics of armor and concrete, and on the effects of weapons on targets. These lectures were given by the heads of the several research sections of the Princeton University Station who were available throughout the course for consultation and guidance of further studies.

Training films, loaned to the station by the Army Air Forces, were used for instructional purposes.

Features of the later training programs were visits to various industrial plants under the guidance of a structural engineer on the staff of the station. These plants were examined for vulnerability to various mechanisms of damage by bombing, and the managers of the plants discussed the critical nature of certain operations and equipment also from the point of view of vulnerability to bombing.

18.2.3 Training by Other Organizations

All formal training groups, except the first, and many of the men who were trained informally received additional training by other organizations, although no group received training by all of the organizations mentioned here. The U. S. Naval Bomb Disposal School gave the men a short course on the characteristics and properties of bombs and fuzes. Division 11, NDRC, sent representatives to Princeton to give lectures on the properties and effects of incendiary bombs. Several of the groups were given additional training in the theory of probability and analysis of data by the Applied Mathematics Panel. Many but not all of the men received further training at the Army Air Forces School of Applied Tactics [AAFSAT]. The last group of trainees received instruction on rockets and their effects from Division 8, NDRC.

18.2.4 Reference Material

All men who were trained for operations analysis prepared personal notebooks containing the most important data and other information acquired in their training course and in study of reports in the Division 2 library. All trainees were given a number of reports to be used in their future work, and provision was made to keep them supplied with revisions and additions to these reports and with other new information. The most important reports given to the trainees are found in the bibliography.[2-6]

Most of the men, on completion of their training, were assigned to operations analysis sections of the Army Air Forces. In the course of their work, these men prepared recommendations on bomb selection and estimates of bomb effectiveness. These reports were distributed among all Army Air Forces operations analysis sections. Copies of these reports were received in the Division 2 library and were used in training new men as operations analysts.

18.3 OTHER TRAINING PROGRAMS

Operations analysis covers a wide variety of subjects, and analysts worked with combat forces in many ways in World War II. Only weapon-effects analysts were trained at Princeton. Most of the operations analysts who worked on weapon selection and damage assessment for the armed forces of the United States were attached to the Army Air Forces or the Navy; two men who had been engaged in research on weapon effectiveness at the Princeton University Station of Division 2 were attached to the Army Ground Forces as operations analysts in weapon effectiveness toward the end of World War II, but such work with the ground forces never received the interest and support given by the air forces. No formal training program for Army Ground Force operations analysts was established.

18.3.1 British Operations Analysis and Training

The British had operations analysis sections attached to most branches of their forces concerned with

combat operations, and used operations analysts to a wider extent than did our own forces. Several men who had taken the Princeton training course also took a training course in bomb selection and bomb damage analysis given by the British, and have described this course in detail.[3]

18.6 RECOMMENDATIONS FOR FUTURE WORK

The need for information on the effectiveness and efficient use of weapons and the need for men trained to use this information has been obvious in World War II. In any future war more complex and more powerful weapons than are now known will be used, and the need for men trained to evaluate the performance and to advise on the use of these weapons will be much greater than it has been in the past. Any future war will require more complete military organization and more interdependence between branches of a Service, between the Services, and between military and civilian organizations than did World War II. Such a complete organization should include a permanent operations analysis division to serve all branches concerned with operations. A single group to serve all forces is desirable since close cooperation of the forces will probably be the future order.

Strategic attack and defense in future wars will be entirely different from attack and defense in World War II and will overshadow tactical attack and defense in importance. The information that has been acquired on the effectiveness and use of weapons will be partly obsolete, but the need for such knowledge and for an adequate supply of men able to use it will be greater than before. The principles of terminal ballistics and the effects of shock waves will not be changed; they must be thoroughly understood so that they may be used correctly in evaluating the performance of new weapons.

18.6.1 Peacetime Functions of Operations Analysis Divisions

The peacetime functions of a permanent operations analysis division must include the following:

1. The collection of information on the performance of weapons as they are developed and the estimation of the performance of weapons as they are planned.
2. The discovery of advantageous uses of existing weapons and recommendation of developments of new weapons.
3. The evaluation of new weapons while still in the planning stage, as a guide to their best development.
4. The procurement and training of suitable men for operations analysis in a future war, before the need for such men arises.
5. The planning of field organizations and methods of operation in preparation for their need.

18.6.2 Training of Future Operations Analysts

The training of suitable men for work as operations analysts in weapon effectiveness and selection must be somewhat broader than it has been in the past, because the actual weapons of the future cannot be predicted very accurately and will certainly show greater variety than the weapons of World War II. Training should be as thorough as possible in the fundamentals of applied physics and applied mathematics, including the fundamental principles of explosive effects and terminal ballistics. The subject matter of the present volume, kept up to date, would be an excellent base for such broad training.

Chapter 19

WEAPON DATA SHEETS

19.1 INTRODUCTION

THE CHIEF FUNCTIONS of Division 2 have been to collect and organize information on the performance of weapons and to supply this information to those needing it. Since it is obvious that the usefulness of such information is always limited by the manner and extent of its distribution, considerable efforts have been made to make the distribution as effective as possible.

The effective distribution of information on weapon performance is made difficult by the fact that such information is particularly useful to individuals who are in or very near the field; the wide dispersal and large numbers of prospective users of weapon data seriously limits the effectiveness of the usual methods of dissemination, such as personal contact and distribution of formal reports. The Weapon Data Sheets are designed to minimize this difficulty by putting weapon data in compact and accessible form suitable for wide distribution and immediate use.

Material has been issued as a looseleaf notebook, entitled *Weapon Data—Fire, Impact, Explosion* (formerly *Effects of Impact and Explosion*). The looseleaf form was chosen so that available material could be issued at once and new sheets and revisions of old ones could be added as they became available. In general, each sheet deals with one aspect of weapon performance, presenting the material in the form of a table, chart, or a combination of these. Incident Summaries have been included to give a detailed description of bomb damage to specific typical targets.

19.1.1 Distribution of the Report

Two sizes of books were issued: a desk size and a pocket book. The first 50 copies of the desk-size looseleaf notebook, containing 15 Weapon Data Sheets and 6 Incident Summaries, were distributed in July 1943. Additional sheets have been prepared and old sheets revised as necessary, and the final edition of the book contains 81 Weapon Data Sheets and 17 Incident Summaries. The distribution list has grown rapidly. The total distribution, including the regular desk-size looseleaf notebook, the pocket edition for field use, and the bound final edition, reached nearly 1,200 copies. In addition to this direct distribution by the Division, the Eighth Air Force reprinted more than 600 copies of the early sheets for the use of ordnance officers, and later, U. S. Strategic and Tactical Air Forces requested 1,500 copies of each new sheet to continue this distribution. In addition, several of the sheets have been reproduced in various reports and manuals of Division 2 and other organizations.

19.1.2 Final Edition of the Report

The final edition of this notebook was issued as OSRD Report 6053, and more than 100 copies were bound and placed in permanent libraries. All sheets of the final edition, with one exception and a few minor corrections, are reprinted as part of this chapter to serve as reference material for other chapters of this report.

19.2 MATERIAL INCLUDED IN THE NOTEBOOK

The notebook was originally conceived as a collection of material useful to air force personnel and others concerned with the performance of bombs; hence all of the early sheets contain only data on the characteristics and performance of aerial bombs. The scope of the notebook was expanded later to include artillery weapons, demolition charges, and land mines, but the final edition still places the greatest emphasis on bombs.

19.2.1 Choice of Subject Matter

The choice of subject matter for the Weapon Data Sheets depended upon the importance of the subject and the availability of information. The ready availability of personnel of the Princeton University Station, Division 2, and of the Committee on Fortification Design [CFD] for consultation has resulted in a large proportion of sheets being on subjects with which the division and the committee were directly concerned. The extensive collection of British reports on bomb damage in the Division 2 library (see Chapter 17) was used for preparation of the early sheets on damage to structures; additional sheets on this subject have been based on bomb damage surveys by the Army

Air Forces Evaluation Boards in the Mediterranean, European and Southwest Pacific theaters, the U. S. Strategic Bombing Survey, the Bombing Analysis Unit (British), and similar groups. The close liaison between Division 2 and various Service organizations such as the Office of the Chief of Engineers, the Ordnance Department, and the Bureau of Ordnance has made much material available and thus influenced the choice of subject matter for Weapon Data Sheets.

The sheets giving quantitative information on the effectiveness of weapons on specific types of targets are based on studies by the Weapon Effects Group of the Princeton University Station, Division 2, and the choice of subject matter was largely dictated by Service requests for target vulnerability studies. These studies were based on bomb-damage reports available in the Division 2 library and on reports from the various theaters, many of which were furnished by the Service organizations requesting the target studies.

Much material prepared by contractors of Division 2 other than the Princeton University Station and by other divisions of NDRC has been included in the notebook. The largest and most important single group of such sheets is the group of incendiary bomb sheets prepared by Section 11.3 of Division 11.

19.2.2 Sources of Information

For each individual sheet an exhaustive survey of all available information was made, using the facilities of the Division 2 library (see Chapter 17), the advice of various Service liaison connections, and other sources described above. The results of the various British researches and reportings of bombing incidents have been made available through the cooperation of the Research and Experiments Department of the Ministry of Home Security.

Whenever possible, one or more experts on each subject were consulted at the beginning of each study for advice on sources of information and again before printing the sheet for approval of what had been done.

Sources of information for each of the Weapon Data Sheets are listed at the end of this chapter, after the sheets themselves.

19.2.3 Presentation of Material

The methods of presentation can best be understood by examination of the sheets making up the bulk of this chapter. Throughout, an effort has been made to present the material in a compact, immediately usable form.

The various subjects treated have been arranged to keep sheets on similar subjects together. The arrangement of sections is as follows:

1. Attacking Weapons
   - 1A Physical Characteristics
   - 1B Striking Velocity and Angle of Impact
   - 1C Aircraft Loading
2. Impact
   - 2A Penetration
   - 2B Scabbing
   - 2C Perforation
3. Explosion
   - 3A Air Blast
   - 3B Earth Shock
   - 3C Underwater
4. Fire (no work done on this section)
5. Fragmentation (no work done on this section)
6. Target Vulnerability
   - 6A Components of Structures
   - 6B Industrial Buildings
   - 6C Special Industrial Targets
   - 6D Military Targets
   - 6E Utilities
   - 6F Transportation
7. Bomb Performance

APPENDIX

0 Miscellaneous Information

Incident Summaries

19.3 RECOMMENDATIONS FOR FUTURE WORK

The success of the looseleaf notebook form of data sheets warrants a continuation of the work, or at least a plan for having such material available for all who may need it at the beginning of any future war. The importance of having as much information as possible conveniently available at the *beginning* of a war is great; many users of the Weapon Data Sheets have expressed regret at receiving sheets only in the last half of World War II when they were sorely needed for guidance of new personnel in the early operations. All material issued in such a form should be subject to constant revision. A large part of the usefulness of such a notebook is in having a wide variety of useful information available in condensed form in *one* book, and this advantage is lost if the material is not kept up to date.

19.3.1 Suggested Changes in the Present Notebook

Not all Weapon Data Sheets that would be desirable in the notebook have been prepared. Sheets on characteristics of certain weapons such as rockets and artillery projectiles, information on terminal ballistics of materials such as brick, stone, and wood, and revision of several of the sheets on concrete perforation and armor perforation were planned but not executed before the end of World War II. Other work that was planned but not completed concerned revision of present sheets and addition of several new sheets for Part 3 on explosive effects.

In the original plan of the notebook, Part 4 was to contain information of a fundamental nature on the effects of incendiaries, and Part 5 was to contain information on fragmentation. A small amount of information on these two subjects is included in Part 6, but no thorough studies of incendiary effects and fragmentation have been included in the notebook. Any continuation of this work should certainly include detailed studies of these two important subjects.

Part 6, dealing with target vulnerabilities, includes sheets based on studies made at the request of the Services. Any future work on a similar notebook or continuation of the present notebook should include studies of the physical vulnerabilities of a wider variety of targets, made along the lines suggested in Chapter 16.

19.4 SOURCES OF INFORMATION FOR THE DATA SHEETS

Each data sheet is based on the best information available to the Division at the time the sheet was prepared. The important sources are listed on each sheet, or are noted by a reference in the lower left corner of the sheet. The references AES, EWT, and OTB followed by numbers refer to the Division 2, NDRC, reports *Air and Earth Shock, Effects of Weapons on Targets,* and *Ordnance and Terminal Ballistics;* the reference PTM refers to *Princeton Technical Memoranda* published by the Princeton University Station of Division 2, NDRC. The numbers following each of these references refer to a particular issue of the report. Some of these references are reports of original research. Others are studies of information from a number of reports and include references to original sources.

The most important sources of information for each sheet are listed below, with no attempt to list all sources. Some remarks on the method of analysis used, and any information that might be useful in extrapolating the information to new weapons or in making further study of the subject are included.

Explosives

Sheet 1A1 summarizes the best available information on the properties and uses of currently used *high-explosive* [HE] fillings for bombs and demolition charges. Information from the following sources was used:

1. *Table of Military High Explosives,* Explosives Research Memorandum No. 10 (first revision), Navy Department, Bureau of Ordnance.

2. *Introduction to Explosives,* OSRD Report No. 5401, Division 8, NDRC, August 1945.

3. *Report on HBX and Tritonal,* OSRD Report No. 5406, Committee on Fillings for Aerial Bombs, Divisions 2 and 8, NDRC, July 1945.

4. Informal communication from Explosives Research Laboratory, Bruceton, Pa., Division 8, NDRC, July 1945.

Physical Characteristics of Weapons

Sheets 1A3, 1A3a*, 1A3b, 1A3c, 1A3d, 1A4a, 1A5a, 1A5b, 1A6*, 1A7a, 1A7b, 1C1 are simple tabulations of the physical characteristics of weapons. Sheets giving characteristics of United States weapons were submitted to the relevant Service organizations before publication. Those listing characteristics of foreign weapons were checked by using several independent references where possible, and certainly are not complete. In using these sheets manufacturing tolerances must be allowed for and it must be remembered that total weights and weights of explosive fillings may vary by 5 per cent from the values given. The most important references for physical characteristics of weapons are listed below.

5. *Catalogue of Standard Ordnance Items,* Technical Division, Office of the Chief of Ordnance, U. S. Army. Continuing looseleaf publication, three volumes and Limited Procurement Supplement.

6. *Catalogue of Enemy Ordnance Material,* Office of the Chief of Ordnance, U. S. Army. Continuing looseleaf publication.

7. *United States Bombs and Fuzes, British Bombs and Fuzes, Enemy Bombs and Fuzes,* and similar publications, United States Navy Bomb Disposal School, Washington. Additions and revisions issued frequently.

8. *Advanced Fuze and Explosive Ordnance Bulletin*, United States Navy Bomb Disposal School, Washington. Published monthly.

9. *Intelligence Bulletin*, United States Navy Bomb Disposal School, Washington. Biweekly publication.

10. *Bomb Disposal Technical Information*, Army Service Forces, Ordnance Department, Ordnance Bomb Disposal Center, Aberdeen Proving Ground, Md. Semimonthly publication.

11. Technical Manuals issued by the War Department. Manuals are published on a variety of subjects. Pertinent manuals were used for each sheet.

12. Ordnance Pamphlets issued by the Bureau of Ordnance, U. S. Navy. Pamphlets are issued for various weapons. Pertinent pamphlets were consulted for each sheet.

13. *Engineer Intelligence Bulletins*, Technical Intelligence Branch, Military Intelligence Division, Office of the Chief of Engineers, Army Service Forces, U. S. Army. Several bulletins on mines and demolition charges. Bulletin No. 3 and revisions tabulate dimensions of United States and foreign mines and demolition charges.

Flight Data for Bombs

Sheet 1B4 is based on calculations of the trajectory of bombs falling in a vacuum. These calculations neglecting air resistance are considered as accurate as more elaborate calculations for bombs dropped from altitudes below 5,000 ft. The equations used are given on the sheet. Sheets 1B5^0-1B21 give striking velocity and angle of impact for bombs as calculated using ballistic coefficients and condensed bombing tables furnished by the Ordnance Department, U. S. Army, and the Ballistic Research Laboratory, Aberdeen Proving Ground, Md. The striking velocities were determined by plotting the striking velocity as abscissa and the reciprocal of the ballistic coefficient for time of flight as ordinate, values being taken from condensed bombing tables. Separate graphs were made for each plane speed, and curves were drawn on the graphs for each altitude. Knowing the ballistic coefficient for time of flight of a given bomb as a function of altitude, a curve was drawn through the points determined by the reciprocal of the ballistic coefficient and the intersection of this value with the corresponding line for each altitude. From this curve, plotted on each of the graphs described above, the striking velocity of the bomb dropped from any altitude at any horizontal plane speed could be determined. A similar method was used for determining the angle of impact, plotting the angle of fall as the abscissa and the reciprocal of the ballistic coefficient for range as ordinate, values being taken from condensed bombing tables. Separate graphs were made for each plane speed, and lines were drawn for each altitude. The procedure described above was followed to determine the angle of impact of the bomb for various combinations of altitude and plane speed, using the ballistic coefficient for range for each bomb. The results were used in drawing the sets of curves shown on the data sheets. The accuracy of 15 per cent in striking velocity and 4 degrees in impact angle is due to inaccuracies in ballistic coefficients and not to inaccuracies in the method of presentation.

Concrete Penetration, Scabbing, and Perforation

Sheet 2A1 is a nomogram of the equation

$$\frac{x}{d} = \left[\tfrac{1}{2} + 282\,S^{-\frac{1}{2}}\left(\frac{w}{d^3}\right)d^{0.215}\left(\frac{V}{1000}\right)^{1.5}\right]\phi(\theta),$$

where x is the penetration measured normal to the surface in inches, d is the projectile diameter in inches, S is the compressive strength of the concrete as measured by cylinders in pounds per square inch, w is the weight of the projectile in pounds, V is the striking velocity of the projectile in feet per second, and θ is the striking obliquity measured from the normal. In constructing the nomogram a graphical function of the projectile diameter, which is very nearly $d^{0.215}$, was used instead of $d^{0.215}$ given in the equation. A graphical function of the obliquity, based on averaged data for a large number of firings of projectiles of various sizes and shapes was used for $\phi(\theta)$.

Sheet 2B1 is based on the nomogram of sheet 2A1 and the relation $s/d = 2.12 + 1.36x/d$, where x/d is from the equation above, s is the thickness of target that can just be scabbed, and d is the projectile diameter; here s, x, and d are measured in the same units.

Sheet 2C1 is based on the nomogram of sheet 2A1 and the relation $s/d = 1.32 + 1.24x/d$, where x/d is from the equation for sheet 2A1, s is the thickness of target that can be perforated, d is the projectile diameter, and s, x, and d are all measured in the same units.

The equations are empirical relations based on analysis of approximately 600 rounds fired in tests of 37-mm, 75-mm, 3-in., 155-mm, 12-in., and 16-in. armor-piercing [AP] projectiles, and about 75 rounds of inert bombs dropped on reinforced-concrete targets. Data are from the following sources:

14. *Penetration and Explosion Tests on Concrete*

Slabs. Report I: Data, Interim Report No. 20 of the Committee on Passive Protection Against Bombing, National Research Council, January 1943.

15. *Armor-Piercing Projectile Tests on Concrete Slabs,* San Francisco District U. S. Engineer Office at the direction of the Chief of Engineers, U. S. Army, May 1942.

16. *Report of Bomb Tests on Materials and Structures,* Passive Defense Bulletin No. 1, War Department, Office of the Chief of Engineers, September 1941.

17. *Armor-Piercing Bomb Test,* Protection Tests, Bulletin No. 3, War Department, Office of the Chief of Engineers, 1941.

18. *Report of Bomb Tests on Burster Slabs, Second Series,* Passive Protection Bulletin No. 8, War Department, Office of the Chief of Engineers, February 1943.

Since these sheets were published, new data have been obtained and a revision of the sheets is desirable. Analysis of recent data indicates that the relations used in sheets 2P1 and 2C1 for scabbing and perforation should be $s/d = 2.28 + 1.13x/d$ and $e/d = 1.23 + 1.07x/d$ instead of the equations given above. Data also show that the dependence of penetration on the strength of the concrete is not so simple as given by the equation above, that the size of the aggregate has a small but definite effect on penetration, that the effect of nose shape of the projectile on penetration is greater and more complicated than indicated by the correction factor of ½ used in the penetration equation, and that if a larger factor is used for nose effect the exponent of velocity in the empirical equation is greater than ⅔. Progress has been made towards a theory of penetration to replace the empirical interpolation formulas used for the nomograms but this has not reached a satisfactory stage at present. The following references contain new material on terminal ballistics of concrete:

19. *Effect of Concrete Properties on Penetration Resistance,* Interim Report No. 27 of the Committee on Fortification Design, National Research Council, July 1944.

20. *Ballistic Tests on Concrete Slabs,* Interim Report No. 23 of the Committee on Fortification Design, National Research Council, July 1944.

21. *Penetration Theory: Separable Force Laws and the Time of Penetration,* NDRC Report No. A-333; OSRD Report No. 5258, Division 2, NDRC, June 1945.

Sheet 2C1a is based on calculations from sheet 2C1, with some corrections using data described in the preceding paragraph. Striking velocities and obliquities were obtained from sheets 1B5*-1B10*. The data on penetration in soil is included for comparison purposes and is taken directly from sheets 2A2* and 2A2a. The data on bomb case breakup was taken from reference 22. The values for perforation of combination targets of soil and concrete were computed by the method described in reference 23, based on small-scale test data. The information on bomb case breakup and on perforation of composite targets is limited, so that the values given on the sheet should be treated as approximations.

22. *Ballistic Data — Performance of Ammunition,* Technical Manual TM 9-1907, War Department, 1945.

23. *Composite Slabs.* Interim Memorandum No. M-13 of the Committee on Fortification Design, National Research Council, July 1945.

The crater profiles shown in sheet 2A3 are copied directly from the following report:

24. *Penetration and Explosion Tests on Concrete Slabs. Report II: Crater Profiles.* Interim Report No. 21 of the Committee on Passive Protection Against Bombing, National Research Council, January 1943.

Soil Penetration

These sheets are based on analysis of penetration tests using small-caliber projectiles, and penetration data for inert bombs dropped on various soils. The graphs in sheet 2A2* are based on an empirical relation between the caliber penetration, x/d, and the striking velocity, where x is the penetration measured along the path of the missile and d is the diameter of the missile, both measured in the same units. It was found that for projectiles having different caliber densities (weight/diameter^3) the caliber penetration at a given velocity was very nearly proportional to the cube root of the caliber density for a range of caliber density from 0.15 to 0.65 lb per cu in. Thus penetration is approximately proportional to the cube root of the projectile weight, as shown on the sheet. The figures given for the relation between the depth below the surface and the length of the curved underground trajectory are based on a small number of measurements of actual bomb penetrations and a large number of measurements of penetration of small-caliber bullets. These figures are used in sheet 2A2a, and are not of great accuracy. Changing these

figures by 25 per cent has small effect on the penetration values given in sheet 2A3a. Sheet 2A3a is based on sheet 2A2*, using striking velocities from various altitudes as in sheets 1B5*-1B9*. The data and analysis for both sheets are given in the following reference:

25. *Penetration in Soils*, Interim Report No. 3C of the Committee on Fortification Design, National Research Council, July 1944.

Ricochet

Sheet 2A5 is based on data for small-caliber projectiles, medium and large artillery shells, and bombs dropped from low altitude. Using the impact angle and striking velocity as variables, a graph was made by plotting each round fired, with indication to show whether ricochet did or did not occur. It was found that a band could be drawn separating the regions of ricochet and no ricochet for each material. The data are for ricochet or no ricochet from thick targets. Ricochet from steel is not treated, since the limit is between ricochet and perforation instead of between ricochet and penetration, and is therefore different for every plate thickness. Most of the ricochet data are from the following sources:

26. *Ricochet Off Land Surfaces*, BRL Report No. 535, Ballistic Research Laboratory, Aberdeen Proving Ground, Md.

27. *Ricochet of Bombs Off Various Surfaces When Released at 300 Miles per Hour*, BRL Report No. 256, Ballistic Research Laboratory, Aberdeen Proving Ground, Md.

28. *The Ricochet of Bombs — Targets on Water*, Service Branch, Technical Division, Office of the Chief of Ordnance, War Department.

29. *The Connexion between Striking Velocity and Ricochet Angle at Low Striking Velocities*, Twenty-fifth Interim Report on Concrete for Defence Works, Road Research Laboratory, Ministry of Supply (British). Note No. MOS/433/ACW.

30. *Ballistic Tests on Concrete Slabs, II: Effect of Nose Shape*, NDRC Report No. A-388, OSRD Report No. 6459, Division 2, NDRC.

See also references 14, 20, and 24.

Plastic Protection

Sheet 2C2 is based on British and American data on the performance of plastic armor in stopping small-caliber bullets. These data were used to determine the thickness plastic protection required for "adequate protection" (5 per cent or less of the bullets perforating). Most of the data came from the following report:

31. *On the Probability of Perforation of Plastic Protection by Caliber .30 AP M-2 Bullets*, NDRC Report No. A-246, OSRD Report No. 3231, Division 2, NDRC, February 1944.

Armor Perforation; Mild Steel Perforation

Sheets 2C3, 2C3a, 2C4, 2C5*, 2C5a, 2C6, 2C7, and 2C8 are based on empirical relations between the scaled variables e/d and $(w/d^3)\,V^2$, where e is the thickness of plate perforated in inches, d is the diameter of the projectile in inches, w is the weight of the projectile in pounds, and V is the striking velocity of the projectile in fps. For small-caliber jacketed bullets, projectiles with cap or windshield which come off on impact, or tungsten-carbide cored projectiles, w and d are the weight and diameter of the core, or part of the projectile which penetrates the plate. An attempt was made to find an empirical equation relating the variables, but the results were unsatisfactory. The sheets show the experimental data in the form of bands which include most of the data for projectiles perforating without shatter of the missile. The curves for individual weapons, given in sheets 2C3a and 2C5a, end at the combination of plate thickness, striking velocity, and obliquity at which shatter or body breakup begins. The other sheets are averages of a large quantity of data for various projectiles and bombs, and the shatter limit is obscured by the method of presentation. The references for all sheets are listed below. References 32-35 are for sheet 2C3; reference 36 is for sheet 2C3a; references 37 and 38 are for sheet 2C4; references 39 and 40 are for sheet 2C5*; sheet 2C5a is based on an earlier edition of reference 40 and should be revised; references 41–46 are for sheet 2C6; references 47 and 48 are for sheet 2C7; references 49 and 50 are for sheet 2C8.

32. *Mechanism of Armor Perforation — 2nd. Partial Report*, Watertown Arsenal Report 710/492, May 1943.

33. *Penetration of Homogeneous Armor by Uncapped Projectiles at 0° Obliquity*, Naval Proving Ground Report 1-43, U. S. Naval Proving Ground, Dahlgren, Va., April 1943.

34. *Armor Penetration Data, Armor Penetration Graphs*. Canadian Military Headquarters, Department of National Defense, 1943.

35. *Ballistic Tests of STS Armor Plate Using 37-mm Projectiles*, NDRC Report No. A-156, Ballis-

tic Research Group, Princeton University Station, Division 2, NDRC, March 1943.

36. *Armor Perforation Curves*, Ballistic Section, Technical Division, Office of the Chief of Ordnance, U. S. Army. Most of these curves are also published in reference 22.

37. *Armor-Piercing Bullet Cores*, Watertown Arsenal Report No. 762/203, May 1943.

38. *Seventh Partial Report on Light Armor Investigation*, and *Eighth Partial Report on Light Armor*, Naval Research Laboratory Reports No. 0-1600 and 0-1745, U. S. Naval Research Laboratory.

39. *Compilation of Data Resulting from Trials to Determine the Explosive Effects of Aircraft Bombs and Means of Protection Therefrom*, Research Department, Woolwich, England, October 1938.

40. *Armor Perforation by Service Bombs*, BuOrd Sketch No. 124400, Rev. B., U. S. Navy Department, Bureau of Ordnance, 1944.

41. *High-Velocity Armor-Piercing Ammunition*, Ordnance Department, U. S. Army, August 1944.

42. *High-Velocity Development*, Ordnance Department, U. S. Army, October 1943.

43. *Proving Center Firing Record P-33104, Ordnance Program 5969*, Aberdeen Proving Ground, Md.

44. *S. D. Technical Artillery Report No. 81*, Canadian Military Headquarters, June 1943.

45. *Trials Carried out in Connection with A.T.D.B. Projects Number 6 and 7*, Army Technical Development Board, Canada, 1944.

46. *Ordnance Board Proceedings* (British), Nos. Q95, Q1471, Q1546, Q1716, Q1834, Q1838, Q1953, Q2521, 25242.

47. *Tactical and Technical Trends*, No. 17, Military Intelligence Division, War Department, Washington, January 1943.

48. *Ordnance Board Proceedings* (British), Nos. Q1834, 26433.

49. *Second Partial Report on Light Armor Investigation*, Naval Research Laboratory Report No. 0-1429, U. S. Naval Research Laboratory, March 1940.

50. *The Ballistic Properties of Mild Steel*, NDRC Report No. A-111, Ballistic Research Group, Princeton University Station, Division 2, NDRC.

Air Blast

Sheets 3A1, 3A2*, and 3A2a are based on analysis of a large quantity of data from various tests of explosives. Individual sets of data were taken from a number of references, and the separate references are not listed here. All data for pressure or impulse were averaged for the sheets. The data for pressure were compared by relating the pressure P in psi to the scaled distance from the charge $r/w^{\frac{1}{3}}$, where r is the distance in feet and w is the charge weight in pounds. The data for impulse were compared by relating the scaled impulse $I/w^{\frac{2}{3}}$ to the scaled distance from the charge $r/w^{\frac{1}{3}}$, I being the impulse in pound-milliseconds per square inch and the other variables as above. The effects of different types of explosive were taken into account by means of multiplicative factors, based on equivalent weight of explosive. The effect of the bomb case on impulse is described in sheet 3A2a and in reference 52 below. The effect of the bomb case on peak pressure has not been determined.

Sheet 3A1 is a nomogram of the equation

$$P = 4120s^{-3} - 105s^{-2} + 39.5s^{-1},$$

where P is the pressure in psi and $s = r/w^{\frac{1}{3}}$, r being the distance from the explosion in feet and w being the weight of explosive in pounds. This equation is based on averaging a large number of pressure measurements, all made prior to June 1943, on bombs filled with various explosives and detonated on the ground. When this is compared to recent pressure-distance curves obtained from explosion of small bare TNT charges in the air it is found to predict pressures which are lower than those that would be expected if ground detonation is taken into account by replacing the weight of charge by twice the weight used for the free air curve. The amount by which the nomogram is lower than the values predicted from the free air curve varies with the distance from the bomb from 50 per cent at $s = 10$ to 3 per cent at $s = 30$. In view of the fact that the peak pressure is different for different explosives and that there may be an effect of the bomb case thickness on pressure, the difference in shape or the pressure-distance curve given by the nomogram and the pressure-distance curve given by the bare TNT charges is not unexpected, since the nomogram is based on simple averaging of measurements involving various types of explosive in cases of various thickness.

A pressure-distance curve for bare TNT charges is given in the upper figure of sheet 3A9.

Experiments using small bare charges of various explosives indicate that the pressures due to detonation of equal weights of various explosives have the following relative values: torpex 2, 1.15; HBX, 1.13; minol 2, 1.09; Composition B (RDX/TNT 60/40), 1.03; tritonal, 1.07; TNT, 1.00; amatol (50/50), 0.93.

Sheet 3A2* and sheet 3A2a are based on the equations given on the sheets. The equations are based on averaging a large quantity of data for charges detonated on the ground. The effect of explosive type on impulse and on pressure, the dependence of pressure and impulse on distance, and the effect of the bomb case on impulse are discussed in the following papers.

51. *Small Charge Air Blast Experiments*, NDRC Report No. A-151, OSRD No. 1518, Division 2, NDRC, June 1943.

52. *Dependence of Positive Impulse of Blast on Charge-Weight Ratio*, AES-4, OSRD No. 4356, Air and Earth Shock, Vol. 4, p. 43, Division 2, NDRC, November 1944.

53. *Relation between Positive Blast Impulse and Charge-Weight Ratio for Bombs*, AES-4, OSRD No. 4356, Air and Earth Shock, Vol. 4, p. 51, Division 2, NDRC, November 1944.

54. *Order of Effectiveness of Explosives, IV*, AES-6, OSRD No. 4649, Air and Earth Shock, Vol. 6, p. 1, Division 2, NDRC, January 1945.

55. *The Air Blast Performance of Some High Explosives*, AES-7, OSRD No. 4754, Air and Earth Shock, Vol. 7, p. 9, Division 2, NDRC, February 1945.

Sheet 3A3 gives a curve for the relation between side-on and face-on blast pressures in air. This curve is calculated from the requirement that the velocity imparted to the gas particles by the oncoming wave is just cancelled by the velocity imparted by the reflected wave. The value of these velocities may be found from the Rankine-Hugoniot equations, which give, among other things, particle velocities as a function of pressure. (See for instance, *Aerodynamic Theory*, edited by W. F. Durand. Division H by G. I. Taylor and J. W. Maccoll. J. Springer, Berlin. 1935.)

Contact Explosions

Sheet 3A4 was prepared directly from reference 56, which describes measurements of the impulse due to explosion of small charges of various shapes in contact with an impulse pendulum.

56. *Impulse Delivered to a Plane Slab by a Contact Explosion, II*, AES-13d, OSRD No. 5506d, Air and Earth Shock, Vol. 13, p. 41, Division 2, NDRC, August 1945.

Cone End Charges

Sheet 3A5 was prepared on the basis of the available experimental data on penetration and perforation of reinforced-concrete slabs by cone and hollow charges detonated under controlled conditions. An attempt to correlate the data was made by plotting the depth of penetration as a function of the weight of explosive used, on log-log paper as shown on the sheet. The straight line giving a best fit to the data, as determined by the method of least squares, has a slope of 0.42. The large scatter in the data is such that this is not significantly different from the value of ⅓ for the slope, given by model laws. An attempt to reduce the scatter in the data by finding correlations with other variables such as type of explosive, thickness and material of cone liner, and cone angle failed. References used include:

57. *Shaped Charges for the Perforation of Concrete*, Eastern Laboratory, Explosives Department, E. I. duPont de Nemours & Co., Inc., Gibbstown, N. J., May 1943.

58. *Theory and Application of the Cavity Effect*, Report for November 1943, E. I. duPont de Nemours & Co., Inc., December 1943.

59. *Sixth Interim Report on Demolition of German Pillboxes*, Road Research Laboratory, Ministry of Supply (British), April 1942.

60. *Fourth and Final Report on Demolition Tests on Concrete Bridge Piers*, Road Research Laboratory, Ministry of Supply (British), August 1942.

Sheet 3A6 is based on reference 61. The sheet is essentially an abstract of the reference.

61. *Performance of Hollow-Charge Weapons*, OTB-12f, OSRD No. 5350f, Ordnance and Terminal Ballistics, Vol. 12, Division 2, NDRC, July 1945.

Effect of Air Burst on Blast

Sheets 3A7, 3A8, and 3A9 are based on experimental studies of small bare charges and of bombs detonated at various heights above ground. The sheets are based on the following references. Some of the graphs given in the sheets are based on new adjustments of data given in the references.

62. *The Effect of Air Burst on the Blast from Bombs and Small Charges: I. Experimental Results*, OSRD Report No. 4246, Underwater Explosives Research Laboratory, Woods Hole, Mass., with collaboration from Stanolind Oil and Gas Company, Tulsa, Okla., Division 8, NDRC, October 1944.

63. *The Effect of Air Burst on the Blast from Bombs and Small Charges: II. Analysis of Experimental Results*, NDRC Report No. A-320, OSRD No. 4899, Division 2, NDRC, April 1945.

64. *Air Burst for Blast Bombs*, NDRC Report No. A-322, OSRD No. 4943, Division 2, NDRC, April 1945.

65. *The Effect of Height of Burst on the Blast Characteristics from 67-lb Bare Cylindrical Charges of RDX/TNT 60/40*, ARD Explosives Report 16/45, Armament Research Department, Ministry of Supply (British), February 1945.

66. *Peak Pressure Dependence on Height of Detonation*, AES-1, OSRD No. 4076, Air and Earth Shock, Vol. 1, p. 1, Division 2, NDRC, August 1944.

67. *Impulse Dependence on Height of Detonation*, AES-2, OSRD No. 4147, Air and Earth Shock, Vol. 2, p. 17, Division 2, NDRC, September 1944.

68. *Mach Reflection of Shock Waves from Charges Detonated in Air*, AES-3, OSRD No. 4257, Air and Earth Shock, Vol. 3, p. 17, Division 2, NDRC, October 1944.

69. *The Effect of Height of Detonation on Peak Pressure and Positive Impulse Measured Close to the Ground*, AES-5, OSRD No. 4514, Air and Earth Shock, Vol. 5, p. 49, Division 2, NDRC, December 1944.

70. *Dependence of Optimum Impulse on Height of Gauge in Air Burst*, AES-9c, OSRD No. 5011c, Air and Earth Shock, Vol. 9, p. 17, Division 2, NDRC, April 1945.

Underground Explosions

Sheet 3B1a* is based on analysis of a large amount of data for craters formed in various soils by explosive charges ranging from a fraction of a pound to more than 3,000 lb. The variables used in plotting the data were suggested by model theory. Separate graphs were made for each soil, and although there was a large scatter in the data a smooth curve was drawn for each set of data. The final curves are shown on sheet 3B1a*. Data were taken from a large number of reports, and most of the measurements are of individual craters made in tests for purposes other than the study of cratering. Since most of the sources list only a few craters, individual references are not listed here. Reference 71 describes extensive tests of cratering by 100- and 1,000-lb general-purpose [GP] bombs. The other references describe tests made with small charges to determine the effect of different types of explosive and the effect of charge shape on crater dimensions.

71. *Supplementary Test of Selection of Bombs and Fuzes for Bombardment Targets*, AAF Proving Ground Command, Project No. 4249C471.6, the Army Air Forces Board, December 1944.

72. *Effect of Charge Shape and Orientation on Cratering in Soil*, AES-3, OSRD No. 4257, Air and Earth Shock, Vol. 3, p. 1, Division 2, NDRC, October 1944.

73. *Weight of Material Required to Fill Bomb Craters (Model Experiments)*, BRL Report No. 488, Ballistic Research Laboratory, Aberdeen Proving Ground, Md., September 1944.

74. *The Comparative Performance of Various Bomb Fillings—Crater and Earthshock Effects. Part I*, REN 452, Research and Experiments Department, Ministry of Home Security (British).

75. *The Order of Effectiveness of Various Explosives in Earth*, AES-13b, OSRD No. 5506b, Air and Earth Shock, Vol. 13, p. 13, Division 2, NDRC, August 1945.

Sheet 3B1b gives diameter of craters formed by detonation of line charges on the surface of the ground. Data from a number of tests were correlated by means of the scale factor $w^{\frac{1}{3}}$ suggested by model theory. The analysis, data, and sources of data are given in reference 76.

76. *Cratering by Line Charges*, AES-13a, OSRD No. 5506a, Air and Earth Shock, Vol. 13, pp. 1, Division 2, NDRC, August 1945.

Sheet 3B2 gives earth displacements due to underground explosions, based on analysis of a large number of tests on bombs and bare charges. The data were plotted in terms of the model-law variables $u/w^{\frac{1}{3}}$ and $r/w^{\frac{1}{3}}$ where u is the displacement, r is the horizontal distance from the explosion, and w is the weight of explosive. Separate curves were obtained for the maximum transient horizontal, maximum transient vertical, permanent horizontal, and permanent vertical displacements. The permanent displacements were determined by measuring the displacement of stakes in the ground. The transient displacements were measured by photographing the motion of a lamp fastened to a stake, or by using an inertia trolley. Data for charges at small depths showed appreciable departure from the other values, and data for detonations in chalk gave smaller displacements than those observed in clay soil. Only the data for charges buried deeper than $1.1w^{\frac{1}{3}}$ in clay soil were used. The data came from the following sources:

77. *Earth Movements Due to Explosions*, Data Compilation No. 14, Research and Experiments Branch, Ministry of Home Security (British), February 1940.

78. *Earth Movement Due to 50-kg Bombs Exploded in Clay Soil at Richmond Park*, RC 328, Road Research Laboratory Report to the Ministry of Home Security (British), May 1942.

79. *Earth Movements in Different Directions Due to Explosion of Buried 50-kg Bombs in Clay Soil*, RC 314, Road Research Laboratory Report to the Ministry of Home Security (British), February 1942.

80. *Earth Movements Due to German Bombs Exploded Below Ground*, RC 259, Road Research Laboratory Report to the Ministry of Home Security (British), August 1941.

81. *Earth Movement Due to German and British Bombs Exploded Below Ground*, RC 153, Road Research Laboratory Report to the Ministry of Home Security (British), November 1941.

82. *Earth Movements Due to 250-kg Bombs Exploded in Clay Soil*, RC 312, Road Research Laboratory Report to the Ministry of Home Security (British), February 1942.

83. *Earth Movement Due to German 250-kg Bombs Exploded Below Ground in Chalk Soil*, RC 313, Road Research Laboratory Report to the Ministry of Home Security (British), February 1942.

84. *Earth Movements Due to Buried Standard Charges*, RC 416, Road Research Laboratory Report to the Ministry of Supply (British), November 1943.

Sheet 3B3* gives nomograms for the pressure and impulse underground due to explosions underground. The nomograms are based on extensive tests of underground explosions described in reference 85. Values of the soil constants are from reference 86. Factors for pressure and impulse due to explosives other than TNT are from reference 87. A recent series of tests on the pressure and impulse at different depths due to explosions at various depths is described in reference 88.

85. *Effects of Underground Explosions* (in three volumes), Interim Report No. 26, Committee on Fortification Design, National Research Council, June 1944.

86. *The Seismic Method of Explorations Applied to Construction Projects*, Military Engineer, September-October 1939.

87. *The Order of Effectiveness of Various Explosives in Earth*, AES-13b, OSRD No. 5506b, Air and Earth Shock, Vol. 13, p. 13, Division 2, NDRC, August 1945.

88. *Final Report on Effects of Underground Explosives*, C. W. Lampson, OSRD No. 6645, NDRC Report No. A 479, submitted on February 20, 1946, and approved March 1946.

Underwater Explosions

The nomogram given on sheet 3C1 is taken directly from reference 89. Data sheet 3C2 was prepared from material in references 90 and 91, as described on the sheet.

89. *Underwater Explosives and Explosions*, Report UE-16, p. 3, Division 8, NDRC, December 1943.

90. *Theory of the Pulsations of the Gas Bubble Produced by an Underwater Explosion*, Report No. C4-ar30-010, Columbia University, Division of National Defense Research, New London, Conn., October 1941.

91. *On the Best Location of a Mine Near the Sea Bed*, AMP Report 37.1R, Applied Mathematics Group, New York University; Applied Mathematics Panel, NDRC, May 1944.

Impulse Criterion—Damage Levels

The method of analysis used in arriving at the conclusions given in sheet 6A0 is described in the sheet. The sheet is based on the references listed below. A discussion of the impulse criterion may be found in pages 17-24 of reference 64.

92. *House Damage by HE Weapons Acting by Blast*, REN 214 Revised, Research and Experiments Department, Ministry of Home Security (British), March 1944.

93. *A Modification of the Impulse Criterion for Blast Damage*, RC 349, Research and Experiments Department, Ministry of Home Security (British), September 1942.

Vulnerability of Components of Structures

Sheet 6A1a* and 6A1b* are based on analysis of column damage taken from reports of building damage. The data for various incidents were correlated by plotting the scaled distance from the explosion as abscissa and the index of column slenderness and aspect as ordinate and separating the plotted values corresponding to different degrees of damage, as shown on the sheet. The index of slenderness and aspect is defined as the area of cross section of the column material divided by the free area of the column exposed directly to the blast. This definition is suggested by a semiquantitative theory which ascribes the damage to air-blast impulse, with the blast wave assumed to act for the length of time required for the diffracted wave to make its way around the column. Data are from the following references:

94. *Effect of German HE Bombs on Industrial Structures*, REN 224, Ministry of Home Security (British), May 1943.

95. *Damage to Single Story Buildings*, R.E. 4,

Data Compilation No. 2, Ministry of Home Security (British), May 1942.

96. *Air Raid Damage Report — Dolphin Court Flats*, Ministry of Home Security (British), November 1940.

97. *Air Raid Damage Report, Serial No. C4*, Ministry of Home Security (British), 1942.

98. *Blast Effect of Bomb on Steelwork*, R.E. 4, Data Compilation No. 27, Ministry of Home Security (British).

99. *Damage to R. C. Framed Buildings*, Data Compilation No. 32, Ministry of Home Security (British), February 1942.

Sheet 6A2 is based on examination of data on bomb damage to British buildings. The data show a rough correlation between the area of concrete floor slab removed and the location and size of the bomb. For a given bomb size it was found possible to make separate analyses of the data for area of floor destroyed for the floors adjacent to the bomb, the floor next above or below the bomb, and the third floor above or below the bomb. The separate curves are shown on the sheet. The curve labeled *total area, all floors* is twice the sum of the area given by the three curves for individual floors. A recent analysis, made since publication of the sheet, shows that although the three lower curves represent the data very well, the damage is not always symmetrical above and below the bomb, and the curve for the total area of all floors does not fit all incidents. This later analysis indicates that a better approach to the problem might be made by correlating the *volume* made unusable with the weight of explosive. If the volume destroyed is determined as the height of each story multiplied by the area of destruction of the floor immediately above or below, whichever is greater, these separate volumes being summed for the entire building, then the relation $V = 140w$ fits the data very well, where V is the volume destroyed and w is the weight of explosive in the bomb. For American GP bombs this relation becomes $V = 70W$, where W is the weight of the bomb. Data on destruction of floor slabs by HE bombs may be found in the following references:

100. *Air Raid Damage Report, Serial No. A4*, Ministry of Home Security (British), February 1943.

101. *Air Raid Damage Report, Serial No. C1*, Ministry of Home Security (British), February 1943.

102. *Air Raid Damage Report, Serial No. C2*, Ministry of Home Security (British), February 1943.

103. *Air Raid Damage Report, Serial No. D4*, Ministry of Home Security (British), February 1943.

104. *Damage to Steel Framed Buildings*, R.E. 4, Data Compilation No. 26, Ministry of Home Security (British), February 1942.

105. *Model (⅛ scale) and Full-Scale Tests of Resistance of Reinforced Concrete to Attack by Bombs Nearby and in Contact*, RC [illegible]8, Road Research Laboratory Report to the Ministry of Home Security (British), September 1942.

106. *Interim Report of a Portion of Bomb Tests Conducted by the Ordnance Department on the Reinforced Concrete Test Structure at Area H, Gunpowder Neck, Aberdeen Proving Ground, Md.*, Corps of Engineers, U. S. Army, December 1942.

See also references 96, 97, and 99.

Sheet 6A3* is based on analysis of available incidents of explosions inside and outside steel framed factory-type buildings. The maximum radius of removal of roofing was plotted as a function of the weight of explosive in the bomb for both asbestos cement and sheet steel roofing. It was found possible to draw separate curves for internal and external explosion for each type of roofing, as shown on the sheet. The second graph on the sheet is a more detailed study of the effect of a German 50-kg SC bomb on the roofs of buildings of different size. Data were from the following sources:

107. *Damage to Light Roofing and Walling Materials*, R.E. 4, Data Compilation No. 8, Ministry of Home Security (British), May 1943.

108. *Damage to Walls*, R.E. 4, Data Compilation No. 10, Ministry of Home Security (British), May 1943.

109. *Variations in the Behavior of Factory Roof Sheetings Subject to Blast*, REN 220, Research and Experiments Department, Ministry of Home Security (British), May 1943.

Sheets 6A5* and 6A6* are based on references 110 and 111 respectively. These describe the methods of analysis and give references to original sources:

110. *Damage to Underground Reinforced Concrete Walls*, EWT-5g, OSRD No. 5405g, Effects of Weapons on Targets, Vol. 5, NDRC, August 1945.

111. *Damage to Reinforced Concrete Wall Panels by Detonation of Contact and Remote Charges*, EWT-3h, OSRD No. 5176h, Effects of Weapons on Targets, Vol. 3. NDRC, June 1945.

Target Vulnerability

The sheets in sections 6B through 6F are studies of the physical vulnerability of various target types. All of these sheets except numbers 6D2 and 6E1 are based on source material and methods of analysis de-

scribed in various articles published in the NDRC report *Effects of Weapons on Targets*. Sheet 6D1 is based on a study of references listed on the sheet. Sheet 6E1 is based on a study of references 123 and 124 listed below. The separate references for each sheet in this group are listed below in the order in which the sheets appear in the book. Sheet numbers are given immediately after the reference number.

112. 6B1 *Direct-Hit Effects of U.S. 500-lb GP Bombs on European Industrial Buildings: HE Structural Damage*, EWT-2f, OSRD No. 5045f, Effects of Weapons on Targets, Vol. 2, NDRC, May 1945.

113. 6B1 *Incendiary Effects of U. S. 500-lb GP Bombs on European Industrial Buildings: Probability of Initiation of Destructive Fires*, EWT-3b, OSRD No. 5176b, Effects of Weapons on Targets, Vol. 3, NDRC, June 1945.

114. 6B1 *Spread of Fire within Single-Story European Industrail Fire Divisions, Mixed HE-IB Attacks*, EWT-3c, OSRD No. 5176c, Effects of Weapons on Targets, Vol. 3, NDRC, June 1945.

115 6B2 *The Probability of Fire-Starting by Incendiary Bombs, I: General Principles and Methods*, EWT-5b, OSRD No. 5405b, Effects of Weapons on Targets, Vol. 5 NDRC, August 1945.

116. 6B2 *The Probability of Fire-Starting by Incendiary Bombs, II: Estimates for the M47 Incendiary Bomb*, EWT-5c, OSRD No. 5405c, Effects of Weapons on Targets, Vol. 5, NDRC, August 1945.

117. 6B2 *The Probability of Fire-Starting by Incendiary Bombs, III: Estimates for the M50 Incendiary Bomb*, EWT-5d, OSRD No. 5405d, Effects of Weapons on Targets, Vol. 5, NDRC, August 1945.

118. 6C1 *Air Attack on Steel Mills*, EWT-6d, OSRD No. 5657d, Effects of Weapons on Targets, Vol. 6, NDRC, September 1945.

119. 6C2a *Attack on Dams*, EWT-5f, OSRD No. 5405f, Effects of Weapons on Targets, Vol. 5, NDRC, August 1945.

120. 6C2b *Attack on Penstocks*, EWT-2b, OSRD No. 5045b, Effects of Weapons on Targets, Vol. 2, NDRC, May 1945.

121. 6D1 *Attack on Open Gun Emplacements*, EWT-6a, OSRD No. 5657a, Effects of Weapons on Targets, Vol. 6, NDRC, September 1945.

6D2 References are listed on the Data Sheet.

122. 6D3 *MAE's Calculated from Ashley Walk Trials*, EWT-6b, OSRD No. 5657b, Effects of Weapons on Targets, Vol. 6, NDRC, September 1945.

123. 6E1 *The Radius of Damage for Underground Services*. RC 290, Ministry of Home Security (British), November 1941.

124. 6E1 *Final Report of Bombing Tests on Underground Piping*, Corps of Engineers, U. S. Army, May 1943.

125. 6F1 *Aerial Bombing Attacks Against Aerodromes—Runways and Landing Grounds*, EWT-1c, OSRD No. 4918c, Effects of Weapons on Targets, Vol. 1, NDRC, April 1945.

126. 6F2 *Attack of Railroads*, EWT-2d, OSRD No. 5045d, Effects of Weapons on Targets, Vol. 2, NDRC, May 1945.

127. 6F3 *Air Attack on Bridges*, EWT-3j, OSRD No. 5176j, Effects of Weapons on Targets, Vol. 3, NDRC, June 1945.

128. 6F4 *Attack of Tunnels*, EWT-2c, OSRD No. 5045c, Effects of Weapons on Targets, Vol. 2, NDRC, May 1945.

Tentative Data—Performance of Large Bombs

Sheet 7A1 gives tentative data for performance of the 12,000-lb GP bomb T10 and the 22,000-lb GP bomb T14. These bombs are essentially the same as the British bombs *Tallboy-M* and *Grandslam* except that the U. S. bombs are filled with Tritonal instead of Torpex D-1. Performance predictions are estimated by extrapolation of the data given in the sheets in Sections 2, 3, and 6 of this book, with use being made of the observed performance of the British bombs where possible. The estimated performance in perforation of concrete, perforation of armor, and cratering in soil agrees very well with the observed performance of the British bombs. No observations of performance for other effects have been reported. Copies of principal papers describing the characteristics and performance of the British *Tallboy-M* and *Grandslam* and a critical discussion of these bombs may be found in reference 129.

129. *Study of the Requirements, Employment, and Effectiveness of Large Bombs*, AAF Project No. 4614A471.3, the Army Air Forces Board, Orlando, Fla., April 1945.

Miscellaneous Information

Sheet 0M1 gives a graphical method for solving the spherical triangle by which the altitude of the sun is determined at any point on the earth's surface and at any date. From the graphs, the ratio of object height to length of shadow on level ground can be determined to a good approximation. The only information that is needed is the latitude and longitude of the place in question, and the date and Greenwich Civil Time

when the shadow was measured. This sheet is useful in determining heights of buildings from aerial photographs. Data on solar declination and Greenwich Hour Angle are from reference 130.

130. *Marine and Air Navigation*, J. Q. Stewart and M. Pierce, Ginn & Co., New York, 1944.

The detailed calculations for sheet 0M2 are given in reference 131.

131. *Bombing Density Calculations for Sloping Targets*, EWT-3g, OSRD No. 5176g, Effects of Weapons on Targets, Vol. 3, NDRC, June 1945.

Incident Summaries

The Incident Summaries are based on the references listed below, the number of the Incident Summary being listed with the reference number.

132. A550 *Air Raid Damage Report, Serial No. A.2*, Ministry of Home Security, February 1943.

133. A1100 *Air Raid Damage Report, Serial No. A.3*, Ministry of Home Security, February 1943.

134. A3100 *Air Raid Damage Report, Serial No. A.5*, Ministry of Home Security, February 1943.

135. A-pm *Air Raid Damage Report, Serial No. A.7*, Ministry of Home Security, February 1943.

136. B110 *Air Raid Damage Report, Serial No. B.1*, Ministry of Home Security, February 1943.

137. B550 *Air Raid Damage Report, Serial No. B.2*, Ministry of Home Security, February 1943.

138. B2200 *Air Raid Damage Report, Serial No. B.4*, Ministry of Home Security, February 1943.

139. B-pm *Air Raid Damage Report, Serial No. B.7*, Ministry of Home Security, February 1943.

C110 See reference 101
C550 See reference 102
C1000 See reference 106
C1100 See reference 96
C2200 See reference 97

140. D110 *Air Raid Damage Report, Serial No. D.1*, Ministry of Home Security, February 1943.

141. D1100 *Air Raid Damage Report, Serial No. D.3*, Ministry of Home Security, February 1943.
D2200 See reference 103.

142. D-pm *Air Raid Damage Report, Serial No. D.7*, Ministry of Home Security, February 1943.

General References

The following publications contain much general material similar to that in *Weapon Data—Fire, Impact, Explosion* or contain information of general interest on the effectiveness of weapons. Much of the material in these works and in the present report is based on the same sources, and in many instances the interpretation used in one of the reports is taken directly from one of the others. Such repetition of information and interpretation should by no means be interpreted as lending authenticity to the material.

143. *Selection of Bombs and Fuses for Bombardment Targets*, the Army Air Forces Board, Project No. 3554A471.6, the Army Air Forces Board, Orlando, Fla., October 1944.

144. *The Relative Effectiveness of Various Type Bombs and Fuses Against Strategic and Tactical Objectives*, Army Air Forces Evaluation Board, Mediterranean Theater of Operations, October 1944.

145. *Selection of Bombs and Fuses to be Used Against Various Targets*, OPNAV-16-V 3A6, Air Intelligence Group, Division of Naval Intelligence, Office of the Chief of Naval Operations, Navy Department, Washington, March 1944.

146. *Selection of Bombs and Fuses for Destruction of Various Targets*, FM 1-110; FTP 224, War and Navy Departments, Washington, April 1945.

147. *Ballistic Data, Performance of Ammunition*, TM 9-1907, War Department, Washington, September 1944.

148. *Selection of Weapons for Fighter Bombers Against Tactical Targets*, Operations Research Section, Ninth Air Force, Memorandum No. 70, February 1945.

149. *Effects of Explosion of HE Bombs: I. General and Air Blast*, BRL Report No. 554, Ballistic Research Laboratory, Aberdeen Proving Ground, Md., June 1945.

150. *Performance of Bombs and Projectiles Against Shore Installations*, Ordnance Pamphlet 1172, Bureau of Ordnance, Navy Department, Washington, May 1944.

151. *Air Attack of Japanese Coast Defense Batteries, Target Analysis*, CINCPAC-CINCPOA Bulletin No. 17-45, February 1945.

152. *Effects of Weapons on Targets*, Volumes 1-6, Divisions 2 and 11 and the Applied Mathematics Panel, NDRC, monthly publication, April-September 1945.

153. *Study of the Physical Vulnerability of Military Targets to Various Types of Aerial Bombardment*, NDRC Report No. A-385, OSRD Report No. 6444, Division 2, NDRC.

154. *Effectiveness of U.S. Incendiary and High Explosive Bombs*, NDRC Report No. A-386, OSRD Report No. 6445, Divisions 2 and 11 and the Applied Mathematics Panel, NDRC.

WEAPON DATA

FIRE, IMPACT, EXPLOSION

Table of Contents

Final Edition

Foreword

WEAPON DATA

1: Attacking Weapons

Physical Characteristics:

Explosive Fillings - Properties & Uses.....1 A1
U.S. Bombs & Fuzes - Fuze Characteristics.....1 A2
American - HE Bombs.....1 A3a*
American - Incendiary Bombs.....1 A3b
American - Incendiary Bomb Clusters.....1 A3c
American - Depth Bombs, A/C Mines, Torpedoes...1 A3d
British - HE Bombs.....1 A4a
German - HE Bombs.....1 A5a
German - Incendiary Bombs, Mines.....1 A5b
Japanese - HE and Incendiary Bombs.....1 A6*
American - Land Mines and Firing Devices.....1 A7a
American - Demolition, Shaped, Line Charges....1 A7b

Striking Velocity and Angle of Impact:

Low Level Bombing.....1 B4
100-lb GP, AN-M30; 250-lb GP, AN-M57.....1 B5*
500-lb GP, AN-M64; 500-lb SAP, AN-M58.....1 B6*
1000-lb GP, AN-M65; 1000-lb SAP; AN-M59.....1 B7*
1000-lb AP, AN-M33; 1000-lb AP, M82A1.....1 B8*
1600-lb AP, AN-M61; 2000-lb GP, AN-M66.....1 B9*
2000-lb SAP, M103; 4000-lb LC AN-M56.....1 B10*
12,000-lb GP, T10; 22,000-lb GP, T14.....1 B12
90-lb Frag. AN-M82; 260-lb Frag. M81.....1 B15
Flight Characteristics of IB's, IB Clusters....1 B20
100-lb IB, AN-M47; 500-lb IB, AN-M76.....1 B21

Aircraft Loading:

Incendiary Bombs and Clusters.....1 C1

2: Impact

Penetration

Reinforced Concrete by Bombs & Projectiles.....2 A1
Bombs into Soil.....2 A2*
Bombs and Small Caliber Bullets into Soil.....2 A2a
Projectile Ballistic Limits and Craters.....2 A3
Ricochet from Water, Soil & Concrete.....2 A4

Scabbing:

Reinforced Concrete by Bombs and Projectiles...2 B1

Perforation:

Reinforced Concrete by Bombs and Projectiles...2 C1
Reinforced Concrete by Specific Bombs & Rockets 2 C1a
Plastic Protection.....2 C2
Homogeneous Armor by Projectiles.....2 C3
Homogeneous Armor by American Projectiles.....2 C3a
Homogeneous Hard Armor by Cal .30 & .50 Bullets..2 C4
Homogeneous Armor by Bombs (General).....2 C5*
Homogeneous Armor by Specific Bombs.....2 C5a
Homogeneous Armor by TC Cored Projectiles.....2 C6
Homogeneous Armor by German Projectiles.....2 C7
Mild Steel by Uncapped AP Projectiles.....2 C8

3: Explosion

Air Blast:

Maximum Peak Pressure.....3 A1
Positive Impulse.....3 A2*
Impulse due to Det. of Bombs, Ground Level.....3 A2a
Side-on vs Face-on Measurement.....3 A3
Impulse - Contact Explosions.....3 A4
Cone-end Charges against Concrete.....3 A5
Cone-end Charges against Homogeneous Armor.....3 A6
Mach Reflection.....3 A7
Optimum Height for Maximum Impulse.....3 A8
Pressure & Impulse on Ground due to Air Burst..3 A9

Earth Shock

Craters in Soil - Diameter and Depth.....3 B1a*
Cratering by Line Charges.....3 B1b
Earth Displacement.....3 B2
Underground Pressure and Impulse.....3 B3*

Underwater:

Pressure and Impulse.....3 C1
Maximum Radius of Bubble.....3 C2

6: Target Vulnerability

Impulse Criterion: Damage Levels.....6 A0

Components of Structures:

Steel Columns - Blast Damage.....6 A1a*
Concrete Columns - Blast Damage.....6 A1b*
Concrete Floor Slabs - Blast Damage.....6 A2
Sheet Roofing - Removal by Blast.....6 A3*
Underground R/C Walls - Damage by Earth Shock....6 A5*
Reinforced Concrete Walls - Damage by Air Blast..6 A6*

Industrial Buildings:

Damage by HE Bombs.....6 B1
Damage by Incendiary Bombs.....6 B2

Special Industrial Targets:

Bombing of Steel Mills.....6 C1
Bombing of Dams.....6 C2a
Bombing of Penstocks.....6 C2b

Military Targets:

Bombing of Gun Positions.....6 D1
Passage of Wire and Obstacles.....6 D2
Frag. Damage - Aircraft, Vehicles, Personnel.....6 D3

Utilities:

Underground Piping.....6 E1

Transportation:

Bombing of Airfield Runways.....6 F1
Air Attack on Railroads.....6 F2
Bombing of Bridges.....6 F3
Bombing of Tunnels.....6 F4

7: Bomb Performance:

12,000-lb GP, T10; and 22,000-lb GP, T14.....7 A1

APPENDIX

Miscellaneous:

Solar Shadow Ratio Chart.....0 M1
Equivalent Horizontal Area for Sloping Target.....0 M2

Incident Summaries:

A: (MS-SF) Multi-story, Steel Frame Construction

550-lb GP Bomb - Office Building.....A 550
1100-lb GP Bomb - Apartment Building.....A 1100
5100-lb AP Bomb - Railway Station.....A 5100
Parachute Mine - Office Building.....A Para-mine

B: (SS-SF) Single-story, Steel Frame Construction

110-lb GP Bombs - Shed Buildings.....B 110
550-lb GP Bombs - Factory Building.....B 550
2200-lb GP Bomb - Factory Building.....B 2200
Parachute Mine - Office Building.....B para-mine

C: (MS-RCF) Multi-story, R/C Frame Construction

110-lb GP Bomb - School Building.....C 110
550-lb GP Bomb - Warehouse.....C 550
1000-lb GP Bomb - American Test Building..C 1000
1100-lb GP Bomb - Apartment Building.....C 1100
2200-lb GP Bomb - Warehouse.....C 2200

D: (MS-W2) Multi-story, Wall Bearing Construction

110-lb GP Bomb - School Building.....D 110
1100-lb GP Bomb - Office Building.....D 1100
2200-lb AP Bomb - Warehouse.....D 2200
Parachute Mine - Factory Building.....D para-mine

Sources of Information

* revised data sheets replacing former equivalent sheets

EXPLOSIVE FILLINGS FOR WEAPONS: PROPERTIES AND USES

| DESIGNATION AND COMPOSITION | DENSITY (gm/cc) | VELOCITY OF DETONATION (m/sec) | RELATIVE PACES (TNT = 100) | | |

UNITED STATES BOMBS AND FUZES

ABBREVIATIONS:

inst	= instantaneous	prim-det	= primer-detonator
mech	= mechanical	adap. boos	= adapter booster
mod(s)	= modification(s)	aux. boos	= auxiliary booster
rpm	= revolutions per minute	AC	= aircraft carrier
air tr	= air travel	grnd	= grazing
pyro	= pyrotechnic	impct	= impact
		AFD	= aircraft

* Time is given in seconds unless noted otherwise, or part of model name or number.

** If air burst setting fails to function, these fuzes will function instantaneously upon impact, providing fuze is armed.

NOTE: The nominal functioning time and the actual range of functioning time of some of the important fuze settings, determined from static firing tests, are given below:

NOMINAL FUNCTIONING TIME, seconds	ACTUAL RANGE OF FUNCTIONING TIME, seconds
Inst. (av. 0.001)	0.0[illegible] to 0.[illegible]
Non-delay (av. 0.[illegible])	0.[illegible] to 0.[illegible]
0.01	0.[illegible] to 0.[illegible]
0.025	0.[illegible] to 0.[illegible]
0.1	0.[illegible] to 0.[illegible]
0.25	- -

A: BOMB-FUZE COMBINATIONS *for High Explosive Bombs*

ARMY "HP" and ARMY-NAVY "AN-HP" BOMBS

BOMB	NOSE FUZE		TAIL FUZE	
model number	model number	functioning time, seconds*	model number	functioning time, seconds*
PENETRATION BOMB - P				
0-lb, P M65 "Butterfly"	-	-	M120 M58 A1 (M168) M46 (M131)	[illegible] air burst** [illegible] nonelec [illegible] anti-disturb.
00-lb, P AN-M59 A1	M110 AN-M110 A1	inst.	-	-
22-lb, P AN-M60 A1 M76 A1	AN-M120 AN-M120A1	inst.	-	-
00-lb, P M64	AN-M120A1 M168 M135	inst., (0.1) 0-02 air burst**	-	-
220-lb, P M66	M135 A1	10-00 air burst**	AN-M100 A1 AN-M100 A2 M168	non-delay, (0.01), (0.025), 0.1, (0.36)
300-lb, P AN-M65	M135 M135 A1	0-30.6 air burst** 10-30.6 air burst**		
	M153, A1; M155 M160, A1; M162	inst., (0.01) inst., (0.025)		
120-lb, P M66	AN-M100 AN-M100A1	inst. inst.	-	-
FRAGMENTATION CLUSTER - FC				
100-lb, FC M30	M110	0-00 air burst**	-	-
500-lb, FC M50	M111 A1 M111 A2	0-00 air burst**		
000-lb, FC M-6	M[illegible]: 0.02 air burst** used in M30 & M50 only.			
000-lb, FC M27	M[illegible] - 0.02 air burst** used in M30 & M27 only.			
GENERAL PURPOSE BOMB - GP				
100-lb, GP AN-M30, A1	AN-M100, A1 M168 M135	inst., 0.1 0-00 air burst**	AN-M100, A1, A2 & M168 series M110 series	non-delay, 0.01, (0.025), 0.1, 0.36 0-01, 0-11
250-lb, GP AN-M57, A1	M135 A1	10-02 air burst**	M111A1 series	0-01, 0-11, 0-15
500-lb, GP AN-M64 AN-M64, A1	M34	0-30.6 air burst**	M115 series M120, A1 series	0-01, 0-11, 0-15 1-144 hrs
1000-lb, GP AN-M65 AN-M65, A1	M135 A1	10-30.6 air burst**	M132 series AN-M-200	10 minutes 25-125 ft of water
2000-lb, GP AN-M66, A1	M110, A1; M155 M168, A1; M168	inst., 0.01 inst., 0.025	M[illegible]-126, 63, 64 & A1 series M231-0 AN-M84, A1	25 ft of water
	M168	Short Pressure-Setting...see Fuze table	M227-0 AN-M66, A1	24 hrs; 36 hrs
	AN-M-200 M132-1 (special)	inst inst or elec. impulse	M228-0 AN-M65, A1; AN-M66, A1 M-200 AN-M65, A1; AN-M66, A1	24 hrs; 30 hrs 25 ft of water
	M228-0 M[illegible]-0	0.01 0.025		
100-lb, GP 250-lb, GP 500-lb, GP	Antipersonnel Bombs		M168	0-15
LIGHT CASE BOMB - LC				
0000-lb, LC AN-M66	A[illegible], A1 M135 M135 A1 M135 M135 A1 M135, A1 M132, A1 M155 [illegible] *10	inst. only 0-02 air burst** 10-02 air burst** 0-30.6 air burst** 10-30.6 air burst** inst. only inst. only Short Pressure inst.	AN-M[illegible] A1 AN-M[illegible] A2 M168	non-delay (to avoid breakup of bomb case)

ARMY "HP" and ARMY-NAVY "AN-HP" BOMBS (continued)

BOMB	NOSE FUZE		TAIL FUZE	
model number	model number	functioning time, seconds*	model number	functioning time, seconds*
SEMI-ARMOR-PIERCING BOMB - SAP				
000-lb, SAP AN-M58 AN-M58 A1 AN-M58 A2	AN-M120, A1 M168 (M168) (M132) (M132 A1) (M132) M135, A1 M168	inst; 0.1 0-02 air burst** 10-02 air burst** 0-30.6 air burst** 10-30.6 air burst** inst; 0.01	AN-M100 A1, A2 M168 M135 M132 A1 M130 M135, A1 M152	non-delay, 0.01, 0.025, 0.1, 0.36 0-01, 0-11 0-01, 0-11, 0-15 1-144 hrs 10 minutes
1000-lb, SAP AN-M59 AN-M59 A1	M168, A1 M168 (M168)	inst; 0.025 Short Pressure	AN-M100 A1, A2 M168	non-delay, 0.01, 0.025, 0.1, 0.36
2000-lb, SAP M103 two nose fuzes	(M132-1 special) M135-0 M132-0	inst or elec. impulse 0.01 0.025	M135 M130 M132	0-01, 0-11, 0-15 1-144 hrs 10 minutes
NAVY "AN" and ARMY-NAVY "AN-Mk" BOMBS				
GENERAL PURPOSE BOMB - GP				
100-lb, GP Mk 1 & mods (obsolescent)	AN-M110 M-231 (special)	inst elec. impulse	-	-
600-lb, GP Mk 13 & mods (obsolescent)	AN-M110 M-231 M-231-1 (special) M-231-0 M-104 AN-M120, A1 M168 M135 M135 A1 M130 M130 A1	inst 0.01 inst or elec. impulse 0.01 0.025 inst; 0.1 0-02 air burst** 10-02 air burst** 0-30.6 air burst** 10-30.6 air burst**	M-223 M-223 AN-M[illegible] A1, A2 M168 M135 M130 A1 M132	0.01 25-125 ft of water non-delay, 0.01, (0.025), 0.1, 0.36 0-01, 0-11 0-01, 0-11, 0-15
1600-lb, GP Mk 13 & mods (obsolescent)	AN-M110 M168 AN-M120, A1 M168 AN-M140, A1 M168 M168	inst; 0.01 inst; 0.1 inst; 0.025 Short Pressure		
ARMOR-PIERCING BOMB - AP				
1600-lb, AP AN-M-53	-	-	AN-M-200 AN-M120 A1, A2 M168	0.00 non-delay, 0.01, 0.025, 0.1, 0.36
1600-lb, AP AN-M-				
DEPTH BOMB - DB				
325-lb, DB AN-M17 AN-M41 AN-M44 AN-M47 (obsolescent)	AN-M110 M-231-1 (special)	inst inst or elec. impulse	AN-M-220 M-[illegible] (Albert only fuse)	25-125 ft of water
325-lb, DB M33 650-lb, DB M34	AN-M120, A1 M119, A1 AN-M120, A1	inst; 10.11 inst; 10.011 inst; 10.0251	AN-M-220 M231-0	25-125 ft of water 25 ft of water
650-lb, DB M17 M30* 900-lb, DB M49 (obsolescent)	M168 M168	Short Pressure inst; 10.11 inst; 10.011	AN-M-220 AN-M-120 (M132, A0 only) (Albert only) M-220 AN-M-220	25-125 ft of water
ANTI-AIRCRAFT BOMB - AA				
0-lb, AA M34	M-227	inst	-	-

NOTE:

Parentheses ( ) enclosing functioning time or fuze number indicate that use is possible but unlikely or not recommended.

* Functioning of the U.S. Army and U.S. Army Dept. Ordnance Schools and the Ballistic Research Laboratory, A.A.A., Aberdeen Proving Ground, Md.

PTM No. 100
April 1945

B-FUZE CHARACTERISTICS *(for High Explosive Bomb Fuzes)*

ARMY "M" and ARMY-NAVY "AN-M" FUZES

MODEL NUMBER	TYPE	RADIAL FUNCTIONING TIME, seconds	ARMING TIME OR DISTANCE, ft	MIN. ALT. TO ARM AT 250 mph, ft	BOMBS USED WITH	COMPANION FUZE	ADDITIONAL COMPONENT PARTS	REMARKS
AN-M100 A1	Tail; mech. impact	non-delay 0.04 0.002 0.1 0.25	720 v. rev		500 GP, AN-M56, A1; 250 GP; 220 FS; 200 F	AN-M100 M343	M16 primer-det M102 adap. bstr. with Navy GP's	non-delay only for 220 F, 4000 LC.....for GP's and SAP's+ delays are generated by tactical use.....the AN-M100 A1 series can be prearmed 300 v. rev; this series is obsolescent
AN-M100 A2			150-170 v. rev 645-680 air fr	40-60				
AN-M101 A1			720 v. rev		500 GP, AN-M43(GAT); 500 SAP			
AN-M101 A2			150-170 v. rev 653 air fr	60-90				
AN-M102 A1			720 v. rev		1000 GP; 500 GP, M121; 2000 GP; 1000 SAP; 4000 LC			
AN-M102 A2			150-170 v. rev 645-680 air fr	60				
AN-M103	Base mech. impact	inst. 0.1	inst: 330 v. rev 700-1000 air fr 0.1: 220 v. rev 510-1000 air fr	inst: 600 0.1: 310	All depth bombs, GP's (except 100 GP, M64) and SAP (except M108) 220 F, 100 F...may be used in SAP's for frag effects; results are inconsistent..... 4000 LB	AN-M99A1, AN series	none	unsafe for dive bombing, not recommended for nose-head attack...AN-M103 not crash-proof, unsafe for CV use...AN-M103 A1 is crash-proof, safe for CV use... modified arming vanes required for use with flat nose bomb
AN-M103 A2								
AN-M105	Base mech. impact	inst.	2.5 seconds aerotechnic	60	23 F, AN-M66; M92 120 F, M90	none	none	sensitive mushroom striker head....being replaced by AN-M130, A1 ..unsafe for CV use
M110	Base mech. impact	inst.	330 v. rev		20 F, AN-M81	none	none	unsafe for CV use...alternate for AN-M103 using M117 adapter booster
AN-M110 A1			350 v. rev	60				
M111	Base mech. time aerial burst	15-55 sec. inst	670 v. rev	450	500 F Clusters: M26 (20 - 28 F's) M27 (8 - 20 F's) M28 (20 - 8 F's)	none	none	not detonator safe...obsolescent; being replaced by TSS E2 M148A1 T71 (M158)
M111 A1		5-22 sec. inst	670 v. rev	450				
M111 A2		5-22 sec. inst	260 v. rev	185	100 F Cluster: M28 (20 - 8 F's)			
M112	Tail; mech. impact pyro. delay	5-5 5-11	18-20 v. rev 100 air fr		100 GP, AN-M30, A1; 250 GP	none	M16 primer-det	these fuses (M112-M114, inclusive) are supersensitive nose fuses and will function at impact angle of 3°...unsafe for CV use...M102 adapter booster used with Navy GP's
M112 A1		5-5 5-11 5-15					M16;M16 A1 primer-det	
M113		5-5 5-11			500 GP; 500 SAP		M16 primer-det	
M113 A1		5-5 5-11 5-15					M16;M16 A1 primer-det	
M114		5-5 5-11			1000 GP; 1000 SAP; 2000 GP; 500 GP; 1000 GP; 4000 LC; AN-M64 A1 nose using M102 adapter bstr & spacer ring		M16 primer-det	
M114 A1		5-5 5-11 5-15					M16;M16 A1 primer-det	
M115	Tail; mech. impact pyro. delay	5-5 5-11 5-15	150-170 v. rev 695 air fr	60-90	100 GP; 250 GP	none	M16;M16 A1 primer-det M102 adap. bstr. with Navy GP's..	minimum altitude bombing fuses.....safe for CV use
M116			150-170 v. rev 535 air fr	60-70	500 GP; 500 SAP			
M117			150-170 v. rev 645 air fr	60	1000 GP; 2000 GP; 1000 SAP; 500 GP; AN-M64, A1; M58 nose using M117 adapter booster			
AN-M120	Base mech. impact	inst.	2.5 sec(120.25) mech. delay		23 F, AN-M33 A1, M72 A1; 120 F, M38 using M117 adapter booster	none		unsafe for CV use.....not available to Navy stations ..for low-level attack, the AN-M120 A1 is preferred
AN-M120 A1			1.9 sec(120.19) mech. delay					
M123	Tail; chem. time anti-removal (to arrest direct drive; earlier model gear reduct)	1, 2, 8, 12, 36, 48, 72, 144 hours	75.6-150 v. rev 370 air fr	180	1000 GP, AN-M65, A1; 250 GP; 220 F; 100 F (A1 nose preferred)	anti-disturbance nose fuse is being developed	M19 primer-det	chemicals in glass ampoule considered unsafe if dropped. ..sensitive to temperature changes...not to be used in temp. over 130°F...delays vary with concentration of alcohol-acetone solution & thickness of cellulold disc ..equipped with ball-locking anti-removal device... cannot be prearmed
M123 A1			4-6 v. rev				M19 A2 primer-det	
M124			75.6-150 v. rev 370 air fr	210	500 GP; 500 SAP (A1 & A2 nose preferred)		M19 primer-det	
M124 A1			4-6 v. rev				M19 A2 primer-det	
M125			75.6-150 v. rev 370 air fr	310	1000 GP; 1000 SAP; 2000 GP (A1 and A2 nose preferred)		M19 primer-det	
M125 A1			4-6 v. rev				M19 A2 primer-det	
M129	Ground or air burst	Impact or air burst	2.5 seconds		4 P,M83 "Butterfly"	none	none	impact has slight inherent delay.....fuse is shipped installed in bomb

FUZE CHARACTERISTICS *(continued)*

ARMY "AP" and ARMY-NAVY "AN-AP" FUZES *(continued)*

MODEL DESIGNATION	TYPE	NOMINAL FUNCTIONING TIME, seconds	ARMING TIME OR DISTANCE, ft	MIN. ALT. TO ARM AT 500 mph, ft	BOMBS USED WITH	COMPANION FUZE	ADDITIONAL COMPONENT PARTS	REMARKS
Type 51 (M130)	mech. time	10,20,30 minutes	3½ rotations of arming spindle		4 F,M88 "Berserkly"	none	none	setting pre-set at factory ..fuze is shipped installed in bomb
T90 (M44)	anti-disturbance	-	about 8 seconds after impact		4 F,M88 "Butterfly"	none	none	supersensitive; vibrations from nearby A/C propeller sufficient to fire fuze... fuze is shipped installed in bomb
M138	Tell-tale chem. time anti-removal	10 minute nominal delay.... range of 8-30 min. delay due to temp. variation	45-65 v.rev 300 air fr		100 GP, AN-M88, A1; 2000	none	M19 primer-det	similar to M135 series, but safer in that solvent is in copper bottom instead of glass ampoule..delays vary with change of temperature but always sufficient to allow forward planes of large formations to drop bombs from low altitude without endangering rear planes....has tell-tale anti-removal device
M139			65-85 v.rev 370 air fr		500 GP,AN-M88,A1; 500 SAP		M19 primer-det	
M140			85-95 v.rev 300-400 air fr		1000 GP,AN-M88,A1; 1000 SAP; 2000 GP			
M135	Boost chem. time air burst	8-30 or inst.inst.	approximately 250 v.rev 750 air fr		All GP's (except 100 GP Mk4) 600LB, may be used in 90 F, 220 F and 260 F (and SAP's)	normally none,unless AN-M103 A2 series is used as an insurance fuze	none	setting can be adjusted to 0.1 second.....will fire accurately to ± one sec... detonator safe; not suitable for naval use....min. setting of 10 sec. recommended
M135 A1		10-30.8 or inp.inst.						
M136	Boost mech. time air burst	8-30.8 or inp.inst.	approximately 250 v.rev 750 air fr		All GP's (except 100 GP Mk4) 600LB, may be used in 90 F, 220 F, and 260 F (and SAP's)	normally none,unless AN-M103 A2 series is used as an insurance fuze	none	improved clockwork, more accurate than M135, A1.... setting can be adjusted to 0.2 second.....will fire accurately ± 0.3 sec..... detonator safe; not suitable for naval use....min. setting of 10 sec recommended
M136 A1		10-30.8 or inp. inst.						
M139 AN-M139 A1	Boost mech. impact	inst. 0.01	inst: 350 v.rev 750-1,000 air fr	inst: 440; 0.01 & 0.025: 310	All depth bombs,GP's (except 100 GP,Mk4) & 90 F,220 F,260 F .. may be used in SAP's ...4000 LB	AN-M100 A2 series	M14 primer-det	companion fuzes to AN-M100 A2 series with shorter delays than AN-M103,A1 .... M139 A1 and M140 A1 are crash-proof
M140 AN-M140 A1		inst. 0.025	0.01 & 0.025: 220 v.rev					
M146	Boost clockwork air burst	8-32 inp. inst	approximately 260 v.rev		100 F Cluster: M28 (24 - 4 F's) 500 F Cluster: M29 (90 - 4 F's)	none	none	detonator safe
M148	Boost mech. impact	inst: 0.1	same as AN-M103	same as AN-M103	Japanese Navy bombs	none	modified booster cup	modified AN-M103
M150	Boost blast pressure or mech. impact	see remarks	12 - 13 v.rev		All GP's (except 100 GP, Mk4,) 1000 LB (and SAP's)	none	none	first bomb of stick detonates on impact; remainder by blast pressure of preceding bomb - about 25 ft apart for 500 GP dropped in train of 0.05 sec. intervals, A/C speed 200 mph, altitude 10,000 feet ..... detonator safe
M151	Tell-tale mech. impact pyro. delay	6 - 18	approximately 12 v.rev		100, 250 GP (anti-ricochet) using M7 parachute and M103 fuze adapter; 500 GP (anti-ricochet) using M8 parachute & M103 fuze adapter	none	M16 A1 primer-det	similar to M12 A1 series with transverse arming vane and accelerator vane
M155	Boost mech. time air burst	6 - 32 inp. inst	6-9 v.rev		500 F Cluster: M28 (20 - 20 F's) M27 (6 - 60 F's)	none	none	supersedes M11 A2 with omission of gear reduction system resulting in quicker arming
M100	Tell-tale mech.impact	non-delay 0.01 0.025 0.1 0.25	720 v.rev 1780-1950 air fr	660	100 GP, AN-M30, All [illegible]	M103 series	M16 primer-det M103 adap.kits with Navy GP's	similar to AN-M103 series except for slower arming designed to prevent premature explosions of bombs within range of releasing aircraft (especially SAP) ...non-delay only for the [illegible]
M101			720 v.rev 1810-2250 air fr	660	[illegible]			
M102			720 v.rev 1710-2580 air fr	1130	[illegible]			
M103	Boost mech.impact	inst. 0.1 inst. 0.01 inst. 0.025	inst: 1710-3430 air fr 0.01 & 0.025: 1160-3430 air fr	1770 910	All depth bombs,GP's (except 100 GP, Mk4) & 90 F,220 F, 260 F and SAP's	M100 series	none	similar to AN-M100, M130, A1, M140,A1 respectively, except for slower arming designed to prevent premature explosions of bombs within range of releasing aircraft(especially SAP)
M104								
M105								

CONFIDENTIAL

E-FUZE CHARACTERISTICS *(continued)*

NAVY "Mk" and ARMY-NAVY "AN-Mk" FUZES

MODEL NUMBER	TYPE	NOMINAL FUNCTIONING TIME, seconds	ARMING TIME OR DISTANCE, FT	MIN. ALT. TO ARM AT 200 mph, FT	BOMBS USED IN	COMPANION FUZE	ADDITIONAL COMPONENT PARTS	REMARKS
AN-Mk219 & mods	Boost mech. impact rotor arm.	inst.	270 r. rev 1400 air fps 2000-2500 air fps for fleimeter depth bombs		all GP's and SAP's	GP's & SAP's Mk238 Navy GP's; AN-M103 A2 and M103 series GP's AN-Mk236 Mk229 AN-Mk230 AN-Mk234	clasp ring & tetryl booster with all GP's and 500 GP, Mk 13 & mods clasp ring & tetryl booster with all 1000 GP and SAP's	will function on impact with water or denser medium providing it has been dropped from sufficient altitude to arm. crush-proof...30° and 45° extension rods available with this fuze
Mk221	Boost mech. impact rotor arm.	0.01	185 r. rev 650-1100 air fps		500 GP, Mk 13 1000 GP, Mk 13	Mk225	none	obsolescent, will fail to fire some of all GP's, but delay may rupture some....400 ft/sec striking velocity is needed to activate fuze on water impact
Mk223 & mods	Tetryl mech. impact rotor arm.	0.01	approximately 150 r. rev 650-1100 air fps		500 GP, Mk12 & mods 1000 GP, Mk 13	AN-Mk219 Mk221 and... see remarks	none	obsolescent...other companion fuzes: AN-M103, AN-M135, A1; M136, A1; AN-M139 A1; AN-M140A1; M149; Mk219; Mk243
AN-Mk220 & mods	Mthacrtable hydrostatic	25, 50, 75, 100, 125 ft of water	completely armed at 12 to 25 ft depth	-	All GP's except Mk58 and Mk59	AN-Mk219; AN-M103; Mk221 and Mk229 in 650 & 700 GP's	spacer ring required with 650 & 700 GP's	obsolescent
Mk227 and 8	Boost mech. impact, centrifugal force arm.	inst.	at sea level 1500 air fps 30,000' alti 3000 air fps		5 AA bomb, M65	none	none	fuze designed for air to air bombing, but proved unsuccessful....limited use against parked aircraft
AN-Mk222 & mods	Tetryl mech. impact rotor arm.	0.08	140-180 r. rev 1100 air fps	200	1000 AP; 1650 AP; (250 GP, Mk12 and 5 1000 GP, Mk13 and 2)	none	none	
Mk229 & mods	Tetryl hydrostatic mech. arming	25, 50, 75, 100, 125 ft of water	110 r. rev 900 air fps	60	650 & 700 GP's 500 GP, Mk13* 1000 GP, Mk13	AN-Mk219 AN-M103 Mk243	none	mod 3 preferred in operational missions for its additional safety features
AN-Mk230 & mods	Tetryl hydrostatic mech. arming	25, 50, 75, 100, 125 ft of water	110 r. rev 300-400 air fps	60	325 GP, M64; 250 GP, M34; 100, 1000, 2000 GP's AN-M64, A1, A2, A mods by removing adapter from M115 adapter booster; 650 & 700 GP's by removing M61 body pellet and inserting 2 M62 booster pellets	AN-Mk219 AN-M103 Mk243	-	mod 1, 3 obsolescent...mod 2 is preferred for its crush-proof features.....mod 2, identical to mod, is converted from Mk229
Mk231 and 8	Tetryl hydrostatic	25 ft of water	40-45 r. rev	60	325 GP, M63; 250 GP, M34; 100, 1000, 2000 GP's AN-M64, A1		none	under development.....no availability date set.... crush-proof and detonator safe
Mk240	Identical to Mk231 but has looper arming also				100 GP, AN-M65, A1 2000 GP, AN-M66, A1			
Mk232 & mods	Boost impact or elec. firing	inst. or electric impulse	0 r. rev		GP's, (SAP's) and 50's except 100 GP, M64	usually none	none	typical dynamite fuze... will not function on impact with water at striking velocity less than 700 ft/sec
Mk238 and 8	Boost elec. firing	electrical impulse			100 GP, M64			special purpose fuze..... limited availability
AN-Mk236 & mods	Mthacrtable hydrostatic	25, 50, 75 100, 125 ft of water	partially armed when dropped... completely armed at 12 to 25 ft depth		all GP's except Mk58 and Mk59	AN-M103 AN-Mk219 Mk221 Mk229	spacer ring required with 650 & 700 GP's	differs from AN-Mk230 in that it has external setting device...not air arming type) not recommended for use....cannot be installed when trinalin bond is used
Mk237 & 8	Tetryl long delay	2, 10, 20 hrs at 60°F	approximately 150 r. rev plus impact		500 GP, AN-M64, A1	none	none	detonator & jettison safe ...anti-removal device... fuze may function without delay on multiple impact... minimum safe altitude same as for instantaneous fuze
Mk239 and 8	Elec. mech. impact rotor arm.	0.01	1100 air fps		1000 GP, AN-M65, A1 2000 GP, AN-M66, A1			
Mk238 and 8	Elec. mech. impact rotor arm.	0.01	1100 air fps		All GP's (except 100 GP, Mk 8) & SAP's	Mk223 for Army bombs use Army fuzes		modified Mk221.....requires 600 ft/sec striking velocity to function on impact with water
Mk240 and 8	Boost mech. impact	0.025	150 r. rev 900 air fps		All GP's (except 100 GP, M64) and SAP's	AN-M100 series AN-Mk230 Mk229	M46 primer-det	designed specifically for use against submarines and ships.....will function on impact with 4" plate, but not with water from altitude of 18,000 ft or at impact angle of less than 45°

WEAPON DATA

1 A3a*
AMERICAN
HIGH EXPLOSIVE BOMBS

PHYSICAL CHARACTERISTICS OF AMERICAN BOMBS

DESIGNATION	TOTAL WEIGHT W, lb	TYPE OF CHARGE	WEIGHT OF CHARGE, lb		CHARGE WEIGHT RATIO w/W, %	MAX. BODY DIA. in	LENGTH OF BOMB, in		WALL THICKNESS in	REMARKS
			w	w%			WITHOUT TAIL	OVER ALL		
GENERAL PURPOSE BOMBS										
*100-lb GP, Mk1 & Mods	116	TNT	65	56.0	56	7.9		48.8		Bomb has teardrop shape
Mk4 Mod 1	120	TNT	65	54.0	46	8.0	28.0	36.2	0.18	Single piece steel forging, cylindrical with ogival nose.
Mk4 Mod 4	105	TNT	55	52.0	52					
*500-lb GP, Mk12 Mod 2	506	TNT	266	52.6	51	14.0	42.6	59.5	0.36	Sling welded to bomb for suspension in torpedo racks
1000-lb GP, Mk13 Mod 2	1006	TNT	511	51.0	51	17.7	53.0	72.6	0.46	
100-lb GP, AN-M30A1	110 115 121	Amatol TNT Tritonal	54 57 68	49.0 49.0 56.0	49 50 52	8.2	28.0	38.0	0.16	All models may have anti-withdrawal fuze. These bombs may have parachute attachment M6 to prevent rapid descent and ricochet of bombs in low-level bombing
250-lb GP, AN-M57A1	256 260 272	Amatol TNT Tritonal	124 128 142	48.0 49.1 52.2	48 50 52	10.8	36.0	46.4	0.27	
500-lb GP, AN-M64 AN-M64A1	510 525 535 545	Amatol TNT Comp. B Tritonal	262 267 276 283	51.4 50.9 51.6 52.0	51 51 51 54	14.2	45.0	56.8	0.3	500-lb AN-M43 and AN-M64; A1 may have parachute attachment M7 to prevent rapid descent and ricochet of bombs in low-level bombing. A1 models may use anti-withdrawal fuze; base plates and adapter boosters cannot be removed. AN-M64, 65, 66 bal models have tail fuze pockets taking hydrostatic fuze AN-M230 (11.5-lbs heavier than AN-M100 series fuzes). AN-M66A2 has slightly heavier nose section.
1000-lb GP, AN-M65 AN-M65A1	985 990 1040 1044	Amatol TNT Comp. B Tritonal	520 529 525 612	52.1 53.2 50.4 58.6	53 66 57 59	18.8	58.1	67.1	0.5	
2000-lb GP, AN-M66 AN-M66A1 AN-M66 A2	2050 2105 2140 2212	Amatol TNT Comp. B Tritonal	1033 1117 1142 1220	10.2 10.4 10.3 10.7	52 53 53 55	23.3	70.0	90.4	0.6	
4000-lb GP, T8	4084 4228	TNT Tritonal	1857 2002	12.3 12.6	46 47	28.0	84.5	118.8	0.88	
12000-lb GP, T10	11750	Tritonal	5100	17.2	43	38	124	252	1.25	Inertia tail fuze. For performance see Data Sheet 7A1. Respectively same as British "Tallboy-MP" and "Grand Slam", but British models filled Torpex D-1
22000-lb GP, T14	22118	Tritonal	9440	21.3	43	46	150	305	1.75	
LIGHT CASE BOMBS										
4000-lb LC, AN-M56A1	4232 4308 4531	Amatol TNT Tritonal	3258 3052 3559	16.8 15.0 16.5	77 60 81	34.0	84.8	117.8	0.37	All models have hoisting at center of gravity as well as provision for suspension in British planes.
SEMI ARMOR-PIERCING BOMBS										
600-lb SAP, AN-M58 AN-M58A1,A2	672 664	TNT TNT	150 162	5.4 5.5	36 33	11.3	46.8	57.0	0.75	A2 mods may use anti-withdrawal fuzes.
1000-lb SAP, AN-M59A1	926	TNT	320	6.8	32	16.1	57.3	69.1	1.0	A1 mod may use anti-withdrawal fuzes. Solid nose construction
2000-lb SAP, M103	2040	Picratol	558	8.2	27	18.7	67.7	83.5		
ARMOR-PIERCING BOMBS										
1000-lb AP, AN-M58	1025	Explosive D	160	6.2	16	12.0	59.0	78.0		
1600-lb AP, AN-Mk1	1530	Explosive D	215	6.0	14	14.0	62.5	83.5	1.3	Recent bombs have grooves on body to position suspension band
ANTI-AIRCRAFT BOMBS										
5-lb AA, M24	5.6	TNT	1.0	1.2	35	3.0	12.0	15.0	0.05	Cluster of 20 bombs in M3 or M3 Mod 1 container

* Obsolescent

*Revised: August 1958

PHYSICAL CHARACTERISTICS OF AMERICAN BOMBS
continued

DESIGNATION	TOTAL WEIGHT W, lb	TYPE OF CHARGE	WEIGHT OF CHARGE, lb W	W'	CHARGE WEIGHT RATIO W/W %	MAX. BODY DIA. in	LENGTH OF BOMB, in WITHOUT TAIL	OVERALL	WALL THICKNESS, in	REMARKS
FRAGMENTATION BOMBS										
4-lb F, M83 (Butterfly)	8.2	TNT	0.47	0.77	15	3.0	3.0		0.25	Adaptation of German SD-2; dropped in clusters
23-lb F, AN-M40;AP M72;A1	23*	TNT	2.7	1.9	10	3.8	11.3	24.7	0.56	Bombs dropped in clusters. M72 is modified version of AN-M40 adapted for vertical suspension. A1 mods facilitate clustering with fused bombs
20-lb F, AN-M41;A1	20	TNT	2.7	1.8	14	3.8	11.3	18.5	0.56	Designed also for vertical suspension, may be dropped in cluster of 6 bombs. A1 mods facilitate clustering with fused bombs
90-lb F, M83	90	Comp. B	11	2.2	12	6.0	19.8	28.0	0.94	Suspended by single lug or in cluster of 6 bombs
120-lb F, M66 (Para)	80**	Comp. B	11	2.2	12	6.0	19.0	66.8	0.94	May be suspended singly or in a two-bomb cluster in a 500-lb bomb station
220-lb F, M66 260-lb F, AN-M81	216 268	Comp. B Comp. B	27 34	3.6 3.2	22 13	8.0 8.0	32.8 32.8	43.7 43.8	1.00 1.25	Horizontal suspension helical steel spring wound around steel tubing

FRAGMENTATION CLUSTERS

DESIGNATION	CLUSTER FUZING	TOTAL WEIGHT pounds	MAX. BODY DIAMETER inches	OVERALL LENGTH inches	REMARKS
100-lb M1 or AN-M1A1 6-20 lb F, AN-M41		125	8.8	46.6	Fuzes shipped installed. Use cluster adapter AN-M1A2
100-lb AN-M1A2 6-20 lb F, AN-M41A1		125	8.8	46.6	Fuzes shipped in sealed cans; installed in the field. Use cluster adapter AN-M1A3
100-lb SIZEL 6-20 lb F, AN-M41		125	8.8	46.6	Navy designation. Use cluster adapter AN-M1A2.
100-lb AN-M4 3-23 lb F, AN-M40		87.2	11	31.0	Use cluster adapter AN-M5. Fuzes shipped installed
100-lb AN-M1A1, A2 3-23 lb F, AN-M40;A1		87.2	11	31.0	Fuzes shipped in sealed cans; installed in field. Use cluster adapter AN-M5, A1.
100-lb M28, M28A1,A2 24 - 4-lb F, M83	M111A2 M146 M155	155	8.0	47.8	Should be released from altitude of 3000-5000 feet with fuze set to function 5(M28) & 8(M29) sec. after release, to form a pattern of approx. 200x300 feet. Use M19,A1,A2 adapters for M28,A1, A2; use M16,A1, A2 for M29, A1.
500-lb M29, M29A1 90-4 lb F, M83		515	16	69.6	
600-lb M26, M26A1,A2 20-20 lb F, AN-M41;A1	M111A2 M146 M155 T77	615	15	53.8	Use cluster adapter M13,A1,A2; can have quick or delayed opening
600-lb M27 6-90 lb F, M83	M111A2 M146 M155	590	15	69.0	Use cluster adapter M14. Has inst. and 5-92 second delay

*Obsolescent **Weight without parachute

NOTES:

Bomb weight given includes weight of standard Army - Navy fuzes, AN-M103 (nose) and AN-M100 (tail); due to slight variations in case thickness and density of filling, weights are accurate to 5%.

The designation Amatol, above, implies a filling of 50% Amm. Nitr. & 50% TNT; TNT represents 100% TNT; Tritonal signifies 80% TNT and 20% Aluminum. Tritonal has been approved as the main charge in GP and LC bombs which are to be used where those loaded TNT were formerly considered suitable. The charge weights of tritonal - filled bombs listed above were calculated using a density of 1.70 for tritonal as compared with 1.56 for TNT.

For Bomb-Fuze combinations, see Weapon Data Sheet 1 AS.

SOURCE: Information supplied by the United States Navy Bomb Disposal School.

Abbreviations:

BOMB TYPE, U. S.	BRITISH DESIGNATION	APPROXIMATE CHARGE-WEIGHT RATIO
General Purpose, GP	MC	50%
Light Case, LC	HC	80%
Semi-Armor-Piercing, SAP	SP	30%
Armor Piercing, AP	AP	15%
Fragmentation, F		
Anti-Aircraft, AA		

WEAPON DATA: INCENDIARIES

PHYSICAL CHARACTERISTICS OF AMERICAN INCENDIARY BOMBS

DESIGNATION nominal weight — model no.	ACTUAL WEIGHT pounds	DIMENSIONS DIAM inches	DIMENSIONS LENGTH inches	INCENDIARY CHARGE	OTHER CHARGES	TOTAL HEAT LIBERATED BTU	FUSING type & number	STRIKING VELOCITY from 20,000 feet/sec	CLUSTER SIZES AND TYPES
100-lb AN-M47A2 AN-M47A3	72* 73*	8.12 8.12	48.9 51.9	40lb. Gasoline Gel	M13 Burster [illegible] 7.9 oz. [illegible] 7.4 oz. [illegible] W.P.-Diss. THF-Ether Tetryl - 0.07 oz.	369,000 (Inclusive heat of White Phos)	Nose Impact M-128A1 or M-100	740	Not clustered but sometimes loaded for multiple suspension on 100-lb. and 500-lb stations
4-lb AN-M50A2	3.6	1.69	21.3	1.1 lb Mag alloy 0.5 lb Therm-Gel	First Fire* 0.7 oz.	13,100	Tail Inertia	420	500-lb size, Aimable 100-lb size, Quick-Opening 500-lb size, Quick-Opening
4-lb AN-M50KA3 (anti-personnel explosive case)	3.7	1.66	21.3	1.0 lb Mag alloy 0.5 lb Therm-Gel	First Fire* 0.7 oz. Tetryl (Type A) 1.6oz Tetryl (Type C) 1.6oz	12,500	Tail Inertia	425	Clustered with AN-M50A2
2-lb AN-M52A1**	1.7	1.69	14.2	0.7 lb Mag alloy 0.5 lb Therm-Gel	First Fire* 0.7 oz.	11,200	Tail Inertia	340	500-lb size, Aimable 100-lb size, Quick-Opening 500-lb size, Quick-Opening
4-lb AN-M54	3.7	1.69	21.3	1.8 lb Thermate	First Fire* 0.7 oz.	2,000	Tail Inertia	420	100-lb size, Quick-Opening 500-lb size, Quick-Opening
6-lb AN-M69**	6.2	2.87	19.5	2.5 lb Gasoline Gel	Black Powder 0.2 Mag Powder 0.2	44,000	Nose Inertia; M1	250	500-lb size, Aimable 100-lb size, Quick-Opening 500-lb size, Quick-Opening
6-lb M69X (anti-personnel incendiary case)	7.0	2.87	19.5	2.25 lb Gasoline Gel	Black Powder 0.1 Mag Powder 0.1 Tetryl 0.2	37,000	Nose Inertia; M1	245	Clustered with AN-M69
10-lb M74	8.4	2.87	19.5	2.8 lb PT-1 mixture	Black Powder 0.0 Mag Powder 0.1 Black Powder 0.0	50,000 (Inclusive heat of White Phos)	Nose Inertia; M142	430	500-lb size, Aimable 100-lb size, Quick-Opening 500-lb size, Quick-Opening
500-lb AN-M76	475	14.8	59.2	175 lb PT-1 mixture	Tetryl 1.0 lb White Phos. 9.0 lb	2,000,000 (Inclusive heat of White Phos)	Nose Inertia AN-M103 Tail Inertia AN-M101A1	965	Not clustered

AN-M69 and M74 are tail ejection type bombs - explosive charge throws incendiary material out of the tail. Other gasoline gel filled bombs are burster types which disperse the incendiary material in chunks in all directions.

From time of impact until explosion of head, AN-M50A3 Type A burns 3-4 min; Type B burns 60-70 sec.

* First Fire is the agent for initiating combustion of main filling.

** Several redesigns of this bomb are now under consideration for standardization.

◆ Weight given is for this bomb with M13-M9 burster-igniter and M128A1 fuse. The M12 burster weighs 3 pounds less than the M13-M9 burster-igniter; the M108 fuse, 0.5 pounds less than M128A1 fuse.

◆◆ New type AN-M69 in production has gross weight of 6.4 lb. and contains 2.8 lb. of gasoline gel, 6.0 oz. of white phosphorus and liberates 41,000 BTU.

December 1944

WEAPON DATA: INCENDIARIES

PHYSICAL CHARACTERISTICS OF AMERICAN INCENDIARY BOMB CLUSTERS

1A3c AMERICAN INCENDIARY CLUSTERS

BOMB TYPE model no. nominal wt.	CLUSTER DESIGNATION nominal size, lb	model number	type	ACTUAL WEIGHT* pounds	NUMBER OF BOMBS**	TOTAL HEAT PER CLUSTER BTU	DISPERSION PATTERN▲ RACE-TRACK▲▲	DISPERSION PATTERN▲ Sq. ft/Bomb (90% of bombs)	FUSING position and model	BOMBING TABLE BTT
AN-M50 (4 lb)	500-lb, AN-M17A1		Aimable	465	110	1,420,000	420 x 630	2,300	Nose: M146◎	500-J-2
	100-lb, AN-M6		Quick-opening	135	34	440,000	700 x 2450	53,000	0.0:no fuse	4-B-1
	500-lb, AN-M7			525	128	1,660,000	700 x 2450	14,000	0.0:no fuse	4-B-1
AN-M52 (2 lb)	100-lb, AN-M10		Quick-opening	105	51	570,000	1100 x 3300	75,000	0.0:no fuse	2-A-1
	500-lb, AN-M11			425	192	2,150,000	1100 x 3300	20,000	0.0:no fuse	2-A-1
AN-M69 (8 lb)	500-lb, M18(E6R2)		Aimable	350	38	1,670,000	240 x 510	4,300	Nose: M146◎	500-K-2
	500-lb, E66		Aimable	425	38	1,670,000	240 x 360	2,200	Tail:2-M152◎	500-Q-1
	100-lb, AN-M12		Quick-opening	105	14	620,000	400 x 1000	28,000	0.0:no fuse	6-A-2
	500-lb, AN-M13			425	60	2,640,000	300 x 1000	6,800	0.0:no fuse	6-A-2
M74 (10 lb)	500-lb, E68		Aimable	525	38	1,440,000	640 x 860	15,400	Tail:2-M152◎	
	100-lb, E68		Quick-opening	140	14	530,000				
	500-lb, E67			550	60	2,280,000				

NOTES

* Weights may vary as much as 5% from average values given.

** All incendiary clusters are supposed to contain 20% of corresponding X-bomb (anti-personnel type), but the percentage may vary with supply and operational requirements.

▲ Patterns given include 90% of the bombs and are for quick-opening clusters dropped from 10,000 feet and for aimable clusters dropped from 20,000 feet and opened at 5,000 feet. Data on quick-opening clusters are less reliable than those on aimable clusters.

▲▲ A *race-track* figure (rectangle with semi-circular ends) was selected as the most suitable figure for representing the patterns of aimable and quick-opening clusters (better than *ellipse, rectangle, circle* or *square*). The area of a race-track is given by $xy - 0.215x^2$, where x = the smaller dimension. In determining dimensions of 90% pattern, axial ratios used were restricted to 1.5, 2.0, 2.5, 3.0, 3.5, 4.0.

◎ M146 (T5GE1), M138 (T3GE1), and M127 (T39) are alternate fuses for these clusters; M146 preferred.

◎ M152 (T53E1), M153 (T73) and M145 (with reversed vanes) are alternate fuses for these clusters; M152 preferred.

February 1945

WEAPON DATA

PHYSICAL CHARACTERISTICS OF AMERICAN DEPTH BOMBS, AIRCRAFT MINES AND TORPEDOES

1A3d
U.S. AMERICAN BOMBS MINES AND TORPEDOES

DESIGNATION nominal weight / model	TOTAL WEIGHT W lbs	TYPE OF CHARGE	WEIGHT of CHARGE pounds W	W^⅔	CHARGE WEIGHT RATIO w/W, %	DIMENSIONS LENGTH OVERALL inches	LENGTH of BODY inches	DIAM inches	WALL THICKNESS inches	FUSING NOSE	FUSING AIRCRAFT SHIP	FUSING TAIL
A DEPTH BOMBS												
325-lb AN-Mk17-3 350-lb AN-Mk44	325 355	TNT TPX	242 266	6.23 6.45	75 76	58.5	51.1	15.0	0.06	AN-Mk219 AN-Mk221	AN-Mk234 AN-Mk224	- -
325-lb AN-Mk41 350-lb AN-Mk47	325 351	TNT TPX	222 248	6.06 6.94	68 71	49.9	37.8	15.0	0.06	AN-M103 AN-Mk219 AN-Mk221	AN-Mk224 AN-Mk234	- -
325-lb Mk53-1 350-lb Mk54-1 *	320 339	TNT TPX	225 252	6.08 6.32	70 74	54.6	30.1	13.5	0.06	AN-M103 AN-Mk219	- -	AN-Mk230
650-lb Mk37 ** Mk58-1 700-lb Mk49-1	655 654 669	TNT TNT RDX	464 425 472	7.74 7.52 7.79	75 67 71	58.5	56.4	17.7	0.12	AN-Mk219 AN-M103	AN-Mk224 AN-Mk234	Mk229 ■ AN-Mk230
AIRCRAFT MINES												
1000-lb,Mk18-0,4,5	1025	TNT	681	8.53	-	69.8	-	19.9	0.12	#0,4: Mag.Induc.Type #5: Acoustic Type		
1000-lb,Mk26-1	1000 1060	TNT TPX	465 528	7.78 8.07	-	68.5	-	18.6	0.12	Magnetic Induction Type		
1000-lb,Mk36	1020 1065	TNT TPX	570 655	8.29 8.59	-	70.6	-	18.6	0.12	Magnetic Induction Type		
1600-lb Mk12-1 4	1595 1725 1606 1690	TNT TPX TNT TPX	1095 1205 1006 1190	10.3 10.7 10.2 10.8	- - - -	134 154	- -	20.8 20.8	0.25 0.25	Magnetic Needle Type Magnetic Needle Type		
1800-lb,Mk10-6,8,9	1850	TNT	420	7.49	-	121.5	-	20.8	0.25	Magnetic Needle Type		
2000-lb,Mk25	1863 2017	TNT TPX	1150 1274	10.58 10.84	-	86.5	-	28.5	0.15	Magnetic Induction Type		
AIRCRAFT TORPEDOES												
Mk 13-3A, 5, 5 Mk 13-6, 7, 9	2140 ● 2223 ●	TNT TPX	600 600	8.45 8.45	-	161.0	-	22.4	0.12	Contact: Mk6-6 Mk8-6		

NOTES:

* This Depth Bomb is currently being filled with TNX instead of Torpex (TPX).
** Because the tail assembly was too weak, the Mk37 was revised producing the Mk58.
● In this group, these fuses are used in the 650-lb Mk37 D.B. only; the Mk58 and Mk49 do not use an aircraft-ship or side fuse.
■ The Mk229 fuse is used only in the Mk37 D.B.; the newer depth bombs, Mk58 and Mk49, use the AN-Mk230.
● The total weight may vary as much as ± 20 pounds from the weight given.

General Purpose bombs (GP 500-lb AN-M64, 1000-lb AN-M65, 2000-lb AN-M66) fitted with the AN-Mk230 hydrostatic tail fuse are also used as depth bombs.

Since Aircraft Mines are usually dropped by parachute, the over all length dimension is given including the parachute pack; without it this dimension is approximately 4 inches less.

SOURCE: Publications of the Bureau of Ordnance and the Bomb Disposal School, U.S.Navy.

1A4a PHYSICAL CHARACTERISTICS

PHYSICAL CHARACTERISTICS OF BRITISH BOMBS

A HIGH EXPLOSIVE BOMBS

DESIGNATION name, type and model	TOTAL WEIGHT- pounds	TYPE of CHARGE	WEIGHT of CHARGE pounds	CHARGE - WEIGHT RATIO per cent	MAX BODY DIAMETER inches	LENGTH without TAIL inches	OVERALL LENGTH inches	BODY WALL THICKNESS inches
20-lb. F, Mk III	20	TNT	3	15	3.9	11.9	21.8	0.35
40-lb. G.P, Mk II	38.5	Amatol 60/40	6.5	17	5.0	15.9	27.3	0.47
250-lb. G.P, Mk IV	230	Amatol 60/40	67	29	10.3	25.6	56.7	0.66
500-lb. G.P, Mk IV	470	Amatol 60/40	143	30	13.0	36.5	70.5	0.72
500-lb. G.P, Mk IV	487	Amatol 60/40	143	31	13.0	36.5	67.5	0.72
1000-lb. G.P, Mk II	1072	Amatol 60/40	357	33	18.2	52.5	72.5	0.77
1600-lb. G.P, Mk II	1785	Amatol 60/40	470	26	18.5	65.5	101.0	1.15
4000-lb. G.P, Mk I or II	3587	Amatol 60/40	1072	30	24.5	81.0	106.0	1.36
250-lb. S.A.P, Mk V	245	TNT	42	17	9.2	31.5	42.2	0.91 — 0.99
500-lb. S.A.P, Mk V	490	TNT	89	18	11.5	41.8	62.0	1.22 — 1.32
500-lb. S.A.P, Mk V	485	TNT	89	19	11.5	41.8	62.0	1.22 — 1.32
2000-lb. A.P, Mk IV	1934	Shellite	166	9	13.5	80.0	113.0	
100-lb. A.S, Mk IV	98	TNT	44	45	8.0	25.0	42.0	0.11
250-lb. A.S, Mk IV	243	TNT	134	55	11.3	36.0	53.0	0.14
500-lb. A.S, Mk IV	490	TNT	282	58	14.3	50.0	73.5	0.18
500-lb. M.C, Mk I or II	447	Amatol 60/40	224	50	12.9	42.0	70.8	0.3
500-lb. M.C, Mk I or II	439	Amatol 60/40	224	51	12.9	42.0	67.8	0.3
500-lb. M.C, Mk IV	510	Amatol 60/40	210	41	12.9	42.0	70.8	0.42
500-lb. M.C, Mk III	502	Amatol 60/40	210	42	12.9	42.0	67.8	0.42
500-lb. M.C, Mk III	440	Amatol 60/40	174	40	12.9	36.5	70.3	0.42
500-lb. M.C, Mk III	437	Amatol 60/40	174	40	12.9	36.5	67.3	0.42
500-lb. M.C, Mk IV	510	Amatol 60/40	210	41	12.9	42.0	70.8	0.42
1000-lb. M.C, Mk I	1021	Amatol 60/40	475	47	17.5	62.5	72.5	0.42
4000-lb. M.C, Mk I		Amatol 60/40 Amatol 60/40 Amatol 60/40 Amatol 60/40 RDX/TNT		56	30.0	74.5	109.5	0.75
2000-lb. H.C, Mk I	1842	Amatol 60/40	1340	73	18.5	99.5	162.0	0.19
2000-lb. H.C, Mk II or IA	1725	Amatol 60/40	1230	71	18.5	80.0	131.0	0.19
4000-lb. H.C, Mk I or IA	3644	Amatol 60/40	2930	75	30.0	82.0	110.0	0.31
8000-lb. H.C, Mk I or IA	7800	Amatol 60/40	5351	68	38.0	nose 47.2 rear 47.5	133.0	0.50
12000-lb. H.C.	11800	Amatex 9	7800	66	38.0		180.0	

ABBREVIATIONS

		AMERICAN EQUIVALENTS	GERMAN EQUIVALENTS
M.C.	MEDIUM CHARGE, charge-weight ratio about 50%	G.P.	S.C.
H.C.	HEAVY CHARGE, charge-weight ratio about 70-75%	L.C.	
G.P.	GENERAL PURPOSE, charge-weight ratio about 30%	S.A.P.	S.D.
A.P.	ARMOR PIERCING, charge-weight ratio about 5-8%	A.P.	
S.A.P.	SEMI-ARMOR PIERCING, chg-wt ratio about 18%		P.C.
A.S.	ANTI-SUBMARINE		
F.	FRAGMENTATION, anti-personnel		

NOTE: COMPILED FROM DATA SUPPLIED BY THE BRITISH MINISTRY OF SUPPLY

December 1945

WEAPON DATA

PHYSICAL CHARACTERISTICS OF GERMAN BOMBS AND MINES

1A5a PHYSICAL CHARACTERISTICS

A HIGH EXPLOSIVE BOMBS

TYPE	TOTAL WEIGHT-pounds	TYPE of CHARGE	WEIGHT of CHARGE pounds	CHARGE-WEIGHT RATIO percent	MAX. BODY DIAMETER inches	LENGTH without TAIL inches	BODY WALL THICKNESS inches	NOSE CORRECTION inches
2 kg. S.C.2 Anti-personnel "Butterfly"	4.4	TNT-cast	7.5 oz.	11	3.0	3.1	3/8	
12-kg. S.C.10 Anti-personnel	26	TNT	2.0	7.7	3.25	15	0.5	
30-33-kg. S.B.S.C. Anti-personnel	66-77	TNT	18		7.0	27	1.75	
10-kg. S.D.C.								
50-kg. S.C.	113	TNT or Amatol	53.7	48	8.0	28-31	3/16	3.83
50-kg. S.D.	113	TNT	36.1	32	8.0	23.5	3/8	3.83
70-kg. S.C.	154	TNT	46.2	30	8.0	28-31	0.39	
100-kg. S.C.	220		110	50	10	33	9/32	
250-kg. S.C.	519	TNT or Amatol	266	55	14.5	46.5 or 47.0	9/32 or 5/16	6.80
250-kg. S.D.	528	TNT	174	33	14.5	36.0	7/8	6.80
500-kg. S.C.	1120	TNT or Amatol	84	43	18, 18.5 or 19	60, 62 or 64.5	9/32 or 5/16	9.59
500-kg. S.D.	1037 1100	TNT/wax TNT-cast	165 165	15 15	15.6 15.0	54.0 52.5	0.9 1.6	8.35 8.35
600-kg. S.D.	1190	TNT	420	35	17.5	54	1.19	
500-kg. P.C. Rocket Bomb	1100	TNT-cast	220	20	15.6	42.7-54.0		
1000-kg. S.C. "Hermann"	2200 2400	TNT-cast & granulated	1190	54 50	26.2	76.0	3/8	12.67
1000-kg. S.C.	2070 ?					65 ?		
1000-kg. S.D. "Esau"	2240	TNT/wax	319	14	19.8	57.9	1.38	
1000-kg. P.C. Rocket Bomb	2200	TNT-cast	308	14	19.8	58.0		11.72
1000-kg. R.B.-P.C.	2200		121	5.5	15.5	47.0		
1200-kg. S.C.	2640		1090	60	26.2	74.0		
1400-kg. S.D. "Fritz"	3010	TNT/wax	660	22	22.0	75.0	1.5	
1400-kg. P.C.	3060		660	21	21.9	76.5		12.06
1700-kg. S.C.D.	3760	TNT-cast	1630	43	25.5	92.0	15/16	11.73
1730-kg. S.C. "Moorhead"	3810		1600	42	25.5	91.5	1.0	
1000-kg. S.C. "Satan"	3300	TNT or Amatol	2100	64	25.9	104	0.4	13.72
1000-kg. R.S.-P.C.	3330		374	9.4				
2500-kg. S.C. "Max"	5300	TNT		Explosive (DD 9)	30-31			

ABBREVIATIONS

S. C. (SPRENGCYLINDRISCH) THIN WALLED, GENERAL PURPOSE....CHARGE-WEIGHT RATIO APPROXIMATELY 50%. USED PRIMARILY FOR GENERAL DEMOLITION....MAIN FILLING USUALLY TNT OR AMATOL.

S. D. (SPRENGDICKWANDIG) THICK WALLED, SEMI-ARMOR-PIERCING OR ARMOR-PIERCING....CHARGE-WEIGHT RATIO, [illegible] APPROXIMATELY 30%....USED PRIMARILY AGAINST SHIPS AND FORTIFICATIONS....CONTAIN TNT PELLETS COATED WITH LIGNITE WAX TO REDUCE THE SENSITIVITY OF THE EXPLOSIVE.

P. C. ARMOR-PIERCING....CHARGE-WEIGHT RATIO APPROXIMATELY 20%.

ALL BOMBS LARGER THAN THE 50-kg. HAVE A COLUMN OF TNT PELLETS WRAPPED IN PAPER AND EXTENDING THROUGH THE CENTER OF THE BOMB TO INSURE HIGH-ORDER EXPLOSION.

COMPILED FROM DATA IN THE U.S. WAR DEPARTMENT TECHNICAL MANUAL, TM-E9-1985 AND FROM DATA SUPPLIED BY THE BRITISH MINISTRY OF HOME SECURITY.

August 1945

CONFIDENTIAL

WEAPON DATA

PHYSICAL CHARACTERISTICS OF GERMAN BOMBS AND MINES (continued).

1Ab PHYSICAL CHARACTERISTICS

B INCENDIARY BOMBS

TYPE	TOTAL WEIGHT pounds	TYPE of CHARGE	WEIGHT of CHARGE pounds	CHARGE-WEIGHT RATIO percent	MAX. BODY DIAMETER inches	LENGTH WITHOUT TAIL inches	BODY WALL THICKNESS inches
B 1-kg. El.	2.05	Thermite	0.44		1.97	9.64	25/64
B 1-kg. El. plus explosive charge	2.05	Thermite TNT	0.44 0.06		1.97	9.64	25/64
B 1.3-kg. Steel Nose	2.76	Thermite	0.44		1.97	9.64	25/64
B 2.2-kg. El-2D3EN (Incend. & expl-person'l)	4 lb-14 oz.	Thermite TNT (in nose)	0.56 0.37		Incend. 1.96 Nose 1.78	16.8	Incend. 25/64 Nose 1/4
50-kg. Thermite Incendiary	75.0	Thermite TNT	— 20.0		8.0	28.0	0.15
50-kg. Phosphorus Incendiary	90.0	Benzine 86% Phosphorus 4% Rubber 10%	30.0	33	8.0	30.0	1/8
50-kg. Sb. C	110		16-17	15		20.3 - 30.3	
110-kg. (Flam) Incendiary	242	Gasoline TNT	110	45	14.5	40.0	1/16
250-kg. (Flam) Incendiary	550	Gasoline TNT			18.0	62.0	1/16
ABB 500 (182-kg) Incendiary Container	336.0	120 1-kg. Incend. Bombs		79	18.4	25.2	0.06

C MISCELLANEOUS BOMBS AND MINES

TYPE	TOTAL WEIGHT pounds	TYPE of CHARGE	WEIGHT of CHARGE pounds	CHARGE-WEIGHT RATIO percent	MAX. BODY DIAMETER inches	LENGTH WITHOUT TAIL inches	BODY WALL THICKNESS inches
Mortar Grenade	2.2	TNT-cast	4.2oz.	12	2.0	4.2	0.16
Hand Grenade Chemical Warfare					1.5	4.1	0.059
Plane Destroying Bomb	6.6	TNT			Dimensions in inches - 7.5 x 6.5 x 2.6		
Ring Charges (Spigot)	A - 2.64 B - 7.04	TNT - compressed			Inside 4.0 Inside 6.9		
Shrapnel	9.0	Tolite (TNT)	1.0	11	3.9	Height 3.7	0.08
Tellermine	19	Tolite (TNT)	11	58	12.6	Height 4.0	1/16
Rail Demolition Charges (2 Uses)	A - 27.5 B - 110.0	TNT TNT					
500-kg. D Parachute-mine	1100		675	60	26.0		
1000-kg. D Parachute-mine	2200		1536	70	26.0		
1000-kg. B Bomb-mine	2200		1616	73	25.5	78.0	

ABBREVIATIONS

Sb. - THERMITE INCENDIARY CONTAINING AN EXPLOSIVE CHARGE.
El. - THERMITE INCENDIARY WITH ELECTRON METAL CASE (?)

COMPILED FROM DATA IN THE U.S. WAR DEPARTMENT TECHNICAL MANUAL, TM-E9-1983, AND FROM DATA SUPPLIED BY THE BRITISH MINISTRY OF HOME SECURITY

August 1943

PHYSICAL CHARACTERISTICS OF JAPANESE HIGH EXPLOSIVE AND INCENDIARY BOMBS

1 A6* JAPANESE HE AND IB BOMBS

A. HIGH EXPLOSIVE AND FRAGMENTATION BOMBS

DESIGNATION	FUZE SETTING	TOTAL WEIGHT W pounds	MAX. BODY DIAM. inches	LENGTH WITHOUT TAIL inches	WALL THICKNESS inches	TYPE OF CHARGE	WEIGHT OF CHARGE w, lb.	CHARGE WEIGHT RATIO w/W, %	REMARKS
1/2-kg AA, grounded, Army	Inst.	0.66	1.6	6.8	0.02	TNT	0.29	32	80° cone-end charge; air burst containers of 30 or 76 bombs.
Bole Bomb, AA Army	Inst.	0.87	2.5	6.4	3/32	Cyclonite and TNT	0.53	60	Parachute attached; air-to-air bombing.
1/2-kg AA, grounded, Army	Inst.	0.90	2.1	5.7	3/64	RDX/TNT	0.44	49	
1-kg AA, Spherical Missile		2.5	5.5	4.5	0.1	Black Powder burster			Paper wall. 32 pellets @ 2/3 oz.
1-kg AA Navy	Inst.	2.2	2.6	8.6	0.07	TNA/NKD	0.69	31	cone-end charge; air burst container of 40 bombs.
1-kg Anti-pers. Navy	Inst.	2.2	2.6	5.6	1/32	TNA/NKD	1.3	60	36 in air-burst container.
10-kg Anti-pers. Type 94, Army substitute	Inst.	22	4.1	18.2	1.0	Black Powder	1.2	5.5	Concrete case; steel central tube.
15-kg Anti-pers. Army	Inst.	32	4.0	16.5	1/32	Picric burster			Cast steel case filled with concrete and steel pellets.
15-kg Anti-pers. Type 92 Army	Inst.	33	3.9	16.6	0.63	Picric	9.7	29	Body wall made of 26 steel rings.
30-kg Anti-pers. Type 1, Army substitute	Inst.	62	5.1	19.8	1/16	Black Powder burster			Cast steel case filled with concrete and steel pellets.
30-kg Anti-pers. Type 2, Army substitute	Inst.	66	5.1	20.6	1/16	Black Powder burster			Cast steel case filled with concrete
30-kg GP, Type 99, Army	Inst; short delay; 15-16 seconds	66	5.9	18.7	0.29	Picric	26	39	
32-kg Streamlined, Navy	Inst.	70	7.6	19.7	1/8				Resembles British Bombs.
50-kg GP, Type 94, Army	Inst; short delay; 15-16 seconds	110	7.1	24.8	0.27	Picric or RDX/TNA	44	40	
50-kg Time Bomb, Type 1 & 94 (mod) Army	15-16 secs 2-24 hrs.	110	7.1	23.2	3/32	Picric	58	40	Type 1 can use anti-withdrawal tail fuze.
60-kg Type 3 Navy	Inst; short delay	143	7.9	21.8	0.28	Picric	86	60	
60-kg Type 97 Navy	In Navy Gaine*	134	7.9	21.8	0.28	Hexanite and TNA	80	61	
60-kg Anti-Sub Type 99 Navy	3½, 10 sec. delays	141	9.4	21.0	0.16	TNA/NKD	86	61	
60-kg Streamlined, Navy	Inst.	130	8.0	25.5			53.9	47	Resembles British Bombs.
63-kg GP, Type 99 Navy	Inst.	139	8.8	25.5	0.25	Picric or TNA/NKD	70	50	
100-kg GP, Type 3 and 94 Army	Inst; short delay; 15-16 seconds	220	8.5	31.2	0.4	Picric	88	45	
100-kg Time, Type 1 and 94 (mod) Army	15-16 secs 2-24 hrs.	238	8.5	30.2	0.4	Picric	106	44	Type 1 can use anti-withdrawal tail fuze.
250-kg GP, Type 1, Navy	Inst; short delay; 1-126 hrs.	550	13.8	35.5	0.25	TNA/NKD	330	60	
250-kg GP, Type 1, Blunt Nose Navy	Inst; short delay	378	11.7	30.4	0.5	TNA/NKD	176	53	May use electric firing mechanism for proximity burets. Explosive-filled tail.
250-kg Anti-Ship, Type 3 Army	2 & 5 secs.	550	11.8	46.8	0.5	Picric & TNT	230	42	
250-kg Explosive-filled Tail Type 3, Navy	In Navy Gaine*	650	12.0	39.6	0.5	TNA/NKD	263	40	Designed for better fragmentation of tail

July 1945

JAPANESE HIGH EXPLOSIVE & INCENDIARY BOMBS
continued

DESIGNATION	FUZE SETTING	TOTAL WEIGHT W pounds	MAX. BODY DIAM. inches	LENGTH WITHOUT TAIL inches	WALL THICKNESS inches	TYPE OF CHARGE	WEIGHT OF CHARGE W, lb.	CHARGE WEIGHT RATIO W/E, %	REMARKS
250-kg GP, Type 98 Army	In Navy Delay*	550	11.7	68.5	1/4	Picric	220	40	Length includes tail cone.
250-kg GP, Type 98 Navy	Inst; short delays 1-120 hrs.	552	12.0	38.6	0.5	Picric or TNA/RDX	220	40	
250-kg Thin, Type 1 Army	0-24 hrs.	527	11.7	68.6	1/4	Picric	220	42	Anti-withdrawal device in cone
250-kg Anti-sub, Type 1 Navy	Inst; short delays 0.5 & 10 secs.	600	10.0	36.6	0.25	TNA/RDX	253	41	Has 1 box anti-ricochet nose ring.
250-kg SAP, Type 98 Navy	In Navy Delay*	540	11.5	38.7	0.75	TNA	130	25	
250-kg Streamline Navy	Inst; short delay	554	10.0	58.5	0.60	Picric	219	41	One-piece cast or forged steel body.
500-kg GP, Type 2 Navy	In Navy Delay*	1100	15.5	38.5	Thick at Base 1	TNA/RDX	440	53	
500-kg GP, Type 92 Army	Inst; short delay	1100	15.5	77.0		Picric	462	46	Length includes tail cone.
500-kg Anti-ship, Type 4 Army	2 & ½ secs.	1122	15.0	57.5	0.56	Picric & TNT	240	48	Explosive-filled tail.
500-kg SAP, Navy	In Navy Delay*	1005	16.5	46.0	Nose 6 Base 1	TNA/RDX	467	46	
800-kg GP, Navy	Inst; short delay	1620	17.5	62.0		TNA	770	48	One-piece forged steel body possibly carried in torpedo racks
800-kg Type 2, #28 Load Emb Navy	Inst; short delay	1604	17.3	71.1	15/32	TNA/RDX	552	48	Also delays incorporates in Navy Delay*
800-kg GP, Type 2 Navy	Inst; short delay	1705	18.0	72.0		Picric	672	48	May use electric firing mechanism for proximity bursts
400-kg. AP, Type 98 Navy	Short delay	1092	16.1	48.3	Nose 6 Base 2	TNA	66	6	One-piece forged machine steel...two base fuzes

B. INCENDIARY BOMBS

1-kg Army	Inst.	2.7	2.1	8.3	3/8	Thermite-filled magnesium containers dropped in clusters.
5-kg	Inst.	11	3.7	6.7	1/8	Thermite filled
12-kg, Type 97 Army	Short delay	26	6.0	19.5	3/16	Thermite-filled magnesium firepots; black powder ignition charges.
22-kg, Shrapnel Type 98, Navy	0-20; 5-30; 8-50 sec. air burst delay	70	5.7	18.5	0.10	196 phosphorus-filled steel pellets; picric acid charge.
50-kg, Type 97 Army	Inst; short delay	110	7.5	26.6	0.2	Gas bomb used as incendiary. CS_2 solution of white phosphorus with 4% rubber charge...picric acid charge.
70-kg, Type 100 Army	Inst; short delay	88	7.0	22.6	0.125	
60-kg, Type 3 Navy	0-20; 5-30; 8-50 sec. air burst delay	116	7.8	22.8	0.42	Three cylindrical containers each containing 87 white phosphorus-filled steel pellets. Explosive tube of TNA/RDX
70-kg /Type 98 Short Delay, Navy	short delay	156	7.5	21.8	0.3	"Electric" firepots filled with thermite scattered by black powder charge.
70-kg, Type 98, Oil Navy	short delay	146	9.5	21.8	0.18	20-lb inflammable mixture, lb thermite scattered by black powder charge.
70-kg, Type 1 Navy	In Navy Delay*	160	9.5	21.8	0.125	Contains 182 cylindrical incendiary pellets and grey powder bursting charge.
216-kg, Type 2 Navy	0-2[illegible]; 5-20; 8-30 sec. air burst delay	420	12.6	68	0.32	700 steel tubes filled with incendiary metallic rubber mixture. 33 kg. bursting charge of H.E. or black powder scatters mixture over 175 yds. radius when air burst occurs 100 ft. above ground.

*Four types of Navy Delay are known. Type A has delays of 0.010, 0.017, 0.025 and 0.041 seconds; Type B is instantaneous; Type C is instantaneous; Type D has selective delay from a fraction of a second to 1.5 seconds.

Source: US Navy Ammo Disposal School and Ordnance Department, US Army.

WEAPON DATA

PHYSICAL CHARACTERISTICS OF AMERICAN LAND MINES AND FIRING DEVICES

1 A7a
AMERICAN LAND MINES

A: LAND MINES

DESIGNATION	THICKNESS OR HEIGHT inches	DIAM OR WIDTH inches	TOTAL WEIGHT pounds	CASE	EXPLOSIVE TYPE	EXPLOSIVE WEIGHT pounds	FUZE	FORCE TO OPERATE pounds	FUZE FUNCTION	REMARKS
Mine, Anti-Tank, M6	4	8 diam	10.6	Steel	Cast TNT	5.5	M2	500 center 250 edge	Pressure cuts shear pin. Balls release striker	No longer in production. Booster integral with fuze. Spider 8.2 in diameter.
Mine, Anti-Tank, M6A1	4	8 diam	10.6	Steel	Cast TNT	5.5	M6A1	500 center 250 edge	Pressure cuts shear pin. Balls release striker	Booster separate from fuze. Spider 8.2in
							M6A2	800 center 250 edge		Same as mine with fuze M6A1 except fuze M6A2 has more powerful detonator to insure high order detonation. Spider 8.2 in diameter.
Mine, Anti-Tank, M6	4	8 diam	10.6	Steel	Cast TNT	5.5	M6	800	"Trident" metal diaphragm snaps striker down	2 activator wells: 1 side, bottom. Internal construction of fuze M6 makes mine safe to re-use. Spider 8.2in diameter.
Mine, Anti-Tank, M7	5.5	10 diam	14.5	Ceramic	TNT or Tetryl pel	5.6	M6 Chem.	275-425	Pressure breaks glass vial. Chem. ignites flash mixture	1 activator well: 1 bottom. Fuze made of plastic.
Mine, Heavy Anti-Tank, M8	3.25	12.5 diam.	20	Steel	Cast TNT	16	M6A2 Chem.	300-400	Piston crushes glass vial. Chem. ignites flash mixture	2 activator wells: 1 side; bottom. Solid pressure plate
Mine, Light Anti-Tank, M7 (or Anti-Personnel-can recycle)	2.8	9.8x7	9.5	Steel	Tetryl pel	3.25	M6A1 Chem.	300-400	Piston crushes glass vial. Chem. ignites flash mixture	1 activator well: 1 side. Any standard firing device may be used in activator well to convert to anti-personnel mine.
Mine, Anti-personnel, M2 (M1, M2A2, M3, M3A1, M4A1)	6.8	Body: 2.8 diam. Base: 5½ diam or 3x4	Shell: 2.8 Total: 6 to 6.5	Steel or malleable iron	Picked TNT	0.35	M2 M2A1	PULL 3-6	PUSH 20-40	Various mods differ in manufacturing details of base. Projects 2½ in shell when detonated 6-8 ft from mine. Lethal range 30-60 ft. Dangerous to 150 ft. Any standard firing device with igniter tube may be used as a fuze.
	6.8						M3	6-10	10-30	
Mine, Anti-Personnel, M3	3.8	3.8x5.8	3.8	Cast iron	Picked TNT	0.35	M3 M3A1	3-4	10-40	Lethal range approx. 30 ft. 2 activator wells: Top, side, and end.
							M7	6-10	10-30	

*Activator wells have standard thread to fit any of the standard firing devices listed below. These may be used for anti-personnel devices or for otherwise booby trapping mines.

Note: In addition to the mines listed above, various demolition charges, the bangalore torpedo, hand grenades, etc. may be equipped with one or more of the standard firing devices listed below and used as anti-tank or anti-personnel mines.

Source: Publications of the Ordnance Department, US Army; Office of the Chief of Engineers, US Army; Bureau of Ordnance, [illegible], and US Navy Bomb Disposal School.

Ref: FEH No. 110
July 1944

CONFIDENTIAL

B: FIRING DEVICES

DESIGNATION	FORCE TO OPERATE, lb	METHOD OF FUNCTIONING	REMARKS
Firing Device, Pull Type, M5	3-4 pull	Pull on release pin releases spring driven striker	
Firing Device, Pull Friction Type, M2	3-8 pull	Pulling coated wire through friction compound ignites compound.	Made of plastic for use in non-metallic mines or booby traps.
Firing Device, Pressure Type, M4A1	20 press (see remarks)	Moving trigger pin inward allows spring driven striker pin to operate	Operates on 5 lb press with trigger spring removed. Has adjustable extension rod with 5 prongs
Firing Device, Release Type, M1	Restraining load at least 2 lb.	Removal of restraining load allows spring driven hammer to drive striker pin.	To shoot metal ban, 1-7/8 x 1-7/8 x 2-3/8 inches
Firing Device, Pull Release Type, M3	6-16 pull or tension release	Pull or release of tension on release pin releases spring driven striker	
Firing Device, Pressure Release Type, M6	Restraining load at least 5 lbs.	Removal of restraining load allows spring driven striker to detonate cap.	To shoot metal ban 1-3/4 x 15/16 x 11/16 inches
Firing Device, Combination, M8	3-6 pull or 20 press	Pressure on cap or pull on release pin releases spring driven striker	With igniter or blasting cap this is fuse M2 or M3 for anti-personnel mines M2 and M3
Fuse Combination, M4	6-10 pull or 10-20 press	Pressure on one or more prongs or pull on release pin releases spring driven striker	Firing devices complete with igniter. M3 has black powder igniter; M7 has blasting cap. Used as fuses in anti-pers. mines M2,M3
Fuse Combination, M7	6-10 pull or 10-20 press	Pressure on one or more prongs or pull on release pin releases spring driven striker	
Firing Device Delay Type, M8	15-25 to crush ampule	Crushing ampule releases corrosive liquid which eats away restraining wire, releasing spring-driven striker pin.	Widely variable delays, color coded on safety tab. Delay is strongly temperature dependent.
Detonator, 15-second Delay, M4	5-20 pull	Pulling coated wire through friction compound ignites flash igniting 15 sec. delay powder train.	Made of plastic. May be used under water. Complete with blasting cap as igniter.
Firing Device (Navy) Demolition, M1 and 0	31 pull, release, or pressure	Pressure on cap or pull or release of trip line releases spring driven striker	M1 and 0 are M1 and 1 differ in mounting details. M1 and 1 ratchet takeup for adjusting trip line. Can be used for pull-release or pressure, but not for both.
Firing Device (Navy) Demolition, M1 and 1	11-16 pull, release or pressure	Pressure on cap or pull or release of trip line releases spring driven striker	
Firing Device (Navy) Demolition, M1 and 0 compression detonator		Air or water pressure gauge discharges through dead center driving striker pin	For sympathetic detonation in air or water up to 12 ft deep. Various arming coils to give arming delays of 0-60 minutes in sea water at 60° F.

All firing devices listed here have standard threaded ampules and may be used to detonate anti-personnel mines, demolition charges, bangalore torpedoes, hand grenades, etc. which have standard threaded activator wells. Igniter tube, non-electric blasting cap, or Activator M1 must be used with all firing devices unless otherwise noted (Fuze M6, Fuze M7, Detonator M3). Primacord, properly attached, may be used to connect firing devices to demolition charge.

1 A7b

PHYSICAL CHARACTERISTICS OF AMERICAN DEMOLITION, SHAPED AND LINE CHARGES

A: DEMOLITION CHARGES

DESIGNATION	LENGTH inches	WIDTH inches	THICKNESS inches	TYPE	WEIGHT pounds	TOTAL WEIGHT pounds	CASE MATERIAL	REMARKS
DEMOLITION CHARGES, U.S. ARMY								
Demolition Block, Chain, M1	11½	8	4½	Tetrytol	20	22	Cloth Bag	8 blocks, strung on pri-cord, in bag.
Demolition Block, M2	11	2	2	Tetrytol	2.5	2.5	Paper	Issued as 8 blocks in bag with strap.
Demolition Block, M3	11	2	2	Comp C-2	20	24	Paper	Issued as 8 blocks in bag with strap.
Demolition Block, M5	8	1	1½	Comp C-2	1	1	Paper	
Block, TNT, ½-lb.	3 1/16	1 1/16	1 1/16	Pressed TNT	½	½	Cardboard	
Block, TNT, ½-lb.	3 1/16	1 1/16	1 1/16	Pressed TNT	½	½	Cardboard Metal Ends	Two ½-lb blocks in one container.
Block, Nitrostarch, ½-lb.	3½	1½	1½	Nitrostarch	½	½	Paper	Three ½-lb blocks wrapped together.
Block, Nitrostarch, ½-lb.	3 1/16	1 1/16	1 1/16	Nitrostarch	½	½	Cardboard Metal Ends	
Block, Nitrostarch, 1-lb.	2½	2½	2½	Nitrostarch	1	1	Paper	Four ½-lb blocks wrapped together.
Demolition Explosive	17	2½-in. diam.		Ammonium Nitrate	40		Metal	
Commercial Dynamite, ½-lb.	8	1½-in. diam.		Dynamite	½	½	Paper	
DEMOLITION CHARGES, U.S. NAVY								
Demolition Charge, M1 and 2	14.2	8.25	8.25	TNT	50½		Steel	For electrical firing
Demolition Charge, M2 Mod 1	14.2	8.25	8.25	TNT	50½		Steel	For electrical or non-chemical firing.
Demolition Charge, M2 Mod 2	14.2	8.25	8.25	TNT	50½		Steel	Has standard threaded detonator well
Demolition Charge, M3	2 1/16	1 1/16	1 1/16	Pressed TNT	½	½	Cardboard Metal Ends	Same as Army Block, TNT ½-lb.
Demolition Charge, M4	2 1/16	1 1/16	1 1/16	Cast TNT	½	½	Cardboard	Two tetryl pellet boosters.
Demolition Charge, M5	13	13	13	TNT	120		Fiber Board	25-lb Tetryl booster (Bootscoord) See M14
Demolition Charge, M8, Mod 0,1	13	13	13	Cast TNT	112	116	Steel	Fitted with standard bomb nose fuze cast for 14-in. fuzes.
Demolition Charge, M10	11	2	2	Tetrytol	2½	2½	Paper	Same as one section of Army Demolition Block, Chain M1, with detonating cord attached. Issued as 8 blocks in cloth bag with strap. Obsolete
Demolition Charge, M10, Mod 0	10	10	6½	Cast TNT	50½	50	Fiber-board	40-lb Cast TNT plus 25-lb tetryl booster. Self-contained detonating cord.
Demolition Charge, M10, Mod 1	10	10	6½	Cast TNT	40	40	Fiber-Board	No booster. Designed for sympathetic detonation.
Demolition Charge, M20	12	2½	4½	Comp C-2	2½	2½	Paper	Issued as 10 blocks in haversack with strap. Two packs issued together as Set, Outfit, M17.

B: SHAPED CHARGES

DESIGNATION	OVERALL LENGTH inches	LENGTH OF BODY inches	STAND-OFF inches	CONE ANGLE degrees	CONE THICKNESS inches	LINER MATERIAL	BURSTER TYPE	BURSTER WEIGHT pounds	TOTAL WEIGHT pounds	CASE MATERIAL	REMARKS
SHAPED CHARGES, U.S. ARMY all have standard threaded detonator well.											
Charge, Shaped, M-3	13.5	8.8	4.7	6	60	0.125	Steel	TNT	8.8	10	Steel	Obsolete.
Charge, Shaped, M-3 M2	16.8	10.2	6.8	6	60	0.20	Steel	Pentolite 50/50	10	12.5	Plastic	Standoff tube 7.5 in. diam.
Charge, Shaped, M-3 M2A1	16.8	8.7	6.8	6	60	0.20	Steel		10	12.5	Impreg-Cloth	Same as M2 with top reduced in length.
Charge, Shaped, M-9, M2A1	16.8	10.8	6.8	6	60	0.20	Steel		21.8	24.7	Fiber-Glass	
Charge, Shaped, M-9 M3	29.8	19.8	14.1	6.5	60	0.16	Steel		29.2	40.5	Steel	Detachable legs
CAVITY CHARGE CONTAINERS, U.S. NAVY											
Cavity Charge Container, M-1	24	9 1/16	8	24	90	0.05	Steel	Comp C-2	2/3		Steel	Empty containers to be filled Comp C-2
Cavity Charge Container, M-2	24	14	8	1	90	0.60	Steel		1		Steel	
Cavity Charge Container, M-3	40	8	8	8	90	0.40	Steel		1 1		Steel	

Ref: FM No. 100
July 1956

CONFIDENTIAL

C: LINE CHARGES

DESIGNATION	OVERALL LENGTH feet	CHARGE LENGTH feet	TOTAL WEIGHT pounds	CHARGE Type	CHARGE Weight pounds	LINEAR CHG. WT. lb/ft	EXPL. CASE MATERIAL	BODY MTRL.	REMARKS
Cable, Detonating Mine Clearing and Anti-Personnel, M6	variable			PETN Primacord		0.036			13 strands of cotton covered PETN Primacord in common outer wrapper. total weight 0.11 lb/ft.
Bangalore Torpedo M1A1	5	5	91	Amatol 80/20	8	1.6	Steel		Sections of 2-1/2 inch diameter pipe, filled Amatol 80/20 with 4 inches TNT each end. Activator well at each end. Sections can be coupled for use in multiple lengths up to 200 ft. Packed in kits containing 10 torpedoes, 10 connecting sleeves, 1 nose sleeve.
Demolition Charge, M3	25	25		Pressed TNT	50	2	Rubber Hose		Obsolete. See Mark 8 and 9.
Demolition Charge, M14 Mod 0 Army	50	25		Pressed TNT	50	2	Rubber Hose		Booster and detonator TNT in each end. Sections can be coupled for use in multiple lengths.
Snake, Mine Clearing & Anti-Personnel, M5	100	100	100	TNT	67	0.67	Paraffin Paper -	Magnesium alloy	Propelled by rocket motor near nose. Fired by 100 foot trip cord. Explosive in paper cartridges, TNT, 8 inches long, one inch diameter
Snake, Demolition M2	400	350	12,500	Amatol 80/20	2240	10 (or 10.6)	Steel	Steel	Front 20 ft. and rear 50 ft. have no charge. Explosive in steel cylinders 4 ft. long, 20 pounds each, filled Amatol 80/20 with 6 inches TNT each end. Can be filled with 4 Bangalore torpedoes each side giving a linear charge weight of 10.4 lb/ft. Bullet impact fuse.
Snake, Demolition M3A1 see figure for M2	400	350	15,000	Amatol 80/20	9000	30	Alum.	Steel	Front 20 ft. and rear 50 ft. have no charge. Explosive in Aluminum elliptical cylinders, 5 ft. long, 35 pounds each, filled Amatol 80/20 with 6 inches TNT each end. Uses two bullet impact fuses.
Snake, Demolition M3 see M2	400	350	8,000	Amatol 80/20	9000	16	Alum.	Alum.	Same as Snake M2A1 except corrugated plates are made of aluminum.
Body for Charge Army Demolition Outfit M1A1 Army	80	40	600 without explosive	Comp C-3 Tetrytol TNT	2116 1500 1700	53 38 37		Steel	Supplied in kits for 80-ft. lengths. Two of these may be used to make a 80-ft. length. Floated by air bags. Detonation of prim-cord along top releases airbags and allows charge to sink. Charge detonated after delay of about 5 minutes. Charge weights are given for unpackaged explosives. Smaller weights result if packaged explosives are used.

Snake, Demolition M2

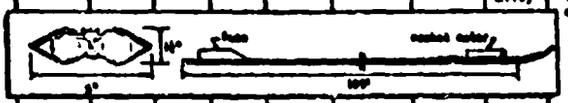

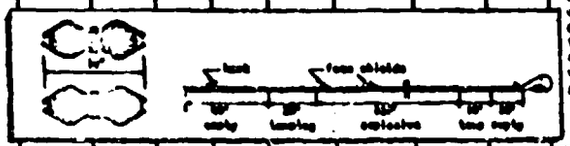

Body for Charge Army Demolition Outfit M1A1 Army

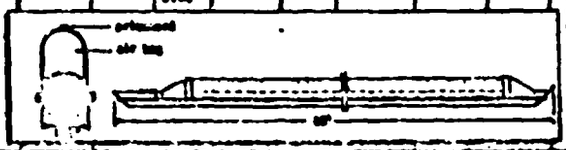

Sources: Publications of the Explosives Research Laboratory, US Army Office of the Chief of Engineers, US Army Corps of Engineers, US Navy and US Navy Bomb Disposal School.

1 B4
1 FLIGHT LOW LEVEL

LOW LEVEL BOMBING

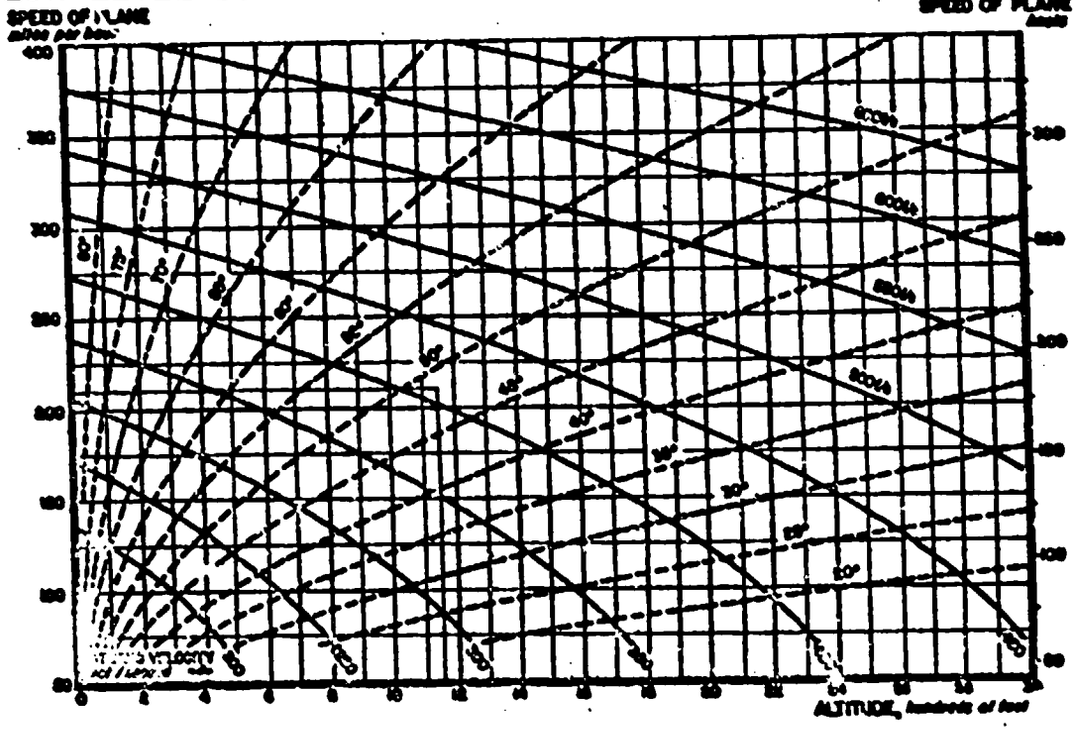

WEAPON DATA

1 B 5 *
FLIGHT
100-lb GP; 250-lb GP

STRIKING VELOCITY AND ANGLE OF IMPACT: 100-lb GP, AN-M30 AND 250-lb GP, AN-M57

100-lb. GP, AN-M 30

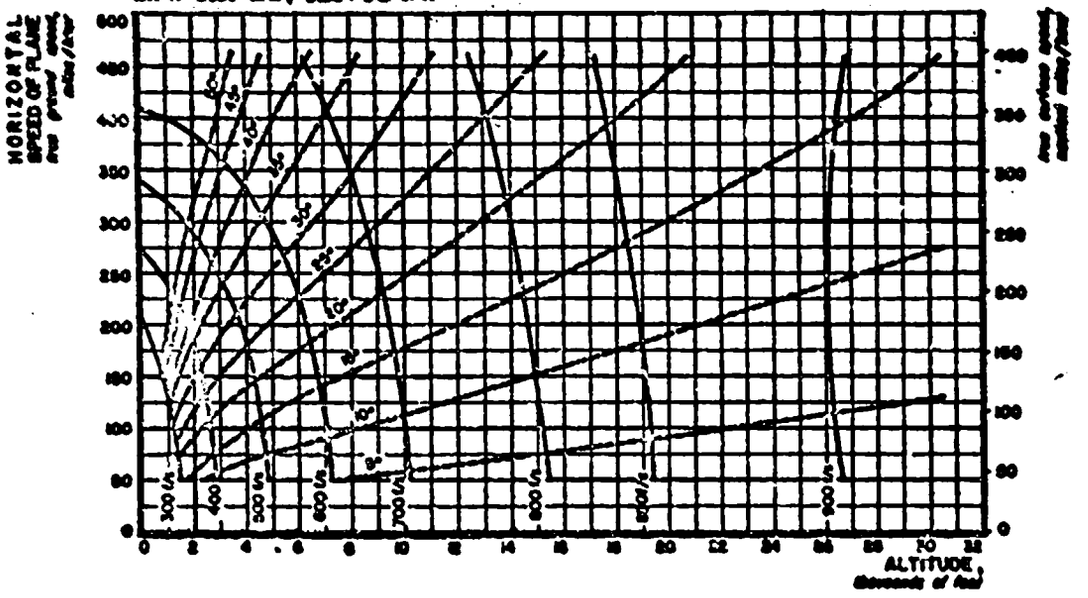

250-lb GP, AN-M 57

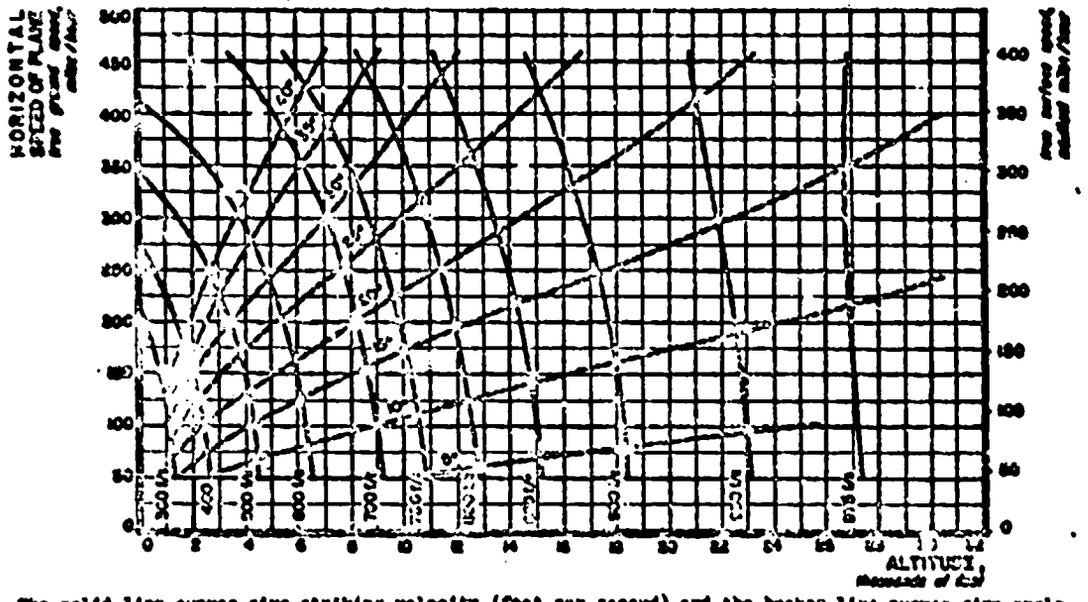

The solid line curves give striking velocity (feet per second) and the broken-line curves give angle of impact (degrees from the vertical) for bombs released from a plane in horizontal flight.

Locate a point by projecting upward from a given altitude and across from the given plane speed. Using this juncture, interpolate between curves to obtain striking velocity or impact angle.

Accuracy: Errors in striking velocity read from the graph will not exceed 1%; in impact angle, 4°.

Prepared from data supplied by the Ballistic Research Laboratory, Aberdeen Proving Ground, Maryland

August 1944

STRIKING VELOCITY AND ANGLE OF IMPACT: 500-lb GP, AN-M64 AND 500-lb SAP, AN-M58

1 B 6 *
FLIGHT
500-lb GP; 500-lb SAP

500-lb GP, AN-M64, AN-M43

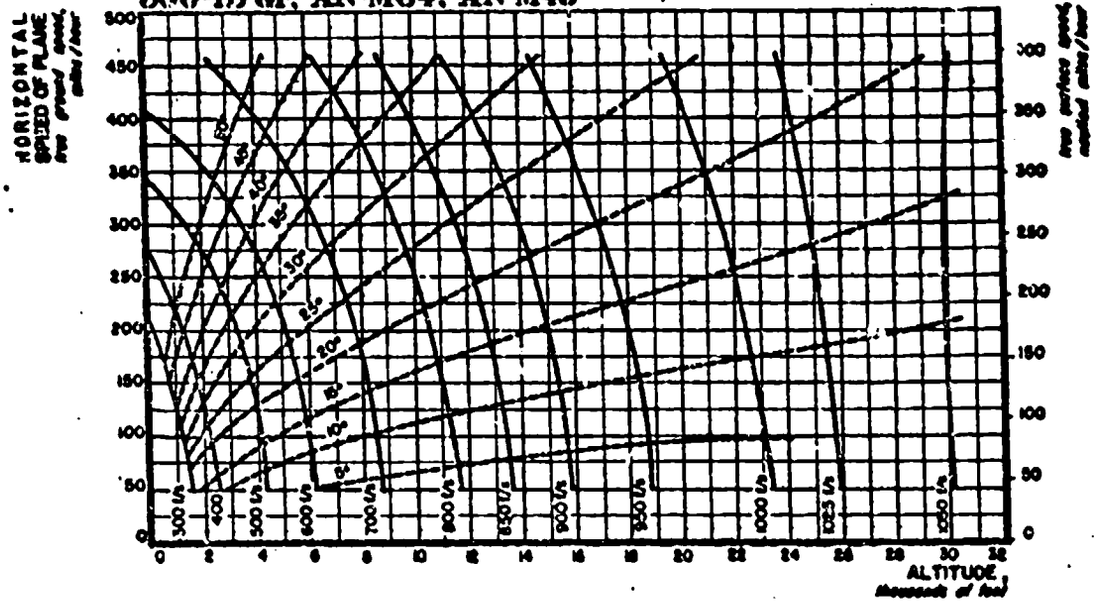

500-lb SAP, AN-M58

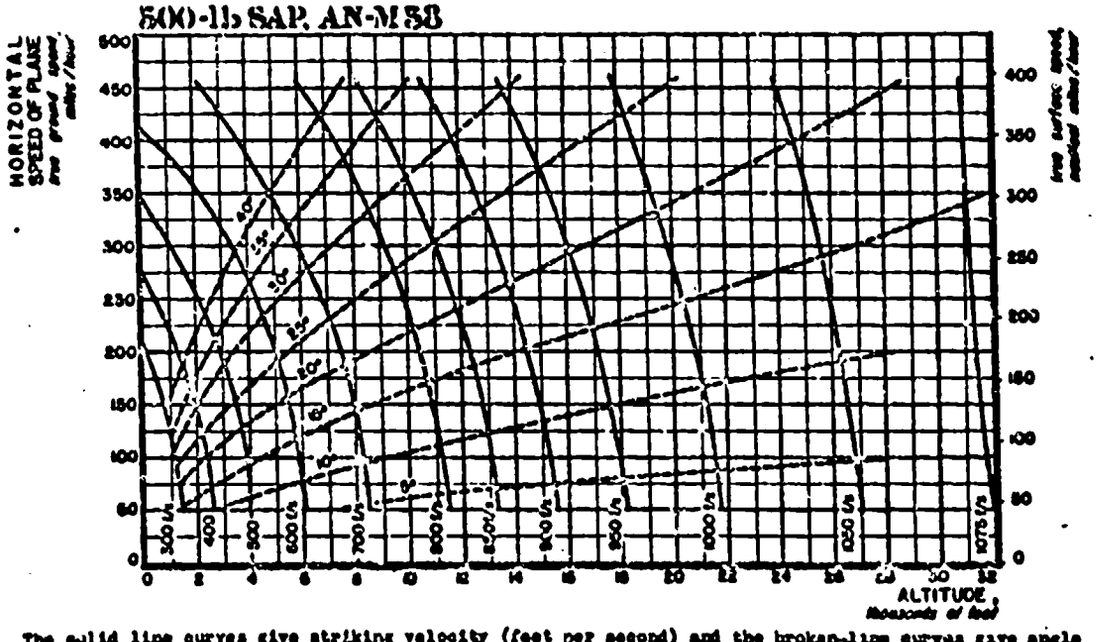

The solid line curves give striking velocity (feet per second) and the broken-line curves give angle of impact (degrees from the vertical) for bombs released from a plane in horizontal flight.

Locate a point by projecting upward from a given altitude and across from the given plane speed. Using this juncture, interpolate between curves to obtain striking velocity or impact angle.

Accuracy: Errors in striking velocity read from the graph will not exceed 1%; in impact angle, 4°.

Prepared from data supplied by the Ballistic Research Laboratory, Aberdeen Proving Ground, Maryland

August 1944

STRIKING VELOCITY AND ANGLE OF IMPACT: 1000-lb GP, AN-M65 AND 1000-lb SAP, AN-M59

1 B7 * FLIGHT
1000-lb GP, 1000-lb SAP

1000-lb GP, AN-M65, AN-M44

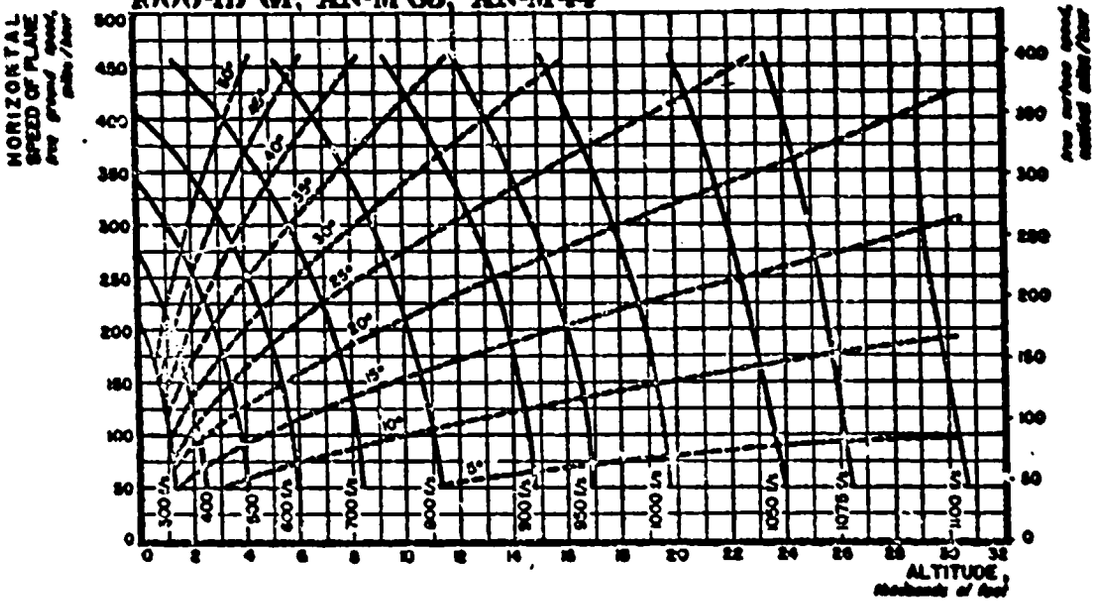

1000-lb SAP, AN-M59

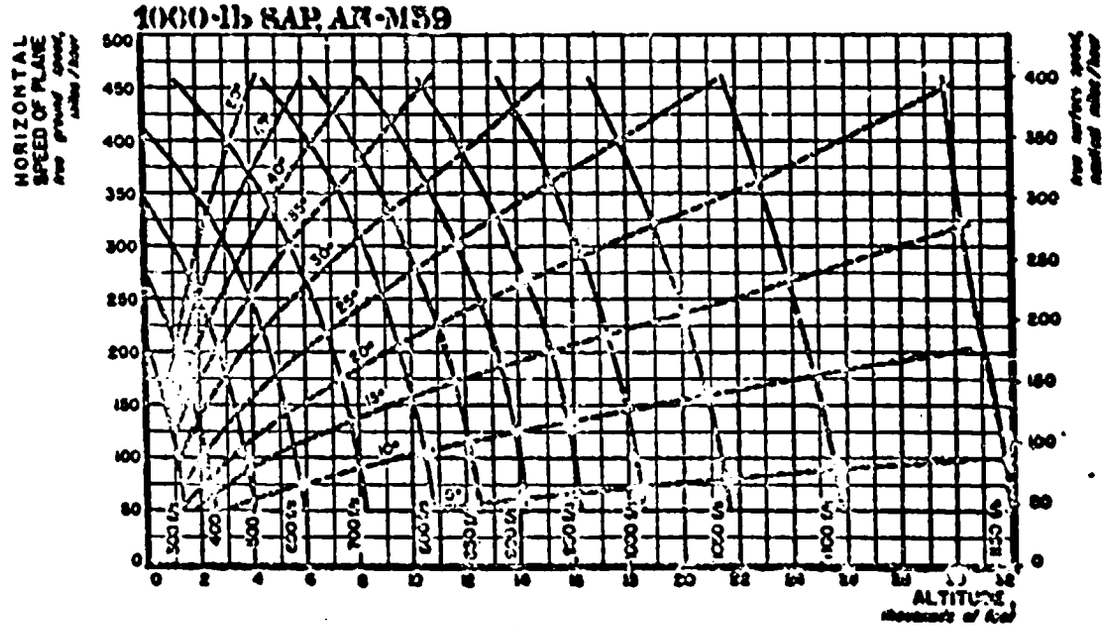

The solid line curves give striking velocity (feet per second) and the broken-line curves give angle of impact (degrees from the vertical) for bombs released from a plane in horizontal flight.

Locate a point by projecting upward from a given altitude and across from the given plane speed. Using this juncture, interpolate between curves to obtain striking velocity or impact angle.

Accuracy: Errors in striking velocity read from the graph will not exceed 10%; in impact angle, 4°.

Prepared from data supplied by the Ballistic Research Laboratory, Aberdeen Proving Ground, Maryland

August 1944

STRIKING VELOCITY AND ANGLE OF IMPACT: 1000-lb AP, AN-Mk33 AND 1000-lb AP, M52 A1

1 B 3 *
FLIGHT
1000-lb AP-lb 33/52

1000-lb AP, AN-Mk33

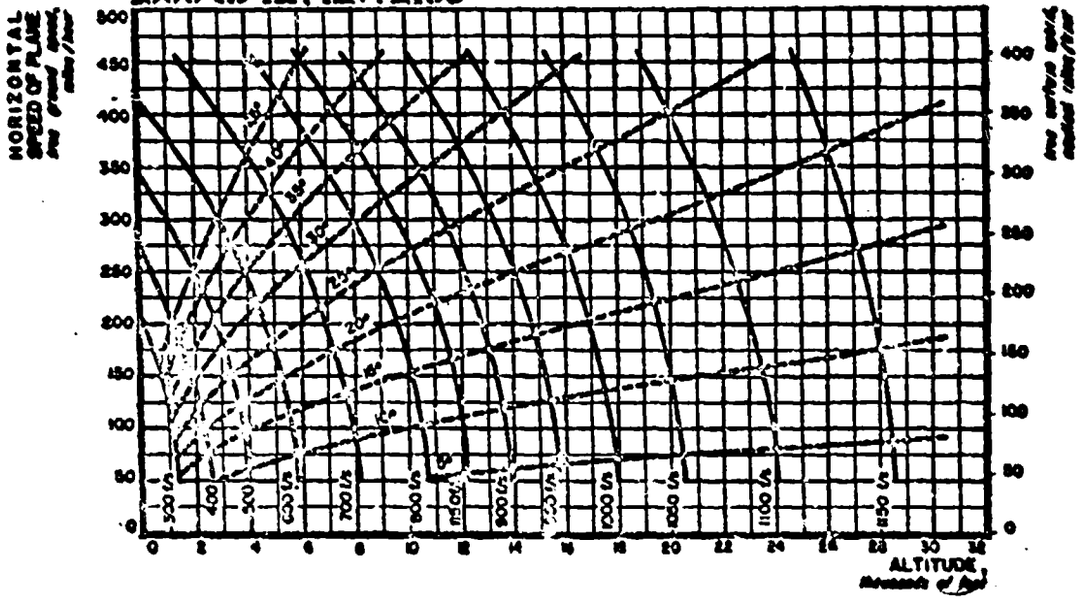

1000-lb AP, M52 A1

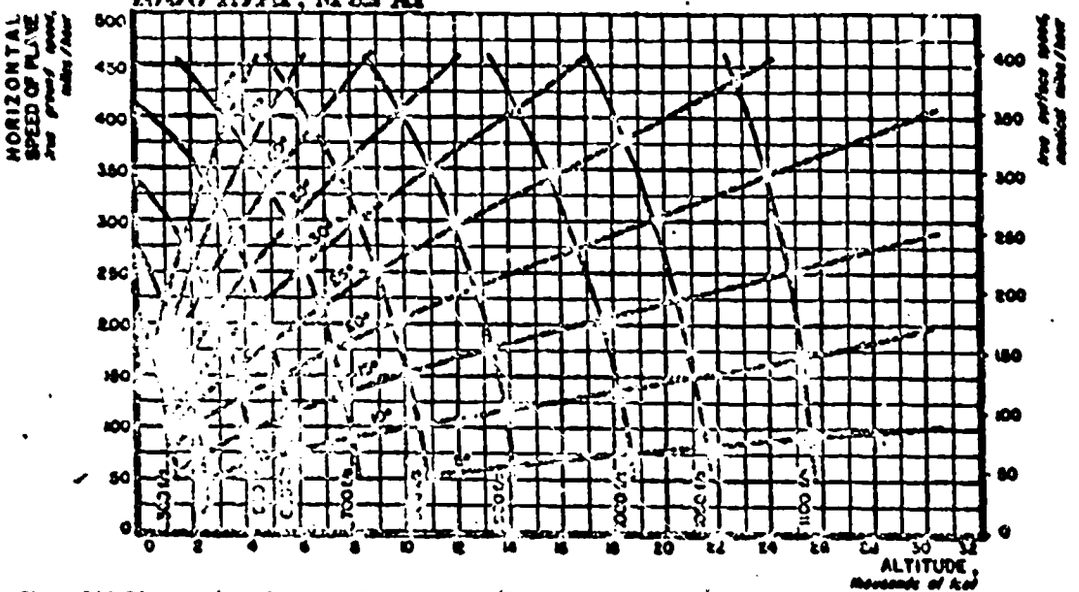

The solid line curves give striking velocity (feet per second) and the broken-line curves give angle of impact (degrees from the vertical) for bombs released from a plane in horizontal flight.

Locate a point by projecting upward from a given altitude and across from the given plane speed. Using this juncture, interpolate between curves to obtain striking velocity or impact angle.

Accuracy: Errors in striking velocity read from the graph will not exceed 1%; in impact angle, 1°.

Prepared from data supplied by the Ballistic Research Laboratory, Aberdeen Proving Ground, Maryland

August 1944

STRIKING VELOCITY AND ANGLE OF IMPACT: 1600-lb AP, AN-Mk1 AND 2000-lb GP, AN-M66

1B9 FLIGHT 1600-lb AP, 2000-lb GP

1600-lb AP, AN-MK1

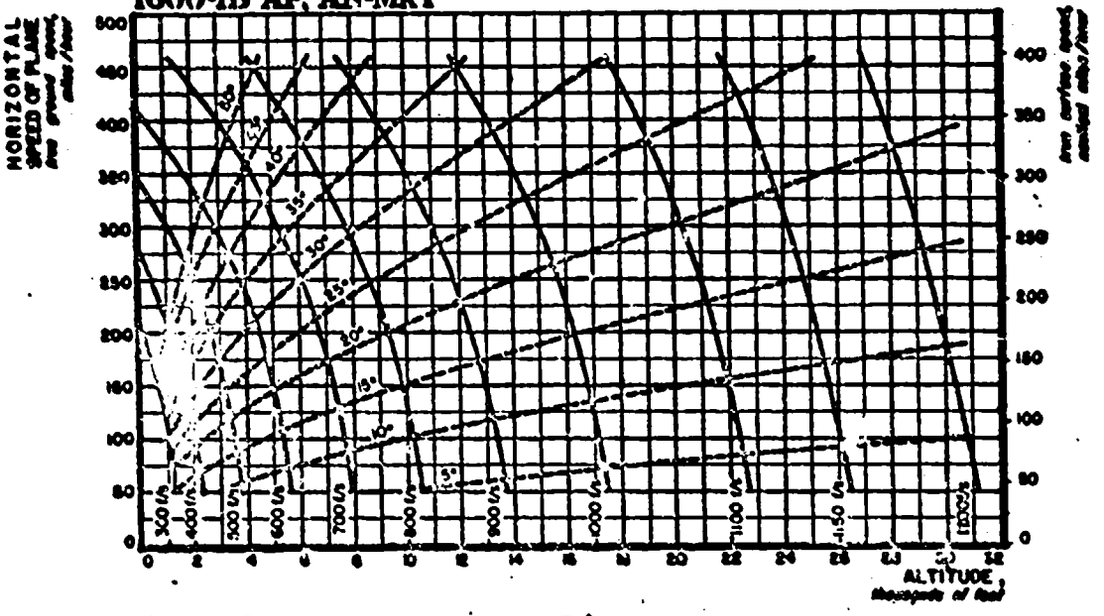

2000-lb GP, AN-M66, AN-M34

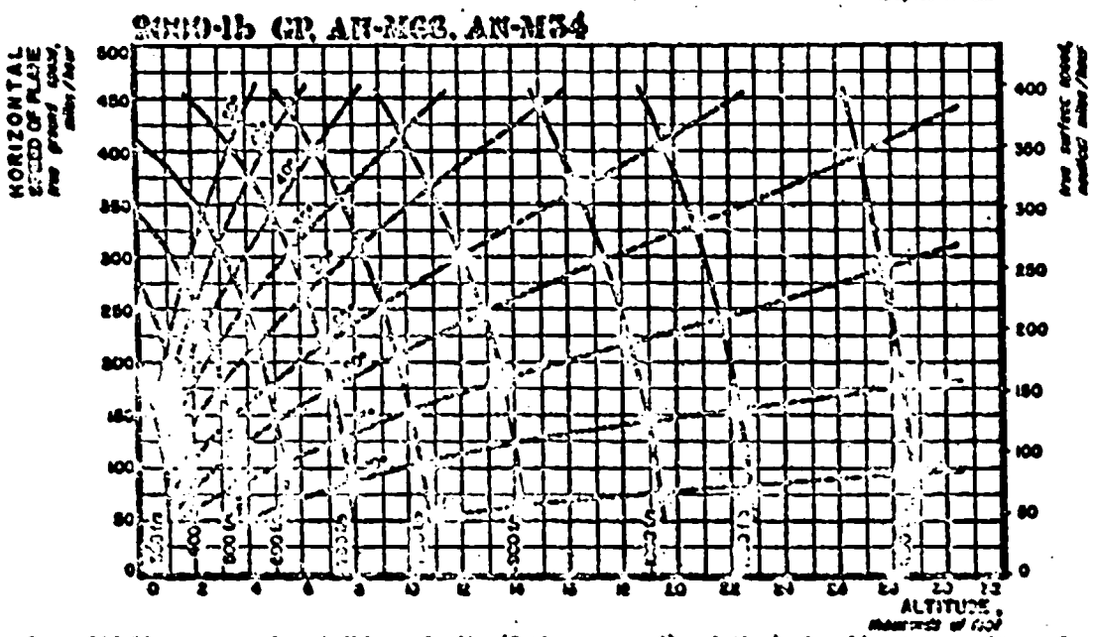

The solid line curves give striking velocity (feet per second) and the broken-line curves give angle of impact (degrees from the vertical) for bombs released from a plane in horizontal flight.

Locate a point by projecting upward from a given altitude and across from the given plane speed. Using this juncture, interpolate between curves to obtain striking velocity or impact angle.

Accuracy: Errors in striking velocity read from the graph will not exceed 16%; in impact angle, 4°.

Prepared from data supplied by the Ballistic Research Laboratory, Aberdeen Proving Ground, Maryland

August 1944

WEAPON DATA

STRIKING VELOCITY AND ANGLE OF IMPACT: 2000-lb SAP, M103 AND 4000-lb LC, AN-M56

1 BIO * FLIGHT 2000-lb SAP; 4000-lb LC

2000-lb SAP, M103

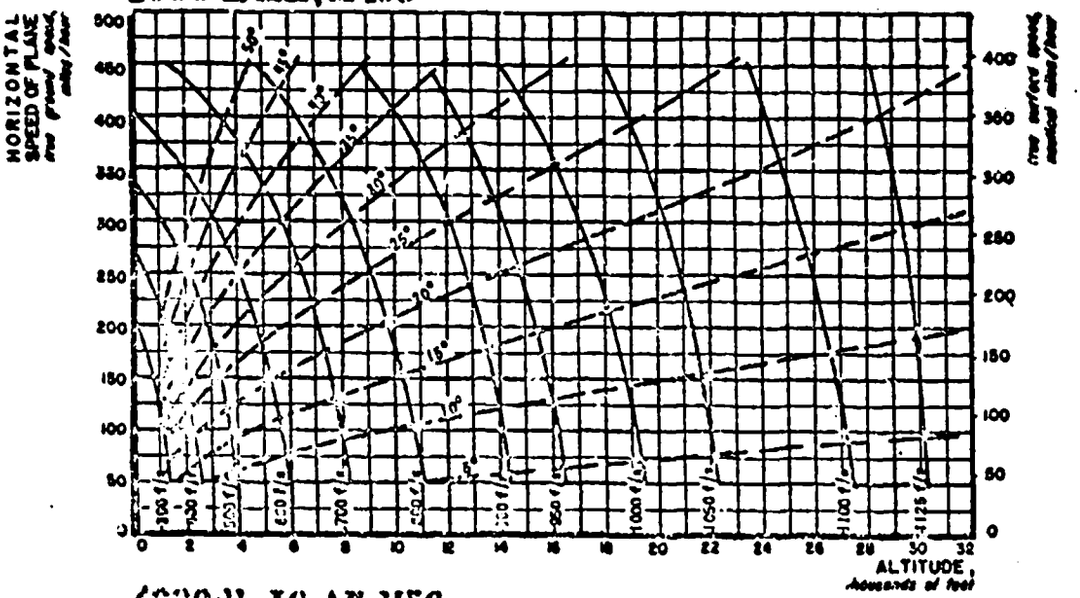

4000-lb LC, AN-M56

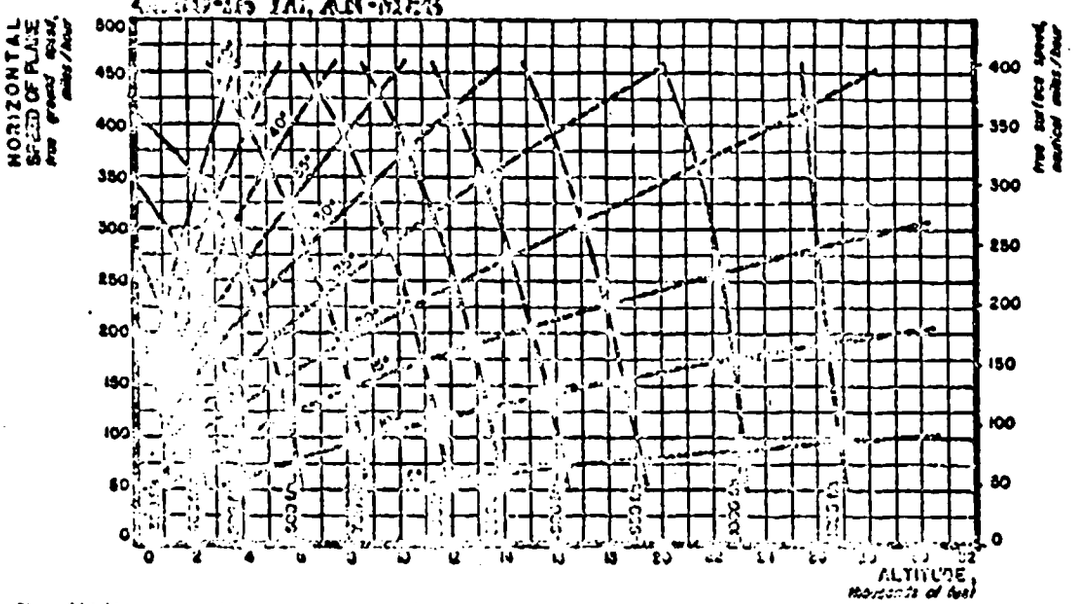

The solid line curves give striking velocity (feet per second) and the broken-line curves give angle of impact (degrees from the vertical) for bombs released from a plane in horizontal flight.

Locate a point by projecting upward from a given altitude and across from the given plane speed. Using this juncture, interpolate between curves to obtain striking velocity or impact angle.

Accuracy: Errors in striking velocity read from the graph will not exceed 15%; in impact angle, 6°.

Prepared from data supplied by the Ballistic Research Laboratory, Aberdeen Proving Ground, Maryland.

Revised
July 1946

WEAPON DATA

STRIKING VELOCITY AND ANGLE OF IMPACT: 12,000-lb GP, T10 AND 22,000-lb GP, T14

1 B 12
FLIGHT
12,000-lb GP; 22000-lb GP

12,000-lb GP, T10

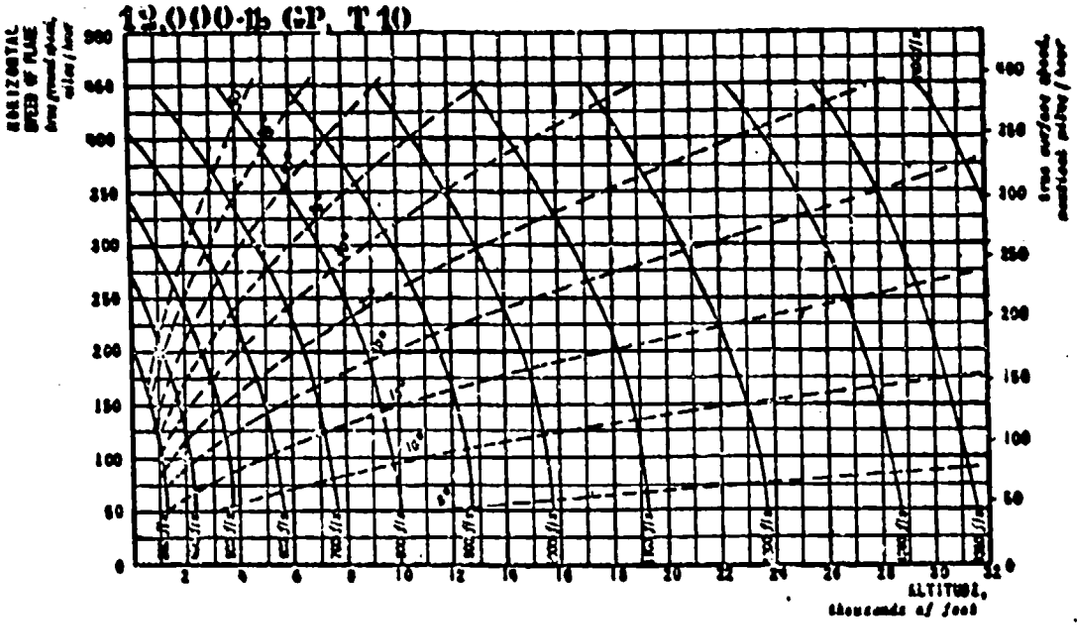

22,000-lb GP, T14

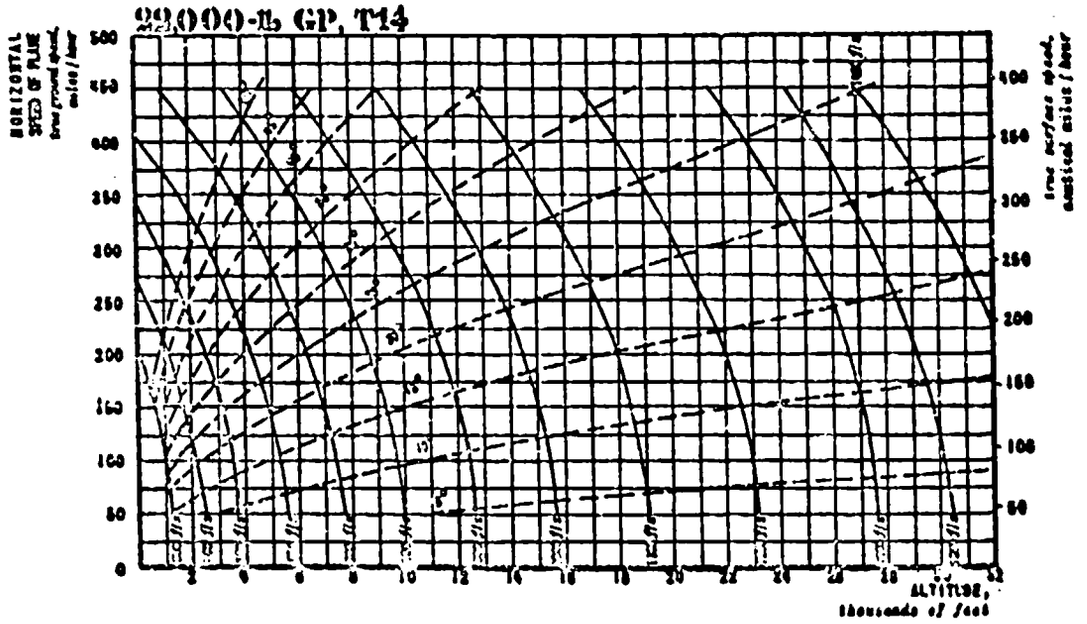

The solid line curves give striking velocity (feet per second) and the broken-line curves give angle of impact (degrees from the vertical) for bombs released from a plane in horizontal flight.

Locate a point by projecting upward from a given altitude and across from the given plane speed. Using this juncture, interpolate between curves to obtain striking velocity or impact angle.

Accuracy: Errors in striking velocity read from the graph will not exceed 15%; in impact angle, 6°.

Prepared from data supplied by the Office of the Chief of Ordnance, U. S. Army.

JUNE 1945

WEAPON DATA

STRIKING VELOCITY AND ANGLE OF IMPACT: 90-lb FRAG. M82 AND 260-lb FRAG., AN-M81

1 B-15
FLIGHT
90-lb F; 260-lb F

90-lb F, M 82

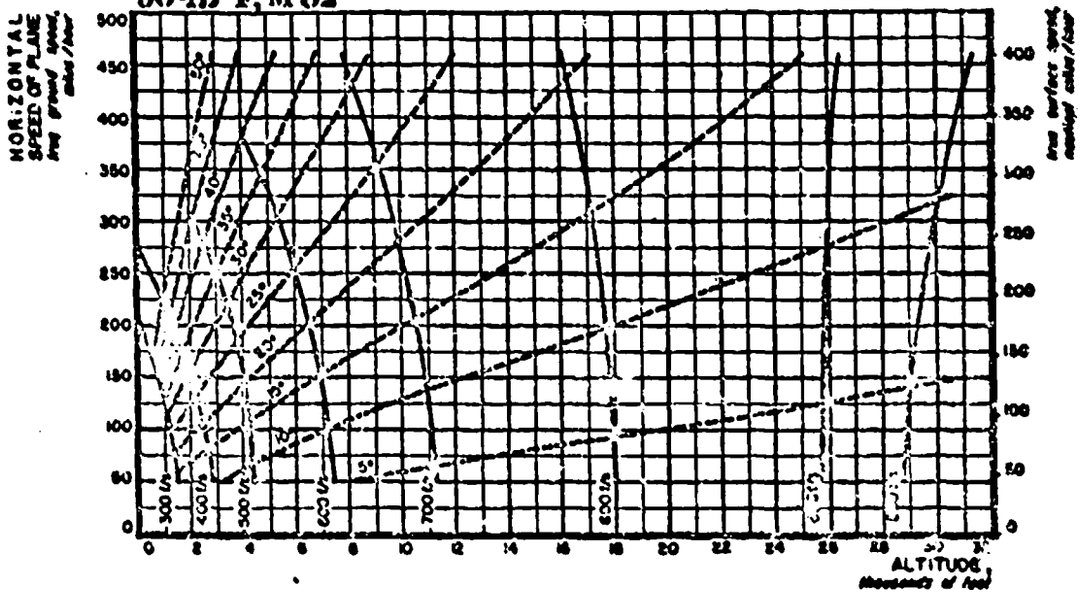

260-lb F, AN-M81

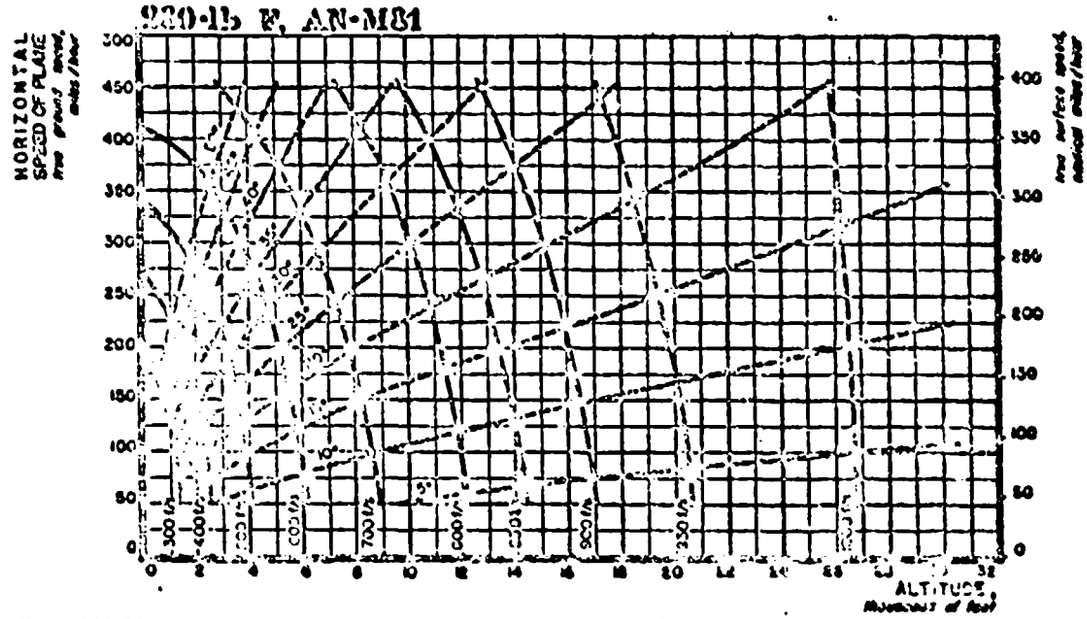

The solid line curves give striking velocity (feet per second) and the broken-line curves give angle of impact (degrees from the vertical) for bombs released from a plane in horizontal flight.

Locate a point by projecting upward from a given altitude and across from the given plane speed. Using this juncture, interpolate between curves to obtain striking velocity or impact angle.

Accuracy: Errors in striking velocity read from the graph will not exceed 10%; in impact angle, 6°.

Prepared from data supplied by the Ballistic Research Laboratory, Aberdeen Proving Ground, Maryland

August 1944

1 B20
1 B FLIGHT
GENERAL

TRAJECTORIES AND BALLISTIC DATA FOR AMERICAN INCENDIARY BOMBS AND CLUSTERS

A: COMPARISON OF TRUE TRAJECTORIES FOR 25,000 ft. RELEASE ALTITUDE & 250 mph A.S.

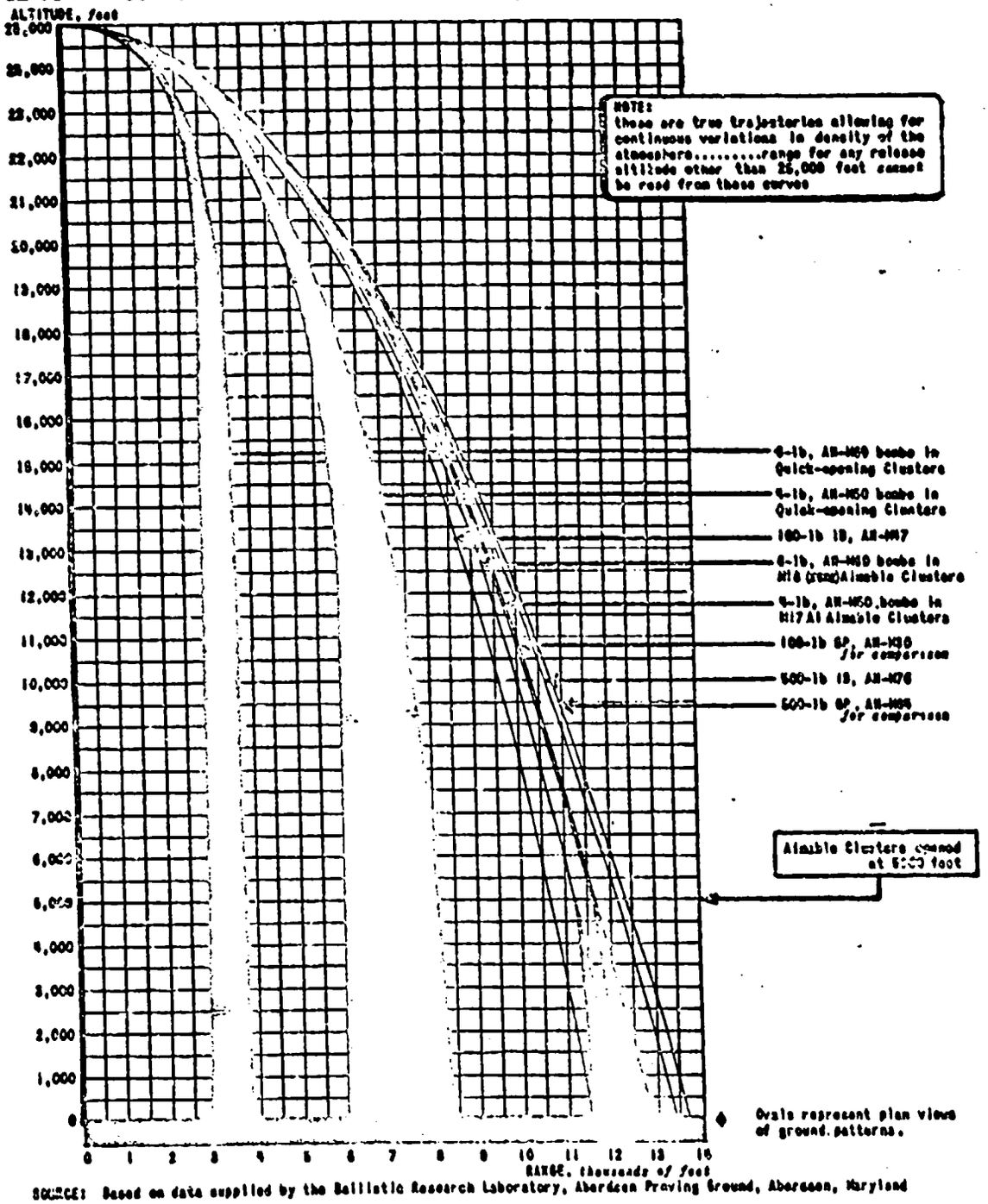

SOURCE: Based on data supplied by the Ballistic Research Laboratory, Aberdeen Proving Ground, Aberdeen, Maryland

April 1945

B: GRAPH OF RANGE FOR ANY DROPPING ALTITUDE

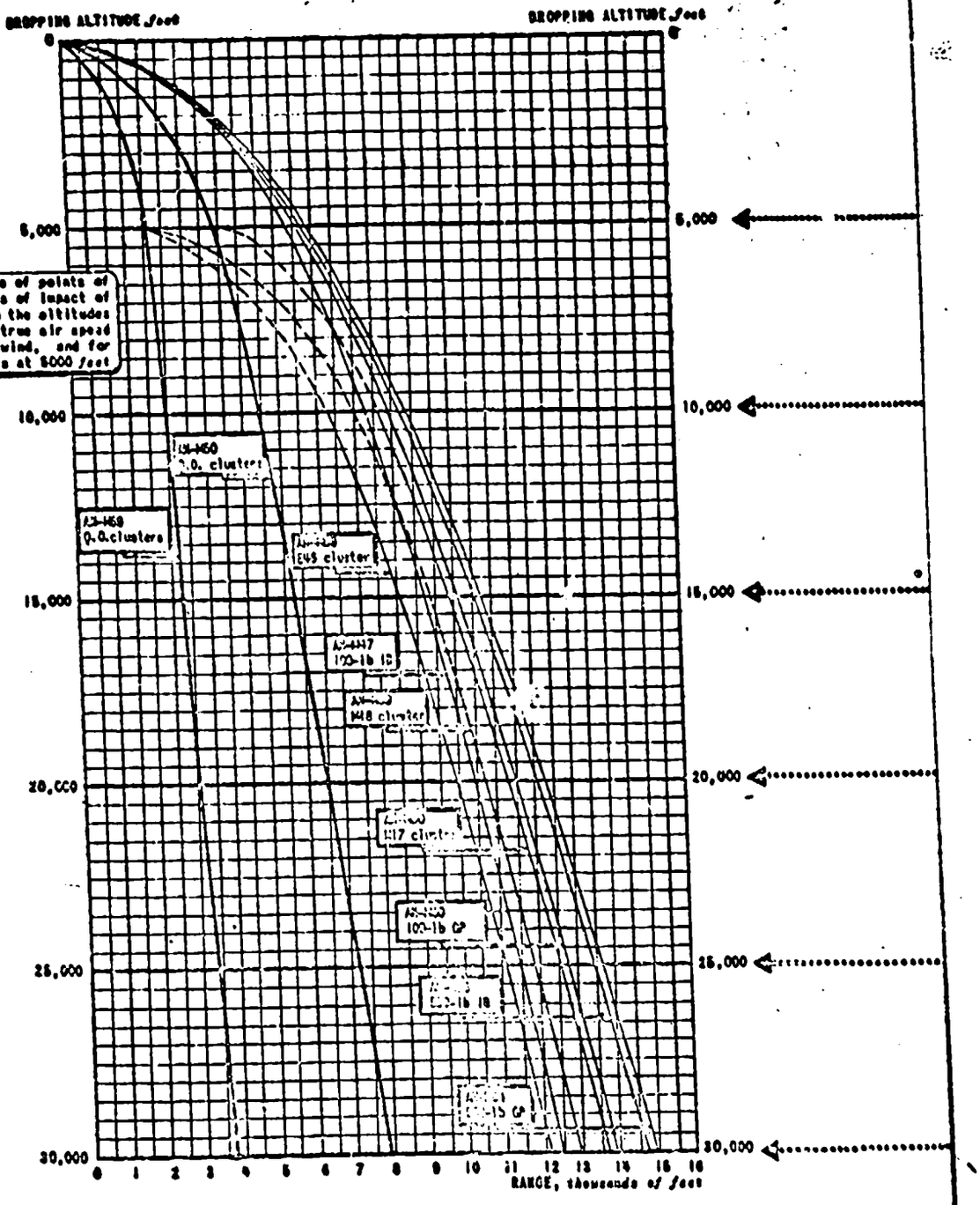

SOURCE: Bases on data in Ordnance Bombing Tables, U. S. Army

C: TABULATION OF COMPARATIVE BALLISTIC DATA

[redacted]

(For true air speed of 250 mph. and zero range wind)

BOMB DESIGNATION	AN-M69	AN-M50	AN-M69	AN-M[illegible]	AN-M69	AN-M50	AN-M30	AN-M76	AN-M64
CLUSTER DESIGNATION	AN-M13	AN-M 7	E46		M18(E6R2)	AN-M17A1*			
CLUSTER TYPE	QUICK-OPENING	QUICK-OPENING	AIMABLE opening at 5000 ft.		AIMABLE opening at 5000 ft.	AIMABLE opening at 5000 ft.			
BOMBING TABLE: BT	6-A-2	4-B-1	500-D-1	100-B-2	500-K-2	500-J-2	100-C-3	500-F-1	500-A-3
6,000 feet									
RANGE, feet	2190	3820	-	5830	-	-	6070	6230	6830
TRAIL, mils	1888	868	-	228	-	-	137	77	54
TRAIL BEHIND AN-M69, feet	6160	2910	-	600	-	-	260	100	0
RELEASE LAG AFTER AN-M64, sec	11.4	6.6	-	1.5	-	-	0.7	0.3	0
DROPPING ANGLE, degrees	29.7	38.1	-	59.6	-	-	50.5	51.3	51.7
TIME OF FLIGHT, sec	32.7	22.8	-	18.91	-	-	18.42	18.06	18.00
STRIKING VELOCITY, ft/sec	230	375	-	530	-	-	575	620	625
10,000 feet									
RANGE, feet	2440	4960	6720	7810	-	8100	8350	8650	8820
TRAIL, mils	1752	810	659	233	-	259	138	78	61
TRAIL BEHIND AN-M69, feet	6350	3360	2100	1010	-	720	460	160	0
RELEASE LAG AFTER AN-M64, sec	17.4	10.6	6.7	2.8	-	2.0	1.3	0.4	0
DROPPING ANGLE, degrees	18.7	26.4	33.8	38.0	-	39.0	39.8	41.0	41.4
TIME OF FLIGHT, sec	54.4	35.8	41.7	27.66	-	29.1	26.57	26.78	25.71
STRIKING VELOCITY, ft/sec	230	410	230	640	-	665	715	790	795
15,000 feet									
RANGE, feet	2750	5750	8530	9240	-	9690	10,090	10,630	10,700
TRAIL, mils	1638	766	642	232	-	216	136	78	65
TRAIL BEHIND AN-M69, feet	7950	4050	2170	1460	-	810	610	170	0
RELEASE LAG AFTER AN-M64, sec	21.6	13.5	8.9	4.0	-	2.2	1.7	0.5	0
DROPPING ANGLE, degrees	10.4	21.0	28.7	31.6	-	33.4	33.8	35.1	35.5
TIME OF FLIGHT, sec	78.4	47.1	59.5	34.74	-	35.7	33.07	31.90	31.77
STRIKING VELOCITY, ft/sec	230	415	230	705	-	810	810	900	910
20,000 feet									
RANGE, feet	3020	6460	9230	10,940	10,880	11,320	11,810	12,090	12,250
TRAIL, mils	1546	722	630	230	378	195	135	78	66
TRAIL BEHIND AN-M69, feet	9250	5620	2360	1610	1000	960	770	190	0
RELEASE LAG AFTER AN-M64, sec	26.2	15.9	6.6	5.0	4.8	2.8	2.1	0.5	0
DROPPING ANGLE, degrees	8.6	17.9	26.6	27.6	28.1	29.5	29.9	31.2	31.6
TIME OF FLIGHT, sec	90.8	57.3	56.0	41.01	49.8	41.5	38.75	37.22	37.04
STRIKING VELOCITY, ft/sec	230	420	230	765	230	850	860	965	980
25,000 feet									
RANGE, feet	3670	7200	11,130	11,890	11,870	12,670	12,770	13,430	13,650
TRAIL, mils	1457	687	468	325	329	187	134	80	68
TRAIL BEHIND AN-M69, feet	10,250	6450	2520	2150	1700	1600	850	220	0
RELEASE LAG AFTER AN-M64, sec	29.0	17.8	6.9	6.8	6.8	3.9	2.4	0.6	0
DROPPING ANGLE, degrees	7.7	16.1	24.0	24.7	25.4	26.7	27.1	28.2	28.7
TIME OF FLIGHT, sec	105.6	66.5	61.2	46.77	54.8	47.1	43.67	42.03	41.65
STRIKING VELOCITY, ft/sec	230	425	230	785	230	855	880	1010	1025
30,000 feet									
RANGE, feet	3740	7820	12,250	12,870	12,880	13,670	13,920	14,070	14,550
TRAIL, mils	-	652	416	322	307	178	134	82	71
TRAIL BEHIND AN-M69, feet	11,160	6970	2680	2430	1920	1230	930	230	0
RELEASE LAG AFTER AN-M64, sec	30.4	19.0	7.3	6.6	8.3	3.4	2.7	0.6	0
DROPPING ANGLE, degrees	7.1	14.8	22.2	22.6	23.4	24.5	24.9	26.1	26.4
TIME OF FLIGHT, sec	-	78.9	67.4	52.17	60.7	51.8	48.02	46.71	46.60
STRIKING VELOCITY, ft/sec	230	500	240	820	250	880	910	1010	1025

*Bombing altitudes of 8,000 to 18,000 feet, instead of 5,000 feet, have recently been recommended for AN-M17A1 cluster

Note for all aimable clusters: (a) Trails given above are true trails. Trails given in bombing tables are fictitious trails for setting into bomb-sight with times of flight and disc speeds given in bombing tables in order to get proper range to target. (b) Trails (true) given above were calculated by the following formula:

$$\text{TRAIL} = \frac{\text{Aiming point offset required for each 10° of drift (trail setting zero)}}{\sin 10° \times (\text{altitude} / 10{,}000)}$$

Times of flight were then calculated from trail and dropping angle by standard formula.

WEAPON DATA: INCENDIARIES

STRIKING VELOCITY AND ANGLE OF IMPACT: 100-lb IB, AN-M47 AND 500-lb IB, AN-M76

1 B24
FLIGHT
100-lb IB; 500-lb IB

100-lb IB, AN-M47

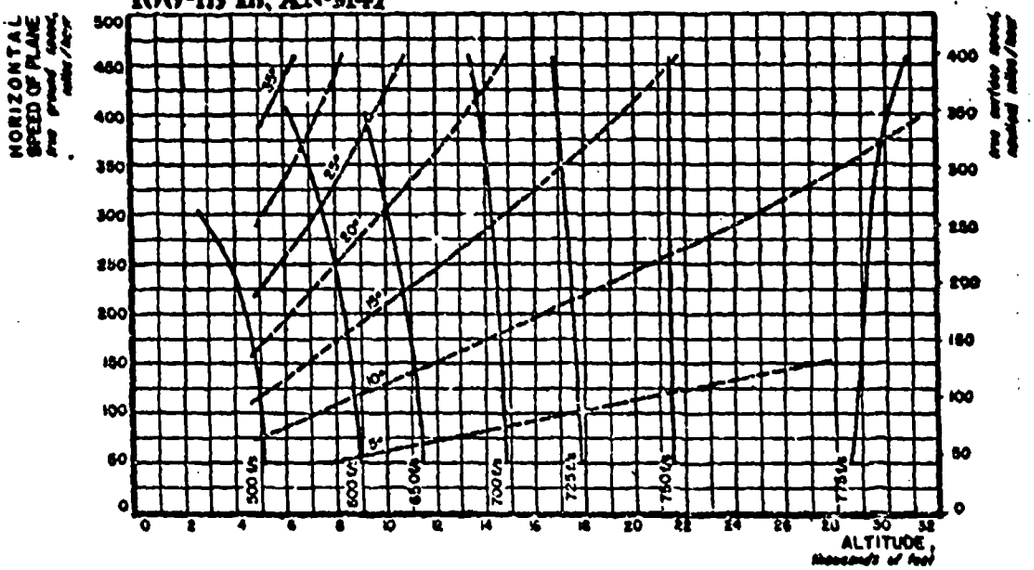

500-lb IB, AN-M76

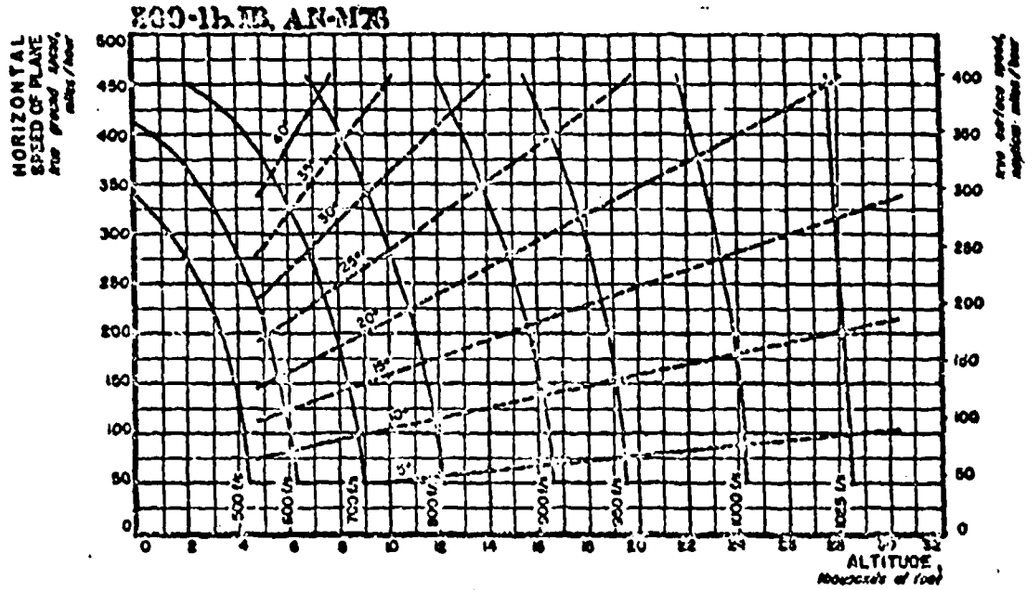

The solid line curves give striking velocity (feet per second) and the broken-line curves give angle of impact (degrees from the vertical) for bombs released from a plane in horizontal flight.

Locate a point by projecting upward from a given altitude and across from the given plane speed. Using this juncture, interpolate between curves to obtain striking velocity or impact angle.

Accuracy: Errors in striking velocity read from the graph will not exceed 15%; in impact angle, 4°.

Prepared from data supplied by the Ballistic Research Laboratory, Aberdeen Proving Ground, Maryland

December 1944

WEAPON DATA: INCENDIARIES

LOADING DATA FOR INCENDIARY BOMBS AND CLUSTERS

1C1 AIRCRAFT LOADING

FOR MAXIMUM LOADING IN ALL CASES ON U.S. ARMY AIRCRAFT WITHOUT BOMB-BAY GAS TANKS OR OTHER SPECIAL EQUIPMENT IN BOMB-BAYS

PLANE	BOMB DESIGNATION → / CLUSTER DESIGNATION → / ACTUAL WEIGHT, pounds →	AN-M47 / None / 72	AN-M50 / AR-M7 / 525	AN-M50 / M17A1 / 485	AN-M52 / AN-M11 / 425	AN-M59 / AN-M15 / 425	AN-M69 / E46 / 425	M74 / E48 / 535	AN-M76 / None / 475	
B-32	No. of clusters	-	40	40	40	40	40	40	-	
	No. of bombs	-	5120	4400	7680	2400	1520	1520	40	
	Total weight, Tons	-	10.5	9.50	8.50	8.50	8.5	10.15	9.50	
	Total heat, million BTU	-	66.2	57.0	86.0	105.6	86.9	57.6	88.4	
B-29	No. of clusters	-	40	40	40	32	40	40	-	
	No. of bombs	144*	5120	4400	7680	1920	1520	1520	40	
	Total weight, Tons	5.18	10.5	9.50	8.50	6.82	8.5	10.15	9.50	
	Total heat, million BTU	96.4	66.2	57.0	86.0	84.5	86.9	57.6	88.4	
B-24 Series	No. of clusters	-	12	12	12	12	12	12	-	
	No. of bombs	52*	1536	1320	2304	720	456	456	12	
	Total weight, Tons	1.87	3.15	2.79	2.55	2.55	2.55	3.15	2.85	
	Total heat, million BTU	34.8	19.8	17.1	25.8	31.7	20.0	17.3	26.5	
B-17 F.G.	No. of clusters	-	12	12**	12	12	12**	12**	-	
	No. of bombs	42*	1536	1320	2304	720	456	456	12	
	Total weight, Tons	1.51	3.15	2.79	2.55	2.55	2.55	3.15	2.85	
	Total heat, million BTU	28.1	19.8	17.1	25.8	31.7	20.0	17.3	26.5	
B-26** Series	No. of clusters	-	6	6	6	6	6	6	-	
	No. of bombs	28*	768	660	1152	360	228	228	6	
	Total weight, Tons	1.01	1.58	1.39	1.28	1.27	1.28	1.57	1.42	
	Total heat, million BTU	18.7	9.9	8.5	12.9	15.8	10.0	8.6	13.5	
B-25 Series	No. of clusters	-	6	6	6	6	4	6	-	
	No. of bombs	24*	768	660	1152	360	228	228	6	
	Total weight, Tons	0.8	1.58	1.39	1.28	1.27	1.28	1.57	1.42	
	Total heat, million BTU	16.0	9.9	8.5	12.9	15.8	10.0	8.6	13.5	
A-26* B	No. of clusters	-	6	6	6	4	6	6	-	
	No. of bombs	16	768	660	1152	240	228	228	6	
	Total weight, Tons	0.58	1.58	1.39	1.28	0.85	0.85	1.57	1.42	
	Total heat, million BTU	10.7	9.9	8.5	12.9	10.6	10.0	8.6	13.5	
A-20* C.G.H. J.K.	No. of clusters	-	4	4	4	4	4	4	-	
	No. of bombs	4	512	440	768	240	152	152	4	
	Total weight, Tons	0.14	1.05	0.93	0.85	0.85	0.85	1.05	0.95	
	Total heat, million BTU	2.7	6.6	5.7	8.6	10.6	6.7	5.8	8.8	
A-36 P-51	No. of clusters	-	2	2	2	2	2	2	-	
	No. of bombs	2	256	220	384	120	76	76	2	
	Total weight, Tons	0.07	0.53	0.47	0.43	0.43	0.43	0.53	0.48	
	Total heat, million BTU	1.3	3.3	2.8	4.3	5.3	3.3	2.9	4.4	
P-47	No. of clusters	-	3	3	3	3	3	3	-	
	No. of bombs	3	384	330	576	180	114	114	3	
	Total weight, Tons	0.11	0.79	0.70	0.64	0.64	0.64	0.79	0.71	
	Total heat, million BTU	2.0	5.0	4.3	6.5	7.9	5.0	4.3	6.6	
P-40	No. of clusters	-	3	3	3	3	3	3	-	
	No. of bombs	3	384	330	576	180	114	114	3	
	Total weight, Tons	0.11	0.79	0.70	0.64	0.64	0.64	0.79	0.71	
	Total heat, million BTU	2.0	5.0	4.3	6.5	7.9	5.0	4.3	6.6	
P-38	No. of clusters	-	2	2	2	2	2	2	-	
	No. of bombs	2	256	220	384	120	76	76	2	
	Total weight, Tons	0.07	0.53	0.47	0.43	0.43	0.43	0.53	0.48	
	Total heat, million BTU	1.3	3.3	2.8	4.3	5.3	3.3	2.9	4.4	

* Internal loading only; for external loading add 4 - 100 lb. or 4 - 500 lb. clusters for A-20 G, H, J, K, and A-20B.

** Omitting aft bomb-bay.

◆ Multiple suspension using toggle wires.

◆◆ Minor interference on two bottom inboard stations might reduce loading from 12 to 10.

December 1944

PENETRATION OF REINFORCED CONCRETE BY AP PROJECTILES AND AP AND SAP BOMBS

BASED ON DATA DEVELOPED FOR THE CHIEF OF ENGINEERS

QA 1 CONCRETE PENETRATION

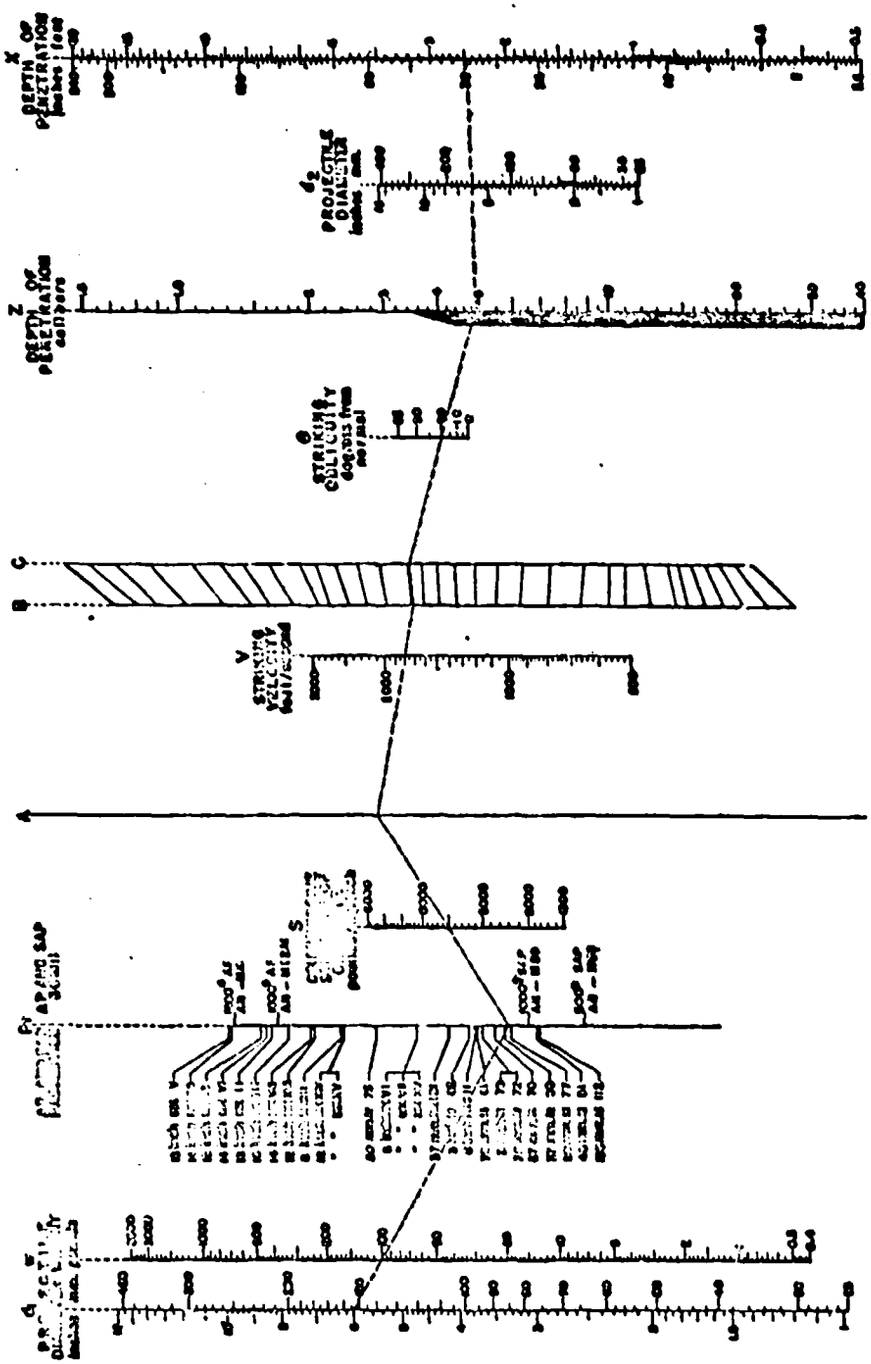

DIRECTIONS: Determine the diameter and weight of the part of the projectile which penetrates the slab. (The total weight minus the weight of the windshield will usually be correct.) Draw a line through the proper points on the d, scale and w scale at the left of the chart to the Pr scale. (If the projectile is a type listed on this scale, the d and w scales will be omitted.) Continue from this point through the S scale to the A scale. From the A scale draw a line through the V scale to the B scale and follow the guide lines to the C scale. From the C scale draw a line through the B scale to the Z scale. (If the point falls within the shaded area the projectile will probably stick in the target.) From the Z scale draw a line through the d scale and read the depth of penetration on the X scale. For oblique fire the depth is the maximum penetration normal to the target face. If the projectile or bomb causes scabbing use 1.8 times the depth of penetration will be somewhat more than shown here. The penetration for oblique fire of velocities above 2000 ft/sec may be somewhat

ACCURACY: This chart gives results accurate within 25 %.

June 1945

PENETRATION OF BOMBS AND PROJECTILES INTO SOIL

2 A2* SOIL PENETRATION

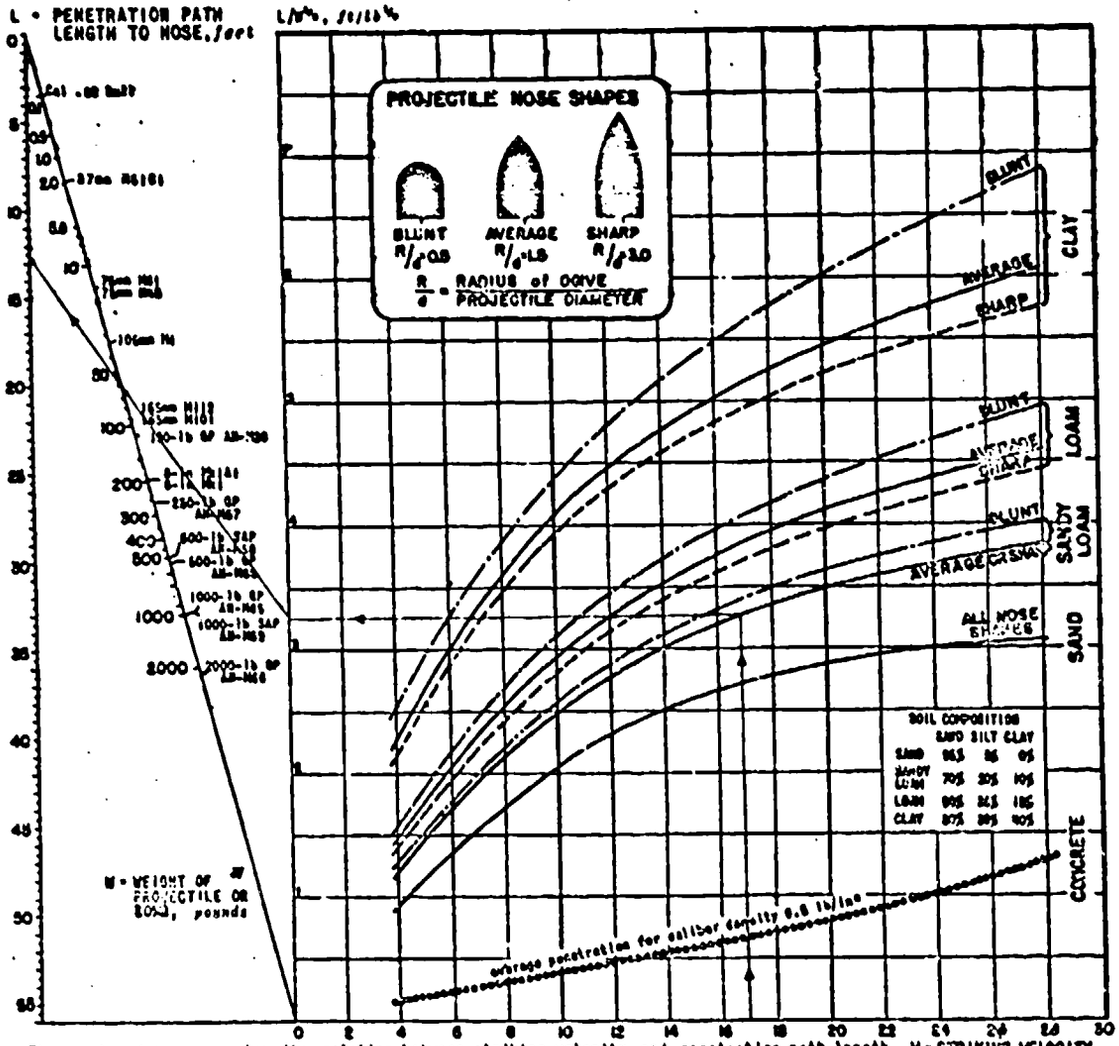

The graph and nomogram give the relation between striking velocity and penetration path length, measured to the nose, for projectiles or bombs of various weights penetrating into several soils. Curves marked *blunt, average, and sharp* are for projectiles of different nose shapes as sketched. Where no appreciable effect of nose shape on penetration has been observed only a single curve is drawn. The dependance of penetration path length on projectile weight, as given by the nomogram, agrees with observations for projectiles or bombs having caliber densities from 0.15 to 0.65 lb/in³. Most bombs and artillery projectiles have caliber density values (weight of projectile in pounds divided by the cube of the diameter in inches) within the above range.

Trajectories in soils are usually straight for two-thirds or more of the path length, but curve near the end of the path (see sketch). For this reason final distance from the surface is usually 10% to 30% less than the penetration path given here.

Curves given are for average soil types. Penetrations into rich plastic clay are approximately 30% greater than those observed in clay. The dotted curve at the bottom of the graph gives average penetration into good quality reinforced concrete, and is added here for rough comparison.

EXAMPLE: The dotted line shows that a projectile of average nose shape and weight of 60 lb striking sandy loam soil with a velocity of 1700 ft/sec will have a path length of approximately 12.5 ft, measured to the nose. Because of the curvature of the underground trajectory, the actual penetration from the surface will be somewhat less.

SOURCE: British and American tests with bombs and large caliber projectiles at velocities below 1100 ft/sec. Small caliber tests for the Corps of Engineers, U.S.A. extending over entire velocity range. The curves agree with measurements to ±20%.

* Revision of 2 A2 dated September 1944

PTM No. 108 February 1945

WEAPON DATA

PENETRATION OF GP BOMBS AND SMALL CALIBER BULLETS INTO SOIL

Q A 2a
SOIL PENETRATION

A - BOMB PENETRATION *for U.S. GP Bombs.*

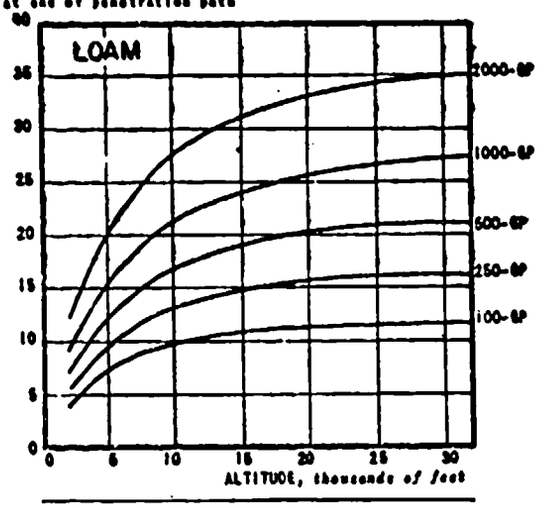

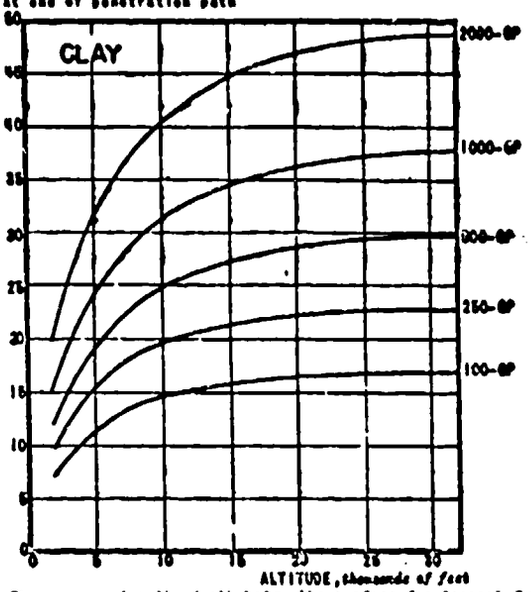

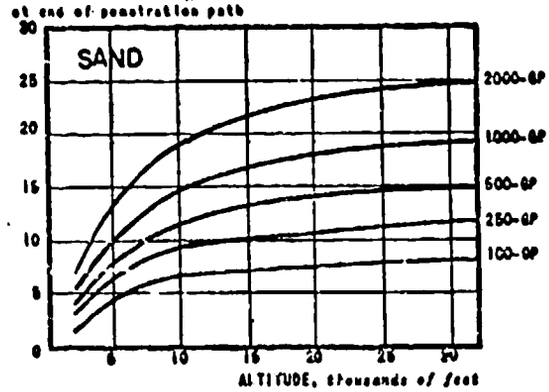

The curves give the depth below the surface for General Purpose bombs dropped from level flight at various altitudes. The depth is that measured from a level surface to the center of the bomb, delay fuzed to permit full penetration.

The designations clay, loam, and sand are for average soil types. For soils of other types interpolation should be made from these curves. For example, the depth in a sandy soil may be expected to be between the values given for sand and the values given for loam.

Bomb penetrations into soil vary due to the irregularities of curvature of the underground trajectory, and may vary appreciably due to inhomogeneities of the soil, water content of the soil, etc. The curves given here agree with the available data to within ± 20%.

B - SMALL CALIBER BULLETS

Penetration of small caliber jacketed bullets into soils is limited by the deformation of the soft tip at low velocities and stripping of the jacket from the core at high velocities. Such deformations result in increased resistance to motion.

The table gives penetration and perforation data for small caliber service ammunition with soft jacket and hard core. The maximum thickness of a soil parapet that can be perforated by a single hit at short range and the recommended minimum thickness of a soil parapet for protection against ten hits close together are given. The protection is adequate only for positions more than twelve inches (25 to 30 calibers) below the top of the parapet.

SOIL	U.S. CALIBER .22 AP				U.S. CALIBER .30 AP			
	Maximum Expected Penetration	Average Penetration, Short Range	Parapet Thickness Perforated	Parapet Thickness for Protection	Maximum Expected Penetration	Average Penetration, Short Range	Parapet Thickness Perforated	Parapet Thickness for Protection
LOOSE SAND	12 in	10 in	13 in	40 in	20 in	18 in	21 in	63 in
COMPACT SAND	9½ in	7½ in	12 in	30 in	15 in	12 in	19 in	48 in
LOAM	16 in	12 in	16 in	44 in	24 in	20 in	26 in	72 in
PLASTIC CLAY	28 in	20 in	28 in	65 in	40 in	30 in	28 in	100 in

SOURCE: The Bomb Penetration Curves are based on British and American tests with bombs and large caliber projectiles. The Small Caliber Bullet Tabulation is based on tests for the Corps. of Engineers, U.S.A.

PTM Sec 103 April 1946

NATIONAL DEFENSE RESEARCH COMMITTEE
DIVISION 2, PRINCETON UNIVERSITY STATION

ENGINEERING DATA

9.4.3
CONCRETE
PROFILES & LIMITS

PENETRATION PROFILES AND BALLISTIC LIMITS FOR REINFORCED CONCRETE SLABS

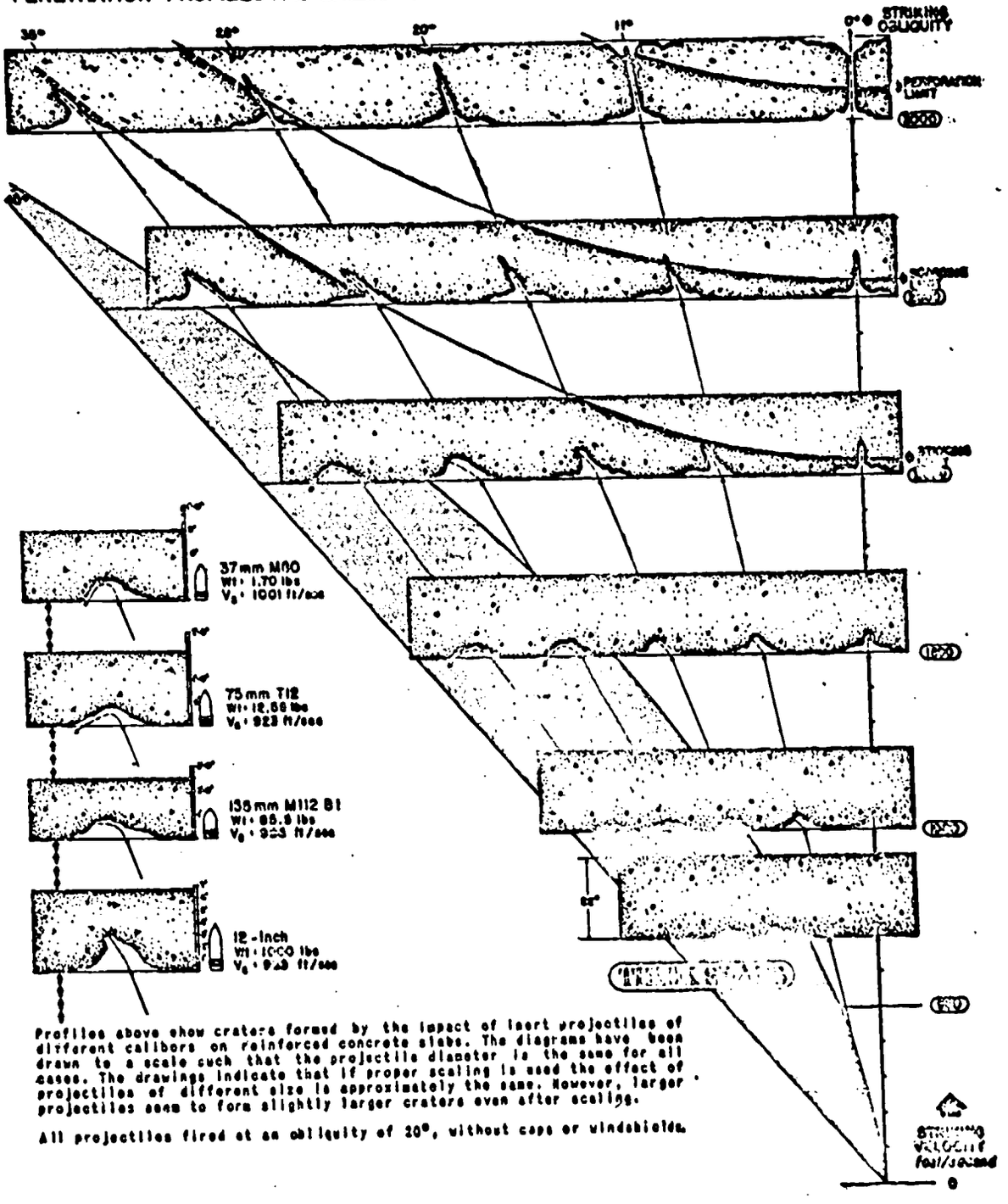

Profiles above show craters formed by the impact of inert projectiles of different calibers on reinforced concrete slabs. The diagrams have been drawn to a scale such that the projectile diameter is the same for all cases. The drawings indicate that if proper scaling is used the effect of projectiles of different size is approximately the same. However, larger projectiles seem to form slightly larger craters even after scaling.

All projectiles fired at an obliquity of 20°, without caps or windshields.

CONFIDENTIAL

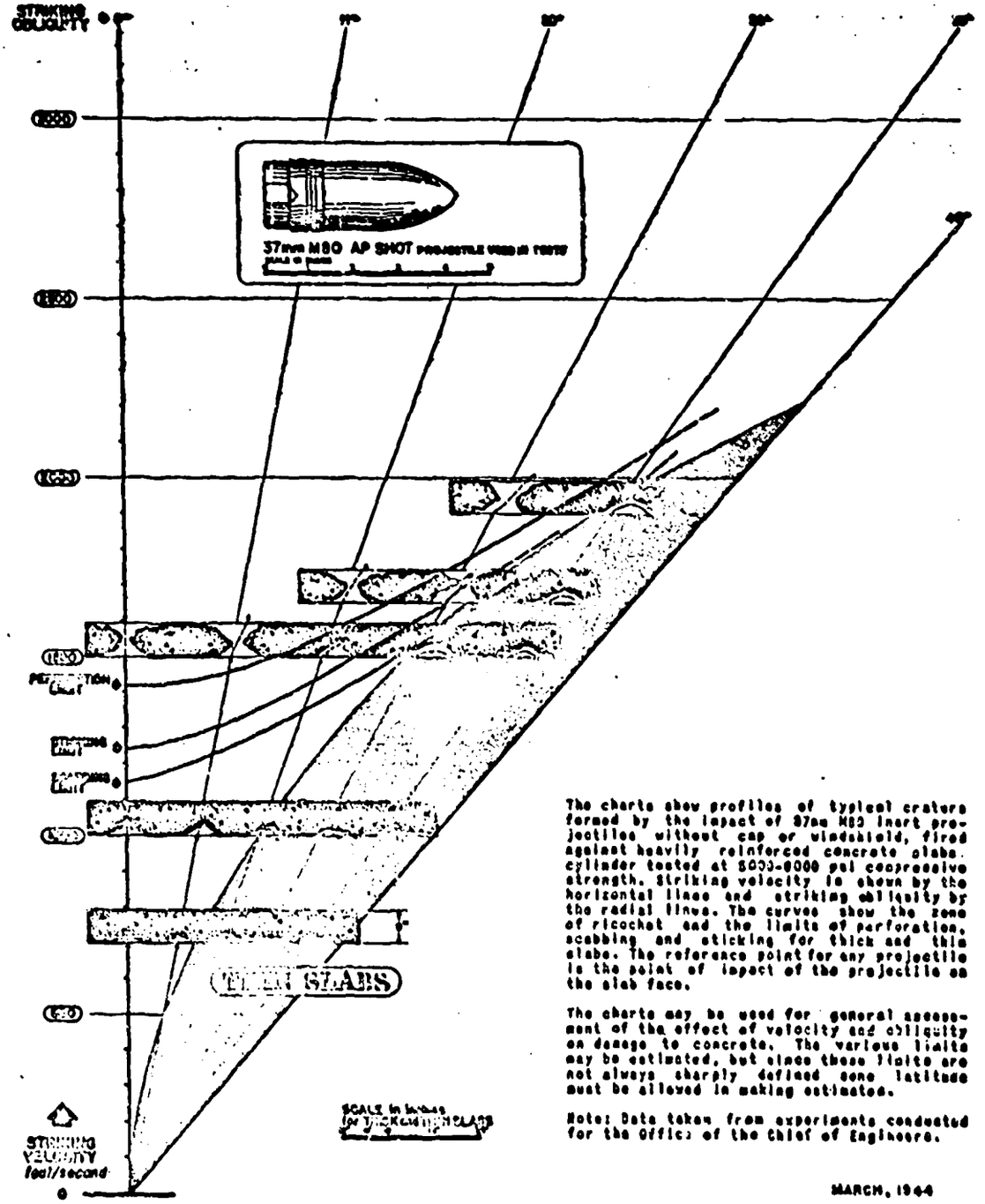

The charts show profiles of typical craters formed by the impact of 37mm M80 inert projectiles without cap or windshield, fired against heavily reinforced concrete slabs cylinder tested at 5000-6000 psi compressive strength. Striking velocity is shown by the horizontal lines and striking obliquity by the radial lines. The curves show the zone of ricochet and the limits of perforation, scabbing and sticking for thick and thin slabs. The reference point for any projectile is the point of impact of the projectile on the slab face.

The charts may be used for general assessment of the effect of velocity and obliquity on damage to concrete. The various limits may be estimated, but since these limits are not always sharply defined some latitude must be allowed in making estimates.

Note: Data taken from experiments conducted for the Office of the Chief of Engineers.

MARCH, 1944

2 A 5
RICOCHET

RICOCHET FROM WATER, SOIL AND CONCRETE

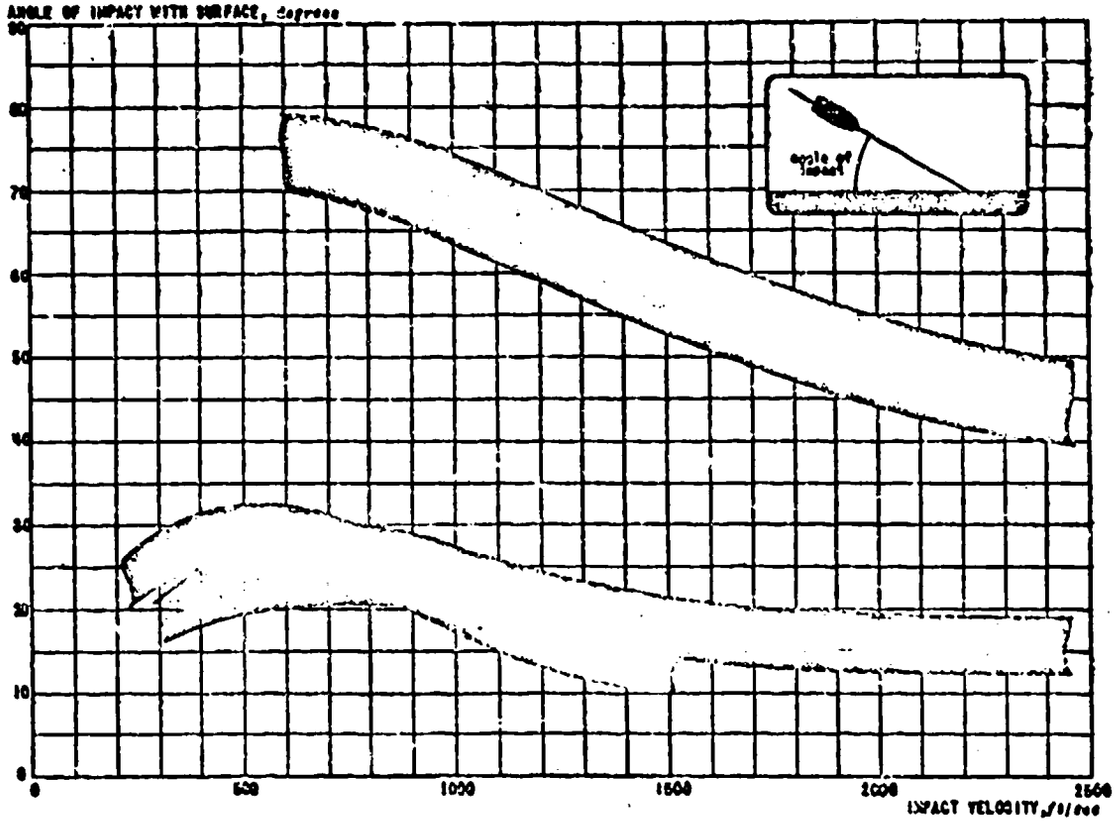

The graph gives the limiting angle separating ricochet and penetration for water, soil or massive concrete as a function of striking velocity. For armor or mild steel plate the limiting angle is different for each plate thickness; these are not treated here. The curves apply to ordinary projectiles and bombs, without special attachments or nose shapes.

The ricochet limits are represented in the form of bands, the width of each band including variation of many factors such as nose shape, moment of inertia, density of the projectile and density of the material. Each band on the graph separates two regions: ricochet occurs for combinations of striking velocity and impact angle below the band, no ricochet occurs for combinations above the band. The portions of each band with dotted edges are based on a small amount of data.

In general, missiles having sharp noses, long slender bodies or low densities will have ricochet limits in the upper part of each band, while those having blunt noses, short bodies or high densities will have ricochet limits in the lower part of each band. Increasing the surface regularity or the density of the target generally shifts ricochet limits toward the lower part of each band.

SOURCE: Soil and water ricochet data are from Aberdeen Proving Ground; concrete ricochet data are from the Office of the Chief of Engineers, U. S. Army.

August 1958

SCABBING OF REINFORCED CONCRETE BY AP PROJECTILES AND AP AND SAP BOMBS

BASED ON DATA DEVELOPED FOR THE CHIEF OF ENGINEERS

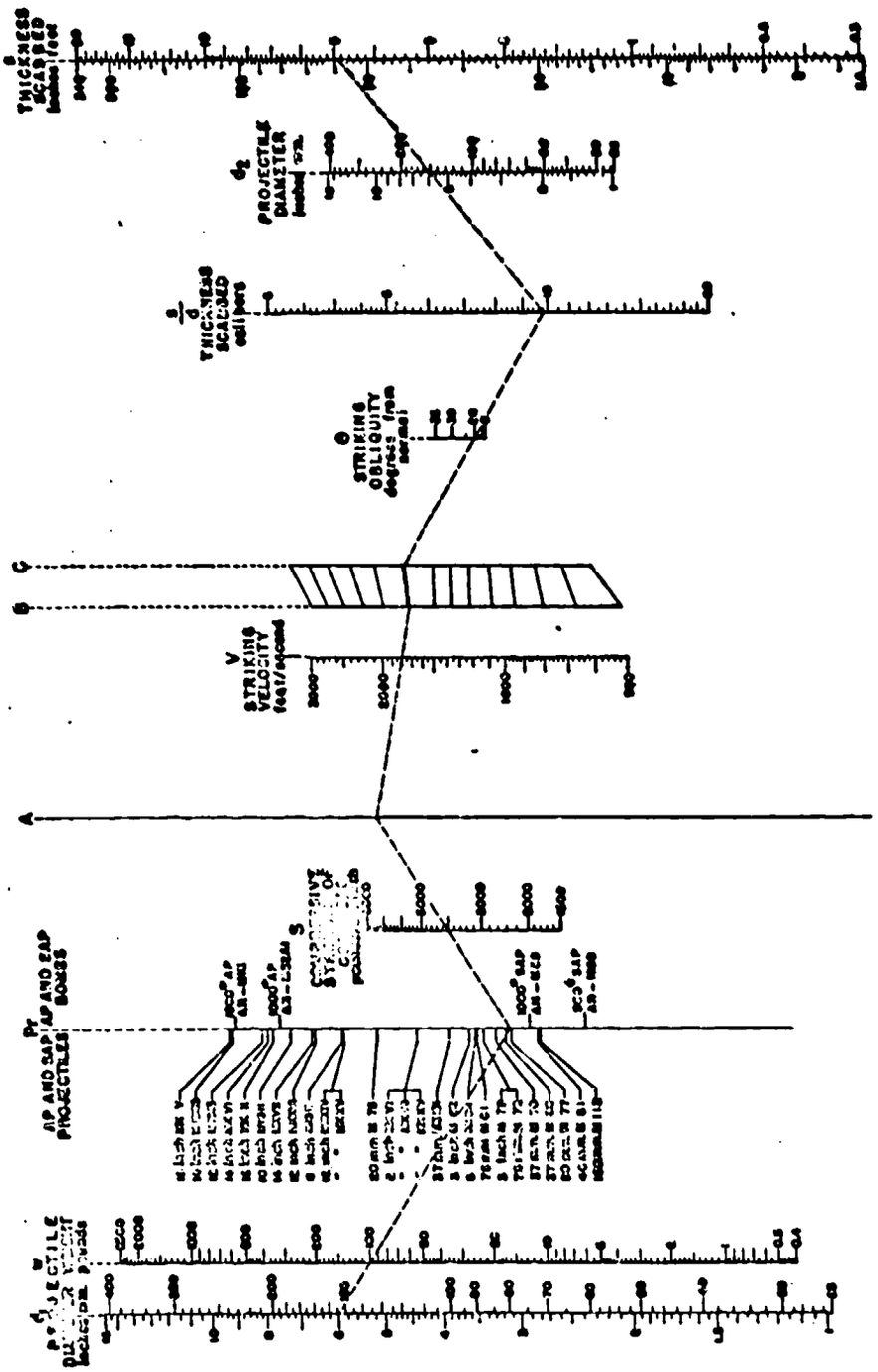

DIRECTIONS: Determine the diameter and weight of that part of the projectile which penetrates the slab. (The *total* weight minus the weight of the windshield will usually be correct.) Draw a line through the proper points on the d_p scale and W scale at the left of the chart to the Pr scale. (If the projectile is a type listed on this scale, the above may be omitted.) Continue from this point through the S scale to the A scale. From the A scale draw a line through the V scale to the C scale and from the C scale draw a line through the θ scale to the $\frac{T}{d_p}$ scale. From this point draw a line through the $\frac{T}{d_p}$ scale to the T scale. The thickness scabbed by oblique fire at velocities above 2000 f/s may be somewhat more than shown here.

ACCURACY: This chart gives results accurate within 15%.

Example: [illegible] 100 pound projectile, striking 2000 f.p.s. normal with a velocity of 1,900 ft/sec at an obliquity of 30° the projectile will scab [illegible] 6.8 inches.

June 1943

WEAPO[illegible]

PERFOR[illegible]ONCRETE BY AP [illegible]ND SAP BOMBS

BASED ON DATA DEVELOPED [illegible]

CONCRETE PERFORATION

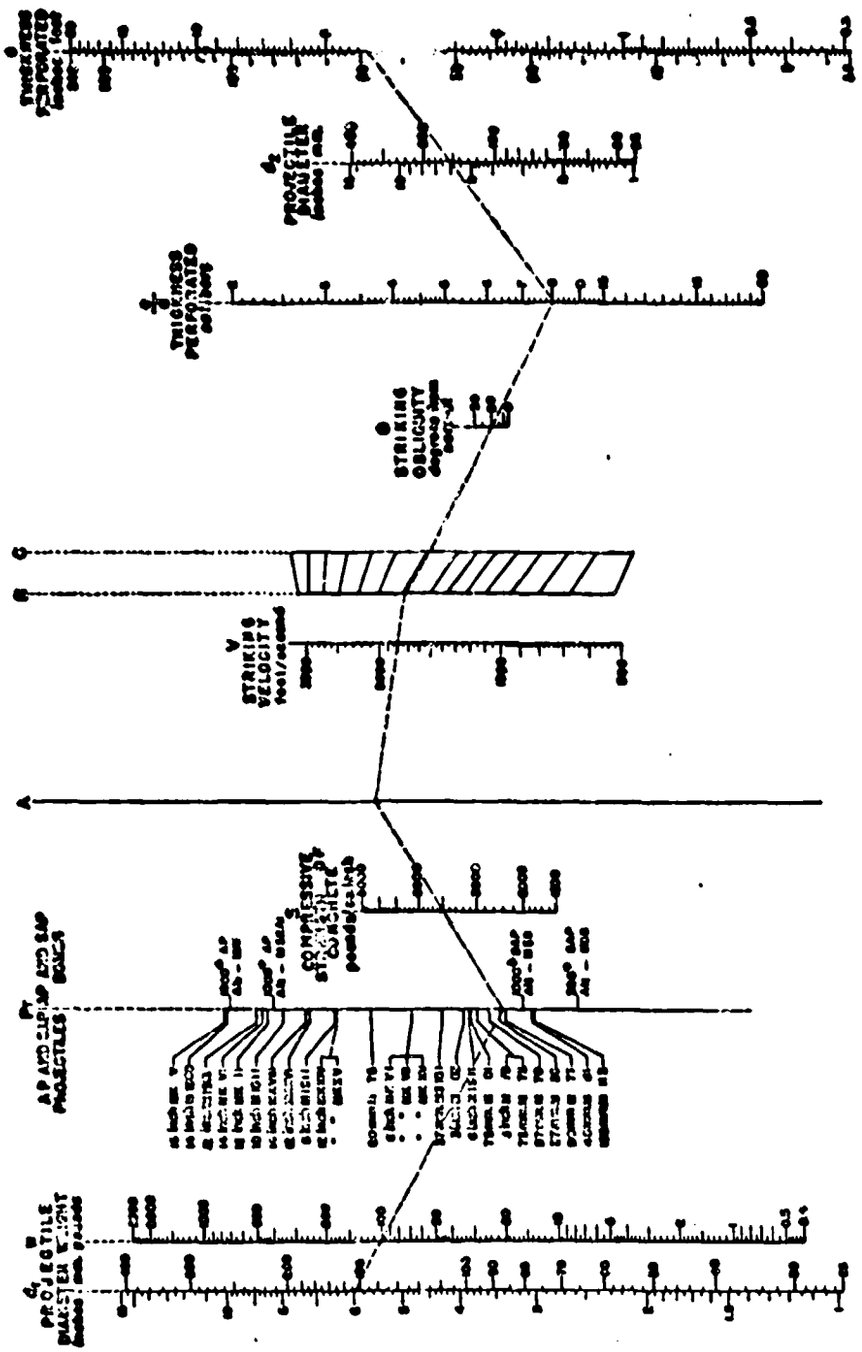

DIRECTIONS: Determine the diameter and weight of that part of the projectile which perforates the slab. (The total weight minus the weight of the windshield will usually be correct.) Draw a line through the proper points on the d_p scale and w scale at the left of the chart to the Pr scale. (If the projectile is a type listed on this scale, the above may be omitted.) Continue from this point through the S scale to the A scale. From the A scale draw a line through the V scale to the B scale and follow the guide lines to the C scale. From the C scale draw a line through the G scale to the e/d scale. From this point draw a line through the d_p scale and read the thickness that will be perforated from the e scale. The thickness perforated by average fire at velocities above 2000 ft./sec may be somewhat more than shown here.

ACCURACY: This chart gives results [illegible]

[illegible]

June 1945

CONFIDENTIAL

WEAPON DATA

9 C1a
PERFORATION OF R/C: SPECIFIC

PERFORATION OF REINFORCED CONCRETE BY SPECIFIC BOMBS AND ROCKETS

BOMB (delay fuzed)	ALTITUDE ft	CONCRETE PERFORATION, feet		SOIL PENETRATION, ft		CONCRETE PERFORATION, ft, WITH SOIL COVER OF VARIOUS THICKNESSES, ft					MINIMUM ALTITUDE ATTACK OF VERTICAL CONCRETE WALLS THICKNESS PERFORATED feet
		3000 psi	5000 psi	Sand	Loam	2 ft	4 ft	6 ft	8 ft	10 ft	By Bombs
100-lb GP AN-M30	5000	1.0 ft limited by case strength	0.75 ft limited by case strength	6	8	0.7	0.5	-	-	-	
	10000			7	10	0.7	0.7	-	-	-	
	15000			7½	11	0.7	0.7	-	-	-	
	20000			8	11½	0.7	0.7	0.5	-	-	
	25000			8	11½	0.7	0.7	0.5	-	-	
250-lb GP AN-M57	5000	1.5 ft limited by case strength	1.0 ft limited by case strength	7	10	1.0	0.8	-	-	-	
	10000			9½	13½	1.0	1.0	0.8	-	-	
	15000			10½	15	1.0	1.0	1.0	-	-	
	20000			11	16	1.0	1.0	1.0	0.8	-	
	25000			11½	16	1.0	1.0	1.0	0.8	-	
500-lb GP AN-M64, M65	5000	1.7 ft limited by case strength	1.5 ft limited by case strength	8	12½	1.3	1.1	0.9	-	-	1.5
	10000			12	17	1.3	1.3	1.3	1.1	-	
	15000			13½	19	1.3	1.3	1.3	1.2	-	
	20000			14½	20½	1.3	1.3	1.3	1.2	1.1	
	25000			15	21	1.3	1.3	1.3	1.3	1.2	
1000-lb GP AN-M44, M65	5000	2.3 ft limited by case strength	1.7 ft limited by case strength	10½	16	1.7	1.7	1.3	1.1	-	1.5
	10000			15	22	1.7	1.7	1.7	1.7	1.3	
	15000			17	26	1.7	1.7	1.7	1.7	1.3	
	20000			18½	26	1.7	1.7	1.7	1.7	1.7	
	25000			19	27	1.7	1.7	1.7	1.7	1.7	
2000-lb GP AN-M66, M65	5000	2.8 ft limited by case strength	2.1 ft limited by case strength	12½	20½	2.1	2.1	2.1	1.9	1.7	2.0
	10000			18½	28	2.1	2.1	2.1	2.1	2.1	
	15000			22	31½	2.1	2.1	2.1	2.1	2.1	
	20000			24	33½	2.1	2.1	2.1	2.1	2.1	
	25000			24½	34½	2.1	2.1	2.1	2.1	2.1	
500-lb SAP AN-M58	5000	2.5	2.0	8	12½	1.7	1.4	1.1	-	-	1.5
	10000	3.0	2.7	12	17	2.4	2.1	1.7	1.3	-	
	15000	3.6	3.1	13½	19	2.7	2.4	2.1	1.8	-	
	20000	3.8	3.3	14½	20½	2.9	2.6	2.3	1.9	1.6	
	25000	4.1	3.5	15	21	3.2	2.8	2.5	2.2	1.8	
1000-lb SAP AN-M59	5000	3.0	2.7	10	16	2.4	2.1	1.8	1.5	-	2.0
	10000	3.8	3.5	15	22	3.2	2.9	2.5	2.2	1.9	
	15000	4.3	4.1	17	24	3.7	3.4	3.1	2.7	2.5	
	20000	5.1	4.9	18½	26	4.0	3.7	3.3	3.0	2.6	
	25000	5.5	4.7	19	27	4.3	4.0	3.7	3.3	3.0	
2000-lb SAP M 103	5000	3.8	3.0	13½	20½	2.7	2.4	2.1	1.8	1.5	
	10000	5.1	4.4	18½	28	4.1	3.8	3.5	3.1	2.8	
	15000	6.1	5.8	22	31½	5.0	4.6	4.3	4.0	3.6	
	20000	6.8	6.6	24	33½	5.4	5.1	4.7	4.4	4.0	
	25000	7.2	6.2	25½	34½	5.8	5.5	5.1	4.7	4.4	
1000-lb AP AN-M 23	5000	2.7	2.5	10½	16	2.2	1.9	1.7	1.1	-	
	10000	4.0	3.8	15	22	3.2	2.9	2.6	2.2	1.9	
	15000	5.2	4.8	17	25	3.8	3.6	3.2	2.9	2.5	
	20000	5.9	5.9	18½	26	4.5	4.1	3.7	3.3	2.9	
	25000	6.4	6.2	19	27	4.8	4.4	4.0	3.7	3.3	
1000-lb AP AN-M 1	5000	3.6	3.0	12½	19	2.7	2.4	2.1	1.8	1.6	
	10000	4.8	4.2	17½	26	3.8	3.5	3.2	2.9	2.6	
	15000	6.2	5.2	20	29	4.8	4.5	4.1	3.8	3.5	
	20000	7.1	6.8	21½	30	5.4	5.0	4.6	4.3	3.9	
	25000	7.8	8.4	22	31	6.0	5.6	5.2	4.7	4.3	

CONCRETE PERFORATION BY ROCKETS
5-inch HVAR M46
2.4 feet
11.75-inch AR M12
4.5 feet

The table gives the thickness of reinforced concrete and thickness of concrete with soil cover that can be perforated by GP, SAP, and AP bombs dropped from planes in level flight at 200 to 300 m.p.h. at various altitudes. The depth of penetration of the same bombs into soil is included for comparison.

Bombs should be fuzed 0.025 seconds delay or longer to insure perforation before detonation. The values given in the table apply to bombs with this fuze delay.

SOURCE: Based on Data Sheets 2A2*, 2C1, and Interim Memorandum No. M-13 of the Committee on Fortification Design.

August 1945

WEAPON DATA:

9.C.2 PLASTIC PROTECTION PERFORATION

PERFORATION OF PLASTIC PROTECTION

DESCRIPTION

PLASTIC PROTECTION CONSISTS OF A MIXTURE, IN PROPORTIONS BY WEIGHT AS GIVEN, OF THE FOLLOWING MATERIALS: COARSE MINERAL AGGREGATE (usually gravel) - 40%; LIMESTONE DUST FILLER - 30%; MASTIC BITUMEN and/or COAL TAR PITCH - 10%. A LAYER OF THIS MIXTURE IS BACKED BY A 1/8-INCH TO 1/4-INCH THICK PLATE OF MILD STEEL. TO INCREASE THE STRUCTURAL STRENGTH AS WELL AS THE STOPPING POWER OF THE MATERIAL, CHICKEN WIRE OR EXPANDED METAL IS EMBEDDED IN THE PLASTIC MIXTURE AT THE CENTER OR NEAR THE FRONT SURFACE. OCCASIONALLY, A FRONT PLATE OF 20-GAUGE (or heavier) STEEL IS APPLIED.

EFFECTIVENESS

STOPPAGE OF THE PROJECTILE IS LARGELY DUE TO THE BREAKING-UP AND YAWING OF THE CORES BEFORE REACHING THE BACK PLATE. INASMUCH AS THIS PROCESS MAY OCCUR IN A LARGE NUMBER OF WAYS, THERE IS NO SHARPLY DEFINED LIMITING VELOCITY FOR A GIVEN THICKNESS OF THE MATERIAL SUCH THAT FOR HIGHER VELOCITIES ALL BULLETS WILL PERFORATE WHILE FOR LOWER VELOCITIES NONE WILL. IT MAY BE SAID ONLY THAT A CERTAIN PERCENTAGE OF PROJECTILES TRAVELING AT A GIVEN VELOCITY WILL BE STOPPED BY A GIVEN THICKNESS OF PLASTIC PROTECTION.

AMOUNTS OF PLASTIC PROTECTION, MILD STEEL AND SPECIAL TREATED STEEL REQUIRED FOR " ADEQUATE PROTECTION "

(50% PERFORATION AT NORMAL IMPACT AND CLOSE RANGE)

PROJECTILE	STRIKING VELOCITY ft./sec.	PLASTIC PROTECTION			MILD STEEL		SPECIAL TREATED STEEL	
		t_b inches	t inches	W lbs./sq.ft.	t inches	W lbs./sq.ft.	t inches	W lbs./sq.ft.
British -303 inch, Mk VI, Ball	2440	1/8	1-1/8	20			1/4	10
American -30 caliber Ball	2580	3/16	1-1/16	23				
British -303 inch AP	2440	3/16	2-1/4	34	1.04 *	42.4 *	.71 *	29 *
American -30 cal., M-2 AP	2580	3/16	3-1/8	44	1.10	43.1	3/4	34
British -.55 inch AP	2400	1/4	5	72				
American -.50 cal., M-2 AP	2900	3/16	5 to 6	70 to 85	2.20 *	89.8 *	1-1/2	60
British -20 mm. AP	2750	1/4	7-7/8	110				
Splinter from U.S. 250-lb. G.P. Bomb at 37.5 feet	-	3/16	1-1/2	26	1.35	55.0	0.9	36

NOTES t_b - thickness of mild steel backing plate
t - total thickness (including backing plate)
W - total weight per unit area (including backing plate)

* these figures are estimates derived from the assumption that the thickness perforated is directly proportional to the mass of the projectile and to the square of the striking velocity and inversely proportional to the square of the caliber.

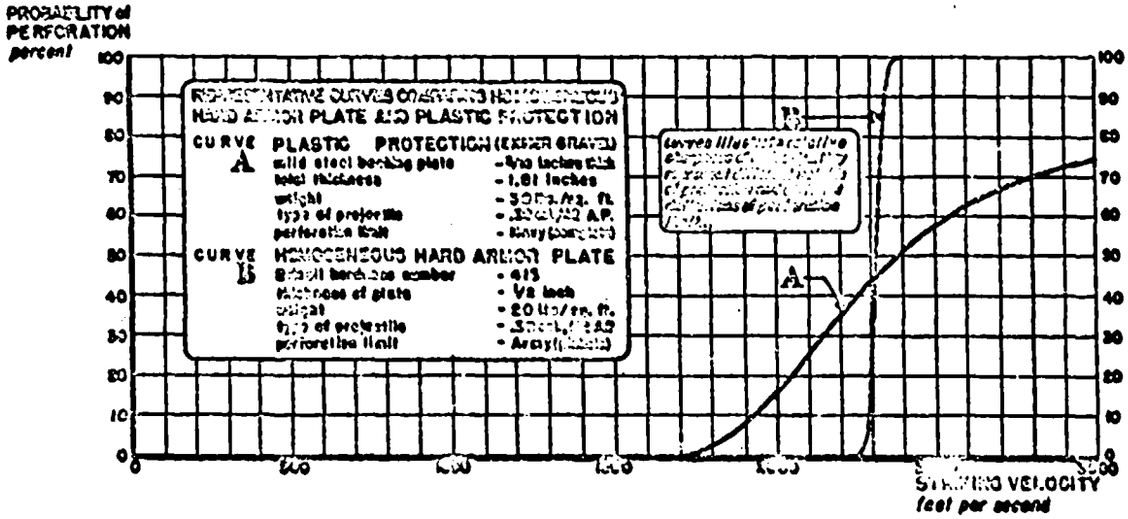

September 1945

CONFIDENTIAL

WEAPON DATA

PERFORATION OF HOMOGENEOUS ARMOR (BHN 250-300) BY UNCAPPED AP PROJECTILES

2 C3 ARMOR PERFORATION

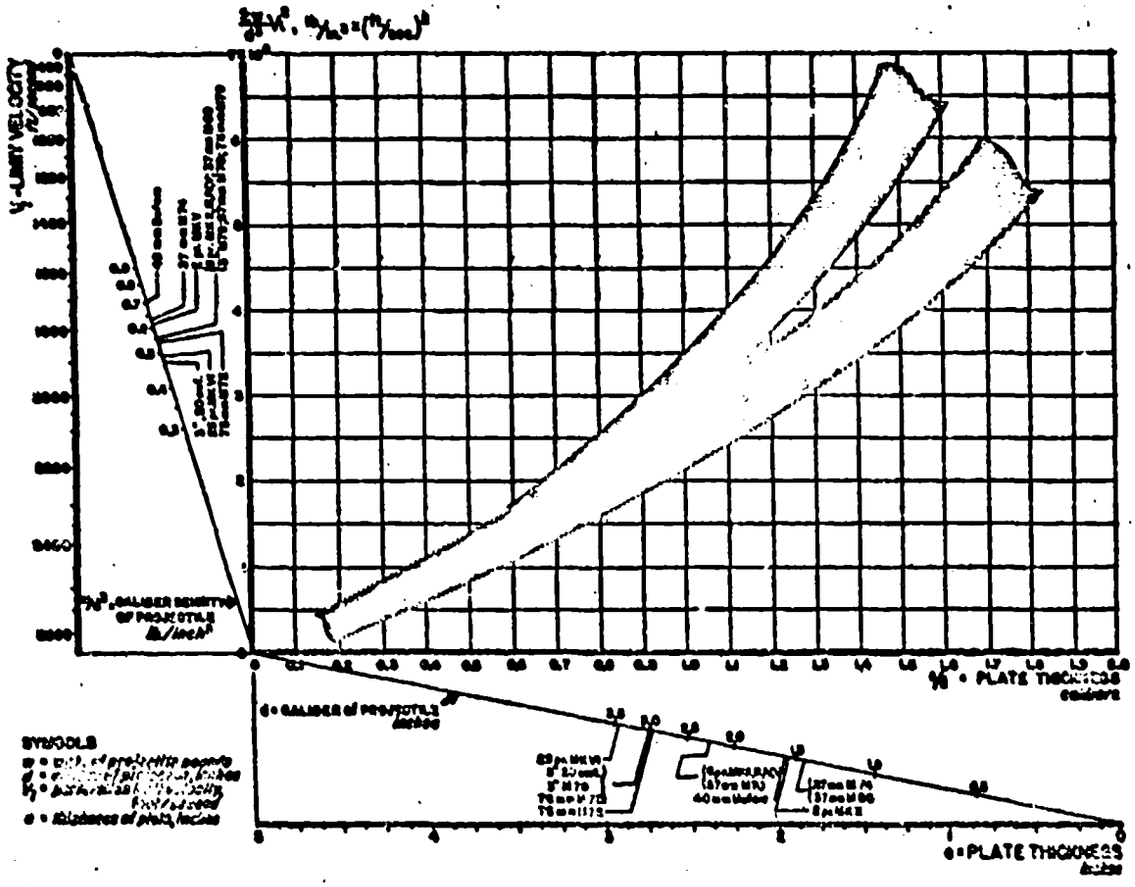

THE GRAPH SHOWS THE RELATION BETWEEN PERFORATION LIMIT VELOCITY AND THICKNESS OF PLATE PERFORATED. THE LIMIT VELOCITY DESCRIBED IS THAT AT WHICH THE PROJECTILE JUST PASSES COMPLETELY THROUGH THE PLATE (very little). THE DATA REPRESENT ARMOR PIERCING (AP) UNCAPPED PROJECTILES RANGING FROM 1.46 inches TO 3.14 inches IN CALIBER AGAINST HOMOGENEOUS ARMOR OF BHN 250 - 300 AT BOTH NORMAL INCIDENCE AND AN OBLIQUITY OF 30 DEGREES.

BECAUSE OF INHERENT SCATTER OF THE DATA, THE RESULTS FOR EACH OF THE TWO ANGLES OF INCIDENCE ARE PRESENTED IN THE FORM OF A BAND. EACH BAND, THEREFORE, MAY BE LOOKED UPON AS SEPARATING TWO REGIONS OF THE GRAPH, CORRESPONDING TO VULNERABILITY (above) AND SAFETY (below).

EXAMPLES:

A) Striking a 75mm M72 projectile striking at 30° obliquity with velocity of 2000 ft./sec., the values of plate thickness for 3-1/2 inches and 3-1/8 inches are read by following the lines to the left of the two borders of the band. It is reasonable to assume that plate thicknesses greater than 3-7/8 inches will be safe against the given projectile, while thicknesses less than 3-3/8 inches will be vulnerable.

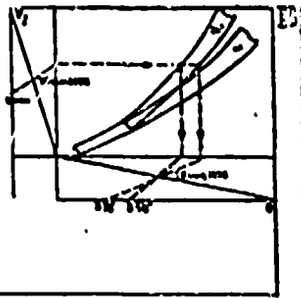

B) Similarly, for the given projectile (example A) fired at a plate 3.5 centimeters thick, two values of the striking velocity result from reading the band. The plate is probably about 50-50 vulnerable. The plate required to be fully safe against striking velocities less than 2000 ft./sec. and vulnerable to velocities greater than 2250 ft./sec.

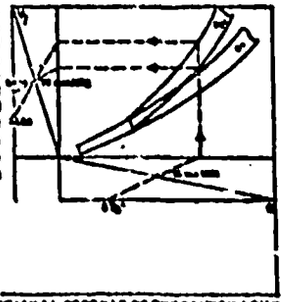

NOTE: GRAPH INCLUDES DATA FROM THE NAVAL PROVING GROUND, DAHLGREN, VA., AND THE DEPARTMENT OF MATHEMATICS OF THE CITADEL

October 1948

PERFORATION OF HOMOGENEOUS ARMOR (BHN 250-300) BY AMERICAN PROJECTILES

2 C3a
PERFORATION OF ARMOR-PROJECTILES

CURVES FOR INDIVIDUAL AP AND APC PROJECTILES

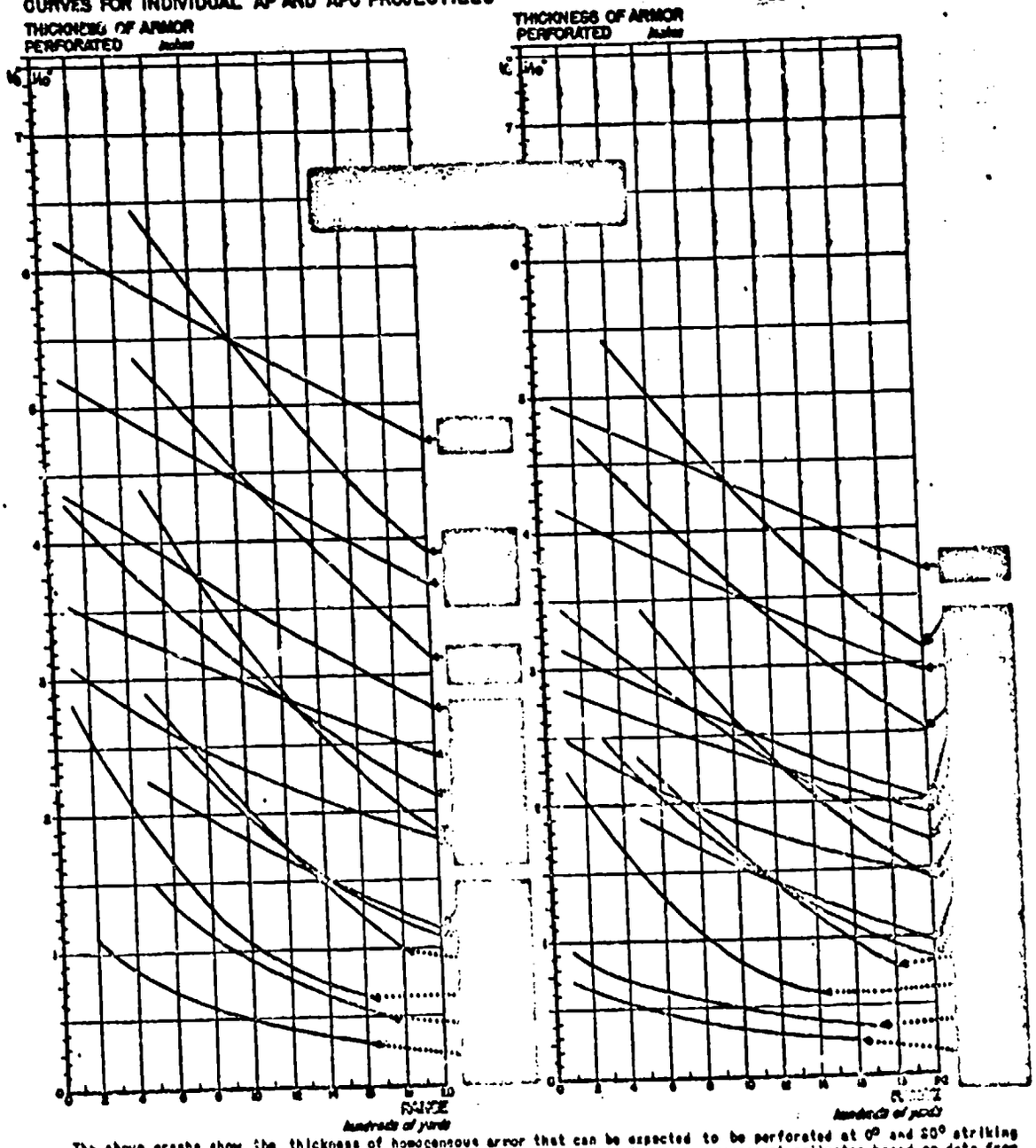

The above graphs show the thickness of homogeneous armor that can be expected to be perforated at 0° and 30° striking angles for various ranges by individual projectiles of known weight. The curves represent estimates based on data from actual firings or extrapolations of results of trials with other projectiles.

For information on perforation of homogeneous armor by other projectiles, see Data Sheet 2 C3.

SOURCE: Ballistic Section, Technical Division, Office of the Chief of Ordnance (U.S.).

PTM No. 112
April 1945

WEAPON DATA

PERFORATION OF THIN HOMOGENEOUS HARD ARMOR BY SMALL CALIBER AP PROJECTILES

2d C4 ARMOR PERFORATION

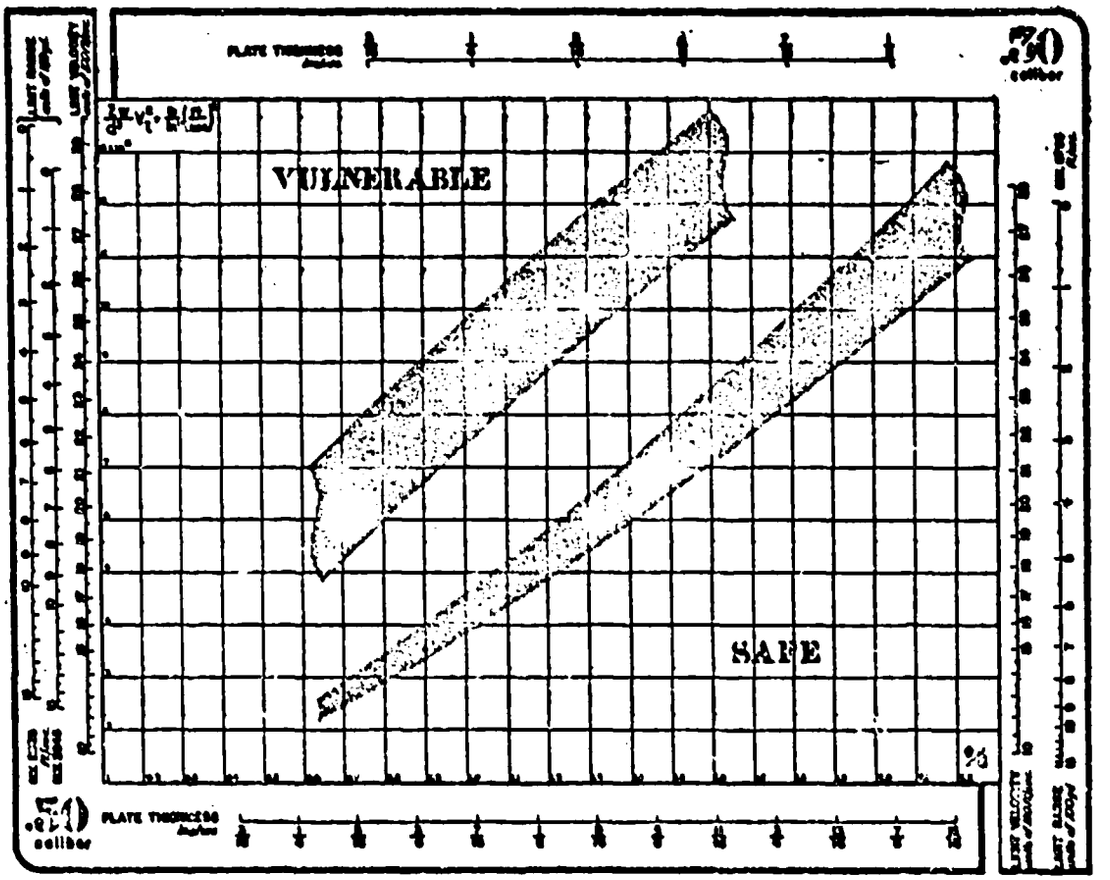

The graph shows the relation between perforation limit striking velocity (perforation limit range) and thickness of plate perforated for Caliber .50 M2 and Caliber .30 M2 AP projectiles fired against Homogeneous Hard Armor of BHN 350-550 at normal incidence and at an obliquity of 30°. The limit velocity concerned is that at which the projectile just passes completely through the plate (Navy Limit). Each value of limit velocity corresponds to a given range, depending on the M.V. of the gun. Range values for service muzzle velocities are given by the appropriate scales at each side of the chart.

Because of inherent scatter of the data, results are presented in the form of a band and may be looked upon as separating two regions of the graph: (a) "vulnerability" above and (b) "safety" below. The 0° band is drawn to include about 95% of the available firing data, while the 30° band includes 80% of the data for this angle.

When thin Homogeneous Hard Armor in this Brinell range is used on aircraft, the limit velocity is considerably increased due to the tipping effect of the skin of the plane. The increase may amount to several hundred feet per second if the bullet is in a sidewise position when striking the armor.

EXAMPLES:

A Given a Cal .50 M2 AP projectile striking at 0° with a velocity of 2500 ft/sec, the values of plate thickness about 5/8 in. and 3/4 in. are read by following the line to each of the two borders of the band. It is reasonable to assume that plate thicknesses greater than 3/4 in. will be safe against the projectile, while thicknesses less than 5/8 in. will be vulnerable.

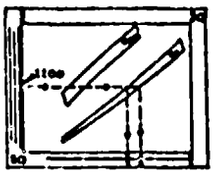

B Similarly, for same projectile striking normally at a plate 3/8 in. thick, the values of striking velocity for the pairs of range values, corresponding to M.V.'s, result by reading to the two borders of the band, namely about 2000 and 2400 f/s or 700 and 850 yds. or 2100 and 2400 yd. The plate reference is to likely to be safe against striking velocities less than 2000 f/s (ranges greater than 700 or 750 yds.) and vulnerable to velocities greater than 2300 f/sec (ranges less than 550 or 600 yds.)

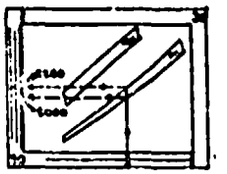

BASED ON DATA FROM THE NAVAL RESEARCH LABORATORY, U.S. NAVAL PROVING GROUND, BALLISTIC RESEARCH LABORATORY, AND WATERTOWN ARSENAL

May 1943

WEAPON DATA

PERFORATION OF HOMOGENEOUS ARMOR BY BOMBS

C 5*
PERFORATION OF ARMOR: BOMBS

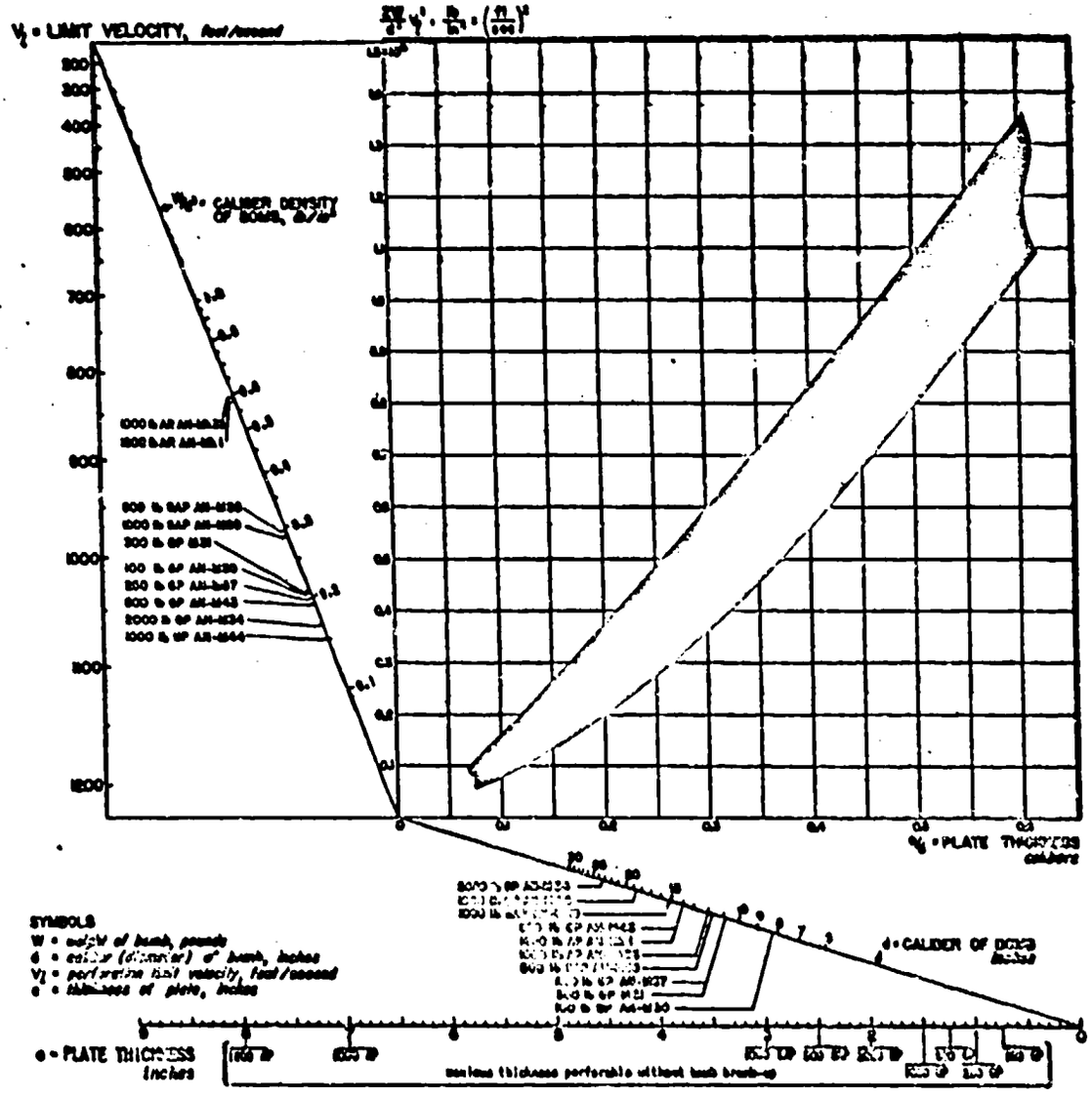

The graph gives the relation between the striking velocity of a bomb and the thickness of homogeneous armor which it will perforate. Due to inherent scatter of the data, the relationship is represented in the form of a band, and strikes at obliquities from 0° to 30° are included in it.

EXAMPLE: Given a 1000-lb AN-[illegible] AP bomb striking with a velocity of 800 ft/sec; it can be expected to remain intact and to have a perforation limit thickness of [illegible] to 6 inches of armor.

SOURCE:
Bureau of Ordnance, U.S.N., Sketch No. [illegible] revision B and Woolwich Bomb Report A4700, Research Dept, Woolwich, England

*Revision of Data Sheet 2 C5, dated July 1944

PTH No.100 February 1945

WEAPON DATA

PERFORATION OF HOMOGENEOUS ARMOR BY BOMBS

CURVES FOR INDIVIDUAL BOMBS BASED ON DATA SHEET 2-C8

9 C5a
PERFORATION OF ARMOR: BOMBS

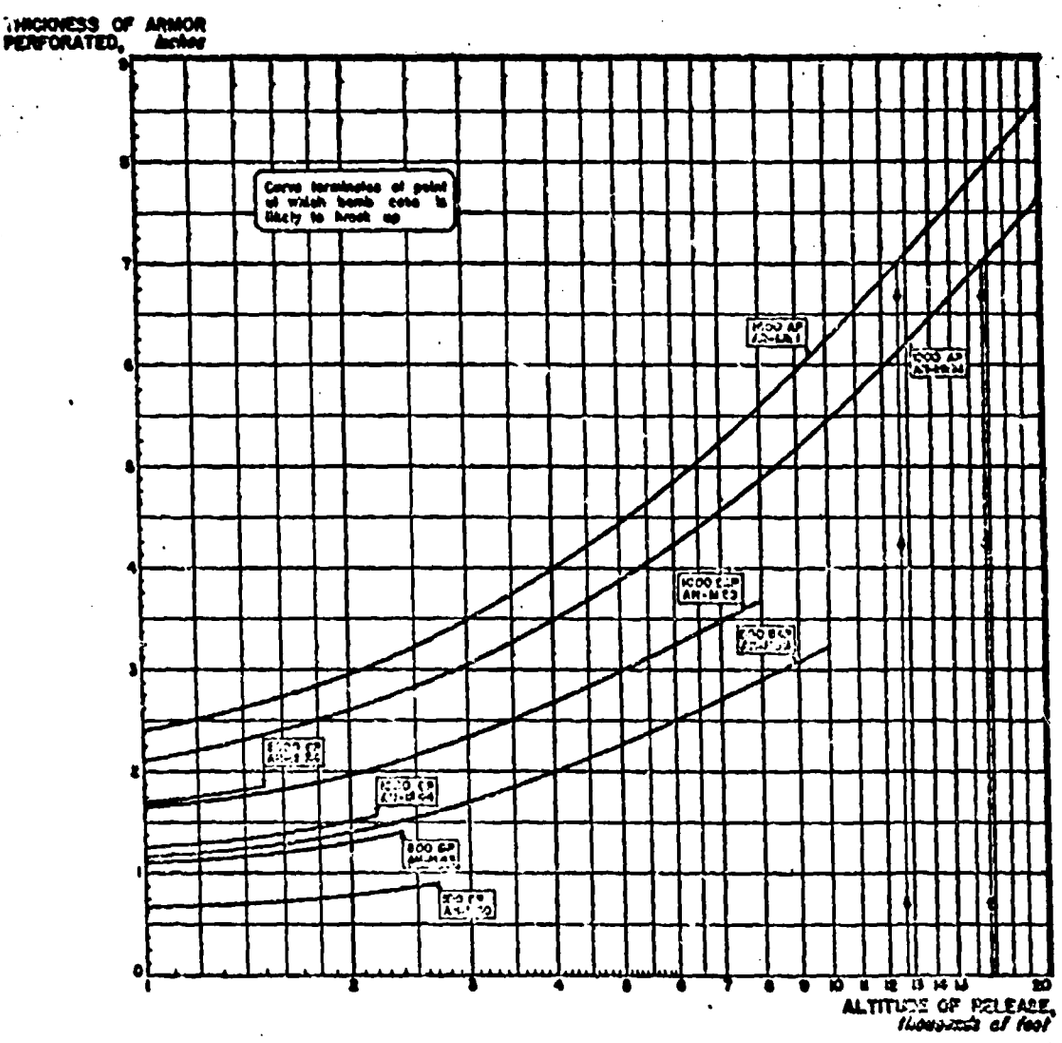

The curves give the thickness of homogeneous armor, in a horizontal position, perforated by a bomb released from a plane in horizontal flight at a ground speed of 200 to 500 m.p.h.

EXAMPLE: The dotted line indicates that in order to perforate 7 inches of armor the 1000-lb. AP bomb should be released above 17,000 feet and the 1000-lb. AP bomb at an altitude above 18,500 feet. All other bombs are likely to break up on striking armor of this thickness.

ACCURACY: Values read from the curves are estimated to be accurate to within 15%.

SOURCE: "Selection of Bombs and Fuses to be Used Against Various Targets", Op-Nav-16-V # A8, Office of the Chief of Naval Operations, and Woolwich Bomb Report A4700, Research Dept., Woolwich, England

August 1944

WEAPON DATA

PERFORATION OF HOMOGENEOUS ARMOR BY TUNGSTEN CARBIDE CORED PROJECTILES

2 CG ARMOR PERFORATION

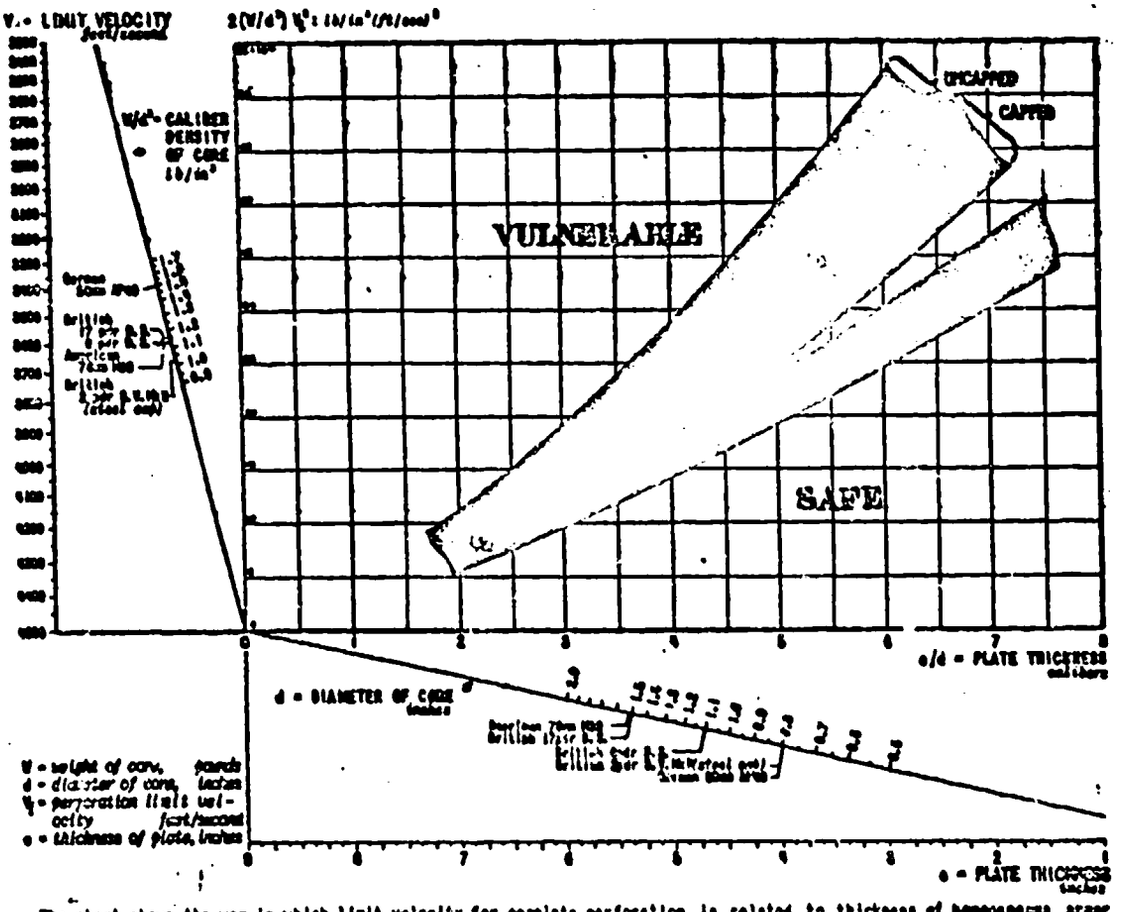

The chart shows the way in which limit velocity for complete perforation is related to thickness of homogeneous armor (BHN 220-280) perforated by capped and uncapped tungsten carbide cored projectiles striking at normal incidence and at 30° to the normal. The data represent projectiles having cores ranging from 0.65 to 1.52 inches in diameter. Indicated on the nomogram scales are projectiles with cores standardized for field use.

Because of inherent scatter of firing data, results are presented as bands. For each obliquity, the band was drawn to include 80% of the points. Capped and uncapped projectiles at 0° scatter randomly through the band; at 30° there is an evident separation as indicated. Tungsten carbide cores usually break up on impact. If there is complete disintegration of the core, perforation of the indicated thickness may not be attained.

EXAMPLE A

Given an uncapped American 76 mm M62 projectile striking at 30° with a velocity of 2270 ft/sec, two values of plate thickness, about 6 inches and 6½ inches, are read by following the line to each of the two borders of the band. It is reasonable to assume that plate thicknesses greater than 6½ inches will be safe against this projectile, while thicknesses less than 6 inches will be vulnerable.

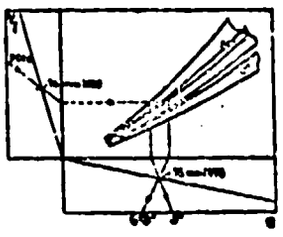

EXAMPLE B

Similarly, for the same projectile (see Example A) fired at a plate about 8 in. thick, two values of the striking velocity are read by following the line to each of the two borders of the band, nearly 2250 and 2750 ft/sec. The plate referred to is likely to be safe against striking velocities less than 2750 ft/sec and vulnerable to velocities greater than 2250 ft/sec.

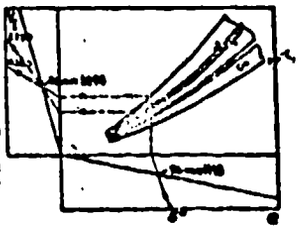

SOURCE: Based on experiments by American, British and Canadian military establishments.

PTM NO. 67
January 1956

CONFIDENTIAL

PERFORATION OF HOMOGENEOUS ARMOR BY GERMAN PROJECTILES

9 C 7
PERFORATION OF ARMOR: GERMAN PROJECTILES

GUN		PROJECTILE			THICKNESS OF HOMOGENEOUS ARMOR PERFORATED, *inches* at RANGES, yards													
Cal. mm	Model	Type	Weight pounds	M.V. f/s	100	200	250	500	400	500	600	750	800	1000	1250	1500	2000	2500
28	KwK 30																	
	KwK 36	APshell	0.227	2625	1.8	1.7		1.6	1.5									
	KwK 38	APCR	0.228	3270	2.2	2.1		1.8	1.7									
28/20	sPzB41	APCR	0.287	4580	3.7	3.5		3.1	2.8	2.6	2.4		1.9					
42/28	Pak 41	APCR	0.79	4600		4.5				3.7		3.2		2.7				
37	KwK																	
	Pak(t)	APshell	1.68	2500		2.2			2.0	1.8	1.6							
	Pak(t)	APCR	0.78	3350	3.1	2.8		2.6	2.3									
47	Flak37																	
	Pak(t)	APCR	3.34	2540	4.2	4.0			3.7		3.5		3.3	3.0				
50	KwK	APC60	1.95	3440			4.6			3.8		3.2		2.6		2.2		
	Pak 38	APC60	1.95	3830			5.0			4.7		3.9		3.3	2.8			
	Pak 38	APC	4.64	2700			3.5			3.1		2.7		2.4	2.1	1.9		
	KwK	APC	4.59	2240			3.4			2.9		2.1		1.9	1.5	1.4		
75/55	Pak 41	APCR		4122						6.7				5.9		5.3	4.6	
75	KwK 42	APC60	18	3674						7.8				6.7		5.7	4.9	4.1
	Pak 40	APC60	9	3250			7.1			6.7		6.2		6.0	5.6	5.2	4.6	
	KwK 42	APCBC	18	3078						5.9				5.2		4.7	4.1	3.6
76.2	Pak 36	APC60	9.25	2690		3.7			3.4		3.2		2.9	2.7				
	Pak 36(r)	APC	16.7	2450						4.6				4.1		3.6	3.1	2.3
	Pak 36	APCBC/HE	14.33	2220		3.9			3.2		3.0		2.9	2.7	2.6	2.4		
88	Flak 41	APC60	18.1	3775						10.0				8.7		7.6	6.6	5.7
	Flak 41	APCBC	22.46	3409						7.3				6.8		6.4	6.0	5.6
	Flak 36	APCBC	21	2600						8.1				6.7		6.3	5.8	5.5
	Pak 43	APCBC	22	3260														
	Pak 43	APC60/43	18	3775														
105	Flak38-39	APC	37.4															
	K 18	APCBC	34.62	2700			6.7			6.5		6.2		6.0	5.8	5.6		
	K 18	APCBC		2370			6.5			6.4		6.2		6.1	6.0	6.0		
	L FH 18	APCBC		1810			3.4			3.3		3.1		3.0	2.9	2.8		
	L FH 18	APCBC		1250			2.7			2.6		2.6		2.6	2.4	2.3		
28	KwK 30																	
	KwK 36	APshell	0.227	2625	1.2	1.1		1.1	1.0									
	KwK 38	APCR	0.223	3270	1.9	1.8		1.8	1.6									
28/20	sPzB41	APCR	0.287	4580	2.7	2.6		2.4	2.2	2.1	1.9		1.6					
42/28	Pak 41	APCR	0.79	4600		3.7				3.0				2.2				
37	KwK																	
	Pak(t)	APshell	1.68	2600		1.7			1.5	1.4	1.3							
	Pak(t)	APCR	0.78	3380	2.7	2.4		2.2	1.9									
47	Flak 37																	
	Pak(t)	APCR	3.44	2540														
50	KwK	APC60	1.65	3440			3.8			2.8		2.1		1.7	1.3			
	Pak 38	APC60	1.65	3830			4.3			3.4		2.7		2.2	1.7			
	Pak 38	APC	4.64	2700			2.6			2.4		2.3		2.0	1.8	1.6		
	KwK	APC	4.58	2230			2.1			1.9		1.7		1.6	1.4	1.2		
75/55	Pak 41	APCR		4123						5.8				5.1		4.5		3.0
75	KwK 42	APC60	18	3674						6.1				5.3		4.8	3.8	2.8
	Pak 40	APC60	9	3250	5.7					5.0				4.4				
	KwK 42	APCBC	18	3078						4.8				4.3		3.8	3.3	2.1
76.2	Pak 36	APC60	9.25	2690														
	Pak 36(r)	APC	16.7	2450				1		3.7				3.2		2.8	2.6	2.2
	Pak 36	APCBC/HE	14.33	2200														
88	Flak 41	APC60	18.1	3775						7.8				6.5		5.4	4.6	3.7
	Flak 41	APCBC	22.46	3409						6.8				5.9		5.5	5.1	4.6
	Flak 36	APCBC	21	2600						4.3				4.1		3.7	3.4	3.2
	Pak 43	APCBC	22	3260	6.0									6.5		5.8		
	Pak 43	APC60/43	18	3775	5.8									7.6		6.7		
105	Flak38-39	APC	37.4											5.5		5.1	4.7	
	K 18	APCBC	34.62	2700			5.7			5.5		5.3		5.1	4.9	4.8	4.6	
	K 18	APCBC		2370			5.9			4.7		4.5		4.4	4.2	4.0	3.7	
	L FH 18	APCBC		1810			2.9			2.7		2.6		2.5	2.4	2.3	2.1	
	L FH 18	APCBC		1250			2.3			2.2		2.1		2.1	2.0	1.9	1.8	

0°

60°

The table gives the thickness of homogeneous armor (BHN from about 255 to 311) that is likely to be perforated at various ranges by German armor piercing projectiles. Distance given is striking range of projectile measured from line perpendicular to plate. Impact velocity in f/s, which are ballistic tests fired either on actual firing data or on extrapolation of results of trials with other projectiles. It should be noted that the tapered bore guns and the tungsten carbide projectiles (APCR and APCBC) have only been in very limited production.

ABBREVIATIONS: Projectiles— AP Armor Piercing; APC Armor Piercing Capped; APCBC Armor Piercing Capped with Ballistic Cap; AP 40 Armor Piercing with Carbide Core; AP 41 Armor Piercing with Tapered Bore gun. Guns— KwK Tank Mounted gun; Flak Anti-aircraft gun; Pak Anti-tank gun; Pak(t) Anti-tank gun (Czech); Pak(r) Anti-tank gun (Russian); Pz B Field gun; s Pz Jgr Heavy anti-tank gun; L FH 18 Light Field Howitzer; K 18 Medium gun.

SOURCE: "Tactical and Technical Trends", No. 17, Catalog of Enemy Ordnance Materiel, Office of Chief of Ordnance, U.S.A.; Prov. of the Brit. Bd. (Brit)

FTM No. 99 February 1945

WEAPON DATA

PERFORMATION OF MILD STEEL ARMOR (BHN 100-150) BY UNCAPPED AP PROJECTILES

9 C 8
MILD STEEL PERFORMATION

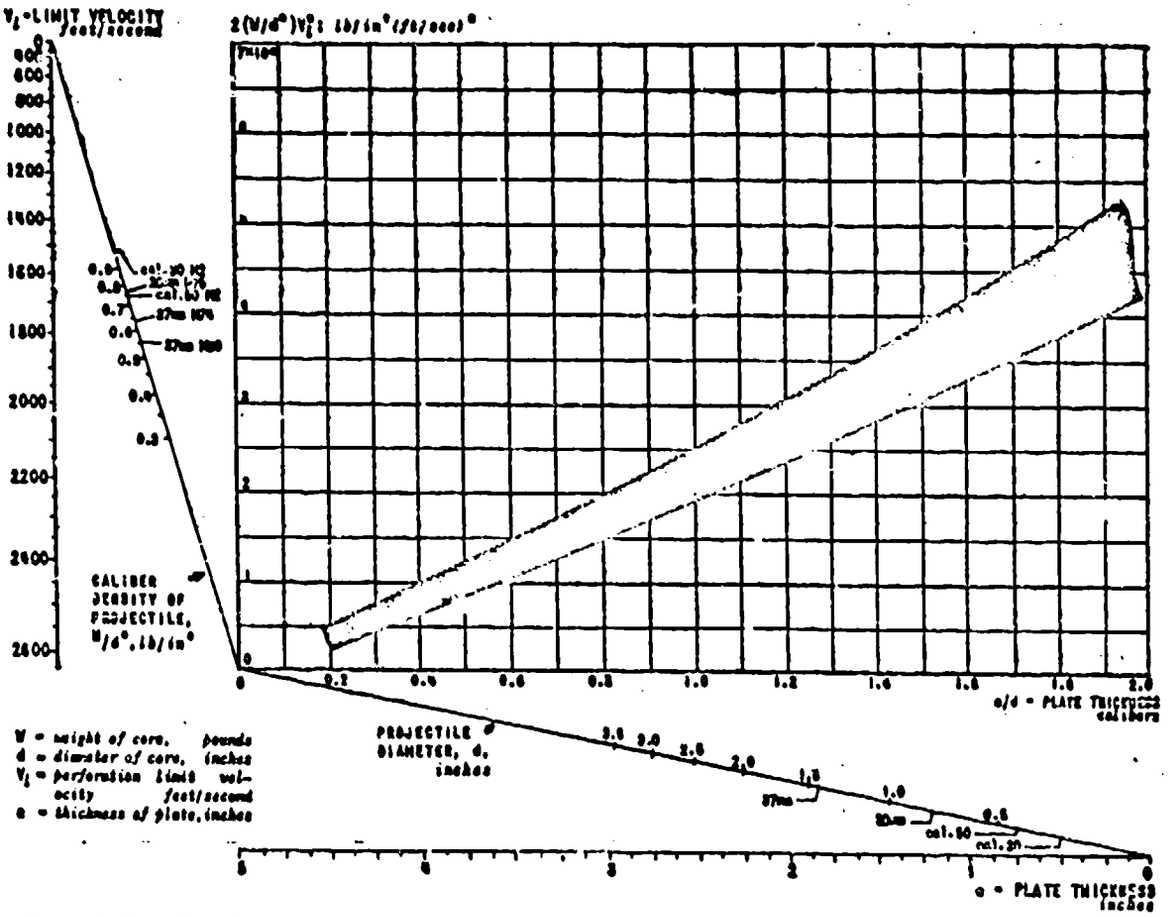

The graph shows the relation between perforation limit velocity and thickness of plate perforated. The limit velocity measured is that at which the projectile just passes completely through the plate (Navy limit). The data represent armor piercing (AP) uncapped projectiles ranging from 0.30 inches to 1.46 inches, and caliber 0.30 and caliber 0.50 jacketed projectiles fired against mild steel armor BHN 100 - 150 at normal incidence.

Because of inherent scatter of data, the results are presented in the form of a band. The band, therefore, may be looked upon as separating two regions of the graph, corresponding to vulnerability (above) and safety (below).

EXAMPLES:

A Given a 37mm M80 projectile striking with a velocity of 1600 ft./sec., two values of plate thickness about 1.6 in. and 2 inches, are read by following the line to each of the two borders of the band. It is reasonable to assume that plate thicknesses greater than 2 inches will be safe against the given projectile, while thicknesses less than 1.6 inches will be vulnerable.

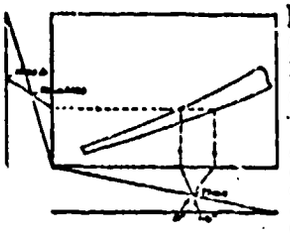

B Similarly, for the given projectile (example A) fired at a plate 2 inches thick, two values of the striking velocity result by reading the two borders of the band, namely about 1550 and 1700 ft/sec. The plate referred to is likely to be safe against striking velocities less than 1550 ft/sec and vulnerable to velocities greater than 1720 ft/sec.

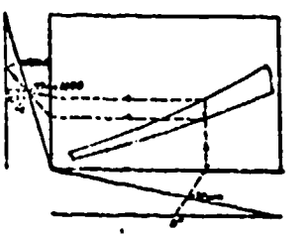

SOURCE:

Graph includes data from the Naval Research Laboratory, Bellevue, D. C., and the National Defense Research Committee, Princeton University.

August 1946

WEAPON DATA

PEAK BLAST PRESSURE AS A FUNCTION OF DISTANCE AND WEIGHT OF EXPLOSIVE

FIG 3A1 PRESSURE

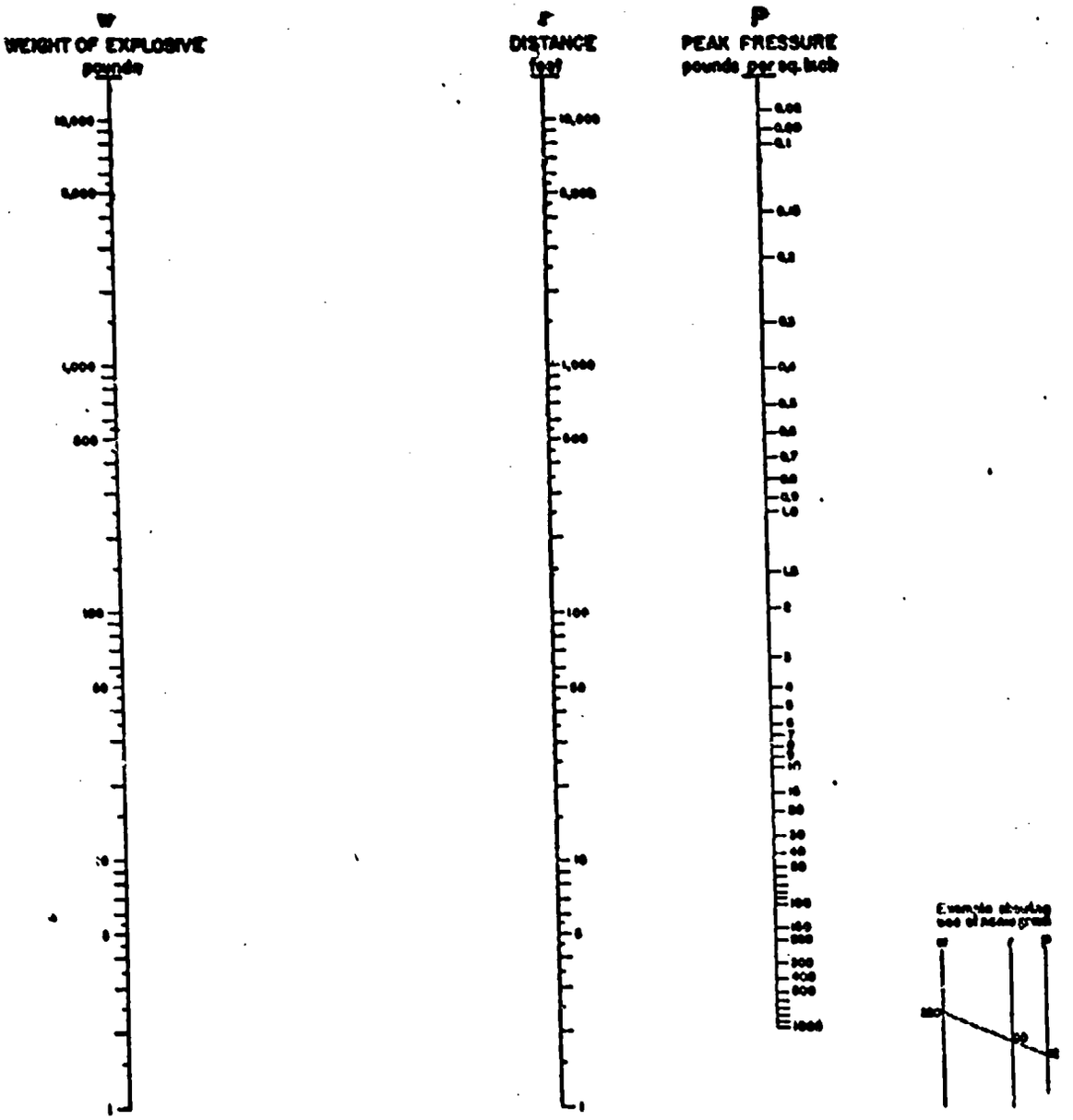

VALUES INDICATED ARE ESTIMATED ACCURATE TO ABOUT 25 PERCENT AND ARE AVERAGES OF A LARGE NUMBER OF MEASUREMENTS ON ALL TYPES OF BOMBS AND EXPLOSIVES
Note: Readings taken with the gauge side-on to the blast wave; for face-on gauge, pressure values should be approximately doubled.

June 1945

WEAPON DATA

POSITIVE IMPULSE AS A FUNCTION OF DISTANCE AND WEIGHT OF EXPLOSIVE

FOR TNT FILLED GENERAL PURPOSE BOMBS

3A2* POSITIVE IMPULSE

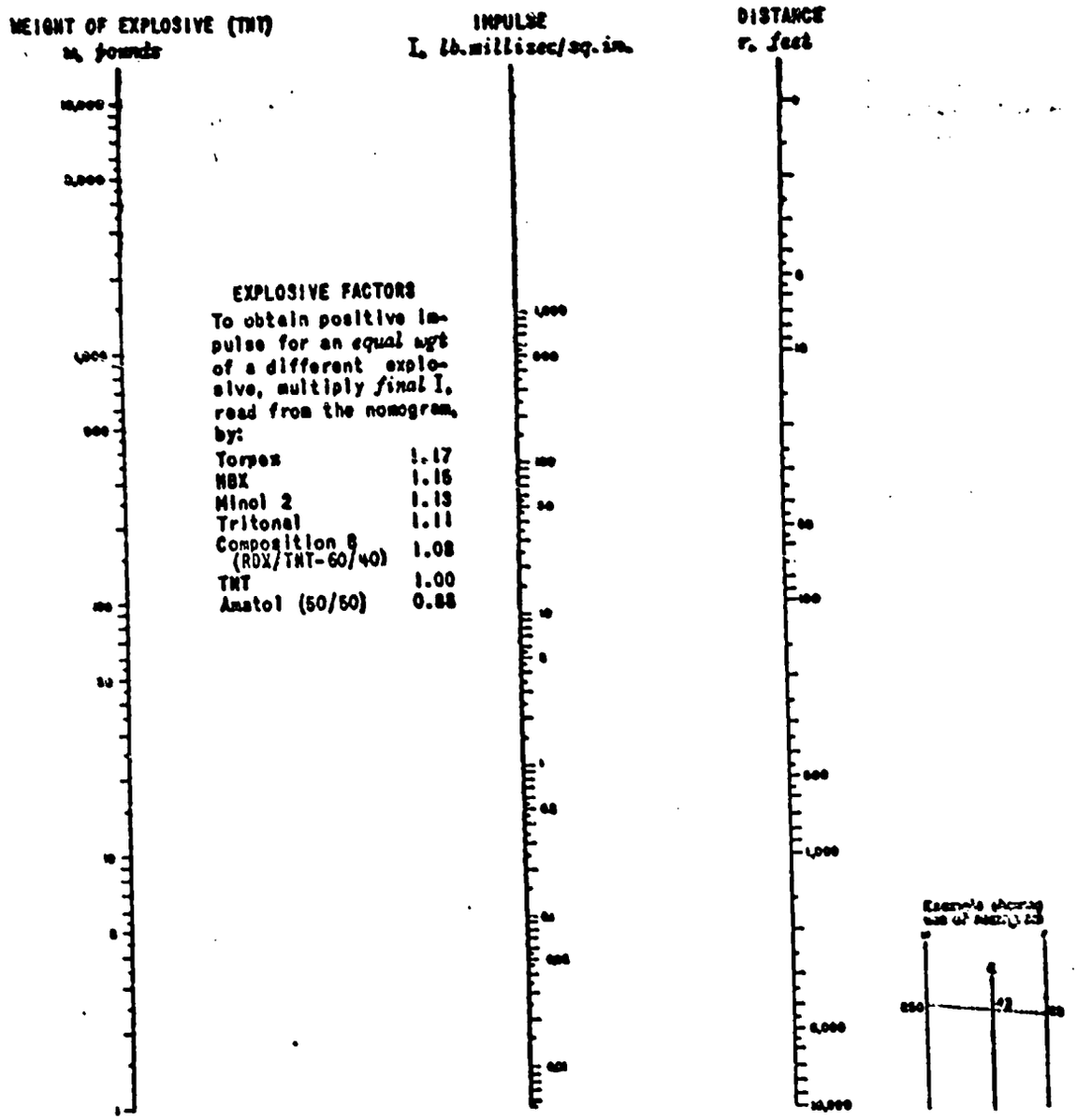

EXPLOSIVE FACTORS

To obtain positive impulse for an *equal* wgt of a different explosive, multiply *final* I, read from the nomogram, by:

Torpex	1.17
HBX	1.16
Minol 2	1.13
Tritonal	1.11
Composition B (RDX/TNT-60/40)	1.08
TNT	1.00
Amatol (50/50)	0.88

This sheet gives values of the positive impulse resulting from detonation of TNT-filled General Purpose (GP) bombs at ground level. Results refer to gauges placed side-on to the blast wave. The nomogram represents the empirical relation $I = \frac{54\,w^{2/3}}{r}$

Where I is the positive impulse (lb-millisec/ins), based on pressure in excess of atmospheric, r is the distance from the explosion (ft) and w is the charge weight (lb). The constant in this equation is an average for American GP bombs. For other explosives, multiply final I, read from nomogram, by factors given in table; for other case weights (bomb types) use sheet 3A2a.

*Revised: August 1945

CONFIDENTIAL

WEAPON DATA

BLAST IMPULSE DUE TO DETONATION OF BOMBS AT GROUND LEVEL

3 A2a POSITIVE BLAST IMPULSE

This sheet gives information on the magnitude of the positive air blast impulse resulting from detonation of bombs near the ground. Impulse values are based on readings of gauges placed side-on to the advancing blast wave.

The table gives a selection of impulse values for American bombs.

BLAST IMPULSE FROM PARTICULAR BOMBS: Positive impulse per unit area, lb-msec/in²

	Weight	Filling	DISTANCE, Feet													
			20	30	40	50	60	70	80	90	100	200	300	400	500	750	1000
	100-lb AN-M30	TNT	42	28	21	17	14	12	10	9.2	8.3	4.2	2.8	2.1	1.7	1.1	0.8
		Tritonal	46	33	25	20	16	14	12	11	9.8	4.9	3.3	2.5	2.0	1.3	1.0
	250-lb AN-M57	TNT	69	46	35	28	23	20	17	15	14	6.8	4.6	3.5	2.8	1.8	1.4
		Tritonal	82	55	41	33	27	23	21	18	16	8.2	5.5	4.1	3.3	2.2	1.6
GP	500-lb AN-M64, M64	TNT	117	78	58	47	39	33	28	24	23	12	7.8	5.8	4.7	3.1	2.3
		Comp.B	128	85	64	51	43	37	32	28	26	13	8.5	6.4	5.1	3.4	2.6
		Tritonal	138	92	69	55	46	40	35	31	28	14	9.2	6.9	5.5	3.7	2.8
	1000-lb AN-M44, M65	TNT			90	72	60	51	45	40	36	18	12	9.0	7.2	4.8	3.6
		Comp.B			101	81	67	56	50	45	40	20	13	10	8.1	5.4	4.0
		Tritonal			106	85	71	61	53	47	42	21	14	11	8.5	5.7	4.2
	2000-lb AN-M34, M66	TNT				119	99	85	75	66	60	30	20	15	12	8.0	6.0
		Comp.B				130	108	93	81	72	65	33	22	16	13	8.7	6.5
		Tritonal				141	118	101	89	78	71	35	24	18	14	9.4	7.1
LC	4000-lb AN-M66	TNT						205	160	160	144	72	48	36	29	19	14
		Comp.B						225	197	176	158	79	52	39	32	21	16
		Tritonal						243	212	189	170	85	57	42	34	23	17
SAP	500-lb AN-M58	TNT		42	32	26	21	18	16	14	13	6.4	4.3	3.2	2.6	1.7	1.3
	1000-lb AN-M59	TNT			48	40	33	28	25	22	20	10	6.6	4.8	4.0	2.6	2.0

Accuracy: It is estimated that the mean of a large number of tests will fall within 5% of the corresponding tabulated value.

The positive impulse in air due to detonation of an explosive charge on the surface of the ground is given by

$$I = E\, e^{S}\left(\frac{w^{2/3}}{r}\right) ;$$

where : I = Positive impulse per unit area, lb-milliseconds/in².
w = Weight of explosive, pounds.
r = Distance from explosion, ft.
E = Explosive factor (values listed below).
S = Equivalent cylinder charge/weight ratio
e = 2.718... a base of natural logarithms.

The equivalent cylinder charge/weight ratio, S, is the ratio of the weight of charge to the total weight of an equivalent cylindrical bomb. An equivalent cylindrical bomb is defined to be one with the same weight of explosive as the actual bomb, enclosed in a cylindrical shell of the same material and with the same internal diameter and internal volume, closed at the ends, the thickness of the shell and ends being equal to the sidewall thickness of the actual bomb. S is given approximately by

$$S = \frac{1}{1 + 4\frac{t\rho_m}{D\rho_e}\left[1 + \frac{t}{6}\right]}$$ for steel cased bombs filled TNT or Tritonal this becomes.....

$$S = \frac{1}{1 + (10 + \frac{0.44}{w/D^3})\frac{t}{D}}$$

where : t = Bomb case thickness, inches.
D = Inside diameter of bomb body, inches.
ρ_m = Density of case material, lb/in³
ρ_e = Density of explosive filling, lb/in³

EXPLOSIVE FACTOR, E	E	$E = e^{S}$
Torpex	25	96
HBX	24	82
Minol	23	80
Tritonal	23	80
Comp.B (RDX/TNT 60/40)	22	66
TNT	20	60
Amatol	18	72

* For uncased charges, where $S = 1$ and $I = E \times (\frac{w^{2/3}}{r})$

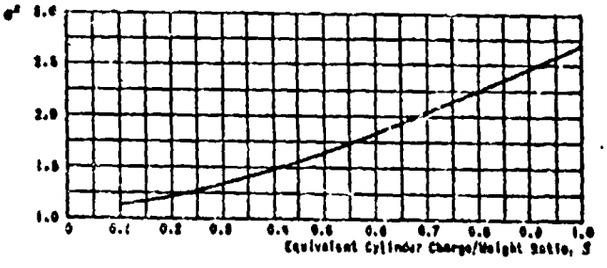

Refs: AES-4, p61, (OSRD-4355)
AES-7, p9 , (OSRD-4764)
August 1945

WEAPON DATA

SIDE-ON AND FACE-ON BLAST PRESSURES IN AIR

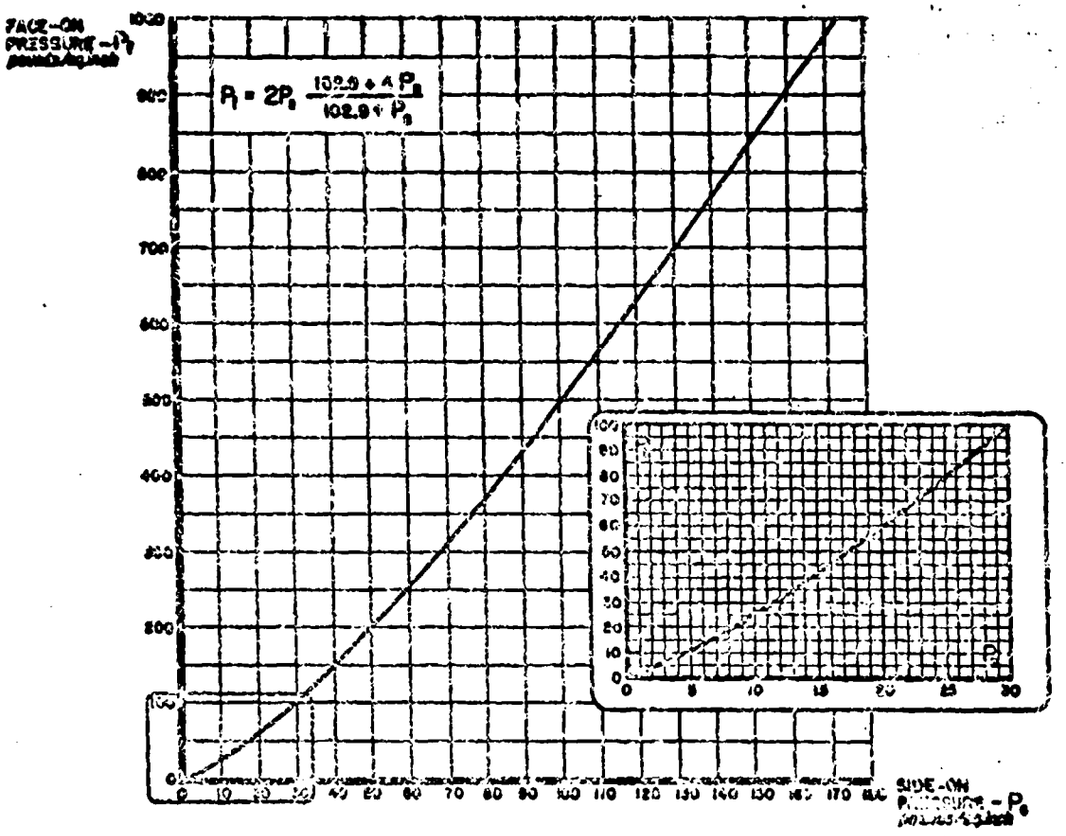

The graph gives the relation between face-on pressure, P_r, recorded by a gauge fixed in an infinite rigid wall facing the blast, and side-on pressure, P_s, measured by a gauge whose face is parallel to the direction of motion of the blast wave.

All pressures indicated are in excess of atmospheric pressure.

This relationship is deduced from the Rankine-Hugoniot equations, assuming the incident blast wave to have a flat top. However, the curve will give the relation between the initial parts of the pressure-time curve obtained from an explosion, where P_s is initial peak pressure in the oncoming wave (as given by a gauge side-on) and P_r is initial peak in the wave reflected from any finite object such as a gauge along.

If a side-on gauge were placed in front of an actual wall (i.e., one of finite extent and rigidity), and if another were set face-on in the wall, then the above relation would apply accurately to the initial phases of the blast pressure record obtained. However, if this relation were applied to the entire pressure-time curve it would predict face-on pressures that are too high at later stages of the record. The reason for the deviation is that the above formula does not consider any motion of the wall or diffraction of the wave around it.

September 1944

CONFIDENTIAL

IMPULSE DELIVERED TO A PLANE SLAB BY A CONTACT EXPLOSION

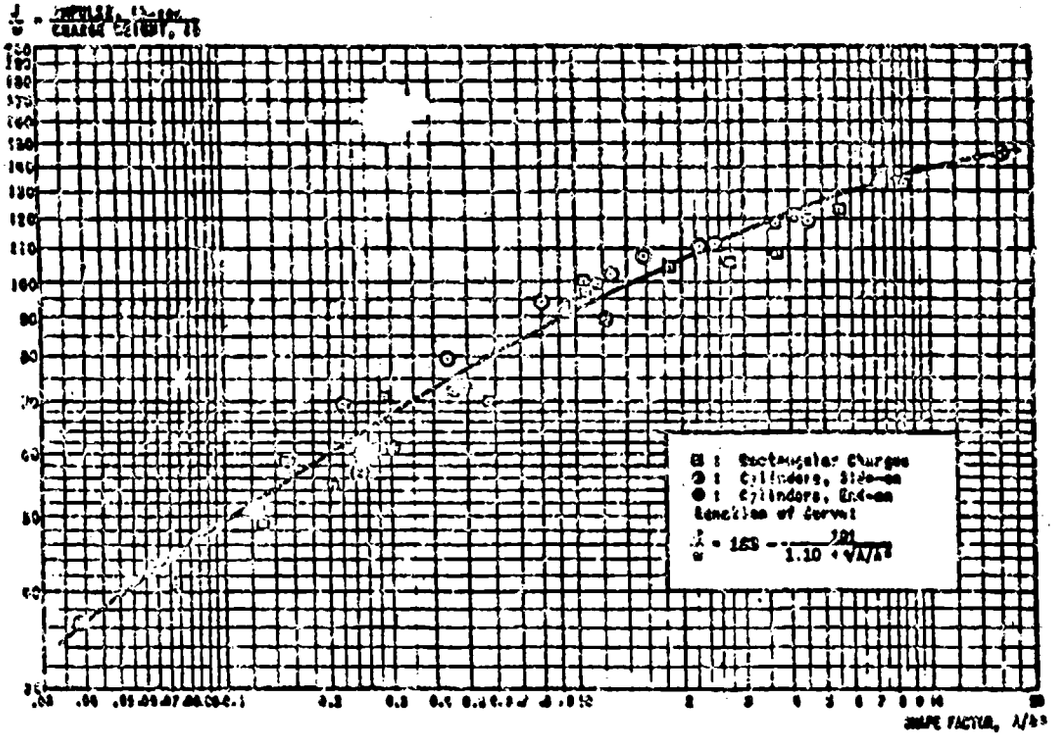

The graph gives the total impulse delivered to an extended plane slab by detonation of a rectangular or cylindrical TNT charge in contact with it. For charges having either of the above forms, the impulse per unit weight can be correlated with the Shape Factor, A/L^2, given by the plan area of the charge divided by the square of its greatest measurement perpendicular to the slab (see sketches).

Measurements were made by means of the impulse pendulum (see source references). Charges used in the tests varied in weight from ¼ to 2-lb, most weights being either ½ or 1-lb. Approximately 76% of the measured impulse values lie within ±5% of the empirical curve, which has the equation given in the graph above, where J is the impulse delivered to the plane slab (lb-msec), w is the weight of charge (lb), A is the plan area of the charge and L is the maximum extension of charge perpendicular to the slab. (All linear dimensions are measured in the same units. A brief series of tests indicates that the values of J/w given by the above relation for TNT should be multiplied by the following factors for other explosives: Tetryl 1.08; RDX-2, Minol-2, Comp.C-3 1.21; Pentolite, Comp.B, Tetrytol, Tritonal, cast TNT 1.11; Amatol 0.85.

For a charge having the form of a circular cylinder or a square-ended rectangular block, the ratio of the impulse delivered when the charge is placed side-on to the slab to that with the charge set end-on is given simply by

$$\frac{J_{side\text{-}on}}{J_{end\text{-}on}} = \frac{2}{3}(s + 1)$$

Here s is the *Slenderness Index* of the charge, conveniently taken to be the length/diameter ratio in the case of a cylinder, or the length-to-side ratio for a square ended block (see sketches). The linear relation is a good approximation for s between 1 and 4.

SQUARE-ENDED BLOCKS

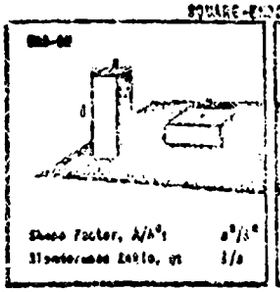

CIRCULAR CYLINDERS

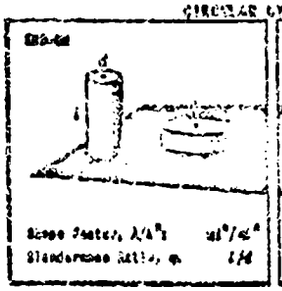

Ref: AEC-12
September 1956

WEAPON DATA

PENETRATION OF CONCRETE BY DETONATION OF CONE-END CHARGES

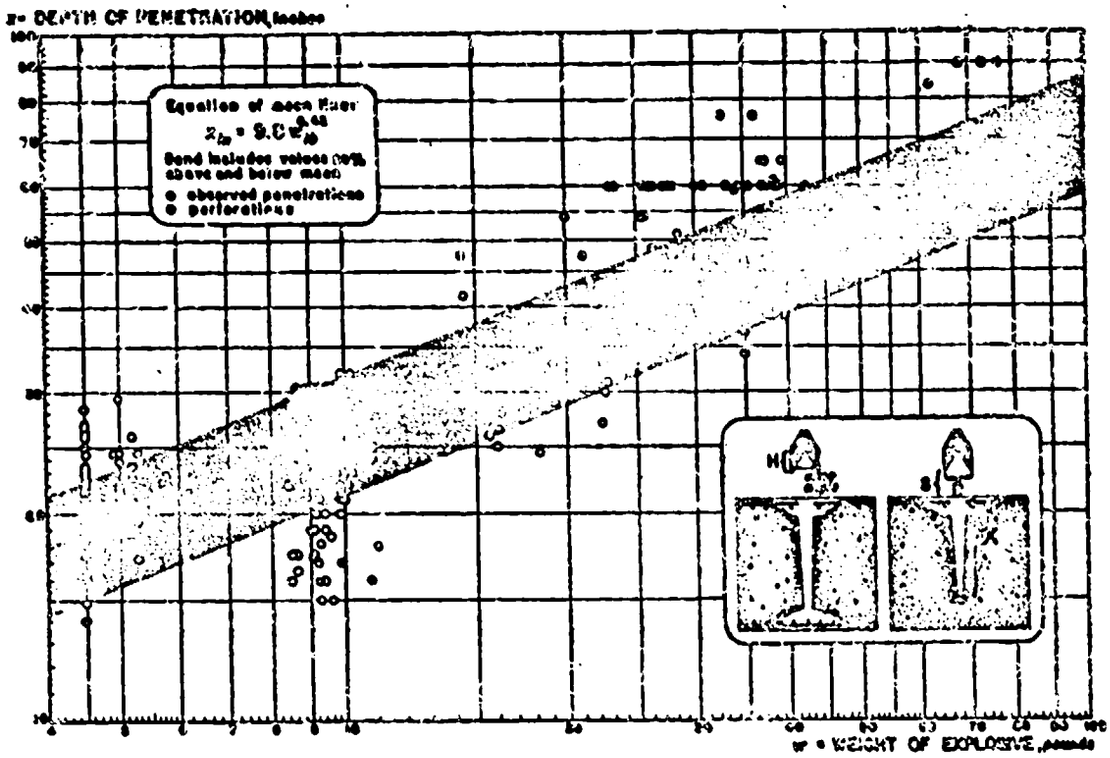

The graph shows depth of penetration produced in concrete by a cone-end charge placed with axis perpendicular to the slab face. The mean line was determined by a least squares reduction; shaded band includes values 20% above and below mean.

Because of scabbing on rear face (see inset sketches) perforation often results even when slab thickness is greater than the penetration depth that would result in massive concrete.

TYPE OF EXPLOSIVE: Effects are not greatly dependent on explosive type provided charge is thoroughly compact and adequately primed.

BEST - TNT/NQV	Plastic H.E.	GOOD - Pentolite	Robel 808	POOR - 60/40 Amatol
TNT/PETN	Cyclotol	TNT	Picric Acid	P. A. A.
TNT/CE	H.E.	Lyddite	Tetrytol	

CONE LINING: Dependence on material and thickness is not great.

Materials: BEST - Pressed steel. Forms large slag which may stick in hole, especially if cone angle is less than about 70°; may thus impair insertion of demolition charge.
GOOD - Glass. Hole somewhat shallower but of larger volume than with steel. Less debris is left in hole. Cast brass and cast manganese bronze also good.

Thickness: Various thicknesses used. Experiments indicate optimum value of about 0.1 inch (steel) for a charge of 8-inch diameter, and weighing approximately 10 lbs.

CONE ANGLE: Not extremely critical, but 65° to 70° usually adopted.

LENGTH-DIAMETER RATIO: Values of H/D (see sketches) between ½ and 1 are recommended.

STAND-OFF DISTANCE: The optimum stand-off, S, appears to be between about ½ and 1½ diameters.

CONCRETE STRENGTH: In general, slightly larger but not deeper holes result in softer concrete.

PILLBOX TESTS: Trials indicate that a 75-lb charge will defeat a 5-ft. thick pillbox wall and throw scab capable of lethal or incapacitating effects on any occupants.

DATA FROM EXPERIMENTS BY U.S. ENGINEER BOARD AND BY BRITISH MINISTRY OF SUPPLY

May 1944

CONFIDENTIAL

WEAPON DATA

PERFORATION OF HOMOGENEOUS ARMOR BY WEAPONS WITH CONE-END CHARGES

3 A 6
ARMOR PERFORATION BY CONE-END WEAPONS

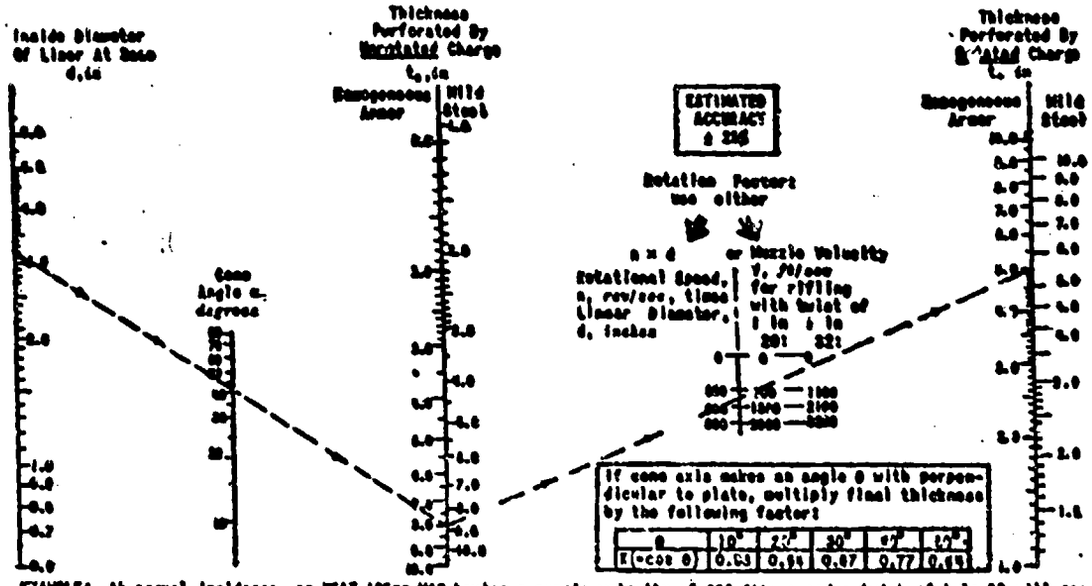

EXAMPLE: At normal incidence, an HEAT 105mm M67 having a muzzle velocity of 850 ft/sec and a twist of 1 in 20 will perforate about 5 in of armor, as shown by the index lines. At 30°, the performance will be about 5 x 0.87 = 4.3 in

The nomogram gives thickness of homogeneous armor perforated by Munroe jets from cone-end hollow charge projected weapons. The underlying empirical equation, deduced from performance records on actual weapons is

$$t = \frac{v \cdot 0.9\, d \cos\theta}{s\,i.(a/s)}\, f(nd)$$

where $f(nd)$ = 1.0, 0.60, 0.57, 0.48, for nd = 0, 300, 600, 900 r.p.s. x in respectively. (See notation on nomogram.)

Factors such as thickness and material of liner, type and density of explosive, confinement of charge, stand-off distance, etc. are not included in the relation, although changes in these quantities are responsible for some variation in observed results. With the empirical relation used, scatter in the data precludes making a distinction between *depth of penetration* in massive plate and *thickness of plate perforated*. Thus the present relation will be useful in estimating performance of any weapon designed according to reasonable practice, but should be considered a rough guide to be used only in the absence of experimental data.

Basic data are mainly for projectiles having steel liners and filled Cyclotol or Pentolite. Explosives combining high power with high rate of detonation give greatest target damage. As the equation above shows, rotated projectiles generally form shallower craters; however, these are likely to be wider than the craters due to static detonation.

PERFORMANCE OF PARTICULAR WEAPONS†

Weapon	Thickness of Armor Perforated, in (normal incidence
US - HEAT M69(Bazooka)	6.5
Grenade M431	3.9
HEAT 57mm T-20 E-2	8
HEAT 75mm M66	8.5
HEAT 105mm M67	6.8
Br - PIAT	3.8
HEAT 3.7-in & 95mm	5.0
Ger- Panzerfaust (30, 60 & 100)	6.0
Panzerschreck (Ger. Bazooka)	6.5
Jap- A.T. Conical Head Grenade	2.8
A.P. Rifle Grenade	2

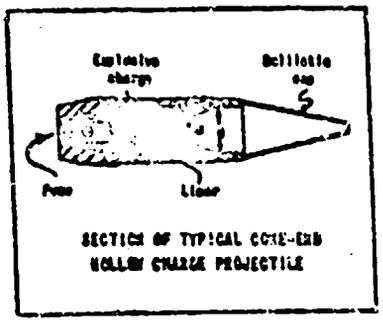

SECTION OF TYPICAL CONE-END HOLLOW CHARGE PROJECTILE

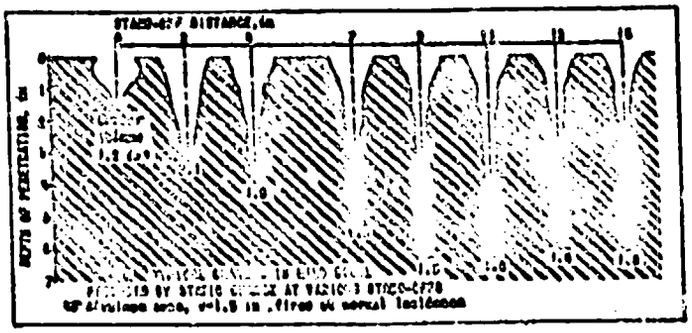

Ref: OTS-129 (6628-536er)
August 1945

MACH REFLECTION

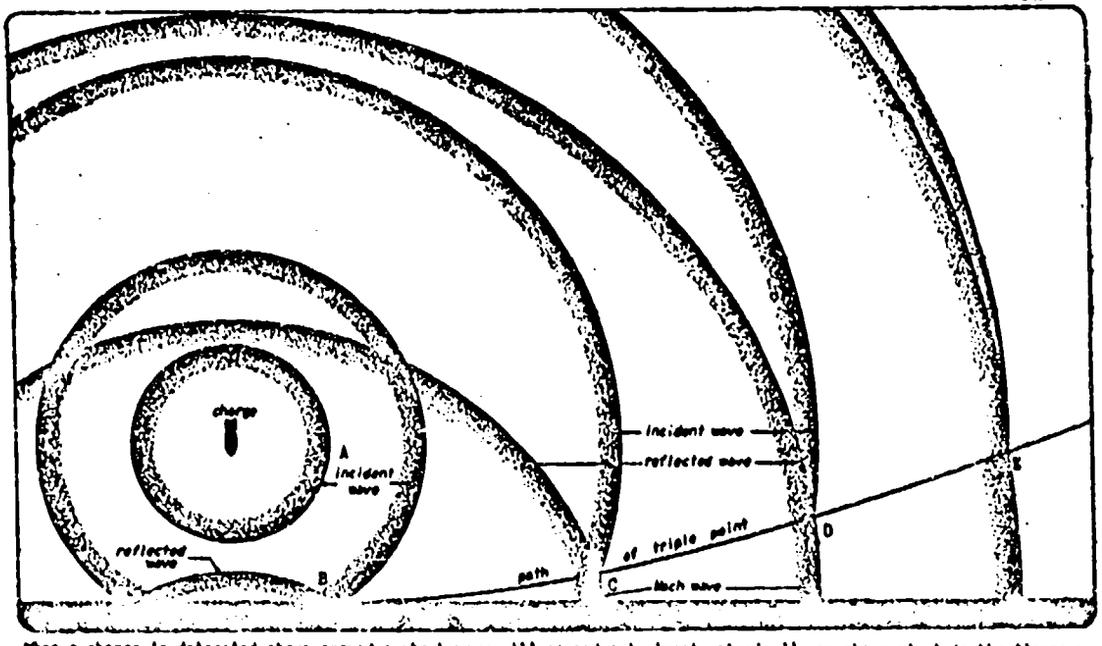

When a charge is detonated above ground a shock wave will spread out almost spherically as shown at A in the figure above, which is a section in a vertical plane passing through the charge. As this shock wave, called the incident wave, strikes the ground it is reflected and the situation is somewhat as shown at B. If the ground were infinitely rigid and if the shock wave were weak (that is, almost a sound wave) the reflected wave could be constructed by imagining that the ground is replaced by air and an equal charge, the so called image charge, detonating at the same time at an equal distance below the ground and in line with the actual charge. In an actual explosion the reflected wave differs from the one constructed in this manner, primarily because the incident wave is stronger than a sound wave.

The angle between the normal to the wave front and the normal to the ground surface is called the angle of incidence. It has been found that for each ratio of the pressure in front of the shock wave to that immediately behind the wave front there is a critical angle of incidence beyond which reflection of the type shown at B is impossible. Thus there is some place along the ground where a new type of reflection called *Mach reflection* takes place. A new wave, called the Mach wave, is formed and the situation is as illustrated at C, D and E in the figure. The intersection of the incident wave, the reflected wave, and the Mach wave is called the triple point.

As the phenomenon progresses the Mach wave grows and the triple point describes a curve through the air. This path has been studied in detail experimentally and a typical path is shown in the figure above. Other paths are shown in the lower figure of sheet 3 A8.

As the Mach wave grows in height it absorbs the incident and reflected waves. Ultimately, at distances very large compared to the height of burst, the whole configuration of shocks becomes approximately a single spherical shock wave intersecting the ground orthogonally.

The pressure and impulse at a point which is a horizontal distance d from the charge & a height H above the ground go through a maximum as the height of burst h of the charge is varied. The height of detonation which maximizes these quantities at a point (d,H) is that which creates a triple point passing approximately through (d,H).

The height of burst which maximizes the pressure and impulse at a point along the ground at a horizontal distance d from the charge is the height for which Mach reflection just forms at the point in question. The relation between d and h for beginning of Mach reflection is given in the graph in terms of the scaled variables $d/w^{1/3}$ & $h/w^{1/3}$ where w is the weight of charge.

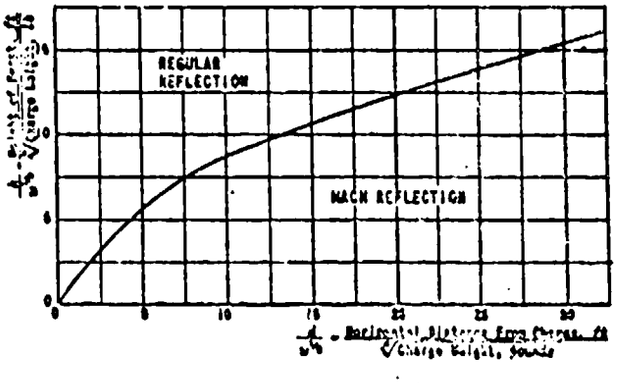

Ref: AES-1, NDRC Report A-328
August 1945

FIG 3 A8 HEIGHT FOR MAXIMUM IMPULSE

OPTIMUM HEIGHT FOR MAXIMUM IMPULSE

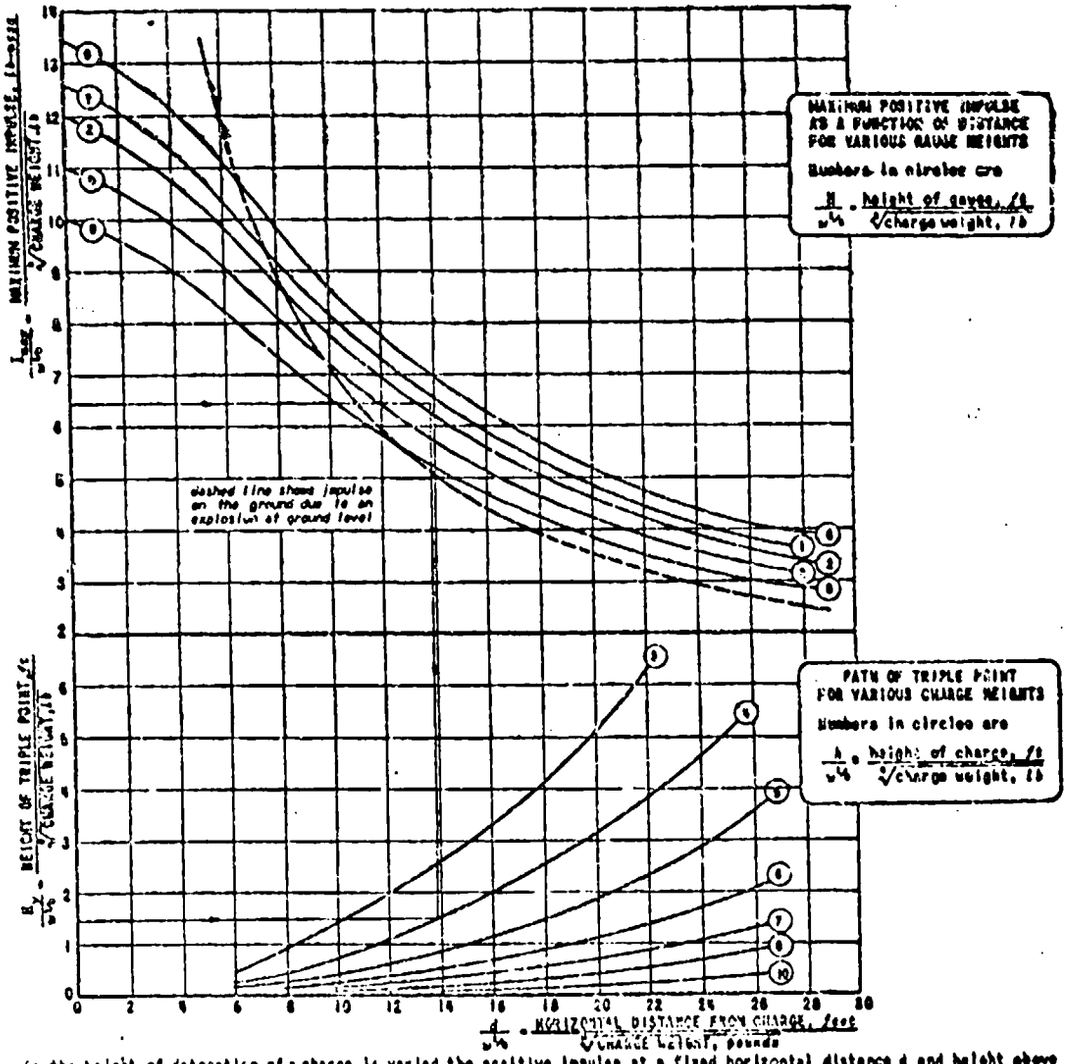

As the height of detonation of a charge is varied the positive impulse at a fixed horizontal distance d and height above ground H goes through a maximum whose value is denoted by I_{max}. The values of $I_{max}/w^{1/3}$ as a function of $d/w^{1/3}$ are plotted in the upper figure for several fixed $H/w^{1/3}$. The height of detonation of the charge which will maximize the impulse at a point (d,H) is the one which will produce a Mach reflection whose triple point passes approximately through the point (d,H). For convenience the impulse on the ground due to a charge detonated on the ground is also given in this figure. In the lower figure each curve is a path of the triple point for a fixed value of $A/w^{1/3}$ where A is the height of detonation of the charge.

The graphs may be used to determine the height of detonation necessary in order to maximize the horizontal distance at which a given level of impulse is formed at a height H above the ground. For example, suppose that a building 40 feet high is to be attacked and that a positive impulse of 80 lb-millisec/in² is necessary to accomplish the desired damage. The impulse should have its maximum at half the height of the wall, so the value of H is 20 feet. Assume that a 4000-lb LC bomb filled Comp. B is to be used. It is found from Sheet 2A2a that this is equivalent to 2730 pounds of bare TNT so $w^{1/3}$ for use in the graphs above is 14. Then $I/w^{1/3}$ is 5.43 and $H/w^{1/3}$ is 1.43. From the upper figure we find that $d/w^{1/3}$ is 13.8 and using this value we find from the lower figure that $A/w^{1/3}$ is 4. Thus the bomb should be detonated at a height 4 x 14 = 56 feet above the ground, and the maximum distance at which damage can be achieved is 13.8 x 14 = 195 feet. From the dashed curve in the upper figure we find that if the charge had been detonated on the ground the impulse level of 80 lb-millisec/in² would have been reached at 155 feet. Thus in this case the airburst increases the radius of damage from 155 to 195 feet, and increases the area over which damage can be achieved by about 63%. The example is shown by dotted lines on the graphs. A change in height of burst of 40% from the optimum height will change the impulse at a point (d,H), from I_{max} by 10%.

Ref: AES-31 AES-86
August 1945

PRESSURE AND IMPULSE ON THE GROUND DUE TO EXPLOSIONS IN AIR

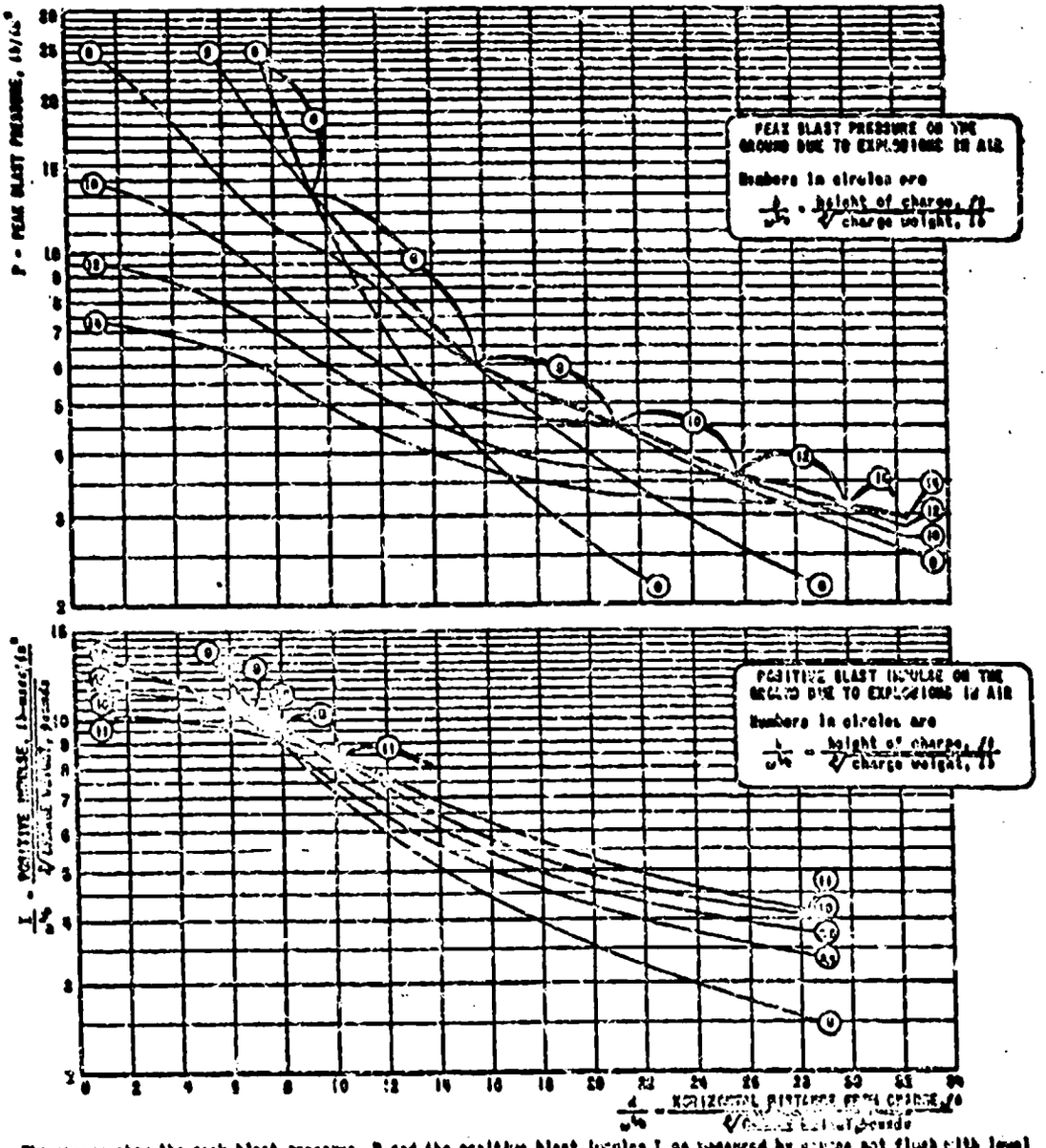

The curves show the peak blast pressure P and the positive blast impulse I as measured by gauges set flush with level ground at a horizontal distance d from a bare charge of w pounds of TNT detonated at a height h above the ground. The pressure curve labeled "0" is obtained from measurements of pressure from a charge detonated in open air on the assumption that the pressure from w pounds detonated on the ground is equivalent to that from 2w pounds detonated at the same distance in open air. The other curves are based on tests using 1-lb bare TNT charges, experiments using mathematically predicted shock waves, and deductions from the theory of regular reflection.

To find the height at which a charge should be detonated to yield maximum peak pressure or positive impulse, at a given distance d, read upward from the proper value of $d/w^{1/3}$ to the curve that is highest at that point and take the value of $h/w^{1/3}$ for that curve. To find the height of detonation that will yield a given peak pressure or positive impulse at the greatest distance, read horizontally from the appropriate value of P or $I/w^{1/3}$ to the curve that lies farthest to the right and take the value of $h/w^{1/3}$ for that curve.

Refs: AEB-1; AEB-2

August 1946

5 B1a
CRATERS: DIAMETER AND DEPTH

CRATERS IN SOIL: DIAMETER AND DEPTH

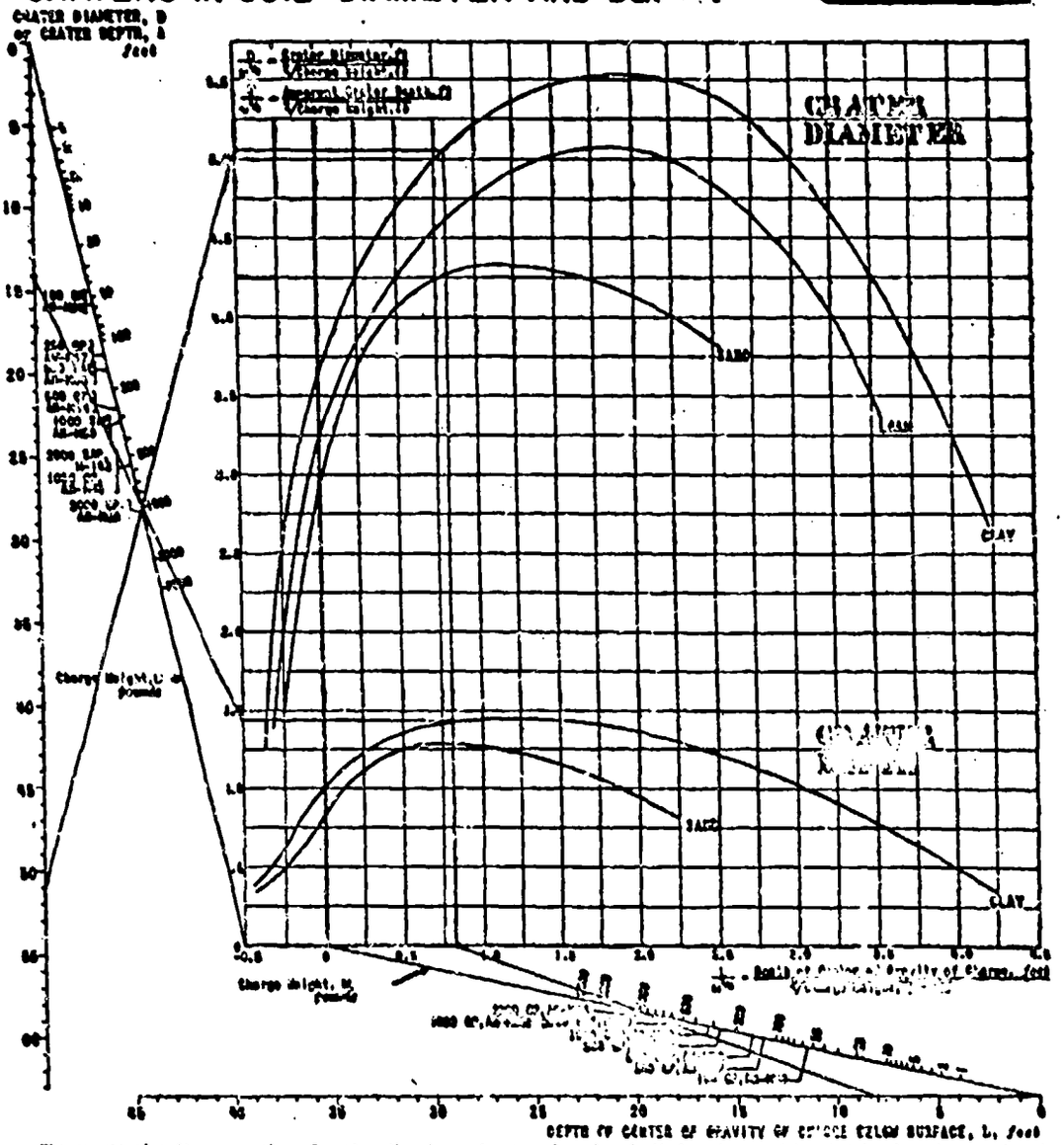

The curves give the mean value of crater diameter and apparent crater depth for charges detonated in clay, loam, or sand as a function of the depth of the center of the charge below the surface of the ground; negative values of depth are included, corresponding to detonation above ground. Deviation between mean and observed values may be as much as 10%.

The curves are for TNT. Craters due to cratration B or Amatol 80/20 are not significantly different. Tactical terms craters approximately 10% larger than given by the curves. Ideal and normal fuze craters approximately 10% larger.

EXAMPLE: The dotted line indicates that a 1000-lb charge detonated at a depth of 9 feet will form a crater 61 feet in diameter and 18 feet in apparent depth in clay.

TYPICAL CRATER PROFILES showing apparent depth, diameter, and position of charge.
A: 1000 lb at reasonable depth, clay or loam
B: 1000 lb at or above ground, any soil.
C: 1000 lb below ground surface, dry sand.

* Devised August 1946

CRATERING BY LINE CHARGES

The width of crater S, in feet formed by explosion of a line charge on various soils is given by the following empirical relations, where w is the linear charge weight in pounds per foot.

Type Soil	Average Crater Width S, feet	70% of Crater Widths Fall Between
Loose Dry Sand	$S = 2.1\sqrt{w}$	$2.0\sqrt{w}$ and $2.4\sqrt{w}$
Packed Wet Sand	$S = 2.4\sqrt{w}$	$2.1\sqrt{w}$ and $2.7\sqrt{w}$
Fine Sandy Silt Loam	$S = 2.2\sqrt{w}$	$2.0\sqrt{w}$ and $2.6\sqrt{w}$
Sandy Clay Loam	$S = 2.6\sqrt{w}$	$2.4\sqrt{w}$ and $2.8\sqrt{w}$
Wet Rich Clay	$S = 2.1\sqrt{w}$	$1.8\sqrt{w}$ and $2.3\sqrt{w}$

Crater widths for line charges exploded under water are greater than those listed here.

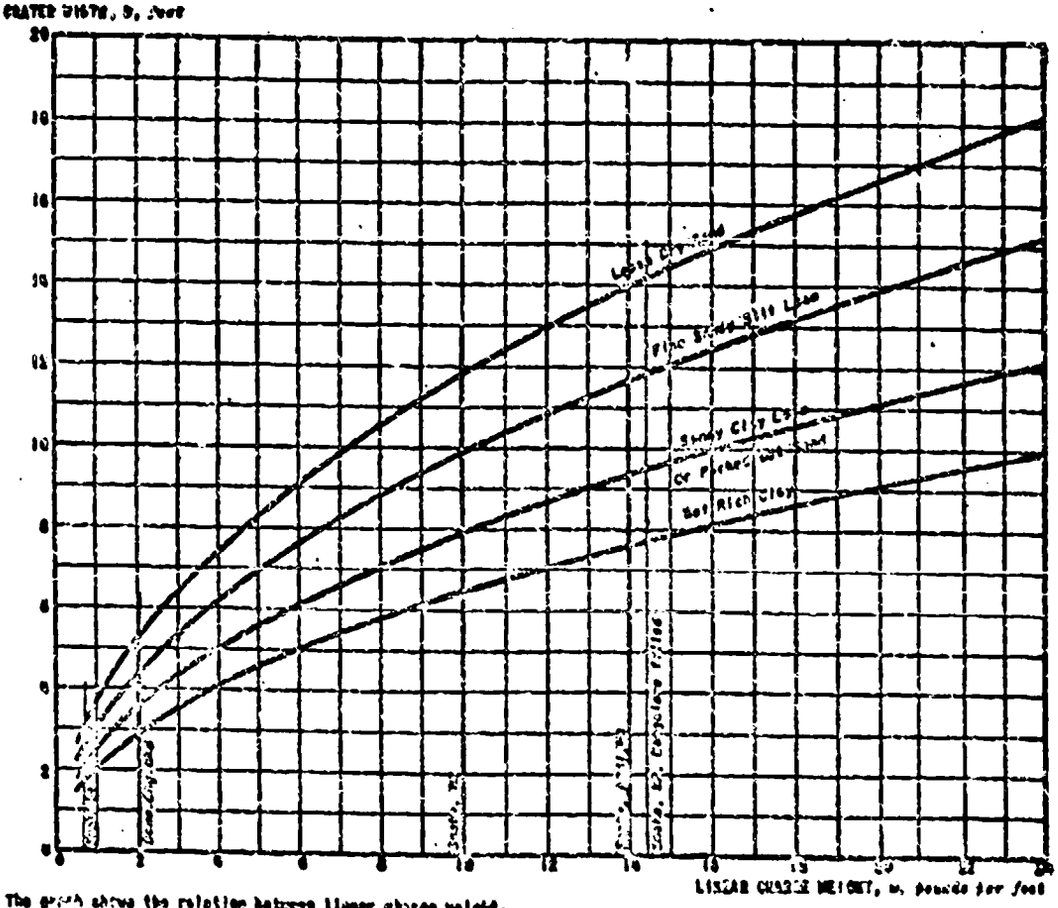

The graph shows the relation between linear charge weight, w, in lb/ft and the width of crater, S, in feet formed by detonating line charges on various soils. This width is measured between the shear shoulders of the crater as shown in the sketch.

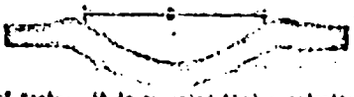

The lines which are drawn are based on the average of a large number of tests. It is expected that a majority (70%) of craters will differ from the average by less than 10%. A minority (30%) of the cases will show extreme variation. Explosive tests include C-4, Amatol, TNT and liquid explosives. Variation in crater width is attributed chiefly to soil conditions; effect of different explosives is masked by this variation.

Example: The M-3 mortar (16 lb/ft) produces craters which should average 18 feet across in dry sand; 12 feet in fine sandy silt loam, 8½ feet in sandy clay loam or packed wet sand, or 7½ feet in wet rich clay.

Sources: Tests by Engineer Board, U.S. Army; and by Joint Army-Navy Experimental Testing Board, U.S.

Draft AES-19
August 1943

WEAPON DATA

EARTH DISPLACEMENTS DUE TO UNDERGROUND EXPLOSIONS IN CLAY SOIL

5B2 EARTH SHOCK DISPLACEMENTS

Data taken from British experiments on detonation of bombs and American experiments with bare charges.

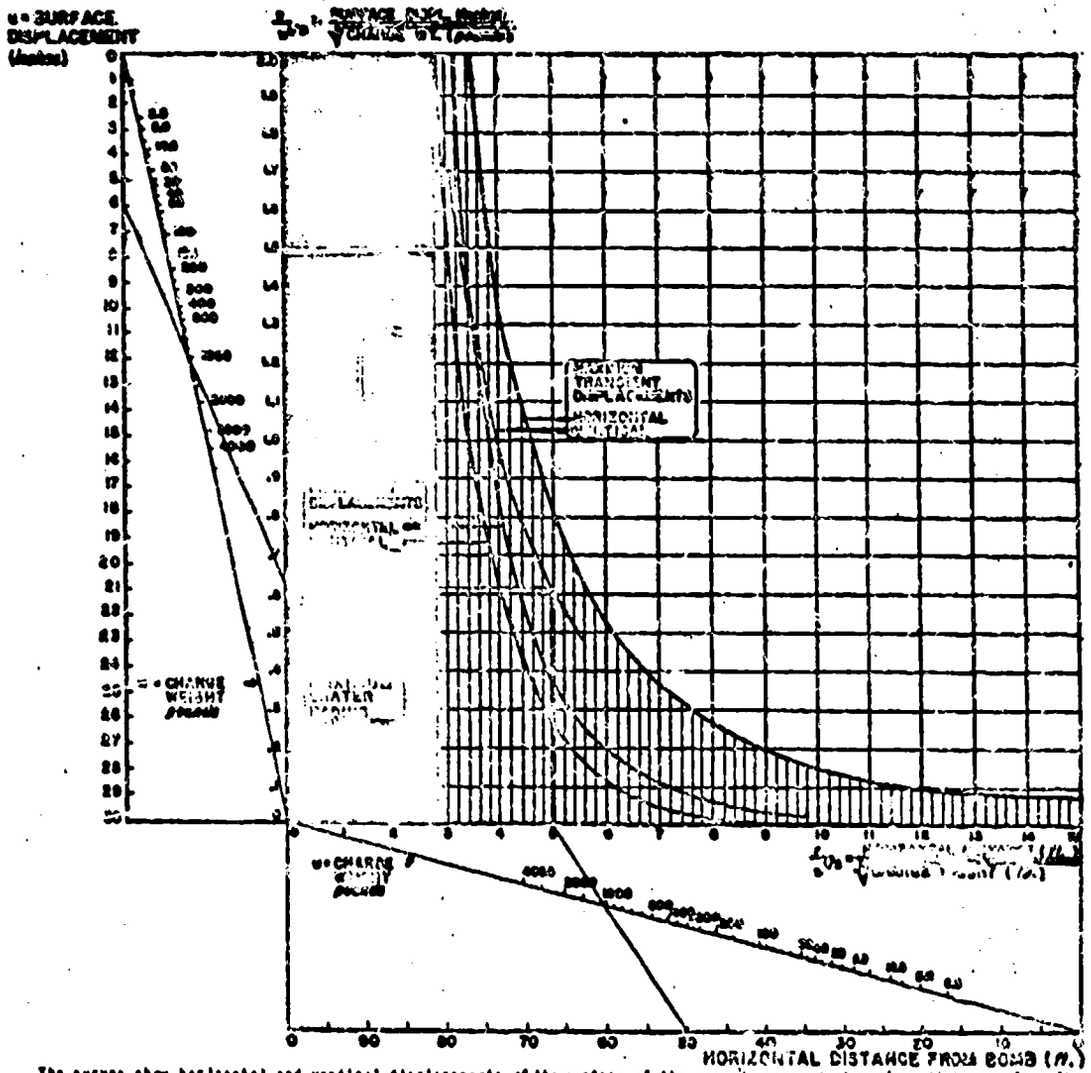

The curves show horizontal and vertical displacements of the surface of the ground measured at various distances from the exploding charge. The phenomena obey a model law, so that results for different weights of charge may be represented on the same curve.

SOIL EFFECTS: Values given are from observations on clay and clay-gravel mixture. Displacements in chalk, not shown on this plot, were found to fall below those in clay.

TYPE OF EXPLOSIVE: The curves are based on experiments using the following types of explosives: T.N.T., 60/40 Amatol, Seratol, Ditholite, Minol, Black Powder and Pyrotite, with charge weights ranging from 2.5 to [illegible] pounds. On the other hand, displacements in clay obtained with Torpex and Hexanite are greater than for equal weights of any of the above explosives.

PRESENCE OR DEPTH EFFECT: The data indicate that for the range of depths tested, the displacements obtained are independent of the depth of burial L provided only that the base of charge is completely buried. Depths in these experiments varied from 7 to 22 feet, and the corresponding values of $L/W^{1/3}$ were between 1.1 and 3.6 ft/(lb)$^{1/3}$.

ACCURACY OF GRAPH: The curves predict displacements over the entire range with an average deviation of 15%.

EXAMPLE: Dotted line indicates that a 1000-lb. charge produces a transient vertical displacement of 8 inches at 80 ft.

November 1943

CONFIDENTIAL

PEAK PRESSURE AND IMPULSE DUE TO EXPLOSION IN EARTH

B 3*
EARTH
PRESSURE - IMPULSE

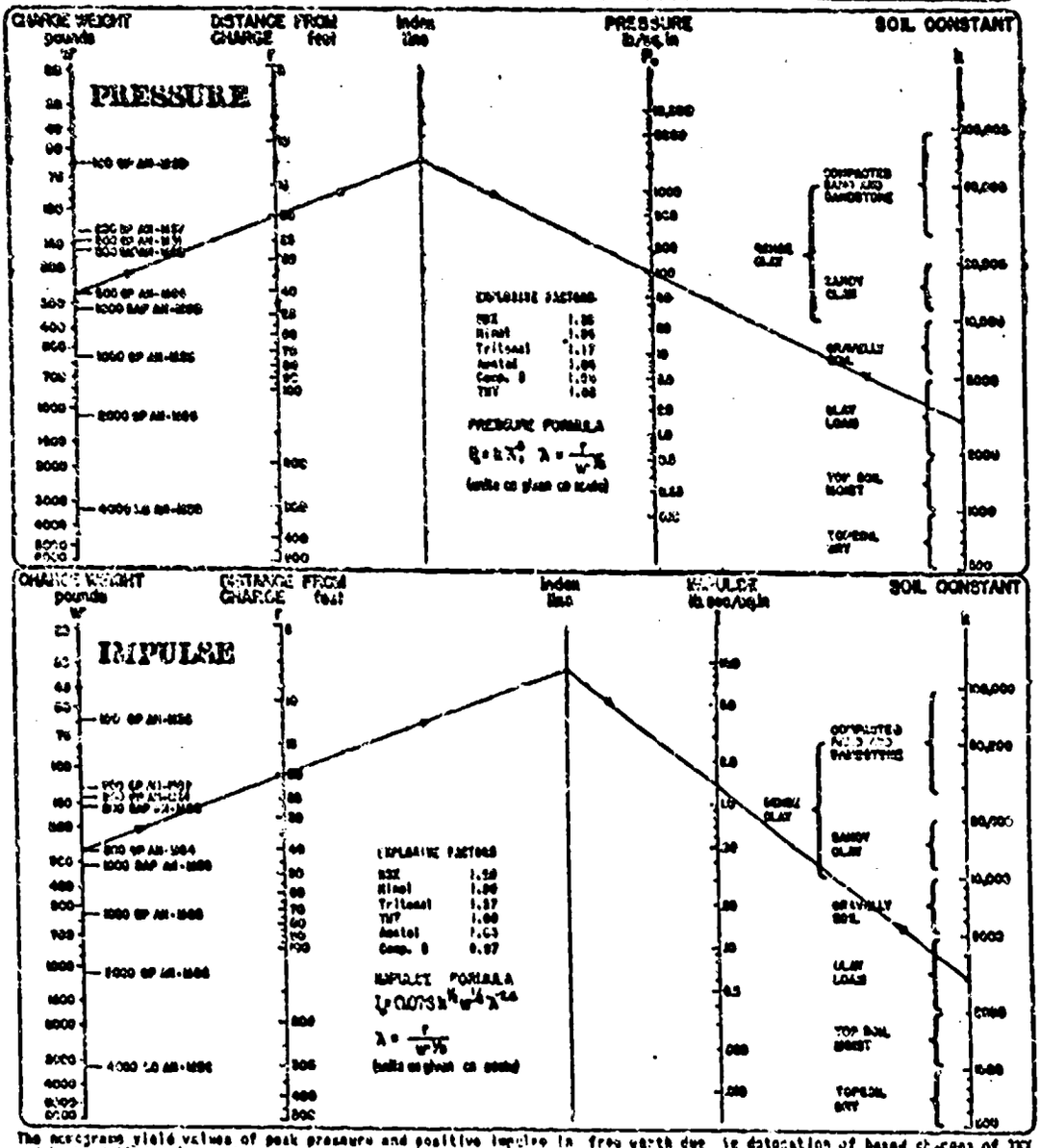

The nomograms yield values of peak pressure and positive impulse in free earth due to detonation of buried charges of TEX and bombs filled 50/50 Amatol. The equations are based on tests for the U. S. Engineers, and extensive small scale tests. In these tests the charge was buried at the depth giving maximum crater diameter ($2.1\ W^{1/3}$) ft and pressure and impulses were measured at the same depth. Under different geometrical conditions the values of pressure and impulse will differ from those given here. With gauges at a constant depth, variations in the charge depth between about $0.9\ W^{1/3}$ and $5\ W^{1/3}$ ft appear to produce negligible change in pressure and impulse values. On the other hand for fixed charge depth alteration of the gauge depth causes appreciable change in pressure approximately, there being a general increase with depth. Values of λ for typical soils are computed from the velocity of seismic waves in the subsurface material. Actually λ depends on many factors and ranges designated for various soil types should be considered a rough guide only. For explosives other than TEX, final values of pressure or impulse read from nomogram should be multiplied by the factors tabulated above.

Pressures measured at the surface of a buried massive target are found to be about twice the free earth values given by the nomograms. Impulse values are approximately 2.5 times the free earth values.

EXAMPLE: The dotted lines indicate that at a distance of 20 ft from a 267-lb charge of TEX the maximum free earth pressure in clay loam will be about 100 lb/in^2 and the impulse about 1.0 lb-sec/in^2.

Soft PTH No. 83
*Revised: September 1948

WEAPON DATA

PEAK PRESSURE AND IMPULSE DUE TO UNDERWATER EXPLOSIONS

Data supplied by the Underwater Explosives Research Laboratory, Division 8, NDRC.

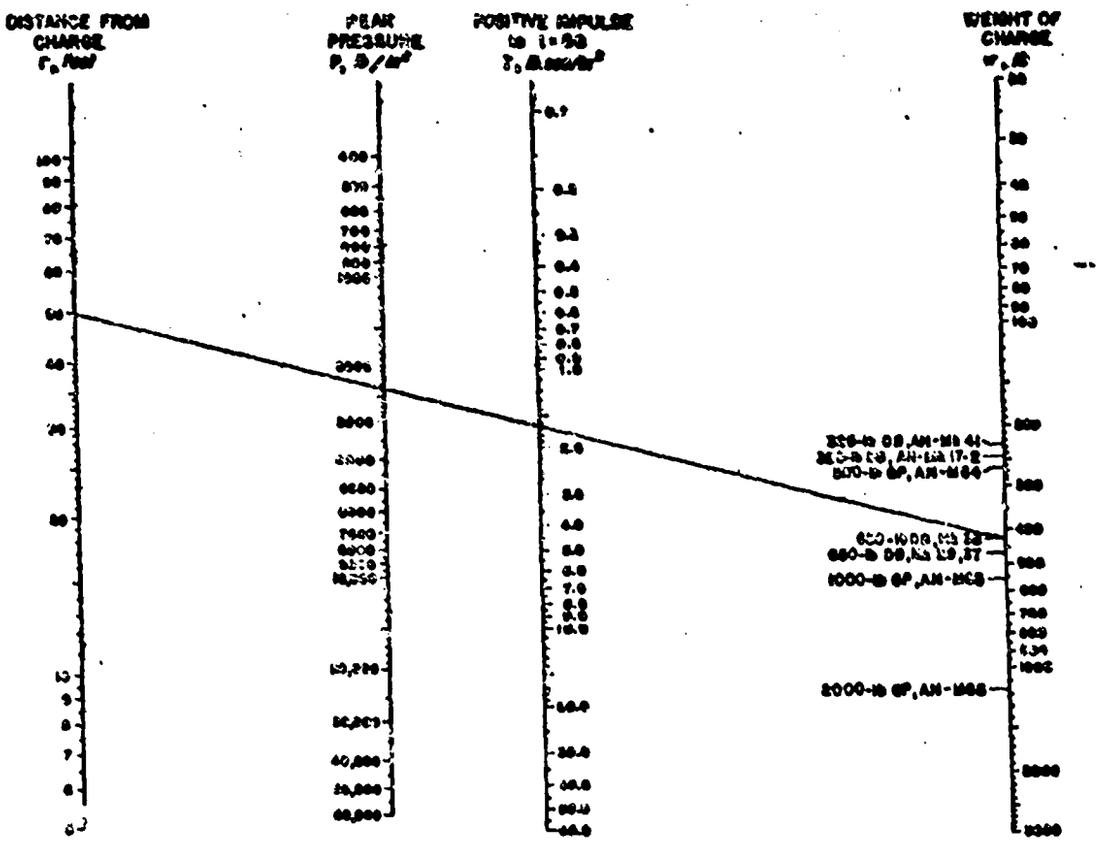

The nomogram yields values of underwater peak pressure and positive impulse due to detonation of charges of cast TNT. Values corresponding to TNT-filled American depth bombs and GP bombs accommodating hydrostatic fuses are indicated on the charge weight scale. Peak pressure measurements on the following explosives range from 10% to 20% higher than for TNT: 80X, Minol, 83Y, Special 80X, 80W, Torpex,— the values increasing in the order given.

The scales correspond to the following empirical equations based on a large number of measurements:

$$P_{max} = 20{,}400\left(\frac{W^{1/3}}{r}\right)^{1.13}, \qquad I_{max} = 1.80\left(\frac{W^{1/3}}{r}\right).$$

Gauges were located in the equatorial plane of the charge and were placed "side-on" relative to the oncoming wave. Average deviation of values obtained from different gauges is of the order of 3% - 6%.

The sketch shows a typical pressure-time record. Since the tail portion of such a curve decreases very slowly, it is necessary to measure t to a chosen point in order to obtain a definite value. This limit has been chosen as $t = \theta$, where θ is the time constant of a decreasing exponential function which fits the initial part of the curve. Absolute values of impulse may be inexact by as much as 15%.

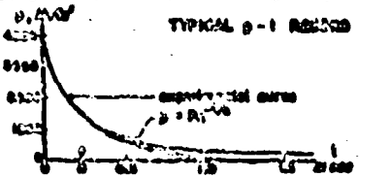

EXAMPLE: At 60 feet a 600-lb Mk 58 depth bomb (charge weight = 425 lbs.) produces a peak pressure of 2400 lb./in^2. and a positive impulse of about 1.7 lb. sec./in^2.

April 11 1944

CONFIDENTIAL

WEAPON DATA

MAXIMUM RADIUS OF BUBBLE OF BURNT GASES FROM AN UNDERWATER EXPLOSION

5C2 UNDERWATER BUBBLE RADIUS

WEIGHT OF CHARGE, pounds	DEPTH OF CHARGE, feet												
	2	3	4	5	10	15	20	25	30	40	50	75	100
0.1	1.8	1.7	1.7	1.7	1.6	1.6	1.5	1.5	1.5	1.5	1.5	1.4	1.4
0.25		2.4	2.4	2.5	2.2	2.2	2.1	2.0	2.0	1.9	1.9	1.8	1.8
0.5		3.0	3.0	3.0	2.8	2.7	2.6	2.5	2.5	2.3	2.2	2.0	1.9
0.75			3.4	3.3	3.2	3.1	3.0	2.9	2.8	2.7	2.5	2.3	2.2
1.00			3.7	3.6	3.5	3.4	3.3	3.2	3.1	2.9	2.8	2.6	2.4
2.00			4.7	4.6	4.5	4.3	4.2	4.0	3.9	3.7	3.5	3.2	3.0
3.00				5.2	5.1	4.9	4.8	4.6	4.5	4.2	4.0	3.7	3.5
5.00				6.2	6.1	5.8	5.6	5.3	5.2	4.9	4.6	4.3	4.0
7.5				7.1	7.0	6.7	6.4	6.3	6.1	5.8	5.5	5.1	4.7
10.				7.8	7.7	7.4	7.1	6.9	6.7	6.4	6.1	5.5	5.1
15.					8.8	8.4	8.1	7.8	7.6	7.3	7.0	6.3	5.8
[illegible]					9.8	9.3	9.0	8.7	8.4	8.0	7.7	7.0	6.4
[illegible]						10.	9.7	9.4	9.1	8.6	8.2	7.5	6.8
50.						11.	10.	10.	9.6	9.2	8.8	8.0	7.2
60.						12.	11.	11.	11.	10.	9.6	8.8	8.1
80.						13.	12.	12.	11.	11.	10.	9.6	8.8
80.						13.	13.	13.	12.	12.	11.	10.	9.3
70.						14.	14.	13.	13.	12.	11.	10.	9.8
80.							14.	14.	13.	13.	12.	11.	10.
90.							15.	14.	14.	13.	13.	12.	11.
100.							15.	15.	14.	14.	13.	12.	11.
150.							18.	17.	16.	15.	15.	14.	13.
200.							19.	19.	18.	17.	16.	15.	14.
250.								20.	19.	18.	18.	16.	15.
300.								21.	21.	20.	19.	17.	16.
400.								23.	23.	22.	21.	19.	18.
500.									25.	23.	22.	20.	18.
750.									29.	27.	26.	23.	22.
1000.										29.	28.	26.	25.
1500.										34.	33.	29.	27.
2000.										37.	36.	32.	30.
4000.											46.	41.	38.

CALCULATED BUBBLE RADIUS FOR TNT, *feet*

To estimate radius for other explosives multiply value in table by:
1.07 for tetryl
1.21 for torpex

WEIGHT CONVERSION TABLE

pounds		grams
0.1	=	45.4
0.25	=	113.6
0.5	=	227.
0.75	=	340.8
1.00	=	454.

The table gives the maximum radius of the bubble formed by burnt gases from an underwater explosion and is based on the equation given below

$$R = k\left[\frac{W}{H + H_a}\right]^{\frac{1}{3}}$$

where: R = maximum radius, *feet*
k = constant dependent on explosive charge = 12.2 lb$^{\frac{1}{3}}$ ft$^{\frac{1}{3}}$ for TNT
W = weight of charge, *pounds*
H = depth of charge, *feet*
H_a = atmospheric head = 33 ft

This equation is derived theoretically in NDRC Report C4-sr20-010. The constant k was determined from the relation between the period of pulsation and the radius which is given in the above report and in the Applied Mathematics Panel Report 27.1R and from measurements of the period at the Underwater Explosives Research Laboratory. The table has been checked at one point by direct measurement of the bubble radius.

January 1945

GAO
IMPULSE
DAMAGE LEVELS

IMPULSE CRITERION-DAMAGE LEVELS

Damage to buildings of wall bearing construction has been divided into the following categories:

A Damage: Buildings completely demolished.
B Damage: Damaged beyond repair and requiring demolition. If one fourth of the wall area is destroyed, the entire building is said to suffer B damage.
C Damage: Seriously damaged and requiring repair before being used.
D Damage: Still habitable, but requiring repairs.

The mean radius and maximum radius of each level of damage due to blast has been calculated as follows: From one incident the value of the maximum radius of damage of a given level is obtained by measuring the distance between the bomb and the furthest point of the furthest building suffering that degree of damage. Averages over a number of incidents of such radii for German instantaneously fuzed bombs against British wall bearing construction are given for various sizes of bombs in REN 219 revised.

The mean radius of a given level of blast damage from a bomb is determined as the radius of the circle with the bomb as center which includes as many buildings which do not suffer the specified degree of damage as there are damaged buildings excluded. For a number of incidents one averages the areas so obtained. The radius of a circle with the average area is then the average mean radius. Such radii are also listed in REN 219, revised.

The mean and maximum radii of a given level of damage are found to be proportional to $w^{1/3}$ where w is the weight of explosive in the bomb in pounds, for bombs which are not too large (less than 3500 lb. of explosive). The constant of proportionality depends on the level of damage as well as on the explosive used, case weight, etc. The distance from a bomb with w pounds of explosive at which a given level of positive impulse is obtained also is proportional to $w^{1/3}$. This suggests that a correlation exists between impulse and damage. (This correlation is supported by theoretical arguments to be found in B.C. 2081). The table below gives the relation between radii of damage and impulse levels, found to exist for British construction.

IMPULSE LEVELS FOR BRITISH CONSTRUCTION Instantaneous Fuzed Bombs	I, lb-millisec/in^2
Mean radius, A Damage	130
Maximum radius, A Damage	90
Mean radius, B damage	72
Maximum radius, B Damage	55
Mean radius, C Damage	40
Maximum radius, C Damage	30

IMPULSE LEVELS FOR GERMAN CONSTRUCTION (Damage Determined by Photocover) Instantaneous Fuzed Bombs	I, lb-millisec/in^2
Mean radius, demolition	130
Maximum radius, demolition	90
Mean radius, visible damage	85
Maximum radius, visible damage	60

Also listed in the table are the categories of damage applied to photo-cover of results of Allied bombing of German wall bearing construction. It was found that the categories of damage A, B, and C could not be distinguished on photo-cover and two categories, demolition and visible damage were introduced. Since German construction is heavier than British, it is to be expected that the impulse level corresponding to a given degree of damage such as A, B, or C would be increased; the amount of increase is given to a first approximation by the ratio of wall thicknesses. Thus, the mean radius of B damage against German construction is expected to correspond to an impulse level of 108 lb-millisec/sq.in. The radius of demolition is thus between the radii for A and B damage whereas that for visible damage is slightly larger than the radius for C damage.

The descriptive of the area of damage from a circle is reflected in the large difference between the maximum radius of a given level of damage and the mean radius. The reason for this is that because of the built-up-ness of the target there is shielding of the blast. The evidence indicates that on the average this shielding can be taken into account by decreasing the maximum radius of a given category of damage by 33% to obtain the mean radius (since impulse is inversely proportional to distance).

Theoretical considerations and operational data show that the impulse criterion does not hold for very large blast bombs. The weight for which it no longer applies depends on the type of construction. For British and German construction the radius of a given level of damage from bombs having between 3500 and 5000 lbs. of explosive is proportional to $w^{1/3}$. For considerably larger bombs it becomes proportional to $w^{1/2}$. The latter is the same as the dependence of the distance for a given level of peak-pressure on the weight of explosive. This is reasonable since as the weight of explosive increases the duration of the blast at a given point increases and so does the impulse; however, the walls of the building will not fail under blast loading with large impulse unless the practically constant pressure (which occurs in this case) is above the static strength of the walls. (See B.C. 2148).

Using the relation given in sheet 2 A2° for impulse due to explosions on the ground, values of the radii for A, B, and C damage due to different bombs have been computed. Results are given in the table below.

Bomb, Instantaneous Fuzing	Mean Radius A Damage, ft	Mean Radius B Damage, ft	Mean Radius C Damage, ft
1000-lb GP AN-M59, TNT Filled	77	112	181
1000-lb GP AN-M59, Tritonal Filled	86	124	196
2000-lb GP AN-M67, TNT Filled	118	170	269
2000-lb GP AN-M67, Tritonal Filled	134	193	305
4000-lb GP AN-M66, TNT Filled	180	259	410
4000-lb GP AN-M66, Comp. B Filled	214	308	487
4000-lb GP AN-M66, Tritonal Filled	233	335	531
1000-lb GP AN-M65, TNT Filled	228	329	520
1000-lb GP AN-M65, Comp. B Filled	254	366	581
1000-lb GP AN-M65, Tritonal Filled	278	400	634
2000-lb GP AN-M66, TNT Filled	325	468	742
2000-lb GP AN-M66, Comp. B Filled	365	526	832
2000-lb GP AN-M66, Tritonal Filled	398	573	908
4000-lb LC AN-M56, TNT Filled	519	748	1185
4000-lb LC AN-M56, Comp. B Filled	581	837	1326
4000-lb LC AN-M56, Tritonal Filled	632	911	1443

September 1945

G 41h*
STEEL COLUMNS

BLAST DAMAGE TO STEEL COLUMNS

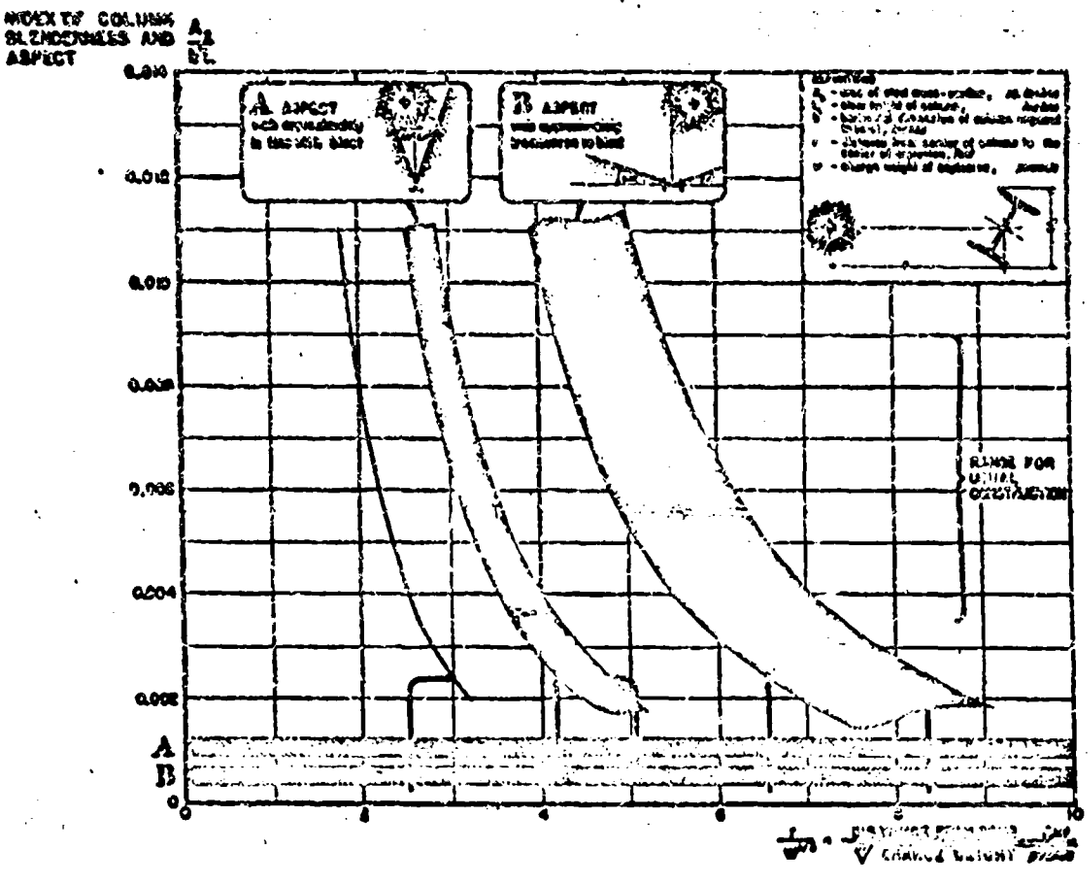

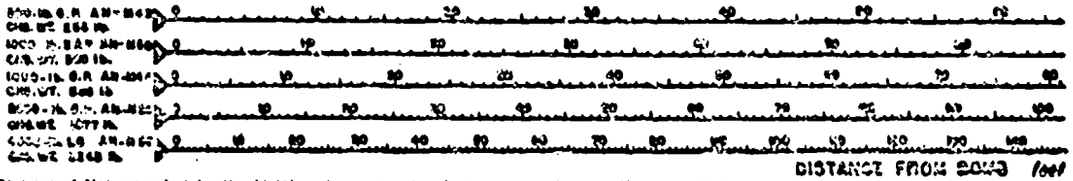

The curves deflect appreciably the limiting distances for various values of $\frac{A}{B}$. At high blast values will be damaged to different ranges, blown out or uncovered, damaged beyond repair either by collapse, or set down for critical repair. The width of the bands is connected to the assumption of reasonable variations in the shape of a representative section assigned to carry a given load. The bottom lines, plotted vertically, is the value of the steel cross-section of the column to the ray normal to the blast. This area is to the product of the length of the column and the projected width on a line perpendicular to the line joining the column to the burst. This value is related to the radius of the ratio of gyration of the cross-section to the length of the column, i.e. large values of the index corresponds to stubby columns and small values to slender columns.

The columns are assumed to have no partitions or walls attached and to be separate to blast on all sides. If there are partitions attached to the columns the radius of damage is likely to be greater, since part of the force on the blanketed structure is transmitted to the columns. Further, in such cases the blast wave cannot so readily wash the way around the column to look it up from behind, as the other hand, where the column is supported by partitions or walls approximately in line with the blast wave, the values of damage should be considerably smaller.

As shown by the curves, the radius of damage is considerably reduced when the brab is attached eccentrically to line with the axis of the column (direct A). For bombs dropped at random in an ordinary building, about 70 - 80% of the cases of damage will be those in which the web is more or less perpendicular to the blast (direct B), and the remainder will be cases in which the web is more nearly in line with the blast.

The chart does not contemplate the destruction of the column by overturning of the loading. Such failures may cause destruction at a value of $\frac{A}{B}$ of about 2.

For charge weights less than about 500 pounds, the radius of damage appears to be less than that given by the chart.

The path of the fragments reported are for single story industrial buildings, with only a few cases of doubtful validity of multi-story framed buildings. All columns are single rolled steel sections.

EXAMPLE: Given a building of average steel-type construction with 4-column 2 in. x 8 in. x 20 in/ft, or 12 ft. unsupported length can exposed to blast whose direction is not from the very long aspect B. Then, $\frac{A}{B} = \frac{12 \text{ in.}}{8 \text{ in.}} = 1.5$, and $\frac{A}{B}$ = 1.5 in., so that $\frac{A}{B}$ = 0.1875, the column lasts under these conditions. It can be expected that such a column will be thrown out or severed by a charge of ammonal some distance away to be about if that the explosive charge of will damage this column beyond repair at distances up to about 80 to 90 feet.

When such detailed information on the construction is not available, it is suggested that the column index be taken as about 0.005, about the upper part of the range for steel construction.

November 1948

6 A4h* CONCRETE COLUMNS

BLAST DAMAGE TO CONCRETE COLUMNS

DATA PREPARED FROM INFORMATION GIVEN IN BRITISH R.C.D. DAMAGE REPORTS AND DATA COMPILATIONS

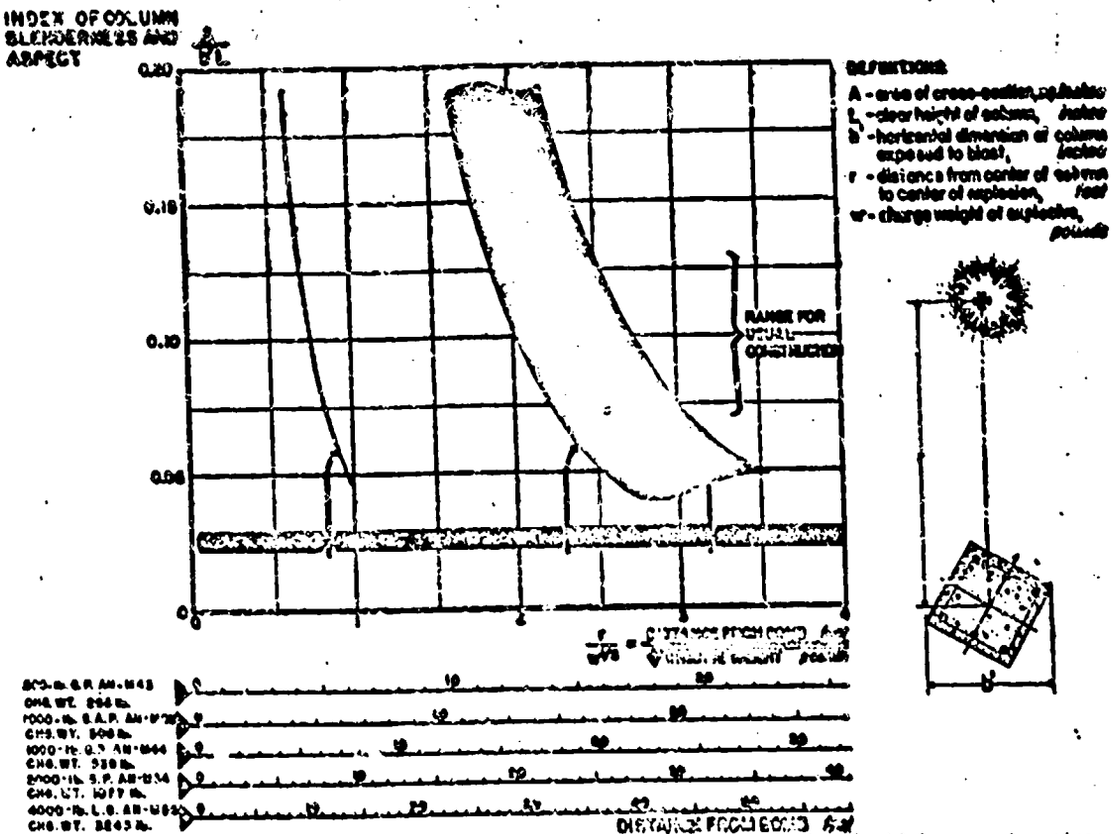

DEFINITIONS

A - area of cross-section, sq.inches
l_c - clear height of column, feet
b - horizontal dimension of column exposed to blast, inches
r - distance from center of column to center of explosion, feet
w - charge weight of explosive, pounds

The curves define approximately the limiting distances from various bombs at which concrete columns will be damaged by blast in different ways - blown out or severed, damaged beyond repair, or not damaged critically. The width of the band is computed on the assumption of reasonable variations in the shape of a cross-section designed to carry a given load. The column index, plotted vertically, is the ratio of the cross-sectional area of the column to the area exposed to the blast. This area is the product of the length of the column and its projected width on a line perpendicular to the line joining the column to the bomb. The index is thus approximately equal to the ratio of the depth of the column to its length, i.e. large values of the index correspond to stubby columns and small values to slender columns.

The columns are assumed to have no partitions or walls attached, and to be exposed to blast on all sides. If there are partitions attached to the columns the radius of damage is likely to be greater, since part of the force on the attached elements is transmitted to the columns. Further, in such cases the blast wave cannot so readily make its way around the column to back it up from behind. On the other hand, where the column is supported by a wall or partition approximately in line with the blast wave, the radius of damage would be considerably smaller.

The chart does not contemplate the destruction of the columns in the lowest story of a building by undermining of the footings. Such an action may cause destruction at a value of $r/w^{1/3}$ of about 8. Neither does the chart consider the action of blast in a relatively confined space, which may cause tensile failure of the column by so-called "uplift" at a greater distance than shown by the chart.

For charge weights less than about 200 pounds, the radius of damage appears to be less than that given by the chart.

EXAMPLE: Given a building of average R/C frame construction having square columns with depth 1/10 the height. Then for blast perpendicular to the face of the column, the column index will be 0.10. It may be expected that such a column will be blown out or severed by a 1000-lb GP AN-M44 bomb at distances up to about 6 feet; the same bomb will damage the column beyond repair at distances up to about 16 to 22 feet.

November 1945

WEAPON DATA

DESTRUCTION OF CONCRETE FLOOR SLABS BY BOMBS

6 A2
CONCRETE FLOOR SLABS

AREA REMOVED,
thousands of square feet

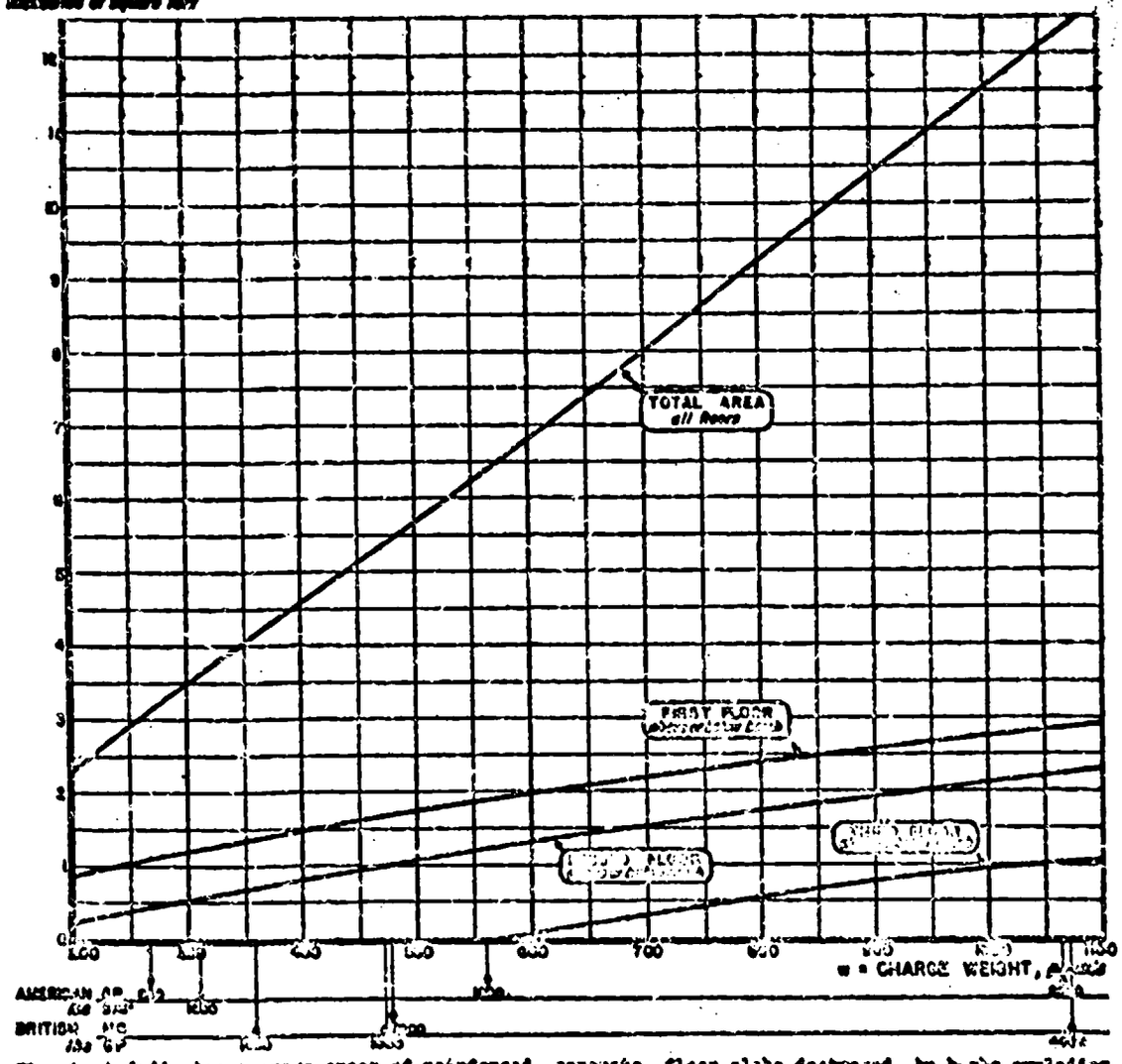

The chart indicates average areas of reinforced concrete floor slabs destroyed by bombs exploding within a building. The curves show, respectively, the average areas of destruction to be expected in the first, second and third floors above or below the bomb and the total area removed on all floors.

It is to be noted that for maximum effectiveness, bombs of about 600 pounds charge weight or less require at least two floors above and below the point of detonation and bombs of charge weight greater than 600 pounds require at least three floors above and below the point of detonation. Bombs of charge weight less than 500 pounds do not appear to produce significant damage.

These curves apply only to ordinary reinforced concrete floor slabs, four to eight inches thick and supported on steel or concrete beams. Waffle joist floors or other such types are not included.

In using the chart it should be remembered that the amount of available data on which this presentation is based is small, and some individual values differ from the average represented by the curve by as much as 100%.

SOURCE: Data Compilations and Incident Summaries of the British Ministry of Home Security.

August 1944

WEAPON DATA

REMOVAL OF LIGHT-WEIGHT SHEET ROOFING BY BLAST

6 A3*
ROOFING

A MAXIMUM RADIUS OF REMOVAL AS A FUNCTION OF THE CHARGE WEIGHT

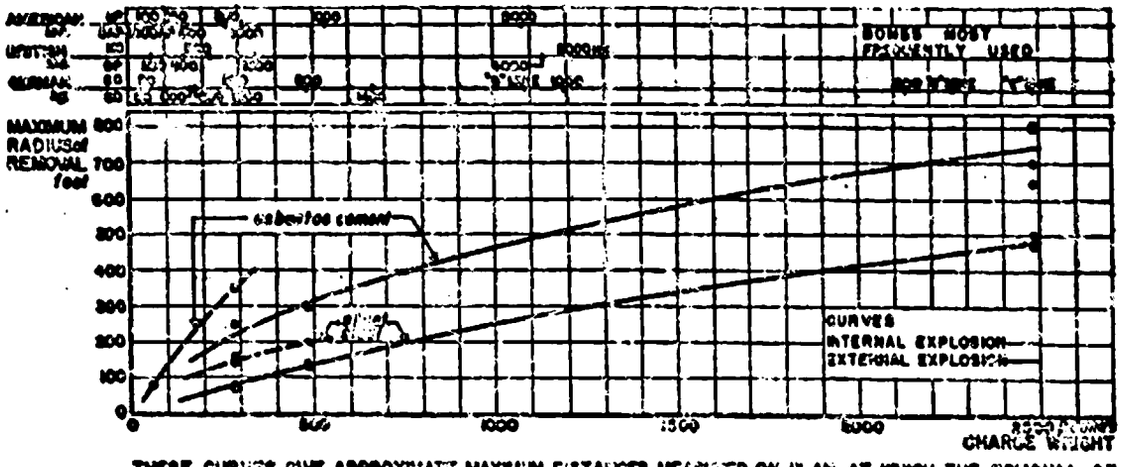

THESE CURVES GIVE APPROXIMATE MAXIMUM DISTANCES MEASURED ON PLAN, AT WHICH THE REMOVAL OF SHEET ROOFING MAY BE EXPECTED DUE TO EXPLOSION OF VARIOUS CHARGES INSIDE OR OUTSIDE OF STEEL-FRAME FACTORY TYPE BUILDINGS. GERMAN MINES APPARENTLY PRODUCE GREATER BLAST EFFECTS THAN BOMBS OF EQUAL CHARGE WEIGHT. ACCORDINGLY, CHARGE WEIGHTS FOR "C" AND "D" TYPE GERMAN MINES SHOULD BE TAKEN ABOUT 60% GREATER THAN THEIR NOMINAL WEIGHTS, WHILE THAT FOR THE TYPE "B" MINE SHOULD BE INCREASED ABOUT 40% IN ORDER TO ALLOW FOR THE EFFECT OF APPARENTLY THICKER STEEL CASE.

B REMOVAL OF ROOFING BY ONE 110-lb (50kg SC) G.P. BOMB EXPLODING INSIDE SINGLE STORY SHED-TYPE BUILDINGS OF VARIOUS VOLUMES

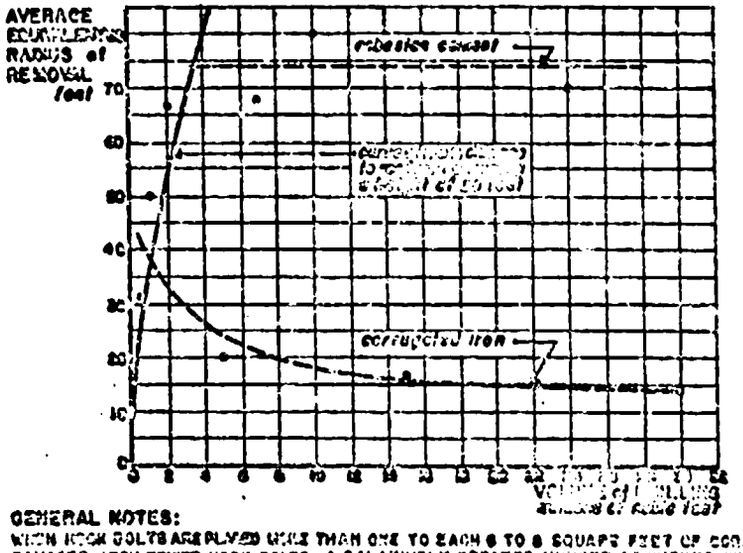

THIS CHART GIVES THE AVERAGE EQUIVALENT RADIUS OF REMOVAL OF SHEET ROOFING BY A SINGLE BOMB OF [illegible] SELECTED EXPLOSIVE WITHIN OF SINGLE STORY SHED BUILDINGS OF VARIOUS VOLUMES. AVERAGE RADIUS IS THE RADIUS OF A CIRCLE OF AREA EQUAL TO THE AREA OF DAMAGE, ALL MEASUREMENTS BEING ON PLAN. THE CHANGE IN HEIGHT OF BUILDING ENVELOPE WITHIN [illegible] TO RANGE [illegible] IS ASSUMED TO AFFECT [illegible] TAKING THIS CHANGE INTO [illegible] EVER, THE LATTER HAS A [illegible] TENDENCY TO CONFINE THE EXPLOSION.

GENERAL NOTES:

WHEN HOOK BOLTS ARE PLACED MORE THAN ONE TO EACH 6 TO 8 SQUARE FEET OF CORRUGATED IRON ROOFING, PURLINS WILL BE DAMAGED; WITH FEWER HOOK BOLTS, A RELATIVELY GREATER NUMBER OF SHEETS WILL BE BLOWN OFF..... INSULATING BOARD PLACED UNDER THE PURLINS PROMOTES TRANSFER OF BLAST UPLIFT EFFECT TO THEM, USUALLY CAUSING GREATER TOTAL DAMAGE..... RADII OF DAMAGE FOR CORRUGATED ROOFS CAN BE TAKEN TO BE APPROXIMATELY 50% LESS THAN THOSE FOR STEEL SHEETS..... FOR SLATES AND TILES ON BATTENS, RADII ARE OF THE SAME ORDER AS THOSE FOR ASBESTOS CEMENT..... CURVES "A" AND "B" ARE BASED ONLY ON INCIDENTS IN WHICH BOMBS EXPLODED AT OR ABOVE [illegible] LEVEL..... DAMAGE WOULD BE EXPECTED TO BE LESS FOR EXPLOSIONS BELOW GROUND.

DATA COMPILED FROM R.E. NOTE 220 AND R.E 4 - DATA COMPILATION NO 6, BRITISH MINISTRY OF HOME SECURITY.

September 1948

EFFECT OF EARTH SHOCK ON UNDERGROUND REINFORCED CONCRETE WALLS

6A5* EARTH SHOCK UNDERGROUND R/C WALLS

MAXIMUM DISTANCE for indicated degree of damage, r in ft																					
WALL THICKNESS, ft	100-lb GP AN-M30			250-lb GP AN-M57 500-lb SAP AN-M58			500-lb GP AN-M64 1000-lb SAP AN-M65			1000-lb GP AN-M66			2000-lb GP AN-M66			12000-lb GP T10			22000-lb GP T14		
	MODERATE	HEAVY	BREACH	MODERATE	HEAVY	BREACH	MODERATE	HEAVY	BREACH	MODERATE	HEAVY	BREACH	MODERATE	HEAVY	BREACH	MODERATE	HEAVY	BREACH	MODERATE	HEAVY	BREACH
1	11.0	7.8	5.6																		
2	8.8	5.8	4.2	12.4	8.7	6.3	18.0	12.6	9.0		17.0	12.3									
3	6.6	4.6	2.8	10.1	7.1	5.0	14.7	10.5	7.5	21.0	14.6	10.6	28.8	20.2	14.7						
4	5.3	3.5		8.5	6.0	4.7	12.7	9.0	6.3	18.2	12.8	9.2	25.9	18.1	13.1		36.0	26.0			
5	4.3	3.0		7.2	5.0		11.1	7.8	5.8	16.2	11.5	8.1	23.0	16.4	11.8	49.0	28.5	24.0		36.0	28.0
6	3.5			6.3	4.6		9.8	6.6	2.5	14.6	10.3	6.8	21.0	14.8	10.6	46.5	32.0	23.0	60.0	38.5	28.0
7				5.3			8.6	5.7		13.2	9.1	6.2	19.3	13.7	9.8	41.5	29.0	21.5	46.0	32.0	23.0
8				4.9			7.6	4.8		11.9	8.1		17.8	12.5	7.8	39.0	27.5	20.0	43.5	30.5	21.5
9							6.6			10.8	7.1		16.5	11.3	6.1	36.5	25.0	18.5	40.5	28.5	20.5
10							6.7			9.8	6.6		15.2	10.4		34.5	24.5	17.5	38.5	27.5	19.5

The bombing efficacy is xr^2/w where xr^2 is the area in square feet within which any walls present will be damaged, and w is the weight of the explosive charge in the bomb, in pounds. For area bombing of underground walls, the efficacy reaches a maximum for $s/w^{1/3}$ between 0.4 and 0.5, where s is the thickness of the wall in feet. This determines the optimum size of bomb for area bombing of underground walls of any known thickness.

Similarly, for area bombing of very long narrow underground targets with reinforced concrete walls, the maximum expectation of damage per pound of explosive will be attained for $s/w^{1/3}$ between 0.8 and 1.0 for breaching or heavy damage.

DAMAGE CRITERIA ASSUMED:

DESCRIPTION OF DAMAGE	TYPE OF SUPPORT		s/R_c, s/ft
	2-edge support	4-edge Support	
SLIGHT	Fine Cracks	Fine Cracks	0.03
MODERATE	Medium Cracks	Light Scabbing	0.1
HEAVY	Heavy Cracks and Scabbing	Severe Scabbing	0.2
BREACHING	Breached	Breached	0.5

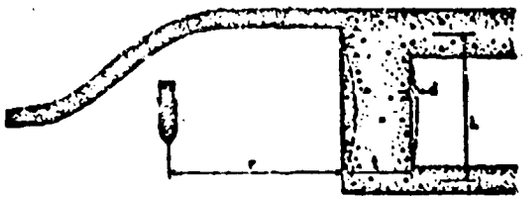

The table gives values of the maximum distance at which various degrees of damage will result from detonation of bombs in earth. The figures given in the table apply to lightly reinforced rectangular concrete wall panels supported along either two opposite edges or along all four edges. The bomb is assumed to be approximately opposite the center of the face of the wall; any marked departure from this position will generally result in less damage. Under the same conditions the 2-edge and 4-edge supported walls will be damaged differently as described by the *Damage Criteria* above, but the ratio of central deflection to span is a good measure of damage for both types.

This information is based on tests of walls whose face dimensions are in the ratio of about 8:5, and whose span to thickness ratio is between 5:1 and 10:1. The test walls were reinforced with mild steel bars, about one percent by volume. Damage and central deflection were measured for bombs detonated at various distances on the earth side of the wall as shown in the sketch. Charge weights used in these tests ranged from 1/8 lb to 1600 lb.

The graph gives the ratio of central deflection to span for various wall thicknesses and charge distances in terms of the scale variables $s/w^{1/3}$ and $r/w^{1/3}$.

Tabulated values based on only meager data are given in italics. Similarly, the corresponding parts of the curves on the graph are dotted.

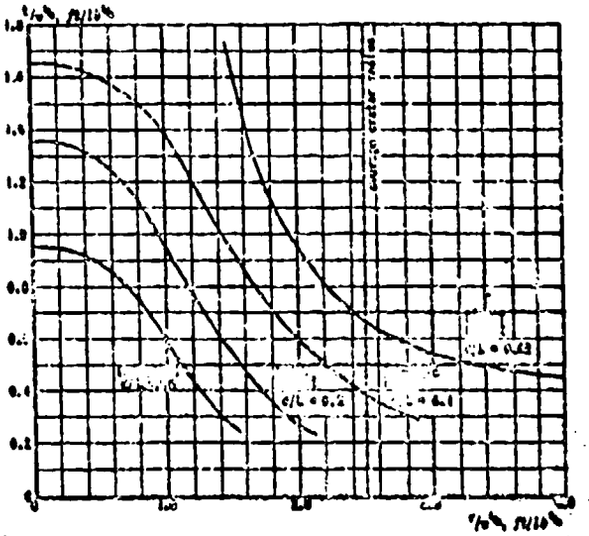

REFERENCES:
Tests by Ministry of Home Security and Road Research Laboratory (British) and by Committee on Fortification Design (U.S.A.)

Ref: SWT-2B (OCRD-5286)
Reviewed: August 1945

WEAPON DATA

DAMAGE TO REINFORCED CONCRETE WALL PANELS BY DETONATIONS IN AIR

6 AG* DAMAGE TO R/C WALLS IN AIR

WALL THICKNESS, ft	MAXIMUM DISTANCE for indicated degree of damage, r in ft																				
	100-lb GP AN-M30			250-lb GP AN-M57 500-lb GAP AN-M59			500-lb GP AN-M64 1000-lb GAP AN-M65			1000-lb GP AN-M66			2000-lb GP AN-M66			4000-lb GP T10			22000-lb GP T10		
	MODERATE	HEAVY	BREACHING	MODERATE	HEAVY	BREACHING	MODERATE	HEAVY	BREACHING	MODERATE	HEAVY	BREACHING	MODERATE	HEAVY	BREACHING	MODERATE	HEAVY	BREACHING	MODERATE	HEAVY	BREACHING
1	3.1	2.2	1.2	8.4	6.4	2.8	9.4	7.8	3.8			8.0									
2	1.3	0.8		3.9	1.8	0.5	5.2	2.8	1.5	7.2	5.6	3.0	11.8	9.8	5.7			18.8			
3	0.5			1.3	0.3		2.9	1.2	0.1	4.4	2.8	1.2	7.4	5.0	2.8	28.7	20.0	12.4	39.0		18.8
4				0.7			1.8	0.8		3.0	1.2		5.2	2.9	1.1	15.8	12.0	10.7	24.2	19.8	11.8
5							1.0			2.1	0.4		3.8	1.7		12.2	8.3	4.8	18.6	14.8	8.3
6										1.5			2.8	0.7		10.3	6.5	3.1	15.7	11.0	5.7
7													2.1	0.1		7.8	5.1	1.2	12.8	8.1	3.8
8													1.5			6.7	3.1	0.3	10.7	6.2	2.0
9																5.8	2.1		9.5	5.0	1.0
10																5.0	1.4		8.1	3.8	0.2

The bombing efficacy is $\frac{Ar^2}{W^{2/3}}$ where Ar is the area in square feet within which any walls present will be damaged, and W is the weight of explosive charge in the bomb, in pounds. For area bombing of reinforced concrete walls the efficacy increases with the charge weight, so the maximum damage per pound of explosive will be attained by use of the bomb with the largest possible charge.

Similar reasoning shows that for area bombing of very long narrow targets having reinforced concrete walls, the bomb with the largest possible charge gives the greatest expectation of damage per pound of explosive.

DAMAGE CRITERIA ADOPTED:

DESCRIPTION OF DAMAGE	TYPE OF DAMAGE	Average Deflection Ratio $\frac{\text{in/ft}}{\text{in/ft}}$
SLIGHT	Slight Cracking and Bending	0.1
MODERATE	Light Punching and Cracking with Possibly Some Spalling	0.5
HEAVY	Heavy Punching, Shattering, or Possible Perforation	1.2
BREACHING	Perforation with Extensive Scabbing, Rare May be Cut or Entirely	---

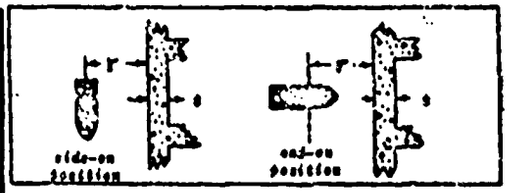

For contact and very near contact shots, nose-on position of a bomb will cause less damage than side-on. Figures given correspond to side-on position, the bomb detonating not far from a point opposite center of wall. Positions appreciably off side usually result in lessened damage.

The table gives max. distance at which an air-backed reinforced concrete wall or wall panel that will experience various degrees of damage due to explosion of TNT-filled bombs in air nearby or in side-on contact with the wall.

These data derive from tests, both model and full scale, on rectangular panels with face dimensions from 8 to 25 times the thickness. Charges used in tests ranged from about $\frac{1}{2}$ oz. to 1000 lb. Test panels were supported along all four edges, and results showed no appreciable difference between freely supported and fixed edges.

Tests involved various degrees of reinforcing and different explosives, but all data were reduced to a basis of 1% steel by volume and bombs filled TNT. Degree of damage and ratio of central deflection to span correlate fairly well for slight, moderate and heavy damage.

Tabulated data refer to about 1% reinforcing steel by volumes. For $\frac{1}{2}$% steel, multiply thickness values by 0.9 for breaching and by 0.7 for other degrees of damage.

Fragments from nearby bomb detonations usually cause surface scars and a few perforations; this type of damage is not included in the present analysis.

The graph gives damage curves in terms of scale variables $r/w^{1/3}$ and $t/w^{1/3}$, where t = wall thickness (ft), r = distance from wall to bomb (ft) and w = weight of charge (lb).

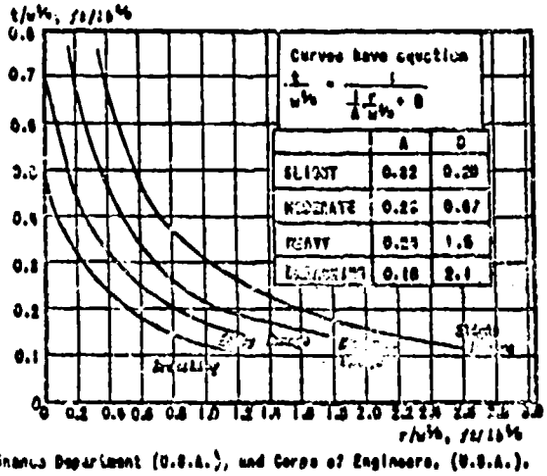

SOURCE: Tests by Ministry of Home Security (British), Ordnance Department (U.S.A.), and Corps of Engineers, (U.S.A.).

PTM No.10B & EXT-6
* Revised: August 1945

WEAPON DATA

DAMAGE TO SINGLE-STORY INDUSTRIAL BUILDINGS BY HE BOMBS

6 B1
HE BOMBS:
INDUSTRIAL BUILDINGS

A. STRUCTURAL DAMAGE DUE TO HIGH EXPLOSIVE BOMBS

The table gives the Mean Area of Effectiveness (MAE) and the near miss distance for common General Purpose bombs (fuzed 0.1 seconds delay nose, 0.01 seconds delay tail) on European Type industrial buildings, and for the 4000-lb LC bomb (fuzed instantaneous). Bombs striking within the near miss distance from the building may be expected to cause damage comparable to that of a direct hit in about one out of ten cases. Bombs striking farther from the building than the near miss distance cause no appreciable structural damage. The effects of the near miss hits are included in the values of MAE tabulated below.

STRUCTURAL CLASS 1, 3 and 5	MAE, sq feet per bomb, and NEAR MISS DISTANCE, r in feet							
	500-lb GP		1000-lb GP		2000-lb GP		4000-lb LC	
	MAE	NEAR MISS DISTANCE	MAE	NEAR MISS DISTANCE	MAE	NEAR MISS DISTANCE	MAE	NEAR MISS DISTANCE
(1) Single story, area > 10000 sq.ft. Principal source of roof support consists of light to heavy concrete or steel roof structural simple beams and columns, arches or rigid frames, trusses, sawtooth trusses, etc. No travelling cranes.	3050 ± 250	13 ft	6400	20 ft	12800	35 ft	32000	80 ft
(3) Single story, area > 10000 sq.ft. Principal source of roof trusses > 50 ft. height to eaves generally 25 ft. Roof structural simple beams, bowstring trusses, arches, rigid frames, etc. No travelling cranes.	5270 ± 550	15 ft	11000	30 ft	22000	55 ft	55000	80 ft
(5) All single story buildings of < 10000 sq.ft. floor area	3100 ± 250	15 ft	6600	20 ft	13000	35 ft	33000	80 ft

Results for the 500-lb GP bomb were obtained from an analysis of 38 USSAF attacks on European industrial targets. The values of the MAE's were determined from the damaged data, and from the number of hits as determined by photointerpretation. The MAE's were determined from the relation $r = A(1-(1-H/A)^{\frac{1}{2}})$ where r is the total area of damage, in square feet, A is the total area of the building in square feet, A is the total number of hits, and H is the MAE per bomb. Bombs used in the raids analyzed were fuzed 0.1 nose and 0.01 tail, or 0.1 nose and 0.025 tail, the majority of the bombs having the shorter fusing. See EWT-2f for averaging process for a number of damaged buildings.

Values given for the 1000-lb and 2000-lb bombs were estimated from the values determined for the 500-lb GP bomb on the assumption that the MAE is proportional to the weight of charge in the bomb. Experience has shown that this assumption is approximately correct.

B. STRUCTURAL AND FIRE DAMAGE DUE TO HIGH EXPLOSIVE BOMBS

Analysis of a number of incidents has shown that the probability of a serious fire being started by a 500-lb GP bomb is 0.17. Thus the overall mean area of effectiveness for structural and fire damage in industrial buildings with 500-lb GP bombs is $0.83(MAE) + 0.17(E)$ where MAE is the mean area of effectiveness for structural damage and E is the average expected damage due to one fire. For combustible buildings, E is the total area of one fire division; for non-combustible buildings, E is approximately 35,000 sq.ft. for large fire divisions and a correspondingly smaller area for fire divisions smaller than 100,000 sq.ft. (see graph on sheet 6 B2). The table gives the gross MAE for both structural damage and fire damage for European industrial type buildings attacked by 500-lb GP bombs fuzed 0.1, nose, and 0.01, tail.

STRUCTURAL CLASS see above	COMBUSTIBLE or NON-COMBUSTIBLE	GROSS MAE, sq ft per bomb for Structural and Fire Damage by 500-lb GP Bombs on Fire Divisions of Different Areas, sq ft					
		7,000	15,000	30,000	60,000	100,000	200,000
1	C	8720	8030	7630	12720	15[illegible]0	[illegible]0
	N	3560	6570	6180	7080	8160	8170
3	C	5660	6920	6[illegible]70	10570	21[illegible]0	[illegible]0
	N	6490	6810	7070	8730	[illegible]0	10210
5	C	3750	6120	7670	12770	15[illegible]0	[illegible]0
	N	3650	6610	6170	7430	8140	8910

DEFINITIONS:

FIRE DIVISION: An area of a building separated from other areas by fire walls or by air gaps, within which a fire is expected to be retained.

COMBUSTIBLE: A building with roof which is constructed of wood sheathing or planking irrespective of whether or not it is supported by wood or non-combustible framing. Tile roofs on wood sheathing are also included in this classification.

NON-COMBUSTIBLE: A building with roof which is constructed of non-combustible material such as gypsum slab, concrete slab, corrugated iron, etc. and supported on encased steel framing.

Once a fire is sufficiently well established to produce "serious" damage the extent of its spread does not depend on whether the fire is facilitated by an incendiary bomb or by a high explosive bomb.

A fire well established in a combustible roof single story fire division will usually burn out the division completely.

The structural classes given in the table are not characteristic of European construction only. Construction practice in various countries shows enough similarity to warrant using the values given for structural damage universally. Differences in roofing material may change the gross MAE materially.

Refs: EWT-2f, 5b, 8a
August 1946

CONFIDENTIAL

WEAPON DATA

DAMAGE TO SINGLE-STORY INDUSTRIAL BUILDINGS BY INCENDIARY BOMBS

6 B2 INCENDIARIES: INDUSTRIAL BUILDINGS

Damage to industrial buildings by incendiary bombs is due to fires started by the bombs. The probability of an incendiary bomb starting a fire in a building depends strongly upon

ROOF – Whether combustible or non-combustible.

HEIGHT – Height to eaves of a single story building. (Height of upper story only for multi-story buildings)

OCCUPANCY – Percentage of floor area covered by combustible material, as estimated by intelligence.

Once a fire is sufficiently well established to cause "serious" damage the extent of its spread does not depend on the origin of the fire. A fire well established in a *combustible roof* fire division will usually burn out the entire fire division. A fire well established in a *non-combustible roof* fire division usually burns out only a part of the fire division.

The Mean Area of Effectiveness, MAE, of incendiary bombs for one fire division of an industrial building with a combustible roof is equal to the area of the fire division times the probability of a fire being started by an incendiary bomb; for an industrial building with a non-combustible roof, the MAE is equal to the area which will be burned out times the probability of a fire being started by an incendiary bomb. Thus the MAE depends on the *roof*, the *height*, the *occupancy* and the *area* of the fire division. The table gives the MAE in square feet per bomb for various combinations of these factors *(See graph below)*

MEAN AREA OF EFFECTIVENESS, (MAE) *square feet per bomb*. FOR INCENDIARY BOMBS AGAINST INDUSTRIAL BUILDINGS

BUILDING CLASSIFICATION		100-lb, IB, AN-M47 Area of One Fire Division, sq ft						4-lb, IB, AN-M50 Area of One Fire Division, sq ft					
Height feet	Occupancy percent	7000	15000	30000	60000	100000	200000	7000	15000	30000	60000	100000	200000
7-9 or 10-19	5	2500	4000	6000	15000	34000	60000	0	0	0	0	0	0
	15	4600	9000	18000	39000	64000	120000	150	300	600	1200	2000	4000
	25	6800	11700	22000	46800	78000	156000	350	750	1500	3000	5000	10000
	35	8300	13400	26700	52400	88000	178000	700	1500	3000	6000	10000	20000
	45	7000	16000	30000	60000	100000	200000	1050	2250	4500	9000	15000	30000
20-29	5	1200	2500	5100	10200	17000	34000	0	0	0	0	0	0
	15	2640	5040	9000	18000	30000	60000	70	150	300	600	1000	2000
	25	2700	5300	11700	23400	39000	78000	210	450	900	1800	3000	6000
	35	3100	6400	13200	26400	44000	88000	350	750	1500	3000	5000	10000
	45	3600	7500	15000	30000	50000	100000	490	1050	2100	4200	7000	14000
30-39	5	600	1200	2400	4800	7000	14000	0	0	0	0	0	0
	15	840	1800	3600	7200	12000	24000	0	0	0	0	0	0
	25	1120	2400	4800	9600	16000	32000	140	300	600	1200	2000	4000
	35	1260	2700	5400	10800	18000	36000	210	450	900	1800	3000	6000
	45	1400	3000	6000	12000	20000	40000	280	600	1200	2400	4000	8000
40-49	5	210	450	900	1800	3000	6000	-	-	-	-	-	-
	15	490	1050	2100	4200	7000	14000	-	-	-	-	-	-
	25	630	1350	2800	5600	9000	18000	-	-	-	-	-	-
	35	630	1350	2700	5400	9000	18000	-	-	-	-	-	-
	45	700	1500	3000	6000	10000	20000	-	-	-	-	-	-
50-59	0-45	0	0	0	0	0	0	-	-	-	-	-	-
all heights	5	0	0	0	0	0	0						
	15	0	0	0	0	0	0						
	25	350	750	1200	1700	3000	3100						
	35	350	1000	2000	3700	5000	5000						

DEFINITIONS:

FIRE DIVISION: An area of a building separated from other areas by fire walls or by air gaps, within which a fire is expected to be retained.

COMBUSTIBLE: A building with roof which is constructed of wood sheathing or sheeting irrespective of whether or not it is supported by wood or non-combustible framing. Tile roofs with wood sheathing are also included in this classification.

NON-COMBUSTIBLE: A building with roof which is constructed of non-combustible material such as gypsum slab, concrete slab, corrugated iron, etc., and supported by composite steel framing.

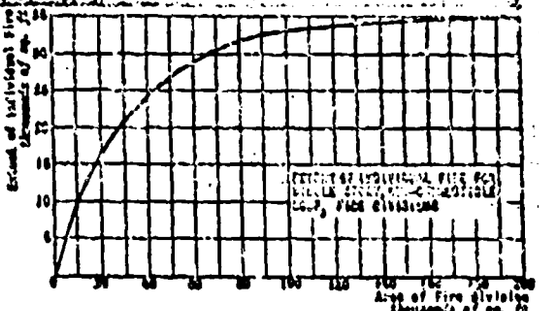

Values given for the B-47 are considered more reliable than those for the B-50.

The information given here was based on analysis of USAAF attacks on European industrial targets. These values can be applied to structures of other types only if the effects of differences in construction, combustibility of the roof, and type and extent of the occupancy are taken into account. (See ENT-b)

Ref: E/T-5b, Wa, 2d
August 1946

GC 1
STEEL MILLS

BOMBING OF STEEL MILLS

In a steel plant large enough for coke ovens and steel furnaces to be used as separate targets, the best bombs are the 500-lb GP fuzed 0.025 sec delay for the coke ovens and the 2000-lb GP fuzed 0.025 or 0.1 sec delay for the steel furnaces. If one overall attack is to be made, the best bomb is the 1000-lb GP fuzed 0.025 sec delay, with the 2000-lb GP fuzed 0.025 sec delay a good second choice.

The principal components of a steel mill in order of their vulnerability to bombing attack, the recommended bomb and fuze delay, and the results to be expected from bombing attack are as follows:

COMPONENT	RECOMMENDED BOMB & FUZE	RESULTS
Coke Ovens	500-lb GP or 1000-lb GP. 0.025 sec delay	One direct hit will disable one section for 3 to 8 months. This will reduce the quantity of coke and gas available to the blast furnaces. Auxilliary equipment such as the aspirating plant, coke loading and ramming equipment, etc. is also highly vulnerable.
Open Hearth Furnaces	2000-lb GP or 1000-lb GP. 0.025 or 0.1 sec delay	At least 25% of the furnaces must be damaged to affect production seriously. Damaged ovens require several months for repairs. Gantry cranes and other equipment are additional targets.
Blooming Mills	2000-lb GP or 1000-lb GP. 0.025 or 0.1 sec delay	These are frequently a bottleneck of the plant. Small, target, but essential to operation and difficult to repair. Smaller bombs could damage controls.
Blast Furnaces and related equipment	2000-lb GP 0.025 or 0.1 sec delay	Direct hits required. Small target. Stoves, hoists, and charging equipment are also vulnerable to smaller bombs. Long repair or rebuilding time if a direct hit is made on furnace
Conveying Equipment and Services	500-lb GP or larger	Good secondary objectives within the target area. Bridge cranes at ore docks, coke pushers, gantry cranes throughout plant, etc. are all essential and vulnerable to direct hits. Services are essential and vulnerable to direct hits or near misses.
Air Compressors	2000-lb GP or larger. 0.1 or 0.025 sec delay	Important, but of very heavy construction. Small target difficult to hit and damage.

Ref: ENT-62
August 1945

6 C2a
DAMS

BOMBING OF DAMS

Planning attacks on dams of all types requires careful engineering investigation of the design. In general, the largest practicable bomb should be used. Many dams will not be vulnerable to any bomb smaller than the 12,000-lb or 22,000-lb GP, or some special weapon.

Attack on a dam should be made when the water level behind the dam is at its highest stage.

Earth dams are best attacked with GP bombs: by deeply cratering the crest if the dam contains no steel or concrete core; by deep penetration and resulting shattering of such a core if present; or by deeply cratering the upstream slope of the seal blanket. The choice of the method depends on the design. Long delay fuzing should be used in most cases.

Masonry and concrete dams should be attacked by the underwater explosion of a large charge in contact with the dam on the upstream side; the details to be carefully worked out for all larger dams. Fuzing should be of short delay, sufficient to develop the full tamping effect of the water.

Gates can be attacked by the adjacent underwater explosion on the upstream side of fairly large bombs with short delay fuzing (0.025 sec) sufficient to develop the full tamping effect of the water.

Operating machinery and control houses are best attacked by the direct hit of intermediate sized bombs fuzed with slight delay (0.025 sec or 0.01 sec) for penetration into the building. There is no appreciable near-miss damage and even total destruction is not too serious.

Ref: [illegible]
Aug. 1945

6 C2b
PENSTOCKS

BOMBING OF PENSTOCKS

The best mode of attack on penstocks is by means of bombs that will penetrate the pipe and explode in the interior. The use of bombs intended to produce large movements of the pipe through earth shock, air blast, or by cratering, is not likely to be effective.

It is recommended that GP bombs, fuzed 0.01 sec nose and tail, be used. Table I shows sizes of bombs required to rupture penstocks when the bomb explodes at the center of the penstock. Generally, an up-slope approach within 30° of the pipe axis, at medium to high altitude gives the largest equivalent horizontal vulnerable area. But the probability of hitting the pipe and of the explosion occurring in the lethal annulus of the pipe must be considered.

Table I

SIZES OF BOMBS REQUIRED TO RUPTURE PENSTOCKS WHEN EXPLODED AT THE CENTER

Diameter of Pipe *ft*	Thickness of PipeWall *in*	Size of Rupturing Charge of TNT *lb*	Size of GP Bomb *lb*
22	1.50	525	1000
16	1.25	240	500
13	1.00	127	250
10	0.75	56	100

If the bomb explodes near the side wall, a smaller bomb than listed above may be sufficient to split the pipe.

A detailed study of the vulnerability of penstocks is given in the first reference. On the basis of model tests made to determine the weight of charge required to rupture a penstock by internal explosion, and of ricochet tests conducted against curved air-backed plates and against water-filled cylinders, recommendations are made as to the weapon to be used in attack. A table of equivalent horizontal vulnerable area factors is given for various slopes of penstocks, angles of fall of bomb, and angles of attack, as an aid to selecting the best combination of bombing conditions and the lowest required bomb density. A procedure for analyzing a penstock installation to determine the type of bombing attack required is given. By means of this analysis, the type, size, and fuzing of bombs and the bombing density can be determined for any desired probability of destruction of the penstock. Diagrams and curves are given to assist in the computation.

Ref: EWT-2b
August 1945

GD1
GUN POSITIONS

BOMBING OF GUN POSITIONS

OPEN GUN EMPLACEMENTS

The table gives the Mean Area of Effectiveness for unserviceability and the Mean Area of Effectiveness for temporary unserviceability in square feet per bomb for light, medium, and heavy guns. Values are for guns that do not have protective shielding of the vulnerable parts.

In the table, guns are classified as *light* (20mm and 37mm), *medium* (75mm to 120mm) and *heavy* (150mm and larger). *Unserviceability* means damage requiring shop repair or more than 24 hours field repair. *Temporary unserviceability* means unserviceable but repairable in less than 24 hours. MAE is defined in data sheet 2 B2.

MEAN AREA OF EFFECTIVENESS PER BOMB FOR VARIOUS BOMBS vs UNSHIELDED GUNS

	BOMB	Crater Radius feet	Fuzing sec	Light Guns: MAE for Unserviceability sq. ft.	Light Guns: MAE for Temporary Unserviceability sq. ft.	Medium and Heavy Guns: MAE for Unserviceability sq. ft.	Medium and Heavy Guns: MAE for Temporary Unserviceability sq. ft.
EXPLOSION (crater produced)	100-lb GP,AN-M30	9.25	1/100	1000	4300	270	1600
	250-lb GP,AN-M57	12.0	or	1800	7200	460	2700
	500-lb GP,AN-M64	16.6	1/40	3000	12000	700	4600
	1000-lb GP,AN-M65	23.75	"	4900	19400	1200	7200
FRAGMENTATION (crater not produced)	20-lb F,AN-M41		Inst.	Lack of data does not warrant prediction of MAE for light guns.		300	600
	20-lb Para.Frag		"			500	600
	90-lb F,AN-M42		"			2400	4800
	100-lb GP,AN-M30		"			2700	7400
	260-lb F,AN-M81		"			7000	14000
	500-lb GP,AN-M64					10400	20800

MEAN AREA OF EFFECTIVENESS for UNSERVICEABILITY

	BOMB	Fuzing	Light Guns: Diameter of Emplacement 20'	30'	40'	50'	60'	Medium Guns: Diameter of Emplacement 20'	30'	40'	50'	60'
FRAGMENTATION (bomb is recovered)	20-lb F,AN-M41	Inst.	300	-	-	-	-	300	-	-	-	-
	20-lb Para.Frag	"	300	-	-	-	-	300	-	-	-	-
	90-lb F,AN-M42	"	600	1100	1800	2600	3600	600	950	1700	2000	2900
	100-lb GP,AN-M30	"	600	1100	1800	2600	3600	600	1100	1800	2300	3200
	260-lb F,AN-M81	"	600	1100	1800	2600	3600	600	1100	1800	2300	3200
	500-lb GP,AN-M64	"	600	1100	1800	2600	3600	600	1100	1800	2300	3200
	"	VT	10400	10400	10400	10400	10400	10400	10400	10400	10400	10400
	"	"	20800 sq.ft. MAE for Temporary Unserviceability for all revetted guns.									

COVERED CONCRETE GUN EMPLACEMENTS

Covered concrete gun emplacements can be destroyed by a bomb perforating the roof and detonating inside of the structure, or seriously damaged by a bomb exploding underground close to the side walls. Bombs should be fuzed 0.025 seconds delay for either type of damage. Data sheet 2C1a may be used to select bombs capable of perforating the roof, and the radii for *breaching* given in Data Sheet 8A5 may be used as near miss distances for damage underground explosion close to the wall. The vulnerable area for *perforation* is the inside plan area of the gun emplacement, and the vulnerable area for *damage by near misses* is the area of a band around the outside of the emplacement, having a width equal to the near miss distance defined above. The most efficient bomb is that bomb having the largest vulnerable area per ton, and is usually the smallest bomb capable of perforating the roof of the gun emplacement.

Refs: CWT-6a
August 1945

G 1) 2
WIRE & OBSTACLES

PASSAGE OF WIRE AND OBSTACLES

BARBED WIRE

Barbed wire may be cleared by aerial bombardment, rocket attack, or ground demolition. The table gives the average radius of clearance of ordinary barbed wire obstacles by various explosive weapons. Within the radius of clearance, trip wires of anti-personnel mines will also be cut.

WEAPON	RADIUS OF CLEARANCE, *feet*
100-lb GP Bomb, fuzed nose inst.	15 - 17
350-lb Depth Bomb, fuzed nose inst.	25 - 30
7.2-in Demo Rocket, fuzed inst.	10 - 12
Bangalore Torpedo, on ground	gap 15 - 20 feet wide

OBSTACLES

Bombing has definitely proven ineffective against obstacles of concrete, stone, wood, or steel. Hand placed demolition charges are usually necessary for destruction of smaller vehicular obstacles, although direct hits with the 7.2-in Demolition Rocket are effective against some types of small obstacles. Obstacles may be demolished by hand placed charges made up of 20-lb Tetrytol packs, using approximately one pound of explosive for each cubic foot of obstacle. The sketches show the proper placing of 20-lb Tetrytol packs for demolition of typical vehicular obstacles.

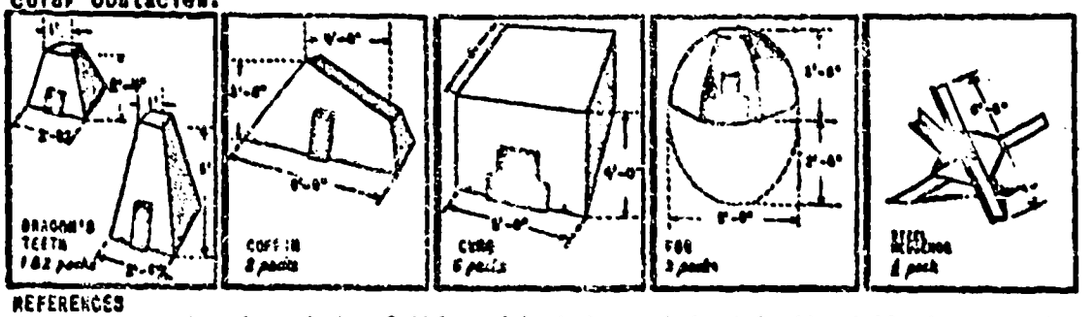

REFERENCES

A very comprehensive study of this subject is contained in the following reports:

The Engineer Board. Interium Reports on the Passage of Beach and Underwater Obstacles.

Joint Army-Navy Experimental and Testing Board. Progress Reports.

Additional reports concerned with particular phases of the problem are:

War Dept., Technical Bulletin. TB Eng 8, February '44. Methods of Passing Beach and Underwater Obstacles.

War Dept., Engineer Field Manual, FM5-30 Obstacle Technique.

Ordnance Section. 12th Air Force. Bomb Damage Survey of Pre-Invasion Targets in Southern France, September 30, 1944

Operational Research Section, 9th Bomber Command, Estimate of Bombing Attacks on the Siegfried Line, September 18, 1944

Observers' Report-Army Ground Forces, May 1945, Removal of Beach and Underwater Obstacles; Iwo Jima and Philippine Campaign.

War Dept., Operations Division, June 1945, Reduction of Beach Defenses and Obstacle Clearance in Normandy.

Army Operational Research Group, Report No. 178 (British), Lethal and Material Effects of Gunfire and Bombing Land Targets.

Refs see above
August 1945

WEAPON DATA

FRAGMENTATION DAMAGE: AIRCRAFT, VEHICLES, PERSONNEL

G D3
DAMAGE BY FRAGMENTS

For discrete targets such as men, guns, tanks, trucks, planes, etc, the mean area of effectiveness (MAE) of a bomb against a target is defined as follows: Using Cartesian coordinates (x,y) in a horizontal plane with the target at $(0,0)$, the probability of target damage of a specified degree or more is a function $\phi(x,y)$ of the coordinates of the bomb. The MAE is then defined to be $\iint \phi(x,y)\,dx\,dy$, the integral being taken over all parts of the x,y-plane for which $\phi(x,y)>0$. Geometrically this may be interpreted as the volume under the surface $z = \phi(x,y)$ and above the x,y-plane. The physical dimensions, however, are those of area.

The above function $\phi(x,y)$, and hence the MAE, depend on (1) type of bomb and fuzing, (2) operational conditions under which bomb is dropped, (3) type of target, (4) degree of damage specified, and (5) ground conditions near target, such as unevenness of ground, presence of shielding objects, etc.

A physical picture of the meaning of an MAE may be obtained as follows: Suppose targets are distributed randomly and uniformly, that is, the expected number of targets in a region is proportional to the area of the region. Then the MAE is the area of a circle centered at the bomb and of a size such that the expected number of targets receiving the specified degree of damage outside the circle equals the expected number not receiving the specified degree of damage inside the circle.

The MAE is used as follows: Suppose that an area contains a number of discrete targets with the same MAE = M; the targets need not be uniformly distributed. If a density of D bombs per unit area is delivered to the target, then the expected fraction F of targets damaged is given by $F = 1 - e^{-MD}$. For light densities D such that MD is small compared with 1, $F = MD$ approximately. The exponential formula is derived under the assumption that the bombs are distributed randomly and uniformly over an area large enough to include all possible positions of a bomb capable of damaging any of the targets under consideration.

MAE FOR SUBSTANTIAL DAMAGE BY FRAGMENTS, *sq. ft per bomb*

TARGET	Ground Burst., Inst. Fusing			Air Burst US 500-lb M[illegible]	
	British 500-lb MC	British 250-lb MC	Cluster of 18 US Frag AN-M41	Height of burst 10 feet	Height of burst 36 feet
Aircraft	70,000	46,000	110,000		
Mechanical transport	44,000	21,000	100,000	83,000	18,000
Men in deep trenches				6,200	4,100
Men in shallow trenches				8,600	8,000
Men prone, unshielded	23,000	22,000	60,000	23,000	24,000

Substantial damage is defined as follows: For aircraft - complete destruction or damage requiring more than 10 man-days for repair. For mechanical transport-damage involving write-off or requiring repair at a second echelon or base workshop. For personnel - incapacitation.

Source: Bombing trials by the British at Ashley Walk.

Ref: EWT-4b
August 1945

WEAPON DATA

G E1
UTILITIES
UNDERGROUND PIPING

DAMAGE TO UNDERGROUND PIPING

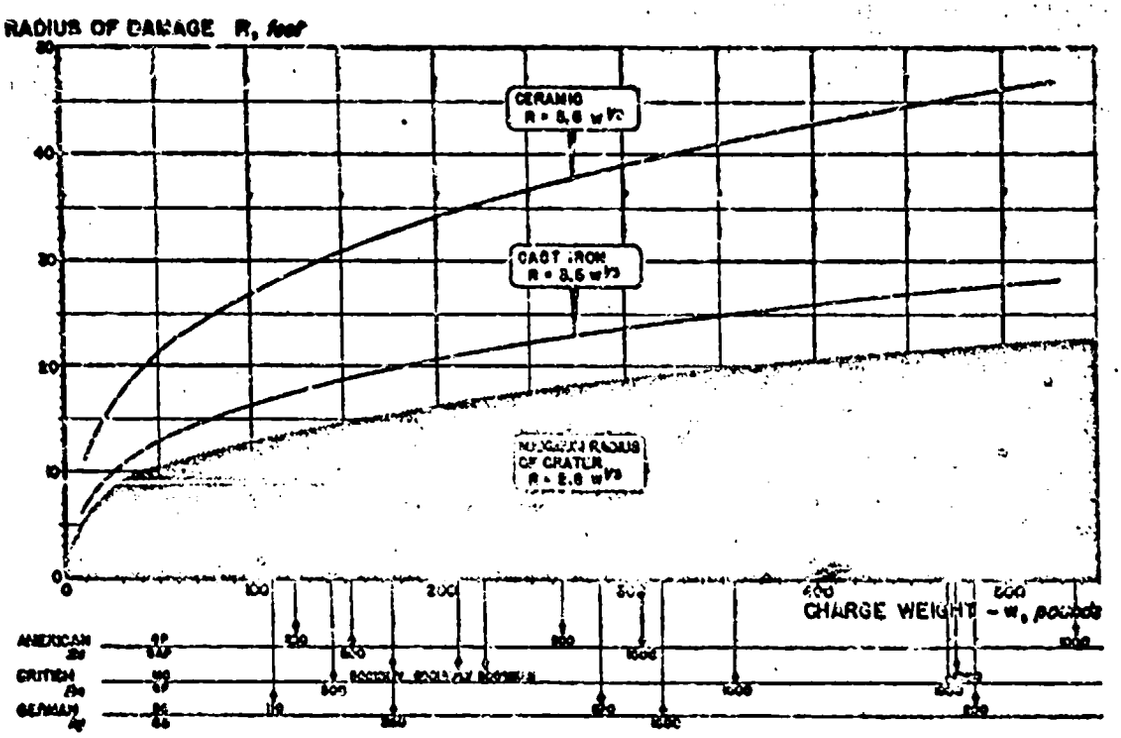

The curves show average radius of damage by medium-sized bombs to pipes made of (a) cast iron and (b) earthenware, brick or tile buried in clay soil. The radius of damage R thus represents roughly the half width of a band within which the pipe will be vulnerable.

SOURCE OF DAMAGE: Damage appears to be caused largely by earth movement rather than by forces transmitted longitudinally through the pipe or through its contents. Services laid in ducts are protected by the "trench effect"; the ducts may be damaged but ground shock will be absorbed, permitting the services to remain intact.

LENGTH OF CAST IRON PIPE DAMAGED: The length of pipe requiring replacement is of the order of one and one-half to two times the radius of damage.

NATURE OF DAMAGE TO CERAMIC PIPE: Earthenware, brick and tile services can be placed in a single category because failure almost always occurs at the joints, which are of comparable strength in all three.

EFFECT OF DEPTH: Data used in compiling results is for services buried at depths of from 2½ to 5 feet, over which range no depth effect is found. Further, the radius of damage depends very little on the depth of the explosion, within the normal limits of bomb penetration.

SIZE OF PIPE: There is no apparent dependence of radius of damage on pipe size within the range commonly used.

MAINTENANCE OF PRESSURE IN WATER SERVICES: In the event that damage to the pipe or its fittings does not result in a complete break, the pressure may hold at a substantial fraction of its normal value for some time. The drop in pressure immediately following the explosion is generally found to increase with $W^{1/3}/r$, where r is the distance from the charge.

OTHER SOILS: Compared with clay, the radius of damage is to be taken slightly smaller in chalk, sand and gravel and slightly more in made ground. If the soil is saturated with water, damage will usually extend to greater distances.*

Source of data: Reports of the British Ministry of Home Security and experiments conducted for the Corps of Engineers, U. S. Army, at Aberdeen Proving Grounds.

* see sheet 3 A

January 1948

CONFIDENTIAL

WEAPON DATA

BOMBING OF AIRFIELD RUNWAYS

6 F 1
BOMBING
AIRFIELD RUNWAYS

The best method for damaging runways and landing grounds is by cratering with general purpose bombs. A given weight of small bombs will disrupt a larger area than the same weight of larger bombs, the volume of soil removed being approximately the same in either case. For immediate immobilization the number of hits is more important than the size of the craters, but for equal number of hits large bombs are preferred.

WEAPON SELECTION: Plane loading characteristics influence the choice of bomb as follows: Multiply the crater area listed in the table by the number of the corresponding bombs that the plane can carry, and choose that bomb giving the largest total area. The height of release and recommended fuzing are to be read from the table. The number of hits required is given in paragraph 2 below.

RECOMMENDED FUZING AND CRATERS EXPECTED FOR AP BOMBS DROPPED ON UNPAVED AIRFIELDS FROM ALTITUDES ABOVE 3500 FEET

(For paved areas, the minimum altitude must be 4500 ft to avoid ricochets; the crater dimensions will be about 10% smaller)

General Purpose bomb	Fuze delay, sec. Unpaved runways	Fuze delay, sec. Paved runways	Crater Diameter feet	Crater Depth feet	Add. Volume to Refill crater cu. yd.	Area Cratered ÷ Weight of Bomb sq. ft/lb bomb	Area Cratered ÷ Weight of Bomb acres/ton
100-lb, AN-M30	0.01 or longer	0.025 or longer	16-18	4-5	16-22	230	0.092
250-lb, AN-M57	0.01 or longer	0.025 or longer	21-26	5-7	35-55	400	0.070
500-lb, AN-M42, M64	0.025 or longer	0.025 or longer	27-31	6-8	70-110	640	0.064
1000-lb, AN-M44, M65	0.025 or longer	0.025 or longer	35-40	8-11	140-220	1060	0.058
2000-lb, AN-M34, M66	0.025 or longer	0.025 or longer	44-50	10-14	280-440	1880	0.037

1. Cratering

For general purpose bombs dropped from any altitude above 3000 feet and fused 0.01 seconds or longer delay, the craters in most airfields do not differ appreciably from the optimum. The additional soil required to refill a crater to compaction varies in individual cases, but on the average 360 cubic yards of soil per ton of GP bombs or about 1000 pounds of soil per pound of explosive are required to refill craters.

If the drainage of an airfield is known to be poor and the water table high, large bombs with long delay fuzes result in deep craters partially filled with water which are difficult to repair.

2. Number of Hits

A statistical study of widely varying data on runways 200 to 300 feet in width shows that 8 hits per thousand feet of runway length render the runway temporarily inoperative and 5 craters per thousand feet usually leave the strip serviceable. Operational data from the SWPA are in agreement with this study and show that the number of hits rather than the size of bomb is the controlling factor.

3. Repair Time

Airfields made inoperative by bombing attack can be made serviceable in a short time by repairing the cratering damage. Japanese engineering records show that when heavy equipment is used an average of 125 man-hours was required to repair craters resulting from 100-lb GP bombs.

The use of mechanical obstacles, small fragmentation bombs with anti-disturbance fuzes, and general purpose bombs with very long delay fuzes is recommended for increasing repair times, but should be considered as additional to the minimum requirement of 8 craters per thousand feet of runway length.

AWT-10 (OSRD Report No. 6518)
July 1945

6 F2
RAILROADS

AIR ATTACK ON RAILROADS

The components of a rail system vulnerable to bombing attack are rail lines, rolling stock, locomotives, and marshalling yards. Small GP bombs (100-lb, 250-lb or 500-lb), fuzed 0.01-sec delay, are the most efficient for attacking rail lines. The 500-lb GP bomb, fuzed instantaneous or 0.01-sec delay, is the best weapon for attacking rolling stock and causes heavy damage if it strikes within about 20 ft of a box car or locomotive. The 1000-lb GP bomb fuzed 0.01 sec delay is slightly less efficient against box cars and slightly more efficient against locomotives. The MAE for damage to rolling stock is 0.29 acre/ton for 500-lb GP bombs.

Strafing and rocket attack of locomotives will result in damage requiring 1 to 35 days and 1 to 60 days, respectively, for repair. Hits with rockets, however, are extremely difficult to attain, and of the two methods strafing is probably to be preferred. These methods are of little use against other forms of rolling stock or against other railroad installations.

The optimum over-all damage to marshalling yards is caused by the 500-lb GP bomb, fuzed 0.01 sec. A density of 1.5 to 2.0 ton/acre on the target is sufficient to completely disrupt a yard.

Table I EXPECTED RESULTS OF DIRECT BOMB HITS ON TRACKS ON THE FLAT

Bomb		Fuze Delay (sec)	Radius for Damage (ft)	Vulnerable Area per foot of Single Track (acre/ton)	Average Time for repair (hr)
Size (lb)	Type				
100	GP	0.01	7-9	0.0080	4
250	GP	.01	9-12	.0042	6
500	GP	.01	12-16	.0029	8
1000	GP	.01	18-23	.0020	13

Table II APPROXIMATE RADII OF DAMAGE DETERMINED FROM FOUR CATEGORIES OF DAMAGE TO LOCOMOTIVES

Bomb		Radius of Damage for Given Degree of Damage (ft)			
Size (lb)	Type	Destroyed	1000 to 3000 man-hours for Repair	250 to 1000 man hours for Repair	Up to 250 man hours for Repair
500	GP	20	23	26	29
1000	GP	40	44	48	52

Ref: CNT-34
August 1944

GF3
ATTACK ON BRIDGES

BOMBING OF BRIDGES

The table gives bomb and fuze selections for bridges with spans of 100 to 800 feet. For light bridges with short spans the next smaller size bomb may be used. For heavy long span bridges larger bombs are often necessary.

BRIDGE	BOMB RELEASE	COMPONENT TO ATTACK	BOMB	FUZING
TRUSS: SIMPLE GIRDER / CONTINUOUS GIRDER; SIMPLE TRUSS / CONTINUOUS TRUSS; CANTILEVER TRUSS; ARCH; TRUSS TYPE	min. altitude low dive or glide	piers or abutments *piers preferred if vulnerable*	Largest bomb F/B can carry to target. See Tables A&B for smallest effective bomb.	8-15 sec. or longer
	high altitude; med. altitude; high dive or glide	superstructure and piers in less than 10 feet of water *preferred target except for multiple short-span bridges*	1000 GP *single track 8-12 ft width* 2000 GP *double track 18 ft. or wider*	0.01; Nose 0.01; Tail
		piers *preferred for multiple short-span bridges*	See TABLE A	8-15 sec. or longer
ARCH: *open spandrel, rib or barrel*; TRUSS TYPE	min. altitude low dive or glide	piers or abutments *piers preferred if vulnerable.*	Largest bomb F/B can carry to target. See Tables A&B for smallest effective bomb.	8-15 sec. or longer
	high altitude; med. altitude; high dive or glide	superstructure *preferred target except for multiple short-span bridges*	1000 GP *single track; 8-18ft width* 2000 GP *double track; 18 ft. or wider*	Inst; Nose, Non-delay; Tail *for trusses or girders < 10 ft deep*..... 0.01; Nose, Non-delay; Tail *for trusses or girders > 10 ft deep.*
		piers *preferred for multiple short-span bridges*	See TABLE A	8-15 sec. or longer
STEEL SUSPENSION	min. altitude low dive or glide	piers or abutments *often too massive*	Largest bomb F/B can carry to target. See Tables A&B for smallest effective bomb.	8-15 sec. or longer
	high altitude; med. altitude; high dive or glide	superstructure	1000 GP *if less than 16 feet wide* 2000 GP *if more than 16 feet wide*	Inst; Nose, Non-delay; Tail
STEEL TRESTLE	min. altitude; low dive or glide	tower footings	Largest bomb F/B can carry to target. See Tables A&B for smallest effective bomb.	8-15 sec. or longer
	high altitude; med. altitude; high dive or glide	superstructure, tower, and footings	1000 GP *single track 8-18ft. width* 2000 GP *double track 18 ft. or wider*	0.01; Nose 0.01; Tail
	min. altitude; low dive or glide	trestle piles	Largest bomb F/B can carry to target. See Tables A&B for smallest effective bomb.	8-15 sec. or longer
	high altitude; med. alt.; high dive or glide	trestle, superstructure, and piles	500 GP *single track* 1000 GP *double track*	0.01; Nose 0.01; Tail
ARCH - GIRDER FILLED	min. altitude; low dive or glide	piers	Largest bomb F/B can carry to target. See Tables A&B for smallest effective bomb.	8-15 sec. or longer
	high altitude; med. altitude; high dive or glide	superstructure	1000 GP *single track 8-18ft width* 2000 GP *double track 18 ft or wider*	.01 or .076; Nose .01 or .125; Tail

TABLE A. BOMB SELECTION FOR BRIDGE PIERS

Pier size, ft x ft	5 x 15	8 x 30	12 x 30	15 x 30
Bomb selection	500 GP	1000 GP	2000 GP	2000 GP Ineffective

TABLE B. BOMB SELECTION FOR BRIDGE ABUTMENTS

Average thickness of abutment, ft	5 to 8	8 to 10	10 to 12	Greater than 12
Bomb selection	500 GP	1000 GP	2000 GP	2000 GP Ineffective

EXT-6 (CNSG Report No. 8178)
July 1946

G F 4
TUNNELS

BOMBING OF TUNNELS

1. A tunnel is a good bombing target only if:
   a. The portion attacked is located in broken, weak rock or poor unconsolidated overburden, structurally weak.
   b. It is lined with a structural material reasonably vulnerable to bombing, such as timbering, standard tunnel-liner segments, reinforced or mass concrete of not too great thickness.
2. Tunnels are best attacked by detonation of a bomb in the soil near the tunnel lining after it has penetrated from the surface of the ground through the overburden (where this is possible). This type of attack requires a bomb and altitude of release combination such that the bomb will penetrate to within the lethal distance from the tunnel lining.

LETHAL DISTANCE OF BOMBS AGAINST TUNNEL LININGS

BOMB size, type	LETHAL DISTANCE, *ft*						
	Slab or Shallow Arch with Some Reinforcing or Massive Concrete Lining						Pressed Steel or Cast Iron Segments
	Thickness, *feet*						
	$\frac{1}{2}$	$\frac{3}{4}$	1	2	3	4	
100-lb, GP	10	8	8	6	5	3	20
250-lb, GP	15	13	12	9	8	6	25
500-lb, GP	18	17	16	12	10	8	30
500-lb, SAP	16	14	13	10	8	7	25
1000-lb, GP	*28*	*24*	*22*	*17*	*15*	*13*	*50*
1000-lb, SAP	*24*	*19*	*17*	*13*	*11*	*10*	*35*
2000-lb, GP	*45*	*37*	*30*	*24*	*20*	*16*	*50*
2000-lb, SAP	*30*	*24*	*22*	*17*	*15*	*13*	*40*
12000-lb, GP	*95*	*80*	*70*	*56*	*44*	*29*	*90*
22000-lb, GP	*125*	*100*	*90*	*67*	*57*	*51*	*105*

Values in *italics* are extrapolations

3. The vulnerable area will be greatest if the penetration is to the level of the tunnel. The fuzing should be a delay of 0.1 sec for deep tunnels or whatever is required for this penetration for shallow tunnels. This attack, which may call for an SAP bomb to penetrate difficult strata, requires a knowledge of the overburden and cannot be used against deep tunnels. Against tunnels under rivers or canals, the bomb must pass through the depth of the channel and then penetrate into the soil or else form a crater large enough to reach the tunnel lining.
4. Advantage may often be taken of the steep slopes usually present at tunnel portals to cause considerable landslides, thus blocking the tunnel entrance. This type of attack is most efficiently carried out by smaller bombs on the basis of results per unit weight of charge, but, both for bomb, a larger one, in general, will produce a somewhat greater slide. The probability of striking the target is increased by dropping the larger number of smaller bombs. The fuzing for this attack should be that required to produce the largest crater, 0.1 sec or more for the larger bombs and 0.025 sec for the 100- or 250-lb GP bombs.

Ref: EWT-2c
August 1945

WEAPON DATA TENTATIVE

BOMB PERFORMANCE
12,000-lb GP, T10 AND 22,000-lb GP, T14

7 A 1
PERFORMANCE
12000-lb GP & 22000-lb GP

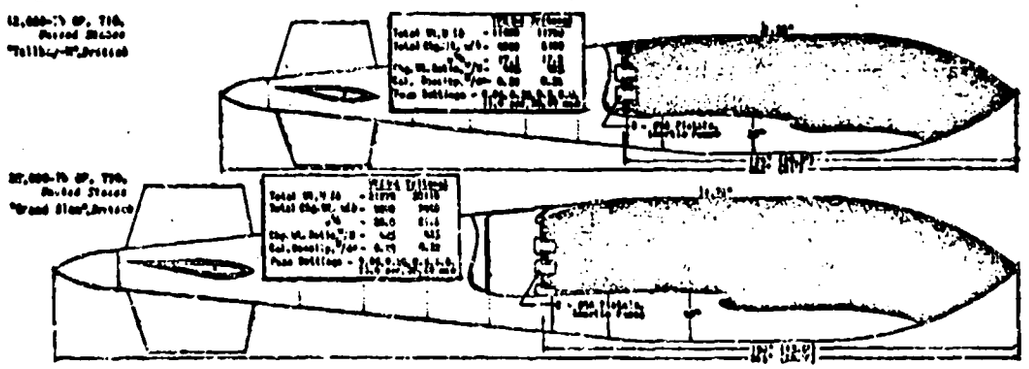

FLIGHT CHARACTERISTICS	Fuze, Bomb, sec	12,000-lb GP, T10 (Tallboy-M) Altitude, ft. 5000	10000	15000	20000	25000	30000	22,000-lb GP, T14 (Grand Slam) Altitude, ft. 5000	10000	15000	20000	25000	30000	REMARKS
Striking Velocity, ft/sec	250	675	676	1010	1160	1260	1365	670	675	1015	1175	1275	1375	
Angle of Impact, degrees	250	33°	21°	20°	15°	10°	10°	33°	20°	20°	17°	11°	10°	
PENETRATION CONCRETE	250													
Max. Thickness Perforated, ft.	250-300	9.0	7.5-8.0	6.0-6.5	Estimated max. for 45° obliquity			9.0	7.5-8.0	7.0-8.0	Estimated max. for 45° obliquity			
REINFORCED CONCRETE	Ordinary Ultimate													
Max. Thickness Perforated, ft. / feet	5000 psi	9.0	8.0	10.1				9.0	11.0	10.0				Standard is thick, on these values may not be realized. Dotted values indicate zone of probable case breakup or premature detonation; values for 30,000 ft. may be considered as limiting thicknesses for higher altitudes.
	8000 psi	7.5*	8.0	10.1				8.0	12.1	10.5				
Max. Thickness Scabbed, ft. / feet	5000 psi	10.1	10.1	10.1				12.5	10.1	17.0				
	8000 psi	10.0	10.1	10.1				12.0	10.1	10.0				
Max. Depth Penetrated, ft. / feet	5000 psi	5.5	6.0	6.9				5.5	6.0	7.7				
	8000 psi	5.0	5.0	7.1				5.0	7.2	8.5				
Max. Thickness Perforated, ft. (Ogival + Cyl. + Base)	5000 psi	8.0*	10.0	11.0	11.0			10.5	12.5	15.0	15.0			
	8000 psi	8.5*	11.0	12.0	12.7			10.0	10.0	10.0	10.0			
Max. Thickness Scabbed, ft. (Ogival + Cyl. + Base)	5000 psi	11.0*	10.7	10.3	10.0			10.0	17.0	10.0	21.0			
	8000 psi	12.1*	10.7	10.0	10.7			10.1	10.0	21.0	20.0			
Max. Depth Penetrated, ft. (Ogival + Cyl. + Base)	5000 psi	5.0*	6.7	7.1	8.0			5.0	7.0	8.0	11.0			
	8000 psi	5.5*	8.0	9.5	10.1			5.7	8.0	11.0	13.0			
Max. Entrance Crater Diam., ft	5-1500 psi	27	30	33	35	35	35	28	36	39	42	43	44	
Peak Crater (Scab) Diameter, ft	5-1500 psi	Varies from heavy breaks at zero drift to 1/2 ft. when perforated						Varies from heavy breaks at zero drift to 1/2 ft. when perforated						
EARTH	Soil Type													
Penetration Depth, ft (With long delay fuze)	Sand	36	38	39	43	45	47	33	41	43	53	55	58	For penetration into Tuffa and Silt to 30 ft to depth values as given for uniform soil.
	Loam	39	40	44	44	45	45	38	42	47	73	77	80	
	Clay	40	43	79	81	85	87	78	85	95	100	105	113	
Cratering Effect	Explosive	Sand			Sandy Loam		Clay	Sand			Sandy Loam		Clay	
Max. Crater Radius, ft.	Torpex D-1	88 - 94			93 - 98		60 - 65	93 - 81			62 - 67		63 - 68	Performance values in EARTH represent open cratering, and based on estimated values for relative effectiveness of explosives.
	Trilenal	57 - 61			91 - 95		90 - 93	96 - 99			90 - 94		99 - 95	
Max. Apparent Crater Depth, ft	TPX or Trit	29 - 37			28 - 29		28 - 31	29 - 32			31 - 34		34 - 38	
Displacement in clay, cubic		Distance from Explosion, ft.						Distance from Explosion, ft.						
		75	85	92	100	110	120	85	90	100	110	120	130	
Horizontal	Torpex D-1	21.2	11.1	7.6	5.0	3.7	2.5	20.3	10.3	10.1	6.5	7.7	5.5	
	Trilenal	20.0	10.5	7.2	5.3	3.5	2.2	27.0	10.0	12.5	8.8	6.7	5.3	
Vertical	Torpex D-1	10.0	6.2	3.6	2.3	2.1		10.6	10.4	7.7	5.3	5.8	4.7	
	Trilenal	12.5	7.0	5.3	3.0	2.0		10.5	10.4	9.2	6.2	4.7	3.5	
Damage of Underground Piping		Cast Iron			Ceramic			Cast Iron			Ceramic			
Dist. from Explosion, ft.	Torpex D-1	68'			104'			77'			104'			
	Trilenal	88'			99'			78'			104'			
Underground R/C Wall Damage (Average Soil)		Distance from Explosion, ft.						Distance from Explosion, ft.						Damage will be greater in wet, or unusually loose or sandy soil.
		0	10	20	30			0	10	20	30	40		
Max. Thickness of Wall Breached, ft.	Torpex D-1	17	10	8				21	20	15	8			
	Trilenal	16	15	8				20	15	15	8			
Max. Thickness of Wall Heavily Damaged, ft.	Torpex D-1	25	23	15	8			28	25	23	15	8		
	Trilenal	23	22	15	8			28	27	22	15	8		
UNDERWATER		Depth Below Surface of Water, ft.						Depth Below Surface of Water, ft.						
Maximum Bubble Radius, ft.		89	110	133	150			85	110	135	150	170		
	TPX or Trit	80	98	98	95			83	81	87	90	91		
Peak Pressure, lbs/sq.in.		Distance from Explosion, ft.						Distance from Explosion, ft.						
		100	200	300	400	500	1000	100	200	300	400	500	1000	
	Torpex D-1	3050	1350	840	610	500	250	3700	1300	1100	760	630	320	
	Trilenal	2740	1210	760	540	440	210	3200	1070	950	670	530	260	
Impulse, lb.sec/sq.in.	Torpex D-1	1250	1040	1700	1200	1000	550	2200	2700	2500	1800	1500	790	
	Trilenal	1500	2140	1845	1250	977	521	2520	2720	2670	1870	1500	750	
AIR														
Peak Pressure, lbs/sq.in.	Torpex D-1	26	8.0	3.1	2.1	1.0	0.5	44	8.0	4.1	2.7	1.9	0.9	
	Trilenal	26	8.2	3.0	2.0	1.0	0.7	42	7.0	3.0	2.0	1.9	0.9	
Impulse, lb.sec/sq.in.	Torpex D-1	170	95	57	42	31	17	250	110	64	44	31	18	
	Trilenal	160	92	53	41	31	16	240	105	61	43	30	25	
PENETRATION														
Thickness Perforable by Fragments at Distance 1000 ft.	TPX or Trit	Oil / Natural 5 - 8		Concrete 10 - 14		Armor 10 - 13		Oil / Natural 11 - 15		Concrete 21 - 25		Armor 12 - 16		

SOURCES: Physical Characteristics from Ordnance Department, U.S. Army; performance data from various British and American model tests

PTR No 118
June 1945

APPENDIX

MISCELLANEOUS, INCIDENT SUMMARIES, SOURCES OF INFORMATION

WEAPON DATA

SOLAR SHADOW RATIO CHART

0 M1
SHADOW RATIO

FOR DETERMINING THE HEIGHT OF AN OBJECT FROM THE LENGTH OF ITS SHADOW

This double page presents a graphical method for determining the height of an object from the length of its shadow as measured, for example, on a vertical aerial photograph. The detailed procedure is explained below.

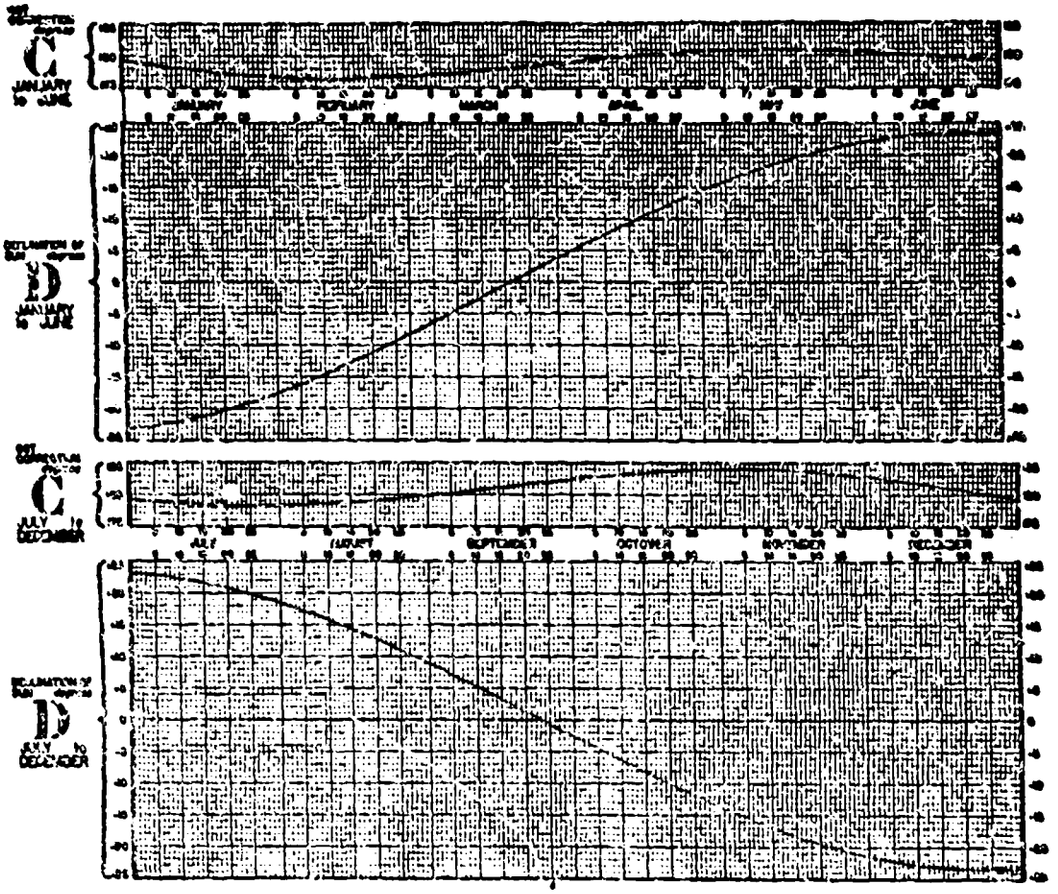

DATA

The following must be known at the time the aerial photograph was taken:

I. MONTH and DAY

II. GREENWICH CIVIL TIME (GCT)
It must be expressed in degrees
1 hr. = 15°

III. LATITUDE (LAT) and LONGITUDE (LONG)
Measured in degrees
North LAT is (+) South LAT is (-)
LONG East is (+) LONG West is (-)

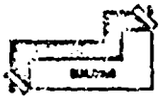

NOTE: Shadow length (S) is as measured on level ground.
For vertical photographs, it is determined by measuring from some point on the object (such as a corner of the roof) to the corresponding point of the shadow on the ground, taking into account the scale of the photograph.

PROCEDURE

1. Read C on the above graph
2. Compute the Local Sun Time (T)
   T = GCT + D + LONG
   NOTE: If T turns out negative, discard the minus sign.
   If T exceeds 360°, subtract 360° from it.
   If T still is greater than 180°, subtract it from 360°
3. Spot T on the bottom scale of the nomogram on the opposite page (see sketch)
4. Read D on the above graph
5. Compute LAT+D and LAT-D
   NOTE: If either result turns out negative, discard the minus sign
6. Spot LAT-D and LAT+D on the nomogram on the opposite page — connect these points with a straight INDEX LINE (see sketch)
7. From the point for T, project upward to the INDEX LINE and across to the right, reading the value of H/S (see sketch)
8. Measure shadow length (S)
9. Object Height (H) = (H/S) × (S)

EXAMPLE

Given: Date = March 8
GCT = 2000 Hours = 300°
LAT = 33° N = +33°
LONG = 84° W = -84°

1. C = 17°
2. T = 300° + 17° + (-84°) = 413°
   413° - 360° = 53°
3. See sketch of nomogram
4. D = -7°
5. LAT - D = 33° - (-7°) = 41°
   LAT + D = 33° + (-7°) = 26°
6. See sketch
7. H/S = 0.46
8. Shadow on photo measures 3mm
   Scale of photo: 1mm = 0.2 ft
   ∴ 5 × 0.2 = 1.0 ft
9. Object Height (H) = 0.46 × 1.0 ft
   = .47 ft

SKETCH OF NOMOGRAM

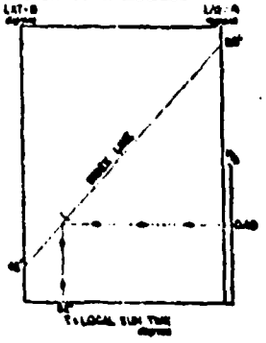

CONFIDENTIAL

SHADOW RATIO NOMOGRAM

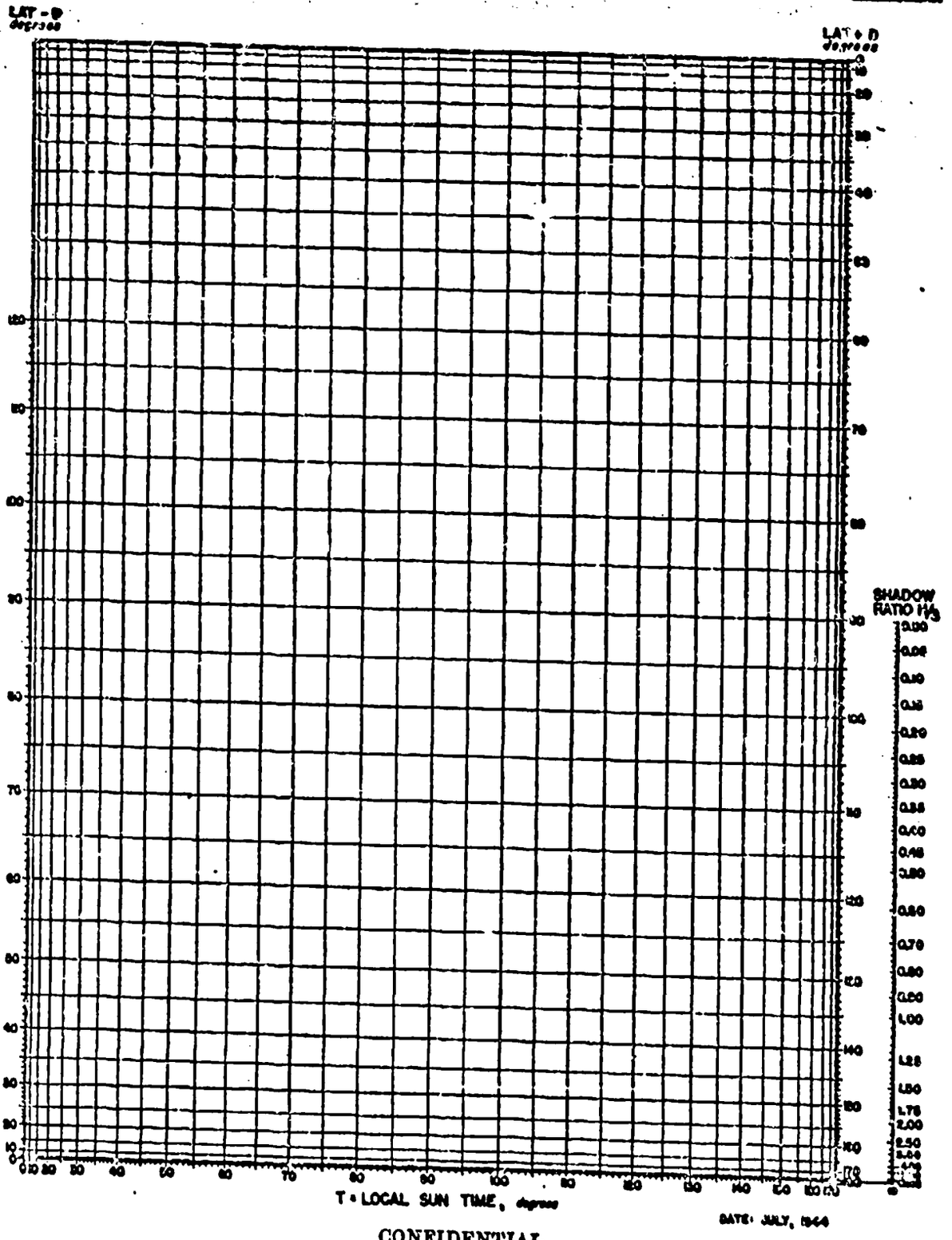

EQUIVALENT HORIZONTAL AREA FOR A SLOPING TARGET

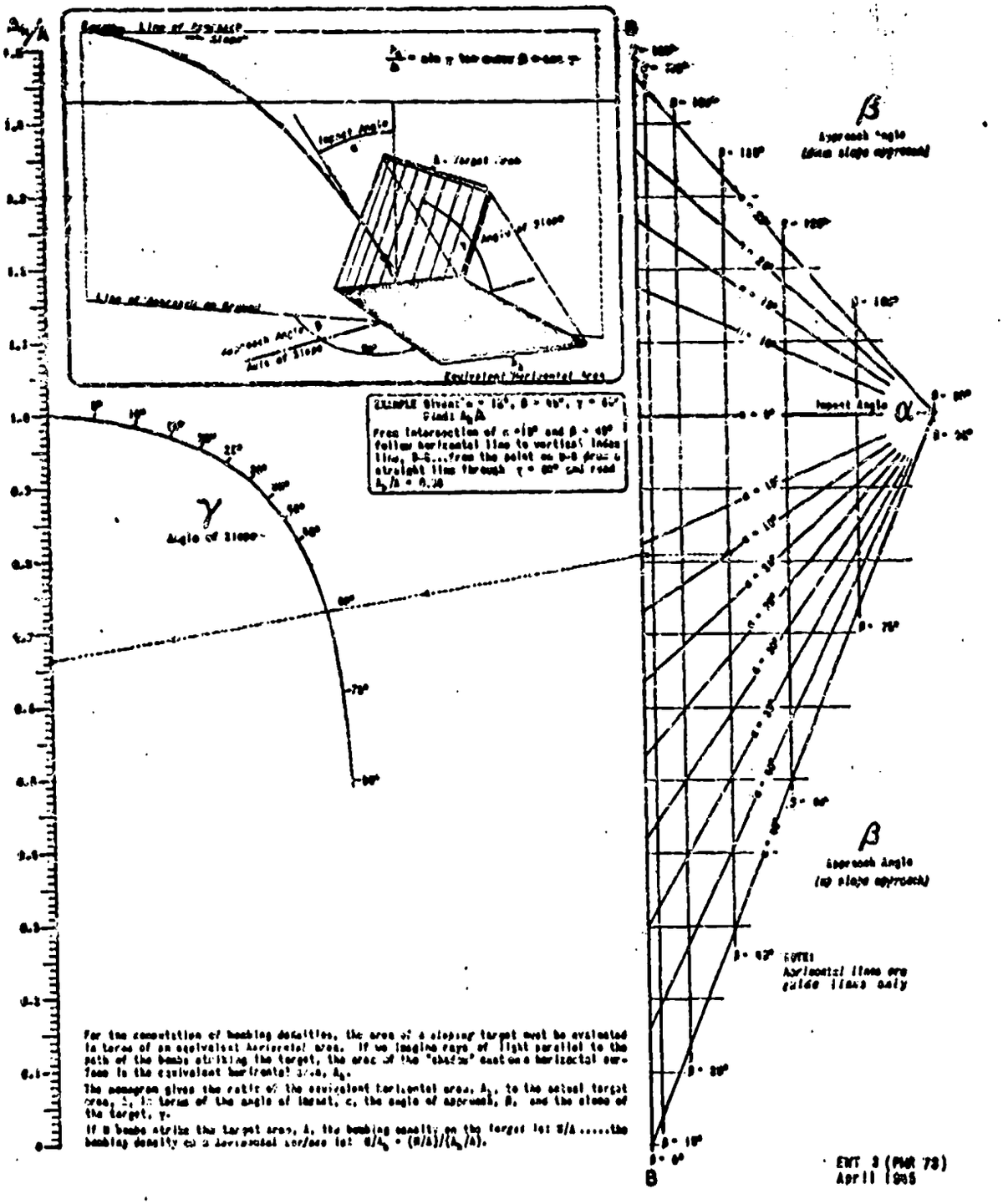

For the computation of bombing densities, the area of a sloping target must be evaluated in terms of an equivalent horizontal area. If we imagine rays of light parallel to the path of the bombs striking the target, the area of the "shadow" cast on a horizontal surface is the equivalent horizontal area, A_e.

The nomogram gives the ratio of the equivalent horizontal area, A_e, to the actual target area, A, in terms of the angle of impact, α, the angle of approach, β, and the slope of the target, γ.

If B bombs strike the target area, A, the bombing density on the target is B/A .....the bombing density on a horizontal surface is $B/A_e = (B/A)/(A_e/A)$.

EWT 3 (PWR 73)
April 1965

INCIDENT SUMMARY

MULTI-STORY, STEEL FRAME OFFICE BUILDING STRUCK BY A 550 lb. G.P. BOMB

A-550 MS-SF INCIDENT ONE

PF-8908/14

(GERMAN 550 k.g. S.C.F obs. at 50%)

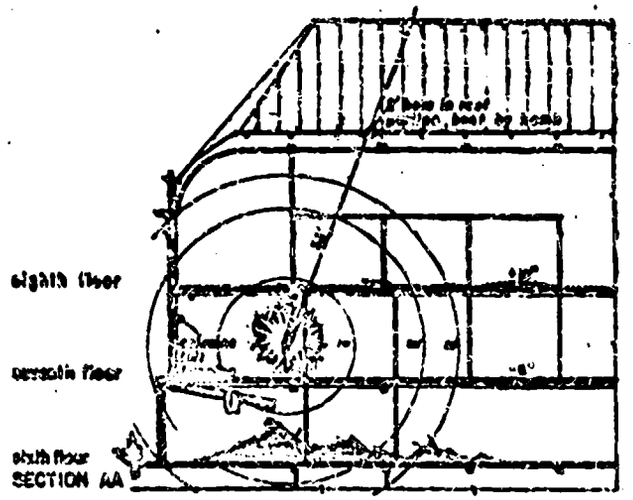

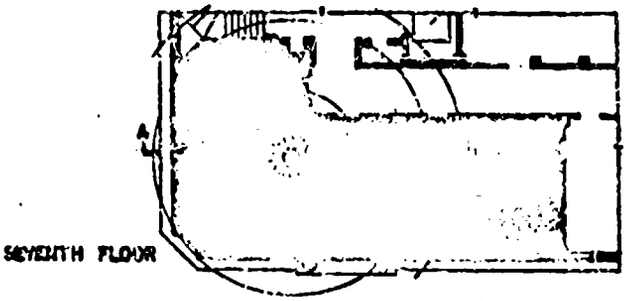

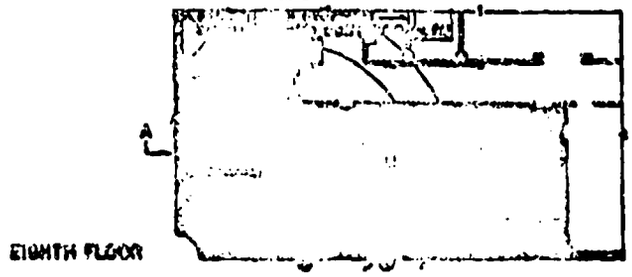

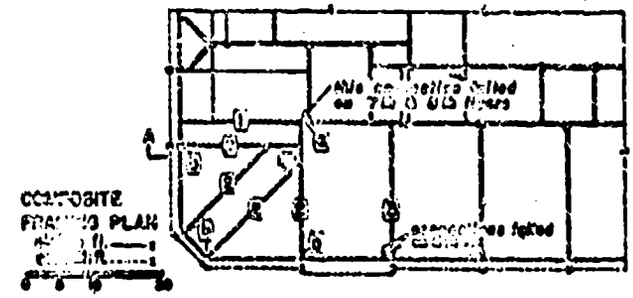

BUILDING

Office Building - basement, sub-basement and eight upper floors.

Construction: Frame - concrete-encased steel frame with bolted connections.
Floor slabs - hollow tile and reinforced concrete joists.
Exterior walls - 13½ in. brick, stone.
Interior partitions - 3" and 4", some 4½ in. and 8" brick.

DAMAGE

Bomb perforated the roof and 8th flr. near one corner of the building and exploded just above the 7th floor. The extensive collapse of the 7th and 8th floor slabs was due to the failure, on both floors, of the connection of beam 1 at column a (see framing plan). This connection provided the only interior support for the entire corner bay floor framing.

On the 7th floor, beams 1 and 2 hinged down from their connections at the exterior wall. Columns b, extending through the 7th and 8th floors, were left hanging from the roof structure, when these supporting beams hinged down. Beam 3 was deflected downward 3 inches.

On the 8th floor, connections of the exterior wall ends of beams 2 failed allowing the entire floor structure to collapse. Beam 3 was deflected upward 4 inches.

Blast damage to doors and windows extended for some distance through building. Exterior walls were blown out where shown crosshatched on the plans and section. Similarly, partitions shown crosshatched were destroyed.

Note: Circles represent the intercept of cones of dispersion with the [illegible]...the center of the cones being at the estimated position of the explosion.

March 1943

INCIDENT SUMMARY

MULTI-STORY STEEL FRAME APARTMENT BUILDING STRUCK BY A 1100 lb. G.P. BOMB

A 1100 MS-SF INCIDENT ONE

PF 5606/18

(Germes 500 Kg S.C. equiv. 500 kg)

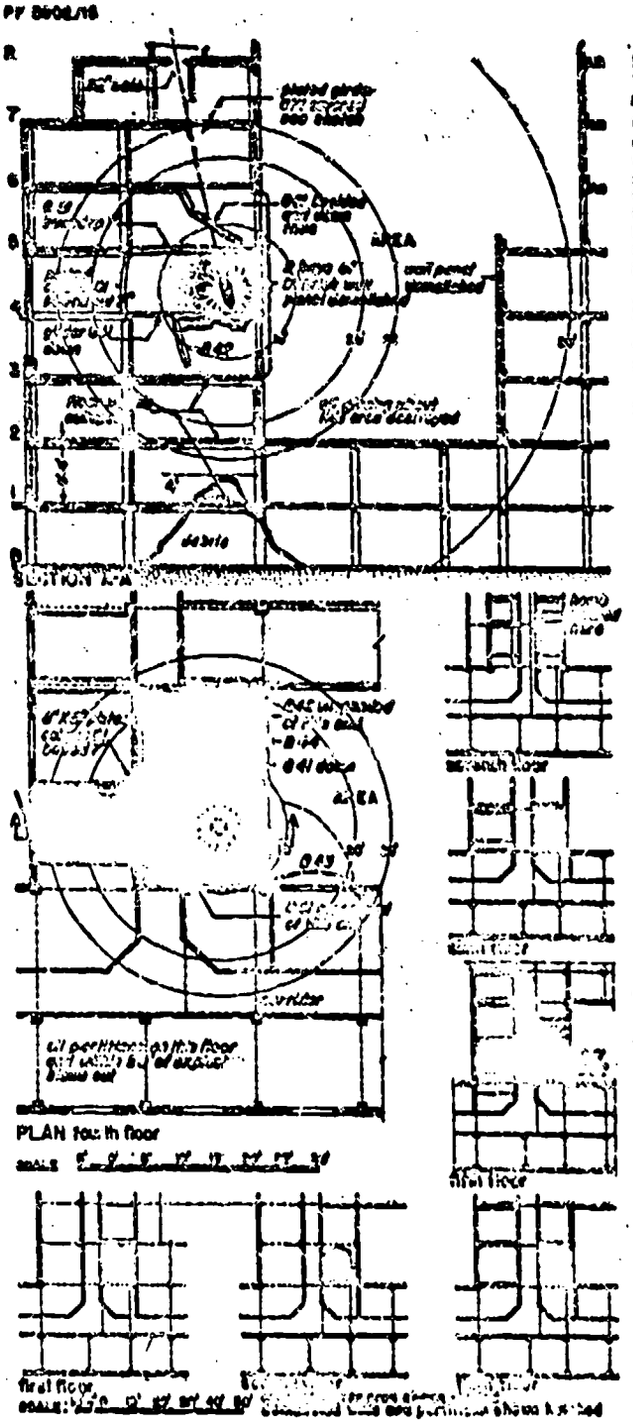

BUILDING

Type: Apartment building consisting of basement and seven upper floors.

Construction: Concrete encased, high tensile steel (Chromador) frame. Floors: 6" hollow tile and 3½" concrete including finish; 1" plaster. Roof: Similar, plus 1" asphalt surface. Exterior Walls: 9" brick with outside tile facing. Partitions: 3" brick or breeze block and 7/8" plaster.

Girders: 87I-plated, 10"x12"; others 15"x 5½"
Beams: All beams 6" x 12" I-beams.

DAMAGE

The bomb perforated the roof and three floors; detonated just above the fourth floor.

Roof: Punched a 12" hole; no structural damage.

Seventh Floor: Plated girder, 87I, severed by impact of bomb. Approx. areas of damage in sq. ft. to: floor - 190; partitions - 900; exterior walls - 0.

Sixth Floor: 66I buckled, and connections were torn but flange held at one end. Approx. areas of damage in sq. ft. to: floor - 190; partitions - 360; exterior walls - 0.

Fifth Floor: 85I deflected up 7"; Beam 85I was bowed out 2", 85Z was bowed up and one column connection severed. Approx. areas of damage in sq. ft. to: floor - 650; partitions-1500; exterior walls - 290.

Fourth Floor: 66I blown down; 85I and 86Z were left hanging by top and connections. Wall beam 86Z, one end torn loose, was wrapped back 90°; 86S and 86E were bowed out 1½"; 86G, one end torn loose, was bent out. Column C1 was bowed 7" and tilted 2°. Approx. areas of damage in sq. ft. to: floor - 700; partitions - 6000 or all within radius of 50 ft.; exterior walls - 400.

Third, Second, First Floors: No structural damage. Approx. areas of damage in sq. ft. to: Floors: 3rd - 160; 2nd - 120; 1st - 120 Partitions: 3rd -1000; 2nd - 800; 1st - 100 Ext. Walls: 3rd - 360; 2nd - 0; 1st - 0

The 8th floor slab was blown up; the 9th was blown down. The single bay of the 3rd, 2nd and 1st floors underneath collapsed under the impact of the debris load. Doors and frames along corridors were damaged; all windows around the area were broken.

DETAIL showing impact damage to girder 87I

April 1944

INCIDENT SUMMARY

A-31(M)
A-MS-SF
INCIDENT ONE

MULTI-STORY, STEEL FRAME RAILWAY STATION STRUCK BY A 3100 lb. A.P. BOMB

PP-3502/17

(German 1400-kg. S.D., Cap.Wt.-52%)

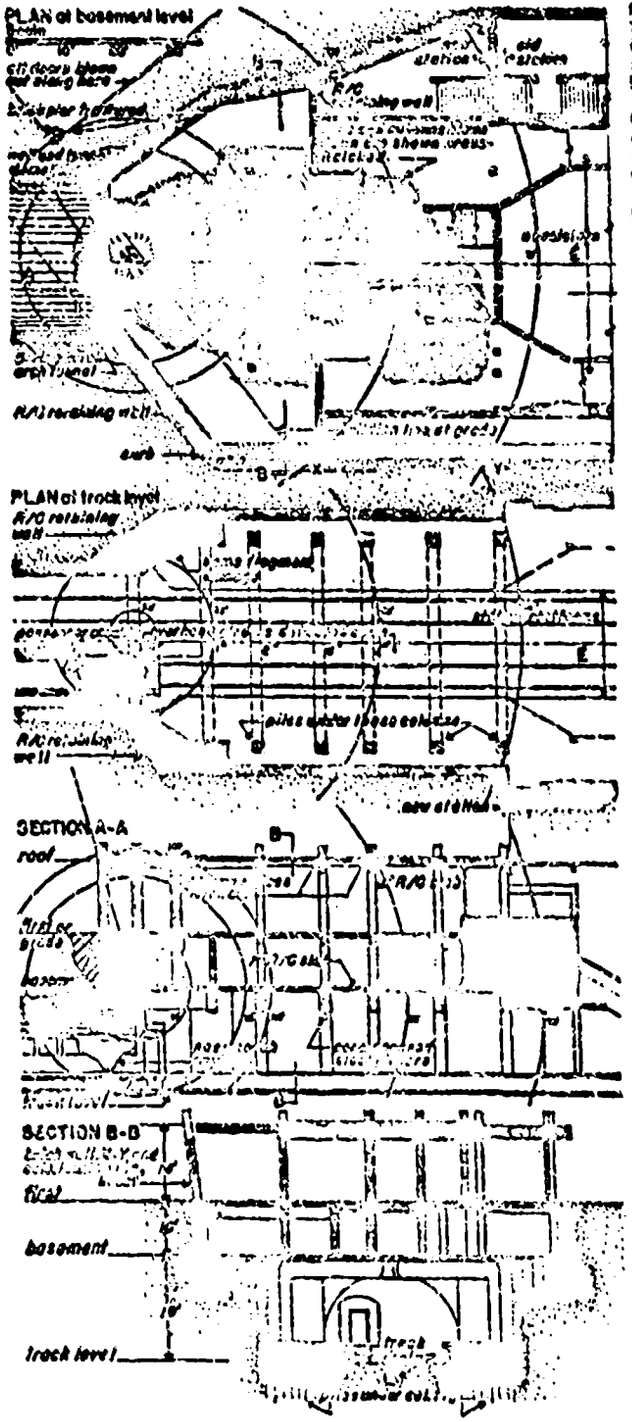

BUILDING

Type: Railway station ticket office, a recent addition to existing old station, consisting of one story above ground, a basement, and the track-level sub-basement.

Construction: Concrete encased steel frame, beam and girder system, 6 ft... and 7 inch two-way R/C floor and roof slabs. Outstanding feature of the construction was the very heavy girders (5'-2" I-beams with cover plates) spanning the tracks. These girders were supported by steel columns set on piles and were designed to carry a proposed 10-story building (see exposed cut, spikes shown on sections). Heavy R/C retaining walls formed the foundation for the exterior walls of the building above grade. The old station was built of single girder, steel arches and light lattice purlins, covered with a patent glazing and corrugated sheathing. Underground tracks were housed in a five-ring brick arch tunnel.

DAMAGE

The bomb perforated the street level or first floor, struck the girder as shown, and exploded. The girder was severely damaged -- I-beam badly bent, plates torn, [illegible]' of concrete encasing stripped off, girder deflected 4". The other girders were deflected (not shown on plan) and the concrete encasings were extensively cracked. Deflections were apparently caused by violent and heavy debris loads. The entire first floor and roof slabs were completely demolished.

A few of the columns and beams remained standing, though twisted and bent. The columns and roof and floor bases between Y and Z remained standing -- connection at Y failed. Failures occurred in the bolted connections between beams and columns -- apparent from the fact that many concrete encased members were strewn about but damaged only at the ends.

The exterior brick walls of the building were blown out except between X-Y and Z-J. (See plan at basement level.) The wall, X-V, and integral columns leaned outward 15° with the vertical but remained intact. A small portion of the brick tunnel was demolished. Adjacent buildings suffered some blast damage.

Damage to the old station was limited to the removal of all sheathing and glazing -- no structural damage.

The bomb was identified by a fragment, 18" x 12" x 3" thick in size. Retaining walls suffered some fragmentation damage. Damage to the retaining walls and girders might have been greater if the bomb had not been stopped by the girder.

Note: Circles represent the intersect of sphere of destruction radius with the floor in question.... the center of the spheres being at the estimated position of the explosion.

September 1948

INCIDENT SUMMARY

MULTI-STORY, STEEL FRAME OFFICE BUILDING STRUCK BY A PARACHUTE MINE

PARA-MINE MS-SF INCIDENT ONE

FP-8508/10

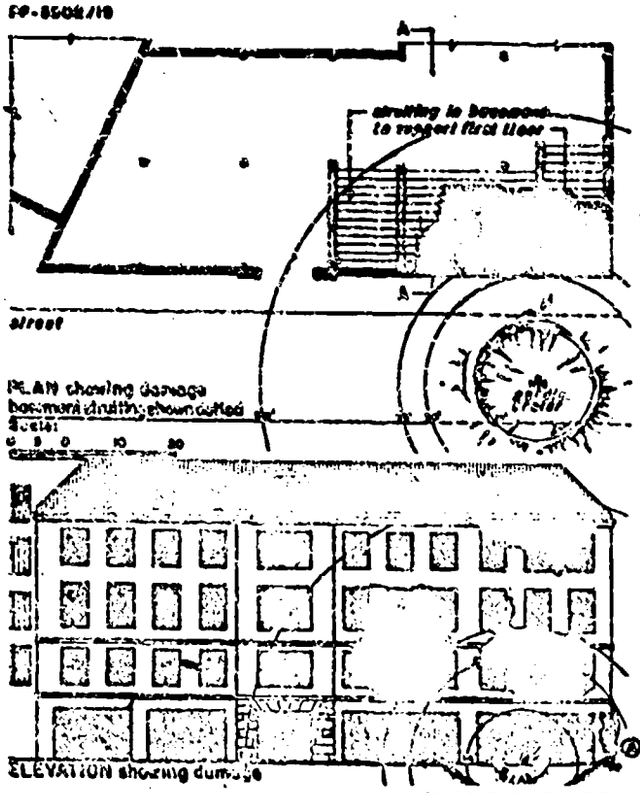

ELEVATION showing damage

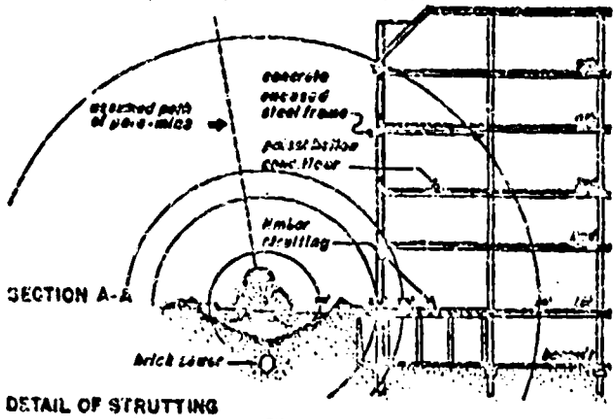

SECTION A-A

DETAIL OF STRUTTING

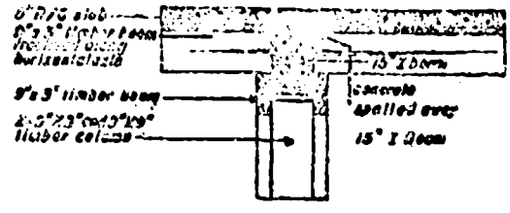

BUILDING
Type: Concrete building consisting of a basement and five upper floors.

Construction: Concrete encased steel columns and beams. First floor slab of 8-inch R/C; upper floors of patent hollow concrete slabs. Walls of 13-1/2-inch brick.

DAMAGE -
The parachute mine fell in the street near one corner of the building, forming a crater about 25 ft. in diameter. The structural framework was generally undamaged. There was some slight spalling at the junction of the floor slab and beams at the first floor. The slab was undamaged but the second floor was broken up directly over the blast.

The basement walls nearest the crater were covered with fine cracks and leaked slightly. Basement partitions were demolished and blast damage to doors, windows and brick facing was considerable. Attention is called to Ⓐ on the elevation showing the characteristic damage to the face-brick and stone caused by the interval of low pressure (suction phase) which directly follows the high pressure (positive phase) of the blast wave; the facing appears to have been sucked from the wall.

The basement was adapted and used as the A.R.P. control. Wood beams and struts, 3"x9" and 6"x9", were installed to support the concrete floor. Some of the beams were split along the horizontal axis. (See detail of strutting.)

Damage to the oil burner lead to localized fires throughout the building.

December 1943

CONFIDENTIAL

INCIDENT SUMMARY

SINGLE STORY, STEEL FRAME SHED BUILDINGS STRUCK BY 110 lb. G.P. BOMBS

B-110 SS-SF INCIDENT ONE

PP - 8908 / 29

(Normee 30 lg 2.6.7 chg. wt. 80%)

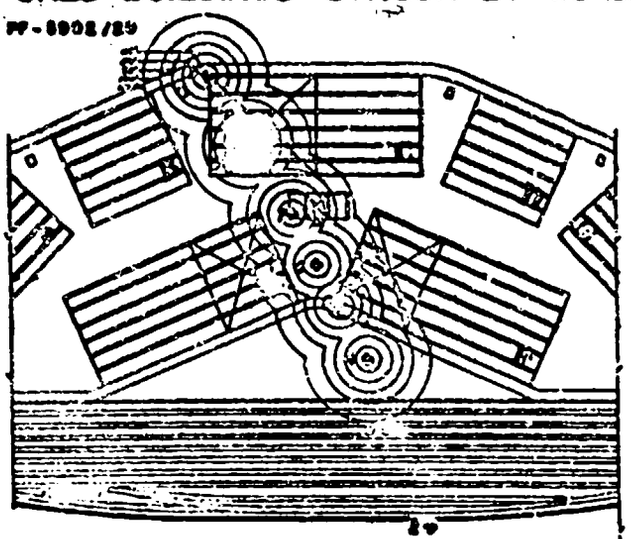

PLOT PLAN
showing location of bomb hits

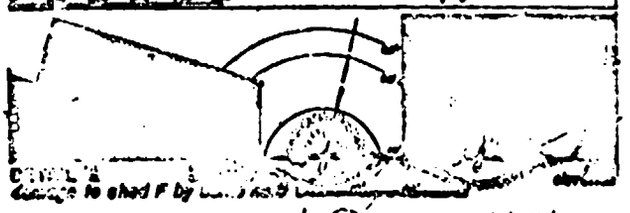

DETAIL A
damage to shed F by bomb no. 5

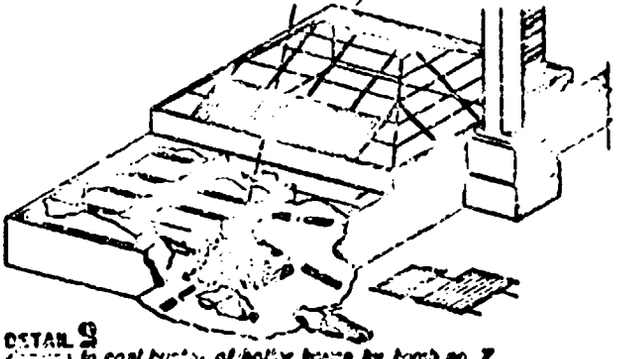

DETAIL B
damage to coal bunker of boiler house by bomb no. 7

DETAIL C
damage to shed C by bombs nos. 3 & 8

BUILDINGS

A group of seven single story, steel framed shed buildings and a boiler house with adjoining coal bunkers was the target of a stick of nine 110 lb. G.P. bombs. Sheds A, C, E and G measured 504'x 240'x 13½' (to eaves); sheds B and D measured 252'x 240'x 13½'.

Construction: Steel saw-tooth trusses, 40' long spaced 12' c.c. with timber purlins, and valley beams 24' long formed 40'x 36' bays. Columns were 8"x6" rolled steel. Roof was sheathed with corrugated asbestos cement sheets. The lower half of the north face of trusses was glazed. Brick walls, 9" thick, had glazing in short, end walls and roller shutter doors (10'x12') in long side walls.

DAMAGE

Bomb no. 1, 2, 3, and 4; see Plot Plan: No damage to buildings, filled ace saw.

Bomb no. 5; see Detail A: A crater, 20' in diameter, 6'6" deep, was formed at the corner of shed F in the 8" R/C roof slab. The slab was cracked and lifted for a maximum distance of 13' from crater edge. The 9" brick walls were cracked by earth shock and the roofing damaged by falling debris to the extent shown. The shutter doors in the side wall were not damaged.

Bomb no. 6; see Plot Plan: Damaged sheds F and G by blast, breaking 60% of the end wall glazing and approximately 5% of the north-light glass in the crossed area. The chimney, 150' high, was marked by about five pieces all striking above a point 60' from the ground.

Bomb no. 7; see Detail B: Direct hit on unfinished, filled coal bunker. Destroyed 13½' brick walls and dislodged several steel roof joists. Roofing on unfinished boiler house was not damaged.

Bomb no. 8; see plan of Detail B: Direct hit on shed C, perforated roofing and formed a crater 7½' in diameter, 3' deep, in 6 inch R/C floor slab. Bomb just missed valley beam. Only 3 timber purlins were destroyed and the valley beam was cut by a few fragments. Sheets of glass and sheets were thrown about. All the cement roofing was completely destroyed in the shaded area (approximately 17,000') and less seriously damaged in the crossed area. The figure indicates the percentage of north-light glazing broken in each 40'x 48' bay.

Bomb no. 9; see elevation of Det. B: Bomb hit exterior wall of shed C forming crater 10'-0" in diameter; nearest edge 4' from wall. The 9 inch brick wall in that area was completely cracked as shown. The front wall (flat) was moved out over one inch, sliding on the damp proof course. Three bays of roof [illegible] only caused by debris. No fragmentation damage. Approximately 60% of the end wall glazing in this shed was broken by bombs no. 8 and 9.

May 1945

INCIDENT SUMMARY

SINGLE STORY, STEEL FRAME FACTORY BUILDING STRUCK BY 2-550 lb. G.P. BOMBS

B-550 SS-SF INCIDENT ORE

(GERMAN 250 kg S.C. (b) or 550 kg)

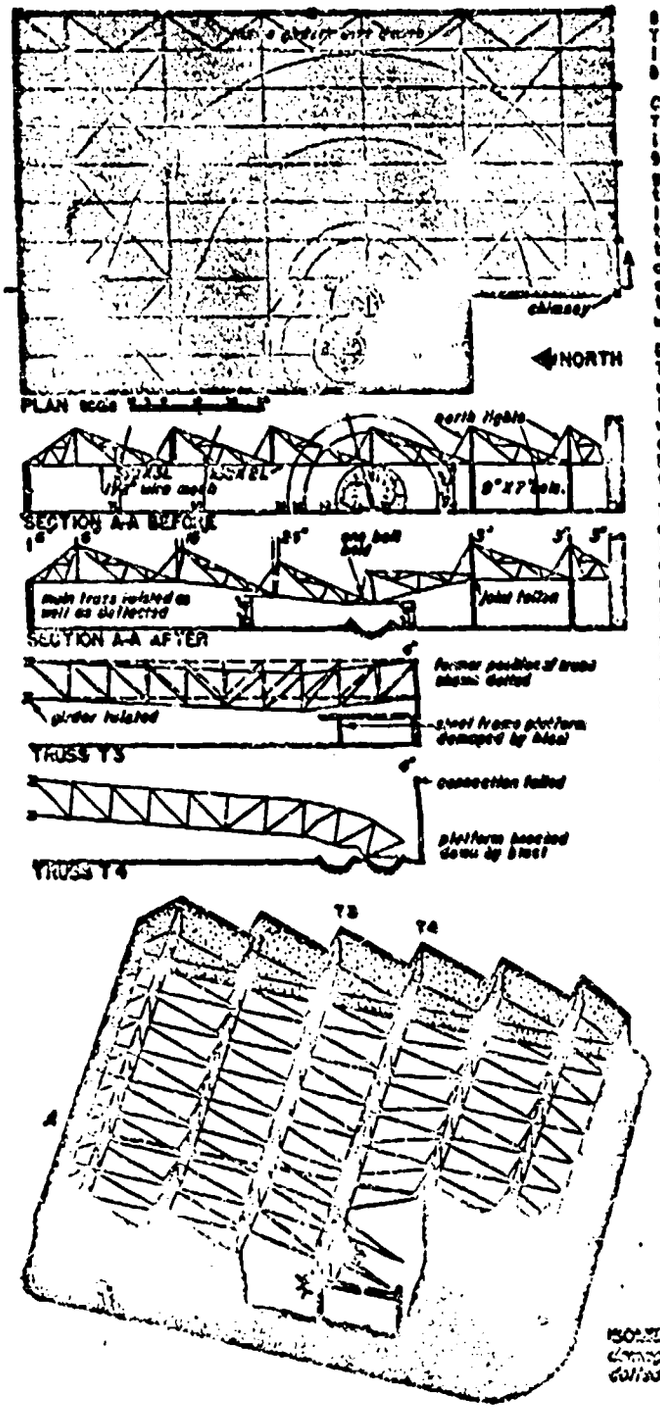

ISOMETRIC of damaged building
Solid lines indicate former position of trusses A-A, T3, T4

BUILDING
Type: Single story factory building forming part of an industrial complex.
Dimensions: 68'-6" x 115'-6"

Construction: Outside walls are of brick. Trusses span the 115-ft. width of the building and are supported on the west side by 9"x7" steel columns, and on the east side by girders spanning 90-ft. door openings. Saw-tooth trusses, spanning 30 ft. and spaced 11.5 ft. apart, were supported on the 115-ft. trusses. North and east end walls supported the ends of the saw-tooth trusses. Roof covering was asbestos sheets supported on steel angle purlins. Ridge plate was of timber. North lights of saw-tooth trusses were enclosed with ¼" wire glass.

DAMAGE
The two bombs perforated the roof and exploded upon contact at the floor. The explosions lifted truss T4 and severed its connection with column 4. That end of truss subsequently collapsed. Three bays of the brick wall were blown down; the saw-tooth trusses, supported there, collapsed.

The saw-tooth trusses along section A-A operated as a chain of tension members allowing a decreasing amount of sag toward the outside walls. The amount that each truss shifted toward the center is shown on the section. All saw-tooth trusses east of section A-A acted similarly but to lesser degree. Columns 3 to 8 were bent toward the collapse, varying in amount from 3" to 5".

The chain of tension members depended on one bolt for its support. However, if it had failed it is probable that the next line of trusses would have taken the load with a correspondingly greater amount of secondary collapse.

All asbestos roofing and glazing were blown off. In general, the purlins remained in place preventing the lateral collapse of the saw-tooth trusses. In the area over the blast, however, the purlins collapsed with the trusses.

One bay of a platform, which was independent of the main structure, was blown down and the adjoining bay was badly bent and deflected by the blast.

The 1½" wire mesh which had been attached to the bottom chords of the trusses caught most of the debris from the roof (except in the area over the blast) and prevented many casualties.

March 1944

CONFIDENTIAL

INCIDENT SUMMARY

SINGLE STORY, STEEL FRAME FACTORY BUILDING STRUCK BY A 2200 lb. G.P. BOMB

B-2200 SS-SF INCIDENT ONE

PF-8902/S5

(German 1000 K.g. S. c. 7 Obg. wt. 50 %)

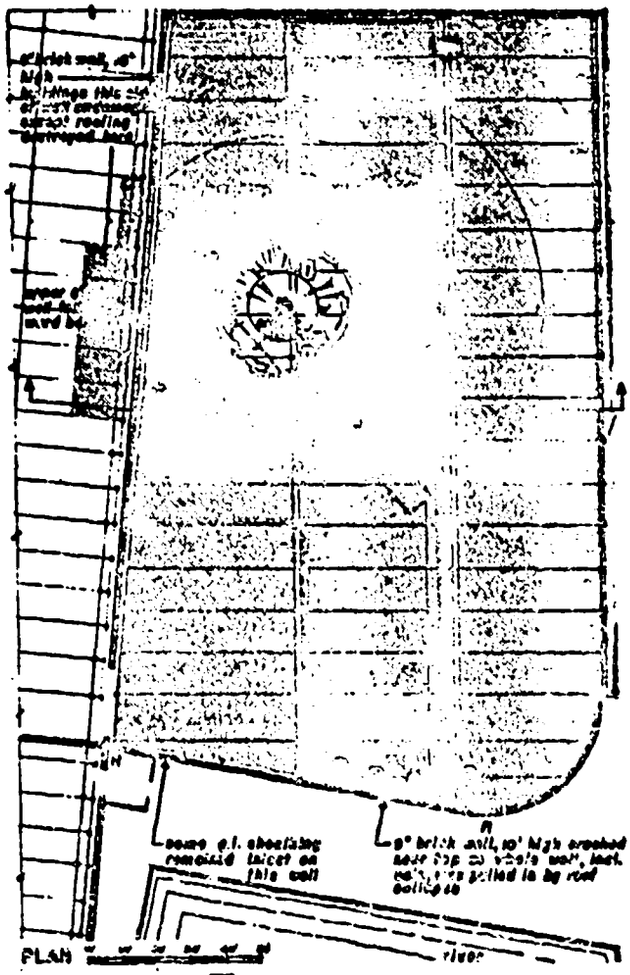

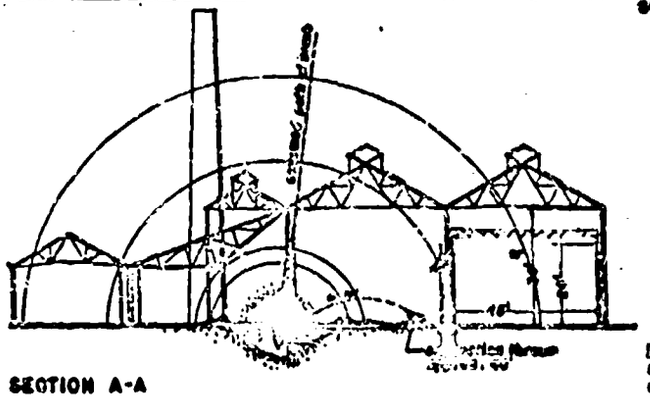

SECTION A-A

BUILDING

A 90'x 225' fully-framed steel shed. Asbestos cement sheathing on steel ∠ purlins. Monitored roof trusses spaced at 12½' on 45' spans carried by braced valley beams. Beams span 25' between columns. 34' to tie level. Columns have extra legs to carry crane girders at 24' level (see sec. A-A), and stand on concrete blocks set on reinforced concrete piles.

DAMAGE

Bomb hit crane girder 1-1 and exploded below level of col. footings. Cols. 1,1 and crane girders 2-1, 1-1 & 1-2 were blown upward. The col. footings were stripped from their piles and the girders were torn upwards from their connections. Valley beam 2-1-1-2 also came down and with it all of the roof structure within the area shown by the heavy shading. The adjacent roof structure, within areas shown in heavy shading, also were pulled toward the collapsed area. At the top of the wall at the river end of the building (R-R) this amounted to approx. 3'-4'. The top of col. 3 (between crane girder & roof) was bent inward about 4'-6". The lighter cols. 4, 5 & 6 bent inward approx. 3'-4' with the wall but remained vertical at bases. The crane girders that fell remained virtually undamaged, failure occurring within the bolts of the connections rather than the members. The chimney, collapsed by earth-shock and blast, crashed through the roof carrying with it a considerable portion of the roof structure.

All of the glazing and all g.i. roofing in entire building gone. Many purlins and light roof members were bent and twisted – their connections also suffering. All exterior wall sheathing, except in end wall R-R, also gone. Attention is called to the displacement of the col. footing (see sec. A-A) it is to be noted that this block of concrete was securely anchored to the R/C piles.

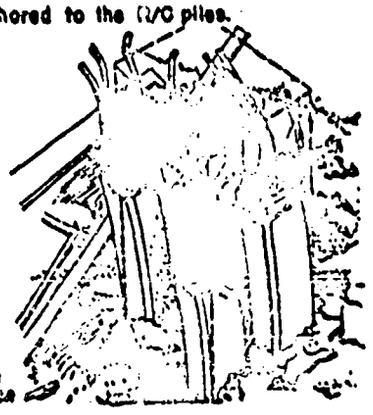

DETAIL

March 1943

INCIDENT SUMMARY

PARA MINE SS-SF INCIDENT ONE

SINGLE STORY, STEEL FRAME FACTORY BUILDING STRUCK BY A PARACHUTE MINE

PP-8808/34

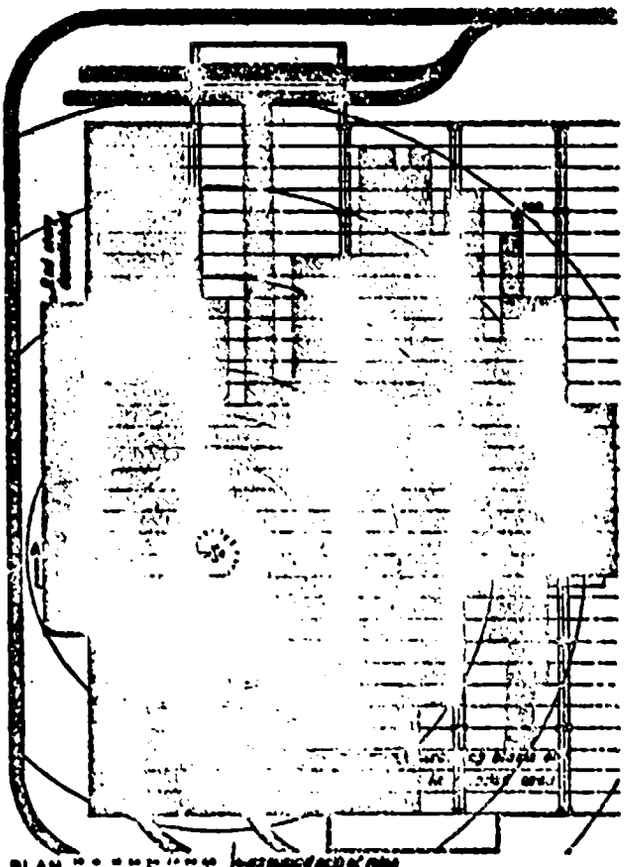

PLAN

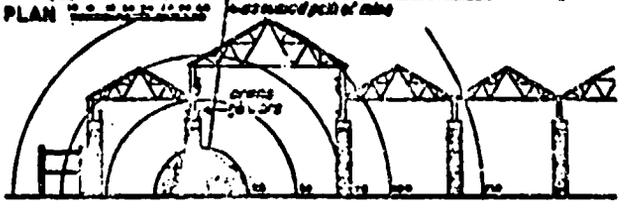

SECTION A-A

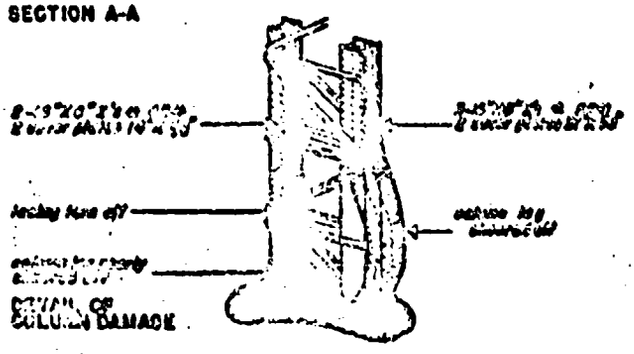

DETAIL OF COLUMN DAMAGE

BUILDING

Type: Single story, steel frame main shop of a steel mill; approximately 570 ft. x 800 ft.

Construction: Interior columns (affected area) - heavy, lattice type; one leg consisting of 2 - 16"x8" I @ 58# with 21"x7/8" cover plates and the other leg of 2 - 16"x6" I @ 42# with 19"x5/8" cover plates. These legs were laced together with steel angles and spaced 5'-7 1/2" o.c. A single built-up column extended upward to the roof and was centered on the lattice column cap.

Girders and Trusses - crane girders, about 5'-3" deep spanning 48'-9" between columns, ran the full length of the building on each side of the columns. They were bolted thru their bottom flanges to the column caps. Above these a third crane girder, facing the Casting Bay, was supported on brackets from the center column. Longitudinal flat trusses, also attached to this center column carried the light pitched roof trusses.

Roofing and Sheathing - corrugated galvanized iron sheets, secured by 5/16" hook bolts to side rails and purlins. The side rails and purlins were 3 1/2"x 3"x5/8" angles.

Two-story Building - brick wall-bearing construction, about 20 ft. x 130 ft., R/C floor slabs, roof of R/C ribs and hollow tile filler.

DAMAGE

The parachute mine perforated the roofing and fell close to the lattice column, detonating upon contact with the floor. Only slight structural damage was done to the main shop building. The column nearest the explosion was distorted considerably: one leg, consisting of three I-sections, was sheared off at the base; the other leg, two I-sections, was almost severed.

Crane girders 1, 2 and 3 (see plan) were blown down when their bolted connections failed in tension. Girders 4, 5 and 6 were torn loose but did not fall down. A few roof purlins and truss members were bent and torn loose by the falling mine. No roof trusses came down.

Almost all of the roofing and wall sheathing was blown off of the building. The hook bolts straightened out but did not tear out of the sheathing.

The two-story brick building, adjacent to the Ladle Stockyard suffered considerable damage. The roof slab and second floor walls were completely demolished by the blast.

January 1944

CONFIDENTIAL

INCIDENT SUMMARY

C 110
MB-RCF
INCIDENT GMZ

TWO STORY, REINFORCED CONCRETE FRAME SCHOOL BUILDING STRUCK BY A 110 lb. G.P. BOMB

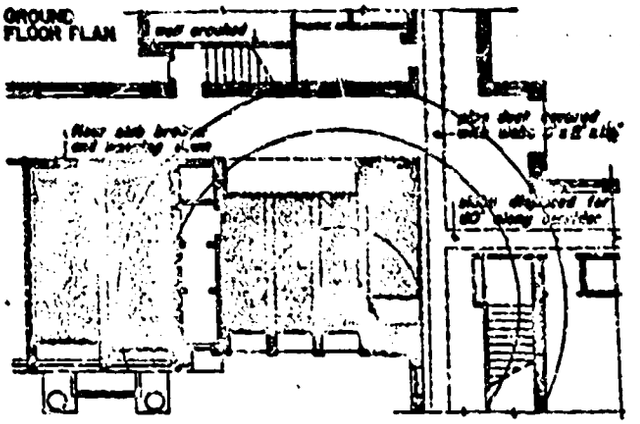

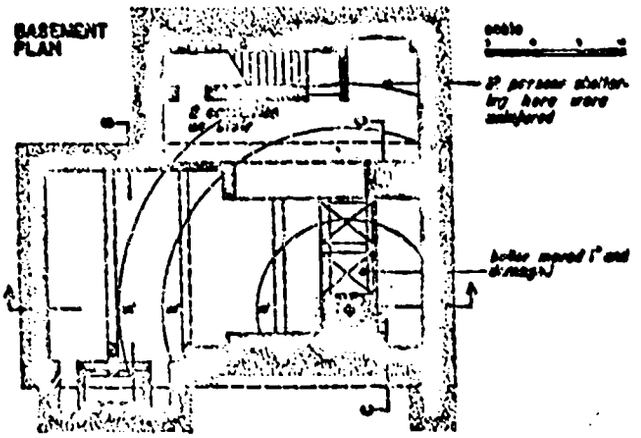

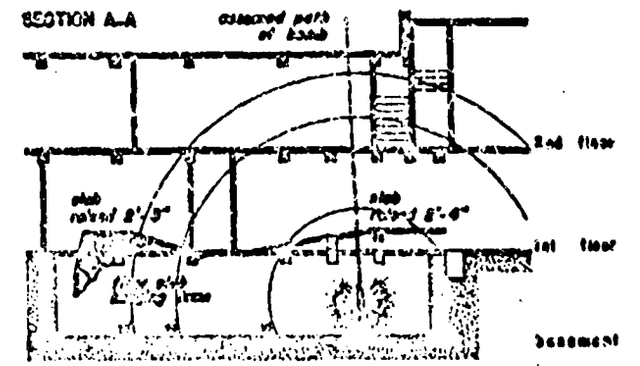

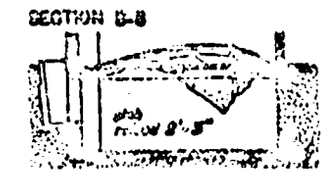

BUILDING
Type: School building consisting of basement and two upper floors in area affected by bomb. Construction: Reinforced concrete frame. Floor slabs 5" concrete. Basement 16" brick walls, exterior walls above basement 13" brick. Partitions 8½" brick.

DAMAGE
The bomb perforated the roof and two floors detonating in the basement. Structural damage was confined to the boiler room (3060 cu. ft.) in which the explosion occurred. The bomb exploded in the 4ft. space between the boiler and the heavy outside wall. The first floor beams (Bm 1,2,3, and 5) were raised upward. Floor slab over bm1, having pulled away from its 8½-in. bearing along the wall, was broken and left hanging down. The floor slab over beams Bm2, 3, and 5 was also raised but beam Bm2 remained in place being supported by the 1st. floor partition. A hole (about 85 sq. ft.) was blown in the floor slab immediately over the blast.

Other damage to the building was minor, consisting of an 11-in. diameter hole in the roof, a small portion of the parapet wall demolished, an 11" x 19" hole in the second floor and some glass damage. A few days after the incident the school was in normal operation although no repairs had been made in the meantime.

Two casualties resulted on the stair when a door was pulled down on top of them. The boiler and chimney effectively screened 12 other persons sheltering in the basement.

The sketch below shows the broken connection of beam Bm1 to column 1 and is typical of concrete beam and column fracture under uplift loading.

May 1944

INCIDENT SUMMARY

THREE STORY, REINFORCED CONCRETE FRAME WAREHOUSE STRUCK BY A 550 lb. G.P. BOMB

C-550
MS-RCF
INCIDENT ONE

PP-5602/56

(German 250kg. S.D.1 Chg. Wt. 50%)

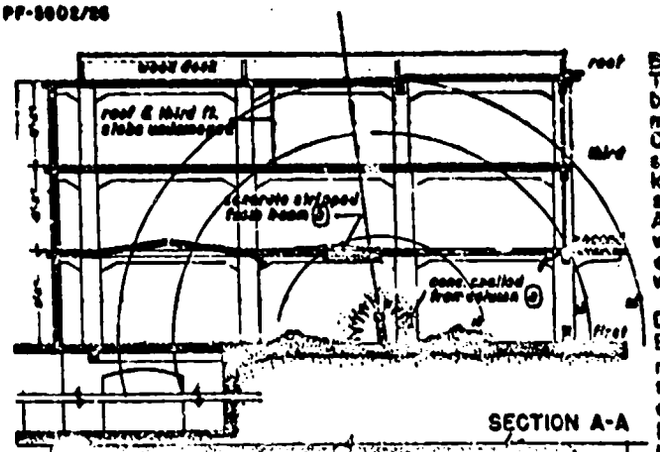

SECTION A-A

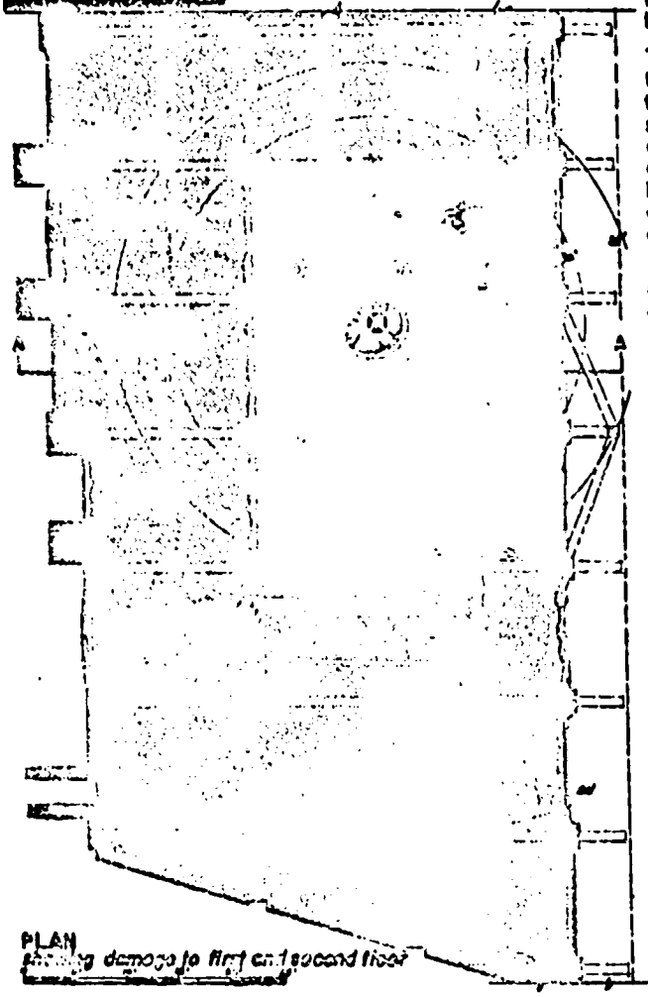

PLAN
showing damage to first and second floor

BUILDING

Type: Wharf warehouse, first, second and third floors; brick vaulted cellar under back row of bays. Overall dimensions 45'x130'.

Construction: Reinforced-concrete frame, beam and slab, 13'x13' bays. Slabs - 8½" thick, designed for a live load of 336 lbs. per sq.ft. (3 cwt). Columns - first floor 24"x24", second fl. - 21"x21", third fl. - 18"x18".

At the time of the incident the first flr. was loaded to within 12" of the ceiling with crates and barrels of eggs, cheese and packing material. The second flr. was not loaded; the third floor was loaded.

DAMAGE

Bomb perforated roof and two floor slabs and detonated centrally in plan at the first floor, forming a small crater in the solid floor. Due to the muffling effect of the goods on this floor and the ease of lifting the unloaded second floor, the force of the blast was upwards. No damage due to fragmentation.

The entire second-floor slab (3930 ft²) was lifted and torn from its supporting beams: Six bays (1170 ft²) of the slab directly over the explosion collapsed. The slab cracked parallel with the one-way reinforcing and remained lifted along lines indicated thus: [illegible] and sagged along lines indicated thus: [illegible]. Maximum lift occurred along the brick wall at the rear of the building. Maximum final lift was 17". Roof and third-floor slabs were not damaged.

The beams lifted with the slab and failed in reverse bending, stirrups pulled out and concrete cracked from reinforcing as shown in sketch below. All second-floor beams suffered similar damage in varying degree. Beam Ⓒ had concrete stripped from steel to the extent shown on plan and section.

Column Ⓓ, 2 feet from the bomb, had a ⅛" metal guard blown away and concrete spalled from its base to a depth of 9" and to a height of 2'-6". No other column damage except light tension cracks at beam haunches.

Wall damage is shown cross-hatched on the plan.

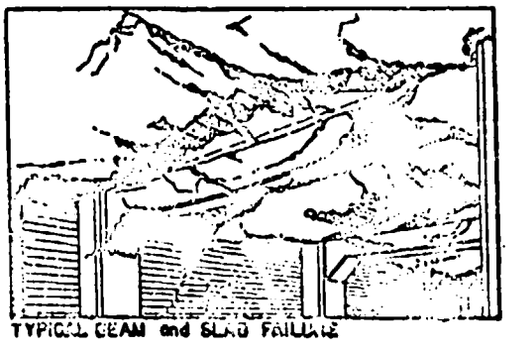

TYPICAL BEAM and SLAB FAILURE

May 1963

CONFIDENTIAL

INCIDENT SUMMARY

TWO STORY REINFORCED CONCRETE FRAME TEST BUILDING STRUCK BY A 1000 lb. G.P. BOMB

C-1000 MS-RCF INCIDENT ONE

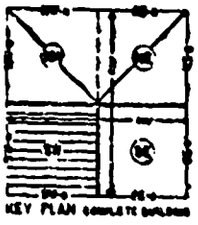
KEY PLAN COMPLETE BUILDING

AREA	FIRST FL	SECOND FLOOR	ROOF	EXTERIOR CURTAIN WALLS-2nd FLR	
NW	8" flat slab, 2-way R/C on column capitals	7 inch slab, 2-way R/C on concrete beams	2 & 3 wood rafters on steel beams, 1" wood sheathing, asbestos cap, 4-ply felt rfg.	[illegible] stock, [illegible] clapboard, wood sash	[illegible] brick, steel sash
NE		8" flat slab, 2-way R/C on column capitals	20 g. steel rib roof, steel beams & girders 1/2" insul, 4-ply rfg.	[illegible] brick, [illegible]	[illegible] concrete [illegible] steel sash
SE		8" slab (expd metal reinf.) on R/C joists (16" x 20" pans)	6" slab (expd metal reinf.) on R/C joists (6" x 20" pans), 4-ply felt rfg. pea gravel on surface	[illegible] load-bearing tile, steel sash	[illegible] brick, steel sash
SW		4" slab (expd metal reinf.) on R/C beams & girders	20 g. corr. g.i. roofing on steel saw-tooth roof trusses, metal & wire-glass lights	[illegible] 20 g. corr. g.i. on steel frame, steel sash	[illegible] 20 g. corr. g.i. on steel frame, steel sash

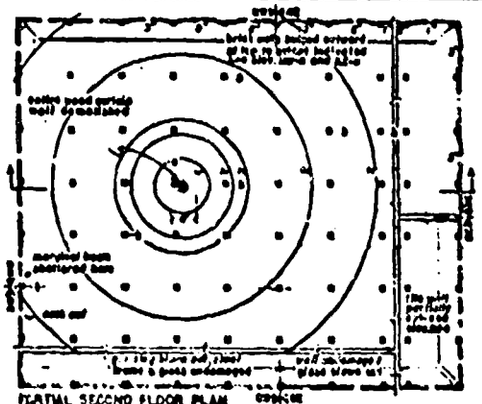
PARTIAL SECOND FLOOR PLAN

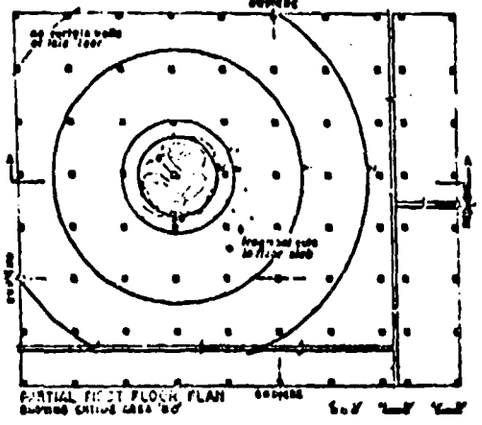
PARTIAL FIRST FLOOR PLAN

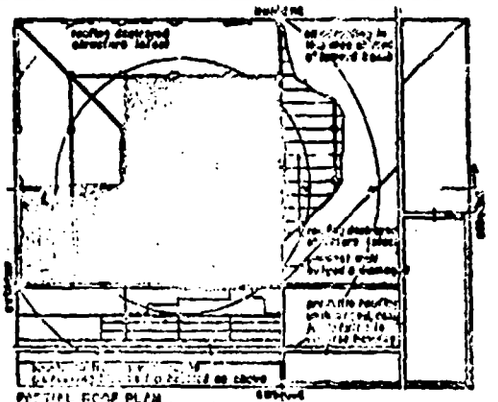
PARTIAL ROOF PLAN

SECTION A-A

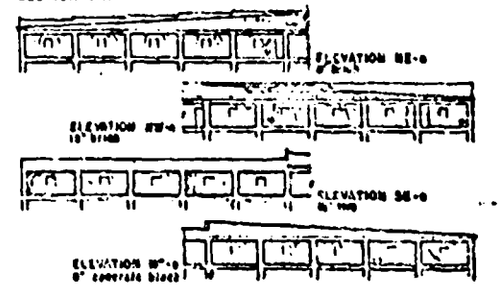

[illegible]

May 1963

CONFIDENTIAL

INCIDENT SUMMARY

MULTI-STORY, REINFORCED CONCRETE FRAME APARTMENT BUILDING STRUCK BY A 1100 lb. G.P. BOMB

C 1100 MS-RCF INCIDENT ONE

P7-5002/B

(GERMAN 500 Kg S.C. ship wt 50 %)

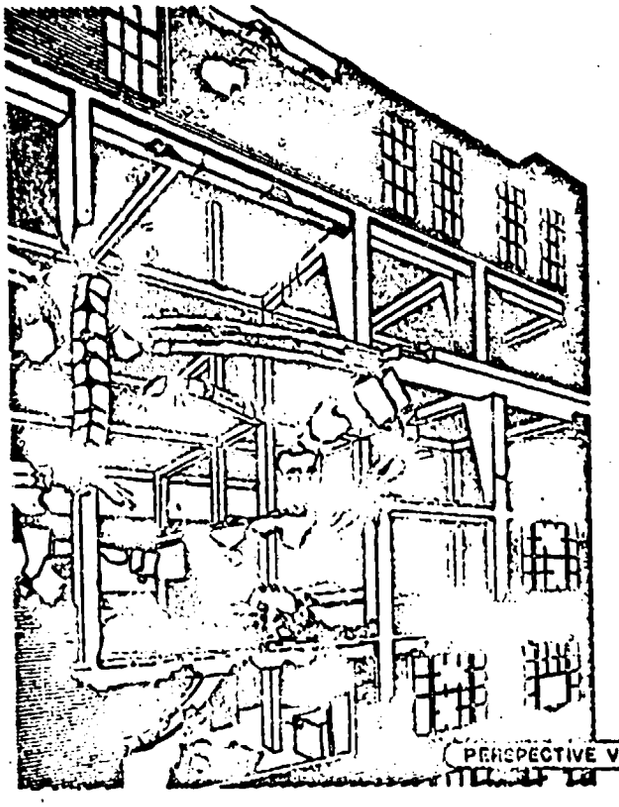

PERSPECTIVE VIEW A

ELEVATION A

roof
ninth
eighth
seventh
sixth
fifth

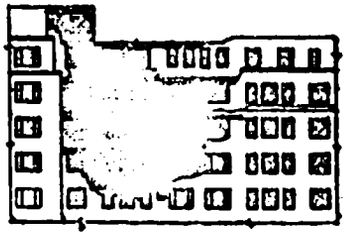

ELEVATION B

roof
ninth
eighth
seventh
sixth
fifth

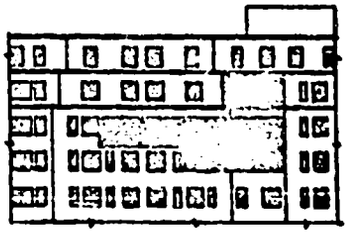

SECTION A A

roof
ninth
eighth
seventh
sixth
fifth

observed path of bomb

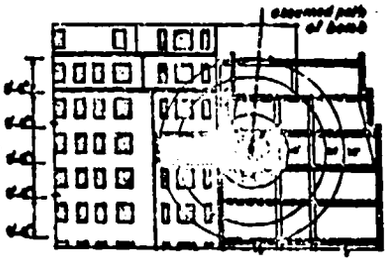

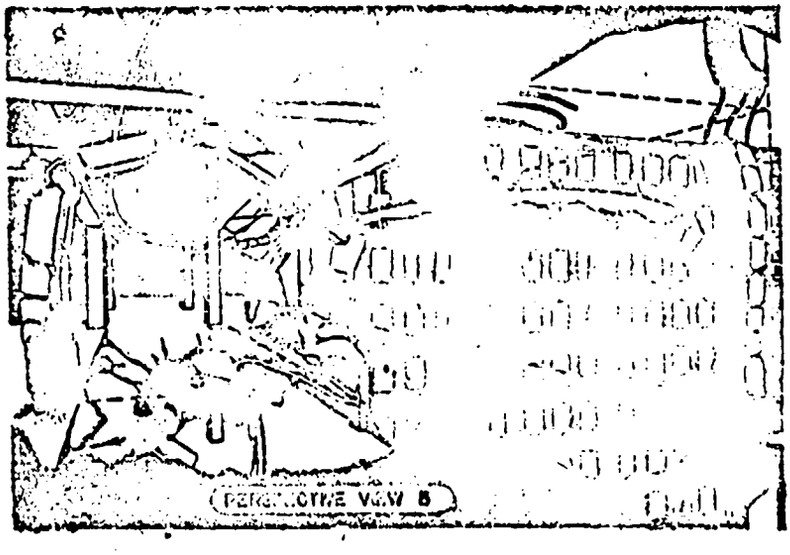

PERSPECTIVE VIEW B

SITE PLAN

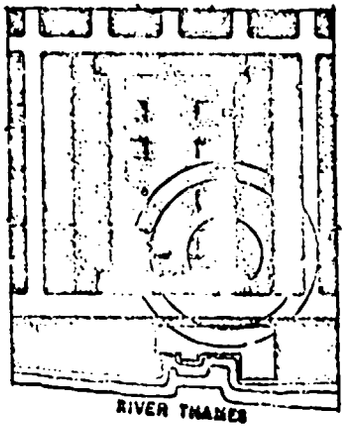

RIVER THAMES

CONFIDENTIAL

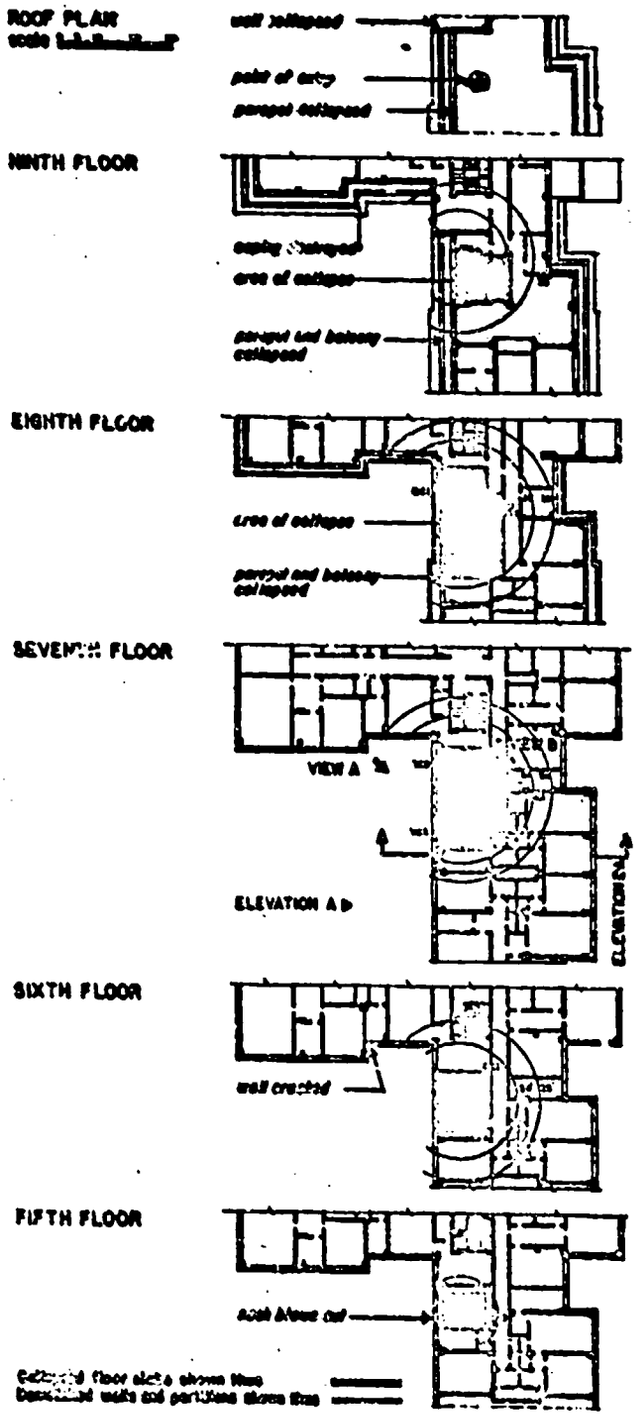

BUILDING

Type: Apartment building consisting of basement, nine upper floors and pent-house on roof. Construction: Reinforced concrete frame. Floor slabs 8" concrete. Exterior walls 11" brick cavity. Partitions 3½" plaster accured to columns with #" wire 24" o.c. 2-2½" walls with 1½" cavity between apartments. Stairway walls 8½" brick. To facilitate erection the reinforcing steel was prefabricated into "cages" and dropped into position between columns with additional straight bars being added for continuity at top and bottom prior to placing of concrete.

DAMAGE

The bomb perforated the roof and two floors detonating between the 7th and 8th floors.

Roof: Beams and columns intact. Bomb punched a 5'x3' hole. Slab bowed upward from blast. Parapet and walls of pent-house collapsed.

8th floor: Beams and columns intact. Approx. areas of damage in sq. ft. to: floor - 184; partitions - 800.

8th floor: Columns intact. 881 and 882 and connections broken, center broken up and bowed upward. 883 and 885 disintegrated. Connection of 884 to CC1 severed, beam sagged down and twisted. Connection of 886 to 8C1 broken. Approx. areas of damage in sq. ft. to: floor - 830; exterior wall - 620; partitions - 1080.

7th floor: Beams and columns most severely damaged. 781, 782, 785 and 786 disintegrated. 783 and 784 bent downward. 787 cage blown up. Columns 7C1 and 7C2 bowed out. 7C3 broken and hanging from column above. Only bowed rods of 7C4 remain. Approx. areas of damage in sq. ft. to: floor - 930; exterior wall - 12401 partitions - 3060.

6th floor: 681 collapsed. Column 6C3 damaged. Approx. areas of damage in sq. ft. to: floor - 620; exterior walls - 890; partitions - 1170.

5th floor: No structural damage. Approx. areas of damage in sq. ft. to: floors - 120; partitions - 360; exterior walls - 0.

Excessive damage to beams and columns may be attributed in part to the use of prefabricated reinforcement "cages" and separate continuity rods. In some cases where beams disintegrated the "cages" were blown out while continuity rods remained in place.

Excessive column damage probably due to bonding partitions to columns, thereby transmitting forces on partitions to columns.

Some fragmentation damage to brick walls and window frames occurred across the courtyard. Damage extended from the third to eighth floors being most severe at the fifth and sixth floors.

Note: Circles represent the intersect of spheres of destructive radius with the floor in question.....the center of the sphere being at the estimated position of the explosion.

April 1944

INCIDENT SUMMARY

C-2200 MS-RCF INCIDENT ONE

MULTI-STORY, REINFORCED CONCRETE FRAME WAREHOUSE STRUCK BY A 2200 lb. G.P. BOMB

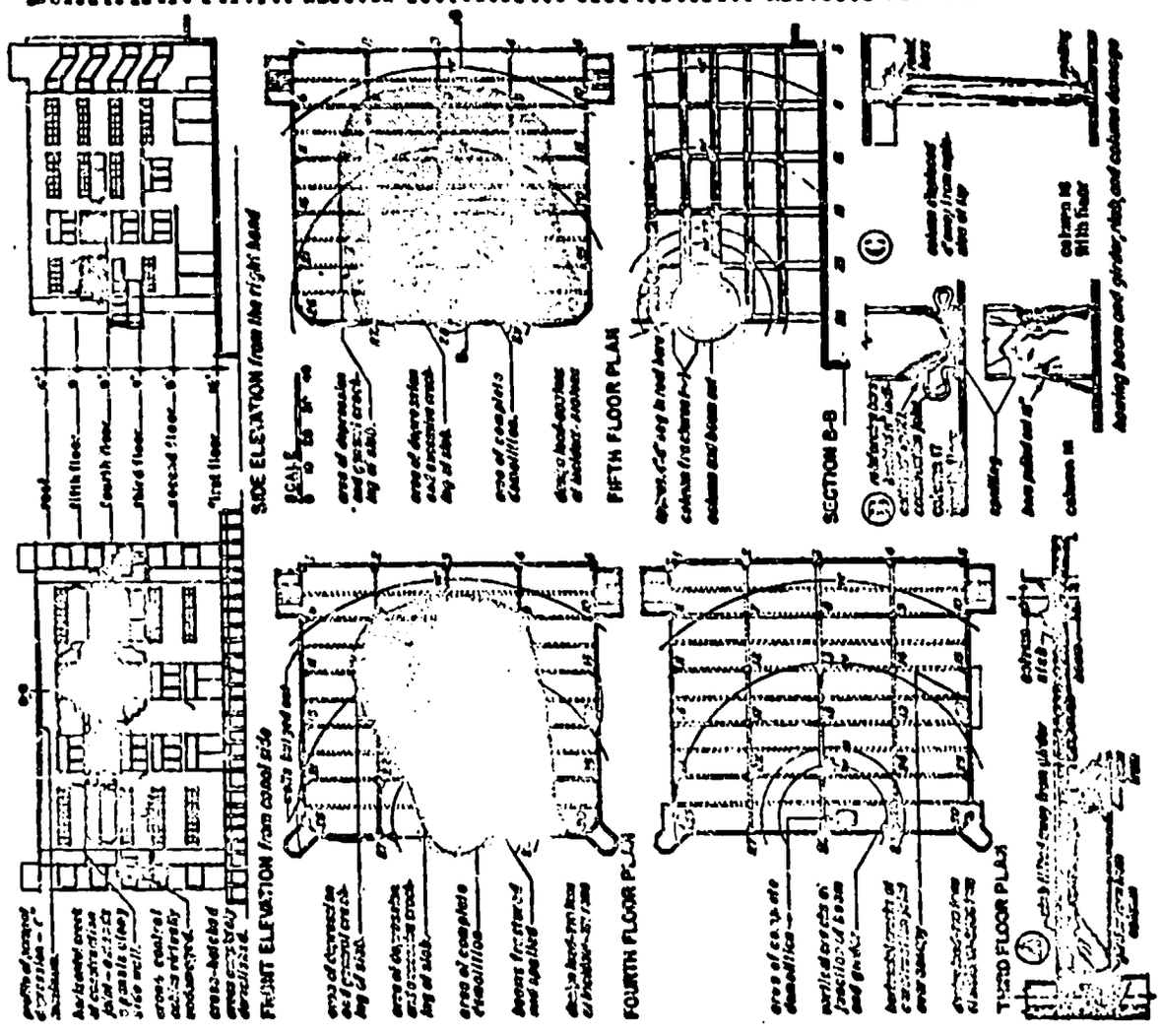

August 1945

INCIDENT SUMMARY

D-110
MS-WB
INCIDENT ONE

MULTI-STORY, WALL BEARING SCHOOL BUILDING STRUCK BY A 110 lb. G.P. BOMB

PF-8908/28

(GERMAN 50 Kg. S.C. 9 deg. W.B.C.%)

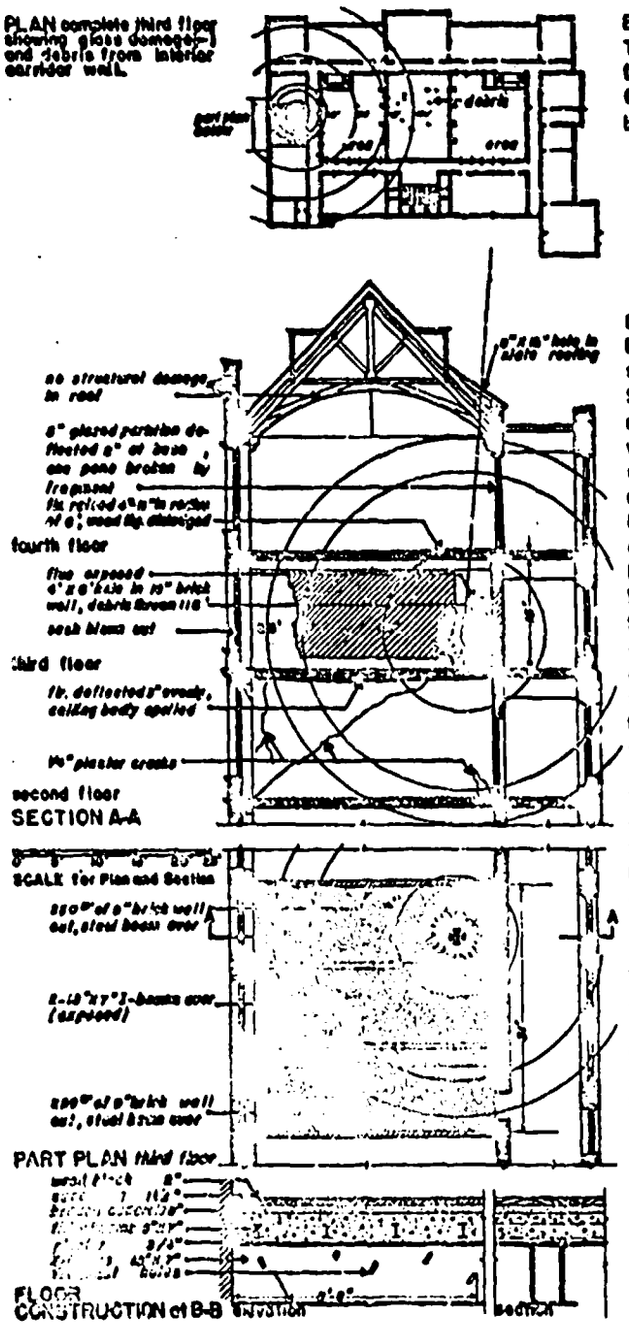

BUILDING

Type: Six-story (basement and four upper floors; five in front). Technical College (ca. 1900)

Construction: Walls—massive, well built brick bearing walls.

Floors—9-inch thick breeze concrete slabs on 3-inch steel filler joists, 2-inch wood block flooring. In this instance the fourth floor was reinforced with steel I-beams.

Roof—slate roofing on timber trusses.

Partitions—9-inch brick panel walls.

DAMAGE

Bomb perforated roof and the 13½-inch fourth floor slab detonating above the third floor as shown in Section A-A. Structural damage was limited to the room (14000 cu. ft.) in which explosion occurred and was confined to an area within 40 feet of the explosion. The bomb exploded about 5 feet from the 18-inch interior corridor wall. A hole 6'X4' was punched in this wall (probably by mass fragmentation) and the debris was thrown horizontally a distance of 116 feet into the Examination Hall in the center of the building. An area of 250 sq. ft. was blown out of each end partition wall. The front exterior bearing wall was moved out about ½ inch. One window sash and the corridor door were blown out. The ceiling (4th. floor slab) within 6 feet of bomb hole was lifted and the third floor was deflected 3 inches uniformly by the blast wave.

The I-beam above the explosion was perforated in web and in flange by fragments. Maximum web perforation was 4"X1"; flange perforations were 1 and 1½ inch in diameter. (See detail of floor construction at B-B)

The brick fireplace was demolished; flue exposed for 10 feet. A small fire was started in the upholstery but was readily extinguished. The skylight in the Area suffered heavily from debris. The pattern of glass damage shows how effectively blast is baffled by the right-angled bends in corridors.

Note: Circles represent the intercept of sphere of designated radius with the floor in question.....the center of the sphere being at the estimated position of the explosion.

July 1943

INCIDENT SUMMARY

MULTI-STORY, WALL BEARING OFFICE BUILDING STRUCK BY A 1100 lb. G.P. BOMB

D 1100 MS-WB INCIDENT ONE

PF 5008/BS

(GERMAN 500 kg S.C. equal 50 %)

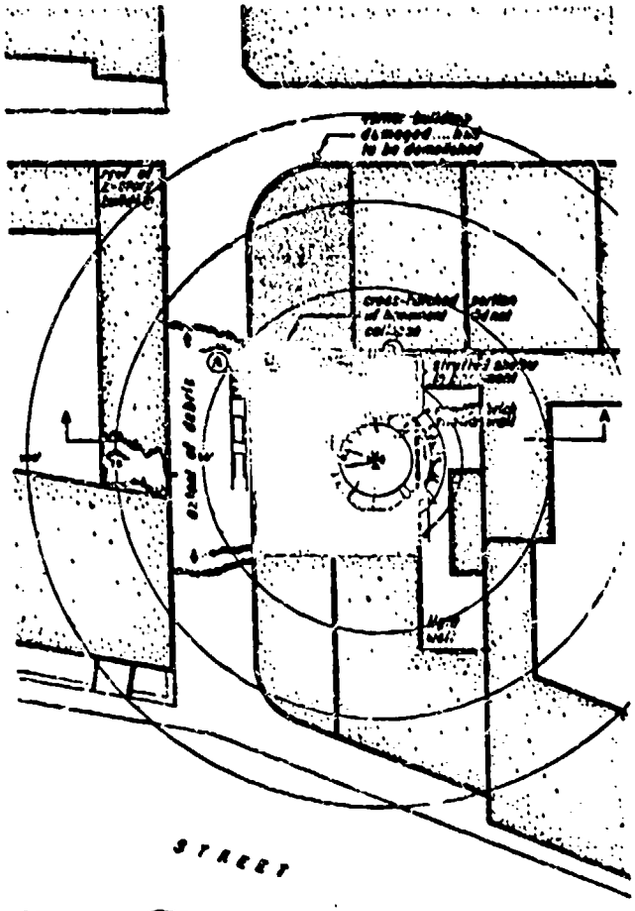

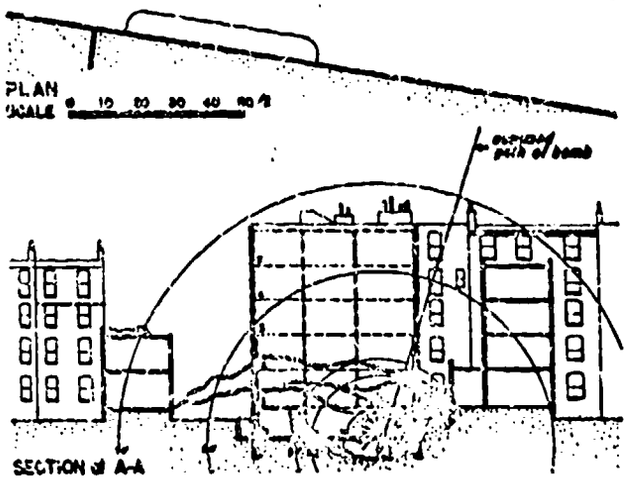

BUILDING
Basement and five upper floors. Overall size approximately 50 ft. by 60 ft.

Construction: Walls - exterior brick load-bearing, 22½ inches thick for basement, first and second floor walls; 18-inch thick walls from third floor to roof. Internal steel frame.
Floors and Roof - breeze concrete and filler joists. Shelter - basement room reinforced with 7"x6" timber struts and beams (set parallel with filler joists), some structural steel and a new 18-inch thick brick wall.

DAMAGE
The bomb apparently fell down the light well between the buildings and perforated the rear exterior wall and basement floor before detonating. A crater, 30 ft. in diameter and 8 ft. deep, was formed in the sandy-clay soil by the explosion. The entire building collapsed filling the basement and pavement at the front of the building with debris. A small part of the shelter (shown cross-hatched on the plan) did not collapse, however, thereby saving the lives of three women. They were rescued, though injured, by means of the emergency exit in the pavement light which was forced through at ①. Others in the shelter were killed when thrown by the blast against the basement wall at ②. The new 18-inch brick shelter wall was demolished. Incendiaries later started fires in the debris.

The corner building, adjacent to the one struck and of similar construction, suffered severely from the effects of the blast and the shock that it had to be demolished later. However, other adjacent buildings did not even suffer glass damage. There was no fragmentation damage.

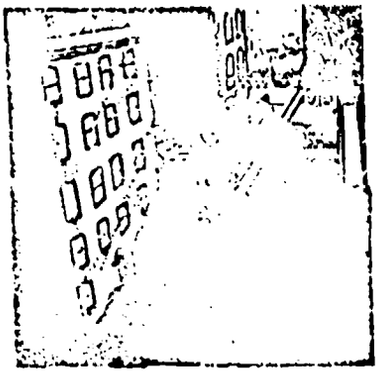

December 1943

INCIDENT SUMMARY

MULTI-STORY, WALL BEARING WAREHOUSE STRUCK BY A 2200 lb. A.P. BOMB

D 2200 MS-WB INCIDENT ONE

PF 8902 / 30

(Curtain 1000 kg G.P. chg. wt. 14%)

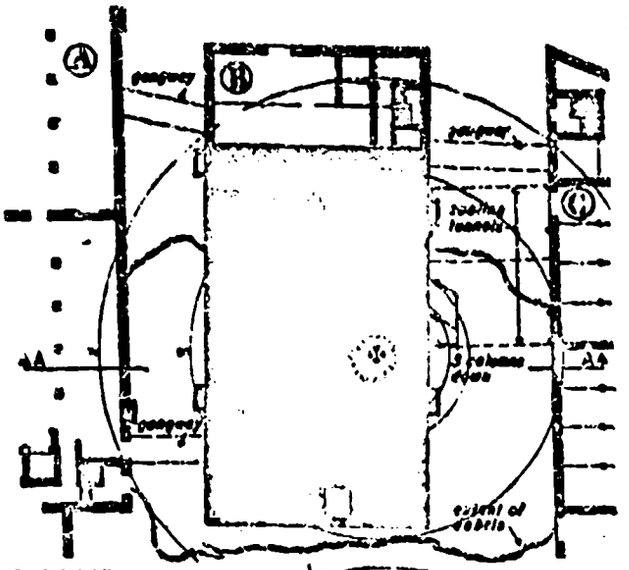

PLAN 1st floor

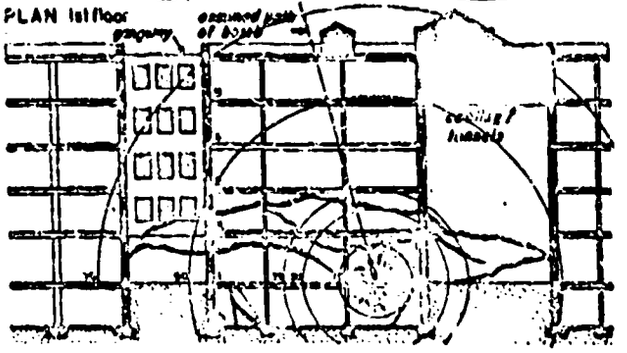

SECTION A-A

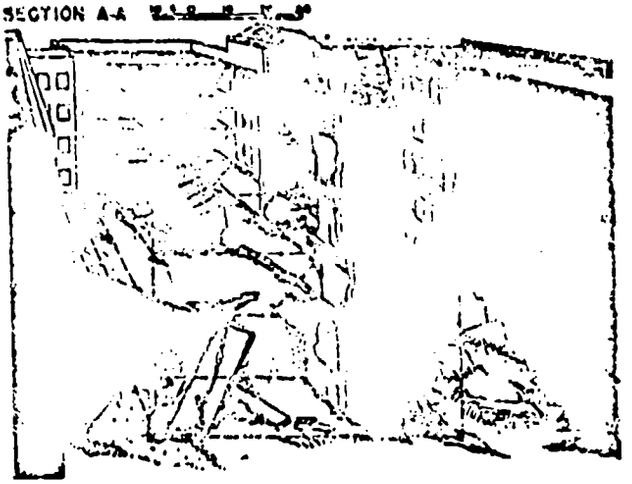

BUILDING

Type: Warehouse B - one of a group of three warehouses - basement and five upper floors and flat roof. Over-all dimensions 60'x180'.

Construction of Warehouse B: brick bearing walls approximately 2' thick. Floors and roof 7" of concrete between 7" steel joists spaced at 2'-6" centers covered with 2" concrete slab. Floors and roof were supported by steel beams and intermediate cast iron columns. Basement beams and columns encased in concrete.

Warehouse (C) of similar construction and warehouse (A) is steel framed enclosed with brick walls.

DAMAGE

The bomb perforated the roof and 3 floors of warehouse (A) and exploded on or near the first floor. The major portion of the warehouse collapsed to the first floor. The first floor collapsed into the basement in the area near to the bomb.

A four story gangway connecting warehouses (A) and (B), and part of the cooling tunnels at the fifth floor between warehouses (B) and (C) collapsed to the ground. The cooling tunnels were used for cooling jam as it passed from warehouse (C) to (B).

The elevator shaft was steel framed and remained standing although considerably damaged.

All windows in warehouses (A) and (C) adjacent to (B) were blown out.

Shelters were provided in the basements of all three buildings and were occupied by 1500 people when the bomb struck. 6 people were killed by the collapse of the first floor of warehouse (B).

January 1944

INCIDENT SUMMARY

D-PARA MINE MS-WB INCIDENT ONE

MULTI-STORY, WALL BEARING FACTORY BUILDING STRUCK BY A PARACHUTE MINE

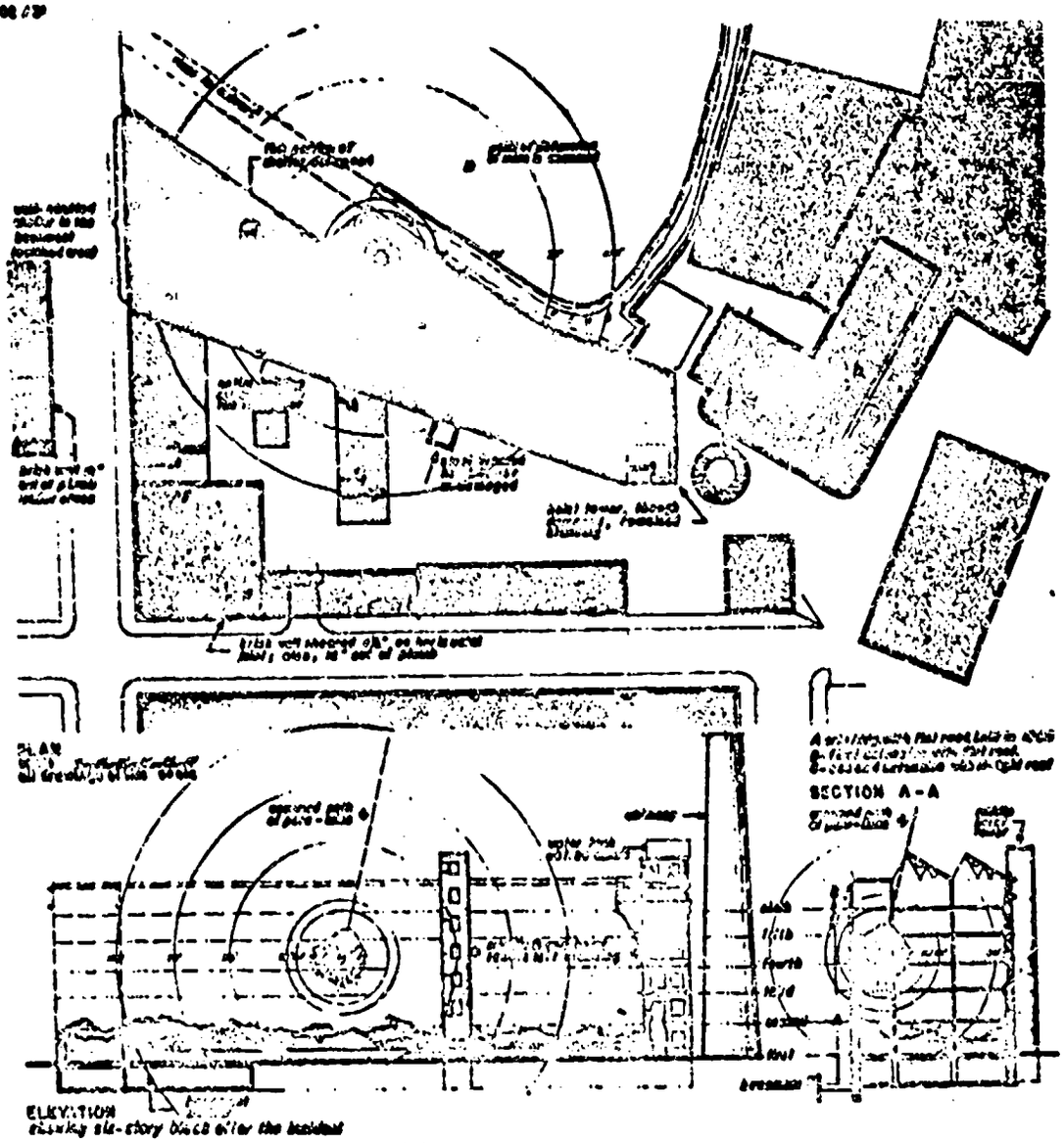

PLAN

SECTION A-A

ELEVATION
Showing six-story block after the incident

BUILDING

DAMAGE

May 1945

GLOSSARY

A. C. Advisory Council on Scientific Research and Development, Ministry of Supply.

ADM. Issued to British Admiralty by Road Research Laboratory, Department of Scientific and Internal Research.

ADP. Ammonium dihydrogen phosphate.

AFTERBURNING. The relatively slow oxidation of the products of the detonation of a high explosive. It may or may not involve atmospheric oxygen.

AIR SHOCK. The disturbance (shock wave) propagated through the air arising from a source of suddenly expanding gases (as from explosions, bursting diaphragms, sparks, etc.).

AMG-NYU. Applied Mathematics Group, New York University.

AMP. Applied Mathematics Panel.

AN. Ammonium nitrate.

APC. Armor-piercing capped projectile.

ARD. Armament Research Department (England).

ARL/S. Admiralty Research Laboratory, Summary.

ARM. Armament Experiment of Royal Aircraft Establishment.

ATM. Atmosphere.

BACK BLAST. The increased blast effects produced at the rear of a gun by a muzzle brake or blast deflector.

BAFFLE (in muzzle brakes and blast deflectors). A plate which intercepts a fraction of the gas and deflects it away from the bore axis.

BARE CHARGE. A charge which is not in a case.

BHN. Brinell hardness number. Obtained by pressing steel ball of 10-mm diameter into the surface under a load of 3,000 kg. The BHN is given by the load divided by the area of the spherical surface of the impression measured in square millimeters (units, kg/mm²).

BLAST DEFLECTOR. A device attached to the muzzle of a gun, such as a muzzle brake, which intercepts and deflects a fraction of the blast.

BOAT-TAIL. Applies to bullets. The back is not plain but partly beveled.

BOOSTER. A quantity of high explosive in which detonation can be more readily initiated (by means of primers) than can the main high-explosive filling. Boosters are used to initiate the main, relatively insensitive high-explosive filling.

BOTTLE (in the blast of a gun). The central, bottle-shaped, supersonic region of a high-pressure jet bounded by stationary shocks in which the main expansion of the gas occurs. In a gun, the neck of the bottle is in the tube.

BRAKE EFFICIENCY. The per cent of reduction in recoil energy produced by a muzzle brake. Brake efficiency depends on brake, gun, and round.

BRINELL HARDNESS. The Brinell method of measuring the surface, or superficial, hardness of a material employs a small hardened steel ball under a force applied for a specified time. The Brinell number is calculated from the dimensions of the resulting permanent impression.

BRISANCE. The property of explosives which describes their shattering power, by virtue of very sudden release of energy. Brisance is usually measured by the depth of the dent produced in a steel plate by a contact explosion.

BRL. Ballistic Research Laboratory, Aberdeen Proving Ground.

BUBBLE MIGRATION. The vertical motion of the gas bubble due to its buoyancy and the forces exerted by nearby surfaces.

BUBBLE PULSE. The pressure pulse emitted by the collapse of the gas bubble.

BURSTER SLAB. A horizontal layer of concrete or masonry at or near the ground surface and surrounding a protective structure. Its purpose is to cause near-miss bombs to break up or to detonate prematurely.

CABLES (coaxial, electric). Electric conductors in the form of one or more conductors provided with insulation and an external conducting envelope, or shield.

CALIBER RADIUS. Radius of curvature of projectile's nose expressed as a multiple of the projectile diameter.

CAMOUFLET. A cavity beneath the surface of the earth caused by an explosion too deep to crater.

CAP. Protective material over the nose of the armor-piercing element. A cap is used to reduce deformation of the projectile proper.

CASE. The jacket or container of a bomb or other projectile. The case is usually made of steel but may also be aluminum, cardboard, plastic, etc.

CAVITATION. The result of negative pressures or tensions applied to water which pull the medium apart and form bubbles of gas or vapor.

CFD. Committee on Fortification Design; original, CPPAB (q.v.).

CHARGE (high-explosive). A quantity of explosive which is prepared for detonation.

COMPOSITE RIGID PROJECTILE. A full-caliber, lightweight projectile with a small armor-piercing core.

CONDENSER-MICROPHONE. A gauge which depends for its action upon the change in electric capacity of a condenser, as the plates of the condenser are deformed by the action of pressure.

COUNTERMINING. The destruction of weapons by means of an explosion.

CPPAB. Committee on Passive Protection against Bombing. This was organized by the National Research Council at the request of the Corps of Engineers to carry out research for the latter. Later called the Committee on Fortification Design (CFD).

CRUSHER CYLINDER OR SPHERE. Used in equipment for measuring maximum pressures in guns or underwater. The crusher, usually made of copper, is placed in a cylinder in contact with a piston that is exposed on its other side to the pressure being measured. The amount of compression given to the crusher is used as a measure of the pressure acting, according to a calibration previously made on similar specimens.

CUP-CONE FRACTURE (of tensile specimen). After fracture, one side of the break resembles a cup with flat bottom and diverging sides. The other part of the break, which fits into the first, is a truncated cone. More complicated breaks can occur.

C/W. Charge/weight ratio.

D-2. Designation of the desensitizer in H3X explosive.

DESENSITIZER. A substance which is added to an explosive to make it less sensitive to detonation.

DETONATION. The extremely rapid chemical reaction which occurs in the explosion of high explosives. Detonation is characterized by its propagation through the mass of explosives as a wave, by its great velocity, by the fact that it can be initiated by a shock or blow, and by the extremely high pressures developed.

DETONATION VELOCITY. The rate at which the decomposition zone or front travels through an explosive after it is detonated.

DIFFUSER. In muzzle brake and blast deflectors, an extension to the muzzle or to a baffle orifice that permits the gas to expand and directs it towards the baffle surface.

DIFFUSOR. In a supersonic wind tunnel, the diverging part of the tunnel downstream from the working section.

DTMB. David Taylor Model Basin (U. S. Navy, Bureau of Ships).

ELASTICITY. The property of a material whereby a straining-unstraining cycle leaves no permanent deformation. The relation between stress and strain during the cycle is usually linear. See *Plasticity*.

ERL. Explosives Research Laboratory, Bruceton, Pennsylvania. (Division 8, NDRC).

FACE-HARDENED PLATE. Hard surface, soft back.

FIELD MUZZLE ATTACHMENTS. Muzzle attachments comparable in size and weight to existing muzzle brakes. Such attachments may be used as field modifications on guns prepared to take a muzzle brake.

FLASH CHARGE. An explosive surrounded by a very thin layer of argon gas. On detonation, an intense flash of light about 1 μsec in duration is emitted.

FLOW STRESS (psi). That part of the longitudinal stress in a tensile specimen that is produced by the tensile force, corrected for the effect of the noncylindrical shape of the neck (if any). Therefore, this does not include the stress produced by any simultaneously acting hydrostatic pressure.

FOLDING SKIRT PROJECTILE. A projectile for use in a tapered bore gun.

FREE AIR. A region in the air well removed from obstacles, the ground, and other reflecting or absorbing surfaces or objects.

FREE PLATE. An idealized plate target which is free to move without restraint when acted on by an impulsive force.

FREE SURFACE. The surface of the sea, i.e., the water-air interface.

GAS BUBBLE, GAS GLOBE. The confined mass of gaseous products resulting from an underwater explosion.

GAUGE LENGTH. In a tensile specimen, the length between the points to which is attached the gauge that measures the extension. In the hydrostatic pressure work (Chapter 16), the length of the uniform part of the specimen, between shoulders.

GP. General purpose.

GUILLOTINE-TYPE TESTING MACHINE. A device constructed at the California Institute of Technology for testing materials at high speeds. It consists of a pair of guide-rails between which slides the hammer. The hammer is attached to the base of the machine by heavy rubber strips. A winch raises the hammer against the tension of the rubber strips.

HARDNESS. Resistance to distortion. Superficial hardness is surface hardness as measured by the Brinell or an equivalent method. *See also* BHN.

HBX. Desensitized Torpex.

HC. High capacity.

HCR2. Designation for a type of plastic protection effective against shaped charges (Chapter 12).

HE. High-explosive shell.

HEAT. High-explosive antitank shell.

HIGH EXPLOSIVE. A substance in which sudden chemical decomposition may be initiated by means of heat, friction, shock, and blows characterized by detonation; confinement is not necessary to the very rapid release of energy in detonation.

H.M.A./S.E.E. His Majesty's Anti-Submarine Experimental Establishment at Fairlie.

HOMOGENEOUS PLATE. Uniform hardness throughout.

HU. Harvard University.

HVAP. High-velocity armor-piercing projectile.

HYDROSTATIC PRESSURE (psi). A pressure uniform in all directions, as is produced on a body immersed in a fluid under pressure.

HYPERVELOCITY. Velocity in excess of 3,000 ft per sec.

ISENTROPIC. Nonconductive flow in which a fluid element suffers no change in entropy. Reversible adiabatic flow.

JACKET. The soft material completely surrounding a hard armor-piercing core.

JET (from the muzzle of a gun). The muzzle blast exclusive of the air shock.

JET SEPARATION. The separation of a jet from the walls of a diffuser when the forward increase in section of the diffuser is too abrupt. Between the separated jet and the diffuser the medium is stagnant and highly turbulent.

LC. Light case.

LEAD RATIO. The ratio of the "leads," in degrees, necessary for the gunner to obtain hits on the fighter in training to the leads necessary in combat, the fighter being at the same point relative to the bomber for both cases.

LETHAL DAMAGE. The damage to a vessel sufficient to sink it or put it out of action.

LIMIT ENERGY. The least energy required to perforate a plate.

LIMIT VELOCITY. The minimum striking velocity required for perforation with zero remaining velocity (Navy limit).

LINE CHARGE. A charge, one of whose dimensions is much greater than the other two.

LINER (of shaped charge). A conical, hemispherical, or other shaped piece of metal or glass whose convex face is backed by an explosive.

LOW EXPLOSIVE (propellant). A substance which, once ignited, burns rapidly without access to air, producing gases having temperature and pressure depending upon confinement. Without confinement, the burning of low explosives is slow and quiet. The burning proceeds from the outer surfaces of the grain inward.

MACH NUMBER. Applies to supersonic flow of a gas. It is the ratio of the velocity of the gas (or of a body moving through it) to the local velocity of sound. *See* Supersonic Velocity.

MACH STEM. The single shock wave which, under the proper conditions, is produced by the reflection of a shock wave from a surface, or by the interaction of two shock waves. The incident and reflected shock waves are coalesced in the Mach stem.

MAE. Mean area of effectiveness.

MC. Medium capacity.

MRL. Maryland Research Laboratory (Division 10, NDRC).

MUZZLE GLOW. A glowing of the gas near the muzzle often observed soon after shot ejection. This glow is due not to burning but to chemical changes taking place in the powder gas composition and, perhaps, to the incandescence of unburned powder particles.

NAVORD. U. S. Navy, Bureau of Ordnance.

NDRC. National Defense Research Committee.

NECKING (of tensile specimen). During a tensile test of a ductile material, the load first increases, reaches a maximum, then decreases. During the first stage, the specimen remains cylindrical. At the instant of maximum load, a neck or local contraction first appears; this becomes more pronounced during the remainder of the test.

NEGATIVE PHASE (suction). The part of the shock wave in which the pressure is less than atmospheric.

NG. Nitroglycerin.

NOL. Naval Ordnance Laboratory.

NORMAL SHOCK. A stationary shock, the front of which is perpendicular to the streamlines.

NOZZLE. In a supersonic wind tunnel, the converging part of the tunnel just upstream from the working section.

OBLIQUE SHOCK. A stationary shock, the front of which makes an angle, other than a right angle, with the streamlines.

OE OSCILLOGRAM. The permanent record of the path of the cathode-ray beam on the fluorescent screen of a cathode-ray tube. Usually, a photographic record.

OSRD. Office of Scientific Research and Development.

OXYGEN BALANCE. Complete oxygen balance requires that enough oxygen be combined in the original explosive so that on detonation every element such as carbon, nitrogen, and hydrogen will be completely converted to its respective oxide.

PARTICLE VELOCITY, MASS VELOCITY. The velocity of the matter in a shock wave. Usually referred to the matter ahead of the wave as stationary.

PEAK PRESSURE. The pressure in the initial part of a shock wave. It is usually, but not always, the highest pressure in the wave.

PETN. Pentaerythritol tetranitrate.

PIEZOELECTRIC. The property, exhibited by certain crystals, of generating an electric charge when subjected to pressure.

PIEZOELECTRICITY. The electric charge produced on the faces of some crystals when they are strained (by the action of applied pressure).

PLANE CHARGE. A charge, two of whose dimensions are much greater than the third.

PLASTIC ARMOR, PLASTIC PROTECTION. The combination of gravel or crushed stone with pitch or bituminous binder and a filler such as limestone dust or wood flour.

PLASTICITY. The property of a material whereby a stressing-unstressing cycle leaves a permanent deformation. *See* Elasticity.

PLC. Projected line charge.

PLUME. The irregular masses of water and burnt gases projected into the air after a shallow underwater explosion.

POSITIVE DURATION. The time during which the pressure in a shock wave is greater than that of the atmosphere.

POSITIVE IMPULSE. The integral $\int_0^{t_0} p\,dt$, where p is the pressure at the time t and t_0 is the positive duration of the wave, measured from the zero of time of the arrival of the shock wave at a gauge; hence, the area under the positive pressure part of the pressure-time curve; hence, the average pressure in this time, times the positive duration.

POSITIVE PHASE. The part of the shock wave whose pressure is greater than that of the atmosphere.

PRIMARY FLASH. A glowing that occurs in the high-temperature region behind the normal stationary shock which terminates the bottle. This glow is due not to burning but to a resumption of the action which produces muzzle glow and which is inhibited when the gases enter the relatively cold bottle.

PRIMERS. Sensitive high explosives which are easily detonated by heat, friction, or shock; used to initiate other, less sensitive high explosives.

PRINCIPLE OF SIMILITUDE. A law describing how the shock wave parameters scale.

PROPELLANT. *See* Low Explosive.

PURSUIT CURVE. An idealized path in space, relative to a bomber, which a fighter may fly in order to obtain continued "hits" on the bomber. The path may be calculated if certain assumptions are made regarding the bomber and fighter velocity, the velocity of the fighter's bullets, and the aerodynamic behavior of the fighter along the path.

PUS. Princeton University Station Division 2, NDRC.

PYROELECTRICITY. The electric charge produced on the faces of some crystals when they are strained (by application of heat).

"RAD" BASIS. The "rad" may be defined as the angle subtended at the eye of the gunner by the radius of the ring in a fixed-ring type sight. In fixed optical sights the value of the "rad" in degrees depends only on the choice of ring size since the ring image is focused at infinity.

RAREFACTION WAVE. In compressible flow, a region of low pressure advancing into one of high pressure. The transition between the pressure levels is gradual in waves of rarefaction.

RATE OF STRAIN EFFECT. The rate at which a metal is deformed alters its strength characteristics.

RDX. Cyclonite (cyclotrimethylenetrinitramine).

RE. Ministry of Home Security, Research and Experiments Department.

RECOIL ENERGY. The kinetic energy of free recoil. It is the kinetic energy the gun tube and recoiling parts would have at the time the gun empties, if the reaction were not impeded by the action of the recoil mechanism and friction on the cleat.

RESIDUAL JET. The fraction of the muzzle blast that goes through the forward hole of a muzzle brake or blast deflector.

REST POSITION (of the bubble). A depth at which no migration of the gas bubble occurs because the buoyancy of the bubble is counterbalanced by a free surface repulsion or a rigid surface attraction.

REVERSAL ANGLE. In muzzle brakes and blast deflectors. The angle in excess of 90 degrees from the bore axis at which a baffle plate is terminated.

ρ (rho). Symbol used for density or mass per unit volume of a material, and equal to weight per unit volume divided by g, the acceleration of gravity.

ROTARY IMPACT MACHINE. A machine for testing materials at high speeds, usually used in tension or compression. It consists of a heavy wheel whose speed can be varied, a dynamometer whose functions are to hold one end of the specimen during the test and to measure the force on it, and a device in the wheel to be thrust out at the proper time to break or compress the specimen.

RRL. Road Research Laboratory, England.

RUPTURE VELOCITY. The velocity at which a projectile suffers initial failure.

SABOT. The carrier for a subcaliber projectile. Discards on leaving gun.

SAP. Semi armor-piercing.

SBX. Slow-burning explosive.

SCALE EFFECT. For projectiles of a similar shape and plates of a given caliber thickness, the specific limit energy decreases with increase in projectile size.

SCALING LAWS. The laws to which the linear dimensions of an explosive charge or a target structure must conform in changing from the full scale to some smaller scale.

SCHLIEREN OPTICAL SYSTEM. A means of determining photographically the variation of density and pressure in a moving gas. It depends on the fact that the refraction coefficient of a gas is a function of the density.

SECONDARY FLASH. The burning of the powder gases mixed with air which occurs in the turbulent shell surrounding the bottle. Secondary flash is the principal flash element in medium- and large-caliber guns.

SELSYN GENERATOR. The selsyn unit used in the "driver" position for remote control of another system.

SHATTER ENERGY. The energy of a projectile having a velocity equal to shatter velocity.

SHATTER GAP. When perforation can be obtained at velocities above and below but not within a certain interval, the interval is called a shatter gap.

SHATTER VELOCITY. As a velocity is increased above this critical value, there is a sudden change in character of hole made in plate and usually an abrupt increase in the energy required for perforation.

SHOCK. A pressure discontinuity in a compressible fluid. A shock always advances into the low-pressure medium.

SHOCK WAVE. A region of compression, propagated through the medium (gas, liquid, or solid) in the front of which the pressure rise is almost infinitely steep.

SHOCK WAVE. In gas, a wave of increasing pressure characterized by its very abrupt rise. Normally of finite intensity (not infinitesimal).

SHIELDING PLATE. A thin plate spaced a considerable distance in front of the main protective armor.

SMOKE RING. A vortex, usually turbulent, which is produced ahead of an orifice through which a jet suddenly emerges. A turbulent smoke ring is always associated with the firing of a gun.

SOC. Stanolind Oil and Gas Company, Tulsa, Oklahoma.

SPECIFIC LIMIT ENERGY. WV_l^2/d^3, where W is projectile weight, V_l limit velocity and d projectile diameter.

SPHERICAL WAVE. A wave originating from a point source or spherically shaped source whose front, as it propagates through the medium, is the surface of a sphere.

SPRAY DOME. The cone-shaped spray of water appearing at the surface immediately after a shallow underwater explosion.

SS. Scientific Section, Mine Design Department of Admiralty.

STABILITY. In projectiles, relative freedom from a tendency to tumble or waver in flight.

STAND OFF. The distance separating target and shaped charge at the instant of detonation.

STATIONARY SHOCK. A shock that does not move with respect to the observer. The low-pressure medium flows into the shock.

STRAIN, ENGINEERING. In the tensile or compressive test this is equal to the change of length of a short element divided by the *original* length of that element. *See* Strain, Natural.

STRAIN-HARDENING. A property of certain materials, especially metals, by which any deformation results in increased resistance to further deformation.

STRAIN, NATURAL. This is defined by the statement that an increment of natural strain equals the corresponding increment of change of length of a short element divided by the actual length of that element (not its original length). For small strains, natural strain and engineering strain (*q.v.*) are equal, but not for large strains. Thus

$$d\epsilon_n = \frac{de_n}{1 + e_n} \quad \text{and} \quad \epsilon_n = \log_e (1 + e_n),$$

where ϵ = natural strain and e = engineering strain. In simple tension or compression

$$\epsilon_n = \log_e \frac{A_0}{A},$$

where A_0 is the initial sectional area of the specimen and A is the area at the instant under consideration.

STRESS, ENGINEERING. Also called nominal or apparent stress. In a tensile or compressive test this is the force at any instant divided by the original sectional area of the specimen. *See* Stress, True.

STRESS, TRUE. In the tensile or compressive test this is the force at any instant divided by the sectional area of the specimen at that instant. After necking in the tensile test, the neck area is used. *See* Stress, Engineering.

SUBCALIBER PROJECTILE. A projectile having a diameter smaller than that of the gun.

SUPERSONIC VELOCITY. The velocity, either of a gas past a fixed object, or of a body through a gas at rest, exceeding the local velocity of sound in the gas.

SW. Interdepartmental Coordinating Committee on Shock Waves, Ministry of Home Security.

SYMPATHETIC DETONATION. The detonation of an explosive by the impact of a nearby explosion.

TAIL (of an underwater shock wave). The later low-pressure, slowly decaying portion of an underwater shock wave.

TANGENT OGIVE. A term describing a particular type of nose shape. The contour of the nose is the arc of a circle which is tangent to the body at the point of juncture.

TENSILE STRENGTH (psi). In the standard tensile test of a material, this is the maximum load during the entire test divided by the cross-sectional area of the specimen. If the original cross-sectional area is used, the strength obtained is that normally specified in engineering design and is called engineering or *apparent strength*. If the actual cross-sectional area (reduced from the original by extension) is used, the value obtained is called the *true strength*.

TERMINAL RAREFACTION. The rarefaction that follows the gun blast caused by the over-emptying of the gun.

THERMOSETTING. Having the property of acquiring strength when heated, usually under high pressure.

TIME CONSTANT (of an underwater shock wave). The time required for the pressure in an underwater shock wave to fall to 1/2.718 of its peak value.

TM. Technical memorandum.

TNT. Trinitrotoluene.

TRACKING RATE RATIO. The ratio, at the same sight point, relative to the bomber, of the angular rate of tracking of a fighter by a bomber gunner in training to the angular rate of tracking necessary in combat.

TRANSIENT JET. A jet in which the flow is variable in time but not periodic, such as the jet from the muzzle of a gun.

TRAVELING SHOCK. A shock that moves with respect to the observer, such as a shock advancing into still air.

TRIPLE POINT. The junction of three shock waves: incident, reflected, and Mach.

TUNGSTEN CARBIDE. Abbreviation for cemented or sintered tungsten carbide. A product of powder metallurgy which is composed of extremely small tungsten carbide particles held together by a binder such as cobalt, iron, or nickel. It is characterized by high density, high hardness, and low transverse rupture strength.

TURBULENCE. The flow of a viscous fluid characterized by the existence of small eddies, usually with strengths and directions distributed at random.

UE. Underwater Explosions: Series of Interim Reports issued by the Underwater Explosives Research Laboratory at Woods Hole.

UERL. Underwater Explosives Research Laboratory, Woods Hole Oceanographic Institution, Woods Hole, Massachusetts (Division 2, NDRC).

UNDEX. Under series of reports issued by the Admiralty Underwater Weapons Establishment, Rosyth.

VT. Variable time.

WA. Weight in air.

WHOI. Woods Hole Oceanographic Institution, Woods Hole, Massachusetts.

WORKING SECTION (of wind tunnel). The test section in which the model is held.

SYMBOLS.

Chapter 1

A	Area of piston of ball crusher gauge.
a_0	Initial radius of a spherical charge.
C	Proportionality constant (see Section 1.2.3).
c	Velocity of sound in sea water.
D	Depth of charge.
d_0	Diameter of surface spray dome base.
E	Energy flux corresponding to the integral $1/\rho c\int P^2 dt$.
e	Base of natural logarithm, or 2.718.
f_1, f_2, f_3, f_4	Unspecified functions of the variable $W^{\frac{1}{3}}/R$.
g	Depth of gauge below the surface.
h_0	Height of the spray dome above the surface.
I	Shock wave impulse (or momentum) per unit area.
K	Proportionality constant (see Section 1.2.6).
k	Scaling factor.
M	Mass.
P, P_m	Peak pressure in the shock wave.
P_0	Pressure in undisturbed medium ahead of the shock wave.
P_t	Pressure at a time t behind the shock front.
R	Distance from charge.
S	Central identification of circular steel diaphragm.
T	Period of the gas bubble oscillation.
t	Time.
U	Propagation velocity of the shock wave.
u	Particle velocity of the water.
V	Velocity of rise of the surface spray dome.
v	Velocity of a target plate under explosive loading.
W	Charge weight.
x	Displacement of piston of ball crusher gauge.
Z	Depth of charge, $D + 33$ ft.
λ	Force constant.
ρ	Density of sea water.
θ	Shock-wave pressure decay constant, or time constant.

Chapter 2

C	Charge.
C'	Image charge.
c_0, c, c'	Velocity of sound in front of incident shock, behind incident shock, and behind reflected shock respectively.
d	Gauge-to-charge distance measured horizontally.
d_0	Distance on ground corresponding to r_{max}.
E	Change in energy content of the gas as it crosses the shock front.
f, F, ϕ	Unspecified function of the variable $r/W^{\frac{1}{3}}$ corresponding to P, I, etc., respectively.
h_c	Height of charge.
h_g	Height of gauge.
H	Total energy liberated by an explosive.
I	Incident wave I_1, I_2 $\cdots$ I_n in successive stages.
I, I_1, I_2	Positive impulse, pressure.
k	Scaling factor.
$I-I$	Path of triple point in Mach reflection.
M	Mach shock.
M	Weight of case.
P, P_1, P_2	Peak pressure (gauge).
P_0	Atmospheric pressure (=0) (gauge)
p_0, p, p'	Pressures (absolute) in undisturbed medium, in incident wave, and in reflected wave, respectively.
ΔP	Increase in pressure in enclosed rooms.
P_I	Incident peak pressure (gauge).
P_R	Reflected peak pressure (gauge).
P_M	Mach peak pressure (gauge).
R	Charge/weight ratio (C/W, W/W_c, or $W/(M+W)$.
R	Reflected wave R_1, R_2 $\cdots$ R_n, successive stages.
r	Radial distance, gauge to charge, if their heights are different.
S	Plane-reflecting surface.
S	Suction phase or negative phase.
S	Slipstream.
T	Triple point.
t	Time.
t_d	Crossing time or positive duration.
t_R	Reflection time.
U, U'	Velocity of shock front propagation of incident and reflected shocks, respectively.
u_0, u, u'	Particle velocities in undisturbed medium, in incident shock, and behind reflected shock, respectively.
V	Volume of enclosed room.
W	Wall.
W, W_1, W_2	Weights of charge (lb) for point charges; weights of charge per foot (lb/ft) for line charges.
W'	Bare charge weight equivalent to cased charge.
W_c	Total weight of charge and its case.
y	Height of Mach stem.
x, z	Directions of air flow in reflection systems.
α	Angle at which incident shock wave meets wall, or angle between tangent to shock and line parallel to wall.
α'	Angle at which reflected shock meets wall.
$\alpha_{extreme}$	Limiting angle of regular reflection.
α_1	Angle of incidence for which δ' has the value for head-on reflection.
α_{min}	Angle of incidence for which δ' is a minimum.
γ	Ratio of specific heats at constant pressure and volume ($\gamma = 1.40$ for air at moderate temperatures).
δ'	p'/p, compression ratio in reflected shock.
δ	p_0/p, inverse of compression ratio in incident shock.
ρ_0, ρ, ρ'	Densities in front of incident shock, behind incident shock, and behind reflected shock, respectively.
ϕ	Angle determined by the triple point T, the point on the wall at which the triple point leaves the wall d_0, and the wall W. The half-angle of the Mach V.

Chapter 3

A	Scale factor (general).
a	Acceleration; also thickness of front wall of underground structure (in.).
a_g	Acceleration in units of g (gravity) [equation (15)].
B	Numerical constant associated with particle velocity and of order 0.7 [equation (10)].
C	Depth factor for cratering.
c	Total crack width in front face of target (in.) [equations (25) and (28)].
D	Displacement (ft) [equations (17), (18), (19), (20), (21)].
d	Depth of charge in earth (ft); also, diameter of reinforcing bars in structure (in).
E	Energy; also, explosive factor for peak pressure (Tables 4, 9, and 10).
E'	Explosive factor for impulse (Tables 6, 8, and 10).
E''	Explosive factor for cratering (Tables 8, 9, and 10).
F	Force; also, coupling factor for peak pressure and impulse [equations (2) and (6)].

g The acceleration of gravity, 384 in./sec^2.
H Vertical dimension of target wall (in.).
h (subscript) Horizontal.
I Impulse per unit area, usually in free earth (psi-sec) [equations (6), (7), (6'), (7')].
I' Total impulse on target wall.
k Soil constant for pressure and for seismic waves, related to k' and k'' (psi) (Table 5).
k' Soil constant for impulse $= 5.5\sqrt{\rho k}$ (Table 7).
k'' Soil constant for cratering $= 1.3k^{\frac{1}{3.4}}$.
L Length; also, horizontal dimension of target wall (in.).
M Mass.
N Number of reinforcing bars that are stretched by bending of target wall.
n An exponent.
P Pressure; in particular, peak pressure (psi) [equations (2) and (3)].
p Pressure; usually less than peak pressure (psi).
Q Participation factor for damage to target wall [equation (28)].
R Crater radius in earth (ft) [equation (22)].
r Distance from charge (ft), see λ; (subscript) reflected.
S Length scale factor; also, strength factor of target [equation (25)].
t Time; scabbing limit thickness of target wall for earth-backed contact explosion [equation (27)].
u Maximum particle velocity (in./sec) [equation (10)].
v Seismic velocity (fps); velocity of any part of pressure wave; (subscript) vertical.
W Weight of explosive charge (lb).
x_0 Maximum center deflection of wall of structure (in.).
δ Strain in a medium.
λ Dimensionless unit of distance from charge $= r/W^{\frac{1}{3}}$.
ρ Density of earth, or weight per cubic inch divided by g in inches per second, approximately 0.00015.
ρ_c Density of concrete, in same units as ρ, approximately 0.00022.
σ Average yielding strength of reinforcing steel in structure (numerically between ordinary yield strength and ultimate strength), (psi), normally of the order 60,000.

Chapter 6

C Ballistic coefficient for determination of velocity losses in flight.
C de Marre terminal ballistic coefficient employed by British Ordnance Department.
e Energy of projectile.
e_F Energy of full-caliber projectile.
e_S Energy of subcaliber projectile.
d Projectile diameter (ft.)
$E(x)$ Ratio of striking energies of two projectiles at range x.
F Thompson terminal ballistic coefficient employed by U. S. Navy.
$F(x)$ Fractional energy retained at range x.
k de Marre terminal ballistic coefficient employed by U. S. Army.
K Drag coefficient.
M Total mass of projectile.
M_s Mass of subprojectile.
M_C Mass of carrier.
M_F Mass of full-caliber projectile.
R Ratio of diameter of subprojectile to that of gun.
t Plate thickness (ft).
V_l Limit velocity (fps).
V_0 Muzzle velocity.
W Projectile weight (lb).
θ Angle of incidence, i.e., angle between trajectory and normal to face of plate.

BIBLIOGRAPHY

Numbers such as Div. 8-100-M1 indicate that the document listed has been microfilmed and that its title appears in the microfilm index printed in a separate volume. For access to the index volume and to the microfilm, consult the Army or Navy agency listed on the reverse of the half-title page.

Chapter 1

1. *List of Titles of Undex Papers 1 to 118, with New Security Classifications*, Admiralty Undex Panel and Subpanel, December 1944.
2. *Introduction to Explosives*, George B. Kistiakowsky, OSRD 5401, OEMsr-202, Service Projects OD-01, OD-04, and NO-290, Carnegie Institute of Technology. Aug. 2, 1945. Div. 8-100-M1
3. *Calculation of Detonation Pressures of Several Explosives*, Stuart R. Brinkley, Jr. and E. Bright Wilson, Jr., OSRD 1231, NDCrc-168, Service Projects OD-02 and NO-144, HU, Mar. 1, 1943. Div. 8-500-M1
4. *Calculation of the Detonation Properties of Some Service Explosives*, Stuart R. Brinkley, Jr., and E. Bright Wilson, Jr., OSRD 1510, NDCrc 168, Service Projects OD-02 and NO-144, HU, June 14, 1943. Div. 8-502-M2
5. *Underwater Explosives and Explosions*, Interim Report, UE-4, NDRC Division 8, UERL, Nov. 15-Dec. 15, 1942, pp. 1-2. Div. 2-130-M1
6. *Underwater Explosives and Explosions*, OSRD 4874, Interim Report UE-32, NDRC Division 2, UERL, Mar. 15-Apr. 15, 1945, pp. 16-36. Div. 2-130-M1
7. *Underwater Explosives and Explosions*, Interim Report UE-19, NDRC Division 8, UERL, Feb. 15-Mar. 15, 1944, pp. 9-19. Div. 2-130-M1
8. *Oblique Reflection of Shocks*, John von Neumann, Explosive Research Report 12, NAVORD, October 1943.
9. *Interaction of Shock and Rarefaction Waves in One-Dimensional Motion*. Richard Courant and Kurt O. Friedrichs, OSRD 1567, OEMsr-944, Service Projects OD-03 and NO-144, AMG-NYU, 38.1, NDRC Division 3, AMP, July 5, 1943. AMP-101.1-M4
10. *The Interaction of Shock Waves*, R. W. Wood, OSRD 1906, OEMsr-773, Service Projects AN-1 and OD-30, Johns Hopkins University, Nov. 4, 1943. Div. 2-120-M4
11. *Regular Reflection of Shocks in Ideal Gases*, H. Polachek and R. J. Seeger, Explosives Research Report 13, NAVORD, February 1944.
12. *Interaction of Shock Waves in Water-Like Substances*, H. Polachek and R. J. Seeger, Explosives Research Report 14, NAVORD, August 1944.
13. *Pinlography of Underwater Explosions*, Paul M. Fye, Ralph W. Spitzer, and John E. Eldridge, OSRD 6246, NDRC A-368.
14. *Underwater Explosives and Explosions*, Interim Report UE-21, NDRC Division 8, UERL, Apr. 15-May 15, 1944, pp. 52-68. Div. 2-130-M1
15. *Diaphragm Gauge Studies of Underwater Explosions*, John E. Eldridge, OSRD 6248, NDRC A-370.
16a. *Underwater Explosives and Explosions*, OSRD 4810, Interim Report UE-30, NDRC Division 2, UERL, Jan. 15-Feb. 15, 1945, pp. 20-31. Div. 2-130-M1
b. *Ibid.*, pp. 32-37.
17. *Theory of the Pulsations of the Gas Bubble Produced by an Underwater Explosion*, Conyers Herring, OSRD 236, NDRC C4-sr20-010, Columbia University Division of War Research, October 1941. Div. 6-510.12-M1
18. *Vertical Motion of a Spherical Bubble and the Pressure Surrounding It*, G. I. Taylor, OSRD Liaison Office H 3-2762, Report SW.12, Aug. 4, 1942. Div. 6-510.2-M2
19. *Radial Motion of Water Surrounding a Sphere of Gas in Relation to Pressure Waves*, E. H. Kennard, Report 577, DTMB, September 1943. Div. 6-510.23-M9
20. *Critical Survey of Bubble Phenomena Based on Information Available up to August 1943*, H. N. V. Temperley, Undex 64, AUE/TRI. 15/RP. 3, Admiralty Undex Works, Rosyth, November 1943.
21. *On the Best Location of a Mine Near the Sea Bed*, Max Shiffman and Bernard Friedman, [OEMsr-945,] Report 37.1R, AMG-NYU 49, AMP, May 1944. AMP-407-M1
22. *Migration of Underwater Gas Globes Due to Gravity and Neighboring Surfaces*, E. H. Kennard, Report R-182, DTMB, December 1943. Div. 6-510.23-M10
23. *Motions of a Pulsating Gas Globe Under Water; Photographic Study*, D. C. Campbell and C. W. Wyckoff, Report 512, DTMB, May 1943.
24. *Small Scale Underwater Explosions Under Reduced Atmospheric Pressure*, D. C. Campbell and C. W. Wyckoff, Report 520, DTMB, November 1943.
25. *The Oscillation of the Gas Bubbles Formed by a Detonator Exploding Under Water: Detailed Comparison of Theory with Experiment*, H. N. V. Temperley, Undex 83, AUW/TRI.73/RP.13, Admiralty Undex Works, Rosyth, March 1944.
26. *Note on the "Second Pulse" Effect for Large Charges*, OSRD Liaison Office WA-556-33, SS Report 1179, Mine Design Department, Great Britain, Feb. 17, 1943. Div. 6-510.23-M15
27. *The Experimental Evidence on the Behavior of the Gas Bubble Due to the Explosion of a Mk VII Depth Charge*, SS Informal Report 1944, Undex 73, Mine Design Department, Great Britain, September 1943.
28. *Measurement of Bubble Pulse Phenomena. I Mark 6 Depth Charges TNT Loaded*, C. P. Slichter, W. G. Schneider, and R. H. Cole, OSRD 6242, NDRC A-364.
29. *Measurement of Bubble Pulse Phenomena. II Small Charges*, A. B. Arons, A. Bordeu, and B. Stiller, OSRD 6578, NDRC A-470.
30. *Underwater Explosions Near the Sea Bed*, H. F. Willis and M. I. Willis, Internal Report 142, Undex 52, H.M.A./S.E.E., Sept. 9, 1943.
31. *The Movement of the Explosion Bubble Produced by 1-Oz. Charge of Polar Ammon Gelignite Detonated Underwater in the Road Research Laboratory Tank*, Undex 78, ADM-162, RRL, February 1944.
32. *Vertical Displacement of the Gas Bubble Formed by an Underwater Explosion*, H. F. Willis and P. T. Ackroyd, Internal Report 123, Undex 36, H.M.A./S.E.E., Fairlie, May 8, 1943.
33. *Damage to Thin Steel Cylindrical Shells by Underwater Explosions*, J. C. Decius and Paul M. Fye, OSRD 6247, NDRC A-369.
34. *Underwater Explosives and Explosions*, Interim Report UE-16, NDRC Division 8, UERL, Nov. 15-Dec. 15, 1943, pp. 34-39. Div. 2-130-M1
35. *Underwater Explosives and Explosions*, OSRD 4671, Interim Report UE-29, NDRC Division 2, UERL, Dec. 15, 1944-Jan. 15, 1945. Div. 2-130-M1
36. *Underwater Craters Formed by Explosions on the Sea*

Floor, John E. Eldridge, Paul M. Fye and others, OSRD 6244, NDRC A-366, OEMsr-569, Service Project NO-203, WHOI, January 1946. Div. 2-132-M3

37. *Measurement of Pressure on the Sea Bed Resulting from Surface Waves Created by Underwater Explosions*, Ralph W. Spitser, OSRD 6245, NDRC A-367, OEMsr-569 and NOrd-9500, Service Project NO-262, WHOI, March 1946. Div. 2-131-M6
38. *Surface Waves Produced by Firing Underwater 32-lb. Charges of Polar Ammon Gelignite at Various Depths*, Undex 122, ADM 223, RRL, February 1945.
39. *Memorandum on the Generation of Surface Waves by an Underwater Explosion*, John G. Kirkwood, Undex 94, August 1944.
40. *Surface Waves from an Underwater Explosion*, G. Hartman, John G. Kirkwood, and R. J. Seeger, report to be published by NAVORD.
41. *Surface Waves in Water of Variable Depths*, AMG-NYU 243, AMP.
42. *Production of Surface Waves by Underwater Explosions*, Ralph W. Spitser and Abraham M. Shanes, OSRD 4259-A, Interim Report Secret Supplement UE-26 SS, NDRC Division 2, UERL, Sept. 15-Oct. 16, 1944. Div. 2-130-M1
43. *Production of Surface Waves by Underwater Explosions. II. Comparison of Distributed and Lumped 1,900-Lb. Charges*, Ralph W. Spitser, OSRD 4259-A, Interim Report Secret Supplement, UE-27 SS, NDRC Division 2, UERL, Nov. 15, 1944. Div. 2-130-M1
44. *The Measurement of Underwater Explosions for Service Weapons at UERL*, J. S. Cole, OSRD 6240, NDRC A-362.
45. *Summary of Underwater Explosive Measurements*, J. S. Cole, OSRD 6241, NDRC A-363.
46. *Measurement of Underwater Explosion Pressures (to Apr. 1, 1942) Part I*, E. Bright Wilson, Jr. and R. H. Cole, OSRD 523, OEMsr-202, Service Project OD-03, Report 223, Carnegie Institute of Technology, Apr. 24, 1942. Div. 2-131-M2
47. *Measurement of Underwater Explosion Pressures (to July 1, 1942) Part II*, E. Bright Wilson, Jr., OSRD 753, OEMsr-202, Service Project OD-03, Report 301, Carnegie Institute of Technology, July 21, 1942. Div. 2-131-M3
48. *Trials of Mark VI and Mark IX Depth Charges Loaded with TNT and with Baronal*, OSRD 1220, OEMsr-569, Service Projects OD-04 and NO-138, NDRC Division 8, UERL, WHOI, Feb. 22, 1943. Div. 2-133-M1
49. *Underwater Explosives and Explosions*, Section B-1, Interim Report UE-1, Division 8, UERL, Aug. 15-Sept. 15, 1943. pp. 1a-3. Div. 2-130-M1
50. *Underwater Explosives and Explosions*, Interim Report UE-9, NDRC Division 8, UERL, Apr. 15-May 15, 1943, pp. 18-23. Div. 2-130-M1
51. *Underwater Explosives and Explosions*, OSRD 5161, Interim Report UE-34, NDRC Division 2, UERL, May 15-June 15, 1945, pp. 2-24. Div. 2-130-M1
52. *Underwater Efficiency of Aluminized Explosives*, Summary M. S. 940/42, AC 3338, WA, Phys./Ex. 372, Mine Design Department, Great Britain. Oct. 22, 1942.
53. *Design of Experiments*, R. A. Fisher, Oliver, and Boyd, Edinburgh, Scotland, 1935.
54. *The Planning of Experiments Requiring Statistical Interpretation*, E. Bright Wilson, Jr., Technical Memorandum 8, UERL, Oct. 2, 1944.
55. *Underwater Explosives and Explosions*, Interim Report UE-22, NDRC Division 2, UERL, May 15-June 15, 1944, pp. 30-32. Div. 2-130-M1
56. *Hugoniot Calculation for Sea Water at the Shock Front*, A. B. Arons, and R. R. Halverson, OSRD 0577, NDRC A-469, OEMsr-569 and NOrd-9500, Service Project NO-223, WHOI, March 1946. Div. 2-131-M7
57. *Depth of Explosion of Aerial Depth Bombs with Some Data on Bomb Trajectories*, R. R. Halverson and W. G. Schneider, OSRD 6268, NDRC A-380.
58. *Determination of Depth of Explosion of Statically-Fired Depth Bombs from Photographs of the Dome Spray*, Chalm L. Pekaris, NDRC Section 6.1, June 1944.
59. *Splashes from Underwater Explosions: Part I. Shallow Charges*, H. Kolsky, M. T. Sampson, Chester I. Snow, and A. C. Shearman, Undex 118, December 1944.
60. *Underwater Explosives and Explosions*, OSRD 4406, Interim Report UE-27, Division 2, UERL, Oct. 15-Nov. 15, 1944, pp. 19-21. Div. 2-130-M1
61. *Design and Use of Tourmaline Gauges for Piezoelectric Measurement of Underwater Explosion Pressures*, A. B. Arons and R. H. Cole, OSRD 6239, NDRC A-361.
62. *The Pressure Wave Produced by an Underwater Explosion, III (to August 15, 1942)*, John G. Kirkwood and John M. Richardson, OSRD 813, OEMsr-121, Service Project OD-03, Report 324, Cornell University, Aug. 24, 1942. Div. 2-131-M4
63. *Calibration of Standard Oil and Gas Company Tourmaline Gauges*, Eginhard Dietze, OSRD 6.1-sr1130-1971, NS-139, Underwater Sound Reference Laboratories, Oct. 31, 1944. Div. 6-554.3-M44

64a. *Journal de l'Ecole Polytechnique*, Hugoniot, Paris, Vol. 57, 1887, p. 3.

b. *Ibid.*, Vol. 58, 1888, p. 1.

65. *Theory of Shock Waves (to August 31, 1943)*, John von Neumann, OSRD 1140, OEMsr-218, Service Projects OD-02 and OD-03, Institute for Advanced Study, January 1943. Div. 2-120-M2
66. *Plane Shock Waves*, George B. Kistiakowsky and E. Bright Wilson, Jr., OSRD 70, NDCrc-35, Service Projects OD-02 and OD-03, Progress Report 7, NDRC Division 8, HU, Jan. 17, 1941. Div. 2-120-M1
67. *The Hydrodynamic Theory of Detonation and Shock Waves (to June 30, 1941)*, George B. Kistiakowsky and E. Bright Wilson, Jr., OSRD 114, NDCrc-30, Service Projects OD-02 and OD-03, Final Report 52, NDRC Division 8, HU, Aug. 15, 1941. Div. 2-131-M1
68. *Pressure-Time Curves for Submarine Explosions, Paper II*, W. G. Penney and H. K. Dasgupta, OSRD Liaison Office II-5-2143, SW 20, RC 333, July 23, 1942.
69. *Comments on the Current Theories of the Pressure Pulse of Submarine Explosions*, W. G. Penney. Undex 72, December 1943.
70. *The Spherical Detonation Wave in TNT and TNT/RDX Mixtures*, H. K. Dasgupta and W. G. Penney, AC-3733, November 1944.
71. *The Theory of Shock Waves for an Arbitrary Equation of State*, H. A. Bethe, OSRD 545, May 1942.
72. *The Pressure Wave Produced by an Underwater Explosion (to May 15, 1944)*, John G. Kirkwood and H. A. Bethe, OSRD 588, May 1942.
73. *The Pressure Wave Produced by an Underwater Explosion*, John G. Kirkwood and E. W. Montroll, OSRD 670, Serial No. 281, Division B, to July 1, 1942.
74. *The Pressure Wave Produced by an Underwater Explosion, II*, John G. Kirkwood and E. W. Montroll, OSRD 676, July 1942.
75. *The Pressure Wave Produced by an Underwater Explosion, IV*, John G. Kirkwood, E. W. Montroll, and John M. Richardson, OSRD 1030, November 1942.
76. *The Pressure Wave Produced by an Underwater Explosion, V*, John G. Kirkwood, Stuart R. Brinkley, Jr., and John M. Richardson, OSRD 2022, November 1943.

77. *The Pressure Wave Produced by an Underwater Explosion, VI, The Cases of Cylindrical Symmetry*, Oscar K. Rice and R. Grinell, OSRD 2023, November 1943.
78. *The Pressure Wave Produced by an Underwater Explosion, VII*, John G. Kirkwood, OSRD 3949, July 1944.
79. *The Pressure Wave Produced by an Underwater Explosion, VIII, The Case of Cylindrical Symmetry, II*, Oscar K. Rice and R. Grinell, OSRD 3950, July 1944.
80. *Underwater Explosives and Explosions*, Interim Report UE-8, NDRC Division 8, UERL, Mar. 15-Apr. 15, 1943, pp. 8-10.
81. *Underwater Explosives and Explosions*, Interim Report UE-24, NDRC Division 2, UERL, July 15-Aug. 15, 1944, pp. 2-6.
82. *Theory of the Propagation of Shock Waves from Explosive Sources in Air and Water*, John G. Kirkwood and Stuart R. Brinkley, Jr., OSRD 4814, NDRC A-318, OEMsr-121, Service Projects OD-03 and NO-224, Cornell University, March 1945. Div. 2-120-M6
83. *Tables and Graphs of the Theoretical Peak Pressures, Energies, and Impulses of Shock Waves from Explosive Sources in Sea Water*, Stuart R. Brinkley, Jr. and John G. Kirkwood, OSRD 5649, NDRC A-342, OEMsr-121, Service Projects OD-03 and NO-224, Cornell University, October 1945. Div. 2-131-M5
84. *The Plastic Deformation of Circular Diaphragms under Dynamic Loading by an Underwater Explosion Wave*. John G. Kirkwood and John M. Richardson, OSRD 4200, OEMsr-121, Service Projects OD-03 and NO-224, NDRC Division 8, Cornell University, Sept. 30, 1944. Div. 2-431.22-M6
85. *Underwater Explosives and Explosions*, Interim Report UE-18, NDRC Division 8, UERL, Jan. 15-Feb. 15, 1944, pp. 10-14. Div. 2-130-M1
86. *Effectiveness of Near Miss Bombs against Warships*, E. Bright Wilson, Jr., Report TM-1, NDRC Division 2, UERL, June 23, 1944.
87. *Underwater Explosives and Explosions*, Section B-1, Interim Report UE-2, NDRC Division 8, UERL, Sept. 15-Oct. 15, 1942, pp. 1-7. Div. 2-130-M1
88. *Underwater Explosives and Explosions*, Section B-1, Interim Report UE-3, NDRC Division 8, UERL, Oct. 15-Nov. 15, 1942, pp. 2-3. Div. 2-130-M1
89. *Underwater Explosives and Explosions*, Interim Report UE-6, NDRC Division 8, UERL, Jan. 15-Feb. 15, 1943, pp. 4-8. Div. 2-130-M1
90. *Underwater Explosives and Explosions*, Interim Report UE-7, NDRC Division 8, UERL, Feb. 15-Mar. 15, 1943, pp. 19-20. Div. 2-130-M1
91a. *Underwater Explosives and Explosions*, Interim Report UE-15, NDRC Division 8, UERL, Oct. 15-Nov. 15, 1943, p. 13. Div. 2-130-M1
b. *Ibid.*, p. 14.
92. *The Plastic Deformation of Marine Structures by an Underwater Explosion*, John G. Kirkwood, OSRD 788, OEMsr-121, Service Project OD-03, Report 303, NDRC Division 8, Cornell University, Aug. 11, 1942. Div. 2-132-M1
93. *The Plastic Deformation of Marine Structures by an Underwater Explosion Wave, II*, John G. Kirkwood, OSRD 1115, OEMsr-121, Service Projects OD-02 and OD-03, Report 450, NDRC Division 8, Cornell University, Dec. 9, 1942. Div. 2-132-M2
94. *Theory of the Plastic Deformation of Thin Plates with Applications*, John M. Richardson, OSRD 5660, NDRC A-344, OEMsr-121, Service Projects OD-03, NO-233, and others, Cornell University, October 1945. Div. 2-431.1-M2
95. *The Distortion Under Pressure of a Diaphragm Which Is Clamped Along Its Edge and Stressed Beyond the Plastic Limit*, G. I. Taylor, OSRD Liaison Office, II-5-2799, Report SW. 24, Sept. 1, 1942.
96. *Underwater Explosives and Explosions*, Interim Report UE-5, NDRC Division 8, UERL, Dec. 15, 1942-Jan. 15, 1943, pp. 2-6. Div. 2-130-M1
97. *Underwater Explosives and Explosions*, Interim Report UE-14, NDRC Division 8, UERL, Sept. 15-Oct. 15, 1943, pp. 8-9. Div. 2-130-M1
98. *Underwater Explosives and Explosions*, Interim Report UE-12, NDRC Division 8, UERL, July 15-Aug. 15, 1943, p. 11. Div. 2-130-M1
99. *Experiments with 1/768 Scale Model of Explosions near ½ Scale Asdic Target*, G. I. Taylor and R. H. Davies, Undex 21, March 1943.
100. *The Attack by Explosive Charges of a 1/11.25 Scale Asdic Target*, Undex 30, ADM/118/ARD, May 1943.
101. *Damage to Submerged Submarines by Underwater Explosions*, A. H. A. Hogg, Undex 56, AUW/TRI.12/RF.2, Admiralty Undex Works, Rosyth, October 1943.
102. *Scale Relationships in 1/11.25-, ½-, and Full-Scale Asdic Trials*, Undex 97, ADM/191, RRL, July 1944.
103. *Dimensional Analysis*, Percey W. Bridgman, Yale University Press, 1931.
104. *The Speed Effect in Copper Crusher Cylinders and Copper Spheres*, Frederick Seitz, Jr., Andrew W. Lawson, and Park H. Miller, Jr., OSRD 619, NDRC A-63, OEMsr-132, Service Projects OD-34, CE-5, and others, University of Pennsylvania, June 1942. Div. 2-431.21-M1
105. *Underwater Explosives and Explosions*, OSRD 5417, Interim Report UE-35, NDRC Division 2, UERL, June 15-July 15, 1945, pp. 2-27. Div. 2-130-M1
106. *Buckling Instability of Thin Cylindrical Shells Under External Static Loading*, John G. Kirkwood, John M. Richardson, and Elaine M. Frankel, OSRD 3780, OEMsr-121, Service Project NO-224, NDRC Division 8, Cornell University, June 15, 1944. Div. 2-431.22-M5
107. *Buckling Instability of Cylindrical Shells under Dynamic Loading*, John G. Kirkwood and John M. Richardson, OSRD 4698, NDRC A-316, OEMsr-121, Service Projects OD-03 and NO-224, Cornell University, February 1945. Div. 2-431.22-M7
108. *Countermining of Japanese Anti-Boat Mines (JE and JG) by Underwater Explosions*, Paul M. Fye, John E. Eldridge, and others, OSRD 6243, NDRC A-365, OEMsr-569, Service Project NO-223, WHOI, November 1945. Div. 2-133-M2
109. *Underwater Explosives and Explosions*, Interim Report UE-17, NDRC Division 8, UERL, Dec. 15, 1943-Jan. 15, 1944, pp. 16-19. Div. 2-130-M1
110. *Nature of the Pressure Impulse Produced by the Detonation of Explosives under Water. An Investigation by the Piezoelectric Cathode Ray Oscillograph Method. Part A. Methods and Apparatus. Part B. Experimental Results.* British Report ARLS/S/12 C. B. 01670 (12), ARL, pp. 442-616.
111. *Construction of Tourmaline Gauges for Piezoelectric Measurement of Explosion Pressures*, Clifford Frendel, OSRD 6253, NDRC A-378, OEMsr-569, Service Projects OD-03 and NO-223, WHOI, January 1946. Div. 2-111.11-M8
112. *Design and Use of Tourmaline Gauges for Piezoelectric Measurements of Air Blast*, A. B. Arons and C. W. Tait, OSRD 6250, NDRC A-372.
113. *Instrumentation for the Measurement of Underwater Explosion Pressures*, M. A. Greenfield and M. M. Shapiro, Report 523, DTMB, September 1944.

114. *Electrical Instruments for Study of Underwater Explosions and Other Transient Phenomena*, R. H. Cole, David Stacey, and R. M. Brown, OSRD 6238, NDRC A-360, OEMsr-569, Service Projects NO-223 and OD-03, WHOI, December 1945. Div. 2-131.1-M2

115. *A Tourmaline Crystal Gauge for Underwater Explosion Pressure*, A. R. Cohen and B. Stiller, Report R-137, DTMB, December 1943.

116. *The Use of Electrical Cables with Piezoelectric Gauges*, R. H. Cole, OSRD 4561, NDRC A-306, OEMsr-569, Service Project NO-223, WHOI, January 1944. Div. 2-111.11-M4

117. *Consistency of the NOL Ball Crusher Gauge*, R. H. Brown, Explosives Report 1, NAVORD, February 1944.

118. *High Speed Compression Testing of Copper Crusher Cylinders and Spheres*, O. C. Simpson, E. L. Fireman, and James S. Kochler, OSRD 3330, NDRC A-257, OEMsr-825, Projects OD-57, NO-7, and PS-301, Carnegie Institute of Technology, March 1944. Div. 2-431.21-M2

119. *High Speed Compression Testing of Copper Crusher Cylinders and Spheres: Part II*, G. H. Winslow, and W. H. Bessey, OSRD 5030, NDRC A-324, OEMsr-825, Service Projects OD-57, NO-7, and NS-109, Carnegie Institute of Technology, April 1945. Div. 2-431.21-M3

120. *Underwater Explosives and Explosions*, Interim Report UE-13, NDRC Division 8, UERL, Aug. 15-Sept. 15, 1943, pp. 11-12. Div. 2-130-M1

121. *Theory of Crusher Gauges*, G. K. Hartman, Memorandum for File A16 (CND) (Ltr3b), NAVORD, Sept. 25, 1942.

122. *An Iterative Method for Calculating the Calibration Curve for a Crusher Gauge*, R. M. Brown, Explosives Research Memorandum 6, NAVORD, Apr. 3, 1944.

123. *Underwater Explosives and Explosions*, Interim Report UE-10, NDRC Division 8, UERL, May 15-June 15, 1943, pp. 21-22. Div. 2-130-M1

124. *Underwater Explosives and Explosions*, OSRD 6116, Interim Report UE-37, NDRC Division 2, UERL, Aug. 15-Sept. 15, 1945. Div. 2-130-M1

125. *Underwater Explosives and Explosions*, OSRD 4259, Interim Report UE-28, NDRC Division 2, UERL, Sept. 15-Oct. 15, 1944, pp. 8-10. Div. 2-130-M1

126. *Underwater Explosives and Explosions*, Interim Report UE-20, NDRC Division 8, UERL, Mar. 15-Apr. 15, 1944, pp. 45-47. Div. 2-130-M1

127. *The Modugno Gauge (Its Construction, Use, and Typical Results)*, Underwater Explosion Report 1942-3, Navy Department, Bureau of Ships, October 1942.

128. *Underwater Explosives Research*, Duncan P. MacDougall, OSRD 1035, OEMsr-202, Report 429, Service Projects OD-03 and OD-04, NDRC Division 8, Carnegie Institute of Technology, Nov. 18, 1942. Div. 2-131.1-M1

129. *Experiments on the Pressure Wave Thrown out by Submarine Explosions*, H. W. Hilliar, R. E. 142/19, December 1919.

130. *The Hilliar Gage*, G. K. Hartman, Confidential Report 531, DTMB.

131. *Underwater Explosives and Explosions*, Interim Report UE-11, NDRC Division 8, UERL, June 15-July 15, 1943, pp. 12-14. Div. 2-130-M1

132. *Underwater Explosives and Explosions*, Interim Report UE-23, NDRC Division 2, UERL, June 15-July 15, 1944, pp. 2-11. Div. 2-130-M1

133. *Underwater Explosives and Explosions*, OSRD 4873, Interim Report UE-31, NDRC Division 2, UERL, Feb. 15-Mar. 15, 1945, pp. 2-21. Div. 2-130-M1

134. *Hydrodynamics*, Horace Lamb, Cambridge University Press, 1932, Chapter IX, p. 363.

135. *Photographs of Surface Phenomena Following Explosion of Mark 54 Aircraft Depth Bombs Fired at Various Depths*, Report TM-11, NDRC Division 2, UERL, June 27, 1943.

136. *Underwater Explosives and Explosions*, OSRD 4142, Interim Report, UE-25, NDRC Division 2, UERL, Aug. 15-Sept. 15, 1944, pp. 35-40. Div. 2-130-M1

137. *Underwater Explosives and Explosions*, OSRD 4407, Interim Report UE-28, NDRC Division 2, UERL, Nov. 15-Dec. 15, 1944, pp. 2-6. Div. 2-130-M1

138. *Underwater Explosives and Explosions*, OSRD 5130, Interim Report UE-33, NDRC Division 2, UERL, Apr. 15-May 15, 1945, pp. 25-30. Div. 2-130-M2

139. *Depth of Detonation of Mark 47 Depth Bombs with Mark 234 Fuses When Dropped from About 135 Feet at Air Speeds of About 150 Knots; Summary of Results by Sound Ranging*, W. G. Schneider, Report TM-4, NDRC Division 2, UERL, August 1944.

140. *Bombing Accuracy as Determined by Overhead Photographs for Mark 47 Depth Bomb When Dropped from About 135 Feet at Air Speeds of About 150 Knots*, Paul M. Fye, Report TM-7, NDRC Division 2, UERL, October 1944.

141. *Underwater Travel-Time of Mark 47 Depth Bombs with Mark 234 Fuses When Dropped from About 135 Feet at Air Speeds of About 150 Knots*, R. R. Halverson, Report TM-3, NDRC Division 2, UERL, July 1944.

142. *Analysis of the Spray Dome*, W. G. Walker, SS Informal Report 1291, Index 102, December 1919.

143. *A Method of Determining Depth of Underwater Explosions*, R. A. Shaw, Report H/ARM/Res 1. B3884, Marine Aircraft Experimental Establishment, Helensburgh, Great Britain, 1941.

144. *A Further Investigation into Dome Analysis Method of Determining the Depth of Underwater Explosions*, R. A. Shaw, Report S. W. 23, H/ARM/Res 3., B3885, April 1942.

145. *Underwater Explosives and Explosions*, OSRD 5433, Interim Report UE-36, NDRC Division 2, UERL, July 15-Aug. 15, 1945, pp 24-28. Div. 2-130-M1

146. *Underwater Trajectory of the Spud Projectile: Part I, the Depth Sinking Time Curve*, W. G. Schneider and R. H. Cole, OSRD 6257, NDRC A-370.

147. *Preparation of Charges for the Study of Explosion Phenomena at the Underwater Explosives Research Laboratory*, Philip Newmark and Ernest L. Patterson, OSRD 6259, NDRC A-381, OEMsr-569 and NOrd-9500, WHOI, March 1946. Div. 2-133-M3

Chapter 2

1. *Air Burst for Blast Bombs*, OSRD 4943, NDRC A-321, OEMsr-260, OEMsr-539, and others, Service Projects OD-03, NO-224, and others PUS, WHOI, and others, April 1945. (A compilation of papers presented at the NDRC Division 2 symposium on air burst for blast bombs.) Div. 2-110-M5

2. *The Hydrodynamic Theory of Detonation and Shock Waves*, George B. Kistiakowsky and E. Bright Wilson, Jr., OSRD 114, Final Report 52, NDCrc-30, Service Projects OD-02 and OD-03, NDRC Division 8, HU, Aug. 15, 1941. Div. 2-131-M1

3. *Calculation of the Detonation Properties of Some Service Explosives*, Stuart R. Brinkley, Jr., and E. Bright Wilson, Jr., OSRD 1510, NDCrc-168, Service Projects OD-02 and NO-144, HU, June 14, 1943. Div. 8-502-M3

4. *The Use of the Rotating Drum Camera for the Measurement of the Velocities of Shell or Bomb Fragments*, G. H. Messerly, OSRD 3000, OEMsr-202, Service Projects NO-110, NO-167, and OD-152, ERL, April 1944. Div. 8-401-M3
5. *Fragment Velocity and Panel Penetration: A Comparison of Haleite and Ednatol with Service Filling, Part I*, R. W. Drake, OSRD 1964, OEMsr-202, Service Projects OD-152 and NO-110, ERL, Oct. 30, 1943. Div. 8-105-M2
6. *Fragment Velocity and Panel Penetration: A Comparison of Haleite and Ednatol with Service Filling, Part II*, R. W. Drake, OSRD 1965, OEMsr-202, Service Projects OD-152 and NO-110, ERL, Oct. 30, 1943. Div. 8-405-M3
7. *Fragment Velocity and Panel Penetration: A Comparison of Haleite and Ednatol with Service Filling, Part III*, R. W. Drake, OSRD-2071, OEMsr-202, Service Projects OD-152 and NO-110, ERL, Nov. 29, 1943. Div. 8-405-M4
8. *Fragment Velocity and Panel Penetration: A Comparison of Haleite and Ednatol with Service Filling, Part IV*, R. W. Drake, OSRD 3022, OEMsr-202, Service Projects OD-152 and NO-110, ERL, Dec. 18, 1943. Div. 8-405-M5
9. *Fragment Velocity and Panel Penetration: A Comparison of Haleite and Ednatol with Service Filling, Part V and Part VI*, R. W. Drake, OSRD 3079, OEMsr-202, Service Projects OD-152 and NO-110, ERL, Jan. 3, 1944. Div. 8-405-M6
10. *Detonation, Fragmentation, and Air Blast*, Interim Reports DFA-1 to 11, DF-12 to 20, Service Projects OD-02, OD-03, and others, NDRC Division 8, August 1943-August 1945. Div. 8-500-M2
11. *Theory of Shock Waves*, John von Neumann, OSRD 1140, OEMsr-218, Service Projects OD-02 and OD-03, NDRC Division 8, Institution for Advanced Study, Jan. 29, 1943. Div. 2-120-M2
12. *A Modification of the Impulse Criterion for Blast Damage*, D. C. Christopherson, R. C. 349, A. C. 2790, S. D. 139, December 1942.
13. *The Design and Use of Tourmaline Gauges for Piezoelectric Measurement of Air Blast*, A. B. Arons and C. W. Tait, OSRD 6250, NDRC A-372.
14. *Development of Explosion Pressure Gauges and Recording Equipment*, OSRD 1739, OEMsr-596, Service Projects OD-03 and NO-144, NDRC Division 8, SOG, Aug. 24, 1943. Div. 2-111.11-M3
15. *Development of Blast Pressure Gauges and Recording Equipment*, Daniel Silverman and H. M. Lang, OSRD 4619, NDRC A-313, OEMsr-596, Service Project OD-03, SOG, January 1945. Div. 2-111.11-M6
16. *Development of Blast Pressure Gauges and Recording Equipment, Part II*, H. M. Lang and Daniel Silverman, OSRD 6317, NDRC A-352, OEMsr-595, Service Projects OD-02, NO-233, and others, SOG, November 1945. Div. 2-111.11-M7
17. *Construction of Tourmaline Gauges for Piezoelectric Measurement of Explosion Pressures*, Clifford Frondel, OSRD 6250, NDRC A-378, OEMsr-569, Service Projects OD-03 and NO-223, WHOI, January 1946. Div. 2-111.11-M8
18. *Characteristics of Air-Blast Gauges: Response as a Function of Pressure Level*, A. B. Arons, C. W. Tait, G. K. Fraenkel, and K. M. Doane, OSRD 4975a, AES-8a, March 1945. Div. 2-100-M1
19. *Characteristics of Air-Blast Gauges, II: Response as a Function of Pressure Level*, C. W. Tait and W. D. Kennedy, OSRD 6271c, AES-11c, June 1945. Div. 2-100-M1
20. *Shock Tube, Piezoelectric Gauges and Recording Apparatus*, J. C. Fletcher, W. T. Read, R. G. Stoner, and D. K. Walnar, OSRD 6321, NDRC A-356, OEMsr-260, Service Projects OD-03 and NO-283, PUS, February 1946. Div. 2-111.11-M10
21. *The Measurement of Transient Stress, Displacement and Pressure*, Curtis W. Lampson, OSRD 756, NDRC A-73, OEMsr-260, Service Projects CE-5, NO-11, and others, PUS, August 1942. Div. 2-111.12-M1
22. *Blast Performances of H. E. Bombs and Charges. Methods Used in the ARD for Recording Blast Characteristics in Air Using Quartz Piezoelectric Gauges*, Explosives Report 48/44, ARD, April 1944.
23. *The Measurement of Blast Pressures in Aberdeen Tests*, Curtis W. Lampson, OSRD 1465, NDRC A-186, OEMsr-260, Service Projects OD-79, NO-11, and others, PUS, June 1943. Div. 2-111-M2
24. *Cable Compensation for Piezoelectric Gages*, Curtis W. Lampson, OSRD 1179, NDRC A-63M, OEMsr-260, Service Projects CE-3, NO-11, and others, PUS, January 1943. Div. 2-111.11-M2
25. *The Use of Electrical Cables with Piezoelectric Gauges*, R. H. Cole, OSRD 4561, NDRC A-303, OEMsr-569, Service Project NO-223, WHOI, January 1944. Div. 2-111.11-M4
26. *Apparatus for the Measurement of Air-Blast Pressures by Means of Piezoelectric Gauges*, G. K. Fraenkel, OSRD 6251, NDRC A-373.
27. *Mobile Oscillograph Laboratory*, Curtis W. Lampson and Walker Bleakney, OSRD 4570, NDRC A-307, OEMsr-575, Service Project OD-70, PUS, January 1945. Div. 2-111.12-M3
28. *A Method of Low-Frequency Compensation of Amplifiers to Reproduce Transients of Long Duration*, Curtis W. Lampson, OSRD 3293, NDRC A-255, OEMsr-260, Service Projects CE-5, NO-12, and others, PUS, March 1944. Div. 2-111.12-M2
29. *Portable Oscillographic Equipment for the Measurement of Blast Pressures*, Curtis W. Lampson, OSRD 5144, AES-10a, May 1945. Div. 2-100-M1
30. *Small Charge Air Blast Experiments*, George T. Reynolds, OSRD 1518, NDRC A-191, OEMsr-260, Service Projects OD-79, NO-11, and others, PUS, June 1943. Div. 2-110-M1
31. *FM System of Blast Measurement*, Phil Weiss, Report 492, BRL, October 1944.
32. *An Improved Indicator for Measuring Static and Dynamic Pressure*, C. E. Grinstead, R. N. Frawley, F. W. Chapman, and H. F. Shults, (presented at the National Material Meeting of the Society of Automotive Engineers at Detroit,) June 1944.
33. *Report on the Use of Condenser Gauges as Pressure-Sensitive Indicators in Pressure Barrels and Automatic Weapons*, RD Explosives Report 255/42, Research Department, Woolwich, September 1942.
34. *A Condenser-Type FM Gauge for Blast Pressure Measurements*, Lincoln G. Smith, OSRD 6320, NDRC A-355, OEMsr-260, Service Projects OD-03 and NO-283, PUS, January 1946. Div. 2-111.11-M9
35. *The Use of General Motors Capacitance Pressure Gauges for Internal Ballistics Measurements on Rocket Propellants*, Charles G. Sage, OSRD 5750, OEMsr-202, Service Project OD-14, ERL, Nov. 1, 1945. Div. 8-607.5-M5
36. *The Taylor Model Basin Diaphragm Blast Gauge*, B. Susebols, Report 503, DTMB, December 1943.
37. *Comparison Tests of the Stanolind Oil and Gas Company Piezoelectric Blast-Pressure Recording Instruments and the David Taylor Model Basin Diaphragm-Type Blast-*

Pressure Recording Equipment, Daniel Silverman and H. M. Lang, OSRD 4257b, AES-3b, October 1944. Div. 2-100-M1

38. *Construction and Performance of the NOL Crusher Gauge*, Report 731, NOL, 1943.
39. *Consistency of the NOL Ball-Crusher Gauge*, R. H. Brown, Explosives Report 1, NAVORD, February 1944.
40. *Theory of the Ball-Crusher Gauge*, G. E. Hartman, Memorandum for File, NAVORD, September 1942.
41. *Mechanical Air-Blast Gauges*, W. E. Gordon, and P. E. Shafer, OSRD 6249, NDRC A-372.
42. *Measurement and Analysis of the Gun-Blast Pressure*, DTMB, Bureau of Ships, Navy Department, August 1942.
43. *A Mechanical Instrument for Recording the Positive Impulse in a Blast Wave*, AC-6656, RRL, July 1944.
44. *The Calibration of Paper Blast Meters*, R. G. Sachs, Report 472, BRL, June 1944.
45. *Theory, Calibration and Use of Diaphragm Blast Meters*, W. T. Read, OSRD 6463, NDRC A-392, OEMsr-260, Service Project OD-03, PUS, April 1946. Div. 2-111.12-M5
46. *An Improved Method for the Measurement of Blast from Bombs*, T. D. Carr, M. Schwarzschild, and Phil Weiss, Report 536, BRL, April 1943.
47. *Review of Flame Velocity Measurements from Bombs and Bare Charges up to January 31, 1943*, AC-3894, RRL, April 1943.
48. *The Formation of Mach or Bridge Waves. I Single Plano-Ended Cylinders*, D. W. Woodhead and R. Wilson, AC-7647, January 1945.
49. *Photographic Investigation of the Reflection of Plane Shocks in Air*, Lincoln G. Smith, OSRD 6271, NDRC A-350, OEMsr-260, Service Projects NO-144 and OD-03, PUS, November 1945. Div. 2-120-M8
50. *Shadowgraphic Determination of Shock Wave-Strength*, Explosives Research Report 11, NAVORD.
51. *Spark Photographs of the Mach Effect*, Paul Lilleaert, Report RC-417, May 1944.
52. *Photographic Observation of a Shock Crossing a Gas Boundary*, D. K. Weimer, Lincoln G. Smith, OSRD 6007b, AES-14b, September 1945. Div. 2-100-M1
53. *High-Speed Cameras for Measuring the Rate of Detonation in Solid Explosives*, W. Payman, W. C. F. Shepherd, and D. W. Woodhead, Paper 99, Safety in Mines Research Board, 1937.
54. *Construction and Operation of the Rotating Mirror Camera*, S. J. Jacobs, OSRD 5614, OEMsr-202, Service Projects NO-201 and OD-04, Carnegie Institute of Technology, Jan. 2, 1945. Div. 8-401-M4
55. *Shock Wave Studies with the Rotating Drum Camera*, Duncan P. MacDougall, Elizabeth M. Boggs, and G. H. Messerly, Interim Report DF-12, NDRC Division 8, August 1944. Div. 8-500-M2
56. *High-Speed Photographic Techniques*, G. M. Cooke, Report 20, Valcartier (Que) Ballistic Laboratory, December 1944.
57. *The Flash Photography of Detonating Explosives*, G. H. Messerly, OSRD 1488, OEMsr-202, Service Project OD-02, ERL, June 1943. Div. 8-401-M2
58. *Physical Optics*, R. W. Wood, The MacMillan Company, 1934, p. 93.
59. *Study of Shock Waves by Interferometry*, J. R. Winckler, C. C. Van Voorhis, H. Panofsky, and R. Ladenburg, OSRD 5204, NDRC A-332, OEMsr-260, Service Projects NO-208 and OD-03, PUS, June 1945. Div. 2-120-M7
60. *Study of Shock Waves by Interferometry*, R. Ladenburg, C. C. Van Voorhis, and J. R. Winkler, OSRD 4514a, AES-5a, December 1944. Div. 2-100-M1
61. *Construction of Resistance Strain Gauges*, Robert J. Hansen, OSRD 1063, NDRC A-59M, OEMsr-260, Service Projects CE-5, NO-11, and others, PUS, November 1942. Div. 2-111.11-M1
62. *A Preliminary Study of Plane Shock Waves Formed by Bursting Diaphragms in a Tube*, George T. Reynolds, OSRD 1519, NDRC A-192, OEMsr-260, Projects NO-144 and NO-207, PUS, June 1943. Div. 2-120-M3
63. *Shock Waves in Air: A Method of Gauge Calibration Based on Velocity Measurements*, W. T. Read, Jr., OSRD 4076b, AES-1b, August 1944. Div. 2-100-M1
64. *Pressures Behind a Shock Wave Computed for Velocity Measurements in the Blast Tube and the Correction for Humidity*, W. T. Read, Jr., OSRD 4257c, AES-3c, October 1944. Div. 2-100-M1
65. *Determination of Shock Wave Pressure in the Blast Tube as a Function of Compression-Chamber Pressure*, W. T. Read, Jr., OSRD 4514b, AES-5b, December 1944. Div. 2-100-M1
66. *Pressure-Velocity Relation for Shock Waves in a "van der Waals" Gas*, W. T. Read, Jr., OSRD 5011a, AES-9a, April 1945. Div. 2-100-M1
67. *Effect of Temperature on Gauge Calibration*, W. T. Read, Jr., OSRD 5144b, AES-10b, May 1945. Div. 2-100-M1
68. *An Experimental Determination of the Point of Catchup of the Rarefaction Wave and the Impulse of the Shock Wave in a Tube*, Curtis W. Lampson, OSRD 4754a, AES-7a, February 1945. Div. 2-100-M1
69. *On the Estimation of Perturbations Due to Flow Around Blast Gauges*, J. K. Lorne MacDonald and Samuel A. Schaaf, OSRD-5639, OEMsr-945, Note 22, AMP, September 1945. AMP-101.1-M14
70. *Prediction of Blast Damage for Experimental Results*, REN 367, Ministry of Home Security, April 1944.
71. *Observations of Blast Damage in Great Britain from German Weapons with Aluminised and Non-aluminised Loadings*, REN 368, Ministry of Home Security, April 1944.
72. *Damaging Effect of Known 8,000-Lb HC Bombs*, AC-4572 (R. E./H. 83), Ministry of Home Security, August 1943.
73. *Effectiveness of 12,000-Lb HC Bombs Filled Torpex 2/ Amatex 3 Against Single Story Reinforced Concrete Buildings*, REN 345, Ministry of Home Security, March 1944.
74. *Radius of Damage from 12,000-Lb HC Bombs Filled Amatex 3. Operational Results*, REN 316, Ministry of Home Security, January 1944.
75. *Study of the Physical Vulnerability of Military Targets to Various Types of Aerial Bombardment*, Walker Bleakney, OSRD 6444, NDRC A-385, OEMsr-260, Service Project AN-29, Weapons Effect Group, PUS, January 1946. Div. 2-530-M3
76. *Reactions of Simple Systems under Blast Loading*, D. Montgomery and A. H. Taub, OSRD 5393a, AES-12a, July 1945. Div. 2-100-M1
77. *Remarks on Reactions under Blast Loading*, D. Montgomery and A. H. Taub, OSRD 6007a, AES-14a, September 1945. Div. 2-100-M1
78. *The Order of Effectiveness of Explosives in Air-Blast*, W. D. Kennedy, OSRD 6252, NDRC A-374.
79. *Measurement of Blast Pressures from 4,000-Lb Bombs*, E. Bright Wilson, Jr., OSRD 1153, OEMsr-334, Service Projects OD-02 and OD-03, NDRC Division 8, HU, Jan. 23, 1943. Div. 2-111-M1
80. *Blast Pressures and Moments from Some Large Bombs*, E. Bright Wilson, Jr., and W. D. Kennedy, OSRD 3046, OEMsr-334, Service Projects OD-02 and OD-03, NDRC Division 8, HU, Nov. 17, 1943. Div. 2-111-M4

81. *Small Charge Air Blast Measurements: Order of Effectiveness of Explosives*, W. D. Kennedy, R. F. Arentzen, G. K. Fraenkel, and Paul C. Cross, OSRD 4076d, AES-1d, August 1944. Div. 2-100-M1
82. *Order of Effectiveness of Explosives, II*, W. D. Kennedy, R. F. Arentzen, G. K. Fraenkel, and Paul C. Cross, OSRD 4147a, AES-2a, September 1945. Div. 2-100-M1
83. *Order of Effectiveness of Explosives, IV. Peak Pressures and Positive Impulses in the Blast from 500-Lb Bombs Filled with HBX, Torpex 2, Composition B, and Tritonal*, W. D. Kennedy, R. F. Arentzen, and C. W. Tait, OSRD 4640a, AES-5a, January 1945. Div. 2-100-M1
84. *Survey of the Performance of TNT/Al on the Basis of Air Blast Pressure and Impulse*, W. D. Kennedy, OSRD 4540b, AES-6b, January 1945. Div. 2-100-M1
85. *The Air-Blast Performance of Some High Explosives*, W. D. Kennedy, OSRD 4754b, AES-7b, February 1945. Div. 2-100-M1
86. *Order of Effectiveness of Explosives, V. Comparison of Blast Pressures and Impulses of PTX-1 and PTX-2 with Those of HBX, Composition B and TNT*, C. W. Tait, W. E. Curtis, and W. D. Kennedy, OSRD 4875b, AES-8b, March 1945. Div. 2-100-M1
87. *Order of Effectiveness of Explosives, III*, W. D. Kennedy, OSRD 4356, AES-4. Div. 2-100-M1
88. *The Effect of Air Burst on the Blast from Bombs and Small Charges*, OSRD 5246, OEMsr-569 and OEMsr-596, Service Project OD-03, NDRC Division 8, UERL, WHOI, and SOG, Oct. 16, 1944. Div. 2-110-M3
89. *Air-Blast Measurements with Tritonal Containing Flake Aluminum and with TNT/Al 60/40 and TNT/Al 40/60*, C. W. Tait and W. D. Kennedy, OSRD 5271d, AES-11d, June 1945. Div. 2-100-M1
90. *Air Blast Measurements of 4-Lb Spherical Pentolite Charges and Cylindrical Charges of Pentolite, Composition B and TNT*, R. F. Arentzen and W. D. Kennedy, OSRD 5271e, AES-11e, June 1945. Div. 2-100-M1
91. *Air Blast Measurements of Various Explosives as a Function of Atmospheric Pressure*, H. M. Long and I. Silverman, OSRD 6007e, AES-14e, September 1945. Div. 2-100-M1
92. *Small Charge Air Blast Measurements: Order of Effectiveness of Explosives*, Paul C. Cross, W. D. Kennedy, and D. F. Hornig, OSRD 3479, OEMsr-569, Service Projects OD-03 and NO-144, NDRC Division 8, WHOI, Apr. 1, 1944. Div. 2-110-M2
93. *Calculation of the Detonation Velocities of Some Pure Explosives*, Stuart R. Brinkley, Jr., and E. Bright Wilson, Jr., OSRD 1707, NDCrc-168, Service Projects OD-02 and NO-144, HU, Aug. 12, 1943. Div. 8-501-M4
94. *Bombs, 500-Lb M. C. Mk III, Blast Performance of Torpex Mixtures Containing 0-42% of Aluminum*, AC-8131, SD-643, March 1945.
95. *Bombs, H. C. 4,000-Lb Mark IV Static Detonation Trials of Minol with Aluminum Content Varying from 0-28%*, Explosives Report 68/44, ARD, July 1944.
96. *Bombs, 500-Lb M. C. Mark III, Filled Minol Mixtures Containing 0-28% Aluminum Powder*, AC-5801, Explosives Report 23/44, ARD, February 1944.
97. *Bombs, HC 4,000-Lb Mark IV, TNT/Al 70/30, TNT/Al 75/25, TNT/Al 80/20, Static Detonation Trials*, AC-7044, SD-533, March 1945.
98. *Bombs, 500-Lb M. C. Mark III Blast Performance of TNT/Al Mixtures Containing 0-40% of Aluminum*, AC-7073, Explosives Report 112/44, ARD, September 1944.
99. *Blast and Fragment Velocity Measurements on 500-Lb GP Bombs of Various Loadings*, R. G. Sachs and W. P. Bidelman, Report 500, BRL, November 1944.
100. *The Effect of Addition of Various Amounts of Aluminum to TNT*, Interim Report DFA-10, NDRC Division 8, UERL. Div. 8-500-M2
101. *Explosive Compositions*, Interim Report PT-25, NDRC Division 8, ERL. Div. 8-109-M3
102. *Measurements of Blast from 4,000-Lb HC Bombs with Minol-2 (36-Dust Al) and 60/40 RDX/TNT Fillings*, AC-5063, March 1944.
103. *Velocities of Shocks Produced in Air from Plane-Ended Charges*, Elizabeth M. Boggs, M. D. Hurwitz, and H. A. Strecker, Interim Report DF-19, NDRC Division 8, July 1945. Div. 8-500-M2
104. *Application of the Law of Dynamical Similarity to the Blast Characteristics from Cylindrical Bare Charges of RDX/TNT, 60/40 Weighing between 8 and 550 Lbs and Fired Resting on the Ground*, Explosives Report 147/44, AC-7673, ARD.
105. *Methods for Computing Data on the Terminal Ballistics of Bombs. II. Estimation of the Air Blast*, U. Fano, Report 524, BRL, February 1945.
106. *Measurement of Blast Pressure from 66-Lb Euro Charges of 60/40 RDX/TNT*, AC-4657, RRL, July 1943.
107. *Contribution of Afterburning to Blast Pressure and Impulse*, W. E. Gordon, OSRD 4147b, AES-2b, NDRC Division 2. Div. 2-100-M1
108. *Note on the Contribution of the Afterburning of Explosive Products to the Positive Impulses in the Blast*, AC-3812, RRL, March 1943.
109. *Measurements of Blast Pressures from Standard Cased Charges of Various Charge-Weight Ratios*, AC-3435, MOS/193/145, RRL, January 1943.
110. *The Effect of Charge Weight Ratio on Equivalent Charge Weight*, RFN 460, Ministry of Home Security, April 1944.
111. *Dependence of Positive Impulse of Blast on Charge Weight Ratio*, Henry Scheffé, OSRD 4356d, AES-4d, November 1944. Div. 2-100-M1
112. *Relation Between Positive Blast Impulse and Charge Weight Ratio for Bombs*, E. J. Tan, OSRD 4356a, AES-4a, November 1944. Div. 2-100-M1
113. *Bombs, HC, 4000-Lb of Increased Charge-Weight Ratio. Static Detonation Trials of Bombs with ¼-In. Mild Steel and 5/16-In. Aluminum Alloy Cases*, AC-7284, ARD, October 1944.
114. *Bombs, 500-Lb MC Filled Minol-2 and Amatol 60/40. Effect of Cast Aluminum Alloy Case on Positive Blast Intensity*, AC-6949, ARD, August 1944.
115. *Measurements of the Air Blast from Mark 6 and Mark 8 Depth Charges, Filled with TNT and RDX-Composition B with Steel, Aluminum and Plastic Cases*, W. P. Bidelman, Report 502, BRL, November 1944.
116. *Blast Measurements of J. B. 2 War Heads with Steel and Aluminum Casings*, W. P. Bidelman, Report 540, BRL, April 1945.
117. *Tables of the Properties of Air Along the Hugoniot Curve and the Adiabatics Terminating in the Hugoniot Curve*, Stuart R. Brinkley, Jr., John G. Kirkwood, and John M. Richardson, OSRD 3550, OEMsr-121 Service Projects OD-03, NO-144, and NO-224, NDRC Division 8, Cornell University, Apr. 27, 1944. Div. 2-120-M5
118. *Oblique Reflection of Shocks*, John von Neumann, Explosives Report BO-12, NAVORD.
119. *Regular Reflection of Shocks in Ideal Gases*, H. Polachek, R. J. Seeger, Explosives Research Report 13, NAVORD, February 1944.
120. "Uber das Gleiten des Elektrischen Funkens," E. Antolik, *Poggendorff's Analen der Physik*, Vol. 154, 1875.
121. "Uber Einige Mechanische Wirkungen des Elektrischen

Funkens," E. Mach and J. Wozyka, *Akademie der Wissenschaften, Sitzungsberichte der Wiener*, Vol. 72, Part 2, 1875.

122. "Uber die Fortpflanzungsgeschwindigkeit von Explosionsschallwellen." F. Mach and J. Sommer, *Akademie der Wissenschaften, Sitzungsberichte der Wiener*, Vol. 75, 1877.

123. "Uber die Fortpflanzungsgeschwindigkeit der Funkenwellen," E. Mach, D. Tumlirz, and C. Kogler, *Akademie der Wissenschaften, Sitzungsberichte der Wiener*, Vol. 77, 1878.

124. "Uber den Verlauf der Funkenwellen in der Ebene und im Raume," *Akademie der Wissenschaften, Sitzungsberichte der Wiener*, Vol. 77, 1878.

125. *Interference of Shock Waves in Air*, E. Bright Wilson, Jr., Interim Reports FS-2 and FS-3, NDRC Division 8, October 1942 and November 1942. Div. 8-400-M1

126. *The Interaction of Shock Waves*, R. W. Wood, OSRD 1906, OEMsr-773, Service Projects AN-1 and OD-03, NDRC Division 8, Johns Hopkins University, Nov. 4, 1943. Div. 2-120-M4

127. *On the Conditions for the Existence of Three Shock Waves*, S. Chandrasekhar, Report 367, BRL, 1943.

128. *Remarks on the Mach Effect*, Kurt O. Friedrichs, Report M5, AMP, July 1943; *Appendix*, Report M6, AMP, July 1943.

129. *On Nearly Glancing Reflection of Shocks*, Valentine Bargmann, OEMsr-1111, Report 168-2R, AMG-Institute for Advanced Study, AMP, March 1945. AMP-101.1-M13

130. *Prandtl-Meyer Zones in Mach Reflection*, Valentine Bargmann, and D. Montgomery, OSRD 5011b, AES-9b, April 1945. Div. 2-100-M1

131. *The Effect of the Height at Which a Bomb Explodes on the Blast Pressures*, Note ARP/255 RJ, August 1941.

132. *General Estimate of the Results of Experiments with the Model Town*, REN 110, August 1941.

133. Ordnance Board (British), Proof Rpt Q1150, April 1943.

134. *Small Charge Air Blast Experiments: Peak Pressure as a Function of Charge-to-Ground Distance*, DFA-5, UERL, January 1944. Div. 8-500-M2

135. *Small Charge Air Blast Measurements: Peak Pressure and Positive Impulse as a Function of Charge-to-Ground Distance, II*, DFA-6, UERL, February 1944. Div. 8-500-M2

136. *Small Charge Air Blast Measurements: Peak Pressure and Positive Impulse as a Function of Charge-to-Ground Distance, III*, DFA-7, UERL, March 1944. Div. 8-500-M2

137. *Small Charge Air Blast Measurements: Peak Pressure and Positive Impulse as a Function of Charge-to-Ground Distance, IV*, DFA-8, UERL, April 1944. Div. 8-500-M2

138. *The Effect of Height of Detonation on Peak Pressure and Positive Impulse Measured Close to the Ground*, W. D. Kennedy and R. F. Arentsen, OSRD 4514d, AES-2d, December 1945. Div. 2-100-M1

139. *Peak Pressure Dependence on Height of Detonation*, A. H. Taub, OSRD 4073a, AES-1a, August 1944. Div. 2-100-M1

140. *The Reflection of Shock Waves in Air*, Lincoln G. Smith, OSRD 4070e, AES-1e, August 1944. Div. 2-100-M1

141. *Impulse Dependence on Height of Detonation*, R. G. Stoner and A. H. Taub, OSRD 4147c, AES-2c, September 1944. Div. 2-100-M1

142. *Mach Reflection of Shock Waves from Charges Detonated in Air*, R. G. Stoner, OSRD 4257d, AES-3d, October 1944. Div. 2-100-M1

143. *The Shape of the Shock-Wave Fronts from Charges Detonated in Air*, R. G. Stoner, OSRD 4516c, AES-5c, December 1944. Div. 2-100-M1

144. *Dependence of Optimum Impulse on Height of Gauge in Air-Burst*, R. G. Stoner and A. H. Taub, OSRD 5011c, AES-9c, April 1945. Div. 2-100-M1

145. *Effect of Height of Burst in the Positive Impulse from Bombs*, Special Preliminary Report, UERL.

146. *Effects of the Height of Burst on the Positive Impulse from Bombs, II*, UERL, June 1944.

147. *Effect of Case Weight on the Positive Impulse from Bombs Filled TNT and Torpex*, W. D. Kennedy, Technical Memorandum 2, UERL, July 1944.

148. *The Effect of Air Burst on the Blast from Bombs and Small Charges. Part II, Analysis of Experimental Results*, R. R. Halverson, OSRD 4899, NDRC A-320, OEMsr-569, Service Project OD-03, WHOI, April 1945. Div. 2-110-M6

149. *The Observed Effects of Proximity Fuzing in the 4000-Lb HC Bomb*, D. G. Christopherson, AC-6442, May 1944.

150. *80th Report of the Static Detonation Committee Meeting Held May 17, 1944*, AC-6343, May 1944.

151. *The Blast Effect of Air-Burst Bombs. History of British Experience. II Commentary on American Investigations*, D. G. Christopherson, AC-6526, June 1944.

152. *Air Burst Bombs. Statement of the Position on October 20, 1944*, D. G. Christopherson, REN 461.

153. *The Effect of Height of Burst on the Blast Characteristics from 67-Lb Bare Charges of RDX/TNT 60/40*, Interim Report, ARD, December 1944.

154. *Effect of Height of Detonation of Bombs on the Blast Pressures and Impulses on Surrounding Buildings—Richmond Park 1/7th Scale Model Town Tests*, AC-6097, RRL, March 1945.

155. *Weapon Data—Fire, Impact Explosion*, OSRD 6053, NDRC Division 2, PUS, September 1945.

156. *The Effectiveness of Explosives in Enclosed Spaces*, W. E. Gordon, OSRD 6255, NDRC A-377.

157. *Studies on SBX, Part II. Comparison of Results Obtained in Part I with Jones' Simplified Theoretical Calculations of SBX Pressure-Time Characteristics*, C. S. Lu, Report 167, MRL, January 1945.

158. *Relative Effectiveness of Explosives Fired in Nearly Enclosed Rooms*, W. E. Gordon and H. M. Lang, OSRD 5011d, AES-9d, April 1945. Div. 2-100-M1

159. *Effect of Confined Blast on Brick Curtain Walls*, A. H. Taub and J. A. Wise, OSRD 6007d, AES-14d, September 1945. Div. 2-100-M1

160. *Development of SBX Fillings*, AC-6644, Incendiary Projectiles Committee of the Static Detonation Committee, July 1944.

161. *Dispersion and Combustion of Metallic Powders in Air*, G. J. Finch, AC-4273, Research and Experiments Department, Ministry of Home Security, June 1943.

162. *Report on Static Trials of SBX-Filled Bombs at the Mansion House, Muirburn*, REN 333, AC-6147, Research and Experiments Department, Ministry of Home Security, April 1944.

163. *Static Trials of a Minol-Filled Bomb at the Mansion House, Muirburn*, REN 350, AC-6148, Research and Experiments Department, Ministry of Home Security, March 1944.

164. *Note On SBX (with Particular Reference to a Suggested Incorporation of Cerium)*, G. J. Finch, AC-6747, July 1944.

165. *On the Possibility of the Use of Combustibles to Amplify the Blast Effect of Bombs*, J. E. Mayer, Report 411, BRL, October 1943.

166. *Use of Flour and Other Dust Explosives in Attacks on Confined Wooden Structures*, C. S. Lu, Report 92, MRL, June 1944.

167. *Dust Explosion Tests in Wooden Houses Located at TVA*

Reservoir Area Near Bryson City, N. C., C. S. Lu, Report 152, MRL, September 1944.

168. *Memorandum on the Latest Dust and Liquid Explosion Tests at Factory Mutual Test Station, Norwood, Mass.*, C. S. Lu, MRL, October 1944.
169. *Use of Dust and Liquid Slow Burning Explosives in Attacks on Confined Structures*, C. S. Lu, Report 183, MRL, February 1945.
170. *Development of Salez*, Norman J. Thompson, Report to W. C. Lathrop, NDRC Division 19, November 1944.
171. *Final Report on Teak*, H. J. Billings and S. Edward Eaton, Jr., OEMsr-1023, Part IX with Arthur Little, Inc., May 1945.
172. *Studies on SBX: Comparison of Various Combustibles vs. SBX Under Confined Conditions*, W. E. Gordon, OSRD 4356a, AES-4a, November 1944. Div. 2-100-M1
173. *The Propagation and Decay of Blast Waves*, G. I. Taylor, RC-39.
174. *The Formation of a Blast Wave by a Very Intense Explosion*, G. I. Taylor, RC-210.
175. *The Development of Suction Behind the Blast Wave in Air and the Energy Dissipation*, W. G. Penney, RC-260, October 1941.
176. *The Numerical Integration of the Equation for a Spherical Shock Wave in Air*, Oscar K. Rice, Interim Report DFA-9, NDRC Division 8, May 1944. Div. 8-500-M2
177. *The Numerical Integration of the Equation for a Spherical Shock Wave in Air*, R. Grinell and Oscar K. Rice, OSRD 4257e, AES-3e, October 1944. Div. 2-100-M1
178. *A New Theory of Shock Wave Propagation with an Application to the Shock Wave Produced in Air by the Explosion of Cast Pentolite*, John G. Kirkwood and Stuart R. Brinkley, Jr., OSRD 4257f, AES-3f, October 1944. Div. 2-100-M1
179. *The Time Constant and Positive Impulse According to the Theory of Shock Wave Propagation of Blast Waves: Results for Cast Pentolite*, John G. Kirkwood and Stuart R. Brinkley, Jr., OSRD 4356f, AES-4f, November 1944. Div. 2-100-M1
180. *The Calculation of the Time Constant and the Positive Impulse from the Peak Pressure-Distance Curves of Blast Waves in Air with an Application to Cast TNT*, John G. Kirkwood and Stuart R. Brinkley, Jr., OSRD 4356g, AES-4g, November 1944. Div. 2-100-M1
181. *Theory of the Propagation of Shock Waves from Explosive Sources in Air and Water*, John G. Kirkwood and Stuart R. Brinkley, Jr., OSRD 4814, NDRC A-313, OEMsr-121, Service Projects OD-03 and NO-224, Cornell University, March 1945. Div. 2-120-M6
182. *Tables and Graphs of the Theoretical Peak Pressure, Energies and Positive Impulse of Blast Waves in Air*, Stuart R. Brinkley, Jr., and John G. Kirkwood, OSRD 5137, NDRC A-327, OEMsr-121, Service Projects OD-03 and NO-224, Cornell University, May 1945. Div. 2-112-M1
183. *Theoretical Blast Wave Curves for Cast TNT*, John G. Kirkwood and Stuart R. Brinkley, Jr., OSRD 5481, NDRC A-341, OEMsr-121, Service Projects OD-03 and NO-224, Cornell University, August 1945. Div. 2-112-M2
184. *The Pressure Distance Relation for TNT, Determined by Measurements of Shock Velocity*, R. G. Stoner, OSRD 6637, NDRC A-474.
185. *Shock Wave Studies with the Rotating Drum Camera*, Duncan P. MacDougall, Elizabeth M. Boggs, and G. H. Messerly, Interim Report DFA-12, NDRC Division 8, August 1944. Div. 8-500-M2
186. *Piezoelectric Measurements of Pressure Impulse and Shock Wave Velocity Close to a One-Half Pound Charge*, Interim Report DFA-7, NDRC Division 8, UERL, March 1944. Div. 8-500-M2
187. *Measurements of Blast Pressure from Bare Charges of 60/40 RDX/TNT, Fired at Richmond Park in the Period April 19-25, 1943*, ARP/408/HS. DJL, RRL, August 1943.
188. *67-Lb Bare Charges of RDX/TNT 60/40 Type D, 100, Fired at Millarsford Between September 25, 1943 and January 31, 1944*, Explosive Report 24/44, AC-5853, ARD, February 1944.
189. *Blast Measurements from Cord Cased Cylindrical Charges of About 60-Lb of Some Service High Explosives*, Report 113/44, AC-7058, ARD, October 1944.
190. *The Air Blast from Line Charges*, G. K. Fraenkel and W. D. Kennedy, OSRD 6253, NDRC A-375.
191. *The Blast Wave in Air Produced by Line Charges*, Stuart R. Brinkley, Jr., John G. Kirkwood, OSRD 5659, NDRC A-343, OEMsr-121, Service Projects OD-03 and NO-224, Cornell University, October 1945. Div. 2-110-M4
192. *Aerial Bombardment of Mine Fields*, Report 860, The Technical Staff, The Engineer Board, Corps of Engineers, U. S. Army, August 1944.
193. *Third Interim Report. Equipment for the Passage of Enemy Minefields*, Report 861, The Technical Staff, The Engineer Board, Corps of Engineers, U. S. Army, September 1944.
194. *Project 112—Aerial Bombing of Mine Fields*, Joint Army-Navy Experimental and Testing Board, Janet Progress Report, Jan-Pro/15, June 1945.
195. *Clearance of Mines by Rocket Barrages from the Woofus*, NDRC 161.1R, OEMsr-860, SRG-P 150, AMP, August 1945. AMP-902-M5
196. *Detonating Cord Cable Kit*, Report 906, The Technical Staff, The Engineer Board, Corps of Engineers, U. S. Army, January 1945.
197. *Snake, Mineclearing, Antipersonnel M1*, War Department Technical Bulletin, TB Eng 65, February 1945.
198. *First Interim Report; Equipment for the Passage of Enemy Mine Fields*, Report 842, The Technical Staff, The Engineer Board, Corps of Engineers, U. S. Army, July 1944.
199. *Second Interim Report; Equipment for the Passage of Enemy Mine Fields*, Report 850, The Technical Staff, The Engineer Board, Corps of Engineers, U. S. Army, August 1944.
200. *Fourth Interim Report; Equipment for the Passage of Enemy Mine Fields*, Report 875, The Technical Staff, The Engineer Board, Corps of Engineers, U. S. Army, October 1944.
201. *Fifth Interim Report; Equipment for the Passage of Enemy Mine Fields*, Report 888, The Technical Staff, The Engineer Board, Corps of Engineers, U. S. Army, November 1944.
202. *Sixth Interim Report; Equipment for the Passage of Enemy Mine Fields*, Report 894, The Technical Staff, The Engineer Board, Corps of Engineers, U. S. Army, December 1944.
203. *Seventh Interim Report; Equipment for the Passage of Enemy Mine Fields*, Report 905, The Technical Staff, The Engineer Board, Corps of Engineers, U. S. Army, January 1945.
204. *Eighth Interim Report; Equipment for the Passage of Enemy Mine Fields*, Report 923, The Technical Staff, The Engineer Board, Corps of Engineers, U. S. Army, April 1945.
205. *Snake, Demolition, M2A1*, War Department Technical Bulletin, TB Eng 47, October 1944.
206. *Snake, Demolition, M3*, War Department Technical Bulletin, TB Eng 60, March 1945.

207. *Mine Clearing Dragon, M-1*, Report 929, The Technical Staff, The Engineer Board, Corps of Engineers, U. S. Army, May 1945.
208. *Piezoelectric Measurements of Blast Pressures in M-4 Tank from Explosive Charges Detonated Outside of Vehicle*, Daniel Silverman and H. M. Lang, OSRD 4307, NDRC A-297, OEMsr-576, Service Project OD-03, SOG, November 1944. Div. 2-111.11-M5
209. *The Effect of Blast on Indicator Mines*, E. Bright Wilson, Jr., A. H. Taub, Curtis W. Lampson, and Thomas Bardeen, OSRD 4276, OEMsr-266, Service Project OD-03, NDRC Divisions 2 and 17, PUS, SOG, and Gulf Research and Development Company, Sept. 28, 1944. Div. 2-113-M1
210. *The Effect of Shock Impulse on Anti-Tank Mines, Parts I and II*, Thomas Bardeen, OSRD 6073, OEMsr-266, Gulf Research and Development Company, Oct. 15, 1945. Div. 17-122.1-M3, M4
211. *Expected Clearance of German and Japanese Anti-Tank and Anti-Personnel Mines by Explosive Mine-Clearing Devices*, Statistical Research Group, AMP 178.1R, PUS, June 1945. AMP-902-M3
212. *The Detonation of TMi-43 Indicator by Blast*, J. L. Brenner, OSRD 5179, NDRC A-331, OEMsr-260, Service Project OD-03, PUS, June 1945. Div. 2-111.12-M4
213. *The Detonation of Universal Indicator Mine by Blast from Point Charges*, J. L. Brenner, OSRD 5271b, AES-11b. Div. 2-100-M1
214. *The Effect of Line Charges on Universal Indicator Mine*, J. L. Brenner and A. H. Taub, OSRD 5144c, AES-10c, May 1945. Div. 2-100-M1
215. *Theoretical Aspects of the Blast Detonation of Teller Mines*, E. B. Philip, PF 3902/89.
216. *On a New Criterion for Measuring the Efficiency of an Explosive Hose*, F. N. David, REN 486, AC-7843, Ministry of Home Security, February 1945.
217. *The Effect of the "Probability Dip" of Alternating the Nature and Weight of Filling of the Conger*, J. L. Alexander, D. C. Brettell and F. N. David, REN 485, AC-7842, Ministry of Home Security, February 1945.
218. *Empirical Laws for Blast Pressures from Line Charges of Ammonal 70/30 B*, E. B. Philip, RC-426, September 1944.
219. *Blast Pressures and Positive Impulses from Cordex Line Charges Fired in Air*, Undex 101, RRL, July 1944.
220. *The Effect of Raising a Line Charge*, F. N. David, REN 348, Ministry of Home Security, March 1944.
221. *The Dependence of Blast on Ambient Pressure and Temperature*, R. G. Sachs, Report 466, BRL, May 1944.
222. *The Effect of Altitude on the Peak Pressure and Positive Impulse from Blast Waves in Air*, John G. Kirkwood, and Stuart R. Brinkley, Jr., OSRD 5271a, AES-11a, June 1945. Div. 2-100-M1
223. *An Examination of the Symmetry of the Positive Blast Impulse Intensity Around Bombs MC 500-Lb, Mark III, Amatol 60/40*, Explosives Report 381/43, ARD, November 1943.
224. *Charge Orientation Tests*, George T. Reynolds, OSRD 1532, NDRC A-193, OEMsr-260, Service Projects OD-76, NO-11, and others, PUS, July 1943. Div. 2-111-M3
225. *Measurements of Blast from Four 1000-Kg German S. B. Bombs Fired at Shoeburyness in the Periods 1st to 9th*, AC-8181, MOS/442/DJL.EK, RRL, April 1945.
226. *Shock Wave Studies with the Rotating Drum Camera*, Duncan P. MacDougall and G. H. Messerly, Interim Report DFA-10, NDRC Division 8, June 1944. Div. 8-500-M2
227. *Blast Pressures Measured Near the Jets from 5-Inch Spin-Stabilized Rockets*, R. F. Arentsen, OSRD 5144d, AES-10d, May 1945. Div. 2-100-M1
228. *Construction and Characteristics of Model Ammunition Storage Magazines*, Nathan M. Newmark, C. P. Atkins, and E. E. Bauer, OSRD 6318, NDRC A-353, OEMsr-1476, Service Project AN-28, University of Illinois, November 1945. Div. 2-540-M2
229. *Observations on the First Model Igloo Test at Camp Edwards, on October 23, 1945*, W. E. Gordon, Technical Memorandum 13, USRL, December 1945.
230. *The Probability of Propagation of an Explosion in a Field of Storage Magazines*, E. Bright Wilson, Jr., OSRD 5271f, AES-11f, June 1945. Div. 2-100-M1

Chapter 3

1. *Final Report on Effects of Explosives in Earth*, Curtis W. Lampson, OSRD, NDRC Report.
2. "A Study of Blasting Recorded in Southern California," Harry O. Wood and Charles F. Richter, *Bulletin of Seismological Society of America*, Vol. 21, No. 1, March 1931, p. 23.
3. *Vibrations Caused by Blasting and Their Effect on Structures*, Edward H. Rockwell, Hercules Powder Company, Wilmington, December 1934.
4. *Earth Vibrations Caused by Quarry Blasting*, F. W. Lee, J. R. Thoenen, and Stephen L. Windes, Report of Investigation 3319, U. S. Bureau of Mines, November 1936.
5. *Earth Vibrations Caused by Quarry Blasting*, J. R. Thoenen and Stephen L. Windes, Report of Investigation 3353, U. S. Bureau of Mines, November 1937.
6. *Earth Vibrations Caused by Quarry Blasting*, J. R. Thoenen and Stephen L. Windes, Report of Investigation 3407, U. S. Bureau of Mines, June 1938.
7. *Seismic Effect of Quarry Blasting*, J. R. Thoenen and S. L. Windes, Bulletin 442, U. S. Bureau of Mines, 1942.
8. *Survey Test on Open Trench after Bombing—Stewartby (Clay Soil)*, R.C. 64, Research and Experiments Branch, Ministry of Home Security, November 1939.
9. *Earth Movement Due to German 50- and 250-Kg and British 250-Lb A. S. Bombs Exploded Below Ground*, R.C. 153, Ministry of Home Security, RRL, November 1940.
10. *Bomb Explosion Test on an Open Trench in Hard Gravel at Hampton Ridge*, R.C. 192, Ministry of Home Security, RRL, January 1941.
11. *A Comparison of the Crater Dimensions and Permanent Earth Movements in Clay, Chalk, and Gravel Soils Due to the Explosion of Buried Bombs*, R.C. 199, Ministry of Home Security, RRL, March 1941.
12. *Earth Movement Due to German 250-, 500-, 1000-Kg G.P. Bombs Exploded Below Ground*, R.C. 259, Ministry of Home Security, RRL, August 1941.
13. *A Preliminary Report on Camouflets in Clay Soil*, R.C. 292, Ministry of Home Security, RRL, November 1941.
14. *Earth Movement Due to 250-Kg Bombs Exploded in Clay Soil*, R.C. 312, Ministry of Home Security, RRL, November 1942.
15. *Earth Movement Due to 50-Kg Bombs Exploded at Different Depths in Clay Soil at Richmond Park*, R.C. 328, Ministry of Home Security, RRL, May 1942.
16. *Earth Movements Due to Buried Standard Charges (Approximately 8.5 Lb in Wt)*, R.C. 416, Ministry of Home Security, RRL, November 1943.
17. *The Radius of Damage for Underground Services*, R.C. 200, Ministry of Home Security, Research and Experiments, Department, October 1941.

18. *The Acceleration of Model Building Due to the Explosion of a Buried Charge*, Note N ARP/366/HJHS, Ministry of Home Security, RRL, August 1942.
19. *A Survey of Information on the Action of Bombs Exploding in Earth*, D. G. Christopherson, R.C. 263, Ministry of Home Security, Civil Defense Research Committee, October 1941.
20. *Preliminary Measurements of Earth Pressures and Movements Under Detonation*, L. W. Blau, W. M. Rust, Jr., W. D. Mounce, and J. M. Lanse, CPPAB Interim Report 18, National Research Council and Humble Oil Company, March 1942. Div. 2-240-M1
21. *Measurements of Earth Pressures and Movements Under Detonations*, W. D. Rust, Jr., and W. D. Mounce, CPPAB Interim Report 19, National Research Council and Humble Oil Company, September 1942. Div. 2-240-M2
22. *Mobile Oscillographic Laboratory*, Curtis W. Lampson and Walker Bleakney, OSRD 4570, NDRC A-307, OEMsr-675, Service Project OD-79, PUS, January 1945. Div. 2-111.12-M3
23a. *Effects of Underground Explosions, Volume I, Subsurface and Target Phenomena*, Curtis W. Lampson, Interim Report 26, Committee on Fortification Design, National Research Council, June 1944. Div. 2-240-M4
23b. *Effects of Underground Explosions, Volume II, Subsurface and Surface Phenomena*, Interim Report 26, Committee on Fortification Design, National Research Council, June 1944. Div. 2-240-M5
23c. *Effects of Underground Explosions Volume III. Resulting Damage to Structures*, David Mayer and Norman C. Dahl, Interim Report 26, Committee on Fortification Design, National Research Council, June 1944. (There is a misplaced decimal point in Appendix A of this reference.) Div. 2-240-M6
24. *The Order of Effectiveness of Various Explosives in Earth*, Curtis W. Lampson, OSRD 5506, NDRC AES-13b, August 1945. Div. 2-100-M1
25. *Effects of Underground Explosions, Volume IV, Influence of Variations of Soil Type and Depths of Charge and Gauge*, Curtis W. Lampson, W. M. Rust, Jr., and others, OSRD 6304, NDRC A-359, OEMsr-260, Service Project OD-03, PUS, February 1946. Div. 2-240-M8
26. *Effects of Subsurface Detonations in Earth, Part II*, B. B. Weatherby, OSRD 3036, NDRC A-238, OEMsr-260, Service Projects CE-5, NO-12, and others, PUS, December 1943, p. 3. Div. 2-240-M3
27. *The Seismic Method of Exploration Applied to Construction Projects*, E. R. Shepard, September to October 1939.
28. *Terminal Ballistics and Explosive Effects*, John E. Burchard, CPPAB, National Research Council, Oct. 1, 1943. Div. 2-200-M2

Chapter 4

1. *The Internal Ballistics of Gun after Shot Ejection*, J. Corner Ballistics Report 54, ARD.
2. *The Interior Ballistics of a Gun after Shot Ejection Applied to the Problem of Dust Deflector Design*, R. D. Buhler, OSRD 5350i (OTB 12i), July 1945. Div. 2-300-M1
3. *On the Emptying of a Gun, Part I*, J. J. Slade, Jr. and C. H. Fletcher, OSRD 5300, NDRC A-336, OEMsr-260, Service Projects OD-154 and OD-160, PUS, August 1945. Div. 2-331-M2
4. *A Study of Blast Deflectors*, Clark B. Millikan, E. E. Sechler, and R. D. Buhler, OSRD 6316, NDRC A-351, OEMsr-1351, Service Projects OD-154 and OD-160, California Institute of Technology, October 1945. Div. 2-330-M3
5. *Muzzle Blast: Its Characteristics, Effects and Control*, J. J. Slade, Jr., OSRD 6462, NDRC A-391, OEMsr-260, Service Projects OD-154, and OD-160, PUS, March 1946. Div. 2-330-M4
6. *Muzzle Blast Deflector*, George T. Reynolds, OEMsr-260, Service Project OD-154, Report PMR-20, NDRC Division 2, PUS, Apr. 15, 1944. Div. 2-330-M1
7. *Reduction of Smoke and Blast Obscuration Effect*, OSRD 5068, NDRC A-325, OEMsr-1343, Service Project OD-154, General Electric Company, May 1945. Div. 2-113-M2
8. *Study of Shock Waves by Interferometry*, R. Ladenburg, C. C. Van Voorhis, and J. R. Winckler, OSRD 4514a, AES 5a, December 1944. Div. 2-100-M1
9. *Study of Shock Waves by Interferometry*, J. R. Winckler, C. C. Van Voorhis, H. Panofsky, and R. Ladenburg, OSRD 5204, NDRC A-332, OEMsr-260, Service Projects NO-208, and OD-03, PUS, June 1945. Div. 2-120-M7
10. *Muzzle Blast Pressure Measurements*, George T. Reynolds, OEMsr-260, Service Project OD-154, Report PMR-21, NDRC Division 2, PUS, Apr. 15, 1944. Div. 2-330-M2
11. *Interaction of Shock and Rarefaction Waves in One-Dimensional Motion*, Richard Courant, and Kurt O. Friedrichs, OSRD 1567, OEMsr-944, Service Projects OD-03 and NO-144, Report 38.1 AMP, July 5, 1943. AMP-101.1-M4
12. *The Study of the Effect of Muzzle Brake Design on the Recoil of Guns, Part I*, Frank R. Simpson and Nicol H. Smith, OSRD 4389, NDRC A-320, OEMsr-1308, Service Project OD-160, The Franklin Institute, November 1944. Div. 2-331-M1
13. *The Effect of Muzzle Brake Design on the Recoil of Guns, II*, Frank R. Simpson and Nicol H. Smith, OSRD 4477g, OTB 5g, December 1944. Div. 2-300-M1
14. *The Effect of Muzzle Brake Design on the Recoil of Guns, III*, Frank R. Simpson and Nicol H. Smith, OSRD 4820g, OTB 8b, March 1945. Div. 2-300-M1
15. *The Effect of Muzzle Brake Design on the Recoil of Guns, IV*, Frank R. Simpson and Nicol H. Smith, OSRD 4948a, OTB 9a, April 1945. Div. 2-300-M1
16. *The Effect of Muzzle Brake Design on the Recoil of Guns, V*, Frank R. Simpson and Nicol H. Smith, OSRD 5462a, OTB 13a, August 1945. Div. 2-300-M1
17. *The Effect of Muzzle Brake Design on the Recoil of Guns*, Frank R. Simpson and Nicol H. Smith, OSRD 6458, NDRC A-387, OEMsr-1368, Service Projects OD-160 and OD-154, The Franklin Institute, February 1946. Div. 2-331-M3
18. *On Dust Raised by a Gun Blast*, J. J. Slade, Jr., OSRD 4148j, OTB 2j, September 1944. Div. 2-300-M1
19. *On Dust Raised by a Gun Blast, II*, J. J. Slade, Jr., OSRD 4477c, OTB 5c, December 1944. Div. 2-300-M1
20. *A Method for Measuring and Recording the Degree of Target Obscuration*, R. D. Buhler, OSRD 4148h, OTB 2h, September 1944. Div. 2-300-M1
21. *On the Design of a Muzzle Blast Deflector*, J. J. Slade, Jr., OSRD 4357g, OTB 4g, November 1944. Div. 2-300-M1
22. *Interior Ballistics, I*, J. O. Herschfelder, R. B. Kershner, and C. F. Curtiss, OSRD 1238, NDRC A-142, OEMsr-51, Carnegie Institution of Washington. Div. 1-210.1-M2
23. *Third Report on Blast Deflectors for the Suppression of Dust*, J. J. Slade, Jr., OSRD 4720c, OTB 7c, February 1945. Div. 2-300-M1
24. *Fourth Report on Blast Deflectors for the Suppression of Dust*, J. J. Slade, Jr., and C. H. Fletcher, OSRD 5094c, OTB 10c, May 1945. Div. 2-300-M1

25. *Shadowgraph Study of Blast with Caliber .30 Blast Deflector*, R. D. Buhler, OSRD 5094f, OTB 10f, May 1945. Div. 2-300-M1
26. *Equipment for Studying Muzzle Blast Effects*, J. R. Bruman, OSRD 4077a, OTB 1a, August 1944. Div. 2-300-M1
27. *Preliminary Report on Blast Deflectors for the Suppression of Dust*, J. J. Slade, Jr., OSRD 4077b, OTB 1b, August 1944. Div. 2-300-M1
28. *Reduction of Smoke and Blast Effect*, S. Neal, OSRD 4077c, OTB 1c, August 1944. Div. 2-300-M1
29. *Effectiveness of Several Devices in Reducing Smoke and Blast Effect*, E. L. Robinson and S. Neal, OSRD 4148i, OTB 2i, September 1944. Div. 2-300-M1
30. *Second Report on Blast Deflectors for the Suppression of Dust*, Ray L. Kramer and J. J. Slade, Jr., OSRD 4258g, OTB 3g, October 1944. Div. 2-300-M1
31. *Investigation of Two New Types of Muzzle Attachments for Reduction of Dust Clouds*, R. D. Buhler, OSRD 4258h, OTB 3h, October 1944. Div. 2-300-M1
32. *Effects of Variations in Design Features in Performance of Dust Suppressors*, R. D. Buhler, OSRD 4357h, OTB 4h, November 1944. Div. 2-300-M1
33. *Dust Suppressor Design for 37-Mm Gun*, E. E. Sechler, OSRD 4477f, OTB 5f, December 1944. Div. 2-300-M1
34. *Effects of Height of Bore on Obscuration of Target when Blast Deflector is Used*, R. D. Buhler, OSRD 4607b, OTB 6b, January 1945. Div. 2-300-M1
35. *Empirical Investigation of Multibaffle Blast Deflectors*, R. D. Buhler, OSRD 4829a, OTB 8a, March 1945. Div. 2-300-M1
36. *Digest of Reports Concerning Muzzle Brakes*, H. M. Schwartz, OSRD 4357i, OTB 4i, November 1944. Div. 2-300-M1

Chapter 6

1. *A Brief History of Tapered Bore Guns*, John S. Purlew, NDRC A-43, OEMsr-51, Service Project OD-52, NDRC Division 1, Carnegie Institution of Washington, Apr. 17, 1942. Div. 1-330-M1
2. *Stability of Subcaliber Projectiles*, Charles L. Critchfield, NDRC A-88, OEMsr-51, Projects PA-260, OD-52, and NO-26, NDRC Division 1, Carnegie Institution of Washington, Sept. 8, 1942. Div. 1-510-M1
3. *On the Occurrence of Shatter*, Milne and Finchliffe, External Ballistic Department Report 30, Appendix to Ordnance Board Proceedings (British) 20,002.
4. Particular reference should be made to projects of the Armament Research Department, England, and the Army Technical Development Board, Canada.
5. *High Velocity Terminal Ballistic Performance of Caliber .30 Armor-Piercing Mark 2 Steel Cores*, Richard J. Emrich and C. W. Curtis, OSRD 3339, NDRC A-282, OEMsr-260, Projects OD-75 and P2-104, PUS, July 1944. Div. 2-210-M9
6. *Subcaliber Steel Projectiles*, C. W. Curtis and Richard J. Emrich, OSRD 4829d, NDRC OTB-8d, March 1945. Div. 2-300-M1
7. *Penetration Mechanism, III*, Report 4-44, U. S. Naval Proving Ground, April 1944.
8. *Tables for Computing the Mass, Center of Gravity, and Moments of Inertia of a Projectile with Tangent Ogival Nose*, C. Koksharova and C. W. Curtis, OSRD 6120d, NDRC OTB-14d. Div. 2-300-M1
9. *The Measurement of Forces Which Resist Penetration of STS Armor, Mild Steel, and 24ST Aluminum*, Report O-2276, U. S. Naval Research Laboratory.
10. *Interim Report on the Measurement of the Deceleration of a Shell Penetrating Armor Plate*, MOS/145/DJM, Ministry of Supply.
11. *An Electromagnetic Method for Measuring Projectile Velocity During Penetration*, Richard A. Beth and E. J. Schaefer, OSRD 5175, NDRC A-329, OEMsr-260, Service Projects CE-36 and NO-12, PUS, June 7, 1945. Div. 2-311-M3
12. *The Mechanics of Armor Perforation, Part I, Residual Velocity*, H. P. Robertson, OSRD 2043, NDRC A-227, OEMsr-260, Service Projects CE-5, NO-11, and others, PUS, November 1943. (A reissue of Report A-16 with corrections and with an addendum by A. H. Taub and C. W. Curtis.) Div. 2-210-M7
13. *Penetration Mechanism, II*, Report 3-44, U. S. Naval Proving Ground.
14. *A Double Pendulum for Use in Studies of the Ballistic Behavior of Armor*, George T. Reynolds and Ray L. Kramer, OSRD 686, NDRC A-52, NDCrc-34, OEMsr-260, Service Projects CE-5, NO-11, and others, PUS, July 1942. Div. 2-210-M1
15. *Sabot—Projectiles for Cannon*, W. D. Crozier, H. F. Dunlap, and others, OSRD 3010, NDRC A-234, NDRC Division 1, University of New Mexico, December 1943. Div. 1-510.1-M1
16. *Free Recoil of a Target and Its Effects on Stopping Power*, Walker Bleakney, Interim Report 17 CPPAB, National Research Council, June 1942. Div. 2-522-M4
17. *Theory of A Two Dimensional Ballistic Pendulum*, V. Rojansky, OSRD 606, NDRC A-66, NDCrc-34, OEMsr-260, Service Projects CE-5, NO-11, and others, PUS, July 1942. Div. 2-210-M2
18. *Short Base Line Projectile Velocity Measurements*, Richard J. Emrich and L. A. Delanasso, OSRD 927, NDRC A-89, OEMsr-260, Service Projects CE-5, NO-11, and others, PUS, October 1942. Div. 2-311-M1
19. *Projectile Velocity Measurements with Light Screens and Spiral Chronograph*, Richard J. Emrich and L. I. Shipman, OSRD 4918k, NDRC OTB-9k, April 1945. Div. 2-300-M1
20. *Thyratron Control of a Spark Discharge Applied to: I; A High-Speed Chronograph; II, Multiple Spark Photography*, C. A. Adams and C. A. Clemmow, Branch Report, RDC 8340/40, Research Department Ballistics, April 1941.
21. *Technique of Multiple Spark Photography Applied to Problems in Terminal Ballistics*, H. R. Calvert and J. Vennart, Terminal Ballistic Report 28/44, ARD, December 1944.
22. *A Further Report on the Application of Mathematical Principles to the Design of Projectiles*, Garnett and Bunting, Terminal Ballistics Report 89/42, ARD.
The Performance of Composite Rigid Projectiles Containing Cores of Various Weights, Garnett and Bunting, Terminal Ballistics Report 8/43, ARD.
Theory of the Composite A.P. Projectile, British Ordnance Board Proceedings, 19835.
23. *Interior Ballistics, Parts I-IV*, J. O. Hirschfelder, R. B. Kershner, and others, OSRD 1236, 1677, and 1740, NDRC A-142, A-180, A-294, and A-293, OEMsr-51, Service Projects OD-52, NO-23, and others, Carnegie Institution of Washington, 1943. Div. 1-310.1-M2
Interior Ballistics. Part V. The Performance of High-Velocity Guns, J. O. Hirschfelder, R. B. Kershner, and others, OSRD 1016, NDRC A-222, OEMsr-51, Service Projects OD-52, NO-23, and others, Carnegie Institution of Washington, October 1943. Div. 1-210.1-M5
Interior Ballistics. Part VI. Pressure-Travel Curves,

Richard E. Johnson, C. F. Curtiss, and R. B. Kershner, OSRD 3255, NDRC A-279, OEMsr-51, Service Projects OD-52, NO-23, and others, Carnegie Institution of Washington, June 1944. Div. 1-210.1-M7

24. *Tables for Interior Ballistics*, A. A. Bennett, Ordnance Department Document 2039, April 1921.
25. *Resistance Functions of Various Types of Projectiles*, Aberdeen Proving Ground, Report 27, BRL.
26. *Mechanism of Armor Penetration, Second Partial Report*, C. Zener and R. E. Peterson, Report 710/492, Watertown Arsenal, May 1943.
27. *Mechanism of Armor Penetration, First Partial Report*, C. Zener and J. H. Holloman, Report 710/454, Watertown Arsenal, September 1942.
28. *A Measurement of the Redistribution of Material in Armor upon Perforation*, Richard J. Emrich and Ray L. Kramer, OSRD 4258f, NDRC OTB-3f, October 1944. Div. 2-300-M1
29. *Penetration Mechanism, I*, Report 1-43, U. S. Naval Proving Ground.
30. *Penetration of Homogeneous Armor by 3-inch Flat-Nosed Projectiles*, Report 7-43, U. S. Naval Proving Ground.
31. *Attempt of a Theory of Armor Penetration*, H. A. Bethe, Frankford Arsenal Report, May 1911.
32. *Penetration of Armor by High Velocity Projectiles and Munroe Jets*, R. Hill, N. F. Mott, and D. C. Pack, Theoretical Research Report 13/44, ARD, March 1944.
33. *Penetration of Homogeneous Plate of One Tensile Strength (110,000 Psi) by 3-In. M79 AP Projectiles: Partial Report*, August 1944.
34. *Effect of Hardness in Plate Performance*, D. G. Sopwith, A. F. C. Brown, and V. M. Hickson, Second Progress Report on the effect of scale in armor penetration (British), A. P. P. Coordinating Subcommittee Paper 50, N. P. L. Engineering Division, February 1943.
35. *Firing Trials at Normal Attack with Geometrically Similar Shot against Homogeneous Armor of Varied Hardness*, A. F. C. Brown and V. M. Hickson, Third Progress Report on effect of scale in armor penetration (British), A. P. P. Coordinating Subcommittee Paper 79, N. P. L. Engineering Division, September 1944.
36. *The Optimum Hardness of Homogeneous Armor for Resistance to Perforation at Normal Attack by Projectiles of Different Sizes*, D. G. Sopwith, Fourth Progress Report on effect of scale in armor penetration (British), A. P. P. Coordinating Subcommittee Paper 80, N. P. L. Engineering Division, September 1944.
37. *The Ballistic Properties of Mild Steel at Normal Attack*, D. G. Sopwith, A. P. P. Coordinating Subcommittee Paper 84, N. P. L. Engineering Division (British), October 1944.
38. *The Ballistic Properties of Mild Steel, Including Preliminary Tests of Armor Steel and Dural*, OSRD 1027, NDRC A-111, OEMsr-230, Service Projects CE-5, NO-11, and others, Ballistics Research Group, PUS, November 1942. Div. 2-210-M4
39. *Ballistic Tests of STS Armor Plate Using 37-mm Projectiles*, Ralph J. Sluts, OSRD 1301, NDRC A-156, OEMsr-260, Service Projects CE-5, NO-11, and others, Ballistics Research Group, PUS, March 1943. Div. 2-210-M5
40. *Modified de Marre Formula: Analysis of AP Trials*, E. A. Milne, Appendix to British Ordnance Board Proceedings 26,399.
41. *Perforation Limits for Nonshattering Projectile against Thick Homogeneous Armor at Normal Incidence*, C. W. Curtis and Ray L. Kramer, OSRD 6164, NDRC A-393, OEMsr-260, Service Projects OD-75 and NO-111, PUS, March 1946. Div. 2-210-M10
42. *Ballistic Tests of Small Armor Plate for the Frankford Arsenal*, George T. Reynolds, Ray L. Kramer, and Walker Bleakney, OSRD 689, NDRC A-67, OEMsr-260, Service Projects CE-5, NO-11, and others, PUS, July 1942. Div. 2-210-M3
43. *Ninth Partial Report on Light Armor*, Report O-1778, U. S. Naval Research Laboratory, September 1941.
44. *The Penetration of Homogeneous Light Armor by Jacketed Projectiles at Normal Obliquity*, Report 14-43, U. S. Naval Proving Ground, July 1943.
45. *The Performance of Shot Against Plates*, Report 20, External Ballistic Department, British Ordnance Board Proceedings 14981, November 1942.
46. *The Testing of Metals in Compression at High Rates of Strain*, Frederick Seitz, Jr., OSRD 1383, NDRC A-174, OEMsr-825, Projects NO-11, NS-109, and P2-303, Carnegie Institute of Technology, April 1943. Div. 2-210-M6
47. *The Scale Effect in Static Penetration*, C. O. Baines, Terminal Ballistics, (British), Report 5/45, ARD, July 1945.
48. *Studies of Size Effect in Heavy Class B Armor Steel*, Progress Report, University of North Carolina, U. S. Naval Research Laboratory, May 1943.
49. *Second Progress Report on Size Effect in Slow Bend Tests of Ni-Cr Armor*, Report O-2245, U. S. Naval Research Laboratory.
50. *Third Progress Report on Size Effect in Slow Bend Test on Ni-Cr Steel*, Report O-2206, U. S. Naval Research Laboratory.
51. *Non-Ballistic Test for Armor Plate*, Maxwell Gensamo, C. S. Barrett, and others, OSRD 2041, NDRC M-87, OEMsr-417, Projects NRC-6 and OD-84, NDRC Division 18, Carnegie Institute of Technology, Nov. 3, 1943. Div. 18-201.1-M1
52. *Principles of Projectile Design for Penetration; Sixth Partial Report*, D. M. Van Winkle, Watertown Arsenal Report 702/231/6, October 1944.
53. *A Statistical Study of the Shatter Velocity of Projectiles at Hypervelocities*, Richard J. Emrich and A. M. Mood, OSRD 4357a, NDRC OTB-2a, September 1944. Div. 2-300-M1
54. *Principles of Armor Protection: Fourth Partial Report*, C. Zener and J. F. Sullivan, Watertown Arsenal Report 710/607/3, June 1944.
55. *Note on Shatter of Shot at Normal Impact—Effect of Hardness of Plate*, H. R. Calvert and J. Vennart, Terminal Ballistic Report 15/44, ARD, June 1944.
56. *The Performance, at High Velocity, of .55-In. AP/CR Tungsten Carbide Core Bullets Against I. T. 80 Plate*, J. T. Harris, Terminal Ballistics Report 4/45, ARD, June 1945.
57. *Terminal Ballistics of Tungsten Carbide Projectiles: Mechanical Strength of Core Material*, C. W. Curtis and Ray L. Kramer, OSRD 6465, NDRC A-394, OEMsr-260, Service Project OD-75, PUS, March 1946. Div. 2-322-M1
58. *Terminal Ballistics of Tungsten Carbide Projectiles: Body Failures*, C. W. Curtis, OSRD 6340, NDRC A-476.
59. *Terminal Ballistics of Tungsten Carbide Projectiles: Length Test*, C. W. Curtis, Richard J. Emrich, and Ray L. Kramer, OSRD 6466, NDRC A-395, OEMsr-260, Service Project OD-75, PUS, March 1946. Div. 2-322-M2
60. *The Effect of Nose Shape on the Ballistic Performance of 15-Lb 3-In. AP Solid Shot Against Homogeneous Armor*, Report 2-43, U. S. Naval Proving Ground.

61. *Terminal Ballistics of Tungsten Carbide Projectiles: Survey and Nose-Shape Tests*, C. W. Curtis, Richard J. Emrich and J. Sproule, OSRD 4720b, NDRC OTB-7b, February 1945. Div. 2-300-M1
62. *Shatter of Caliber .80 Monobloc Steel Projectiles*, Richard J. Emrich, OSRD 4148c, NDRC OTB-2c, September 1944. Div. 2-300-M1
63. *Principles of Projectile Design for Penetration: First Partial Report*, C. Zener and R. E. Peterson, Report 762/231, Watertown Arsenal, October 1943.
64. *Oblique Impact with Tungsten Carbide Projectiles*, C. W. Curtis, OSRD 4948i, NDRC OTB-9i, April 1945. Div. 2-300-M1
65. *Effect of Armor-Piercing Cap on Perforation Limits*, C. W. Curtis and Richard J. Emrich, OSRD 5004g, NDRC OTB-10g, May 1945. Div. 2-300-M1
66. *Comparison of Capped and Monobloc Steel Projectiles at Hypervelocities*, Richard J. Emrich, J. Sproule, and C. W. Curtis, OSRD 4258e, NDRC OTB-3e, October 1944. Div. 2-300-M1
67. *Capped Projectiles at Hypervelocities*, Richard J. Emrich, OSRD 4077f, NDRC OTB-1f, August 1944. Div. 2-300-M1
68. *Terminal Ballistics of Tungsten Carbide Projectiles: Effect of Carrier, Part I*, E. R. Jones, C. W. Curtis, and Richard H. Emrich, OSRD 5370a, NDRC OTB-12a, July 1945. Div. 2-300-M1
69. *Terminal Ballistics of Tungsten Carbide Projectiles: Effect of Carrier, Part II*, Richard J. Emrich, OSRD 6407, NDRC A-396, OEMsr-260, Service Projects OD-75 and NO-11, PUS, March 1946. Div. 2-322-M3
70. British Ordnance Board Proceedings Q3369.
71. British Ordnance Board Proceedings Q3173.

Chapter 7

1. *Final CFD Report*, John E. Burchard, National Research Council, December 1944, (on the program of research conducted by the Committee for the Corps of Engineers, U.S. Army, summarizing the work of the Committee on Fortification Design and the Committee on Passive Protection Against Bombing). Div. 2-530-M2
2. *Terminal Ballistics*, H. P. Robertson, CPPAB, National Research Council, January 1941. Div. 2-200-M1
3. *Final CPPAB Report, Part I*, for year ending June 1941.
4. *Penetration of Projectiles in Concrete*, Richard A. Beth, Interim Report 3, CPPAB, National Research Council, November 1941. Div. 2-220-M1
5. *AP Bomb Test—Comment*, Richard A. Beth, Interim Report 9, CPPAB, National Research Council, April 1942. Div. 2-220-M2
6. *A Brief Summary of Recent Data on Penetration in Concrete at Various Scales*, Richard A. Beth, Interim Report 18, CPPAB, National Research Council, June 1942. Div. 2-220-M3
7. *Penetration and Explosion Tests on Concrete Slabs, Report I: Data*, Richard A. Beth and J. Gordon Stipe, Jr., Interim Report 20, CPPAB, National Research Council, January 1943. Div. 2-220-M5
8. *Penetration and Explosion Tests on Concrete Slabs, Report II: Crater Profiles*, J. Gordon Stipe, Jr., Interim Report 21, CPPAB, National Research Council, January 1943. Div. 2-220-M6
9. *Resistance of Laminated Concrete Slabs to Perforation*, Robert J. Hansen, Interim Memorandum M-9, CPPAB, National Research Council, May 1943. Div. 2-220-M7
10. *Terminal Ballistics and Explosive Effects*, John E. Burchard, CFD, National Research Council, October 1943. Div. 2-200-M2
11. *Concrete Properties Survey, Effect of Concrete Properties on Penetration Resistance*, Richard A. Beth, J. Gordon Stipe, Jr., Marinus E. DeReus, and John T. Pittenger, Interim Report 27, CFD, National Research Council, July 1944. Div. 2-220-M11
Concrete Properties Survey, Preparation and Physical Tests of Concrete, Marinus E. DeReus, Interim Report 27, Appendix A, CFD, National Research Council, June 30, 1944. Div. 2-220-M12
Concrete Properties Survey, Penetration Data, Richard A. Beth, J. Gordon Stipe, Jr., and John T. Pittenger, Interim Report 27, Appendix B, CFD, National Research Council, June 30, 1944. Div. 2-220-M13
12. *Ballistics Tests on Small Concrete Slabs*, J. Gordon Stipe, Jr., Marinus E. DeReus, John T. Pittenger, and Robert J. Hansen, Interim Report 28, CFD, National Research Council, June 30, 1944. Div. 2-220-M14
Ballistics Tests on Small Concrete Slabs, Tables of Data, J. Gordon Stipe, Jr., Marinus E. DeReus, John T. Pittenger, and Robert J. Hansen, Interim Report 28, Appendix A, CFD, National Research Council, June 30, 1944. Div. 2-220-M15
13. *Repeated Fire and Edge Fire Effects on Small Concrete Slabs*, J. Gordon Stipe, Jr., Interim Memorandum M-12, CFD, National Research Council, July 1944. Div. 2-220-M18
14. *Composite Slabs*, J. Gordon Stipe, Jr., Interim Memorandum M-13, CFD, National Research Council, June 30, 1944. Div. 2-220-M17
15. *Penetration Theory: Estimates of Velocity and Time During Penetration*, Richard A. Beth, OSRD 4720, NDRC OTB-7, Feb. 15, 1945. Div. 2-300-M1
16. *Concrete Penetration*, Richard A. Beth, OSRD 4856, NDRC A-310, OEMsr-260, Service Projects OD-75 and NO-11, PUS, Mar. 20, 1945. Div. 2-220-M21
17. *An Electromagnetic Method for Measuring Projectile Velocity during Penetration*, Richard A. Beth, and E. J. Schaefer, OSRD 5175, NDRC A-320, OEMsr-260, Service Projects CE-36, and NO-12, PUS, June 7, 1945. Div. 2-311-M3
18. *Penetration Theory: Separable Force Laws and the Time of Penetration*, Richard A. Beth, OSRD 5253, NDRC A-353, OEMsr-260, Service Projects CE-36 and NO-12, PUS, June 28, 1945. Div. 2-311-M3
19. *Ballistic Tests on Concrete Slabs, Part II. Effect of Nose Shape*, J. Gordon Stipe, Jr., OSRD 6038, NDRC A-112M, OEMsr-260, Service Projects GD-75, CE-36, and NO-11, PUS, March 1946. Div. 2-220-M33
20. *Concrete Penetration*, Richard A. Beth, OSRD 6460, NDRC A-388, OEMsr-260, Service Projects OD-75 and NO-11, PUS, March 1946. Div. 2-220-M24
21. *Report on AP Projectile Tests on Large Concrete Slabs Conducted at Fort Cronkhite, California*, U. S. Engineer Office, San Francisco District, May 1942.
22. *Discussion of Recent British Papers on Penetration in Concrete*, Richard A. Beth, OEMsr-260, PUS, Oct. 6, 1943. Div. 2-220-M19
23. *Comment on Concrete Penetration Equations*, J. Gordon Stipe, Jr., OEMsr-260, Technical Memorandum PTM-23, PUS, Aug. 14, 1944. Div. 2-220-M19
24. *Remarks on Fortification Design*, A. H. Taub and Walker Bleakney, Interim Memorandum M-10, CFD, National Research Council, November 1944. Div. 2-530-M1
25. "Action and Effects of Bombs," Part 13, *Civil Protection*, Sweedy and Hamann, London, 1939.

26. *Tests and Design of Bombproof Structures of Reinforced Concrete*, C. A. Trexel, Bureau of Yards and Docks, Navy Department, Sept. 30, 1941.
27. *AP Bomb Test, Protection Tests*, Bulletin No. 3, Office of the Chief of Engineers, War Department.
28. *Projectile and Bomb Penetration in Concrete and Steel (Introduction)*, Information Bulletin 135, Office of the Chief of Engineers, Army Service Forces, Nov. 11, 1943.
29. *Bomb Tests on Building Prototype*, Technical Bulletin TB Eng 6, War Department, Feb. 7, 1944.
30. *First Partial Report on Test of German Type Concrete Pillboxes, and First Report on Ordnance Program No. 5937*, Army Ordnance Department, Aberdeen Proving Ground, June 7, 1943.
Second Report on Test of German Type Concrete Pillboxes and Second Report on Ordnance Program No. 5937, Army Ordnance Department, Aberdeen Proving Ground, July 12, 1943.
Third Report on Test of German Type Concrete Pillboxes and Third Report on Ordnance Program No. 5937, Army Ordnance Department, Aberdeen Proving Ground, Aug. 21, 1943.
Fourth Report on Test of German Type Concrete Pillboxes and Fourth Report on Ordnance Program No. 5937, Army Ordnance Department, Aberdeen Proving Ground, Jan. 27, 1944.
31. *Effect of Projectiles on Concrete Pillboxes*, Technical Bulletin TB ENG 2, War Department, December 1943.
32. *First Partial Report on Development of Fuze, Nose, Concrete Penetration, T-105, for Anti-concrete Projectiles, and First Report on Ordnance Program No. 6071*, Army Ordnance Department, Aberdeen Proving Ground, Jan. 24, 1944.
Second Report on Development of Fuze, Nose, Concrete Piercing, T-105 for Anti-Concrete Projectiles, and Third Report on Ordnance Program No. 6071, Army Ordnance Department, Aberdeen Proving Ground, Mar. 14, 1944.
33. *The Design of Bombproof Structures*, notes reference R. C. 392 and Bulletin A.6, Ministry of Home Security, Research and Experiments Department.
34. *Estimated Penetration of AP Bombs into Concrete*, ARD Explosives Report 72/43, Anti-Concrete Committee, Advisory Council on Scientific Research, Ministry of Supply, March 1943.
35. *Attack of Concrete*, Proceedings of the Ordnance Board Q1378, June 22, 1943.
36. *General Formula for Penetration of Projectiles into Concrete*, Proceedings of the Ordnance Board Q2312, June 1944.
37. *Penetration of Projectiles into Concrete: Velocity at Any Point of the Path*, Research and Experiments Department, Ministry of Home Security, June 1944, (revised December 1944).
38. *First Interim Report on Concrete for Defense Works*, Report for the Ministry of Supply, Note MOS/16, Department of Scientific and Industrial Research, RRL, April 1941.
39. *Second Interim Report on Concrete for Defense Works, Protection Against 0.303-In. Armour-Piercing Bullets*, Report to the Ministry of Supply, Note MOS/20/ACW, HWWP, Department of Scientific and Industrial Research, RRL, July 1941.
40. *Fourth Interim Report on Concrete for Defense Works, the Use of Model Targets and Projectiles in Penetration Tests*, Report to the Ministry of Supply, Note MOS/26/ACW.HWWP, Department of Scientific and Industrial Research, RRL, October 1941.
41. *Fifth Interim Report on Concrete for Defense Works, Tests on Model Targets to Investigate a Proposed Design for Strengthening Existing Reinforced Concrete Pill-Boxes to Withstand 6-Pr. Attack*, Report to the Ministry of Supply, Note MOS/44/ACW.HWWP, Department of Scientific and Industrial Research, RRL, December 1941.
42. *Sixth Interim Report on Concrete for Defense Works—Reinforced Concrete to Resist 6-Pr. Attack, Model Tests*, Report to the Ministry of Supply, Note MOS/72/CW.HWWP, Department of Scientific and Industrial Research, RRL, March 1942.
43. *Seventh Interim Report on Concrete for Defense Works—Concrete to Resist Multiple 6-Pr. Attack—Detailed Results of Model Tests*, Report to the Ministry of Supply, Note MOS/84/ACW.HWWP, Department of Scientific and Industrial Research, RRL, April 1942.
44. *Eighth Interim Report on Concrete for Defense Works, Preliminary Tests to Determine the Connexion between the Striking Velocity of AP Shot and Their Penetration into Plain Concrete*, Report to the Ministry of Supply, Note MOS/106/ACW, RRL, May 1942.
45. *Ninth Interim Report on Concrete for Defense Works—Full-Scale Targets on Reinforced Concrete Designed to Resist Multiple 6-Pr. Attack and Their Relation to Model Tests*, Report to the Ministry of Supply, Note MOS/107/ACW.HWWP, Department of Scientific and Industrial Research, RRL, May 1942.
46. *Tenth Interim Report on Concrete for Defense Works—Reinforced Concrete to Resist the Attack of Mortar Bombs*, Report to the Ministry of Supply, Note MOS/109/ACW, Department of Scientific and Industrial Research, RRL, June 1942.
47. *Thirteenth Interim Report on Concrete for Defense Works, Summary of the Position of Experimental Work, General Experimental Relationships*, Extra-Mural Research F. 72/212, Note MOS/223/ACW, Anti-Concrete Committee, Advisory Council on Scientific Research and Technical Development, RRL, April 1, 1943.
48. *Fourteenth Interim Report on Concrete for Defense Works—Thicknesses of Reinforced Concrete Necessary to Resist Certain Forms of Attack*, Extra-Mural Research F.72/212, Note MOS/224/ACW, Anti-Concrete Committee, Advisory Council on Scientific Research and Technical Development, RRL, April 1943.
49. *Sixteenth Interim Report on Concrete for Defense Works—The Penetration of Oblique Shot*, Extra-Mural Research F.72/212, Note MOS/234/ACW, Anti-Concrete Committee, Advisory Council on Scientific Research and Technical Development, RRL, July 1943.
50. *Seventeenth Interim Report on Concrete for Defense Works—The Effect of Sectional Density on the Penetration Into Concrete of AP Shot and the Derivation of a General Penetration Formula*, Extra-Mural Report F.72/212, Note MOS/311/ACW, Anti-Concrete Committee, Advisory Council on Scientific Research and Technical Development, RRL, February 1944.
51. *Twentieth Interim Report on Concrete for Defense Works—The Penetration Characteristics of the German 15 Cm. Anti-Concrete Shell*, Extra-Mural Research F.72/212, Note MOS/363/ACW, Anti-Concrete Committee, Advisory Council on Scientific Research and Technical Development, RRL, June 1944.
52. *Twenty-First Interim Report on Concrete for Defense Works—Summary of Experimental Results Obtained During Period May 1943 to May 1944*, Extra-Mural Research F.72/212, Note MOS.E.355/ACW, Anti-Concrete Committee, (Projectile Penetration), Advisory Council on Scientific Research and Technical Development, RRL, May 1944.

53. *Twenty-Second Interim Report on Concrete for Defense Works—Suggestions for Further Experiments on the Penetration of Projectiles*, Extra-Mural Research P.72/212, Note MOS/369/ACW, Anti-Concrete Committee, Advisory Council on Scientific Research and Technical Development, RRL, June 1944.
54. *Contact Explosions on Concrete*, Donald G. Kretsinger, Interim Report 29, CFD, National Research Council, June 30. Div. 2-220-M16
55. "German Hollow Charge Shells and Bombs," *Tactical and Technical Trends*, No. 45, Apr. 1, 1944, pp. 33-37.
56. *Summary of Tests on Breaching of Walls by Gunfire*, A. A. Ziegler, Jr., Technical Memorandum PTM-24, OEMsr-260, Research Project P2-204, PUS, May 4, 1944. Div. 2-220-M10
57. "German Anti-Concrete Shell," *Tactical and Technical Trends*, No. 18, Feb. 11, 1943, p. 23.
58. *Electricity and Magnetism*, Third Edition, Article 718, Vol. II, pp. 358-359.

Chapter 8

1. *The Probability of Perforation of Plastic Protection by Caliber .30 Armor-Piercing Mark 2 Bullets*, Lincoln G. Smith, OSRD 3231, NDRC A-246, OEMsr-260, Service Projects CE-5, NO-11, and others, PUS, February 1944. Div. 2-230-M1
2. *The Resistance of Welded Unit-Construction-Plates to Attack by Grenades, Mortar Bombs, and Rifle Bullets*, Report to the Ministry of Supply MOS/121/ACW/DBW., Department of Scientific and Industrial Research, RRL, July 1942.
3. *Armor Using Plastic and Composite Materials*, OSRD 3042, NDRC A-272, OEMsr-213, Service Projects CE-5, NO-11, and others, The Polaroid Corporation, May 1944. Div. 2-230-M2

Chapter 9

1. *Penetration in Soils*, J. Gordon Stipe, Jr., Interim Report 30, CFD, National Research Council, July 1944. Div. 2-240-M7
2. *The Penetration of Projectiles into Chalk, Clay, Sand and Shingle*, OSRD Liaison Office WA-2738-9, Report to the Ministry of Supply, Note MOS/359/ACW, AC-6523/C152, Department of Scientific and Industrial Research, RRL, June 1944.
3. *Second Report on the Penetration of Projectiles into Soil*, OSRD Liaison Office WA-4116-12, Report to the Ministry of Supply, Note MOS/429/ACW.HLDP.KLCF, AC-7880/C229, Department of Scientific and Industrial Research, RRL, February 1945.
4. *Composite Slabs*, J. Gordon Stipe, Jr., Interim Memorandum M-13 CFD, National Research Council, June 30, 1944. Div. 2-220-M17
5. *Bombs, Aircraft*, OSRD Liaison Office WA-841-14C, Proceedings of the Ordnance Board Q 95, A.M.S./33,433, January 6, 1939.
6. *Penetration of Bombs and Shells (Other than Incendiary Bombs)*, OSRD Liaison Office W-127-2q, Data Compilation 17, Research and Experiments Branch, A.R.P. Department, Ministry of Home Security, 1941.
7. *Tests on Bombproof Structures, Burster Courses and Building Prototype*, (located at Area "H," Edgewood Arsenal, Maryland), U. S. Engineer Office, Baltimore, 1941.
8. *Field Fortifications*, Engineer Field Manual FM5-15, Table VI, War Department, 1940, p. 48.
9. *Terminal Ballistics*, H. P. Robertson, CPPAB, National Research Council, January 1941. Div. 2-200-M1
10. *Terminal Ballistics and Explosive Effects*, John H. Burchard, CPPAB, National Research Council, Oct. 1, 1943. Div. 2-200-M2

Chapter 10

1. *The Frangible Bullet for Use in Aerial Gunnery Training*, P. M. Gross, OSRD 6625, NDRC A-473, Duke University, March 1946.
2. *Deformable Projectiles for Flexible Gunnery Training*, OSRD 1788, NDRC A-210, OEMsr-260 and OEMsr-1284, Research Project P2-105, PUS, and Duke University, BRL, September 1943. Div. 2-321-M1
3. *Characteristics of Frangible Projectiles Suitable for Flexible Gunnery Training*, Marcus E. Hobbs and P. M. Gross, OSRD 4077d, OT3-1d, Duke University, August 1944. Div. 2-300-M1
4. *Velocity-Loss and Time-of-Flight Measurements of Frangible Projectiles*, C. W. Curtis, Richard J. Emrich, and Ray L. Kramer, OSRD 4077e, OTB-1e, PUS, August 1944. Div. 2-300-M1
5. *Temperature Effect on the Frangible Projectile Round and Armor, and the Influence of Lead Characteristics on the Properties of the Projectile: Part I*, A. J. Weith, Jr. and J. H. Saylor; *Part II*, A. J. Weith, Jr., and H. Scheraga, OSRD 4357b, OTB-4b, Duke University, November 1944. Div. 2-300-M1
6. *The Effect of Different Molding Conditions and Accelerated Aging Tests on the Limit Impact Velocity of the T44 Frangible Projectile*, A. J. Weith, Jr. and J. H. Saylor, OSRD 4607a, OTB-6a, Duke University, January 1945. Div. 2-300-M1
7. *Armor Penetration and Impact Strength of Frangible Projectiles*, K. Jeffers, Marcus E. Hobbs, and C. Deal, OSRD 4148a, OTB-2a, Duke University, September 1944. Div. 2-300-M1
8. *Damage Tests with Caliber .50 Frangible Projectile*, Ray L. Kramer and C. W. Curtis, OSRD 4148b, OTB-ab, Princeton University, September 1944. Div. 2-300-M1
9. *Armor for Use Against Frangible Projectiles and Powders for the Frangible Projectile Round: Part I*, Marcus E. Hobbs, A. J. Weith, Jr. and H. Scheraga; *Part II*, A. J. Weith, Jr. and Marcus E. Hobbs, OSRD 4258a, OTB-3a, Duke University, October 1944. Div. 2-300-M1
10. *The Effect of Moisture Content of DuPont No. 4759 Smokeless Powder on the Average Muzzle Velocity of the T44 Round*, Marcus E. Hobbs and A. J. Weith, Jr., OSRD 4329c, OTB-8c, Duke University, March 1945. Div. 2-300-M1
11. *Preliminary Investigation of the Muzzle Velocity of the T44 Projectile When Fired Through Machine-Gun Barrels with Different Histories*, A. J. Weith, Jr. and J. H. Saylor, OSRD 4477b, OTB-5b, Duke University, December 1944. Div. 3-300-M1
12. *The Effect of Projectile Diameter on the Average Muzzle Velocity for the T44 Projectile*, A. J. Weith, Jr., J. H. Saylor, and Marcus E. Hobbs, OSRD 4720c, OTB-7c, Duke University, February 1945. Div. 2-300-M1
13. *The Effect of Temperature on the Muzzle Velocity of Several Production Lots of T44 Ammunition*, B. C. Eastham and A. J. Weith, Jr., OSRD 4648c, OTB-9c, Duke University, April 1945. Div. 2-300-M1
14. *Additional Investigation of the Effect of Temperature on the Muzzle Velocity of the T44 Ammunition*, A. J. Weith, Jr., OSRD 5220c, OTB-11c, Duke University, June 1945. Div. 2-300-M1

15. *A Further Investigation of the Effect of Projectile Diameter on the Average Muzzle Velocity of the T44 Projectile*, B. C. Eastham and A. J. Weith, Jr., OSRD 10h, Duke University, May 1945.
16. *Development of the Henderson Instructor's Turret*, M. E. Hobbs, J. H. Saylor, and others, OSRD 5220d, OTB-11d, Duke University, June 1945. Div. 2-300-M1
17. *Calculated Leads for Aerial Gunners Using the API-M8 Caliber .50 Projectile and the T44 Caliber .30 Frangible Projectile*, H. Scheraga and Marcus E. Hobbs, OSRD 4720d, OTB-7d, Duke University, February 1945. Div. 2-300-M1
18. *Calculated Leads for Aerial Gunners Using the API-M8 Caliber .50 Projectile and the T44 Caliber .30 Frangible Projectile for Parallel Flight Case*, H. A. Scheraga and Marcus E. Hobbs, OSRD 4948b, OTB-9b, Duke University, April 1944. Div. 2-300-M1
19. *Calculated Leads for Aerial Gunners Using the API-M8 Caliber .50 Projectile and the T44 Caliber .30 Frangible Projectile, III*, G. E. Bowden and H. A. Scheraga, OSRD 5350g, OTB-12g, July 1945. Div. 2-300-M1
20. *Calculated Leads for Aerial Gunners Using the API-M8 Caliber .50 Projectile and T44 Caliber .30 Frangible Projectile, IV*, G. E. Bowden and H. A. Scheraga, OSRD 5350h, OTB-12h, Duke University, July 1945. Div. 2-300-M1
21. *Calculated Leads for Aerial Gunners Using the API-M8 Caliber .50 Projectile and the T44 Caliber .30 Projectile*, G. E. Bowden and H. A. Scheraga, OSRD 5462b, OTB-13b, Duke University, August 1945. Div. 2-300-M1
22. *Calculated Leads for Aerial Gunners Using the API-M8 Caliber .50 Projectile and the T44 Caliber .30 Frangible Projectile*, G. E. Bowden and Marcus E. Hobbs, OSRD 6120a, OTB-14a, Duke University, October 1945. Div. 2-300-M1

Chapter 11

1. *The Model Supersonic Wind-Tunnel Project*, Allen E. Puckett, OSRD 3560, NDRC A-269, NDCrc-36, Projects OD-24, NO-3, and P2-401, California Institute of Technology, May 1944. Div. 2-410-M4
Proposal and Tentative Plans for a Supersped Wind Tunnel, Theodor von Kármán, OSRD 13, NDRC A-9, California Institute of Technology, July 1941. Div. 2-410-M1
The Supersped Wind Tunnel, Theodor von Kármán, OSRD 14, NDRC A-10, Service Project OD-24, California Institute of Technology, September 1941. Div. 2-410-M2
The Model Supersonic Wind Tunnel, Theodor von Kármán, OSRD 510, NDRC A-38, NDCrc-36, Service Project OD-24, California Institute of Technology, April 1942. Div. 2-410-M3
2. "Gasdynamik," A. Busemann, *Handbuch der Experimental Physik*, Vol. 4, Part 1, 1931.
3. "Conversion of the Stanton 3-In. High Speed Wind Tunnel to the Open Jet Type," A. Bailey and S. A. Wood, *Proceedings of the Institute of Mechanical Engineers*, London, Vol. 135, 1937, pp. 445-466.
4. "Nozzles for Supersonic Flow Without Shock Fronts," Ascher H. Shapiro, *Journal of Applied Mechanics*, Vol. 2, No. 2, June 1944.

Chapter 12

1. "Effects of Momentary Stresses in Metals," Bertram Hopkinson, *Proceedings of the Royal Society of London*, Vol. 74, 1904.
2. *Zwanglose Mitteilungen des Deutsches Verbandes für Materialprüfung*, F. Körber, No. 8, 1926, p. 91.
3. "The Yield Point of Mild Steel," C. W. MacGregor, *Transactions of the American Society of Mechanical Engineers*, Vol. 53, 1931.
4. "The Influence of Rate of Deformation on the Tensile Test with Special Reference to the Yield Point in Iron and Steel," C. F. Elam, *Proceedings of the Royal Society of London*, Vol. 165, 1933, p. 568.
5. "The Effect of the Speed of Stretching and the Rate of Loading in the Yielding of Mild Steel," E. A. Davis, *Transactions of the American Society of Mechanical Engineers*, Vol. 60, 1938.
6. "High Speed Tension Tests at Elevated Temperatures," Parts II and III, A. Nadai and M. J. Manjoine, *Transactions of the American Society of Mechanical Engineers*, Vol. 63, 1941.
7. "High Velocity Tension Impact Tests," H. C. Mann, *Proceedings of the American Society of Testing Materials*, Vol. 36, 1936, p. 85.
8. "The Influence of Impact Velocity on the Tensile Characteristics of Some Aircraft Metals and Alloys," Donald S. Clark, Technical Note 868, National Advisory Committee for Aeronautics, October 1942.
9. "Stress-Strain Relations Under Tention Impact Loading," Donald S. Clark and G. Dätwyler, *Proceedings of the American Society of Testing Materials*, Vol. 38, 1938, p. 93.
10. "Rapid Tension Tests Using the Two-Load Method," Deforest, C. W. MacGregor, and Anderson, *Metals Technology*, December 1941.
11. "Influence of Rate of Strain and Temperature on Yield Stresses of Mild Steel," M. J. Manjoine, *Journal of Applied Mechanics, Transactions of the American Society of Mechanical Engineers*, Vol. 66, 1944.
12. "Über die Fortpflansung Ebener Luftwellen von Endlichen Schwingungsweite," B. Riemann, *Abhandlungen Gesellschaft der Wissenschaften zu Göttingen*, Math-Phys., Vol. 8, 1860, p. 43, or *Collected Works*, 1876, p. 144.
13. "Longitudinal Wave Transmission and Impact," L. H. Donnell, *Transactions of the American Society of Mechanical Engineers*, Vol. 52, 1930, p. 153.
14. *On the Propagation of Plastic Deformation in Solids*, Theodor von Kármán, OSRD 365, NDRC A-29, Service Projects CE-5 and CE-6, January 1942. Div. 2-430-M1
15. *Preliminary Experiments on the Propagation of Plastic Deformation*, Pol E. Duwes, OSRD 380, NDRC A-33, Service Projects CE-5 and CE-6, February 1942. Div. 2-430-M2
16. *The Permanent Strain in a Uniform Bar Due to Longitudinal Impact*, Merit P. White and LeVan Griffis, OSRD 742, NDRC A-71, Service Projects CE-5, NO-11, and others, July 1942. Div. 2-434-M1
17. *Comments on White and Griffis' Theory of the Permanent Strain in a Uniform Bar Due to Longitudinal Impact*, H. F. Bohnenblust, OSRD 781, NDRC A-47M, Service Projects CE-5, NO-11, and others, August 1942. Div. 2-434-M2
18. *Propagation of Plastic Waves, A Comparison of Reports NDRC A-29 and RC-329*, H. F. Bohnenblust, OSRD 910, NDRC A-53M, OEMsr-343, Service Projects CE-5, NO-11, and others, California Institute of Technology, September 1942. Div. 2-433-M1
19. *The Plastic Wave in a Wire Extended by an Impact Load*, G. I. Taylor, RC-320, June 1942.
20. *A Note on von Kármán's Theory of the Propagation of Plastic Deformation in Solids*, H. F. Bohnenblust, OSRD 684, NDRC A-41M, OEMsr-260, Service Projects CE-5, NO-11, and others, PUS, June 1942. Div. 2-430-M4

21. *Addendum to von Kármán's Theory of the Propagation of Plastic Deformation in Solids*, C. Zener, and J. H. Hollomon, OSRD 859, NDRC A-37M, Service Projects CE-5 and CE-6, June 1942. Div. 2-430-M3

22. *The Propagation of Plastic Waves in Tension Specimens of Finite Length; Theory and Methods of Integration*, Theodor von Kármán, H. F. Bohnenblust, and D. H. Hyers, OSRD 942, NDRC A-103, OEMsr-348, Service Projects CE-5, NO-11, and others, California Institute of Technology, October 1942. Div. 2-433-M2

23. *Graphical Solutions for Problems of Strain Propagation in Tension*, H. F. Bohnenblust, Joseph V. Charyk, and D. H. Hyers, OSRD 1204, NDRC A-131, OEMsr-348, Service Projects CE-5, NO-11, and others, California Institute of Technology, January 1943. Div. 2-434-M6

24. *The Behavior of Longitudinal Stress Waves Near Discontinuities in Bars of Plastic Material*, LeVan Griffis, OSRD 1799, NDRC A-212, Projects NO-11, NS-109, and P2-303, September 1943. Div. 2-434-M8

25. *Discussion of Energy Measurements in Tension Impact Tests at the California Institute of Technology*, Pol E. Duwez, Donald S. Clark, and D. S. Wood, OSRD 1829, NDRC A-217, OEMsr-348, Projects NO-11, NS-109, and P2-303, California Institute of Technology, September 1943. Div. 2-432-M1

26. *Wave Propagation in a Uniform Bar Whose Stress-Strain Curve Is Concave Upward*, Merit P. White and LeVan Griffis, OSRD 1302, NDRC A-152, Projects NO-11, NS-109, and P2-303, March 1943. Div. 2-434-M7

27. *The Force Produced by Impact of a Cylindrical Body*, Merit P. White, OSRD 1285, NDRC A-157, Projects NO-11, NS-109, and P2-303, March 1943. Div. 2-431.22-M2

28. *The Propagation of Plastic Strain in Compression*, Pol E. Duwez, Donald S. Clark, and H. E. Martens, OSRD 3886, NDRC M302, OEMsr-348, Projects NS-109 and NRC-82, California Institute of Technology, July 7, 1944. Div. 18-902.11-M6

29. *Theory, Calibration, and Use of Diaphragm Blast Meters*, W. T. Read, OSRD 6403, NDRC A-392, OEMsr-260, Service Project OD-03, PUS, March 1946. Div. 2-111.12-M5

30. *The Behavior of Long Beams under Impact Loading*, Pol E. Duwez, Donald S. Clark and H. F. Bohnenblust, OSRD 1028, NDRC A-216, OEMsr-348, Projects NO-11, NS-109, and P2-303, California Institute of Technology, September 1943. Div. 2-420-M3

31. *The Behavior of Clamped Beams under Impact Loading*, Pol E. Duwez, H. E. Martens and Donald S. Clark, OSRD 4043, NDRC M-338, OEMsr-348, Projects NS-109 and NRC-82, California Institute of Technology, Aug. 16, 1944. Div. 18-902.13-M6

32. *Applications des Potentiels*, Boussinesq, Paris, 1885.

33. *Deflection and Perforation of Steel Plates at Impact Velocities up to 150 Feet per Second*, Pol E. Duwez, D. S. Wood, and Donald S. Clark, OSRD 1402, NDRC A-175, OEMsr-348, Projects NO-11, NS-109, and P2-303, California Institute of Technology, April 1943. Div. 2-434.11-M3

34. *On the Static and Dynamic Plastic Bending of Plates*, D. H. Hyers, OSRD 2018, NDRC A-228, OEMsr-348, Projects NO-11, NS-109, and P2-303, California Institute of Technology, November 1943. Div. 2-431.1-M1

35. *The Behavior of Large Plates under Impact Loading*, Pol E. Duwez, Donald S. Clark, D. S. Wood and D. H. Hyers, OSRD 3202, NDRC A-254, OEMsr-348, Projects NO-11, NS-109, and P2-303, California Institute of Technology, February 1944. Div. 2-420-M5

36. *On the Propagation of the Plastic Deformation Produced by an Expanding Cylinder*, James S. Koehler and Frederick Seitz, Jr., OSRD 1214, NDRC A-139, OEMsr-336, Service Projects CE-5, NO-11, and others, University of Pennsylvania, January 1943. Div. 2-431.22-M1

37. *The Stress Waves Produced in a Plate by a Plane Pressure Pulse*, James S. Koehler and Frederick Seitz, Jr., OSRD 3230, NDRC A-245, OEMsr-825, Projects NO-11, NS-109, and P2-303, Carnegie Institute of Technology, February 1943. Div. 2-434-M9

38. *An Attempt at a Theory of Armor Penetration*, H. A. Bethe, Ordnance Laboratory, Frankford Arsenal, 1945.

39. *A Preliminary Investigation of the Mechanism of Penetration, from the Standpoint of Strain Propagation*, Pol E. Duwez and Donald S. Clark, OSRD 3957, NDRC M-317, OEMsr-348, Projects NS-109 and NRC-82, California Institute of Technology, July 19, 1944. Div. 18-902.11-M7

40. *The Plastic Properties of Metals at High Rates of Strain*, Frederick Seitz, Jr., Andrew W. Lawson, and Park H. Miller, Jr., OSRD 495, NDRC A-41, OEMsr-132, Service Projects OD-34, CE-5, and CE-6, University of Pennsylvania, April 1942. Div. 2-431-M1

41. *High-Speed Compression Testing of Copper Crusher Cylinders and Spheres*, O. C. Simpson, E. L. Fireman, and James S. Koehler, OSRD 3330, NDRC A-257, OEMsr-825, Projects OD-57, NO-7, and P2-303, Carnegie Institute of Technology, March 1944. Div. 2-431.21-M2

42. *The Speed Effect in Copper Crusher Cylinders and Copper Spheres*, Frederick Seitz, Jr., Andrew W. Lawson, and Park H. Miller, Jr., OSRD 610, NDRC A-63, OEMsr-132, Service Projects OD-34, CE-5, and others, University of Pennsylvania, June 1942. Div. 2-431.21-M1

43. *The Testing of Metals in Compression at High Rates of Strain*, Frederick Seitz, Jr., OSRD 1388, NDRC A-174, OEMsr-825, Projects NO-11, NS-109, and P2-303, Carnegie Institute of Technology, April 1943. Div. 2-210-M6

44. *High-Speed Compression Testing of Copper Crusher Cylinders and Spheres, Part II*, G. H. Winslow and W. H. Beesey, OSRD 6039, NDRC A-324, OEMsr-825, Service Projects OD-57, NO-7, and NS-109, Carnegie Institute of Technology, April 1945. Div. 2-431.21-M3

45. *The Set Added to Compressed Cylinders after Impact*, E. L. Fireman, James S. Koehler, and Frederick Seitz, Jr., OSRD 3331, NDRC A-258, OEMsr-825, Projects OD-57, NO-7, and P2-301, Carnegie Institute of Technology, March 1944. Div. 2-431.22-M4

46. *The Propagation of Plastic Strain in Tension*, Pol E. Duwez, D. S. Wood, and Donald S. Clark, OSRD 631, NDRC A-90, OEMsr-348, Service Projects CE-5, NO-11, and others, California Institute of Technology, October 1942. Div. 2-434-M3

47. *The Influence of Specimen Length on Strain Propagation in Tension*, Pol E. Duwez, D. S. Wood, and Donald S. Clark, OSRD 957, NDRC A-105, OEMsr-348, Service Projects CE-5, NO-11, and others, California Institute of Technology, October 1942. Div. 2-434-M4

48. *The Effect of Stopped Impact and Reflection on the Propagation of Plastic Strain in Tension*, Pol E. Duwez, D. S. Wood, Donald S. Clark, and Joseph V. Charyk, OSRD 988, NDRC A-103, OEMsr-348, Service Projects CE-5, NO-11 and others, California Institute of Technology, November 1942. Div. 2-434-M5

49. *The Influence of Impact Velocity on the Tensile Properties of Plain Carbon Steels and of a Cast-Steel Armor Plate*, Pol E. Duwez, Donald S. Clark, and D. S. Wood,

OSRD 1274, NDRC A-154, OEMsr-348, Projects NO-11, NS-109 and P2-303, California Institute of Technology, March 1943. Div. 2-432.1-M1

50. *Factors Influencing the Propagation of Plastic Strain in Long Tension Specimens*, Pol E. Duwez, D. S. Wood, and Donald S. Clark, OSRD 1304, NDRC Report A-159, OEMsr-348, Projects NO-11, NS-109, and P2-303, California Institute of Technology, March 1943. Div. 2-433-M3

51. *Dynamic Tests of the Tensile Properties of SAE-1020 Steels, Armco Iron and 17ST Aluminum Alloy*, Pol E. Duwez, D. S. Wood, and Donald S. Clark, OSRD 1490, NDRC A-182, OEMsr-348, Projects NO-11, NS-109 and P2-303, California Institute of Technology, May 1943. Div. 2-432.1-M2

52. *The Influence of Impact Velocity on the Tensile Properties of Class B Armor Plate, Heat-Treated Alloy Steels, and Stainless Steel*, Pol E. Duwez, D. S. Wood, and Donald S. Clark, OSRD 1641, NDRC A-195, OEMsr-348, Projects NO-11, NS-109, and P2-303, California Institute of Technology, July 1943. Div. 2-432.1-M3

53. *The Influence of Specimen Dimensions and Shape on the Results of Tensile Impact Tests*, D. S. Wood, Pol E. Duwez, and Donald S. Clark, OSRD 3028, NDRC A-237, OEMsr-348, Projects NO-11, NS-109, and P2-303, California Institute of Technology, December 1943. Div. 2-432-M2

54. *The Influence of Velocity on the Tensile Properties of a Carbon Steel, Two National Emergency Steels, and a Manganese Steel*, Donald S. Clark, Pol E. Duwez, and D. S. Wood, OSRD 3180, NDRC A-241, OEMsr-348, Projects NO-11, NS-109, and P2-303, California Institute of Technology, January 1944. Div. 2-432.1-M4

55. *The Influence of Impact Velocity on the Tensile Properties of Four Magnesium Alloys and 24S Aluminum Alloy*, Donald S. Clark, Pol E. Duwez, and D. S. Wood, OSRD 3256, NDRC A-249, OEMsr-348, Projects NO-11, NS-109, and P2-303, California Institute of Technology, February 1944. Div. 2-432.2-M1

56. *The Influence of Impact Velocity on the Tensile Properties of Three Types of Ship Plate: MS, HTS, STS*, Donald S. Clark, Pol E. Duwez, and D. S. Wood, OSRD 3420, NDRC A-261, OEMsr-348, Projects NO-11, NS-109, and P2-303, California Institute of Technology, March 1944. Div. 2-432.1-M5

57. *Influence of Impact Velocity on the Tensile Properties of NE 8715, NE 9415, SAE 1045, and SAE 1090 Steels*, Donald S. Clark, Pol E. Duwez, and D. S. Wood, OSRD 3605, NDRC M-257, OEMsr-348, Projects NO-11, NRC-82, and others, California Institute of Technology, May 9, 1944. Div. 18-002.12-M13

58. *Influence of Impact Velocity on the Tensile Properties of Furniture Steel Sheets*, Pol E. Duwez, Donald S. Clark, and H. E. Martens, OSRD 3603, NDRC M-264, OEMsr-343, Projects NO-11, NRC-82, and others, California Institute of Technology, May 9, 1944. Div. 18-002.12-M12

59. *Influence of Impact Velocity on the Tensile Properties of Some Metals and Alloys*, Pol E. Duwez and Donald S. Clark, OSRD 3637, NDRC M-288, OEMsr-348, Projects NO-11, NS-109, and NRC-82, California Institute of Technology, June 10, 1944. Div. 18-002.12-M14

60. *The Influence of Hardness and Type of Heat Treatment on the Static and Impact Tensile Properties of SAE 4340 Steel*, Pol E. Duwez, H. E. Martens, Donald S. Clark and D. A. Elmer, OSRD 4775, NDRC M-462, OEMsr-348, Projects NS-109 and NRC-82, California Institute of Technology, Feb. 19, 1945. Div. 18-002.12-M15

61. *Some Static and Dynamic Properties of Zamac II, Die-Cast Alloy in Relation to Use in Mark 140 (HIR-5) Fuse*, Donald S. Clark, Pol E. Duwez and D. S. Wood, OSRD 3425, NDRC M-234, OEMsr-348, Projects NO-11, NS-109, and NRC-82, California Institute of Technology, Mar. 27, 1944. Div. 18-002.13-M5

62. *The Propagation of the Plastic Zone Along a Tension Bar of a Material Having a Well-Defined Plastic Limit*, Julius Miklowitz, OSRD 3864, NDRC A-230, OEMsr-891, Projects NO-11, and P2-303, Western Electric and Manufacturing Company, Inc., July 1944. Div.2-433-M4

63. *The Initiation and Propagation of the Plastic Zone in a Mild-Steel Tension Bar*, Julius Miklowitz, OSRD 4612, NDRC A-309, OEMsr-891, Service Project NO-11, Western Electric and Manufacturing Company, Inc., January 1945. Div. 2-433-M5

64. *Behavior of Metals Under Dynamic Conditions—Progression of Yielding*, Pol E. Duwez, H. E. Martens and Donald S. Clark, OSRD 4453, NDRC M-400, OEMsr-348, Project NS-109, California Institute of Technology, Dec. 9, 1944. Div. 18-002.11-M8

65. *The Influence of Pure Strain Rate on the Tensile Properties of Three Types of Ship Plate*, Pol E. Duwez, H. E. Martens, D. A. Elmer, and Donald S. Clark, OSRD 4773, NDRC M-459, OEMsr-348, Projects NS-109 and NRC-82, California Institute of Technology, Feb. 19, 1945. Div. 18-002.15-M2

66. *The Application of Pure Strain Rate Tests to an Investigation of Two 76 MM Gun Tubes*, Pol E. Duwez, H. E. Martens, D. A. Elmer and Donald S. Clark, OSRD 4720, NDRC M-460, OEMsr-348, Projects NS-109 and NRC-82, California Institute of Technology, Feb. 19, 1945. Div. 18-002.15-M1

67. *A Preliminary Study of the Influence of Rapid Loading and Time at Load on the Initiation of Plastic Deformation in Tension*, Pol E. Duwez, H. E. Martens and Donald S. Clark, OSRD 4021, NDRC M-450, OEMsr-348, Projects NS-109 and NRC-82, California Institute of Technology, Jan. 22, 1945 Div. 18-002.14-M1

68. *The Design of a Hydropneumatic Machine for Rapid Load Tensile Testing*, D. A. Elmer, Donald S. Clark and D. H. Hyers, OSRD 4774, NDRC M-461, OEMsr-348, Projects NS-109 and NRC-82, California Institute of Technology, Feb. 19, 1945. Div. 18-002.14-M2

Chapter 13

1. "Recent Work in the Field of High Pressures," Percey W. Bridgman, *The American Scientist*, Vol. 31, 1943, p. 29.

2. *Sixth Partial Report on Light Armor—The Dynamics of Armor Penetration by Light Projectiles*, Report O-1591, Naval Research Laboratory, February 1940.
Measurements of Forces Which Resist Penetration of STS Armor, Mild Steel, and 24ST Aluminum, Report O-2276, Naval Research Laboratory, April 1944.

3. *Plastic Deformation of Steel Under High Pressure*, Percey W. Bridgman, OSRD 910, NDRC A-65, OEMsr-201, Service Projects CE-5, NO-11, and others, HU, September 1942. Div. 2-431.11-M1

4. *Plastic Deformation of Steel Under High Pressure*, Percey W. Bridgman, OSRD 1347, NDRC A-103, OEMsr-201, Projects NO-11 and P2-302, HU, March 1943. Div. 2-431.11-M2

5. *Plastic Deformation of Steel Under High Pressure*, Percey W. Bridgman, OSRD 1929, NDRC A-218, OEMsr-201, Projects NO-11 and P2-303, HU, September 1943. Div. 2-431.11-M4

6. *The Plastic Properties of Steel Under Large Strains and High Stresses*, Percey W. Bridgman, OSRD 4256, NDRC A-294, OEMsr-201, Service Project NO-11, HU, October 1944. Div. 2-431.11-M6
7. *Distortion of an Armor-Plate Steel Under Simple Compressive Stress to High Strains*, Percey W. Bridgman, OSRD 3019, NDRC A-235, OEMsr-201, Projects NO-11, and P2-302, HU, December 1943. Div. 2-431.11-M5
8a. "The Measurement of Hydrostatic Pressure to 30,000 Kg/Cm^2," Percey W. Bridgman, *Proceedings of the American Academy of Arts and Sciences*, Vol. 74, 1940, pp. 1-10.
b. "The Linear Compression of Iron to 30,000 Kg/Cm^2," Percey W. Bridgman, *Proceedings of the American Academy of Arts and Sciences*, Vol. 74, 1940, pp. 11-20.
c. "The Compression of 46 Substances to 50,000 Kg/Cm^2," Percey W. Bridgman, *Proceedings of the American Academy of Arts and Sciences*, Vol. 74, 1940, pp. 21-51.
9. "The Stress Distribution at the Neck of a Tension Specimen," Percey W. Bridgman, *Transactions of the American Society of Metals*, Vol. 32, 1944, pp. 553-574.
10. *Effect of Prestressing in Tension on Behavior of Steel in Tension*, Percey W. Bridgman, Experimental Report WAL 111/7-6, Watertown Arsenal Laboratory, June 1944.
11. *Tension Tests on Tubes under Hydrostatic Pressure*, Percey W. Bridgman, Experimental Report WAL 111/7-4, Watertown Arsenal Laboratory, January 1944.
12. "The Latent Energy Remaining in a Metal After Cold Working," G. I. Taylor, and H. Quinney, *Proceedings of the Royal Society of London*, Vol. 143, 1933-1934, p. 323.

Chapter 14

1. *Protection Against Shaped Charges*, Emerson M. Pugh, OSRD 6384, NDRC A-334, OEMsr-950, Service Project AN-1, Carnegie Institute of Technology, February 1946. Div. 2-510-M4
2. *Defense Against Hollow Shaped Charges, Part I*, Emerson M. Pugh, OSRD 3109, NDRC A-242, OEMsr-950, Projects AN-1 and P2-206, Carnegie Institute of Technology, January 1944. Div. 2-510-M1
3. *A Theory of Target Penetration of Jets*, Emerson M. Pugh, OSRD 3762, NDRC A-274, OEMsr-950, Projects AN-1 and P2-206, Carnegie Institute of Technology, June 1944. Div. 2-310-M1
4. *Fundamental Principles of Jet Penetration: Secondary Penetration in Hollow-Charge Targets*, Robert J. Eichelberger, OSRD 4148g, OTB-2, September 1944. Div. 2-300-M1
5. *Fundamentals of Jet Penetration: Theory of Jet Penetration*, Emerson M. Pugh and E. L. Fireman, OSRD 4357f, OTB-4, November 1944. Div. 2-300-M1
6. *Note on the Theory of the Munroe Effect*, J. L. Tuck, (British), A. C. 3696.
7. *A Formulation of Mr. Tuck's Conception of Munroe Jets*, G. I. Taylor, (British), A. C. 3734, March 1943.
8. *Mathematical Jet Theory of Lined Hollow Charges*, Garrett Birkhoff, Report 370, BRL, June 1943.
9. *The Mechanism of Action of Cavity Charges*, George B. Kistiakowsky, Duncan P. MacDougall, and G. H. Messerly, OSRD 1538, OEMsr-202, ERL, Carnegie Institute of Technology, April 12, 1943. Div. 8-495-M1
10. *Penetration by Munroe Jets*, R. Hill, N. F. Mott, and D. C. Pack, (British), A. C. 5756.
11. *Penetration of Armour by High Velocity Projectiles and Munroe Jets*, R. Hill, N. F. Mott, and D. C. Pack, (British), A. C. 6024.
12. *A Review of Certain Aspects of Research on Munroe Jets*, D. C. Pack, Theoretical Research Survey 1/44, ARD.
13. *Remark on the Hill-Mott-Pack Theory of Penetration by Munroe Jets*, Garrett Birkhoff, Report 497, BRL, October 1944.
14. *High Speed Radiographic Studies of Controlled Fragmentation*, L. B. Seely and J. C. Clark, Report 368, BRL, June 1943.
15. *High Speed Radiographic Studies of Controlled Fragmentation*, L. B. Seely and J. C. Clark, Report 488, BRL, September 1944.
16. *Studies of Shaped Charges with the Rotating Drum Camera*, H. A. Strecker and M. H. Hurwitz, OSRD 5615, OEMsr-202, Service Project AN-1, ERL, Carnegie Institute of Technology, Jan. 15, 1946. Div. 8-401-M5
17. *Tests of Plastic Materials*, Emerson M. Pugh, Robert J. Eichelberger, and Robert J. Lew, OSRD 4046, NDRC A-288, OEMsr-950, Service Project AN-1, Carnegie Institute of Technology, August 1944. Div. 2-230-M2
18. *Review of Principles Involved in Protecting Armored Vehicles Against Shaped-Charge Weapons*, Emerson M. Pugh, OSRD 4498, NDRC A-103M, OEMsr-950, Service Project AN-1, Carnegie Institute of Technology, December 1944. Div. 2-510-M3
19. *Protection of Armored Vehicles Against Shaped Charges: Static Tests of Plastic and Steel Armor Combinations*, Emerson M. Pugh and Robert J. Eichelberger, OSRD 4148d, OTB-2, September 1944. Div. 2-300-M1
20. *Protection of Armored Vehicles Against Shaped Charges: Dynamic Tests of Plastic and Steel Armor Combinations*, Emerson M. Pugh, OSRD 4148e, OTB-2, September 1944. Div. 2-300-M1
21. *Correlation Between Residual Penetration of Shaped Charges in Mild Steel and Percentage Perforations in Homoplate*, Emerson M. Pugh and Robert J. Eichelberger, OSRD 4258b, OTB-3, October 1944. Div. 2-300-M1
22. *Protection Against Shaped Charges Afforded by Spaced Armor*, Emerson M. Pugh and Robert J. Eichelberger, OSRD 4258c, OTB-3, October 1944. Div. 2-300-M1
23. *Protection of Armored Vehicles Against Shaped Charges: Effect of Particle Size, Grading, and Composition upon Stopping Power of Lileaville Gravel Plastics*, Emerson M. Pugh and Robert J. Eichelberger, OSRD 4357e, OTB-4, November 1944. Div. 2-300-M1
24. *Fundamental Principles of Jet Penetration: Secondary Penetration in Hollow-Charge Targets*, Emerson M. Pugh and Robert J. Eichelberger, OSRD 4357e, OTB-4, November 1944. Div. 2-300-M1
25. *Dynamic Tests on HCR8 at Aberdeen*, Emerson M. Pugh and Robert J. Eichelberger, OSRD 4477e, OTB-5, December 1944. Div. 2-300-M1
26. *Protection of Armored Vehicles Against Shaped Charges: Use of Chemical Compounds*, Emerson M. Pugh and Robert J. Eichelberger, OSRD 4820f, OTB-8, March 1945. Div. 2-300-M1
27. *Defense of Armored Vehicles Against Shaped Charges: Weights and Thicknesses of Protective Slabs*, Emerson M. Pugh and E. Fireman, OSRD 4820g, OTB-8, March 1945. Div. 2-300-M1
28. *Defense of Concrete Fortifications Against Shaped Charges*, Emerson M. Pugh and G. H. Winslow, OSRD 4148, OTB-2, September 1944. Div. 2-300-M1
29. *Scaling Laws for Concrete Targets Attacked by Shaped Charges*, Emerson M. Pugh and G. H. Winslow, OSRD 4258d, OTB-3, October 1944. Div. 2-300-M1
30. *Defense of Concrete Fortifications Against Shaped Charges*, Emerson M. Pugh and G. H. Winslow, OSRD 4357d, OTB-4, November 1944. Div. 2-300-M1

...g Pene... ...by ...ts, E. Fireman and ... ...Pugh, ...29b, OTB-8, March 1945. Div. 2-300-M1

32. ... ...ade ... ...aded No. 8 Detonators ... ...ng ... ...ed Charges, Robert J. ... Robert J. ... OSRD 3715, NDRC ...-C2-..., OEMsr-... ...N-1 and P2-206, Car... ...une 1944. Div. 2-510-M2

33. ... ...ent ... ...et Penetration: Studies of Control... ...sey, Robert J. Eichelberger, A. G. Stra... ...Emerson M. Pugh, OSRD 4477d, OTS-5, December 1944. Div. 2-300-M1

Chapter 15

1. *Static Detonation Trials of Three Framed Houses at Area "J" Aberdeen Proving Ground, Parts I and II*, John E. Burchard, Herbert L. Beckwith, Ernest N. Gelotte, and Norman C. Dahl, Interim Report 23, CPPAB, National Research Council, April 1943. Div. 2-521-M3
2. *Effects of Confined Blast on Brick Curtain Walls*, A. H. Taub and J. A. Wise, OSRD 6007d, NDRC AES-14d, September 1945. Div. 2-100-M1
3. *Contact Explosions on Concrete*, Donald G. Kretsinger, Report 29, CFD, National Research Council, June 30, 1944. Div. 2-220-M16
4. *Contact Explosions Against Concrete*, I. M. Freeman, Donald G. Kretsinger, and A. H. Taub, OSRD 6319, NDRC A-354, OEMsr-260, Service Project AN-29, PUS, December 1945. Div. 2-220-M22
5. *Relation Between Shape of Cylindrical Charges and Dimensions of Craters Produced—Tests of a Flat Slab at Shoeburyness*, (British) A. C. 5713/C39, May 1944.
6. *Nose Versus Tail Initiation of Contact Charges*, Walker Bleakney, Donald G. Kretsinger, and A. H. Taub, OSRD 5506c, NDRC AES-13c, August 1945. Div. 2-100-M1
7. *Impulse Delivered to a Plane Slab by a Contact Explosion*, Donald G. Kretsinger, Interim Memorandum M-11 CFD, National Research Council, June 30, 1944. Div. 2-210-M8
8. *Impulse Delivered to a Plane Slab by a Contact Explosion, II*, I. M. Freeman, Donald G. Kretsinger, and A. H. Taub, OSRD 5506d, NDRC AES-13d, August 1945. Div. 2-100-M1
9. *The Limit Design of Structures Subjected to Impulsive Loads, with Application to Military Structures*, Merit P. White, OSRD 4192, NDRC A-293, Service Projects CE-36, NO-11, and NO-12, October 1944. Div. 2-420-M6
10. *Impact Tests of Reinforced Concrete Beams, Part I*, Frank E. Richart and Nathan H. Newmark, OSRD 1105, NDRC A-125, OEMsr-318, Service Projects CE-5, NO-12, and others, University of Illinois, December 1942. Div. 2-220-M4
11. *Impact Tests of Reinforced Concrete Beams, Part II*, Nathan M. Newmark and Frank E. Richart, OSRD 1751, NDRC A-213, OEMsr-318, Projects CE-5, NO-12, and P2-304, University of Illinois, August 1943. Div. 2-220-M8
12. *Impact Tests of Reinforced Concrete Beams, Part III*, W. H. Munse and Frank E. Richart, OSRD 4490, NDRC A-304, OEMsr-318, Service Projects CE-36, NO-11, and NO-12, University of Illinois, December 1944. Div. 2-220-M20
13. *The Reactions of Thin Beams and Slabs to Impact, Part I, General Theory*, H. P. Robertson and Ralph J. Sluts, Interim Report 13, CPPAB, National Research Council, June 1942. Div. 2-420-M1
14. *The Reactions of Thin Beams and Slabs to Impact Loads, Part II, Beams*, H. P. Robertson and Ralph J. Sluts, Interim Report 14, CPPAB, National Research Council, June 1942. Div. 2-420-M2
15. *The Analysis of Elastic Structures Acted upon by Impulsive Loadings*, John B. Wilbur, OSRD 1915, NDRC A-219, OEMsr-468, Service Projects CE-5, NO-12, and others, The Massachusetts Institute of Technology, October 1943. Div 2-420-M4
16. *Reactions of Simple Systems under Blast Loading*, D. Montgomery and A. H. Taub, OSRD 5303a, NDRC AES-12a, July 1945. Div. 2-100-M1
17. *Remarks on Reactions under Blast Loading*, D. Montgomery and A. H. Taub, OSRD 6007a, AES-14a, September 1945. Div. 2-100-M1
18. *A Modification of the Impulse Criterion for Blast Damage*, D. G. Christopherson, (British), R. C. 349, September 1942.
19. *The Impact Resistance of Reinforced Concrete Beams*, Department of Scientific and Industrial Research (British) R. C. 128, July 1940.
20. *Further Tests on the Impact Resistance of Some Reinforced Concrete Beams*, (British) R. C. 345, RRL, August 1942.
21. *Further Tests on the Impact Resistance of Some Reinforced Concrete Beams*, (British) R. C. 369, ARP/385/LGS, November 1942.
22. *Further Tests on the Impact Resistance of Some Reinforced Concrete Units*, (British) R. C. 379, ARP/398/LGS.

The following are not referred to specifically in this chapter, but are pertinent to it:

23. *Fundamental Principles of Structural ARP*, John E. Burchard, CPPAB, National Research Council, December 1942. Div. 2-520-M6
24. *Remarks on Fortification Design*, Walker Bleakney and A. H. Taub, Interim Memorandum M-10, CFD, National Research Council, November 1944. Div. 2-530-M1
25. *The Failure of Diaphragms under Uniform Pressure*, Merit P. White, OSRD 1376, NDRC A-167, Projects NO-11, NS-109, and P2-303, April 1943. Div. 2-431.22-M3
26. *Suggestions Based on Observations of Results of Tests at Edgewood Arsenal, May 21, 1941*, Frank E. Richart and Nathan M. Newmark, Interim Report 1, CPPAB, National Research Council, August 1941. Div. 2-521-M1
27. *The Problem of Defeating an Explosive Projectile. Part I, Introduction. Direct Hit*, CPPAB, National Research Council, June 30, 1941. Div. 2-520-M1
The Problem of Defeating an Explosive Projectile. Part II, Nearby Hit and Collateral Questions, CCPAB, National Research Council, June 30, 1941. Div. 2-520-M2
The Problem of Defeating an Explosive Projectile. Part III, Economics of Structural Air Raid Protection, CCPAB, National Research Council, June 30, 1941. Div. 2-520-M3
The Problem of Defeating an Explosive Projectile. Part IV, Summary. Rational Design—Suggestions for Further Research, CCPAB, National Research Council, June 30, 1941. Div. 2-520-M4
28. *Exploratory Tests on Underground Bursters*, Donald G. Kretsinger and David Mayer, Interim Report 10 CPPAB, National Research Council, May 1942. Div. 2-522-M1
29. *Incendiary Bomb Test*, Robert J. Hansen, Interim Report 11, CPPAB, National Research Council, May 1942. Div. 2-522-M2
30. *Investigation of Uplift Effect of Explosion Within a Building, the Design of the Test Buildings*, David Mayer, Interim Report 12, CPPAB, National Research Council, May 1942. Div. 2-521-M2

31. *Blast Reduction Effect of Trulock Screens*, Curtis W. Lampson, Interim Report 15, CPPAB, National Research Council, June 1942. Div. 2-522-M3
32. *CPPAB Final Report* (for year ending June 30, 1942), National Research Council, June 30, 1942. Div. 2-520-M8
33. *The Use of Bamboo for Reinforcement in Concrete*, Norman C. Dahl, Interim Report 22, CPPAB, National Research Council, February 1943. Div. 2-522-M5
34. *Relative Safety of Basements and Upper Stories of Frame Houses in Air Raids*, Henry Scheffé, Interim Report 24 CPPAB, National Research Council, May 1943. Div. 2-521-M4
35. *CPPAB Final Report*, (for year ending June 30, 1943). National Research Council, June 30, 1943. Div. 2-520-M7
Terminal Ballistics and Explosive Effects, John E. Burchard, Appendix to CPPAB Final Report for year ending June 30, 1943. National Research Council, Oct. 1, 1943. Div. 2-200-M2
36. *Effects of Underground Explosions. Volume I, Subsurface and Target Phenomena*, Curtis W. Lampson, Interim Report 26, CFD, National Research Council, June 30, 1944. Div. 2-240-M4
Effects of Underground Explosions. Volume II, Subsurface and Surface Phenomena, Interim Report 26, CFD, National Research Council, June 30, 1944. Div. 2-240-M5
Effects of Underground Explosions. Volume III, Resulting Damage to Structures, David Mayer and Norman C. Dahl, Interim Report 26, CFD, National Research Council, June 30, 1944. Div. 2-240-M6
37. *Final Report on the Program of Research Conducted by the Committee for the Corps of Engineers, U. S. Army, Summarizing the Work of the CFD and CPPAB*, John E. Burchard, National Research Council, December 1944. Div. 2-530-M12

Chapter 16

Note: Many of the references listed below are studies of target vulnerability made by Division 2, based on operations reports and on reports on fundamental investigations of terminal ballistics and effects of explosions. These reports contain references to original sources.

References 4, 5, 7, 8, 9, 10, 11, and 14 are reprinted together in reference 15.

1. *Theory of Probability, with Applications*, Henry Scheffé, OSRD 1918, NDRC A-224, OEMsr-260, Service Projects CE-5, CE-6, and NO-12, PUS, February 1944. Div. 2-540-M1
2. Various reports by Army Operations Analysis Sections should be consulted. See, for example, ORS 8th Bomber Command, Report 19 and 25; ORS Mediterranean Allied Air Forces, Report 27; ORS 9th Army Air Force, Report 68.
3. *Joint Target Group Memorandum M-8*, Joint Target Group, AC/AS Intelligence.
4. *MAE's Calculated from Ashley Walk Trials*, OSRD 5657b, EWT-6b, September 1945.
5. *Attack on Open Gun Emplacements*, OSRD 5657a, EWT-6a, September 1945.
6. *Remarks on Fortification Design*, Walker Bleakney and A. H. Taub, Interim Memorandum M-10, CFD, National Research Council, November 1944. Div. 2-530-M1
7. *Attack of Railroads*, OSRD 5046d, EWT-2d, May 1945.
8. *Air Attack on Bridges*, OSRD 5170j, EWT-3j, June 1945.
9. *Attack of Tunnels*, OSRD 5045c, EWT-2c, May 1945.
10. *Attack on Earth Slopes*, OSRD 5176i, EWT-3i, June 1945.
11. *Aerial Bombing Attacks against Aerodromes—Runways and Landing Grounds*, OSRD 4918, EWT-1c, April 1945.
12. *Striking Power of Air-Borne Weapons*, OpNav-16-V A43, Air Intelligence Group, Division of Naval Intelligence, Office of the Chief of Naval Operation, Navy Department, July 1944.
13. *Effectiveness of U. S. Incendiary and High Explosive Bombs*, OSRD 6445, NDRC A-386.
14. *Air Attack on Steel Mills*, OSRD 5657d, EWT-6d, September 1945.
15. *Study of the Physical Vulnerability of Military Targets to Various Types of Aerial Bombardment*, Walker Bleakney, OSRD 6444, NDRC A-385, OEMsr-260, Service Project AN-29, PUS, January 1946. Div. 2-530-M3

Chapter 18

1. *Notes on a Course of Instruction in Bomb Damage, A Course Given by the Ministry of Home Security*, Research and Experiments Department, Princes Risborough, England, from July 6, 1944, through Aug. 4, 1944; Bomb Damage; Prediction and Assessment, OpNav 16-V A58, prepared by Air Intelligence, September 1944.
2. *Weapon Data—Fire, Impact, Explosion*, (formerly *Effects of Impact and Explosion*), continuing looseleaf report by Division 2, the final edition was issued as OSRD 6053 (see Chapter 19).
3. *Terminal Ballistic and Explosive Effects*, John E. Burchard, Appendix to Final Report for year ending June 30, 1943, CPPAB, National Research Council, Oct. 1, 1943. Div. 2-200-M2
4. *Theory of Probability, with Applications*, Henry Scheffé, OSRD 1918, NDRC A-224, OEMsr-260, Service Projects CE-5, CE-6, and NO-12, PUS, February 1944. Div. 2-540-M1
5. *Fundamental Principles of Structural ARP*, John E. Burchard, CPPAB, National Research Council, 1943. Div. 2-520-M6
6. *U. S. Bombs and Fuzes, Enemy Bombs and Fuzes*, and similar publications of U.S. Navy Disposal School were given to all men who received additional training there.

OSRD APPOINTEES

DIVISION 2

Chiefs

E. BRIGHT WILSON (since June 4, 1944)
J. E. BURCHARD (up to June 4, 1944)

Officers

H. P. ROBERTSON, *Chief Advisor*
WALTER BLEAKNEY, *Deputy Chief*
BURNHAM KELLEY, *Special Assistant to the Chief*

Technical Aides

R. J. SLUTZ
M. P. WHITE

Members

H. L. BOWMAN
W. E. LAWSON
D. P. MACDOUGALL
J. VON NEUMANN
S. A. VINCENT

Consultants

JOHN B. ARMENTROUT
C. W. BARBER
R. A. BETH
F. H. BOHNENBLUST
P. W. BRIDGMAN
W. T. BRIGHTMAN, JR.
JOHN S. BURLEW
L. A. BROTHERS
R. W. CARLSON
D. S. CLARK
R. H. COLE
P. C. CROSS
C. W. CURTIS
L. A. DELSASSO
J. W. DUNHAM
W. M. FIFE
P. M. FYE
N. GELOTTE
J. W. GREIG
P. M. GROSS
R. J. HANSEN
M. E. HOBBS
W. D. KENNEDY
J. G. KIRKWOOD
C. W. LAMPSON
R. R. MARTEL
A. NADAI
STANFORD NEAL
N. M. NEWMARK
E. M. PUGH
CHESTER LEROY POST
F. E. RICHART
V. ROJANSKY
A. C. RUGE
W. M. RUST
F. SEITZ, JR.
L. G. SMITH
H. D. SMYTH
A. W. STEPHENS
R. STEPHENS, JR.
A. H. TAUB
T. VON KÁRMÁN
B. B. WEATHERBY
J. B. WILBUR

Special Representatives [a]

NORMAN C. DAHL
ROBERT H. DIETZ
FRANCIS R. SMITH

[a] These men were employees under the contract but were appointed Special Representatives in order that they might travel to the European Theater of Operations to represent Division 2.

CONTRACT NUMBERS, CONTRACTORS, AND SUBJECTS OF CONTRACTS

Contract Number	*Name and Address of Contractor*	*Subject*
NDCrc-34	Princeton University Princeton, New Jersey	Terminal ballistics and explosive effects
NDCrc-36	California Institute of Technology Pasadena, California	Designing, constructing, and operating a continuously functioning supersonic wind tunnel
OEMsr-127	Cornell University Ithaca, New York	Theoretical investigation of explosives
OEMsr-132	University of Pennsylvania Philadelphia, Pennsylvania	Rapid rates of strain
OEMsr-201	Harvard University Cambridge, Massachusetts	Study of plastic properties of steel under high pressure
OEMsr-213	Polaroid Corporation Cambridge, Massachusetts	Development and testing of plastic materials for military purposes
OEMsr-260	Princeton University Princeton, New Jersey	Research on problems of terminal ballistics, penetration of projectiles, and effects of impact and detonation
OEMsr-318	University of Illinois Urbana, Illinois	Impact tests of concrete
OEMsr-336	University of Pennsylvania Philadelphia, Pennsylvania	Rapid rates of strain
OEMsr-348	California Institute of Technology Pasadena, California	Rapid rates of strain
OEMsr-424	Herbach and Rademan 522 Market Street Philadelphia, Pennsylvania	Construction of laboratory unit
OEMsr-468	The Massachusetts Institute of Technology Cambridge, Massachusetts	Engineering principles of design of fortifications and other structures
OEMsr-569	Woods Hole Oceanographic Institution Woods Hole, Massachusetts	Study of characteristics and effects of explosions in air and underwater
OEMsr-596	Stanolind Oil and Gas Company Tulsa, Oklahoma	Construction of piezoelectric gauges for study of shock waves
OEMsr-641	The Massachusetts Institute of Technology Cambridge, Massachusetts	Studies of rapid rates of strain
OEMsr-675	Princeton University Princeton, New Jersey	Design and construction of mobile laboratory unit
OEMsr-751	Cornell University Ithaca, New York	Development of methods of calculating damage due to underwater explosions
OEMsr-825	Carnegie Institute of Technology Pittsburgh, Pennsylvania	Impact testing of steel and other materials
OEMsr-891	Westinghouse Electric and Manufacturing Company East Pittsburgh, Pennsylvania	Stress-strain characteristics of metals under dynamic loads
OEMsr-950	Carnegie Institute of Technology Pittsburgh, Pennsylvania	Defense against shaped charges
OEMsr-1284	Duke University Durham, North Carolina	Development of frangible projectile for flexible gunnery training
OEMsr-1343	General Electric Company Schenectady, New York	Reduction of smoke and blast effect
OEMsr-1351	California Institute of Technology Pasadena, California	Reduction of smoke and blast effect
OEMsr-1398	Franklin Institute Philadelphia, Pennsylvania	Fundamental design of muzzle brakes
OEMsr-1476	University of Illinois Urbana, Illinois	Construction of model explosive storage shelters
OEMsr-1498	Arthur D. Little Company 30 Memorial Drive Cambridge, Massachusetts	Evaluation of relative and absolute effectiveness of various aerial weapons

SERVICE PROJECT NUMBERS

The projects listed below were transmitted to the Executive Secretary, OSRD, from the War or Navy Department through either the War Department Liaison Officer for NDRC or the Office of Research and Inventions (formerly the Coordinator of Research and Development), Navy Department.

Service Project Number	*Subject*
	Army Projects
AC-73	Utilization of frangible projectile in flexible gunnery training.
AN-1	Study of defense against shaped charges.
AN-23	Studies of combined He-IB attack on precision targets.
AN-28	Model scale explosion studies.
AN-29	Study of physical vulnerability of military targets to various types of aerial bombardment.
CE-5	Passive defense of civil population and utilities against aerial bombing.
CE-6	Passive protection of military aircraft and airport facilities against bombing.
CE-36	Requirements for protective structures.
OD-01	Study of PTX compositions.
OD-03	Study of shock waves.
OD-24	Supersonic wind tunnel development.
OD-57	Copper pressure cylinder versus copper balls for use in chamber pressure measurements.
OD-75	Investigation of the penetration of homogeneous and face-hardened armor at striking velocities of 3,000 fps and above.
OD-79	Equipment for measuring and recording blast pressures (mobile laboratory unit).
OD-121	Mine case M3A1.
OD-145	Study of bomb effectiveness.
OD-154	Reduction of smoke and blast effect.
OD-160	Fundamental design of muzzle brakes.
	Navy Projects
NO-3	Supersonic wind tunnel development.
NO-7	Copper pressure cylinder versus copper balls for use in chamber pressure measurements.
NO-11	Structural defense—testing facilities.
NO-12	Testing facilities, concrete, detonation effect—blast, earth shock, structures.
NO-138	Determination of proper booster system for large explosive charges.
NO-144	Photographic examination of shock waves in air.
NO-208	Interferometric examination of air jets.
NO-223	Investigation of explosives for use in underwater munitions.
NO-224	Theoretical investigation of explosion phenomena, Parts B, C, and D (Part A remained in Division 8).
NO-237	Determination of depth of underwater explosions from surface observations.
NO-262	Production of water waves by explosions.
NO-263	Cratering properties of explosives.
NO-267	Study of physical vulnerability of military targets to various types of aerial bombardment.
NO-283	Air-blast measurements.
NS-109	Determination of properties of materials at high rate of loading in structures subjected to shock loading.
NS-145	Systematic investigation of the nonmetallic ballistic material known as plastic protection for the purpose of a better understanding and a further development of the material.
NS-267	NDRC assistance in underwater explosion measurements on submarine models.

INDEX

The subject indexes of all STR volumes are combined in a master index printed in a separate volume. For access to the index volume consult the Army or Navy Agency listed on the reverse side of the half-title page.

Aberdeen chronograph, 234
Aberdeen Proving Ground
  air-blast measurements, 65
  frangible bullet for gunnery training, 242
  supersonic wind tunnel, 251
  terminal ballistics of concrete, 192
Accelerometers, 118
ADP (ammonium dihydrogen phosphate) gauge, 51, 70
Aerial gunnery training
  coupled instructor's turret, 246
  frangible bullet, 242-248
  hit indicator system, 245
  recommendations, 247
  target airplanes, 245-246, 248
Aerial torpedoes, physical characteristics, 368
Afterburning of explosives, 66-67, 80, 91-92
Air-blast measurements, 69-78
  blast tube, 75-76
  gauges, 69-74
  height effect on pressure and impulse, 418-421
  peak pressure, 77, 411
  photography of explosions, 74-75
  positive impulse, 67-68, 77-78, 412-413
  shock-wave velocity, 74
  side-on vs. face-on pressure, 414
Air-blast waves
  see Shock waves in air
Airburst explosives
  see Explosions in air
Airburst fuze, 320-321, 329-330
Aircraft armor, 243
Aircraft Laboratory, Wright Field, 245
Aircraft mines, characteristics, 368
Aircraft weapons, 307-308
Alcoa 24 ST dural armor, 243
Algas (aluminum gasoline), 94
Aluminized explosives, 76-79
  clearance of mine fields, 106
  explosive power, 33
Aluminum cases for bombs, 82
Amatex, 78
Amatol
  composition, 20, 78
  effectiveness for underground explosions, 127
  in underwater weapons, 30
  properties and uses, 359
American Time Products Company
  frangible bullet, 242
  hit indicator system in target airplanes, 246
Ammonium dihydrogen phosphate gauge, 51, 70
Amplifiers for electrical gauges, 70
Amplitude-modulated gauges, 71-72
Anti-concrete projectiles
  see Concrete targets, projectile penetration
Anti-personnel mines, 102, 374
Anti-tank mines, 101-102, 374
AP 40 (German hypervelocity gun), 160
AP bombs (armor-piercing), 307, 312, 406-407
  penetration of reinforced concrete, 393, 397
  physical characteristics, 364
AP projectiles
  see Projectiles, armor-piercing
Applied Mathematics Panel
  calibration studies of gauges, 75
  evaluation of weapons, 77
  training of operations analysts, 340
Armor, pressure deformation
  see Steel, pressure deformation
Armor, terminal ballistics
  see Armor perforation
Armor for aircraft, 243
Armor perforation, 160-190
  see also Projectiles, armor-piercing
  angle of attack, 179-184
  homogenous armor, 170
  perforation formulas, 171-176
  photography, 164-165, 167
  plate hardness, 163, 174-175
  plate suspension, 165
  plate vulnerability, 171-172, 174
  resisting forces during impact, 164-165
  shatter velocity, 177, 181
  spalling from plates, 171
  terminal ballistic coefficients, 172-174
  thickness of plate, 181-183
Armor-piercing bombs, 307, 312, 322, 406-407
Armor-piercing cap, 162, 163
  prevention of shatter, 171
Artillery weapons, 308-309
Atomic bomb
  height of burst, 89
  peak pressure, 42, 69, 77
  soil penetration, 240

Bakelite Corporation, frangible bullet, 242
Ball crusher gauge
  deformation on copper spheres, 53
  evaluation, 73
  operation, 53
  peak pressure measurement, 53, 72
  theory, 53-54
Ballistic pendulum, 151, 166
Ballistic studies
  armor, 160-190
  bombs, 378-390
  concrete, 191-228
  plastic protection, 229-232
  soil, 233-241
  theory of terminal ballistics, 155-159
Bangalore torpedoes, 309, 323-324
Baronal for explosive fillings, 78-79
Bazooka, rocket launcher, 277-278
Bell Aircraft Corporation, 245-246
Blast measurements in air
  see Air-blast measurements
Blast tube, 75-76, 84
Blast waves in air
  see Shock waves in air
"Blunderbus" extensions for guns, 133
Bombing attacks, force requirements for damage, 317-318
Bombs
  airburst, 64-111
  armor-piercing, 307, 312, 364
  ballistic studies, 378-390
  British, 369
  concrete-piercing, 396-400
  depth bomb, 308, 314, 368
  explosive fillings, 78, 91-93, 127, 359
  flight characteristics, 378-390
  fragmentation, 307, 314, 320-322, 325-328, 365
  fuses, 360-363
  German, 370-371
  GP bombs, 307, 312-317, 324-332, 364, 440
  high explosive, 307, 315-316, 328
  incendiary, 307-308, 315-316, 320, 329-330, 366-367, 391
  Japanese, 372-373
  LC (light case), 307, 312, 330, 364
  loading efficiency, 316-317
  proximity fusing, 82, 86, 91
  soil penetrating, 237
Boosters, explosive, 66
Brakes, gun-muzzle, 142-146
  design, 143-145
  efficiency factors, 145
  M-2 brake, 133
  requirements, 144
British research
  air-blast tests, 76-77, 87
  bombs, 369
  breaching of concrete anti-tank walls, 212
  hypervelocity gun, 160
  materials under dynamic loads, 255
  operations analysis, 340
  plastic armor, 155, 229-232
  standard bomb, 90
  Telecon cable, 118
  underground trajectory of bombs, 238
Bullets for aerial gunnery training
  see T-44 frangible bullet
Bureau of Ordnance, 27

California Institute of Technology
  gun muzzle attachments, 134
  materials under dynamic loads, 255
  supersonic wind tunnel, 251

Cap attachment for armor-piercing projectile, 162, 163, 170
Carpet-roll torpedo, 102
Cavitation
  effect on damaging power of explosive, 42-43
  photographic experiments, 43-45, 57-58
Chapman-Jouguet detonation state of explosives, 95
Chronograph for projectile velocity measurement, 234
Composition A (explosive filling) properties and uses, 359
Composition B (explosive filling)
  composition, 78
  effectiveness for underground explosions, 127
  explosive effect, 79
  open air effectiveness, 92
  properties and uses, 359
Composition C (explosive filling) properties and uses, 359
Concrete targets, projectile penetration, 191-228
  see also Fortification damage
  ballistic limits of concrete penetration, 396
  bombs, 399-400
  conditions for maximum damage, 207, 210
  contact explosions, 120, 285-288
  delayed fused bombs, 322
  dispersion of points of impact, 211
  explosive projectiles, 207-211
  mathematical formulae, 192-194, 212-227
  nose fuze, 210-211
  perforation of target, 199, 206, 218
  projectile properties, 194, 207-209, 217, 221-223
  quality and thickness of concrete, 193, 201-202, 211, 290-291
  ricochet and sticking of projectile, 193-199, 213-214, 220, 396-398
  rockets, 401
  scabbing of target, 199, 208, 214, 218, 285-286, 291, 399
  shaped charges, 416
  striking angle and velocity of projectile, 101, 108, 207, 211, 215-217, 219-220
  time and velocity of penetration, 194, 199, 225-226, 228
  vulnerable areas, 214-216
Concrete targets, types
  see Fortification design
Condenser-microphone gauge, 71-72
Conductivity gauge, 51
Cone-end charges, 376
Contact explosions, 285-288
  cratering in concrete, 285-286
  impulse produced by, 287-288, 415
  scabbing of concrete, 285-286
Copper, compression testing, 262-263
Cornell University, study of shock wave properties, 40, 45
Crater formation, destructive effect, 324-327, 422-423
Cyclonite (cyclomethylene trinitramine), 20

Damage gauges, 73-74
DBX (explosive), 78-79
Deflectors for guns, 145-150
  control of jet, 149-150
  reduction of blast effects, 145-149
  suppression of dust, 146-149
  suppression of flash, 148
Demolition charges, characteristics, 376
Depth bombs, 33-35
  Mark 54; 33, 60
  physical characteristics, 368
Destruction techniques
  see Target damage techniques
Detonating cord, line charge, 102, 105
Detonation wave, 66-67
Detonator caps, 49
Diaphragm gauges, 44-45, 54, 73-74
  Modugno gauge, 54
  paper blast meter gauge, 73
  peak pressure measurement, 54
  steel diaphragms, 54
Dragon hose, line charge, 102
Duke University, frangible bullet research, 242
duPont de Nemours Company, frangible bullet research, 242
duPont powder No. 4759; 244
Dural armor, Reynolds, 243

Ednatol for explosive fillings, 78-79
Eglin Field, Florida, frangible bullet research, 242
Elastic wave propagation, 255-257
Electro-magnetic blast pressure gauge, 118
Euler-Robins theory, projectile penetration, 194, 227
Explosions, contact, 285-288
  cratering in concrete, 286-287
  impulse produced by, 287-288
  scabbing of concrete, 285-286
Explosions, photography
  see Photography of explosions
Explosions in air, 64-109
  see also Shock waves in air
  afterburning process, 66-67, 81, 91-92
  air-blast measurements, 69-72, 95-99
  Chapman-Jouguet detonation state, 95
  chemical reactions of explosives, 66-67, 81, 91-92
  composition of explosive, 76-79
  damage, 76-77, 326, 328
  evaluation of explosives, 65, 77-80, 86-87
  flame velocity, 74, 107
  fragmentation of bombs, 95, 314-315
  fuzes for bombs, 314-315
  gas formations, 66-67, 81
  height of burst, 86-91
  low order explosions, 307
  measuring instruments, 72-74
  model town tests, 37
  physical properties of explosives, 78-83, 107
  principle of similitude, 80-81
  skin effect of explosives, 81
  slow-burning explosives, 93-94
  theory, 66-69
Explosions in enclosed rooms, 91-94
  blast impulse, 93
  effect of ventilation, 92
  effectiveness, 91-93
  high explosives, 91-93
  slow-burning explosives, 93-94
Explosions on ground, 99-100
Explosions under ground, 110-132
  comparison of explosives, 127
  crater formations, 112-114, 126, 127, 313, 422-423
  damage to structures, 127-132, 285, 297-301, 312, 321-328
  earth shock waves, 112-126, 312-313, 424
  film recording, 118
  gas formation, 112
  measuring instruments, 118-119
  model tests, 114-116
  peak pressure and impulse, 121-122, 425
  recommendations for future work, 132
  soil factors, 116-117, 131
  transient and permanent effects, 117
Explosions under water, 20-63
  see also Shock waves under water
  comparison of explosives, 32-40
  craters produced, 3
  damage produced, 41-43
  description of underwater weapon, 19-20
  detonation process, 20-21
  effect of cavitation, 42-43
  effect of charge-weight and depth, 44, 46-48
  gas bubble formation, 28-31, 46-48, 314, 427
  high explosives, 20-21
  measuring instruments, 44-45, 49-56
  methods of locating source, 59-61
  noncontact explosions, 41-42
  photographic methods of analysis, 56-59
  pressure and impulse, 42, 426
  pressure inside an explosive, 21-22, 39-41
  research facilities, 62-63
  surface phenomena, 31-32, 59
  sympathetic detonation, 50
Explosive D, properties and uses, 359
Explosive fillings
  airburst explosives, 78
  bombs, 359
  underground explosives, 127
  underwater weapons, 20
Explosives, afterburning, 66-67, 80, 91-92
Explosives, high
  see High explosives
Explosives, low (propellants), 66
Explosives, magazines, 103

Explosives, mine clearing
see Mine clearing explosives
Explosives, slow-burning
see Slow-burning explosives

Factory Mutual Research Corporation, Salex burster, 93
Firing devices, characteristics, 375
Flintkote Company, protective panels for tanks, 281
Follmeter gauge, 74
Folding skirt projectile, 188
Formulas
armor perforation, 171, 175
concrete penetration, 192-194, 216-228
crater volume in concrete, 287
plastic bending of a concrete beam, 295
prediction of bombing damage, 309-310
required density of bombing, 318
scabbing limit of concrete, 285
soil penetration, 237
velocity of elastic wave propagation, 256
Fort Pierce, Florida, mine clearing explosives, 102
Fort Worth Headquarters, AAF, Training Command, frangible bullet, 242
Fortification damage
see also Concrete targets, projectile penetration; Explosions under ground; Target damage techniques; Target vulnerability
by AP projectiles, 393, 397, 399-400
contact explosions, 129, 285-288
crater formations, 197-200, 280-287, 313
damage criteria, 429
damage to structural components, 313, 430-435
explosion after penetration, 208
force requirement for bombing attack, 317-318
impact tests on concrete, 288-292, 296-297
noncontact charges, 128-129
prediction of damage, 220, 296, 315-316
pressure measurements, 128
relative effectiveness of explosives, 288
repeated fire effect, 193, 211-212
tests, 127-132
theory, 130-132, 297-301
underground explosions, 285, 297-301, 322
underground structures, 127-132, 313, 434, 444
vulnerable areas, 214-216
Fortification design
aggregate size in concrete, 202
concrete "cover", 203
control of scabbing, 204-205, 209, 286
cured concrete, 201
elastic versus plastic design, 292-300
face mats, 203-204
laminated concrete, 193, 206, 210
plastic protection, 220-292
quality of concrete, 201-202, 291
recommendations for future work, 294-295
reinforced concrete, 197-199, 202-212, 288-292
vulnerable area diagrams, 214
Fragmentation bombs, 320-322, 325-328
on aircraft, 327-328, 443
on freight yards, 326
on light guns, 321
on light targets, 320
on open gun emplacements, 321
on transformer substations, 330
personnel destruction, 320, 443
physical characteristics, 365
Frangible bullet
see T-44 frangible bullet
Frankford Arsenal, frangible bullet, 242
Franklin Institute, muzzle brakes, 134
Frequency-modulated gauges, 71-72
Fuses
airburst, 320-321, 329, 330
delay, 329-330, 332
for bombs, 360-363
for concrete piercing projectiles, 210-211
for high explosive bombs, 360-363
for mines, 374
instantaneous, 329, 330

Gauges for pressure measurement
ADP, 51, 70
ball crusher, 44, 53-54, 72-73
calibration, 70-71, 75-76
condenser-microphone, 71-72
conductivity, 51
diaphragm, 37, 44-45, 54, 73-74
electro-magnetic, 118
follmeter gauge, 74
magnetostriction, 51, 72
Modugno, 33, 54
paper blast meter, 73
piezoelectric, 33, 49-51, 69-71, 118
piston, 54-56, 72-73
quartz, 51, 70
recording methods, 51-52
resistor, 51, 71-72, 75, 118
Rochelle salt, 51, 70
rotating drum, 73
tourmaline, 38-39, 50-51, 69-70
UERL gauge, 44, 72-73
Williams gauge, 73
General Electric Company, gun muzzle attachments, 134
General purpose bombs
see GP bombs
German research
anti-concrete projectiles, 210
armor-piercing projectiles, 409
Bazookas, 277-278
bombs, 370-371
hypervelocity gun, 160
mines, 370-371
Panzerfaust, 280, 281
pressure-operated mines, 32
reinforcement of fortifications, 286
steel projectiles, 187
V2 rocket, 309
GP bombs (general purpose), 312-317, 324-332
dropped on aircraft landing grounds, 327-328
dropped on bridges, 326
dropped on coke ovens, 331-332
dropped on docks, 327
dropped on freight yards, 326
dropped on light factory constructions, 329-330
dropped on railway track, 324
dropped on transformer substations, 330
dropped on tunnels, 325
efficiency, 316
fragmentation, 315
mean area of effectiveness, 326
performance data, 449
physical characteristics, 364
soil penetration, 395
Groundburst charges, 99-100
Guillotine type machines for testing materials, 258
Gulf Research and Development Company
simulated Japanese anti-boat horn mines, 49
universal indicator mine, 102-103
Gun deflectors, 145-150
control of jet, 149-150
reduction of blast effects, 145-149
suppression of dust, 148-149
suppression of flash, 148
Gun muzzle brakes, 142-144
design, 143-145
efficiency factors, 145
M-2 brake, 133
requirements, 144
Gunnery training
see Aerial gunnery training
Guns, hypervelocity
see Projectiles, hypervelocity
Guns, muzzle blast from
characteristics, 135-139, 146-147
control, 141-152
effects, 133-134, 139-141, 146

Harvard University, air-blast measurements, 65
HBX (explosive filling)
aircraft depth bombs, 35
composition, 20, 78
effectiveness for airburst explosions, 92
effectiveness for underground explosions, 127
explosive effect, 79
in underwater weapons, 20, 35
properties and uses, 359
sensitivity, 79
HCR2 plastic armor, 280
Heiland recording oscillograph, 141
Hexanite, 79
High explosives
bomb fuses, 360-363

bombs, 307
damage to factory machinery, 326
definition, 19
detonation process, 20-21
fire starting efficiency, 315-316
in enclosed rooms, 91-93
nitro compounds, 20
theory of detonation, 66-67
Hilliar piston type momentum gauge, 54-55
Hit indicator system in target airplanes, 246
Hollow charges
see Projectiles, shaped charge
Hopkinson law of scaling, 24, 46
Hugoniot relations for shock waves, 40, 95
HVAP (hypervelocity armor-piercing gun), 160
Hypervelocity projectiles, 160-162
see also Projectiles, armor-piercing
energy loss in flight, 169
steel projectiles, 187
tungsten carbide projectiles, 188-189

Impulse in shock waves
see Peak pressure and positive impulse
Impulse pendulums, 285, 288
Incendiary bombs
aircraft loading, 391
clusters, 315
damage to structures, 330
effect of target combustibility, 316
fire starting efficiency, 315
physical characteristics, 366-367
use on grounded aircraft, 320
Indicator mines, 102-103
Infantry snake (line charge), 102, 105, 323
Interferometer, use in studying shock waves, 75, 134, 137

Japanese anti-boat horn mines, 49
Japanese bombs, 372-373
Japanese steel plants, vulnerability, 331-333
Jessop steel armor, 243
Jet smoke rings, 137

Land mines, characteristics, 374
Laredo Army Air Field, Texas, frangible bullet, 242
LC bombs (light case), 307, 312, 330
physical characteristics, 364
Lead azide, 19, 66
Light case bombs (LC), 307, 312, 330
physical characteristics, 364
Line charges, 102
aluminized explosives, 106
Bangalore torpedoes, 309
clearance of minefields, 103-106
cratering effect, 423
definition, 100
detonating cord, 102, 105
dimensions and weights, 105
Dragon hose, 102
on wire barricades, 323
physical characteristics, 377
pressure and impulse-distance curves, 103-106
snakes, 102, 105, 309, 323-324, 377
tank hose, 102, 105
use against defended towns, 106
Low explosives, 66
"Lulu" burster, 93

M2 muzzle brake, 133
M2 service projectiles, 235-236
M3 snake, 105
Mach number, definition, 253
Mach reflection of shock waves
height effect on pressure and impulse, 419-421
interaction of shock waves, 85
Mach stem, 68-69
Machines for testing materials
compression testing, 262
for testing steel under high pressure, 267
guillotine type, 256, 258, 264
pneumatic impact-testing machine, 290
rotary type, 256, 258, 264
tensile testing, 264
MAE (mean area of effectiveness), explosives, 309-311
fragmentation damage, 443
GP bombs, 329
Magazines for explosives, 108
Magnetostriction pressure gauge, 51, 72
Mark 1 hydrophone, 59
Mark 6 depth charge, 33
Mark 13 aerial mine, 33, 49
Mark 54 depth bomb, 33, 60
Massachusetts Institute of Technology, 255
Materials, stress-strain relation
see Stress-strain phenomena in terminal ballistics
Mean area of effectiveness of explosives, 309-311
fragmentation damage, 443
GP bombs, 329
Mercury fulminate, 19, 66
Mine clearing explosives, 101-106
aerial bombardment of mines, 102, 106
aluminized explosives, 106
carpet-roll torpedo, 102
comparison of point and line charges, 106
countermining of horn mines, 49
detonating cord, 102
disadvantages, 102-103
Dragon hose, 102
effect of mine's depth, 103
evaluation of, 102
factors determining distance from charge, 103
line charge blasts, 103-106
projected line charge, 102
skip effect, 103
snakes, 102, 323
tank hose, 102
Mines
aircraft, 368
anti-personnel, 102, 376
anti-tank, 101-102, 374
damage to ships, 328
effective countermining radius, 49
fuses, 374
German, 32, 370-371
land mine characteristics, 376
position of underwater mines, 29
simulated mines for tests, 102-103
tellermine, 103
types of mines, 101
universal indicator mine, 102-103
Minol (explosive filling)
aluminum content, 79
composition, 30, 78
effectiveness as open air explosive, 92
effectiveness for underground explosions, 127
explosive effect, 79
for underwater weapons, 20, 36
in British bomb, 90
properties and uses, 359
Modugno gauge, 33, 54
Monobloc projectiles, 176-187
Munroe jet action, 35, 308
Muzzle-blast characteristics, 135-139
air shock, 135-137
blast pressure, 137-139
detonation process, 135-136
jet characteristics, 135-139, 140-147
muzzle glow, 137
rarefaction front, 137-139
Muzzle-blast control, 141-152
blunderbus extensions, 133
control of jet, 140-150
deflectors, 145-150
field attachments, 141-142
muzzle brake, 133-134, 142-146, 151
recommendations for future research, 151-152
reduction of blast effects, 145-149
reduction of gun's recoil energy, 139, 142-143
Muzzle-blast effects, 133-134, 139-141, 146
blast damage to structures, 139
dust formation, 133, 140
effect of charge weight, 139
effect of gun tube length, 139
effect of muzzle velocity, 133, 139
excessive flash from gun, 133, 141
obscuration of target, 133, 140-141, 146
personnel injury, 140-141
recoil of gun, 139
shock wave impact, 140

Naval Ordnance Laboratory (NOL)
ball crusher, 53-54, 72-73
hydrophone, 59
Nomograms for projectile penetration of concrete, 220

Oblique reflection, application to air-burst bombs, 88-91

Operations analysts, 339-341
peacetime functions, 341
selection of men, 340
Optical distortion method, analysis of shock waves, 57

Panzerfausts (shaped charges), 280-281
Paper blast meter gauge, 73
Peak pressure and positive impulse
charge in free air, 95-96
comparison of charges, 100-101, 103-106
definition, 67-68
destructive effect, 77
distance and weight of explosive, 411-412
effect of atmospheric pressure, 106-107
effect of charge container, 82
effect of distance from explosive, 77, 95-100, 114
effect of height of bomb burst, 86-91
effect of size of explosive, 77
electrical methods for measuring, 69-72
ground-level pressures, 99-100
impulse factors, underground, 121-122, 425
Mach reflection of shock waves, 419-421
measurement for various explosives, 79
mechanical gauges, 72-74
methods of estimating pressure, 38-39
pressure factors, underground, 119-122, 425
Rankine-Hugoniot equations, 83
ratio for common explosives, 69
relative positive impulses, 94
underwater explosions, 426
velocity method of measurement, 74, 83
Pendulum, ballistic, 151, 166
Pendulum, impulse, 285, 288
Pentolite, 24, 99
composition, 78
explosive effect, 79
in shaped charges, 277
properties and uses, 359
Petn, properties and uses, 359
Pétry concrete penetration theory, 227
Photography of armor perforation, 164-165, 167
Photography of cavitation, 43-44, 57-58
Photography of explosions
air cover photographs, 77, 86
flash charge photography, 56-58
high speed motion pictures, 48, 53-56, 75
interferometry, 75, 137
light sources, 75
optical distortion method, 57
rotating drum camera, 75
Schlieren technique, 75
spark photographs, 135, 137, 167
X-ray photographs, 179
Picratol, 78-79, 359
Piezoelectric gauges
ADP, 51, 70
auxiliary apparatus, 70-71
calibration, 39, 50-51, 70-71
comparison of various crystals, 51
compressive impact measurement, 263
effect of gauge mounting, 70
evaluation, 69, 71
measurable quantities, 118
piezoelectric substance, 69
pressure measurements, 69-71, 118
pyroelectric activity, 70-71
quartz, 51, 70
recording of signals, 71
reliability tests, 38-39
Rochelle salt, 51
sensitivity of crystals, 70
tourmaline, 50-51, 70
Piston gauges, 54-55, 72-73
ball crusher gauge, 72
rotating drum gauge, 73
split piston gauge, 73
spring piston gauges, 72, 74
testing of underwater explosives, 33
wave impulse measurement, 54-55, 73
Plane charges, 102
Plastic armor
see Plastic protection
Plastic bullet
see T-44 frangible bullet
Plastic protection, 229-232
comparison with steel, 230
description of material, 229
effect of variation of components, 231-232
for tank protection, 280-281
penetration by projectiles, 229-231, 402
proportions of materials, 231
protection against explosions, 231
protection against shaped charges, 280
ricochet, 230
specifications of components, 231
Plastics
definition of plastic material, 256
elastic limit, 256
particle velocity, 257
propagation of waves, 257-255
tensile impact, 257-258
velocity of plastic waves, 257
"Plate denting index" of explosives, 287
PLC (projected line charge), 102
Pneumatic impact-testing machine, 200
Point charges, 102
Poncelet force law of concrete penetration, 192, 194, 227
Positive phase in shock waves, 67
Pressure measurements in shock waves
see Peak pressure and positive impulse
Pressure wave
see Shock waves
Pressure-time curve for explosions
detonation inside a building, 91
oscillogram, 71, 107
piston gauges, 73
underground wave propagation, 113
Primers, explosives, 68
Probability dip, mine detonation, 198
Projected line charge, 102
Projectile deformation
comparison of steel and tungsten carbide, 179
density of projectile material, 185
effectiveness of projectile cap, 186-187
impact conditions, 176-183
length of projectile, 185
nose shape of projectile, 184
shatter velocity, 179-183
strength of material, 183-184
striking velocity, 179-183
Projectile design
capped projectiles, 186-187
causes of failures, 183
criteria for good projectile, 184
density of material, 185
increase in muzzle velocity, 167-169
length of projectile, 185
mechanical strength of material, 183-184
monobloc projectiles, 186-187
nose shape, 184-185
optimum diameter, 176
prevention of shatter, 183
recommendations, 190
size of core, 187
size of projectile, 176, 185
stability factor, 169-170
Projectiles, armor-piercing, 160-190
see also Armor perforation
armor-piercing cap, 162, 186-187
bombs, 307, 312, 322, 364, 406-407
deceleration during impact, 164
deformation of projectile, 176-183
effect of weight, 176
fortification damage, 393, 397, 399-400
German, 409
monobloc projectiles, 176-187
muzzle energy measurement, 167-169
non-deforming projectile, 170-176
prediction of projectile performance, 176
residual energy, 164
rupture velocity, 177
sabot projectiles, 165, 167, 189
shaped charges, 417
shatter velocity, 177-179, 184
small caliber bullets, 405
stability factor, 169-170
steel projectiles, 184, 189
striking energy, 170
tungsten carbide projectiles, 176, 184, 188-189, 408
uncapped, 403-409
velocity measurement, 166-167
Projectiles, artillery, 308-309
Projectiles, concrete-piercing
see Concrete targets, projectile penetration
Projectiles, flight velocity measurement, 251
Projectiles, hypervelocity, 160-162
see also Projectiles, armor-piercing
effect of armor thickness, 173

UNCLASSIFIED

energy loss in flight, 169
steel projectiles, 187
tungsten carbide projectiles, 188-189
Projectiles, shaped charge, 277-282
armor-piercing, 417
Bazooka, 277-278
cone-end charge, 376
design, 282
effect of sensitive nose fuze, 281
Panzerfaust, 280-281
perforation of armor, 417
perforation of concrete, 416
physical characteristics, 376
protection against, 279-280
residual penetration, 279
tank protection against 280-281
theory of jet penetration, 277-280
Projectiles, soil penetrating, 233-239
see also Soil penetrated by projectiles
effect of projectile mass, 237
fuzes for, 240
GP bombs, 395
instability, 239-240
M2 service projectile, 235
perforation limit velocity, 236
recommendations for future work, 235-236
rocket projectiles, 237
shape and density of projectile, 235-237
shape of projectile nose, 234, 238
striking velocity, 234-235, 237
underground trajectory, 238
Propellants (low explosives), 66
Proximity fuzes, 82, 86, 91

Quartz pressure gauge, 51, 69-70

Rankine-Hugoniot relations, 39, 83
Rarefaction waves in air, 67
Rayleigh waves, underground, 113
RDX-Composition B, 20
Recommendations for future research
air blast phenomena, 103-109
fortification design, 294-295
muzzle blast control, 151-152
projectile design, 190
soil penetrating projectiles, 235-236
underground explosion, 132
weapon effectiveness, 333
Reddy fox charge, 377
Reeves Sound Laboratory, 50
Remington Arms Company, Connecticut, 242
Resistor gauge
auxiliary apparatus, 72
evaluation, 51, 72
measurement of strain, 75
pressure measurement, 118, 287
Reynolds .301 T dural armor, 243
Richardson, properties of air, 83
Riemann, propagation of air waves, 255
Robins-Euler theory, penetration of concrete, 194, 227
Rochelle salt gauge, 51, 69-70
Rockets
airborne, 308, 320
artillary, 308
blast pressure measurements, 107
German V2; 309
on armored vehicles, 323
on locomotives, 326
on open gun positions, 321
on ships, 326
penetration into concrete, 401
penetration into soil, 237
Rotary type machines for testing materials, 264
Rotating drum cameras, 75, 164
Rotating drum gauge, 73
Rupture velocity of projectiles, definition, 177

Sabot projectile, 165, 167, 189
Salex burster, 93
SAP bombs (semiarmor-piercing)
description, 307
dropped on bridge abutments, 325
dropped on coke ovens, 331
dropped on heavy roof construction, 329
dropped on tunnels, 325
fragmentation from, 315
targets used against, 312
SBX (slow-burning explosives)
see Slow-burning explosives
Scaling of models, 23-25, 45-46, 80-81
Schlieren optical system, 75, 251
Schnacke Manufacturing Company, Indiana, 242
Seismic wave, 121
Shadow ratio chart, 452-453
Shaped charge
see Projectiles, shaped charge
Shatter velocity of projectiles, definition, 177-179
Shock tube, 84
Shock waves in air, 64-109
destruction caused by, 68-69, 76-77, 311-312
detonation wave, 66-67
duration, 311
effect of distance from charge, 94-100
explosions in enclosed areas, 91-93
formation, 67
incident wave, 68-69
Mach reflection, 85-86
oblique reflection, 84-91
particle velocity, 67-68, 83
peak pressure, 67, 77
photography of explosions, 74-75
positive impulse, 67-68, 76-77
pressure measurement, 67-68
propagation, 67-68, 74, 95
recommendations for further study, 108-109
reflection, 68-69, 83-85
shape, 67
shock tube, 84
slipstream boundary, 85
temperature of medium, 67-68, 106-107
velocity measurement, 74
wave front, 67
Shock waves in earth, 112-126, 312-313
crater formation, 422-423
damage to bridge abutments, 326
displacement of earth, 424
effect of soil, 114, 116
particle acceleration and displacement, 122-125
peak pressure, 112-117, 122-125, 426
propagation of shock wave, 118-121
reflection, 113
shape of wave, 119
stress-strain curve, 115
velocity, 114, 116
Shock waves under water, 20-63
cavitation, 25
cut-off time, 24-25
damaging factors, 43-44, 314
destruction, 48-49, 313-314
duration, 23-24
effect of charge shape, 57
energy, 21, 23-24, 37, 43
equations for parameters, 37-39
impulse, 37
low pressure tail, 23
measurement of characteristics, 23
methods of estimating peak pressure, 38-39
momentum of, 22-24
optical distortion method of analysis, 57
peak pressure, 22-26, 37-39, 49
pressure decay, 21-24
pressure measuring instruments, 49-56
propagation, 20-21, 38-41
properties, 21-25
reflection, 24-28
similitude principle, 23-25
surface phenomena, 31-32
theoretical calculation of properties, 39-41
wave front, 21-22
Similarity law of explosives, 80-81
application, 80
limitations, 80-81
"skin effect," 81
statement of principle, 80
Similitude principle of shock waves, 23-25
Slow-burning explosives (SBX), 93-94
aluminum and gasoline mixtures, 94
comparison with HE explosive, 94
for sabotage devices, 93
"Lulu" burster, 93
pressure time oscillogram, 94
"Salex" burster, 93
Snakes (line charges), 102, 105, 309
application, 323-324
physical characteristics, 377
Soil penetrated by projectiles, 233-239
see also Projectiles, soil penetration
mathematical formulas, 237
moisture content of soil, 235
physical properties of soil, 233
recommendations for future work, 235-236
ricochet of projectile, 306-308
sand bag experiments, 238
sectional energy and pressure theories, 239

UNCLASSIFIED

UNCLASSIFIED

soil parapets, 238
Soil penetrated by projectiles, tests, 234-236
clay, 236
concrete slabs with soil covering, 236
experimental method, 234-235
loam, 235-236
parapets of soil, 236
physical characteristics of soils used, 235
sand, 235
sand bags, 236
Sound ranging, detection of underwater explosions, 59-60
Spark shadowgraphs of projectiles, 178
Sperry Gyroscope Company, 246
Split-piston gauge, 73
Spring piston gauge, 72, 74
Steel, pressure deformation, 255-273
blast damage to steel columns, 430
critical impact velocity, 260
ductility of steel, 269
effect of underwater explosions, 44-49
elastic limit velocity, 261
flow stress, 271
fracture, 269-270, 272
hardness tests, 268, 272
heat-treatments, 269
hydrostatic stress, 267
mechanism of deformation, 266-267
method of measurement, 267
orientation of specimens, effect on strength, 271
plastic deformation, 45
punching of steel, 272-273
rate of strain, 263
rupture, 267
strain-hardening, 270
stress limit, 255
tensile tests, 264, 268
uniaxial state of stress, 267
Steel projectiles, 168, 184-190
comparison of monobloc and capped projectiles, 187
conventional length, 185
hardness, 184
hypervelocity projectile, 187
shatter velocity, 184-185
Strain gauge
auxiliary apparatus, 72
evaluation, 51, 72
pressure measurement, 118, 267
strain measurements, 75
Stress-strain phenomena in terminal ballistics, 255-273, 292-294
compression tests, 259-263
critical impact velocity, 260
critical impulse, 260-261
critical tensile velocity, 258
deformation of steel under pressure, 266-273
elastic versus plastic design, 292-293
elastic waves, 256-257
flow stress, 269
force deformation curves, 263
impact tests, 256, 260-261, 293-294
impulsive loading, 260-261
natural strain, 267
particle velocity in medium, 257
propagation of plasticity in solids, 256-261
rapid loading tests, 260, 265
rupture of materials, 267
strain rate tests, 255-256, 265
tensile impact tests, 256, 264-265
true stress, 267, 269
unstraining, 258-259
Supersonic wind tunnel, design problems, 251-254
Surface waves, explosion generated
effect on mines, 32
measurement of, 59

T-44 frangible bullet, 242-248
ballistic coefficient, 242
evaluation, 248
limit velocity, 242-243
limitations in aerial gunnery training, 247
performance on glass, 244
propellant, 244-245
range, 242
use with K-15 sight, 246
use with piston gun, 245
Tank hose (line charge), 102, 105
Tank protection against shaped charges
plastic armor, 280-281
spikes on panels, 281
Target airplanes for aerial gunnery training, 245-246, 248
Target damage techniques, 310-333
air blast, 311-312, 328
confined blast, 312, 328-329
cratering attacks, 327
equivalent horizontal area for sloping target, 41
external blast, 328
fire, 315-316, 328
force requirement, 317-318
fragmentation, 314-315, 326
mining of harbor entrances, 327
prediction of damage, 310-311, 319
radius of damage, 314-315
shadow ratio chart, 452-453
training of operations analysts, 339-341
underground explosion, 312-313, 321, 327-328, 330
underwater explosion, 313-314
weapon selection, 319-333
Target vulnerability, 318-333
air transportation, 326-328, 445
domestic construction, 284-285, 330, 456, 459, 463, 465-467, 469
industrial targets, 328-333, 436-437, 460-462, 464, 468, 471-472
Japanese steel industry, 331-333
military targets, 319-324, 441-442
rail and highway transportation, 324-326, 446, 448, 457
steel mills, 438
underground structures, 323
utilities, 330
warehouses, 330
water transportation, 327-328, 433, 447
Taylor Model Basin
air-blast measurements, 65
cables for electrical pressure gauges, 52
resistor gauge, 51, 71-72
Telecon (British) cable, 113
Tellermine, 43; 103, 106
Tensile testing machines, 262
Terminal ballistics
see Ballistic studies
Testing materials, machines
see Machines for testing materials
Tetryl charges
destructive effect, 46-48, 284
properties and uses, 359
tetryl booster, 66, 93
Tetrytol, properties and uses, 359
Thompson, J. J., shock wave pressure measurement, 50
TMI-43 (tellermine), 103, 106
TNT
peak pressure and positive impulse, 78-79
properties and uses, 359
Torpedoes
aerial, 308, 368
Bangalore, 309, 323-324
carpet-roll, 102
effect on water transportation, 327
Torpex
aluminum content, 79
bubble period, 35
composition, 20, 78
effective range, 35
explosive effect, 79
properties and uses, 359
sensitivity, 35
torpex D-1; 79
underwater weapons, 20
Tourmaline gauges
advantages, 51
calibration methods, 38-39
description, 50, 70
sensitivity, 70
Trauzl lead block test of explosives, 65
Trialen, 78-79
Tritonal
aluminum content, 79
composition, 20, 78
evaluation, 92, 94, 127
explosive effect, 79
properties and uses, 359
Tungsten carbide projectiles
angle of attack, 179
ballistic coefficient, 169
bond strength, 184
effect of projectile cap, 187
effect on German tanks, 189
perforating ability, 176, 185, 408
stability, 170
standard length, 185
striking velocity, 178
types, 188

UERL spring-piston gauge, 72-73

UNCLASSIFIED

Underground explosions
see Explosions under ground; Shock waves in earth
Underwater explosions
see Explosions under water; Shock waves under water
Underwater Sound Reference Laboratory, 39
U. S. Naval Bomb Disposal School, 340
Universal indicator mine, 102, 106
University of Illinois, 255
University of Pennsylvania, 255

V2 rocket, 309
Von Neumann, reflection of shock waves, 83-85
VT (proximity) fusing, 82, 87
Watertown Arsenal Experimental Laboratory, 255
Weapon data sheets, 342-354, 357-472
Weapons, airborne, 307-308
Weapons, artillery, 308-309
Weapons, effectiveness, 305-307, 309-311
mean area of effectiveness, 309-311
methods of studying, 305-307
prediction of damage, 309-311
radius of damage, 310-311
recommendations for future work, 333
Weapons, selection principles, 319-333
airborne rockets, 320
AP bombs, 322
artillery projectiles, 321
cratering bombs, 327-328
delay fused bombs, 322
fragmentation bombs, 320, 327-328, 330
GP bomb, 321-332
high explosive bombs, 329
incendiary bombs, 320, 330
instantaneously fused bombs, 328
LC bomb, 330
line charges, 323-324
rockets, 321, 323, 326
SAP bombs, 325, 329, 332
torpedoes, 326
Westinghouse Research Laboratories, 255
Williams gauge, 72
Wind tunnel, supersonic, design problems, 251-254
Woods Hole Oceanographic Institution, 62
Wright Field, Ohio, 242

RECEIVED FEB 2 1948 RDB